CFTRI MYSORE
5578
Investigation of

TECHNIQUE OF ORGANIC CHEMISTRY

ARNOLD WEISSBERGER, *Editor*

Volume VIII—Part II

INVESTIGATION OF RATES AND MECHANISMS OF REACTIONS

Second completely revised and augmented edition

Part II

TECHNIQUE OF ORGANIC CHEMISTRY

ARNOLD WEISSBERGER, *Editor*

Volume I:	Physical Methods of Organic Chemistry *Third Edition*—Parts I to IV
Volume II:	Catalytic, Photochemical and Electrolytic Reactions *Second Edition*
Volume III:	*Second Edition* Part I. Separation and Purification Part II. Laboratory Engineering
Volume IV:	Distillation
Volume V:	Adsorption and Chromatography
Volume VI:	Micro and Semimicro Methods
Volume VII:	Organic Solvents *Second Edition*
Volume VIII:	Investigation of Rates and Mechanisms of Reactions *Second Edition*, in Two Parts
Volume IX:	Chemical Applications of Spectroscopy
Volume X:	Fundamentals of Chromatography
Volume XI:	Methods of Systematic Degradation

TECHNIQUE OF ORGANIC CHEMISTRY
Volume VIII—Part II

INVESTIGATION OF RATES AND MECHANISMS OF REACTIONS

Second Completely Revised and Augmented Edition

Editors

S. L. FRIESS, E. S. LEWIS, and A. WEISSBERGER

Authors of Part II:

Myron L. Bender
Charles E. Boozer
G. M. Burnett
Britton Chance
L. De Maeyer
Manfred Eigen
S. L. Friess
Frank M. Huennekens
Maurice M. Kreevoy
Edward S. Lewis
Sir H. W. Melville
Richard M. Noyes
George Porter
F. J. W. Roughton
William H. Saunders, Jr.
H. Strehlow
A. Weller

1963
INTERSCIENCE PUBLISHERS, DIV., JOHN WILEY & SONS
NEW YORK, LONDON

5578

Dt. 9.10.63

E1,5:f",1,N49

N48.8B

Library of Congress Catalog Card Number 45-8533

Copyright 1953, 1961, 1963 by Interscience Publishers, Inc.

First Edition 1953
Second Revised Edition, 1961, 1963

All Rights Reserved. *This book or any part thereof must not be reproduced in any form without permission of the publisher in writing. This applies specifically to photostat and microfilm reproductions.*

CFTRI-MYSORE
5578
Investigation of

PRINTED IN THE UNITED STATES OF AMERICA BY MACK PRINTING CO., EASTON, PA.

INTRODUCTION

Organic chemistry, from its very beginning, has used specific tools and techniques for the synthesis, isolation, and purification of compounds, and physical methods for the determination of their properties. Much of the success of the organic chemist depends upon a wise selection and a skillful application of these methods, tools, and techniques, which, with the progress of the science, have become numerous and often intricate.

The present series is devoted to a comprehensive presentation of the techniques which are used in the organic laboratory and which are available for the investigation of organic compounds. The authors give the theoretical background for an understanding of the various methods and operations and describe the techniques and tools, their modifications, their merits and limitations, and their handling. It is hoped that the series will contribute to a better understanding and a more rational and effective application of the respective techniques. Reference is made to some investigations in the field of chemical engineering, so that the results may be of assistance in the laboratory and help the laboratory chemist to understand the problems which arise when his work is stepped up to a larger scale.

The field is broad and some of it is difficult to survey. Authors and editors hope that the volumes will be found useful and that many of the readers will let them have the benefit of their criticism and of suggestions for improvements.

Part 2 of Volume VIII is the first book in this series which is published since the death of my wife, Dr. Louise Harris Weissberger. She was a biochemist by education. She had a deep interest in style and language and particularly in the succinct documentation of research. Her interest in my work was a steady source of encouragement and help. Her companionship and devotion, her sincerity and warmth, her patience and love have contributed immeasurably to my life.

ARNOLD WEISSBERGER

Research Laboratories
Eastman Kodak Company
Rochester, New York

GENERAL PLAN OF THE SERIES

Volume I (Third Edition—in four parts). **Physical Methods of Organic Chemistry.** *Authors:* A. E. Alexander, D. H. Anderson, J. R. Anderson, J. C. Arthur, Jr., E. D. Bailey, N. Bauer, G. L. Beyer, E. R. Blout, L. O. Brockway, L. M. Corliss, A. H. Corwin, R. L. Custer, B. P. Dailey, G. Donnay, J. D. H. Donnay, K. Fajans, D. D. Fitts, G. K. Fraenkel, A. L. Geddes, H. S. Gutowsky, F. A. Hamm, W. D. Harkins, J. M. Hastings, W. Heller, E. E. Jelley, W. Klyne, C. G. Le Fevre, R. J. W. Le Fevre, S. Z. Lewin, W. N. Lipscomb, W. J. Mader, H. Mark, L. Meites, D. H. Moore, L. D. Moore, Jr., O. H. Muller, J. B. Nichols, W. C. Nixon, G. Oster, A. C. Parker, M. A. Peacock, R. B. Pontius, J. G. Powles, H. A. Scheraga, P. W. Selwood, T. Shedlowsky, R. Signer, D. R. Simonson W. M. Siri, E. L. Skau, C. P. Smyth, M. Spiro, D. W. Stewart, J. M. Sturtevant, W. Swietoslawski, J. F. Swindells, C. Tanford, G. W. Thomson, B. M. Tolbert, R. Ullman, M. J. Vold, R. D. Vold, R. H. Wagner, H. Wakeham, C. E. Waring, S. Wawzonek, W. West, N. B. Woodall and N. Wotherspoon

Volume II (Second Edition). **Catalytic Reactions,** V. I. Komarewsky, C. H. Riesz, and F. L. Morritz; **Photochemical Reactions,** C. R. Masson, V. Boekelheide, and W. A. Noyes, Jr.; **Electrolytic Reactions,** S. Swann, Jr.

Volume III (Second Edition)

Part I. Separation and Purification. C. M. Ambler, G. Broughton, D. Craig, L. C. Craig, A. B. Cummins, F. B. Hutto, Jr., A. L. Jones, K. Kammermeyer, F. W. Keith, Jr., E. MacWilliam, E. G. Scheibel, R. E. Stauffer, and R. S. Tipson.
Part II. Laboratory Engineering. J. W. Axelson, R. S. Egly, R. F. Eisenberg, M. P. Hofmann, R. R. Kraybill, G. H. Miller, J. H. Rushton, W. C. Streib

Volume IV. Distillation. J. R. Bowman, C. S. Carlson, A. L. Glasebrook, J. C. Hecker, E. S. Perry, A. Rose, E. Rose, R. S. Tipson, and F. E. Williams.

Volume V. Adsorption and Chromatography. H. G. Cassidy

Volume VI. Micro and Semimicro Methods. N. D. Cheronis. With contribution by A. R. Ronzio and T. S. Ma

Volume VII. Organic Solvents. A. Weissberger and E. S. Proskauer. *Second Edition* by J. A. Riddick and E. E. Toops, Jr.

Volume VIII (Second Edition—in two parts). **Investigations of Rates and Mechanisms of Reactions.** *Editors:* S. L. Friess, E. S. Lewis, and A. Weissberger. *Authors:* J. C. Balaceanu, M. L. Bender, S. A. Bernard, C. E. Boozer, J. F. Bunnett, G. M. Burnett, B. Chance, L. DeMaeyer, M. Eigen S. L. Friess, J. Higgins, F. M. Huennekens, J. C. Jungers, M. Kreevoy, E. S. Lewis, R. Livingston, A. Maccoll, E. F. MacNichol, Jr., H. W. Melville, B. K. Morse, R. M. Noyes, G. Porter, F. J. W. Roughton, G. A. Russell, W. H. Saunders, Jr., H. Strehlow, A. Weller

Volume IX. Chemical Applications of Spectroscopy. *Editor:* W. West. *Authors:* A. B. F. Duncan, W. Gordy, R. N. Jones, F. A. Matsen, C. Sandorfy, and W. West

Volume X. Fundamentals of Chromatography. H. G. Cassidy

Volume XI. Methods of Systematic Degradation. *Editor:* K. W. Bentley. *Authors:* B. Belleau, K. W. Bentley, K. Beimann, J. C. D. Brand, A. R. H. Cole, P. deMayo, J. K. N. Jones, J. F. King, E. Leete, S. McLean, F. J. McQuillin, K. H. Overton, M. B. Perry, N. Polgár, K. T. Potts, A. I. Scott, E. Y. Spencer, J. B. Stothers, G. A. Swan, Z. Valenta, B. C. L. Weedon

Investigation of Mechanisms of Reactions

PREFACE TO THE SECOND EDITION

The search for information about the changes which compounds undergo is of the very essence of chemistry, not only because of the end-products formed, but also in view of the intermediates and the transformations which control the over-all reactions. Investigations of the mechanisms of reactions have therefore been undertaken since the beginning of modern chemistry. In recent years they have become one of the most important branches of physical organic chemistry. From a practical point of view, detailed information on the rates and mechanisms of reactions can be most valuable in guiding operations and choosing optimum conditions for synthetic and for analytical work.

This volume is concerned with the theoretical and experimental tools used to establish the mechanisms of reactions. Foremost among these ranks the determination of the rates at which a reaction proceeds as a whole and in its various parts. Several of the physical methods used in the handling of kinetic problems have been discussed in earlier volumes of this series, to which reference is made in order to avoid duplication. But it is the application and adaptation of experimental techniques to the various reactions, as well as the theoretical interpretation of the results, which present the most intricate and highly individual problems. These applications and adaptations, the special methods which have been devised for the study of reaction rates and mechanisms and the relevant theories are discussed in detail; examples of investigations are given as models for related reactions together with appropriate comment on possible variations or refinements.

In the eight years which have elapsed since this was said in the preface to the first edition of this volume, highly significant advances have been made in both the experimental and the theoretical methods for the study of reaction mechanisms, and a new edition rather than a reprinting has become necessary. For this the title of the book has been changed in view of the importance of the non-kinetic methods for the elucidation of reaction mechanisms, and the new edition has been divided into two parts, I dealing with the kinetic methods and II in which the non-kinetic methods are discussed.

A general survey of the methods useful in determining reaction mechanisms is given in a new introductory chapter (Lewis), and new chapters have been added on "Time Measurements and the Recording of Kinetic Data" (MacNichol), "The Interpretation of Rate Data" (Bunnett), "Use of Computers" (Chance, Higgins), "Kinetic Isotope Effects" (Saunders), and "Heterogeneous Reactions and Catalysis" (Jungers and Balaceanu). Most of the old chapters have been thoroughly revised—some have been entirely rewritten—by new authors, "Competing Reactions" (Russell), "Homogeneous Gas Phase Reactions" (Maccoll), "Homogeneous Catalysis" (Bernhard).

The emergence of powerful new methods for following reactions with half-lives much smaller than a second has given rise to a section on the study of very rapid reactions. The organization of this section owes much to Dr. M. Eigen who has written an introduction. Chapters XV to XX deal respectively with: "Electrochemical Methods" (Strehlow), "Photostationary Methods" (Noyes and Weller), "Magnetic Resonance Methods" (Strehlow), "Relaxation Methods" (Eigen and DeMaeyer), "Flash Photolysis" (Porter), and "Determination of Active Intermediates in Reactions" (Melville and Burnett).

Part II contains a new set of chapters on nonkinetic techniques, beginning with Chapter XXIII which deals with "Thermodynamics and Reaction Mechanism" (Kreevoy). It is followed by chapters on "The Product Criterion of Mechanism" (Lewis, Boozer), "Evidence for Formation of Intermediates in Organic Chemical Reactions" (Bender), "Use of Isotopes and Tagged Groups" (Saunders), and "Stereochemistry and Mechanism of Reactions" (Friess).

While all the chapters deal with the elucidation of reaction mechanisms and the pertinent methods, the individual topics are so different that no attempt has been made to impose on the authors rules aiming at uniformity. Rather, the authors have been encouraged to develop their themes in accordance with the essence and the immanent structure of their material. Some overlapping has been accepted so that the integrity of the respective presentations would not be disturbed and because each exposition has its intrinsic value by virtue of the particular point of view and experience of the author.

We hope that by the discussion of the theoretical and practical aspects of work on reaction mechanisms a treatise has been obtained which will provide the student and the advanced research worker with stimulating information and the knowledge needed for a well-directed approach to new problems, point the way to the pertinent literature, and help in the further development of a field fascinating because of its difficulty and its importance.

We thank the Publishers and their staff for their skillful assistance in the preparation of this volume.

S. L. Friess
Naval Medical Research Institute
Bethesda, Maryland

E. S. Lewis
Department of Chemistry
William M. Rice University
Houston, Texas

A. Weissberger
Research Laboratories
Eastman Kodak Company
Rochester 4, New York

Investigation of Rates and Mechanisms of Reactions

CONTENTS

PART ONE

I. General Methods of Determining Reaction Mechanisms. By E. S. Lewis

Kinetic Methods

II. General Theory of Rate Process. By Robert Livingston
III. Fundamental Operations and Measurements in Obtaining Rate Data. By Robert Livingston
IV. Time Measurements and the Recording of Kinetic Data. By Edward F. MacNichol, Jr.
V. Evaluation and Interpretation of Rate Data. By Robert Livingston
VI. The Interpretation of Rate Data. By Joseph F. Bunnett
VII. Use of Computers. By Joseph Higgins
VIII. Competing Reactions. By Glenn A. Russell
IX. Kinetic Isotope Effects. By William H. Saunders, Jr.
X. Homogeneous Gas Phase Reactions. By Allan Maccoll
XI. Homogeneous Solution Reactions. By B. Kathlfen Morse
XII. Homogeneous Catalysis. By Sidney A. Bernard
XIII. Heterogeneous Reactions and Catalysis. By J. C. Jungers, and J. C. Balaceanu

PART TWO

Preface to the Second Edition vii
XIV. Rapid Reactions. By F. J. W. Roughton and Britton Chance 703

Very Rapid Reactions in Solution

Introduction to Chapters XV to XX. By Manfred Eigen 793
XV. Electrochemical Methods. By H. Strehlow 799
XVI. Photostationary Methods. By Richard M. Noyes and A. Weller. 845
XVII. Magnetic Resonance Methods. By H. Strehlow 865
XVIII. Relaxation Methods. By Manfred Eigen and L. de Maeyer 895
XIX. Flash Photolysis. By George Porter 1055
XX. Determination of Active Intermediates in Reactions. By G. M. Burnett and Sir H. W. Melville 1107
XXI. Polymerization and Polymer Reactions. By G. M. Burnett 1139

XXII. Enzymic Reactions 1231
Part 1. Measurement of Enzyme Reactions and General Theory of Enzyme Kinetics. By Frank M. Huennekens
Part 2. Enzyme Kinetics in the Transient State. By Britton Chance

Nonkinetic Methods

XXIII. Thermodynamics and Reaction Mechanism. By Maurice M. Kreevoy 1361
XXIV. The Product Criterion of Mechanism. By Edward S. Lewis and Charles E. Boozer 1407
XXV. Evidence for the Formation of Intermediates in Organic Chemical Reactions. By Myron L. Bender 1427
XXVI. Use of Isotopes and Tagged Groups. By William H. Saunders, Jr. .. 1519
XXVII. Stereochemistry and Mechanism of Reactions. By S. L. Friess 1549

CHAPTER XIV

RAPID REACTIONS

F. J. W. Roughton, *University of Cambridge*
Britton Chance, *University of Pennsylvania*

Part 1. General Principles of Measurement of Velocity of Rapid Reactions in Solution. F. J. W. Roughton 704
I. Historical Introduction 704
II. Scope of Present Chapter 707
III. Common Factors in Rapid Reaction Measurements by Various Techniques . 708
1. Reagent Containers 708
2. Methods of Fluid Drive 708
3. Mixing Chambers 709
4. Tests of the Efficiency of Mixing 711
5. Construction of Observation Tubes 714
6. Character of Flow in Observation Tube 714
7. Magnitude of Errors Due to Deviations from "Mass" Flow 717
8. Magnitude of Errors Due to Mixing Time and Slit Length 720
9. Multiple Mixers 724
10. Standard Reactions for the Testing of Rapid Flow Apparatus 725
11. Solvent and Temperature Changes 726
References 727
Part 2. Accelerated and Stopped Flow Methods Using Spectrophotometric Measurements. Britton Chance 728
I. Introduction 728
II. Survey of Current Designs of Flow Apparatus 731
1. Detailed Description of Chance's Apparatus 733
2. Description of Gibson's Apparatus 741
3. Apparatus of Dalziel and O'Brien 745
References 748
Part 3. The Regenerative Flow Apparatus. Britton Chance 749
I. Regenerative Features 751
II. Applications 751
1. The Rapid Recording of Absorption Spectra in the Visible and Ultraviolet Regions 752
2. Application to the Rankine Balance 754
3. Application to Electron Spin Resonance 755
III. Summary 757
References 757
Part 4. The Thermal Measurement of Rapid Reactions in Solution. F. J. W. Roughton 758
I. Introduction 758

II. Present Method for Measurement of Rapid Reactions with Total Temperature Changes of 0.05 to 0.5°C. . . . 759
1. General Set-Up of Apparatus (Exclusive of Temperature-Measuring System) . . . 759
2. Measurement of Temperature . . . 760
3. Procedure in an Actual Experiment . . . 763
4. Accuracy and Use of the Method . . . 765
III. Earlier Work on Rapid Reactions with Temperature Changes of Less Than 0.05°C. . . . 767
1. Points of Difference in Earlier Procedure . . . 767
2. Residual Blank Effects Due to Physical Factors . . . 768
IV. Summary of Reactions Studied: Present and Possible Future Scope of Rapid Flow Thermal Methods . . . 773
1. Range of Reactions and Determination of Heats of Reactions Inaccessible by Classical Calorimetry . . . 773
2. Résumé of Present Scope and Limitations . . . 775
3. Possible Developments . . . 776
References . . . 778
Part 5. Quenching, Electrometric, and Other Rapid Reaction Techniques. F. J. W. ROUGHTON . . . 778
I. The Quenching Method . . . 779
II. Electrometric Methods . . . 781
1. Electrical Conductivity . . . 782
2. Reversible Electrode Potentiometry . . . 783
3. Polarographic Determination of H_2O_2 and O_2 . . . 785
III. The Gasometric Method . . . 787
IV. The Ultrafiltration Method . . . 788
1. Dirken and Mook's Technique . . . 789
2. Recent Filtration Technique . . . 790
References . . . 791
General References . . . 792

Part 1. *GENERAL PRINCIPLES OF MEASUREMENT OF VELOCITY OF RAPID REACTIONS IN SOLUTION*

I. HISTORICAL INTRODUCTION

Until 1923 there existed no direct, generally applicable method for measuring the velocity of rapid chemical reactions in the liquid phase with half-times of less than about 10 sec. In that year, however, Hartridge and Roughton (1) extended the observable time range about 10,000-fold by devising a method which could be used to follow reactions with half-periods ranging from 10 sec. (or more) down to 0.001 sec. The principle of their method was that the two solutions which were to react were placed in sep-

arate containers and driven thence into a special mixing chamber: the emerging mixed fluid passed down an observation tube, at various cross sections of which the composition of the streaming fluid was determined by optical, thermal, electrical, chemical, or other methods of analysis applicable to rapidly moving fluids. If d is the distance in cm. between the mixing chamber and the cross section under examination, and $\bar{u}$ is the average linear velocity in cm./sec. of the streaming fluid, then the average time for which the reaction has proceeded before reaching the place of observation is simply $d/\bar{u}$ sec. Thus if the cross section under examination is 3 cm. from the mixing chamber and $\bar{u}$ = 1,000 cm./sec., the corresponding time is $^3/_{1,000}$ or 0.003 sec. (3 millisec.). The value of $\bar{u}$ is given by $\bar{v}/A$, where $\bar{v}$ is the average volume velocity of the streaming fluid as measured in cc./sec. and A is the cross-sectional area of the observation tube. From observations at 5 or more cross sections the usual type of concentration-time curve could readily be plotted. Alternatively, the observations could be all made at a fixed distance, e.g., 1 cm., from the mixing chamber and the velocity of fluid flow varied either in discrete steps, as in Millikan's (2) procedure, or continuously as in the accelerated flow method of Chance (3), the latter of which has the great advantage of minimal fluid requirements.

By interposing dead spaces, of volume up to 3 liters, between the mixing chamber and point of observation, Hartridge and Roughton (4) were able to extend the time of observation up to several minutes and thus to "overlap" their method with the classical methods previously in use for relatively slow chemical reactions. In certain instances (see Roughton (5)) they also made use of the "stopped flow" method, which consists in suddenly arresting the flow of two reacting liquids and then immediately following, by optical or other suitable technique, the progress of the chemical change in the "stopped flow" in the observation tube. Forty or so years ago, there were no photocells, electronic, or cathode ray tube equipment generally available, and the visual and other methods at the disposal of Hartridge and Roughton only permitted them to study by the stopped flow method processes taking several seconds for completion. With the advent of the rapid electronic methods of registration during the past twenty years the "stopped flow" method has become a cardinal feature (see Chance (3), Gibson (6), and later workers) in the measurement of rapid chemical reactions. The stopped flow method has several advantages over the continuous flow method: (*1*) it is independent of the rate and character of flow down the observation tube, (*2*) a permanent record can be obtained of the progress of the reaction over a period starting at a few milliseconds after mixture and extending as long as desired, (*3*) it is free from the distorting effect of mechanical disturbances, (*4*) the volume of reagents required are minimal. On the other hand the stopped flow method

is less sensitive and the methods of possible observation are more restricted: furthermore it can so far cope only with reactions about one fifth as fast as the most rapid within the compass of the moving fluid method.

Before the present day forms and potentialities of the rapid reaction technique are described in detail, some reference may be made to earlier work which contained one or more of the ideas used by Hartridge and Roughton in their 1923 method.

An application of the flow principle (but without mixing) was made by Rutherford (7) in his measurements of the coefficient of recombination of gaseous ions. A steady stream of gas was passed down a long tube at the entrance to which was placed a layer of uranium oxide. This supplied a constant source of ionizing rays so that the gas was all ionized to the same extent. At various points along the observation tube were placed electrodes which could be connected to an electrometer. Measurement of the saturation current at each of the electrodes gave the number of ions left in the streaming gas at the corresponding point in the observation tube, and from the rate of gas flow and the distance between the electrodes the rate of recombination of the ions was thus readily obtained. A similar use of the flow method 25 years later by Hartridge and Roughton (8) enabled them to make their first kinetic measurements on the reactions of hemoglobin with carbon monoxide and oxygen. In this work a solution of carboxyhemoglobin flowed up a vertical tube which was illuminated by a beam of light from a powerful arc lamp. Under the influence of the light the carbon monoxide in combination with the hemoglobin was photochemically displaced by dissolved oxygen. The solution, after flowing through the brightly illuminated tube, passed into a dark tube wherein the initial dark state of equilibrium was progressively regained. The amount of the return reaction in the flowing fluid at various distances along the dark tube was estimated by the reversion spectroscope. Hartridge and Roughton also followed the kinetics of the same reaction by displacing a stationary solution of carboxyhemoglobin from equilibrium by means of light and then following the return to the dark equilibrium. Their work may perhaps be regarded as a crude forerunner of the flash photolysis methods of Porter and Norrish (9).

Two earlier examples of the application to gas reactions of the principles which Hartridge and Roughton and their successors subsequently developed for rapid reactions in solution have been found in the literature. In 1905 Raschig (10) made kinetic studies of the rapid reaction between NO and O_2 by driving the two gases into a T-shaped glass mixer and thence, through glass tubing of varying volume, into an absorbing solution which stopped the reaction. The time during which the reaction had proceeded was calculated from the volume rate of gas flow and the volume of inter-

mediary tubing between the mixer and the absorbing solution: times ranging from 0.025 to 25 sec. are quoted in the original paper. Raschig's technique was thus a direct precursor of one of the main developments of the Hartridge-Roughton principle, namely the chemical or "quenching" method. In 1922 Stewart and Edlund (11) drove a mixture of C_2H_4 and Br_2 vapor into a mixer and thence into a reaction tube. By suddenly turning off the stream of mixed gases, and following the changes in the reaction tube manometrically the course of the reaction $C_2H_4 + Br_2 \rightarrow C_2H_4Br_2$ was continuously followed. Though the timing was rather slow, i.e., of the order of 0.25 minutes and upwards, the method of Stewart and Edlund is obviously a precursor of the "stopped flow" method.

Finally, reference should be made to the continuous flow calorimetry of (*1*) Callendar and Barnes (12) as applied to measurements of the specific heat of water, and (*2*) Keyes, Gillespie, and Mitsukuri (13) on the heat of neutralization of HCl and NaOH. This technique may be regarded in some degree as a forerunner of the thermochemical method of measuring the velocity of rapid reactions, a subject treated in detail later in this chapter.

II. SCOPE OF PRESENT CHAPTER

The principles introduced by Hartridge and Roughton in 1922 through 1923 still form the basis of the greatly improved methods available today. While some of the details of technique are governed by the particular method of observation employed—optical, thermal, chemical, electrical, etc.—there are numerous features and factors which are encountered in all the methods of observation, namely:

(*1*) Nature of reagent containers.
(*2*) Mode of driving the reagents to the mixing chamber and down the observation tube.
(*3*) Construction of the mixing chambers.
(*4*) Tests of the efficiency of mixing.
(*5*) Nature of the observation tubes.
(*6*) Character of flow down the observation tube, including the problem of cavitation.
(*7*) Magnitude of errors due to deviations from ideal or "mass" flow.
(*8*) Magnitude of errors due to slit length and finite size of mixing chamber.
(*9*) Multiple mixing.

Part 1 of the chapter is devoted to the discussion of these general features. There follows in Parts 2 and 4 a detailed description of the technique used in the two most widely applicable methods of observation, namely the photoelectronic and the thermal methods, together with references to the application of these two methods to a number of actual chem-

ical reactions. A briefer descriptioins given in Part 3 of the regenerative flow apparatus and in Part 5 of the quenching and electrometric methods, and of other techniques of powerful but limited application, together with appropriate practical examples.

III. COMMON FACTORS IN RAPID REACTION MEASUREMENTS BY VARIOUS TECHNIQUES

1. Reagent Containers

In the early apparatus of Hartridge and Roughton, the volumes of each reagent required for a single experiment were of the order of 3 to 4 liters. Large stoneware bottles, with bottom outlets and capacities of 5, 10, or even 20 liters were used as containers. Such bottles are capable of standing up to 2 atmospheres pressure and hence were serviceable when compressed gas was used as the driving agent. Subsequent work led to progressive reduction in fluid requirements by powers of 10 down, finally, in the Chance apparatus, to volumes as low as 0.1 cc. or less. For volumes of 0.1 to 25 cc., the use of syringes, which were first introduced by Dirken and Mook (14), has been generally adopted. The metal plunger type is superior to the all-glass syringe as regards mechanical sticking but may be dangerous for use with metal-sensitive systems. For volumes in the range 100 to 1,000 cc. glass containers with rubber stoppers and leads through them to the mixing chamber are still widely used.

2. Methods of Fluid Drive

In current methods, using fluid volumes of over 100 cc., e.g., that of Dalziel (15), the fluid drive is usually by compressed gas at constant pressures up to 2 atmospheres. The fluids should be filtered of grease or other debris, otherwise variations may occur both in the total rate of flow and in the relative contributions from the two reagent containers, due to obstruction of the jets of the mixing chamber. With care, however, a constancy in relative and total fluid delivery rates of about 1% can be attained. With the more generally used syringes, constancy in relative delivery is assured if the syringes are leak tight and the plungers are both acted on by a rigid platform, the movement of which forces the plungers to deliver their fluids into the mixing chamber. The movement of the platform has been brought about manually, hydraulically, or by direct coupling to a geared electric motor. In the case of the first two methods of platform drive, the velocity of movement of the platform varies continuously during an obser-

vation, and the instantaneous rate of movement is therefore recorded electronically as in Chance's apparatus; with direct electric motor drive a steady and repeatable rate of syringe discharge can be secured, this rate being readily measurable by collecting the fluid delivered in a given time.

3. Mixing Chambers

In their early work Hartridge and Roughton employed fairly small conical chambers fed by sharply tapering rectangular section jets milled out from solid metal. The general construction of this type of chamber and its lining-up with the rest of the apparatus is shown in Figure 1.1, in which a mixing chamber with eight jets is illustrated. It will be noticed that the jets deliver tangentially rather than radially and thus impart a rotary motion to the fluid in the mixing chamber: tests showed that this improved not only the speed and efficiency of the mixing, but also the character of

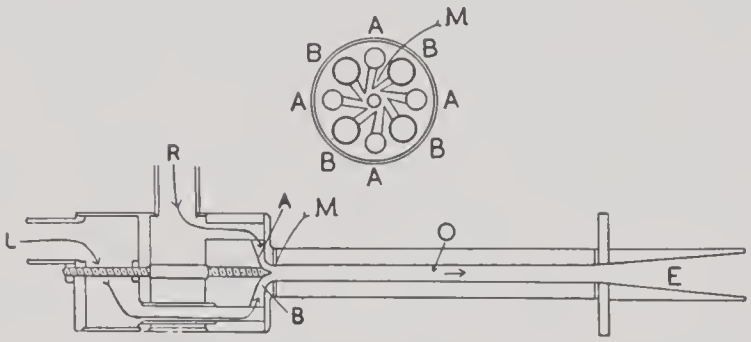

Fig. 1.1. Early rapid reaction apparatus used by Hartridge and Roughton. (*a*) Cross section of mixing chamber to show arrangement by which the two reagents are brought into mixing chamber by alternate jets A, B, A, B, A, B, A, B, delivering tangentially into M. (*b*) Diagrammatic longitudinal section of whole apparatus. The reagents enter, respectively, through the pipes L and R. They are then forced through the four jets A and the four jets B, respectively, and enter the mixing chamber M, from which they pass immediately into the observation tube O, to flow finally out at the exit tube E.

the subsequent fluid flow down the observation tube (except as regards "cavitation," the danger of which Chance has shown is best avoided by a compromise between tangential and radial placement of the jets (see later discussions). With arrangements of this kind Hartridge and Roughton were able to study unimolecular and bimolecular reactions of half-times down to 0.001 sec. The quantity of fluids required for each experiment was, however, excessive (e.g., 3 to 6 liters), and in some cases contact of the reagents with metal produced deleterious results. Accordingly, during the past 20 years, the use of metal has been discontinued and smaller-scale mixing chambers have, instead, been made either of glass or transparent plastic.

A. GLASS MIXING CHAMBERS

(*1*) An ordinary commercial three-way glass T-tap of capillary bore, i.e., 1 to 2 mm., provides fairly good mixing and can be used for reactions with half-times of 0.01 sec. or more (see Table 1.I). (*2*) For faster reactions, recourse must be had to glass taps with conical bores, to the two-jet T glass mixers of Dalziel (15) and of Trowse (16) or, best of all, to the special four-jet glass mixer of Chance and Graham. Dalziel's mixer is made by drilling into the wall of a glass capillary tube (1–2 mm. bore), first with a fine drill until the tip just enters the capillary and then with a cylindrical grinding tool. One end of the capillary mixing chamber is closed and the other end is cemented to an observation tube of precision glass tube ground to fit the mixing chamber. The following dimensions were found convenient: jets, 2 to 3 cm. long and 1.5 to 1 mm. in diameter; mixing chamber, 1 to 2 mm. in diameter and 2 mm. in depth; observation tube, 2 mm. in diameter and length up to 30 cm. Trowse's mixer is similar in size and in number and diameter of jets, but was constructed by delicate glass blowing; for fuller information reference should be made to the original description of the author. (*3*) The glass mixers of Chance and Graham (3) are made as follows. A length of glass capillary is melted at one end and by means of a heated tungsten wire (of diameter less than the desired bore of jet) four holes are made in the heated end of the capillary by a quasi-drilling movement. The capillary is then annealed. The holes are next polished and enlarged with steel needles and Carborundum (600) until they are of the desired width. In order to taper the internal bore to that of the four inlet capillaries (e.g., 0.5 mm.), the holes are closed with glass buttons and repunctured with large tapered tungsten wire. Four inlet capillary tubes are then melted on (without blowing) and afterwards bent and joined to form two Y-tubes, the stems of which are each fused to leads from a double T-tap as in Figure 2.7 (see also Figs. 2.3 and 2.4). Of the other leads from the double tap, two are fused to a pair of 1-cc. all-glass (tuberculin) syringes and the other two, which are open, can be connected as desired to filling reservoirs.

B. PLASTIC MIXING CHAMBERS

(*a*) Millikan's mixer, in transparent Bakelite, was one of the earliest of this type. The construction is as follows. A Bakelite key is ground into the barrel of a three-way glass capillary-bore tap and the mixing chamber is then made in the key of the tap, the stem of which forms the observation tube and the two arms of which form the delivery tubes for the reagents. The holes forming the mixer are drilled with dentist drills ground down to make 0.5-mm. holes: as in the chambers of Hartridge and Roughton, the

jets—either two or four in number—were arranged to deliver tangentially into the mixing chamber, which is placed at the very surface of the key. In a typical case the diameter of the chamber was 1.0 mm. and its depth 2.5 mm. The end of the observation tube (cross-sectional area ranging from 0.5 to 3.0 sq. mm.) is taper ground into the tap barrel and cemented into it, in such a way as to eliminate all dead space between the mixing chamber and the observation tube. For fuller details reference should be made to Millikan's paper (2). (*b*) The manufacture of mixing chambers in polystyrene or Lucite has been extensively adopted by Chance and by those who have followed him. The following directions for the construction of one of Chance's chambers may be taken as representative of this general type. "First, drill the two holes for the syringe tips. Draw a line between the ends of the two holes. Heat the observation tube (it may not be quite as long as the available drill) and plunge it into the styrene at the mid point of the line. Take the drill that just fits the observation tube and drill up through the end of the observation tube to clear out the styrene that has solidified there. Continue drilling until the hole is 2 mm. past the end of the observation tube. Now drill two 2-mm. holes in toward the end of the observation tube. These holes will intersect the two syringe holes at right angles and follow the line drawn between their ends. Bring these holes to within 2 mm. of the extension of the observation tube. Now follow up the hole with a 0.5-mm. drill and drill two jet holes on each side into the extension of the observation tube. These two jets should be side by side along the axis of the observation tube. Now tap the syringe holes, screw the syringes into the proper hole, and seal in glass plugs for the other two. A four-jet mixer is now completed. An eight-jet mixer has been made by drilling two jets in from each of four larger holes, much in the way described."

For further information the reader is referred to Chance's paper (3, pp. 738–42 and Figs. 17–20).

4. Tests of the Efficiency of Mixing

It is obviously of paramount importance that the time taken to mix the two reagents should be small in comparison with the half-time of the reaction under study. Tests of the efficiency of mixing were, accordingly, introduced by Hartridge and Roughton (1) at the outset and have been frequently applied in many of the subsequent apparatus. The tests have been either chemical or physical in nature.

The chemical method consists in measuring with the apparatus the apparent extent of a bimolecular reaction which is known (or believed) to be complete in a time much smaller than the minimum time measurable

by the system. The times in the observation tube at which the reaction is observed to be apparently 95, 97, and 99% complete must then be greater than or at least equal to the times required for the corresponding degrees of mixture. In this way a minimal estimate of the speed and efficiency of the mixing process is obtained. The reaction which has been most used for this purpose has been the neutralization of acid by carbonate-free alkali of exactly equivalent titer, the method of observation being either colorimetric (with the aid of one of the normal series of colored pH indicators, the members of which usually react in less than 0.001 sec.) or, better, thermal (depending on the heat of neutralization). The rate of combination of iodine with sodium thiosulfate of equivalent titer has also been employed by Roughton, by Chance (3), and by Trowse (16), the apparent extent of the reaction being followed photocolorimetrically.

The physical method, as used by Dubois (17) and by Trowse (16), consists in mixing together two solutions of different optical properties and using the approach to optical homogeneity as a criterion of the extent of mixing. Dubois applied a "Schlieren" method to the fluid in the observation tube, while Trowse followed the light transmission changes after mixing together water and 20% aqueous ammonium sulfate in his apparatus. While the fluids are mixing, there is an appearance of turbidity due to multiple refractions of the illuminating light and there is in consequence a reduction in the intensity of the transmitted light. As mixing proceeds, the solution clears and the intensity of the transmitted light returns to normal.

The thermochemical mixing test has been in continuous and satisfactory use for over 30 years and as regards simplicity and reliability is much to be recommended. Fuller details of operation will be deferred until the section dealing with the thermal measurement of rapid reactions, in order to avoid duplication. Mixing tests involving the measurement of light transmission are an obvious corollary of the photoelectronic rapid reaction methods, which are described later, and need only brief reference there. They are probably not quite so exact as the tests by the thermal method. Thus in the colorimetric mixing tests used by Chance there was a possible photoelectric error of 2% so that his estimate of 98% mixing in 0.0004 sec. for his eight-jet polystyrene apparatus operating at the highest rate of flow (viz., 23 m./sec.—with no stopcocks between the syringes and the mixer) may be a conservative one.

Table 1.I summarizes the results of mixing tests by the above methods, as recorded by various workers over the past 40 years. The tests were all done at room temperature (15–25°C.). It should, however, be noted that the mixing process has a significant temperature coefficient, being of the order of 3 times faster at 40°C. than at 20°C. The time of mixing in the

TABLE 1.I
Summary of Results of Mixing Tests by Various Authors

Authors	Apparatus	Test	Method of observation	Rate of flow in observation tube		Maximum time, sec., for		
				cm./sec.	cc./sec.	95% mixing	97% mixing	99% mixing
Hartridge and Roughton	8-jet metal mixer	HCl + NaOH	Colorimetric	345	68	—	0.0003	—
	8-jet ebonite mixer	HCl + NaOH	Thermochemical	1,000	63	—	0.0004	—
Roughton	3-way glass T-taps bore 1.5 mm.	HCl + NaOH	Thermochemical	400	6	0.0100	—	—
Millikan	4-jet Bakelite tap mixer, jets 0.5 mm. bore	HCl + NaOH	Thermochemical	268	2.7	—	0.0005	0.0020
		HCl + NaOH	Thermochemical	175	1.7	—	0.0015	0.0070
		HCl + NaOH	Thermochemical	100	1.0	—	0.0040	0.0100
Chance (plastic)	8-jet polystyrene mixing jets 0.4 mm., tube bore 1.0 mm.	$I_2 + Na_2S_2O_3$	Colorimetric	2,300	18	—	0.0004	—
Dalziel	2-jet glass mixer (0.5 mm. bore)	H_2SO_4 + NaOH	Thermochemical	140	4.4	—	—	0.0050
	2-jet glass mixer (1.0 mm. bore)	H_2SO_4 + NaOH	Thermochemical	280	8.8	—	—	0.0050
	2-jet glass mixer (1.0 mm. bore)	H_2SO_4 + NaOH	Thermochemical	140	4.4	—	—	0.0080
Trowse	2-jet glass mixer (0.7 mm. bore)	H_2O + 20% $(NH_4)_2SO_4$	Light transmission	440	8.8	0.0009	0.0013	0.0030
	2-jet glass mixer (0.5 mm. bore)	H_2O + 20% $(NH_4)_2SO_4$	Light transmission	995	10.0	0.0005	0.0006	0.0008
Chance and Graham (glass)	4-jet all glass mixer, 0.5 mm. jets, bore 1.0 mm.	Peroxidase and hydrogen peroxide	Colorimetric	1,000	8	—	0.001	—

early Hartridge-Roughton mixers is seen to be quite as short as in the later more micro-models, but only at a cost of 5 to 50 times greater volume flow of fluid per second. Millikan's (2) and Dalziel's (15) figure show clearly the improvement obtained with a given apparatus by speeding up the rate of flow. If Millikan's results on percentage mixing are plotted against distance from the mixing chamber to the point of observation (instead of against time, as in his diagrams) the point of 97% mixing moves toward the mixing chamber as the flow velocity is increased. In general it may be concluded that complete mixture, to within 2 to 3%, can be attained with the present types of apparatus within a few ten-thousandths of a second, and no substantial improvement along the present lines is in sight unless the driving pressures can be raised to values of the order of 100 atmospheres. This extension might well bring in its train many and serious technical difficulties. Such high pressure work is a matter for the future, if and when the need arises for studying, by the flow methods, reactions with half-times of 0.0001 sec. or less. Ultra-rapid reactions in this time range have, of course, been studied in recent years by relaxation methods (18), but the chemical reactions for which the latter are available are at present more limited in scope.

5. Construction of Observation Tubes

In measurements involving optical analyses of the moving fluid the observation tubes have usually been circular in cross section and made of glass or quartz. Tubes drilled in ebonite or transparent plastic have sometimes proved more suitable, especially in the rapid thermal and quenching methods. In certain rapid reaction velocity techniques, e.g., those of Dirken and Mook (14), special observation arrangements are necessary.

The bore of the observation tubes has usually ranged from 0.5 to 15 mm., though in some early work on rather slow reactions, optical depths of as much as 20 to 200 cm. were examined. The length of the tubes has ranged from 1 to 100 cm. or more, the longer lengths being generally used in conjunction with the wider bores, wherein the resistance to flow is less.

The observation tubes have been joined to the mixing chambers either (*a*) in one piece, in the cases of all-glass tap mixers or of apparatus made from a single block of plastic, or (*b*) by cement, after grinding to fit, or (*c*) by means of rubber washers and screwed rods as in Hartridge and Roughton's early apparatus (Fig. 1.1).

6. Character of Flow in Observation Tube

In the moving fluid method, all parts of the reacting solution should, ideally, reach the place of observation in the same time, otherwise the

chemical reaction would not have proceeded to the same extent throughout the fluid and a "blurring" of the time axis would result. Such homogeneity would only be realized if the fluid moved as a solid body (i.e., "mass flow"). In practice, the central parts of the fluid always tend to move faster than the average, whereas the peripheral parts move more slowly. Such deviations from mass flow are much more marked with stream-line than with turbulent flow. All investigators have, in consequence and wherever possible, used rates of flow in excess of the critical velocity for turbulent flow, hoping thereby to reduce the errors in the computation of the velocity constants, which might result from the "blurring" of the time axis through deviations from mass flow. In the next subsection the possible magnitude of these errors is discussed, and is fortunately found to be very small in the case of turbulent flow.

The critical velocity for turbulent flow, u_c, is given approximately by Reynolds' formula:

$$u_c = \frac{1{,}000\ \eta\ (\text{viscosity in poises})}{\rho\ (\text{density}) \times r\ (\text{radius of tube in cm.})} \tag{1}$$

At 20°C., the critical velocity for water in a tube of 1-mm. bore is about 200 cm./sec., and in a tube of d-mm. bore $200/d$ cm./sec. The corresponding volume rates are 1.6 and 1.6 d cc./sec.

Turbulent flow has the further advantages: (*1*) The longitudinal motion down the tube is accompanied by constant eddying, which therefore gives rise to components of flow velocity transverse to the main length of the tube. Any such transverse component will take some of the fluid either towards or away from the center and will thus tend to mix the faster and slower moving portions, thus reducing the difference between them. (*2*) The rate of flow down the tube is proportional to the square root of the pressure, and is therefore less sensitive to variations in pressure than is stream-line flow, the rate of which is directly proportional to the pressure. (*3*) Although the critical velocity is higher when the viscosity is increased, the rate of flow once the critical velocity is exceeded becomes progressively less and less dependent on the viscosity. In stream-line flow, on the other hand, the rate of flow is always inversely proportional to the viscosity, and the time scale is therefore much more sensitive to variations in the latter.

Chance (3) has made a detailed experimental study of the relations between pressure drop and velocity of turbulent flow for mixing chambers with varying lengths of observation tubes attached. His results were expressible by the formula:

$$P = K'u^2 = (\rho\bar{u}^2/2)[A'(L/d) + B'] \tag{2}$$

where P is the pressure drop in lb./sq. in., ρ is the density of the fluid, $\bar{u}$ is the linear velocity of flow in m./sec., L is the length and d the diameter of the observation tube, and K', A', and B' are constants.

The empirical values of K', A', and B' agreed reasonably well with those to be expected from the Prandtl-Karman equations for turbulent flow in tubes with sharp entrances. The numerical values of A' and B' are such that the $A'L/d$ term in Equation (2) is unimportant in comparison with the B' term when L/d is less than 40. At higher values of L/d the resistance offered by the length of the tube is seen to affect linearly the requisite pressure drive. K' for four-jet mixers was found to be only slightly lower than for two-jet mixers. From such empirical values of K', the driving pressures necessary to produce a desired rate of flow in a given apparatus can be readily calculated, and the best conditions of design worked out therefrom. Thus in a typical case of a mixing chamber, with 4 jets of 0.6-mm. diameter, and an observation tube 2.7 cm. long and diameter 1.05 mm., $K' = 0.425$. ΔP, for a flow velocity of 10 m./sec., $= 0.425 \times 10^2$ or 42.5 lb./sq. in.

Cavitation. At high rates of flow there are considerable variations in the hydrostatic pressure of the streaming fluid at different parts of the apparatus and the phenomenon of cavitation may occur. This consists of the formation of a stream of very fine bubbles, with consequent turbidity of, and a sharp (and large) decrease in light transmission by, the fluid in the observation tube. It can therefore be a serious disturbing factor in the measurements of the rate of rapid reactions by optical methods, though presumably less so in cases of certain other methods of observation, e.g., thermal or chemical. The control for cavitation is simply to discharge water through the observation tube at all values of flow velocity used in actual experiments and then to measure the light transmission. With his eight-jet polystyrene mixer, Chance (3) found no cavitation at flow velocities up to 23 m./sec. Trowse (16), in his apparatus, observed cavitation if there was a constriction between the mixing chamber and the observation tube, but on eliminating the constriction he could then detect no cavitation up to the highest flow rates he used, i.e., 13 m./sec.

In much of the earlier work with the flow method the reagents only contained small amounts of dissolved air or other difficultly soluble gases. Cavitation troubles are, however, much aggravated—as Sirs (19) has shown—if the reagents contain moderate amounts of more soluble gases such as carbon dioxide. Until this factor was properly controlled Sirs was unable to get concordant results for the velocity of combination of carbon dioxide with hydroxide ions, by rapid thermal methods and by rapid optical or electrical conductivity methods.

7. Magnitude of Errors Due to Deviations from "Mass" Flow

As pointed out in the preceding section (III.6), the observed extent of reaction at any distance along the observation tube will not in general be the same as the true value corresponding to the average time of arrival of the fluid (as calculated from the measured volume flow rate). The difference will depend on the distribution of fluid flow velocity and also on the method of observation.

Roughton and Millikan (20) were the first to estimate, by a numerical approximation method, the possible errors which might arise (owing to deviations from mass flow) in the computation of the velocity constants for unimolecular and bimolecular reactions, in the case of optical analysis of the moving fluid. In their theoretical treatment they divided the fluid passing down the observation tube into ten equal blocks each of which was assumed to move as a solid body, but with a velocity greater or less in varying degree than the average velocity. The distribution of velocities between the blocks was chosen to correspond either to the conditions found in (*1*) stream-line flow or (*2*) a type of flow intermediate between stream-line and turbulent flow.

If $\bar{t}$ is the time of arrival at a given cross section X, corresponding to the average velocity $\bar{u}$, and t and u are the corresponding time of arrival, and velocity for any particular block, then $t = \bar{t}\bar{u}/u$.

If an arbitrary value be assigned to $\bar{t}$, the actual extent of chemical reaction corresponding thereto could be readily calculated from the velocity constant and order of the reaction, as could also the corresponding extents of chemical reaction in each of the ten blocks. The mean of these last ten values was assumed to be the "apparent" extent of reaction and was therefore compared with the calculated extent of the reaction corresponding to $\bar{t}$, which was considered to be the "true" extent of reaction. The discrepancies between the "apparent" and "true" extents of the reaction were found to be appreciable for the stream-line case, but barely so for the "semi-turbulent" case. The results for unimolecular and bimolecular reactions were substantially the same.

Table 1.II shows the results of more recent and improved calculations by Trowse (16) and Dalziel (15) independently. The discrepancies between the true and apparent extents of reaction were estimated for unimolecular and bimolecular reactions, both with stream-line and fully turbulent flow. The same general principle of calculation was used, namely that of dividing up the fluid into ten solid-moving elements and summing the individual contributions of these elements. The latter were, however, more correctly taken as concentric cylinders, coaxial with the axis of the observation tube. In one case (Dalziel), namely that of a bimolecular reaction with

stream-line flow, analytical rather than numerical integration was possible. The reason why the results given by the two authors are not quite the same is that in Trowse's calculations, the analyzing light beam was assumed to be focussed on the center of the observation tube, whereas in Dalziel's case the observation tube was illuminated by a parallel beam of light, of breadth equal to half the diameter of the tube.

TABLE 1.II

Calculated Values for Observed Extent (in %) of a Unimolecular Reaction and a Bimolecular Reaction with Stream-line and Turbulent Flow in the Observation Tube

Reaction, true percentage	Stream-line flow		Turbulent flow	
	Dalziel	Trowse	Dalziel	Trowse
		Unimolecular Reaction		
6.7	—	—	—	6.34 (−5.5)
12.90	16.3 (+29)[a]	—	12.50 (−3.3)	—
29.30	33.0 (+16)	—	28.5 (−3.2)	27.86 (−5.8)
50.00	50.9 (+2.7)	—	48.6 (−3.7)	47.87 (−6.0)
75.00	71.5 (−8.7)	—	73.4 (−4.2)	72.64 (−6.5)
		Bimolecular Reaction		
9.1	11.2 (+12.6)	8.4 (−8.3)	8.8 (−3.5)	8.6 (−5.9)
33.3	35.0 (+7.6)	31.2 (−9.3)	32.5 (−3.8)	32.0 (−6.0)
50.0	50.1 (+0.4)	47.3 (−10.3)	49.0 (−4.0)	48.4 (−6.2)
66.7	65.5 (−5.1)	64.1 (−10.7)	65.7 (−4.2)	65.1 (−6.5)
80.0	78.5 (−8.7)	78.0 (−11.4)	79.7 (−1.8)	78.9 (−6.5)

[a] Figures in parentheses denote corresponding percentage errors in computed velocity constants.

The following formulas were used for the longitudinal fluid velocity, u, at distance y from the axis of the tube (radius r).

(a) For stream-line flow (Poiseuille's equation):

$$u = u_m(r^2 - y^2) = 2\bar{u}(r^2 - y^2) \tag{3}$$

where u_m is the maximum rate of flow at the axis and $\bar{u}$ is the average rate of flow

(b) For turbulent flow (Prandtl's equation):

$$u = u_m[(r - y)/r]^{1/7} = 1.225\ \bar{u}[(r - y)/r]^{1/7} \tag{4}$$

Inspection of Table 1.II shows that with turbulent flow the differences between the apparent and true extents of reaction never exceed 2.5% of the whole reaction and are often much less. The figures in brackets indicate the corresponding errors in the velocity constants, as computed from

the apparent extents of the reactions, a negative sign meaning that the computed value is too low. The errors only range from 3 to 7% of the true values of velocity constants. Even these small percentages are, in all probability, overestimates for in obtaining them it has been assumed that no mixing of the elements takes place through eddying and furthermore that the velocity distribution, characteristic of turbulence, is set up as soon as the fluid enters the observation tube, whereas in practice the fluid flow at the inlet must be of the mass type and only gradually gives way to the turbulent type corresponding to Equation (4). If these two factors could be allowed for, they would both tend to bring the apparent extent of the reaction nearer to the true extent and thus reduce the systematic errors in the computed velocity constants.

The figures for stream-line flow are seen to be far less favorable, the possible errors in the computed constants being sometimes greater than 10%. Furthermore, the two factors, which make the calculated errors too high in the case of turbulent flow, will be much less operative in the case of stream-line flow.

In general, it may be concluded from this rather lengthy discussion that with turbulent flow the errors, in unimolecular and bimolecular constants, caused by deviations from mass flow are probably no more than 2 to 3%—a figure of the same order as, or less than, the errors due to other factors. With reaction velocity curves containing sharp bends, the errors may be somewhat larger. Stream-line flow should, wherever possible, be avoided but especially so in the latter case. That the claim for 2 to 3% accuracy with turbulent flow is not unduly exaggerated is shown by the agreement, in many instances, between the results obtained thereby and the results by "stopped flow" and other methods, in which errors due to deviation from mass flow do not arise. The following examples of such agreement may be quoted:

(*1*) The velocity constant, k'', of the reaction $CO_2 + OH^- \rightarrow HCO_3^-$ has been measured over the range 0 to 40°C. by one continuous flow method (thermal (21)), two stopped flow methods (photoelectric (19) and electrical conductivity (19)), and two classical methods (quenching (22) and manometric (23)). The results by all these five independent methods agree within their respective experimental errors and are expressible by the equation

$$\ln k'' = 31.30 - (13{,}210/RT)$$

The time scales in this work ranged from milliseconds (in the flow methods) to seconds or minutes (in the classical methods). Further reference to this reaction is made in Part 4 of the present chapter.

(*2*) The rate of displacement of oxygen from combination with hemo-

globin by carbon monoxide (5) has been measured by the continuous flow method, by the stopped flow method, by a rapid photolysis method, and a classical manometric method. The results by all four methods agreed within the limits of experimental error.

(3) Gibson (25) obtained concordant results for the velocity constant of the bimolecular reaction carbon monoxide + myoglobin → carboxymyoglobin with his stopped flow method and his flash photolysis method.

8. Magnitude of Errors Due to Mixing Time and Slit Length

There are two other factors, besides deviation from mass flow, which lead to lack of homogeneity in the reacting fluid under the conditions in which it is submitted to analysis in the observation tube:

(*a*) Some parts of the fluid entering the mixing chamber mix completely, and therefore commence to react almost at once, whereas other parts may not become completely mixed until the exit of the mixing chamber or beyond. Furthermore, the fluid which enters the side of the jets distal to the observation tube has a greater length to travel (and therefore a longer time in which to react) than has fluid which enters at the near side of the jets. The extent of the heterogeneity due to this factor clearly depends on the speed of reaction, on the speed of fluid flow, and on the time and conditions of mixing, the last of which Hartridge and Roughton (1) roughly expressed in terms of a certain "equivalent length of observation tube." This equivalent mixing length, L_0, may be taken as equal to the product of t_m (the time for mixing to be almost—say 98%—complete) and $\bar{u}$, the average velocity of fluid flow in cm./sec. For their early apparatuses they gave approximate values of L_0 ranging from 0.12 to 0.75 cm.

(*b*) Most methods of analyzing moving fluids involve the examination of a certain finite width of fluid in the observaton tube. This width which, in the case of optical methods of analysis, has been called the "slit length," can usually be kept 2 or more times smaller than the equivalent mixing length, and the error therefore should be correspondingly smaller.

The effect of these two somewhat similar factors on the determination of the velocity constants of unimolecular and bimolecular reactions has been investigated both by experimental tests and by theoretical calculations.

A simple direct control as to the sum of the errors from these two sources, together with that due to deviation from mass flow, can be obtained by carrying out the reaction velocity measurements with two widely different rates of fluid flow, both, however, in excess of the critical velocity. The "slit length" is unaffected by the rate of flow, whereas the equivalent mixing length decreases somewhat with increase of flow, and so also should any deviation from mass flow: with faster rates of flow the heterogeneity

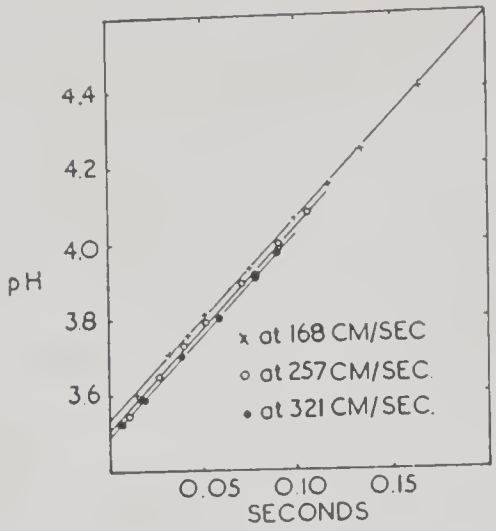

Fig. 1.2. Measurements of rate of reaction of 0.02*M* $NaHCO_3$ with 0.01*N* HCl at three different rates of flow of mixed fluid in observation tube (168 cm./sec., 257 cm./sec., and 321 cm./sec.). Temperature, 19°C.

of the fluid under analysis must accordingly be less than with slower rates of flow. If, however, the results obtained at the two rates of flow agree within experimental error, it seems fair to conclude that they would also agree with the true results in entire absence of heterogeneity from all three factors (slit length, mixing, and deviation from mass flow). *A fortiori* then, the error from any one of these factors should be negligible, since all tend to act in the same direction. Hartridge and Roughton (24), with their early apparatus, did tests on a unimolecular reaction with a half-time of 0.003 sec. and a bimolecular reaction with a half-time of 0.0015 sec., but were unable to discover any significant difference between the measurements when the rate of flow was varied 3-fold. Figure 1.2 shows the results of some rapid reaction experiments by Dalziel (15) on the rate of pH change, which occurs when 0.02*M* $NaHCO_3$ is mixed with 0.01*N* HCl, each containing 0.005% bromphenol blue. As shown by Brinkman, Margaria, and Roughton (26), there should be almost linear relation between pH and time, corresponding very closely to the equation

$$k_1 = 2.303 \times 1.09[(pH_2 - pH_1)/(t_2 - t_1)]$$

where k_1 is the velocity constant of the unimolecular reaction $H_2CO_3 \rightarrow CO_2 + H_2O$, and pH_1, pH_2 are the respective values of pH corresponding to times t_1 and t_2.

The points obtained at three different rates of flow, viz. 168, 257, and 321 cm./sec. all fall on lines of the same slope. These three rates were all greater than the critical velocity, which was about 110 cm./sec. The differences in intercept on the pH axis are due to slight differences in the relative deliveries of the two reacting fluids in the three cases.

Similar successful tests at different rates of flow have been made by other observers, and should wherever possible be used as checks in the case of any and every rapid reaction measured by the continuous flow method. The effect of slit length alone has been studied by Dalziel (15) in measurements of the same reaction, i.e., 0.02*M* $NaHCO_3$ + 0.01*M* HCl, at a constant rate of flow of 153 cm./sec. but with slit length varying from 0.5 to 5.0 mm., which correspond to time intervals of 0.00033 to 0.0033 sec. and to pH changes of roughly 0.003 to 0.03. No effect was seen with such variations of slit length, though it must be admitted that the unimolecular reaction was not a very rapid one, and therefore not particularly suited to bringing out any errors due to slit length. Similar tests could, however, be applied to faster reactions, though the theoretical investigations now to be described make it most unlikely that any significant errors would be revealed.

Calculations of the error due to the slit length have been given by Chance (3) for unimolecular reactions. His formula, in simplified form, runs

$$\text{percentage error}/100 = (\sinh \phi/\phi) - 1 \tag{5}$$

where

$$\phi = [(s_2 - s_1)/(s_1 + s_2)] \ln (c/c_0) \tag{6}$$

and s_2, s_1 are the respective distances from the mixing chamber of the two edges of the analyzing beam of light, c_0 is the initial concentration of the reacting substance, $c = c_0 \exp [-k_1(t_1 + t_2)/2]$, $t_1 = s_1/\bar{u}$, $t_2 = s_2/\bar{u}$, $\bar{u}$ is the average velocity of flow in cm./sec., and k_1 is the velocity constant of the reaction.

The error is taken as a percentage of the measured concentration rather than as a percentage of the initial concentration. From Equation (5) it may be seen that the sign of the error must be positive, which means that the measured value of c must always be greater than the value which would be obtained if there were no slit-length error. The minuteness of the slit-length error is shown by the following extreme example of a unimolecular reaction, half complete in the first half-centimeter of the observation tube, and with a slit length of 0.5 cm., i.e.,

$$c = 0.5c_0,\ s_1 = 0.25 \text{ cm.},\ s_2 = 0.75 \text{ cm.},$$

then:

$$\phi = -0.3466$$

and

$$(\sinh \phi/\phi) - 1 = 0.02.$$

The measured value of c is thus in error by $0.02 \times 0.5c_0$, i.e., by $0.01c_0$ and the calculated value of the velocity constant is in error by

$$100 \times [(\ln c_0 - \ln 0.49c_0)/(\ln c_0 - \ln 0.5c_0)] \%$$

i.e., by 2.9% of itself.

Even in this example, which is beyond the limit to which the method would ordinarily be pressed, the error in the computed velocity constant due to slit length is only very small. Under more normal conditions of working, the errors as calculated from Equations (5) and (6) should be quite negligible. Chance, indeed (Part 2), takes advantage of the small slit-length error to get more light through the observation tube.

In Chance's calculation it is implicitly assumed that the optical density of the solution is so low that the light absorption can be taken as directly proportional to the concentration of absorbing substance. Trowse (16) has investigated the more general case of a unimolecular reaction in which there is the usual exponential relation between light absorption and concentration of absorbing substance, but here again finds that the error from "slit length" is of only the same small order of magnitude as that given by Chance's formulas.

By similar analysis Chance found that the slit-length error for a bimolecular reaction is somewhat less than that for a unimolecular reaction. For reactions with highly inflected kinetic curves, however, the slit-length errors will be larger and special calculations are advisable in cases in which such curves are experimentally obtained.

The error due to the finite time of mixing may, to a rough approximation, be treated in the same way as the slit-length error, the equivalent mixing length, L_0, being substituted for $s_2 - s_1$, while $(s_1 - s_2)/2$ is, as before, the mean distance from the mixing chamber to the part of the observation tube under examination. A more exact physical picture of the problem has been given by Trowse (16) and approximate calculations have been made by him on this basis, for unimolecular reactions with velocity constants ranging from 25 to 3,200. In the more efficient of the two apparatuses considered by him (diameter of mixing jets, 0.5 mm.; bore of observation tube, 0.112 cm.; flow rate, 995 cm./sec.), the percentage error in the velocity constant, k, at various times after mixing was only found to be appreciable with extremely rapid reactions, e.g., $k \geqq 800$ and half-time less than about 0.001 sec. With $k = 800$, the percentage errors due to the mixing factor, at 0.0005, 0.001, and 0.002 sec. after mixing were found to be 7, 1.1, and 0.028 respectively, whereas with $k = 1{,}600$ the corresponding percentage errors at the same three intervals after mixing were calculated to be 9.5, 2.2, and 0.12 respectively.

It may thus be concluded that with the most efficient apparatus the

errors in the velocity constant of unimolecular reactions due to imperfect mixing will generally be negligible or slight, provided that the velocity constant does not exceed about 1,600, and the half-time is not less than about 0.0005 sec. With bimolecular reactions, the percentage error in the velocity constant should also be negligible or slight, provided again that the half-time exceeds 0.0005 sec.: reactions with sharply inflected kinetic curves will, however, be more subject to mixing errors as well as to slit-length errors.

9. Multiple Mixers

The apparatus so far described in this chapter has only contained a single mixing chamber with attached observation tube. Hartridge and Roughton (4), however, pointed out various cases in which the use of multiple mixers in series would be of value. The principle involved may be explained as follows:

By means of a reaction velocity apparatus of the usual type, solutions of two substances A and B are caused to mix and react with one another with the production of a new substance C. If it is desired that the substance C should forthwith react with a fourth substance D this reaction may be rapidly brought about by causing the fluid containing C, which has just left the first reaction velocity apparatus, to enter a second apparatus of similar design by which it is mixed and caused to react with D. If C and D produce a new substance E, the kinetics of reaction of E with yet another substance F may be similarly studied by the use of a third reaction velocity apparatus and so on. Thus by connecting several sets of apparatus in cascade, it is readily possible to study multiple reactions of considerable complexity (Fig. 1.3).

The multiple mixing arrangement also forms the basis of the *chemical* or *quenching* method of measuring the velocity of rapid reactions.

In this method the two solutions, L and R, which are to react, are driven into a mixing chamber, M_1, and thence, after passing through an intermediary tube of suitable volume, into a second mixing chamber, M_2, where they meet a solution of a "quenching" agent, Q, which fixes the reaction between L and R at the stage reached at the end of the time of travel between the first and the second mixing chambers. The fluid emerging from the second chamber is then analyzed at comparative leisure by ordinary methods of chemical analysis. It is the essence of this method that the time taken by Q to fix the reaction between L and R should be short in comparison with the time of reaction between L and R. Unfortunately the cases in which such a rapid quencher Q can be found are not very numerous, but when such a reagent is available the method is both an accurate and

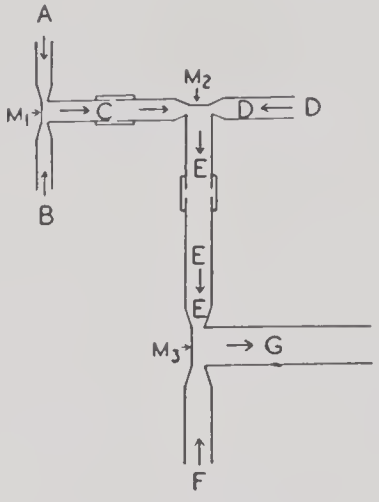

Fig. 1.3. Arrangement of mixing chambers in series. The first two fluids A and B mix in M_1, the mixed fluid from which (i.e., C) enters a second mixing chamber, M_2, where it mixes with a third fluid, D. The mixed fluid, E, emerging from M_2 enters a third mixing chamber, M_3, where it mixes with F, and so on.

powerful one. Some actual applications of the method are given in Part 4, Section I, of this chapter.

Another, and allied, application of mixing chambers in cascade is the study of the formation and behavior of transient intermediate compounds. If two solutions, L and R, are rapidly mixed and react together to form a short-lived compound, T, the physicochemical properties and kinetic behavior of the transient T can sometimes be followed by causing T to mix with further solutions in a second mixing chamber, etc. Some examples of this use of multiple mixers have been given by Roughton (27).

More recently an apparatus having multiple mixers has been described by Ruby (27a), in which three mixers can be connected in cascade for mixing four solutions in sequence. The reaction path length between any two mixers can be varied by insertion of calibrated spacers. By variation of flow velocity and/or path length, reaction times from 1 msec. to 1 sec. can be covered. Physical measurements can be made at any point along the flow path by insertion of an appropriate unit or the chemical stop method can be used by employing two or more mixers. This apparatus has been used extensively by Tong *et al.* (27b) in the study of the reactions involved in dye formation in color photography. In this work, the chemical stop method is especially useful since there may be several reaction products. This method allows one to separate, analyze, and characterize the reaction mixture by conventional methods.

10. Standard Reactions for the Testing of Rapid Flow Apparatus

The unimolecular dehydration of carbonic acid at acid pH has been used as a test reaction not only in photocolorimetric work (15), as in Dalziel's

applications referred to above, but also for checking the validity of electrical conductivity measurements (19) and pH measurements by the glass electrode (28) in the case of the continuous flow and the stopped flow methods. Further details in regard to the reaction are given in Part 4 of this chapter. Its main advantages are:

(*1*) The half-times of the reaction vary from about 400 to 8 msec. over the temperature range 0 to 40°C., and can thus cover all but the fastest time scales over which the flow methods have been used.

(*2*) Suitable known concentrations of the reagents (in the range 0.005 to 0.05*M*) are readily prepared. (The variable carbonate content of the bicarbonate can, if necessary, be reduced to less than 1% of the latter by equilibrating the solution with 5% CO_2 (29).)

Unfortunately, however, there are at present unresolved discrepancies between the values of k_1, the velocity constant of the reaction, as measured by thermal (29) and electrical (30) conductivity methods on the one hand, and by photocolorimetric (15) and glass electrode (28) methods on the other hand. Thus, at 18°C., k_1 (thermal, electrical conductivity) = 14.2 sec.$^{-1}$, whereas k_1 (photocolorimetric, glass electrode) = 12.3 sec.$^{-1}$ This 15% difference is believed to be greater than can be accounted for by experimental error. In the case of the thermal method (29) it might be in part due to the higher ionic strengths used, but this explanation does not cover the electrical conductivity results (30). Until the cause of the discrepancies has been cleared up it would seem safest to average the results of the various methods, according to which

$$\ln k_1 = 31.20 - (16{,}700/RT)$$

The combination of carbon dioxide with hydroxide ions can also be used as a test reaction with the advantage that there are no outstanding discrepancies in the values of the velocity constant, k'', by the various methods. Standard concentrations of CO_2 are, however, somewhat more troublesome to prepare and, as already indicated, special care must be exercised in regard to cavitation. Sirs (19) states that, as regards the latter factor, the maximum tension of dissolved CO_2, which can be tolerated in the mixed solution, is of the order of one quarter of an atmosphere.

11. Solvent and Temperature Changes

Many of the earlier applications of the rapid flow methods were to reactions of biological interest, in dilute aqueous solution and with temperatures in the range 0 to 40°C. In recent years there have been increasing uses of the methods in nonaqueous media (e.g., Prince (31)), the apparatus being necessarily all glass (Pyrex) in construction. Recently Allen, Brook, and

Caldin (32) have adapted the stopped flow technique, for nonaqueous media, down to temperatures as low as −100°C. Tests at room temperature, at about −50°C. and at about −100°C., on efficiency of mixing, stopping time, and flow velocity showed that the performance was satisfactory.

References

1. H. Hartridge and F. J. W. Roughton, *Proc. Roy. Soc. London*, **A104**, 376 (1923).
2. G. A. Millikan, *Proc. Roy. Soc. London*, **A155**, 277 (1936).
3. B. Chance, *J. Franklin Inst.*, **229**, 455, 613, 737 (1940).
4. H. Hartridge and F. J. W. Roughton, *Proc. Cambridge Phil. Soc.*, **23**, 450 (1926)
5. F. J. W. Roughton, *Proc. Roy. Soc. London*, **B115**, 473 (1934).
6. Q. H. Gibson, *Discussions Faraday Soc.*, **17**, 137 (1954).
7. E. Rutherford, *Phil. Mag.*, **44**, 422 (1897).
8. H. Hartridge and F. J. W. Roughton, *Proc. Roy. Soc. London*, **B94**, 336 (1923).
9. R. G. W. Norrish and G. Porter, *Discussions Faraday Soc.*, **17**, 40 (1954).
10. F. Raschig, *Z. angew. Chem.*, **18**, 281 (1905).
11. T. D. Stewart and K. R. Edlund, *J. Am. Chem. Soc.*, **48**, 1014 (1923).
12. H. L. Callendar, *Trans. Roy. Soc. London*, **A199**, 55 (1902). H. T. Barnes, *ibid.*, **A199**, 149 (1902).
13. F. G. Keyes, L. J. Gillespie, and S. Mitsukuri, *J. Am. Chem. Soc.*, **44**, 709 (1922).
14. M. N. J. Dirken and H. J. Mook, *J. Physiol.*, **70**, 373 (1930).
15. H. Dalziel, *Biochem. J.*, **55**, 79 (1953).
16. F. W. Trowse, Ph.D. Dissertation, Leeds (1952).
17. D. Dubois, *J. Biol. Chem.*, **137**, 123 (1941).
18. M. Eigen, *Discussions Faraday Soc.*, **17**, 194 (1954).
19. J. A. Sirs, *Trans. Faraday Soc.*, **54**, 201 (1958).
20. F. J. W. Roughton and G. A. Millikan, *Proc. Roy. Soc. London*, **A155**, 258 (1936).
21. B. R. W. Pinsent, L. Pearson, and F. J. W. Roughton, *Trans. Faraday Soc.*, **52**, 1512 (1956).
22. C. Faurholt, *J. Chim. Phys.*, **21**, 400 (1925).
23. B. R. W. Pinsent and F. J. W. Roughton, *Trans. Faraday Soc.*, **47**, 263 (1951).
24. H. Hartridge and F. J. W. Roughton, *Proc. Cambridge Phil. Soc.*, **22**, 426 (1924).
25. Q. H. Gibson, *J. Physiol.*, **134**, 112 (1956).
26. R. Brinkman, R. Margaria, and F. J. W. Roughton, *Trans. Roy. Soc. London*, **A232**, 65 (1933).
27. F. J. W. Roughton, *Proc. Roy. Soc. London*, **B115**, 495 (1934).
27a. W. R. Ruby, *Rev. Sci. Instr.*, **26**, 460–62 (1955).
27b. L. K. J. Tong, *J. Phys. Chem.*, **58**, 1090 (1954). L. K. J. Tong and M. C. Glesmann, *J. Am. Chem. Soc.*, **78**, 5827 (1956); *ibid.*, **79**, 583 (1957); *ibid.*, **79**, 4310 (1957). L. K. J. Tong, M. C. Glesmann, and R. L. Bent, *ibid.*, **82**, 1988 (1960).
28. J. A. Sirs, *Trans. Faraday Soc.*, **54**, 207 (1958).
29. F. J. W. Roughton, *J. Am. Chem. Soc.*, **63**, 2930 (1941).
30. R. G. Pearson, R. E. Meeker, and F. Basolo, *J. Am. Chem. Soc.*, **78**, 709 (1956).
31. R. H. Prince, *Trans. Faraday Soc.*, **54**, 838 (1958).
32. C. R. Allen, A. J. W. Brook, and E. F. Caldin, *Trans. Faraday Soc.*, **56**, 788 (1960).

Part 2. *ACCELERATED AND STOPPED FLOW METHODS USING SPECTROPHOTOMETRIC MEASUREMENTS*

I. INTRODUCTION

By 1935 Roughton and Millikan (1) had perfected a rapid flow apparatus for investigating chemical kinetics of blood pigments obtainable in quantities of 10 cc. to 1 liter of a $10^{-3}M$ solution. Similarly large supplies of the muscle pigment, myoglobin, were available. In 1935 Theorell prepared reasonably large quantities and subsequently prepared about one-half kilogram of the pure crystalline material in a single process (2). But pure crystalline enzymes were unavailable except in small amounts: catalase and peroxidase were not crystallized until about 1940 and then only in milligram quantities. Thus, the development of a rapid flow apparatus for the study of labile intermediates in enzyme reactions, as suggested by Roughton and Millikan in 1938, presented a number of problems. Some of the stringent design requirements for such an instrument were known. Haldane estimated the velocity constant for the combination of catalase and hydrogen peroxide to be about as large as that for the combination of myoglobin and oxygen (3). The preparative procedures of Keilin and Hartree for catalase or peroxidase gave at best 100 cc. of a $10^{-4}M$ solution of partially purified enzyme after several weeks of intensive work. Thus a method with a time resolution of less than 1 millisec. and a fluid requirement of less than 1 cc. of a $10^{-5}M$ enzyme solution was needed.

A study of Millikan's apparatus soon revealed that the limiting factor in fluid economy was the 1.2-sec. period galvanometer used for measuring the current of the selenium photocell. With the development of suitable electronic techniques that included an automatic control circuit for the light intensity (4), it became possible not only to measure more sensitively but to reduce the response time of the recorder to less than 0.01 sec. by replacing the galvanometer with a cathode ray oscilloscope. With such a rapid recording system, however, the motor-driven syringes of Millikan gave insufficiently rapid starting and stopping times and were superseded by a manual drive in which the syringe plungers were given a short sharp push. The discharge may be rapidly halted mechanically (11) or hydraulically (5). Since the volume discharged per kinetic curve need be only about 0.1 cc., Millikan's 10-cc. syringes could be replaced by 1-cc. syringes. In order to measure the continuously variable flow velocity during the manual discharge, a potentiometer was attached to the syringe plungers by means of a pulley and a chain in order to produce a potential proportional to the amount of fluid discharged. This quantity is directly recorded or

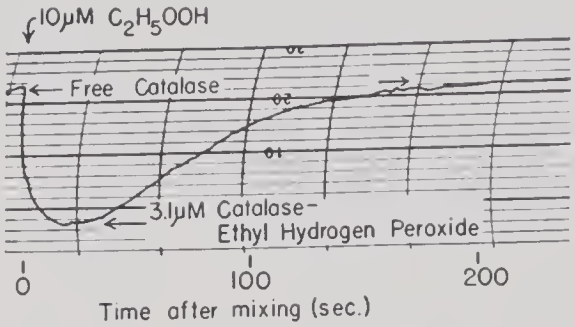

Fig. 2.1. An illustration of the "cycle" of the formation and the disappearance of catalase–ethyl hydrogen peroxide complex I. 5 7 μM horse liver catalase hematin iron; $\lambda = 405$ mμ, pH = 6.7, 0.01M PO_4^{3-} buffer (Expt. 77) (6).

may be differentiated electrically to give a voltage that is proportional to flow velocity.

An incompletely foreseen benefit arising from the quick stopping feature of the accelerated flow method was the extended time range of the stopped flow method which has the considerable advantages enumerated in Part 1, Section I of this chapter. The minimum time measured by the stopped flow method was conservatively estimated in 1940 as 0.03 sec. and is now, with current apparatus, measured as about 4 millisec. Gibson (5) gives a time of about 2 millisec.

In actual practice it has been found that both the stopped and accelerated flow methods are required for the study of enzyme reactions. In order to demonstrate that the combination of enzyme and substrate is a second-order reaction, it is necessary to carry out kinetic studies over a very wide range of times and concentrations. Table 2.I represents a typical experiment in which a range of 0.3 sec. to 8 millisec. is covered (6). Studies of enzyme–substrate complexes involve not only the measurement of the kinetics of appearance of the complex but also the kinetics of disappearance of the complex, which may require a rather long recording interval as illustrated in Figure 2.1. Thus long time stability of the spectrophotometric circuits also is required.

TABLE 2.I

Velocity Constants for Formation and Spontaneous Decomposition of Primary Catalase–Methyl Hydrogen Peroxide Complex (6)

1.9 μM hematin iron guinea pig liver catalase; pH 6.7, 0.01M phosphate, $\lambda = 405$ mμ (Expt. 120b)

Initial methyl hydrogen peroxide, μM	0.58	1.5	2.9	15	58
Concentration of complex I at t, μM	0.24	0.60	0.95	0.95	0.62
t, sec.	0.33	0.39	0.30	0.06	0.0086
Second-order velocity constant, $k_1 \times 10^{-6}\ M^{-1} \times$ sec.$^{-1}$	0.90	0.84	0.96	0.76	0.80

A novel feature of this rapid flow apparatus is the ability to obtain with it the absorption spectra of unstable compounds that may have a lifetime of only a few hundredths of a second. By illuminating an observation tube of a known optical depth with monochromatic light and by using appropriately calibrated photoelectric circuits, the molecular extinction coefficient of a labile intermediate formed from the reaction of the substrate with a known concentration of the enzyme is accurately measured a few millisec. after mixing. If then the reaction is repeated at various wavelengths, the absorption spectrum may readily be plotted. It often happens that the enzyme itself has absorption so that the molecular extinction

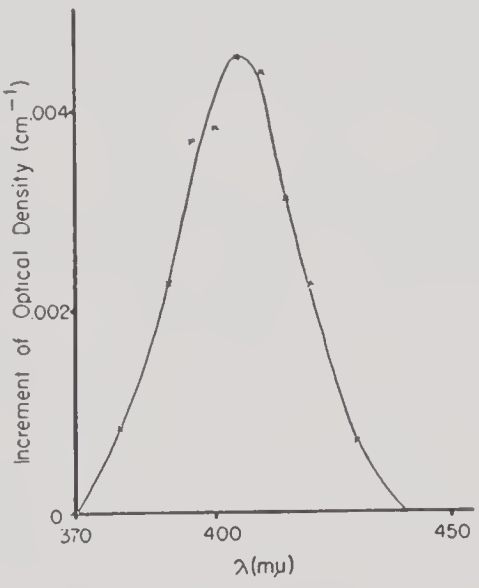

Fig. 2.2. A "difference" spectrum for the catalase–hydrogen peroxide complex I. An absolute spectrum for complex I as illustrated in Figure 2.9 may be obtained by applying the optical density increments plotted here to the spectrum of free catalase as obtained with an ordinary spectrophotometer. 3.5 μM horse blood catalase, 7.5 μM H_2O_2, pH = 6.7, 0.01M PO_4^{3-} buffer (Expt. 51b,d) (7).

coefficients measured represent changes with respect to the free enzyme, i.e., the spectrum obtained in the flow apparatus represents the difference between the absorption of the intermediate complex and that of the free enzyme. The spectrum of the catalase–hydrogen peroxide complex was first obtained in this manner and the original result is reproduced in Figure 2.2 (7). The experimentally determined difference spectrum of Figure 2.2 is applied to the known catalase spectrum to give that of the catalase–hydrogen peroxide complex discussed in Chapter XXII, Part 2, Figure 10.

More recently, double beam spectrophotometric systems have been developed for the purpose of observing the formation of unstable compounds in the presence of large amounts of interfering pigment. An example of

this is the study of the compound of reduced diphosphopyridine nucleotide (DPNH), and of alcohol and lactic dehydrogenase (8,9). Formation of this compound requires a large excess of DPNH and causes only a small shift of the DPNH absorption maximum at 340 mμ. In order to detect this change, the effect of the DPNH absorption is eliminated by means of a double beam spectrophotometer which subtracts the optical density changes at 353 and 328 mμ, two wavelengths of equal DPNH absorption. Thereby the photoelectric circuit is rendered insensitive to the presence of DPNH alone, but readily detects the formation of the enzyme–DPNH complex even though the ratio of the absorption of DPNH to that of the complex is as great as 40:1. Kinetic studies of such complexes have also been carried out with the accelerated and the stopped flow methods (9). It is now obvious that the fluorometric method is more suitable for a study of these dehydrogenase–DPNH intermediates (10).

In summary, these techniques represent a rapid flow system of high fluid economy, utilizing both the accelerated and stopped methods, which is combined with an extremely sensitive and versatile spectrophotometric system, is required for exploratory research on new enzyme systems. But often straightforward kinetic studies are readily carried out with much simpler apparatus when spectroscopic data on unstable intermediates are not required or a wide range of times need not be covered. We shall also describe designs for such an apparatus because they may be constructed more economically and may be easier to maintain and operate.

II. SURVEY OF CURRENT DESIGNS OF FLOW APPARATUS

Table 2.II gives data for seven current models of spectrophotometric flow apparatuses. Five of these apparatuses are of the "Chance" type, with rapid recording of the spectrophotometric data and with rather fast stopping fluid drives. The apparatus of Gibson is very efficient and will be described in detail below. The designs of Forrest, Lu Valle, and Gibson incorporate a mechanical or hydraulic means for driving the syringe plungers. Many designs employ monochromators and thus may be used to study unstable intermediate compounds. Trowse's apparatus has a wide time range. The apparatus of Dalziel is a continuous flow apparatus specialized for hemoglobin studies and is patterned after the original Hartridge-Roughton design but uses a Beckman spectrophotometer; it has a very large fluid requirement caused by the slow response speed of the manually operated photoelectric system, but covers a wide range of wavelengths and absorbancy values.

TABLE 2.II
Spectrophotometric Flow Apparatuses

Constructor	Type	General purpose	Optics: Monochromator	Optics: Optical slit, mm.	Optics: Min. distance from mixing to observation, mm.
Chance	AFM[a], SFM[b]	Kinetics and identification of enzyme-substrate compounds	Double grating, f = 3.5	0.2 × 7	7
Gibson	SFM	Kinetics of hemoglobin and lipoate dehydrogenase	Prism, f = 4	2 × 2	10
Forrest	AFM, SFM	Kinetics of CO_2 hydration	Chance filters (glass)	0.3 × 1	30
Trowse	CFM[c] (and scanning), SFM	Proton transfer reactions	Ilford filters (gelatin)	0.07 × 0.6	4
Dalziel	CFM	Kinetics of hemoglobin and related studies	Quartz, f = 7.5	~4 × 8	25 (?)
Lu Valle		Kinetics of dye formation in color processes	Double prism, f = 6	0.4 × 0.1	3
Sutin	SFM, CFM	Kinetics of oxidation-reduction reactions	Quartz. f = 7.5	2 × 1	20

[a] Accelerated flow method. [b] Stopped flow method. [c] Continuous flow method.

Constructor	Hydraulics: Max. flow rate, m./sec.	Hydraulics: Fluid drive	Hydraulics: Volume delivery, cc./sec.	Mixer: Number of jets	Mixer: Jet diameter mm.	Mixer: Observation tube diameter, mm.
Chance	15	Manually driven syringes	10	4	0.5	1.0
Gibson	30	Hydraulically driven syringes	30	8	0.5	2.0
Forrest	15	Hydraulically driven syringes	45	4	0.5	2.0
Trowse	10	Motor-driven syringes	10	2	0.5	1.12
Dalziel	10	Gas pressure drive	15	2	0.5	2.0
Lu Valle	3	Mechanical hammer driven by air pressure	3	4	0.5	1.0
Sutin	1	Motor-driven syringes	12	4	0.7	2.0

Constructor	Electronics: Photocell: Type	Electronics: Photocell: Surface	Electronics: Recorder	Electronics: Response speed, sec.	Electronics: Temperature control
Chance	929	Cs-Sb	Pen-and-ink, galvanometer oscillograph	0.03–5	Yes
Gibson	EMI 6260 multiplier	Cs-Sb	CRT[d]	0.001	Yes
Forrest	929	Cs-Sb	CRT	0.002	No
Trowse	931A multiplier	Cs-Sb	CRT	0.001–0.1	Yes
Dalziel	Beckman	Cs-Sb	Manual	2	Yes
Lu Valle	931A, 1P21	Cs-Sb	CRT	3×10^{-4}	Yes
Sutin	1P28	Cs-Sb	Leeds and Northrup Speedomax	0.2	Yes

[d] Cathode ray tube oscillograph.

TABLE 2.II (*continued*)

Over-all Performance							
Constructor	Min. time, millisec. SFM	Min. time, millisec. AFM, CFM	Volume per curve, cc.	Min. optical density change	Max. first-order velocity constant actually measured, sec.$^{-1}$	Max. second-order constant actually measured, M^{-1} sec.$^{-1}$	Reference
Chance	4	1	0.1	1×10^{-5}	200	2×10^{7}	11,12
Gibson	2.4	—	0.4	1×10^{-4}	100	8×10^{7}	5
Forrest	?	2	0.1		200	5000	13
Trowse	—	0.4	6		500	600	14
Dalziel	10^{3}	5	500	2×10^{-3}	20	$\sim 5 \times 10^{6}$	15
Lu Valle	<10	1	0.2	2×10^{-4}	22	2×10^{5}	16
Sutin	500	5	10	5×10^{-4}	40	2×10^{7}	17–23

1. Detailed Description of Chance's Apparatus

The apparatus that will now be described is the one with which nearly all the catalase and peroxidase studies were carried out in the interval 1946–1950. A summary of the results of this work is given in reference 6 and in Chapter XXII of this volume.

The monochromator and associated electronic equipment were originally constructed as a sensitive spectrophotometer without a rapid flow attachment (24), but studies of catalase and peroxidase with the colorimeter (24,25) soon proved the necessity for monochromatic illumination of the observation tube in order to obtain spectroscopic data on unstable enzyme–substrate compounds. Complete data (26) of the flow apparatus using this spectrophotometer appeared in 1951 and will be briefly summarized here. An earlier apparatus specialized for kinetics work at fixed wavelengths used Corning filters (27) and the results appear in references 25 and 28.

The construction of the all-glass syringe unit, stopcock, and mixer has already been referred to in Part 1, Section III.3. This unit is mounted on the monochromator as shown in Figure 2.3 and it is enclosed together with reservoirs in a water-jacketed housing for temperature control and for thermal equilibration of the reactants. The pushing block for the syringes is mounted on a slider that runs smoothly along a track. The block is attached by a tape to the pulley mounted on the shaft of the potentiometer used in the flow velocity measurement circuit. The friction drag which gives quick stopping is provided partly by the slider and track and partly by a phosphor bronze spring mounted between the pulley and the frame. The syringe plungers themselves are cemented into aluminum caps that fit snugly into the pushing block, one syringe plunger in the photograph having been removed from the holder to show its construction.

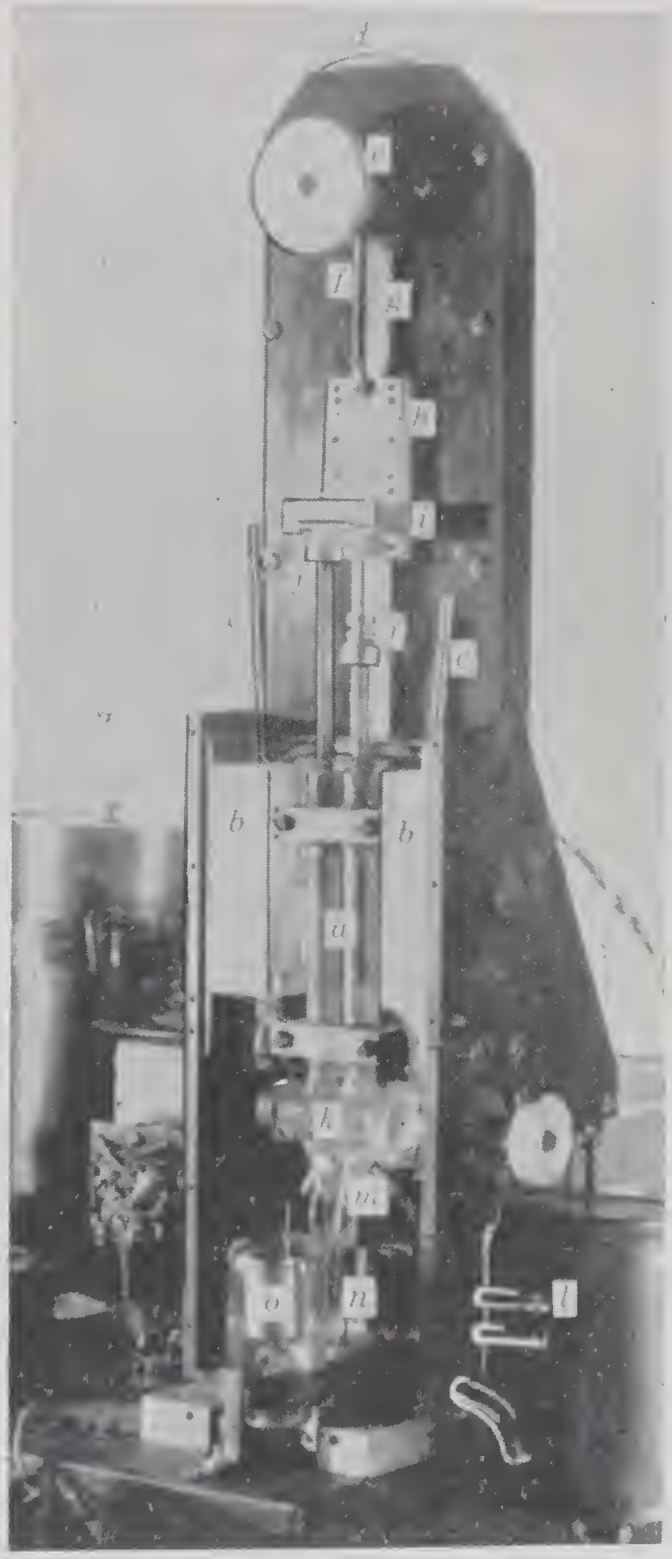

d, Potentiometer

e, Pulley

f, Tape
g, Track

h, Slider

i, Pushing block
j, Caps attached to syringe plunger

c, Stirring rods

b, Thermostated reservoir for reactants

a, 1-cc. Pyrex syringes

k, Stopcock

m, Mixing chamber

n, Observation tube
o, Photocell
l, Inlet for coolant

Fig. 2.3. A view of the Chance rapid flow apparatus showing the pushing block and track, the syringe unit, stopcock, observation tube, and photocell (FA 10).

The details of the cooling system and the observation tube are shown more clearly in Figure 2.4. The relationships of the flow apparatus and the optical and electronic components are shown in Figure 2.5. The flow unit is fastened directly to the casting of the monochromator which is

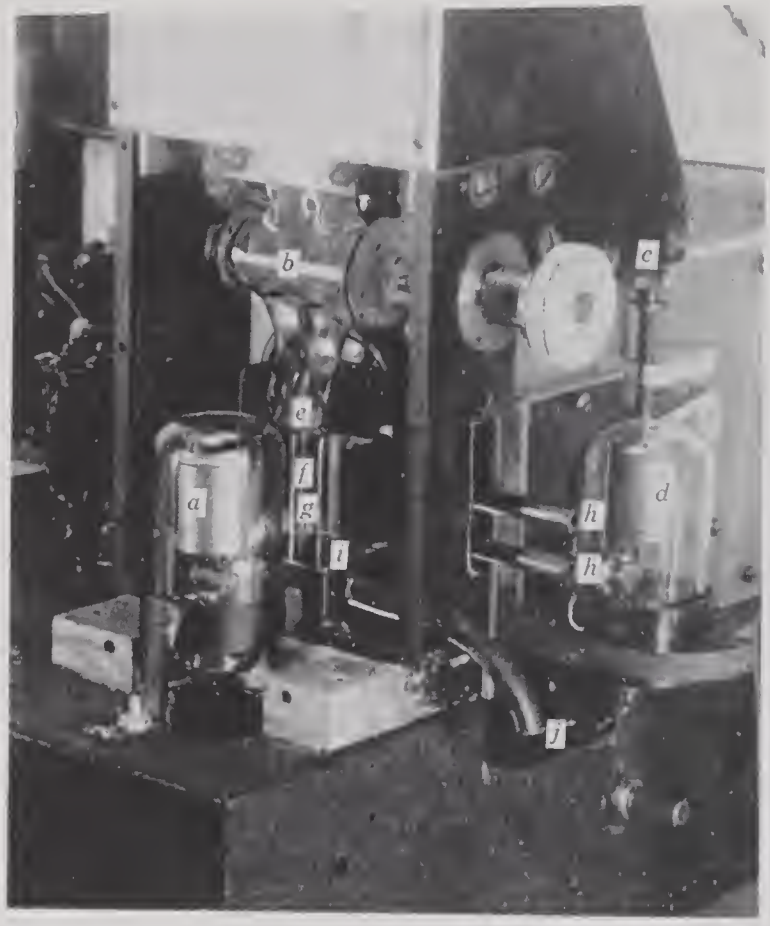

b, Stopcock
c, Shutter screw for compensating photocell

e, Mixer
f, To exit slit of monochromator
a, Photocell
g, Observation tube
d, Compensating photocell
h, Coolant
i, Cup

j, Drain

Fig. 2.4. A close-up of the apparatus in Figure 2.3 illustrating the cooling system for the mixing chamber and observation tube. Used reactants are removed via a cup and drain tube. The measurement and compensating photocells are shown as is the shutter screw for the compensating photocell (FA 11).

in turn mounted in the steel chassis for the electronic components. The complete apparatus including the power supply, recorders, and connections to the thermostat is shown in Figure 2.6. The extra pen-and-ink recorder is used for polarographic (platinum microelectrode) data on oxygen or hydrogen peroxide and the mirror galvanometer oscillograph (General Electric type PM-10-B2) has three elements for flow velocity, spectrophotometric, and polarographic recordings (see Chapter XXII, Figs. 2.3, 2.11, and 2.12).

The relationship between the output data and a typical oscillograph record is illustrated in Figure 2.7. The operation of the apparatus in the measurement of reaction kinetics is discussed in Chapter XXII, Part 2.

A. OPTICAL DETAILS

The monochromator is of the double replica-grating type obtained from Coleman Electric Company (Maywood, Illinois) and is suitable for studies in the region 370 to 1,000 mμ. The spectral interval is set at 5 to 10 mμ

and a photocurrent of about 10^{-7} amp. is obtained at 400 mμ at normal lamp voltage. The calibration of the monochromator is stable and only a simple adjustment is required when the lamp is replaced. The compactness of

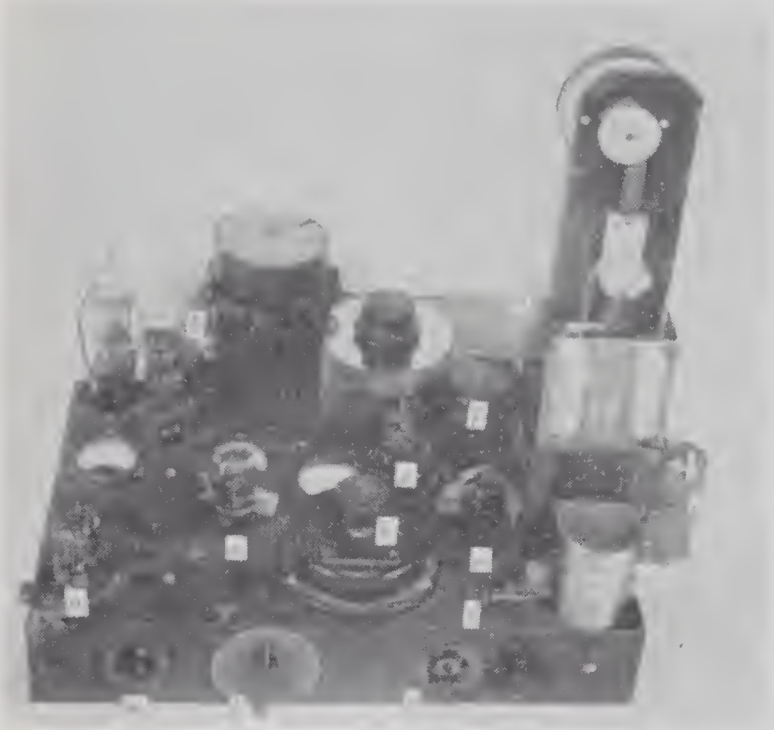

a, Amplifiers
b, Lamp voltage control
c, Fan
d, Monochromator
e, Wave length dial
f, Demodulator
g, Compensating photocell
h, Measurement photocell
i, Modulator
j, Response speed
k, Fine signal voltage
l, Coarse signal voltage
m, Gain

Fig. 2.5. The relationship of optical and electronic components to the flow unit depicted in Figure 2.3 (FA 12).

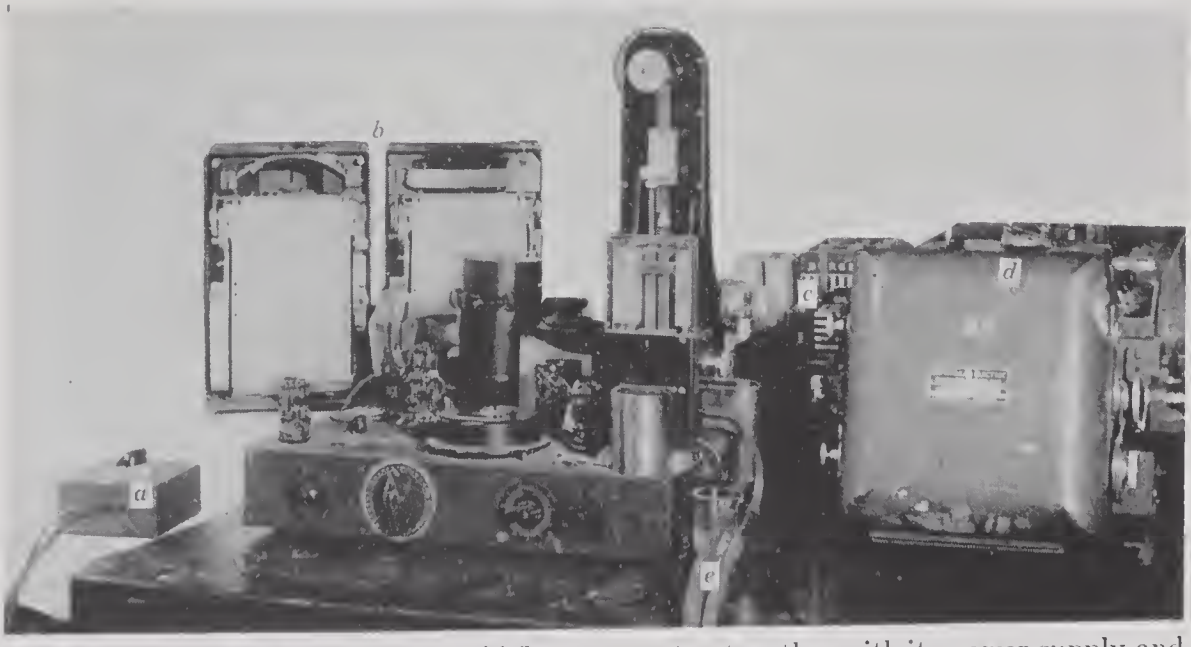

Fig. 2.6. The complete Chance rapid flow apparatus together with its power supply and recording systems (FA 13).

a, Recorder switches
b, Pen-and-ink recorders
c, Power supply
d, Mirror galvanometer oscillograph
e, Coolant from thermostat

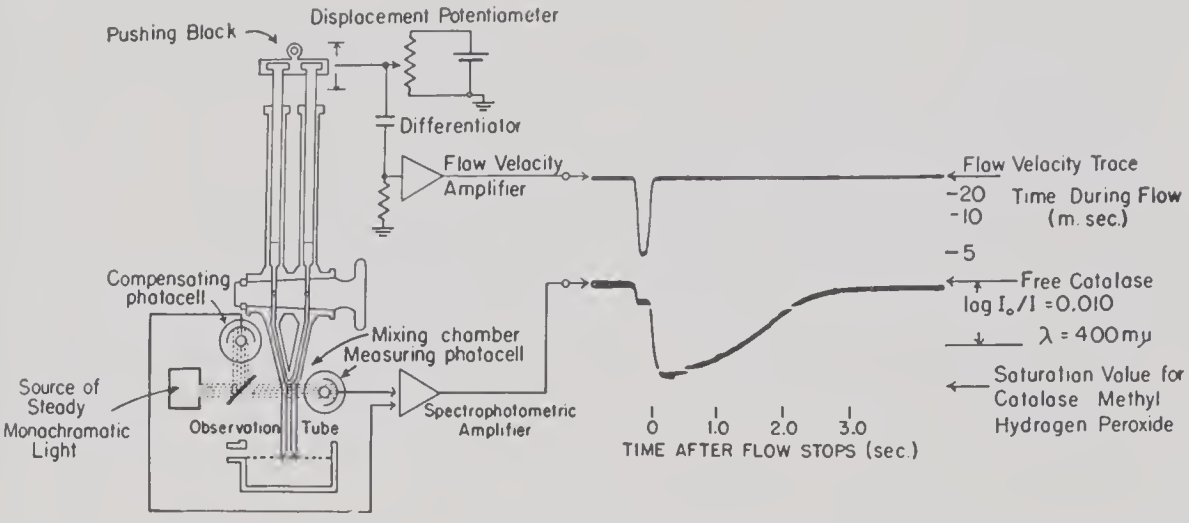

Fig. 2.7. A schematic representation of the stopped and accelerated flow methods with a typical oscillograph record of the formation and decomposition of the catalase–methyl hydrogen peroxide complex in the presence of ethanol (Expt. 468).

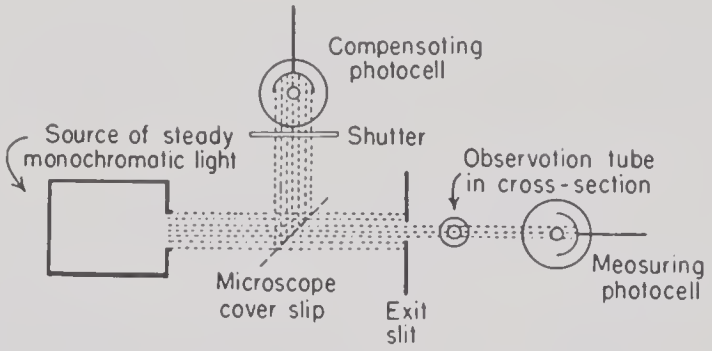

Fig. 2.8. The optical system in an apparatus utilizing a compensating photocell for light intensity control. The shutter is used for the zero adjustment that equalizes the current output of the two photocells (468).

the monochromator, its small f number (3.5), and the slit dimensions (0.4 × 10 mm.) make it excellently suited to the flow methods that utilize capillary observation tubes. In addition, we take advantage of the fact that the slit length error is not serious and illuminate the observation tube over a length of 2 to 12 mm. from the point of mixing (see Part 1, Section III.8). A portion of the light incident upon the exit slit is reflected upon a compensating photocell by means of a microscope cover slip as illustrated by Figure 2.8.

B. ELECTRONIC DETAILS

The electronic circuit is shown in Figure 2.9. The current passed by the measurement and the compensating photocells is adjusted to equality by means of a shutter in front of the latter. The chopper amplifier then

measures any small change of light transmission through the observation tube, caused by the chemical reaction, and these changes are recorded directly as shown in Figure 2.7.

The chopper amplifier is selected because of its simplicity and reliability, although equally satisfactory results could be obtained with a carefully adjusted direct-coupled amplifier. The chopper amplifier is especially suited for a circuit using a compensating photocell because it accepts a differential input signal. The fastest response that can be obtained at a 60 c.p.s. chopping frequency is about 0.03 sec., but choppers with nearly identical characteristics are available for 400 c.p.s. operation and would permit a response speed of about 0.004 sec. A direct coupled amplifier would respond in a fraction of a millisecond.

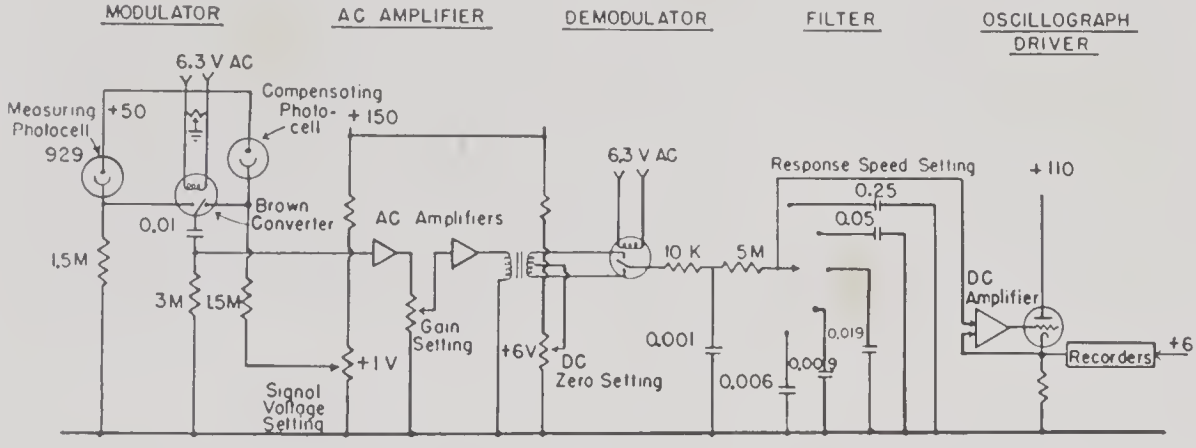

Fig. 2.9 A block diagram of an electronic circuit for amplifying the difference of the photocurrents by means of a chopper amplifier. Each a-c amplifier has a gain of 10^3 (MD-4).

A great simplification of the electronic circuits is now possible, since the components described in Fig. 2.7 are available commercially. Chopper amplifiers are obtainable from Millivac, Keithley, and Magnetic Instruments companies. Also there are several oscilloscopes with built-in d-c amplifiers that are adequately stable for use with a photomultiplier (Tektronics, etc.). Where high stability for operation directly from a photocell is desired, the design of d-c amplifier described in reference 27 is recommended, particularly for fast response at low signal levels.

The use of a fast and a slow recorder is almost essential if it is desired to obtain complete records of the rapid formation and slow disappearance of the enzyme–substrate compounds. We use the pen-and-ink recorder not only for its slow time scale but also as a monitor for the oscillograph to insure that the proper gain and zero setting are used. A satisfactory alternative is a triple beam oscillograph with a fast and a slow time base, but the monitoring of the traces that are photographed is not always convenient.

C. PHOTOCELLS

In this circuit we use the RCA-929 phototube with a Cs-Sb surface. It is possible to eliminate the chopper amplifier if a photomultiplier is used and the output can be directly connected to the filter of Figure 2.9 or to an oscilloscope as described above. However, photomultipliers could not be used in the compensating circuit of Figure 2.9 without some difficulty in the accurate equalization of their gains. At the very high light intensities demanded by sensitive spectrophotometry, photomultipliers may fatigue and this fatigue lasts for several minutes and differs from tube to tube.

D. LIGHT INTENSITY CONTROL

As shown in Figure 2.10 the light intensity is controlled by the potential applied to the lamp. This circuit has been quite satisfactory in our hands. A simpler circuit is one which uses a photocell for controlling the light intensity (26). Since a compensating photocell is used in the circuit of Figure 2.9 the circuit is relatively insensitive to light intensity fluctuations and a fairly simple light intensity controller is adequate.

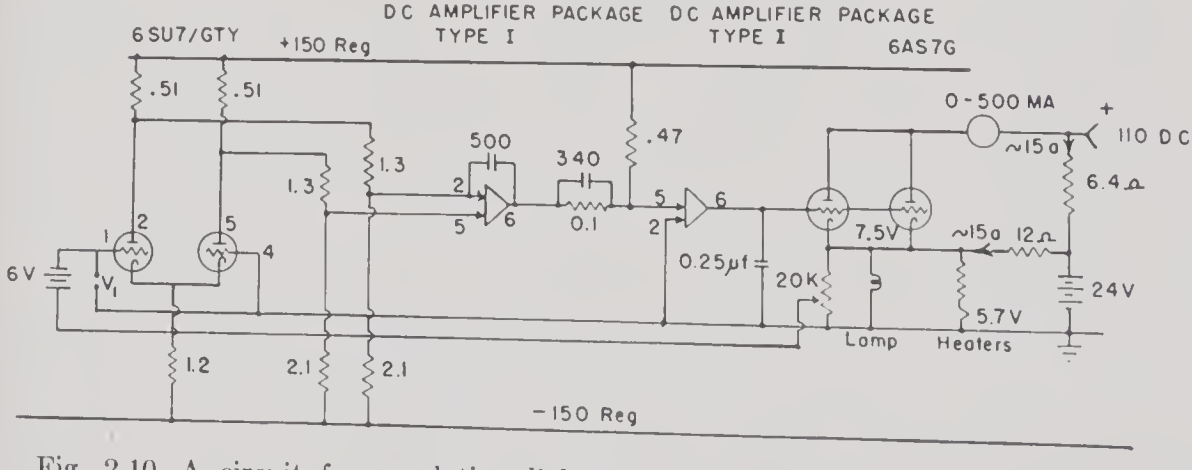

Fig. 2.10. A circuit for regulating light intensity through lamp voltage control. Resistance values are in megohms and capacitance in $\mu\mu$f. unless otherwise noted. The direct coupled amplifier gain is 10^3 per unit (MD-3).

We do not favor the direct use of a battery supply because the continuous decrease in the battery voltage results in a corresponding decrease in the sensitivity of the photoelectric circuit—a rather undesirable feature in spectroscopic studies where a constant day-to-day sensitivity is needed.

Recent developments in solid-state power supplies make the latter very attractive, particularly those that can readily be controlled by the amplified photocell output.

In the current discussion (see Fig. 2.9) we recommend the use of a compensating photocell whereas we had previously concluded (26) that such a circuit could have only 1/1.4 the performance of a single photocell circuit, provided the light intensity control circuit were operating ideally. Since the highly efficient light control circuit of Figure 2.10 may be difficult to duplicate we feel that others would have a better chance of success with the circuit that employs a compensating photocell.

E. OVER-ALL PERFORMANCE

Table 2.II gives performance data for this apparatus in comparison with that of contemporary designs. It is clear that this apparatus excels in its photoelectric sensitivity and can operate with very dilute solutions and hence measure a large value of a second-order velocity constant. The fluid economy of the apparatus could be improved by a factor of two by incorporating the quick stopping feature of Gibson's apparatus.

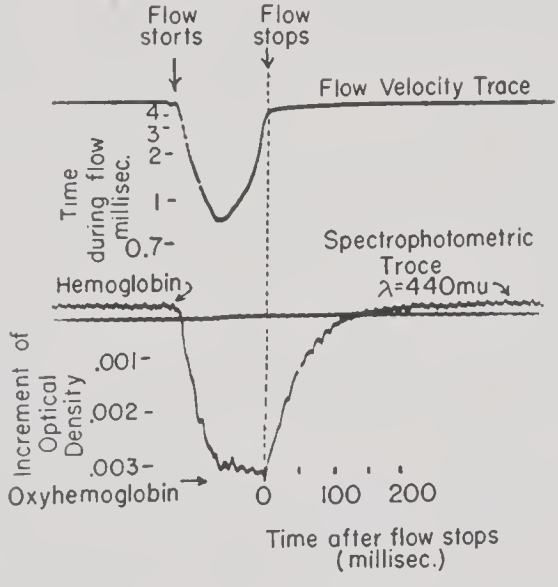

Fig. 2.11. A direct reading of the disoxygenation of hemoglobin made by the rapid flow method of Chance. The trace is recorded by the mirror galvanometer oscillograph seen in Figure 2.6 (Expt. 19).

The limitations of this apparatus for the measurement of rapid reactions by the stopped flow method are shown by Figure 2.11 where the disoxygenation of oxyhemoglobin is recorded—a reaction for which this apparatus was not specifically designed, but a good reaction for a comparison of the performance of Chance's and Gibson's apparatus designs (*cf.* Fig. 2.14). The observation tube is filled with hemoglobin from a previous experiment and, on initiating the flow, the hemoglobin is cleared out in 50 millisec. after the flow starts as shown by comparing the flow velocity and spectro-

photometric traces. The observation tube then contains mixed oxyhemoglobin and hydrosulfite which gives a nearly horizontal trace corresponding to approximately zero extent of the reaction because the time after mixing (see "time during flow" scale) is small compared to the half-time of the reaction. The total optical density change is 0.003. 80 millisec. after the flow starts the pushing block is released. 50 millisec. later the flow comes to a halt as clearly shown by the rise in the flow velocity trace. The deceleration is quite rapid (about 400 m./sec.^{2}) and the fluid which stops at the point of observation reaches there in only 5 millisec. The disoxygenation reaction then proceeds with a half-time of 45 millisec. The spectrophotometric trace contains irregularities (ripple) because the smallest value of filter condenser was used to obtain the rapid response time (see Fig. 2.9—0.006 μf.).

A record of a typical use of this apparatus in measuring the velocity constant for the formation of the catalase–hydrogen peroxide complex is given in Figure 2.10. In this case the reaction is more rapid and is half complete at the most rapid flow velocity.

2. Description of Gibson's Apparatus

Basically this apparatus is similar to that just described, but is especially adapted for stopped-flow studies. Gibson (5) obtains a stopping time of about 1 millisec. by means of a hydraulic stopping device. The outflow of the flow apparatus drives a piston against a stop, and if the elasticity is almost negligible, the flow stops instantaneously.

In order to obtain more rapid response times of the photocell, Gibson employed an electron multiplier phototube and, since his longest recording interval is about 30 sec., neither slow fatigue of the photomultiplier nor slow discharge of the batteries that supply the lamp cause appreciable difficulty except with regard to the calibration of the optical density scale.

The details of the apparatus construction are shown in Figures 2.12 and 2.13. The pushing block is guided by the Lucite ways and bears against the plungers of the two 2-cc. metal-to-glass syringes ("Record" type). These syringes can be filled from their respective reservoir syringes by turning the stopcocks. The reservoir syringes are convenient for hemoglobin studies since no undesirable gas exchanges can occur. The fluids are delivered from the syringes to the mixing chamber and the 2-mm.-bore observation tube. Light from a tungsten lamp passes through an interference filter or a monochromator and is focussed as a 2×2 mm. image on the observation tube and thence downward to a lens, 45° mirror, and onto an electron multiplier phototube. The fluid from the observation tube then drives the arresting piston against its stop and rapidly halts the

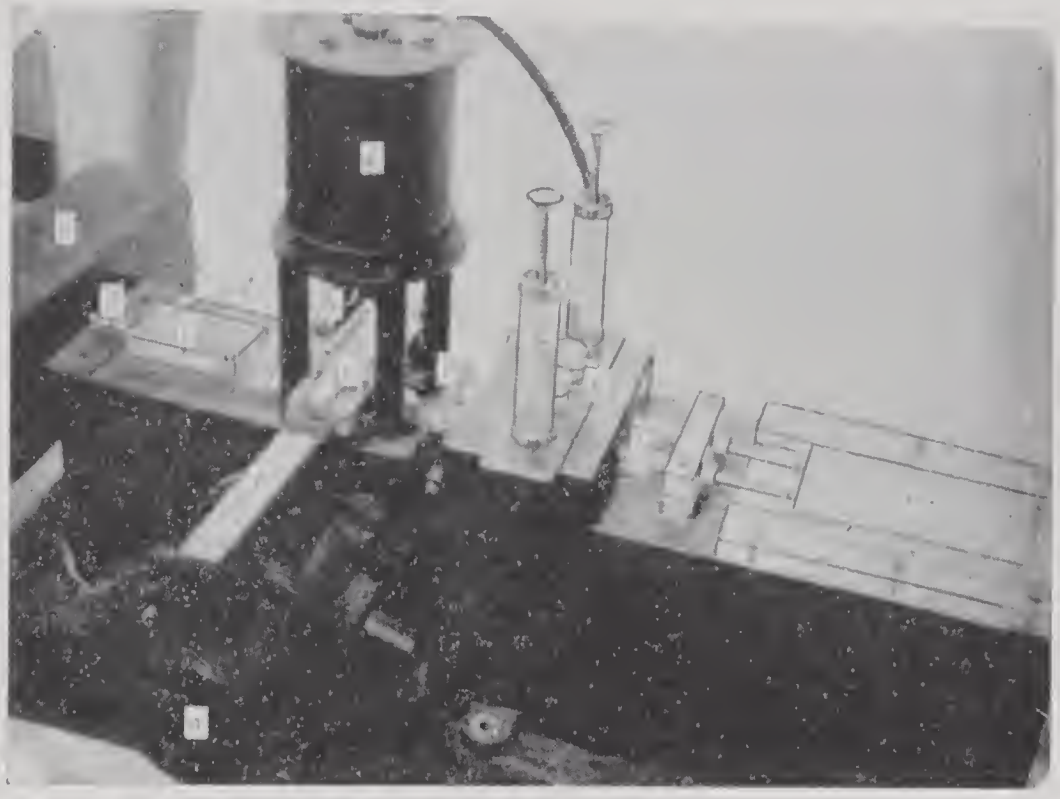

Fig. 2.12. The mixing and observation units of Gibson's stopped flow apparatus.

a, Photomultiplier casing
b, Filter
c, Observation tube
d, Signal flag for piston displacement
e, Housing for piston displacement photomultiplier
f, Arresting piston
g, Lamp housing
h, Lens
i, Mixer
j, 10 cc. reservoir syringes
k, Stopcocks for admitting reactants
l, 2 cc. driving syringes
m, Syringe plunger pushing block

flow. In order to repeat the experiment some fluid is removed from the cylinder of the arresting piston via the stopcock shown in Figure 2.12, permitting the piston to be reset.

In order to measure precisely the moment at which the flow stops, the arresting piston drives a rod that extends into the box (shown in Fig. 2.12) that contains a second lamp and photocell. As the arresting piston moves the rod, a vane alters the intensity of the light falling on the photocell, thereby giving an electric signal of magnitude proportional to the position of the arresting piston. (The function of these parts is identical to that of the displacement potentiometer of the Chance apparatus. The photocell and vane arrangement used by Gibson has the advantage of having considerably less inertia, and hence is more satisfactory for quick stopping.)

The output of the photomultiplier is sufficiently large to operate directly the direct coupled amplifier of the Cossor Model 1049 oscilloscope. The oscilloscope has two separately controllable electron beams so that the second can be used to record the displacement of the arresting piston. The assembled apparatus is shown in Figure 2.13.

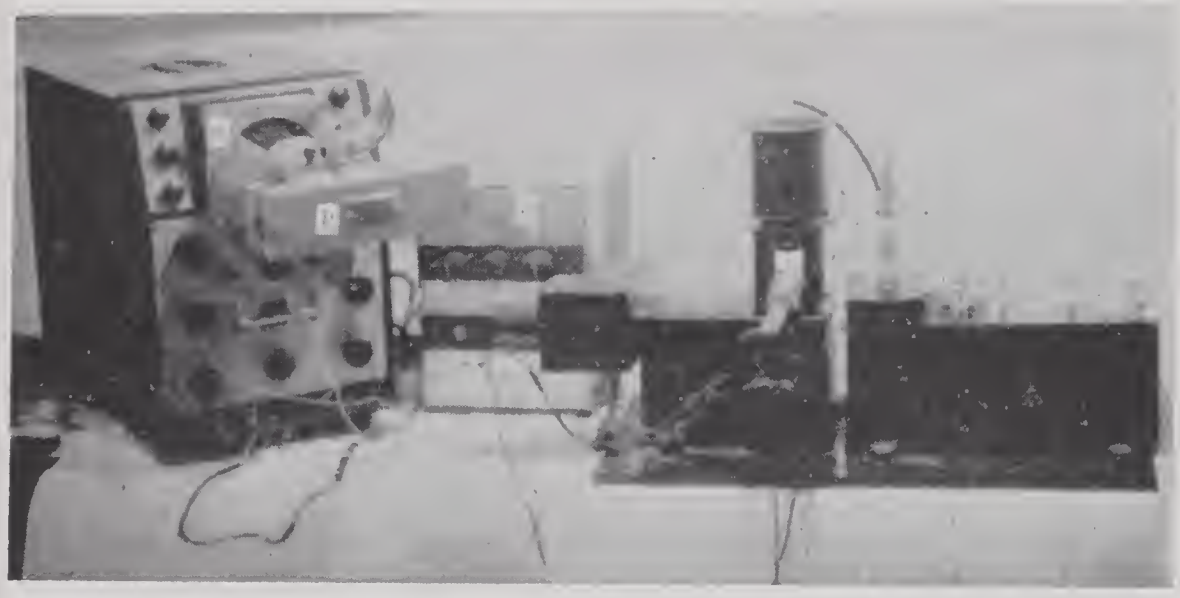

Fig. 2.13. An over-all view of Gibson's apparatus showing power supply, recording cathode ray tube oscilloscope, and stopped flow apparatus. *a*, CRT oscilloscope. *b*, Camera. *c*, Power supply.

A typical record (Fig. 2.14) illustrates the operation of Gibson's apparatus in measuring the disoxygenation of hemoglobin. The two dots on the left-hand side of the figure represent static calibrations with hemoglobin and with oxyhemoglobin, an upward deflection representing an increase in optical density at 475 mμ of a magnitude equal to 0.0045. When the kinetic run is begun, the observation tube is filled with hemoglobin remaining from the preceding experiment. The traces rise rapidly in their

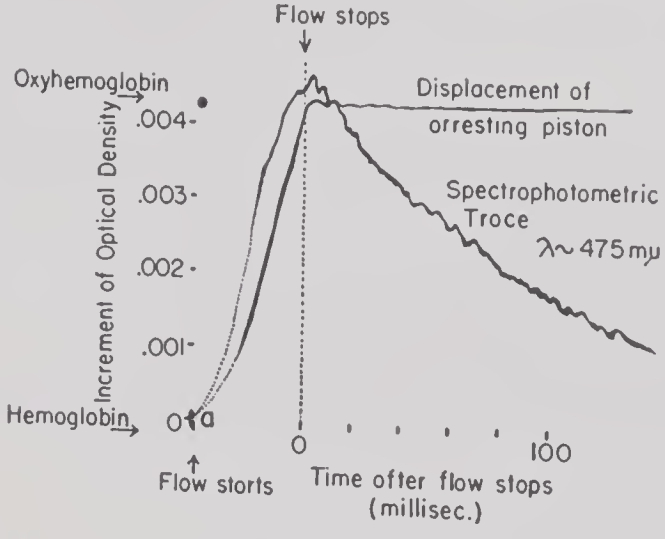

Fig. 2.14. A typical recording of the disoxygenation of hemoglobin made by Gibson's apparatus which should be compared with the kinetic curve of Figure 2.11. The trace here is made by a cathode ray oscilloscope and recorded by means of a camera shown in Figure 2.13.

initial phases, and 40 millisec. after starting the flow the observation tube is cleared of hemoglobin and filled with oxyhemoglobin flowing at the rate of 7.5 m./sec. The piston displacement curve shows that the piston stops in about 1 millisec. with very little "bounce." The disoxygenation of hemoglobin then proceeds with a half-time of 64 millisec.

A general feature of a new design by Gibson (29,30) is flexibility in the choice of observation path, whereby values from 2 to 20 mm. are possible. In addition, the apparatus is easy to manipulate and highly reliable.

The apparatus is indicated in Figure 2.15, which shows a side elevation. The reagents are transferred to the 25-ml. storage syringes A, from which they are transferred by appropriate manipulation of the valves to the driving syringes C. The valves do not require grease, and unlike stopcocks cannot be forced out by the higher pressures given by the hydraulic unit. To make a determination, driving syringes are forced in together by the pressure of a hydraulic unit, causing the reactants to pass through the mixers D, and the mixture to flow past the observation window E. From there the mixture flows into the stopping syringe F, driving its plunger upwards until the handle strikes the stop G. At this time, flow is arrested suddenly without having been previously slowed down, and observation is made by means of a photomultiplier, whose position is indicated at H, on the stationary portion of fluid in front of the observation window. To repeat the observation, the port valve I is opened, allowing the spent-reaction mixture in the stopping syringe F to drain away through

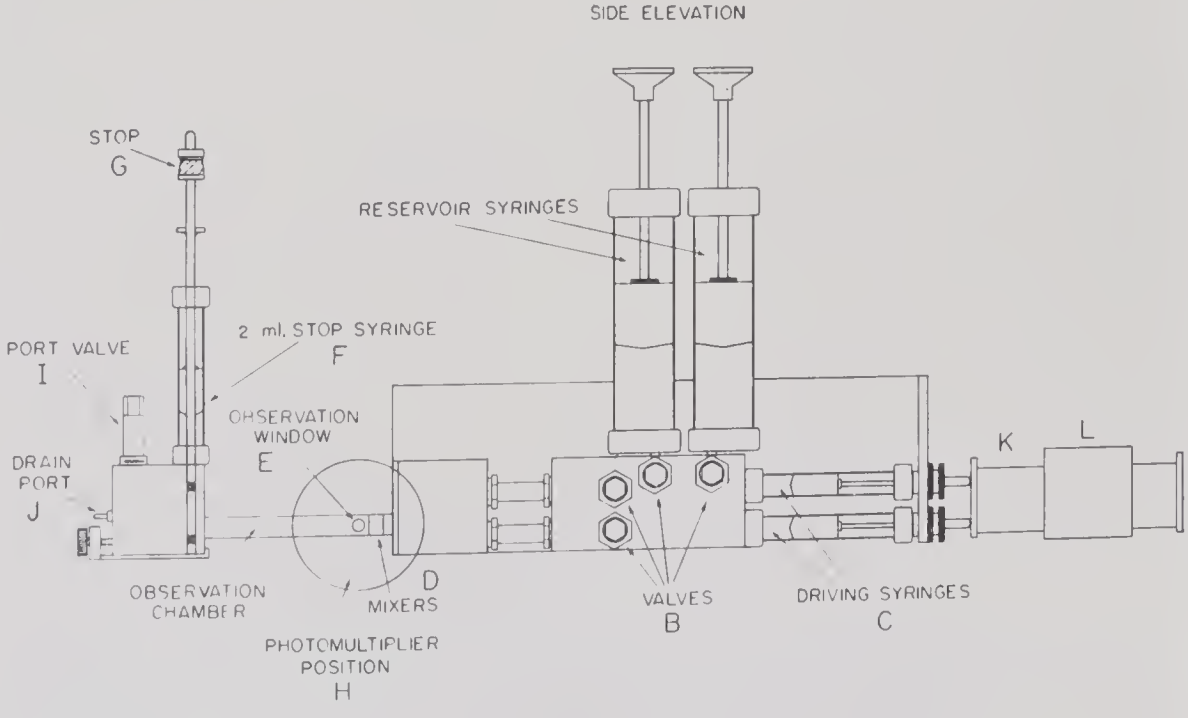

Fig. 2.15. Gibson's flow apparatus in its most recent form.

the drain port J; the port valve I is then closed, and the observation is repeated by operating the hydraulic actuator.

Detailed construction plans are available upon request from Q. H. Gibson (29) and include a double 8-jet mixer and suitable connections to the observation tube. The apparatus can be accurately temperature-controlled, and it can be equipped with a Hilger D246 monochromator (glass prism).

Performance. The apparatus is suitable for measuring a first order reaction of $k = 80$ sec.$^{-1}$, and an extinction change of 0.01. For a highly absorbing material at a concentration of 10^{-7} M, the second-order constant would approach 10^9, and a value of 8×10^7 M^{-1} sec.$^{-1}$ has actually been measured.

3. Apparatus of Dalziel and O'Brien

This apparatus is described here because it is, in the writer's opinion, the one that could be constructed, operated, and maintained by a person quite unfamiliar with electronic apparatus, inasmuch as it employs the well-known Beckman spectrophotometer. In order to use this slowly re-

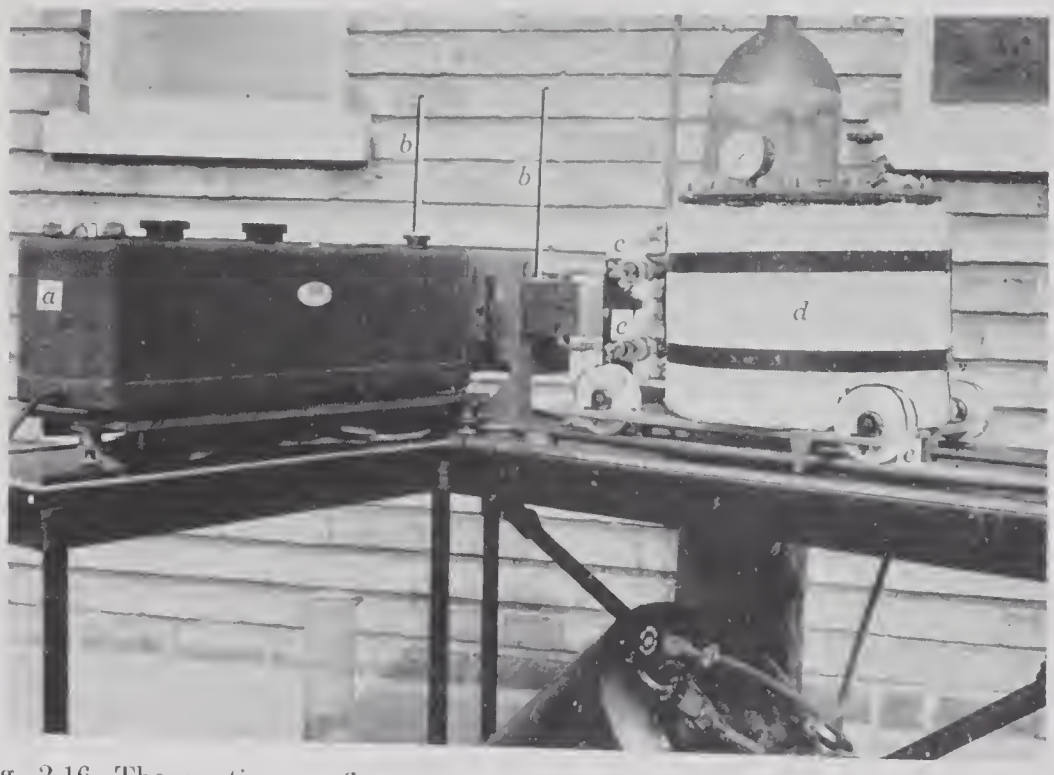

Fig. 2.16. The continuous flow apparatus of Dalziel showing the relation of the fluid drive units and pressure reservoirs to the Beckman spectrophotometer.

a, Beckman spectrophometer
b, Thermometers
c, Cocks for stopping the flow of reactants
d, Thermostated pressure tank containing reservoir for 4 liters of reactants
e, Track and rollers for adjusting the distance from mixing to observation

sponding, manually operated instrument, a continuous flow is maintained for an interval of several seconds. Thus a large expenditure of fluid is required and the pressure system originally used by Hartridge and Roughton provides the most satisfactory type of fluid drive.

The complete apparatus is shown in Figure 2.16. The pressure tank is usually set to 40 lb./sq. in. after the reservoirs have been filled with one liter of the reagents. After thermal equilibration has taken place, the calibration of the initial and final values for the reaction are obtained by filling the observation tube with the appropriate reactants and by reading the scale of the Beckman spectrophotometer in the usual fashion. The kinetic run is started by opening both stopcocks shown in Figure 2.17.

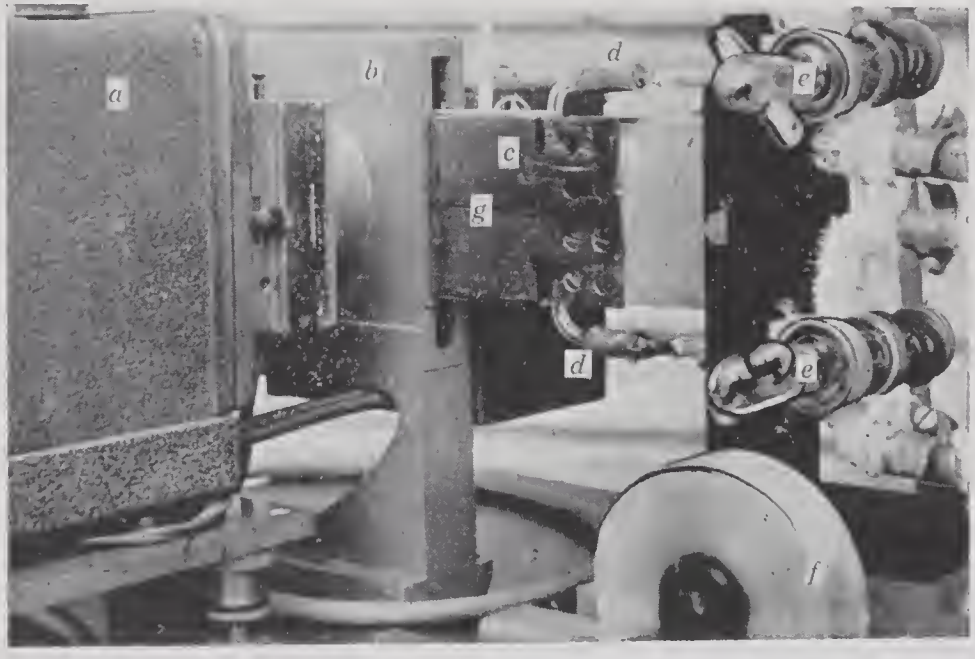

Fig. 2.17. A detail of the flow components of the apparatus in Figure 2.15.

a, Spectrophotometer
b, Guide for observation tube
c, Mixer
d, Reactants
e, Stopcocks
f, Roller for moving tank containing reactants
g, Slit for admitting light to observation tube

The extent of the reaction is determined for various distances from mixing to observation, which are varied by moving the whole pressure reservoir and observation tube with respect to the spectrophotometer. The zero point of the Beckman scale is set by running the less colored reactant through the observation tube. An illustration of the performance of this method in measuring the velocity constant for the dissociation of oxyhemoglobin is given in Figure 2.18 and more recent data are afforded by reference 31.

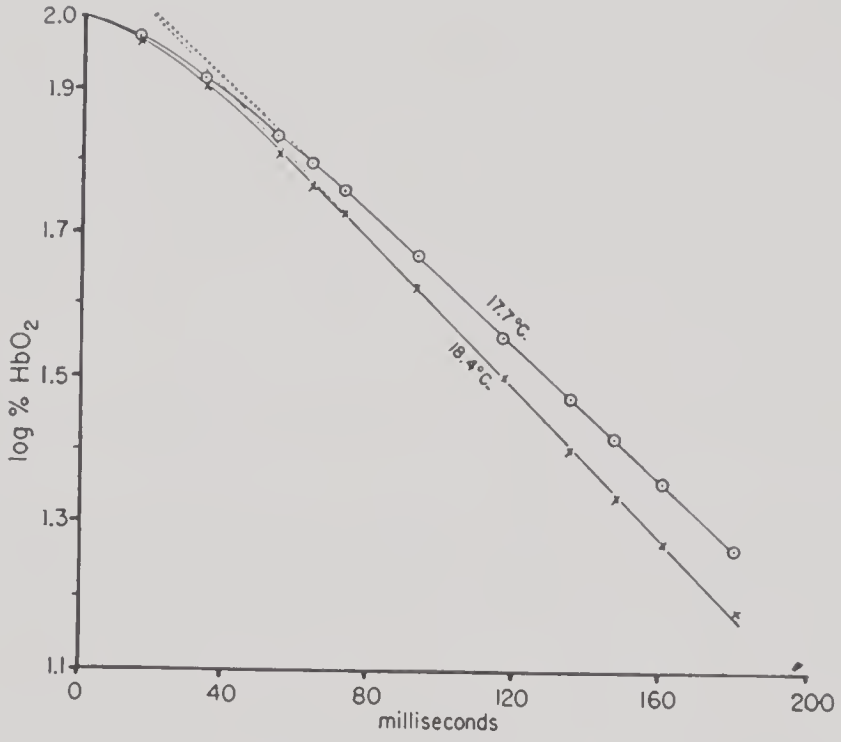

Fig. 2.18. Kinetic curves for the disoxygenation of hemoglobin as measured by the continuous flow apparatus of Dalziel.

The inherent difficulty that characterizes the continuous flow method in which the observation tube is scanned by the spectrophotometer is that optical irregularities in the observation tube may give artifacts as great as the change in transmission due to the chemical reaction. This effect is not so apparent with Dalziel's apparatus because the sensitivity of the Beckman spectrophotometer is not very high and satisfactory performance may be obtained. In practice, Dalziel corrects for this error by calibrating the instrument at each point.

For reactions such as the rate of combination of dissolved oxygen with hemoglobin, it is essential that the reagents should not be affected by exposure to the driving gas in the pressure tank. The Dalziel apparatus, which was never intended for this purpose, has been modified and is in operation at Roughton's laboratory (see Forrest in Table 2.II, pages 732–733, and Fig. 1 of the paper by Forster, *et al.* (32)).

Dalziel's method is suited only for the study of the kinetics of reactions in optically clear homogeneous solutions. A satisfactory extension of the mechanical features of Dalziel's method to the kinetics of reactions in heterogeneous turbid media (such as the rate of uptake of oxygen by hemoglobin in intact suspensions of red blood cells) has been made by means of a simple application of the differential principle (27,32). Light

from a tungsten filament lamp (12V 24W) is focussed on the center of the observation tube and after passing through the latter, falls on a half-silvered mirror, by which it is split into two beams at right angles. Each beam passes through a separate interference filter onto a separate phototube, the two filters being so chosen that the amounts of scattered light at their respective wavelength transmissions are about the same, whereas the amounts of light absorbed by the two pigments under study are very different. The difference between the electrical outputs of the two phototubes, which is amplified and recorded in a conventional way, is thus mainly due to the color change associated with the chemical reaction under study, and noise due to variations of light scattering in the turbid system is almost, if not entirely, eliminated. The observation tube must be calibrated at each point, preferably during each experiment.

Sirs (33) has recently applied the same differential principle to Gibson's stopped flow apparatus, and has thereby extended the use of the latter to the recording of color changes in suspensions of red blood cells.

References

1. F. J. W. Roughton and G. A. Millikan, *Proc. Roy. Soc. London*, **155A**, 258, 269, 279 (1936).
2. H. Theorell and A. Ehrenberg, *Acta Chem. Scand.*, **5**, 823 (1951).
3. J. B. S. Haldane, *Proc. Roy. Soc. London*, **108B**, 559 (1931).
4. B. Chance, *Electronics*, **13**, 2 (1940).
5. Q. H. Gibson, *J. Physiol.*, **117**, 49P (1952); *Discussions Faraday Soc.*, **17**, 137 (1954).
6. B. Chance, *J. Biol. Chem.*, **179**, 1341 (1949).
7. B. Chance, *Acta Chem. Scand.*, **1**, 236 (1947).
8. B. Chance and J. B. Neilands, *J. Biol. Chem.*, **199**, 383 (1952).
9. H. Theorell and B. Chance, *Acta Chem. Scand.*, **5**, 1127 (1951).
10. H. Theorell, *Advances in Enzymol.*, **20**, 31 (1958).
11. B. Chance, *J. Franklin Inst.*, **229**, 455, 613, 737 (1940).
12. B. Chance, *Advances in Enzymol.*, **12**, 153 (1951).
13. W. W. Forrest, unpublished data.
14. F. W. Trowse, Ph.D. dissertation, University of Leeds, 1952.
15. K. Dalziel, *Biochem. J.*, **55**, 79 (1953).
16. J. E. Lu Valle, personal communication.
17. N. Sutin and B. M. Gordon, *J. Am. Chem. Soc.*, **83**, 70 (1961).
18. M. H. Ford-Smith and N. Sutin, *J. Am. Chem. Soc.*, **83**, 1830 (1961).
19. B. M. Gordon, L. L. Williams, and N. Sutin, *J. Am. Chem. Soc.*, **83**, 2061 (1961).
20. M. H. Ford-Smith, N. Sutin, and R. W. Dodson, *Discussions Faraday Soc.*, **29**, 134 (1960).
21. N. Sutin, *Nature*, **190**, 438 (1961).
22. N. Sutin and D. R. Christman, *J. Am. Chem. Soc.*, **83**, 1773 (1961).
23. G. Dulz, Ph.D. thesis, Columbia University, work in progress.
24. B. Chance, *Rev. Sci. Instr.*, **18**, 601 (1947).
25. B. Chance, *J. Biol. Chem.*, **151**, 553 (1943).
26. B. Chance, *Rev. Sci. Instr.*, **22**, 619 (1951).

27. B. Chance, *Rev. Sci. Instr.*, **13**, 158 (1942).
28. B. Chance, E. N. Harvey, F. Johnson, and G. A. Millikan, *J. Cell. Comp. Physiol.*, **15**, 195 (1940).
29. Q. H. Gibson, personal communication.
30. Q. H. Gibson and E. Antonini, *Biochem. J.*, **77**, 328 (1960).
31. K. Dalziel and J. R. P. O'Brien, *Biochem. J.*, **78**, 236 (1961).
32. R. E. Forster, F. J. W. Roughton, F. Kreuzer, and W. A. Briscoe, *J. Applied Physiol.*, **11**, 260 (1957).
33. J. A. Sirs, *J. Physiol.*, **150**, 18P (1960).

Part 3. *THE REGENERATIVE FLOW APPARATUS*

Two general requirements, of physical apparatus on one hand and of turbid biological materials on the other, are met by an instrument which we have chosen to name a "regenerative flow apparatus" (1,2). Its fulfillment of the second requirement is most easily explained. In studies of the reaction kinetics of turbid heart muscle preparations which carry out the rapid oxidation of succinic acid, it was found that the usual form of flow apparatus in which equal volumes of substrate are mixed with equal volumes of enzyme was unsatisfactory since the two-fold dilution of the turbid suspension caused a very large diminution of absorbancy. Furthermore it was difficult to maintain with sufficient precision the relative deliveries of flow of the two reagents necessary to achieve the required degree of constancy of optical density in the diluted turbid suspension. Although considerable improvements were possible in the relative delivery of flow of enzyme and substrate, it appeared simpler to deliver volumes of substrate about 1% those of the enzyme. Mixing unequal volumes of enzyme and substrate requires special consideration in the design of the mixing chamber because of the greater possibilities of laminar flow for these smaller volumes of material delivered. A number of designs have been considered (1). The most satisfactory is a two-stage mixing chamber in which the enzyme and mixed solutions are combined in a second set of mixing jets. The design of such a mixer is illustrated in detail in Figure 3.1. Good mixing over a wide range of flow velocities is highly desirable for studies of the type mentioned below where the flow is prolonged over times up to a minute.

The second requirement is that of certain types of physical measurements for the evaluation of the extent of the chemical reaction in which the response time and the sensitivity are limited. Three examples which will be discussed here are:

(*1*) The recording of spectra of labile intermediates in turbid biological material where light scattering of the material diminishes the light intensity available for the spectrophotometric measurement.

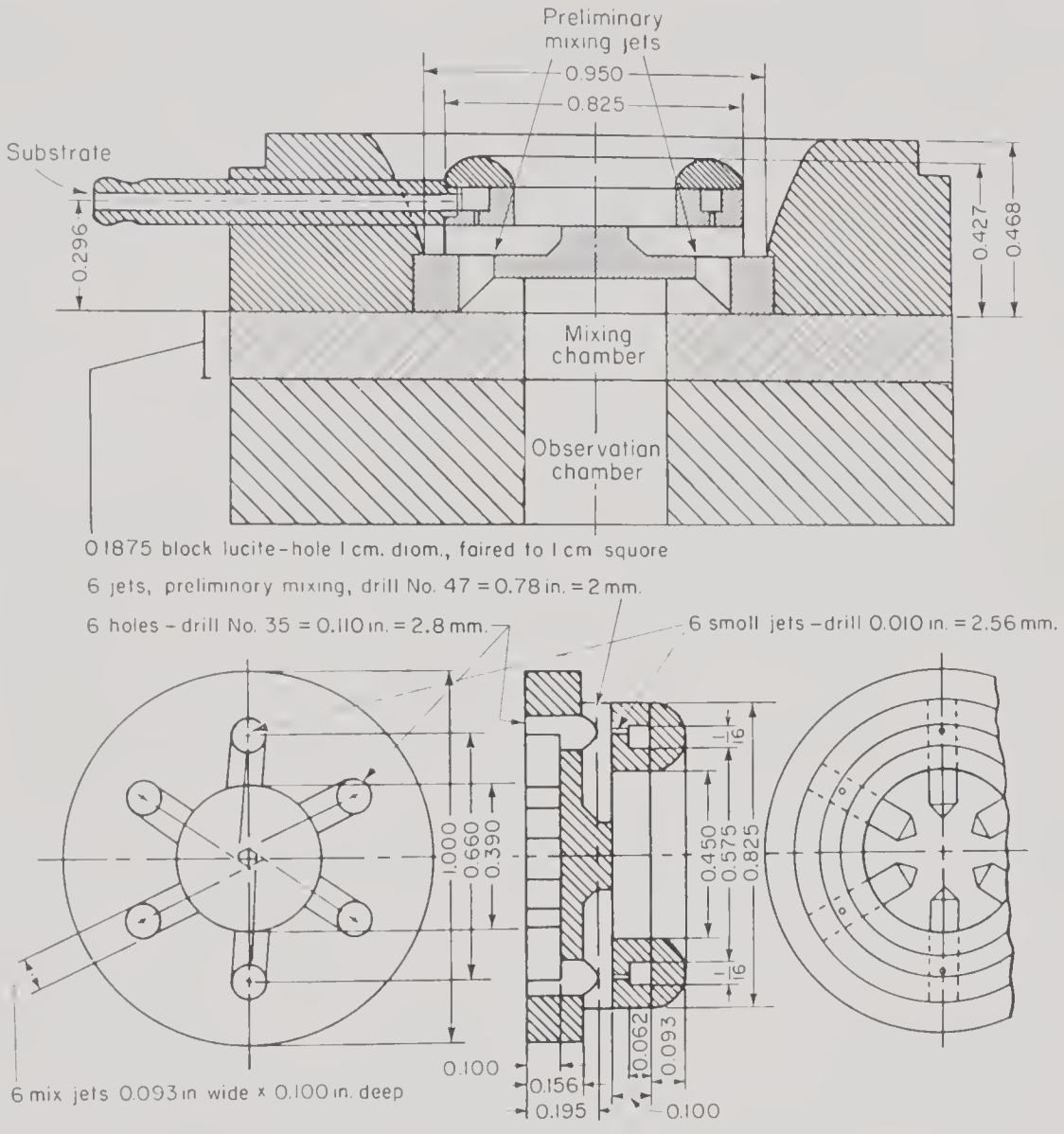

Fig. 3.1. Two-stage mixing chamber for regenerative flow apparatus. The first chamber into which substrate and enzyme are injected has 6 jets of 0.25 mm. bore for the former and 12 jets of 2 mm. bore for the latter. The second chamber has 6 jets of 2.5 mm. bore. The distance from mixing to observation is 11 cm. (FA-24) (1).

(*2*) The measurement of rapid changes of volume magnetic susceptibility by means of the Rankine balance.

(*3*) The measurement of labile free radical signals with electron spin resonance apparatus.

With each of these methods, it is possible to obtain a clearer recording of the electrical signals with a slower response time provided the flow method is used to maintain a steady concentration of the intermediate for the required time interval. Without this precaution, signals due to a labile intermediate would be missed. The required interval depends upon the apparatus; for the recording of the spectrum over the spectral interval

from 50 to 100 mμ, a corresponding number of seconds may be required. For the recording of a spin resonance signal, a comparable or even longer time may be required. The volume magnetic susceptibility method will respond in a few seconds. Thus the design of the flow apparatus depends upon the particular time requirements of the physical method.

I. REGENERATIVE FEATURES

When the reaction of enzyme and substrate is largely irreversible, for example in the case of the reduction of peroxide or oxygen to water by iron porphyrin enzymes, repeated additions of a small volume of the oxidant to the enzyme solution may be made. This technique has been found useful in studies of the reaction of peroxidase with hydrogen peroxide or of cytochrome oxidase with oxygen. For this reason the regenerative flow apparatus provides either (*1*) a *continuous* circulation of reagents through the mixing chamber and into a reservoir, the capacity of which will allow decomposition of the intermediate or utilization of the added oxidant or (*2*) an *intermittent* flow of reagents through the mixing chamber into a reservoir which will contain sufficient material for a flow through the chamber of about a minute (such a chamber is usually in the form of a syringe). Under these conditions one may wait a considerable time interval for the exhaustion of the added substrate.

In both cases the material is reintroduced into the mixing chamber: in case (*1*) by means of a continuous pumping system and in case (*2*) by discharging the collecting syringe back into the driving syringe, the delivery of substrate being interrupted during this interval.

It is important here to indicate possible difficulties in using regenerative flow apparatuses of the intermittent type with a substrate which is added in large excess. Under such conditions, the driving syringe must be continuously refilled with fresh reagent since a mixture of fresh enzyme and enzyme mixed with substrate would only serve to convert the fresh enzyme to the state of the reaction products. If the driving syringes are separated from the observation chamber by a large stopcock, no difficulty is encountered in this mode of operation. In devices in which a higher fluid economy and a state of simplicity of constructon has been achieved by elimination of this stopcock, care must be taken to avoid any flow of substrate remaining in the mixing jets into the driving syringe.

II. APPLICATIONS

As mentioned above, apparatuses of this type have been designed for extending the sensitivity and time ranges of spectroscopic, volume magnetic

susceptibility, and electron spin resonance apparatuses. Since these flow devices are similar in principle and differ only in details of execution, redundant details of the designs will be omitted and only the general principles stressed. In each case the apparatus is designed so that constant flow may be maintained by weights applied to the driving plunger.

1. The Rapid Recording of Absorption Spectra in the Visible and Ultraviolet Regions

The spectrophotometric technique for accurately recording small differences in absorbancy between the time zero and after the material that has reacted with substrate for several milliseconds involves measurement of the absorbancy ratio in the two solutions. For this reason the flow apparatus is designed with a pre-mixing and a post-mixing observation chamber. The light from the spectrophotometer is flickered through these two chambers 30 times per second in order to permit satisfactory registration by the ratio-measuring circuits. The fluid pathways that permit this are indicated by Figure 3.2.

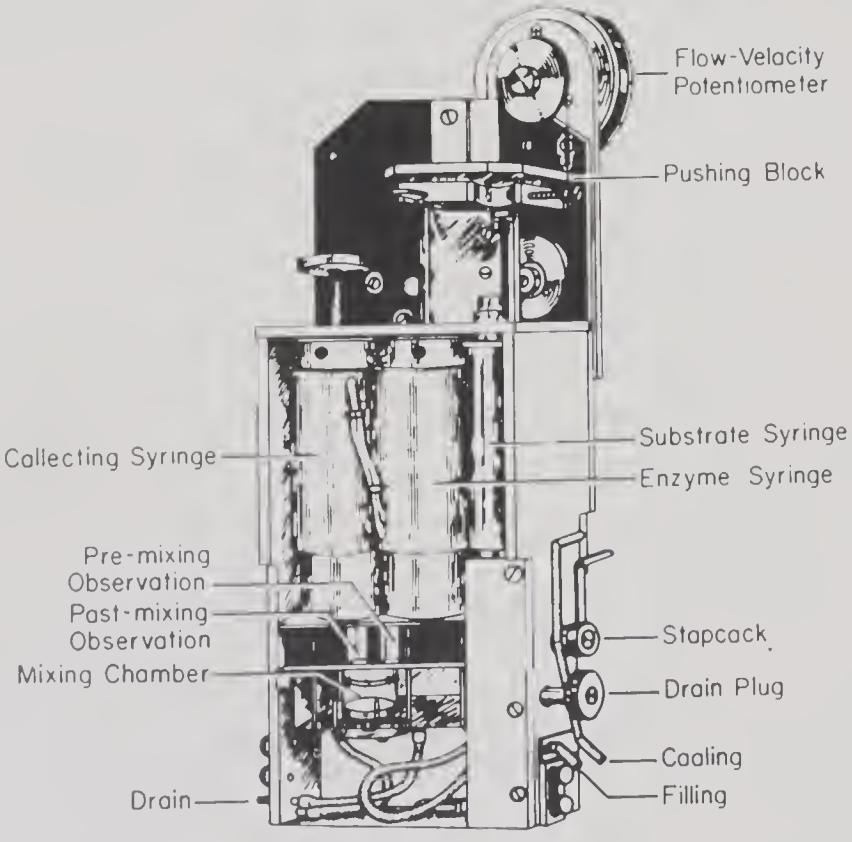

Fig. 3.2. A regenerative flow apparatus using the two-stage jet mixer of Figure 3.1. The apparatus records difference spectra between the pre- and post-mixing observation chambers. The time after mixing is 9 millisec. The ratio of the volumes of enzyme and substrate syringes is ~100:1 (FA-45).

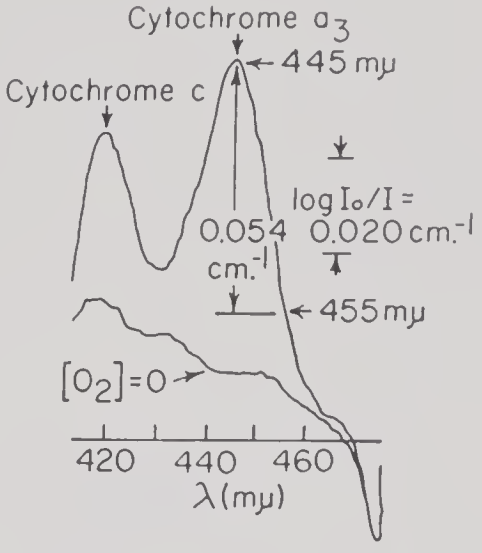

Fig. 3.3. Spectrophotometric record of the kinetics of oxidation of cytochrome of baker's yeast, obtained with the apparatus illustrated in Figure 3.2. Time after mixing, 9 millisec. at 25°C. (Expt. 471b) (2).

The enzyme and substrate are delivered in syringes having a volume ratio of approximately 100:1. The plungers for both syringes are driven by the pushing block as indicated by the diagram, the flow-velocity potentiometer being directly connected to the pushing block. In this particular apparatus, where good equilibration with the coolant was required, stainless steel syringe barrels were used and the plungers were packed with "0" rings. Material from the enzyme syringe first passed through the pre-mixing observation chamber and then downward to the bottom of the mixing chamber where mixing with the substrate occurs. The mixed reactants then flow through the post-mixing observation chamber and thence into the collecting syringe. The substrate syringe can be refilled with fresh reactant from the stopcock shown and the contents of the collecting syringe can be drained after a particular experiment or can be forced back into the enzyme syringe providing the substrate added is irreversibly exhausted by the enzyme activity.

This apparatus is particularly suitable for recording spectra of labile intermediates several milliseconds after mixing enzyme with substrate. The absorption bands of an intact yeast cell suspension that disappear 9 millisec. after adding oxygen to the previously anaerobic material are shown in Figure 3.3. As a control the contents of the enzyme syringe are discharged without the addition of substrate in order to give the base line labelled $[O_2] = 0$.

Significant advantages are obtained with this combination of components. First, the spectrum can be scanned in approximately 50 sec. Second, the time resolution is good (9 millisec.) and could be further im-

TECHNICAL RESEARCH LIBRARY

proved by using higher flow velocities. Third, a rather small absorbancy is measured (the noise level is less than 0.001 in optical density) in spite of the fact that a turbid cell suspension is used (considerably better optical accuracy would be obtained with clear solutions). Fourth, the recording is directly in terms of log I_0/I and thus large absorbancies are accurately measured and nonspecific absorbancy differences between the two chambers as well as variations of light source emissivity, photocell sensitivity, etc., are compensated for. Fifth, the wavelength scale is linear due to the use of a grating monochromator. The apparent inflexibility of a design with a fixed post-mixing observation chamber has not so far been a serious difficulty with this apparatus, since a reasonable variation of the flow velocity is possible with proper design of the mixing chamber and the experimental concentrations can be changed to vary the extent of the reaction at a particular time after mixing.

2. Application to the Rankine Balance

A similar application of flow apparatuses to the Rankine balance has been made by Dr. A. S. Brill of this laboratory (4,5). Here the problem is not one of scanning through a variety of experimental parameters, for example in the case of the wavelength scan mentioned above, but of obtaining a single measurement corresponding to a time after mixing of 40 to 100 millisec. with an apparatus of a response time of several seconds. One use of this apparatus is the detection of the volume magnetic susceptibility of primary enzyme substrate intermediates prior to their conversion to the secondary compound. Another use is in the detection of free radical oxidation products of enzyme reactions.

A schematic diagram of the arrangement of the components is given in Figure 3.4. The enzyme and substrate solutions flow successively through the pre-mixing, mixing, and the post-mixing portions of the reaction chamber. Thus the magnet moves in a differential field due to the difference in volume magnetic susceptibility between the pre-mixing and post-mixing solutions. This feature is essential since the volume magnetic susceptibility of the solvent is large compared to the quantities measured. In fact, the temperature coefficient of the latter requires accurate temperature equilibration of the materials so that pre- and post-mixing temperatures will be nearly identical. The quartz fiber suspension records the movement of the magnet toward the paramagnetic solution and a mirror system picks off this movement and feeds back a portion of the signal to restore the magnet to its original position. Changes in feedback current are recorded. A detailed study of the performance of this apparatus has been made (4,5) and errors in Δk as small as 5.7×10^{-12} are obtainable.

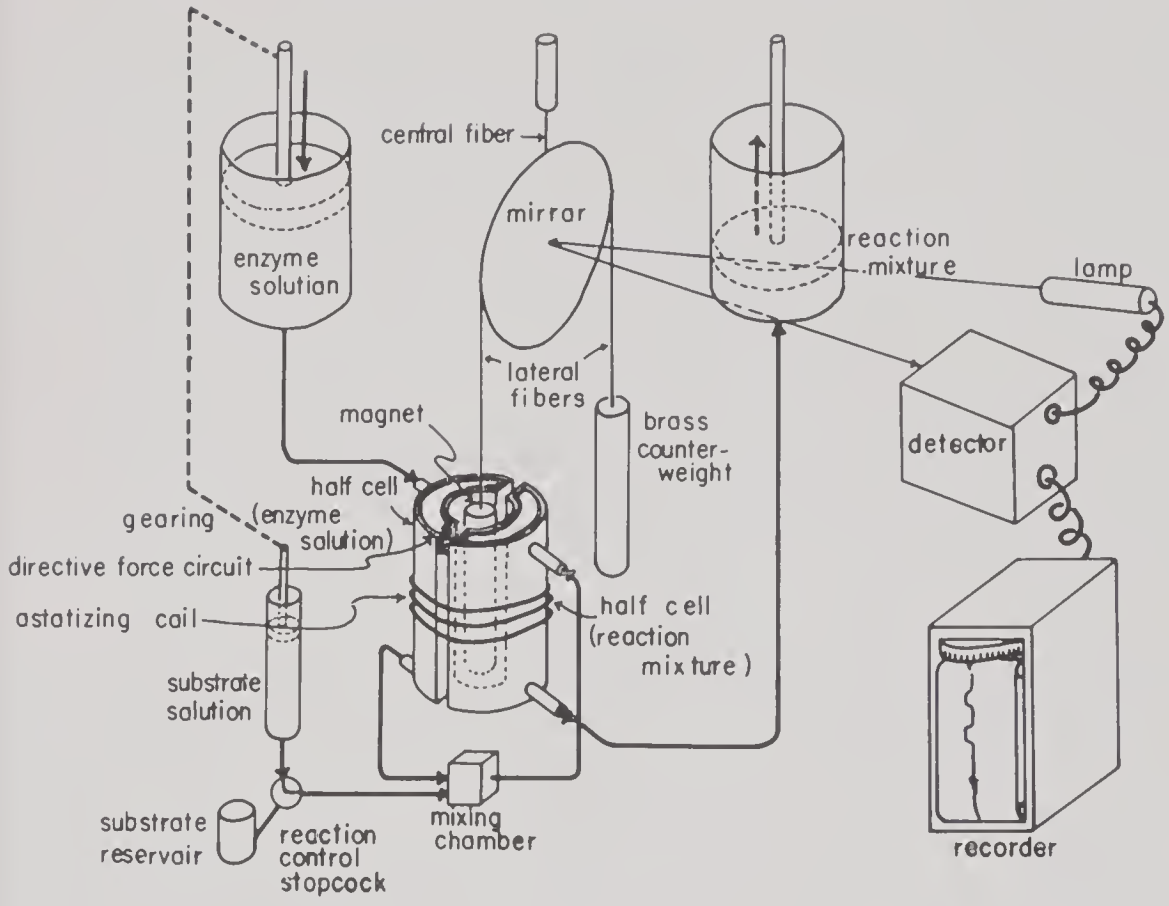

Fig. 3.4. A schematic diagram (after A. Brill) of the application of a regenerative flow apparatus to the Rankine balance (courtesy of T. Yonetani) (3).

The apparatus is readily used with biological materials which have sensitivities of 1×10^{-11} c.g.s. emu.

3. Application to Electron Spin Resonance

Apparatuses for measuring electron spin resonance are often used with time constants of several seconds for which corresponding rise times are in the range of 5 to 150 sec. We have designed a flow apparatus for increasing the time range of the spin resonance apparatus under these conditions so that times after mixing between 3 and 30 millisec. are measurable even though the response time of the recorder corresponds to 5 and 50 seconds, respectively. In electron spin resonance, certain restrictions are placed on the dimensions of the observation tube in order to avoid detuning and loss of heat of the cavity, i.e., the dimensions can be increased in the plane of a small electric field (nodal plane) but not appreciably in a direction perpendicular to this. Therefore rectangular observation chambers 8.5 mm. in length and 0.5 mm. in width are required. If a mixing chamber of the type usually employed with circular tubes is used, then inevitable dead

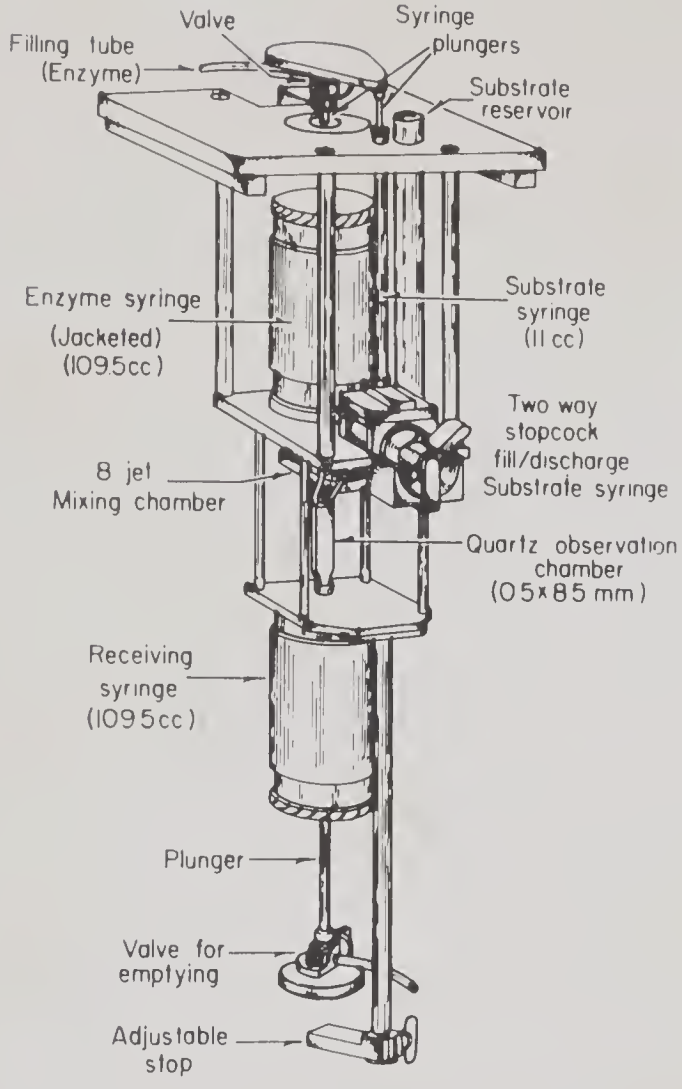

Fig. 3.5. A regenerative flow apparatus applicable to electron spin resonance measurements (FA-48) (3).

space intervenes between the mixing chamber and the observation tube. While this has not yet been a serious limitation in the application of the flow apparatus, an improved design would take advantage of mixing techniques developed for entering rectangular tubes (6) in order to reduce this dead space to a minimum. An apparatus designed with a mixing chamber appropriate to a circular observation tube is illustrated by Figure 3.5. The components of this apparatus are similar to those of Figure 3.2, and the 100:1 volume ratio of the enzyme and substrate syringes is maintained. This apparatus has the additional feature that the enzyme and receiving syringes may be filled separately through hollow plungers with appropriate valves so that it may be used not only in cases in which substrate is irreversibly expended by the enzyme action but also in cases in which the reaction is reversible or in which the reaction products interfere. When used in the latter fashion, the receiving syringe is emptied through

its valve and the enzyme syringe is filled with fresh solution, the contents of the receiving syringe never being returned into the enzyme syringe, as would be the case with regenerative flow operation. The receiving syringe can be detached from the bottom of the observation chamber in order to pass the quartz observation tube through the cavity of the spin resonance apparatus (Varian 100 kc modulation model). The receiving syringe is then reassembled and operation of the flow apparatus is carried out in the usual manner. Varian Associates manufacture a modification of Berger's apparatus for electron spin resonance (7).

Experiments show that mechanical disturbances due to discharge of the plunger do not affect the signal-to-noise ratio of the apparatus.

III. SUMMARY

These specific applications of the regenerative flow apparatus illustrate its adaptability to the requirements of the specific physical technique employed. It is worthwhile to reiterate those features which have been of particular use in the studies described.

(*1*) The application of the regenerative feature to those reactions in which substrate is irreversibly expended and in which the reaction products do not interfere—for example, those involving oxygen or hydrogen peroxide—results in an extremely high fluid economy with very limited amounts of rapidly reacting components.

(*2*) Its applicability to the study of intracellular reaction kinetics which requires deliveries of enzyme and substrate in volume ratios on the order of 100:1 in order to avoid unreasonable accuracy in relative deliveries.

(*3*) The extension of the time range of slowly responding physical techniques such as wavelength recording spectrophotometry, volume magnetic susceptibility, and electron spin resonance.

References

1. B. Chance, *Discussions Faraday Soc.*, **17**, 123 (1954).
2. B. Chance, *Discussions Faraday Soc.*, **20**, 205 (1955).
3. B. Chance, L. Bicking, and V. Legallais, *Free Radicals Biol. Systems, Proc. Symp. Stanford, Calif, 1960*, 101.
4. A. S. Brill, H. den Hartog, and V. Legallais, *Rev. Sci. Instr.*, **29**, 383 (1958).
5. A. S. Brill, A. Ehrenberg, and H. den Hartog, *Biochim. Biophys. Acta*, **40**, 313 (1960).
6. B. Chance and V. Legallais, *Rev. Sci. Instr.*, **22**, 627 (1951).
7. L. H. Piette, T. Yamazaki, and H. S. Mason, *Free Radicals Biol. Systems, Proc. Symp., Stanford Calif,, 1960*, 196.

Part 4. *THE THERMAL MEASUREMENT OF RAPID REACTIONS IN SOLUTION*

I. INTRODUCTION

In most chemical reactions in solution there is an evolution or absorption of an appreciable amount of heat. The corresponding temperature changes can accordingly be used to follow quantitatively the progress of many chemical processes, provided that the total heats of the latter are known. To adapt this principle to the general rapid reaction method of Hartridge and Roughton (1), it is necessary to insert thermocouples, thermistors, or other accurate temperature-measuring devices into the observation tube, and thence to determine the temperature of the streaming fluid at various distances from the mixing chamber. The technique is not specially difficult, and it is perhaps rather surprising that its application, during the past 30 years, has been limited to some ten rapid reactions and to about the same number of scientific papers, the majority of which have come from Roughton's laboratories.

In addition to the heat effects due to the chemical reactions there are, in rapidly mixed and streaming fluids, a number of physical factors which also give rise to temperature changes, namely: (*1*) fluid friction; (*2*) thermoelastic effects, due to variations in the hydrostatic pressure in different parts of the apparatus; (*3*) heat conduction; and (*4*) local disturbances in the neighborhood of the thermojunction or other thermal measuring instrument. Roughton (2) made a detailed investigation of these physical factors, by means of both control experiments and of theoretical calculations, and found that, although these factors might—at currently used rates of flow down the observation tube—give rise to collective temperature effects of the order of 0.01°C., they could in practice be cancelled out (to the extent of at least 90%), by means of the simple experimental procedure described later. The residual blank effects do not then exceed 0.0007°C. and can thus be neglected in rapid reactions, in which the total temperature change is greater than 0.1°C.; they must, however, be taken into account whenever the total temperature change lies within the range 0.05 to 0.003°C., the latter figure representing the limit to which the rapid thermal method has so far been pressed. Most of the experimental investigation of the blank effects was carried out over 25 years ago (3) with a slowly responding, cumbersome but very sensitive and accurate apparatus. More recently, however, the technique, and especially the thermoelectric recording, have been modernized: the later apparatus has given very satisfactory results, but has so far been mainly applied to processes with total

temperature changes in the range 0.05 to 0.5°C. Part 4 of Chapter XIV is accordingly divided into the following further sections:

II. A detailed description of the method now in current use.
III. A résumé of the earlier methods, with special reference to processes with temperature changes of less than 0.05°C.
IV. A summary of the rapid reactions studied by the thermal method.
V. Discussion of scope and development of the method.

The application of the rapid thermal method to the kinetics of chemical reactions requires, as has already been mentioned, a knowledge of the heat of the reaction under study. Though this quantity is often obtainable by classical calorimetric technique, there are cases (see later discussions) in which such an approach is not possible and the desired heat can only be gotten by a special application of the rapid thermal method itself. The determination of the heats of reactions, which are not accessible by the usual methods, is thus an occasional, but valuable, by-product of the rapid thermal technique. An example of such an application is given later (see Fig. 4.6).

II. PRESENT METHOD FOR MEASUREMENT OF RAPID REACTIONS WITH TOTAL TEMPERATURE CHANGES OF 0.05 TO 0.5°C.

1. General Set-Up of Apparatus (Exclusive of Temperature-Measuring System)

The main elements of the apparatus used in Roughton's laboratory during the last 10 years are shown in Figure 4.1. The reagent containers L and R, the leads, the mixing chamber M, and the observation tube O are all mounted as a single assembly in a metal frame, which is immersible in a well-stirred 40 gallon water thermostat. The temperature of the latter is regulated to ±0.0015°C. by a mercury–toluene regulator. L and R are 500 cc. glass bottles with top and bottom outlets, each closed with rubber bungs. One of the two leads through each top bung connects with the source of compressed gas which is used to drive the reagents, whereas the other lead, which goes to the bottle, is used for filling and for occasional stirring of the contents by hand. The glass leads (internal diameter, 5 mm.) through each bottom outlet connect with the mixing chamber via glass taps, T and T′, the cocks of which are controlled from above by brass rods as shown. The mixing chamber, M, is made in a Lucite block, and consists of four tangential jets, each of 1 mm. diameter and length about 1.5 mm. The observation tube, O, is of glass and has an internal

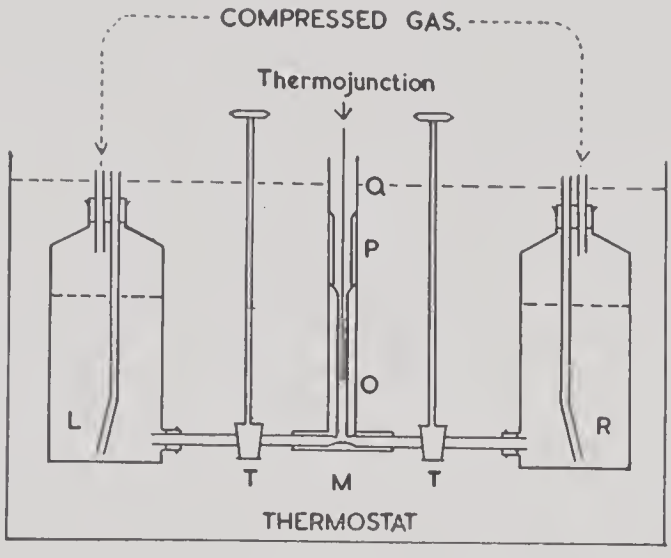

Fig. 4.1. General arrangement (exclusive of electrical connections) of apparatus for thermal measurement of velocity of rapid reactions; description of various parts in text. Glass mantle enclosing P and Q is not shown.

diameter of about 2 mm. and an external diameter of 7 mm.; its length is 10 cm., but this is easily convertible according to requirements. It is fixed to the mixing chamber by an arrangement of metal plates and screwed rods similar to that used by Hartridge and Roughton (1). The upper end of O is cemented to a wider glass tube, P (internal diameter, 5 mm.; external diameter, 20 mm.; length, 4 cm., and the upper end of P is in turn cemented to a still wider tube Q (internal diameter, 10 mm.; external diameter, about 20 mm.; length, 4 cm.). P and Q are enclosed by a glass mantle, of diameter about 7 cm. which is not shown in the figure. (More recently the observation tube, O, has also been surrounded by an air-jacket, so as to reduce heat conduction between the streaming fluid and its surroundings.) The purpose of the wider tubes P and Q is to provide sufficient volume to enable the total heat of the reaction in the streaming fluid to be determined, in cases in which the reaction takes 0.1 to 0.5 sec. to reach practical completion.

2. Measurement of Temperature

Both in our present and our previous techniques, the temperatures have been measured with thermocouples and sensitive direct current galvanometers, with or without photoamplification of the latter. Recently Giladi, Lifshitz, and Perlmutter-Hayman (4) have described the application of thermistors in a 1.6 mm. bore observation tube. The temperature sensitivity was about ± 0.001°C., but the quoted accuracy is appreciably lower than that in the thermocouple apparatus now being considered.

A. CONSTRUCTION OF THERMOCOUPLE

The thermocouple consists of a single pair of junctions, one of which, θ, is placed in the streaming fluid while the other—the reference junction, θ_s—is placed in a glass tube containing a few cc. of mercury, and immersed in the thermostat so as to maintain it at a standard known temperature. The junction for the observation tube is made of 30-gage (B.S.I.) copper wire and 30-gage constantin wire, and is insulated with Bakelite varnish—its effective diameter is about 0.5 mm., and the length of the junction is not more than 0.5 mm. It is attached to a rack and pinion, by means of which it can be readily adjusted to any desired position in the observation tube. The reference junction is made of 20-gage copper and constantin wires. The total resistance of the thermocouple system is about 4 ohms, and the sensitivity at 20°C. is about 40 μv./°C. This figure, which of course varies somewhat with the mean temperature, is determined by calibration with known differences of temperature as estimated with a standard thermometer. (Mr. A. C. Downing has kindly constructed for the writer a thermocouple with five pairs of junctions, and of diameter no greater than that of the single-pair thermocouple just described.)

B. GALVANOMETER RECORDING SYSTEM

Downing (5) and A. V. Hill (6) have, in the past 15 years, developed very quick and sensitive galvanometer systems primarily for following thermoelectrically the rapid heat effects in muscle and nerve during physiological activity. Their methods have proved very suitable for the present purpose.

The thermocouple is connected to a Downing galvanometer which has the following characteristics: period, 0.011 sec. (without feedback—with feedback the period can be reduced to about 0.003 sec.); resistance, 10 ohms; critical damping resistance, about 30 ohms; sensitivity at one meter, 10 mm./μamp. By optical and electronic amplification, using twin photocells, an output of 9 v./°C. is obtained. It was originally intended to apply this output to a cathode ray oscillograph, but for the reactions studied up till now it has proved more convenient to apply the output to a pointer microammeter with 12,000 ohms in series, the microammeter thus functioning as a voltmeter. A temperature change of 0.1°C. gives 75 to 80 divisions deflection, the latter being readily readable to one-half of a division ($\sim$0.0007°C.). The time for each reading is not more than 4 sec. Further details of the amplifying and electrical arrangements follow.

Photocell Amplifier (Fig. 4.2). The reflected beam of light from the galvanometer falls on the twin photocells (C.M.V. 28). The resultant photocell output is amplified by a balanced d.c. amplifier and the amplifier

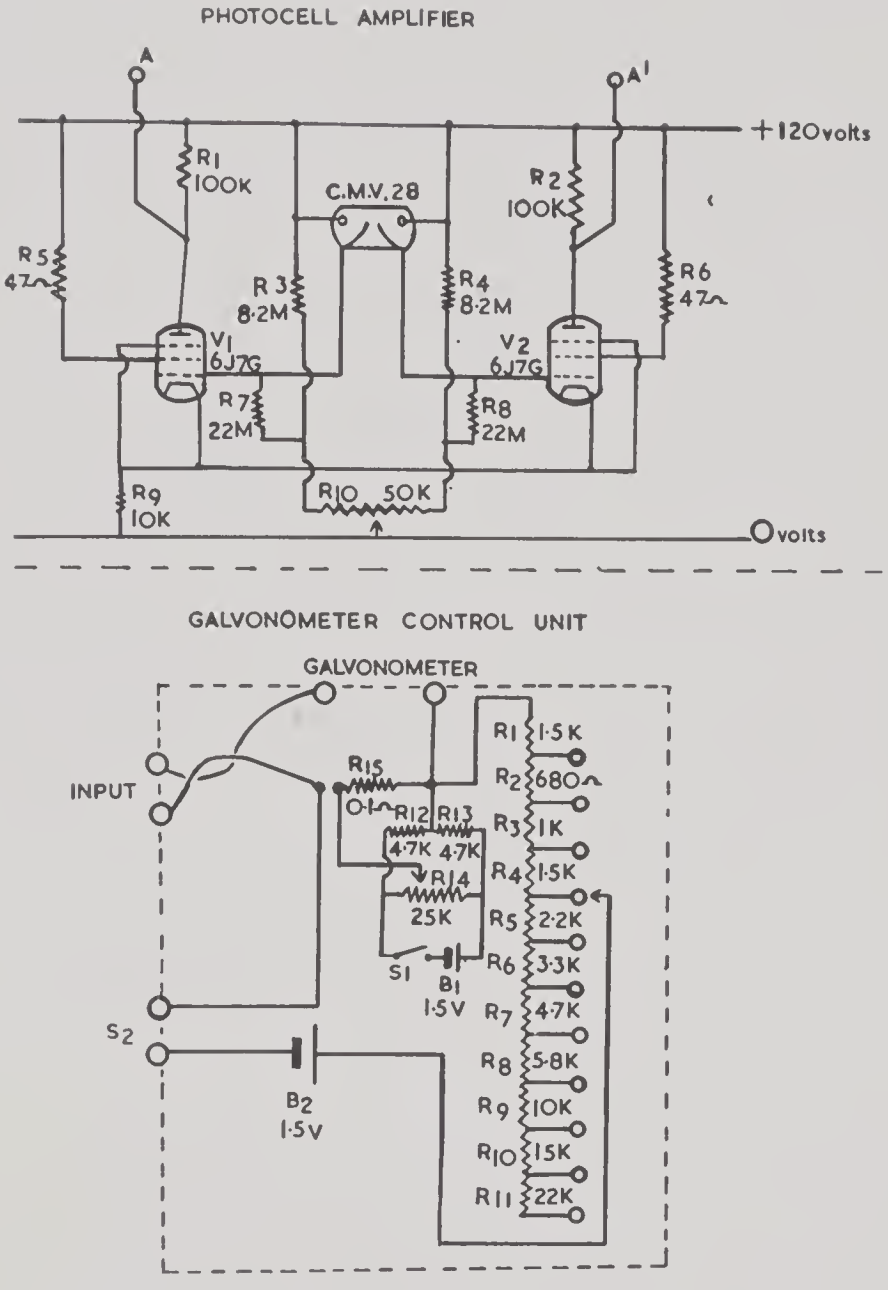

Fig. 4.2. Circuits of photocell amplifier of Downing galvanometer. Circuits for control and calibration of Downing galvanometer.

output AA′ recorded on an oscilloscope or on a microammeter used as a voltmeter. The amplifier balance can be adjusted by R_{10} (wire wound). High stability resistances are used in the circuit. The period of the galvanometer may be decreased if necessary by applying negative feedback from the amplifier to the galvanometer.

Galvanometer Control Unit (Fig. 4.2). The galvanometer control unit is used to adjust the base position of the galvanometer and to supply standard signals for calibration. The thermocouple is connected to the all-copper input terminals. By closing S_1 and adjusting R_{14} the galvanom-

eter can be set at any required base reading. By closing S_2 and plugging into any required resistance between R_I and R_{II} a standard current for calibration can be passed through the galvanometer. Wire-wound, 1% tolerance resistances are used.

The Downing Galvanometer, in this set up, was one of a limited stock made individually to private order, but has worked so well over the years that the above details of its operation have seemed fully worthy of inclusion. Electronic instruments for the amplification and rapid registration of the small microvoltages met with in refined thermoelectric work (and not involving the use of rapid and sensitive primary galvanometers), are commercially available and have been successfully tried out to a limited extent. Thus with an apparatus otherwise similar to the above, but employing a British "Sunvic" Amplifier, D. C. Type DCA1 Mk II and a Weston millivoltmeter (full scale deflection, 73.5 μamp.; resistance, 129.8 ohms shunted with 449 ohms; time of response, about half a second) a sensitivity of 2×10^{-4}°C. was obtained with a double-junction copper-Constantan thermocouple connected to the input of the "Sunvic" Amplifier (Research Laboratory of I.C.I. Alkali Division, Winnington, Cheshire, England). The mean value, at 25°C., of the velocity constant of the reaction $CO_2 + NH_3 \rightarrow NH_2COOH$ (see later discussions) as measured with this "Sunvic" apparatus, agreed to within 5% with the value for the same reaction when measured with the Downing Galvanometer apparatus.

3. Procedure in an Actual Experiment

The metal frame, with the attached apparatus, is lifted out of the thermostat and the two bottles L and R are charged with 400 cc. of their respective reagents. The assembly is then returned to the thermostat and left therein until temperature equilibrium is attained. This takes about 1 hour at 20°C., and up to 2 hours at 0 or 40°C. Just before the experiment proper is started, samples are drawn from L and R and their composition determined by chemical analysis. The sensitivity of the recording system is also checked by sending several known currents through the galvanometer. Compressed N_2 (or other indifferent gas) is next applied to L and R, usually at a constant pressure of 25 cm. mercury. The thermojunction is then placed at a suitable position in the observation tube, as measured by a scale on the rack and pinion device, and readings are taken with fluid L running alone (i.e., tap T open, T′ closed), then with fluids L and R running (tap T and T′ both open) together, and finally with fluid R running alone (tap T closed, tap T′ open)—each reading taking about 4 sec. The running fluid overflows into a glass mantle, from which it is continuously removed by suction.

If L', B', R' are the corresponding readings, and x is the relative delivery of fluid R to fluid L when both fluids are running, then the temperature change due to the chemical reaction plus heats of dilution (other physical effects being neglected):

$$= B' - (xR' + L')/(x + 1)$$

The procedure is then repeated at other positions in the observation tube, up to 12 in all. The fraction $(xR' + L')/(x + 1)$ is nearly zero and usually drifts so slightly during the time of the experiment (*ca.* 10 minutes) that it is only necessary to check it at 3 or 4 out of the 12 places of observation. A repetition of the measurement of the temperature difference at a given place usually gives a figure concordant to within ± 0.001°C. At the end of the experiment the sensitivity of the recording system is rechecked with the same known currents as at the start.

To determine the rate of flow and relative delivery, the two bottles L and R are marked with volume calibrations. If L'' and R'' are the respective volumes delivered from L and R in t sec., then the rate of volume flow is

$$= (L'' + T'')/t \text{ in cc./sec.}$$

and the relative delivery of R to L, i.e., x, $= R''/L''$. With the solutions for which the apparatus has so far been used, the rates of volume flow (at 25 cm. Hg driving pressure) have ranged from 6.5 to 8.5 cc./sec. according to (*1*) the viscosity and temperature of the solutions and (*2*) the position of the thermojunction in the observation tube; the corresponding linear rates are 230 to 290 cm./sec. The relative deliveries have usually been very nearly equal, though with concentrated salt in one bottle the delivery may be depressed by about 20%. The procedure may be illustrated by the following example which is taken from an experiment on the rate of combination of CO_2 with OH ions at 20°C.:

Reagents used:

$$\text{L} = 0.0165M\ CO_2 \qquad \text{R} = 0.095M\ \text{NaOH}$$

Readings obtained with thermojunction at 1 cm. from mixing chamber:

$$L' = 2 \text{ div. (division)} \qquad B' = 79 \text{ div.} \qquad R = 5 \text{ div.}$$

$$1 \text{ div.} = 0.00153\text{°C.}$$

$$x = 1.03$$

Temperature change:

$$= 79 - (1.03 \times 5 + 2)/(1 + 1.03) = 75.5 \text{ div.} = 0.105\text{°C.}$$

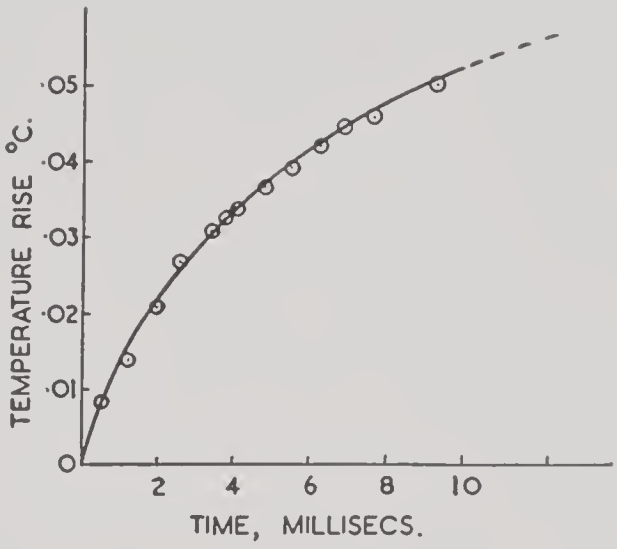

Fig. 4.3. Thermal measurement of rate of combination of 0.00735M CO_2 with 0.0404M NaOH at 20°C. Total temperature rise when reaction is completed = 0.0758°C.

Distance of point of observation from mixing chamber = 1 cm.

Rate of flow = 275 cm./sec.

Time of reaction = 0.0036 sec.

In the example just quoted the heat of dilution was neglected. In cases in which it is appreciable the value is determined in the apparatus by mixing the reagent with CO_2-free water.

Figure 4.3 shows the complete results obtained in an experiment on the rate of combination of 0.00735M CO_2 with 0.040M NaOH at 20°C. The total temperature rise when the reaction is completed is 0.0758°C., so that the time for the half-reaction in this example is about 6 millisec.

4. Accuracy and Use of the Method

As already mentioned, the temperature measurements are generally repeatable to ±0.001°C. That the total heat of rapid reactions is measurable to this precision is shown by two pieces of evidence:

(*1*) In blank experiments in which bottles L and R contained plain water, no temperature effects could be detected (i.e., $B' - (xR' + L')/(x + 1)$ was not greater than ±0.0008°C.). This proves that the heat effects due to fluid friction, thermoelastic effects, and local disturbances in the neighborhood of the thermojunction have been effectively cancelled out by the procedure adopted, but it does not exclude possible errors due to heat conduction between the streaming fluid in the observation tube and the thermostat water. That such effects are negligible is, however, shown by the following.

(*2*) Comparison of the heat of neutralization of HCl and NaOH, as determined in the rapid reaction velocity apparatus, with the standard value, as measured by classical calorimetry. If heat conduction from the fluid in the observation tube to its surroundings is appreciable the temperature rise in the observation tube will be too small, and the heat of neutralization, by the rapid reaction method, will be lower than the accepted value. Actual tests, however, failed to reveal significant discrepancies. Thus when 0.0239*M* HCl was mixed with 0.06*M* NaOH a total temperature rise of 0.165°C. was observed, the corresponding heat of neutralization being 13,800 cal. This compares very favorably with the accepted value at 20°C. of 13,700 cal., on the basis of which the total temperature rise should have been 0.1635°C.

Although the accuracy of the method, as regards the measurement of the total heat of "instantaneous" reactions is thus established, there still remain further possibilities of error in the use of the method for studying the kinetics of rapid reactions of measurable speed. Discussion of such errors will be reserved until Section III.2.B.

The chief applications of the method have been to the measurement, over the range 0 to 40°C., of the velocity constants of two rapid carbon dioxide processes (7,8), viz.:

$$\left.\begin{aligned} CO_2 + OH^- &\rightarrow HCO_3^- \\ \text{followed by the proton exchange reaction} & \\ HCO_3^- + OH_3^- &\rightarrow CO_3^{2-} + H_2O \end{aligned}\right\} \quad (1)$$

and

$$\left.\begin{aligned} CO_2 + NH_3 &\rightarrow NH_2COOH \\ \text{followed by the proton exchange reaction} & \\ NH_2COOH + NH_3 &\rightarrow NH_2COO^- + NH_3 \end{aligned}\right\} \quad (2)$$

In both processes, the proton exchange reaction is so much faster than the first reaction that the overall rate of disappearance of CO_2 is conditioned by the first reaction and is therefore kinetically bimolecular. The thermal effect of disappearance of each CO_2 molecule, however, corresponds to the *sum* of the heats of the two reactions, which is conveniently large, i.e., of the order of 20,000 cal. for reaction (1) and 12,000 cal. for process (2). Concentrations of CO_2 down to 0.002*M* have therefore been feasible. The results have been very consistent, and, as already mentioned in Part 1 of this chapter (page 726) show good numerical agreement, in the case of the reaction $CO_2 + OH^- \rightarrow HCO_3$, with the values for the velocity constant as obtained by four other, quite independent, methods. In the case of the reaction $CO_2 + NH_3 \rightarrow NH_2COOH$, the values of the velocity constant by

the rapid thermal method tally satisfactorily with the values previously obtained by Faurholt (9), using a classical method.

The highest bimolecular velocity constant so far measured with the above technique has been 24,000 M^{-1} sec.$^{-1}$ for reaction (1) at 40°C., corresponding to a half-time of about 2 millisec. By increasing the pressure drive it might be possible to shorten the measurable half-time down to about 1 millisec., but this is probably the limit obtainable with this apparatus. Bimolecular reactions with still higher velocity constants would only be measurable if they had very large heats of reaction, so that the concentrations of the reagents could be reduced. The lowest velocity constant measured has been 80 M^{-1} sec.$^{-1}$ for reaction (2) at 0°C. Bimolecular reactions with lower velocity constants than 30 M^{-1} sec.$^{-1}$ can also be followed if they have higher heats of reaction, so that an appreciable temperature rise is developed in the elapsed time measurable in the observation tube. In most experiments values for the velocity constant have been reproducible to ±7%.

III. EARLIER WORK ON RAPID REACTIONS WITH TEMPERATURE CHANGES OF LESS THAN 0.05°C.

1. Points of Difference in Earlier Procedure

In the earlier work (3), the arrangements in regard to (*a*) the reagent containers, (*b*) the driving of the fluids to the mixing chamber, (*c*) the adjustment of the thermojunctions in the observation tube, and (*d*) the thermostatting of the whole assembly, were in general similar to those just described in the present set-up, but there were several important differences:

(*1*) The leads from the containers to the mixing chamber, and the observation tube were all air-jacketed instead of being immersed directly in the water thermostat.

(*2*) The galvanometer (type Zb, Kipp & Zonen, Delft, Holland) was not amplified, its deflection on a scale at 2 to 4 m. distance being, instead, read by eye. At maximum sensitivity 1 mm. deflection at 4 m. corresponded to 0.0083 μv., or to a temperature difference of 0.0002°C., when measured with a low-resistance copper–constantan thermocouple, consisting of only a single pair of junctions. In favorable circumstances the deflection could be read to 0.1 to 0.2 mm., corresponding to temperature differences of 0.00002 to 0.00004°C. The time of indication of the galvanometer was, however, much slower and in consequence each reading took 20 sec. instead of 4 sec. This gave opportunity for large temperature

drifts of the solutions during the run, but these were satisfactorily allowed for by taking 5 readings at each point of the observation tube, i.e., L alone, L + R together, R alone, L + R together, L alone—or alternatively the sequence R, L + R, L + R, R. In this way the mean of the L readings alone and the mean of the R readings alone, corresponded in time with the mean of the L + R readings together.

(*3*) This more drawn-out procedure led to a much greater consumption of fluids in each experiment. It was, in fact, necessary to provide 4 to 5 liters, instead of 400 cc., of each reagent. The initial time of temperature equilibration was about twice as great with 5 liter as with 500 cc. bottles, with the result that only one experiment, or at most two, could be carried out in a single day.

(*4*) In spite, however, of the method being more cumbersome, it was nevertheless possible to obtain good results on reactions with temperature changes of only 0.003 to 0.05°C., especially if the temperature gradient in the observation tube was measured, as well as the actual temperature of the streaming fluid at various points. This was easily done by a simple modification of the previously described thermocouple. A third length of 32-gage copper wire was soldered to a point, θ', 3 cm. distant from θ, the junction normally introduced into the observation tube. θ, θ', and θ_s (the reference junction) were connected to the terminals of a six-point, double-throw, all-copper switch so that either the $\theta - \theta_s$ combination (referred to as the *absolute thermocouple*) or the $\theta - \theta'$ combination (referred to as *differential thermocouple*) could be connected to the galvanometer. In this way the difference of temperature between two points in the running fluid, or the actual temperature at a single point could be determined merely by adjusting $\theta - \theta'$ to the appropriate position in the observation tube.

2. Residual Blank Effects Due to Physical Factors

With the 10-fold greater sensitivity in the temperature measurements it is no longer necessarily permissible to neglect the temperature changes due to fluid friction, thermoelasticity, heat conduction, and local effects in the neighborhood of the thermojunction. These factors could affect the temperature readings on the running fluid, both at point in the observation tube at which the reaction is complete, and at points at which it is still in progress and where there is therefore a temperature gradient along the tube. The effects of the first two factors were readily ascertained by further blank experiments with plain water in each bottle and by additional neutralization experiments, and will accordingly be considered first.

A. EFFECTS OF FLUID FRICTION, THERMOELASTICITY, AND THERMAL CONDUCTION BETWEEN THE FLUID IN THE OBSERVATION TUBE AND ITS SURROUNDINGS

Table 4.I shows the result of blank determinations with water in both bottles, and with the tip of the thermocouple, θ, at 2, 5, and 8 cm. distance from the mixing chamber. The driving pressure was 20 cm. Hg and the relative deliveries of water from the two bottles were equal. The length of the observation tube was 12 cm. and its bore 0.2 cm., and was thus similar in dimensions to the tube used in Section II.1. The temperature differences were as before given by the difference between the reading when L and R were both delivering and the mean of the readings when L and R were delivering separately, the mean being weighted according to the relative deliveries of the two bottles. With the differential thermocouple, the galvanometer deflection settled down more quickly and remained more stable than with the absolute thermocouple: the blank temperature differences did not at most exceed 0.00037°C. and were repeatable to within the limits of visual reading of the galvanometer deflection (i.e., to within 0.00003°C.). With the absolute thermocouple the blank effects were around twice as large and individual readings showed a small, though appreciable scatter. Approximate theoretical calculations suggest that the blank effects must have been in the main due to fluid friction.

TABLE 4.I

Tests for Blank Corrections with L = R = Water

Absolute Thermocouple			
Distance of $\theta - \theta'$, from mixing chamber, cm.	2	5	8
Temp. diff., mm. galv. deflection	+2.3	+2.1 (±0.3)	2.0 (±0.5)

1 mm. deflection = 0.00032°C.

The + sign means that the reading with both fluids running is warmer than the mean of readings L and R.

Differential Thermocouple			
Distance of $\theta - \theta'$, from mixing chamber, cm.	2–5	5–8	8–11
Temp. diff., mm. galv. deflection	+0.8 (±0.1)	+1.4 (±0.1)	+1.5 (±0.1)

1 mm. deflection = 0.00025°C.

The + sign means that the junction distal to the mixing chamber is warmer.

Confirmation of the validity of the blank corrections of Table 4.I was obtained by comparisons of the expected and observed temperature rises,

when very dilute solutions of HCl were mixed with NaOH solutions of higher titer. Two such tests gave:

Observed rise = 0.0340 ± 0.0004°C., expected rise =

0.0343 ± 0.0004°C. (3)

Observed rise = 0.0009 ± 0.0002°C., expected rise =

0.0008 ± 0.0002°C. (4)

The uncertainties in the "expected" rises were due to the difficulty of measuring accurately the titer of such dilute HCl solutions. If the residual blank corrections of Table 4.I had not been subtracted there would have been discrepancies of up to 0.001°C.

Beyond the point in the observation tube at which mixture was complete, no change in the temperature of the running fluid could be detected. This confirms again (as in Section II.4 (*2*)) that there were no appreciable errors due to heat conduction from the fluid in the observation tube to the surroundings. Indeed, any errors due to the latter factor would be expected to be *proportionally* the same with reactions involving large temperature changes as with reactions involving only small temperature changes.

B. EFFECT OF LONGITUDINAL THERMAL CONDUCTION IN THE OBSERVATION TUBE AND OF LOCAL STIRRING CONDITIONS IN THE NEIGHBORHOOD OF THE THERMOJUNCTIONS

These factors have specially to be considered when there are temperature gradients in the streaming due to chemical reactions therein as it travels along the observation tube.

Longitudinal Thermal Conduction in the Observation Tube. There are two effects to be considered: (*1*) thermal conduction down the streaming fluid due to the longitudinal temperature gradient therein and (*2*) thermal conduction down the electrical wires leading to the thermojunction. In the case of exothermic reactions these two factors would cause the steady state temperature of the thermojunction to be higher than the actual temperature of the streaming fluid in its immediate neighborhood—vice versa with endothermic reactions.

Local Stirring Conditions Near the Thermojunctions. It is generally held that whenever a stationary object (such as a thermojunction) is placed in a moving fluid, films of relatively stagnant fluid form in the immediate neighborhood of the object, the thickness of such films decreasing as the rate of fluid movement is increased. In such films the chemical reaction would have proceeded further than in the average fluid streaming through

the cross section of the observation tube at which the thermojunction is located. This factor would also, in the case of an exothermic reaction, tend to cause the temperature reading of the junction to be too high.

In his first full paper on the rapid thermal method, Roughton (2) devised and carried out specific individual controls on each of these two factors. His "stagnant film" controls were uniformly negative, but his conduction controls suggested that the observed temperature difference between two points in the observation tube might be about 3% too low, on account of heat conduction. Details of these tests will not be repeated here since the joint effect of these two sources of error can be more readily and definitely assessed from measurements on the same rapid reaction at two different

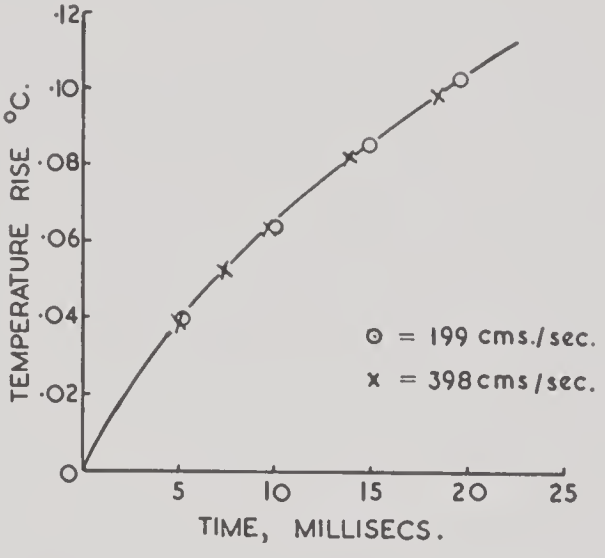

Fig. 4.4. Thermal measurement of rate of reaction of 0.0362M CO_2 with 0.197M NH_3 in 0.0992M NH_4Cl at 20°C. at two different rates of flow. This control eliminates errors due both to heat conduction and to stagnant films.

rates of flow. At a faster rate of flow, the reaction would be spread over a greater length of observation tube and the longitudinal temperature gradient per centimeter length of tube would be less; consequently any error due to heat conduction along the leads to the junction would be reduced. Since the thickness of the "stagnant film" is diminished as the velocity of fluid flow is increased, any error due to this factor would also be reduced at the faster rate of flow. If then it be found that variation of flow rate has no appreciable influence on the observed velocity of reaction, then it may be concluded that these two effects are both singly, and jointly, of no significance.

An example of such a test is shown in Figure 4.4, which gives the results of thermal measurements on the rate of reaction of 0.0362M CO_2 with a solution containing 0.197M NH_3 and 0.0992M NH_4Cl at 20°C. at two

different rates of flow. The effect of a 2-fold variation in linear rate of flow is seen to be within the limits of error of the temperature measurements. The effect of stagnant films and heat conduction down the leads are thus negligible in the case of this particular reaction, when measured in the modern apparatus which is sensitive to ±0.001°C. Further evidence in the same direction is provided by the agreement, already mentioned, between the value of the velocity constant of the reaction $CO_2 + OH^- \rightarrow HCO_3^-$ by the rapid thermal method, and by other methods in which thermal conduction and stagnant fluids do not enter.

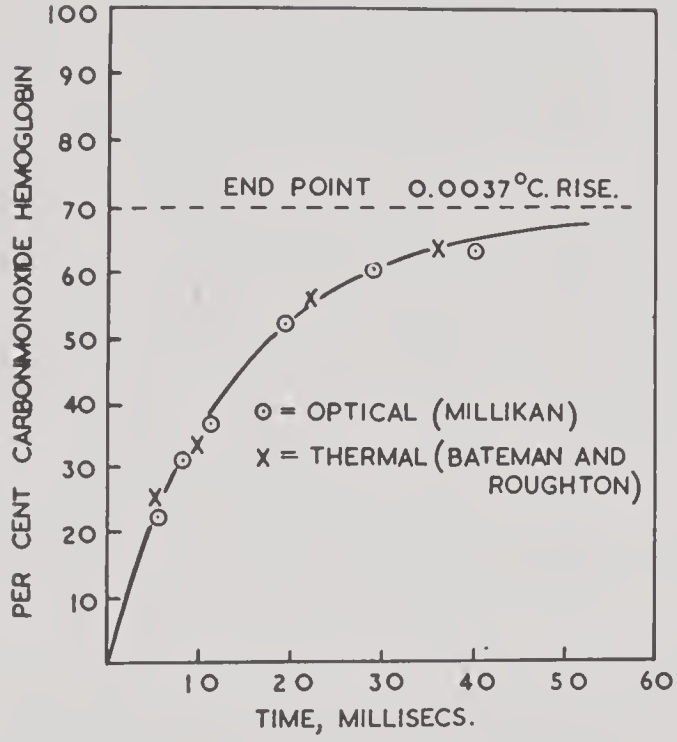

Fig. 4.5. Comparison of optical and thermal measurements of the rate of reaction of 0.001M CO with 0.0014M hemoglobin.

Any errors due to longitudinal thermal conduction in the observation tube and/or to the presence of stagnant films near the thermojunctions should be *proportionately* the same in the case of reactions with large temperature effects as in reactions with small temperature effects. It is probably, therefore, not a serious criticism of the older, more sensitive, method (3) that no controls were done with it at varying rates of flow. On the other hand, the lack of importance of these two factors was strongly indicated by the success of the comparison shown in Figure 4.5. The rate of combination of carbon monoxide with hemoglobin was measured both by the rapid thermal method (3) (with the old, more sensitive apparatus) and by the rapid photocolorimetric method of Millikan, identically the same reagent solutions being used in the two separate determinations.

The results by the two methods agreed within experimental error, even though the total temperature rise was only 0.0037°C.

IV. SUMMARY OF REACTIONS STUDIED: PRESENT AND POSSIBLE FUTURE SCOPE OF RAPID FLOW THERMAL METHODS

1. Range of Reactions and Determinations of Heats of Reactions Inaccessible by Classical Calorimetry

Table 4.II lists the reactions (or reaction types) hitherto studied by the rapid thermal method, together with the appropriate references. Three of the inorganic reactions, viz., A, B, and D were timed by apparatus of the type described in Section II. Reaction C and the three hemoglobin proc-

TABLE 4.II
Range of Reactions Studied by Rapid Thermal Method

	Velocity constant		
	Uni-molecular, k'	Bi-molecular, M^{-1} sec.$^{-1}$	Reference
A. $CO_2 + OH^- \rightarrow HCO_3^-$	—	1,000 at 0°C. 24,000 at 40°C.	(7)
B. $CO_2 + NH_3 \rightarrow NH_2COOH$	—	74 at 0°C. 1,000 at 40°C.	(8)
C. $H_2CO_3 \rightarrow CO_2 + H_2O$	2 at 0°C. 80 at 38°C.	—	(10)
D. $H_2O + Cr_2O_7^{2-} \rightarrow 2HCrO_4$	8.8 at 25°C.	—	(11)
E. CO + hemoglobin → CO hemoglobin (in homogeneous solution)	—	100,000 at 20°C.	(3)
F. CO + hemoglobin (in red blood cells) → CO hemoglobin (in red blood cells)	—	50,000 at 18°C.	(3)
O_2 + hemoglobin (in red blood cells) → O_2 hemoglobin (in red blood cells)	—	80,000 at 18°C.	(3)
G.			
H. $H^+ + OH^- \rightarrow H_2O$	too fast for rapid thermal measurement—require relaxation methods		(2)
I. $H^+ + A^- \rightleftharpoons HA$			
J. $H^+ + B \rightleftharpoons HB^+$			
K. $H^+ + Z^- \rightleftharpoons HZ^+$			
L. $H^+ + Z^+ \rightleftharpoons HZ^+$			

A^- = Anion of weak acid, e.g., acetate or aminoacetate ($NH_2CH_2COO^-$)
B = Molecule of weak base, e.g., ammonia
Z^- = Anion of protein (at alkaline pH)
$Z\pm$ = Zwitterion of protein (at isoelectric pH)
HZ^+ = Cation of protein (at acid pH)

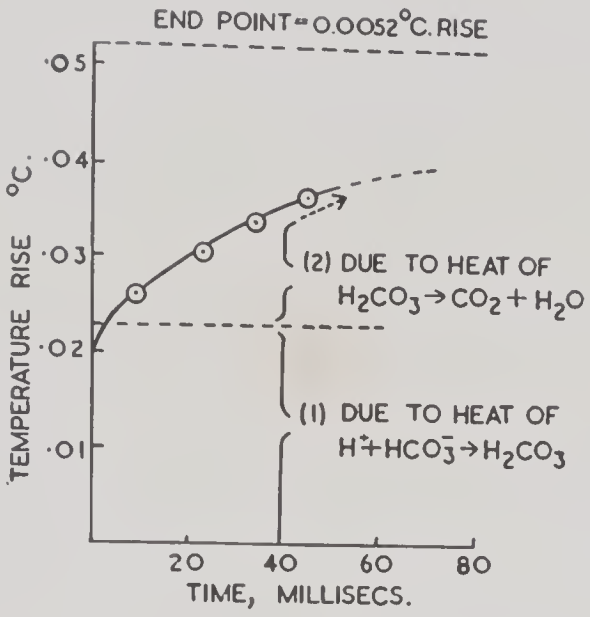

Fig. 4.6. Time course of temperature rise on rapid mixture of 0.059*M* HCl with 0.039*M* $NaHCO_3$ at 18°C.

esses (E, F, G) were followed by the more sensitive, but more laborious method just described. The ionic reactions H, I, J, K, L, are included as examples, which were tested in the early apparatus (2), but, as expected, proved too fast to follow by the rapid flow method.

As regards reaction C, Figure 4.6 shows the time course of the temperature changes following mixture of 0.059*M* HCl with 0.039*M* $NaHCO_3$ (10) at 18°C. This reaction takes place in two stages, viz., $H^+ + HCO_3^- \rightarrow H_2CO_3$, followed by $H_2CO_3 \rightarrow CO_2 + H_2O$. The corresponding heat liberation is also clearly divisible into two parts: (*1*) An "instantaneous" phase due to the heat, ΔH_1, of the ionic reaction $H^+ + HCO_3^- \rightarrow H_2CO_3$. (*2*) A progressive phase due to the heat, ΔH_2, of the molecular reaction $H_2CO_3 \rightarrow CO_2 + H_2O$. From similar experiments over the range 0 to 40°C., it was found that:

$$-\Delta H_1 = 10{,}170 - 31\ T \text{ cal.}$$

where T = absolute temperature. The usual methods only give the heat of the overall reaction:

$$H^+ + HCO_3^- \rightarrow CO_2 + H_2O, \text{ i.e., } \Delta H_1 + \Delta H_2.$$

Subtracting from the latter the values of ΔH_1 as given by (*1*), leads to values of ΔH_2 over the range 0 to 40°C. With a knowledge of ΔH_2 it was then simple to calculate from the second (progressive) phase of Figure 4.6, the value of k_1, the velocity constant of the reaction $H_2CO_3 \rightarrow CO_2 + H_2O$.

The present case is, therefore, an example, in which it is possible with the rapid thermal method to determine not only the velocity constant of a reaction, but to obtain also the heats of two individual reactions, neither of which were accessible by the usual methods.

A similar principle applies to reaction D of Table 4.II, the time course of which was followed thermally by La Mer and Read (11). When NaOH is mixed with $Na_2Cr_2O_7$ there is again a biphasic liberation of heat, due to the following 3-stage mechanism

$$Cr_2O_7^{2-} + H_2O \rightarrow 2HCrO_4^- \text{ (rapid, but measurable by flow method)} \quad \text{(D1)}$$

$$HCrO_4^- \rightarrow H^+ + CrO_4^{2-} \text{ (ultra-rapid)} \quad \text{(D2)}$$

$$H^+ + OH^- \rightarrow H_2O \text{ (ultra-rapid)} \quad \text{(D3)}$$

The rapid thermal measurements yielded not only the velocity constant of the reaction (D1), but also the individual heats of the reactions (D1) and (D2), which were hitherto inaccessible to measurement.

2. Résumé of Present Scope and Limitations

The rapid thermal techniques so far developed are suited to reactions with total temperature changes of 0.005°C. and upwards. For reactions with heats ranging from 1,000 to 10,000 cal. the minimal concentration of reagents required range from 0.005 to 0.0005*M*. These figures are around 1,000 times higher than the minimal concentrations required, under favorable conditions, in the photoelectronic methods. With bimolecular reactions, the highest velocity constants measurable by the thermal method are thus of the order of 10^4 to 10^5, as against 10^7 to 10^8 by Chance's method. With unimolecular reactions, in which the half-times are independent of reagent concentration, there is no such discrepancy, the maximum velocity constant measurable by either method being of the order of 10^3.

Since the total volume of solution needed for a thermal experiment is at present not less than 300 cc., the actual amount of solute required for a velocity constant determination is at least 1,000 times greater than in the photoelectronic method. A further advantage of the latter is that the time occupied by a complete experiment is only of the order of a few minutes as against the 2 to 3 hours required for a thermal experiment

On the other hand the rapid thermal method has the advantages of being applicable to a wider range of reactions, of sometimes furnishing new data as to heats of reactions not accessible by other methods, and in many cases of yielding more accurate values for velocity constants. Furthermore, in

the case of reactions involving ions (e.g., $CO_2 + OH^- \rightarrow HCO_3^-$) the thermal method has a great advantage over electrometric methods or colorimetric methods with indicators, namely that the stoichiometric extent of the reaction is obtainable directly from the temperature readings, without the need of activity corrections, which are often rather dubious and are sometimes impossible to make satisfactorily.

It may thus be concluded that the rapid thermal method, as so far developed, is an accurate tool of wide range in the study of the kinetics of rapid reactions, in which shortage of material is not a limiting factor and in which—in the case of bimolecular reactions—the velocity constants do not exceed 10^5 at most. In some cases it has advantages over other rapid reaction methods.

3. Possible Developments

A. SENSITIVITY OF TEMPERATURE MEASUREMENTS

This could certainly be increased, e.g., by multiplying the number of thermojunctions, but it would not seem profitable to do so unless the residual blank effects can be further cancelled out. Until then the limits of the method are ± 0.0002 to ± 0.0004°C. with the absolute thermocouple and ± 0.00004°C. with the differential thermocouple.

B. ECONOMY OF SOLUTIONS

It should be feasible to reduce substantially the present requirement of about 300 cc. of solution per experiment by a combination of the following measures:

(*1*) Reduction of the bore of the observation tube from 0.2 to 0.1 cm. (with corresponding reduction in the diameter of the thermocouple). Expected economy: 4-fold.

(*2*) Use of an additional galvanometer recording system to record simultaneously, instead of successively, the readings of the absolute and differential thermocouples. Expected economy: 2-fold.

(*3*) Speeding up of the galvanometer readings from 4 sec. to 1 to 2 sec. [as in the slight modification described in the "Sunvic" apparatus (see above)]. Expected economy 2- to 4-fold.*

These various economies are multiplicative, so that if all three were put into successful operation, there might be a total reduction of: $4 \times 2 \times 4$, i.e., of 32-fold. This would make it possible to work with 5 to 15 cc. of solutions, and thus would bring the thermal method to the same stage as had been reached in the photoelectric methods at the time Chance started

* This measure has recently been put into practice, and the fluid requirement is now about 100 cc. per experiment.

his work. Any further substantial reductions would seem to involve the incorporation of the "stopped flow" and "accelerated flow" techniques in the rapid thermal method.

C. POSSIBILITY OF THERMAL MEASUREMENTS ON "STOPPED FLOW" FLUID

So far the only published observations of this kind have been those of Bateman and Roughton (3), with their very slow recording galvanometer system. These authors followed the temperature in a "stopped" mixture of hemoglobin and oxygen solutions over a period of 90 sec. With the Downing galvanometer now in use, there is no electrical difficulty in starting records at about 0.05 sec. after the stoppage flow and continuing them indefinitely. Preliminary tests have recently been carried out by Sirs and Roughton, with a thermojunction responding within 0.01 sec. and situated in a thin nylon observation tube, surrounded with an air jacket, the whole being immersed in a thermostat. The arrangement was in other respects similar to that shown in Figure 4.1, a Gibson stopped flow device being joined to the end of the observation tube (see Fig. 2.12). Promising results have been obtained in the case of a reaction involving a temperature rise of about 0.01°C. and a half-time of about 0.5 sec. Temperature changes due to heat conduction in the stopped fluid were found to be of the order of 3% of the total temperature change per second. There is clearly much scope for further work in this field, for the possible advantages of the stopped flow principle in rapid thermal work are just as obvious as in the other types of technique to which this principle has been successfully applied.

Further developments of the thermal apparatus shown in Figure 4.1, are to be reported in a forthcoming article by R. L. Berger (*Temperature, Its Measurement and Control in Science and Industry*, C. M. Herzfeld, ed., Vol. III, Reinhold, New York, 1962) along the lines of the preliminary tests described by Sirs and Roughton in the last paragraph. With the stopped flow method, heat changes of the order of 0.001 to 0.002°C. have been measured to within 0.00002°C. by a single thermocouple with a time of response of 0.01 sec. A 10-junction thermocouple gives a 10-fold further increase of sensitivity, the ultimate limit being set by the Brownian movement of the primary (Downing) galvanometer. The following are the main improvements.

(*1*) The actual reaction velocity apparatus is mounted in an inner water thermostat which is in turn mounted in a second large thermostat. For the most refined work the reaction velocity apparatus is furthermore enclosed in a 12 inch diameter aluminum block. In the latter case temperature stabilization of $\pm 10^{-6}$°C. has been reached.

(*2*) Much of the electronic circuitry has been transistorized.

(*3*) Mixing chambers capable of handling very viscous liquids (viscosity up to 200 centipoises) have been included.

(*4*) By means of light-pipe arrangements the progress of the reaction is also followed optically in the same observation tube as that used for the thermal measurements. Comparative experiments of the type illustrated in Figure 4.5 can be very readily performed, thus adding greatly to the power of the whole technique. As an example, the time course of the heat liberated by the hemolysis of red blood cells has been compared with the time course of the concomitant changes in light scattering as revealed by optical transmission records. The two processes appear to synchronize well, the half-time in each case being about 7.3 sec.

References

1. H. Hartridge and F. J. W. Roughton, *Proc. Roy. Soc. London*, **A104**, 376 (1923).
2. F. J. W. Roughton, *Proc. Roy. Soc. London*, **A126**, 439, 470 (1930).
3. J. B. Bateman and F. J. W. Roughton, *Biochem. J.*, **29**, 2622, 2630 (1935).
4. E. Giladi, A. Lifshitz, and B. Perlmutter-Hayman, *Bull. Res. Council, Israel*, **A8**, 75 (1959).
5. A. C. Downing, *J. Sci. Instruments*, **25**, 230 (1948).
6. A. V. Hill, *J. Sci. Instruments*, **25**, 225 (1948).
7. B. R. W. Pinsent, L. Pearson, and F. J. W. Roughton, *Trans. Faraday Soc.*, **52**, 1512 (1956).
8. B. R. W. Pinsent, L. Pearson, and F. J. W. Roughton, *Trans. Faraday Soc.*, **52**, 1594 (1956).
9. C. Faurholt, *J. Chim. Phys.*, **22**, 1 (1925).
10. F. J. W. Roughton, *J. Am. Chem. Soc.*, **63**, 2930 (1941).
11. V. K. LaMer and C. L. Read, *J. Am. Chem. Soc.*, **52**, 3098 (1930).

Part 5. *QUENCHING, ELECTROMETRIC, AND OTHER RAPID REACTION TECHNIQUES*

The optical and thermal flow methods have been described at length in Parts 2 and 4 because of their previous wide application and possible further applicability to rapid reaction work in solution, and also on account of the illustrations they provide of the general principles governing all such work by flow methods. Several other types of technique have, however, also been developed either for confirmatory purposes or—more often—for cases in which the optical and/or thermal methods are much less suitable or competent. These methods will be discussed in this part of the chapter.

I. THE QUENCHING METHOD

The general principle of this method has already been described under the heading "Multiple Mixers" (Part 1). Table 5.I gives a list of some reactions to which the method has been successfully applied. The reaction times, τ, are given by the equation

$$\tau = V/\bar{v}$$

TABLE 5.I
Some Reactions That Have Been Studied by the Quenching Method

Reaction	Reaction time, sec.	Quenching agent	Authors
1. CO + hemoglobin	0.1–1	O_2 (in soln.)	Roughton (1)
2. $H_2O_2 + Br_2$	0.5–6	I^-	Bray and Livingston (2)
3. $H_2O_2 + Cl_2$	0.2–5	I^-	Makower and Bray (3)
4. $NaNO_2 + H_2SO_4$	*ca.* 1	NaOH	Schmid (4)
5. CO_2 + buffer (± carbonic anhydrase)	0.1–1.0	Dimethylamine (± sulfanilamide)	Faurholt (5) Clark and Perrin (6) Pinsent (7)
6. $2H_2O_2$ (catalase)	0.1–0.4	H_2SO_4	Chance (7a)

where V = volume (cc.) between the first mixer M_1 (in which the two primary reagents L and R meet) and the second mixer M_2 (in which the L + R mixer meets the quenching reagent Q), and $\bar{v}$ = rate of flow (in cc./sec.) of the L + R mixture between the first and second mixing chambers. V and $\bar{v}$ are readily adjustable to give any desired values of τ within the range shown. In all the cases listed in Table 5.1 the time taken by the quenching reaction to proceed to 98% completion was not greater than one-fiftieth of the reaction times of the respective primary reactions. A useful experimental control is to vary the concentrations of the quencher: if the latter is fully efficient the observed extent of the primary reaction should be unaffected. If, conversely, the apparent extent of the primary reaction is reduced when the quencher concentration is increased, it might be possible—though, so far as the writer is aware, there is no case yet in which this has been done—to extrapolate to an "infinite" quencher concentration (i.e., complete quenching efficiency) by plotting the observed extent of the primary reaction against the reciprocal of quencher concentration. In this way the true rate of the primary reaction might be indirectly determined.

Figure 5.1 shows a convenient quenching arrangement due to Pinsent (7). The mixing chambers, M_1 and M_2, are made in two Lucite blocks which are

then clamped together to form a single block. The mixers M_1 and M_2 each have eight 1 mm. jets arranged in two sets of four jets; the first set enters the observation tube, M_1 M_2, at a tangent to produce a clockwise swirl, whereas the second set enters 1 mm. further along the observation tube tangentially so as to produce an anticlockwise swirl. Such an arrangement not only improves the efficiency of mixing, but also reduces greatly the pressure needed to drive the solutions. The syringes L′, Q′, R′ (containing respectively the primary reagents L and R, and the quenching

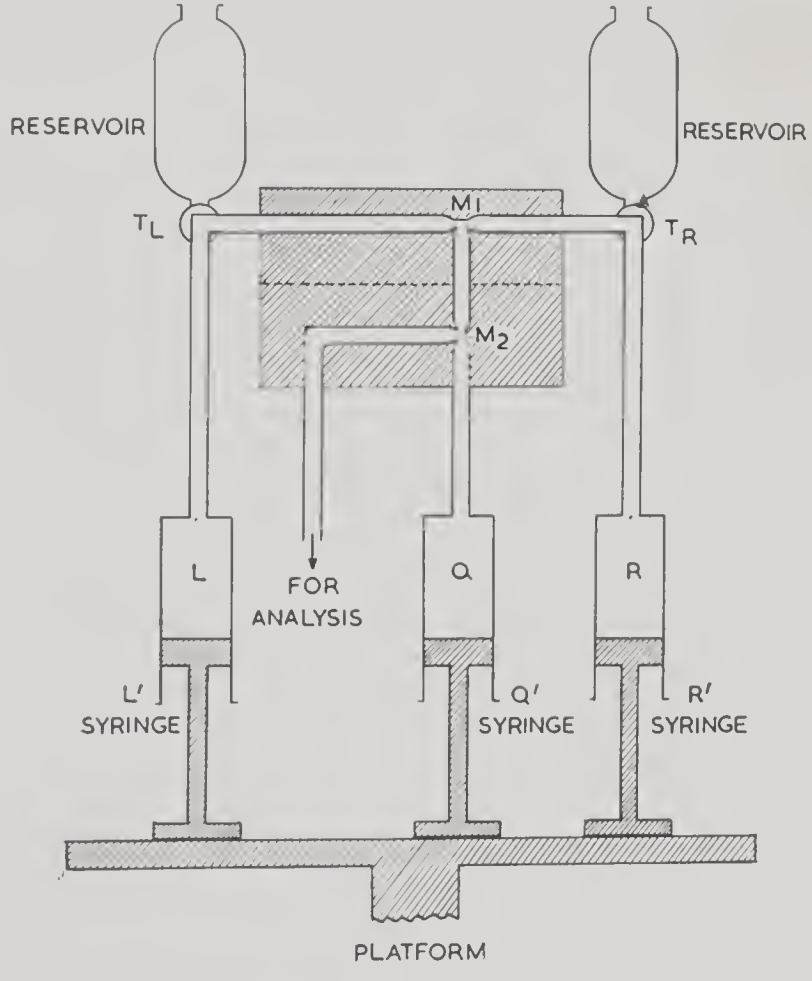

Fig. 5.1. Schematic diagram of Pinsent's quenching apparatus. For detailed description, see text.

reagent Q) are of 5 or 10 ml. capacity. Their plungers all rest on the platform P, which can be driven upwards by a hydraulic drive, operated by a hand lever. It is easy, by maintaining a steady pressure on the lever, to raise the platform at a practically uniform rate, the constancy of which is checked by timing the movement of the platform. This can be done by means of a rod attached to the platform and consisting of alternate brass and Lucite sections. As the platform moves up, the rod passes two con-

tacts connected to a pen recorder and alternately makes and breaks the circuit. The syringes L′ and R′ are filled from reservoirs through the 3-way taps T_L and T_R. Q′ has a similar reservoir not shown in the diagram. The taps are turned to connect the syringes with the mixing chamber and the platform driven up. The solutions L and R are mixed at M_1 and then pass along the observation tube M_1 M_2 into M_2 where they are mixed with the quenching solution. The final mixture emerges through the exit tube, and, after discarding the portion at the beginning of the run, is collected in a vessel for subsequent analysis by standard chemical methods. In the practical use of the method, samples should be obtained for at least 4 different reaction times, either by varying the pressure drive or by varying the volume between the two mixing chambers (or by both procedures). In the case of the reaction studied by Pinsent, viz., $CO_2 + OH^- \rightarrow HCO_3^-$, L = CO_2 solution, R = carbonate/bicarbonate buffer solution, Q = $2M$ dimethylamine solution. With a half-time of reaction of 0.4 sec., Pinsent obtained results reproducible to $\pm 7\%$.

The advantages of the rapid quenching method are: (*a*) It is economical of reagents, only some 20 ml. being required. (*b*) Only simple and inexpensive apparatus is needed. The whole set-up can easily be thermostatted if necessary. (*c*) The analysis of the final mixed fluid can be carried out at leisure by standard chemical methods, which can often be brought to a higher degree of precision than is possible in the analysis of moving fluids by physical methods.

The two main drawbacks of the method are the relative rarity of the cases in which a suitable quencher can be found, and the uncertainty as to its applicability for reaction times of less than about 0.01 sec. In cases in which it can satisfactorily be used the quenching method may well, however, prove to be the most accurate of all methods for determining the velocity of rapid reactions by flow methods.

II. ELECTROMETRIC METHODS

The following types of electrical measurement have been applied to the measurement of the rates of rapid reactions in solution by the flow methods:

1. Electrical conductivity (8,9,10,11,12)
2. Reversible electrode potentiometry
   - A. pH
     - (1) Hydrogen electrode (8,9)
     - (2) Glass electrode (13,14,15)
   - B. Redox potentials (8,16,17,18)
3. Polarographic determinations of O_2 and H_2O_2 (19)

All the work with the hydrogen electrode and redox potentials was done some 30 years ago and it therefore seems better to refer the reader to the original papers of those times for details of the techniques, and the purposes to which they were applied, rather than to supply much description here. The electrical conductivity, glass electrode, and polarographic methods have been increasingly used in the last 5 years or so and therefore call for further discussion.

1. Electrical Conductivity

Saal (8,9) was the first worker in this field. He used a continuous flow method with platinum electrodes sealed into glass observation tubes of 8-mm. bore; his times of reactions ranged from 0.004 to 2 sec. No further electrical conductivity studies were reported until 28 years later.

Pearson, Meeker, and Basolo (10) describe a simple continuous flow arrangement in which a 1 mm. bore glass capillary observation tube, with 2 platinum wires fused through slots in the walls of the latter to form the conductivity cell, is joined to a conventional type Lucite mixer. The slots do not face each other directly but are staggered 2 mm. for structural strength. Three different cells were provided, having volumes ranging from 0.13 to 0.70 cc., giving reaction times varying from 30 millisec. to a few seconds when the reagents were driven through the apparatus by applying various air pressures to the reservoirs containing them. The electrical resistances were measured with a conductivity bridge using alternating current at 1,000 cycles per second, with a cathode ray oscilloscope for null point determination. This apparatus appears to be quite a simple one, requiring little knowledge of electronics.

Two years later Sirs (11) adapted the stopped flow method to electrical conductivity measurements, and in the same year Prince (12) described a method available both for continuous flow and stopped flow procedures. For the latter purpose it is obviously necessary that the period of the alternating current should be far shorter than the chemical reaction under study.

Sirs' apparatus consists of a constant voltage 50 kc./sec. oscillator, an electrode supply and calibration network, the rapid reaction chamber (including a Gibson syringe device for sudden stoppage) and electrode system, an a-c amplifier which is followed by a rectifier and filter, and finally a d-c amplifier and cathode ray oscilloscope; traces appearing on the latter being recorded photographically. For details of the electronic arrangements the original paper should be consulted. The mixing chamber and observation tube are constructed in Lucite, along similar lines to those used by Chance and Gibson. The diameter of the Lucite observation tube is

3 mm. The electrodes consist of two tapped 1.2-mm. diameter stainless-steel rods screwed into the Lucite block at a distance of 12 mm. from the mixing chamber. The reagents are contained in two (platform-driven) 2-cc., all-glass syringes connected through 3-way glass taps to the Lucite block. The whole apparatus is readily immersible in a thermostat. The apparatus has so far been applied mainly to the kinetics of the reaction $CO_2 + OH^- \rightarrow HCO_3^-$. Tests showed that, provided the artefact due to dissolved gas was controlled (see Part 1, page 716), the method gave values of the velocity constant of this reaction correct to $\pm 5\%$. The apparatus has so far been limited to experiments involving a 10% overall change of conductivity, but this degree of sensitivity can probably be increased.

Prince's (12) apparatus was specially designed, in the first instance, for the study of reaction mechanisms in organometallic compounds dissolved in nonaqueous solvents. Plastics, such as Lucite, could not therefore be used for the mixing chamber and the observation tube, which were of all-glass construction, the mixing chamber being made by the method of Chance and Graham (20). For continuous flow work there are six 22-gage platinum wires sealed into the 4-mm. diameter observation tube, at intervals ranging in volume from 0.043 to 0.97 cc., the conductivity cell constants being determined with 0.01*N* KCl solution in the usual way. The reactants were contained in 500-cc. flasks and driven thence into the mixing chamber by nitrogen at constant pressure. In the case of reagents of differing viscosity, equality of delivery was ensured by adjusting a tap connecting the liquid of lower viscosity to the mixing chamber. Volume flow rates of 5 to 7 cc./sec. gave velocity constants agreeing within $\pm 7\%$. The stopped flow version of Prince's original apparatus was subsequently improved in various ways, especially as regards its application to slower reactions with a half-time of a second or so: in such cases the measurements were sometimes spoiled by diffusion of reagent solutions from the jets of the mixing chamber down the observation tube. In the later apparatus this difficulty was eliminated by dividing it into two parts in series, separated by glass taps, the first part being for rapid reactions with times of less than a second, and the second part for slower reactions of times greater than 1 sec. For full details of the electronic (mechanical and thermostatic) arrangements and the performance characteristics the reader should consult the original papers of Prince.

2. Reversible Electrode Potentiometry

A. pH

Hydrogen Electrode. Saal (8,9), the sole worker with this technique, listed the "very great" precautions necessary to get satisfactory results.

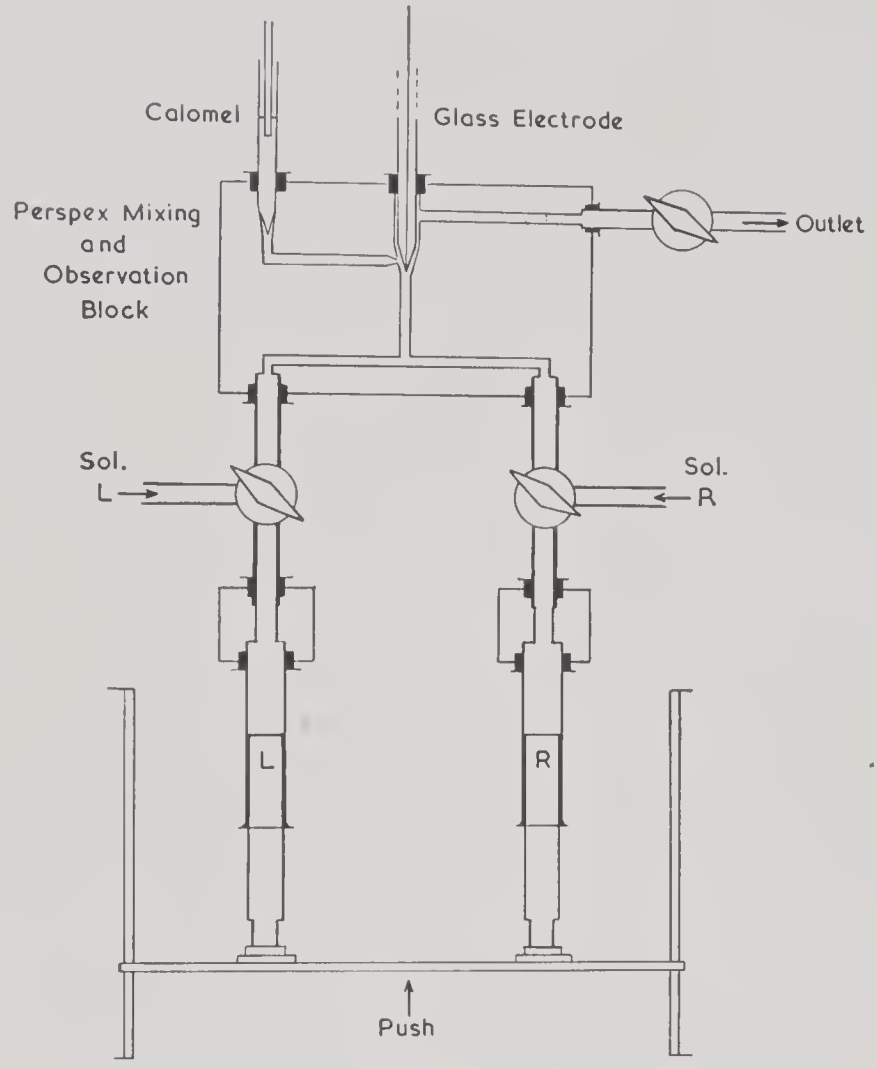

Fig. 5.2. Schematic diagram of Sirs' pH stopped flow apparatus.

His results on the reaction $H_2CO_3 \rightarrow CO_2 + H_2O$, showed a 40 to 50% scatter about the mean. (He also tried out quinhyddrone, copper, silver, and silver iodide electrodes for measuring changes of concentration of H^+, Cu^{2+}, Ag^+, and I^- respectively in streaming fluids. Of these, only the silver electrode proved satisfactory.)

Glass Electrode. The glass electrode has been used in flowing streams by Steinhardt and Zaiser (13). The geometry of their apparatus and their driving pressure gave them a resolution time of less than 3 sec. Love, using the stopped flow method, found that he could record pH changes occurring about 0.06 sec. after mixing, which is the calculated response time of his system. In a further development of the stopped flow method, Sirs (15) was able to shorten the response time of the amplifier so as to be able to measure reactions with half-times down to 0.05 sec. By means of a correction method (21), which is also applicable to electrical conductivity work, he found it possible to follow reactions with half-times down to 0.01

sec. A schematic diagram of Sirs' reaction apparatus is shown in Figure 5.2. The original paper should be consulted for details as to the glass electrode input amplifier and the intermediate amplifier circuit leading finally to a d-c oscilloscope.

B. REDOX POTENTIALS

Inorganic Systems. Saal (8) made a survey of a dozen or so oxidation-reduction reactions and found the rates of many to be measurable. Using white platinum electrodes, he later (16) made a more detailed study of the velocity constants of the rapid bimolecular reactions (*a*) $Fe^{2+} + S_2O_8^{2-}$ and (*b*) $I_2 + Fe(CN)_6^{4-}$.

Unstable Organic Systems. Ball and co-workers (17,18) made use of the rapid flow method to study the redox potentials of 13 systems, of which the reductants (catechol, benzohydroquinone, or their derivatives) are stable, but the oxidants are unstable. Such systems are thus inaccessible to the ordinary redox methods. The technique consisted of driving an inorganic oxidant, e.g., ceric sulfate, and the organic reductant into an all-glass mixing chamber and thence over a series (usually 4) of gold-plated, platinum gauze electrodes. After flowing past the last electrode, the mixture formed a flowing, liquid junction with a saturated calomel half-cell. Data were thus obtained, at 30 and 37.4°C. and at various pH values for: (*a*) E'_0, the redox potential at 50% reduction and a specified pH; (*b*) $-dE_h/dt$, the rate of chance of redox potential with time, after the primary oxidation is complete. The values of $-dE_h/dt$ were found to be very dependent on pH: thus for epinephrine, at 30°C., $-dE_h/dt$ at pH 1.28 = 0.03 mv./sec., but at pH 7.66 = 150 mv./sec. The corresponding values of the velocity constant of decomposition of the oxidant of epinephrine are 0.0023 at pH 1.28, and 11.5 at pH 7.66.

3. Polarographic Determination of H_2O_2 and O_2

A. OXYGEN

The dropping mercury electrode for which so many uses have been described (see Ref. 19 as a general reference) is unsuitable for measurements in rapidly moving flow streams. The platinum microelectrode as described by Davies and Brink for the measurement of oxygen concentration with cathodic polarization (22) is much more suitable mechanically and has been used by Chance (23) for measurement of the oxygen consumption of the glucose oxidase system. The microelectrode (about 0.2 mm. in diameter) was inserted into the observation tube of the flow apparatus of Figure 2.3 so that the platinum tip lay in the zone of photoelectric observa-

tion. Although the electrode gave an increased current when the reactants were flowing down the observation tube, this artefact terminated a few seconds after the flow stopped, and then the oxygen concentration was followed with satisfactory accuracy. A sensitivity of the order of $1 \times 10^{-6}M$ oxygen (corresponding to about 0.5 mm. Hg pressure of dissolved O_2 at 20°C.) is often attainable. Various methods to avoid the "flow artefact" of the platinum microelectrode have been tried. Probably the simplest solution is to maintain the flow velocity constant and calibrate the electrode for these conditions.

In the past five years a valuable development of the oxygen electrode has been made by Clark (24) and others. The Clark electrode, or its modifications, is suitable for use in a far wider range of solutions or media than were hitherto accessible by electrometric methods of this type. It has recently been applied by Staub, Forster, and Bishop to the measurement, by the Hartridge-Roughton continuous flow method, of the rate of uptake of oxygen by human red blood cells at 37°C. In their technique a suspension of red blood cells, equilibrated with a suitable gas pressure of oxygen (ranging from 0 to 200 mm. Hg or upwards), is mixed with a saline solution equilibrated with a higher pressure of dissolved oxygen, and the oxygen concentrations at different positions along a precision-bore observation tube are then measured. The oxygen electrode consists of a 0.002 in. platinum-in-glass cathode, a silver wire anode, and KCl electrolyte. The membrane covering the cathode is Teflon, 0.00025 in. thick (recently Teflon membranes 0.005 in. thick have been used). This combination gives a sensitive, rapid system with times of response of the order of 2 to 10 sec. The relation between electric current and oxygen concentration in watery fluids is linear: the input, after amplification, is written on a pen recorder. A sensitivity of $1 \times 10^{-6}M$ oxygen is again easily obtainable. In the work on red blood cell suspensions so far carried out, the Clark electrode has been located at distances from the mixing chamber corresponding to reaction times of 3, 7, 14, 31, 52, and 700 millisec. For fuller details the reader should consult the papers of Staub, Bishop, and Forster (24a).

B. HYDROGEN PEROXIDE

Chance has found that the platinum microelectrode polarized as an anode responds satisfactorily to hydrogen peroxide and has used this method for catalase assay where hydrogen peroxide is decomposed into water and oxygen (25). A typical record is shown in Figure 5.3. In this case the particular electronic circuit employed considerably reduced the flow artefact.

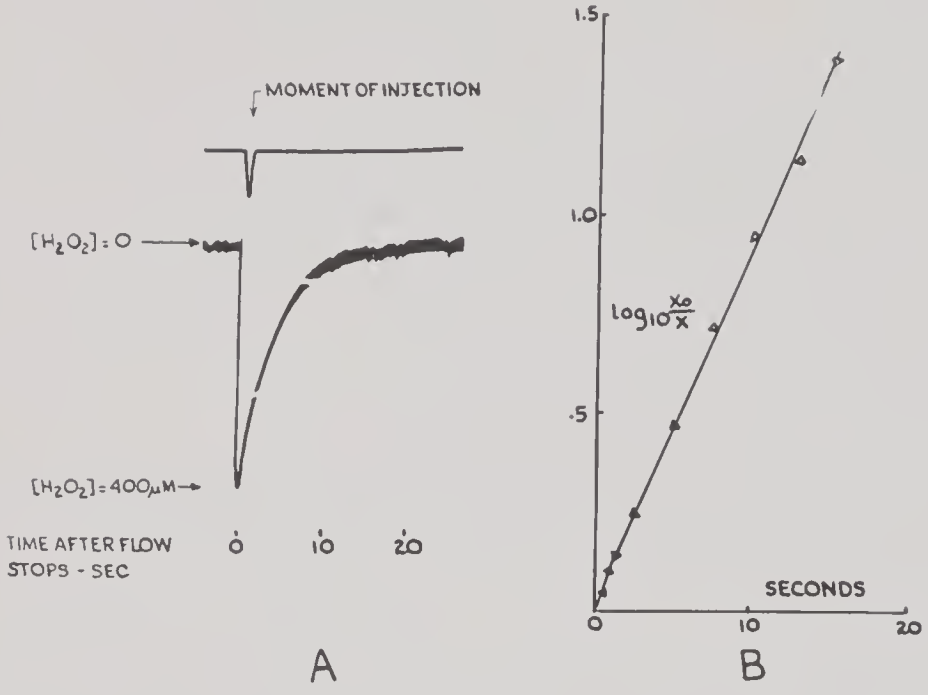

Fig. 5.3. The catalytic decomposition of hydrogen peroxide as measured by the platinum microelectrode with anodic polarization. The original data in A, recorded by a mirror oscillograph is plotted in B as a first-order reaction. $5.7 \times 10^{-9} M$ horse liver catalase, 400 μM hydrogen peroxide, 0.01M buffer, pH 6.5, $T = 25°$C., electrode polarized at +IV, $k_1 = 4 \times 10^7$ liter mole^{-1} sec.$^{-1}$ (Expt. 90C) (25).

III. THE GASOMETRIC METHOD

Dirken and Mook (26) have described a special method for rapid reactions of CO_2 in solution, which may possibly have other applications. The outlines of the method were as follows. The two solutions which are to react are driven into a mixing chamber and thence, in the form of a fine vertical jet (diameter *ca.* 1.2 mm.) through a small gas chamber containing CO_2 at atmospheric pressure (Fig. 5.4). The rate of CO_2 absorption by the jet is measured either by noting the movement of a drop of kerosene in a capillary attached to the chamber or by a delicate membrane manometer with mirror, and is found to depend solely on the CO_2 tension of the fluid in the jet. From calibration experiments with fluids containing known CO_2 tensions it is thus possible to estimate the CO_2 tension developed in a reacting fluid during the time taken to travel from the mixing chamber to the center of the gas chamber. Times of reaction varying from 0.07 to 15 sec. are obtained by interposing intermediary volumes between the mixing and gas chambers, a specially convenient device being designed for this purpose. The total quantity of reagent required for an experiment is from 10 to 20 cc. The results by the method are somewhat rough, but agree fairly well with those obtained by other methods.

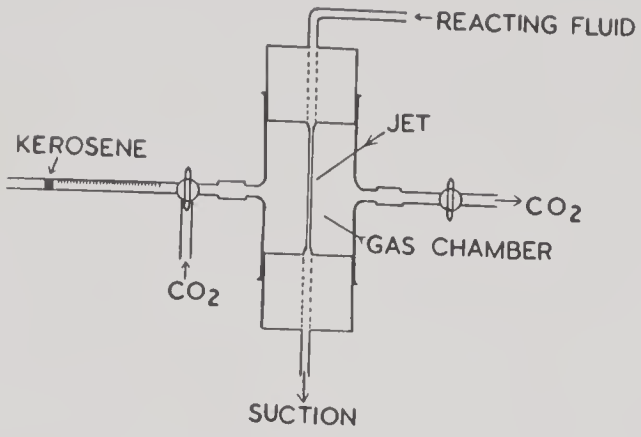

Fig. 5.4. Enlarged view of gas chamber in which CO_2 tension in jet of reacting fluid is estimated from rate of absorption of CO_2 by jet as indicated by movement of kerosene in graduated tube.

The method has been applied to (*1*) the reactions of $NaHCO_3$ with HCl and with lactic acid (*2*) the reactions of dissolved CO_2 with buffer solutions in presence and in absence of the enzyme carbonic anhydrase. It is presumably applicable to reactions of other gases of similar (or greater) solubility to that of CO_2, e.g., N_2O, C_2H_2, H_2S, SO_2, etc. For difficultly soluble gases such as O_2 and CO (the reactions of which are of much biological interest) the rate of absorption in the gas chamber is so slow that the apparatus, in the form designed by Dirken and Mook is not suitable.

IV. THE ULTRAFILTRATION METHOD

The object of this method is to measure the rate of chemical interchanges between a continuous medium (e.g., blood plasma) and a disperse phase (e.g., red blood cells). An apparatus for this purpose was developed 30 years ago by Dirken and Mook (27), who applied it in a very fruitful manner to studies on the rate of exchange of O_2, CO_2, HCO_3^-, and Cl^- between mammalian red blood cells and their surrounding fluid, all these processes being rapid and of much interest to physiologists. The subject then remained dormant until a few years ago when Paganelli and Solomon (28) and Tosteson (29) modified the Dirken and Mook apparatus and applied it to the study of the rate of exchange of isotope-labelled water and isotope-labelled halide respectively, between the inside and outside of red blood cells. Roughton and Rupp (30) have recently used a slightly altered form of Tosteson's apparatus for measuring the rate of exchange of Cl^- and HCO_3^- between the outside and inside of bullock red blood cells at 37°C. In the present Section a brief description is given of Dirken and Mook's original method, followed by a similar outline of the more recent methods.

1. Dirken and Mook's Technique

The two reagents were contained in rubber bags located in steel cylinders completely filled with water. By pumping further water into the cylinders, the bags were forced to discharge their contents into a mixing chamber and thence, after varying reaction times (from 0.1 sec. upwards), into a special ultrafiltration chamber, in which about 1 cc. of filtrate was obtained from each 100 cc. of passing fluid. Analysis of the filtrate for any desired constituent gave the concentration of the latter in the continuous medium at the time taken by the fluid to travel from the mixing chamber to the center of the ultrafiltration chamber. The construction of the latter is illustrated in Figure 5.5. For study of the rate of interchange processes in blood, Dirken and Mook used commercial membranes containing a large number of fine pores of roughly equal size (i.e., about 0.5 μ, which is much less than the dimensions of the red blood cells).

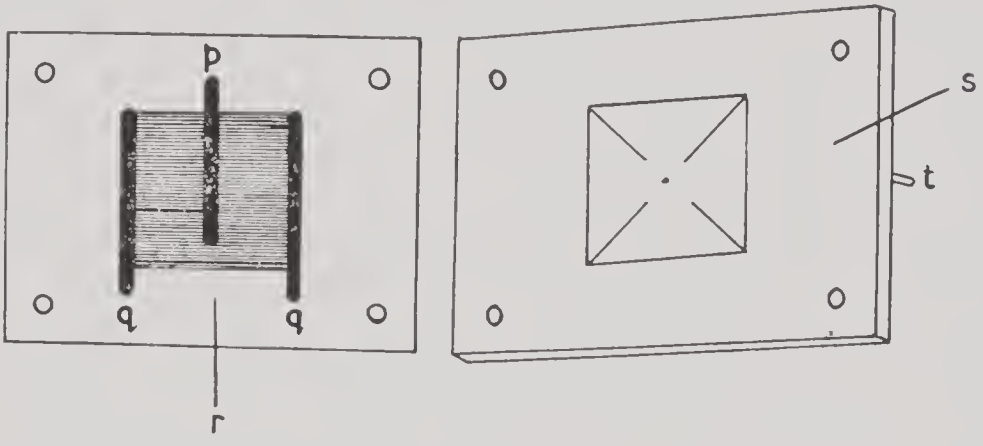

Fig. 5.5. Arrangement of ultrafiltration chamber. The membrane is clamped between the plates r and s. The reacting fluid enters at the upper end of groove p and leaves by grooves q, q which are connected with p by 80 shallow grooves (length 10 mm., width 0.4 mm., depth 0.1 mm.). The ultrafiltration is removed by the capillary tube t.

The authors pointed out rates of exchange as determined by this technique are possibly greater than the true rates for the following reason. The fluid passing through the filter must be drawn from the periphery of the grooves, where presumably the motion is slower than that of the average fluid in the grooves. The time recorded in each experiment is, however, that taken by the average fluid to reach the middle of each groove, and may therefore be *less* than the time value for the fluid which is filtered. The motion of the fluid in the grooves is, however, very turbulent and the time spent in each groove is only about 0.02 sec. (i.e., one-tenth, or less, of the half-time of all the processes investigated in 1930 through 1931),

so that the authors consider—no doubt correctly—that the rates as observed by them are not likely to be far from the true rates.

2. Recent Filtration Technique

In the modification by Paganelli and Solomon (28) the reagents were contained in 1,500 cc. stainless steel beakers fitted with pressure-tight tops made from $^1/_4$ in. brass plate. They were driven by gas pressure (of the order of 1 to 3 atmospheres) into a Lucite mixing chamber and thence into a filtration chamber formed from stainless steel tubing (No. 12 gage, 0.085 in. inner diameter, 0.012 in. wall thickness), imbedded in a Lucite block ($3^1/_4$ in. $\times$ 1 in. $\times$ $^5/_{16}$ in.). Four cylindrical surfaces of $^{11}/_{32}$ in. radius, at 2 cm. intervals, were milled into the Lucite block and the wall of the steel tubing until the latter was very thin. Then four $^1/_{16}$ in. holes were drilled through the wall of the steel tubing at the thin spots. Seven mm. diameter circles of Millipore paper (0.8 μ pore diameter, Aerosol Assay, Millipore Filter Corporation, Waltham, Massachusetts) supported by circles of ordinary No. 42 Whatman filter paper were placed in position over the holes in the wall of the steel tube. The filters were held tightly in place by segments of cylinders of $^{11}/_{32}$ in. radius, bolted to the Lucite block. Holes in these segments allowed passage of filtrate through the filters. With this set-up, four samples could be filtered simultaneously, thus giving, in a single experiment, four points on a kinetic curve (with times ranging from 2 to 8 millisec. in a typical experiment). A total of about 0.1 cc. filtrate was generally produced from 500 cc. of reacting mixture. For further details of the apparatus the reader is referred especially to Figures 1, 2, and 3 of the original paper.

Tosteson's (29) arrangement permits the measurement of somewhat slower processes (i.e., half-times between 10 and 0.05 sec. or less). The main differences are that (*a*) the reagents are driven by pumps, rather than by compressed gas, into the Lucite mixing chamber and (*b*) the filtration chamber consists of a 34 cm. long Lucite channel, in the form of a rectangular slit, 1.0 cm. wide and 0.1 cm. thick. At 5 cm. intervals the wall of the Lucite tube is replaced by six 1 sq. cm. discs of 0.8 μ pore Millipore filter paper. During continuous flow small (0.1 to 0.5 cc.) samples of the continuous medium filter through the six discs and are subsequently analyzed by standard methods. In Rupp's modification there is a sliding arrangement by which the filtrate is collected in two separate chambers, the advantage of this being that the contents of the first chamber, i.e., the earliest portions of the filtrate, can be discarded.

Further tests for efficiency of mixing, besides those described in the earlier part of this chapter, are required when flow apparatus is used for

concentrated mixed suspensions, such as whole blood. Paganelli and Solomon (28) consider that their special mixing tests with human red cells labelled with $Cr^{51}O_4^{2-}$ validated their apparatus as regards this point. They also argue, both on theoretical grounds and from the results of their experiments, that deviations from mass flow down the observation tube and effects of the stagnant layer of fluid present at the boundary between the moving fluid and the filter ports were jointly unimportant in the applications so far made by them. In this matter they thus agreed with the earlier opinion of Dirken and Mook (27) to the same effect.

The filtration procedures, in the hands of both their original and their recent exponents, have given self-consistent and seemingly very satisfactory results as regards rapid red blood cell exchange problems, some of which are not accessible—or not readily accessible—by other methods. It is, however, the opinion of the writer that, wherever possible, the results by any one rapid reaction velocity technique should be tested by some quite independent method and that this principle applies with particular force to work with the filtration technique.

References

1. F. J. W. Roughton, *Proc. Roy. Soc. London*, **B115**, 451, 464, 473, 495 (1934).
2. W. C. Bray and R. S. Livingston, *J. Am. Chem. Soc.*, **50**, 1654 (1928).
3. B. Makower and W. C. Bray, *J. Am. Chem. Soc.*, **55**, 4765 (1933).
4. H. Schmid, *Z. Physik. Chem.*, **141**, 41 (1929).
5. C. Faurholt, *J. chim. phys.*, **21**, 400 (1924).
6. A. N. Clark and D. D. Perrin, *Biochem. J.*, **48**, 495 (1951).
7. B. R. W. Pinsent, *Discussions Faraday Soc.*, **17**, 140 (1954).

7a. B. Chance in D. E. Green, ed., *Currents in Biochemical Research*, Interscience, New York–London, 1956, p. 311.

8. R. N. J. Saal, *Rec. trav. chim.*, **47**, 73 (1928).
9. R. N. J. Saal, *Rec. trav. chim.*, **47**, 264 (1928).
10. R. G. Pearson, R. E. Meeker, and F. Basolo, *J. Am. Chem. Soc.*, **78**, 709 (1956).
11. J. A. Sirs, *Trans. Faraday Soc.*, **54**, 201 (1958).
12. R. H. Prince, *Trans. Faraday Soc.*, **54**, 838 (1958).
13. J. Steinhardt and E. M. Zaiser, *J. Biol. Chem.*, **90**, 197–210 (1951).
14. J. Meier and G. Schwarzenbach, *Helv. Chim. Acta*, **40**, 907 (1957).
15. J. A. Sirs, *Trans. Faraday Soc.*, **54**, 207 (1958).
16. R. N. J. Saal, *Rec. trav. chim.*, **47**, 385 (1928).
17. E. G. Ball and T.-T. Chen, *J. Biol. Chem.*, **102**, 691 (1931).
18. E. G. Ball and W. M. Clark, *Proc. Natl. Acad. Sci. U.S.*, **17**, 347 (1931).
19. I. M. Kolthoff and J. J. Lingane, *Polarography*, 2nd ed., Interscience, New York 1952.
20. B. Chance, *J. Franklin Inst.*, **229**, 455, 613, 737 (1940).
21. J. A. Sirs, *J. Sci. Instr.*, **35**, 419 (1958).
22. P. W. Davies and F. Brink, *Rev. Sci. Instr.*, **13**, 524 (1942).
23. B. Chance, *Biochem. J.*, **46**, 387 (1950).

24. L. C. Clark, *Trans. Am. Soc. Art. Int. Organo*, **11**, 41 (1956).
24a. N. C. Staub, J. M. Bishop, and R. E. Forster, *J Applied Physiol.*, **16**, 511 (1961), **17**, 21 (1962).
25. R. Bonnichsen, B. Chance, and H. Theorell, *Acta Chem. Scand.*, **1**, 685 (1947).
26. M. N. J. Dirken and H. J. Mook, *J. Physiol.*, **70**, 373 (1930).
27. M. N. J. Dirken and H. J. Mook, *J. Physiol.*, **73**, 349 (1931).
28. C. V. Paganelli and A. K. Solomon, *J. Gen. Physiol.*, **41**, 259 (1957).
29. D. C. Tosteson, *20th Intern. Congr. Physiol.* (1956).
30. F. J. W. Roughton and J. C. Rupp, *Ann. N. Y. Acad. Sci.*, **75**, *Art I*, 157 (1958).

General References to Parts 1 through 5

Chance, B., The accelerated flow method for rapid reactions, *J. Franklin Inst.*, **229**, 455, 613, 737 (1940).

Hartridge, H., and Roughton, F. J. W., A method of measuring the velocity of very rapid chemical reactions, *Proc. Roy. Soc.* (*London*), **B104**, 376 (1923).

Roughton, F. J. W., The time course of the heat effects in rapid chemical changes, *Proc. Roy. Soc.* (*London*), **A126**, 439 (1930).

Roughton, F. J. W., and Millikan, G. A., Photoelectric methods of measuring the velocity of rapid reactions, *Proc. Roy. Soc.* (*London*), **A155**, 258 (1936).

The Study of Fast Reactions. *Discussions of the Faraday Society*, **No. 17** (1954).

Bericht über das Internationale Kolloquium über Schnelle Reaktionen in Lösungen, *Z. Elektrochem.*, **64** (1960).

INTRODUCTION TO CHAPTERS XV–XX

Very Rapid Reactions in Solution

M. Eigen, *Max-Planck-Institut für physikalische Chemie, Göttingen*

Only one decade ago a reaction in solution with a half time shorter than 1 msec. would usually have been called "infinitely fast" or—with a little more reserve—"immeasurably fast."

This situation has changed appreciably within the last few years as demonstrated in Chapters XV–XX, the subjects of which were not included in the last edition (1953) of this volume. Since then, the measurable time range of chemical kinetics has been extended by almost as many orders of magnitude as apply in the former range of classical kinetics. If it is asked how this highly progressive development was initiated during the last few years, no unique new discovery could be named. The bases of most methods described in these chapters were known at least ten or twenty, or even more, years ago. Certainly, a good part of the recent development is simply a consequence of improved instrumentation, which has led to higher time resolution and sensitivity. However, the significant advances in the application of these techniques can be related to the approach to the problem, which can be characterized in this manner: "How can one use modern techniques or new principles in order to obtain information about the kinetics and mechanism of a given chemical reaction?" instead of, "What chemical systems are available in order to demonstrate certain physical effects?" The latter attitude toward the problem was as necessary for the earlier stages of development, as the former one was effective in its application to the problems of chemistry. As a result, many important elementary reactions in solution, such as radiational excitation, electron or proton transfer, ligand substitution, and structural transformation (isomerism, H-bond formation, hydration), have now been studied in great detail. These studies, in turn, permit analysis of more complex reaction mechanisms, such as enzymatic transformation or other processes of biological interest, although most such studies are still in a very early stage.

How can a reaction in solution proceeding in times shorter than one millisecond be studied experimentally? The following chapters will give many answers to this question. Before going into detail, it may be instructive to give a comparative survey of the different methods, their principles, application ranges, and restrictions.

There are two problems which arise during the study of fast reactions. The first concerns the initiation of the reaction and the second, the observation of its time course.

In one of the preceding chapters it has been shown how the classical principle of initiating a reaction by mixing the reactants can be extended to times of the order of milliseconds, utilizing flow techniques (*cf.* F. J. W. Roughton, Chapter XIV). Any further extension requires some new principle which avoids mixing. Two principal approaches proved to be useful:

1. The reaction system can be steadily disturbed by some (physical) kinetic process competing with the chemical transformation. If the physical process is known, the resulting stationary state of the system will give information about the chemical reaction rates. We shall call all the (indirect) methods utilizing this principle "competition methods."

2. A system that is in equilibrium or in a steady state of reaction can be subjected to a rapid perturbation (e.g., by changing external parameters, such as temperature or pressure, or by irradiation) and the resulting equilibration process is observed directly. This group of (direct) methods will be called "perturbation methods."

Let us begin with a survey of the first group, the competition methods. The *constant-flow technique*, as discussed in the preceding chapter, may be considered a typical example of this group. Competition occurs between the flow transport of the reaction mixture and the chemical change, and thus leads to a stationary distribution of reaction products in the observation tube. As already mentioned, the resolution time of this method is about 10^{-3} sec. Apart from this restriction, the method is most versatile when combined with sensitive detectors (*cf.* B. Chance, Chapter XIV).

Other transport processes that can be brought into competition with a chemical reaction are diffusion and ionic migration. On these processes are based the different *electrochemical methods* (*cf.* H. Strehlow, Chapter XV). If a homogeneous chemical reaction is involved in the depolarization process at an electrode, it will influence the current-voltage relationship. The polarographic technique, extensively described in Chapter XV, utilizes this principle. As diffusion in liquids is a comparatively slow process, in which the time constant is related to the mean square of displacement, the competitive influence of a fast chemical process will be decisive only in the very close vicinity of the electrodes. This, on the other hand, will set a lower limit of detectable reaction times. The behavior in a region of less than 10–20 A. around an electrode can hardly represent that of a homogeneous solution. Thus, the interpretation of results concerning the fastest chemical processes in aqueous solution, the protolytic reactions, may not be very reliable in some cases, even with respect to orders of magnitude. The most precise results are obtained with the method of catalytic currents

(*cf.* p. 806). Among other variants of the electrochemical methods, the so-called galvanostatic (p. 830) and potentiostatic (p. 838) methods deserve special mention. Here, the temporal changes of voltage or current that occur when a constant current or voltage, respectively, is applied to the electrode system are recorded. Although they utilize the competition principle, most of these electrochemical methods are only quasi-stationary with respect to the chemical reaction. A real stationary method is exhibited by a high-field technique, where competition between chemical reaction (i.e., charge production) and ion transport occurs in the well-defined space between the electrodes. (*cf.* p. 837). Unfortunately, this method is applicable only to liquids or solids of very low conductivity (i.e., some nonaqueous systems, ice crystals, etc.). The inverse of this method is also known. Particles that are consumed by a reaction can be supplied from an electrolysis process. In case of fast reactions the resulting stationary concentrations are quite low and the methods of their detection have to be sufficiently sensitive.

The principle of the last-mentioned method is rather similar to that of *photostationary techniques*, where a steady influx of light quanta (or other kind of radiation) is utilized to produce a stationary concentration of reactants, whose disappearance by chemical reaction competes with their production (p. 847). The method, of course, is restricted to photo- or radiation-chemical processes. It requires quantum yield measurements as well as the detection of the photoproduct. The time resolution depends essentially upon how small a concentration of photoproduct can be detected (*cf.* also H. W. Melville and S. M. Burnett, Chapter XX).

Generally, any physical process involving a finite lifetime, which depends upon the chemical state of the species, may be utilized in a competition method. A very elegant procedure is the measurement of *fluorescence transformation* (*cf.* p. 850). The chemical reaction of an electronically excited molecule results in detectable changes in the fluorescence spectrum. Since the lifetime of such an excited state is of the order of 10^{-8} sec., only reactions competing in this time range can be studied. On the other hand, the relative yields in the fluorescence spectrum can be measured so accurately that the rate constants derived from these data are quite precise. Rate constants of protolytic reactions have been measured by this method. Restrictions are primarily a result of the requirement of fluorescence transformation and of the finite time range of about 10^{-8} sec.

A chemical reaction usually is characterized also by production or consumption of heat. Thus not only matter transport but also heat transport processes can be utilized for a competition method. Measurements of this type have indeed been carried out (*cf.* R. P. Bell in ref. 1: "Thermal Maximum Method").

A special group, intermediate between the competition and perturbation methods, is that of *magnetic resonance* (electron spin and nuclear magnetic resonance). (*Cf.* H. Strehlow, Chapter XVII.) A finite lifetime of the chemical state of the species contributes to the broadening of the resonance line. In special cases, the (reciprocal) chemical lifetime can be directly related to the line width, the absolute value of which is independent of the frequency of the resonance line. Therefore, in a certain sense, the method might be compared to the direct methods, e.g., the relaxation methods. However it is not the chemical state but the spin system which is perturbated by the magnetic field. As in isotope techniques, the spin system serves only as a mode of labeling the different chemical species. Technically, the half-width of a resonance line can be determined only in relation to its frequency or frequency separation from the neighboring line of the transformed species. These frequencies serve as "clocks" for the determination of chemical half-lives, and this implies some similarity to the competition methods. The frequency separation of two lines also determines the time limits of the chemical processes that can be studied. For proton magnetic resonance, the detectable times from frequency separation are quite long, i.e., around 10^{-2} to 10^{-3} sec. (*cf.* p. 869 ff.). In other cases, they may become shorter, especially for T_2 (transverse relaxation) measurements involving paramagnetic nuclei. As the frequencies of electron spin resonance lines are appreciably higher than for nuclear spin lines, the detectable time constants become essentially shorter and may even reach 10^{-8} to 10^{-9} sec. Many variants of nuclear and electron spin techniques have been applied to the study of fast exchange reactions in solution. (Hitherto only magnetic resonance line broadening has been utilized for chemical rate studies, although, in principle, these effects might also be found with other resonance lines, e.g., in infrared spectra.)

Finally, the direct or *perturbation methods* deserve consideration. The stopped-flow technique (Chapter XIV) may be considered a classical analog of these methods. In this case, the perturbation is represented by the mixing process, followed subsequently by a direct observation of the proceeding reaction. Much higher time resolution can be realized if the perturbation is effected by other (external) means, e.g., an input of radiant energy. Absorption of energy from light quanta or accelerated particles yields unstable products, such as excited molecules or radicals which are far from their equilibrium state. Their disappearance during the re-establishment of equilibrium can be followed spectrophotometrically or conductometrically. The *flash photolysis methods* (*cf.* G. Porter, Chapter XIX) utilize this principle. The time resolution of present methods lies in the microsecond range. With time sampling, it was even possible to measure fluorescence decay processes in the mμ-sec. region. Restrictions are essentially a result of the types of reactions that can be initiated this way.

Another very general approach of studying fast reactions directly is represented by the *relaxation methods* (*cf.* M. Eigen and L. De Maeyer, Chapter XVIII). The principle of these techniques consists of rapidly changing an external parameter—such as pressure, temperature or electrical field density—which results in a perturbation of the equilibrium or steady state of reaction, with subsequent observation of the re-equilibration process. If the perturbation leads to only small shifts in the equilibrium concentrations, linearized rate equations can be applied and the equilibration process can be characterized by a discrete spectrum of relaxation times (the number of which is given by the number of independent reaction steps). The relaxation studies usually involve only such linear processes (small perturbations), but this restriction is not significant as long as a mathematical treatment of the non-linear process is practicable. The different methods (described in Chapter XVIII) include step or pulse techniques (pressure-shock-, T-jump, and electrical-pulse methods) as well as periodic oscillations where relaxation processes cause phase shift between external and internal parameters (e.g., sound-absorption and dielectric-loss techniques). At present, these methods cover the time range between 1 and $\lesssim 10^{-9}$ sec. The restrictions are set by the requirement of an equilibrium state, which, however, can be very much to one side (e.g., with a molar ratio of 10^{-8}, or even less, depending on the sensitivity of detection). The absorption and dispersion techniques however, require, a relatively high concentration of the reacting species (usually $>10^{-3}M$), which is a very restrictive condition for many chemical problems. The other relaxation techniques are better adjusted to the requirements of chemical studies, especially if they are combined with specific methods of detection, such as spectrophotometry, conductimetry, or polarimetry. The equilibrium should depend on one of the parameters mentioned above; but even this is not a necessary condition, if coupling to another p-, T-, or E-*dependent* equilibrium (e.g., a buffer) is possible.

Generally, the direct methods have some advantages in the study of complex reaction systems, as the different steps of a chemical transformation occur directly on the time or frequency axis. Also, the interpretation of a directly measured time function generally involves only minor difficulties, whereas the data obtained by competition methods still require theoretical treatment. On the other hand, there are processes, such as the transfer of a proton or an electron between two identical species, which cannot be detected by direct methods, as they do not represent a macroscopic reaction. Furthermore, some of the indirect techniques are appreciably simpler to work with, since direct measurements made at times less than 1 μsec. usually require relatively extensive and expensive instrumentation. We may conclude our survey with a graph (see Fig. 1) summarizing the

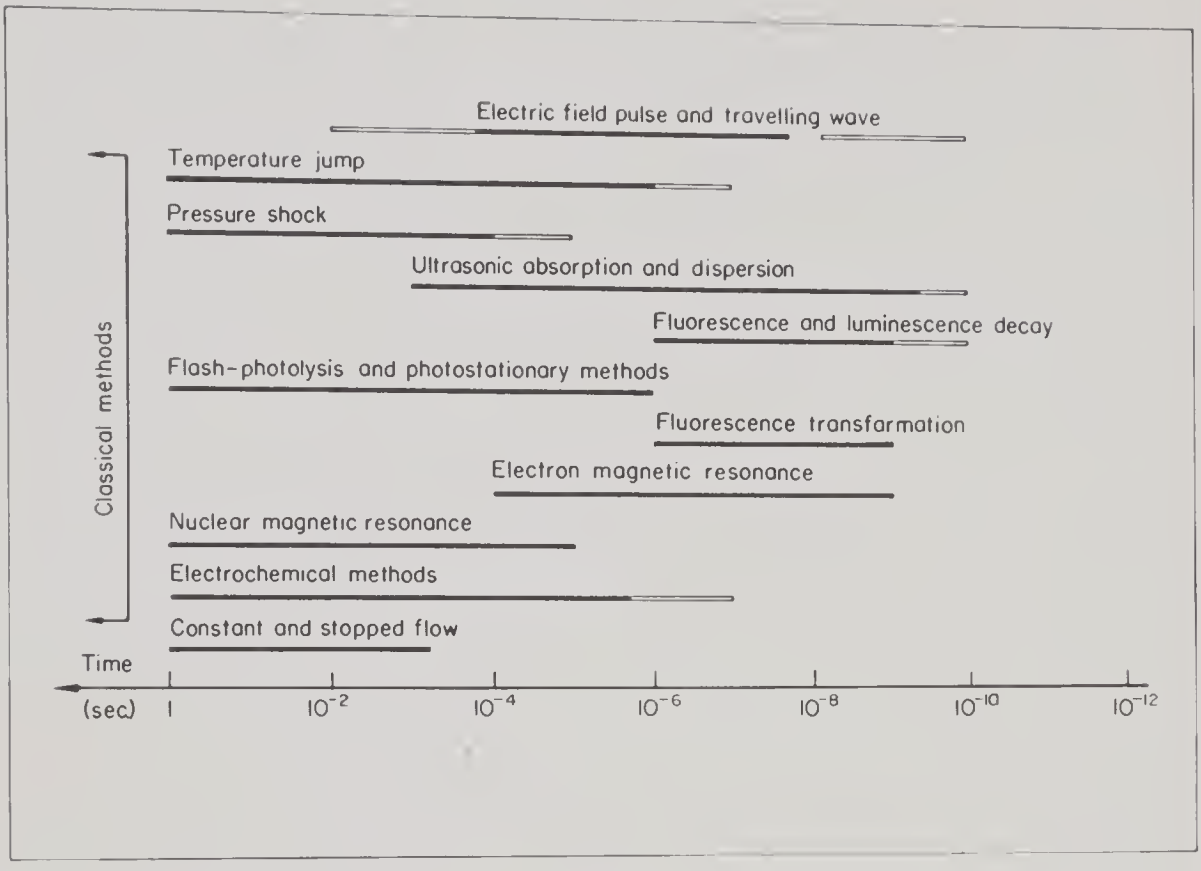

Figure 1

principal methods and their approximate ranges of applicability. There remains only a very small range in which processes, normally considered "chemical," are not yet accessible for experimental observation. Of course, each of the methods has its particular restrictions, but the methods are supplementary and their variety is large enough to permit one to hope that most problems will "find" their method.

General References*

"The Study of Fast Reactions," *Discussions Faraday Soc.* **17** (1954).

"Fast Reactions in Solution," *Z. Elektrochem., Ber. Bunsenges. physik. Chem.* **64**, No. 1 (special issue) (1960).

* References to the original papers are to be found in the corresponding chapters. The different authors therefore have not been named in this comparative survey.

CHAPTER XV

ELECTROCHEMICAL METHODS

H. Strehlow *Max-Planck-Institute für physikalische Chemie, Göttingen*

I. Introduction 799
II. The Polarographic Method 801
1. The Reaction Layer Concept 801
2. Calculated Ratios $\bar{i}/\bar{i}_d$ for Different Reaction Schemes 807
3. Experimental Arrangement and Estimation of Errors 812
4. The Reaction Rate for the Recombination of Protons with Anions of Weak Acids 815
5. Experimental Results for Non-Protolytic Reactions 818
III. Electrolysis under Constant Current. Chronopotentiometry 824
1. The Transition Time τ 824
2. Kinetic Currents in Chronopotentiometry. The Reaction Layer Concept 827
3. Calculated Transition Times for Different Reaction Schemes 828
4. Experimental Technique 830
5. Experimental Results 832
IV. Other Electrochemical Methods for the Measurement of Fast Reaction Rates 834
1. The Rotating Disc 834
2. The Stationary-Field Method 837
3. The Potentiostatic Method 838
4. Further Possible Methods 840
References 840
General References 843

I. INTRODUCTION

This chapter is concerned with methods of measuring fast reactions that are of a more indirect nature than relaxation methods or flash photolysis. Whereas, in the latter cases, concentration changes are observed directly as a function of time, in polarography (and other electrochemical methods), the competition between diffusion and reaction determines, in a rather complicated way, the intensity of an electric current. But these disadvantages are at least partly outweighed by the fact that in polarography much experimental and theoretical knowledge has been gained from non-kinetic applications. Well-designed and practically approved apparatus

is commercially available. The electrochemical methods are in rapid progress.

In this chapter, polarographic and other electrochemical applications to the study of fast reactions will be discussed. Following a simplified introduction to the underlying physical principles, the more rigorous solutions for different kinetic systems are given, omitting their complex derivations. These were obtained mainly by Koutecký and co-workers. This may prove useful, since many important papers in the field are published in Czechoslovakian journals and are, therefore, not easily accessible to many interested readers. Rate constants calculated from polarographic or chronopotentiometric data are given in tables. Critical remarks are made on some of the results, and the conditions necessary for obtaining reliable results are outlined.

Since the experimental procedures for polarography have been dealt with elsewhere in this series, and in other monographs, only a few comments of special relevance to the application to kinetic research will be added here. This chapter should, therefore, be considered a supplement to the existing monographs cited at the end of the chapter.

Since Wiesner and Brdička (1) first demonstrated the applicability of polarography to the measurement of very fast reaction rates in 1943, many papers have appeared on this new method. Theoretical progress was made, especially by Koutecký, by solving the rather involved mathematical equations that govern the kinetically determined electric current to the dropping mercury electrode. Experimentally, many chemical reactions of organic and inorganic substances have been investigated. Furthermore, promising new electrochemical experimental procedures have been developed with certain advantages over polarography. Of these methods, electrolysis under constant current, the rotating disc electrode, and the potentiostatic method will be dealt with in subsequent sections.

Though considerable progress has been made during the last fifteen years and although much valuable information has been obtained, the kinetics of the investigated systems in some cases seem more complicated than assumed by the authors With protolytic reactions, especially results are not always in harmony with data from nonelectrochemical methods. Nevertheless, electrochemical processes are a valuable and promising means of obtaining kinetic data of fast reactions, if critically applied.

An important advantage of polarography and other electrochemical methods described in this chapter is the simple and inexpensive equipment required, compared with the more recent experimental techniques discussed in other chapters of this volume. On the other hand, the theoretical evaluation of kinetic constants from the measured quantities may be rather an intricate process.

II. THE POLAROGRAPHIC METHOD

Polarography can be used as a powerful tool in kinetic research in two different ways. A very obvious application is given by the fact that polarography is a microanalytical method. A series of many analyses can be effected, each within the drop time (about 2 sec.), and practically without change in the solution under investigation. The recorder of the polarograph is used to register the change of concentration with time, the polarizing voltage being kept constant at a suitable value. Such measurements have been carried out to a large extent but obviously can only be applied if the reaction time is greater than about 30 sec. So this method (2) does not apply to very fast reactions and will not be considered here. Another less important drawback, which is valid for all electrochemical kinetic methods, is the necessity of working in relatively concentrated solutions of an inert electrolyte.

There is, however, an indirect polarographic method by which even the most rapid reactions can be measured. The main contributions in this field have been made by Czechoslovakian workers, although some important papers have also been published by Japanese, American, and German authors.

1. The Reaction Layer Concept

The two most important reaction schemes will be discussed here on the basis of the reaction layer concept in order to provide a qualitative picture of the underlying physical principles (2a).

The electrochemical reaction is preceded by a chemical reaction which is kinetically of the first order.

$$\mathrm{B} \underset{k_2}{\overset{k_1}{\rightleftharpoons}} \mathrm{A} \xrightarrow{e} \mathrm{R} \qquad \text{(I)}$$

(In the following, the depolarizer will be designated by the letter A and the product of the electrode reaction by R. Electro-inactive reacting substances, which are not reduced or oxidized at the electrode at the voltage in question, are denoted by B, C, etc.) As an example of reaction scheme (I), we may consider the recombination of a proton with the anion of a α-ketocarbonic acid, e.g., pyruvic acid.

$$\mathrm{CH_3COCOO^-} + \mathrm{H^+} \underset{k_2}{\overset{k_1}{\rightleftharpoons}} \mathrm{CH_3COCOOH} \xrightarrow{e,\ \mathrm{H^+}} \mathrm{CH_3CHOHCOOH} \qquad \text{(Ia)}$$

or, as an abbreviation,

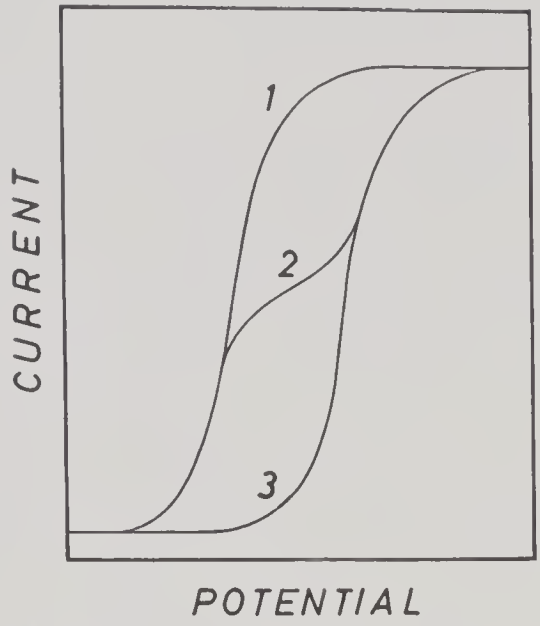

Fig. 1. Polarograms of pyruvic acid at three pH values. Curve 1: pH = 4, curve 2: pH = 6; curve 3: pH = 8.

$$A^- + H^+ \underset{k_2}{\overset{k_1}{\rightleftharpoons}} HA \xrightarrow{e,\ H^+} R \qquad \text{(Ia)}$$

In a well-buffered solution, this reaction is pseudomonomolecular. The acid HA is reduced at a more positive voltage than the anion (Fig. 1). At low pH, only the wave of the free acid results and in alkaline solution only the wave of the anion; at intermediate pH values (about pH 6) a double wave is observed.

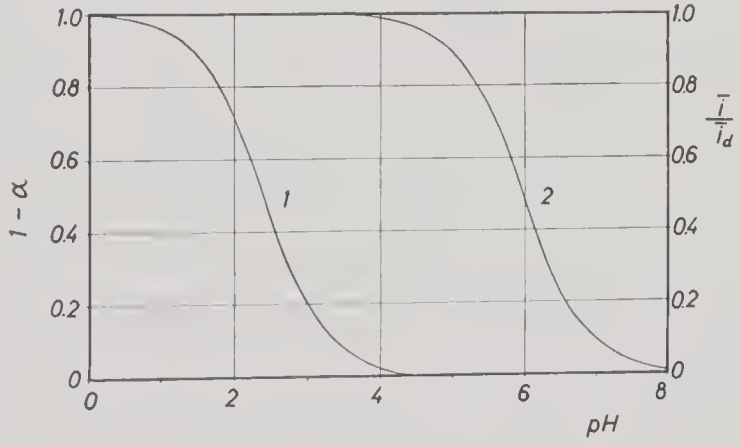

Fig. 2. $1 - \alpha$ and $\bar{\imath}/\bar{\imath}_d$ for pyruvic acid plotted against pH. Curve 1, $1 - \alpha$; curve 2, $\bar{\imath}/\bar{\imath}_d$.

In Figure 2 the ratio of the first to the second wave is plotted against pH. The curve strongly resembles a dissociation-pH diagram of a weak acid with $pK = 6$, if we take

$$\bar{\imath}/\bar{\imath}_d = (1 - \alpha) = [HA]/([HA] + [A^-]) \qquad (1)$$

where α is the degree of dissociation. But, in fact, pyruvic acid is rather a strong acid ($pK = 2.4$), and this simple explanation of the double wave fails.

The equilibrium concentration of the free acid [HA] at pH 6 is only a minute fraction of the concentration of the anion. The diffusion current from this small equilibrium concentration of HA is immeasurably small and may be safely neglected.

In the diffusion layer at the electrode, the concentration of HA is reduced still further, the equilibrium (Ia) is disturbed, and undissociated acid is formed according to

$$d[\mathrm{HA}]/dt = k_1[\mathrm{A}^-][\mathrm{H}^+] - k_2[\mathrm{HA}] \tag{2}$$

with $k_2/k_1 = K_D$.

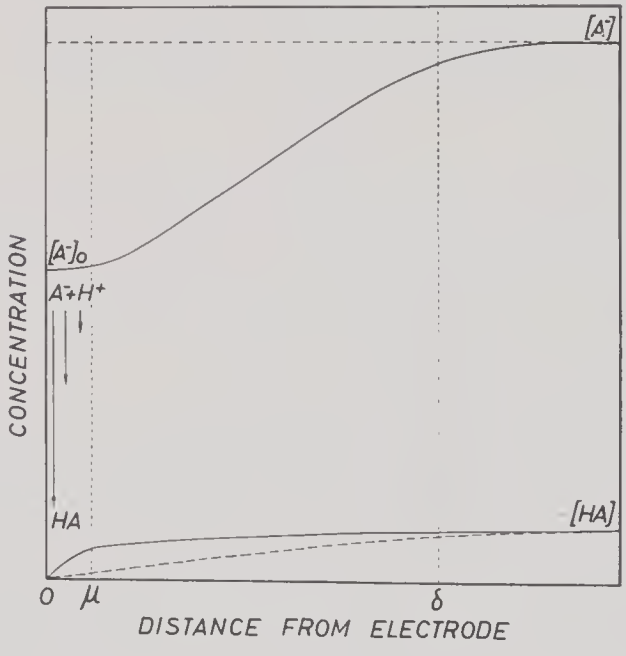

Fig. 3. Concentration-distance diagram for the reduction of pyruvic acid.

The situation is clarified by Figure 3. The concentration of A^- and HA are plotted against the distance x from the electrode for pH 6, at a voltage suitable for the first wave and for the end of the drop time t. For clarity, the concentration [HA] is grossly exaggerated. Here, δ is the thickness of the Nernst diffusion layer at a dropping mercury electrode.

$$\delta \equiv c/(\partial c/\partial x)_{x=0} = (3\pi Dt/7)^{1/2}$$

If there were no reaction, the reaction profile would be given by the dotted curves. The lengths of the arrows symbolize the rate of the reaction, which, according to Equation (2), is greatest in the immediate neighborhood of the electrode where [HA] = 0. The chemical reaction changes the con-

centration profile to the solid curves. The concentration gradient of [HA] at $x = 0$ becomes much steeper, and the current, which is proportional to the concentration gradient of the reducible substance, is correspondingly increased. A "thin reaction layer" of thickness μ may now be defined, similar to the much thicker diffusion layer δ (3). Of course, the anions, which react in the reaction layer, must diffuse there through the diffusion layer. The kinetic current $\bar{\imath}_k$, averaged over the drop time, is given by the product of the mean production rate of HA per unit volume $d[\mathrm{HA}]/dt$ in the reaction layer, the reaction volume $A\mu$, where A is the averaged electrode area, and the charge zF necessary for the reduction of one mole of HA.

$$\bar{\imath}_k = zF(d[\mathrm{HA}]/dt)A\mu = zF\, k_1[\mathrm{A}^-]_0[\mathrm{H}^+]A\mu \tag{3}$$

$[\mathrm{A}^-]_0$ is the almost constant concentration of A^- within the reaction layer.*

The current is also determined by the diffusion of anions to the electrode, according to the well-known Ilkovič equation for diffusion-controlled currents,

$$\bar{\imath}_k = \kappa([\mathrm{A}^-] - [\mathrm{A}^-]_0) \tag{4}$$

where κ is the known proportionality constant between diffusion current and concentration. $\kappa[\mathrm{A}^-]$ is equal to $\bar{\imath}_d$, the diffusion current given by the second wave, so that

$$[\mathrm{A}^-]_0 = (\bar{\imath}_d - \bar{\imath}_k)/\kappa \tag{5}$$

With Equation (5), the unknown $[\mathrm{A}^-]_0$ may be eliminated from Equation (3), and, after rearrangement of terms, we get

$$\bar{\imath}_k/\bar{\imath}_d = (zF\mu A k_1[\mathrm{H}^+])/(\kappa + zF\mu A k_1[\mathrm{H}^+]) \tag{6}$$

Since κ is proportional to $D^{1/2}At^{-1/2}$, where t is the drop time of the electrode, Equation (6) may be written

$$\bar{\imath}_k/\bar{\imath}_d = (a\mu D^{-1/2}k_1[\mathrm{H}^+]t^{1/2})/(1 + a\mu D^{-1/2}k_1[\mathrm{H}^+]t^{1/2}) \tag{7}$$

where a may be calculated from the known value of κ, and turns out to be $(7/3\pi)^{1/2}$. The only unknown quantities in Equation (7) are the required k_1 and the thickness of the reaction layer μ. For an estimate of μ, we assume equilibrium outside μ and a stationary state within the reaction layer, which is approximately true. In other words, the HA molecules produced in the reaction layer are transported to the electrode by diffusion. There-

* If the area A is given in cm.^{2} and concentrations in moles per liter instead of moles per cm.^{3}, the Faraday constant F in Equation (3) must be replaced by $F/1000$ in order to obtain $\bar{\imath}_k$ in amperes. This remark applies to all following equations for the polarographic current.

fore, by Fick's first law, the current $\bar{i}_K$ is proportional to the concentration gradient of HA at $x = 0$.

$$\bar{i}_K = zFAD(\partial[\mathrm{HA}]/\partial x)_{x=0} \tag{8}$$

or with the definition of μ in mind,

$$\bar{i}_K = zFAD([\mathrm{HA}]_\mu/\mu) \tag{9}$$

where $[\mathrm{HA}]_\mu$ is the concentration of HA at $x = \mu$. From Equations (3) and (9), we have

$$\mu^2 = (D[\mathrm{HA}]_\mu)/(k_1[\mathrm{A}^-]_0[\mathrm{H}^+]) \tag{10}$$

Since equilibrium exists at $x = \mu$,

$$([\mathrm{A}^-]_0[\mathrm{H}^+])/[\mathrm{HA}]_\mu = K_D$$

and

$$\mu = [D/(k_1 K_D)]^{1/2} \tag{11}$$

with a possible factor of the order of magnitude one. Combining Equations (11) and (7), we have

$$\frac{\bar{i}_k}{\bar{i}_d} = \frac{a[(k_1/K_D)t]^{1/2}[\mathrm{H}^+]}{1 + a[(k_1/K_D)t]^{1/2}[\mathrm{H}^+]} \tag{12}$$

According to a more rigorous calculation (4), the constant a has the value 0.886. Different diffusion coefficients of HA and A^- and spherical diffusion lead to minor corrections of formula (12), as given later in Equation (17). For the rate of recombination of protons and pyruvate ions, $k_1 = 1.3 \times 10^{10}$ l./mole sec. has been obtained (5). (See Table IV, p. 816.) For a monomolecular reaction which precedes the proper electrode reaction,

$$\mathrm{B} \underset{k_2'}{\overset{k_1'}{\rightleftharpoons}} \mathrm{A} \xrightarrow{e} \mathrm{R} \qquad \text{with } k_2'/k_1' = K' \tag{I}$$

k_1 in Equation (12) must be replaced by $k_1'/[\mathrm{H}^+]$, and K by $[\mathrm{H}^+]K'$. Thus, for a reaction which proceeds according to reaction scheme (I), we have

$$\frac{\bar{i}_k}{\bar{i}_d} = \frac{0.886[(k_1'/K')t]^{1/2}}{1 + 0.886[(k_1'/K')t]^{1/2}} \tag{12a}$$

The applications of formula (12) to specific cases are given below, (4,5) together with a discussion of the conditions necessary for a correct kinetic interpretation of polarographic data.

Another important case of polarographic kinetic currents is given when the product of depolarization R reacts with a third electroinactive substance B, with the reformation of the depolarizer.

$$A \xrightarrow{e} R \qquad R + B \underset{k_2}{\overset{k_1}{\rightleftharpoons}} A + R' \tag{VI}$$

B is not reduced at the electrode potential at which the electrode reaction of scheme (VI) proceeds. The net reaction of scheme (VI) is $B \xrightarrow{e} R'$, so that A, the depolarizer, acts as a catalyst for the reduction of B. Therefore polarographic currents that are the consequence of a reaction proceeding according to reaction scheme (VI) have been called catalytic currents. The dependence of catalytic currents on the parameters involved will, again, be treated first with the reaction layer concept to provide a basic physical understanding.

To be specific, we shall discuss the reduction of hydroxylamine by Fe^{2+} ion (6).

$$Fe^{3+} \overset{e}{\rightleftharpoons} Fe^{2+} \qquad Fe^{2+} + NH_2OH \xrightarrow{k'} Fe^{3+} + NH_2\cdot + OH^- \tag{VIa}$$

The radical $NH_2\cdot$, the primary reduction product of NH_2OH, oxidizes another Fe^{2+} in a very fast reaction.

$$Fe^{2+} + NH_2\cdot + H_2O \rightarrow Fe^{3+} + NH_3 + OH^-$$

The concentration of NH_2OH is made far greater than that of Fe^{3+}, so that $[NH_2OH]$ is practically constant. Figure 4, which is analogous to

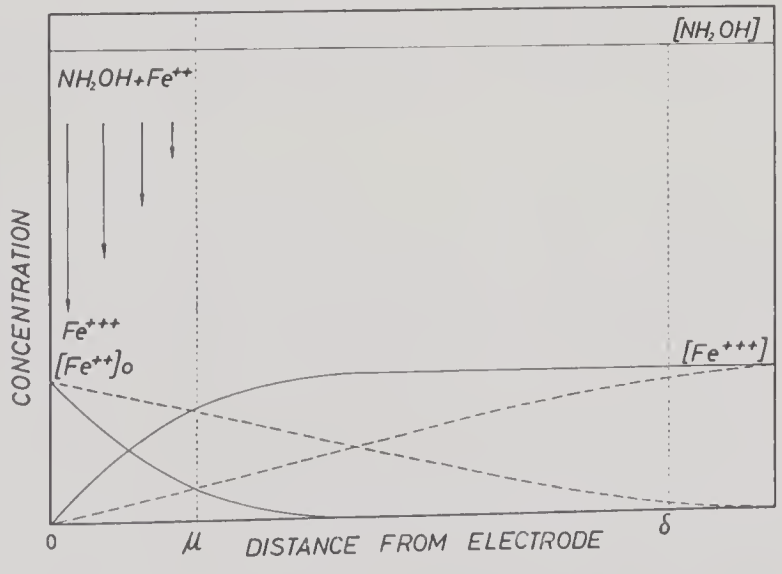

Fig. 4. Concentration-distance diagram for the catalytic reduction of hydroxylamine by ferrous ion.

Figure 3, shows the concentration-distance diagram. The kinetic current is given by [compare Equation (3)]

$$\bar{i}_k = zFA\mu k[NH_2OH][Fe^{2+}]_0 \tag{13}$$

where $k = 2k'$ because of the following rapid reactions of scheme (VIa). The equivalent equation to Equation (9) is

$$\bar{i}_K = zFA(\partial[Fe^{3+}]/\partial x)_{x=0} = zFAD([Fe^{3+}]_\mu/\mu) \approx zFAD[Fe^{2+}]_0/\mu \tag{14}$$

From Equations (13) and (14) we obtain, for μ,

$$\mu = (D/k[NH_2OH])^{1/2} \tag{15}$$

and

$$\bar{i}_k = zFA(Dk[NH_2OH])^{1/2}[Fe^{2+}]_0 = zFA(Dk[NH_2OH])^{1/2}[Fe^{3+}] \tag{16}$$

$[Fe^{2+}]_0$ is equal to $[Fe^{3+}]$ (provided the diffusion coefficients of Fe^{2+} and Fe^{3+} are equal). Since the diffusion current due to the reduction of Fe^{3+} is proportional to $AD^{1/2}t^{-1/2}[Fe^{3+}]$ and the total current $\bar{i}$ is the sum of the kinetic current $\bar{i}_k$ and the diffusion current $\bar{i}_d$, Equation (16) may be written:

$$\bar{i}/\bar{i}_d = a(k[NH_2OH]t)^{1/2} + 1 \tag{16a}$$

The proportionality a becomes 0.813, according to rigorous calculation (7). It must be borne in mind, however, that Equation (16a) is only an asymptotic solution for high concentrations of NH_2OH. At low hydroxylamine concentration, Equation (16a) must fail because reaction (VIa) is no longer pseudomonomolecular. Furthermore, the reaction layer must be small compared to the diffusion layer, or $k[NH_2OH]t \gg 1$. The complete solution of the problem is given below [Equation (25)].

The reaction constant k, which was obtained by Koryta for reaction (VIa) with triethanolamine, ferric ions, and NH_2OH, is 396 l./mole sec., and therefore $k' = 198$ l./mole sec. By using a direct method, a value of 186 was determined for k', which compares very favorably with the polarographic result (6).

2. Calculated Ratios $\bar{i}/\bar{i}_d$ for Different Reaction Schemes

In this section, the results obtained by Koutecký and co-workers are given in a condensed form. Applications will be dealt with in Section II.4

Case 1. The electrode reaction is preceded by a monomolecular (or pseudomonomolecular) reaction according to

$$B \underset{k_2}{\overset{k_1}{\rightleftharpoons}} A \xrightarrow{e} R \qquad k_2/k_1 = K \tag{I}$$

In the more general case (8) of $D_A \neq D_B$ and correcting for spherical diffusion (9), Equation (12a) (ref. 4) becomes

$$\frac{\bar{i}}{\bar{i}_d} = \frac{0.886[(k_1/K)t]^{1/2}M}{1 + 0.886[(k_1/K)t]^{1/2}M} - \frac{11D^{1/2}m^{-1/3}t^{1/6}(k_1t/K)^{1/4}M^{1/2}}{1 + 0.14(k_1t/K)M^2} \tag{17}$$

with

$$D = (D_A + KD_B)/(1 + K) \quad \text{and} \quad M = (D/D_B)(D_A/D_B)^{1/2} \tag{17a}$$

The last term approximates a function tabulated by Koutecký and Čižek (9); it is a correction term for spherical diffusion that does not exceed about 5% of the first term on the right side of Equation (17) and, therefore, may often be ignored; m is the outflow of mercury (in milligrams per second), and t is the drop time of the electrode. Equation (17) holds if $K \gg 1$ and $(k_1 + k_2)t \gg 1$, that is, only for sufficiently rapid reactions.

Case 2. The electrode reaction is preceded by two consecutive monomolecular (or pseudomonomolecular) reactions according to

$$A_1 \underset{k_2}{\overset{k_1}{\rightleftharpoons}} A_2 \underset{k_4}{\overset{k_3}{\rightleftharpoons}} A_3 \xrightarrow{e} R \tag{II}$$

$\bar{i}_k/\bar{i}_d$ is then given by (10)

$$\bar{i}/\bar{i}_d = 0.886\, ht^{1/2}/(1 + 0.886\, ht^{1/2}) \tag{18}$$

with

$$h \equiv \frac{\bar{k}_1\bar{k}_3}{\sqrt{D}\,\bar{k}_4}\left\{(\lambda_2^{1/2} + \lambda_3)^{1/2}\left[\bar{l}_1 + \frac{\bar{l}_1^2 + \bar{k}_2\bar{k}_3}{(\lambda_2\lambda_3)^{1/2}}\right]\right\}^{-1} \tag{18a}$$

$$\bar{l}_1 \equiv \bar{k}_1 + \bar{k}_2 \qquad \bar{l}_2 \equiv \bar{k}_3 + \bar{k}_4$$

$$\bar{k}_1 \equiv k_1/D_1 \qquad \bar{k}_2 \equiv k_2/D_2 \qquad \bar{k}_3 \equiv k_3/D_3 \qquad \bar{k}_4 \equiv k_4/D_3$$

$$\lambda_{2,3} \equiv {}^1/_2\{\bar{l}_1 + \bar{l}_2 \pm [(\bar{l}_1 + \bar{l}_2)^2 + 4\bar{k}_2\bar{k}_3]^{1/2}\}$$

and

$$D \equiv \frac{D_1 + (k_1/k_2)D_2 + [(k_1k_3)/(k_2k_4)]D_3}{1 + (k_1/k_2) + [(k_1k_3)/(k_2k_4)]}$$

The rate constants evaluated by Equation (18), show a rather sensitive dependence on the exact values of the equilibrium constants k_1/k_2, k_3/k_4, and D_1/D_2.

Case 3. A bimolecular reaction precedes the electrode reaction according to

$$B \underset{k_2}{\overset{k_1}{\rightleftharpoons}} 2A \xrightarrow{e} R \tag{III}$$

We define $x = k_1 t[\mathrm{B}]K$, where t is the drop time and $K = k_2/k_1 = [\mathrm{B}]/[\mathrm{A}]^2$. [B] is the concentration of the dimer and [A] that of the monomer in the solution. Then, if $[\mathrm{B}] \gg [\mathrm{A}]$ and $k_1 t \gg 1$, the following relation exists between x and $\bar{i}/\bar{i}_d$:

$$x = 2.20 \frac{(\bar{i}/\bar{i}_d)}{[1 - (\bar{i}/\bar{i}_d)]^{3/4}} - 2.68\ (\bar{i}/\bar{i}_d)^5 \qquad (19)$$

Equation (19) is a close approximation of a function tabulated by Koutecký and Hanuš (11). The first term on the right side of Equation (19) is of the same form as the approximate solution obtained with the reaction layer concept (12). The diffusion current $\bar{i}_d$ would be measured if k_1 were infinitely great.

Case 4. The electrode reaction is preceded by a rapid bimolecular reaction according to

$$\mathrm{B} \underset{k}{\rightleftharpoons} \mathrm{A} + \mathrm{C} \qquad \mathrm{A} \xrightarrow{e} \mathrm{R} \qquad \text{(IV)}$$

If the reaction is rapid and the equilibrium is shifted to the left, the ratio $\bar{i}/\bar{i}_d$ is given by (13)

$$\bar{i}/\bar{i}_d = G(\beta) \qquad (20)$$

where β is defined by

$$\beta = (kK^2 t/[\mathrm{B}]) \cdot (D_\mathrm{A}/D_\mathrm{B}) \cdot (D_\mathrm{C}/D_\mathrm{B})^{1/2} \qquad \text{and} \qquad K = ([\mathrm{A}][\mathrm{C}])/[\mathrm{B}] \qquad (21)$$

and the function G is tabulated for different values of β in Table I.

TABLE I

β	$G(\beta)$	β	$G(\beta)$	β	$G(\beta)$
7.29×10^{-5}	0.037	7.29×10^{-2}	0.304	15.8	0.84
5.83×10^{-4}	0.073	0.126	0.349	37.3	0.87
1.97×10^{-3}	0.106	0.299	0.429	72.9	0.91
4.67×10^{-3}	0.139	0.583	0.496	126	0.921
9.12×10^{-3}	0.169	1	0.553	200	0.946
1.58×10^{-2}	0.199	1.60	0.601	299	0.950
2.50×10^{-2}	0.227	2.39	0.642	583	0.96
3.73×10^{-2}	0.254	3.40	0.677	4670	0.99
5.32×10^{-2}	0.279	4.67	0.71		

Case 5. A substance B undergoes rapid dismutation into a depolarizer A and another substance C, which is identical with the product of depolarization.

$$\mathrm{B} \underset{k}{\rightleftharpoons} \mathrm{A} + \mathrm{C} \qquad \mathrm{A} \xrightarrow{e} \mathrm{C} \qquad \text{(V)}$$

In this case, the ratio $\bar{\imath}/\bar{\imath}_d$ is given by (13)

$$\bar{\imath}/\bar{\imath}_d = G(\beta/2) \tag{22}$$

where β and G are again defined by Equation (21) as in Table I.

Case 6. The depolarization product R reacts in a pseudomonomolecular reaction, producing the depolarizer A. This is the case of catalytic currents, which has already been treated with the reaction layer concept.

$$\mathrm{A} \xrightarrow{e} \mathrm{R} \qquad \mathrm{R} \underset{k_2}{\overset{k_1}{\rightleftharpoons}} \mathrm{A} \tag{VI}$$

For $(k_1 + k_2)t > 10$, the solution of the problem is given by (7)

$$\bar{\imath}/\bar{\imath}_d = 0.812[(k_1 + k_2)t]^{1/2} + 1.92[(k_1 + k_2)t]^{-7/6} \tag{23}$$

Formula (23) has not yet been corrected for spherical diffusion. If we call $(k_1' + k_2')$ the uncorrected value of the sum of the kinetic constants obtained by the application of formula (23), the true constants k_1 and k_2 are given approximately by

$$k_1 + k_2 = (k_1' + k_2')(1 - 35D^{1/2}m^{-1/3}t^{1/6})^{-2} \tag{24}$$

where D, m, and t have the same meaning as in Equation (17). The cor-

TABLE II

x	$\Psi(x)$	$\phi(x)$
0	1	0
0.05	1.013	0.0075
0.1	1.027	0.0156
0.2	1.054	0.0314
0.4	1.104	0.0605
0.6	1.154	0.0902
0.8	1.204	0.1202
1.0	1.250	0.1479
1.2	1.297	0.1765
1.4	1.342	0.2042
1.6	1.386	0.2314
1.8	1.428	0.2574
2.0	1.47	0.28
2.5	1.56	0.34
3.0	1.66	0.40
3.5	1.75	0.46
4	1.84	0.52
5	2.01	0.63
6	2.17	0.74
7	2.31	0.83
8	2.45	0.93
9	2.57	1.01
10	2.69	1.09

rected form, Equation (24), is justifiable since Equations (23) and (24) have proved fairly reliable (see Table V). For values of $(k_1 + k_2)t < 10$, the ratio $\bar{\imath}/\bar{\imath}_d$ is given by (7,14)

$$\bar{\imath}/\bar{\imath}_d = \Psi[(k_1 + k_2)t] - 50.4D^{1/2}m^{-1/3}t^{1/6}\,\phi[(k_1 + k_2)t] \qquad (25)$$

The two functions $\Psi(x)$ and $\phi(x)$ are given in Table II for arguments $0 < x < 10$.

Case 7. The depolarization product R is decomposed under the action of a catalyst C, producing a half mole of the depolarizer A.

$$\mathrm{A} \xrightarrow{e} \mathrm{R} \qquad \mathrm{R} + \mathrm{C} \xrightarrow{k} {}^1/_2\,\mathrm{A} + \mathrm{C} \qquad \text{(VII)}$$

With $x = k[\mathrm{C}]t$, we have (15)

$$\bar{\imath}/\bar{\imath}_d = 1 + x/(7.42 + 1.25x) \qquad \text{for } 0 < x < 10 \qquad (26)$$

For large values of x, an approximate solution is given by

$$\bar{\imath}/\bar{\imath}_d = 2(0.886x^{1/2})/(1 + 0.886x^{1/2}) \qquad (27)$$

Case 8. The depolarization product R undergoes irreversible dismutation into the depolarizer A and another substance R′.

$$2\mathrm{A} \xrightarrow{e} 2\mathrm{R} \xrightarrow{k} \mathrm{A} + \mathrm{R}' \qquad \text{(VIII)}$$

The ratio $\bar{\imath}/\bar{\imath}_d$ is given by (16)

$$\bar{\imath}/\bar{\imath}_d = f(2[\mathrm{A}]kt) \qquad (28)$$

where the function $f(z)$ is given in Table III.

TABLE III

z	$f(z)$	z	$f(z)$
0.5	1.022	3.0	1.110
1.0	1.043	3.5	1.124
1.5	1.062	4.0	1.137
2.0	1.079	4.5	1.15
2.5	1.095	5.0	1.16

Case 9. The depolarization product R reacts in a bimolecular reaction with another substance B with the reformation of the depolarizer A.

$$\mathrm{A} \xrightarrow{e} \mathrm{R} \qquad \mathrm{R} + \mathrm{B} \xrightarrow{k} \mathrm{A} + \mathrm{C} \qquad \text{(IX)}$$

Further, the possibility is considered that C reacts very fast with $\alpha - 1$ moles of R to give $\alpha - 1$ more moles of A, so that, altogether, α moles of A are formed in the total reaction, which is kinetically determined by the bimolecular reaction (IX). (See the discussion of the catalytic reduction of NH_2OH by Fe^{2+} in Section II.1. In that case, $\alpha = 2$.) The ratio $\bar{i}/\bar{i}_d$ is given by (17,18)

$$\bar{i}/\bar{i}_d = (\bar{i}/\bar{i}_d)_\infty[(0.37u + 1)^{1/2} - 0.37u] \tag{29}$$

where

$$u = [\mathrm{A}][(kD_\mathrm{R}l)/(\alpha[\mathrm{B}]D_\mathrm{B})]^{1/2}$$

and

$$(\bar{i}/\bar{i}_d)_\infty = 0.812([\mathrm{B}]k\alpha t)^{1/2}$$

is the ratio of $\bar{i}/\bar{i}_d$ when $[\mathrm{B}] \gg [\mathrm{A}]$ and we have *Case 6*, the catalytic current with a pseudomonomolecular reaction. Equation (29) is only valid for $\bar{i}/\bar{i}_d \geq 3$.

Case 10. A substance A is reduced (or oxidized) at the electrode and the product reacts to an electrode inactive compound C

$$\mathrm{A} \xrightarrow{e} \mathrm{R}$$

$$\mathrm{R} \underset{k_2}{\overset{k_1}{\rightleftharpoons}} \mathrm{C} \qquad K = k_1/k_2 \tag{X}$$

If the redox potentials A/R and A/C are different, the half-wave potential $E_{1/2}$ at a dropping mercury electrode will depend on the velocity of reaction (X) according to (ref. 18a).

$$E_{1/2} = E_{1/2(k=\infty)} - (RT/zF) \ln 0.886\ [(D_\mathrm{R}/D_\mathrm{C})(k_2/K)t]^{1/2} \tag{30}$$

$E_{1/2(k=\infty)}$ is the redox potential that is not influenced by the kinetics of the reaction and may be obtained at an equilibrium electrode. An example of *Case 10* has been given by Koryta (18b).

3. Experimental Arrangement and Estimation of Errors

From an experimental standpoint, it is of great advantage for the polarographic determination of rate constants that polarography is a well-developed and relatively simple experimental method and that good equipment is commercially available. The polarographic technique proper has been dealt with elsewhere (19) so that only two specific points for the study of kinetically determined current need be considered here.

A fairly simple procedure allows one to recognize whether a polarographic current is a diffusion current or is determined by kinetic rate processes. According to the equation of Ilkovič, the diffusion current $\bar{\imath}_d$ is proportional to $m^{2/3}t^{1/6}$. With a given capillary, m is proportional to h, the height of the mercury head, and t is inversely proportional to h so that

$$\bar{\imath}_d = kh^{1/2} \tag{31}$$

If $\bar{\imath} \ll \bar{\imath}_d$, i.e., if the current is determined only by a chemical reaction, $\bar{\imath}$ is proportional to the electrode surface, i.e., to $m^{2/3}t^{2/3}$, and, therefore, is independent of the height of the mercury reservoir [see Equations (3), (12), (13), and (16)]. This criterion may prove very helpful in ascertaining the kinetic character of polarographic currents (20). Currents controlled partly by diffusion and partly by chemical reaction, so that $\bar{\imath}$ is comparable to $\bar{\imath}_d$, show a dependence on h, which is approximately of the form

$$\bar{\imath} = kh^n \qquad \text{with } 0 < n < {}^1/_2$$

It must be remembered, however, that, if allowance is made for spherical diffusion (21), Equation (31) changes to

$$\bar{\imath}_d = kh^{1/2} + k' \tag{31a}$$

where k' is a correction term. Therefore, there may be observed small deviations from Equation (31), but these do not necessarily indicate kinetically determined currents.

Sometimes the polarographic diffusion current $\bar{\imath}_d$ cannot be measured in the system under investigation because the current is not purely diffusion controlled under any experimentally attainable condition. If that is so, one must resort to indirect methods. A very simple, and often sufficiently accurate, method consists of measuring the diffusion current of another substance under the same polarographic conditions. The molecules of that substance must be of about the same size as those of the kinetically reduced substance, so that the respective diffusion coefficients are practically equal. If the concentrations and the number of electrons necessary for reduction and oxidation, respectively, are the same for both substances, the values of $\bar{\imath}_d$ may be taken as equal. Another method of evaluating k, when values of $\bar{\imath}_d$ are not known, has been proposed by Rüetschi (22).

This procedure is only applicable for *Cases* 1 and 2 if $\bar{\imath}$ and $\bar{\imath}_d$ are comparable. Equation (12), and similarly (18), may be written as

$$\begin{aligned} \bar{\imath}t^{1/2} &= \bar{\imath}_d t^{1/2} - (\bar{\imath}K^{1/2})/(0.886k_1{}^{1/2}M) \\ &= \text{const} - (0.886)^{-1}M(K/k)^{1/2}\bar{\imath} \end{aligned} \tag{32}$$

For a given capillary, $\bar{i}_d t^{1/2}$ is independent of the drop time [see discussion of Equation (31)]. Therefore, a plot of $\bar{i}t^{1/2}$ obtained, with different drop times, against the corresponding value of $\bar{i}$ results in a straight line with a slope from which k_1 may be calculated.

The error introduced by neglecting spherical diffusion is small and may be safely neglected with this kind of plotting. Equation (32) should be compared with Equation (48) for the relation between $\bar{i}$ and the transition time τ in chronopotentiometry, which is treated in Section III. The similarity of Equations (32) and (48) is of a merely formal character.

The relative error of a measured value of k is composed of different parts and will be discussed for the recombination of a proton with a pyruvate anion, a case which has been treated above. For the sake of brevity, we define $y = \bar{i}/\bar{i}_d$; y is the polarographically measured quantity.

From Equation (12a), we have

$$\Delta k/k = (\partial \ln k/\partial \ln y)(\Delta y/y) + (\Delta K/K) + 2 \times 2.303 \Delta \mathrm{pH} + d \ln k/dT\, \Delta T \quad (33)$$

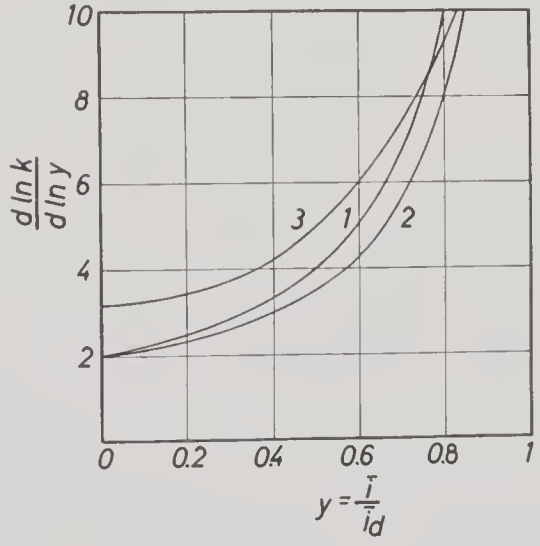

Fig. 5. Diagram for estimating the error in the rate constant k for a given experimental error in $y = \bar{i}/\bar{i}_d$. The numbers of the curves refer to the number of the cases discussed in Section II.2

The quantity $\partial \ln k/\partial \ln y$ is plotted against y in Figure 5 for some of the cases discussed above.* The relative error in y amounts to at least 1% if the wave is well developed and will often be much greater. Therefore, an error of only 10% in k may be considered quite satisfactory. Polarographic measurements are made in fairly concentrated solutions so that activity coefficients will differ appreciably from unity, and K must be cor-

* For catalytic currents, $\partial \ln k/\partial \ln y$ is only 2 for $y = \infty$ and even less for smaller y.

rected for this effect. Furthermore, the pH value in concentrated solutions is a rather ill-defined quantity (23), and errors in k of 30% and more may arise from the third term on the right of Equation (33). Since reaction rates are strongly temperature dependent, a suitably constant temperature must be maintained. Thus, in the case of kinetic currents, the kinetic constants can be determined only with rather large experimental errors. The situation for catalytic currents is far more favorable, and here the agreement between rate constants obtained polarographically and by other methods is quite satisfactory.

4. The Reaction Rate for the Recombination of Protons with Anions of Weak Acids

In Table IV, rate constants for the recombination of protons with anions of weak acids are presented. In column 3 the pK values of the acids are listed.

Since a bimolecular reaction cannot proceed faster than the diffusion of the reactants, resulting in a rate constant of some 10^{10} l./mole sec., some of the data listed in Table V are theoretically unsound. On the other hand, other methods, e.g., relaxation methods and the fluorescence method, have shown that the recombination of all investigated anions with protons is a diffusion-controlled reaction, so that values of k far below 10^{10} l./mole sec. must also be viewed with some reserve.

In addition to the experimental errors discussed in Section II.3, there are three possible causes which may seriously falsify polarographically determined rate constants for protolytic reactions (47a).

First, Equation (11) shows that, if $k = 3 \times 10^{10}$ l./mole sec. and $D = 10^{-5}$ cm.^{2}/sec., $\mu = 1.6 \times 10^{-8}/K^{1/2}$ cm. If K is fairly large (as, for example, $K = 6 \times 10^{-2}$ for phenylglyoxylic acid), μ is of the order of only a few angstrom units, and the application of Fick's law in these thin layers is physically unsound. The reaction becomes quasi-heterogeneous. It may be shown that the neglect of this fact results in the calculation of rate constants that are too large. Furthermore if μ is only some few angstrom units thick, the reaction proceeds within the region of the diffuse electrical double layer with two consequences: The concentrations of cations and anions are modified by the electric potential (47b), and the reactions constants are changed by the dissociation field effect (47c).

Second, it may be possible that proton donors other than H_3O^+ are involved in the protolytic reaction and contribute to the formation of undissociated acid in comparable or even greater amounts than H_3O^+. This effect has been discussed by several authors (25,43,42) and may be responsible for what appears to be a very high rate constant. This kind of dis-

TABLE IV

Acid	k(l./mole sec.)	pK	Lit. ref.
Pyruvic acid	1.3×10^{10}	2.40	5,24,48
Trimethylpyruvic acid	5.7×10^{6}	2.30	24
Phenylpyruvic acid	2.6×10^{10}	2.68	24
Diphenylpyruvic acid	6.6×10^{10}	2.78	24
3,4-Dimethoxyphenylpyruvic acid	5.8×10^{11}	3.10	24
Phenylglyoxylic acid	1.2×10^{12}	1.20	5,25,26
Nicotinic acid	1.4×10^{6}	4.75	27
Picolinic acid	6.8×10^{11}	5.45	28
Isonicotinic acid	1.3×10^{12}	4.90	28
Isonicotinic acid	1.2×10^{7}	4.90	29
Quinolinic acid	1.2×10^{11}	2.41	30
Quinolinate	5.3×10^{10}	5.05	30
Cinchomeronic acid	1.7×10^{11}	2.60	30
Cinchomeronate	3.5×10^{11}	5.07	30
Maleic acid	2.0×10^{10}	1.85	31
Fumaric acid	1.7×10^{9}	3.02	31
Citraconic acid	1.2×10^{9}	2.29	31
Oxalic acid	5.5×10^{7}	1.42	32
Phthalic acid	1.4×10^{7}	2.9	33
Phthalate	2.2×10^{8}	5.3	33
Monobenzylphthalate	2.7×10^{7}	3.55	33
cis-β-Acetylacrylic acid	3.9×10^{9}	4.56	34
trans-β-Acetylacrylic acid	2.9×10^{11}	3.57	34
Urocanic acid (Veronal–acetate buffer)	8.6×10^{12}	3.5	35
Urocanic acid (Britton–Robinson buffer)	8.7×10^{13}	3.5	35
Urocanate (Veronal–acetate buffer)	9.2×10^{10}	5.9	35
Hydroxylamine	1.9×10^{13}	6.05	36
O-Methylhydroxylamine	7.8×10^{11}	4.65	37
Nitrosohydroxylamine	8.3×10^{9}	4.28	38
N-Nitrosopyrrolidine	5.0×10^{14}	−1.28	39
N-Nitrosoproline	1.9×10^{12}	−1.44	39
N-Nitrosooxyproline	2.6×10^{10}	−1.68	39
Folic acid	4.3×10^{13}		40
p-Azobenzenemonocarbonic acid	5.5×10^{13}	4.7	41
Benzaldehyde-*p*-dimethylammonium ion	5×10^{14}	6.8	42
Acetic acid	4.4×10^{10}	5.33	22
Hydrogen chromate ion	7.4×10^{12}	6.5	43
Boric acid	2.0×10^{12}	9.20	44
Iodic acid	2.5×10^{11}	0.78	45
Nitrous acid	7.7×10^{4}	3.4	46
Sulfurous acid	4×10^{11}	1.77	47

turbance can be recognized by varying the kind and concentration of the buffer used. See the values for phenylglyoxylic (5,25,26), isonicotinic (28,29), and urocanic acid [β-imidazolylacrylic acid (35)] in different buffers (Table IV). From the measurements of polarographic currents of

pyruvic acid in mixed buffers, Becker and Strehlow (47d) were able to determine the rate constant for the reaction

$$CH_3COO^- + C_3N_2H_5^+ \xrightarrow{k} CH_3COOH + C_3N_2H_4$$

Here, $C_3N_2H_4$ is imidazole, and k was found to be $(3.5 \pm 1) \times 10^6$ l./mole sec.

A third possible cause of erroneous results is a reaction preceding the recombination reaction proper. For some α-ketocarbonic acids, it has been proved that the hydrated keto group dehydrates at a finite rate before the anion of the dehydrated acids combines with a proton (48). Neglect of this effect results in calculated rate constants that are lower than the true ones.

The requirement that μ should be large compared to molecular dimensions and that $\bar{\imath}$ should differ sufficiently from $\bar{\imath}_d$ leads to an upper limit for the pseudomonomolecular rate constant k_1 in Equation (17).

If $\bar{\imath}$ is to differ by at least 9% from $\bar{\imath}_d$, this inequality holds.

$$0.886\ [(k_1/K)t]^{1/2}M < 10$$

or approximately

$$(k_1/K)^{1/2} < 10$$

Further, if the reaction layer is to be thicker than about 3×10^{-7} cm., we have, from Equation (11),

$$\mu = (D/k_1K)^{1/2} > 3 \times 10^{-7}\ \text{cm.}$$

or approximately

$$(1/k_1K)^{1/2} > 10^{-4} \qquad \text{and} \qquad k_1K < 10^8$$

Therefore, for the pseudomonomolecular rate constant k_1, we have as an upper polarographically accessible limit

$$k_1 < 10^5\ \text{sec.}^{-1} \tag{34}$$

Furthermore, for a reaction of the type (Ia) $H^+ + A^- \overset{k_1}{\rightleftharpoons} HA$, which is diffusion controlled, we have for the rate constant of the bimolecular reaction k_1

$$k_1 \approx 3 \times 10^{10}\ \text{l./mole sec.}$$

and, with Equation (11)

$$\mu = (D/3 \times 10^{10}\ K)^{1/2} > 3 \times 10^{-7}\ \text{cm.} \qquad \text{and} \qquad K < 3 \times 10^{-3} \tag{35}$$

So, the pK of the acid whose rate of recombination is investigated polarographically must be greater than 2.5 if the result is to be regarded as meaningful.

For acids that are not reducible at the dropping electrode, the kinetic constants may be obtained by measuring the reduction current of H^+ ions. Rüetschi (22) determined the recombination of protons with acetate ions in a solution buffered with respect to the anion (49) (1M CH_3COONa; 0.05M CH_3COOH). In this case the reducible depolarizer H^+ is supplied by the reaction

$$HA \underset{k_2}{\overset{k_1}{\rightleftharpoons}} A^- + H^+ \qquad K = k_1/k_2 \tag{36}$$

which is pseudomonomolecular with respect to H^+. Equation (17) reads, in this case,

$$\bar{\imath}/\bar{\imath}_d = 0.866(k_1Kt/[A^-])^{1/2}M/\{1 + 0.866(k_1Kt/[A^-])^{1/2}M\} \tag{17b}$$

Rüetschi worked with solutions that were 0.01N with respect to azobenzene and contained 48 vol. % C_2H_5OH. Azobenzene is reduced with the consumption of H^+, and the well-developed diffusion current of this substance is a measure of the supply of H^+. Rüetschi's method works for $K < 2 \times 10^{-6}$ if $\bar{\imath}/\bar{\imath}_d$ is to be smaller than 0.9 and μ greater than 3×10^{-7} cm. [This requirement is not fulfilled with acetic acid, but nevertheless the results of Rüetschi conform with data obtained by dissociation field effect measurements (50)].

5. Experimental Results for Nonprotolytic Reactions

Table V presents the results of polarographic kinetic measurements as obtained by different authors. When possible, the corresponding nonpolarographic data are given in the fourth column for comparison. In all such cases the data are in good, or at least reasonable, agreement.

The reduction of formaldehyde in unbuffered solution has been investigated by Brdička (51). The dehydration of methylene glycol is autocatalyzed according to the following reaction scheme:

$$CH_2(OH)_2 \overset{k}{\rightleftharpoons} CH_2O$$

$$CH_2O + 2H_2O \overset{e}{\rightarrow} CH_3OH + 2OH^-$$

The hydroxyl ions evolved in the electrode reaction catalyze the dehydration reaction

$$k = k_0 + k_{OH^-}[OH^-] \tag{37}$$

TABLE V

Reaction Rate Constants Determined by the Polarographic Method

Reaction	Case	Rate constant k		Temp., °C.	Remarks	Lit. ref.
		Polarographic	Classical			
$CH_2(OH)_2 \overset{k}{\rightleftharpoons} CH_2O + H_2O$	1	$k_0 = 3.4 \times 10^{-2}$ sec.$^{-1}$			$K_H = [CH_2O]/[CH_2(OH)_2] = 4.4 \times 10^{-4}$ (53a)	51
		$k_{OH^-} = 1.3 \times 10^3$ l./mole sec.			$k = k_0 + k_{OH^-}[OH^-] + k_{H_2BO_3^-}[H_2BO_3^-]$	52
					In borate- and NaOH buffer	
		$k_{H_2BO_3^-} = 3.0$ l./mole sec.			In unbuffered solutions see below	53
$CdX^- + H^+ \overset{k}{\rightleftharpoons} Cd^{2+} + HX^{2-}$	1, 4	7.8×10^5 l./mole sec.		25	Ionic strength 0.1	54a
$CdX^- \overset{k}{\rightleftharpoons} Cd^{2+} + X^{3-}$		2.2×10^{10} sec.$^{-1}$		25	Acetate buffer, compare (55)	54
$MnX^- + H^+ \overset{k}{\rightleftharpoons} Mn^{2+} + HX^-$	1	2.2×10^5 l./mole sec.			Ionic strength 0.1	54b
$MnX^- \overset{k}{\rightleftharpoons} Mn^{2+} + X^{3-}$	1	6.8×10^8 sec.$^{-1}$			Ionic strength 0.1	54b
$PbX^- + H^+ \rightleftharpoons Pb^{2+} + HX^-$ H_3X = nitrilotriacetic acid	1	1.5×10^8 l./mole sec.			Ionic strength 0.1; see also (55)	54c
$CdHY^- \underset{k_2}{\overset{k_1}{\rightleftharpoons}} Cd^{2+} + HY^{3-}$	2	$k_1 = 2.7 \times 10^3$ sec.$^{-1}$ $k_2 = 3.7 \times 10^9$ l./mole sec.			Ionic strength 0.5; pH = 2.9 – 4.4	
				25	Heat of activation for k_1 = 15 kcal./mole	56
					Simplified theoretical treatment	
					Compare (10)	
H_4Y = ethylenediaminetetra-acetic acid	10	$k_2 = 10^9$ l./mole sec.				53a, 56a

(*continued*)

TABLE V (*continued*)

Reaction	Case	Rate constant k		Temp., °C.	Remarks	Lit. ref.
		Pylarographic	Classical			
$Cd(CN)_3^- \underset{k_2}{\overset{k_1}{\rightleftharpoons}} Cd(CN)_2 + CN^-$	1	$k_1 = 2.7 \times 10^8$ sec.$^{-1}$ $k_2 = 4 \times 10^{10}$ l./mole sec			Ionic strength 0.1	57
$Ti^{3+} + ClO_3^- + 2H^+ \overset{k}{\rightarrow} Ti^{4+} + ClO_2 + H_2O$ $5Ti^{3+} + ClO_2 + 4H^+ \rightarrow 5Ti^{4+} + 2H_2O + Cl^-$ (very fast)	6	2×10^4 l /mole sec.			In acid solution	61
$Fe^{2+} + H_2O_2 + H^+ \overset{k}{\rightarrow} Fe^{3+} + OH + H_2O$		75 l./mole sec.	58–66 l./mole sec.	21–24		62
		68 l./mole sec.		31	In acid solution	65,7
$Fe^{2+} + OH + H^+ \rightarrow Fe^{3+} + H_2O$ (very fast)	6	11 l./mole sec.	Lit. (64)	1		63 63
$Fe^{2+} + H_2O_2 + H^+ \overset{k}{\rightarrow} Fe^{3+} + H_2O + OH$	6	6.8×10^3 l./mole sec.			pH = 4.8	66
$Fe^{2+} + OH + H^+ \rightarrow Fe^{3+} + H_2O$ (very fast)	9	7×10^3 l./mole sec.		25	In ethylenediaminetetraacetate	67
$Fe^{2+} + H_2O_2 \overset{k}{\rightarrow} Fe^{3+} + OH^- + OH$ $Fe^{2+} + OH \rightarrow Fe^{3+} + OH^-$ (very fast)	9	6.3×10^8 l./mole sec.			In 0.5N KOH; evaluated with $\bar{\imath}/\bar{\imath}_d = 0.81\{2k[H_2O_2]$ $(1 - (\bar{\imath}/\bar{\imath}_{dH_2O_2})t\}$ where $\bar{\imath}_{dH_2O_2}$ is the sum of $\bar{\imath}_d$ for both waves	18 53a

$Fe^{2+} + H_2O_2 \xrightarrow{k}$ $Fe^{3+} + OH^- + OH$ $Fe^{2+} + OH \rightarrow Fe^{3+} + OH$ (very fast)	6	3.2×10^6 l./mole sec.			In 1*M* NaOH + triethanolamine	67a
H_2O_2 + catalase $\xrightarrow{k}$ $H_2O + {}^1/_2O_2$ + catalase	7	1.72×10^7 l./mole sec.	1.73×10^7 l./mole sec.			15 68
$UO_2^+ + H^+ \rightleftharpoons UOOH^{2+}$		$k_{0Cl} = 250$ l./mole sec.			$k = k_0 [H^+]$	69
$UO_2^+ + UOOH^{++} \xrightarrow{k}$ $UO_2^{2+} + UOOH^+$	8	$k_{0ClO_4} = 143$ l./mole sec.			In 0.5*M* Cl^- and in 0.5*M* ClO_4^-	70,71
$Z \xrightarrow{e} Y$ $O \xrightarrow{e} R$ $R + Z \xrightarrow{k} Y' + O$	9	800 l./mole sec.	1,200 l./mole sec.	25	Z = eumene hydroperoxyde O = ferric ethylenediaminetetra-acetate R = ferrous EDTA The nonlinear differential equations have been solved numerically	72
$W^{5+} + HClO_4 + H^+ \xrightarrow{k}$ $W^{6+} + H_2O + ClO_3$ $7W^{5+} + ClO_3 + 6H^+ \rightarrow$ $7W^{6+} + 3H_2O + Cl^-$ (very fast)	6	$\frac{1630 \text{ sec.}^{-1}}{8 \times 12 \text{ mole/l.}} = 17$ l./mole sec.		25	The catalytic current is suppressed by 1*M* HCl	73

(*continued*)

TABLE V (*continued*)

Reaction	Case	Rate constant k		Temp., °C.	Remarks	Lit. ref.
		Polarographic	Classical			
$S_2O_4^{2-} \overset{k}{\rightleftharpoons} 2SO_2^-$	3	$k/K^{1/2} = 6 \times 10^{-3}$ mol.$^{1/2}$ l.$^{-1/2}$ sec.$^{-1}$		40	$K = [S_2O_4^{--}]/[SO_2^-]^2$ The total reduction of dithionite is a complex reaction	58
$Ti^{3+} + NH_2OH \overset{k}{\rightarrow} Ti^{4+} + NH_2 + OH^-$ $Ti^{3+} + NH_2 + H^+ \rightarrow Ti^{4+} + NH_3$ (very fast)	6	42 ±1.2 l./mole sec.	42 l./mole sec.	25		59
$Fe^{2+} + NH_2OH \overset{k}{\rightarrow} Fe^{3+} + NH_2 + OH^-$ $Fe^{2+} + NH_2 + H_2O \rightarrow Fe^{3+} + NH_3 + OH^-$ (very fast)	6	198 l./mole sec.	186 l./mole sec.		In 1M NaOH + triethanolamine	6
$U^{3+} + NO_3^- + 2H^+ \overset{k}{\rightarrow} U^{4+} + NO_2 + H_2O$ $4U^{3+} + NO_2 + 4H^+ \rightarrow 4U^{4+} + 2H_2O + {}^1/_2N_2$ (very fast)	6	1.6×10^6 l./mole sec.			In acid solution	60

For this autocatalyzed reaction, Koutecký (53) derived an equation for $\bar{i}/\bar{i}_d$, which is valid for relatively high concentrations of formaldehyde,

$$\bar{i}/\bar{i}_d = 0.966[(D_{CH_2(OH)_2})/(D_{OH^-})]K_H k_{OH^-}[CH_2(OH)_2]t \qquad (38)$$

where K_H is the constant defined in the first line of Table V.

Another interesting case of kinetic currents was found in the reduction of sugars (74–76). The height of the reduction wave of sugars is much smaller than the diffusion current of a reducible substance of the same concentration. Wiesner showed that only a sugar with a free carbonyl group is reducible and that the current is determined by the rate of the reaction

$$\text{cyclohemiacetal} \underset{k_1'}{\overset{k_1}{\rightleftharpoons}} \text{free carbonyl} \xrightarrow{e} \text{R} \qquad (39)$$

In an interesting paper (75), Wiesner and co-workers accounted for the kinetic mechanism of mutarotation of glucose. According to these authors, the reaction proceeds as follows:

$$\alpha\text{-glucose} \underset{k_1'}{\overset{k_1}{\rightleftharpoons}} \text{aldehyde form} \underset{k_2}{\overset{k_2'}{\rightleftharpoons}} \beta\text{-glucose} \qquad (39a)$$

The reducible free aldehyde is present in only a minute fraction, i.e., $k_1' \gg k_1$ and $k_2' \gg k_2$. Under these circumstances, the reaction layer μ is simply given by

$$\mu = [D/(k_1' + k_2')]^{1/2} \qquad (40)$$

[Compare Equation (11). Paldus and Koutecký (77) have obtained the rigorous solutions of the problem and have shown that, under the given conditions, Equation (40) leads to the correct result.]

Starting at time $t = 0$ with pure α-glucose, the kinetic current is a function of time by virtue of the mutarotation reaction, and is given by

$$i_k(t) = 493z(mt)^{2/3}[D/(k_1' + k_2')]^{1/2}$$
$$[k_1 a - (k_1 - k_2)x_\infty + (k_1 - k_2)x_\infty e^{-kt}] \qquad (41)$$

In this equation, a is the initial concentration of α-glucose, x_∞ is the equilibrium concentration of β-glucose present after a sufficient time, for equilibrium, and k, the time constant of mutarotation, is given by

$$k = (k_1 k_2' + k_1' k_2)/(k_1' + k_2') \qquad (42)$$

On using Equations (41) and (42) and also the values of i_k $(t = \infty)$ and the equilibrium constant of the two cycloacetal forms $x_\infty/(a - x_\infty) = 1.740$, the four rate constants were obtained; they are given in Table VI.

TABLE VI

The Rate Constants of the Reaction α-Glucose $\underset{k_1'}{\overset{k_1}{\rightleftharpoons}}$ Aldehyde Form $\underset{k_2}{\overset{k_2'}{\rightleftharpoons}}$ β-Glucose and the Rate Constant k of Mutarotation[a]

Buffer conc.	KCl conc.	Ionic strength	$k \times 10^3$ sec.$^{-1}$	$k_1 \times 10^3$ sec.$^{-1}$	$k_2 \times 10^3$ sec.$^{-1}$	k_1' sec.$^{-1}$	k_2' sec.$^{-1}$
0.070	0.1	0.27	3.1	5.5	1.8	64	37
0.112	—	0.27	4.0	7.3	2.2	96	51
0.112	0.2	0.47	4.6	7.6	2.7	108	66
0.153	0.1	0.47	5.6	9.8	3.2	139	78
0.194	—	0.47	6.8	12.7	3.8	212	110

[a] T = 25°C.; pH = 6.9; $D = 6.16 \times 10^{-6}$ cm.^{2} sec.$^{-1}$; $a = 0.655$ mole./l.; phosphate buffer.

III. ELECTROLYSIS UNDER CONSTANT CURRENT. CHRONOPOTENIOMETRY

Electrolysis under constant current has been developed in recent years as a promising new method for measuring rate constants. Here a time-independent current is forced through the electrolytic cell, and the rate of voltage change is observed. For given conditions (current density j, concentration of reducible substance A, and kinetic constants k), the voltage changes very rapidly at a certain time τ, the "transition time" (78), and a new electrode process starts. Calculation of rate constants from measurements of τ is based on the relation $\tau = \tau(j, c, k)$. In the following sections, this method will be discussed qualitatively. A competent and thorough treatment is given in Chapter 8 of Delahay's monograph (see General References, #3).

1. The Transition Time τ

In this discussion, we shall assume a flat electrode of constant area, no convection, and a large excess of a supporting electrolyte to avoid electric migration. Furthermore, the substance reduced at the electrode is assumed to diffuse into the bulk of the solution. Since the current is proportional to the gradient of the reducible substance at $x = 0$, this gradient is constant in the case of chronopotentiometry. In Figure 6, the concentration profile at an electrode is shown for different times, assuming constant current. At a finite time τ, the concentration [A] of the reducible substance at $x = 0$ is zero and cannot be further reduced. In place of A, another substance—the alkali ions of the supporting electrolyte—is then reduced by the current, and the electrode potential jumps to the more negative reduction potential pertaining to this new electrode process. In

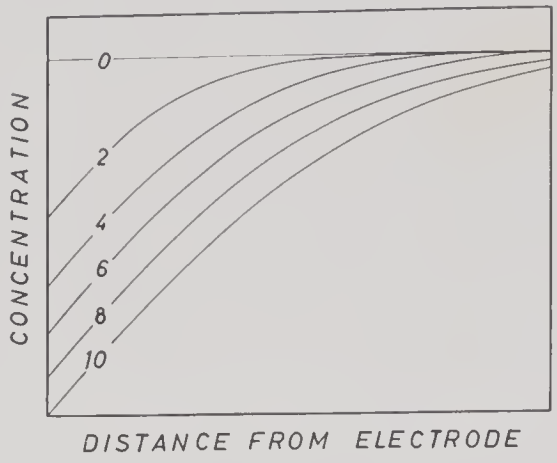

Fig. 6. Concentration-distance diagram for chronopotentiometric electrolysis of a substance A for different times. The time in seconds is given as the parameter on each curve. The transition time is 10 sec. in the example given.

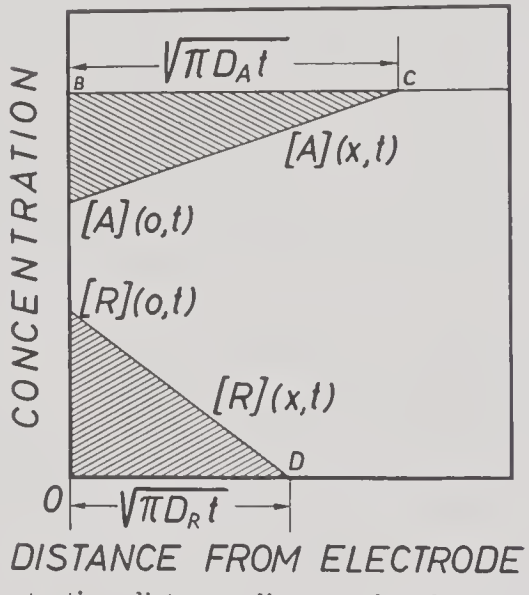

Fig. 7. Schematic concentration-distance diagram for the chronopotentiometric reduction of a substance A to a reduction product R.

Figure 7 the concentration of the substance in the oxidized state [A] and in the reduced state [R] is given as a function of distance from the electrode for time t. The two shaded areas are both equal to jt/zF, by Faraday's law. According to the laws of free diffusion, $BC = (\pi D_A t)^{1/2}$ and $OD = (\pi D_R t)^{1/2}$ and

$$jt/zF \approx {}^1/_2(\pi D_A t)^{1/2}\{[A] - [A](O, t)\} = {}^1/_2(\pi D_R t)^{1/2}[R](O, t) \quad (43)$$

Therefore

$$[A]\,(O, t) = [A] - \{2jt^{1/2}/[(\pi D_A)^{1/2} zF]\} \quad (44)$$

and

$$[R]\,(O, t) = (2jt^{1/2})/[(\pi D_R)^{1/2} zF] \quad (44a)$$

At time τ, when $[A](O, \tau) = 0$, we have

$$j\tau^{1/2} = \{[A](\pi D_A)^{1/2} zF\}/2 \tag{45}$$

Despite this simplified derivation, Equation (45) and the numerical factor are correct (78). Equation (45) is the basis for analytical applications of chronopotentiometry (79,80). By a suitable choice of the current density j, a conveniently measurable transition time τ may be obtained. Introducing Equations (44) and (44a) into the Nernst equation and bearing Equation (45) in mind, we have

$$\begin{aligned} E(t) &= E^\circ + \frac{RT}{zF} \ln \frac{f_A[A](O, t)}{f_R[R](O, t)} \\ &= E^\circ + \frac{RT}{zF} \ln \frac{f_A D_R{}^{1/2}}{f_R D_A{}^{1/2}} + \frac{RT}{zF} \ln \frac{\tau^{1/2} - t^{1/2}}{t^{1/2}} \end{aligned} \tag{46}$$

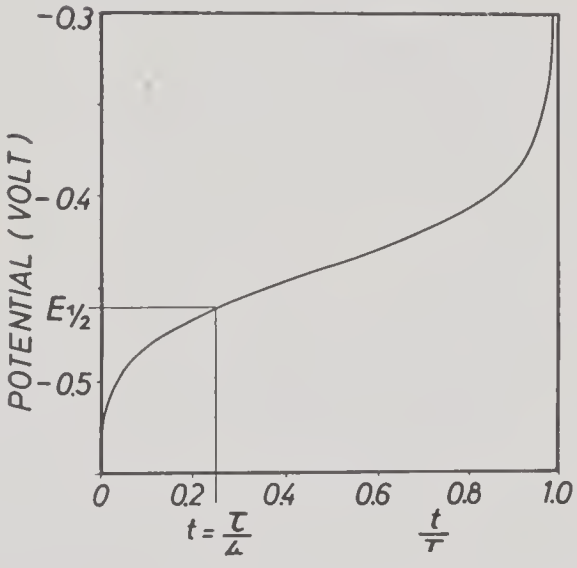

Fig. 8. Electrode-potential as a function of time (fraction of transition time τ) for the chronopotentiometric reduction of Tl^+ ions.

The first two terms on the right side of Equation (46) may be recognized as the polarographic half-wave potential $E_{1/2}$, so that the potential time relationship in chronopotentiometry reads

$$E(t) = E_{1/2} + RT/zF \ln [(\tau^{1/2} - t^{1/2})/t^{1/2}] \tag{46a}$$

[In the case of chronopotentiometric oxidation, the sign on the right side of Equation (46a) must be changed.] Equation (46a) is valid for purely diffusion-controlled currents.

Figure 8 shows the variation of potential with time as given by Equation (46a). Here, $t^{1/2}$, plotted against the electrode potential, shows a curve quite analogous to a polarographic wave, where $\tau^{1/2}$ corresponds to the

diffusion current. Whereas the proportionality constant κ between polarographic diffusion current and concentration [Equation (3)] cannot be varied significantly, the proportionality constant between $\tau^{1/2}$ and the concentration is inversely proportional to the applied current density [Equation (45)] and can, therefore, be assigned a wide variety of values.

τ may be evaluated graphically from the measured $E - t$ curves. If the half-wave potential of the redox system is known, τ may also be obtained from the relation

$$E(\tau/4) = E_{1/2} \tag{47}$$

2. Kinetic Currents in Chronopotentiometry. The Reaction Layer Concept

The influence of the rate of homogeneous reactions on j will be discussed with reference to the example of the reduction of pyruvic acid, which was treated above with the polarographic method.

$$A^- + H^+ \underset{k_2}{\overset{k_1}{\rightleftharpoons}} HA \qquad HA \xrightarrow{e} R \tag{Ia}$$

Again the concentration profile is given by Figure 3, in which the concentration gradient of A^- outside the reaction layer μ is now constant. Whereas Equation (3)

$$j = i/A = zFk_1[A^-]_0[H^+]\mu \tag{3}$$

is also valid, Equation (4), which is the second equation for $[A^-]_0$, must be replaced, in the case of chronopotentiometry (80), by

$$[A^-](O, \tau) = [A^-] - \{[2j\tau^{1/2}]/[(\pi D)^{1/2}zF]\} \tag{43}$$

The condition represented in Figure 3 refers to the time at which $[HA]_0$ becomes equal to zero, i.e., time τ. Thus $[A^-](O, \tau)$ does not vanish at that time, provided the current is determined by the rate of a chemical reaction.

Eliminating $[A^-]$ (O, τ) from Equation (3), using Equation (43) and rearranging, we have

$$j\tau^{1/2} = \{(\pi D)^{1/2}zF[A^-]\}/2 - [(\pi D)^{1/2}/(2k_1\mu[H^+]j)] \tag{48}$$

or introducing

$$\mu = [D/(k_1K)]^{1/2} \qquad \text{and} \qquad \{[(\pi D)^{1/2}zF]/2\}[A^-] = j\tau_d^{1/2}$$

where τ_d is the transition time for a purely diffusion-controlled current. Equation (48) reads

$$j\tau^{1/2} = j\tau_d^{1/2} - \frac{\pi^{1/2}}{2}\frac{1}{(k_1/K)^{1/2}[H^+]}j = \text{const} - \frac{\pi^{1/2}}{2}\frac{1}{(k_1/K)^{1/2}[H^+]}j$$

Therefore, by measuring τ for different values of j and plotting $j\tau^{1/2}$ against j, we obtain a straight line, from the slope of which the rate constant k_1 may be obtained. Equation (48) should be compared with Equation (32).

3. Calculated Transition Times for Different Reaction Schemes

Case 1. The electrode reaction is preceded by a monomolecular (or pseudomonomolecular) reaction according to

$$\mathrm{B} \underset{k_2'}{\overset{k_1'}{\rightleftharpoons}} \mathrm{A} \xrightarrow[e]{e} \mathrm{R} \qquad k_2'/k_1' = K' \tag{I}$$

The rigorous solution has been given by Delahay and Berzins (81), and reads

$$j\tau^{1/2} = \frac{\pi^{1/2}zF([\mathrm{B}] + [\mathrm{A}])D^{1/2}}{2} - \frac{\pi^{1/2}j}{2K'(k_1' + k_2')^{1/2}} \operatorname{erf}\,[(k_1' + k_2')\tau]^{1/2} \tag{49}$$

erf (z) is the well-known error function

$$\operatorname{erf}\,(z) = (2/\pi^{1/2}) \int_0^z e^{-x^2}\,dx$$

For values of $z > 2$; $\operatorname{erf}(z) \approx 1$; and, under this condition, Equation (49) reads

$$j\tau^{1/2} = \frac{\pi^{1/2}zF([\mathrm{B}] + [\mathrm{A}])D^{1/2}}{2} - \frac{\pi^{1/2}j}{2K'(k' + k')^{1/2}} \tag{49a}$$

This equation is equivalent to Equation (48a) if $[\mathrm{B}] \equiv [\mathrm{A}^-]$

$$[\mathrm{A}] \equiv [\mathrm{HA}] \ll [\mathrm{A}^-] \qquad k_1' \equiv k_1[\mathrm{H}^+] \ll k_2' \qquad \text{and} \qquad K' \equiv [\mathrm{H}^+]/K$$

For the case in which D_A and D_B, the diffusion coefficients of A and B, are unequal according to Matsuda (81a), Equation (49a) reads

$$j = \frac{\pi^{1/2}zF([\mathrm{B}] + [\mathrm{A}])D^{1/2}}{2} - \frac{\pi}{2K'(k_1' + k_2')^{1/2}} (D_\mathrm{B}/D)(D_\mathrm{B}/D_\mathrm{A})^{1/2}j \tag{49b}$$

with

$$D = (D_\mathrm{B} + K'D_\mathrm{A})/(1 + K')$$

The range of applicability of Equations (49) and (49a), respectively, will be discussed in Section IV.1.

Case 2. The depolarization product R reacts, producing an electroinactive substance C.

$$\mathrm{A} \overset{e}{\rightleftharpoons} \mathrm{R} \qquad \mathrm{R} \underset{k_2}{\overset{k_1}{\rightleftharpoons}} \mathrm{C} \qquad k_2/k_1 = K \tag{X}$$

In this case, the relation $E = E(t)$ is changed from Equation (46a) to

$$E = E_{1/2} + (RT/zF) \ln [(\tau^{1/2} - t^{1/2})/t^{1/2}] - (RT/zF) \ln Z$$

with

$$Z = 1/(1 + K) + (\pi^{1/2}/2)[K/(1 + K)]\{\text{erf } [(k_1 + k_2)t]^{1/2}/[(k_1 + k_2)t]^{1/2}\} \quad (50)$$

For high current densities, τ is small, and Z tends to unity, that is, $E_{\tau/4} = E_{1/2}$. With low current densities and high values of K, Z is approximately given by $Z = 1/K$. The measurement of $E_{\tau/4}$, for intermediate values of j, yields information about the desired rate constants.

Case 3. The depolarization product R reacts in a pseudomonomolecular reaction with B, producing the depolarizer A (82).

$$\text{A} \overset{e}{\rightleftharpoons} \text{R} \qquad \text{R} + \text{B} \overset{k}{\rightarrow} \text{A} \qquad \text{(VI)}$$

The ratio of the transition time τ to the transition time τ_d which would be observed in a purely diffusion-controlled current, is given by

$$(\tau/\tau_d)^{1/2} = [2(k[\text{B}]\tau)^{1/2}]/[\pi^{1/2} \text{ erf } (k[\text{B}]\tau)^{1/2}] \quad (51)$$

If the reaction rate is quite large, the current density j may be too small to remove the depolarizer A and no transition time τ is observed. The condition for obtaining a finite τ may be written

$$\tau_d < \pi/k[\text{B}] \quad (52)$$

[(see Koutecký and Čižek (83)]. For very small arguments of the error function in Equation (51), i.e., for a slow reaction, τ is equal to τ_d, whereas for large arguments no transition time is observed. A careful choice of j and of the concentrations [A] and [B] is therefore essential for obtaining reliable results.

Case 4. The depolarization product R is decomposed under the action of a catalyst C producing half a mole of the depolarizer (83)

$$\text{A} \overset{e}{\rightarrow} \text{R} \qquad \text{R} + \text{C} \overset{k}{\rightarrow} {}^1/_2\text{A} + \text{C} \qquad \text{(VII)}$$

In this case we have

$$2(\tau_d)^{1/2}/\tau^{1/2} = 1 + [\pi^{1/2} \text{ erf } (k[\text{C}]\tau)^{1/2}]/[2(k[\text{C}]\tau)^{1/2}] \quad (53)$$

Case 5. The depolarizer is formed by a very rapid reversible monomerization (83)

$$\text{B} \overset{k}{\rightleftharpoons} 2\text{A} \qquad \text{A} \overset{e}{\rightarrow} \text{R} \qquad \text{(III)}$$

Case 6. The depolarization product undergoes a very rapid irreversible dimerization (83)

$$A \xrightarrow{e} > R \qquad 2R \rightarrow B \tag{X}$$

Case 7. The depolarization product undergoes a slow bimolecular reaction producing the depolarizer A, according to (83)

$$2A \xrightarrow{e} > 2R \qquad 2R \xrightarrow{k} A + R' \tag{VIII}$$

Koutecký and Čižek (83) have solved the boundary value problems for bimolecular reactions, *Cases* 5–7, but their results are given in a rather complex form, which is not suitable for practical application. Since no applications of chronopotentiometry to these cases are known to the writer, the interested reader is referred to the original literature.

Mamentow and Delahay (84) (see also Koutecký and Čižek, reference 83) considered the case of chronopotentiometry on a spherical electrode. Differences from the case of semi-infinite linear diffusion are only to be expected when the thickness of the diffusion layer is comparable to the radius of the sphere, that is,

$$(\pi D\tau)^{1/2} \approx r_0$$

Under these circumstances, natural convection as a result of density gradients is very likely to occur. The derived expressions, therefore, are not of great practical importance and will not be considered further.

4. Experimental Technique

Since competent and thorough discussions of experimental methods in chronopotentiometry have been given elsewhere (see General References, #3, #5), only a short outline will be given here.

A chronopotentiometric apparatus consists of three essential parts: (1) the galvanostat—a device to force a constant current through an electrolytic vessel with a time-dependent polarization, (2) the electrolytic vessel, and (3) a device to measure the electrode potential as a function of time. A simple galvanostat (Figure 9), which works well in chronopotentiometric measurements, consists of a constant voltage source of some 100 volts feeding a variable resistance R_x and the electrolytic cell C, connected in series. More than 99% of the voltage drop takes place across R_x, so that the variations of cell polarization with time will not measurably influence the current. Before the experiment is started, the current flows across the auxiliary resistance R_c, which is equalized to the cell resistance, and hence the current can be adjusted to the desired value with R_x and the amper-

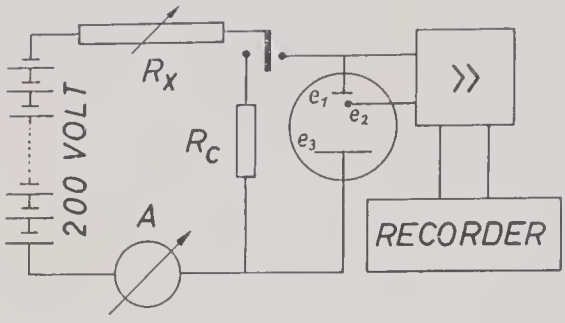

Fig. 9. Schematic circuit for a chronopotentiometric setup.

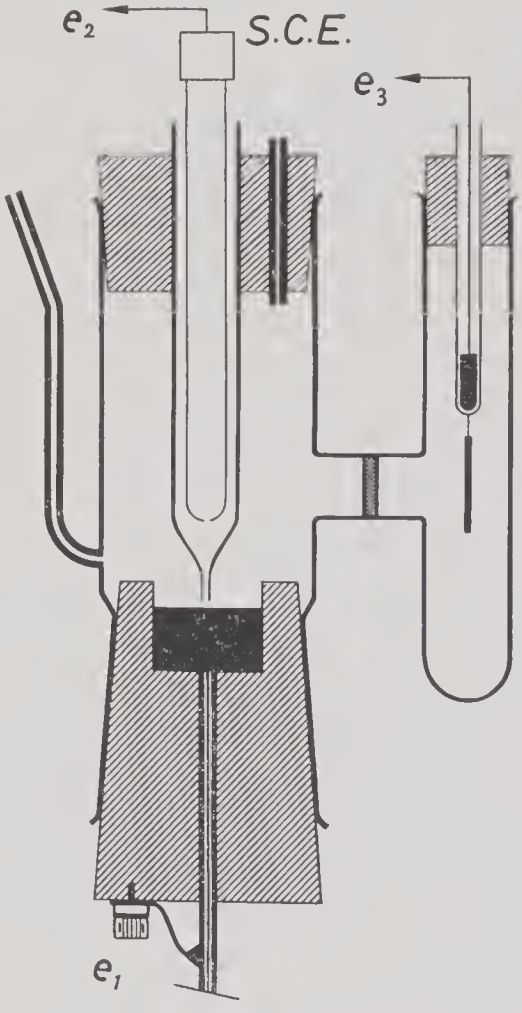

Fig. 10. Electrode vessel for chronopotentiometry according to Delahay (82) e_1: working electrode; e_2: reference electrode; e_3: counter electrode.

emeter A. (A precision resistance may be used, instead of A, in which the IR drop can be accurately measured with a potentiometer.)

An electrolytic cell suitable for electrolysis under constant current is drawn in Figure 10. The tip of the Haber-Luggin capillary making electrolytic contact to the reference electrode e_2 is placed about 1 mm. above the working electrode e_1. The vessel for the electrode proper consists of

a non-wetting material since, with glass vessels, a creeping of the solution between mercury and glass leads to ill-defined current densities.*

For work with high current densities and short transition times, the hanging stationary mercury drop has proved to be a very suitable electrode. Small currents are sufficient for quite high current densities, since the area is small, although well defined. Convection trouble is more serious in this kind of electrode but is not likely to be of importance if the transition times are very short.

A recording potentiometer P is quite convenient for measuring long transition times, $\tau \geq 10$ sec. For short times, a cathode-ray oscilloscope must be used.

As in polarography, the charging of the electrode capacity is a disturbing factor in chronopotentiometric measurements. Let C be the electrode capacity assumed constant, ΔE the potential difference passed in the time interval, and j the applied current density. Then the ratio of electric charge Q_c used for charging the double-layer capacity to the charge Q_e used for the reduction of the depolarizer is given by (85)

$$Q_c/Q_e = C\Delta E/j\tau \tag{54}$$

or, introducing (45),

$$Q_c/Q_e = (4jC\Delta E)/(\pi^2 z^2 F^2 [\mathrm{A}]^2 D) \tag{54a}$$

Therefore, with large current densities (short transition times), the ratio Q_c/Q_e becomes large, and the values of τ are incorrect. The finite electrode capacity leads to a lower limit for measurable τ, which is of the order of 10^{-2} sec. An ingenious method of lowering this limit by about one order of magnitude has been proposed by Gerischer and Krause (86). For application, of this method, the original paper should be consulted.

For the evaluation of poorly defined transition times, the derivative chronopotentiometric technique as developed by Iwamoto may prove helpful (see General References, #6).

5. Experimental Results

Despite the promising potentialities of chronopotentiometry in the field of homogeneous chemical reactions, only a very few measurements of this kind have been published; see Table VII.

* Another efficient means of avoiding the creeping of solution between mercury and glass has been described by Giner and Vielstich. [*Z. Elektrochem.*, **64**, 128 (1960).] An amalgamated platinum ring separates the glass-solution and glass-mercury boundaries.

TABLE VII

Reaction Rate Constants Determined by the Chronopotentiometric Method

Reaction	Case	Rate constant k		Temp., °C.	Remarks	Lit.
		Chronopotentiometric	Polarographic			
$CH_3COO^- + H^+ \xrightarrow{k} CH_3COOH$	1	2.7×10^{10} l./mole sec.		25	In H_2O with *p*-nitraniline as proton acceptor	86a
$CH_3COO^- + H^+ \xrightarrow{k} CH_3COOH$	1	9×10^{10} l./mole sec.	4.5×10^{10} l./mole sec.	25	In 1:1 H_2O/C_2H_5OH	87
$HCOO^- + H^+ \xrightarrow{k} HCOOH$	1	$\geq 2 \times 10^{10}$ l./mole sec.				86a
$Cd(CN)_4^{2-} \underset{k_2}{\overset{k_1}{\rightleftharpoons}} Cd(CN)_3^- + CN^-$	1	$k_1 = 3.9 \times 10^4$ sec.$^{-1}$ $k_2 = 1.5 \times 10^8$ l./mole sec.			See also Koryta (57) and Table IX	88
$Ti^{3+} + NH_2OH \xrightarrow{k} Ti^{4+} + NH_2 + OH^-$ $Ti^{3+} + NH_2 + H^+ \rightarrow Ti^{4+} + NH_3$ (very fast)	3	30 l./mole sec.	42 l./mole sec. (59)	30	The polarographic results of Blazek and Koryta (59) were confirmed by Delahay and co-workers; this value seems to be the more reliable one.	82

IV. OTHER ELECTRO CHEMICAL METHODS FOR THE MEASUREMENT OF FAST REACTION RATES

In this section some further electrochemical methods, which have not been applied to any large extent, will be briefly outlined.

1. The Rotating Disc

Polarography and chronopotentiometry are non-stationary method, and the theoretical implications are therefore considerable. A far simpler electrode—from a theoretical point of view—is the rotating disc electrode (89). At such an electrode, there exists a diffusion layer thickness, independent of time and of radial distance from the axis of revolution. The diffusion layer thickness does depend on the angular velocity of revolution in a theoretical calculable manner, which is borne out by experiment. Koutecký and Lewitsch (90) derived equations for the current at the rotating disc, where the current is limited by homogeneous reaction rates in the electrode layer. These calculations have been extended by Dogonadze (91) to the case in which the reacting species have different diffusion coefficients.

Case 1. B reacts in a monomolecular (or pseudomonomolecular) reaction to form a depolarizer A, which is reduced at the rotating disc electrode.

$$\mathrm{B} \underset{k_2}{\overset{k_1}{\rightleftharpoons}} \mathrm{A} \qquad \mathrm{A} \xrightarrow{e} \mathrm{R} \qquad \text{with} \quad k_2/k_1 = K \tag{I}$$

Then

$$\frac{1}{\omega^{1/2}} = \frac{zFD^{2/3}([\mathrm{A}] + [\mathrm{B}])}{1.61\nu^{1/6}} - \frac{KD_\mathrm{B}}{1.61\mathrm{D}^{1/3}\nu^{1/6}D_\mathrm{A}} \frac{1}{[(k_2/D_\mathrm{A}) + (k_1/D_\mathrm{B})]^{1/2}} j \tag{55}$$

where j is the current density, ω is the angular frequency of the rotating disc, ν is the kinematic viscosity of the medium ($\nu = \eta/\rho$), D_A and D_B are the diffusion coefficients of A and B, respectively, and D is given by

$$D = (k_1D_\mathrm{A} + k_2D_\mathrm{B})/(k_1 + k_2) \tag{55a}$$

Equation (55) has been written similarly to Equations (32) and (48) and indicates how measurements may be simply evaluated: j is measured for different speeds of rotation, and $j(1/\omega^{1/2})$ is plotted against j. From the slope of the resulting straight line, the kinetic constants may be evaluated. The first term on the right side of Equation (55) may be recognized as the value of $j(1/\omega^{1/2})$ for purely diffusion-controlled currents. Equation (55) is applicable only if the reaction layer $\delta_K \ll \delta$, where

$$\delta_K = 1/[(k_2/D_\mathrm{A}) + (k_1/D_\mathrm{B})] \tag{56}$$

and the diffusion layer δ is given by

$$\delta = 1.61(D/\nu)^{1/3}(\nu/\omega)^{1/2} \tag{57}$$

Case 2. For the case of a catalytic current proceeding according to

$$\mathrm{B} \underset{k_2}{\overset{k_1}{\rightleftharpoons}} \mathrm{A} \qquad \mathrm{A} \xrightarrow{e} \mathrm{B} \tag{VIb}$$

the equation for the current reads

$$j = zF[\mathrm{B}]k_1\{(D_\mathrm{A}/D_\mathrm{B})[D/(k_1 + k_2)]\}^{1/2} \tag{58}$$

and is valid for $j \gg j_d$, where j_d is the current density under diffusion-controlled conditions.

Case 3. Koutecký and Lewitsch (90) calculated the case for the reversible monomerization of an electro-inactive dimer in the reducible monomer (equal diffusion coefficients are assumed).

$$\mathrm{B} \underset{k_2}{\overset{k_1}{\rightleftharpoons}} 2\mathrm{A} \qquad \mathrm{A} \xrightarrow{e} \mathrm{R} \tag{IIIa}$$

The solution is given by

$$j = zFD\{(2[\mathrm{B}] - \psi_0)/[1.61(D/\nu)^{1/3}(\nu/\omega)^{1/2}]\} \tag{59}$$

where ψ_0 is the root of the equation

$$\psi_0^{3/4} + (D/K\delta)(\psi_0 - 2[\mathrm{B}]) = 0 \tag{59a}$$

δ in Equation (59a) is given by Equation (57) and K by

$$K = (k_1^3/k_2D^2)^{1/4}(1/18^{1/4}) \tag{59b}$$

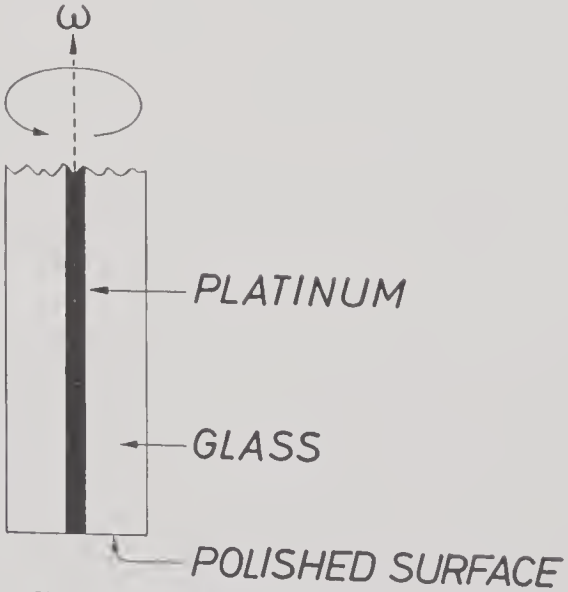

Fig. 11. Rotating disc electrode.

The condition of applicability of Equation (59) is

$$[\omega/(k_1k_2[\mathrm{B}])]^{3/2}(D/\nu)^{1/2} \ll 1 \tag{59c}$$

The equations for the rotating disc have been derived with the assumption that a liquid streams radially on a disc of infinite radius. In order to fulfill these boundary conditions satisfactorily, the disc electrode is sealed in a glass tube as shown in Figure 11. The micro roughness of the platinum electrode seems to have no great influence on the results as indicated by the data of Table VIII.

TABLE VIII
Reaction Rate Constants Determined by the Rotating Disc Method

Reaction	Case	Rate constant k	Temp. °C	Remarks	Lit. ref.
$CH_3COO^- + H^+ \xrightarrow{k} CH_3COOH$	1	2.6×10^{10} l./mole sec.	25	Compare Table VII	91a
$HCOO^- + H^+ \xrightarrow{k} HCOOH$	1	$\geq 1 \times 10^{10}$ l./mole sec.	25	Compare Table VII	91a

An interesting comparison of the ranges of applicability of polarography, chronopotentiometry, and the rotating disc electrode to protolytic reactions has been given by Vielstich (92).

The three equations may be written as follows:

$$it^{1/2} = \text{const} - \frac{1}{0.866\, M(k_1/K)^{1/2}[\mathrm{H}^+]}\, j \qquad \text{polarography} \tag{32}$$

$$j\tau^{1/2} = \text{const} - \frac{\pi^{1/2}}{2}\,\frac{1}{(k_1/K)^{1/2}[\mathrm{H}^+]}\, j \qquad \text{chronopotentiometry} \tag{48}$$

$$j(1/\omega^{1/2}) = \text{const} - \frac{D^{1/6}}{1.61\,\nu^{1/6}}\,\frac{1}{(k_1/K)^{1/2}[\mathrm{H}^+]}\, j \qquad \text{rotating disc electrode} \tag{55}$$

The minimum drop time t_{min} that can be used in polarography is about 2 sec.; for the transition time, there is a lower limit of about 10^{-2} sec., owing to the charging of the double-layer capacity (see ref. 86). For the rotating disc electrode, an upper limit for the rotation speed is given by the condition for laminar flow $\omega_{max} \approx 2000$ sec.$^{-1}$ (89). If the second terms on the right sides of Equations (32), (48), and (55) are to be larger than about 10% of the first terms, the following inequalities arise:

$$(k_1/K)^{1/2}[H^+] \leq 12/{t_{min}}^{1/2} \approx 10 \quad \text{polarography} \quad (60a)$$

$$(k_1/K)^{1/2}[H^+] \leq 9/{\tau_{min}}^{1/2} \approx 100 \quad \text{chronopotentiometry} \quad (60b)$$

$$(k_1/K)^{1/2}[H^+] \leq 10D^{1/6}{\omega_{max}}^{1/2}/1.61\nu^{1/6} \approx 70 \quad \text{rotating disc electrode} \quad (60c)$$

For the case in which the anion is buffered and the proton reduced, the expression $(k_1/K)^{1/2}[H^+]$ in Equations (60) must be replaced by $(Kk_1^{1/2})/[A^-]^{1/2}$ and for true monomolecular reactions by $(k_1/K)^{1/2}$. With the condition that the reaction layer μ is to be greater than 3×10^{-7} cm., the conditions (60a) to (60c) become

$$k_1[H^+] \leq 10^5 \text{ sec.}^{-1} \quad \text{polarography} \quad (61a)$$

$$k_1[H^+] \leq 10^6 \text{ sec.}^{-1} \quad \text{chronopotentiometry} \quad (61b)$$

$$k_1[H^+] \leq 5 \times 10^5 \text{ sec.}^{-1} \quad \text{rotating disc electrode} \quad (61c)$$

In the inequalities (61) $k_1[H^+]$ has to be replaced by Kk_1 in the case of anion buffering and by k_1 for monomolecular reactions. Chronopotentiometry is, therefore, the best electrochemical method for measuring very fast reactions.

2. The Stationary-Field Method

An electrochemical method developed by Eigen and De Maeyer (93) allows the measurement of ionic reaction rates in solutions of very low ionic concentration ($c < 10^{-7}$ mole/l.). It may be applied to non-aqueous solutions and to semiconductors, and has been applied by the authors to the neutralization reaction in highly purified ice. If a solution with low ionic content between two electrodes of small separation (e.g., 0.01 cm.) is exposed to a high voltage (e.g., 1,000 volts), the electric field will draw all ions to the electrodes, and the final saturation current will be determined solely by the rate of formation of new ions; in the case of ice, this formation consists of the dissociation of water molecules into protons and hydroxyl ions.

$$H_2O \underset{k_2}{\overset{k_1}{\rightleftharpoons}} H^+ + OH^- \quad (62)$$

The current is then given by [compare Equation (3)]

$$i_k = zFAl(d[H^+]/dt) = zFAlk_1[H_2O] \quad (63)$$

Here, l is the distance between the electrodes, and A is their area; l plays the role of the reaction layer thickness μ in polarography but is of macroscopic dimensions and a known experimental parameter.

When complications occur, e.g., when currents are not completely controlled by reaction rate or when the influence of the dissociation field effect must be taken into account, the paper quoted above should be consulted. The rate of dissociation in ice has been found by Eigen and De Maeyer (93) to be some orders of magnitude lower than that in water, whereas the rate of recombination turns out to be higher.

3. The Potentiostatic Method

Classical polarography is, in principle, a potentiostatic method since a definite potential is applied to the electrode and the resulting current is determined. Normally, however, the instantaneous current is not obtained, but its value is averaged over the drop time. As indicated by Equation (60a), much greater reaction rates can be measured when the measuring time t_{min} is appreciably shorter than polarographic drop times t_{pol} ($\geq$2 sec.). Furthermore, an electrode of constant area can be used, which greatly simplifies the analysis.

Let again be assumed that a (pseudo)monomolecular reaction precedes the much faster electrode reaction

$$\mathrm{B} \underset{k_2}{\overset{k_1}{\rightleftharpoons}} \mathrm{A} \xrightarrow{e} \mathrm{R} \qquad k_2/k_1 = K \tag{I}$$

Then the limiting current density, determined by reaction and diffusion, is given by (93a)

$$j = zF([\mathrm{A}] + [\mathrm{B}])\, D^{1/2} K k_1^{1/2} \exp(\lambda^2)\, \mathrm{erfc}(\lambda) \tag{62}$$

with $\lambda = (K k_1 t)^{1/2}$ and $\mathrm{erfc}\, x \equiv 1 - (2/\pi^{1/2}) \int_0^x \exp(-y^2) dy$.

For $\lambda \ll 1$, that is for a short time t,

$$\exp(\lambda^2)\, \mathrm{erfc}(\lambda) \approx 1 - (2/\pi^{1/2})\lambda$$

and the current is determined by the reaction rate, whereas for a long time or $\lambda \gg 1$

$$\exp(\lambda^2)\, \mathrm{erfc}(\lambda) \approx 1/\pi^{1/2}$$

Then j will be diffusion controlled and independent of the rate constant k_1.

Gerischer (93b) and (independently) Delahay and Oka (93c) applied the potentiostatic method to the measurement of fast reactions. The electrode potential, as measured with respect to a reference electrode, was held constant with an electronically regulated potentiostat (94d). Indeed, for most purposes, a low ohmic potentiometer should work as well. Figure 12 shows the principle of an experimental arrangement.

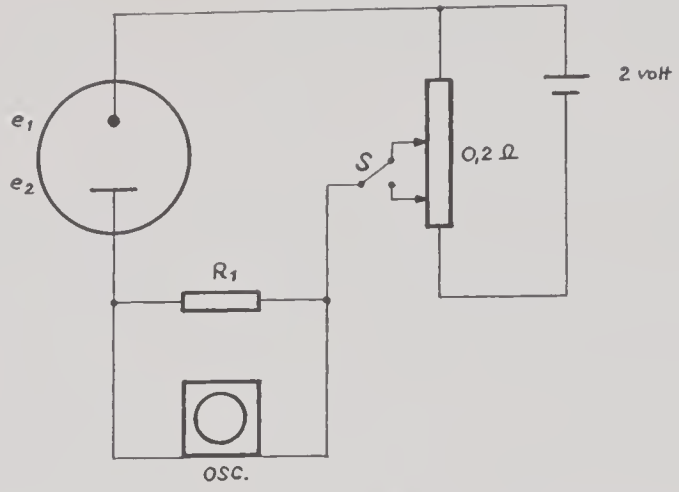

Fig. 12. Schematic diagram of a potentiostatic arrangement for the measurement of fast reaction rates. e_1: working electrode: e_2: counter electrode; *osc.*: cathode-ray oscilloscope; *S:* switch.

By operating switch S, a sufficiently negative potential is applied to the electrode e_1 (at the same time the oscilloscope is triggered), and reaction (I) starts. The current drawn for charging the double-layer capacity in the very beginning of the experiment is considerable, and the potentiostatic device must, accordingly, have a rather low resistance. The current is measured as a function of time by the oscilloscope *osc.* The polarizing voltage E must be negative enough so that, at all times, the electrode potential $E - iR$ is in the region of limiting currents; R is the total resistance of the circuit. With high resistances of the cell and/or of R_1, a potentiostat in connection with a reference electrode and a Haber-Luggin capillary must be used (93b). The hanging mercury drop electrode (93e) has proved a useful electrode for the potentiostatic method.

TABLE IX
Reaction Rate Constants Determined by the Potentiostatic Method

Reaction	Case	Rate constant k	Temp., °C.	Remarks	Lit. ref.
$Cd(CN)_4^{2-} \underset{k_2}{\overset{k_1}{\rightarrow}} Cd(CN)_3^- + CN^-$	1	$k_1 = (2 \pm 0.5) \times 10^4$ sec.$^{-1}$ $k_2 = (8 \pm 2) \times 10^7$ l./mole sec.	25	In 3N $NaClO_4$; compare Table VI	93b
$ClCH_2COO^- + H^+ \overset{k}{\rightarrow} ClCH_2COOH$	1	$(1.3 \pm 0.3) \times 10^{10}$ l./mole sec.	25	In 1:1 H_2O/C_2H_5OH; method analogous to Rüetschi (22) and Delahay and Vielstich (87)	93c

Results obtained by the potentiostatic method are summarized in Table IX.

4. Further Possible Methods

The influence of homogeneous reactions that precede the electrode reaction proper on the electrode impedance, as measured by alternating currents, has been discussed by Gerischer and Vetter (94) and by Gerischer (95). Applications have not yet been reported.

The streaming mercury electrode has been successfully applied to the measurement of kinetic currents (96). For this type of electrode, the equivalent of the polarographic drop time is much shorter than 1 sec., and, therefore, the electrode is better suited for the measurement of very rapid reactions. Since it is cumbersome to use, however, it has not found any extensive application.

The influence of reaction rates on the electrolysis current with periodically changing electrode potential has been discussed theoretically by Weber (97) for the case of a flat and a spherical stationary electrode.

Dubois (98) succeeded in determining the rate constants of fast reactions in a rather ingenious and simple manner. By coulometric generation, the concentration of one reactant (bromine) of a bimolecular reaction (the bromination of olefinic derivatives) was held constant on a very low level so that the rate was slow enough to be measured directly. The rate of the reaction is proportional to the Coulometric current and can be followed very conveniently. Rate constants of the order of 10^3 l. mole^{-1} sec.$^{-1}$ have thus been determined. Of course, the method cannot be applied to reactions of the first order, but, by virture of its simplicity and directness, it should prove helpful in other applications.

References

1. K. Wiesner, *Z. Elektroehem.*, **49**, 164 (1943); R. Brdička, and K. Wiesner, *Naturwissenschaften*, **31**, 247, 391 (1943).

2. For a review see H. Berg, *Chem. Teeh.* (Berlin), **8**, 5 (1956).

2a. Compare: V. Hanuš, *Chem. zvesti*, **8**, 702 (1954).

3. K. Wiesner, *Chem. listy*, **41**, 6 (1947).

4. J. Koutecký, *Collection Czeeh. Chem. Communs.*, **18**, 597 (1953); K. H. Henke and W. Hans, *Z. Elektrochem.*, **57**, 591 (1953); J. Weber and J. Koutecky, *Colleetion Czech. Chem. Communs.*, **20**, 980 (1955).

5. R. Brdička, *Collection Czeeh. Chem. Communs.*, **12**, 212 (1947).

6. J. Koryta, *Colleetion Czech. Chem. Communs.*, **19**, 666 (1954).

7. J. Koutecký, *Colleetion Czeeh. Chem. Communs.*, **18**, 311 (1953); P. Delahay and G. L. Stiehl, *J. Am. Chem. Soe.*, **74**, 3500 (1952).

8. J. Koutecký, *Colleetion Czeeh. Chem. Communs.*, **19**, 857 (1954).

9. J. Koutecký and J. Čižek, *Colleetions Czech. Chem. Communs.*, **21**, 836 (1956).

10. J. Koutecký, *Collection Czech. Chem. Communs.*, **19**, 1093 (1954).
11. J. Koutecký and V. Hanuš, *Collection Czech. Chem. Communs.*, **18**, 337 (1953).
12. V. Hanus, *Chem. zvesti*, **8**, 702 (1954).
13. J. Čižek, J. Koryta, and J. Koutecký, *Collection Czech. Chem. Communs.*, **24**, 663 (1959).
14. J. Koutecký and J. Čižek, *Collection Czech. Chem. Communs.*, **21**, 1063 (1956).
15. J. Koutecký, R. Brdička, and V. Hanuš, *Collection Czech. Chem. Communs.*, **18**, 610 (1953).
16. J. Koutecký and J. Koryta, *Collection Czech. Chem. Communs.*, **19**, 845 (1954).
17. J. Koutecký, *Collection Czech. Chem. Communs.*, **20**, 160 (1955).
18. M. Brezina, *Collection Czech. Chem. Communs.*, **22**, 339 (1957).
18a. J. Koutecký, *Collection Czech. Chem. Communs.*, **20**, 116 (1955); see also D. M. H. Kern, *J. Am. Chem. Soc.*, **76**, 1011 (1954).
18b. J. Koryta, *Electrochim. Acta*, **1**, 26 (1959); R. Brdicka, *Z. Elektrochem.*, **64**, 16 (1960).
19. See General References.
20. See General References; #1, p. 274.
21. J. J. Lingane and B. A. Loveridge, *J. Am. Chem. Soc.*, **72**, 438 (1950); H. Strehlow and M. v. Stackelberg, *Z. Elektrochem.*, **54**, 51 (1950); T. Kambara and I. Tachi, *Bull. Chem. Soc. Japan*, **23**, 226 (1950); J. Koutecký, *Czechoslov. J. Phys.*, **2**, 50 (1953).
22. P. Rüetschi, *Z. physik. Chem. N. F.*, **5**, 323 (1955).
23. R. Bates, *Chem. Revs.*, **42**, 1 (1948).
24. E. G. Clair and K. Wiesner, *Nature*, **165**, 202 (1950).
25. K. Wiesner, M. Wheatley, and J. M. Loos, *J. Am. Chem. Soc.*, **76**, 4858 (1954).
26. W. Hans and K. H. Henke, *Z. Elektrochem.*, **57**, 595 (1953).
27. R. Brdička, *Prace Konferenceji Polarografieznej* Warszawa, 1936, p. 31.
28. J. Volke and V. Volková, *Collection Czech. Chem. Communs.*, **20**, 1332 (1955).
29. Y. Nagata, and I. Tachi, *Bull. Chem. Soc. Japan*, **27**, 290 (1954).
30. J. Volke, *Collection Czech. Chem. Communs.*, **22**, 1777 (1957).
31. V. Hanuš and R. Brdička, *Chem. listy*, **44**, 291 (1950) (quoted in 28).
32. J. Kůta, *Collection Czech. Chem. Communs.*, **21**, 697 (1956).
33. A. Ryvolova and V. Hanuš, *Collection Czech. Chem. Communs.*, **21**, 853 (1956).
34. V. Nikolajenko, *Dissertation Prag* 1952, (quoted in 27).
35. J. Kůta and E. Krejči, *Collection Czech. Chem. Communs.*, **24**, 258 (1959).
36. Z. Vodrážka, *Chem. listy*, **45**, 293 (1951).
37. Z. Vodrážka, *Chem. listy*, **46**, 210 (1952).
38. I. M. Kolthoff and A. J. Liberti, *J. Am. Chem. Soc.*, **70**, 1885 (1948).
39. R. Zahradnik, E. Svatek, and M. Chvapil, *Collection Czech. Chem. Communs.*, **24**, 347 (1959).
40. O. Hrdý, *Chem. listy*, **52**, 1058 (1958).
41. P. Rüetschi and G. Trümpler, *Helv. Chim. Acta*, **35**, 1947 (1953).
42. E. T. Bartel, Z. R. Grabowski, W. Kemula, and W. Turnowska-Rubaszewska, *Roczniki Chem.*, **31**, 13 (1957).
43. J. H. Green and A. Walkley, *Australian J. Chem.*, **8**, 51 (1955).
44. J. Kůta, *Collection Czech. Chem. Communs.*, **22**, 1411 (1957).
45. V. Čermak, *Collection Czech. Chem. Communs.*, **21**, 1344 (1956).
46. J. Masek, *Collection Czech. Chem. Communs.*, **21**, 1347 (1956).
47. A. Foffani and G. Dall'Aglio, *Contributi Teorici e Sperimentali di Polarografia* (1952), p. 107. According to V. Čermak (*Collection Czech. Chem. Communs.*, **23**, 1871 (1958) the polarographic reduction of sulfurous acid is a rather complicated process, so that no reliable recombination rate constants may be obtained.

47a. H. Strehlow, *Z. Elektrochem.*, **64**, 45 (1960).
48. M. Becker and H. Strehlow, *Z. Elektrochem.*, **64**, 129, 813 (1960).
47b. J. Koryta, *Z. Elektrochem.*, **64**, 23 (1960). L. Gierst and H. Hurwitz, *Z. Elektrochem.*, **64**, 36 (1960).
47e. L. Onsager, *J. Chem. Phys.*, **2**, 599 (1934); P. Delahay and W. Vielstich, *J. Am. Chem. Soc.*, **77**, 4955 (1955).
47d. M. Becker and H. Strehlow, *Z. Elektrochem.*, **64**, 42, 818 (1960).
48. M. Becker and H. Strehlow, *Z. Elektrochem.*, **64**, 129; 813.
49. See also Kůta (38) and Hanuš (12).
50. M. Eigen and J. Schön, *Z. Physik. Chem. N. F.*, **3**, 126 (1955).
51. R. Brdička, *Z. Elektrochem.*, **59**, 787 (1955).
52. K. Veselý and R. Brdička, *Collection Czech. Chem. Communs.*, **12**, 313 (1947); R. Bieber and G. Trümpler, *Helv. Chim. Acta*, **30**, 706 (1947).
53. J. Koutecký, *Collection Czech. Chem. Communs.*, **21**, 653 (1956).
53a. R. Brdička, *Z. Elektrochem.*, **64**, 16 (1960).
54. J. Koryta, *Z. physik. Chem., Leipzig Sonderheft*, 1958, p. 157.
54a. J. Koryta, *Collection Czech. Chem. Communs.*, **24**, 3057 (1959).
54b. J. Bjernat and J. Koryta, *Collection Czech. Chem. Communs.*, **25**, 38 (1960).
54c. M. Pryszczewska, R. Ralea, and J. Koryta, *Collection Czech. Chem. Communs.*, in press.
55. K. Morinaga and T. Nomura, *J. Chem. Soc. Japan*, **79**, 200 (1958).
56. N. Tanaka, R. Tamamushi, and M. Kodama, *Z. physik. Chem. N. F.*, **14**, 141 (1958).
56a. J. Koryta and Z. Zabransky, *Collection Czech. Chem. Communs.*, **24**, 3075 (1959).
57. J. Koryta, *Z. Elektrochem.*, **61**, 423 (1957).
58. V. Čermak, *Collection Czech. Chem. Communs.*, **23**, 1471 (1958).
59. A. Blažek and J. Koryta, *Collection Czech. Chem. Communs.*, **18**, 326 (1953).
60. J. Koryta, *Collection Czech. Chem. Communs.*, **20**, 667 (1955).
61. J. Koryta, *Chem. listy*, **48**, 462 (1954).
62. Z. Pospišil, *Collection Czech. Chem. Communs.*, **18**, 337 (1953).
63. P. Delahay and G. L. Stiehl, *J. Am. Chem. Soc.*, **74**, 3500 (1952).
64. D. H. Baxendale, M. G. Evans and G. S. Park, *Trans. Faraday Soc.*, **42**, 155 (1946).
65. I. M. Kolthoff, and E. P. Parry, *J. Am. Chem. Soc.*, **73**, 3718 (1951).
66. B. Matyska and D. Duskova, *Collection Czech. Chem. Communs.*, **22**, 1747 (1957).
67. B. Matyska, *Collection Czech. Chem. Communs.*, **22**, 1758 (1957).
67a. J. Koryta, *Collection Czech. Chem. Communs.*, **19**, 666 (1954).
68. R. Brdička and K. Wiesner, *Collection Czech. Chem. Communs.*, **12**, 138 (1947).
69. J. Koryta and J. Koutecký, *Collection Czech. Chem. Communs.*, **20**, 423 (1955).
70. E. F. Orlemann and D. M. H. Kern, *J. Am. Chem. Soc.*, **75**, 3058 (1953).
71. J. Koutecký and J. Koryta, *Collection Czech. Chem. Communs.*, **19**, 845 (1954).
72. W. C. Reynolds and S. Prager, *J. Chem. Phys.*, **26**, 1006 (1957).
73. H. A. Laitinen and W. A. Ziegler, *J. Am. Chem. Soc.*, **75**, 3045 (1953).
74. K. Wiesner, *Collection Czech. Chem. Communs.*, **12**, 64 (1947).
75. J. M. Los, L. B. Simpson, and K. Wiesner, *J. Am. Chem. Soc.*, **78**, 1564 (1956); **75**, 6346 (1953).
76. P. Delahay and J. E. Strassner, *J. Am. Chem. Soc.*, **74**, 893 (1952).
77. J. Paldus and J. Koutecký, *Collection Czech. Chem. Communs.*, **23**, 376 (1958).
78. I. A. V. Butler and G. Armstrong, *Proc. Roy. Soc. (London)*, **A139**, 406 (1933); *Trans. Faraday Soc.*, **30**, 1173 (1934); H. F. Weber, *Wied. Ann.*, **7**, 536 (1879); H. J. S. Sand, *Phil. Mag.*, **1**, 45 (1901); Z. Karaoglanoff, *Z. Elektrochem.*, **12**, 5 (1906); T. R. Rosebrugh and W. L. Miller, *J. Phys. Chem.*, **14**, 816 (1910).

79. F. G. Cottrell, *Z. physik. Chem.*, **42**, 385 (1902); A. Rius, J. Llopis, and S. Polo, *Anales fis. y quim. (Madrid)*, **45**, 1029 (1949); N. Ibl and G. Trümpler, *Helv. Chim. Acta*, **33**, 2162 (1950); **35**, 363 (1952), M. v. Stackelberg, M. Pilgram, and V. Toome, *Z. Elektrochem.*, **57**, 342 (1953).

80. L. Gierst and A. Juliard, *Proc. Intern. Comm. Electrochem. Thermodynam. and Kinet.*, 2. *Meeting Tamburini, Milan*, 1950, pp. 117, 279.

81. P. Delahay and T. Berzins, *J. Am. Chem. Soc.*, **75**, 2486 (1953).

81a. H. Matsuda, *J. Am. Chem. Soc.*, **82**, 331 (1960).

82. P. Delahay, C. C. Mattax, and T. Berzins, *J. Am. Chem. Soc.*, **75**, 5319 (1954); P. Delahay, *Discussions Faraday Soc.*, **17**, 205 (1954).

83. J. Koutecký and J. Čižek, *Collection Czech. Chem. Communs.*, **22**, 914 (1957).

84. G. Mamontov and P. Delahay, *J. Am. Chem. Soc.*, **76**, 5323 (1954).

85. L. Gierst, Thesis University of Brussels, 1952.

86. H. Gerischer and M. Krause, *Z. physik. Chem. N. F.*, **10**, 264 (1957).

86a. J. Giner and W. Vielstich, *Z. Elektrochem.*, **64**, 128 (1960).

87. P. Delahay and W. Vielstich, *J. Am. Chem. Soc.*, **77**, 4955 (1955).

88. H. Gerischer, *Z. physik. Chem. N. F.*, **2**, 79 (1954).

82. P. Delahay, *Discussions Faraday Soc.*, **17**, 205 (1954).

89. W. G. Lewitsch, *Discussions Faraday Soc.*, **1**, 37 (1947); W. Vielstich, *Z. Elektrochem.*, **57**, 646 (1953).

90. J. Koutecký and W. G. Lewitsch, *Doklady Akad. Nauk SSSR*, **117**, 441 (1957).

91. R. R. Dogonadze, *Zhur. Fiz. Khim.*, **32**, 2437 (1958).

91a. W. Vielstich and D. Jahn, *Z. Elektrochem.*, **64**, 43 (1960).

92. W. Vielstich (private communication).

93. M. Eigen and L. De Maeyer, *Z. Elektrochem.*, **60**, 1037 (1956).

93a. J. Koutecký and R. Brdička, *Collection Czech. Chem. Communs.*, **12**, 337 (1947).

93b. Gerischer, H., *Z. Elektrochem.*, **64** 29 (1960).

93c. P. Delahay and S. Oka, *J. Am. Chem. Soc.*, **82**, 329 (1960).

93d. H. Gerischer and K. E. Staubach, *Z. Elektrochem.*, **61**, 789 (1957); potentiostats are now commercially available from H. Wenking, Elektronische Werkstätten, Göttingen, Germany.

93e. H. Gerischer, *Z. Elektrochem.*, **59**, 604 (1955).

94. H. Gerischer and K. J. Vetter, *Z. physik. Chem.*, **197**, 92 (1951).

95. H. Gerischer, *Z. physik. Chem.*, **198**, 286 (1951); *Z. physik. Chem. N. F.*, **1**, 278 (1954).

96. J. Koryta, *Chem. listy*, **46**, 246 (1952), *Collection Czech. Chem. Communs.*, **19**, 433 (1954), *ibid.*, **20**, 1125 (1955).

97. J. Weber, *Collection Czech. Chem. Communs.*, **24**, 1770 (1959); see also J. Koutecký, *Collection Czech. Chem. Communs.*, **21**, 433 (1956).

98. J. E. Dubois, *Z. Elektrochem.*, **64**, 143 (1960).

General References

1. I. M. Kolthoff and J. J. Lingane, *Polarography*, Interscience Publishers, New York, 1952.

2. L. Meites, *Polarographic Techniques*, Interscience Publishers, New York, 1955.

3. P. Delahay, *New Instrumental Methods in Electrochemistry*, Interscience Publishers, New York, 1954.

4. O. H. Müller, Polarography in A. Weissberger, ed., *Technique of Organic Chemistry*, Vol. I, 3rd Edition, Interscience Publishers, New York, 1960, ch. 48.

5. C. N. Reilly, G. W. Everett, and R. H. Johns, *Anal. Chem.*, **27**, 483 (1955).

6. R. T. Iwamoto, *Anal. Chem.*, **31**, 1062 (1959).

CHAPTER XVI

PHOTOSTATIONARY METHODS

R. M. Noyes, *University of Oregon, Eugene*
A. Weller, *Technische Hochschule, Stuttgart*

I. Introduction 845
II. Recombination of Radicals 846
1. Formulation of Problem 846
2. Measurement of Steady-State Concentration, X 847
3. Measurement of Quantum Yield, ϕ 847
4. Validity of Methods 848
5. Critique 849
III. Processes Competing with Fluorescence 850
1. Introduction 850
2. Experimental Methods 853
A. Intensity Measurements 853
B. Lifetime Measurements 854
3. Results 855
A. Quenching of Fluorescence 855
B. Energy Transfer 855
C. Complex Formation 856
D. Acid-Base Reactions 856
4. Critique 860
IV. Photochemical Space Intermittency 806
References 862

I. INTRODUCTION

Most methods of studying fast reactions either observe the system at a known time after mixing or else follow changes during periods comparable to the lifetimes of the reactive species. However, kinetic information can also be obtained by measurements on a time-independent system provided a continuous external influence produces a *steady state* significantly different from the position of equilibrium that would exist in the absence of that influence.

Maintenance of a non equilibrium steady state requires continuous energy dissipation in the system. The present chapter is concerned only with the effects of visible and ultraviolet light because the primary effects of energy absorption are more clearly understood for these influences. Steady-state concentrations of chemical species can also be produced by

ultrasonic and by ionizing radiations, but the mechanisms of producing the species are so obscure that quantitative kinetic conclusions are usually very difficult to derive. Infrared radiation does not produce new chemical species, but it does cause steady-state concentrations of vibrationally and rotationally excited molecules; studies in such systems could be used in principle to learn about kinetics of energy transfer.

Photostationary techniques have been used in two ways to study kinetics when light is absorbed homogeneously. Section II discusses recombination of radicals and illustrates methods where the quantum yields and absolute concentrations of species must both be known. Section III discusses fluorescent intensity techniques for studying competitive reactions of excited species. Since these reactions are all first order in the products of light absorption, it is not necessary to know absolute concentrations of reactants.

Steady-state techniques can also be applied to systems exhibiting macroscopic concentration gradients. Then diffusion becomes the process that is competing with chemical reaction. Some of the electrochemical methods of Chapter XV illustrate such competition. A photochemical application discussed in Section IV shows how steady states can be used to study the kinetics of the diffusion process itself.

II. RECOMBINATION OF RADICALS

1. Formulation of Problem

Many symmetrical molecules such as the halogens can be photochemically dissociated to radical fragments that recombine to form the original compound. The steady state arises because of identical rates for the processes:

$$X_2 + h\nu \rightarrow 2X \tag{1}$$

$$X + X \rightarrow X_2 \tag{2}$$

Since the two rates are equal,

$$k = \phi q / X^2 \tag{3}$$

where k = rate constant in l./mole sec. for Process (2) as written, if the ragments came originally from different X_2 molecules; ϕ = quantum yield for producing a pair of radical fragments that escape permanently from each other; q = rate of absorption of light in einstein/l. sec; X = steady-state concentration in mole/l. of fragments destined to combine with fragments that were not their original partners.

If the three quantities on the right side of Equation (3) can be measured, the rate constant, k, can be calculated. The rate of light absorption, q, is obtainable by standard techniques such as absorptimetry, actinometry, and spectrophotometry; they are discussed in other volumes of this series and need not be considered here. The other two quantities require more specialized techniques.

2. Measurement of Steady-State Concentration, X

The steady-state concentration can be calculated from measurements of either the increase in concentration of fragments or the decrease in concentration of X_2 molecules. The latter approach was employed by Rabinowitch and Wood (1–3) during studies of bromine and iodine dissociation. The photostationary state was produced by an intense beam of light in one direction, and the concentration of molecular halogen was measured spectrophotometrically with a weak beam of a different frequency, perpendicular to the main illumination.

The technique worked very well for gaseous systems (1,2) where the rate constants for halogen atom recombination are low because a third molecule must be near if two colliding atoms are to recombine. The technique was much more difficult to apply to a liquid phase (3) where the values of k are much greater. Concentrations of X_2 never changed by more than about 0.03%, and the measurements had to be made rapidly because the light absorption caused a thermal expansion of the solution that also decreased the halogen concentration. It is a great tribute to the experimental ability of the investigators that they obtained reliable data for this system with pre-war equipment.

Because the concentration of X_2 changes by such a small fraction, it is tempting to study these systems by measuring the concentration of X directly. The radical concentrations attained should be detectable by modern electron spin resonance techniques, and halogen atom optical absorption spectra are also known. Illumination of the solution will produce a much greater percentage change in a signal measuring X than in a signal measuring X_2. However, this singal must be calibrated so that it can measure the *absolute* concentration of X, and such calibration is difficult for species that cannot be formed in concentrations greater than about 10^{-7} mole/l. The signal based on X_2 has the advantage that it can be calibrated directly against known concentrations.

3. Measurement of Quantum Yield, ϕ

In gas phase, molecular absorption spectra can sometimes be interpreted with enough confidence to say that the quantum yield for dissociation is

unity in certain wavelength regions of continuous absorption. For these cases, application of Equation (3) is simple.

Quantum yields in solution are always less than unity because of geminate recombination (4) of the fragments. The yields can be measured if it is possible to find a scavenger that reacts efficiently with X but does not react significantly with X_2 during the time needed for an experiment. If the rate of photochemical reaction is independent of scavenger concentration over a considerable range, it is reasonably safe to conclude that the scavenger is capturing all X fragments that escape their original partners and that the rate of reaction is equal to the rate of photochemical production of X by Equation (1).

This type of technique was first developed by Rutenberg and Taube (5) who showed that cerous ions and that manganous ions in pyrophosphate are effective scavengers for halogen atoms formed in aqueous solutions. Lampe and Noyes (6) subsequently showed that air-saturated solutions of allyl iodide are good scavengers for iodine atoms produced photochemically in organic solvents. The atoms react to form iodine molecules and allyl radicals that then react irreversibly with oxygen; hence the rate of iodine production becomes a direct measure of the rate of photochemical dissociation. Air-saturated solutions of benzyl iodide can be used in identical fashion (7).

4. Validity of Methods

The rate constants for radical recombination reactions can also be measured directly by the flash-photolysis techniques described in Chapter XIX. The two methods can be compared particularly readily in gas phase where Rabinowitch and Wood could assume quantum yields of unity for bromine and iodine dissociation. The comparison is not entirely satisfactory. Russell and Simons (8) found that rate constants for iodine recombination in several inert gases were about a factor of two lower when measured by flash photolysis than were the values of Rabinowitch and Wood (2) measured by the steady-state method. It was subsequently found (9) that iodine molecules are unusually efficient at promoting the recombination of atoms, and appropriate corrections for this effect would be needed for a careful comparison of the methods.

Although rate constants for iodine atom recombination are consistently lower when measured by flash photolysis than by the steady-state method, the reverse is observed with gaseous bromine. The flash photolysis rate constant for bromine atoms in argon (10) is 3.6×10^9 l.^{2}/mole^2 sec., while Rabinowitch and Wood (1) obtained 2.4×10^9.

Comparison of methods in liquid phase is more difficult because quantum

yields are less than unity and must be measured independently. Additional comparisons are possible because the lifetimes of halogen atoms have also been measured by the methods of intermittent illumination discussed in Chapter XX. These measurements lead to the relation:

$$\tau = 1/2kX \tag{4}$$

where τ is the average time between formation and combination of atoms that do not recombine with their original partners.

The combination of Equations (3) and (4) permits the rate constant, k, to be calculated from independent measurements of any two of the three quantities ϕ, X, and τ. Since all three have been measured, and since k has also been determined by flash photolysis, several comparisons are possible. Table I by Rosman and Noyes (11) shows such comparisons for

TABLE I
Rate Constants (reported as $10^{-9}k$ in l./mole sec.) for Iodine Atom Combination in Different Solvents

Quantities measured	C_6H_{14}	CCl_4	References
$X + \phi$	12.5 ± 2.7	6.7 ± 1.0	3, 6
$X + \tau$	11.4 ± 2.8		3, 12
	12.8 ± 3.0	7.4 ± 2.0	3, 11
$\phi + \tau$	10.3 ± 1.4		6, 12
	13.0 ± 1.6	8.2 ± 2.1	6, 11
k	22[a] ± 4	7.2 ± 1.1	13
		5.7 ± 0.5	14
	18 ± 6	6.9 ± 0.6	15

[a] These measurements were in heptane instead of hexane.

iodine atom recombination at 25° in hexane and carbon tetrachloride.

The results certainly show that photostationary methods can be used to measure rate constants for some very fast reactions. Although different techniques sometimes agree to well within the estimated errors, occasional discrepancies are as large as a factor of 2. Since these rate constants are larger by several powers of 10 than any that could be measured until a few years ago, even the present uncertainties represent a considerable advancement in techniques.

5. Critique

Rates of radical recombination can be studied by photostationary methods provided it is possible to measure both the quantum efficiency for radical production and the absolute concentration of radicals. In the ap-

plications reported here, the combination reaction regenerated the original chemical species. If the radical fragments from dissociation reacted irreversibly in some other way such as with a scavenger, a quasi-stationary concentration of radicals would be established in the system undergoing irreversible change. Measurements of this concentration and of the quantum efficiency for radical formation could permit calculation of the rate constant for the reaction of the radical. Such techniques apparently have not been applied to measure rate constants of radical reactions because of the difficulties of measuring absolute radical concentrations.

III. PROCESSES COMPETING WITH FLUORESCENCE

1. Introduction

Absorption of light may produce a molecule in an electronically excited state which can return to the ground state by various processes including the emission of fluorescence. Illumination for any significant time will produce a steady state in which the rate of production of excited molecules is equal to the rate of their deactivation by all processes, and for a constant intensity of illumination the intensity of fluorescence will be proportional to the steady-state concentration of excited molecules.

Since a molecule in the fluorescent state, $\mathring{A}$, differs from a ground-state molecule, A, with respect to both energy and electron wave function, a difference in chemical reactivity is to be expected. Thus excited molecules can undergo reactions that occur to a much lesser extent or not at all in the ground state. These reactions in the excited state compete with fluorescence emission. Measurements of fluorescent intensity provide information on the efficiency of this competition and can, therefore, be used to establish the kinetics and rate constants of the reactions of excited molecules. Since the mean lifetime, τ_0, of molecules in the fluorescent state is typically of the order of 10^{-8} sec., it is possible by this method to study kinetics when reaction times are of this order.

Let n_f and n_d be the rate constants (sec.$^{-1}$) of the radiative and nonradiative transitions, respectively, to the ground state. Then the mean lifetime is given by

$$\tau_0 = 1/(n_f + n_d) \tag{5}$$

and the quantum yield of fluorescence by

$$\varphi_0 = n_f \tau_0 \tag{6}$$

If the solution also contains a species B capable of reacting in some way with $\overset{*}{A}$, then

$$\overset{*}{A} + B \xrightarrow{k} \text{products} \tag{7}$$

where k is the second-order rate constant of the process. This reaction reduces the quantum yield of fluorescence to

$$\varphi = n_f/(n_f + n_d + kc) = \varphi_0/(1 + kc\tau_0) \tag{8}$$

where c is the concentration of B molecules.

Under conditions of constant absorption of the exciting light, the relative quantum yield, φ/φ_0, is equal to the corresponding intensity ratio. Thus measurements of fluorescent intensity can be used to obtain the relative rate constants $k\tau_0$. Similarly, the temperature dependence of the mean lifetime can be obtained from intensity measurements with the aid of the following relation:

$$\varphi_0(T_1)/\varphi_0(T_2) = \tau_0(T_1)/\tau_0(T_2) \tag{9}$$

This follows from Equation (6) because n_f is virtually independent of temperature. Analogous equations apply to the influence of ionic strength and of solvent on τ_0.

A more refined treatment of Reaction (7) has to take into account the fact that the time required for the incipient reactivity of an excited molecule to decrease to the stationary reactivity, kc, is comparable to the average reaction time (16,17). Thus the time-average reactivity is greater than kc. The effect of this transient excess reactivity increases with increasing efficiency of the reaction, with increasing viscosity of the solvent, and with decreasing lifetime of the excited molecules. It can be handled (17,18) (so that stationary rate constants can be obtained from measurements of fluorescent intensity) in terms of a characteristic volume of reaction, V_D (l./mole), around $\overset{*}{A}$. The probability that no B molecule is in that volume is then given by

$$W = \exp(-V_D c) \tag{10}$$

This also is the fraction of excited molecules that react at the stationary rate, whereas the fraction $(1 - W)$ may be regarded as having reacted with a B molecule immediately after excitation.

Often the reaction of excited molecules produces species which are still excited and can fluoresce with a different spectrum from the original $\overset{*}{A}$. When this *fluorescence transformation* occurs, the new fluorescence spectrum, being typical for the species formed, provides information on the type of the

reaction. The following classification of reactions which have been investigated so far by the fluorescence method is based on this information.

(*a*) Quenching of fluorescence:

$$\overset{*}{\mathrm{A}} + \mathrm{B} \rightarrow \mathrm{A} + \mathrm{B} \tag{11}$$

(*b*) Energy transfer:

$$\overset{*}{\mathrm{A}} + \mathrm{B} \rightarrow \mathrm{A} + \overset{*}{\mathrm{B}} \tag{12}$$

(*c*) Complex formation:

$$\overset{*}{\mathrm{A}} + \mathrm{A} \rightarrow \overset{*}{\mathrm{A}}_2 \tag{13a}$$

$$\overset{*}{\mathrm{A}} + \mathrm{B} \rightarrow \overset{*}{\mathrm{AB}} \tag{13b}$$

(*d*) Acid-base reactions:

$$\overset{*}{\mathrm{AH}} + \mathrm{B} \rightarrow \overset{*}{\mathrm{A}}^- + \mathrm{HB}^+ \tag{14a}$$

$$\overset{*}{\mathrm{A}} + \mathrm{HB} \rightarrow \overset{*}{\mathrm{AH}}^+ + \mathrm{B}^- \tag{14b}$$

The quantum yield for fluorescence of the species formed in fluorescence transformation is given by

$$\varphi' = \varphi_0' \frac{kc}{n_f + n_d + kc} = \varphi_0' \frac{kc\tau_0}{1 + kc\tau_0} \tag{15}$$

Here φ' is the quantum yield for fluorescence of the transformed species and φ_0' is the limiting quantum yield for this fluorescence when the efficiency of transformation is unity (as $c \rightarrow \infty$). By contrast, φ_0 is the limiting quantum yield of the original fluorescence as $c \rightarrow 0$.

It is seen that

$$(\varphi/\varphi_0) + (\varphi'/\varphi_0') = 1 \tag{16}$$

Any side reaction which quenches the fluorescence of one or the other species makes this sum smaller than unity. Thus measurements of the relative quantum yield φ'/φ_0' (which can be obtained by intensity measurements under constant absorption) are necessary in order to make due allowance for such side reactions and to avoid misinterpretations.

In order to obtain absolute values of rate constants from fluorescent intensity measurements, the mean lifetime of the excited molecules must be known. However, measurements of relative fluorescent intensities alone can be used to study secondary effects such as the influence of temperature, ionic strength, or solvent on the rates of fast reactions. Such small effects require, of course, high-precision intensity measurements.

2. Experimental Methods

A. INTENSITY MEASUREMENTS

When the fluorescent intensities of two solutions are to be compared, equal absorption of exciting light by these solutions is required. This can be achieved in two ways, provided monochromatic light is used for excitation. (*i*) With solutions of high enough optical density so that practically all exciting light is absorbed within a short distance (of the order of a few millimeters) the intensities of fluorescence emitted through the front window may be compared favorably. (*ii*) In those cases where high concentrations of the fluorescent substance should be avoided because of concentration quenching, it is necessary that both solutions have equal optical density with respect to the exciting wavelength. Measurement of fluorescent

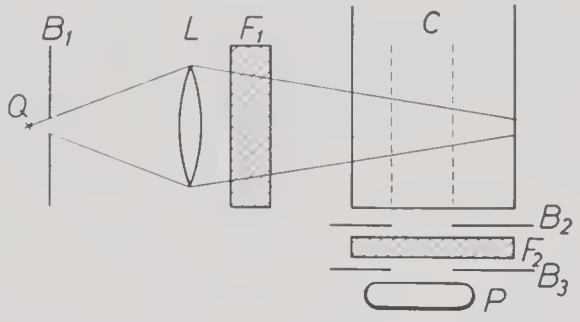

Fig. 1. Apparatus for the measurement of relative intensity of fluorescence.

intensity perpendicular to the exciting beam is then recommended. Figure 1 shows the plan of an apparatus (19,20) which has proved useful for measurements of the second type. The exciting light is isolated by means of appropriate light filters (F_1) from a high-pressure mercury lamp (Q), whose power supply is stabilized. The fluorescence is measured at right angles to the incident beam after filtering through a light filter (F_2) with the aid of photo-cell or multiplier (P), amplifier, and galvanometer. (Either light filter may be replaced by a monochromator if necessary.) Suitable placing of the apertures (B_2 and B_3) with respect to the cuvette makes the signal almost independent of the optical density of the solution over a wide range even at low concentrations. A 10% change of an optical density as low as 0.1 cm.$^{-1}$ changes the galvanometer deflection by less than 0.3%. Two quartz cuvettes containing the solutions whose relative intensities are required can be placed in the light path in turn. Water from a thermostat flows either through coils placed in the solutions or else through the outer space when double-walled cuvettes are used.

For fluorescence transformation studies the light filters F_2 must be properly selected so that the relative fluorescence yield of either component can be measured separately. Let I/I_0 and I'/I_0' be the relative intensities measured behind the selected filters F_2 and F_2', respectively; then the relative quantum yields are given by:

$$\frac{\varphi}{\varphi_0} = \frac{I}{I_0} - p\frac{\varphi'}{\varphi_0'} \text{ and } \frac{\varphi'}{\varphi_0'} = \frac{I'}{I_0'} - p'\frac{\varphi}{\varphi_0} \tag{17}$$

where p and p' are the respective reciprocal selectivities. (For highly selective filters, p approaches zero.) It follows:

$$\frac{\varphi}{\varphi_0} = \frac{(I/I_0) - p(I'/I_0')}{1 - pp'} \text{ and } \frac{\varphi'}{\varphi_0'} = \frac{(I'/I_0') - p'(I/I_0)}{1 - pp'} \tag{18}$$

B. LIFETIME MEASUREMENTS

Direct measurement of τ_0 is generally carried out with the exciting light modulated in intensity at a frequency, ν, of the order of 10^7 c.p.s. Then the intensity of the fluorescent light oscillates with the same frequency, but is shifted in phase with respect to the exciting light. From this phase shift, $\Delta\phi$, the lifetime can be obtained.

$$\tau_0 = \frac{\tan \Delta\phi}{2\pi\nu} \tag{19}$$

Gaviola (21), who was the first to measure lifetimes of fluorescence, used Kerr cells consisting of nitrobenzene between crossed polarizing prisms. These cells transmit light only when the nitrobenzene is subjected to an electric field. Thus light modulation can be brought about by application of high-frequency oscillations. Ultraviolet light also can be modulated by use of the Debye-Sears effect in which ultrasonic standing waves in a liquid cause it to act as an intermittent diffraction grating (22,23). Using the nonzero-order part of the diffraction pattern, one obtains almost 100% modulation (24).

The quantum yield of fluorescence is known (at least approximately) more often than the lifetime. An estimate of the lifetime can then be made using Equation (5). The rate constant for emission, n_f, can be calculated [with the use of equations developed by Lewis and Kasha (25)] from the absorption spectrum integrated over the long wavelength part which corresponds to the fluorescence spectrum. A useful rule of thumb is

$$n_f \approx \epsilon_{max} \cdot \tilde{\nu}_{max}^2 \cdot 10^{-5} \text{ (sec.}^{-1}\text{)} \tag{20}$$

where ϵ_{max} is the maximal molar decadic extinction coefficient at wave number $\tilde{\nu}_{max}$ (cm.$^{-1}$) of the long wavelength absorption band.

3. Results

A. QUENCHING OF FLUORESCENCE

A great deal of information on the kinetics of fast reactions in solution has been gained from studies of fluorescence quenching. However, very little is known about the detailed mechanism of quenching itself. A reversible electron transfer, as suggested by Baur (26) and by Weiss (27), seems to be highly probable, but there exists no direct experimental proof of this mechanism.

B. ENERGY TRANSFER

Equation (12) represents a transfer of electronic excitation. Hence the fluorescent intensity of $\overset{*}{A}$ will decrease when that of $\overset{*}{B}$ increases. Some reactions of this type are very fast, because the energy apparently can be transferred over a distance of some 30 A. and more. Under these conditions, the characteristic volume of reaction, V_D, becomes very large so that the simple relations (8) and (15) are no longer valid. Förster (28) has

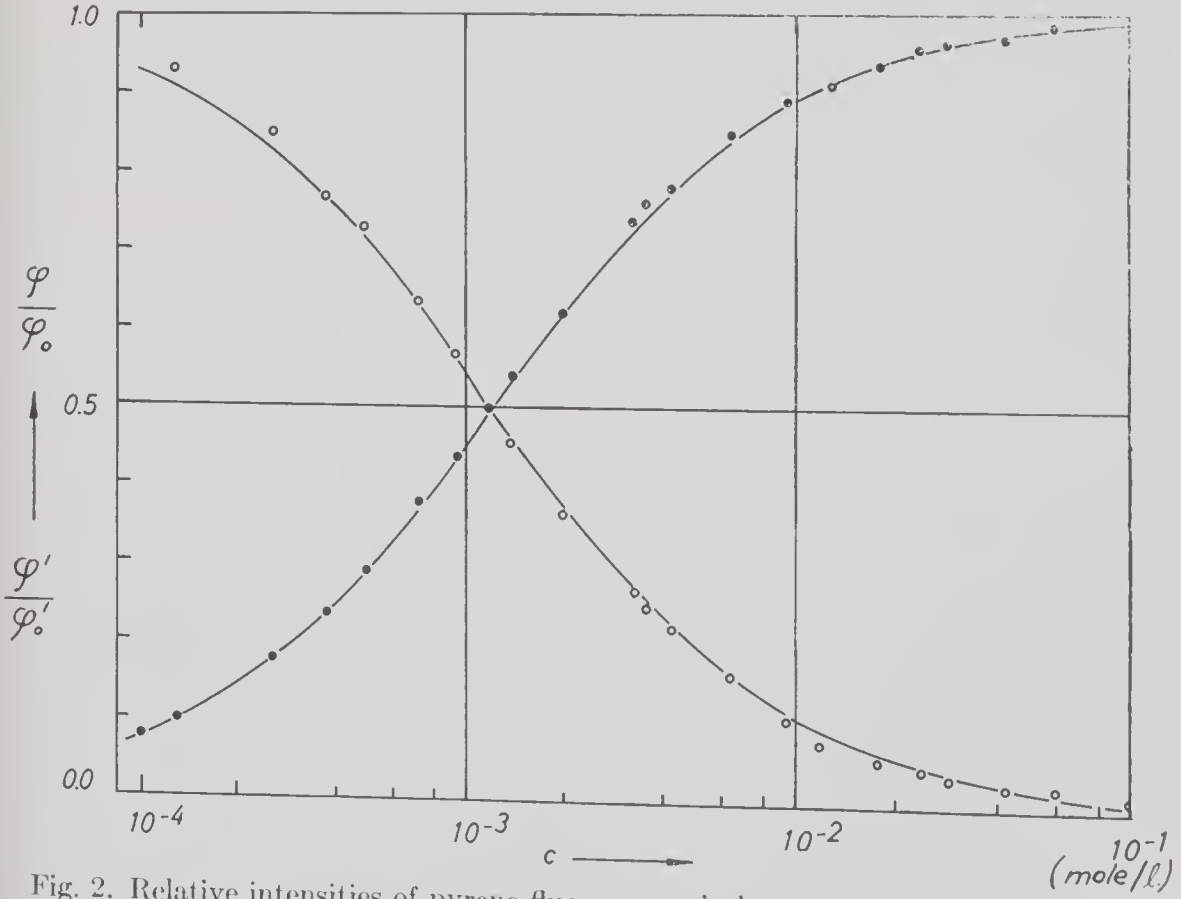

Fig. 2. Relative intensities of pyrene fluorescence in benzene as a function of pyrene concentration (32). Open circles indicate relative intensity of monomer fluorescence (φ/φ_0); filled circles indicate relative intensity of dimer fluorescence (φ'/φ'_0).

discussed the theory of this type of process and given references to a number of examples. Some very efficient transfer reactions have been investigated by Bowen (29,30).

C. COMPLEX FORMATION

In a dimerization process represented by Equation (13a) the spectrum of fluorescence varies with the concentration of A. Förster and co-workers (31,32) have studied the dimerization of pyrene and pyrene derivatives in different solvents. Figure 2 illustrates the two spectral intensities for the fluorescence of pyrene in benzene. The curves are calculated with the use of Equations (8) and (15), respectively, with $k\tau_0 = 840$ l./mole. Since the mean lifetime of excited pyrene is of the order of only 10^{-7} sec. the resulting bimolecular rate constant k of the order of 10^{10} l. mole^{-1} sec.$^{-1}$ clearly indicates a diffusion-controlled reaction. Intermolecular formation of hydrogen bonds is represented by Equation (13b) and can also be investigated by fluorescence measurements (33).

D. ACID-BASE REACTIONS

Much of the interest in fluorescence transformation arises from its use for the study of acid-base reactions of excited molecules [cf. Equations (14a) and (14b)]. In these cases the back reaction (with the rate $k'c'$) has also to be considered. This consideration leads to the following expressions:

$$\frac{\varphi}{\varphi_0} = \frac{1 + k'c'\tau_0'}{1 + kc\tau_0 + k'c'\tau_0'} \tag{21}$$

and

$$\frac{\varphi'}{\varphi_0'} = \frac{kc\tau_0}{1 + kc\tau_0 + k'c'\tau_0'} \tag{22}$$

where τ_0' is the mean lifetime of the excited species formed in the forward reaction.

Let us consider one example in more detail. Acridine (Acr) is a weak base ($pK_a = 5.5$). Thus in aqueous solutions with pH < 5 it mainly exists as acridinium cation ($AcrH^+$), whereas the neutral form predominates at pH > 6. In ammonium-buffered aqueous solutions the following reactions can occur:

$$\overset{*}{Acr} \cdot H_2O \rightarrow \overset{*}{AcrH}^+ + OH^- \tag{23}$$

$$\overset{*}{Acr} + NH_4^+ \rightarrow \overset{*}{AcrH}^+ + NH_3 \tag{24}$$

Spectra emitted from these solutions consist of the blue acridine

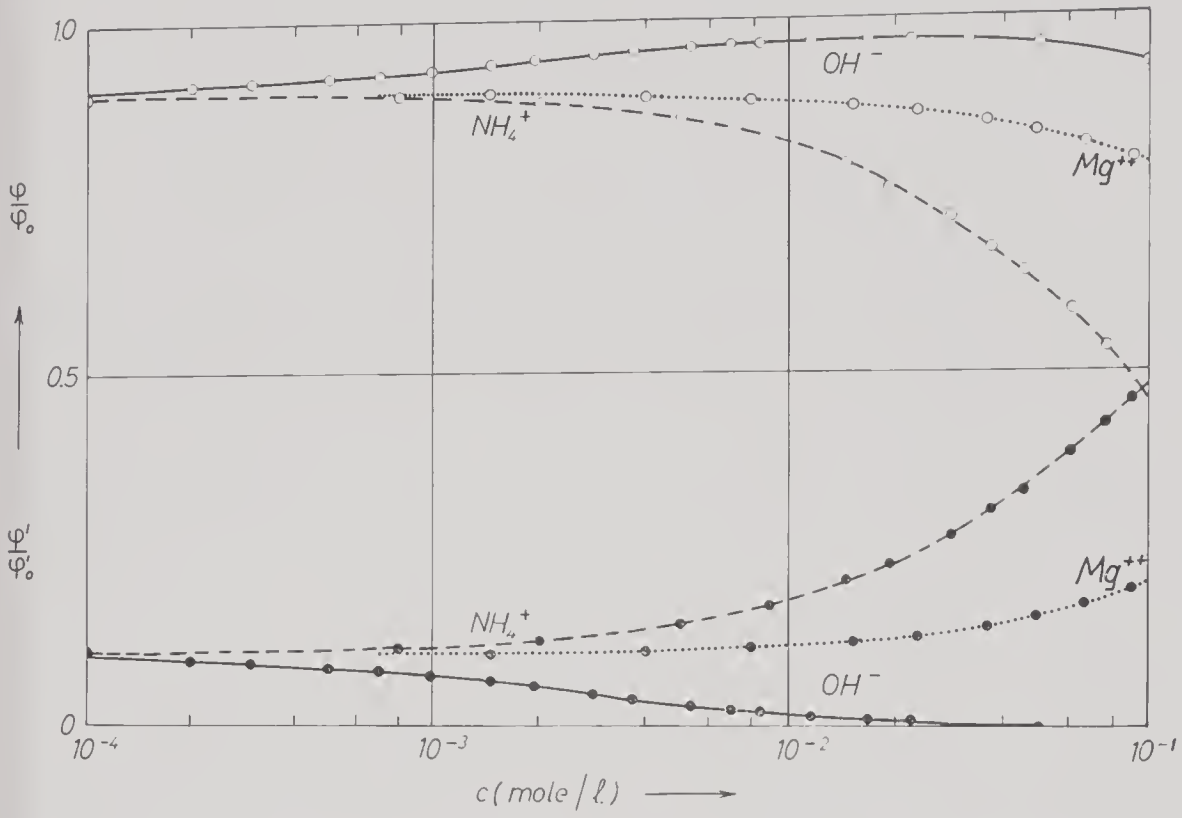

Fig. 3. Relative intensities of acridine fluorescence in water at 25°C. as a function of OH^- (——), of ammonium (— — —), and of $Mg(ClO_4)_2$ (. . . . . .) concentration, respectively. Open circles indicate relative intensity of acridine fluorescence (φ/φ_0); filled circles indicate relative intensity of acridinium fluorescence (φ'/φ'_0). ($\varphi'/\varphi'_0 = 1$ is reached in acidic aqueous solution at pH < 3.)

fluorescence and the green acridinium fluorescence in different amounts. Separate measurement of the relative intensities of these components yields the results given in Figure 3. As long as the buffer ratio $[NH_3]/[NH_4^+]$ is kept small, the back reaction of (24) need not be considered. It is seen from Figure 3, as the buffer concentration approaches zero, that some 10% of excited acridine molecules are protonated. This, evidently, is due to Reaction (23). The back reaction of this process can be studied as a function of OH^- concentration in nonbuffered solutions. The curves denoted by Mg^{++} are obtained when $Mg(ClO_4)_2$ is added to aqueous solutions (pH 8.3) of acridine. The observed effect is based on the process:

$$\overset{*}{\mathrm{Acr}} + [Mg(H_2O)_n]^{++} \rightarrow \overset{*}{\mathrm{AcrH}}^+ + [Mg(H_2O)_{n-1}OH]^+ \qquad (25)$$

The back reaction can be neglected because $[Mg(H_2O)_{n-1}OH]^+$ at pH 8.3 is at low concentration.

The results of these and other measurements are summarized in Table II. This also contains the equilibrium constants, K, the reaction enthalpies, ΔH, and the activation energies, E_A, obtained from Arrhenius plots. All

TABLE II
Acid-Base Reactions of Excited Molecules in Water at 25°C.

Reactant and Lifetimes	Reaction	K	ΔH (kcal./mole)	k / k' (l./mole·sec.)	E_A / E_A' (kcal./mole)	Ref.
Acr = 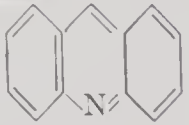	$\overset{*}{\text{Acr}}\cdot H_2O \rightleftharpoons \overset{*}{\text{AcrH}}^+ + OH^-$	$4.5\cdot10^{-4}$[a]	1.6	$8.4\cdot10^{6}$[b] $1.85\cdot10^{10}$	5.7 4.1	34
$\tau_0 = 1.4\cdot10^{-8}$ sec.	$+ NH_4^+ \rightleftharpoons + NH_3$	25	0.6	$5.7\cdot10^{8}$ $(2.3\cdot10^{7})$	4.1 (3.5)	34
$\tau_0' = 3.3\cdot10^{-8}$ sec.	$+ [Mg(H_2O)_n]^{++} \rightleftharpoons + [Mg(H_2O)_{n-1}\cdot OH]^+$	0.15	—	$9.4\cdot10^{7}$[c] $(6.3\cdot10^{8})$	— —	35
	$+ H_3BO_3\cdot H_2O \rightleftharpoons + B(OH)_4^-$	26	−8.5	$3.8\cdot10^{8}$ $(1.5\cdot10^{7})$	— —	35
AH = 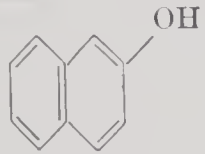	$\overset{*}{\text{AH}}\cdot H_2O \rightleftharpoons \overset{*}{\text{A}}^- + H_3O^+$	0.00154[a]	0.6	$7.3\cdot10^{7}$[b] $4.8\cdot10^{10}$	4.1 3.5	20,36
	$+ C_2H_5COO^- \rightleftharpoons + C_2H_5COOH$	115	0.8	$2.86\cdot10^{9}$ $(2.5\cdot10^{7})$	4.5 (3.7)	20
$\tau_0 = 7.6\cdot10^{-9}$ sec.	$+ C_3H_7COO^- \rightleftharpoons + C_3H_7COOH$	102	1.3	$2.76\cdot10^{9}$ $(2.7\cdot10^{7})$	4.7 (3.4)	20
$\tau_0' = 8.0\cdot10^{-9}$ sec.	$+ CH_3COO^- \rightleftharpoons + CH_3COOH$	89	0.7	$2.90\cdot10^{9}$ $(3.3\cdot10^{7})$	4.4 (3.7)	20
	$+ HCOO^- \rightleftharpoons + HCOOH$	8.7	0.6	$2.40\cdot10^{9}$ $(2.8\cdot10^{8})$	4.5 (3.9)	20
	$+ H_2PO_4^- \rightleftharpoons + H_3PO_4$	0.22	2.4	$6.0\cdot10^{8}$ $(2.8\cdot10^{9})$	— —	37
	$+ SO_4^{--} \rightleftharpoons + HSO_4^-$	0.15	5.8	$6.9\cdot10^{8}$ $(4.6\cdot10^{9})$	— —	20

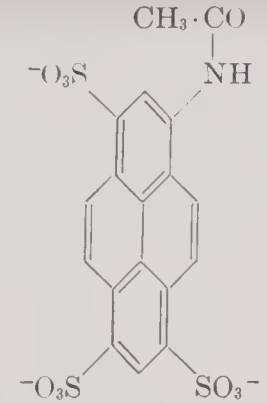

AH^{3-} =	$\overset{*}{A}H^{3-} + OH^- \rightleftharpoons \overset{*}{A}^{4-}\cdot H_2O$	$1.3\cdot10^{7}$[d]	−13.0	$1.48\cdot10^{9}$ $(1.1\cdot10^{2})$[b]	— —	38
	$+ (CH_3)_2NH \rightleftharpoons + (CH_3)_2NH_2^+$	8000	−11.3	$4.5\cdot10^{8}$ $(5.6\cdot10^{4})$	— —	38
$\tau_0 = 4.0\cdot10^{-9}$ sec.	$+ CH_3\cdot NH_2 \rightleftharpoons + CH_3\cdot NH_3^+$	5200	−12.5	$4.6\cdot10^{8}$ $(8.8\cdot10^{4})$	— —	38
$\tau_0' = 5.0\cdot10^{-9}$ sec.	$+ (CH_3)_3N \rightleftharpoons + (CH_3)_3NH^+$	800	−8.4	$2.2\cdot10^{8}$ $(2.7\cdot10^{5})$	— —	38
	$+ NH_3 \rightleftharpoons + NH_4^+$	210	−11.8	$2.3\cdot10^{8}$ $(1.1\cdot10^{6})$	3.7 (15.5)	38
	$+ CH_3COO^- \rightleftharpoons + CH_3COOH$	0.0072	+0.6	$7.8\cdot10^{6}$ $1.1\cdot10^{9}$	— —	38

[a] In this instance K has the dimensions (mole/l). [b] This rate constant has the dimension ($sec.^{-1}$). [c] With other metal ions the following values were obtained: Ca^{++}, $5.4\cdot10^{7}$; Ba^{++}, $4.7\cdot10^{7}$; Li^+, $2.0\cdot10^{7}$; Na^+, $1.1\cdot10^{7}$. [d] In this instance K has the dimensions (l./mole).

rate constants represent true stationary rate constants and have been extrapolated to zero ionic strength when necessary. Those given in parentheses have not been measured directly but have been obtained from the relationship $k = k'K$.

The experimental errors of the rate constants given in Table II depend essentially on those of the corresponding τ_0 values. The usual error in k is probably smaller than $\pm 10\%$. Values of the Arrhenius activation energy are experimentally significant to ± 0.5 kcal./mole.

4. Critique

Photostationary measurements of fluorescent intensity can be used to determine rate constants for some very fast reactions of electronically excited molecules. Although the fluorescence measurements themselves are truly photostationary, the data cannot be used to compute absolute bimolecular rate constants unless it is possible to measure the rate constant for the decay of excited molecules in pure solvent. Most of the methods of measuring this quantity do not involve photostationary techniques, and these methods introduce the time element into the bimolecular rate constants ultimately calculated.

IV. PHOTOCHEMICAL SPACE INTERMITTENCY

The photostationary applications discussed above require systems that are illuminated uniformly, and they are most accurate when the intensity of the incident light is not rapidly attenuated by absorption. If the illumination is not uniform, photostationary gradients are established in the concentrations of photochemically produced species. The magnitudes of the gradients depend upon the diffusion coefficients of these species, and photostationary experiments with nonuniform illumination offer the best promise for measuring the transport properties of unstable species that can never be prepared in high concentrations.

Such methods are particularly attractive if destruction of active species depends upon a power other than first of the concentration of these species. Then the space-average concentration throughout a system will depend upon the sizes and shapes of the areas of illumination as well as upon the total light incident on the system. The effect is similar to that of time-intermittent illumination as discussed in Chapter XX where the time-average concentration depends upon the rate of rotation of a sector as well as upon the angle of the opening in the sector.

The theory has been worked out in detail for the recombination of species like halogen atoms that are produced in pairs and destroyed by second-order

processes (39). If sharply defined light and dark areas exist in the system, a stationary state is produced such that the following equations apply:

$$D\nabla^2 c + 2\phi q - 2kc^2 = 0 \quad \text{(in light)} \tag{26}$$

$$D\nabla^2 c - 2kc^2 = 0 \quad \text{(in dark)} \tag{27}$$

where c is the local concentration of radical fragments, D is their diffusion coefficient, and the other symbols are the same as those given for Equation (3).

Detailed solutions are illustrated in Figure 4 for different systems illumi-

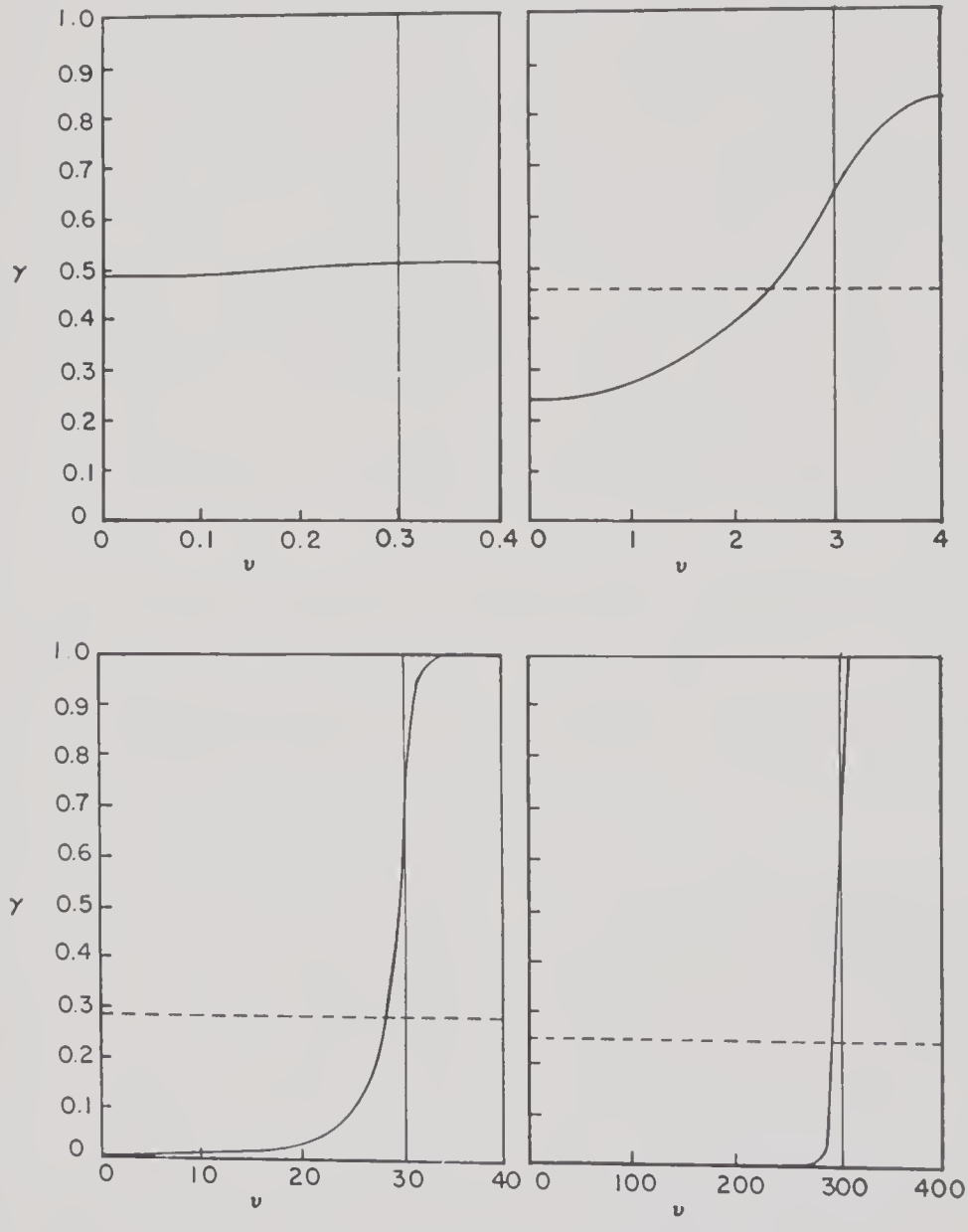

Fig. 4. Fragment concentrations for four different zebra patterns with dark strips three times as wide as light. Each plot goes from the center of a dark stip to the center of a light one. Average fragment concentrations (usually indicated with dashed lines) are 0.4999, 0.4557, 0.2898, and 0.2544.

nated by a "zebra" pattern consisting of parallel light strips one-third as wide as the dark strips between them. In these plots, γ is a normalized concentration defined to be unity for a system illuminated entirely with light of the same intensity as that in the strips. The abscissa, ν, is defined to be unity for a distance equal to $1/\sqrt{2}$ times the root-mean-square distance a fragment diffuses during an average lifetime in a solution under homogeneous illumination of the same intensity. Even though the total illumination is the same in the examples of Figure 4, the average value of γ falls from 0.5 to 0.25 as the width of individual strips increases.

The effects can be magnified by illumination in a "leopard" pattern consisting of a two-dimensional grid of circular light areas each of which has six nearest neighbors. An apparatus to employ these principles has been constructed by Dr. G. A. Salmon at the University of Oregon; it is being used to measure the diffusion coefficient of iodine atoms in hexane. These experiments have demonstrated the predicted effect does indeed exist and that it is of the anticipated magnitude (40).

The interest in these systems arises because the rate of recombination of atoms in solution is determined by diffusion together. If diffusion is slow enough compared to the reaction so that an atom has much less chance to be found near another atom than near an arbitrary point in solution, and if the medium can be regarded as an isotropic continuum even when two atoms are almost in contact, then the rate constant (l./mole sec.) is given by

$$k = 4\pi\rho DN/1000 \tag{28}$$

where ρ is the diameter of an atom in centimeters and N is Avogadro's number. All the quantities in this equation except D have already been measured independently. Measurement of D will provide a test of the isotropic continuum model upon which the derivation is based.

References

1. E. Rabinowitch and W. C. Wood, *Trans. Faraday Soc.*, **32**, 907 (1936).
2. E. Rabinowitch and W. C. Wood, *J. Chem. Phys.*, **4**, 497 (1936).
3. E. Rabinowitch and W. C. Wood, *Trans. Faraday Soc.*, **32**, 547 (1936).
4. R. M. Noyes, *J. Am. Chem. Soc.*, **77**, 2042 (1955).
5. A. C. Rutenberg and H. Taube, *J. Am. Chem. Soc.*, **72**, 5561 (1950); **73**, 4426 (1951).
6. F. W. Lampe and R. M. Noyes, *J. Am. Chem. Soc.*, **76**, 2140 (1954).
7. I. J. Gardner and R. M. Noyes, *J. Am. Chem. Soc.*, **83**, 2409 (1961).
8. K. E. Russell and J. Simons, *Proc. Roy. Soc. London*, **A217**, 271 (1953).
9. M. I. Christie, A. J. Harrison, R. G. W. Norrish, and G. Porter, *Proc. Roy. Soc. London*, **A231**, 446 (1955).
10. R. L. Strong, J. C. W. Chien, P. E. Graf, and J. E. Willard, *J. Chem. Phys.*, **26**, 1287 (1957).

11. H. Rosman and R. M. Noyes, *J. Am. Chem. Soc.*, **80**, 2410 (1958).
12. J. Zimmerman and R. M. Noyes, *J. Chem. Phys.*, **18**, 658 (1950).
13. R. Marshall and N. Davidson, *J. Chem. Phys.*, **21**, 2086 (1953).
14. R. L. Strong and J. E. Willard, *J. Am. Chem. Soc.*, **79**, 2098 (1957).
15. S. Aditya and J. E. Willard, *J. Am. Chem. Soc.*, **79**, 2680 (1957).
16. R. M. Noyes, *J. Am. Chem. Soc.*, **79**, 551 (1957); *J. Phys. Chem.*, **65**, 763 (1961); *Progr. Reaction Kinetics*, **1**, 129 (1961).
17. A. Weller, *Z. physik. Chem. N. F.*, **13**, 335 (1957).
18. A. Weller, *Z. physik. Chem. N. F.*, **15**, 438 (1958).
19. A. Weller, *Z. Elektrochem.*, **56**, 662 (1952).
20. A. Weller, *Z. physik. Chem. N. F.*, **17**, 224 (1958).
21. E. Gaviola, *Z. Physik*, **42**, 853 (1927).
22. O. Maerks, *Physikal. Z.*, **37**, 562 (1936); *Z. Physik*, **109**, 685 (1938).
23. L. A. Tumerman and W. Szymanowski, *Compt. Rend. Acad. Sci. URSS*, **15**, 323 (1937).
24. For details see e.g. A. Schmillen, *Z. Physik*, **135**, 294 (1953); E. A. Bailey, Jr., and G. K. Rollefson, *J. Chem. Phys.*, **21**, 1315 (1953); B. D. Venetta, *Rev. Sci. Instr.*, **30**, 450 (1959).
25. G. N. Lewis and M. Kasha, *J. Am. Chem. Soc.*, **67**, 994 (1945). Also cf. Th. Förster, *Fluor. org. Verb.*, Vandenhoeck & Ruprecht, Göttingen, 1951, 158.
26. E. Baur, *Z. physik. Chem.* **B16**, 465 (1932).
27. J. Weiss and H. Fischgold, *Z. physik Chem.*, **B32**, 135 (1936).
28. Th. Förster, *Discussions Faraday Soc.*, **27**, 7 (1959); *Z. Elektrochem.*, **64**, 157 (1960); also in *Comparative Effects of Radiation*, John Wiley, New York, 1960, 300–319.
29. E. J. Bowen and R. Livingston, *J. Am. Chem. Soc.*, **76**, 6300 (1954).
30. E. J. Bowen and B. Brocklehurst, *Trans. Faraday Soc.*, **51**, 774 (1955).
31. Th. Förster and K. Kasper, *Z. Elektrochem.*, **29**, 976 (1955).
32. E. Döller, Dissertation, Stuttgart, 1960.
33. K. H. Grellmann and A. Weller, *Z. Elektrochem.*, **64**, 145 (1960).
34. A. Weller, *Z. Elektrochem.*, **61**, 956 (1957).
35. H. Leonhardt, Diplomarbeit, Stuttgart, 1958; H. Leonhardt and A. Weller *Naturwiss.*, **47**, 58 (1960).
36. A. Weller, *Z. physik. Chem. N. F.*, **3**, 238 (1955).
37. M. Gurr, Diplomarbeit, Stuttgart, 1959.
38. A. Weller, *Z. physik. Chem. N. F.*, **18**, 163 (1958).
39. R. M. Noyes, *J. Am. Chem. Soc.*, **81**, 566 (1959).
40. G. A. Salmon and R. M. Noyes, *J. Am. Chem. Soc.*, **84**, 672 (1962).

CHAPTER XVII

MAGNETIC RESONANCE METHODS

H. STREHLOW, *Max-Planck-Institut für physikalische Chemie, Göttingen*

I. Introduction 865
II. The Evaluation of Rate Constants of Rapid Reactions by Nuclear Magnetic Resonance 866
1. Qualitative Discussion of Nuclear Magnetic Resonance 866
2. Nuclear Relaxation Times and Line Widths 869
3. The Bloch Equations 872
4. Chemical Shift and Electron-Coupled Spin Interaction 875
5. Chemical Exchange Reactions and Nuclear Magnetic Resonance 876
6. The Measurement of Line Widths and the Relaxation Time T_2 879
7. The Protolysis of Methyl Ammonium Ion; An Application of Nuclear Magnetic Resonance to Reaction Kinetics 881
8. Results 883
9. The Measurement of Rate Constants for Paramagnetic Pulse Reactions by Nuclear Magnetic Resonance 885
10. Exchange Broadening on Nuclei with Quadrupole Moments 887
III. The Evaluation of Rate Constants of Rapid Reactions by Electron Spin Resonance 888
1. Kinetic Line Broadening in ESR 888
2. Experimental Results 889
References 891
General References 892

I. INTRODUCTION

Nuclear magnetic resonance (NMR) and electron spin resonance (ESR) have proven to be most useful tools for the elucidation of structures of chemical compounds. These two methods make use of the Zeeman splitting of nuclear or electron energy levels, which depends on the chemical environment of the magnetic moments. If the magnetic field is in the kilogauss region the resonance frequency is of the order of megacycles per second for nuclear moments and of kilomegacycles per second for electron spin moments. Among other factors the measured line widths depend upon the average lifetime of the spin state in question. Thus kinetic information can be obtained for systems which are in a (dynamic) state of equilibrium. Since the line widths for nuclear magnetic resonance, and

electron spin resonance spectra are appreciably different, the range of lifetimes measurable by the two methods differ by orders of magnitude. In the case of NMR lifetimes of about 1 to 10^{-4} sec. are measurable while with ESR lifetimes between 10^{-4} and 10^{-9} sec. have been investigated.

Since NMR spectra are in general much simpler than ESR spectra, and since more kinetic investigations have been performed with the former, this method will be treated first, in Section II. The underlying physical principles are outlined so far as seems necessary for an understanding of the applications in fast-reaction kinetics. Section II is concluded by a compilation of experimental results and a short introduction to recently developed special methods for the investigation of fast reactions by NMR.

Section III is devoted to the application of ESR to kinetic problems.

A great advantage of the methods described in this chapter is that measurements are made under equilibrium conditions. The serious experimental difficulties of other methods used in this field, namely establishing a well-defined disturbance of the equilibrium state, do not apply here.

Of course, like all experimental methods, those using NMR and ESR spectra have their drawbacks. Thus NMR can only be applied to nuclei with a finite spin (e.g., O^{16} and C^{12} have none) and ESR can only be applied to substances with unpaired electron spins. Furthermore the experimental equipment of either method is not very simple and is quite expensive. Nevertheless, there is a growing use of these modern techniques in the field of fast-reaction kinetics.

II. THE EVALUATION OF RATE CONSTANTS OF RAPID REACTIONS BY NUCLEAR MAGNETIC RESONANCE

1. Qualitative Discussion of Nuclear Magnetic Resonance

Since nuclear magnetic resonance is discussed elsewhere in this series, and, since other good introductions to the general field are available, (1) in this section the physical basis of nuclear magnetic resonance will be treated only so far as is necessary for an understanding of its application in reaction kinetics. For the same reason experimental procedures are discussed only briefly.

Many atomic nuclei have a nuclear spin different from zero, and, combined with the spin, a magnetic moment. The order of magnitude of the angular momentum p is $\hbar$, and that of the magnetic moment is a nuclear magneton $e\hbar/2m_pc$, which is about 2000 times smaller than the Bohr magneton since the mass of the proton m_p is so much greater than that of the electron m_e. Therefore paramagnetism, which is the consequence of nuclear

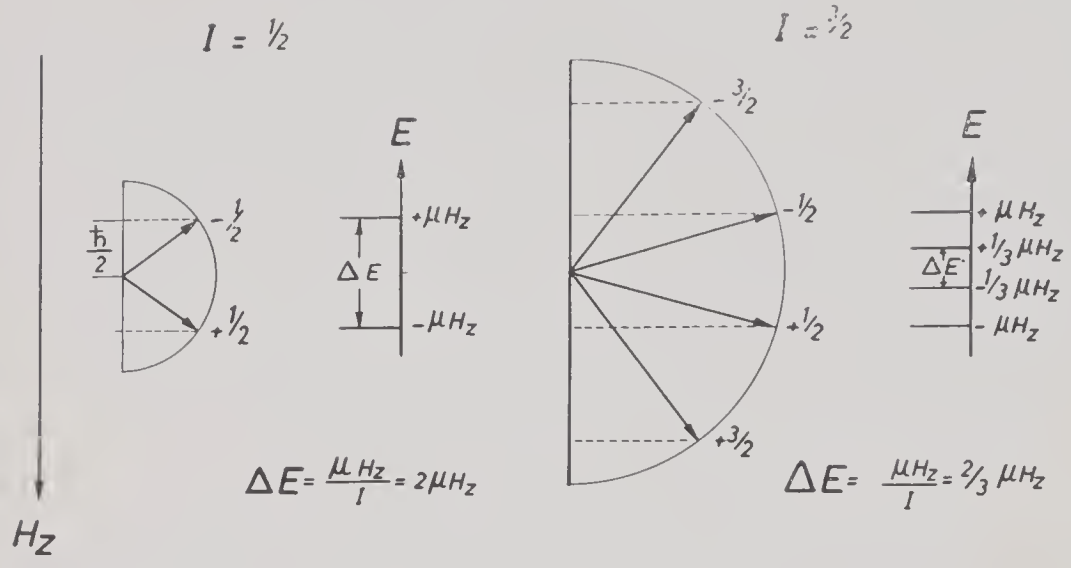

Fig. 1. Orientation and energy for nuclei with nuclear spin quantum numbers $I = 1/2$ and $I = 3/2$ in a magnetic field H_z.

magnetic moments, is very small compared with normal diamagnetism and can only be observed at extremely low temperatures. If a sample containing nuclei with spin quantum number I is put into a strong magnetic field H_z, the magnetic dipoles μ orient themselves in $2I + 1$ allowed directions relative to the z axis. Different energies correspond to these orientations and the energy levels are occupied according to Boltzmann's law. Because of the torque L exerted on the magnetic moments by H_z the moments precess about the z axis with an angular frequency ω. The torque is given by

$$L = \mu H_z \sin(z,\mu) \tag{1}$$

On the other hand we have for L

$$L = \omega p \sin(\omega,p) \tag{2}$$

Since the angle between z and μ is the same as that between ω and p, we have

$$\omega = (\mu/p)H_z = \gamma H_z \tag{3}$$

The precession frequency ω (Larmor frequency) is therefore proportional to the magnetic field strength H_z. The constant of proportionality γ, known as the gyromagnetic ratio, is the quotient of magnetic moment and angular momentum and is constant for a given atomic nucleus. For magnetic field strengths of 10^4 gauss, which are experimentally attainable, the Larmor frequencies are of the order of 10^7 sec.$^{-1}$.

If a weak alternating magnetic field of the Larmor frequency ω is applied perpendicular to the z axis, e.g., in the direction of the x axis, jumps between different energy levels are induced. The probability of emission and absorption are equal but since occupation numbers of low energy levels

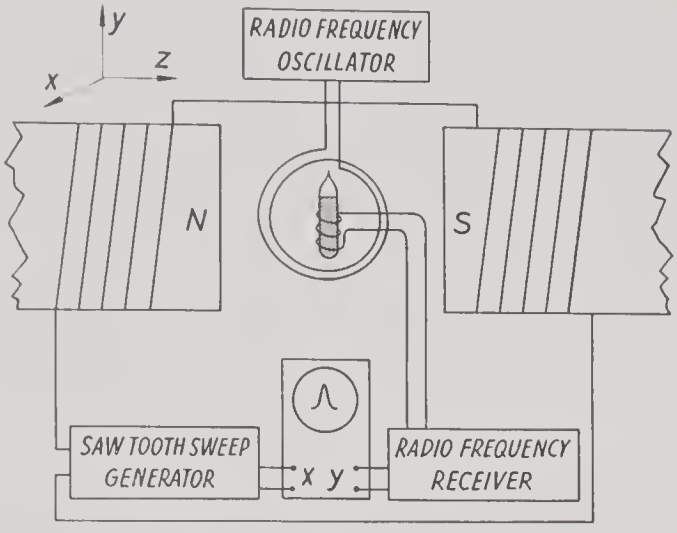

Fig. 2. Schematic diagram of a Bloch nuclear magnetic resonance apparatus

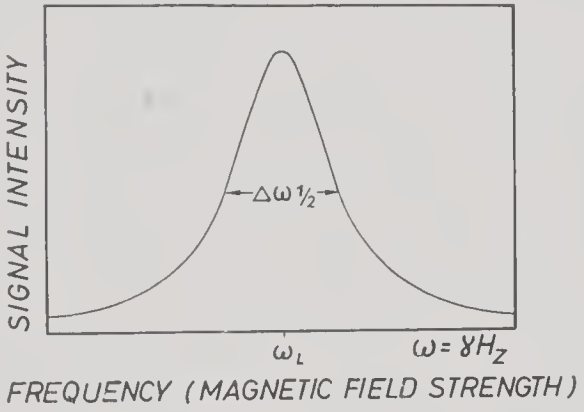

Fig. 3. Signal intensity as function of frequency (or magnetic field strength).

are greater than those of high energy levels, a net absorption takes place. This absorption, which corresponds to an energy increase of the spin system, can be followed experimentally. According to Bloch (2) a receiver coil is arranged in the y direction perpendicular to the magnetic field and to the transmitter coil (x axis). The alternating nuclear magnetic moments induce a voltage in the receiver coil, which may be amplified and measured. (According to Purcell and co-workers (3), the energy taken from the transmitter coil can be measured directly without a receiver coil. At the Larmor frequency the resistance of the transmitter coil increases and its change with frequency can be measured in a bridge arrangement. In the following discussion, however, only the Bloch method will be considered, since this forms the basis of the commercially available instruments.)

A signal can only be observed in the receiver coil if the angular frequency ω of the alternating magnetic field coincides with the Larmor frequency defined by Equation (3). Nuclear magnetic resonance can either be measured at constant magnetic field with variable frequency, or with fixed frequency

and a modulated magnetic field. In practice, the latter method is preferred. Figure 2 represents the principle of a Bloch nuclear magnetic resonance apparatus. The magnetic field H_z is modulated with a magnetic saw-tooth field of low frequency and amplitude. The horizontal plates of the oscilloscope are coupled to the same frequency. When the total magnetic field H_z has the value prescribed by Equation (3) for resonance, a voltage is induced as shown in Figure 3. The half widths of such absorption lines may be extremely small in liquids and in fact are often due to the unavoidable inconstancy of the magnetic field over the sample volume during the time of measuring.

2. Nuclear Relaxation Times and Line Widths

For further treatment we shall confine our discussion to the most important case of proton magnetic resonance. The spin quantum number I is $^1/_2$ for the proton. In the magnetic field there are therefore two Zeeman levels whose occupation numbers are in the ratio:

$$\frac{\exp\,(-\mu H_z/kT_s)}{\exp\,(\mu H_z/kT_s)} \sim \left(1 - \frac{2\mu H_z}{kT_s}\right) : 1 \tag{4}$$

Here $\mu H_z/kT$ at room temperature and at the highest available field strength H_z is only of the order of 10^{-5}, and the two energy levels are therefore nearly equally populated. If an alternating magnetic field with the Larmor frequency is applied, this small difference almost vanishes since the probability of absorption and emission is equal. Formally this means that the "spin temperature" T_s defined by Equation (4) rises and may acquire very high values. Since the spin system and the lattice system* are nearly adiabatically insulated from each other, the energy taken up by the spin system can only slowly be transferred to the lattice system. The relaxation time of this energy transfer is called the spin-lattice relaxation time T_1. This process is caused by the Fourier component of the Larmor frequency ω_L of the magnetic noise which in turn is a consequence of the thermal agitation of nuclear moments or of any existing paramagnetic substances.

A characteristic time, which oriented electric dipoles of radius a need to attain statistical distribution in a medium of viscosity η at a temperature T, is given according to Debye by

$$\tau_D = 4\pi\eta a^3/kT \tag{4a}$$

For nuclear magnetic moments the correlation time τ_c is similarly given by

$$\tau_c = 4\pi\eta a^3/3kT \tag{4b}$$

* Lattice system, in this connection, denotes the molecular surrounding into which the nucleus in question is embedded. It is not necessarily a solid.

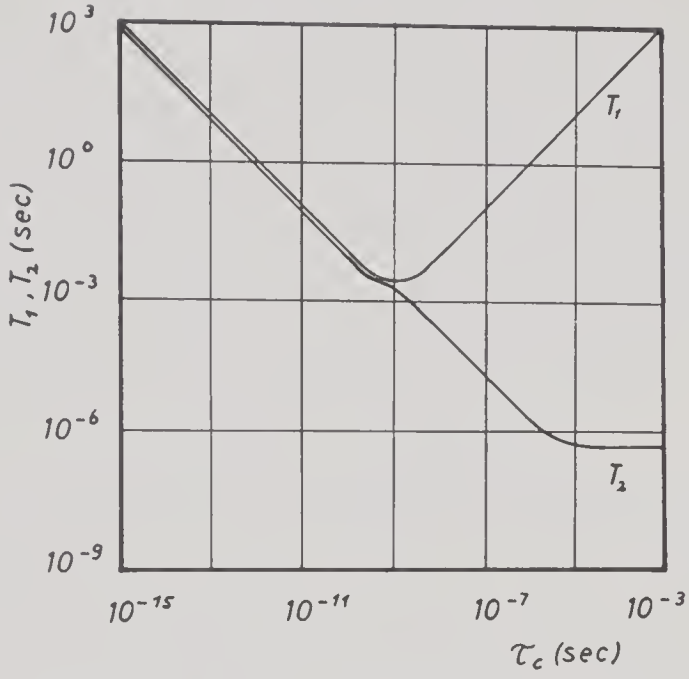

Fig. 4. Nuclear relaxation times T_1 and T_2 as a function of the correlation time τ_c.

The Fourier coefficient of magnetic noise will therefore be at a maximum when $\omega \approx 1/\tau_c$. If the Larmor frequency is of this order of magnitude, a rapid energy transfer from the spin system to the lattice system is possible: T_1 is a short time. For smaller and for larger τ_c the relaxation times T_1 are larger, the Larmor frequency ω_L being held constant. In Figure 4 (upper curve) T_1 is plotted as a function of τ_c. Thus T_1 is the time constant with which the magnetization M_z grows after the magnetic field H_z is switched on. Therefore T_1 is sometimes called the longitudinal relaxation time.

Not only is the building up (or decay) of the magnetization in the z direction a process which needs finite times for completion, but the attainment of the stationary state for the rotating magnetic field in the xy plane is also related to a relaxation time T_2. The application of the rotating magnetic field forces the precessing moments into phase. Macroscopically this corresponds to a rotating transversal magnetization. After switching off H_x, the phase relations decay with the time constant T_2. There are several physical reasons for a finite T_2. By virtue of the magnetic field exerted on any one nucleus by neighboring nuclear moments, the total magnetic field at this nucleus fluctuates with an amplitude of about $\Delta H_{\text{loc}} \sim 1$ gauss, and therefore the Larmor frequency is not exactly the same for every nucleus but varies by about $\Delta\omega = \gamma \Delta H_{\text{loc}}$. If at time $t = 0$ all moments are in phase and the field H_x is switched off, then at $t = T_2' \sim 1/\Delta\omega$ the phases of the precessing moments are distributed over one radian and the rotating magnetization has decayed to $1/e$ of its original value. The time T_2' which may be called the "phase memory time" is reduced still further

by another effect. The moment of a proton can be switched over to the alternative direction if at the same time another nucleus changes in the opposite sense. The energy does not change by such a process but the phase relation of the two nuclei is lost and the transversal magnetization is thereby diminished.

The relation between T_2' and τ_c may be qualitatively understood in the following way: In a medium with small τ_c [low viscosity, high temperature, see Equation (4b)], ΔH_{loc} is averaged out by Brownian molecular movement during one revolution of precession, and the transversal magnetization is not affected. An energy exchange between two nuclei is only possible if the nuclei are in neighboring positions for a sufficiently long time. For small τ_c, T_2' is thus inversely proportional to τ_c. Only when T_2' becomes of the order of magnitude of τ_c, will the decay of the transversal magnetization attain its maximum value. The minimum value of T_2' is about 10^{-6} sec. Except by the discussed mechanisms every change of magnetic moment from one energy level to another related to the relaxation time T_1 results in a loss of phase relation. Therefore the relaxation time T_2 is shorter than T_2' and is given by

$$1/T_2 = (1/T_2') + (1/2T_1) \tag{5}$$

(The factor 2 in the denominator of the second term of Equation (5) accounts for the fact that for every jump the difference between the occupation numbers of the two energy levels changes by 2.) T_2 is called the spin-spin relaxation time or, according to Bloch, the transversal relaxation time. The dependence of T_2 on the correlation time is given by the lower curve of Figure 4 and is qualitatively understood by the foregoing discussion. For liquids (with low η) $T_1 \simeq T_2' \sim T_2$.

The precessing nuclear moments are distributed about the Larmor frequency with $\Delta\omega \sim 1/T_2$, and therefore the signal in the receiver must show a half line width of about this magnitude. A more rigorous calculation shows that

$$\Delta\omega_{1/2} = 2/T_2 \tag{6}$$

For water at room temperature, T_2 is about 2 sec. and therefore $\Delta\omega_{1/2} = 1$ sec.$^{-1}$. With an irradiation frequency $\omega = 2\pi\nu = 10^8$ sec.$^{-1}$ we have therefore

$$\Delta\omega/\omega = 10^{-8}$$

The constancy of the frequency ω and of the magnetic field H_z, which is proportional to ω according to Equation (3), must be better than $1:10^8$ if the natural line width is to be resolved. The measured line width is therefore

$$\Delta\omega_{\text{obs}} = (2/T_2) + \gamma\Delta H_z = 2/T_{2\text{eff}} \tag{6a}$$

ΔH_z is the inhomogeneity of the magnetic field and, with fluids, often determines the observed line width. The inhomogeneity broadening $\gamma \Delta H_z$ can be appreciably reduced by an ingenious experimental device proposed by Bloch. The sample is rotated with an angular frequency $\omega_{rot} \gg 1/T_2$. The inhomogeneities of the magnetic field are thereby averaged out to a considerable extent. The nuclear moments "see" the average of the magnetic field H_z.

Another possible cause of line broadening is the presence of nuclear quadrupole moments. Only nuclei with spin quantum number $I > 1/2$ possess quadrupole moments and therefore this matter will only be mentioned briefly. Nuclear quadrupoles precess under the influence of gradients of electric field strength and thereby influence the energy levels. The spin-lattice relaxation times for quadrupole moments, because of the noise of inhomogeneities of the electrical field, are often small compared with T_2 and T_2'. Therefore a shortening of T_2 occurs [analogous to Equation (5)] and line broadening is observed.

3. The Bloch Equations

A quantitative discussion of the phenomena described in the foregoing sections has been given by Bloch. His differential equations and some of his results of practical importance are given in this section.

For a single nucleus, according to Equation (3), the magnetic moment μ and the angular moment p are proportional to each other. With $\mu = \gamma p$, and Equation (1)

$$L = \frac{dp}{dt} = \frac{1}{\gamma}\frac{d\mu}{dt} = \mu \times H \tag{7}$$

(Because of the rotating magnetic field, H is not given exactly by H_z.) Summing over all nuclear moments within 1 cm.^{3} we obtain for the macroscopically observable magnetization

$$dM/dt = \gamma M \times H \tag{8}$$

This time-dependence of M is superimposed on the spin-lattice and the spin-spin relaxations

$$\frac{dM_z}{dt} = \frac{M_0 - M_z}{T_1}, \quad \frac{dM_x}{dt} = -\frac{M_x}{T_2}, \text{ and } \frac{dM_y}{dt} = -\frac{M_y}{T_2} \tag{9}$$

M_z, M_x, and M_y are the instantaneous values of the components of magnetic action, and M_0 the stationary value which builds up under the field strength H_z after sufficient time if $H_x = H_y = 0$.

In the x direction a periodic magnetic field of angular frequency H_x is applied: $H_x = 2H_1 \cos \omega t$. This field can be thought of as the superposition of two circularly polarized fields, $H_1 \cos \omega t + H_1 \sin \omega t$ and $H_1 \cos \omega t - H_1 \sin \omega t$, with opposite senses of rotation. Only the field which has the same sense of rotation as the precessing moments can cause a jump of nuclear moments. With positive γ we have for the effective field

$$H_x = H_1 \cos \omega t \text{ and } H_y = -H_1 \sin \omega t \tag{10}$$

Combining Equations (8), (9), and (10) we get for the three components of dM/dt the Bloch equations:

$$\begin{aligned} \frac{dM_x}{dt} &= \gamma \left[M_y H_z + M_z H_1 \sin \omega t\right] - \frac{M_x}{T_2} \\ \frac{dM_y}{dt} &= \gamma \left[M_z H_1 \cos \omega t - M_x H_z\right] - \frac{M_y}{T_2} \\ \frac{dM_z}{dt} &= \gamma \left[-M_x H_1 \sin \omega t - M_y H_1 \cos \omega t\right] + \frac{M_0 - M_z}{T_1} \end{aligned} \tag{11}$$

A general solution of (11) is rather involved, but some special cases are of practical interest. Compared to the relaxation times H_z is so slowly modulated that the time necessary for passing the resonance line is long. The signal then measured in the receiver coil has the form shown in Figure 3. For this case of slow passage through the resonance and for a weak high-frequency field

$$\gamma H_1 (T_1 T_2)^{1/2} \ll 1$$

the half line width is calculated as

$$\Delta H_{1/2} = \frac{1}{\gamma} \Delta \omega_{1/2} = \frac{1}{\gamma} \frac{2}{T_2} \tag{9}$$

The signal intensity $U_{\max}$ at resonance under these conditions is dependent on the parameters according to

$$U_{\max} = \text{const. } n H_z^2 \frac{I(I+1)}{T} \frac{\gamma^4 H_1 T_2}{1 + \gamma^2 H_1^2 T_1 T_2} \tag{12}$$

Here n is the number of nuclei/cm.^{3} with spin quantum number I and gyromagnetic ratio γ. The constant contains the geometric and electrical values of the receiver coil; $U_{\max}$ increases linearly with magnetic field strength H_z and is inversely proportional to the temperature. The dependence of $U_{\max}$ on the irradiated field strength H_1 is shown in Figure 5. For small H_1, $U_{\max}$ increases linearly with H_1, and passes through a maxi-

mum; at large H_1, U_{max} decreases as $1/H_1$. The physical meaning of this decrease has already been discussed in Section II-2. The populations of the two energy levels equalize at high field strength H_1, while the spin temperature tends to infinity. At equal occupation absorption and emission are also equal and the signal disappears. The optimal signal is given if

$$(H_1)_{opt} = 1/\gamma(T_1T_2)^{1/2} \tag{13}$$

Equation (12) shows that $U_{max} = 0$ if $T_2 = 0$ or if $T_1 = \infty$. In the first case the magnetic moments cannot be forced into phase with the rotating field, since the phase relation decays infinitely rapid. For $T_1 = \infty$, the nuclear magnetic moments are ideally insulated from the lattice system; the spin

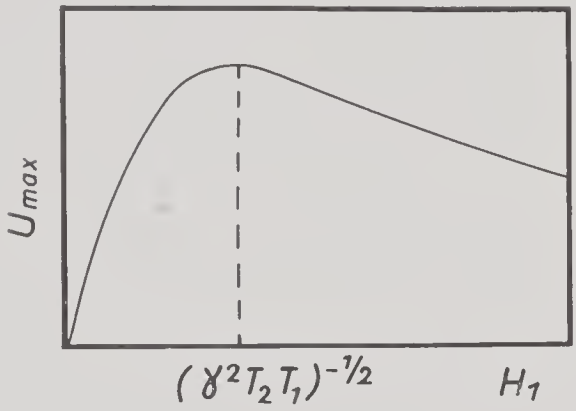

Fig. 5. Signal intensity at resonance frequency as function of the intensity H_1 of the irradiating field.

system is accordingly heated to the temperature $T_s = \infty$ and saturation occurs even with the smallest field strength. For the ratio of the signal U to the noise level N one calculates, after collecting all constants,

$$\rho = \frac{U}{N} = \text{const. } n_0 p H_z^{3/2} \left(\frac{T_2}{\Delta f T_1}\right)^{1/2} \approx \text{const. } \frac{n_0 p H_z^{3/2}}{(\Delta f^{1/2})} \tag{14}$$

where p, the filling factor, is the volume fraction of the receiver coil which is filled by the sample. Since T_2 and T_1 are about equal, in liquids, their influence on ρ may be neglected; Δf is the band width of the receiver arrangement. To obtain the most favorable signal-to-noise ratio for a given number of nuclei it is therefore advisable to work with the highest available magnetic field strength. By using for example a suitable lock-in detector with very small band width (down to 0.01 sec.$^{-1}$) even very weak signals can be measured. But it must be remembered that the resonance line must be passed in a time which is longer than about $10/\Delta f$, so that very long measuring times may be necessary, and the requirements of time constancy of the magnetic field may become critical.

4. Chemical Shift and Electron-Coupled Spin Interaction

After the introduction of the nuclear magnetic resonance method by the groups of Bloch and Purcell, gyromagnetic ratio values of different nuclei were obtained with a high degree of accuracy. To a very good approximation this quantity is independent of the chemical compound in which the nucleus in question is bound. But as early as 1950 (4) it was found that with sufficiently high resolution a weak dependence of the resonance frequency on the state of binding of the nucleus can be observed. The principal reason for this "chemical shift" is the weak diamagnetism of the electronic environment of the nucleus. The field at the position of the nucleus is thereby reduced to the value H where

$$H = H_z - \sigma H_z \tag{15}$$

The shielding constant σ is characteristic of the type of chemical binding. Generally, for any given nucleus one selects a definite compound as reference substance, setting $\sigma_{\text{ref.}}$ for the reference nucleus equal to zero. Then we have

$$\sigma = (H_z - H_{\text{ref}})/H_z \tag{15a}$$

where the resonance field strength of the nucleus in question is H_z and of the reference nucleus H_{ref}. For protons σ is of the order of magnitude of 10^{-6} whereas for other nuclei it can be as large as 10^{-2}. The chemical shift therefore allows a determination of the kind and quantity of differently bound atoms in the nuclear magnetic resonance spectrum. Figure 6 shows the nuclear magnetic resonance spectrum of ethyl alcohol. The areas under the maxima are in the ratio 1:2:3 corresponding to the number of protons bound as OH, CH_2, and CH_3, respectively. The chemical shift method has developed into an extremely valuable tool in chemical structural research. For the problem of the kinetics of rapid reactions it provides the means of recognizing nuclei, e.g., protons, in definite binding states. As

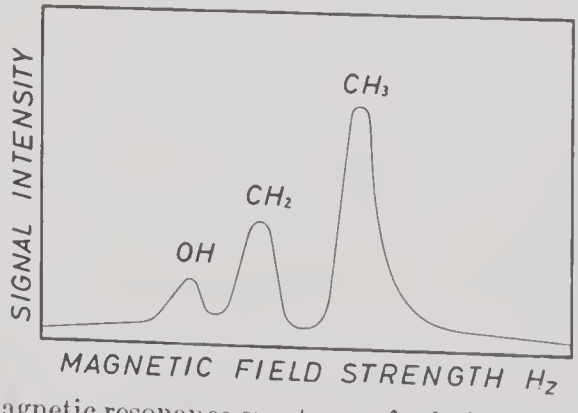

Fig. 6. Nuclear magnetic resonance spectrum of ethyl alcohol. Low resolution.

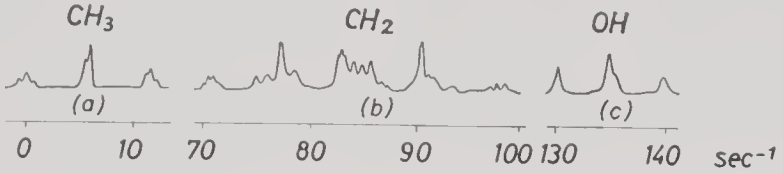

Fig. 7. Nuclear magnetic resonance spectrum of ethyl alcohol at 30.5 Mc sec^{-1}. High resolution (Arnold†).

shown in the next section the observed line width gives information about the lifetimes of the nuclei in these binding states. With these lifetimes the rate constants of the involved exchange reactions can be calculated.

A further splitting of the signal from protons (and other nuclei), known as the electron-coupled spin interaction, or more simply, spin-spin interaction, may be observed with still higher resolution of the nuclear magnetic resonance spectrometer. Figure 7 shows the spectrum of ethyl alcohol at high resolution. The three lines of Figure 6 now show a hyperfine structure.† This new splitting is caused by a partial polarization of the binding electrons due to the nuclear magnetic moments, and the thereby altered resonance condition of neighboring protons. Such alternating polarization may occur over more than one bond. As an example we shall discuss the splitting of the lines of CH_3 and OH protons in C_2H_5OH. The two protons in the CH_2 group together may have the spins $+1$, 0, or -1 (with the probabilities of the binominal coefficients 1:2:1).

These spin orientations split the energy levels of the protons of CH_3 and OH into triplets with relative intensities 1:2:1. This kind of splitting is evidently independent of the external field strength and may consequently be distinguished from the chemical shift, which is proportional to the field. This, of course, is only possible if two frequencies (and therefore field strengths) are available in the nuclear magnetic resonance spectrometer.

It must be borne in mind that there is no electron-coupled spin interaction between equivalent protons. This hyperfine structure similar to the chemical shift may provide information of a kinetic nature.

5. Chemical Exchange Reactions and Nuclear Magnetic Resonance

The change of appearance of a nuclear magnetic resonance spectrum under the influence of chemical exchange reactions will be described in terms of the following example. Protons exchange rapidly between two substances AH and BH according to

$$AH^* + BH \rightleftharpoons AH + BH^* \tag{16}$$

† Figure 7 has been taken from an important paper of Arnold [J. T. Arnold, *Phys. Rev.*, **102**, 136 (1956)] who also demonstrated the exchange of protons on the hydroxyl group of ethyl alcohol.

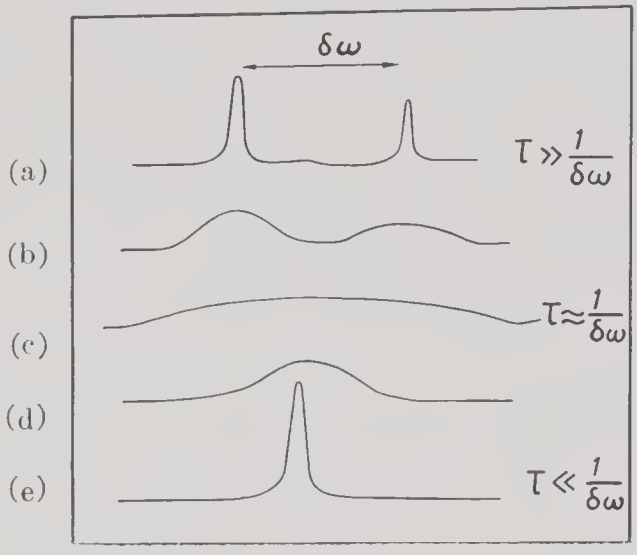

Fig. 8. Nuclear magnetic resonance spectrum of two proton exchanging substances HA and HB for different rates of exchange. $\delta\omega$ = chemical shift between HA and HB; τ = average lifetime of proton in a given species.

The resonance lines of AH and BH are separated by a chemical shift $\delta\omega$. If the average lifetimes τ_A and τ_B of the protons in the two states are very long compared with $(\delta\omega)^{-1}$ the two lines are resolved sharply. This is evident for the case $\tau \to \infty$ when no reaction occurs at all [Figure 8(a)]. The intensities of the two resonance lines are in the ratio of the mole fractions p_A and p_B of the protons in the two states. If, on the other hand, τ_A, $\tau_B << (\delta\omega)^{-1}$ only one sharp line is observed [Figure 8(e)] whose frequency is the weighted average of the two lines separated by $\delta\omega$ (i.e., $\omega = \omega_A p_A + \omega_B p_B$). The intermediate cases are shown in Figures 8(b, c, and d). As long as the two lines are broadened by the rate of exchange but do not yet overlap, they may be treated as two independent systems with the uncertainty principle. According to that principle the uncertainty ΔE of a measured energy multiplied by the uncertainty Δt of the appropriate measuring time is given by $\Delta E \cdot \Delta t \simeq \hbar$.

Identifying $\Delta E/\hbar$ by $\Delta\omega_{\text{exchange}}$ and Δt by the average lifetime τ we have

$$\Delta\omega_{\text{exchange}} = 1/\tau$$

The collapsing of two overlapping broad lines into a single sharp line, with τ becoming very short (Figure 8), may be understood as follows: The exchanging protons switch their Larmor frequency from ω_A to ω_B at every exchange jump, where $\omega_A - \omega_B = \delta\omega$. To simplify the argument, we shall assume that $p_A = p_B$. Now we shall refer to a co-ordinate system rotating with an angular frequency $\omega_{1/2} = (1/2)(\omega_A + \omega_B)$ about the z axis. In this system the magnetic moments of the protons move either with $+\delta\omega/2$ or $-\delta\omega/2$ depending on the momentary state of the protons. The

switching occurs at the moment of exchange. For very short lifetimes τ_A (or τ_B), the vector of the rotating moments, makes an angle with the axis of the order of ${}^1/_2\tau_A\,\delta\omega$. At the limit $\tau_A = 0$ the system behaves as if there were only nuclei with the Larmor frequency $\omega_{1/2}$, and in the spectrum a single sharp line is observed at this frequency. A careful analysis of this problem has been given by Gutowsky and co-workers (5) in 1953. For the rotating magnetization M, which determines the signal intensity, these authors solve the Bloch differential equation modified for chemical exchange and obtain

$$M = i\gamma H_1 M_0 \frac{(\tau_A + \tau_B) + \tau_A\tau_B(\alpha_A p_B + \alpha_B p_A)}{(1 + \alpha_A\tau_A)(1 + \alpha_B\tau_B) - 1} \tag{17}$$

The symbol stands for the complex quantities $\alpha_A = (1/T_2) - i[\Delta\omega + (\delta\omega/2)]$ and $\alpha_B = (1/T_2) - i[\Delta\omega - (\delta\omega/2)]$. M_0 is the magnetization component in the z direction and $\Delta\omega = \omega_{1/2} - \omega$ the deviation of the momentary value of ω from $\omega_{1/2}$. In a resonance experiment the imaginary component of the complex expression (17) is proportional to the measured signal intensity. For the special case of very slow reactions, that is τ_A, $\tau_B \gg (\delta\omega)^{-1}$, we obtain from (17)

$$M_v = -\frac{\gamma H_1 M_0}{T_2}\frac{p_A}{(1/T_2^2) + [\Delta\omega + (\delta\omega/2)]^2} + \frac{p_B}{(1/T_2) + [\Delta\omega - (\delta\omega/2)]^2} \tag{17a}$$

That is, two separated lines are found at ω_A and ω_B with an intensity ratio $p_A : p_B$.

If, on the other hand, the reaction is extremely rapid $[\tau_A, \tau_B \ll (\delta\omega)^{-1}]$ Equation (17) reads

$$M_v = -\frac{\gamma H_1 M_0}{T_2}\frac{1}{(1/T_2) + [\Delta\omega - (\delta\omega/2)\,(p_B - p_A)]^2} \tag{17b}$$

This is the equation for a single sharp line with maximum intensity at a frequency $\omega = p_A\omega_A + p_B\omega_B$.

In the case shown in Figure 8(b), where two exchange broadened lines do not yet overlap, (17) simplifies to

$$1/T_2' = (1/T_2) + (1/\tau) \tag{17c}$$

T_2' is the apparent value of T_2 which is shortened by exchange, and T_2 the relaxation time without exchange; τ is the mean lifetime of the proton in the chemical bond for which the resonance line is characteristic.

For a fairly rapid reaction, which is still slow enough for the resulting single line to be broadened by exchange, we have

$$1/T_2' = (1/T_2) + (\delta\omega)^2 p_A^2 p_B^2 (\tau_A + \tau_B) \qquad (17d)$$

If Equation (17) must be applied in the unshortened form, the use of the graphical methods described in the literature (6) is recommended.

6. The Measurement of Line Widths and the Relaxation Time T_2

As shown in the preceding section, the experimental task in the application of nuclear magnetic resonance to kinetic problems consists of measuring line widths with and without chemical reaction. The values of T_2 in Equation (17) are effective values as defined by Equation (6a). Since the widths of lines, which are not broadened by chemical exchange or quadrupole relaxation, are often practically determined by the inhomogeneity of the magnetic field, $T_{2\text{eff}}$ is independent of the nucleus on which it is measured in the absence of the discussed broadening mechanisms. Therefore, T_2 can be measured directly from the width of a strong line, e.g., a non-exchanging solvent line.

Since line widths and $\delta\omega$ must be known in absolute units (sec.$^{-1}$) the spectra must be calibrated according to frequency. Some commercially available apparatus provide a so-called side band technique for this purpose. An alternating current of known low frequency, e.g., 100 sec.$^{-1}$, is superimposed on the signal. This frequency beats with the high frequency and for every line produces two side bands separated from the central line by ± 100 sec.$^{-1}$. If the spectrum contains many lines of similar intensity, this technique may prove to be troublesome and a different method of frequency calibration, which is generally applicable, is recommended. The sample containers consist of glass tubes into which the substances are sealed (Figure 9). In the bottom of the actual sample tube a thinner tube (melting-point tube) is sealed containing a fluid mixture which produces a certain number of lines (two is sufficient) of known frequency separation and of about equal intensity. Of course not only the frequency separation, but also the chemical shift relative to the reference substance (e.g., water), must be known. For the influence of sample shape on frequency marks thus obtained the reader is referred to the monographs cited.

A more exact method than the direct measurement of line width is that of wiggle decay. In the discussion, so far, we have assumed that the reso-

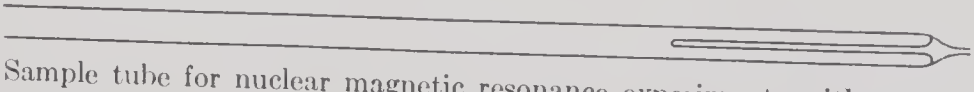

Fig. 9. Sample tube for nuclear magnetic resonance experiments with small tube for reference substance.

nance curve was passed in a time which is long compared with T_2. If the saw-tooth frequency ν_m is comparable with, or even greater than, $1/T_2$ a resonance curve is measured which is shown in Figure 10(b). The physical reason for the wiggles, shown in Figure 10(b), is interference of the following kind: At the resonance frequency the rotating field H_1 forces the moments

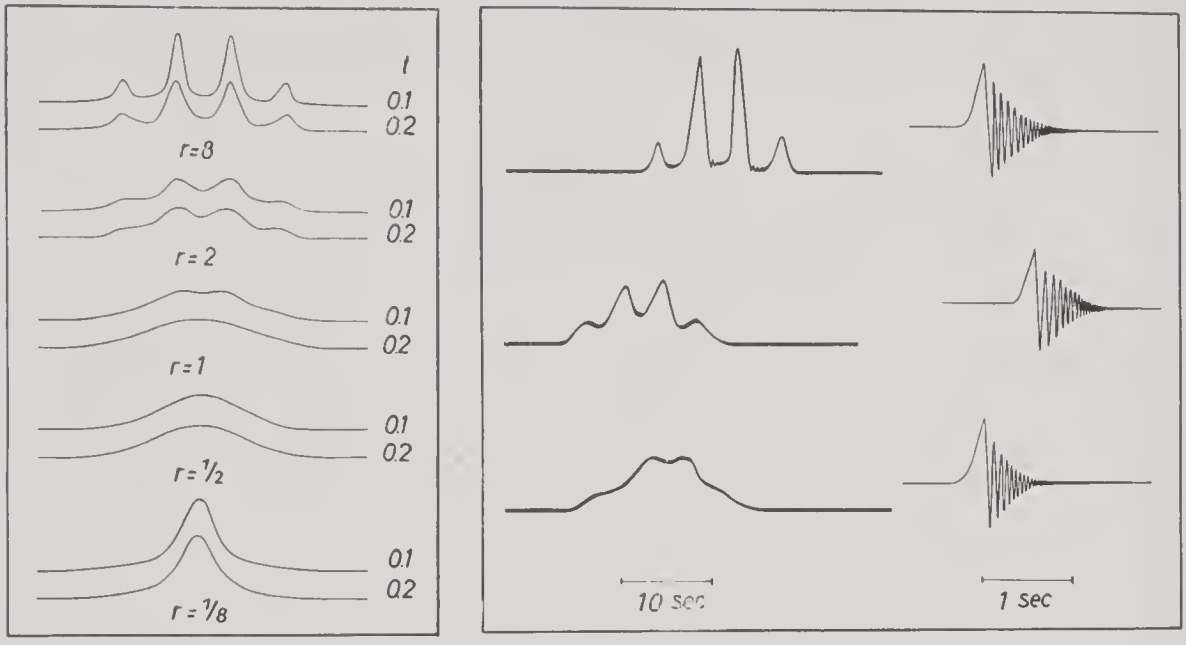

(a) (b)

Fig. 10. (a) Calculated line shapes for the CH_3 quadruplet of CH_3NH_3Cl for different exchange rates. $r = 2\ \tau\delta\omega$ and $t = 1/T_2\delta\omega$. (b) Observed line shapes for the CH_3 quadruplet of CH_3NH_3Cl. The curves on the right show the wiggles of the water line in the same solution for fast passage. The time constant of the wiggle is taken as T_2. (6)

into phase with a frequency γH_z. If H_z is changed appreciably during T_2 the original phase will not yet have decayed and will interfere with the new value of ω. The total phase difference ϕ at time t is then given by

$$\phi(t) = \int_o^t \gamma[H_z(t) - H_z(\mathrm{O})]dt = \frac{1}{2}\gamma\dot{H}_z t^2 \tag{18}$$

if H_z is saw-tooth modulated. Since the amplitude of the interference decays with a time constant T_2 the wiggle signal U is of the form:

$$U = U_0 \exp\left(-\frac{t}{T_2}\right)\cos\left(\frac{1}{2}\gamma H_z t^2\right) \tag{19}$$

From the envelope of the curve [Figure 8(b)] the effective T_2 may be obtained.

7. The Protolysis of Methyl Ammonium Chloride; An Application of Nuclear Magnetic Resonance to Reaction Kinetics

The method, which has been treated theoretically in the preceding sections, will now be applied to a specific example. Grunwald, Loewenstein, and Meiboom (6) analysed the kinetics of the protolysis of methylammonium ion with nuclear magnetic resonance. Figure 11 shows the nuclear magnetic resonance spectra of CH_3NH_3Cl at different pH values. The

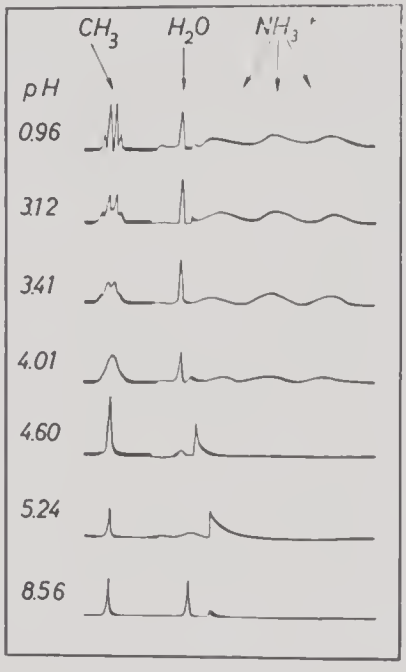

Fig. 11. Proton magnetic resonance spectra (6) of 4.47 M solutions of CH_3NH_3Cl in water of different pH (31.65 Mc sec.$^{-1}$). Different groups were recorded at different amplifications. Relative intensities have therefore no significance.

resonance of the methyl protons is split into a quadruplet due to the spin-spin interaction with the three protons attached to the nitrogen atom, with relative intensities 1:3:3:1. The merging of this quadruplet into a single sharp line with increasing pH supplies the most important kinetic information. The protons at the nitrogen atom show a triplet because of the spin quantum number of nitrogen $I = 1$. The quadrupole moment of the nitrogen broadens these lines, so that the quadruplet splitting due to the methyl protons is not resolved. The NH_3^+ resonance lines coincide at high pH values with the water line, which at intermediate pH also shows exchange broadening.

The broadening of the methyl quadruplet is a measure of the mean lifetime of the spin states of the NH_3^+ protons and thereby for the exchange

of protons at the nitrogen. At the pH values investigated only the following reactions may be discussed for proton exchange:

$$CH_3NH_3^+ + H_2O \xrightarrow{k_1} CH_3NH_2 + H_3O^+ \quad (20a)$$

$$CH_3NH_3^+ + OH^- \xrightarrow{k_2} CH_3NH_2 + H_2O \quad (20b)$$

$$CH_3NH_3^+ + H_2NCH_3 \xrightarrow{k_3} CH_3NH_2 + {}^+H_3NCH_3 \quad (20c)$$

For the reaction rate, *R.R.*, we have

$$\frac{R.R.}{[CH_3NH_3^+]} = k_1 + \frac{k_2 K_w}{[H^+]} + k_3 K_a \frac{[CH_3NH_3^+]}{[H^+]}$$

where K_w is the ionic product of water and K_a the acidity constant of methylammonium chloride. Since the exchange of spin orientation at NH_3^+ is, kinetically, of the first order relative to the concentration of methylammonium, we have

$$\frac{R.R.}{[CH_3NH_3^+]} = k = \frac{1}{\tau} = \frac{2\delta\omega}{r}$$

where r is defined as $r = 2\ \tau\delta\omega$. In Figure 8(a) calculated curves for the methyl quadruplet are shown for different values of r and T_2. Figure 10(b) shows measured curves, together with wiggle curves measured on the water line, for the evaluation of T_2 as discussed in the previous section. The shortening of the effective relaxation times in the lower curves is caused by a proton exchange in water, which manifests itself as a broadening of the water line in Figure 11 at intermediate pH values. The authors have evaluated the spectra by comparing measured and calculated ratios of the maximum to the inner minimum of the quadruplet. For higher pH values, calculated and observed line widths were compared. From the results of these measurements it is concluded that the proton exchange proceeds almost exclusively by Reaction (20c). Reactions (20a) and (20b) are too slow in the investigated range of pH. For the kinetic constant k_3 a value of $(5.9 \pm 0.7) \cdot 10^8$ l./mole sec. was obtained at 19 ± 2°C. The uncertainty is caused, at least partly, by insufficient constancy of temperature.

The broadening of the water line shows that water molecules are also involved in proton exchange. According to Grunwald, Loewenstein, and Meiboom (6) Reaction (20d) proceeds at a rate comparable to that of (20c)

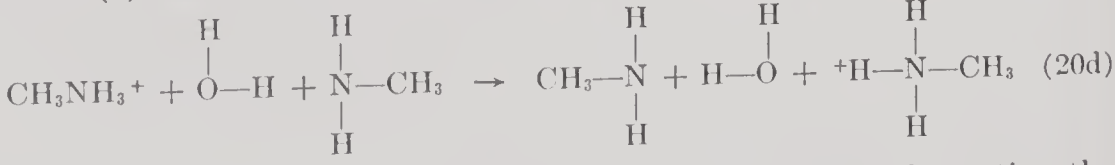

(20d)

(see also Table I in the following section). For further information the original paper should be consulted.

8. Results

In this section data of reaction kinetics obtained by the nuclear magnetic resonance method are presented.

In a recent paper, Patterson and Ettinger (12) discuss the hydration rate of CO_2 measured by the nuclear magnetic resonance of C^{13}. While the average lifetime of an unhydrated CO_2 molecule is about 40 sec. at 25°C., under the catalyzing influence of carbonic anhydrase ($5 \cdot 10^{-4}$ by weight), this lifetime becomes as short as $1.6 \cdot 10^{-3}$ sec.

According to Meiboom, Luz, and Gill (13) the formation and decay of hydrogen bonds in water are catalyzed by H_3O^+ and OH^- ions. At medium pH values (4–10) the rate constant for this process may be written

$$k = k_1 + k_2[H_3O^+] + k_3[OH^-]$$

with $k_1 = 2.2 \cdot 10^5$ sec.$^{-1}$; $k_2 = 5.7 \cdot 10^{10}$ l./mole sec., and $k_3 = 1.3 \cdot 10^{10}$ l./mole sec.

Gutowsky and Holm (14) investigated the inner rotation of dimethylformamide and dimethylacetamide, which in the temperature range 236–269°K., occur mainly in the coplanar form

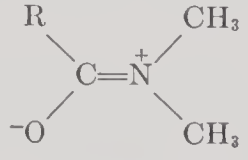

The two methyl groups have different magnetic surroundings and show a chemical shift. For the reaction:

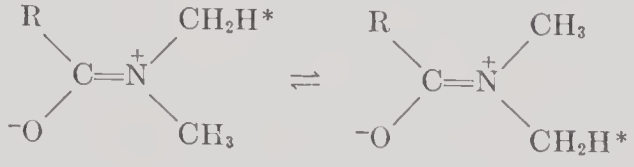

a rate constant $k = \nu_0 \exp(-E_A/RT)$ is found, where ν_0 and E_A are as shown.

Substance	ν_0	E_A
Dimethylformamide	10^3 to 10^7	7 ± 3
Dimethylacetamide	10^7 to 10^{10}	12 ± 2

Further observations of a qualitative nature are given in Table II.

TABLE I
Rate Constants of Chemical Reactions Obtained by Nuclear Magnetic Resonance

Reaction	k	T°C.	Ref.
$NH_4^+ + NH_3 \rightleftharpoons NH_3 + NH_4^+$	$(10.6 \pm 1.0)\cdot 10^8$ l./mole sec.	21	7
$NH_4^+ + O{-}H\ NH_3 \rightleftharpoons NH_3\ H{-}O + NH_4^+$ (H, H)	$(0.9 \pm 0.1)\cdot 10^8$ l./mole sec.	21	7
$CH_3NH_3^+ + H_2NCH_3 \rightleftharpoons CH_3NH_2 + {}^+H_3N{-}CH_3$	$(2.5 \pm 0.3)\cdot 10^8$ l./mole sec.	19	6
$CH_3NH_3^+ + O{-}H\ H_2NCH_3 \rightleftharpoons CH_3NH_2\ H{-}O + {}^+H_3NCH_3$ (H, H)	$(3.4 \pm 0.4)\cdot 10^8$ l./mole sec.	19	6
$(CH_3)_2NH_2^+ + HN(CH_3)_2 \rightleftharpoons (CH_3)_2NH + {}^+H_2N(CH_3)_2$	$(0.4 \pm 0.3)\cdot 10^8$ l./mole sec.	22	8
$(CH_3)_2NH_2^+ + O{-}H\ HN(CH_3)_2 \rightleftharpoons (CH_3)_2NH\ H{-}O + {}^+H_2N(CH_3)_2$ (H, H)	$(5.6 \pm 0.3)\cdot 10^8$ l./mole sec.	22	8
$(CH_3)_3NH^+ + N(CH_3)_3 \rightleftharpoons (CH_3)_3N + {}^+HN(CH_3)_3$	$(0.0 \pm 0.3)\cdot 10^8$ l./mole sec.	22	8
$(CH_3)_3NH^+ + O{-}H\ N(CH_3)_3 \rightleftharpoons (CH_3)_3NH{-}O + {}^+HN(CH_3)_3$ (H, H)	$(3.1 \pm 0.3)\cdot 10^8$ l./mole sec.	22	8
$H_2O_2 + H_3O^+ \rightleftharpoons H_3O_2^+ + H_2O$	$(1.6 \pm 0.2)\cdot 10^7$ l./mole sec.		9
$HO_2H + H^*OH + HO_2^- \rightleftharpoons HO_2H^* + H_2O + HO_2^-$	$(7.3 \pm 1.0)\cdot 10^7$ l./mole sec.		9
$CH_3CONHCH_3 + OH^- \rightleftharpoons CH_3CON^-CH_3 + H_2O$	$(5.2 \pm 1.0)\cdot 10^2$ l./mole sec.	21	10
$CH_3CONHCH_3 + H_3O^+ \rightleftharpoons CH_3CONH_2{}^+CH_3 + H_2O$	$(3.8 \pm 0.4)\cdot 10^2$ l./mole sec.	23	10
$C_2H_5OH + OH^- \rightleftharpoons C_2H_5O^- + H_2O$	$2.8 \cdot 10^6$ l./mole sec.	22 ± 2	11
$C_2H_5OH + C_2H_5O^- \rightleftharpoons C_2H_5O^- + C_2H_5OH$	$1.4 \cdot 10^6$ l./mole sec.	22 ± 2	11
$C_2H_5OH + H_3O^+ \rightleftharpoons C_2H_5OH_2{}^+ + H_2O$	$2.8 \cdot 10^6$ l./mole sec.	22 ± 2	11
$C_2H_5OH + C_2H_5OH_2{}^+ \rightleftharpoons C_2H_5OH_2{}^+ + C_2H_5OH$	$1.1 \cdot 10^8$ l./mole sec.	22 ± 2	11
$C_2H_5OH^* + H_2O \rightleftharpoons C_2H_5OH + HOH^*$	0.8 l./mole sec.	22 ± 2	11
$CH_3OH + OH^- \rightleftharpoons CH_3O^- + H_2O$	$2.6 \cdot 10^6$ l./mole sec.	22 ± 2	11
$CH_3OH + CH_3O^- \rightleftharpoons CH_3O^- + CH_3OH$	$9.5 \cdot 10^6$ l./mole sec.	22 ± 2	11
$CH_3OH + CH_3COH_2{}^+ \rightleftharpoons CH_3OH_2{}^+ + CH_3OH$	$8.8 \cdot 10^7$ l./mole sec.	22 ± 2	11
$CH_3OH + CH_3OH^* \rightleftharpoons CH_3OH^* + CH_3OH$	0.08 sec.$^{-1}$	22 ± 2	11

TABLE II
Chemical Reactions Investigated Qualitatively by Nuclear Magnetic Resonance

Reaction	Remarks	Ref.
$NH_2H^* + NH_3 \rightarrow$ $NH_3 + NH_2H^*$	Very rapid with traces of water Slow in carefully dried ammonia In the gas phase slow even in the presence of water vapor	15
C_2H_5OH	Protolysis	16
Glycine Glycine methyl ether Sarcosine	Protolysis in very acidic solutions Only mean lifetimes of protons are given	17
$AlF^{++} + AlF^+ \rightleftharpoons$ $AlF^+ + AlF^{++}$	$1M$ $Al(NO_3)_3 + 1M$ NaF; $\tau \geq 8 \cdot 10^{-3}$ sec. $2M$ $Al(NO_3)_3 + 2M$ NaF; $\tau \geq 5 \cdot 10^{-3}$ sec.	18 19
$SnF^+ + F^- \rightleftharpoons SnF_2$	$0.8M$ $SnCl_2 + 1M$ NaF $+ 0.3M$ HF; $\tau \geq 7 \cdot 10^{-5}$ sec.	19
$ZnF^+ + F^- \rightleftharpoons ZnF_2$	$;\tau \geq 2 \cdot 10^{-4}$ sec.	19

9. The Measurement of Rate Constants for Paramagnetic Pulse Reactions by Nuclear Magnetic Resonance

McConnell and co-workers (20,21) have shown how average lifetimes may be determined in the presence of paramagnetic ions. These lifetimes may be much shorter than those attainable by the method discussed in the preceding sections. Let us consider this possibility with a specific example. The relaxation time T_2 of Cu^{63} of (diamagnetic) $1M$ CuCl, as a complex with HCl, has been found (20) to be $2 \cdot 10^{-5}$ sec. The reason for this short relaxation time T_2 is an additional relaxation mechanism by the quadrupole moment of Cu^{63} as discussed at the end of Section II-2. Only minute additions of cupric ions (e.g., $10^{-3}M$) shorten this time T_2 appreciably. The quadrupole broadening is superimposed by an exchange broadening of the electron exchange reaction between the two ionic species Cu^+ and Cu^{++}.

$$1/T_{2DP} = (1/T_{2D}) + (1/T_{2P}) \tag{21}$$

with T_{2DP} the measured relaxation time in a mixture containing $[Cu^{++}]$ mole/l. paramagnetic cupric ions, T_{2D} is T_2 in pure diamagnetic CuCl, and T_{2P} is the (hypothetical) relaxation time of an ion without a quadrupole moment but shortened by the electron exchange with paramagnetic Cu^{++} ions.

In an exchange reaction: $Cu^+ \rightarrow Cu^{++} \rightarrow Cu^+$ the nucleus experiences a strong magnetic pulse during the time ($\sim 10^{-8}$ sec.) when it is in Cu^{++}

form. The nucleus will loose its phase relation completely if $\tau_{Cu^{++}}$ is only $\geq 10^{-9}$ sec. (20). Since $\tau_{Cu^{+}} \gg \tau_{Cu^{++}}$ ($\tau_{Cu^{+}}/\tau_{Cu^{++}} = [Cu^{+}]/[Cu^{++}]$), T_{2P} is practically given by $\tau_{Cu^{+}}$. If the rate of the exchange reaction

$$Cu^{+} + Cu^{++} \overset{k}{\rightleftharpoons} Cu^{++} + Cu^{+}$$

is proportional to $[Cu^{+}][Cu^{++}]$, the constant k is given by

$$k = \frac{1}{[Cu^{++}]}\left[\frac{1}{T_{2DP}} - \frac{1}{T_{2D}}\right] \tag{22}$$

with $[Cu^{++}] = 10^{-3}$ mole/l. and $T_{2D} = 2 \cdot 10^{-5}$ sec., T_{2DP} has been found to be $1 \cdot 10^{-5}$ sec. Therefore k turns out to be $0.5 \cdot 10^{8}$ l./mole sec.

A more extensive treatment of this method has been given by McConnell and Berger (21). It has been applied also to a reaction with an organic radical ion. The results are summarized in Tables III, IV, and V.

An analogous application of the paramagnetic pulse procedure has been made in measuring the rate of exchange for complex ligands bound to para-

TABLE III

Rate Constants of Chemical Reactions Obtained by the Paramagnetic Pulse Method

Reaction	k (l./mole sec.)	Ref.
$Cu^{+} + Cu^{++} \overset{k}{\rightleftharpoons} Cu^{+} + Cu^{++}$	$0.5 \cdot 10^{8}$	20
$(CH_3)_2N{-}C_6H_4{-}N(CH_3)_2 + (CH_3)_2N{-}C_6H_4{-}\overset{+}{N}(CH_3)_2 \overset{k}{\rightleftharpoons} (CH_3)_2N{-}C_6H_4{-}\overset{+}{N}(CH_3)_2 + (CH_3)_2N{-}C_6H_4{-}N(CH_3)_2$	$2.5 \cdot 10^{4}$	22

TABLE IV

Rate Constants (sec.$^{-1}$) for Exchange of H_2O and CH_3OH Molecules on Paramagnetic Ions

Ion	H_2O (23)	CH_3OH (24) measured with resonance of: CH_3 proton	CH_3OH (24) measured with resonance of: OH proton
Cr^{3+}	Slow	$3.2 \cdot 10^{3}$	$1.1 \cdot 10^{4}$
Fe^{3+}	$1 \cdot 10^{6}$	$1.0 \cdot 10^{4}$	$2.0 \cdot 10^{4}$
Mn^{++}	$4 \cdot 10^{7}$ (25)	$1.8 \cdot 10^{4}$	$2.5 \cdot 10^{5}$
Co^{++}	$>2 \cdot 10^{5}$	$1.7 \cdot 10^{3}$	$1.1 \cdot 10^{4}$
Ni^{++}	$>4 \cdot 10^{4}$	$2.2 \cdot 10^{3}$	$2.5 \cdot 10^{3}$
Cu^{++}	$>6 \cdot 10^{5}$	$1.0 \cdot 10^{4}$	$1.0 \cdot 10^{4}$
Ce^{3+}		$0.8 \cdot 10^{2}$	$2.5 \cdot 10^{4}$

TABLE V
N—H Exchange Rates for Chromium Complexes in Water at 25°C. (24)

Compound	$[OH^-]$	k (l./mole sec.)
$[Cr(en)_3](ClO_4)_3$[a]	pH = 9.8	$2 \cdot 10^2$
$[Cr(en)_3](ClO_4)_3$	pH > 11	$3.7 \cdot 10^6$
$[Cr(NH_3)_6](ClO_4)_3$	0.044	$1.7 \cdot 10^6$
$[Cr(NH_3)_6](ClO_4)_3$	0.027	$2.5 \cdot 10^6$
$[Cr(NH_3)_5H_2O](ClO_4)_3$	0.062	$1.2 \cdot 10^6$
$K[Cr(NH_3)_2(SCN)_4]$	0.5	$3 \cdot 10^4$

[a] Solution contained 1M excess en and 0.5M en·2HCl. The rate constant is for the acid-base reaction $Cr(en)_3^{3+}$ + en.

magnetic ions with similar molecules in the diamagnetic bulk of the solution. Experimental results are given in Tables IV and V.

10. Exchange Broadening on Nuclei with Quadrupole Moments

A further possibility of measuring fast reactions might be called "quadrupole relaxation pulse method." As in Section II-9, a very efficient mechanism of nuclear relaxation takes place in one of the reactants. The argument of this section is therefore very similar to that of the preceding one.

Nuclei with sufficiently high quadrupole moments will have measurable resonance signals in the liquid phase only if they occur in the form of atomic ions. With a covalent bond to another atom large inhomogeneities of electric field strength arise. Accordingly quadrupole broadening is so large that the signal amplitude becomes unmeasurably small.

With Br^{79} and Br^{81}, nuclear magnetic resonance is observed only in completely dissociated bromides. By adding cadmium ions to a solution of KBr, the covalent compounds $CdBr^+$, $CdBr_2$, and $CdBr_3^-$ are formed, each with a characteristic average lifetime.

For the measured effective relaxation time T_2 an equation analogous to (21) holds

$$1/T_2 = (1/T_{2o}) + (1/T_{2c}) \tag{21a}$$

where T_{2o} is the observed effective relaxation time of Br^- without addition of Cd^{++} and T_{2c} is the average lifetime of free Br^- ions in the presence of Cd^{++}.

Results obtained by Hertz (26) for this system and measurements on the system $I^- + I_2 \rightleftharpoons I_3^-$ by Myers (27) are summarized in Table VI.

TABLE VI
Reaction Rate Measured by Exchange Broadening of Br^{81} and I^{127}

Reaction	Equilibrium constant K (mole/l.)	Rate constant k (l./mole sec.)	Ref.
$Cd^{++} + Br^- \overset{k}{\rightleftharpoons} CdBr^+$	$7 \cdot 10^{-3}$	$7 \cdot 10^8$	26
$CdBr^+ + Br^- \overset{k}{\rightleftharpoons} CdBr_2$	$1 \cdot 10^{-2}$	$1.8 \cdot 10^7$	26
$CdBr_2 + Br^- \overset{k}{\rightleftharpoons} CdBr_3^-$	0.27	$1.4 \cdot 10^7$	26
$I^- + I_2 \overset{k}{\rightleftharpoons} I_3^-$	$1.8 \cdot 10^{-3}$	$(4.1 \pm 0.4) \cdot 10^{10}$	27

III. THE EVALUATION OF RATE CONSTANTS OF RAPID REACTIONS BY ELECTRON SPIN RESONANCE

1. Kinetic Line Broadening in ESR

Since the underlying physical principles of electron spin resonance have been outlined by Fraenkel in this series (general references Fraenkel and also Wertz and Ingram), only a very short presentation of the matter will be given here. This section is intended to show the analogies and differences between NMR and ESR as applied to rapid-reaction kinetics.

Unpaired electrons in molecules, crystals, or metals exhibit a magnetic moment by virtue of their spins quite analogously to the behavior of nuclei. Furthermore there are orbital moments for electrons which may be coupled with the electron spin moment. The resulting moment will precess about an external magnetic field. The equation for the precessional frequency corresponding to Equation (3) is usually written in the form:

$$h\nu = g\mu_B H_z \tag{23}$$

where g, the Landé factor, is 2.0023 for free electrons and μ_B is the Bohr magneton. Since the Bohr magneton is 3 orders of magnitude greater than the nuclear magneton, the gyromagnetic ratio of the electron exceeds that of the nucleus by a similar factor. Therefore electron magnetic resonance in the megacycle region will be observed with magnetic fields of only about 10 gauss. These resonances are intense enough to be observed, but in many cases the line widths are much greater than 10 gauss. It is therefore advisable to work with higher magnetic fields, of the order of a few kilogauss. The resonance frequency is then in the microwave range of about 10^{10} cycles/sec. The absorption of the irradiated energy is observed in a microwave guide. The measured ESR spectra often show a quite complex

structure. The reason for this complexity is hyperfine splitting of the electron resonance by nuclear spins in the molecule.

In solid substances the crystal field masks these hyperfine splittings but in magnetically diluted systems spectra with many lines have been observed, especially when the free electron is smeared out over a molecule and is thereby coupled to many nuclear spins.

The relaxation times T_1 and T_2 are much shorter for ESR than they are in the case of NMR since the moments are much less shielded from magnetic noise (see Section II-2). In fact, T_1 has been found to be about 10^{-7} sec. in liquids, while T_2 is even somewhat shorter [see Equation (5)]. The line widths are then of the order of 10^7 cycles/sec. or, in magnetic field units, roughly 10 gauss. Thus line broadening by chemical exchange, as discussed in Section II-5, can only be observed by ESR, when the average lifetimes are smaller than the reciprocal line widths, i.e., $\tau \lesssim 10^{-5}$ sec.

Some cases of kinetic broadening have been reported in the literature and will be dealt with in the following section. A recent review has been given by Weissman (28).

2. Experimental Results

A good example of the application of ESR to fast-reaction kinetics has been supplied by Gardner and Fraenkel (29). These authors investigated the electron spin resonance of liquid sulfur in the temperature range between 216° and 414°C. The sulfur was recognized as polymer chains, the ends of which formed the sites of unpaired electrons. From intensity considerations the concentration of the free radicals was estimated to be $(1.1 \pm 0.6)\cdot 10^{-3}$ mole/l. (at 300°C.). The line width w (in gauss) could be represented as a function of temperature by

$$\log w = 2.9812 - 673/T \tag{24}$$

The calculated broadening by neighboring dipoles was smaller than the observed effect even when motional narrowing was disregarded. Spin orbital coupling ($g = 2.024$), an anisotropic g factor or nuclear spin splitting (in sulfur there are only very few nuclei with $I \neq 0$) could only explain a much smaller broadening than the measured value. Therefore all possible line-broadening effects except chemical exchange broadening could not account for such large line widths. The authors discuss chemical exchange broadening due to the following reactions:

$$\text{.....S}\cdot + \cdot\text{S.....} \rightleftharpoons \text{.....S-S.....} \tag{I}$$

and

$$\text{.....S}\cdot + \text{.....S-S.....} \rightleftharpoons \text{.....S-S.....} + \cdot\text{S.....} \qquad \text{(II)}$$

Because of the small concentration of free radicals Reaction (I) was ruled out. The reaction constant k is connected with the average lifetime τ by

$$\text{Rate} = -d[\text{S}\cdot]/dt = k[\text{S}][\text{S}\cdot] \qquad (25)$$

and

$$k = (\tau[\text{S}])^{-1} \qquad (26)$$

On disregarding the natural line width, Equation (17c), applied to this problem, reads

$$\tau = 6.47 \cdot 10^{-8}/w \qquad (27)$$

where τ is in seconds and w in gauss. The rate constant of Reaction (II) as a function of temperature was evaluated from the experimental results and is given by

$$k = (2.8 \pm 1.0) \cdot 10^{8} \exp\left\{-(3.08 \pm 0.75) \cdot 10^{3}/RT\right\} \qquad (28)$$

Some further applications of ESR to the kinetics of rapid reactions have been reported by Weissman and co-workers. The naphthalene negative ion exchanges its surplus electron according to (30)

$$C_{10}H_8^- + C_{10}H_8 \rightleftharpoons C_{10}H_8 + C_{10}H_8^- \qquad \text{(III)}$$

In solutions of the potassium, lithium, or sodium salts of the anion a spectrum of 28 lines is observed. These lines are hyperfine components arising from interaction between the magnetic moment of the free electron and the nuclear moments of the protons in the naphthalene negative ion. The lines are appreciably broadened by the addition of enough naphthalene to increase the rate of Reaction (III) sufficiently. The kinetic results for different salts in the solvents 1,2-dimethoxyethane (DME) and tetrahydrofuran (THF) are summarized in Table VII.

TABLE VII

Positive ion	Solvent	k(l./mole sec.)
K^+	DME	$(7.6 \pm 3) \cdot 10^{7}$
K^+	THF	$(5.7 \pm 1) \cdot 10^{7}$
Na^+	DME	$(1.3 \pm 0.7) \cdot 10^{9}$
Na^+	THF	$(1.3 \pm 0.6) \cdot 10^{7}$
Li^+	THF	$(4.6 \pm 3) \cdot 10^{8}$

Adam and Weissman (28,31) investigated the reaction of the sodium ketyl of benzophenone with benzophenone. By comparing the spectra of the lithium or potassium ketyls with that of sodium ketyl it was shown that a splitting of 1 gauss ($2.7 \cdot 10^6$ cycles/sec.) occurs with the nuclear moment of Na^{23} ($I_{Na^{23}} = {}^3/_2$). It must therefore be concluded that every ketyl molecule holds its sodium atom for at least $3 \cdot 10^{-7}$ sec.

With added benzophenone the following exchange reaction occurs:

$$(C_6H_5)_2CONa + OC(C_6H_5)_2 \rightleftharpoons (C_6H_5)_2CO + NaOC(C_6H_5)_2 \qquad (IV)$$

The question whether the electron and sodium ion exchanged independently, or whether there was a sodium atom transfer, could be answered from the structure of the spectrum. In the former case with Reaction (IV) proceeding at very high rates a single line is expected, whereas for atom transfer, the electron resonance is then expected to split into four components because of interaction with the sodium nuclear moment. With high concentrations of benzophenone, Reaction (IV) became fast enough so that the very complex spectrum of the ketyl collapsed into a quadruplet indicating an atom transfer mechanism. Limits could be obtained for the rate constant of (IV) and for mean lifetimes

$$k \geq 5 \cdot 10^7 \text{ l./mole sec.}, \quad \tau_K \leq 10^{-8} \text{ sec., and } \tau_{Na} \geq 3 \cdot 10^{-7} \text{ sec.}$$

Here τ_K is the mean lifetime of a ketyl molecule and τ_{Na} the mean lifetime of a sodium ion and electron considered together.

Similarly for the electron transfer of the reaction

$$W(CN)_8^{4+} + W(CN)_8^{3+} \rightleftharpoons W(CN)_8^{3+} + W(CN)_8^{4+} \qquad (V)$$

an upper limit for the rate constant could be obtained (32) by ESR methods: $k > 4 \cdot 10^8$ l./mole sec.

These examples clearly demonstrate the potentialities of ESR in the field of rapid-reaction kinetics.

References

1. See "General References."
2. F. Bloch, W. Hansen, and M. Packard, *Phys. Rev.*, 69, 680 (1946).
3. E. Purcell, H. Torrey, and R. Pound, *Phys. Rev.*, 69, 37 (1946).
4. W. G. Procter and F. C. Yu, *Phys. Rev.*, 77, 717 (1950).
5. H. S. Gutowsky, D. W. McCall, and C. P. Slichter, *J. Chem. Phys.*, 21, 279 (1953); H. S. Gutowsky and A. Saika, *J. Chem. Phys.*, 21, 1688 (1953); H. McConnell, *J. Chem. Phys.*, 28, 430 (1958); P. Diehl, *Helv. Physica Acta*, 31, 685 (1958).
6. E. Grunwald, A. Loewenstein, and S. Meiboom, *J. Chem. Phys.*, 27, 630 (1957).
7. S. Meiboom, A. Loewenstein, and S. Alexander, *J. Chem. Phys.*, 29, 969 (1958)
8. A. Loewenstein and S. Meiboom, *J. Chem. Phys.*, 27, 1067 (1957).

9. M. Ambar, A. Loewenstein, and S. Meiboom, *J. Am. Chem. Soc.*, **80**, 2630 (1958).

10. A. Berger, A. Loewenstein, and S. Meiboom, *J. Am. Chem. Soc.*, **81**, 62 (1959).

11. Z. Luz, D. Gill, and S. Meiboom, *J. Chem. Phys.*, **30**, 1540 (1959).

12. A. Patterson, Jr., and R. Ettinger, *Z. Elektrochem.*, **64**, 98 (1960).

13. S. Meiboom, Z. Luz, and D. Gill, *J. Chem. Phys.*, **27**, 1411 (1957).

14. H. S. Gutowsky and C. H. Holm, *J. Chem. Phys.*, **25**, 1228 (1956).

15. R. A. Ogg, Jr., *J. Chem. Phys.*, **22**, 560 (1954); *Discussions Faraday Soc.*, **17**, 215 (1954); H. M. McConnell and D. D. Thompson, *J. Chem. Phys.*, **26**, 958 (1957); H. S. Gutowsky and S. J. Fujiwara, *ibid.*, **22**, 1782 (1954).

16. J. T. Arnold, *Phys. Rev.*, **102**, 136 (1956); I. Weinberg and J. R. Zimmermann, *J. Chem. Phys.*, **23**, 748 (1955).

17. S. Meiboom and M. Sheinblatt, *Final Tech. Rept.*, 61 (052) 03 (1958); M. Takeda and O. Jardetzky, *J. Chem. Phys.*, **26**, 1346 (1957).

18. R. E. Connick and R. E. Poulson, *J. Am. Chem. Soc.*, **79**, 5153 (1957).

19. R. E. Connick (private communication).

20. H. M. McConnell and H. E. Weaver, *J. Chem. Phys.*, **25**, 307 (1956).

21. H. M. McConnell and S. B. Berger, *J. Chem. Phys.*, **27**, 230 (1957).

22. C. R. Bruce, R. E. Norberg, and S. I. Weissmann, *J. Chem. Phys.*, **24**, 473 (1956)

23. Measured with O^{17} resonance: R. E. Connick and R. E. Poulson, *J. Chem. Phys.*, **30**, 759 (1959).

24. R. G. Pearson, J. Palmer, M. M. Anderson, and A. L. Allred, *Z. Elektrochem.*, **64**, 110 (1960).

25. With the proton resonance $7 \cdot 10^7$ sec.$^{-1}$ has been obtained for Mn^{++} by R. A. Bernheim, T. H. Brown, H. S. Gutowsky, and D. E. Woessner, *J. Chem. Phys.*, **30**, 950 (1959).

26. H. G. Hertz, *Z. Elektrochem.*, **64**, 53 (1960).

27. O. E. Myers, *J. Chem. Phys.*, **28**, 1027 (1958).

28. S. I. Weissman, *Z. Elektrochem.*, **64**, 47 (1960).

29. D. M. Gardner and G. K. Fraenkel, *J. Am. Chem. Soc.*, **78**, 3279 (1956).

30. R. L. Ward and S. I. Weissman, *J. Am. Chem. Soc.*, **76**, 3612 (1954); **79**, 2086 (1957).

31. F. C. Adam and S. I. Weissman, *J. Am. Chem. Soc.*, **80**, 1518 (1958).

32. S. I. Weissman and C. S. Garner, *J. Am. Chem. Soc.*, **78**, 1072 (1956).

General References

Andrew, E. R., *Nuclear Magnetic Resonance*, Cambridge University Press, Cambridge, 1956.

Wertz, J. E., *Chem. Rev.*, **55**, 829 (1955).

Kopfermann, H., *Kernmomente*, Akademische Verlagsgesellschaft, Frankfurt/M., 1956.

Roberts, J. D., *Nuclear Magnetic Resonance*, McGraw-Hill Book Company, New York, 1959.

Pople, J. A., Schneider, W. G., and Bernstein, H. J., *High-Resolution Nuclear Magnetic Resonance*, McGraw-Hill Book Company, New York, 1959.

Gutowsky, H. S., Nuclear Magnetic Resonance, in A. Weissberger, ed., *Physical Methods of Organic Chemistry*, 3rd ed. (Vol. I of *Technique of Organic Chemistry*), Interscience, New York-London, 1960, Ch. 41.

Fraenkel, G. K., Paramagnetic Resonance Absorption, in A. Weissberger, ed., *Physical Methods of Organic Chemistry*, 3rd ed. (Vol. I of *Technique of Organic Chemistry*), Interscience, New York-London, 1960, Ch. 42.

Ingram, D. J. E., *Free Radicals as Studies by Electron Spin Resonance*, Butterworths Scientific Publications, London, 1958.

Laukien, G., *Kernmagnetische Hochfrequenz-Spektroskopie* (*Handbuch der Physik XXXVIII/1*), Springer, Berlin, 1958.

Strehlow H., *Magnetische Kernresonanz und Chemische Struktur*, Steinkopff, Darmstadt, 1962.

CHAPTER XVIII

RELAXATION METHODS

M. Eigen and L. de Maeyer
Max-Planck-Institut für physikalische Chemie, Göttingen

I. Introduction 896
References 900
General References 900
II. Theoretical Basis of Relaxation Methods 901
1. Linearized Rate Equations and Relaxation Times 901
A. Single-Step Reactions 901
*B. Relaxation Times and Thermodynamic Conditions 905
*C. Multiple-Step Systems (Relaxation Spectra) 907
D. Analysis of Relaxation Spectra 914
References 915
2. Principal Procedures 916
A. Transient and Forced Solutions of Relaxation Equations 916
B. Measurement of Transient Response 917
C. Measurement of Forced Response (Stationary Methods) 924
References 928
3. Perturbation of Chemical Equilibrium (Thermodynamic Relations) 928
A. Forcing Parameters 928
B. The Enforced Change of Concentration 929
*C. Chemical Contributions to Equations of State 941
*D. Dynamic Equations of State 948
E. Wave Phenomena (Sound Absorption and Dispersion) 952
References 963
4. Concluding Remarks 964
References 966
III. Experimental Techniques 966
1. Transient Methods 967
A. Detection of Concentration Changes 967
B. Temperature-Jump Methods 969
C. Pressure-Shock Methods 981
D. Electric Field-Pulse Methods 988
E. Radiation Methods 1001
F. Prospective Developments in Transient Methods 1002
References 1003
2. Stationary Methods 1004
A. Acoustical Methods (Sound Absorption and Dispersion) 1005

* For those who wish information about the principal problems of kinetic applications and methods only, it is not necessary to read the chapters marked with an asterisk or the sections printed in "small print."

B. Evaluation and Interpretation of Sound Absorption Data 1017
C. Electrical Methods (High Field Techniques) 1022
References 1029
IV. Survey on Results and Conclusions 1031
References 1049
Appendix: List of Symbols 1051

I. INTRODUCTION

The term "relaxation," in connection with a molecular process, is widely used by physicists to describe any (retarded) process of self-adjustment of a perturbed molecular system to its thermostatic equilibrium. Its early origin dates from the middle of the last century when Maxwell (1) introduced his theory of stress-strain relations for viscoelastic systems. Classic examples of molecular relaxation phenomena are the dipolar orientation processes as represented by the (complex) relationship between dielectric displacement and density of the (alternating) electric field [according to Debye (2)], or their magnetic analogues [*cf.* Gorter and Kronig (3)]. Similarly, molecular relaxation processes are of importance in the thermo-"dynamic" behavior of a system (in the real meaning of the word dynamic), and express themselves in dynamic relationships between pressure and volume as found in acoustical relaxation phenomena.

The "chemical relaxation" process may also be defined as a relation between two conjugate variables. These variables, characteristic of the chemical state, are the affinity and the "extent of reaction" (*cf.* Section II. 3. B). The definition includes any rate process readjusting the chemical equilibrium as a consequence of perturbation of the concentrations of reactants, either by change of a state parameter or by some other external forces influencing the equilibrium. It is related to the internal process only, and will be used regardless of whether this process is detected directly or as a contribution to electrical, acoustical, or other relaxation phenomena.

Our definition will also include processes studied by a special flash technique, where an equilibrium in the ground state is disturbed through transformation of the excited molecules which deactivate after reaction (*cf.* p. 1001). However, the reactions of the usual flash or radiation products, which are almost completely absent under normal equilibrium conditions, will not be included here. They are treated separately in Chapter XVI. (Trivial applications to slow rate processes are, of course, not included here though they may fulfill the above definition.)

In a more restricted sense, the relaxation studies deal only with rate phenomena that are close to equilibrium and can be represented by linear relationships (*cf.* Section II.1.A). The linear relaxation process is characterized by a time constant, the "relaxation time," which, for a one-step

reaction under defined external conditions, can be simply related to the rate constants. A multiple-step system is represented by a whole spectrum of relaxation times; these, in general, do not correspond to the single steps of the reaction but are related to normal modes of the coupled reaction system, analogous to the detectable vibration frequencies in a system of coupled oscillators. A treatment of larger deviations from equilibrium (nonlinear phenomena) usually involves considerable mathematical difficulties, especially in the case of a multiple-step system.

Insofar as the relaxation technique serves only as a means of studying fast reactions, it is advantageous (and usually possible) to maintain the conditions of linear approximations. However, the nonlinear phenomena are also of interest as problems themselves, quite apart from the possibilities of shifting an unsymmetrical equilibrium to the extent that the minor compound becomes detectable (*cf.* p. 965).

The first theoretical treatment of a chemical relaxation process was given by Einstein (4), who considered a dissociating gas subjected to rapid adiabatic compression and dilatation in a sound wave. At frequencies where the chemical transformations cannot follow the rapid change of temperature, phase shifts occur, and sound absorption and velocity dispersion should be observable. Corresponding experiments with the N_2O_4–NO_2 system had been previously suggested by Nernst (5). However, the technique at that time was not yet adequate for a detection of such small effects, and it was only recently that this particular system could be studied successfully as an example of a chemical relaxation process in the gas phase (*cf.* p. 1019). Instead, other molecular relaxation processes, resulting from energy transfer between different molecular degrees of freedom, were discovered some years later by Herzfeld and Rice (6), Kneser (7), Henry (8), and Eucken *et al.* (9), and absorbed the interest of physicists working in this field. It would be beyond the scope of this chapter to list all papers dealing with ultrasonic relaxation that followed these first studies (for reviews see the general references), as they are only slightly related to our subject. The very rigorous theoretical treatment of relaxation phenomena on the basis of "thermodynamics of irreversible processes" by Meixner (10) deserves special mention, however, as it includes a consideration of chemical processes.

New possibilities arose when techniques for more precise studies of sound absorption in liquids became available, about 15 years ago. Again, most of the early measurements were made from a purely physical point of view; they were usually related to structural analysis or even to practical acoustical problems (e.g., absorption by sea water, etc.). Nevertheless, such studies led to the first observation of typical chemical relaxation processes. For example, the very strong sound absorption found in solutions of 2:2 electrolytes (*cf.* p. 1021) proved representative for chemical processes, al-

though their complex reaction mechanisms—characterized by several (in some cases 3 or even 5) relaxation times as a result of coupled dissociation and hydrolysis—allowed a satisfactory explanation and quantitative description only quite recently. Typical weak electrolytes, such as NH_3 in aqueous solution, were among the first systems whose dissociation and recombination kinetics could be studied quantitatively (*cf.* p. 1021). In these cases, the known equilibrium parameters permitted prediction of the absolute values of (maximum) absorption coefficients. Also, the extensive work on sound absorption in pure liquids with molecules exhibiting configurational isomerism, as well as the numerous studies of molecular association, should be quoted here, although, in these cases, the molecular process does not always represent an actual "chemical" transformation (see Section IV and the general references).

Sound absorption or dispersion represents an important method in certain cases, but one that is not always well suited to the requirements of chemical studies; one of its disadvantages is the relatively large amount of substance needed. Also, the concentration of a substance to be investigated must be at least 10^{-3} to 10^{-2} M, which is too restrictive a condition in many cases. In this respect, the pressure-shock method (*cf.* p. 981) in combination with sensitive means of detection has great advantages. Further, the nonspecificity of sound methods with respect to single compounds makes the analysis of more complicated reaction mechanisms difficult.

Once the usefulness of the principle of relaxation methods was recognized, it was a natural development to find new methods which avoid these difficulties. Aqueous solutions are of particular interest, since their importance with respect to biological processes presents a variety of challenges. It is apparent that these studies require more sensitive and more specific means of detection. These requirements are not always met by sound absorption methods.

Among other external parameters influencing a chemical equilibrium, the electrical field density proved useful in certain cases. As was found by Wien (11) and his school, and theoretically explained by Onsager (12), weak electrolytes in solution show an increase in conductivity at high electric field strengths because of increased dissociation. The relaxation of this "dissociation field effect" gives information about the chemical kinetics, as the chemical transformations are coupled to the electrostatic processes of ionization. Many systems have been studied by this method, which is very sensitive to small amounts of reactants, though, again, it is rather restricted in scope because of the ionization requirement. The most useful parameter for perturbing chemical systems is the temperature since most equilibria are associated with a finite heat of reaction. Thus, it was almost a requirement to develop methods which allow fast (step-wise) temperature changes in aqueous solutions. Such methods, utilizing the

electric properties of aqueous systems (rather than adiabatic compression and dilatation, which, owing to the density anomaly, are not effective in water) have been developed (*cf.* p. 969 ff.). When combined with sensitive means of detection such as conductimetry, spectrophotometry, or polarimetry, they represent methods that are optimally adjusted to the requirements of chemistry and, particularly, of biochemistry. It is possible to detect reactants with molar fractions of as little as 10^{-8} in the presence of other substances of much higher concentration (apart from the solvent). If the temperature dependence of the system to be studied is small, coupling with a temperature-dependent buffer may serve as a means of shifting the equilibrium. Similarly, indicators may be used for the spectrophotometric observation of nonabsorbing reactants. These two possibilities appreciably enlarge the range of this method.

The time range covered by the relaxation methods includes more than nine orders of magnitude (see Figure 1, p. 919) and is still being extended. Such a "band-width" is of importance when a complicated reaction mechanism is to be studied. The analysis of a relaxation spectrum requires knowledge of the different time constants, which usually are not simply related to the rate constants because of coupling between the various reaction steps. Normally, a complete analysis of the reaction mechanism is possible only when all the time constants can be measured.

This chapter is planned to present a survey of methods and techniques suitable for *chemical* relaxation studies. In accord with the title of the series it is designed for practical applications. No attempt has been made to give a complete survey of all kinds of molecular relaxation studies. Furthermore, the applications deal primarily with solution kinetics. There are few applications of the techniques to be described which are connected with chemical kinetics in the gas phase. There has been, however, extensive work on shock waves, detonations, and flame reactions (for reviews see reference 13); these descriptions are beyond the scope of this chapter.

Theory is included in so far as it is necessary for an understanding of the principles underlying the methods and for the treatment of data. The presentation might sometimes be a little more detailed than in other chapters of this book. The reason for this is that, in contrast to conventional methods, a complete treatment of chemical relaxation is missing in the literature. For more general problems of the theory of irreversible processes, energy transfer, etc., the original papers as listed in the general references should be consulted.

A survey of some general results is given in the last section (IV). The data are presented to demonstrate the applicability of methods. A more detailed discussion of special reaction mechanisms studied by relaxation techniques may be found in a monograph (see general references), in preparation.

References

1. J. C. Maxwell, *Phil. Mag. (IV)*, **35**, 134 (1868).
2. P. Debye, *Ber. deut. physik. Ges.*, **15**, 777 (1913).
3. C. J. Gorter and R. de L. Kronig, *Physica*, **3**, 1009 (1931).
4. A. Einstein, *Sitzber. preuss. Akad. Wiss., Physik. math. Kl.*, **1920**, 380.
5. W. Nernst, see *Diss. F. Keutel*, Berlin, 1910; E. Grüneisen and E. Goens, *Ann. Phys.*, **72**, 193 (1923).
6. K. F. Herzfeld and F. O. Rice, *Phys. Rev.*, **31**, 691 (1928); *cf.* also G. W. Pierce, *Proc. Am. Acad. Arts Sci.*, **60**, 271 (1925).
7. H. O. Kneser, *Ann. Phys.*, **11**, 761, 777 (1931).
8. P. S. H. Henry, *Proc. Cambridge Phil. Soc.*, **28**, 249 (1931).
9. A. Eucken, *Naturwissenschaften*, **20**, 85 (1932); *cf.* also *Lehrbuch der Chemischen Physik* Leipzig, 1943, Vol. II, pp. 360ff.
10. J. Meixner, *Ann. Phys.*, **43** (5) 470 (1943); *Kolloid-Z.*, **134**, 3 (1953).
11. M. Wien and J. Schiele, *Z. Phys.*, **32**, 545 (1931).
12. L. Onsager, *J. Chem. Phys.*, **2**, 599 (1934).
13. E. F. Greene and J. P. Toennies, *Chemische Reaktionen in Stosswellen*, Steinkopf, Darmstadt, 1959.

General References

Chemical Relaxation

"The Study of Fast Reactions," *Discussions Faraday Soc.*, **17** (1954).
"Fast Reactions in Solution," *Z. Elektrochem.*, **64** (1) (1960).
M. Eigen, *Chemische Relaxation*, Steinkopf, Darmstadt (in preparation).

Related Molecular Relaxation Processes

K. F. Herzfeld and T. A. Litovitz, *Absorption and Dispersion of Ultrasonic Waves*, Academic Press, New York, 1959.
H. O. Kneser, *Ergeb. exakt. Naturw.*, Springer, 1949, p. 121 (review).
D. Sette, *Nuovo cimento*, **6**, 1 (1949) (review).
R. O. Davies and J. Lamb, *Quart. Rev.*, **9**, (2), 134 (1957) (review).
K. F. Herzfeld, *Relaxation Phenomena in Gases* (*High Speed Aerodynamics and Jet Propulsion*, Vol. I) Princeton, 1953.
W. Nosdrew, *Ultraacoustic Applications in Molecular Physics*, State Publ. of Phys. Math. Lit., Moscow, 1958; in Russian, containing many references from Russian literature.
D. Tabuchi, *Reaction Velocity* (*Experimental Methods of Chemistry*, Vol. 6), Maruzen Publishing Co., Tokyo, 1956, Chap. 3, pp. 121–199 (in Japanese).

General Theory

"The Relaxational Behaviour of Matter," *Kolloid-Z.*, **134**, 1 (1953).
J. Meixner, *Thermodynamik der irreversiblen Prozesse*, Aachen, 1954 (collection of papers 1941–1949).
B. Gross, *Mathematical Structure of the Theory of Viscoelasticity*, Paris, 1953.
I. Prigogine and R. Defay, *Thermodynamique Chimique*, Desoer, Liège, 1950.
S. R. de Groot, *Thermodynamics of Irreversible Processes*, North-Holland Publ. Co., Amsterdam, 1951.

II. THEORETICAL BASIS OF RELAXATION METHODS

1. Linearized Rate Equations and Relaxation Times

A. SINGLE-STEP REACTIONS

A set of externally fixed parameters (e.g., over-all concentrations of reactants, temperature, pressure, etc.) defines the thermodynamic equilibrium for any chemical system. The equilibrium may actually not be established, depending on the previous history of the system. Any deviation, however, will tend to vanish, the system approaching its stable equilibrium in a manner described by the rate equations. As long as these deviations from the equilibrium are small, a linearization of the rate equations with respect to the time-dependent concentration variable is possible. Thus, the rate of disappearance of a (small) difference between the actual and equilibrium concentrations is proportional to this difference itself. The reciprocal of the proportionality factor has the dimension of time and is called the relaxation time.

Let us consider, first, a system in which only a single-step reaction (of arbitrary order) takes place. The linearized rate can be generally expressed as

$$dx_i/dt + (1/\tau)x_i = (1/\tau)\bar{x}_i \qquad \text{(II.1.1)}$$

in which x_i and $\bar{x}_i$ are defined as concentration* differences of a reacting species i. $x_i = c_i - c_i^0$ is the difference between the actual concentration c_i and a time-independent reference value c_i^0 (i.e., the concentration belonging to reference external conditions). $\bar{x}_i = \bar{c}_i - c_i^0$ is the corresponding difference between the (possibly time-dependent) equilibrium concentration $\bar{c}_i$ and the reference value c_i^0. Equation (II.1.1) is valid only under the condition

$$\bar{x}_i - x_i \ll c_i \qquad \text{(II.1.2)}$$

This may be shown explicitly for the following example:

$$\mathrm{A} + \mathrm{B} \underset{k_{21}}{\overset{k_{12}}{\rightleftharpoons}} \mathrm{C}$$

* The proper choice of concentration variables, which are characteristic of the chemical transformations only, is discussed in Section II.3.B.

The complete rate equation is given by

$$-dc_A/dt = -dc_B/dt = dc_C/dt = k_{12}c_Ac_B - k_{21}c_C \qquad \text{(II.1.3)}$$

By using the above definitions of x_i and $\bar{x}_i$,

$$\begin{aligned} c_A &= c_A^0 + x_A & \bar{c}_A &= c_A^0 + \bar{x}_A \\ c_B &= c_B^0 + x_B & \bar{c}_B &= c_B^0 + \bar{x}_B \\ c_C &= c_C^0 + x_C & \bar{c}_C &= c_C^0 + \bar{x}_C \\ x_A &= x_B = -x_C & \bar{x}_A &= \bar{x}_B = -\bar{x}_C \end{aligned} \qquad \text{(II.1.4)}$$

We can write, for small differences $(\bar{x}_i - x_i)$,

$$\begin{aligned} dc_A/dt = dx_A/dt &= k_{21}(\bar{c}_C + x_C - \bar{x}_C) \\ &\quad - k_{12}(\bar{c}_A + x_A - \bar{x}_A)(\bar{c}_B + x_B - \bar{x}_B) \\ &= k_{21}\bar{c}_C + k_{21}(\bar{x}_A - x_A) \\ &\quad - k_{12}\bar{c}_A\bar{c}_B + k_{12}(\bar{c}_A + \bar{c}_B)(\bar{x}_A - x_A) \end{aligned} \qquad \text{(II.1.5)}$$

$k_{21}\bar{c}_C = k_{12}\bar{c}_A\bar{c}_B$ represents the equilibrium condition; thus we obtain

$$dx_A/dt + [k_{21} + k_{12}(\bar{c}_A + \bar{c}_B)]x_A = [k_{21} + k_{12}(\bar{c}_A + \bar{c}_B)]\bar{x}_A \qquad \text{(II.1.6)}$$

which is equivalent to Equation (II.1.1) with

$$\tau = [k_{21} + k_{12}(\bar{c}_A + \bar{c}_B)]^{-1} \qquad \text{(II.1.7)}$$

For a weak binary electrolyte, we may introduce a degree of dissociation α and substitute $c_A = c_B = \alpha c_0$; $c_C = (1 - \alpha)\, c_0$ (c_0 = over-all electrolyte concentration). Then the relaxation time can be expressed as

$$\tau = [k_{21} + 2k_{12}\alpha c_0]^{-1} \qquad \text{(II.1.8)}$$

It may be noted that, for single-step systems, a complete solution of the nonlinearized rate equation is also possible as a rule. For instance, if we write Equation (II.1.3) using the definitions (II.1.4) and (II.1.7) with $\bar{x} = 0$ in the form

$$dx/dt = -(x/\tau) - k_{12}x^2 \qquad \text{(II.1.9)}$$

the solution with $x_{t=0} = x_0$ will be

$$x(t) = x_0/\{x_0k_{12}\tau[1 - \exp(t/\tau)] + \exp(t/\tau)\} \qquad \text{(II.1.10)}$$

which, for small perturbations ($x_0 \ll \bar{c}_A : x_0 \ll 1/k_{12}\tau$), reduces to the solution of the homogeneous relaxation equation (*cf.* Section II.2).

$$x = x_0 \exp(-t/\tau) \qquad \text{(II.1.11)}$$

For nonlinear multiple-step systems, an explicit solution cannot usually be given. In such cases, the use of computers, as described by Higgins in Chapter VII, is advisable.

As may be seen from the above example, the analytical expression for τ always contains the contributions from the forward and backward reactions additively. This means that, close to equilibrium, both processes compete for the equilibration, and τ is independent of the sign of perturbation (corresponding to either increased or decreased dissociation). Other examples of important one-step reaction systems are listed in Table II.1. As may

TABLE II.1

(1) $A \underset{k_{21}}{\overset{k_{12}}{\rightleftharpoons}} B$	$1/\tau = k_{12} + k_{21}$
(2) $A + C \rightleftharpoons B + C$ (C = catalyst)	$1/\tau = k_{12}\bar{c}_C + k_{21}\bar{c}_C$
(3) $2A \rightleftharpoons A_2$	$1/\tau = 4k_{12}\bar{c}_A + k_{21}$
(4) $A + B \rightleftharpoons C$ (B = buffered: $x_B \approx 0$)	$1/\tau = k_{12}\bar{c}_B + k_{21}$
(5) $A + B \rightleftharpoons C + D$	$1/\tau = k_{12}(\bar{c}_A + \bar{c}_B) + k_{21}(\bar{c}_C + \bar{c}_D)$
(6) $A + B + C \rightleftharpoons D$	$1/\tau = k_{12}(\bar{c}_A\bar{c}_B + \bar{c}_A\bar{c}_C + \bar{c}_B\bar{c}_C) + k_{21}$

be seen from example (2) in Table II.1 the concentration of a catalyst appears as a constant factor only in combination with the rate constant (i.e., $x_{cat} \approx 0$), in contrast to the behavior of an ordinary reaction partner. A similar behavior is shown by a buffered compound [example (4)], if the buffer equilibrium is established rapidly enough (compare also the discussion of multiple-step systems).

If any of the reactions proceeds through intermediates present in undetectably small (quasi-stationary) amounts, their concentrations will not appear explicitly in the expression for the relaxation times, which is related to the over-all mechanism only. Higher-order reactions [as represented by example 6] usually involve such intermediates.

As another example we may consider the exchange equilibrium (II.1.12),

$$\begin{array}{ccc} \text{(I)} & & \text{(II)} \\ AB + C & \underset{k_{21}}{\overset{k_{12}}{\rightleftharpoons}} & AC + B \\ & {\scriptstyle k_{31}} \searrow \nwarrow {\scriptstyle k_{13}} \quad {\scriptstyle k_{32}} \swarrow \nearrow {\scriptstyle k_{23}} & \\ & A + B + C & \\ & \text{(III)} & \end{array} \qquad \text{(II.1.12)}$$

where only the compounds of states I and II are present in detectable concentrations. The relaxation time for the equilibration between state I and II is given by

$$\tau = \{[k_{12} + k_{13}k_{32}/(k_{31}\bar{c}_B + k_{32}\bar{c}_C)](\bar{c}_{AB} + \bar{c}_C) + [k_{21} + k_{23}k_{31}/(k_{31}\bar{c}_B + k_{32}\bar{c}_C)](\bar{c}_{AC} + \bar{c}_B)\}^{-1} \qquad \text{(II.1.13)}$$

This expression may be derived easily by using the stationary condition for state III: $dc_A/dt = 0$, together with the condition of conservation of the components A, B, and C and their compounds. (Note that the terms

$$k_{13}\,k_{32}/(k_{31}\bar{c}_B + k_{32}\bar{c}_C) \qquad \text{and} \qquad k_{23}\,k_{31}/(k_{31}\bar{c}_B + k_{32}\bar{c}_C)$$

commonly used in the description of stationary intermediates, enter the expression for τ as constant rate coefficients, the concentration terms being time-independent equilibrium values.) This type of reaction is a very common one [examples: proton or electron exchange reactions; substitution of a proton by a metal ion in a complexing compound such as $EDTAH^{3-} + Me^{2+} \rightleftharpoons EDTAMe^{2-} + H^+$].

For ionic reactions in particular, the rate constants usually include concentration-dependent terms, primarily as a result of electrostatic interactions with other ions present in the system. Let us again consider the example [Equation (II.1.3)] treated above, where A and B now represent charged particles. Let us further assume that the reaction proceeds slowly enough, so that all diffusive processes such as the establishment of a configurational distribution of ions (ionic atmosphere) are stationary. The ionic interactions then can be described by an activity factor of the form $\Pi f = f_+ f_- / f_\pm$, which occurs in k_{12}, whereas k_{21} remains concentration independent. As long as the ionic strength of the system is determined by an indifferent electrolyte rather than by the reacting species themselves, Equation (II.1.7) remains valid with $k_{12} = k_{12}^\circ \Pi f$. If, however, the ionic strength does not remain constant during the reaction, i.e., if it is determined by the reacting ions, the variation of Πf due to a finite concentration change has to be considered and Equation (II.1.7) is replaced by

$$\tau = [k'_{12} + k_{21}]^{-1}$$

with

$$k'_{12} = k_{12}^\circ \cdot \Pi f \left[\bar{c}_A \left(1 + \frac{\partial \ln \Pi f}{\partial \ln \bar{c}_B} \right) + \bar{c}_B \left(1 + \frac{\partial \ln \Pi f}{\partial \ln \bar{c}_A} \right) \right] \qquad \text{(II.1.14)}$$

In more complicated reaction systems, where Πf depends on the concentrations of different ionic species, an evaluation of τ in terms of rate constants might become rather difficult. In such a case, it is advisable to work at constant ionic strength, e.g., in $0.1M$ solution of a 1:1 electrolyte. (The conditions are especially appropriate for the investigation of biochemical reactions.)

Needless to say, these influences are only of importance at higher electrolyte concentrations. If the reactions are diffusion controlled, a separation of ionic atmosphere and reaction effects is not possible since equilibration of both processes occurs at comparable rates. At small reactant

concentrations, the reaction can be treated formally as a normal chemical rate process (recombination and dissociation). Ionic interaction is restricted to the reacting pair of ions. At higher concentration, however, a whole (continuous) spectrum of relaxation times will appear, owing to the infinite number of possible ionic arrangements, among which the configuration at the reaction distance is only a special case (*cf.* Section II.1.C).

*B. RELAXATION TIMES AND THERMODYNAMIC CONDITIONS

The relaxation time was introduced in Section II.1.A from the point of view of conventional chemical kinetics; i.e., only the temporal change of the variable, characteristic of the chemical state, was taken into account. It is evident that any treatment of chemical change requires the definition of the thermodynamic conditions. (*cf.* also Section II.3.C). If the relaxation process can be initiated by a change in thermodynamic variables, the equilibration process necessarily will produce a secondary shift of these variables unless they are fixed by some internal or external means. For instance, if a chemical equilibrium can be directly disturbed by a change in temperature, which means that the heat of reaction is finite, there will be a secondary absorption or evolution of the latter during the equilibration causing a small secondary temperature change which will be opposite to the primary one. Thus, if no heat exchange with the surroundings takes place (i.e., under adiabatic conditions), the final temperature shift after the input of a certain amount of heat will be lower than that under isothermal conditions, where the primary temperature shift is kept constant by heat exchange. As the concentration shift is proportional to the temperature change, the equilibration will be effected sooner under adiabatic than under isothermal conditions. However, it is easily seen that these influences will be negligible in solution reactions, where the concentration of the reacting solute is usually small with respect to the solvent concentration. Here the solvent will act as a "thermostat" and maintain fixed conditions during the chemical equilibration of the solute, provided that the internal equilibration of the solvent (solvent relaxation processes) does not interfere in this time range. Actually, these conditions will be fulfilled in most of the applications discussed. In certain cases, however, the differences in thermodynamic conditions can have some influence (e.g., for relaxation phenomena in pure liquids, H-bond formation, etc.).

A quantitative treatment of these influences based on the thermodynamics of irreversible processes was given by Meixner (1) [in an important paper to which the reader is referred for a more extensive discussion; compare also ref. (3)]. It can be shown that

$$\tau_{SV} \leq \tau_{TV} \leq \tau_{TP} \qquad \text{and} \qquad \tau_{SV} \leq \tau_{SP} \leq \tau_{TP} \qquad \text{(II.1.15)}$$

a condition which is closely related to the principle of Le Chatelier and Braun. Using a definition introduced by Planck (4) and Wagner (5), one may generalize this statement as follows: The relaxation time is shorter when during equilibration the extensive variables (such as S, V) instead of the intensive variables (such as T, P) are kept constant [*cf.* Schlögl (6)]. This statement should also hold for generalized variables such as electric field density $\mathbf{E}$ (intensive) and its conjugate extensive variable $\mathbf{D}^*$ [for definition see Equation (II.3.62)] as far as these quantities influence the affinity† of the chemical system (7).

According to Meixner (1), the difference between the relaxation times disappear under the following conditions:

$$\begin{aligned}
\tau_{SV} &= \tau_{TV} && \text{if } (\partial\xi/\partial T)_{V,A} = 0 \\
\tau_{SV} &= \tau_{SP} && \text{if } (\partial\xi/\partial P)_{S,A} = 0 \\
\tau_{SP} &= \tau_{TP} && \text{if } (\partial\xi/\partial T)_{P,A} = 0 \\
\tau_{TV} &= \tau_{TP} && \text{if } (\partial\xi/\partial P)_{T,A} = 0 \\
\tau_{\mathbf{D}^*Z_iZ_k} &= \tau_{\mathbf{E}_iZ_iZ_k} && \text{if } (\partial\xi/\partial\mathbf{E})_{Z_i,Z_k,A} = 0
\end{aligned} \tag{II.1.16}$$

Thus we have $\tau_{SV} = \tau_{TV} = \tau_{SP} = \tau_{TP} = \tau_{\mathbf{E}Z_iZ_k}$, if the equilibrium value of ξ is independent of T,P,$\mathbf{E}$, etc. For chemical equilibria in solutions, this condition—though not exactly fulfilled—generally holds with sufficient accuracy, even if ξ depends strongly on one of the state parameters. This is because the solvent, which is present at much higher concentration, maintains constant conditions. As the difference between $\tau_{Z_iz_k}$ and $\tau_{Z_iZ_k}$ is given by $(\partial\xi/\partial Z_k)_{Z_iA}\ (\partial Z_k/\partial A)_{Z_iz_k}$, the condition here is $(\partial\xi/\partial Z_k)_{Z_iA} \ll (\partial A/\partial Z_k)_{Z_iz_k}$. (The small letters z_iz_k denote general extensive, the capital letters Z_iZ_k general intensive, variables.) By using relations derived in Section II.3.C, Meixner's conditions (II.1.16) can be written for one-step relaxation systems as

$$\begin{aligned}
\tau_{SV} &= \tau_{TV}\,(1 - \bar{c}_V^{\,ch}/\bar{c}_V) \\
\tau_{SP} &= \tau_{TP}\,(1 - \bar{c}_P^{\,ch}/\bar{c}_P) \\
\tau_{TV} &= \tau_{TP}\,(1 - \bar{\kappa}_T^{\,ch}/\bar{\kappa}_T) \\
\tau_{SV} &= \tau_{SP}\,(1 - \bar{\kappa}_S^{\,ch}/\bar{\kappa}_S) \\
\tau_{\mathbf{D}^*Z_iZ_k} &= \tau_{\mathbf{E}Z_iZ_k}\,(1 - \bar{\epsilon}_{Z_iZ_k}^{\,ch}/\bar{\epsilon}_{Z_iZ_k})
\end{aligned} \tag{II.1.17}$$

where $\bar{c}_V$, $\bar{c}_P$, $\bar{\kappa}_T$, $\bar{\kappa}_S$, and $\bar{\epsilon}_{Z_iZ_k}$ are the specific heats at constant volume and pressure, the isothermal and adiabatic compressibilities, and the elec-

† The affinity A is introduced according to De Donder (10) (*cf.* Section II.3.B). The conjugate variable to A is the extent of reaction ξ. Thermodynamically, the quantity $Ad\xi$ may be introduced as a term of the total differential of the internal energy U of the system: $dU = TdS - PdV - Ad\xi$ [*cf.* Guggenheim (8)].

tric permittivity at constant A, Z_iZ_k, respectively.* The "chemical" terms, denoted by ch, represent the corresponding (equilibrial) parts due to chemical transformation as derived in Section II.3.C, e.g., for†

$$\bar{c}_V = \frac{1}{\rho V}\left(\frac{\partial U}{\partial T}\right)_V \qquad \bar{c}_V^{ch} = \frac{1}{\rho V}\left(\frac{\partial U}{\partial \xi}\right)_{T,V}\left(\frac{\partial \xi}{\partial T}\right)_{V,A}$$

$$c_P = \frac{1}{\rho V}\left(\frac{\partial H}{\partial T}\right)_P \qquad \bar{c}_P^{ch} = \frac{1}{\rho V}\left(\frac{\partial H}{\partial \xi}\right)_{T,P}\left(\frac{\partial \xi}{\partial T}\right)_{P,A}$$

$$\kappa_T = -\frac{1}{V}\left(\frac{\partial V}{\partial P}\right)_T \qquad \bar{\kappa}_T^{ch} = -\frac{1}{V}\left(\frac{\partial V}{\partial \xi}\right)_{T,P}\left(\frac{\partial \xi}{\partial P}\right)_{T,A}$$

$$\bar{\kappa}_S = -\frac{1}{V}\left(\frac{\partial V}{\partial P}\right)_S \qquad \bar{\kappa}_S^{ch} = -\frac{1}{V}\left(\frac{\partial V}{\partial \xi}\right)_{S,P}\left(\frac{\partial \xi}{\partial P}\right)_{S,A}$$

$$\bar{\epsilon}_{Z_iZ_k} = \frac{1}{V_e\epsilon_0}\left(\frac{\partial \mathbf{D}^*}{\partial \mathbf{E}}\right)_{Z_iZk} \qquad \bar{\epsilon}_{ZiZ_k}^{ch} = \frac{1}{V_e\epsilon_0}\left(\frac{\partial \mathbf{D}^*}{\partial \xi}\right)_{\mathbf{E},Z_i,Z_k}\left(\frac{\partial \xi}{\partial \mathbf{E}}\right)_{Z_i,Z_k,A}$$

These chemical terms can be related to directly measurable quantities as will be shown in Sections II.3.B and C. They generally become small if the mole fraction of solute is small with respect to that of the solvent, regardless of the relative shift of ξ with the external variable. In most cases of solution kinetics, the relaxation times, as introduced in Section II.1.A, can be used, where rate constants are related to constant T and P, and volume changes are negligible.

*C. MULTIPLE-STEP SYSTEMS (RELAXATION SPECTRA)

In the above treatment we preferred to consider some specific single-step reaction systems. From these considerations, a generalization to any reaction order is readily possible. In practice, however, there is little need of such generalized expressions for single-step relaxation. Higher-order reactions usually do not proceed in one single step and therefore cannot be represented by a single relaxation time. The more general case, therefore, requires the treatment of a system of rate equations resulting in a spectrum of relaxation times.

It is obvious that the number of discrete relaxation times in a spectrum depends on the number of independent reaction steps. As there may be interrelations between different reaction paths leading to the same state,

* Only at very high field densities does $\bar{\epsilon}_{Z_iZ_k}^{ch}$ have detectable values. Then the definition of ϵ must include the conditions of the other thermodynamic variables [*cf* Equation (II.1.18)].

† For definition of V_e and ϵ_0 see Equation (II.3.65)ff

the number of relaxation times usually will be smaller than the number of actual reaction steps.

For example, the transformation between two states such as A $\rightleftharpoons$ B, even if effected by n different parallel reaction paths, is characterized by only one relaxation time, containing the sum of all rate constants of the simultaneous reactions. Consecutive reaction systems, however, will generally possess more than one relaxation time, unless all intermediates are present at undetectably small concentrations.

The single relaxation times in a multiple-step system generally do not correspond to the single reaction steps. This is a consequence of the coupling between the different reactions, analogous to the coupling of vibrations in a multiple-oscillator system (such as a molecule containing many atomic groups). The resulting resonance frequencies of such a system correspond to the normal modes of vibration rather than to the single vibrational modes of the isolated oscillators. Similarly, the relaxation times of coupled reaction systems correspond to normal modes of reactions, as can be seen from the following treatment.

The temporal change in the concentration of a reactant, dc_i/dt, may depend on all the concentrations of other reactants present. Therefore Equation (II.1.1) will then have the form

$$(dx_i/dt) + \sum_k a_{ik}x_k = \sum_k a_{ik}\bar{x}_k \qquad \text{(II.1.19)}$$

where the x_i have the above meaning and the a_{ik} represent coefficients containing rate constants and equilibrium concentrations, according to the stoichiometry and molecularity of the reactions. There will be n such equations if n variables x_i are present. In order to find the relaxation times corresponding to the definition of Equation (II.1.1), we have to transform the x_i into a new system of concentration coordinates y_i, for which

$$(dy_i/dt) + b_{ii}y_i = b_{ii}\bar{y}_i \qquad \text{(II.1.20)}$$

These new concentration variables may be considered principal axes of the system, obtained by an affine coordinate transformation. They are linear combinations of the true concentration variables x_i.

$$y_i = \sum_k m_{ik}x_k \qquad \text{and} \qquad x_i = \sum_k m'_{ik}y_k \qquad \text{(II.1.21)}$$

The b_{ii} represent the reciprocal relaxation times $(1/\tau_i)$. They are the eigenvalues of the characteristic equation, which, in determinant form, reads

$$\begin{vmatrix} (a_{11} - b) & a_{12} & \cdots & a_{1n} \\ a_{21} & (a_{22} - b) & \cdots & \vdots \\ \vdots & \vdots & \ddots & \vdots \\ a_{n1} & \cdots & \cdots & (a_{nn} - b) \end{vmatrix} = 0 \qquad \text{(II.1.22)}$$

Written in this form, Equation (II.1.22) yields only real and positive values for $1/\tau_i$ (roots of b), a result of the principle of microscopic reversibility, or the principle of detailed balance (as it is often called for chemical systems).† Generally, these restrictions apply only to closed systems near equilibrium. It follows that for such systems only stable (i.e., decaying exponentials), but no periodical, solutions are possible. The term "periodical" includes damped harmonic oscillations that can be written as complex expressions; it does not include a finite number of maxima which are possible by a superposition of different exponential terms, the pre-exponential coefficients of which have different signs. In such a case, it can be shown that the number of maxima is smaller than the number of independent steps by at least one. [For more details see also ref. (15).]

The determination of the spectrum of relaxation times requires only the solution of Equation (II.1.22). If, however, a knowledge of the extent of perturbation of each concentration is required, the transformation matrices must also be calculated. As can be mentioned here, the choice of normal variables for a multiple-step system is not independent of the thermodynamic conditions under which the chemical transformation takes place. The present considerations are valid for changes at constant intensive variables such as T, P, and $\mathbf{E}$, to which the equilibrium conditions refer. They may be adapted, also, to changes at constant extensive variables such as S, V, and $\mathbf{D}^*$ (*cf.* Section II.3.D).

The problem may be formulated by considering the variables x_i and y_i as components of a vector $\mathbf{X}$ and $\mathbf{Y}$, respectively. If $\mathbf{A}$ and $\mathbf{B}$ are the corresponding matrices of coefficients [according to Equations (II.1.19) and (II.1.20)], $\mathcal{E}$ the unit matrix, and $\mathfrak{D}$ the differential operator d/dt, the rate equations in the primary and in the transformed form then can be written

$$(\mathfrak{D}\mathcal{E} + \mathbf{A})\mathbf{X} = \mathbf{A}\bar{\mathbf{X}} \qquad (\mathfrak{D}\mathcal{E} + \mathbf{B})\mathbf{Y} = \mathbf{B}\bar{\mathbf{Y}} \qquad \text{(II.1.23)}$$

with

$$\mathbf{X} = \mathbf{M}^{-1}\mathbf{Y} \qquad \text{and} \qquad \mathbf{Y} = \mathbf{M}\mathbf{X} \qquad \text{(II.1.24)}$$

where the matrix $\mathbf{M}^{-1}$ is the inverse to the transformation matrix $\mathbf{M}$: $\mathbf{M}\mathbf{M}^{-1} = \mathcal{E}$. The quality of $\mathbf{M}$ is such that $\mathbf{B} = \mathbf{M}\mathbf{A}\mathbf{M}^{-1}$ is of the diagonal form (i.e., $b_{ik} = 0$ for $i \neq k$). Explicit solutions of this very common problem of principal axis transformation can be found in textbooks of mathematics. It might be more instructive here to give an example (17,18).

† Because of these conditions, the matrix of coefficients $\mathbf{A}$ is symmetrical, as shown explicitly for the analogous case of a general system of first-order reactions by Jost (11) [*cf.* Bauer (12)]. The same conditions are implied in Meixner's general thermodynamic treatment (1), where they are equivalent to Onsager's reciprocity relations [*cf.* refs. (13,14)]

Let us consider the reaction system

$$\underset{(1)}{A^+ + B^-} \underset{k_{21}}{\overset{k_{12}}{\rightleftharpoons}} \underset{(2)}{AB} \underset{k_{32}}{\overset{k_{23}}{\rightleftharpoons}} \underset{(3)}{C} \qquad \text{(II.1.25)}$$

where the intermediate (e.g., an ion pair) is present at finite concentration. This system represents the more general case of an electrolytic dissociation equilibrium. The linearized rate equations can be written as

$$\begin{aligned} dx_1/dt &= -k'_{12}x_1 + k_{21}x_2 \\ dx_2/dt &= k'_{12}x_1 - (k_{21} + k_{23})x_2 + k_{32}x_3 \\ dx_3/dt &= k_{23}x_2 - k_{32}x_3 \end{aligned} \qquad \text{(II.1.26)}$$

with $x_1 = c_A - c_A^\circ = c_B - c_B^\circ$; $x_2 = c_{AB} - c_{AB}^\circ$; $x_3 = c_C - c_C^\circ$, and k'_{12}, according to Equation (II.1.14) [if ionic atmosphere effects are negligible, k'_{12} reduces to $k_{12}(\bar{c}_A + \bar{c}_B)$]. The reciprocal relaxation times $1/\tau_i = b_{ii}$ are[†]

$$1/\tau_{I,II} = {}^1/_2[\sum \mathbf{k} \pm \sqrt{(\sum \mathbf{k})^2 - 4\Pi \mathbf{k}}] \qquad \text{(II.1.27)}$$

where

$$\sum \mathbf{k} = k'_{12} + k_{21} + k_{23} + k_{32}$$

and

$$\Pi \mathbf{k} = k'_{12}(k_{23} + k_{32}) + k_{21}k_{32}$$

The transformation matrix is given by

$$\mathbf{M} = \begin{pmatrix} \dfrac{k'_{12}}{k'_{12} - 1/\tau_I} & 1 & \dfrac{k_{32}}{k_{32} - 1/\tau_I} \\ \dfrac{k'_{12}}{k'_{12} - 1/\tau_{II}} & 1 & \dfrac{k_{32}}{k_{32} - 1/\tau_{II}} \\ 1 & 1 & 1 \end{pmatrix} \qquad \text{(II.1.28)}$$

There are only two relaxation times, because of the condition of conservation $\sum x_i = 0$ $(= y_{III})$, which reduces the number of independent variables by one.

The physical meaning of the single terms becomes more apparent if we consider the special case of $\tau_I \ll \tau_{II}$, which is equivalent to the assumption of very rapid equilibration of the step $1 \rightleftharpoons 2$ as compared to $2 \rightleftharpoons 3$. (This case is a very common one, since $1 \rightleftharpoons 2$ may represent a diffusion-controlled reaction.) The relaxation times then reduce to

[†]The positive sign holds for τ_I, the negative for τ_{II}.

$$\begin{aligned} \tau_{\mathrm{I}} &= [k'_{12} + k_{21}]^{-1} \\ \tau_{\mathrm{II}} &= \{k_{32} + [(k_{23}k'_{12})/(k'_{12} + k_{21})]\}^{-1} \end{aligned} \qquad \text{(II.1.29)}$$

Here, τ_{I} represents the equilibration process for $1 \rightleftharpoons 2$, which is independent of the other step, since, during the fast transformation of 1 and 2, state 3 remains unchanged. The second relaxation time, however, is not simply related to step $2 \rightleftharpoons 3$, but has to account also for the fast equilibration shift $1 \rightleftharpoons 2$ during the change of 3. As $y_{\mathrm{III}} = x_1 + x_2 + x_3 = 0$, and therefore $x_3 = -(x_1 + x_2)$, the transformed equations can be simply written as

$$\begin{aligned} y_{\mathrm{I}} &= -[k'_{12}/(k'_{12} + k_{21})]x_1 + [k_{21}/(k'_{12} + k_{21})]x_2 \\ y_{\mathrm{II}} &= \qquad -x_1 \qquad\qquad -x_2 \end{aligned} \qquad \text{(II.1.30)}$$

and

$$\begin{aligned} x_1 &= -y_{\mathrm{I}} - [k_{21}/(k'_{12} + k_{21})]y_{\mathrm{II}} \\ x_2 &= y_{\mathrm{I}} - [k'_{12}/(k'_{12} + k_{21})]y_{\mathrm{II}} \end{aligned} \qquad \text{(II.1.31)}$$

where the schemes of coefficients represent the matrices $\mathbf{M}$ and $\mathbf{M}^{-1}$ with the condition: $k'_{12}, k_{21} \gg k_{23}, k_{32}$. (The properties of such a system of equations are not changed, if y_i, or $\mathbf{Y}$, is multiplied by a constant factor or a diagonal matrix, respectively.)

It is obvious that the evaluation may become rather complicated if more than two independent concentration variables are involved. However, in most cases, sufficiently accurate approximations are possible. (The above example was especially chosen to demonstrate this possibility.) Since chemical processes (in contrast to other physical relaxation phenomena) proceed with discrete time constants, which usually differ by orders of magnitude, a separation of the rate equations is possible. For instance, the above case may easily be generalized to an n-step reaction, where each consecutive step proceeds slowly with respect to the preceding one. Then, as shown for τ_{II} above, the relaxation time of each step is given by the sum of the corresponding rate constants, where the constant of the forward reaction is multiplied by an equilibration factor representative of the preceding equilibrated steps [such as $k'_{12}/(k'_{12} + k_{21})$ in τ_{II}].

Thus a further step in reaction scheme (II.1.25) (with $k'_{12}, k_{21} \gg k_{23}$, $k_{32} \gg k_{34}, k_{43}$) results in a new relaxation time.

$$\tau_{\mathrm{III}} = [k_{43} + [k'_{23}/(k'_{23} + k_{32})]k_{34}]^{-1} \qquad \text{with}$$

$$k'_{23} = [k'_{12}/(k'_{12} + k_{21})]k_{23} \qquad \text{(II.1.32)}$$

in addition to τ_{I} and τ_{II}, as given above. (It is important to note that, for higher than first-order reactions, the equilibration factor involves a differential quotient of equilibrium concentrations, rather than only equilibrium constants, e.g., $k'_{12}/(k'_{12} + k_{21}) = 1/(1 + k_{21}/k'_{12}) = 1/(1 + \delta\bar{c}_{\mathrm{A}}/\delta\bar{c}_{\mathrm{AB}})$.)

Other examples of coupled multiple-step reactions have been discussed in the literature. They include mechanisms of reactions in solution such as metal-complex formation (16–21), buffer action and pH indication (22), general hydrolysis (22), chain association (23), enzymatic catalysis (24,25), as well as gas-phase processes such as coupled energy transfer and dissociation (26–28).

We may briefly discuss two more cases, which are representative of the method:

(1) A coupled protolysis and metal-complex mechanism, according to the reaction scheme II.1.33, where the horizontal (metal-complex) reactions

$$\begin{array}{ccccc} & & (1)\ XH_2 & \rightleftharpoons & MeXH_2\ (4) \\ & & \downarrow\uparrow & & \downarrow\uparrow \\ & & (2)\ XH & \rightleftharpoons & MeXH\ (5) \\ \uparrow +H^{(+)} & & \downarrow\uparrow & & \downarrow\uparrow \\ \rightarrow +Me^{(n+)} & & (3)\ X & \rightleftharpoons & MeX\ (6) \end{array} \qquad \text{(II.1.33)}$$

are slow compared to the vertical (protolytic) reactions.

(2) A metal-activated enzyme reaction, according to scheme II.1.34,

$$\begin{array}{lcl} (1)\ EMe + S & & EMe + P\ (5) \\ \rightleftharpoons & & \rightleftharpoons \\ & EMeS \rightleftharpoons EMeP & \\ \rightleftharpoons & (3)\quad (4) & \rightleftharpoons \\ (2)\ E + MeS & & E + MeP\ (6) \end{array} \qquad \text{(II.1.34)}$$

where the transformation from S (substrate) to P (product) is the slow step. In these examples, two rapidly equilibrating two-step systems are separated from one another by a slow connecting reaction. The solutions for the separated two-step systems are analogous to those given in Equation (II.1.27) (two roots of a quadratic equation). They can be given explicitly and yield, for each of the above reaction systems, four relaxation times representative of the fast processes [protolytic reactions in scheme (II.1.33), enzyme-metal-substrate-complex formation in scheme (II.1.34)].† The fifth relaxation time (a system with six states does not possess more than five relaxation times) is then representative of the slow connecting process and therefore of the total equilibration.

This relaxation time will contain the rate constants of the slow processes and the equilibrium constants of all fast (equilibrated) steps. As variables, one may use the sum of X compounds [scheme (II.1.33) or S compounds [scheme (II.1.34)] the changes of which are equal to those of the

† There may also be a connection between (1) and (2), (or (5) and (6), respectively) via the states E, Me, S (or P), a consideration of which would further complicate the expressions of the relaxation times.

sum of MeX or P compounds, respectively. The individual concentrations can be related to these sums via the equilibrium constants (of the fast steps) and some conservation conditions (e.g., for E or Me compounds, etc.). The numerical expressions may be relatively complicated and it is important to adjust the conditions properly, in order to make the evaluation as simple as possible. It is, for instance, possible to buffer c_H and c_{Me} in the system (II.1.33), after the fast processes ($1 \rightleftharpoons 2$; $2 \rightleftharpoons 3$ and $4 \rightleftharpoons 5$; $5 \rightleftharpoons 6$) have been studied in unbuffered solutions. The relaxation time τ_v is then given by

$$\frac{1}{\tau_V} = \left\{ \frac{k_{14}}{1 + (k_{12}/k_{21}c_H)[1 + (k_{23}/k_{32}c_H)]} + \frac{k_{25}}{1 + (k_{23}/k_{32}c_H) + (k_{21}c_H/k_{12})} + \frac{k_{36}}{1 + (k_{32}c_H/k_{23})[1 + (k_{21}c_H/k_{12})]} \right\} c_{Me}$$

$$+ \left\{ \frac{k_{41}}{1 + (k_{45}/k_{54}c_H)[1 + (k_{56}/k_{65}c_H)]} + \frac{k_{52}}{1 + (k_{56}/k_{65}c_H) + (k_{54}c_H/k_{45})} + \frac{k_{63}}{1 + (k_{65}c_H/k_{56})[1 + (k_{54}c_H/k_{45})]} \right\} \quad \text{(II.1.35)}$$

(pMe and pH buffered).

Similarly, it is possible to work at high substrate concentrations (c_S and c_{MeS}) in the system (II.1.34) where the predominant part of E will be present in the form of the double complexes EMeS or EMeP. The relaxation time τ_v will then become concentration-independent (corresponding to the maximum velocity of the enzyme reactions),

$$\tau_V = [k_{34} + k_{43}]^{-1} \quad \text{(II.1.36)}$$

The complete numerical expression of $1/\tau_V$ is quite involved, but can be explicitly calculated.

A continuous superposition of relaxation times, i.e., a continuous relaxation spectrum, usually will not be found for chemical transformations, because of their discrete nature. (Continuous relaxation spectra are quite common in the dielectric and mechanical relaxation of high polymers, e.g., as a consequence of a continuous particle length distribution.) However, for very rapid reactions where diffusion of reactants becomes significant, such continuous relaxation spectra may be found even with chemical processes. An example is provided by the bimolecular ionic reaction considered in Section II.1.A. The two ionic partners interact with each other (and with other ions of the ionic atmosphere) electrostatically at each distance of approach. The great variety of possible configurations, described by a

distribution function, which varies continuously with distance of separation, will cause a continuous relaxation spectrum for the diffusive encounter process as well as the rearrangements in the ionic atmosphere [for further details see ref. (17)]. As a consequence, thermodynamic activity coefficients as introduced in Equation (II.1.14) cannot be used in such a case since they represent an equilibrial spatial distribution of ions. The diffusion-controlled recombination can be considered a discrete reaction step according to the rate equation (II.1.3) only when the ion-pair formation is followed by a chemical transformation, according to scheme (II.1.25). The ionic concentration has to be low enough to permit one to neglect the concentration of ion pairs (AB) with respect to the free ions (A and B) and to the products (C). For univalent reaction partners, e.g., protons and the anions of weak acids, this condition is usually fulfilled sufficiently for $c_A < 10^{-2}M$, corresponding to $\tau > 10^{-9}$ sec.

D. ANALYSIS OF RELAXATION SPECTRA

The analysis of a relaxation spectrum may involve considerable difficulties, if the single time constants differ by less than one order of magnitude. For instance, if the relaxation response to a stepwise change of external conditions can be expressed as a sum of exponential functions $\sum_k A_{ik} \exp(-t/\tau_k)$ (corresponding to the solutions of the system of homogenous differential equations, see Section II.2.B), the single relaxation process occurs as a discrete step in a log t plot only if $\tau_i \ll \tau_{i+1}$. Similar behavior will be found for any other form of temporal change of external conditions, listed in Section II.2.B. The resolution is restricted by the nature of the relaxation process itself, in contrast to resonance, where a separation of two processes (i.e., two neighboring resonance lines) can usually be effected by an improvement in experimental conditions. Problems of this kind are still more important for other molecular relaxation processes. As has been shown by Hiedemann and Spence (2), the form of relaxational response in the case of spectra with a continuous distribution of time constants is very insensitive to the distribution function (see also the discussion in Section II.2.D). Particularly, it is very difficult to distinguish a continuous relaxation spectrum from a discrete spectrum with several time constants which are of the same order of magnitude. Fortunately, this problem is not as severe in chemical relaxation, since chemical processes generally are of a discrete nature. Moreover, the pertinent mechanisms are usually known from the reactants present in the system, so that the problem consists merely of a separation of a known number of time constants, if these processes overlap at all in a narrow time range.

There are, of course, mathematical procedures by which a separation of two or more time constants is possible in principle. As an example let us consider two relaxation processes represented by

$$x = A_{\mathrm{I}} \exp(-t/\tau_{\mathrm{I}}) + A_{\mathrm{II}} \exp(-t/\tau_{\mathrm{II}}) \qquad \text{(II.1.37)}$$

where τ_{I} is slightly smaller than τ_{II}. Repeated differentiation with respect to t and a plot of the respective ratios of differential quotients

$$(d^n x/dt^n)/\{[d^{(n+1)}x/dt^{(n+1)}]\}$$

as a function of n will yield τ_{I} by extrapolation to large n, since the quotient $(\tau_{\mathrm{I}}/\tau_{\mathrm{II}})^n$ will approach zero if n is sufficiently high.

It is obvious that the application of such mathematical procedures requires very accurate measurements; thus, time resolution is here again closely related to the accuracy and sensitivity of measurements. With the sensitivity of present methods, the above procedure in even optimal cases will require that $\tau_{\mathrm{II}} \gtrsim 2\tau_{\mathrm{I}}$. In such a case, the original relaxation curve may not yet exhibit discrete structure.

A further important factor in the analysis of chemical relaxation is the dependence of the relaxation times on the concentrations of the different reaction partners. If, in a coupled-reaction system, only one step is of higher molecularity, all relaxation times may become concentration dependent. If they all can be measured as a function of concentration, the information for an unequivocal evaluation of the rate constants may be quite complete. The study of the concentration dependence is especially important in the first identification of the relaxation times of unknown mechanisms. As Equation (II.1.7) shows, both rate constants of a single-step transformation can be determined if the reaction is of higher than first order and if the concentration dependence can be studied. Further valuable information may be obtained from measurements at different temperatures, changes of solvent, etc. For stationary methods such as sound absorption, it is important to determine the relaxation times directly from the frequency dependence. Otherwise, it will be difficult to determine any multiple-step reaction mechanism, since the information will not be sufficient.

The methods should be arranged so that they yield the necessary information for a clear analysis of the reaction mechanism and determination of the rate constants. The time or frequency range should include several orders of magnitude, and the sensitivity should allow measurements at concentrations as low as possible.

References

1. J. Meixner, *Kolloid-Z.*, **134**, 3 (1953).
2. E. Hiedemann and R. D. Spence, *Z. Physik*, **133**, 109 (1952).
3. R. O. Davies and J. Lamb, *Proc. Phys. Soc. (London)*, **B69**, 293 (1956).

4. M. Planck, *Vorlesungen über Thermodynamik*, 10th ed. (by M. von Laue), W. de Gruyter & Co , Berlin, 1954, pp. 266 ff.
5. C. Wagner, in *Thermodynamik* by W. Schottky, H. Ulich, and C. Wagner, Springer-Verlag, Berlin, 1929.
6. R. Schlögl, *Z. physik. Chem. N.F.*, **9**, 259 (1956).
7. K Bergmann, M. Eigen and L. De Maeyer, *Z. physik. Chem. N. F.* (in preparation).
8. E. A. Guggenheim, *Thermodynamics*, 4th ed., North-Holland Publishing Co., Amsterdam, 1959, Chapter 11.
9. H. S. Frank, *J Chem. Phys.*, **23**, 2023 (1955).
10. Th. de Donder, *Affinity*, Stanford University Press, 1936.
11. W. Jost, *Z. Naturforsch.*, **20**, 159 (1947); *Z. physik. Chem.*, **195**, 317 (1950).
12. S. H. Bauer, *J. Chem. Phys.*, **21**, 1888 (1953).
13. S. R. de Groot, *Thermodynamics of Irreversible Processes*, North-Holland Publishing Co., Amsterdam, 1952.
14. J. Prigogine, *Etude Thermodynamique des Processus Irréversibles*, Dunod, Paris, and Desoer, Liège, 1947.
15. M. Eigen, *Chemische Relaxation*, Steinkopf, (in preparation).
16. M. Eigen, *Z. Electrochem.*, **64**, 115 (1960).
17. M. Eigen, *Discussions Faraday Soc.*, **24**, 25 (1957).
18. M. Eigen and K. Tamm, *Z. Elektrochem.*, **66**, 93 (1962).
19. G. Czerlinski and M. Eigen, *Z. Elektrochem.*, **63**, 652 (1959).
20. H. Diebler and M. Eigen, *Z. physik. Chem., N.F.*, **20**, 299 (1959).
21. H. Diebler, M. Eigen, and G. G. Hammes, *Z. Naturforsch.*, **15b**, 554 (1960).
22. M. Eigen, W. Kruse, G. Maass and L. De Maeyer, *Progresses of Reaction Kinetics*, G. Porter (Ed.) (in press).
23. W. Maier, *Z. Elektrochem.*, **64**, 132, (1960).
24. R. A. Alberty and G. G. Hammes, *Z. Elektrochem.*, **64**, 124 (1960).
25. M. Eigen and G. G. Hammes [to be published in *Advances in Enzymology* **25**].
26. J. Meixner, *Ann. Phys.*, **43**, 470 (1943).
27. S. H. Bauer and M. R. Gustavson, *Discussions Faraday Soc.*, **No. 17**, 69 (1959).
28. G. Sessler, H. O. Kneser, (Göttingen) and H. Bauer, Papers presented at the third International Congress on Acoustics, Stuttgart, 1959.

2. Principal Procedures

A. TRANSIENT AND FORCED SOLUTIONS OF RELAXATION EQUATIONS

In Equation (II.1.19) the (measurable) dependent variables $x_i(t)$ and the independent variables $\bar{x}_i(t)$ occur separately. By removing the right-hand term, a homogeneous system of linear first-order differential equations with constant coefficients remains. The solution of this homogeneous equation system, called the transient solution, can be expressed as a sum of n linearly independent solutions of the homogeneous system, each multiplied by an integration constant A_{ik}, see Equation (II.1.21):

$$x_i(t)_{\text{trans}} = \sum_{k=1}^{k=n} A_{ik} e^{-t/\tau_k} \qquad \text{(II.2.1)}$$

The function that specifies the independent variables $\bar{x}_i = f(t)$ is called the forcing function.

Any particular solution of the complete system of nonhomogeneous equations (II.1.19) is called the forced solution. The complete solution of the system is the sum of the transient solution and the forced solution. The n constants A_{ik} may be found after n initial conditions for the dependent variables x_i have been specified, and an expression for the forced solution has been determined. Actually, we have supposed that the reaction mechanism is known, or at least that adequate assumptions have been made to allow one to write a sufficient number of equations for the different A_{ik} in terms of rate and equilibrium constants. With these equations, then, the rate constants may be calculated, provided the relaxation times are known.

In order to determine the relaxation times of the system, it is necessary to have measured a number of concentration variables or related properties. These variables will be called the measured parameters. In view of Equation (II.2.1), one single measured parameter is sufficient to obtain all the relaxation times of the system. In principle, the nature of the forcing function is unimportant, as long as it is possible to find a particular (forced) solution for the equation system. In practice, there are some types of forcing functions that allow a relatively easy determination of the relaxation times.

The transient solutions depend upon the initial conditions of the dependent variables and also upon the forcing function. They effectively disappear for sufficiently long times. The forced solutions depend upon the differential equation system and upon the forcing function, but not upon initial conditions.

There are two different approaches for an experimental study of relaxation behavior. The first is based upon the determination of the transient behavior. There is a special class of forcing functions that are most appropriate for such determinations (impulse forcing functions). The second type of experiment determines the steady-state forced behavior that is described only by the forced solution. Periodic forcing functions are most useful for such methods.

B. MEASUREMENT OF TRANSIENT RESPONSE

The form of the transient solution for a given system of linear differential equations is determined uniquely by the dependent variables [Equation (II.2.1)]. This form always includes a number of integration constants (which are equal to the number of linearly independent first-order equations). In any particular case, the values of these constants depend upon

the forcing function and upon initial conditions for the dependent variables. When these constants have been properly determined, the transient solution describes the variation of the dependent variables during the "period of transition" required for them to change from their initial values to the steady-state forced values.

For our purposes the initial conditions imposed on the dependent variables will be quite simple. The chemical system to be studied will generally be assumed in equilibrium for $t < t_0$, where t_0 is the time at which the forcing disturbance is applied. Our dependent variables x_i (deviations from a reference state) will therefore be constants, and their time derivatives vanish for $t < t_0$.

There are a number of specific forcing functions which either are physically easy to realize, or have properties making the mathematical derivation of the integration constants simple. The functions allow the experimental determination of relaxation times by simple inspection of the complete solution in the transient range.

Rectangular Step Function. Theoretically (not always experimentally), the most simple forcing function is the rectangular step. The independent variables then have the form

$$\begin{aligned} \bar{x}_i &= 0 && \text{for } t < 0 \\ \bar{x}_i &= \text{const.} = \bar{x}_{i_0} && \text{for } t \geqslant 0 \end{aligned} \qquad \text{(II.2.2)}$$

The initial condition is

$$x_i = 0 \qquad \text{for } t < 0 \qquad \text{(II.2.3)}$$

In the more general case of a multiple-step system, the variables x_i are to be replaced by the normal variables y_i as introduced in Section II.1.C. The initial conditions remain the same for the y_i (or $\bar{y}_i$, respectively), which will be used directly in the following. The complete solution of the differential equation

$$dy_i/dt + y_i/\tau_i = \bar{y}_i/\tau_i$$

[*cf.* Equation (II.1.20)] under the above conditions reads

$$y_i(t) = \bar{y}_i(1 - e^{-t/\tau_i}) \qquad \text{(II.2.4)}$$

as can be easily verified. This behavior, i.e., the one-step transient concentration change for a rectangular step change of external conditions, is represented in Figure II.1(a).

Similarly, a fast disturbance can most easily be generated by suddenly removing an existing constant perturbation

$$\begin{aligned} \bar{y}_i &= y_i = \bar{y}_{i_0}; \quad \dot{y}_i = 0 && \text{for } t < 0 \\ \bar{y}_i &= 0 && \text{for } t \geqslant 0 \end{aligned} \qquad \text{(II.2.5)}$$

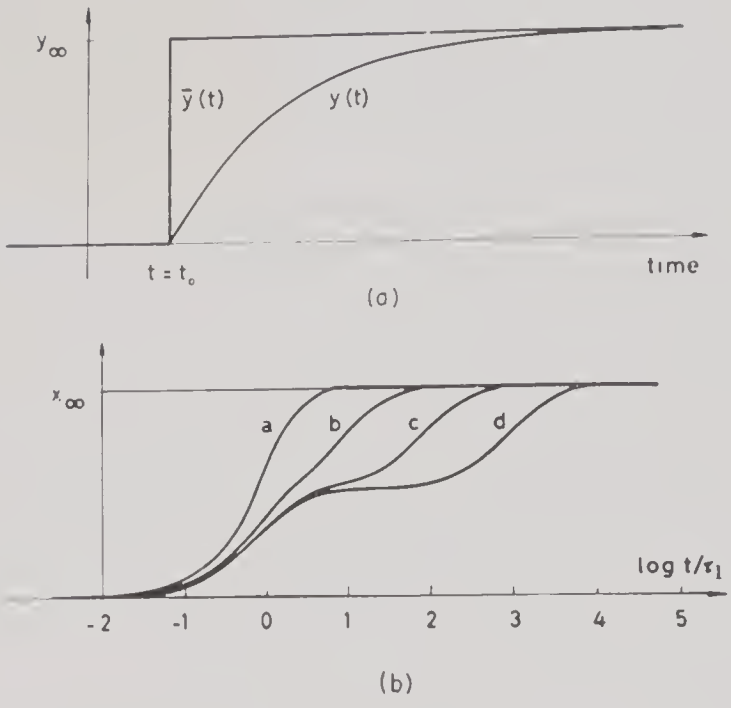

Fig. II.1. Relaxational response for a rectangular step-forcing function. (a) One-step mechanism (linear time base). (b) Two-step mechanism (logarithmic time base) for different relaxation times τ_{II} at fixed τ_I (a: $\tau_{II} = \tau_I$; b: $\tau_{II} = 10\tau_I$; c: $\tau_{II} = 100\ \tau_I$; d: $\tau_{II} = 1000\tau_I$).

The solution is

$$y_i = \bar{y}_{i_0} e^{-t/\tau_i} \tag{II.2.6}$$

We can use relation (II.1.21) to express the solution (II.2.4) for a multiple-step system in terms of the actual concentration variables x_i:

$$x_i(t) = \sum_k m'_{ik} \bar{y}_k (1 - e^{-t/\tau_k}) \tag{II.2.7}$$

or

$$\begin{aligned} x_i(t) &= \sum_k m'_{ik} \sum_j m_{kj} \bar{x}_j (1 - e^{-t/\tau_k}) \\ &= \sum_k A_{ik} (1 - e^{-t/\tau_k}) \end{aligned} \tag{II.2.8}$$

with

$$A_{ik} = m'_{ik} \sum_j m_{kj} \bar{x}_j \tag{II.2.9}$$

If the various τ_k's differ sufficiently, a log t plot of $x_i(t)$ yields a number of separated steps, as shown in Figure II.1(b). Experimentally, this course could be directly recorded using a logarithmic sweep on an oscillograph. It yields a quick detection of the whole relaxation spectrum, but, of course, it is not as accurate as a measurement with linear sweep. The kinetic analysis does not usually require the knowledge of the A_{ik} values,

which can be measured from the height of the different steps. These A_{ik} values are given solely by equilibrium parameters, since they are representative of the normal modes of concentration at equilibrium. Only the analysis of these values in terms of parameters of the actual reaction steps requires the application of the matrices of transformation.

In the following discussion of other forcing functions, we shall focus our interest on the temporal behavior (τ_i) only. We shall therefore express this behavior in terms of the variables y_i, which can easily be transformed to the variables x_i, as shown above.

Step Function with Linear Increase. In practical cases, a step-forcing function will have a finite rise time. When the observed relaxation times are long with respect to this rise time, expressions (II. 2.4) or (II. 2.6), respectively, may still be used. In other cases, the finite rise time has to be taken into account. When the forcing function increases linearly with time in the range $0 \leqslant t \leqslant t_1$, and then remains constant, the expression (II. 2.11) may be derived, with initial conditions (II. 2.10):

$$\begin{aligned} &\bar{y}_i = 0 \qquad \text{for } t < 0; \qquad \dot{y}_i = 0 \qquad \text{for } t < 0 \\ &\bar{y}_i = \bar{y}_{i\infty}(t/t_1) \qquad \text{for } 0 \leqslant t \leqslant t_1 \\ &\bar{y}_i = \bar{y}_{i\infty} \qquad \text{for } t_1 \leqslant t \end{aligned} \tag{II.2.10}$$

$$y_i = \left[1 - \frac{\exp(t/\tau_i) - 1}{t/\tau_i} \cdot \exp(-t/\tau_i)\right](t/t_1)\bar{y}_{i\infty} \qquad \text{for } 0 \leqslant t \leqslant t_1$$

$$y_i = \left[1 - \frac{\exp(t_1/\tau_i) - 1}{t_1/\tau_i} \exp(-t/\tau_i)\right]\bar{y}_{i\infty} \qquad \text{for } t_1 \leqslant t \tag{II.2.11}$$

This behavior is represented in Figure II.2.

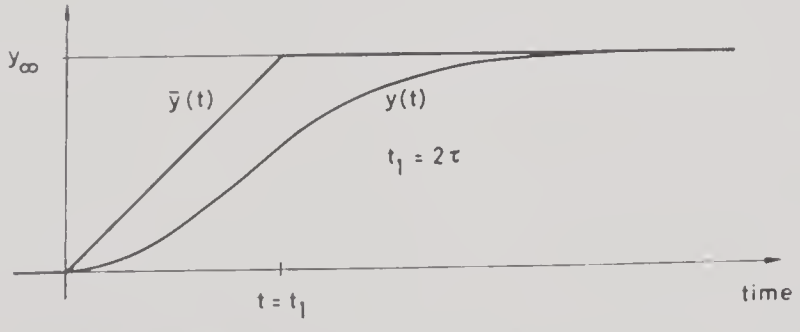

Fig. II.2. Relaxational response for a step-forcing function with linear increase.

Step Function with Exponential Increase or Decrease. As will be seen in Section III, it is easy to realize a step function of the following form:

$$\bar{y}_i = \bar{y}_{i\infty}(1 - e^{-t/\tau_s}) \qquad y_{t=0} = 0 \tag{II.2.12}$$

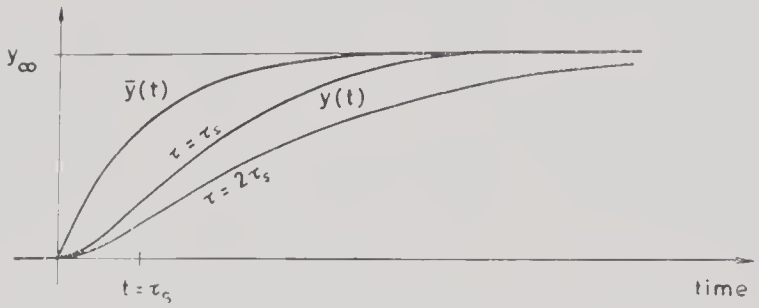

Fig. II.3. Relaxational response for a step-forcing function with exponential increase.

Then we obtain (*cf.* Figure II.3, for different τ_i at given τ_s)

$$y_i = [1 + \frac{\tau_s}{\tau_i - \tau_s} e^{-t/\tau_s} - \frac{\tau_i}{\tau_i - \tau_s} e^{-t/\tau_i}]\bar{y}_{i\infty} \tag{II.2.13}$$

$$y_i = [1 - (1 + t/\tau)e^{-t/\tau}]\bar{y}_{i\infty} \qquad \text{for } \tau_i = \tau_s = \tau$$

or, correspondingly, for the exponential decrease,

$$\begin{aligned} \bar{y}_i &= y_i = \bar{y}_{i_0} && \text{for } t < 0 \\ \bar{y}_i &= \bar{y}_{i_0} e^{-t/\tau_s} && \text{for } t \geqslant 0 \end{aligned} \tag{II.2.14}$$

$$y_i = [1/(\tau_i - \tau_s)][\tau_i e^{-t/\tau_i} - \tau_s e^{-t/\tau_s}]\bar{y}_{i_0}$$

$$y_i = \bar{y}_{i_0}(1 + t/\tau)e^{-t/\tau} \qquad \text{for } \tau_i = \tau_s = \tau \tag{II.2.15}$$

Rectangular Pulse. A rectangular pulse function with a duration Θ may be described by

$$\begin{aligned} \bar{y}_i &= 0 && \text{for } t < 0 \text{ and } t > \Theta \\ \bar{y}_i &= y_{iR} && \text{for } 0 \leqslant t \leqslant \Theta \end{aligned} \tag{II.2.16}$$

In the region $0 \leqslant t \leqslant \Theta$, the expression for y_i is the same as for the rectangular step function (II.2.4),

$$y_i = \bar{y}_{iR}(1 - e^{-t/\tau_i}) \qquad \text{for } 0 \leqslant t \leqslant \Theta \tag{II.2.17}$$

For $t > \Theta$, an expression may be found using the decreasing step function (II.2.5) with different initial conditions.

$$\begin{aligned} y_i &= \bar{y}_{iR}(1 - e^{-\Theta/\tau_i}) \\ & && \text{for } t = \Theta \\ \dot{y}_i &= \bar{y}_{iR}(1/\tau_i)e^{-\Theta/\tau_i} \end{aligned} \tag{II.2.18}$$

The solution is

$$y_i = \bar{y}_{iR}[e^{-(t-\Theta)/\tau_i} - e^{-t/\tau_i}] \qquad \text{for } t > \Theta \tag{II.2.19}$$

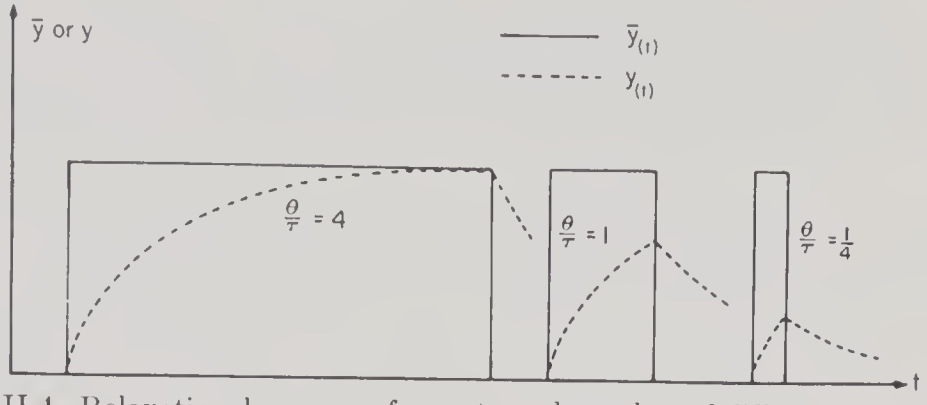

Fig. II.4. Relaxational response for rectangular pulses of different duration Θ.

For a determination of τ_i, it may be sufficient to determine the ratio of $y_{i_{max}}$ to $\bar{y}_{iR}$ as a function of impulse duration Θ. From Equation (II.2.18) this ratio is seen to be

$$y_{i_{max}}/\bar{y}_{iR} = y_{i(t=\theta)}/\bar{y}_{iR} = (1 - e^{-\theta/\tau_i}) \qquad \text{(II.2.20)}$$

An example is shown in Figure II.4 for a system with a single relaxation time. As may be seen, the maximum value, which y_i can reach, decreases with decreasing Θ. At the same time the center of this maximum is shifted to the right. This is in principle the same behavior as that found for periodical solutions (compare below), i.e., amplitude dispersion and phase shift.

Damped Harmonic Oscillation. The transient response for a damped harmonic oscillation-forcing function is of interest because such a function is easily realized experimentally (*cf.* Section III). When the damping constant b has been properly chosen, a damped harmonic oscillation represents a good approximation for a short single pulse. With

$$y_i = \bar{y}_i = 0; \qquad \text{for } t < 0$$

and (II.2.21)

$$\bar{y}_i = A_i e^{-bt} \sin \omega t \qquad \text{for } t \geqslant 0$$

the change of the concentration variable y_i is given by

$$y_i = A_i \{e^{-bt}/[(1 - b\tau_i)^2 + \omega^2\tau_i^2]^{1/2}\} \sin(\omega t - \varphi_i) + (\sin \varphi_i)\, e^{-(1-b\tau_i)\, t/\tau} \qquad \text{(II.2.22)}$$

with

$$\tan \varphi_i = \omega\tau_i/(1 - b\tau_i) \qquad \text{and} \qquad \sin \varphi_i = \{\omega\tau_i/[(1 - b\tau_i)^2 + \omega^2\tau_i^2]^{1/2}\} \qquad \text{(II.2.23)}$$

This behavior is shown in Figure II.5. The relaxation behavior can be measured by recording the maximum values $y_{t_{max}}$, which decrease with increasing frequencies (compare the behavior at periodic perturbation).

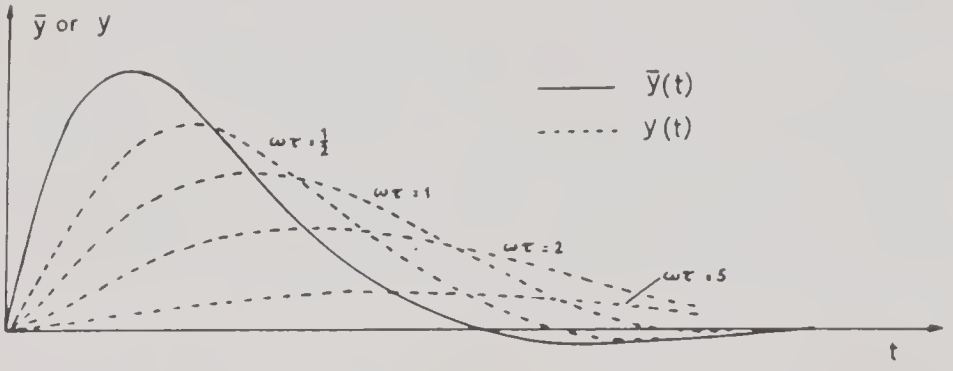

Fig. II.5. Relaxational response for a strongly damped harmonic forcing function.

For the aperiodic case with

$$\bar{y}_i = A_i t e^{-bt} \qquad \text{for } t \geqslant 0 \tag{II.2.24}$$

one obtains

$$y_i = A_i[e^{-bt}/(1 - bt)^2]\{t(1 - b\tau_i) - \tau_i[1 - e^{-t/\tau_i(1 - b\tau_i)}]\} \tag{II.2.25}$$

General Forcing Function. The above five examples represent special solutions of the relaxation equation (II. 1.20), which can be experimentally realized with relative ease [*cf.* refs. (1–3)]. In principle, any forcing function $f(t)$ can be inserted:

$$dy_i/dt + y_i/\tau_i = f_i(t)/\tau_i \tag{II.2.26}$$

yielding the general solution

$$y_i(t) = [\exp(-t/\tau_i)/\tau_i] \int_0^t \exp(\Theta/\tau_i) f(\Theta) d\Theta \tag{II.2.27}$$

under the condition $y_i = 0$ for $t = 0$. It is a general property of this solution that, for $f_i(t \to \infty) \equiv$ const, $y_i(t \to \infty)$ reaches the same (constant) value [for details see ref. (4)].

The transient methods require a direct observation of the relaxation response as a function of time. In most cases this observation is made in a single experiment, where the response is followed over the whole time range of interest. For very rapid processes, this requires a relatively large frequency bandwidth for the recording equipment (*cf.* Section III). As a measure of concentration change, any property of the system that can be followed instantaneously may be utilized. Electric conductivity, dielectric constant, or other properties, which can be easily converted to electric quantities (e.g., optical properties such as light transmission, fluorescence emission, refraction, optical rotation, etc.), prove especially useful.

For accurate measurements, it is advisable to use differential methods in order to distinguish between chemical relaxation processes and other physical effects following a change in external parameter.

C. MEASUREMENT OF FORCED RESPONSE (STATIONARY METHODS)

In contrast to the transient methods, which depend upon the complete solution of the differential equations (including initial conditions), the stationary methods require only the particular (forced) solution, for which the forcing function is decisive. If the forcing function can be written as a complex exponential of the form (e.g., for harmonic oscillations)

$$\bar{y}(t) = Ae^{pt} \tag{II.2.28}$$

the stationary relation between y and $\bar{y}$ can be expressed simply by

$$y(t) = \mathfrak{S}\bar{y}(t) \tag{II.2.29}$$

where $\mathfrak{S}$ represents a time-independent function which we shall call the transfer function. The transfer function contains all necessary information for the determination of the relaxation times.

Relation (II.2.29) can be easily verified in the following way: If the forcing function is represented by a harmonic oscillation

$$\bar{y}_i = Ae^{j\omega t} \tag{II.2.30}$$

(with $\omega = 2\pi\nu$, ν = frequency of oscillation, and A a real amplitude factor), the forced solution y_i must also be harmonic, i.e., y_i will also oscillate with the same frequency:

$$y_i = Be^{j\omega t} \tag{II.2.31}$$

The pre-exponential factor B can be complex, and then includes the description of a phase shift between $\bar{y}_i$ and y_i. Thus the relaxation equation (II.1.20)

$$\tau_i(dy_i/dt) + y_i = \bar{y}_i \tag{II.2.32}$$

with $dy_i/dt = j\omega y_i$ reads

$$j\omega\tau_i y_i + y_i = \bar{y}_i \tag{II.2.33}$$

or

$$y_i = \bar{y}_i/(1 + j\omega\tau_i) = \mathfrak{S}\bar{y}_i \tag{II.2.34}$$

More rigorously, the forced solution for any forcing function $\bar{y}(t)$ can be obtained from solution (II.2.27)†

† If $y_i \neq 0$ at $t = 0$, the complete solution reads

$$y_i(t) = e^{-F}[y_i(\vartheta) + (1/\tau_i)\int_{\vartheta}^{t} e^{F} f(\Theta)d\Theta]$$

with $F = (t - \vartheta)/\tau_i$, where $y_i(\vartheta)$ is an adjustable constant, i.e., the value of y at $t = \vartheta$. For the present applications, this value is fixed to be 0 for $\vartheta = 0$. For the stationary solution this term is unimportant because it decays with exp $(-t/\tau_i)$ (transient term).

$$y_i(t) = \frac{\exp(-t/\tau_i)}{\tau_i} \int_0^t \exp(t/\tau_i) \cdot f(\Theta)\, d\Theta$$

by extrapolating to large t ($t \gg \tau_i$), since transient terms will then have decayed.

For instance, inserting $\bar{y}_i = f(\Theta) = A \exp(j\omega t)$ yields

$$\begin{aligned} y_i(t) &= [\exp(-t/\tau_i)/\tau_i]\, [A\, \tau_i/(1 + j\omega\tau_i)]\, \{\exp[(1 + j\omega\tau_i)\, t/\tau_i] - 1\} \\ &= [A \exp(j\omega t) - A \exp(-t/\tau_i)]/(1 + j\omega\tau_i) \end{aligned} \tag{II.2.35}$$

which, for $t \gg \tau_i$, reduces to

$$y_i(t) = [A \exp(j\omega t)]/(1 + j\omega\tau_i) = \bar{y}_i(t)/(1 + j\omega\tau_i) \tag{II.2.36}$$

A similar treatment is possible for any other periodic function which can be represented by a Fourier spectrum of frequency terms; e.g., $\bar{y} = \sum_k F_k e^{j\omega_k t}$. The relation between y and $\bar{y}$ is then not simply given by a factor $\mathfrak{S}$, but every term of the sum will be multiplied by its individual frequency factor $1/(1 + j\omega_k\tau)$. This behavior can be expressed by use of an operator S instead of $\mathfrak{S}$. S is inversely related to the differential operator $(1 + \tau d/dt)$, which, applied to y, yields Equation (II.1.20):

$$(1 + \tau d/dt)y = \bar{y}.$$

If we make the following *formal* expansion:

$$y = \bar{y}/(1 + \tau d/dt) = [1 - \tau(d/dt) + \tau^2(d/dt)^2 - \tau^3(d/dt)^3 + \ldots]\bar{y}$$

where the operator is now applied to $\bar{y}$, we obtain for $\bar{y} = \sum_k F_k \exp(j\omega_k t)$

$$\begin{aligned} y &= \sum_k F_k[1 - j\omega_k\tau + (j\omega_k\tau)^2 - (j\omega_k\tau)^3 + \ldots.] \exp(j\omega_k t) \\ &= \sum_k [F_k \exp(j\omega_k t)]/(1 + j\omega_k\tau) \end{aligned}$$

which is the correct solution. However, with this treatment, we have only introduced a formalism (which generally has to be handled with care). Its justification in the above case can be given by a Laplace transformation (5), but it is mathematically quite complicated. The use of operators in the above sense is quite common in textbooks dealing with the theory of electrical networks, which, in a formal sense, have much in common with the phenomena discussed in this chapter.

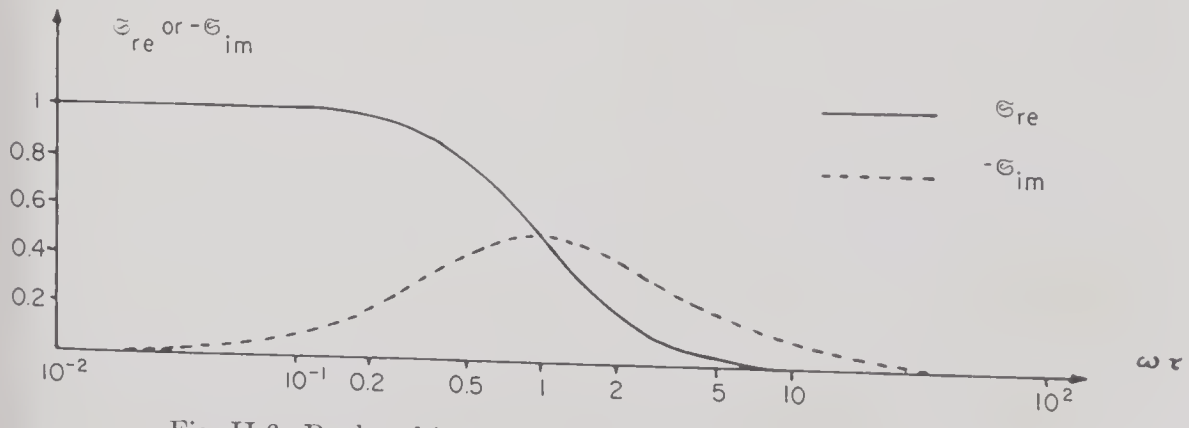

Fig. II.6. Real and imaginary part of the transfer function $\mathfrak{S}$.

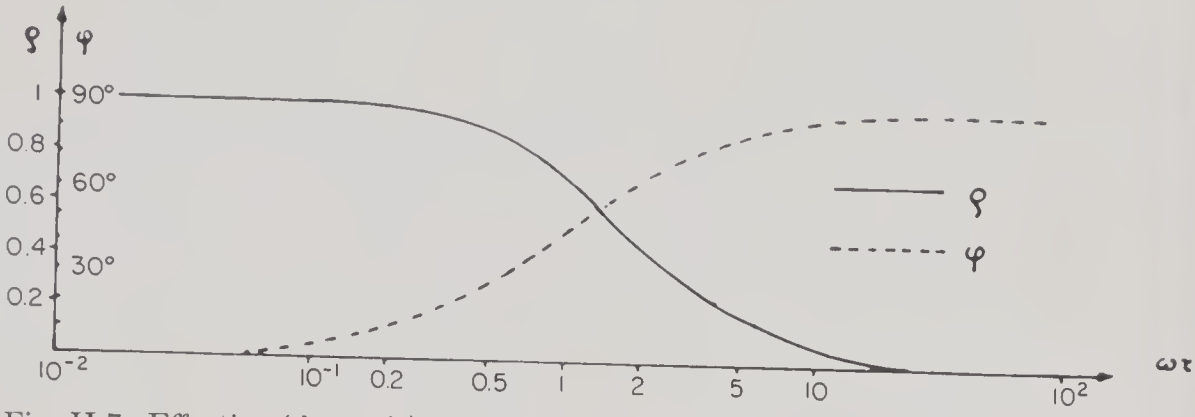

Fig. II.7. Effective (dynamic) amplitude ratio ρ and phase angle φ of stationary relaxation behavior.

The complex transfer function $\mathfrak{S}_i = 1/(1 + j\omega\tau_i)$ can be written in the form

$$\mathfrak{S} = \mathfrak{S}_{re} + j\mathfrak{S}_{im}$$

$$\text{with } \mathfrak{S}_{re} = 1/(1 + \omega^2\tau^2) \quad \text{and} \quad \mathfrak{S}_{im} = -\omega\tau/(1 + \omega^2\tau^2) \tag{II.2.37}$$

The terms $\mathfrak{S}_{re}$ and $\mathfrak{S}_{im}$, as a function of frequency, are shown in Figure II.6. They are directly related to the frequency dependence of measurable quantities such as sound velocity and absorption coefficient (per wavelength), or dielectric constant and energy loss (*cf.* below and Section II.3.C). By using some well-known trigonometric relationships, we may also express Equation (II.2.37) in the form

$$\mathfrak{S} = \rho\,(\cos\varphi - j\sin\varphi) = \rho\, e^{-j\varphi} \tag{II.2.38}$$

Then ρ and φ are given by

$$\rho = (\mathfrak{S}_{re}^2 + \mathfrak{S}_{im}^2)^{1/2} = (1 + \omega^2\tau^2)^{-1/2} \tag{II.2.39}$$

$$\cos\varphi = 1/(1 + \omega^2\tau^2)^{1/2} \qquad \sin\varphi = \omega\tau/(1 + \omega^2\tau^2)^{1/2}$$

$$\tan\varphi = -\mathfrak{S}_{im}/\mathfrak{S}_{re} = \omega\tau \text{ (}cf.\text{ Figure II.7).}$$

With $\mathfrak{S}$ according to Equation (II.2.38) and $\bar{y}_i = A\exp(j\omega t)$, y_i can be written

$$y_i = \mathfrak{S}\bar{y}_i = [A\exp j(\omega t - \varphi_i)]/(1 + \omega^2\tau_i^2)^{1/2} \tag{II.2.40}$$

The physical meaning is that y_i lags behind $\bar{y}_i$ with a phase angle φ_i that will increase with increasing frequency. It reaches 45° for $\nu = 1/2\pi\tau_i$ (i.e., $\omega\tau_i = 1$), but never exceeds 90° ($\tan\varphi \to \infty$). At the same time, the amplitude of y_i—in contrast to the constant amplitude A of the forcing function—will decrease to zero because of the factor $(1 + \omega^2\tau_i^2)^{-1/2}$. In other words, at low frequencies ($\omega \ll 1/\tau_i$), y_i will be almost completely in equilibrium with the oscillating external conditions ($y_i = \bar{y}_i$), whereas

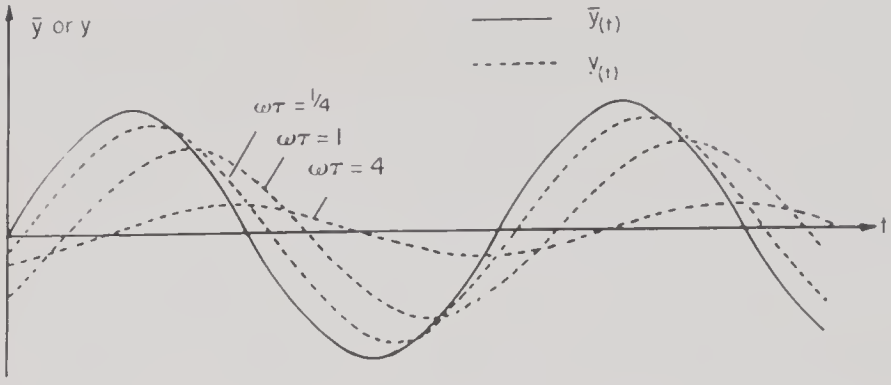

Fig. II.8. Relaxational response for a periodic forcing function.

at high frequencies ($\omega \gg 1/\tau_i$), y_i will not be able to follow the rapid oscillation but finally becomes constant. This behavior is represented in Figure II.8. Since the above considerations apply to the normal variables y_i, the measurable relaxation spectrum can be expressed in additive terms; e.g.,

$$x_i = \sum_k m'_{ik}\, \mathfrak{S}_k \bar{y}_k = \sum_k m'_{ik}\, \bar{y}_k\, [(1 - j\omega\tau_k)/(1 + \omega^2\tau_k{}^2)]$$

This treatment holds for a discrete chemical relaxation spectrum, supposing that physical equilibrium (spatial and energetic distribution) is always established (*cf.* Section II.3.D). Two general methods follow from the above considerations of stationary solutions.

(1) One method is concerned with the real part of the transfer function $\mathfrak{S}_{re} = 1/(1 + \omega^2\tau^2)$ or its square root "ρ." Plots of these functions against ω are shown in Figure II.6. For $\omega = 1/\tau$, the quantities $\mathfrak{S}_{re}$ and ρ amount to 1/2 and $(1/2)^{1/2}$ respectively. As mentioned earlier, some measurable quantities are directly related to the real part of the ratio of the instantaneous values $\mathfrak{S}_{re}$ or to the ratio of effective amplitudes ρ of concentration parameters $\bar{y}_i$ and y_i, or of two variables to which $\bar{y}_i$ and y_i are related, such as pressure and volume or electric field density and displacement. A readily measurable quantity of this kind is the sound velocity (*cf.* Section II.3.E), which, for a relaxing system, will show a frequency dependence according to $\mathfrak{S}_{re}$. This frequency dependence (in analogy to the corresponding optical case) is called sound dispersion. Accordingly, we shall call the whole group of methods utilizing the frequency behavior of $\mathfrak{S}_{re}$ "dispersion methods."

(2) The other group of methods is related to the imaginary part $\mathfrak{S}_{im}$: $-\omega\tau/(1 + \omega^2\tau^2)$. As will also be shown in Section II.3.E, this imaginary part is representative of energy loss (per period of oscillation), owing to relaxation. Any phase shift between two conjugate variables (as a consequence of a phase shift between $\bar{y}_i$ and y_i) will cause such a loss of energy. According to the form of $\mathfrak{S}_{im}$, the energy loss per period will show a maxi-

mum at $\omega = 1/\tau_i$, which can be directly measured by suitable methods (*cf.* Section III.2). Sound absorption methods, especially, have found wide application. Since the basis for all methods utilizing $\mathfrak{S}_{im}$ is the measurement of energy absorption, we shall call this group "absorption methods."

Steady-state response measurements can be carried out over a period of time, which is long compared to the reciprocal frequency of the forcing function. Therefore, very sensitive methods with greatly reduced bandwidth may be used. However, the total energy input to the system must be small for the total duration of the experiment, or else heating and nonlinear effects will occur. The resulting equilibrium displacements are, consequently, also very small. In sound absorption and dispersion they are, in fact, so small that, with present methods, it is quite difficult to detect directly the periodic concentration changes.

References

1. M. Eigen, *Discussions Faraday Soc.*, **No. 17**, 194 (1954).
2. M. Eigen and J. Schoen, *Z. Elektrochem.*, **59**, 483 (1955).
3. L. de Maeyer, *Z. Elektrochem.*, **64**, 65 (1960).
4. E. Kamke, *Differentialgleichungen*, 6th ed., Akad. Verlagsgesellschaft, Leipzig, 1959.
5. G. Doetsch, *Einführung in Theorie und Anwendung der Laplace Transformation*, Birkhäuser-Verlag, Basel, 1958.

3. Perturbation of Chemical Equilibrium (Thermodynamic Relations)

A. FORCING PARAMETERS

A classification of the different experimental techniques for a study of chemical relaxation may be made on the basis of the external (forcing) parameters, which are used for perturbation of the initial equilibrium. We shall discuss the application of (*1*) temperature, (*2*) pressure, and (*3*) electrical field density as forcing parameters. In principle, magnetic fields could also be used in order to disturb directly a chemical equilibrium between paramagnetic species (as far as they change their magnetic moments upon reaction). However, such applications, (which would refer to a vanishingly small effect) have not yet been reported and therefore will not be considered explicitly here. (The formal treatment is analogous to that given below for electric dipolar species.) On the other hand, there exist some other external means, by which a chemical equilibrium can be disturbed, such as electromagnetic or particle radiation, which will be considered at the end of Section III. 1.

In order to make any quantitative calculation, it is important to have defined the conditions under which the chemical change occurs. In cer-

tain cases, these thermodynamic conditions may be decisive even for the temporal course of equilibration as has been shown in Section II.1.B. We shall return to a discussion of these questions in Section II.3.C. The forcing parameter will usually affect not only the chemical equilibrium, but also physical properties of the system such as solvent structure (e.g., density, dipolar orientation, etc.). The dynamic relation between a forcing parameter and such properties may also be represented by a system of (linear) differential equations describing some mechanical or electrical relaxation processes. If these processes interfere with the chemical relaxation (for solutions, this may happen at times less than 10^{-9} sec.), an analysis might become rather difficult.

Furthermore, an instantaneous change in these properties may also complicate the relations for the relaxation of the chemical system. It is therefore important to define the chemical variables x_i and $\bar{x}_i$ or y_i and $\bar{y}_i$ respectively [*cf.* Equation (II.1.19 or 20)] in such a way that these complications are avoided.

In the following paragraphs we shall consider how a chemical equilibrium can be shifted by means of the above-mentioned forcing parameters.

B. THE ENFORCED CHANGE OF CONCENTRATION

For the following treatment, a knowledge of the fundamental thermodynamic functions and relations is supposed. By starting with the total differential of Planck's function $Y = -G/T$ (G = Gibbs free energy), which can be written as (1):

$$dY/R = (H/RT^2)\,dT - (V/RT)\,dP + (A/RT)d\xi \tag{II.3.1}$$

some general relations may be derived, which follow simply from cross-differential identities. [H is the enthalpy, A the affinity according to De Donder: $A = -\Sigma\nu_i\mu_i = -(\partial G/\partial\xi)_{TP} \equiv -\Delta G$; ξ is the extent of reaction with the definition $n_i = (n_i^0 + \nu_i\xi)$; n_i^0 is a constant initial mole number, all changes due to reaction being represented by ξ. The stoichiometric coefficients ν_i are negative for participants in the forward ($\rightarrow$) and positive for those in the reverse ($\leftarrow$) reactions. The other symbols have their obvious meanings (1,3) (see also list of symbols).]

At constant pressure we can write

$$[\partial(H/RT^2)/\partial\xi]_{T,P} = -[\partial(\Sigma\nu_i\mu_i/RT)/\partial T]_{P,\xi} = \Sigma\nu_i H_i/RT^2 \equiv \Delta H/RT^2 \tag{II.3.2}$$

where ΔH is the reaction enthalpy at given composition (H_i = partial molar enthalpy of species i).

Similarly, for constant temperature we have

$$[\partial(V/RT)/\partial\xi]_{T,P} = [\partial(\Sigma\nu_i\mu_i/RT)/\partial P]_{T,\xi} = (\Sigma\nu_i V_i)/RT = \Delta V/RT \quad \text{(II.3.3)}$$

Here ΔV is the (isothermal) volume of reaction (i.e., the difference of partial molar volumes V_i of products and reactants at given composition).

By using extended equations [see Equation (II.3.62)ff.] with inclusion of external field terms, analogous expressions may be derived for the dependence of chemical equilibria on electric or magnetic field density, e.g.,†

$$[\partial(\mathbf{D}^*/RT)/\partial\xi]_{T,P,\mathbf{E}} = -[\partial(\Sigma\nu_i\mu_i/RT)/\partial\mathbf{E}]_{T,P,\xi} = (\Sigma\nu_i\mathbf{D}^*_i)/RT = \Delta\mathbf{D}^*/RT \quad \text{(II.3.4)}$$

$\mathbf{D}^*$ is the conjugate variable to the electric field density $\mathbf{E}$, as introduced with Equation (II.3.62). We may call $\Delta\mathbf{D}^*$ the "polarization" of reaction, i.e., the difference of partial molar "polarizations" of products and reactants at given composition (though it differs from the common meaning of the term "polarization" in electrostatics by inclusion of a volume. For a more detailed discussion see Section II.1.B.)

We may note that the symbol Δ employed here generally has the meaning of an operator $(\partial/\partial\xi)$, which is related to constant intensive variables (see Section II.3.C).

Let us now consider the function $A/RT = (-\Sigma\nu_i\,\mu_i/RT)$, which we may write as a function of the extent of reaction ξ and two other general intensive variables Z_1 and Z_2, e.g., T,P or $T,P,\mathbf{E}$;

$$d(A/RT) = [\partial(A/RT)/\partial\xi]_{Z_1Z_2}\,d\xi + [\partial(A/RT)/\partial Z_1]_{\xi,Z_2}\,dZ_1 + [\partial(A/RT)/\partial Z_2]_{\xi,Z_1}\,dZ_2 \quad \text{(II.3.5)}$$

If we express A in terms of standard chemical potentials μ_i^0 and activities a_i with

$$\mu_i \equiv (\partial G/\partial n_i)_{T,P,nj\neq i} = \mu_i^0 + RT\ln a_i \quad \text{(II.3.6)}$$

we have

$$-A/RT = \Sigma\nu_i\,\mu_i^0/RT + \Sigma\nu_i \ln a_i \quad \text{(II.3.7)}$$

The condition of chemical equilibrium is defined as $A \equiv 0$, yielding

$$-\Sigma\nu_i\,\mu_i^0/RT = \Sigma\nu_i \ln \bar{a}_i \quad \text{(II.3.8)}$$

or

$$\prod_i (\bar{a}_i^{\nu_i}) \equiv K_0 \equiv \exp(-\Sigma\nu_i\mu_i^0/RT)$$

† For isothermal, isochoric systems, one may use the Massieu function $J = -F/T$ [F = Helmholtz free energy (*1*)] instead of the Planck function. Similar extended functions can be defined for systems with the electrical field density as independent variable [*cf.* ref. (1), p. 412, Equation II.05.8].

where K_0 is the equilibrium constant. The standard chemical potential does not depend upon the composition of the system, but is a function of the intensive variables $Z_1, Z_2, \ldots$ (e.g., T, P, etc.). (In solutions, μ_i^0 also depends on the nature of the solvent. The standard state is then defined as a hypothetical state of the pure compound having properties that result from an extrapolation of the partial molar properties in the given solvent to infinite dilution.)

From Equation (II.3.5) we obtain, for chemical equilibrium, where A is maintained at zero with $d(A/RT) = 0$:†

$$(\partial\xi/\partial Z_1)_{(A/RT)Z_2} = -\{[\partial(A/RT)/\partial Z_1]_{\xi,Z_2}/[\partial(A/RT)/\partial\xi]_{Z_1,Z_2}\} \quad \text{(II.3.9)}$$

In the denominator, the standard chemical potentials can be omitted if Z_1, Z_2 represent intensive variables. With $a_i = c_i f_i$, where c_i is a concentration variable expressed in a suitable normalized unit (see below) and f_i the corresponding activity coefficient, which is a function of c_i and the Z_i's, Equation (II.3.9) yields

$$\left(\frac{\partial\xi}{\partial Z_1}\right)_{Z_2,A} = -\frac{[(\partial\Sigma_i \nu_i\mu_i/RT)/\partial Z_1]_{\xi,Z_2}}{(\partial\Sigma_i \nu_i \ln c_i/\partial\xi)_{Z_1,Z_2} + (\partial\Sigma_i \nu_i \ln f_i)/\partial\xi_{Z_1,Z_2}} \quad \text{(II.3.10)}$$

or

$$(\partial\xi/\partial Z_1)_{Z_2,A} = -\Gamma^*[(\partial\Sigma\nu_i\mu_i/RT)/\partial Z_1]_{\xi,Z_2} \quad \text{(II.3.11)}$$

with

$$\Gamma^* = \Gamma/[1 + \Gamma(\partial\Sigma\nu_i \ln f_i/\partial\xi)_{Z_1,Z_2}]$$

$$\Gamma = [\partial\xi/(\partial\Sigma\nu_i \ln c_i)]_{Z_1,Z_2},$$

and $[(\partial\Sigma\nu_i\mu_i/RT)/\partial Z_1]_{\xi Z_2}$ according to Equations (II.3.2) to (II.3.4

For any practical application, it is important to choose an appropriate concentration variable. Correctly, the c_i and f_i would have to be expressed in mole fractions γ_i and mole fraction activity coefficients $f_{\gamma i}$ (see below). Certain other concentration variables, however, have practical advantages, especially when applied to solutions.

The extent of reaction ξ is related to the mole number n_i by $n_i = (n_i^0 + \nu_i\xi)$. For a closed system which does not exchange matter with its surroundings, the initial composition n_i^0 can be considered constant, and changes of composition because of reaction are expressed by ξ.

$$(d \ln n_i)_{\text{chem}} = (\nu_i/n_i)\, d\xi \quad \text{(II.3.12)}$$

This relation also holds for any concentration variable in which the mole numbers are normalized by constant factors, e.g., for mass concentrations (normalized by the constant mass of the whole system or a reference system such as solvent), or mole ratios r_i

†Near equilibrium the condition $d(A/RT) = 0$ is equivalent to $dA = 0$, since in $d(A/RT) = (dA/RT) - A(dT/RT^2)$ the second term vanishes because of $A = 0$.

(normalized by the mole number of a chemically indifferent solvent). For solutions, the molalities m_i, defined as number of moles per 1,000 g. of solvent, are very convenient units.

The mole fractions

$$\gamma_i = n_i/\Sigma_j n_j = (n_i^0 + \nu_i\xi)/[\Sigma_j(n_j^0 + \nu_j\xi)] \qquad \text{(II.3.13)}$$

are related to ξ in a more complicated manner since, for $\sum_j \nu_j \neq 0$, the total number of moles depends on ξ. Here we have

$$(d \ln \gamma_i)_{\text{chem}} = (\nu_i/n_i)d\xi - (\Sigma_j \nu_j/\Sigma_j n_j)\, d\xi \qquad \text{(II.3.14)}$$

In the case of solutions, the second term reduces to a small and usually negligible correction term, if the mole number of the solvent is large with respect to that of the chemically reacting solute, i.e., if $\Sigma_j n_j \approx n_{\text{solvent}} \gg n_i$. Then the Γ term in Equation (II.3.11) has the same form, regardless of whether mole fractions or molalities are used. If the correction term is important, it may be considered in the definition of f_i when c_i is expressed in molalities. This inclusion is justified since μ_i contains these terms as a sum of logarithms.

Some precaution is necessary if volume concentrations (e.g., molalities = number of moles per 1000 cm.^{3} of solution) are used. With

$$c_i = n_i/V = n_i(\rho/m) = (n_i^0 + \nu_i\xi)(\rho/m) \qquad \text{(II.3.15)}$$

(V = total volume, m = total mass, ρ = density of the system) no difficulties will occur if studies are made at a constant volume or density. If, however, volume changes have to be considered explicitly, we have to write (with n_i^0 = const)

$$\begin{aligned}(\partial\bar{c}_i/\nu_i)/\partial Z &= [(\partial c_i/\nu_i)/\partial\xi]_{\rho,Z}\,(\partial\xi/\partial Z) + [(\partial\, c_i/\nu_i)/\partial\rho]_{\xi,Z}(\partial\rho/Z) \\ &= (\rho/m)(\partial\xi/\partial Z) + (c_i/\nu_i)/(\partial \ln \rho/\partial Z) \qquad \text{(II.3.16)}\end{aligned}$$

Thus, Equation (II.3.11), if written in the form of Equation (II.3.16), will be modified by addition of a term which reads

$$\begin{aligned}&\text{for } Z = T \text{ and constant } P: && -[(\bar{c}_i/\nu_i)\,\alpha_P] \\ &\text{for } Z = P \text{ and constant } T: && +[(\bar{c}_i/\nu_i)\,\kappa_T] \qquad \text{(II.3.17)} \\ &\text{for } Z = \mathbf{E} \text{ and constant } P,T: && +[(\bar{c}_i/\nu_i)\,\lambda_{P,T}]\end{aligned}$$

where α_P denotes the coefficient of thermal expansion [$\alpha_P \equiv (1/V)(\partial V/\partial T)_P$], κ_T the isothermal compressibility [$\kappa_T \equiv -(1/V)(\partial V/\partial P)_T$], and $\lambda_{P,T}$ the coefficient of (isothermal and isobaric) electrostriction of the system [$\lambda_{P,T} = -(1/V)(\partial V/\partial \mathbf{E})_{P,T}$].

These additional terms, of course, are not related to chemical relaxation, because they affect the independent variables $\bar{c}_i$ as well as the dependent variables c_i in the same way. They only describe some mechanical consequences of changing external parameters. It is therefore advisable to adjust the definition of the concentration variables $\bar{x}_i$ and x_i or $\bar{y}_i$ and y_i, respectively (introduced in Section II.1), to this behavior by including the concentration change due to the terms (II.3.17) in the reference concentration c_i^0 [defined in Equation (II.1.2)]. This adjustment is allowed if the volume changes can be considered instantaneous as compared to chemical relaxation. The relaxational part

of thermodynamic functions (*cf.* Section II.3.C) then does not contain these terms (II.3.17).†

For a discussion of Equation (II.3.10) and its physical implications we may write this relation in a more convenient form. If $\bar{x}_i$ again denotes a small equilibrium shift of a general concentration variable (as introduced in Section II.1.A), the relation (II.3.10) can be expressed by three multiplicative terms.

$$[\bar{x}_i/\nu_i]_{Z_2} = \Gamma \left\{ [\partial \ln K_0/\Pi(f_i^{\nu_i})]/\partial Z_1 \right\}_{Z_2} \delta Z_1 \qquad \text{(II.3.18)}$$

(The introduction of K_0 implies a restriction to a consideration of intensive variables Z_i only.)

(1) δZ_1 represents the applied change of intensive variable, e.g., δT, δP, or $\delta \mathbf{E}$ under certain conditions (constant P or T, etc.). Its temporal course determines the form of the solution of the relaxation equation (forced or transient solution, see Section II.2).

(2) The second term corresponds to the (negative) fractional one in Equation (II.3.10) and describes the change of the function $K_0/\Pi(f_i^{\nu_i})$—which we call the equilibrium function—with the intensive variable Z_1 at constant Z_2. A finite change of the equilibrium function requires finite reaction quantities as introduced in Equations (II.3.2) to (II.3.4). If consideration of activity coefficients can be neglected ($\Pi(f_i^{\nu_i}) \to 1$ and $\Gamma\,(\partial \Sigma \nu_i \ln f_i/\partial \xi)_{Z_1,Z_2} \ll 1$) the equilibrium function is equal to the equilibrium constant, then we have:

$$\begin{aligned} (\partial \ln K_0/\partial T)_P &= \Delta H_0/RT^2 \\ (\partial \ln K_0/\partial P)_T &= -\Delta V_0/RT \\ (\partial \ln K_0/\partial \mathbf{E})_{P,T} &= \Delta \mathbf{D}_0^*/RT \end{aligned} \qquad \text{(II.3.19)}$$

If $(\partial \Pi(f_i^{\nu_i})/\partial Z_1)_{Z_2}$ is finite, although its dependence upon the extent of reaction can be neglected (e.g., for ionic reactions in solutions whose ionic strength is maintained by a reference electrolyte in excess concentration), the relations (II.3.19) formally remain valid. However, the equilibrium constants K_0 have to be replaced by the equilibrium functions $K_0/\Pi(f_i^{\nu_i})$ and ΔH_0, ΔV_0, $\Delta \mathbf{D}_0^*$ by ΔH, ΔV, and $\Delta \mathbf{D}^*$, which now relate to the (constant) condition of ionic strength. If ionic reactions are to be studied at concentrations where activity coefficients cannot be neglected, it is advisable to work under such conditions of defined constant ionic strength.

† The relaxation times calculated in Section II.1.A are related to constant T and P (maintenance of a constant equilibrium state). Any secondary volume change which might be of influence to the k values is negligible for small perturbations. (Since τ is a factor of the small quantity $(x - \bar{x})$, such changes of k or τ, respectively, lead to small perturbation terms of higher order.)

If, finally, the dependence of $\sum \nu_i \ln f_i$ on the extent of reaction cannot be neglected, the general factor

$$1/\{1 + \Gamma\,[(\partial \Sigma \nu_i \ln f_i)/\partial \xi]_{Z_1,Z_2}\} \tag{II.3.20}$$

enters into Equation (II.3.19) with ΔH, ΔV, and $\Delta \mathbf{D}^*$ instead of ΔH_0, ΔV_0, and $\Delta \mathbf{D}_0^*$. Its explicit form depends on the choice of the concentration variable (compare below).

(3) The factor Γ is independent of Z_i. It simply relates the change of concentration to the change of the equilibrium function. If we use molalities as concentration variables, we have with $m_i = n_i/1000$ g. solvent and $\xi_m = \xi/1000$ g. solvent,

$$\bar{x}_i = d\bar{m}_i = \nu_i d\bar{\xi}_m$$

(*cf.* Equation II.3.12), and

$$d \ln K_0/(\Pi f_i^{\nu_i}) = \sum \nu_i d \ln \bar{m}_i = [\sum (\nu_i^2/\bar{m}_i)]\, d\bar{\xi}_m$$

with the definition

$$\Gamma_m = d(\bar{m}_i/\nu_i)/d\sum(\nu_i \ln \bar{m}_i)$$

we obtain

$$\Gamma_m = 1/\sum \nu_i^2/\bar{m}_i \tag{II.3.21}$$

The index of Γ indicates the kind of concentration variable used. The ξ in Equation (II.3.20) then refers to the same concentration variable (i.e., $\xi = \xi_m$).

Similarly, other concentration variables can be inserted. If the use of mole fractions $\bar{\gamma}_i$ is required, one can readily derive, from Equation (II.3.14),

$$\Gamma_\gamma = (d\bar{\gamma}_i/\nu_i)/(d\textstyle\sum_i \nu_i \ln \bar{\gamma}_i) = [1 - (\bar{\gamma}_i/\nu_i)\sum_i \nu_i]/[\sum_i(\nu_i^2/\bar{\gamma}_i) - \sum_i \sum_j \nu_i \nu_j] \tag{II.3.22}$$

For $\bar{\gamma}_i \ll 1$ (i.e., γ solvent $\gg \bar{\gamma}_i$), Γ_γ reduces to

$$\Gamma_\gamma = 1/(\sum \nu_i^2/\bar{\gamma}_i) \tag{II.3.23}$$

If volume concentrations are used, one has to remember Equation (II.3.16). Thus, Γ_c occurs only in the first term, i.e., the term describing the change of $\bar{c}_i$, a result of chemical shift at constant density:

$$\Gamma_c = (\partial \bar{c}_i/\nu_i)/(\partial \sum \nu_i \ln \bar{c}_i)\rho = 1/(V\sum \nu_i^2/\bar{n}_i) = 1/(\sum \nu_i^2/\bar{c}_i) \tag{II.3.24}$$

Other more specific concentration parameters, such as degree of transformation or dissociation "α," will be considered below in a discussion of some examples. Such dimensionless parameters have certain advantages, e.g., they are characteristic of the progress of the transformation as is the "extent of reaction."

Let us consider some applications. The following two examples of simple one-step transformations have been discussed already with respect to their kinetics:

Example 1:

$$A \rightleftharpoons B \tag{II.3.25}$$

With $m_A = \alpha\, m_0$, $m_B = (1 - \alpha)\, m_0$, m_0 = over-all concentration $(m_A + m_B)$ = const, $f_A/f_B = 1$, $K_0' = \bar{\alpha}/(1 - \bar{\alpha}) = 1/K_0$, we obtain for $Z = T$,

$$(\partial \bar{m}_A/\partial T)_P = m_0(\partial \bar{\alpha}/\partial T)_P = -\, m_0\, \bar{\alpha}(1 - \bar{\alpha})\Delta H_0/RT^2 \tag{II.3.26}$$

with $\Gamma_m = m_0\, \Gamma_\alpha$ and $\Gamma_\alpha = \bar{\alpha}(1 - \bar{\alpha})$.

Figure (II.9) shows Γ_α as a function of α. There is a maximum for $\bar{\alpha} = 50\%$, indicating the optimal change of m_A and m_B with T. Also Γ_α can be expressed as a function of K_0':

$$\Gamma_\alpha = K_0'/(1 + K_0')^2 \tag{II.3.27}$$

The relative changes of m_A and m_B at constant P are

$$\delta m_A/m_A = -\, (1 - \bar{\alpha})\, (\Delta H_0/RT)\, (\delta T/T) \tag{II.3.28}$$

$$\delta m_B/m_B = +\, \bar{\alpha}\, (\Delta H_0/RT)\, (\delta T/T)$$

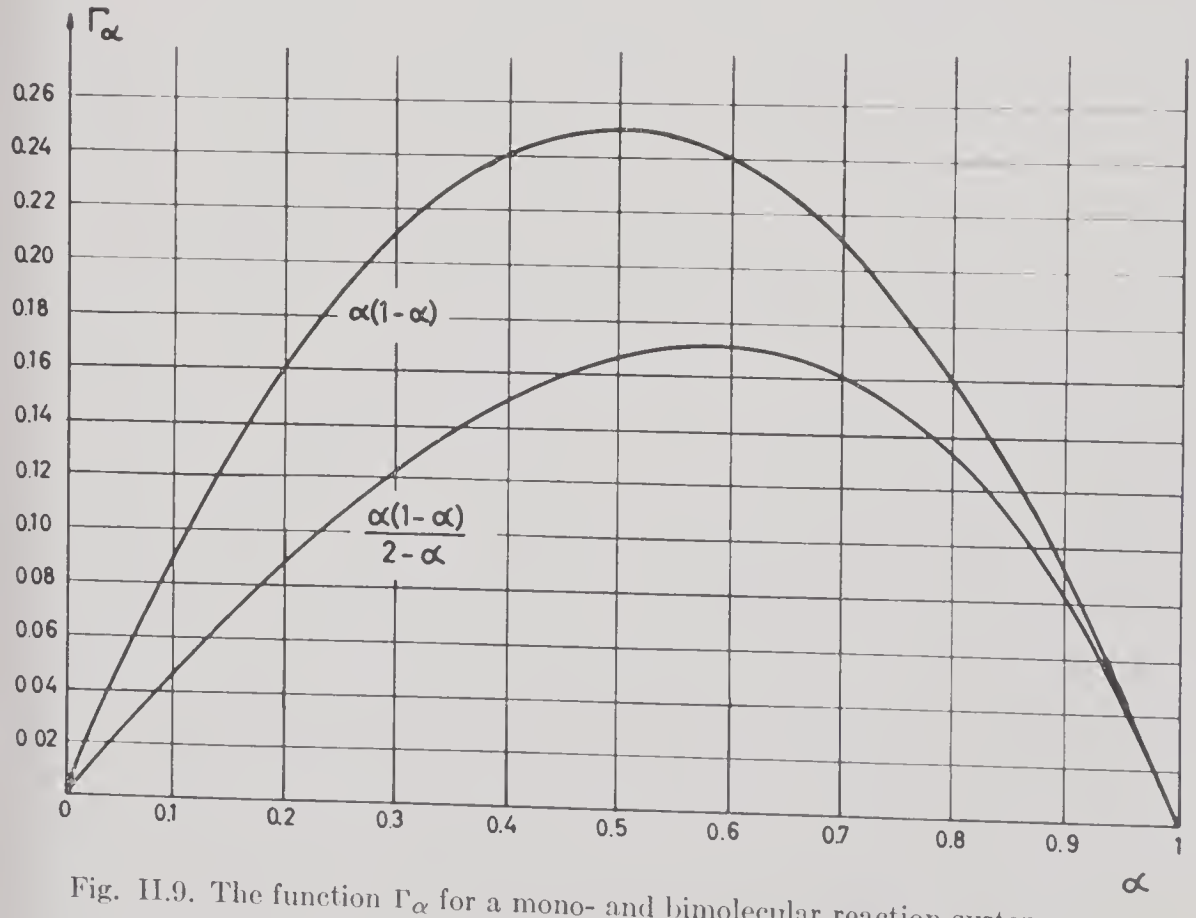

Fig. II.9. The function Γ_α for a mono- and bimolecular reaction system.

and become zero for $\bar{\alpha} \rightarrow 1$ or $\bar{\alpha} \rightarrow 0$, respectively.

Example 2:†

$$A^+ + B^- \rightleftharpoons AB \tag{II.3.29}$$

With $\bar{m}_A = \bar{m}_B = \bar{\alpha} m_0$ and $\bar{m}_{AB} = (1 - \bar{\alpha})\, m_0$, and m_0 = over-all electrolyte concentration

$$K' = 1/K_0 = \bar{\alpha}^2 \bar{f}^2 m_0/(1 - \bar{\alpha})$$

(dissociation constant = reciprocal stability constant; $\bar{f}^2 = f_A f_B$; $f_{AB} = 1$) and the absolute change of m_A with P at constant T is given by

$$(\partial \bar{m}_A/\partial P)_T = m_0\, (\partial \bar{\alpha}/\partial P)_T = m_0 \left\{ \bar{\alpha}(1 - \bar{\alpha})/(2 - \bar{\alpha}) \right\} (\Delta V/RT)$$

$$[1 + (1 - \bar{\alpha})/(2 - \bar{\alpha})\ 2 \cdot (\partial \ln \bar{f}/\partial \ln \bar{\alpha})_{T,P}]^{-1} \tag{II.3.30}$$

The function $\Gamma_\alpha = \alpha(1 - \alpha)/(2 - \alpha)$ is also shown in Figure (II.9). Its maximum occurs at almost symmetrical equilibrium, but not exactly at $\alpha = 50\%$ ($\alpha_{max} = 0.586$). The expression of Γ_α in terms of the equilibrium function $K_0'/\bar{f}^2$ is somewhat more complicated then in the first example:

$$\Gamma_m = m_0\, \Gamma_\alpha = (K'/2\bar{f}^2) \left\{ [(1 + 2m_0 \bar{f}^2/K')/(1 + 4m_0 \bar{f}^2/K')] - 1 \right\} \tag{II.3.31}$$

The relative change of A and B will again become zero for $\alpha \rightarrow 1$, whereas for $\alpha \rightarrow 0$ the relative change of AB will disappear. The latter conditions are important in the direct observation of relaxation phenomena. They show which component under given conditions is most sensitive to a change of the external variable. The factor Γ_m, on the other hand, shows where optimal effects of energy absorption (*cf.* sound absorption, Section II.3.E) are to be expected.

In the more general case of a multiple-step reaction system, the normal variables y_i, as introduced in Section II.1.C, will replace the concentration variables x_i. The analogue of Equation (II.3.18) again can be written in terms of equilibrium constants and reaction quantities of the single steps by use of the transformation $y_i = \sum_k m_{ik} x_k$. For these purposes, i.e., the calculation of absolute values of concentration shift, the transformation matrices must be known (whereas the analysis of the time spectrum only

† The equilibrium constants for these and the following examples have been defined throughout as reciprocal K_0 values. The relations for many second-order reaction systems are more conveniently written in terms of "dissociation constants" rather than "stability constants." On the other hand, the relaxation times are numbered in the way outlined in Section II.1.C for practical reasons whereby it is convenient to write the recombination from left to right. Note that relations (II.3.19) change the signs if K_0 is replaced by K_0', but the reaction quantities remain unchanged [*cf.* (II.3.2) to (II.3.4)].

requires the solution of the characteristic equation, i.e., the calculation of the eigenvalues). The procedure may be demonstrated by considering an example, i.e, the two-step reaction

$$A^+ + B^- \underset{k_{21}}{\overset{k_{12}}{\rightleftharpoons}} AB \underset{k_{32}}{\overset{k_{23}}{\rightleftharpoons}} C$$

where equilibration in the first stage is much faster than in the second. This example has also been discussed previously with respect to kinetics (*cf.* Section II.1.C). The transformation matrices were given by Equations (II.1.30) to (II.1.31).

The physical meaning of the normal variables and their different derivatives becomes apparent if we introduce the following expressions: $m_A = m_B = \alpha m_0$ with $m_0 = m_A + m_{AB} + m_C$ = total (molality) concentration (invariant). The quantity α has the meaning of an over-all degree of dissociation, which is related to the over-all dissociation constant K'_0 by the law of mass action.

$$m_A m_B \bar{f}^2_{A,B}/(m_{AB} + m_C) = [\alpha^2 \bar{f}^2 m_0]/(1 - \alpha) = K'_0$$

$$= K'_{12}K'_{23}/(1 + K'_{23}) \quad \text{(II.3.32)}$$

(It is assumed that only activity coefficients of the ionic species A^+ and B^- have to be taken into consideration.) The single-step equilibrium constants K'_{12} and K'_{23} are defined as

$$K'_{12} = m_A m_B \bar{f}^2_{A,B}/m_{AB} = [\alpha^2 \bar{f}^2 m_0]/[\beta(1 - \alpha)]$$

$$K'_{23} = m_{AB}/m_C = \beta/(1 - \beta) \quad \text{(II.3.33)}$$

where $\beta = m_{AB}/(m_{AB} + m_C)$ is defined as a degree of transformation. The normal variables then have the form [*cf.* Equation (II.1.30)]:

$$y_I = -[k'_{12}/(k'_{12} + k_{21})]\, x_1 + [k_{21}/(k'_{12} + k_{21})]\, x_2 \quad \text{(II.3.34)}$$

$$y_{II} = -(x_1 + x_2) = x_3 \quad \text{(II.3.35)}$$

where $x_1 = m_0\delta\alpha$, $x_2 = m_0\delta[\beta(1 - \alpha)]$, and $x_3 = m_0\delta[(1 - \beta)(1 - \alpha)]$. They are related to the relaxation times τ_I and τ_{II} according to Equation (II.1.29).

We obtain with $Z = T$ or P for Equation (II.3.18),

$$\bar{y}_I = \{m_0\Gamma_I/[1 + \Gamma_I(\partial \ln \bar{f}^2/\partial\alpha)]\}\, (\Delta H_I/RT)\, (\delta T/T) \quad \text{at const. } P$$

$$\bar{y}_I = -\{m_0\Gamma_I/[1 + \Gamma_I(\partial \ln \bar{f}^2/\partial\alpha)]\}\, (\Delta V_I/RT)\, \delta P \quad \text{at const. } T \quad \text{(II.3.36)}$$

$$\bar{y}_{II} = \{m_0\Gamma_{II}/[1 + \Gamma_0(\partial \ln \bar{f}^2/\partial\alpha)]\}\, (\Delta H_{II}/RT)\, (\delta T/T) \quad \text{at const. } P$$

$$\bar{y}_{II} = \{m_0\Gamma_{II}/[1 + \Gamma_0(\partial \ln \bar{f}^2/\partial\alpha)]\}\, (\Delta V_{II}/RT)\, \delta P \quad \text{at const. } T \quad \text{(II.3.37)}$$

with

$$\Gamma_{\mathrm{I}} = \alpha(1 - \alpha)/(2 - 2\alpha + \alpha/\beta),$$

$$\Gamma_{\mathrm{II}} = \Gamma_0 (1 + k'/k_{21})/(1 + k_{32}/k_{23}), \quad \Gamma_0 = \alpha(1 - \alpha)/(2 - \alpha) \qquad \text{(II.3.38)}$$

and

$$\Delta H_{\mathrm{I}} = \Delta H_{12} = H_{\mathrm{AB}} - H_{\mathrm{A}} - H_{\mathrm{B}}$$

$$\Delta H_{\mathrm{II}} = \Delta H_{23} + [k_{21}/(k_{12} + k_{21})]\, \Delta H_{12} \qquad \text{(II.3.39)}$$

where $\Delta H_{23} = H_{\mathrm{C}} - H_{\mathrm{AB}}$ and ΔV_i correspondingly [k'_{12} according to Equation (II.1.14)].

For $\beta \to 1$, $\bar{y}_{\mathrm{I}}$ becomes identical with the expression for a one-step dissociation equilibrium ($\mathrm{A}^+ + \mathrm{B}^- \rightleftharpoons \mathrm{AB}$), and $\bar{y}_{\mathrm{II}}$ disappears ($k_{32}/k_{23} \gg 1$), whereas for $\beta \to 0$, $\bar{y}_{\mathrm{I}}$ disappears, and we have for $\bar{y}_{\mathrm{II}}$ a one-step equilibrium ($\mathrm{A}^+ + \mathrm{B}^- \rightleftharpoons \mathrm{C}$) with a negligible intermediate AB (if $k'_{12}/k_{21} \ll 1$). Then ΔH_{II} is given simply by the sum $\Delta H_{12} + \Delta H_{23} = H_{\mathrm{C}} - H_{\mathrm{A}} - H_{\mathrm{B}}$.

The expressions $\Delta H_{\mathrm{I,II}}$ or $\Delta V_{\mathrm{I,II}}$, respectively, are related to the normal variables y_i, but ean be expressed in terms of partial molar quantities as usually defined:

$\delta H = (\delta H)_{n_{\mathrm{A}}, n_{\mathrm{B}}, n_{\mathrm{AB}}, n_{\mathrm{C}} = \text{const.}} + H_{\mathrm{A}}\delta n_{\mathrm{A}} + H_{\mathrm{B}}\delta n_{\mathrm{B}} + H_{\mathrm{AB}}\delta n_{\mathrm{AB}} + H_{\mathrm{C}}\delta n_{\mathrm{C}}$
$\delta n_{\mathrm{A}} = \delta n_{\mathrm{B}} = x'_1; \quad \delta n_{\mathrm{AB}} = x'_2; \quad \delta n_{\mathrm{C}} = -(x'_1 + x'_2)$ from $\delta n_{\mathrm{A}} + \delta n_{\mathrm{AB}} + \delta n_{\mathrm{C}} = 0$. (The x' here are related to the mole numbers n_i.)

Using the transformation $\mathbf{X} = \mathbf{M}^{-1}\mathbf{Y}$ according to Equation (II.1.31) we obtain

$$\delta H = (\delta H)_{y_{\mathrm{I}}, y_{\mathrm{II}} = \text{const.}} + \Delta H_{\mathrm{I}} y_{\mathrm{I}} + \Delta H_{\mathrm{II}} y_{\mathrm{II}}$$

with $\Delta H_{\mathrm{I}} = \Delta H_{12}$
and

$$\Delta H_{\mathrm{II}} = [k_{21}/(k'_{12} + k_{21})]\, \Delta H_{12} + \Delta H_{23} \qquad \text{(II.3.40)}$$

In the same way, the formally identical volume terms $\Delta V_{\mathrm{I,II}}$ or polarization terms $\Delta \mathbf{D}^*_{\mathrm{I,II}}$ can be obtained. Like $\Delta H_{\mathrm{I,II}}$ they are partial molar quantities but now related to the normal coordinates of concentration, e.g., $\Delta H_{\mathrm{I}} = (\partial H/\partial y_0)_{y_i \neq \mathrm{I}}$, etc. (with $dy_i = \lim y_i \to 0$).

If more than two reaction steps are involved, the explicit expressions may become rather complicated. However, in most cases, certain conditions such as those mentioned in the discussion of the examples in Section (II.1.C) are fulfilled, allowing accurate approximations to be made. In these cases, the law of mass action has to be defined by suitable quantities [such as expressions (II.3.32) to (II.3.33)] which can be simply related to the y_i variables [compare the treatment of three-step reaction system in ref. (4)].

For numerical evaluations, both the equilibrium constants and the reaction quantities ΔH, ΔV, or $\Delta \mathbf{D}^*$ have to be known. These quantities

can be determined experimentally, either from measurements of thermodynamic functions (e.g., heat content, density, or from their differential quotients with respect to T or P) if a splitting into the individual contributions is possible by comparison with known quantities, or—more directly—from the (static) change of equilibrium constant with the corresponding intensive variable (e.g., by spectrophotometric, conductimetric, or other methods). The concentration dependence of the reaction quantities, again, can be either determined directly or can be calculated from measurements of the T or P dependence of activity coefficients, e.g.,

$$\Delta H - \Delta H_0 = -RT^2[(\partial \sum \nu_i \ln f_i)/\partial T]_{P,m_i}$$

The ΔH values are usually finite and large enough to produce a considerable T dependence of the equilibrium constant. At room temperature ($\sim$293°K.), a temperature shift of 10° will cause a relative change in K of about 6% if ΔH amounts to only 1 kcal./mole. If $|\Delta H|$ is appreciably smaller, as is the case for some weak acids and bases in aqueous solutions with pK values around 5 (ln K then is predominantly given by $\Delta S/R$), the equilibrium may be coupled to a buffer equilibrium with stronger T dependence.

The ΔV values are usually relatively small so that a directly observable shift of K requires quite high pressures. Appreciable ΔV values can be found for ionic reactions in aqueous solution, which involve a neutralization of charge [e.g., $H^+ + OH^- \rightleftharpoons H_2O$; ΔV ($= V_{H_2O} - V_{H^+} - V_{OH^-}$) $\approx$ 22 cm.^{3}/mole]. These large changes are primarily a result of a rearrangement of water structure upon charge neutralization (dehydration, etc.). For ΔV = 22 cm.^{3}/mole, a pressure change of about 65 atm. is necessary to give the same relative change in K (i.e., 6%) as was calculated for the above example of T dependence.

Similarly, very high electric field strengths are required to produce observable changes in equilibrium constants. For reactions between dipolar species, which include a compensation of dipole moments (e.g., dimerization of carboxylic acids

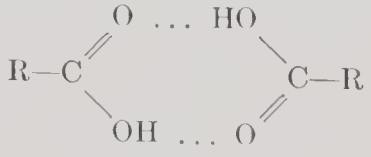

in nonpolar solvents) the relative shift of K remains considerably below 1% even at the highest field densities which can be reached experimentally. (For benzoic acid in toluene, with $K_{dim} \simeq 2 \times 10^{-3}$ mole/l., one may expect a shift of about 0.1% in K, if a field of 3×10^5 v./cm. is applied.) However, the very sensitive methods for determination of dielectric constants and losses make it feasible to think of such applications. Consider-

ably larger effects can be found, if ionic reactions are involved (dissociation field effect). Since the ions will migrate in an external field, the resulting effect may include irreversible contributions. It is therefore important to direct the experiments in such a way (*cf.* Section III.1.D) that the quasi-equilibrial shift of dissociation only is recorded. A theoretical treatment was given by Onsager (5) from a kinetic point of view, i.e., the calculation of the field dependence of K from the rates of dissociation and recombination in a one-dimensional external field. According to Onsager, $K(\mathbf{E})$ can be expressed for moderate field densities ($b < 1$) as a series in powers of $b = B_z[(4\pi|\mathbf{E}|e_0^3)/(2\epsilon\epsilon_0 k^2T^2)]$

$$K(\mathbf{E}) = K(\mathbf{E}=0)\left\{1 + b + (b^2/3) + (b^3/18) + (b^4/180) + \cdots\right\} \quad \text{(II.3.41a)}$$

where $B_z = |z|^3$ for a z–z electrolyte, z = valency, e_0 = elementary charge, ϵ = dielectric constant of solvent, k = Boltzmann's constant, and $\epsilon_0/4\pi$ a conversion factor [*cf.* the discussion following Equation (II.3.65)]. For high field densities ($b > 3$), the approximation

$$K(\mathbf{E}) = K(\mathbf{E}=0)\,(2/\pi)^{1/2}(8b)^{-3/4}\exp(8b)^{1/2}\left[1 - \frac{3}{8(8b)^{1/2}} - \frac{15}{128(8b)} - \frac{105}{1024(8b)^{3/2}} - \cdots\right] \quad \text{(II.3.41b)}$$

holds.

In aqueous solutions the linear relationship from Equation (II.3.41) is applicable throughout, since the field densities which can be obtained will hardly exceed some 10^5 v./cm. For a weak 1:1 electrolyte in water, K will shift by about 15%, if, in the linear range, $\mathbf{E}$ is raised by 10^5 v./cm. The relative change in ionic concentration will amount to half this value, if the dissociation of the electrolyte is small ($\alpha \ll 1$). (At field densities less than 30 kv./cm. some deviations from the linear relationship because of ionic interactions are observed. Thus the optimal range for a determination of K as a linear function of $\mathbf{E}$ lies between 30 and 150 kv./cm. in aqueous solution.)

Chemical effects are influenced much less by magnetic than by electric fields, since magnetic moments are comparatively weaker. (The susceptibilities scarcely exceed values of 10^{-3}.) Corresponding applications have not yet been reported.

In the case of multiple-step systems, the reaction quantities of the single steps are usually not known. An experimental detection of the individual terms is possible only by relaxation methods. A sufficient number of independent data (concentration dependence, etc.) has to be collected in order to allow an unambiguous evaluation. For coupled systems, the single step does not necessarily have to involve a finite reaction quantity

(ΔH, ΔV, or $\Delta \mathbf{D}^*$), in order to contribute to relaxation. As an example we may consider an ionic equilibrium in which only the ion-pair dissociation depends essentially on the electric field strength. Then, the whole equilibrium shift and all individual relaxation steps can, in principle, be measured from the dissociation field effect and its time dependence, though only the first step (the ion-pair equilibrium) is appreciably affected by the field. Similarly, a complete multiple-step equilibrium can be disturbed by T or P if only one step includes a finite ΔH or ΔV [*cf.* Equation (II.2.1)].

The above considerations show how the equilibrium concentration parameter $\bar{y}_i$ is related to the change of intensity (P, T, or $\mathbf{E}$).

The treatment, however, implies defined conditions of the intensive variables during the chemical change, e.g., δc_i as function of T (or P) at constant P (or T). More generally, we would have to write

$$\delta \bar{c}_i = (\partial c_i/\partial T)_P \delta T + (\partial c_i/\partial P)_T \delta P \qquad \text{(II.3.42a)}$$

or a corresponding expression for changes with $\mathbf{E}$. If in an experiment T or P is changed isochorically or adiabatically, respectively, both dependences of $\delta \bar{c}_i$ must be taken into consideration, where

$$(\delta P)_V = (\alpha_P/\kappa_T)(\delta T)_V \qquad (\delta T)_S = (T\alpha_P/\rho c_P)(\delta P)_S \quad \text{(II.3.42b)}$$

(with α_P the expansion coefficient, c_P the specific heat at constant pressure, κ_T the isothermal compressibility, and ρ the density). Relations of this kind will be discussed in more detail below. It will be shown that, more correctly, α_P, c_P, and κ_T have to be replaced by α_P^∞, c_P^∞, and κ_T^∞, i.e, the quantities at a constant extent of reaction. These differences, however, are usually negligibly small, just as are the differences between τ_{TP}, τ_{SP}, and τ_{TV} (*cf.* Section II.1.B).

The actual concentration shift y_i again is related to $\bar{y}_i$ by a time function as was shown in Section II.2. Thus, all the information for a theoretical treatment of the transient methods, i.e, the direct observation of a concentration change (y_i or x_i, respectively) as a consequence of a shift in P, T, or $\mathbf{E}$, is now available.

*C. CHEMICAL CONTRIBUTIONS TO EQUATIONS OF STATE

It has already been shown that any change in concentration also results in a change of extensive parameters such as volume (if $\Delta V \neq 0$), entropy or heat content (if $\Delta H \neq 0$), or polarization (if $\Delta \mathbf{D}^* \neq 0$). Therefore, the relation between y_i and $\bar{y}_i$ can be expressed as a term in the relation between any two conjugate variables ($V - P$, $S - T$, or $\mathbf{D}^* - \mathbf{E}$). For periodic changes of P, T, or $\mathbf{E}$, this term will contain the complex transfer function $\mathfrak{S}_i$ as introduced in Section II.2. The quantities $(\partial V/\partial P)$,

$(\partial S/\partial T)$, or $(\partial \mathbf{D}^*/\partial \mathbf{E})$ will then be dynamic functions containing the contributions from chemical relaxation. It is only for changes which are slow in comparison with chemical rates that these functions become identical with the usual equilibrium functions (e.g., compressibility, specific heat, electrical permittivity, etc.). For a theoretical treatment of the stationary methods, the knowledge of these quantities, and especially their chemical terms, is required.

Let us first calculate these terms under the assumption that the chemical system remains in equilibrium according to the external conditions. This condition may be expressed by $dA = 0$, which means (as we are always in or near equilibrium) that the affinity A is kept constant at zero. The following relations between the extensive variables (S, V, $\mathbf{D}^*$) and their conjugate intensities may thus be derived.

Entropy–Temperature. The relation between S and T is reflected (and can be measured) by the heat capacities C_P, C_V or, if related to the mass unit, by the specific heats c_P, c_V of the system†

$$\bar{C}_P = (\partial H/\partial T)_{P,A} = T(\partial S/\partial T)_{P,A}$$
$$\bar{C}_V = (\partial U/\partial T)_{V,A} = T(\partial S/\partial T)_{V,A} \qquad \text{(II.3.43)}$$

As mentioned already, the meaning of the subscript A for equilibrium systems is not only $dA = 0$ but also $A = 0$. Then the above identities follow directly from the total differentials of H and U, which in the absence of external fields may be written as

$$dH = TdS + VdP - Ad\xi$$
$$dU = TdS - PdV - Ad\xi \qquad \text{(II.3.44)}$$

We now define a residual (C_P^{∞}) and a chemical term $(\bar{C}_P^{\mathrm{ch}})$ by

$$T\,(\partial S/\partial T)_{P,A} = T(\partial S/\partial T)_{P,\xi} + T(\partial S/\partial \xi)_{T,P}\,(\partial \xi/\partial T)_{P,A} = C_P{}^{\infty} + \bar{C}_P^{\mathrm{ch}} \qquad \text{(II.3.45)}$$

and correspondingly for $\bar{C}_V$. The index ∞ in the residual part is already related to the consideration of relaxational behavior. It simply means that the response of S to a change in T (at constant P and ξ) is supposed to be instantaneous. In other words, C_P^{∞} remains finite and constant for high-frequency temperature oscillations, whereas C_P^{ch} disappears at these frequencies, owing to finite relaxation times. (The index ∞ for changes in S or other extensive variables is to be understood only as relative in comparison to changes in ξ; it has no absolute meaning; compare below).

†The symbol $\bar{C}_P$ (etc.) means that C_P is related to complete chemical equilibration ($A = 0$).

In order to calculate $\bar{C}_P^{ch}$ and $\bar{C}_V^{ch}$, we make use of some well-known thermodynamic relations. With

$$(\partial\xi/\partial T)_{Z,A} = -(\partial A/\partial T)_{Z,\xi}/(\partial A/\partial\xi)_{Z,T} \qquad Z = P \text{ or } V \quad \text{(II.3.46)}$$

and

$$(\partial A/\partial T)_{P,\xi} = -[(\partial/\partial T)(\partial G/\partial\xi)_{P,T}]_{P,\xi} = (\partial S/\partial\xi)_{P,T}$$
$$(\partial A/\partial T)_{V,\xi} = -[(\partial/\partial T)(\partial F/\partial\xi)_{V,T}]_{V,\xi} = (\partial S/\partial\xi)_{V,T} \quad \text{(II.3.47)}$$

we obtain

$$\bar{C}_Z^{ch} = -T(\partial S/\partial\xi)^2_{Z,T}/(\partial A/\partial\xi)_{Z,T} \qquad Z = P \text{ or } V \quad \text{(II.3.48)}$$

The quantity $(\partial A/\partial\xi)_{P,T}$ can be written as $-RT/\Gamma_\xi^*$, where Γ_ξ^* can be identified with the corresponding expression introduced by Equation (II.3.11). Since (by definition) the first term of

$$-A = \Sigma\nu_i\mu_i^0(P,T) + RT\sum\nu_i \ln a_i$$

does not change, if P and T are kept constant, Γ_ξ^* simply follows from differentiation of $\Sigma\nu_i \ln a_i$ with respect to ξ [*cf.* Equation (II.3.11)]. In contrast, a change of ξ at constant V and T will yield

$$(\partial A/\partial\xi)_{V,T} = (\partial A/\partial\xi)_{P,T} + (\partial A/\partial P)_{\xi,T}(\partial P/\partial\xi)_{V,T}$$
$$= -(RT/\Gamma_\xi^*) + [(\partial V/\partial\xi)^2_{P,T}/(\partial V/\partial P)_{\xi,T}]$$
$$= -(RT/\Gamma_\xi^*)(\bar{\kappa}_T/\kappa_T^\infty) \quad \text{(II.3.49)}$$

where $\bar{\kappa}_T$ and κ_T^∞ are the isothermal compressibilities as introduced below [*cf.* Equations (II.3.53) and (II. 3.59)].

We may, furthermore, introduce the reaction quantities ΔH and ΔV, using the symbol Δ as an operator $(\partial/\partial\xi)_{P,T}$:

$$(\partial S/\partial\xi)_{V,T} = (\partial S/\partial\xi)_{P,T} + (\partial S/\partial P)_{\xi,T}(\partial P/\partial\xi)_{V,T}$$
$$= (\Delta H/T) - \Delta V(\alpha_P^\infty/\kappa_T^\infty) \quad \text{(II.3.50)}$$

with $\alpha_P^\infty = (1/V)(\partial V/\partial T)_{P,\xi}$.

The final expressions for the chemical parts of the heat capacities read

$$\bar{C}_P^{ch} = \Gamma_\xi^*(\Delta H)^2/RT^2 \quad \text{(II.3.51)}$$

$$\bar{C}_V^{ch} = [\Gamma_\xi^*(\Delta H - \Delta V\cdot T\alpha_P^\infty/\kappa_T^\infty)^2/RT^2]\,(\kappa_T^\infty/\bar{\kappa}_T) \quad \text{(II.3.52)}$$

The term $T(\partial S/\partial\xi)_{V,T} = \Delta H - \Delta V\cdot T\alpha_P^\infty/\kappa_T^\infty$ is often written as ΔU.

In contrast, we shall use the symbol Δ throughout for "differentiations with respect to ξ at constant intensive variables." We shall therefore also express $(\partial V/\partial\xi)_{S,P}$ by a function of ΔV and ΔH, rather than by the use of a new symbol. We note that, even if we were to introduce the term ΔU, $\bar{C}_V^{ch}$ and $\bar{C}_P^{ch}$ would not be symmetrical in ΔU and ΔH because of the factor $\kappa_T^\infty/\bar{\kappa}_T$. However, they would become equal for $\Delta V = 0$. If we relate

$\bar{C}_P^{ch}$ to the unit mass, we obtain as the chemical part of the specific heat c_P^{ch}:

$$\bar{c}_P^{ch} = \Gamma_\xi^*(\Delta H)^2/(RT^2\rho V) = \Gamma_c^*(\Delta H)^2/(\rho RT^2) \qquad \text{(II.3.51a)}$$

For a first-order system with Γ according to Equation (II.3.27), $\bar{c}_P^{ch}$ will pass a maximum since K_0 depends exponentially on T [*cf.* ref (18).]

Volume–Pressure. We must, again, define two relations representing the isothermal and adiabatic compressibilities

$$\bar{\kappa}_T = -(1/V)(\partial V/\partial P)_{T,A} \qquad \bar{\kappa}_S = -(1/V)(\partial V/\partial P)_{S,A} \qquad \text{(II.3.53)}$$

With these definitions, we can write for the chemical part of the isothermal compressibility

$$\bar{\kappa}_T^{ch} = -(1/V)(\partial V/\partial \xi)_{T,P}(\partial \xi/\partial P)_{T,A} = \bar{\kappa}_T - \kappa_T^\infty \qquad \text{(II.3.54)}$$

and, for the corresponding part of the adiabatic compressibility,

$$\bar{\kappa}_S^{ch} = -(1/V)(\partial V/\partial \xi)_{S,P}(\partial \xi/\partial P)_{S,A} = \bar{\kappa}_S - \kappa_S^\infty \qquad \text{(II.3.55)}$$

In analogy to the above considerations, we may use the relations

$$(\partial \xi/\partial P)_{Z,A} = -(\partial A/\partial P)_{Z,\xi}/(\partial A/\partial \xi)_{Z,P} \qquad Z = T \text{ or } S \qquad \text{(II.3.56)}$$

$$(\partial A/\partial \xi)_{S,P} = (\partial A/\partial \xi)_{T,P} + (\partial A/\partial T)_{P,\xi}(\partial T/\partial \xi)_{S,P}$$
$$= -(RT/\Gamma_\xi^*)(\bar{c}_P/c_P^\infty) \qquad \text{(II.3.57)}^\dagger$$

and

$$(\partial V/\partial \xi)_{S,P} = (\partial V/\partial \xi)_{T,P} + (\partial V/\partial T)_{P,\xi}(\partial T/\partial \xi)_{S,P}$$
$$= \Delta V - \Delta H(\alpha_P^\infty/\rho c_P^\infty) \qquad \text{(II.3.58)}$$

[ρ = density (mass/vol.) and $c_P^\infty = c_P^\infty/\rho V$ = specific heat under constant pressure and composition.]

The final expressions for the reaction contributions to compressibility are then

$$\bar{\kappa}_T^{ch} = [\Gamma_\xi^*(\Delta V)^2/RTV] \qquad \text{(II.3.59)}$$

$$\bar{\kappa}_S^{ch} = [\Gamma_\xi^*(\Delta V - \Delta H\alpha_P^\infty/\rho c_P^\infty)^2/RTV](c_P^\infty/\bar{c}_P) \qquad \text{(II.3.60)}$$

If $\Delta V = 0$, we have $\bar{\kappa}_S^{ch} = \bar{c}_P^{ch}[(\alpha_P^\infty)^2 T/\rho c_P^\infty c_P]$, where $\bar{c}_P^{ch}$ is the chemical part of the specific heat according to Equation (II.3.51a). Correspondingly, we may define a chemical part of the coefficient of thermal expansion ($\alpha_P^{ch} = \bar{\alpha}_P - \alpha_P^\infty$)

$$\bar{\alpha}_P^{ch} = (1/V)(\partial V/\partial \xi)_{T,P}(\partial \xi/\partial T)_{P,A} = (\Gamma_\xi^* \Delta H \Delta V)/(VRT^2) \qquad \text{(II.3.61)}$$

† Compare the relations (II.3.49) to (II.3.51).

Electric Displacement—Field Density. If we define, in analogy to the Gibbs free energy, the function

$$G^* = U + PV - TS - \mathbf{E}\mathbf{D}^* \tag{II.3.62}$$

[*cf.* Guggenheim (1)] with the total differential being

$$dG^* = VdP - SdT - \mathbf{D}^*d\mathbf{E} - Ad\xi \tag{II.3.63}$$

we may derive relations between $\mathbf{D}^*$ and $\mathbf{E}$ which are similar to those obtained above. Some precaution is necessary if the pressure within the field space is to be used as an independent variable (6). Usually the volume of this field space (i.e., the volume between the plates of a condenser) will have to be considered a constant; however, one can think of experimental arrangements where this restrictive condition does not necessarily apply (7, 8). For the expression $(\partial\mathbf{D}^*/\partial\mathbf{E})$, four different relations can be derived that are closely related to the electrical permittivity, which is usually defined as the ratio of displacement and field density. For a correct treatment, however, $(\partial\mathbf{D}^*/\partial\mathbf{E})$, will depend upon the conditions maintained during the change of $\mathbf{E}$. For practical reasons, we write these relations as

$$\bar{\epsilon}_{T,P} = (1/V_e\epsilon_0)(\partial\mathbf{D}^*/\partial\mathbf{E})_{T,P,A} \qquad \bar{\epsilon}_{T,V} = (1/V_e\epsilon_0)\,(\partial\mathbf{D}^*/\partial\mathbf{E})_{T,V,A} \tag{II.3.64}$$

$$\bar{\epsilon}_{S,P} = (1/V_e\epsilon_0)(\partial\mathbf{D}^*/\partial\mathbf{E})_{S,P,A} \qquad \bar{\epsilon}_{S,V} = (1/V_e\epsilon_0)(\partial\mathbf{D}^*/\partial\mathbf{E})_{S,V,A} \tag{II.3.65}$$

where V_e relates to the volume of field space, which may or may not be variable (according to the experimental conditions). If $\mathbf{D}^*$ and $\mathbf{E}$ are given in amp. sec. cm. and v./cm. respectively, for ϵ_0 the value 8.8543×10^{-14} amp. sec./v. cm. is to be used (rational system). If $\mathbf{D}^*$ and $\mathbf{E}$ are given in c.g.s. units, ϵ_0 must be replaced by $\epsilon_0/4\pi$, but ϵ_0 can be taken as unity. The differences between $\bar{\epsilon}_{T,P}$, $\bar{\epsilon}_{T,V}$, $\bar{\epsilon}_{S,P}$, and $\bar{\epsilon}_{S,V}$ disappear for $\mathbf{E} \rightarrow 0$ (compare below); all four quantities then become identical with the dielectric constant ϵ of the usual definition, and for homogeneous media $\mathbf{D}^*$ can be written as $\epsilon_0\epsilon V_e\mathbf{E}$. The quantity $\mathbf{D} = \epsilon_0\epsilon\mathbf{E}$ is usually called "electric displacement"; it differs from $\mathbf{D}^*$ by the volume V_e.

As will be seen later, a chemical contribution to $\bar{\epsilon}_{Z_i,Z_k}$ according to the definition

$$\bar{\epsilon}^{\mathrm{ch}}_{Z_i,Z_k} = (1/V_e\epsilon_0)(\partial\mathbf{D}^*/\partial\xi)_{Z_i,Z_k,E}\,(\partial\xi/\partial\mathbf{E})_{Z_i,Z_k,A} = \bar{\epsilon}_{Z_i,Z_k} - \epsilon^{\infty}_{Z_i,Z_k} \tag{II.3.66}$$

$$\epsilon^{\infty}_{Z_i,Z_k} = 1/V_e\epsilon_0(\partial\mathbf{D}^*/\partial\mathbf{E})_{Z_i,\,Z_k,\xi} \tag{II.3.67}$$

will occur only at higher field densities, where $\mathbf{D}^*$ is no longer linearly related to $\mathbf{E}$. On the other hand, the usual (high frequency) methods for determination of ϵ are related to a linear change of displacement with field density. It is therefore advisable to carry out the experiments in a constant high field with the strength $\mathbf{E}_0$, upon which is superimposed a (high

frequency) modulation field $\delta\mathbf{E}$ (in the same direction) with low amplitude. All changes with respect to $\delta\mathbf{E}$ can then be linearized, and the previously described analysis can be applied. However, all thermodynamic quantities are now related to the reference state $\mathbf{E}_0$, just as all dynamic S-T and V-P relations above belong to a reference state such as $T = 298°\text{K.}$, $P = 1$ atm.

Among the four relations between $\mathbf{D}^*$ and $\mathbf{E}$, the isochoric, isentropic change is of primary practical importance for relaxation experiments. The frequencies will usually be high enough so that all transformations occur under adiabatic and isochoric conditions. (For standard cell dimensions, the latter condition will be fulfilled at $\nu > 10^6$ c/sec., the former at much lower frequencies.) We shall therefore consider only the case of ϵ_{SV} in the following material. Furthermore, we shall omit all terms including ΔV, as they are of only minor importance for the practical applications considered below (8). As a consequence we do not need to pay special attention to how the pressure within the field space differs from external pressure. (Also, the question whether V_e is a constant, is unimportant if we make measurements under conditions of constant V.) The chemical contribution to $\bar{\epsilon}_{SV}$ can then be obtained in complete analogy to the calculation of $\bar{\kappa}_S$, as shown above:

$$\bar{\epsilon}_{SV}^{\text{ch}} = (\Gamma_\xi^*/\epsilon_0 V_e RT)[\Delta\mathbf{D}^* + \Delta H(\beta_{V\mathbf{E}}^{\infty}/\rho c_{V\mathbf{E}}^{\infty})]^2(c_{V\mathbf{E}}^{\infty}/\bar{c}_{V\mathbf{E}}) \qquad \text{for } \Delta V = 0 \tag{II.3.68}$$

with

$$\Delta\mathbf{D}^* = (\partial\mathbf{D}^*/\partial\xi)_{P,T,\mathbf{E}} \qquad \text{and} \qquad \beta_{V\mathbf{E}}^{\infty} = -(1/V)(\partial\mathbf{D}^*/\partial T)_{E,V,\xi}$$

This part of ϵ_{SV} occurs in addition to ϵ_{SV}^{∞}, which includes all nonchemical contributions such as dipolar orientation and polarization. Since the chemical equilibrium is field dependent the number of dipoles has also been stationarily increased due to $\mathbf{E}_0$, and this increased number of dipoles means an increase in ϵ_{SV}^{∞} which is contrary to the Langevin saturation term.† This contribution, however, is to be distinguished from $\bar{\epsilon}_{SV}^{\text{ch}}$, since it is related to the orientation of the additional number of dipoles (produced by $\mathbf{E}_0$), whereas $\bar{\epsilon}_{SV}^{\text{ch}}$ is directly related to the finite chemical production $(\partial\xi/\partial\mathbf{E})_{S,V,A}$ in the alternating field $\delta\mathbf{E}$ at high $\mathbf{E}_0$. (Note that this quantity does not depend on the amplitude of the alternating field $\delta\mathbf{E}$—if $\delta\mathbf{E} \ll \mathbf{E}_0$—but only on the constant $\mathbf{E}_0$.) In some cases, $\bar{\epsilon}_{SV}^{\text{ch}}$ may even be appreciably higher than the secondary ($\mathbf{E}_0$-dependent term) in ϵ_{SV}^{∞}. Moreover, $\bar{\epsilon}_{SV}^{\text{ch}}$ may be finite for systems which do not include dipolar or polarizable particles. The only condition, then, is that ΔH is finite and that the whole solution has a dielectric constant that changes with temperature at constant volume. This fact may be surprising, but it is simply a result of the adiabatic condition. Similarly, $\bar{\kappa}_S$ contains chemical terms, owing to a finite ΔH, even if the reaction is not com-

† In very strong fields, a decrease of the permittivity should occur as a result of orientational saturation (first described by Langevin).

bined with a finite volume change ΔV. To estimate the magnitude of $\bar{\epsilon}^{ch}_{SV}$, we may consider a dipolar equilibrium, such as the dimerization of acetic or benzoic acid in a nonpolar solvent (e.g., benzene, CCl_4, etc.). For $\mathbf{E}_0 = 10^5$ v./cm. and $c_0 = 0.1$ to $1M$, $\bar{\epsilon}^{ch}_{SV}$ would be of the order of magnitude of 10^{-6} (increasing with the second power of $\mathbf{E}_0$). This may be just beyond the resolution of present techniques. However, since the relation II.3.68 or 69 resp. for $\bar{\epsilon}^{ch}_{SV}$ corresponds to a fourth power dependence of the dipole moments, appreciably larger effects can be expected for substituted compounds (such as *p*-nitrobenzoic acid, *p*-nitrophenol etc.). As may be estimated, the relaxation of the chemical equilibrium occurs at frequencies $\sim 10^7$ c/sec., whereas the relaxation frequencies of the terms in ϵ_{SV} (including the field-dependent increments) occur at frequencies $\nu > 10^{10}$ c/sec. As a consequence, the loss factor because of dispersion of $\bar{\epsilon}^{ch}_{SV}$ reaches, in the Mc range, the same order of magnitude as that due to dipolar relaxation (which is almost field-independent) and should be detectable by sensitive methods† (compare below).

For the estimation of $\bar{\epsilon}^{ch}_{SV}$, we may express $\mathbf{D}^*$ by $\epsilon_0 \epsilon V_e \mathbf{E}$, with constant ϵ and $\mathbf{E} = \mathbf{E}_0 + \delta\mathbf{E}$, which, even at $\mathbf{E}_0 = 3 \times 10^5$ v./cm. means that small higher-order terms may be neglected. Then we have for an equilibrium $2A \rightleftharpoons A_2$

$$\bar{\epsilon}^{ch}_{SV} = (\Gamma_\xi^* \epsilon_0 \mathbf{E}_0^2/RT)(c^{\infty}_{V\mathbf{E}}/\bar{c}_{V\mathbf{E}}) \left\{ [(\partial\epsilon/\partial c_{A_2}) - 2(\partial\epsilon/\partial n_A)]_{T,P,\mathbf{E}} - (\Delta H/\rho c^{\infty}_{V\mathbf{E}})(\partial\epsilon/\partial T)_{E,V,\xi} \right\}^2 \quad \text{(II.3.69)}$$

As mentioned above, $\bar{\epsilon}^{ch}_{SV}$ is proportional to the square of the field density (in this case, to the constant $\mathbf{E}_0^2$). It disappears for $\mathbf{E}_0 \to 0$. If the reaction consists of a dimerization of dipolar molecules involving a compensation of their moments the first term in the brackets will be the predominant one. The second term will usually be too small to give a detectable effect (unless methods improve appreciably in sensitivity). ΔH is usually negative for this reaction type so that both terms have the same sign. Among other possible dipolar reactions, the transformation between the molecular and zwitterion state in amino acids, and rotational isomerism (involving compensation of group moments) are to be mentioned. The above example of dimerization by hydrogen bonding is different in character from the more unspecific electrostatic interaction which can always be observed in dipolar media (at high concentration of the dipolar species). The relaxation of these unspecific effects occurs at frequencies that are not far different from those for single dipolar rotation. Equilibrium effects of the latter kind have been observed by measurements of ϵ as a function of field density. This field dependence is a result of superposition of Langevin saturation and disturbance of dipolar interaction (9).

Similar considerations are possible for magnetic fields. For instance, one could derive an expression for the chemical contributions to magnetic permeability. However, these contributions, even at the highest obtainable magnetic field strengths, are comparatively smaller than the corresponding electric effects and therefore not detectable, unless the sensitivity of present methods could be increased by some orders of magnitude.

The above relations for $\bar{c}^{ch}_P$, $\bar{c}^{ch}_V$, $\bar{\kappa}^{ch}_T$, and κ^{ch}_S (and also correspondingly

† Corresponding effects have meanwhile been detected (8).

for the generalized quantities in electric fields) are not independent of each other. One may easily verify that

$$\bar{c}_P\bar{\kappa}_S = \bar{c}_V\bar{\kappa}_T \tag{II.3.70}$$

with

$$c_P - \bar{c}_V = (T\bar{\alpha}_P^2)/(\rho\bar{\kappa}_T) \qquad \text{and} \qquad \bar{\kappa}_T - \bar{\kappa}_S = [T(\bar{\alpha}_P)^2]/(\rho\bar{c}_P)$$

Since the same relations hold for the quantities c_P^∞, c_V^∞, κ_T^∞, and κ_S^∞, one obtains for the chemical terms,

$$[1 - (\bar{c}_P^{ch}/\bar{c}_P)][1 - (\bar{\kappa}_S^{ch}/\bar{\kappa}_S)] = [1 - (\bar{c}_V^{ch}/\bar{c}_V)][1 - (\bar{\kappa}_T^{ch}/\bar{\kappa}_T)] \tag{II.3.71}$$

The factors occurring in this equation are identical with those occurring in the interrelations of the different relaxation times τ_{SV}, τ_{TV}, τ_{SP}, and τ_{TP} (*cf.* Section II.1.B). Equation (II.3.71) could have been obtained as a direct consequence of the equations (II.1.17), but now, these relations can be expressed explicitly.

*D. DYNAMIC EQUATIONS OF STATE

The above considerations were restricted to the condition of chemical equilibrium, expressed by $A = 0$. We shall now return to a treatment of relaxation phenomena.

All chemical terms derived above contain the differential quotient of ξ with respect to an intensive variable (T, P, or $\mathbf{E}$) under different thermodynamic conditions. The real change of ξ, however, will generally differ from the equilibrium change of ξ, corresponding to the externally enforced variations of T, P, or $\mathbf{E}$. (As we have seen in Section I.1.A, any small deviation from equilibrium will result in relaxation processes.) For stationary periodic variations, the change $\delta\xi$ is simply related to the equilibrium change $\delta\bar{\xi}$ by a complex transfer function $\mathfrak{S}$, as was shown in Section II.2.C. Thus, we obtain dynamic quantities $(\partial\xi/\partial Z_i)_{Z_k}$ and from them the dynamic chemical terms c_P^{ch}, c_V^{ch}, κ_S^{ch}, κ_T^{ch}, ϵ_{SV}^{ch}, etc., which are related to the static terms (condition $A = 0$) by the complex transfer function. According to the definition of different relaxation times, the transfer functions $\mathfrak{S}_i(\omega)$ are dependent upon the conditions kept constant. Thus for a dynamic change of ξ with respect to P at constant S, the transfer function will be related to $\tau_{S,P}$. This relation and the corresponding equations for constant T,P or V,T, etc., have been first derived by Meixner (10).

In Meixner's thermodynamic treatment the reaction rate (with ξ, for instance, being a function of S and P) is written as

$$\partial\xi(S,P)/\partial t = kA(S,P,\xi) \tag{II.3.72}$$

Since A is a very small quantity, close to equilibrium, we may expand and obtain for constant S,

$$(\partial\xi/\partial t)_S = k(\partial A/\partial\xi)_{S,P}\delta\xi + k(\partial A/\partial P)_{S,\xi}\delta P \qquad \text{(II.3.73)}$$

or for periodic changes,

$$j\omega\delta\xi = -(\delta\xi/\tau_{SP}) + k(\partial A/\partial P)_{S,\xi}\delta P \qquad \text{(II.3.74)}$$

with the definition

$$1/\tau_{SP} = -k(\partial A/\partial\xi)_{S,P}$$

The adiabatic change of ξ with P can then be written as

$$(\partial\xi/\partial P)_S = -[(\partial A/\partial P)_{S,\xi}/(\partial A/\partial\xi)_{S,P}][1/(1 + j\omega\tau_{SP})] = (\partial\xi/\partial P)_{A,S}\,\mathfrak{S}_{SP} \qquad \text{(II.3.75)}$$

with

$$\mathfrak{S}_{SP} = 1/(1 + j\omega\tau_{SP})$$

Accordingly, we obtain a "dynamic equation of state":

$$(\partial V/\partial P)_S = (\partial V/\partial P)_{S,\xi} + (\partial V/\partial\xi)_{S,P}(\partial\xi/\partial P)_{S,A}\,\mathfrak{S}_{SP} \qquad \text{(II.3.76)}$$

These procedures are applicable only for very small variations. In practice (especially for solutions), the differences between τ_{SP}, τ_{TP}, etc., are usually negligibly small, but they can be of importance in certain extreme cases. It should be emphasized at this point that, to be correct, the expressions of τ, derived from the phenomenological rate equations, as conventionally introduced in chemical kinetics, always belong to the conditions of constant intensive variables.

If more than one single chemical transformation is involved, the τ_i values belong to normal variables ξ_i (e.g., the variables y_i introduced in Section II.1.C). Some care, however, is required, if changes at constant S or V are treated. Consider the expressions for c_V, κ_S, and ϵ_{SV}. In contrast to c_P and κ_T, these expressions contain terms which are multiplied by quantities with the index ∞. In other words, these quantities depend on how many normal variables have been introduced. The choice of normal variables in Section II.1.C was contingent upon the condition that, at constant P and T, the y_i are independent of each other, i.e., that $(\partial V/\partial\xi)_{T,P}$ and $(\partial S/\partial\xi_i)_{T,P}$ are independent of $\xi_{k\neq i}$. This condition is equivalent to $(\partial A_i/\partial\xi_k)_{T,P} = 0$ for $k \neq i$, or $\{-(\partial A_i/\partial\xi_k)_{T,P}\}$ being a diagonal tensor, where $-(\partial A_i/\partial\xi_i)_{T,P} = RT/\Gamma_{\xi i}{}^*$. In order to obtain a similar condition for changes at constant S and/or V, we must introduce new normal variables ξ for which the tensor with the elements $-(\partial A_i/\partial\xi_k)_{S,V}$ etc., becomes diagonal, i.e., $(\partial A_i/\partial\xi_k)_{S,V} = 0$ for $i \neq k$ (*cf.* Meixner). Such an introduction of new normal variables would complicate the interpretation of relaxation spectra greatly. However, it is required only in extreme cases, where the τ_{TP} differ considerably from the τ_{TV} values, etc., i.e., where the reacting species represent a predominant part of the total system and essentially determine its thermodynamic functions (e.g., some transformations in pure liquids or gases especially at very low temperatures). For solutions, where $\bar{\kappa}_S^{ch}$, $\bar{c}_P^{ch}$, etc., are small with respect to κ_S^{∞}, c_P^{∞}, etc., these difficulties disappear [as may be directly seen from Equations (II.3.49) and (II.3.57) according to which, for instance $(\partial A/\partial\xi)_{S,P} = (\partial A/\partial\xi)_{T,P}(c_P/c_P^{\infty})$]. The neglect of these differences in normal variables

leads to the same accuracy as the neglect of the differences between τ_{TP}, τ_{SP}, etc., and the replacement of α_P^∞, c_P^∞, κ_T^∞, by $\bar{\alpha}_P$, $\bar{c}_P$, and $\bar{\kappa}_T$. The latter (equilibrium) values are independent of the choice of normal coordinates.

For a multiple-step system the (dynamic) chemical terms of c_P, c_V, κ_S, κ_T, ϵ_{SV}, etc., can generally be written as a sum, for instance,

$$c_P^{ch} = \sum_i \bar{c}_P^i \, \mathfrak{S}_{TP}^i \qquad \text{(II.3.77)}$$

The index i belongs to the ith chemical normal variable y_i, which is related to the equilibrium variable $\bar{y}_i$ by a transfer function $\mathfrak{S}_i$ [*cf.* Equation (II.1.20)] In order to express $\bar{c}_P^i$ in terms of quantities such as ΔH_i or K_i belonging to single steps in the reaction systems, we need both the transformation from x_i to y_i and that from y_i to x_i (Equation II.1.21). The calculation of such single terms as $\bar{c}_P^i$, κ_S^i, etc., follows the procedure outlined above (examples on p. 960 ff.). Such calculations have been carried out for specific cases.

Since the dynamic functions are complex, there will exist, in principle, two methods of measurement. One method makes use of the real part of $\mathfrak{S}$, the other one is related to the imaginary part. Both parts are, of course, not independent of each other, but connected by general relations, which hold whatever the number and distribution of relaxation steps. These relations are known in optics (e.g., for ϵ) as "Kronig-Kramers relations" (11). They have also been shown to be valid for acoustical relaxation phenomena (i.e., for κ_S) by Ginzberg (12). [see also refs. (13) and (14)]. Their practical use requires the knowledge of either the real or the imaginary part of ϵ_{SV}, κ_S, etc., over the whole frequency range (a condition which for the present applications is usually not fulfilled).

If both the real and the imaginary parts of a dynamic function can be determined, the well-known semicircle plot of the real against the imaginary part gives information about the distribution of relaxation times [*cf.* Cole and Cole (15)]. A regular semicircle indicates a single relaxation time, whereas a compressed circle (axis ratio of imaginary and real part less than 1) indicates a distribution of relaxation times. Certain empirical relations (15,16) have been introduced for the description of dielectric relaxation phenomena. They are of minor importance for chemical relaxation effects, which, for the most part, are sufficiently discrete. In many cases, a simultaneous determination of the real and imaginary part (e.g., sound dispersion and absorption, compare below) is very difficult.

Measurements of the dynamic system behavior permit two major applications.

(1) The determination of relaxation times. As shown in Section (II.2.C), the real part of the transfer function $\mathfrak{S}_i$ changes in a stepwise manner;

the absolute value of the imaginary part shows a maximum at $\omega = 1/\tau_i$. Thus, a detection of such steps or maxima simply allows the determination of single relaxation times, if these differ sufficiently. This application—the chief concern of this chapter—does not require the use of detailed thermodynamic relations, but only the analysis of the time spectrum. In some cases the experimental method does not directly yield the transfer function, but some combination of terms containing $\mathfrak{S}$ (compare sound absorption, dispersion, etc.). The steps or maxima may then not occur exactly at $\omega = 1/\tau$ and it becomes necessary to estimate the importance of the deviation, which usually is not significant.

(2) The measurement of the dynamic behavior allows one to discriminate between different molecular interactions. In contrast, the static behavior expresses the sum of all interactions present and does not permit the separation of single terms without additional theoretical considerations. In the dynamic behavior, we have one more parameter. The static function is, so to speak, expanded on a frequency axis, and the single terms may occur separately at different frequencies. Measurements have been made that have led to the distinguishing of different ionic interactions in aqueous electrolytic solutions (4,17). The analysis of those data requires the thermodynamic treatment of the whole multiple-step system, as outlined above. A concrete example is given in the discussion of sound absorption.

For an experimental determination of dynamic behavior, a periodic variation of an intensive variable is required. A direct temperature oscillation (periodic heating) in general can not be effected rapidly enough because of limitations in heat conduction. However, the temperature may change secondarily in adiabatic variations of other intensive variables, such as P and $\mathbf{E}$ (*cf.* κ_S and ϵ_{SV}). Rapid oscillations of these variables can readily be obtained, as will be shown in Section III.

There are two principal possibilities for measuring the stationary response: One is to use stationary (mechanical or electric) circuits and to record their resonance properties (e.g., line width), the other is to measure the properties of propagating waves. In the latter case, the wavelength has to be small with respect to the dimensions of the vessel. For acoustical waves, this can be realized at relatively "low" frequencies ($\lambda \approx 1$ cm. for $\nu \approx 10^5$ c/sec.). For electromagnetic waves, these conditions will be fulfilled only at frequencies that are about five orders of magnitude higher. Therefore the study of acoustical wave phenomena is most appropriate, whereas the study of electromagnetic wave phenomena is not as suitable as far as chemical relaxation is concerned. Since high electric fields are required, the use of stationary electrical methods is restricted to special (nonconducting) systems. For the conducting systems, the use of transient methods is of advantage.

It will be shown in Section III.2 how a stationary measurement of κ_S and ε_{SV}, respectively, and their chemical terms can be carried out. We have to consider how these quantities and especially their "relaxing" chemical terms are related to directly detectable wave parameters, such as phase velocity and absorption coefficient. For practical reasons we restrict these considerations to acoustical wave phenomena. A treatment of similar electromagnetic phenomena, based upon Maxwell equations and involving dynamical permittivities with chemical contributions, would be analogous but of less practical importance for experimental applications.

E. WAVE PHENOMENA (SOUND ABSORPTION AND DISPERSION)

The theoretical treatment of sound propagation in fluids is essentially based on three fundamental equations: (1) the equation of continuity of mass flow; (2) Newton's second law, relating mass acceleration with force; and (3) an equation of state: $V = f(P,T)$, of which, however, only the existence has to be supposed.

The usual form of a wave equation can be obtained upon the linearization of these relations, if only small perturbations of density are to be considered.

For the one-dimensional case, by neglecting dissipative influences, this can be done in the following simple manner: On considering only a small change of density, ρ, given by the "condensation" s, due to $\rho = \rho_0 (1 + s)$, the equation of continuity reads

$$\partial s/\partial t + \partial \mathrm{u}/\partial \mathrm{x} = 0 \qquad \text{(II.3.78)}$$

$\mathrm{u}(= \mathrm{u_x})$ = particle velocity, x = space coordinate. The mass in the volume element $\delta V = q\delta \mathrm{x}$ (q = area) changes with the rate $\rho_0 q\delta \mathrm{x}(\partial s/\partial t)$, which must be equal to the net flow $\rho_0 \delta V$ div u $= \rho_0 q\delta \mathrm{x}(\partial \mathrm{u}/\partial \mathrm{x})$.

Newton's second law, on the other hand, can be written as

$$\rho_0(\partial \mathrm{u}/\partial t) = -(\partial P/\partial \mathrm{x}) \qquad \text{(II.3.79)}$$

since the force acting on an element of the fluid of thickness δx and area q,$q\delta \mathrm{x}(\partial P/\partial \mathrm{x})$, is equal to $\delta m(\partial \mathrm{u}/\partial t) = \rho_0 q\delta \mathrm{x}(\partial \mathrm{u}/\partial t)$. A combination of both equations yields

$$\partial^2 P/\partial \mathrm{x}^2 = \rho_0(\partial^2 s/\partial t^2) \qquad \text{(II.3.80)}$$

With the dynamic equation of state, which can be expressed by $(P - P_0) = (1/\kappa_S)s$, we obtain

$$\partial^2 P/\partial t^2 = (1/\rho_0\kappa_S)(\partial^2 P/\partial \mathrm{x}^2) \qquad \kappa_S = \kappa_S^{\infty} + \kappa_S^{\mathrm{ch}}\, \mathfrak{S}_{SP} \qquad \text{(II.3.81)}$$

with $(\rho_0\kappa_S)^{-1/2} = \mathrm{v}$ having the dimension of a velocity. In this derivation, use has been made of the fact that only small perturbations are involved

(allowing linearization,† replacement of material by partial differential quotients, relation of κ to P_0, and replacement of the stress tensor by hydrostatic pressure).

Details of the theoretical procedures leading to the complete wave equation and its solution can be found in textbooks of physics and special monographs (13). It is not possible here, because of space limitations, to give a thorough discussion of all physical questions connected with sound propagation in fluids. Instead—following the scope of the preceding chapters—we shall concentrate our interest on a more rigorous treatment of the chemical influences. All other effects are discussed only in so far as they emphasize the limitations of the methods as a "means of studying chemical kinetics." (Of course, apart from this coverage, there exist many other interesting problems of sound dispersion in relation to molecular physics which cannot be treated here at all.)

We may start our discussion with the statement (following from the solution of the wave equation), that, for a plane sound wave, propagated in the direction of the x axis, pressure and density will be periodic functions in t and x, expressed by the term

$$\exp\{j\omega(t - \mathrm{x}/\mathrm{v})\} \tag{II.3.82}$$

The velocity v does not simply represent the phase velocity of sound. For any real system—even in the absence of chemical or other molecular relaxation processes—v will be a complex quantity, due to the presence of dissipative processes such as viscous behavior and heat conduction causing dispersion and absorption of sound. These dissipative processes can be directly included in the fundamental equations, as will be shown later.

Let us first consider the influence of chemical relaxation processes only, exhibited by complex terms in the pressure-volume relationship, derived in the preceding section. The expression for the (dynamic) adiabatic compressibility was written as

$$\kappa_S = \kappa_S^{\infty} + \sum_i \bar{\kappa}_S^i \, \mathfrak{S}_i \tag{II.3.83}$$

where only the chemical terms were assumed to be complex functions. The assumption of a real term κ_S^{∞} is equivalent to the neglect of the above-mentioned dissipative (and, for instance, other structural relaxation) effects. As will be shown, the splitting of κ_S into these terms is justified as long as all volume changes, which are not related to chemical transformations, occur

† This linearization implies some restrictions for the sound intensities to be applied in experiments the interpretation of which is based on the theoretical expressions given in this paragraph. In general, the conditions are fulfilled as long as intensities remain appreciably below 1 w./cm.^{2}, as is usually the case for the equipment described below. The conditions can be tested by measurements at different intensities.

almost "instantaneously," i.e., sufficiently fast with respect to any chemical change. The (complex) sound velocity $\mathbf{v}$, introduced above, is directly related to the dynamic compressibility κ_S by

$$\mathbf{v} = [(\partial P/\partial \rho)_S]^{1/2} = [\rho\kappa_S]^{-1/2} \tag{II.3.84}$$

Since κ_S includes complex terms, $\mathbf{v}$ must also be complex and can be written in the form

$$1/\mathbf{v} = (1/\mathbf{v}_{re}) - (j\alpha/\omega) \tag{II.3.85}$$

defining a phase velocity $\mathbf{v}_{re}$ (real) and an attenuation coefficient α (dimension, cm.$^{-1}$). The physical meaning of α can be easily seen, if $1/\mathbf{v}$ is inserted into the complex expression $\exp\{j\omega[t - (x/\mathbf{v})]\}$, yielding a (real) damping factor $\exp(-\alpha x)$. The decrease of energy is accordingly characterized by a factor $\exp(-2\alpha x)$, since energy density will be proportional to the square of the pressure amplitudes. Apart from these definitions, the "absorption per wavelength" (λ = wavelength)

$$\mathfrak{u} = 2\alpha\lambda = 4\pi\alpha\mathbf{v}_{re}/\omega \tag{II.3.86}$$

is also often used in the representation of data. This quantity is related to the decrease of energy within the distance of one wavelength: $\exp[-(2\alpha\lambda)(x/\lambda)]$. Both $\mathbf{v}_{re}$ and α (or $\mathfrak{u}$, respectively) are frequency-dependent because of the relaxing terms in κ_S. Equation (II.3.84), combined with (II.3.85), yields

$$\rho\kappa_S = [(1/\mathbf{v}_{re}^2) - (\alpha^2/\omega^2)] - j(2\alpha/\omega\mathbf{v}_{re}) \tag{II.3.87}$$

or, by comparing with the real and imaginary parts of κ_S,

$$\mathbf{v}_{re}^2 = -2\,\mathrm{Re}(\kappa_S)/\rho[\mathrm{Im}(\kappa_S)]^2\{1 - [1 + (\mathrm{Im}(\kappa_S)/\mathrm{Re}(\kappa_S)^2]^{1/2}\} \tag{II.3.88a}$$

$$\mathfrak{u} = 4\pi\,\mathrm{Re}(\kappa_S)/\mathrm{Im}(\kappa_S)\{1 - [1 + (\mathrm{Im}(\kappa_S)/\mathrm{Re}(\kappa_S))^2]^{1/2}\} \tag{II.3.88b}$$

The symbols Re and Im designate the real and imaginary parts of κ_S:

$$\mathrm{Re}(\kappa_S) = \kappa_S^\infty + \sum_i [\bar{\kappa}_S^i/(1 + \omega^2\tau_i^2)] \qquad \mathrm{Im}(\kappa_S) = -\sum [\bar{\kappa}_S^i\omega\tau_i/(1 + \omega^2\tau_i^2)]$$

Since the chemical contributions $\sum_i \bar{\kappa}_S^i$ are usually very small as compared to κ_S^∞, which means $\mathrm{Im}(\kappa_S) \ll \mathrm{Re}(\kappa_S)$, we obtain the approximations

$$\mathbf{v}_{re} \approx [\rho\mathrm{Re}(\kappa_S)]^{-1/2} \tag{II.3.89a}$$

and

$$\mathfrak{u}^{ch} \approx -2\pi[\mathrm{Im}(\kappa_S)/\mathrm{Re}(\kappa_S)] \tag{II.3.89b}$$

($\mathfrak{u}^{ch}$ = chemical contribution to $\mathfrak{u}$). If (in solution) $\mathfrak{u}^{ch}$ is related to the solute, we may divide by n^0N_A, the total number of solute molecules per

cm.^{3}, obtaining a quantity $[Q\lambda]$, where Q is called the "absorption cross section" of a solute molecule (cm.^{2}/molecule) and λ is the wavelength. $[Q\lambda]$ may also be given (after multiplication by $N_A/10^3$) in M^{-1}.

For most practical applications (especially for solutions), the above approximations hold with sufficient accuracy. Inserting the expressions for $\mathrm{Im}(\kappa_S)$ and $\mathrm{Re}(\kappa_S)$ from Section II.3.D we obtain, with the approximation $\Sigma\kappa_S^i \ll \kappa_S^\infty$,

$$\mathbf{v}_{re} \approx [\rho\kappa_S^\infty]^{-1/2} \left\{ 1 - {}^1/_2 \sum_i [(\bar{\kappa}_S^i/\kappa_S^\infty)/(1 + \omega^2\tau_i^2)] \right\} \qquad \text{(II.3.90a)}$$

with $[\rho\kappa_S^\infty]^{-1/2} \equiv \mathbf{v}_{re}^\infty$, and

$$\mathfrak{y}^{ch} \approx 2\pi \sum_i [(\bar{\kappa}_S^i/\kappa_S^\infty)\, \omega\tau_i/(1 + \omega^2\tau_i^2)] \qquad \text{(II.3.90b)}$$

As may be seen from Equation (II.3.90a), the above approximation is directly equivalent to a small velocity dispersion (which, indeed, is usually <1%). Then, the contribution of a single relaxation step to $\mathbf{v}_{re}$† and $\mathfrak{y}$ exhibits directly the frequency dependence of $\mathfrak{S}_i$, e.g., a maximum of $\mathfrak{y}$ at $\omega \approx 1/\tau_i$. Both quantities ($\mathbf{v}_{re}$ and $\mathfrak{y}$) can be considered, therefore, direct measures of the real and imaginary parts of $\mathfrak{S}_i$. An experimental determination of their frequency dependence can immediately yield the relaxation times τ_i. It is with these applications of sound absorption and dispersion measurements that we are primarily concerned here. For such applications, it is important to cover a large frequency range in order to allow a complete determination of the different $\mathfrak{S}_i$ terms. Measurements at one frequency—even in the case of a one-step mechanism—would require the knowledge of all thermodynamic parameters involved in $\bar{\kappa}_S^i$, in order to allow a separate determination of the transfer function $\mathfrak{S}_i$ or relaxation time τ_i, respectively.

We have, however, to remember that the expressions (II.3.90) only represent approximations. Note that according to the presence of the (frequency-dependent) term $\mathrm{Re}(\kappa_S)$ in the denominator, the maximum in $\mathfrak{y}$ does not occur exactly at $\omega = 1/\tau_i$, (see below) and, furthermore, that τ_i is here given by τ_{SP}, which differs from τ_{TP}, the relaxation time at constant intensive variables according to the relations given in Section II.1.B. The usual rate equations in chemical kinetics [and also the normal variables introduced in Section II.1.C] are related to constant intensive variables.

There is an alternate derivation of the expressions for $\mathbf{v}_{re}$ and $\mathfrak{y}$ by using the definition $\mathbf{v}_{re}^2 = (\partial P/\partial\rho)_S = (V/\rho)(\partial P/\partial V)_S$ directly. The transfer functions entering $(\partial P/\partial\xi)_{S,V}(\partial\xi/\partial V)_{S,A}\mathfrak{S}_i$ are then related to $\tau_{S,V}$. The correct final expressions, of course, come out to be the same as above, if the relation between τ_{SV} and τ_{SP} is taken into consideration. This relation comes into play as soon as the approximate substitution of Equation (II.3.90) for (II.3.88) begins to fail. Expressions reported in the litera-

† The contribution of the real part of $\mathfrak{S}_i$ occurs in $\mathbf{v}_{re}$ with inverted sign, i.e., $\mathbf{v}_{re}$ increases around $\omega = 1/\tau_i$, whereas $\mathfrak{S}_i$ decreases.

ture are given in either one of the different forms. They agree with the correct expressions given above, as long as the thermodynamic conditions for the chemical transformations are stated correctly [*cf.* refs. (4) and (18)]. They usually differ slightly from the correct expressions (by practically negligible terms, as in the above approximation) if these conditions are not specified, (19–26).† The above approximation, Equations (II.3.90), still holds for the ω_{max} of a single absorption maximum with an accuracy of better than 1%, if κ_S^{ch} remains smaller than $0.4\kappa_S^{\infty}$ [as reported by Davies and Lamb (18)]. However, it has to be taken into consideration that the relation $\omega_{max}\tau_{SP} \approx 1$ is not fulfilled with the same degree of approximation. It follows, nevertheless, from the correct expression, that $\omega_{max}\tau_{SP} = (\bar{\kappa}_S/\kappa_S^{\infty})^{1/2}$ and, therefore:

$$\mathfrak{y}_{max}^{ch} = \pi\kappa_{S_i}^{ch}/(\bar{\kappa}_S\,\kappa_S^{\infty})^{1/2}$$

[*cf.* Eq. (34) in ref. (18); the quantity $\mathfrak{y}$ in this chapter, which is related to energy absorption, corresponds to $2\mathfrak{y}$ in ref. (18)]. For reactions in solution where the solute represents only a small fraction of the total matter, $\bar{\kappa}_S$ and κ_S^{∞} are almost equal, and ω_{max} is given by $1/\tau_{SP}(\approx 1/\tau_{TP})$ with an accuracy essentially higher than that of the present experimental determination. Correctly, the maximum of $\mathfrak{y}^{ch}$ occurs, according to Equation (II.3.88), at

$$1/\omega_{max} = (\kappa_S^{\infty}/\bar{\kappa}_S)^{1/2}\tau_{SP} = [(c_P^{\infty}c_V^{\infty}\kappa_T^{\infty})/(\bar{c}_P\bar{c}_V\bar{\kappa}_T)]\tau_{TP}$$

[*cf.* also Herzfeld and Litovitz (13), p. 82, where, for thermal relaxation processes: $\kappa_T^{\infty} = \bar{\kappa}_T$ is assumed]. The expression for $1/\omega_{max}$ can also be written as $1/\omega_{max} = (\tau_{SV}\tau_{SP})^{1/2} \equiv \tau_S$ if use is made of relation (II.1.17). This result indicates that there is no preference for P or V, the changing conjugate variables, but for S which is kept constant.

All these differences, however, are usually negligible, but can be taken into consideration (according to the relations given above) where necessary.

A more serious neglect in the above treatment is that of the dissipative processes such as heat conduction and viscous behavior, as well as of other, e.g., structural relaxation processes.

The latter processes could be treated in formal analogy to the chemical processes, as, in fact, has been done (27,28). They will therefore contribute terms to v_{re} and $\mathfrak{y}$ which have the same form as the chemical terms. Usually, the relaxation times for structural rearrangements in liquids are so short that the corresponding maxima in $\mathfrak{y}$ cannot be reached experimentally ($\omega_{max} > 10^{10}$ c/sec.). Then, these structural rearrangements may be considered almost in equilibrium with the forcing parameters during the process of chemical equilibration. The thermodynamic reaction parameters (ΔH, ΔV, K), entering $\bar{\kappa}_S^{ch}$, usually hold for such a condition of physical equilibration of solvent structure, etc. The structural equilibration itself will have practically no effect on the frequency dependence of v_{re} [since $1/(1 + \omega^2\tau^2) \approx 1$, the corresponding κ term is included in κ_{re}^{∞} as a constant] but will contribute to α (or $\mathfrak{y}$) a separate term that is proportional to ω^2 (or ω, respectively). If, on the contrary, these physical equilibration processes interfere in their time dependence with the chemical processes, they cannot be treated separately, but have to be considered in the choice of normal coordinates of the whole coupled

† Most of the expressions are related either to the temperature (22,24–26) or to the pressure dependence (21,23) of the equilibrium. The expressions quoted in ref. 24, though applied to electrolytes (for which the pressure dependence usually is decisive), do not describe correctly the pressure dependence (the ΔV^2 term is missing), and can therefor be used only for temperature-dependent systems.

reaction system (cf. Section II.1.C). This might be the case for reaction processes in the gaseous state which are coupled to energy transfer among the different degrees of freedom, occurring with time constants similar to those of the chemical transformations.

Dissipation of sound energy by heat conduction and viscous behavior can be taken into consideration by additional terms in the fundamental equations.

It would be beyond the scope of this chapter to give a more detailed treatment of these "classical" effects of sound absorption and dispersion (which can be found in the literature quoted above). Calculations of these terms have been carried out first by Stokes (29) (for the influence of shear viscosity) and by Kirchhoff (30) and Langevin (for the influence of heat conduction). The absorption coefficient α_{class} and the change of phase velocity v_{re}, as compared to the "low-frequency value" v_{re}^0, describing these "classical" effects, can be written approximately as

$$\alpha_{class} = \frac{\omega}{4\pi v_{re}} \mu_{class} = \frac{2}{3} \frac{\omega^2}{v_{re}^3 \rho} \left[\eta + \frac{3}{4} (\gamma - 1) \frac{\lambda_h}{c_P} \right] \quad \text{(II.3.91a)}$$

$$\left(\frac{v_{re}^0}{v_{re}} \right)^2 = 1 - \left[\left(\frac{2}{3} \eta - \frac{\gamma - 1}{2} \frac{\lambda_h}{c_P} \right)^2 - (\gamma - 1) \left(\frac{\lambda_h}{c_P} \right)^2 \right] \frac{\omega^2}{\rho^2 v_{re}^4} \quad \text{(II.3.91b)}$$

(η = shear viscosity, $\gamma = c_P/c_V$, c_P and c_V = specific heats at constant pressure and volume, respectively, λ_h = heat conductivity, and ρ = density). The second term in brackets, which describes the influence of heat conduction, is usually much smaller than the first one (i.e., the viscosity term). Structural and other relaxation effects could be included formally in the above treatment by replacing the shear viscosity η by $\eta + (3/4)\eta_b$, where η_b is defined as bulk or volume viscosity. This definition is related to the excess of α over α_{class}; η_b contains contributions of shear and dilatational viscosity: $\eta_b = \eta' + (2/3)\eta$, where η' is the dilatational viscosity (31). In most fluids, the measured values of α exceed appreciably α_{class}, owing to delayed energy exchange between external and internal molecular degrees of freedom and structural or chemical relaxation processes. In associated liquids, the structural influences may be predominant. As an example, we may consider pure water. With a shear viscosity of 1.0×10^{-2} poise (g. cm.$^{-1}$ sec.$^{-1}$) and a sound phase velocity of 1.48×10^5 cm. sec.$^{-1}$ we may calculate a value of about 8×10^{-17} sec.^{2} cm.$^{-1}$ for α_{class}/ν^2 at 20°C. The measured value of α/ν^2 amounts to about 25×10^{-17} sec.^{2} cm.$^{-1}$ at 20°C., the difference being primarily related to the relaxation of water structure. (For comparison, the value α/ν^2 for a 0.1M $MgSO_4$ solution at $\nu = 10^4$ c/sec., due to chemical relaxation, amounts to about 3×10^{-14} sec.^{2} cm.$^{-1}$.) The influence of heat conduction in α_{class} is especially small for water, since $c_P \approx c_V$ (as a result of the density anomaly at 4°C.). The factor $(\gamma - 1)$ is therefore almost zero, which means that, even at 20°C., the adiabatic temperature oscillation is still very small. For liquids, the order of magnitude of λ_h/c_P is usually 10^{-3} (g. cm.$^{-1}$ sec.$^{-1}$) as compared to viscosities of around 10^{-2} (g. cm.$^{-1}$ sec.$^{-1}$). Since $3/4\,(\gamma - 1) < 1$, the heat conduction term may generally be neglected in fluids. The influence of the dissipative processes in v_{re} is very small. With the data given above, the relative change of $1/v_{re}^2$ with respect to $1/v_{re}^{0\,2}$ amounts to only about 10^{-4} at $\nu = 5 \times 10^8$ c/sec. (the upper-frequency limit for studies in liquids).

It is important to note that α_{class} increases with the square of the frequency, as is characteristic of a relaxation process at frequencies $\omega \ll 1/\tau$. The above expressions, indeed, are valid only at frequencies that are appreciably below a "relaxation time" of the order of magnitude of reciprocal frequencies of molecular collisions. However, our considerations should not be extended to such high frequencies, where the validity of

continuum theory may be questioned. For liquids, the frequencies at which deviations of α_{class} from proportionality to ω^2 should occur are far above the experimental range. For gases, this may not always be the case.

The above treatment suggests that sound absorption data, generally, may be represented by an expression of the form

$$\mathfrak{y} = A'\omega + \sum_i B'_i[\omega\tau_i/(1 + \omega^2\tau_i^2)] \qquad \text{(II.3.92)}$$

or

$$\alpha = A''\omega^2 + \sum_i B''_i[\omega^2\tau_i/(1 + \omega^2\tau_i^2)]$$

Here the second term represents the coupled chemical relaxation processes as expressed by Equation (II.3.90), whereas the first term includes all dissipative, structural (and eventual further fast chemical) effects, which in the experimental frequency range may be considered (almost completely) equilibrated.

Meixner (32) has given a more general treatment, where the transport effects are not handled separately from other molecular relaxation effects. As a result, he obtains a determinant equation, similarly as in the treatment of coupled chemical reactions in Section II.1.C, but with the inclusion of the dissipative transport processes. The question, therefore arises whether a representation of data by separate chemical, structural, and "classical" terms is justified at all. For the present applications, this justification can be given and has also been demonstrated by experiments with systems (33) in which the complete chemical terms could be calculated from the known ΔV, ΔH, and K values. The validity of a separate treatment is contingent upon certain conditions. A trivial condition would be that the classical (and structural) effects are negligibly small compared to the chemical effects. This may not be the case for chemical effects in less concentrated solutions. However, another (sufficient) condition has already been mentioned: The equilibration of the chemical processes has to be slow enough, so that structural spatial and energy distribution can be considered almost completely in equilibrium according to thermodynamic conditions. (This condition is, in most cases, fulfilled for the frequency range of present applications.) Similarly, fast chemical steps must be considered in the treatment of slower steps only with their equilibrium properties (*cf.* Section II.1.C). The "static" reaction parameters ΔV, ΔH, and K are also related to a complete equilibration of the physical state of the solution. Meixner's treatment, therefore, is important in order to show the limitations of the methods, as far as they are used for a study of chemical kinetics. If the conditions are such that cross relations between chemical and other relaxation effects come into play, the quantitative interpretation of data may become very complicated and the method becomes useless, as far as analysis of chemical reaction mechanisms is concerned.

In the expressions of $\mathfrak{v}_{re}$, corresponding to Equation (II.3.92), only the chemical terms may contribute to a (measurable) frequency dependence. However, as the part $\mathfrak{v}_{re}^{\infty}$ is usually very large, in comparison with the chemical terms, very sensitive methods would be required. On the other hand, the relative extent of the chemical terms in $\mathfrak{y}$ is much higher, so that

sound absorption methods are usually more appropriate for chemical relaxation studies. For measurements in solution, relatively high concentrations of the solute (in most cases greater than $10^{-2}M$) are required in order to allow a separation of the A' and B' terms. This requirement implies some disadvantage with respect to the more sensitive transient methods (*cf.* Section III). A very convenient mode of evaluation is to plot the quantity α/ν^2 against frequency, yielding a constant for the A'' term, but frequency dependencies for the B'' terms around $\omega\tau_i \approx 1$ (*cf.* Figure II.10).

An evaluation may become complicated, if the τ_i values differ only slightly (*cf* Section II.1.D). Real continuous relaxation spectra are not to be expected for chemical processes because of their discrete nature. For

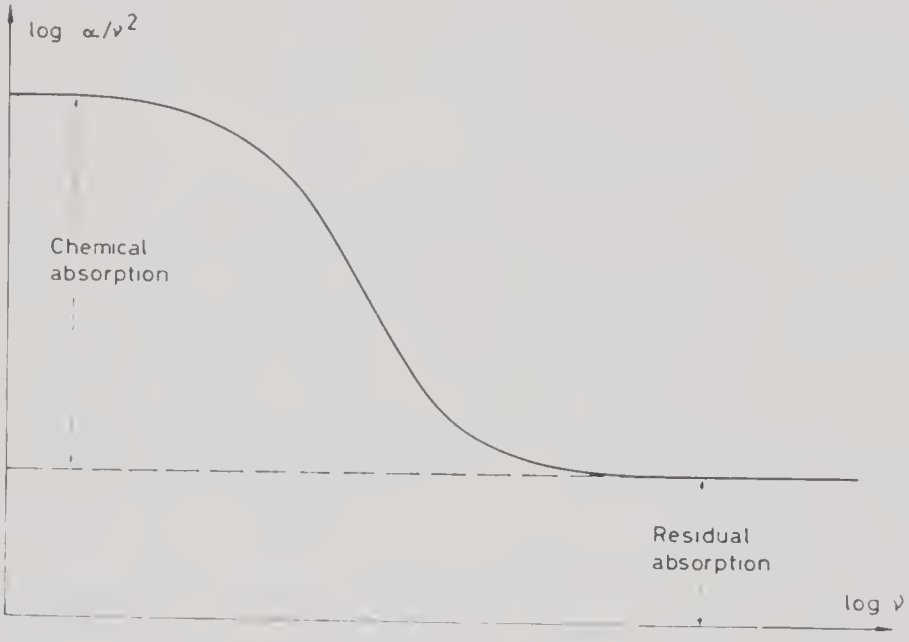

Fig. II.10. α/ν^2 as a function of ν representing chemical and residual parts of sound absorption.

ionic reactions there might be some coupling to the relaxation of the ionic atmosphere, which is characterized by a continuous spectrum of relaxation times (*cf.* Section II.1.C) The effect of relaxation of the ionic atmosphere on sound absorption has been calculated by Leontovic (34) and Hall (35). These calculations are related to small concentrations, in which the approximations of the Debye-Hückel theory of electrolytes are applicable. At these concentrations, however, the absolute contributions to μ would become—for ordinary frequencies undetectable—very small. For higher concentrations, the theoretical suppositions are no longer fulfilled. The relaxation times then become very small, so that the ionic atmosphere directly contributes only to the A' term (which can be determined empirically). For the coupling to the slower chemical transformations (B' terms),

only the equilibrated ionic atmosphere is of importance and the use of activity coefficients is justified [*cf.* ref. (17)].

For a determination of the A' terms in solution, it is not sufficient to measure only the excess absorption of the solution relative to that of the pure solvent, since the solvent absorption itself may change when solute is present at higher concentration (e.g., breaking of water structure in the presence of electrolytes). The only correct way is to take measurements over the whole frequency range, where the B' terms under discussion contribute to the absorption. If the above-mentioned restrictions are taken into consideration the sound-absorption method can give quite reliable information about the kinetics of fast reactions.

We may conclude our discussion by considering again as example (17) the two-step mechanism of ionic recombination in solution:

$$A^+ + B^- \underset{21}{\overset{12}{\rightleftharpoons}} AB \underset{32}{\overset{23}{\rightleftharpoons}} C \qquad (\text{with } k'_{12},\ k_{21} \gg k_{23},\ k_{32})$$

Kinetics and equilibrium have already been treated in Sections II.1.C and II.3.B, respectively [*cf.* Equations (II.1.25) ff., and (II.3.32) ff.]. A sufficiently accurate treatment, using the normal variables (and transformation matrices) derived in Section II.1.C, is possible, as the chemical contributions $\bar{\kappa}_S^{ch}$ are small with respect to κ_S^∞. This, also, implies that $\tau_{SP} \approx \tau_{TP}$, $c_P^\infty \approx \bar{c}_P$ and is equivalent to small velocity dispersion. The complete expressions for excess sound absorption (corresponding to the B' terms) are:

$$\mathfrak{u}^{ch} = \mathfrak{u}^{I} + \mathfrak{u}^{II} = (2\pi\bar{\kappa}_S^{I}/\kappa_S^\infty)[\omega\tau_I/(1+\omega^2\tau_I^2)] + (2\pi\bar{\kappa}_S^{II}/\kappa_S^\infty)[\omega\tau_{II}/(1+\omega^2\tau_{II}^2)] \quad \text{(II.3.93)}$$

with

$$\bar{\kappa}_S^{I} = \{n_0\Gamma_I/[1+\Gamma_I(\partial\ln\bar{f}^2/\partial\alpha)_{T,P}]\}\{[\Delta V_I - (\alpha_P^\infty/\rho\bar{c}_P^\infty)\Delta H_I]^2/RTV\} \quad \text{(II.3.94)}$$

related to the relaxation time [*cf.* Equation (II.1.29)]

$$\tau_I = 1/(k'_{12} + k_{21})$$

and

$$\bar{\kappa}_S^{II} = \{n_0\Gamma_{II}/[1+\Gamma_0(\partial\ln\bar{f}^2/\partial\alpha)_{T,P}]\}\{[\Delta V_{II} - (\alpha_P^\infty/\rho\bar{c}_P^\infty)\Delta H_{II}]^2/RTV\} \quad \text{(II.3.95)}$$

related to the relaxation time [*cf.* Equation (II.1.29)]:

$$\tau_{II} = 1/[k_{32} + k_{23}k'_{12}/(k'_{12} + k_{21})]$$

The reaction parameters $\Gamma_{I,II}$, Γ_0, $\Delta V_{I,II}$, and $\Delta H_{I,II}$ have been introduced in Section II.3.B [*cf.* Equations (II.3.36) to (II.3.39)]. The quantity α (to be distinguished from the residual expansion coefficient α_P^∞) represents the total degree of dissociation: $\alpha = m_A/(m_A + m_{AB} + m_C)$, f^2 the mean square of the activity coefficients of the ions (f_{AB} and f_C are assumed to be unity). The omission of factors like c_P^∞/c_P in $\bar{\kappa}_S^i$ [*cf.* Equation (II.3.60)] and τ_i [*cf.* Equation (II.1.17)] as well as the replacement of α_P^∞ and c_P^∞ by $\bar{\alpha}_P$ and $\bar{c}_P$ is justified, since even at higher concentrations of the solute any neglect of this kind remains within the present limits of experimental error. In the above expressions, the term $\mathfrak{y}^I$ is related to the fast equilibration of step 1–2, where 3 remains almost unchanged. Expressions of the same form hold for a one-step dissociation equilibrium. The term $\mathfrak{y}^{II}$ is related to the slower equilibration of step 2–3, whereby step 1–2 is always maintained at equilibrium. Therefore, $\mathfrak{y}^{II}$ representing the complete equilibration, contains parts which are related to step 2–3 as well as to 1–2. However, only the ratio of k_{12}' to k_{21}, which is a function of the equilibrium constant K_{12}, not the single rate constants, enters the relaxation time. If k_{12}' were zero ($\alpha = 0$), $\mathfrak{y}^{II}$ would be representative of a one-step first-order transformation.

For reactions in aqueous solutions, the ΔV term is usually much larger than the term $(\alpha_P^\infty/\rho c_P^\infty)\Delta H$, for three reasons:

(i) The ΔV values are relatively large (several cm.^{3}/mole), since a charge neutralization involves considerable changes of solvent structure such as desolvation, etc. (e.g., $NH_4^+ + OH^- \rightleftharpoons NH_3 \cdot H_2O$: $\Delta V = V_{NH_3 \cdot H_2O} - V_{NH_4^+} - V_{OH^-} \approx 28$ cm.^{3}/mole).

(ii) The ΔH values are relatively small (i.e., a few kcal./mole), as far as electrolytes with pK values between 2 and 8 are concerned. (For $pK > 8$ the dissociation will be too weak to give any measurable contribution to sound absorption.) In this range, the pK values of electrolytes are primarily determined by the relatively large ΔS values.

(iii) The quantity $\alpha_P^\infty/\rho c_P^\infty$ is especially small for aqueous solutions (it is even zero for water at 4°C.). Some values are quoted below:

ϑ[°C.]	0	10	20	40
$10^3(\alpha_P^\infty/\rho c_P^\infty)$[l./kcal.]	−0.06	0.09	0.21	0.39

Thus, at room temperature a $|\Delta H|$ of 1 kcal./mole contributes considerably less to $\bar{\kappa}_S^{ch}$ than a $|\Delta V|$ of 1 cm.^{3}/mole. The differences of $\bar{\kappa}_S^{ch}$ and $\bar{\kappa}_T^{ch}$ are, therefore, for many aqueous electrolyte systems, beyond the accuracy of experimental detection. Furthermore, the term $(\partial \ln f^2/\partial\alpha)_{T,P}$ is negligible for small ionic concentrations, or in the presence of an excess of indifferent electrolyte (constant ionic strength, buffered solution). Even for higher concentrations of reacting ions ($\sim 0.1M$), the term remains relatively

small, since activity coefficients generally exhibit a flat minimum and subsequent rise at higher concentrations.† The relaxation of the ionic atmosphere is not included in the above expressions. For low concentrations of ions, the numerical contribution to $\mathfrak{y}$ would be negligible. At higher concentrations, e.g., greater than $0.1M$, the relaxation time of the ionic atmosphere equilibration becomes less than 10^{-9} sec. so that, up to frequencies greater than 10^8c/sec., this contribution is included in $\mathfrak{y} - \mathfrak{y}^{ch}$, having the form $A'\omega$.

As a numerical example, we estimate $\mathfrak{y}^{ch}_{max}$ for a one-step electrolytic dissociation equilibrium (NH_3 in aqueous solution) with $\alpha^2 c_0/(1 - \alpha) = K'_0/\bar{f}^2 = 1.7 \times 10^{-5}$ mole/l. ($f^2 \approx$ const ≈ 1), $c_0 = 0.5$ mole/l., $\Delta V = 2.8 \times 10^{-2}$ l./mole, $(\alpha^\infty_P/\rho c^\infty_P)\Delta H$ negligible, e.g., $\Delta H < 1$ kcal./mole, $\kappa_{H_2O} = 4.5 \times 10^{-5}$ atm.$^{-1}$, and $T = 298°$K. ($R = 8.205 \times 10^{-2}$ l. atm./mole deg. The maximum value of $\mathfrak{y}^{ch}$ at $\omega = 1/\tau$, according to Equation (II.3.94), would be:

$$\mathfrak{y}^{ch}_{max} \approx (\pi \bar{\kappa}^{ch}_T/\bar{\kappa}_T) = (\pi/RT\kappa_{H_2O})(\Gamma_\xi/V)[\Delta V]^2$$

$$\mathfrak{y}^{ch}_{max} \approx 2.9 \times 10^3[\text{mole/l.}]\, c_0\Gamma_\alpha[\Delta V]^2[\text{l./mole}] \approx 3.3 \times 10^{-3} \tag{II.3.96}$$

or

$$[Q\lambda]_{max} \approx 4.8 \times 10^{-24}[\text{mole}^2/\text{cm.}^3]\, \Gamma_\alpha[\Delta V]^2[\text{cm.}^6/\text{mole}^2] \approx 10^{-23}[\text{cm.}^3]$$

Both numerical factors* hold only for aqueous solutions at $T = 298°$K. With $\Delta H = 1$ kcal./mole we would have for $(\tau_{TP} - \tau_{SP})/\tau_{TP} \approx 6.6 \times 10^{-5}$. Thus τ_{SP} can be replaced by τ_{TP}, as obtained from the kinetic expression in (Section II.1.A).

The expressions (II.3.94) and (II.3.95) have been tested quantitatively for a number of protolytic and metal complex reactions in aqueous solution (4,33,36,37). The metal-complex formation can, in many cases, be represented as a two- or three-step mechanism, where ion-pair formation is followed by a (slower) substitution of H_2O molecules from outer- and inner-coordination spheres of the metal ions.

For nonelectrolytes and especially for nonaqueous solutions, the situation may be just the reverse; i.e., the ΔV values are usually smaller (less than 1 cm.^{3}/mole), the ΔH values larger (e.g., 10 kcal./mole and more) and

† It is important to note that the activity coefficients to be inserted should include only the contributions from general ionic interactions, but not the specific interactions of the reacting ions. The literature values for many electrolytes include both influences (In the simplest case such values would correspond to $\alpha\bar{f}$.)

* Note, that with the definitions introduced in Section II.3.B: $n_0\Gamma_\alpha = \Gamma_\xi$, $\Gamma_\alpha = \alpha(1 - \alpha)/(2 - \alpha)$ (for this example) and $n_0/V = c_0$.

the factor $\alpha_P^\infty/\rho c_P^\infty$ becomes larger than 1 cm.^{3}/kcal. As an example, we may estimate $\mathfrak{y}_{\max}^{ch}$ for the dimerization of benzoic acid with toluene as the solvent. With $K' = [A]^2/[A_2] = 2.3 \times 10^{-3}$ mole/l. (activity coefficients ≈ 1) $c_0 = 10^{-1}$ mole/l.; $\alpha_P^\infty/\rho c_P^\infty \approx 3.05$ ($c_P \approx 0.42$ cal./deg. g., $c_V \approx 0.3$ cal./deg. g.), $\Delta H = 5.7$ kcal./mole (ΔV negligible e.g. $\leqslant 1$ cm.^{3}/mole), $\kappa_{tol} = 8.7 \times 10^{-5}$ atm.$^{-1}$, the maximum value of $\mathfrak{y}^{ch}$ for $\omega = 1/\tau$ is

$$\mathfrak{y}_{\max}^{ch} \approx (\pi/\bar{\kappa}_S)(\Gamma_\xi/RTV)[(\alpha_P/\rho c_P^\infty)\Delta H]^2 = (\pi/\kappa_{tol})(\bar{\alpha}^2{}_P/\rho \bar{c}_V)(\bar{c}_P^{ch}/c_P) \tag{II.3.97}$$

$$\mathfrak{y}_{\max}^{ch} \approx 4.3 \times 10^{-3} \text{ (at } T = 298°\text{K.)}.$$

If a dimerization includes the formation of two hydrogen bonds, the general mechanism may be similar to the above two-step mechanism. [For experimental studies of this kind see ref. (26).]

Expressions for mechanisms with more than two subsequent steps (with monotonously decreasing rate constants (i.e., $k_{12}', k_{21} \gg k_{23}, k_{32} \gg k_{34}, k_{43}$, etc.) can be explicitly derived, and are formally similar to those given above [*cf.* ref. (4)].

References

1. E. A. Guggenheim, *Thermodynamics 4th* ed., North Holland Publ. Co. Amsterdam, 1959.
2. Th. De Donder, *Bull. Acad Roy. Belg. (Cl. Sc.) (5)*, **7**, 197, 205 (1922).
3. (a) I. Prigogine and R. Defay, *Chemical Thermodynamics*, Longmans Green and Co., London, 1954. (Translation from French edition: Maison Desoer Ed., Liege, Belgium 1944 and 1946.) (b) W. Schottky, H. Ulich, and C. Wagner, *Thermodynamik*, Springer Verlag, Berlin, 1929.
4. M. Eigen and K. Tamm, *Z. Elektrochem.*, **66**, 93 (1962).
5. L. Onsager, *J. Chem. Phys.*, **2**, 599 (1934).
6. Reference 1, pg. 412.
7. H. S. Frank, *J. Chem. Phys.*, **23**, 2023 (1955); *cf.* also F. O. Koenig, *J. Phys. Chem.*, **41**, 597 (1937).
8. K. Bergmann, M. Eigen, and L. DeMaeyer, *Z. physik Chem.*, 1963.
9. A. Piekara and A. Chetkowsky, *J. Chem. Phys.*, **25**, 794 (1956).
10. J. Meixner, *Kolloid-Z.*, **134**, 3 (1953).
11. R. de L. Kronig, *J. Opt. Soc. Am.*, **12**, 547 (1926); H. A. Kramers, *Physik. Z.*, **30**, 522 (1929).
12. V. L. Ginzberg, *Soviet Phys.—Acoustics*, **1**, 32 (1957).
13. K. F. Herzfeld and T. A. Litovitz, *Absorption and Dispersion of Ultrasonic Waves*, Academic Press, New York, 1959.
14. W. Fuller Brown Jr., in *Encyclopedia of Physics*, Vol. XVII, Springer, Berlin, 1956, pg. 119ff
15. K. S. Cole and R. H. Cole, *J. Chem. Phys.*, **9**, 341 (1941).
16. R. M. Fuoss and J. G. Kirkwood, *J. Am. Chem. Soc.*, **63**, 385 (1941).
17. M. Eigen, *Discussions Faraday Soc.*, **24**, 24 (1957).
18. R. O. Davies and J. Lamb, *Quart. Revs.*, **11**, No. 2, 134 (1957).
19. L. Liebermann, *Phys. Rev.*, **76**, 1520 (1949).

20. R. Barthei, *J. Acoust. Soc. Am.*, **24**, 313 (1952).
21. M. Manes, *J. Chem. Phys.*, **21**, 1791 (1953).
22. E. Freedman, *J. Chem. Phys.*, **21**, 1784 (1953).
23. M. Eigen, G. Kurtze, and K. Tamm, *Z. Elektrochem.*, **57**, 103 (1953).
24. D. Tabuchi, *J. Chem. Phys.*, **26**, 993 (1957).
25. J. Lamb, *Z. Elektrochem.*, **64**, 135 (1960).
26. W. Maier, *Z. Elektrochem.*, **64**, 132 (1960).
27. L. Hall, *Phys. Rev.*, **73**, 772 (1948).
28. R. N. Barfield and W. G. Schneider, *J. Chem. Phys.*, **31**, 488 (1959).
29. G. Stokes, *Trans. Cambridge Phil. Soc.*, **8**, 287 (1845).
30. G. Kirchhoff, *Poggendorf's Ann. Phys.*, **134**, 177 (1868).
31. *American Institute of Physics Handbook*, McGraw-Hill, New York, 1957, p. **3**, 28.
32. J. Meixner, *Ann. Phys.*, **43**, 470 (1943).
33. M. Eigen, *Chemische Relaxation* (*loc. cit.* Sec. I.).
34. M. Leontovic, *Expt. Theor. Phys.* (*USSR*), **8**, 40 (1938).
35. L. Hall, *J. Acoust. Soc. Am.*, **24**, 704 (1952).
36. M. Eigen, *Z. physik. Chem. N. F.*, **1**, 176 (1954).
37. M. Eigen, G. Maass, and G. Schwarz, *Z. physik. Chem. N. F.*, in preparation.

4. Concluding Remarks

The extensive theoretical treatment given in Section II may lead to the impression that, for the application of relaxation methods, many suppositions have to be fulfilled and that the interpretation of the results involves excessive theoretical considerations. This is not the case, however.

The relaxation methods represent *direct* methods, just as the classical techniques of chemical kinetics do. In the transient methods, the temporal change because of chemical transformation is *directly* recorded. In the stationary methods, it is converted into a characteristic frequency dependence, which can again be recorded so as to yield *directly* the relaxation times. In general, these determinations do not depend on a quantitative knowledge of the shift of equilibrium or its dependence on T, P, or $\mathbf{E}$. It is only supposed that such a dependence exists, regardless of whether the considered chemical change is initiated primarily or secondarily via a coupled-reaction system. Therefore, the theoretical treatment given in Section II.3 is necessary only in so far as it shows the appropriate conditions for chemical applications and the limitations. (A more complicated behavior, for instance, is present, if the considered chemical change contributes predominantly to the thermodynamic functions of the total system. The relaxation times then become dependent on the thermodynamic conditions maintained. These difficulties are usually not present for studies in solutions where the concentrations of reactants are not too high.) For chemical rate studies, the methods are the more useful the more specific they are with respect to the reacting species.

In Section II.2 it was shown how the relaxation times can be determined from the temporal or frequency response of the system. This procedure,

of course, is characteristic of any kinetic method making use of integrated reaction rate equations.

The results of Section II.1 are important for the interpretation of the properly determined relaxation times. For single-step systems (Section II.1.A) an analysis is quite trivial; reaction order and rate constants can readily be obtained from studies at different concentrations. Difficulties may arise in the analysis of relaxation spectra of multiple-step systems (Section II.1.C). These difficulties may, however, be less serious than when they occur in the usual studies of chemical kinetics, since the linearized rate equations allow a general mathematical representation of the temporal behavior in the form of a time or frequency spectrum. Such a comprehensive representation is usually not possible for higher-order reaction processes far from equilibrium. Any difficulties in the numerical evaluation of relaxation spectra are not a result of the method, but are due to the reaction mechanism, which must anyway be given a rigorous kinetic treatment.

An important requirement for the theoretical description given above was the assumption of small perturbations of equilibrium. This requirement, of course, imposes some restrictions on the application of relaxation methods. On the other hand, there is no reason why the methods should be applicable to equilibrium systems only. Any stationary reaction state, which is characterized by a zero net rate of transformation, could be perturbed in the above sense (e.g., by the use of a flow or photostationary technique in combination with a relaxation method), allowing a similar theoretical treatment of the resulting relaxation processes. In many cases, the stationary state involves an intermediate which is itself in true equilibrium; then, no principal difference from the above treatment will exist. [Such studies have been carried out, for instance, with unstable semiquinones (1).] From a more general point of view, however, the stationary state differs considerably from the equilibrium by the fact that it represents an "open" chemical system with in- and out-flux of energy and matter. For such a system, the conditions of microscopic reversibility are not necessarily fulfilled for every reaction step. For the general treatment of equilibration, the condition of microscopic reversibility is important as it implies the nonexistence of true periodic solutions of the rate equations which would lead to resonance instead of relaxation (*cf.* ref. 2–4). In principle, periodic reactions may exist in homogeneous *open* systems, if nonlinear terms occur in the primary rate equations.

Another problem, not treated here, is that of nonlinear relaxation effects, i.e., equilibration upon very strong perturbations of equilibrium. A general treatment of these processes does not exist, though specific reaction problems have been handled in monographs on reaction kinetics. Relaxa-

tion studies of this kind (apart from shock-wave studies) have scarcely been carried out, though methods are known by which equilibria can be shifted by many orders of magnitude upon rapid change of T, P (5), or **E** (*cf.* Section III.1).

References

1. H. Diebler, M. Eigen, and P. Matthies, *Z. Naturforsch.*, **16b**, 629 (1961).
2. A. I. Lotka, *Elements of Physical Biology*, Williams and Wilkins, Baltimore, 1925, chapter VIII, pg. 77.
3. K. F. Bonhoeffer, *Z. Elektrochem.*, **51**, 24 (1948).
4. W. Jost, *Z. Naturforsch.*, **2a**, 159 (1947).
5. S. D. Hamann and H. G. David, *Trans. Faraday Soc.*, **55**, 72 (1959).

III. EXPERIMENTAL TECHNIQUES

In Section (II.2) a distinction has been made between transient and forced relaxation behavior, and it has been related to different mathematical forms of the forcing function, i.e., the temporal course of the external parameter disturbing the equilibrium. This distinction is also reflected in two groups of experimental methods, because the determination of a rapid transient or of a long-lasting stationary state corresponds to two quite different experimental situations. Transient and stationary methods will therefore be treated separately.

There is, of course, a large variety of instrumental possibilities for the determination of given quantities. It is almost impossible to give detailed technical descriptions of the various types of apparatus which have been found appropriate in special cases. The basic principles underlying different experimental techniques will be shown, and the approximate range of their applicability given. For a unified treatment of different techniques that have been applied to the study of chemical relaxation, we may use the fact that any experimental method has two different requirements: First, the equilibrium state of the chemical system to be studied must be disturbed in a known manner, and second, the resulting effect must be recorded. In some cases the experimental equipment may reflect quite directly this double aspect of relaxation measurements, in that either task is assumed by different and separated parts of the instrument. In other cases this distinction may not be obvious at first appearance; it is useful, however, to characterize a measuring technique (*1*) by the external variable that is changed in order to obtain a displacement of the equilibrium (pressure, temperature, electric field, magnetic field, and radiation energy) and (*2*) by the internal variable used for the determination of subsequent chemical changes.

1. Transient Methods

In transient methods, the chemical changes are directly measured as a function of time. In many cases, transient methods have certain advantages over stationary ones, because they can be more easily adapted to specific requirements and may then lead to greatly increased sensitivity of measurement. Because of the special form of forcing functions required for transient studies (impulse functions), the system to be studied can be subjected to much greater disturbances than is generally possible using periodic changes of external parameters, and the corresponding displacements of the chemical equilibrium can be much larger. At the same time, special analytical methods are used for the detection of concentration changes. These methods may be specific for the concentration variation of a given compound so that measurements are possible at a very low concentration of this compound. Another advantage of transient methods is that they are inherently adapted to measurements on small samples of the system [for a survey of techniques see also refs. (1) and (2)]. The ultimate sensitivity of transient methods is limited by the band-width requirements and the corresponding noise level of the measuring equipment (*cf.* Section III.1.F).

A. DETECTION OF CONCENTRATION CHANGES

The changes in a chemical system can be followed using any quantity related to the number of atoms, ions, molecules, or compounds of a particular species present in the system and undergoing the chemical transformation.

It is obvious that a direct chemical analysis of the composition (e.g., by titration) is usually too slow to be applied to studies of fast reactions; physical analytical methods will, in general, be used. Many of these physical methods do not detect the total number of moles of the species in the system, but they measure the number of moles in a given volume,which is representative of the whole system. A consideration of volume changes accompanying the disturbance of the forcing parameter will be necessary. In most cases, however, such volume changes are much faster than the concentration changes, so that they do not interfere with the measurement of relaxation times. If special difference techniques are used (see below), the volume changes can also be canceled.

(1) *Optical properties* are especially suitable for the determination of concentration changes, as such properties may be specific for one of the components of the reacting system. The variation of optical properties can be followed very rapidly and with great sensitivity using photoelectric transducers (photomultipliers). Absorption spectrometry has already been

used in a method with temperature as the forcing variable (3,4). The use of fluorescence spectrometry may increase the sensitivity at low concentrations (5). Refractometric or polarometric techniques (measurement of optical rotation) may also be very efficient for special problems (6).

(2) *Electric properties* of the system give information on the chemical composition if ionic or dipolar species are involved. Reactions accompanied by formation or disappearance of ions may be followed most easily by measurement of electrical conductance (7–10). The main advantages are the high sensitivity of such measurements and the high accuracy that can be obtained by bridge circuits, which are easily adapted for difference measurements (deviations of $\sim 1\%$ are easily detected and can be measured accurately in very short times).

The dielectric constant of a medium may also be dependent upon its chemical composition. With present experimental techniques, high relative accuracy and fast measurements are possible (11).

(3) Among *mechanical properties* the pressure change in a chemical system at constant volume is a rapidly measurable quantity especially suitable for studying the course of gas-phase reactions that are accompanied by a variation in the number of molecules. Such pressure changes can be followed, for instance, by a microphone or by piezoelectric transducers. Although no such technique has been used in the study of chemical relaxation, this possibility may be mentioned.

(4) *Thermal properties* of the reaction system may also be utilized in the study of a fast chemical transformation. A rapid calorimetric method in which heat of reaction is measured has been described (12), although the time resolution is not very high.

(5) In some cases, it is preferable to introduce a *chemical indicator*, which is coupled by a very rapidly established equilibrium to the other components the relaxation behavior of which is to be studied (13). Many such indicators have been used for a long time in analytical work, because their concentrations can be easily and accurately measured, owing to their specific light absorption or fluorescence properties. The relaxation time of the indicator equilibrium should be measured separately. This relaxation time should be short compared to the relaxation times of the system to be studied, if the measurements are to lend themselves to easy interpretation. According to the same principle, a coupled buffer equilibrium which strongly depends on external parameters may be used to generate appreciable concentration changes in a system that alone is too insensitive with respect to the forcing parameter (3).

It must be emphasized that almost any of the above-mentioned physical properties do not depend only upon chemical composition; they are generally disturbed by the forcing parameter as a result of changes in the

physical state of the system. Therefore, practically every measurement, with the purpose of an accurate determination of the change of a chemical variable, will be carried out by a difference method. In such a method, one of the systems, the reference system, does not contain the chemical components whose transformation is to be studied, but in all other aspects, especially in regard to the physical interdependence of the forcing and the measured variables, it should be as similar as possible to the other system in which chemical transformation takes place.

Another advantage of difference methods is the increased sensitivity and relative accuracy that can be obtained. When electric properties are measured, the customary bridge arrangements can be used. For optical measurements, a split-beam technique will be most appropriate (3–6). In those cases where a direct difference measurement is difficult, a reference system can be studied in the same apparatus under identical conditions. In this case, however, measuring techniques with sufficient sensitivity and precision are required.

B. TEMPERATURE-JUMP METHODS

One of the most appropriate techniques for rapidly disturbing a chemical reaction equilibrium is a sudden change of temperature: almost any chemical reaction equilibrium is either temperature dependent or may be coupled to another temperature-dependent equilibrium.

Disturbances may easily be applied in the form of a rectangular step (1, 3). In an electrically conducting medium (such as aqueous solutions) a sudden increase of temperature can be obtained by a fast input of electric energy. The energy ($^1/_2\ CU_0^2$), stored in a high-voltage capacitor, is suddenly dissipated in the system when an electrode cell containing the sample under study is connected across the capacitor (e.g., by a triggered spark gap).

When C represents the capacitance in farads, L the circuit inductance in henrys, R the total circuit series resistance in ohms, and U_0 the initial voltage on the capacitor, the current is given by:

$$\begin{aligned} \mathrm{I} &= (U_0/\omega L)\, e^{-bt} \sin \omega t && \text{if } {}^1/_2\, RC < 2L/R \\ &= (U_0/\omega L)\, te^{-bt} && \text{if } {}^1/_2\, RC = 2L/R \\ &= jU_0/\omega L\, e^{-bt} \sin \mathrm{h}\,(-j\omega t) && \text{if } {}^1/_2\, RC > 2L/R \end{aligned} \qquad \text{(III.1.1)}$$

for the underdamped (oscillatory), critically damped and overdamped (aperiodic) cases, respectively, with $b = R/2L$ and $\omega = (1/LC - R^2/4L^2)^{1/2}$ or

$$\mathrm{I} = (U_0/R)\, e^{-t/RC} \qquad \text{if } {}^1/_2\, RC \gg 2L/R \qquad \text{(III.1.2)}$$

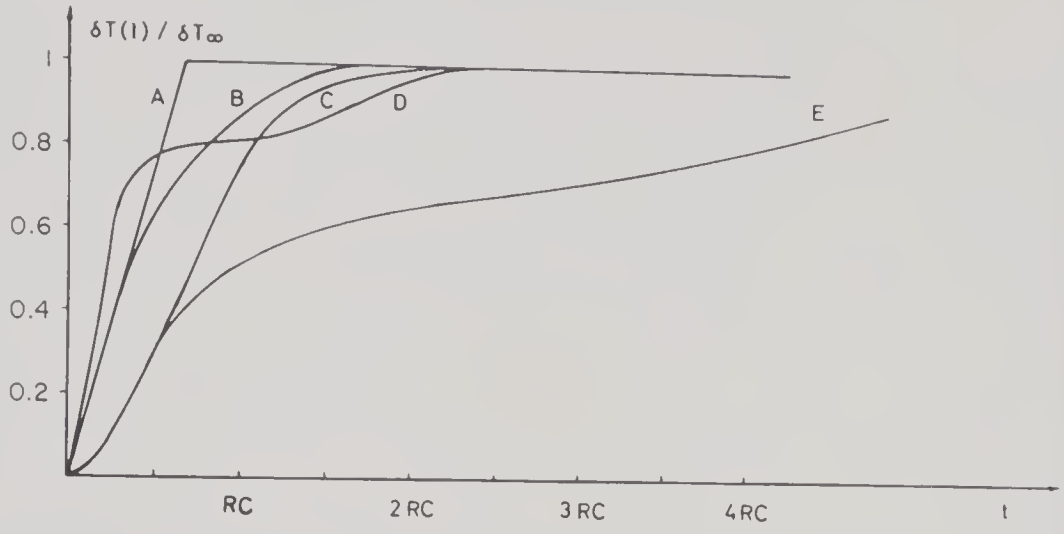

Fig. III.1. Temperature rise as a function of time for different forms of the heating pulse. A = square pulse; B = exponential discharge ($L \rightarrow 0$); C = critically damped harmonic pulse ($L = R^2C/4$); D = harmonic pulse ($L = R^2C/2$); E = harmonic pulse ($L = 2R^2C$).

for the pure exponential case ($L \rightarrow 0$); R includes the resistance R_c of the sample cell and also contains all other circuit losses (skin effect, eddy currents, radiation losses, etc.).

The temperature change at constant pressure (for a homogeneous current density in the sample cell with a total heat capacity $ql\rho c_P$) is then given by

$$\delta T = \int_0^t (\mathrm{I}^2 R_c / ql\rho c_P) dt \qquad \text{(III.1.3)}$$

Here ql is the cell volume (i.e., the space between the electrodes) in cm.^{3}, ρ the density of the system in g.cm.$^{-3}$, and c_P the specific heat at constant pressure in w. sec. g.$^{-1}$ deg.$^{-1}$. If the heating occurs faster than thermal expansion can proceed, the specific heat c_P has to be replaced by c_V in order to give the initial temperature rise. Since the rate of propagation of volume changes is approximately given by the sound velocity, the expansion times are of the order of magnitude of some 10^{-5} to 10^{-6} sec. (depending on the dimensions of the sample cells, which usually have a size of a few centimeters). In such cases strong pressure changes occur at the first moment, causing some problems which are considered below.

The temperature change as a function of time is given in Figure III.8 (a slight change in R_c because of changing temperature and dissociation field effect has not been taken into account in these curves). If values for R and C have been specified, the shape of the curve is determined by the circuit inductance L, which should be smaller than $R^2C/4$ in order to avoid an oscillatory discharge. A constant rate of change of temperature (curve

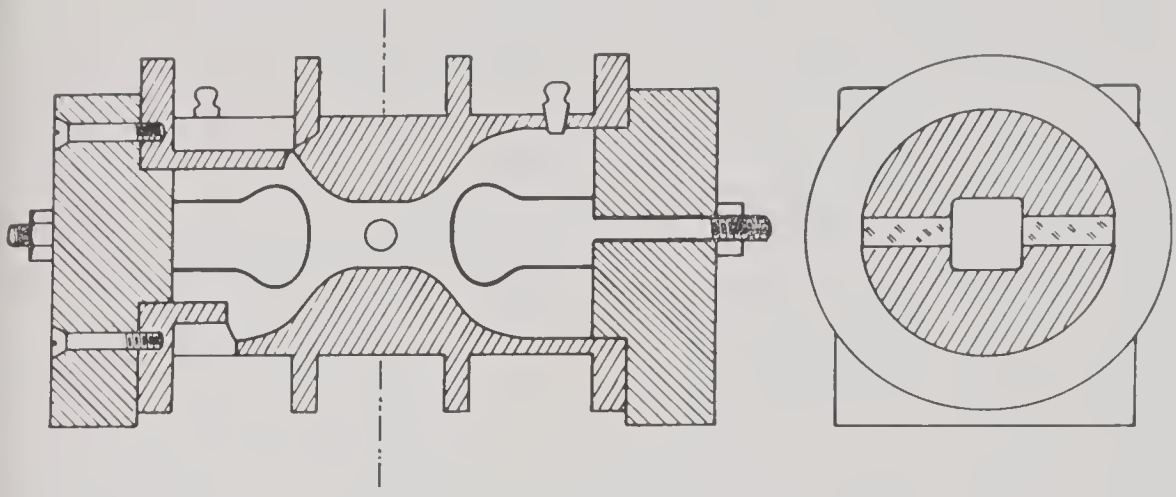

Fig. III.2. Sample cell of temperature-jump method (demonstrating the shape of the electrode space).

A in Figure III.1) can be obtained if a constant voltage is applied to the cell. This constancy can be realized if the discharge capacitor has the form of a coaxial line; the resistance of the sample cell must, in this case, be equal to the characteristic impedance of the line (*cf.* Figure III.12).

For an exponential discharge (curve B in Figure III.1), one obtains (with neglect of a T dependence of R, c_P, and ρ and with $R = R_c$) using Equations (III.1.2) and (III.1.3):

$$\delta T(t) = (CU_0^2/2)(1/ql\rho c_P)e^{-2t/RC} \qquad \text{(III.1.4)}$$

Thus the "time constant" of the temperature rise is $RC/2$.

The ultimate value of temperature change (at sufficiently large t) can be calculated from the total energy stored in the capacitor. If changes of R, c_P, and ρ with T can be neglected, one obtains

$$\delta T_\infty = (CU_c^2/2)(1/ql\rho c_P)(R_c/R) \qquad \text{(III.1.5)}$$

If the time course of the temperature change is to be known exactly, an experimental determination is easier than the exact evaluation of the integral in Equation (III.1.3). An experimental determination can be made using an indicator equilibrium with a very short relaxation time compared to the time constant of the discharge. For approximate calculations, a risetime ϑ can be arbitrarily defined for an aperiodic discharge as the time in which the temperature change reaches 90% of its ultimate value:

$$\int_0^\vartheta \mathrm{I}^2 dt = 0.9 \int_0^\infty \mathrm{I}^2 dt \qquad \text{(III.1.6)}$$

yielding $\vartheta \approx 1.3RC$.

For a specified risetime ϑ and amplitude of the temperature change δT (assuming aperiodic discharge), the capacitance of the storage capacitor

and the value of the charging voltage are fixed and depend upon the heat capacity and the resistance of the sample cell, thus

$$C \leqslant 0.77\vartheta/R \tag{III.1.7}$$

$$U_0^2 \geqslant 2.6ql\rho c_P(R^2/R_c)(\delta T/\vartheta) \tag{III.1.8}$$

For systems with a relatively low conductivity, the voltage to be used may become prohibitively high (a limit is given by spark breakdown in the sample cell). Voltages as high as 100 kv. have been used. A careful design of the electrode shape in the sample cell is required (Fig. III.2).

In some cases where the use of added electrolytes for lowering the resistance of the sample cell is not possible, absorption of electromagnetic energy in the dielectric dispersion frequency region of the solvent (for water at about 10 kMc.) may be useful to obtain rapid heating (14). Generators for such high frequencies with sufficient impulse power capabilities (magnetrons) are available at present; they are currently used for radar applications.

Similarly, a high-intensity light flash could be used if the optical density of the system provided sufficient absorption of the light. Very high absorption will lead to inhomogeneous heating, however. The efficiency of the method may therefore be low if homogeneous heating is necessary. At the same time, unwanted photochemical effects may be produced.

Furthermore, transient temperature changes can be produced by rapid adiabatic compression or dilatation (as shown for sound waves in the paragraph on stationary techniques, compare also Section II.3.E). This method will be most effective for gases. Since these techniques (e.g., shock-wave techniques) are closely related to the pressure methods, they will be discussed in Section III.1.C.

In the procedures described above a certain amount of energy is dissipated in the system within a very short time. The question arises as to how this energy is distributed to produce a fast homogeneous rise of temperature. The distribution of energy among the translational and rotational degrees of freedom is a very rapid process; for liquids, it is usually effected within 10^{-12} sec. or less, i.e., within a few molecular collisions. The transfer of energy to vibrational modes, however, may involve some delay. This delay can become appreciable, as has been shown for gases (here even the excitation of rotational degrees of freedom may proceed with a finite time lag). In this connection, we may refer to the extensive sound absorption and dispersion studies in gases as described in the work quoted under Section I [general references]. Since the presence of polyatomic molecules catalyzes the energy transfer, these processes are usually very rapid in the quasi-lattice structure of the liquid phase, where such relaxation

effects have scarcely been observed. Thus, for the aqueous phase, we may suppose a complete equilibration of energy distribution within the risetime of temperature for all present procedures.†

After initial heating the temperature can be kept constant for a relatively long time (≈ 1 sec.) if heat conduction and convection remain within safe limits. The geometric dimensions of the cell, especially the electrode distance, are to be chosen appropriately.

Another problem is that of thermal expansion. A very rapid heating of the solution takes places essentially at constant volume, because inertia prohibits the volume change from instantaneously following the temperature change. Therefore, at the first instant, the temperature change is accompanied by a relatively great increase in pressure, which will propagate through the liquid as a shock wave. The reflection of this shock wave at the walls of the sample cell may be accompanied by phase reversal of the pressure, and, in this way, cavitation effects may occur. The initial pressure change may be quite appreciable. It is given by

$$(\partial P/\partial T)_V = -(\partial V/\partial T)_P/(\partial V/\partial P)_T = \alpha_P/\kappa_T \qquad \text{(III.1.9)}$$

Even for water, where α_P at room temperature is quite small because of the density anomaly, the pressure will rise to about 50 atm. if T rises from 20 to 30°C. For the equipment described below, the pressure effects are only important if heating occurs in times less than 10^{-5} sec. They can be completely avoided if the measurements are made around 4°C., e.g., if temperature is raised from 0 to 8°C. ($\alpha_P = 0$ for H_2O at 4°C.). Practically, the effects disappear if studies are made below 10–15°C.

Measurements of chemical relaxation effects are made by recording the transient behavior of the system. It would be possible to use electric properties of the system (e.g., the conductivity) as a measuring parameter if no inert electrolytes had been added to the system for lowering its resistivity; otherwise (as in buffered solutions), the sensitivity of the measurements will be very low. Conductivity measurements may be practical in the case of dielectric heating. The use of conductivity as a measuring parameter is described in more detail in Section III.1.C (pressure-jump method).

In most cases, a photometric measurement of system variables has a number of advantages.

Spectrophotometric Recording. The change in transmitted light intensity is related to the change in volume concentration by the Beer-Lambert law. This law relates the decrease of light intensity with the

† Very strong delays of energy transfer are to be found if processes of electronic excitation, or spin distribution, are involved. These processes, however, are not important with respect to the present application.

thickness l of the medium and the volume concentration c_i of the absorbing substance i, thereby defining a molar extinction coefficient ϵ'_i:

$$I = I_0 e^{-\epsilon'_i c_i l} \tag{III.1.10}$$

(Usually the decadic extinction coefficient $\epsilon'' = \epsilon'/\ln 10 = \epsilon'/2.303$ is given in tables.)

For a disturbance in concentration: $c_i(t) = c_{i\text{ref}} + \delta c_i$, with $I(t) = I_{\text{ref}} + \delta I(t)$, we may write

$$\delta I = I_{\text{ref}} (e^{-\epsilon'_i \delta c_i l} - 1) = -I_{\text{ref}} \epsilon'_i l \{\delta c_i - [(\delta c_i)^2 \epsilon'_i l/2] + \ldots\}$$

or, for $\epsilon'_i \delta c_i l \ll 1$,

$$\delta I / I_{\text{ref}} = -\epsilon'_i l \delta c_i \tag{III.1.11}$$

The change in volume concentration δc_i is due partly to the chemical reaction taking place and partly to the temperature dependence of the density; ϵ'_i is practically independent of temperature. For a small temperature jump δT, we may write

$$\delta I/I_{\text{ref}} = -[\epsilon_i' l \delta T (\partial \bar{c}_i/\partial \ln K_c)(\Delta H/RT^2)] (1 - e^{-t/\tau}) - \epsilon_i' l \delta T \bar{c}_i (\partial \ln \rho/\partial T) f(t) \tag{III.1.12}$$

($f(t)$ describes the time lag of volume expansion.) By using difference techniques, the last term can be canceled out. Moreover, $\alpha_P = -(\partial \ln \rho/\partial T)_P$ is small in aqueous solutions in the neighborhood of 4°C. When only the first term is considered, we get, for a rectangular temperature step δT,

$$(\delta I/I_{\text{ref}})_{\text{relax}} = \epsilon_i' \, l(\Delta H/RT)[\nu_i/\textstyle\sum_i(\nu_i^2/\bar{c}_i)] \, (\delta T/T)(1 - e^{-t/\tau}) \tag{III.1.13}$$

in the case of a single one-step chemical equilibrium. [If activity coefficients are to be considered, this expression has to be modified according to Equation (II.3.11).]

In practice, it is not the relative change in light intensity, $\delta I/I_{\text{ref}}$, which is important, but the signal to noise ratio (S/N) for the particular detecting equipment. The noise is essentially shot-noise, produced by the constant illumination background I_{ref} at the photomultiplier cathode. Therefore we can write

$$\frac{S}{N} = \frac{\delta I S_\lambda A_\varrho}{1.25[2e_0 \Delta f]^{1/2}[I_{\text{ref}} S_\lambda A_\varrho]^{1/2}} = \frac{\delta I [I_0 S_\lambda A_\varrho]^{1/2}}{I_{\text{ref}} 1.25 [2e_0 \Delta f]^{1/2}} \cdot \exp(-\epsilon_i' c_i l/2) \tag{III.1.14}$$

In this equation e_0 represents the electron charge, Δf the frequency bandwidth of the recording equipment. S_λ is the photosensitivity of the photo-

multiplier cathode (in amp./lumen), whereas A_g is a geometrical factor with the dimensions of a solid angle, and represents the geometrical efficiency of the optical arrangement (including monochromator optics, light source condensor etc.). For a given optical arrangement I_0 depends upon the light intensity (candle-power) of the (point) source (for light sources, which are not pointshaped, the surface brightness is important). I_0A_g is then the effective light flux falling on the photocathode when the sample cell is removed. $I_0A_gS_\lambda$ can be evaluated from the measured anode current I_{an} of the photomultiplier and its gain G:

$$I_0A_gS_\lambda = \mathbf{I}_{an}/G \qquad \text{(III.1.15)}$$

A factor 1.25 has been included in the above formula to take into account an approximately 25% increase in the noise due to statistical fluctuations of the secondary emission factor at the dynode surfaces.

It is easily seen that for maximum signal to noise ratio a multiplier tube with large sensitivity together with high light intensity should be used. This may eventually drive the photomultiplier into saturation. It is then advisable to work at lower multiplier gain by decreasing the dynode acceleration voltages, or by shorting the last dynodes to the anode, so that the number of multiplying stages is reduced. In any case, photomultipliers with the largest possible cathode current capability should be used, so that saturation does not occur at the cathode.

For the case of absorption spectrophotometry we may obtain from equations (III.1.13) and (III.1.14) by maximizing with respect to ϵ_i':

$$\partial \ln (S/N)/\partial\epsilon_i' = 0 = 1/\epsilon_i'(\max) - \bar{c}_i l/2 \qquad \text{(III.1.16)}$$

or

$$\epsilon_i''\bar{c}_i l = 2/2.303 = 0.868 \qquad \text{(III.1.17)}$$

This result shows that the most sensitive measurements can be carried out at a spectral region where the absorption in the sample cell is relatively large (optical density = 0.868). In this calculation it was supposed that only the substance i, whose concentration changes are to be followed, absorbs in this range. Similar calculations may be carried out when other absorbing substances are present. The path length l may also be varied (by the use of different cell shapes) in order to obtain an optimum or an acceptable signal to noise ratio. The same equation applies if optical indicators are used, whose concentrations may then be adjusted for optimum performance.

Attempts are being made at present to extend the applicability of T-jump methods to times far below the microsecond range, using high field pulses produced in coaxial discharge devices. For such applications the above

considerations are especially important. Very intense light pulses and highly focusable beams as obtainable by means of optical masers (which are being tested at present) are required for such purposes.

Fluorophotometric Recording. For the selective detection of substances which are present at low concentrations, fluorophotometric measurements may be of special interest. The fluorescence intensity I_f can be taken proportional to the total amount of light absorbed by the fluorescing substance. This assumption is only valid for the fluorescence intensity observed at the front end (i.e., the end directed toward the illuminating light source) of a fluorescent body. Then,

$$I_f = gI_0 (1 - e^{-(\epsilon'_{\lambda e} + \epsilon'_{\lambda f})c_i l}) \qquad \text{(III.1.18)}$$

where $\epsilon'_{\lambda e}$ and $\epsilon'_{\lambda f}$ are the molar extinction coefficients at the wave lengths λ_e and λ_f of the exciting and fluoresced light, respectively, and g is a proportionality factor.

One obtains, if only a small fraction of light is absorbed, $[(\epsilon'_{\lambda e} + \epsilon'_{\lambda f})cil \ll 1]$, and for a small change in concentration $\delta\bar{c}i \ll \bar{c}i$

$$\delta I_f / I_{f\text{ref}} = \delta ci/\bar{c}i \qquad \text{(III.1.15)}$$

A comparison of this equation with Equation (III.1.11) shows that, in the case of absorption spectrometry, the relative (percentage) change of measured light intensity is proportional to the absolute change of concentration, whereas it is proportional to the relative change in concentration in the case of fluorophotometry. Whether absorption or fluorescence measurements are more sensitive for the detection of a small change in concentration, will depend upon the quantity $\epsilon'_i c_i l$; if this quantity is very much smaller than one, fluorescence measurements can be of advantage (provided that requirements for fluorescence are fulfilled).

Polarimetric Recording. Optical rotation may be a quite selective and sensitive parameter for the observation of chemical relaxation phenomena in biochemical systems, especially for a study of the rate of cooperative hydrogen-bond formation (helix-random coil transformation, etc.). A sufficiently long light path is required; this requirement leads to a special construction of the sample cell. If the temperature change is to be effected by electric discharge, long rod-shaped electrodes, which are mounted in parallel with a small slit between them, may be used, so that the total volume to be heated remains small. A plane-polarized light beam passes parallel to the electrodes in the region of homogeneous temperature change. This beam then passes through a Nicol prism, which is properly oriented for minimum light transmission. Any change in concentration that causes a change in polarization can then be detected as a change in light intensity. A difference method that discriminates between variations in light intensity

(owing to fluctuations of the light source) will be most appropriate, since the effects to be studied are relatively small. In this case, the light beam is split after having passed the sample cell. Two Nicol prisms (one for each light beam) then have to be used. They are oriented in such a way that the transmission is the same for each of the light beams, but that a change in the plane of polarization of the two beams gives an increase in transmission for the first, and a decrease in transmission for the other one. If two photomultipliers are used in a differential circuit, a very sensitive detection of changes in the plane of polarization is possible.

General Requirements. The optical effects to be measured in any of these photometric methods are small. The use of photomultipliers, with their inherent rapid response and great amplification factor, has many advantages. They should be operated with the greatest anode load resistor compatible with band-width requirements; simple cathode followers are used for removing the parallel capacitance of connecting cables. A well-stabilized power supply delivering a stepwise variable voltage is recommended; d.c. amplifiers and d.c. coupling should be used throughout.

For a maximum signal-to-noise ratio, all optical parts should be carefully designed so that the energy available from the light source is efficiently used. The light source should have a high surface brightness: high-pressure xenon or mercury lamps may be used, but they suffer from some arc instability. This effect may introduce some difficulties if split-beam techniques are used. The use of secondary light sources (illuminated slit) is recommended.

Temperature-jump equipment has been developed which allows spectrophotometric, polarimetric, and fluorimetric determination of relaxation times as short as 10^{-7} sec. (3–5). A schematic diagram of such equipment is given in Figure III.3. The discharge circuit contains a capacitor bank, which can be connected in different parallel and series combinations; the maximum charging voltage is 100 kv., the capacitance is then 0.02μf. In a different connection and using a lower voltage, the maximum energy that can be stored is about 120 w.sec. Spark gaps switch the sample cell (which may be shunted by a reference cell if relaxation times between 10^{-7} and 10^{-5} sec. are to be measured) across the capacitors which discharge in about 10^{-7} sec. if the smallest capacitance is used. A certain amount of energy is absorbed by eddy current losses in the copper conductors and by the necessary electrostatic and magnetic shielding surrounding the discharge equipment. An homogeneous temperature rise of about 6° can be obtained in less than 10^{-7} sec. in a sample volume of 1 cm^3.

Spark gaps are currently used for switching the sample cell to the energy storage capacitor. If the latter is charged slowly (using a high series resistance) from a high-voltage supply, the discharge will

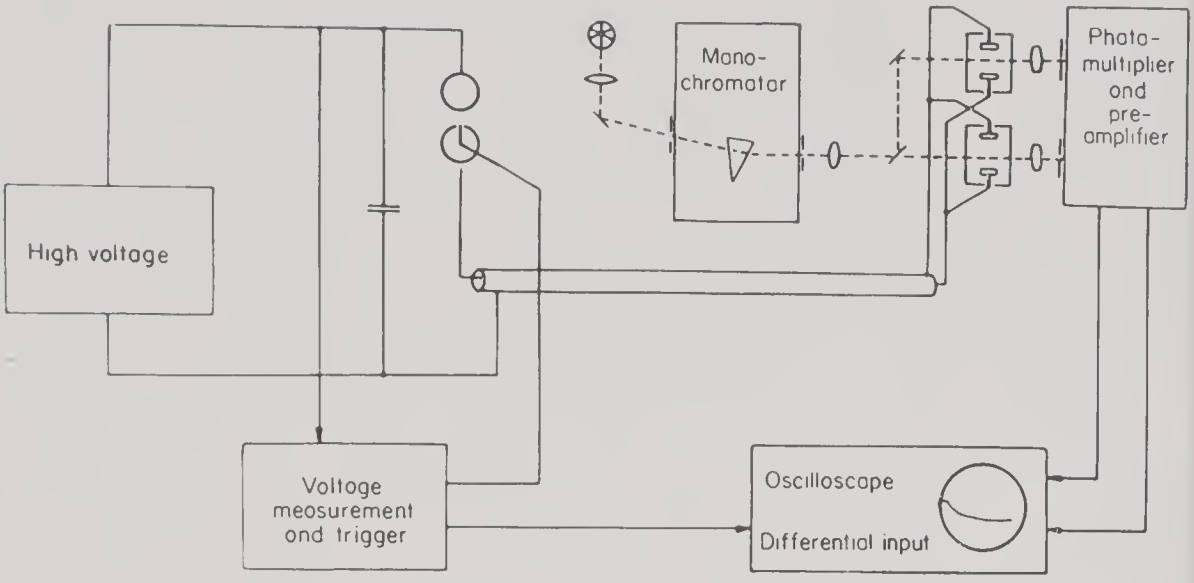

Fig. III.3. Temperature-jump arrangement (schematic).

automatically occur when the breakdown voltage of the spark gap has been reached. For well-shaped spark gaps of the spherical or homogeneous field type, this voltage depends primarily upon the spark gap distance and will be reproduced accurately within a few per cent if it is not lower than about 20 kv. (Illumination by ultraviolet light also improves the reproducibility.) For smaller voltages, triggered spark gaps (trigatrons) or thyratrons may be useful. The trigger pulse may be derived at a pre-set voltage from comparison circuits that are easily incorporated in voltage measurement devices. Variable delays incorporated in the trigger signals are useful for synchronization of the oscillograph sweep, etc. For simple equipment, a sweep trigger is easily obtained from a small length of unshielded wire (antenna), which extends into the shielding container surrounding the discharge equipment. Heavy electrostatic and magnetic shielding is necessary, especially if very sensitive transducers (e.g., photomultipliers) are mounted in the vicinity of the sample cell. In the setup shown in Figure III.3, the difference in light transmittance through the sample and the reference cell is detected by two photomultipliers. Both cells have quartz windows which are especially constructed so that the light beam cuts the field lines between the electrodes perpendicularly *cf.* Figure III.2. This construction is necessary because the refractive index of the solution depends on the temperature. The curvature of the field lines outside the electrode region produces a temperature profile with corresponding changes in the refractive index, distorting the optical path (lens effect), and giving rise to uncontrollable changes in the light intensity received by the photomultiplier. Also, the light beam should not pass the sample cell in too close proximity to the electrodes, since discharge products (occurring at the elec-

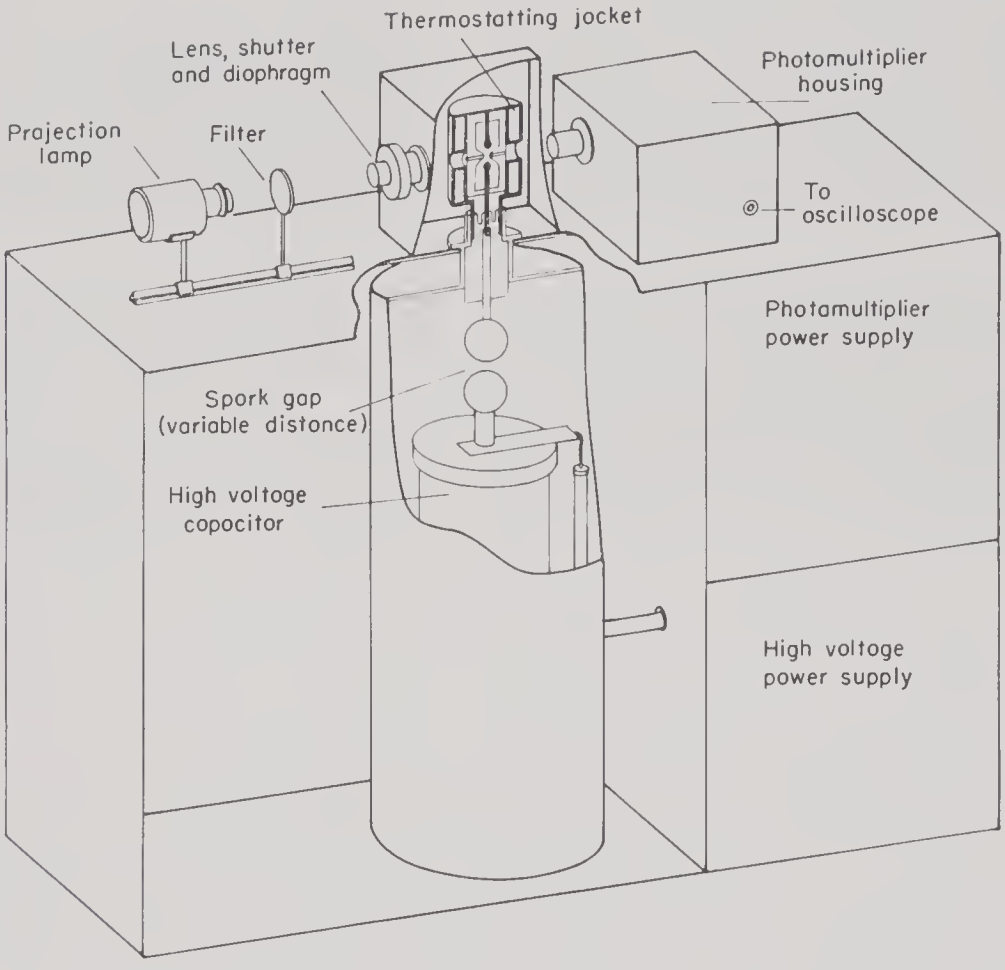

Fig. III.4. Simple temperature-jump arrangement (with single beam, coaxial construction of the discharge unit).

trodes) may influence the chemical composition. The diffusion length from electrodes to the light beam region should be large enough so that such influences cannot become effective during the time of measurement ($\lesssim 1$ sec.) If such influences are present, they can easily be recognized from the unreproducibility of the data.

The wavelength of the light can be varied by a monochromator throughout the visible and the ultraviolet region. The difference signal of the photomultipliers is displayed on a wide-band oscillograph (e.g., Tektronix 545). If measurements are carried out in a time range that is long compared to the discharge time and the time necessary for the establishment of pressure equilibrium in the sample cell, the reference cell may be omitted; the total energy in the storage capacitor is then available for the sample cell only, allowing larger temperature changes. In this case, the differential photoelectric circuit is used only for discrimination of variations in the emission of the light source. An appropriate arrangement of the discharge circuit, the sample cell, and the photometric equipment (in their simplest

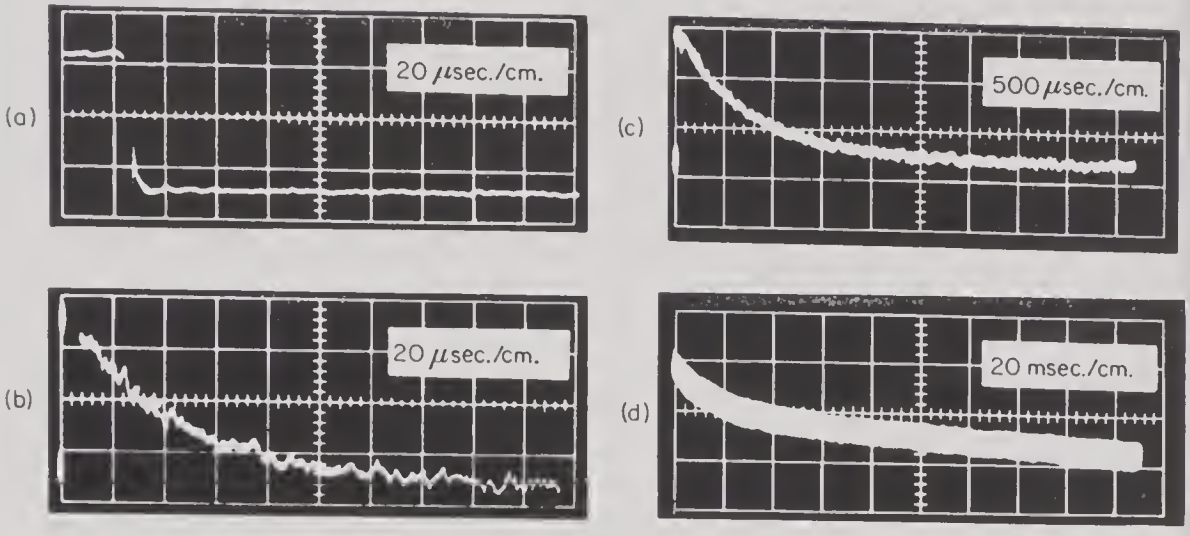

Fig. III.5. Oscillogram patterns: (a) Temperature jump (measured with highly concentrated glycine buffer and phenolphthalein as indicator; no relaxation); (b) relaxational response in the Ca^{2+}/ATP system; (c) relaxational response in the $Fe(CN)_6^{3-}$/$Fe(CN)_6^{4-}$ dichlorophenol-indophenol system; (d) two-step relaxational response in the $BeSO_4$ system.

form) is shown in Figure III.4. The discharge capacitor is coaxially mounted in a shielding compartment; the shortest connections possible are used to minimize circuit inductance. The special cell design gives very efficient shielding. A reduction of the risetime of temperature (using the same energy input) seems possible, if matched coaxial lines instead of capacitors are used (*cf.* Section III.1.D).

Figure III.5 shows four oscillogram patterns, obtained in temperature-jump experiments. In (a) (glycine buffer containing phenolphthalein) the transmitted light intensity changes in phase with temperature (the solution is heated within a few microseconds). Owing to a high buffer concentration, the relaxation time is appreciably smaller than 1 μsec. Constancy of temperature over about 1 sec. can be shown by a second deflection of the oscillograph sweep after 1 sec. In (b), a typical relaxation effect (related to a protolytic reaction in a Ca^{++}/ATP solution) and in (c) the single-step relaxation response of electron transfer (between $Fe(CN)_6^{4-}$ and the redox indicator dichlorophenol-indophenol) are shown. Trace (d) shows an example of a two-step equilibrium with two discrete relaxation times (hydrolysis reactions in $BeSO_4$ solution at pH 3.5).

A number of fast chemical reactions of different types have already been studied by means of the temperature-jump method. Among protolytic reactions, of which a number of examples are given in Section IV, the rate of reaction of pH indicators and buffers was of special interest (15). In this important group of reactions, the reaction rates are usually determined by rate-limiting diffusion processes and steric and electrostatic influences.

This is not generally the case for electron transfer (as studied with Fe^{II}/Fe^{III} complexes and redox indicators) (16) and metal-complex formation (studied with weak sulfate and phosphate as well as strong complexes of the EDTA type) (3,4,13). In combination with a rapid mixing technique, fast reactions of unstable intermediates (such as the semiquinone radical) could also be investigated (17,18). This example shows that the application of the method is not restricted to stable equilibria, but may also be used (e.g., in combination with a flow or photostationary technique) for studies in stationary reaction systems.

The temperature-jump method proved especially valuable for the investigation of biochemically important fast processes: Metal-enzyme-complex formation (19), antibody-hapten reactions, as well as structural transformations in proteins and nucleic acids, have been or are being investigated. A short discussion of some results is given in Section IV.

C. PRESSURE-SHOCK METHODS

A rectangular step-forcing function is realized by sudden application or release of the static pressure acting on the system (pressure-jump method) (9). It is obvious that in this way the risetime of the rectangular step is limited by the velocity of propagation of the pressure wave front. Therefore, very short relaxation times cannot be measured by this technique, but the method provides a useful downward extension of the time range covered by acoustical absorption methods, which become quite difficult in the lower sonic range (<10 kc./sec.). The pressure change is usually accompanied by an appreciable temperature change as a result of the adiabatic condition (*cf.* Sections II.3.B and C). This temperature change will also influence the measurable parameters and will be included in the following considerations. It must then be assumed that no heat conduction and convection will interfere during the time of observation.

Very rapid pressure and accompanying temperature changes occur within the very thin transition region of a *progressing shock wave*. The transition times may be as short as 10^{-10} sec., for a transition region (thickness of the wave front), which amounts to only a few mean free path lengths in gases. However, it would be very difficult to observe chemical changes in such a small transition zone, so that applications usually deal with reaction times greater than 10^{-6} sec. Such investigations have been performed by studying the temporal change of physical properties (light absorption, refractive index, etc.) in relatively thin regions traversed by a plane shock wave (19). In the shock wave, the kinetic energy of the medium (which can be considered as moving relatively to a co-ordinate system being fixed with respect to the wave front) is transformed into thermal energy and mechanical work (compression). In gases, very high temperature changes

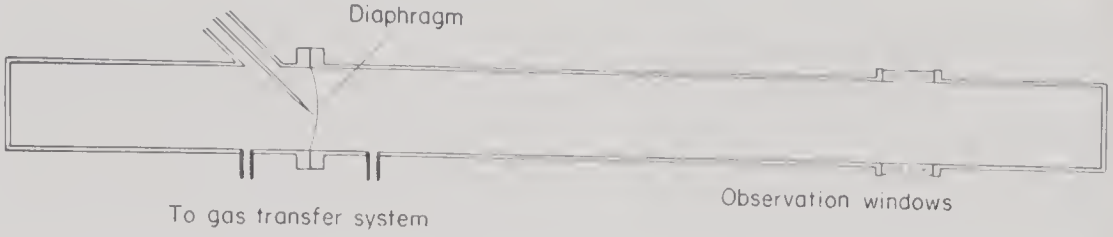

Fig. III.6. Shock-tube arrangement (schematic).

(several 1000°K.) can be obtained with moderate pressure shocks [for details *cf.* refs. (22) and (23)]. In condensed systems the temperature changes are smaller, but considerable pressure changes can be realized (up to above 10^5 atm.) by the use of explosives (21). Studies of chemical kinetics in liquids have not yet been reported, though this method seems to offer many possibilities. In shock waves, the equilibrium displacements are usually so great that the linearized treatment of the rate equations is no longer allowed. This situation may lead to difficulties in the interpretation of the data obtained. The advantage of the shock-wave techniques is that experiments can be carried out under extreme conditions of pressure and temperature, which in some cases are unattainable by other techniques.

Among experimental methods for the production of shock waves in gases, the shock-tube technique is mostly used. In such a tube (Figure III.6) (which may be made of steel, brass, or glass with a diameter between about 2 and 50 cm.) two compartments are separated by a thin membrane (metal or plastic foil) filled with gas at different pressures. These compartments may have different lengths, usually about 100–200 cm. for the high-pressure and 200–400 cm. for the low-pressure part. For a given pressure difference, the membrane will be destroyed; a shock wave will then rapidly form and propagate uniformly in the low-pressure compartment, which will contain the necessary measuring equipment (probes, observation windows, etc).

The theoretical treatment of shock-wave phenomena in gases and the description of special suitable techniques for the measurement of shock-wave velocity, temperature, pressure change, etc. is given in specialized literature [as quoted most extensively in ref. (23)]. A more detailed description would be beyond our scope here.

In condensed systems (liquids and solids), shock waves are usually generated by means of specially shaped explosives, which assure uniform propagation of the shock wave. Such experiments of course, require special testing laboratories [see ref. (24)].

A further technique for obtaining rapid equilibrium disturbance in gases related to pressure-change methods has also been applied to studies of

chemical relaxation by Bauer (25). This method is due to Kantrowitz (26) who devised it for studying vibrational relaxation phenomena. A relatively slow expansion of the gas mixture (at initial pressure P_0, temperature T_0, and extent of reaction ξ_0) is obtained by flow through a properly shaped smooth nozzle. Thermal and chemical energy of the gaseous system is thereby converted isentropically into kinetic energy of mass motion, if we may assume that chemical time lags are short compared to the time during which pressure decreases in the nozzle. The streaming mass flow is then again compressed very rapidly (within a few microseconds) in front of an obstacle (impact tube) set in the stream parallel to the flow lines. The kinetic energy ($^1/_2\, mu^2$, where u is the mass velocity at the nozzle exit) is thereby again converted into random thermal motion. The compression time can be calculated from hydrodynamic considerations and may be varied over a relatively large range by changing the expansion rate. The final state of the gas will be found to be P_f, T_f, ξ_f. From the observed pressure differences, $P_0 - P_f$, and their dependence upon compression times, an evaluation of relaxation times is possible if the compression time is comparable to the time lag of chemical equilibrium. This method is neither a transient nor a stationary method in the strict sense of the definition given in Section II.2; it may be considered a steady-state disturbance method.

The pressure-jump methods in which small samples are subjected to sudden changes in static pressure (mentioned at the beginning of this paragraph), have been applied to the study of transient behavior of electrolytes in solution. Electrolytic dissociation equilibria in aqueous solution are pressure dependent because of the relatively large volume changes involved in the formation of charged particles in the solvent (electrostriction, hydration). The transient relaxation behavior of electrolytes in solutions can most easily be followed by means of electric conductivity. However, the changes in conductivity are not only a result of changes in ionization, but also of changes in volume concentration because of solvent compression or dilatation and of the effect of pressure (and temperature) on the mobilities of the ions (viscosity changes).

The specific conductivity σ_{el} (in ohm^{-1} cm.$^{-1}$) of an electrolyte solution can be expressed as

$$\sigma_{el} = \mathbf{F}/1000 \sum c_i \, |z_i| \, u_i = (\rho \mathbf{F}/1000) \sum m_i \, |z_i| \, u_i \quad \text{(III.1.16)}$$

if z_i is the valency of the ion "i", u_i its electrical mobility (i.e., the absolute value of velocity at unit field strength, in cm.^{2}v.$^{-1}$ sec.$^{-1}$), c_i and m_i the molarity and molality, respectively, and $\mathbf{F}$ the Faraday constant (i.e., 96,493 absolute coulombs equivalent^{-1}).

If the (small) changes in molality, mobility, and density are denoted by δm_i, δu_i, $\delta\rho$ it follows, by neglecting second-order terms, that

$$\delta\sigma_{el} = (\mathbf{F}/1000)\{\sum |z_i|\ \bar{u}_i\,\bar{\rho}\delta m_i + \sum |z_i|\ \bar{m}_i\,\bar{\rho}\delta u_i + \sum |z_i|\ \bar{u}_i\bar{m}_i\delta\rho\} \tag{III.1.17}$$

Only the first term of the right-hand member of this equation describes the chemical relaxation process; the other changes follow the pressure change almost instantaneously. They can be cancelled out by suitable difference methods.

Bridge arrangements are especially adapted for such difference measurements. It will be necessary to apply a voltage of relatively high frequency to the bridge, if rapid conductivity changes are to be followed. Resistance changes in one of the bridge arms are then measured as an amplitude modulation of the high-frequency voltage appearing at the terminals of the bridge. [Direct current cannot be used because of polarization effects occurring at the electrodes. Furthermore, as electrolytic resistances are shunted by the cell capacitance, there is a frequency dependence of the bridge sensitivity for changes in the Ohmic part, *cf.* Equation (III.1.19).]

Some precautions are necessary for obtaining sufficient sensitivity and precision with high-frequency Wheatstone bridges. The total changes in conductance in the sample cell may be as low as 0.1%. The driving voltage should be stable, of constant frequency, and must be completely free from harmonics, because it is extremely difficult to obtain a bridge balance that is frequency independent. This effect is due to the fact that it is almost impossible to make a sample and a reference cell with exactly the same cell constant and reference solutions with exactly the same conductivity and an identical high-frequency behavior of electrode capacitance. Auxiliary means for adjusting the bridge balance condition are therefore required, and since these will generally disturb the exact symmetry of the impedances compared in the bridge, slight frequency dependencies are introduced.† If the bridge is then balanced for the fundamental frequency, the harmonic content of the driving voltage may still cause a remaining signal. It is preferable to use the bridge arrangement which is shown in Figure III.7. The bridge is driven from a balanced ungrounded source; this avoids the necessity of a differential amplifier for the amplification of the voltage appearing at the measuring terminals, or the introduction of a differential transformer. The rejection ratio of differential amplifiers is usually too low and not constant over the whole frequency region

† The impedance of such a bridge arm cannot be exactly represented by a frequency-independent Ohmic resistance with a capacity in parallel.

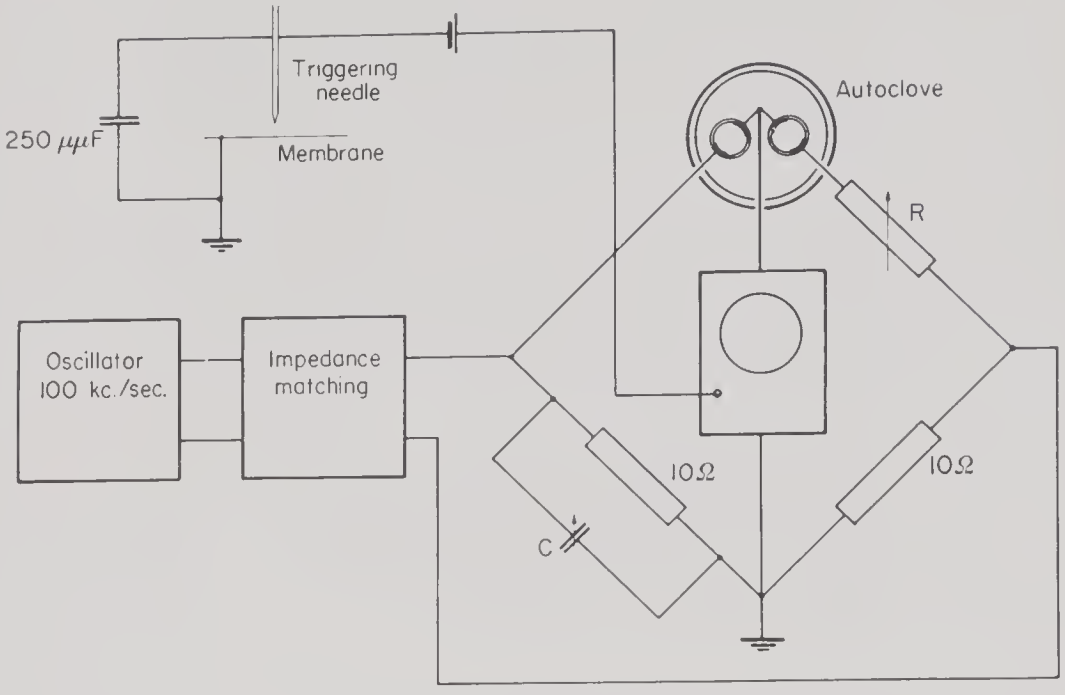

Fig. III.7. Pressure-jump arrangement (schematic).

of interest. The differential transformer, although well adapted to the problem, in principle, should be a broad-band transformer (see below); this is difficult to obtain with high enough accuracy.

The use of low-valued comparison resistors in the setup shown in Figure III.7 reduces the influence of stray capacitances of the signal source and electrostatic pickup. Low-inductance precision resistors with small temperature coefficients should be used.

A relatively high-powered signal generator is necessary. The harmonic content of ordinary *RC* generators is usually sufficiently low, and the frequency and voltage stability is good enough for the short duration of a single experiment. However, most commercial generators do not provide an ungrounded or balanced voltage adapted to the bridge load. If a power amplifier is used, it should be carefully designed to have low distortion (no d.c. magnetization of the output transformer, class A power stages, degenerative feedback).

Untuned amplifiers must be used for the amplification of the signal. The frequency of the driving voltage (carrier) and the band-width of the amplifiers will depend upon the fastest transients to be measured. As the relaxation times measurable with the pressure-jump method are usually restricted to times larger than about 10^{-5} sec., a carrier frequency of about 100 kc. may be adequate in most cases. The pass band of the amplifier should then at least extend from a few 1000 c/s to 200 kc.

Ljunggren and Lamm (10) describe a technique in which pressure is applied to a conductivity cell contained in a stainless steel pressure vessel.

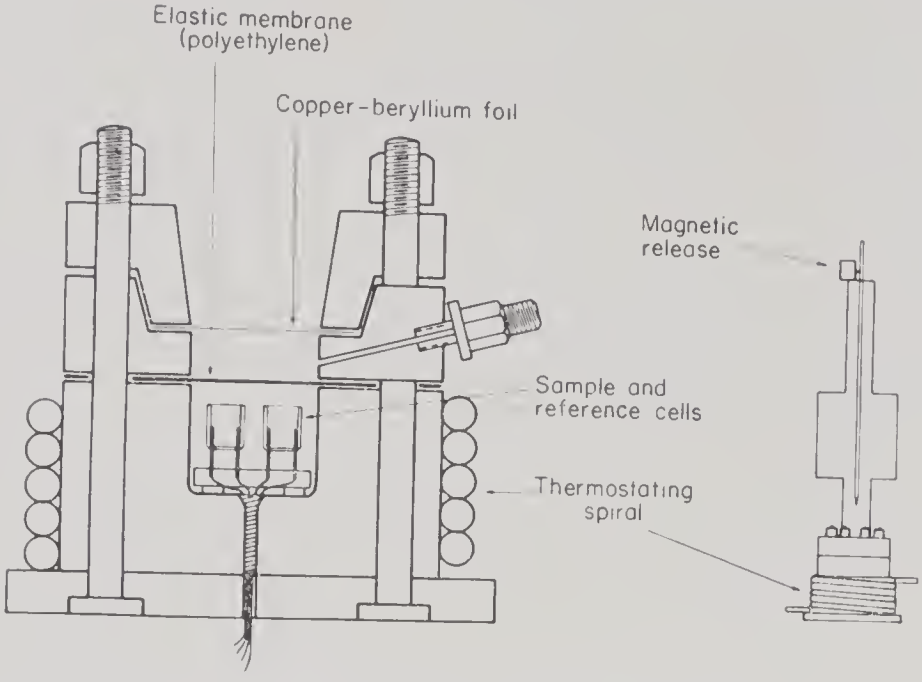

Fig. III.8. Construction of pressure-jump autoclave.

The pressure is applied by means of a transmitting medium (water or paraffin oil), which is separated from the solution to be measured by means of a short elastic polyethylene tube closing the conductivity cell. A short pressure risetime (~0.05 sec.) is obtained simply by connecting the pressure vessel to a 150 atm. nitrogen cylinder, which is opened rapidly.

The conductivity cell forms one arm of a Wheatstone bridge, which is fed from an audio-oscillator. For low degrees of unbalance, the detector signal is proportional to the relative resistance variation of the cell. This signal, after amplification by an untuned amplifier, is rectified and recorded by a fast, direct-writing recorder. With this apparatus, Ljunggren and Lamm studied the hydration equilibrium of carbon dioxide in water. A different technique has been described by Strehlow and Becker (9), who extended the time range of pressure-jump methods down to 10^{-4} to 10^{-5} sec. A very rapid pressure change is obtained by sudden release of a static pressure applied to a small autoclave in which a sample and a reference conductivity cell are contained. This sudden release is obtained by the destruction of a "bursting membrane" of copper beryllium bronze (Figure III.8).

The sample and the reference cells are part of a Wheatstone bridge circuit fed from a 100 kc./sec. generator. The a.c. detector voltage is amplified by an untuned amplifier and displayed on a cathode-ray oscillograph. Sweep triggering is made by an electrical contact closed by the needle which also initiates the bursting of the membrane. (This bursting occurs instantaneously if a sharp needle falls on the membrane

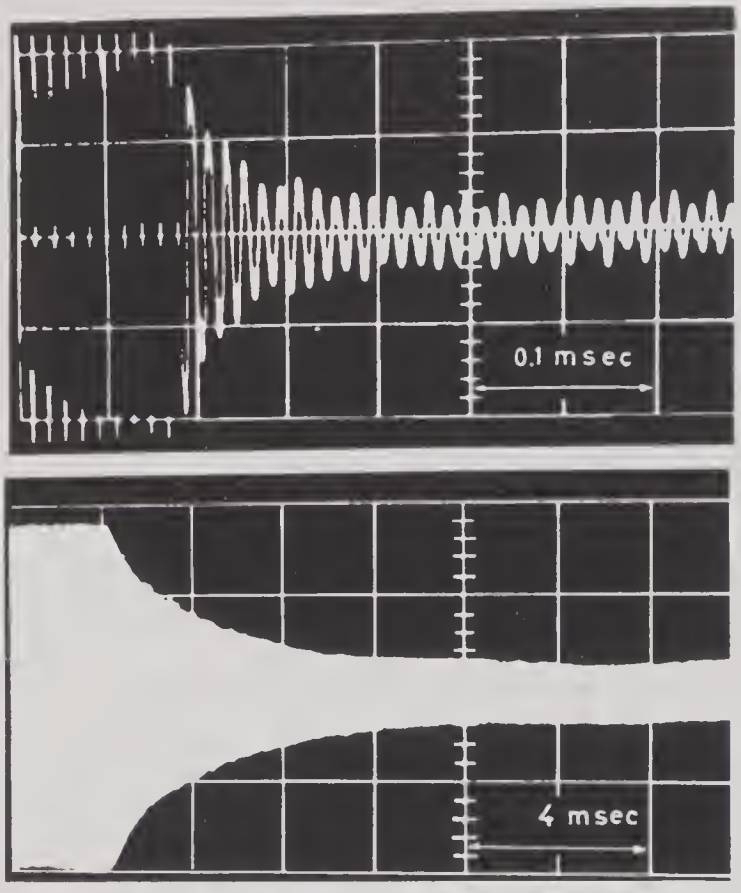

Fig. III.9. Oscillogram patterns: (a) Pressure-jump (without relaxation); (b) relaxational response in the Fe^{3+}/Cl^- system.

under pressure.) It is advantageous to use a sound muffling tube (*cf.* Figure III.8) to prevent microphonic effects. Again a pressure transmitting fluid is used; pressure is obtained from a 55-atm. air cylinder. The air space, closed at one side by the bursting membrane, is separated from the transmitting fluid and the conductivity cells by a polyethylene membrane. The Wheatstone bridge arrangement may be balanced at atmospheric pressure. Static pressure is then applied; the bridge becomes unbalanced. When pressure is released, the bridge again reaches balance within the transient period, from which relaxation times are determined.

The use of this difference technique, which allows compensation of the density and mobility effects, leads to greater sensitivity and precision of the measurements.

As an example, two oscillograms obtained by the pressure-jump technique are given in Figure III.9. Trace (a) essentially shows the time course of the pressure change, indicated by the envelope of the modulated sine wave. In this case, the relaxation time of the dissociation equilibrium investigated ($MgSO_4$ at sufficient concentration) is much shorter than the pressure risetime. In trace (b) a typical example of chemical relaxation (formation of Fe^{III} monochloro complexes in aqueous solution) is shown.

The applicability of the pressure-jump method to ionic reactions has been demonstrated by Strehlow and Becker (9) in some preliminary experiments. More extensive studies of the kinetics of metal-complex reactions (e.g., Fe^{3+}, Be^{2+}, and Al^{3+} with SO_4^{2-}, SCN^-, Cl^-, and Br^- and formation of polynuclear hydroxo complexes) are reported by Strehlow (27) and Wendt (28) (*cf.* Section IV).

D. ELECTRIC FIELD-PULSE METHODS

As shown in Section II.3, chemical equilibria involving ions, dipolar, or polarizable species may depend on electric field strength. Primarily, transient methods have been used for such studies (7,8). Here our considerations will be restricted to ionic equilibria, since these are the only ones that have previously been studied by field methods. (For dielectric methods, see the stationary techniques in Section III.2.C.)

According to the considerations in Section II.3, very high field densities are required for media with high dielectric constants, such as water, to produce measurable changes (of a few per cent) in the degree of ionization. At the same time, the field causes changes in conductivity, owing to a disturbance of the ionic atmosphere [first Wien effect, see refs. (34,35)]. This ionic atmosphere field effect is relatively small in comparison to the dissociation field effect, especially at high dilution, and can be cancelled out by suitable difference measurements.

More severe restrictions are to be expected from secondary effects which occur when a conducting medium is subjected to a high electric field. We have to consider especially the Joule heat, which is dissipated in the system (compare the estimation in Section III.1.B on temperature-jump methods). To keep such effects small enough, single-pulse methods must be used. The electric conductivity of the system has to be kept sufficiently low (depending on the pulse length), so that heating does not exceed a few hundredths of a degree. (The conductivity must be much lower than that in temperature-jump experiments where extra electrolyte usually is added.) Since the temperature dependence of conductivity usually amounts to a few per cent per degree temperature change (owing to changes in mobilities, etc.), the above limit will allow an accuracy of a few per cent in the determination of field effects (at $\sim 10^5$ v. cm.$^{-1}$ in water). As a result, only the very short relaxation times of protolytic equilibria could be studied by this method.

Among other secondary influences, electrode polarization and space charge effects have to be considered. These effects can be kept negligible only, if first, the conductivity is again low; second, the pulse duration is short; and third, the electrode distance is large enough so that the extension of any space charge or double layer remains small and its potential

negligible, with respect to the applied voltage. (The influence of discharge products on the conductance of the cell will then also be small.) The last condition requires high voltages (up to 10^5 v.), since the electrode distance should not be smaller than a few millimeters. Considerable difficulties are to be expected if ordinary voltages are applied to very small distances in order to obtain high field densities. Furthermore, the field strength should be homogeneous in order to allow an easy interpretation of results. The above-mentioned conditions are usually met in studies of the very rapid protolytic reactions.

Less drastic is the influence of other secondary effects, such as pressure rise due to the isochoric field change (*cf.* Section II.3), which, even in water ($\epsilon \approx 80$), remains below 1 atm. at the highest experimental field strengths, causing only minor changes in conductivity.

All these effects can be omitted in suitable difference measurements, in which the sample solution is compared with a solution of a strong electrolyte consisting of ions with properties similar to those studied. This reference electrolyte has the same specific conductivity as the weak electrolyte (comparable ion concentrations) and is subjected to the same field conditions (the same cell geometry). The major difference of field action in both solutions is then given by the dissociation field effect, the time dependence of which has to be followed.

Different procedures for relaxation measurements using high electric-field pulses have been described. To meet the requirements of sensitivity, bridge methods were used throughout for recording the changes in conductance. We shall begin, therefore, with a discussion of general requirements for such bridge arrangements (1) and later continue with a description of some pulse methods (2) and (3), which are specially adapted to chemical relaxation measurements. Conductance bridges or bridgelike arrangements have already been used in the early investigations of "static" field effects by Wien (29), Malsch (30), Schiele (31) and co-workers ("baretter" methods), as well as later in the highly developed differential transformer technique of Patterson and co-workers (32,33).† The major point in these methods was a high absolute accuracy. The methods which have been developed for relaxation studies (7,8) are especially adapted to a high time resolution as well as being of a sufficient relative accuracy.

High-field Bridge Arrangements. The band-width of the signals to be measured and the high voltage (usually between 10 and 200 kv.) to be ap-

† Studies of static-field effects have also been reported by other authors. [We refer to a survey in references (34) and (35).] A detailed discussion of this work would be beyond the scope of this chapter. Our discussion will be restricted to well-defined measurements of the time dependence of the field effect and especially to chemical applications.

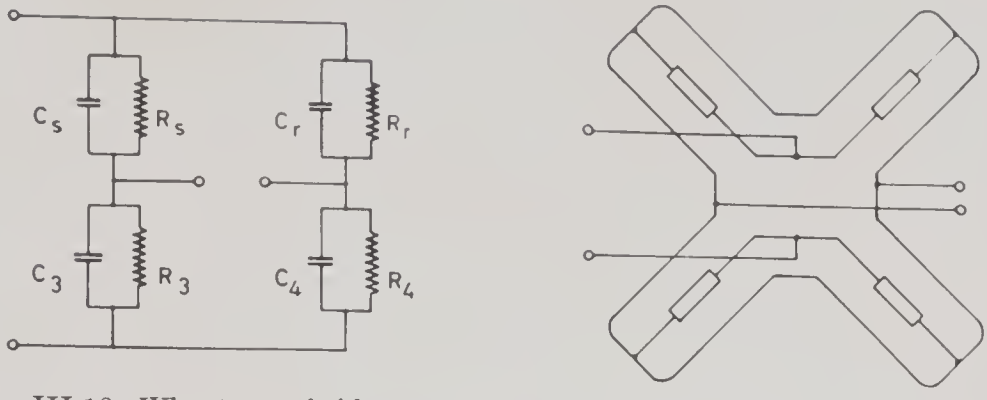

Fig. III.10. Wheatstone bridge arrangement for high field pulse measurements.

plied require a special bridge design. A number of advantages are obtained if the bridge elements have coaxial form. They can then be easily mounted perpendicularly to each other giving a cross-shaped arrangement. The coaxial construction and perpendicular arrangement together with a well-shielded container of appropriate dimensions avoid dissymmetrical stray capacitances and mutual inductive coupling between the bridge arms (which may be quite disturbing for rapidly changing strong fields, *cf.* Figure III.10). The high-voltage connections are close together and must be well insulated. They may be brought through the wall of the shielding container in the form of a coaxial cable, if a single-ended high-voltage pulse is to be applied to the bridge, or as a bifilar line if a balanced pulse (symmetrical against the reference ground potential) is to be applied. All conductors should have a sufficient diameter; preferably hollow tubing should be used, avoiding sharp bends. Connections should be soldered where possible; plug-in connectors, which are used for removable bridge elements (sample and reference cells, comparison resistances or cells, shunting capacitors), must be carefully designed for the high voltage. Good insulating material should be used, because any spurious point discharge will deteriorate the signal, and the reproducibility and accuracy of the measurement will suffer.

If a balanced-voltage pulse is used, a symmetrical bridge arrangement with four equal resistances has many advantages: The diagonal points of the bridge (connected to the oscillograph or amplifier) will remain essentially at ground potential. These points are therefore represented by the outer shields of the coaxial elements. A Wagner ground, also made of coaxial elements, is recommended in this case.

With single-ended voltage pulses, a completely symmetrical bridge is disadvantageous, because the bridge diagonal will rise to half the applied driving voltage. It is preferable to use low comparison resistances R_3 and R_4 (Figure III.10). The loss in sensitivity of such an arrangement must be compensated for by a wide-band differential amplifier, which should

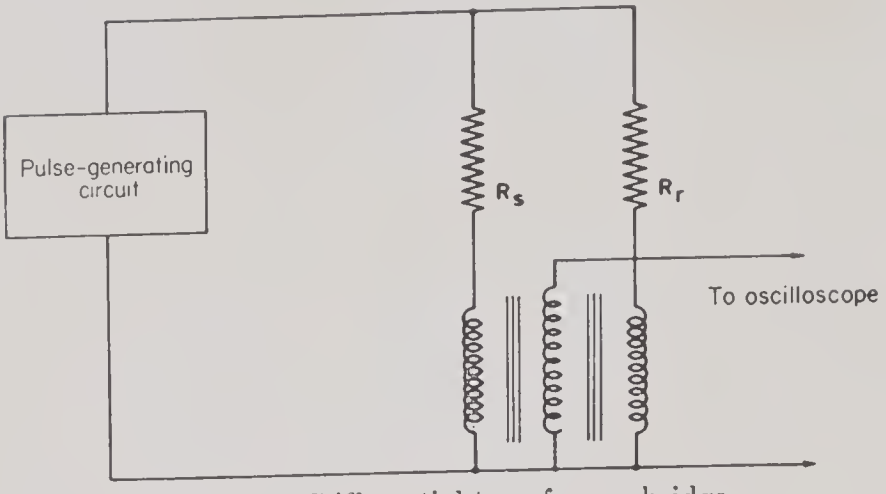

Fig. III.11. Differential transformer bridge.

have a good rejection ratio for in-phase signals. A differential transformer arrangement can also be used (32,33) (*cf.* Figure III.11). Such a transformer needs careful design and construction to avoid "ringing" resulting from spurious oscillation circuits formed by the primary or secondary inductances and their associated capacitance.

The construction of the sample cell and the reference cell deserves special mention. The coaxial arrangement allows a sturdy construction of electrode-supporting glass tubes. This is necessary because the high field strength may cause appreciable mechanical forces (especially in media of high dielectric constant), owing to electrostatic attraction. The electrode edges are to be rounded. The radius of curvature should not be too small, otherwise a region of inhomogeneous field density will exist, prohibiting the use of such a cell at high voltages. A reliable electrode set [*cf.* ref. (7)] consists of 0.5–1 mm. thick platinum sheet pressed to a flat cap (with round edges) in a suitable die. This cap is fused onto a closed glass tube to an exact fit. Platinum used in high field work must be polished (no black platinized electrodes can be used) and aged in pure water to exhaust any content of adsorbed ions.

Electrode spacing should be such that a high field strength is obtained (considering the above-mentioned restrictions). The electrode surface must be large enough so that edge effects may be neglected. The reference cell may be identical to the sample cell. In this case, the reference cell is filled with a strong electrolyte (completely dissociated into ions) of the same conductivity and with ionic mobilities similar to those in the solution under study. It is also possible to use a reference cell containing the same solution as the sample cell, if a different electrode geometry is used (greater electrode distance and surface, so that the cell constant is the same). The field strength in the reference cell is then smaller than in the sample cell and relative field effects can be measured. (For relaxation measure-

ments, the absolute value of the field effect is unimportant.) In this case, however, the secondary effects do not disappear, because their magnitude differs in both cells. Therefore, this method should be used only for solutions with very low conductivity (e.g., pure water).

The impedance of sample and reference cells should, in any case, be made as equal as possible. Therefore, the reference cell must be specially constructed, to allow a small variation of the cell resistance with a change of the electrode distance. This is important if a zero method is used: The conductivity change (owing to the high field) in the sample cell can thus be compensated by a variation in the reference cell resistance. The micrometer screw to be used for this purpose can be calibrated directly in resistance change if the reference "cell constant" is accurately measured as a function of electrode distance. Such measurements (in an ordinary impedance bridge) should be made at sufficiently high frequencies in order to avoid excess resistance and polarization capacitance.

The other comparison resistances in the Wheatstone bridge are preferably also electrolytic cells with variable and large electrode distances, if a symmetrical bridge arrangement is used. They are then easily adapted to the resistance of the system to be investigated; also, for sufficiently large electrode distances any primary and secondary field effects are negligible.

Wagner ground elements may be of the same construction. Variable shunting capacitors are usually necessary for at least two of the bridge arms in a symmetrical arrangement. They are also of coaxial construction.

Square-Pulse Method. Rectangular pulses can be obtained from a capacitor discharge. By using a triggered spark gap, the voltage on a charged capacitor C is switched to the bridge in less than 10^{-7} sec. The capacitance of the condenser and the total resistance of the bridge must be large enough so that the voltage remains practically constant during the time of investigation. Thereafter the capacitor can be shorted by a second spark gap, fired by a delayed trigger, in order to avoid too much heating of the bridge resistances by the current (Figure III.12).

With this method, it is difficult to generate balanced pulses. Rectangular pulses are therefore used with a single-ended bridge (one point is grounded), containing very low comparison resistances R_3 and R_4 (8), or a differential transformer (33). Such low resistances are also necessary if resistance changes are not determined by a compensation method, but are derived from the deflection of the zero instrument connected to the bridge terminals. The voltage difference appearing at the bridge terminals for a given (small) change in the Ohmic part of the sample cell is frequency dependent, because the electrolytic resistances always contain a shunting capacitance (*cf.* Figure III.10).

In the vicinity of bridge balance, a deflection sensitivity "S" may be

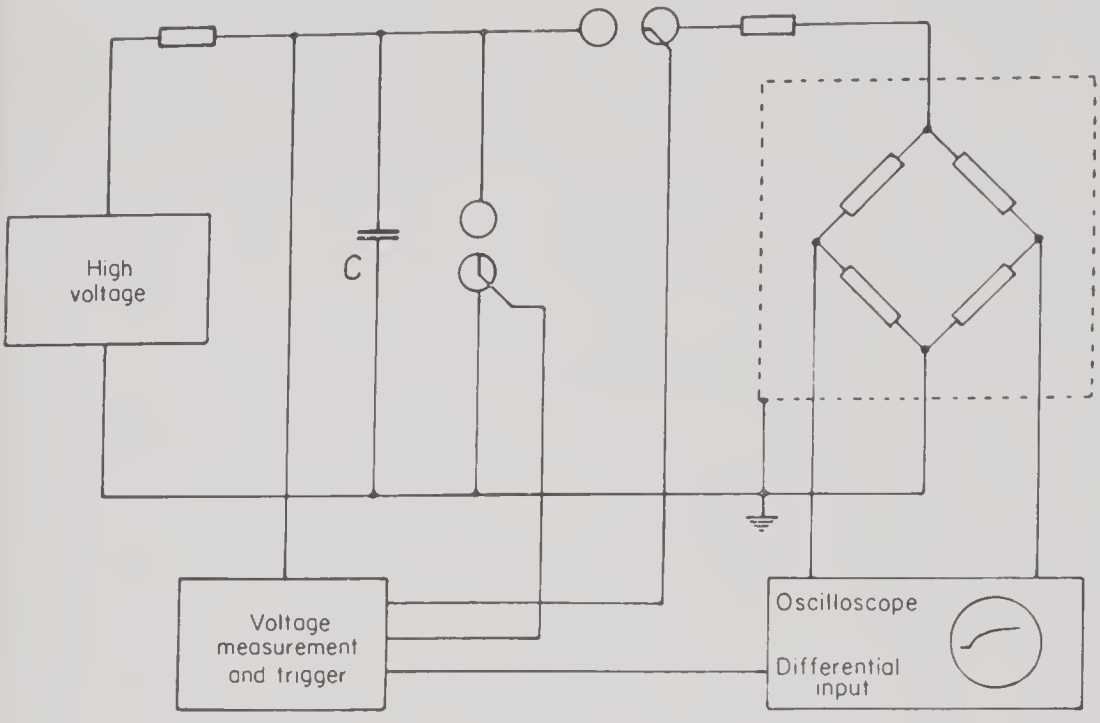

Fig. III.12. High-voltage square-pulse generator.

defined as the voltage amplitude δU appearing at the bridge terminals for a given relative resistance change $\delta R/R$ in one of the upper bridge arms, divided by the total voltage U_d applied to the bridge:

$$S(\omega) = (\delta U/U_d)/(\delta R/R) \qquad \text{(III.1.18)}$$

If $C_s = C_r$ and $R_s = R_r$ are the capacitances and the Ohmic resistances of the sample and reference cell, (cf. Figure III.10.) $R_3 = R_4$ are the comparison resistances (since we assume that they are small, their capacitive parts may be neglected), one obtains for the frequency dependence of the sensitivity for an Ohmic change:

$$S(\omega) = R_3 R_s/[(R_3 + R_s)^2 + \omega^2 R_3^2 R_s^2 C_s^2] \qquad \text{(III.1.19)}$$

The sensitivity is constant for small ω but falls to $^1/_2$ of its original value at $\omega_b = (R_3 + R_s)/R_3 R_s C_s$ or (for $R_3 \ll R_s$) $\omega_b = 1/R_3 C_s$. We may call ω_b the band-width of the bridge arrangement. As will be pointed out in Section III.1.F, this band width must be greater than the Fourier spectrum of $\delta R(t)$, if the relaxation transient is to be observed without distortion from direct measurement of $\delta U(t)$. By making R_3 and R_4 small, the band-width is increased at the expense of sensitivity; therefore, amplification will be necessary. A non-overloading differential amplifier with a high dynamic range and a good discrimination for in-phase input signals is necessary.

Very short rectangular pulses are generated by the discharge of delay

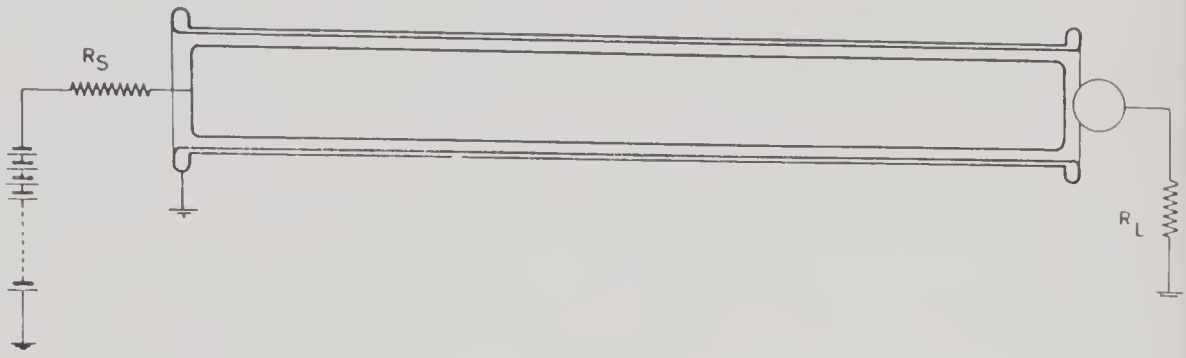

Fig. III.13. Coaxial discharge line.

lines or coaxial lines into a resistance, which is equal to their characteristic impedance. The bridge arrangement, which is coupled to the line, may be shunted with a suitable resistance to fullfill this requirement. The pulse height, which can be obtained in this way, is one-half the charging voltage of the line, unless impulse transformers are used. Such transformers, however, will deteriorate the risetime and the rectangular shape of the pulse, and it is difficult to design them for the high voltage required.

By using very short pulses, it may be possible to avoid spark breakdown occurring, usually, at very high field strengths. A statistical time lag is generally observed in the formation of a spark. For very short pulses (less than 10^{-8} sec.), the breakdown field strength can therefore be appreciably exceeded.

If short pulses are transmitted through a coaxial line containing a field-dependent dielectric, a very steep wave front can be obtained, because the propagation velocity is greater at high than at low field amplitudes. A setup with a coaxial line 3 m. long and a characteristic impedance of about 1 ohm is being tested (Figure III.13). This method should allow an extension of the time range of directly detectable chemical processes down to the mμsec-range.

The rectangular impulse method is very useful for measurements in highly diluted solutions of low conductance, which are usually very sensitive to impurities or foreign substances. A single high pulse allows a direct determination of relaxation behavior. It can easily be calculated that, for a sufficient electrode distance, impurities adsorbed on the electrode and released by the high field cannot diffuse very far into the solution during a single pulse. A few high-voltage pulses will sufficiently clean the electrodes. If a great number of pulses, however, is applied to the same solution, its composition may change as a result of the discharge processes taking place at the electrodes.

Amplitude Dispersion Method. This method is based on the considerations in Section II.2, Equation (II.2.21ff.). A forcing function having the form of a single (strongly damped) harmonic oscillation may be generated

quite easily using a simple series resonance circuit consisting of inductance, capacitance, and resistance (*cf.* Equation III.1.1). The Wheatstone bridge arrangement is shunted across the damping resistance, which may serve at the same time as a Wagner ground.

The arrangement can easily be adapted for the generation of balanced pulses, using two inductances, two capacitors, and a single spark gap (Figure III.14). Energy is stored in the capacitors from a high-voltage supply. When the capacitors are charged, the series resonance circuit is closed by the triggered or self-firing spark gap. The frequency of the strongly damped oscillation (consisting almost of a single cycle) can be varied easily by changing the inductance and the damping resistance.

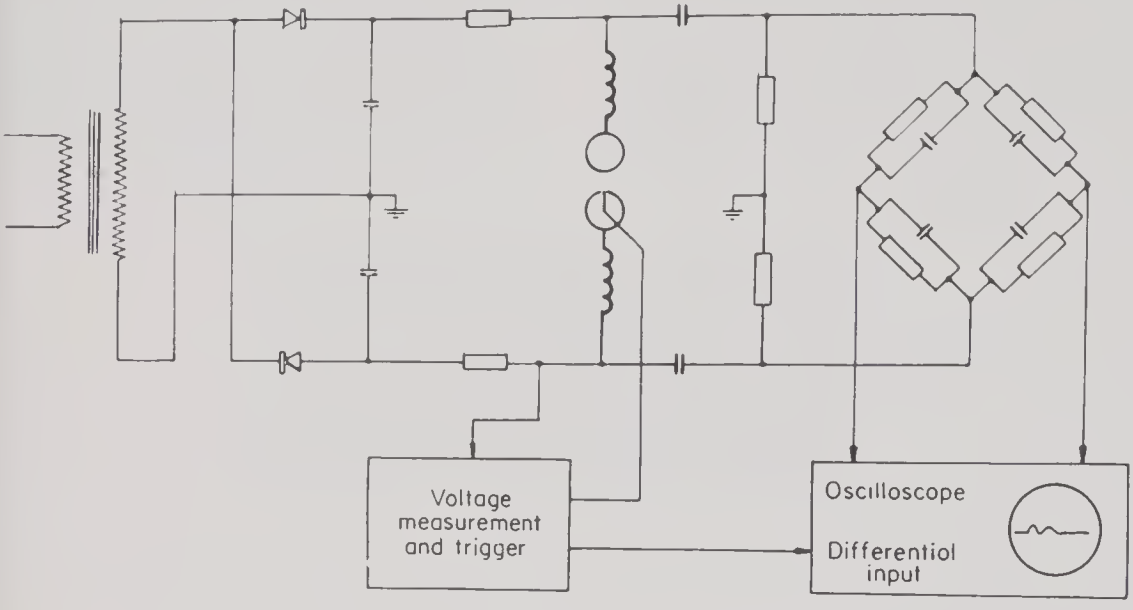

Fig. III.14. Circuit for generation of harmonic high-voltage pulses (amplitude dispersion).

A symmetric bridge giving maximum sensitivity and frequency independent balance can then be used. The bridge sensitivity will strongly depend upon frequency. The relaxation behavior, therefore, cannot be studied from the frequency dependence of the maximum value of the deflection obtained with a high-voltage pulse at a previously balanced bridge. It is essential to use a zero method, in which the conductivity change in the sample cell is compensated by a change of the resistance of the reference cell. The resistance of the sample cell, however, is field dependent, and therefore a function of time, whereas the compensating reference cell resistance is constant. The voltage appearing at the bridge terminal will then be given by:

$$\delta U(t) = U_d(t)\{[\delta R_s(t)/R_s] - (\delta R_r/R_r)\} \qquad \text{(III.1.20)}$$

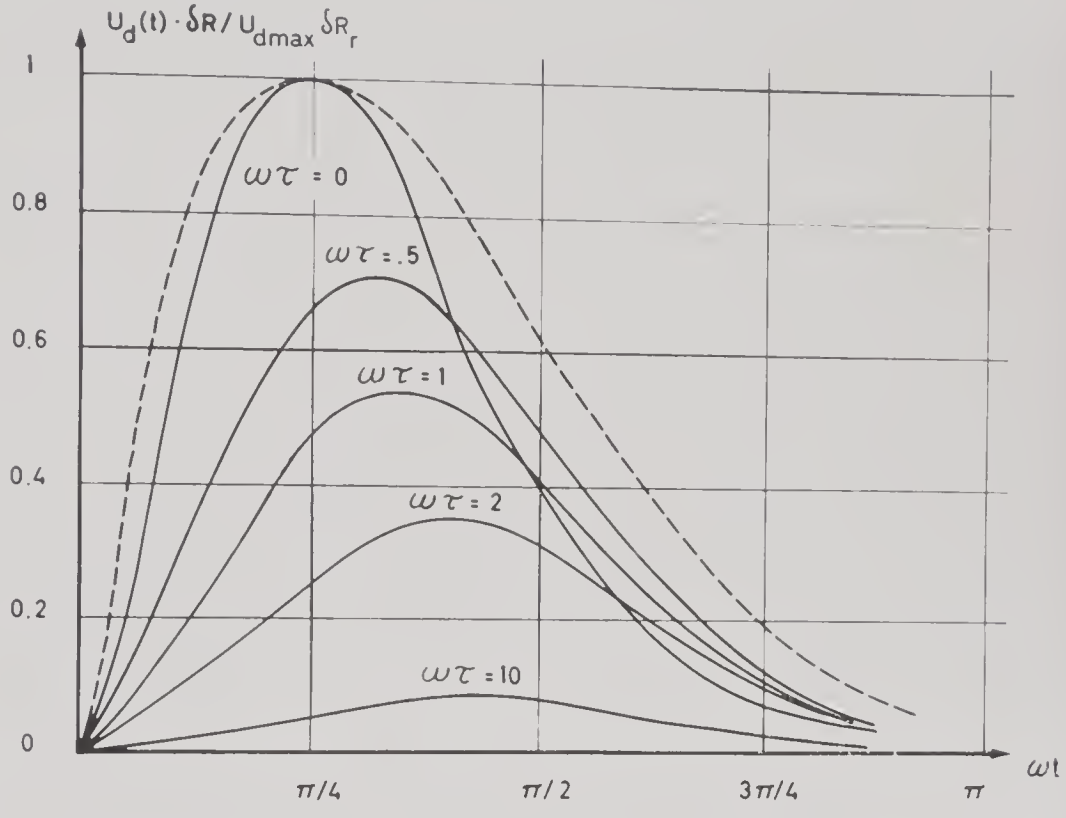

(a)

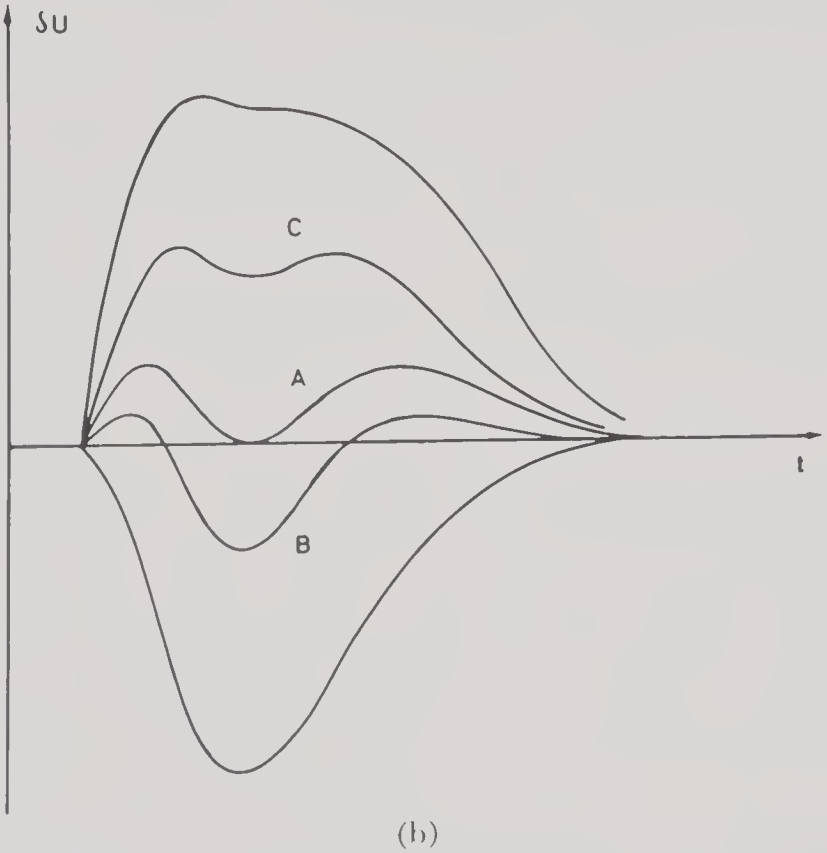

(b)

Fig. III.15(a). Currents (normalized) in the measuring (solid line) and reference (broken line) bridge branches (excess currents due to dissociation field effect and corresponding compensation). (b). Voltage at the bridge terminals (balance patterns) in the presence of a field-dependent Ohmic resistance (compensated by a constant δR_r). A = balanced; B = underbalanced; C = overbalanced.

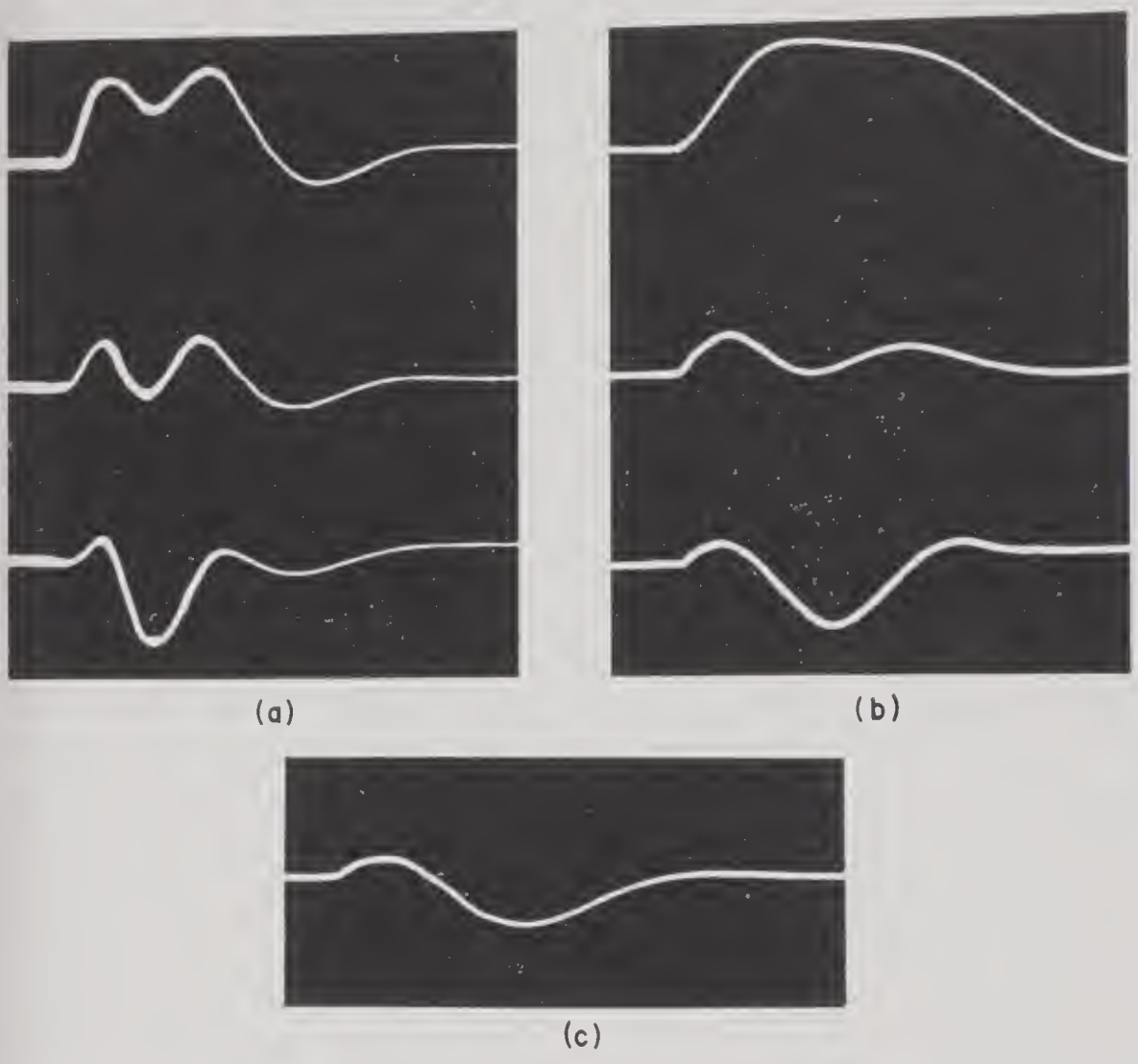

Fig. III.16. Oscillographic balance patterns; a,b: dissociation-field-effect (*cf.* Figure III.15b) (note the entirely different pattern (c) for unbalanced capacitances).

The change $\delta R_s(t)$ is related to the driving voltage $U_d(t)$ (damped oscillation). The relationship includes a phase shift and an amplitude dispersion and is described by Equation II.2.22 (see also Figure II.5). The time-independent quantity δR_r is the compensating change introduced in the reference bridge arm. The terms $U_d(t)\delta R_s(t)/R_s$ and $U_d(t)\delta R_r/R_r$, both normalized by their amplitudes for $\omega \to 0$, are shown in Figure III.15a. Their differences [Equation (III.1.20)] for several values of δR_r is shown in Figure III.15b.

An exact balance of the bridge will thus be obtained only at the single instant at which both changes are equal. If the constant compensating reference change has been made exactly equal to the maximum value of the time-dependent change in the sample cell, the voltage at the measuring terminal will be zero at that maximum. The balance diagram (which is displayed on an oscilloscope) then shows two maxima and a valley, which

touches the zero line exactly at the instant of balance (Figure III.16; *cf.* also Figure III.15b, curve A). If the compensating change was too small, the zero line will be crossed twice; if it was too large, the valley will not reach the zero line. This type of balance pattern provides a very sensitive zero method for measuring the maximum amplitude of the relaxing field-dependent conductivity change. This maximum value can be read from the calibrated micrometer screw on the reference cell, once the desired zero pattern has been observed on the oscilloscope. A good capacitive balance of the bridge is necessary. Capacitive unbalances can be easily detected from the waveshape displayed on the oscilloscope; they will always produce a waveform of odd symmetry (charging and discharging a capacitance involves currents of opposite directions *cf.* Figure III.16c). Changing the electrode distance in the reference cell for compensating Ohmic changes in the sample cell will at the same time produce a variation of capacitance of the reference cell. However, this variation can also be calibrated and compensated by a shunting capacitor parallel to the reference or to the sample cell. The maximum value of the conductivity change can also be easily measured as a function of the impulse voltage. This dependency should correspond to Onsager's equation for sufficiently long pulses [for very high fields, higher-order terms should be included according to Equation (II.3.41)]. The voltage applied to the bridge is not equal to the charging voltage on the energy storage capacitors. The bridge voltage may be measured with a peak voltmeter using a suitable frequency-compensated divider, or it can be measured with calibrated spark gaps. In the symmetrical bridge, one-half this voltage is applied to the sample cell.

From the frequency dependence of the Wien effect measured in this way, the relaxation behavior can be determined. In contrast to the square-pulse technique this method does not allow determination of the relaxation time in a single experiment. Measurements at different frequencies are at least necessary, and measurements at different voltages will greatly enhance the accuracy obtained. Moreover, a number of impulses is necessary before the exact value of the compensating reference change is found. A system to be studied will therefore be subjected to a considerable number of successive impulses. Concentrations used may not be too low (ionic concentration $\geq 10^{-5}M$) since impurities ordinarily adsorbed on the electrode surfaces and released by subsequent discharges will change the properties of the system. (The upper limit of the ionic concentration will be determined by the minimum required damping resistance.) The accuracy which can be obtained is very high. It is possible to measure relative resistance changes of about 1% with an accuracy of 1% in less than 10^{-6} sec.

Measurements should be made in the linear range of field dependence of R_s, and the amplitude values of conductivity changes should be related to a linear extrapolation to zero-field strength (*cf.* Figure III.17). A plot of these corrected amplitude values $[(\sigma_E - \sigma'_0)/\sigma'_0]$, normalized by the

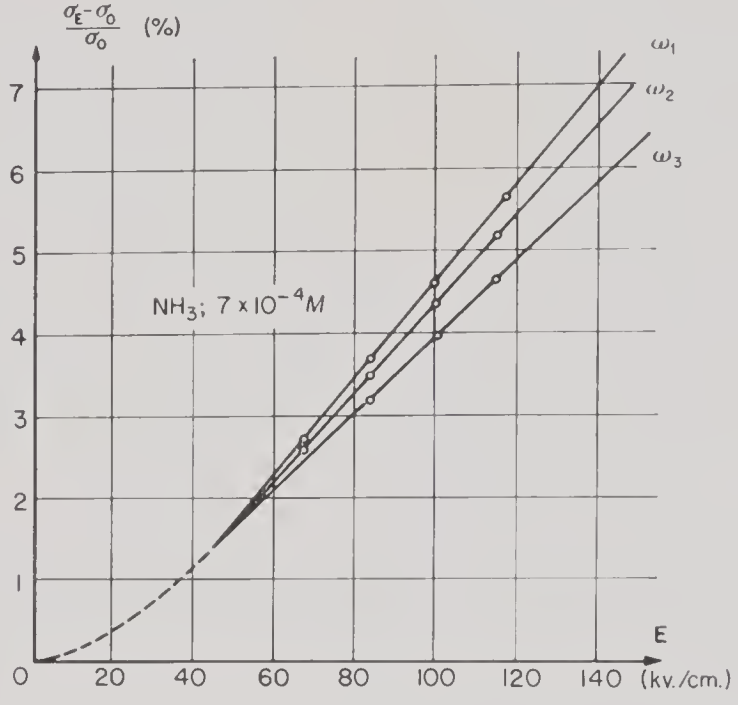

Fig. III.17. Field dependence of conductance, owing to dissociation field effect (at different pulse lengths).

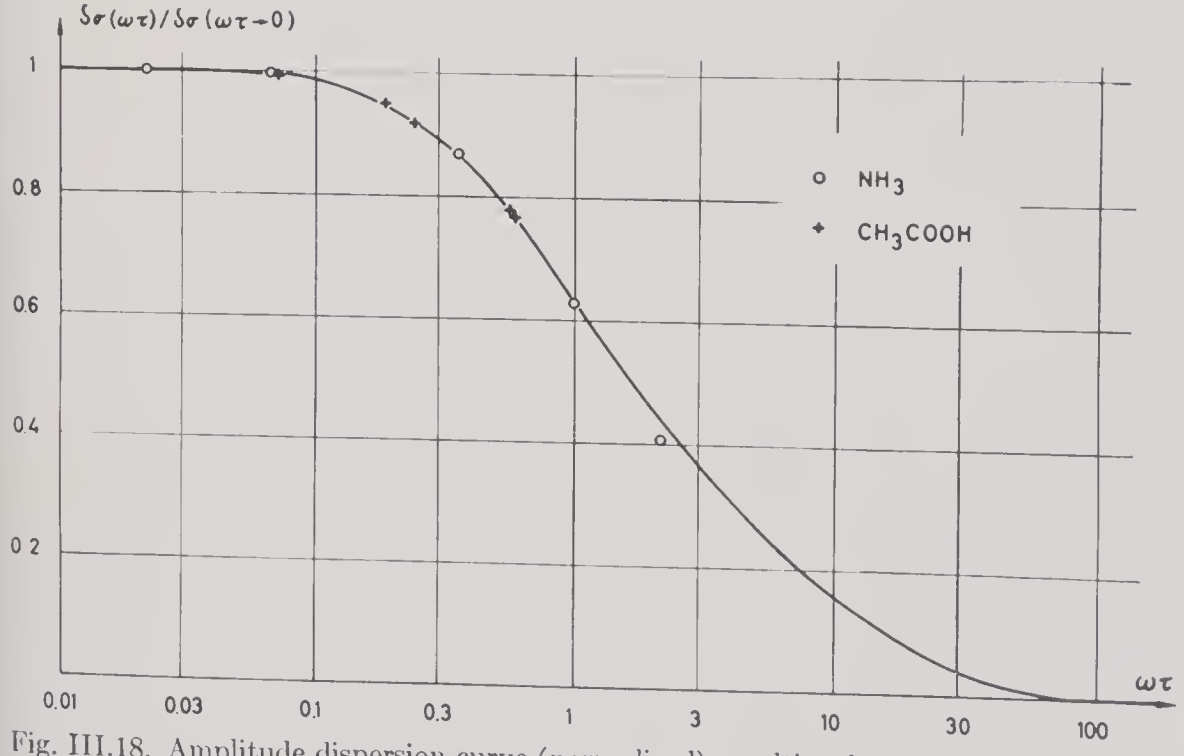

Fig. III.18. Amplitude dispersion curve (normalized) resulting from relaxation of dissociation field effect.

"equilibrium" amplitude values $[(\sigma_E - \sigma'_0)/\sigma_0']_{\omega\to 0}$, against normalized frequency $\omega/\omega_{relax} = \omega\tau$ is shown in Figure III.18 for two examples (NH_3 and CH_3COOH in aqueous solution). The relaxation time is readily determined from a theoretical curve [according to Equation (II.2.22), *cf.* Figure II.5], which is made to coincide with the experimental points merely by a displacement parallel to the abscissa. Some general precautions for all high-field methods should be mentioned: the systems to be investigated should be well degassed, and no air bubbles should be present at the electrodes. When air bubbles are present, spark breakdown will invariably result if field strengths higher than 10 kv./cm. are reached. This may lead to the eventual destruction of the electrode cell.

Discharge circuits should be heavily shielded, since stray pulses may interfere with the signals to be observed. Unlike the temperature-jump method, the observation of small signals is necessary during the application of the high voltage. Careful analysis of best grounding conditions must be made; eventually different signal and chassis grounds may be necessary.

It is important that sufficient security precautions be incorporated in any equipment using high-power, high-voltage generators. The low-duty cycle of the discharge circuits will usually allow the use of low-powered generators.

Among the applications of the field methods, the investigation of protolytic dissociation equilibria is to be mentioned especially. The method is well adapted to the measurement of the very fast relaxation times that are generally to be expected for reaction equilibria belonging to this group, the main advantage being the requirement of only small samples of the solution, which may be of very low concentration. The rate constants of H_2O dissociation and of the recombination of H^+ and OH^- in pure water could be determined by this method (8). From the investigation of a number of other weak bases and acids [NH_3(7), $N(CH_3)_3$(36), imidazole(37), HF(38), CO_2(39), formic, acetic, and propionic acid, *o*- and *p*-nitrophenol (40)] the influence of steric and electrostatic effects on the recombination rates could be studied in detail. All these recombination reactions are characterized by diffusion-limited rate constants. The permeability of the hydration shell of the cation or anion for OH^- and H^+, respectively, by a special mechanism of charge migration (high mobility of protons and "defect protons" in the H-bond-linked structure) reduces any activation barrier (decomposition of the hydration shell) for the charge neutralization.

High-field techniques have also been used for the investigation of relaxation effects in polyelectrolyte solutions, where relaxation of the dissociation field effect (41,42) is accompanied by (relatively slow) orientational re-

laxation of large induced dipoles (polarization of the inner part of the ionic atmosphere of the poly-ion) (43). The orientation of these dipoles in the field gives rise to conductivity changes due to the anisotropy of the mobility of the long rod-shaped poly-ion.

E. RADIATION METHODS

It has been mentioned that equilibrium disturbances may be produced by secondary concentration changes induced by coupled chemical reactions. These coupled chemical reactions may proceed because of their dependence on external parameters, but in some cases one can take advantage of their dependence on specific photochemical activation. Breitschwerdt and Weller (44) described such a technique for the investigation of the relaxation of protolytic dissociation equilibria. In the reaction scheme

$$\begin{array}{ccc} R^*OH + H_2O & \rightleftharpoons & R^*O^- + H_3O^+ \\ \uparrow h\nu & & \downarrow h\nu' \\ ROH + H_2O & \rightleftharpoons & RO^- + H_3O^+ \end{array}$$

the dissociation equilibrium in the excited state may be very different from that in the ground state, owing to the different electronic structure. [Acidic pK values are generally displaced by orders of magnitude in the excited state (45).]

By using a flash-photolysis method, a measurable fraction of the molecules ROH are brought to the excited level R*OH where they dissociate very rapidly. Under fluorescent emission, the R^*O^- ions formed return to the ground state. The lifetimes of the excited states are very short, so that immediately after the photolysis flash one can observe the re-establishment of the equilibrium in the ground state, which is a normal relaxation process. The experimental procedure is similar to normal flash-photolysis methods; the re-establishment of the ground-state equilibrium is observed by photometric measurement of the concentration of the reaction partners in the ground state.

Transient radiation methods are currently used in radiation chemistry for the determination of lifetimes and kinetics of excited molecules. Pulsed X-rays or particle radiation may be used for the production of the excited states. After a stationary concentration has been produced, irradiation is interrupted. The decay of luminescence may be recorded as a measure of the remaining concentration of excited molecules (46).

In this case, the displacement from the equilibrium state is usually quite large, and such methods are, in principle, nonlinear relaxation methods. However, the return to equilibrium will, most often, be determined by first- or pseudo-first-order processes, as the concentrations of the different reaction partners for the excited molecules will practically remain constant.

In this way, the formal analogy to relaxation methods as described above remains established.

Flash-photolysis techniques are described in detail in chapter XIX of this volume (*cf.* also chapter XVI for a discussion of fluorescence methods).

F. PROSPECTIVE DEVELOPMENTS IN TRANSIENT METHODS

Improvement of the sensitivity of transient methods will be possible if different techniques for band-width reduction of repetitive fast signals (of identical shape), known as "time-sampling" techniques are used. At first, such methods appear similar to stationary methods. Actually, it is not the stationary (forced) response, but the transient response of the chemical system that is observed and analyzed. It is well known that the band-width requirements of the measuring equipment are inversely proportional to the risetime of the signals, which are to be observed without introducing serious distortion. In our case, the risetime is determined by the smallest relaxation times which are to be measured. If the signal to be observed is derived from the transient response to a rectangular pulse-forcing function [Equation (II.2.17), Figure II.4], it is usually the leading edge that is to be observed. The frequency spectrum of the observed signal is given by its Fourier transform:

$$F(j\omega) = \int_{-\infty}^{+\infty} f(t)e^{-j\omega t}dt = \int_{0}^{\vartheta} f(t)e^{-j\omega t}dt \qquad \text{(III.1.12)}$$

($f(t) = 0$ for $t < 0$ in transient methods, ϑ is the duration of the observation). If the signal is to be passed without distortion through the measuring system (which is assumed to be linear), the latter should have a flat (constant) amplitude characteristic over the whole frequency spectrum of the input signal, and its phase characteristic should be a linear function of frequency over the same interval. If any part of the measuring system does not correspond to those conditions, it will be necessary to introduce phase or amplitude equalizing networks, so that the conditions hold for the over-all frequency characteristics of the measuring equipment.

Although the present standard of available instrumentation will, in general, allow the fulfillment of band-width requirements, there will remain an inherent limitation on the time-resolving power, owing to the statistical fluctuations of signal level (noise), which will always be present where small effects are to be observed. These fluctuations may deteriorate the observed signal to such an extent that accurate measurements on a single experiment become impossible. The signal-to-noise power ratio is inversely proportional to the band-width required, and therefore it becomes increasingly difficult to make accurate measurements as the duration of the experiment decreases.

One may, of course, repeat a great number of identical experiments, from which the quantity to be measured is obtained by taking the statistical average.

A great variety of data handling and sampling techniques can solve this problem and may be directly incorporated in the measuring equipment. At the same time the band-width requirements for other parts of this equipment can be reduced. The repetitive application of an appropriate forcing function (generally, impulse-forcing functions will be used in this case) will reduce the effective band-width by a factor which is proportional to the square root of the number of successive experiments, and will therefore improve the signal-to-noise ratio (47).

In general, the measuring equipment will no longer be a true linear system; it may remain a linear system with time-varying coefficients, but nonlinear elements may also be incorporated for a further improvement of noise discrimination. A detailed description of such circuits, however, will not be discussed further here.

The range of application of relaxation methods may be extended if a combination with other techniques for the study of rapid reactions is made. Reactions of intermediates can be studied in a combination of relaxation methods and flow techniques if the flow method provides a sufficient concentration of the intermediate. In such a case the effects of small perturbations from a stationary equilibrium instead of a true equilibrium are studied. It will be necessary to make an exact analysis of the thermodynamic conditions that are implied and to consider any consequences for the time-dependent behavior of the measured quantities.

References

1. M. Eigen, *Discussion Faraday Soc.*, **17**, 194 (1954).
2. L. De Maeyer, *Z. Elektrochem.*, **64**, 65 (1960).
3. G. Czerlinski and M. Eigen, *Z. Elektrochem.*, **63**, 652 (1959).
4. H. Diebler, Dissertation, Göttingen, 1960.
5. G. Czerlinski, *Z. Elektrochem.*, **64**, 78 (1960).
6. M. Eigen and L. De Maeyer (to be published).
7. M. Eigen and J. Schoen, *Z. Elektrochem.*, **59**, 483 (1955).
8. M. Eigen and L. De Maeyer, *Z. Elektrochem.*, **59**, 986 (1955).
9. H. Strehlow and M. Becker, *Z. Elektrochem.*, **63**, 457 (1959).
10. S. Ljunggren and O. Lamm, *Acta Chem. Scand.*, **12**, 1834 (1958).
11. K. Bergmann, M. Eigen and L. De Maeyer (to be published).
12. U. Schoedel, R. Schlögl, and M. Eigen, *Z. physik. Chem. N. F.*, **15**, 350 (1958).
13. H. Diebler, M. Eigen, and G. G. Hammes, *Z. Naturforsch.*, **15b**, 554 (1960).
14. H. Gerischer, *Z. Elektrochem.*, **64**, 86 (1960).
15. M. Eigen and G. G. Hammes, *J. Am. Chem. Soc.*, **82**, 5951 (1960).
16. H. Diebler, *Z. Elektrochem.*, **64**, 128 (1960).
17. H. Diebler, M. Eigen, and P. Matthies *Z. Naturforsch.*, **16b**, 629, (1961).

18. P. Matthies, Dissertation, Göttingen, 1961.
19. M. Eigen and G. G. Hammes, *Advances in Enzymology*, 25. (to be published).
20. D. Britton, N. Davidson, and G. Schott, *Discussions Faraday Soc.*, 17, 58 (1954).
21. H. Lawton and I. C. Skidmore, *Discussions Faraday Soc.*, 22, 188 (1956).
22. R. Courant and K. O. Friedrichs, *Supersonic Flow and Shock Waves*, Interscience, New York, 1948.
23. E. F. Greene and J. P. Tönnies, *Chemische Reaktionen in Stosswellen*, Steinkopf, Darmstadt, 1959.
24. S. D. Hamann and H. G. David, *Trans. Faraday Soc.*, 55, 72 (1959).
25. S. H. Bauer and M. R. Gustavson, *Discussions Faraday Soc.*, 17, 69 (1954).
26. A. Kantrowitz, *J. Chem. Phys.*, 14, 150 (1946).
27. H. Strehlow and H. Wendt, *Z. Elektrochem.*, 64, 131 (1960).
28. H. Wendt, Dissertation, Göttingen, 1960.
29. M. Wien, *Physik. Z.*, 23, 399 (1922); *Ann. Physik.*, 73, 161 (1924); 83, 327 (1927); *Physik. Z.*, 32, 545 (1931).
30. J. Malsch and M. Wien, *Ann. Physik.*, 83, 305 (1927).
31. J. Schiele, *Physik. Z.*, 35, 632 (1934); *Ann. Physik*, 13, 811 (1932).
32. J. A. Gledhill and A. Patterson, Jr., *J. Phys. Chem.*, 56, 693 (1954).
33. J. A. Gledhill and A. Patterson, Jr., *Rev. Sci. Instr.*, 20, 960 (1949); F. R. Kotter, *Rev. Sci. Instr.*, 28, 178 (1957).
34. H. Falkenhagen, *Elektrolyte* 2nd ed., S. Hirzel Verlag, Leipzig, 1953.
35. H. C. Eckström and C. Schmelzer, *Chem. Revs.*, 24, 367 (1939).
36. W. Fuchs and K. Tesch, *Z. Physik.*, 148, 53 (1957).
37. M. Eigen and L. De Maeyer (to be published).
38. J. S. Johnson, K. Kustin, and A. Wittig (unpublished data).
39. M. Eigen, G. G. Hammes, and K. Kustin, *J. Am. Chem. Soc.*, 82, 3482 (1960).
40. M. Eigen, K. Kustin, *J. Am. Chem. Soc.*, 82, 5952 (1960).
41. M. Eigen, K. Kustin, R. Munson, *Z. physik. Chem.*, (in preparation).
42. F. E. Bailey, A. Patterson, Jr., and R. M. Fuoss, *J. Am. Chem. Soc.*, 74, 1845 (1952).
43. M. Eigen and G. Schwarz, *Symposium on Electrolytes, Triest* 1959, Pergamon Press, London, 1961.
44. K. Breitschwerdt and A. Weller, *Z. Elektrochem.*, 64, 395 (1960).
45. Th. Förster, *Z. Elektrochem.*, 54, 42 (1950); 54, 531 (1950).
46. M. Burton and H. Dreeskamp, *Phys. Rev. Letters*, 2, 45 (1959); *Z. Elektrochem.*, 64, 165 (1960); S. S. Brody, *Rev. Sci. Instr.*, 28, 1021 (1957); *Z. Elektrochem.*, 64, 187 (1960).
47. H. T. Witt, *Z. Elektrochem.*, 64, 87 (1960); B. Chance, *ibid.*, 64, 88 (1960).

2. Stationary Methods

The term "stationary method" will be used for any experimental method related to the determination of transfer functions. It includes absorption methods, based on the measurement of frequency-dependent energy losses caused by chemical relaxation phenomena, and dispersion methods involving the determination of frequency-dependent properties of the system [such as compressibility (sound velocity), dielectric constant, or other quantities related to the relative amplitudes of actual concentration changes]. Because of the unambiguous relationship between amplitude

and phase in linear first-order systems, as described by Equation (II.1.20ff.), the information obtained from either method is the same and is sufficient for a complete description of the kinetically important quantities (relaxation times).

In acoustical methods, the periodic adiabatic pressure and accompanying temperature changes present in a sound field will influence chemical equilibria that are pressure or temperature dependent. In this case, the experimental procedures are the same, regardless of whether pressure or temperature change is actually the driving force of the equilibrium displacement. It is, in fact, the acoustical behavior of the system that is studied and interpreted using the concepts derived in Section (II.3.E).

In a similar way, the electromagnetic properties of the system (permittivity, conductivity, permeability) permit an analysis of chemical relaxation, if electric or magnetic fields or accompanying changes of other parameters (T, P) are able to displace the chemical equilibrium. The nonlinear relation between the forcing function $\bar{y}(t)$ and an electric or magnetic forcing parameter may be utilized advantageously in a few special measuring techniques.

A. ACOUSTICAL METHODS (SOUND ABSORPTION AND DISPERSION)

Measurable acoustical quantities that are directly related to energy absorption are the attenuation constant (for a progressive wave) or the decay constant (for stationary waves). The attenuation constant represents the real part of the acoustical propagation constant. Sound velocity or wavelength are measurable quantities related to the imaginary part of the propagation constant. This constant appears in the solution of the first-order (small signal) equations (1) of classic acoustics, which read, in the one-dimensional case (*cf.* Equation II.3.81),

$$(\partial^2 p_1/\partial t^2) - \mathrm{v}^2(\partial^2 p_1/\partial \mathrm{x}^2) = 0 \qquad \text{(III.2.1)}$$

with the solution

$$p_1 = p_{10} \exp(j\omega t) \exp\{-[\alpha + j(\omega/\mathrm{v_{re}})]\mathrm{x}\} \qquad \text{(III.2.2)}$$

for a plane wave. The quantity $[\alpha + j(\omega/\mathrm{v_{re}})]$ is called the propagation constant, $\omega/\mathrm{v_{re}}$ the phase constant.* Similar equations can be written for u_1, ρ_1, and ϑ_1. In these cases, p_1, u_1, ρ_1, and ϑ_1 represent the first-order increment values of pressure, particle velocity,† density, and temperature,

* Since, in Equation (II.3.82), $j\omega$ occurs as a factor of the complex sound velocity v, the real constant α is related to the imaginary part of compressibility, as shown in Section (II.3.E).

† "Particle velocity" is the instantaneous velocity (due to the sound wave) of an infinitesimally small part of the medium.

respectively, in a sound field. If higher-order increment values of these quantities are also considered, more complicated wave equations result, for which no general solution has been given. The second-order equation, however, introduces a number of new concepts which are necessary for the description of some acoustical phenomena, of which the most important, for measuring purposes, is the existence of "radiation pressure" (a quantity proportional to the average energy density and that can be measured as a mechanical force exerted on an obstacle exposed to the sound field). Another consequence of second-order effects is a (measurable) streaming potential arising in a sound field and related to sound absorption (gradients of radiation pressure).

For the investigation of relaxation phenomena, measurements in sound fields covering a very wide frequency range are desirable, especially when multiple-step reactions are to be studied. In general, a wide frequency range cannot be studied using a single experimental technique. Obviously, for measurements based on resonators or stationary waves, the linear dimensions of the measuring vessel must be proportional (or even comparable) to the wavelength, or inversely proportional to the frequency, and it will hardly be possible to cover more than one frequency decade with a single piece of measuring equipment. For progressive waves, the frequency range of a single apparatus is even more restricted. This is a result of the normal thermoviscous behavior of fluids, which leads to a dissipation of energy that increases with the square of frequency. At low frequencies (less than 50 kc.), no observable absorption takes place from a plane wave that travels a distance of several meters, whereas, at high frequencies (greater than 100 Mc.), practically all the energy is absorbed after a few millimeters of propagation.

For kinetic purposes a high absolute accuracy of energy absorption or of wavelength is not as important as a good relative accuracy in the determination of the differences between a reference solution (or pure solvent) and the solution containing the reacting chemical compounds. Difference measurements may be carried out either in sequence in the same apparatus, or simultaneously by suitable comparison methods. Some experimental techniques will now be described (2–6).

(1) Low-frequency region: resonance methods (100 c.p.s.–50 kc.). An appropriate method for the determination of sound absorption in this region is the measurement of the sharpness of the resonance curve of a single simple vibration mode for a given volume of the solution in a resonator. It is also possible to measure the decay time of such a vibration. The accuracy of the measurement is limited by losses from deformation of the enclosing walls, friction between the walls and the enclosed liquid, radiation losses, etc. The resonating container therefore has smooth thin

walls constructed of a material with very low acoustical loss (quartz, glass, or aluminum). Radiation loss is minimized by mounting the resonating container in a chamber that can be evacuated to a few millimeters of mercury during measurement.

Dispersion methods may consist of an exact measurement of the harmonically related resonance frequencies of different vibration modes of the same resonator, first filled with the reference solution and then with the system to be studied.

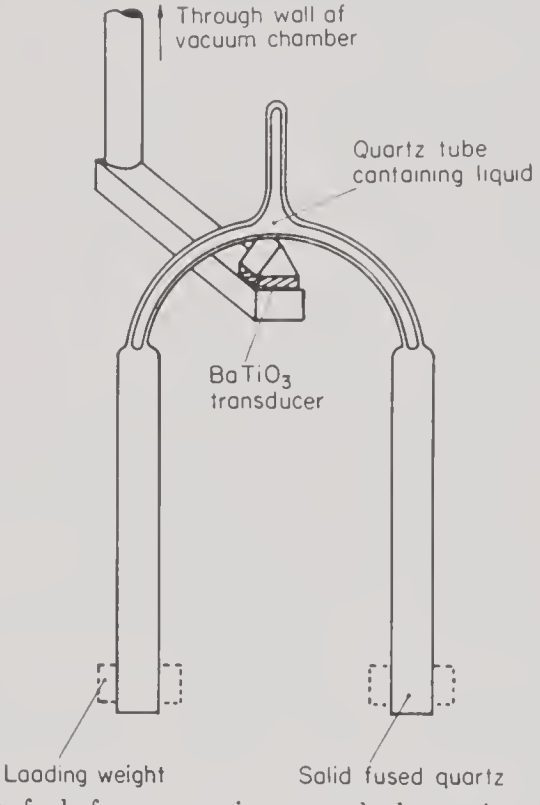

Fig. III.19. Tuning fork for measuring sound absorption at low frequencies.

A *tuning fork resonator* with a hollow arch containing the solution to be investigated has recently been described by J. H. Andreae *et al.* (7) for measurements at frequencies as low as 100 c.p.s. (Figure III.19). The fork is excited into vibration by a sharp tap on the heavy metal support that extends through the vacuum chamber. A small $BaTiO_3$ transducer allows detection of the vibrations, their rate of decay being determined from an oscillographic display. Excess absorption because of compressional relaxation is determined from measurements relative to the pure solvent. The decay rates are first determined with a small vapor bubble present, then with the hollow arch completely filled with liquid. In the first case, there may be a small dissipation, owing to viscous flow of the liquid (which will be neglected in the following), but the pressure change to which the latter is subjected is almost negligible. In the second case,

the liquid contributes to the elasticity of the arch of the tuning fork. In both cases, the moment of inertia of the fork will be very nearly the same. The contribution of the liquid to the total loss can then be easily calculated if the resonance frequency ω_B and the rate of decay $1/T_B$ (in neper sec.$^{-1}$) for the fork with the vapor bubble and the same quantities ω_F and $1/T_F$ for the full fork are determined. The energy absorption per period in the liquid is then given by

$$\mathfrak{y}_L = \mathfrak{y}_F[\omega_F^2/(\omega_F^2 - \omega_B^2)] - \mathfrak{y}_B[\omega_B^2/(\omega_F^2 - \omega_B^2)] = [4\pi/(\omega_F^2 - \omega_B^2)][(\omega_F/T_F) - (\omega_B/T_B)] \quad \text{(III.2.3)}$$

The resonance frequency of the tuning fork can be changed if loading weights are attached to the quartz tines of the fork. Only small amounts of liquid are required; the accuracy of this method, however, still needs some improvement.

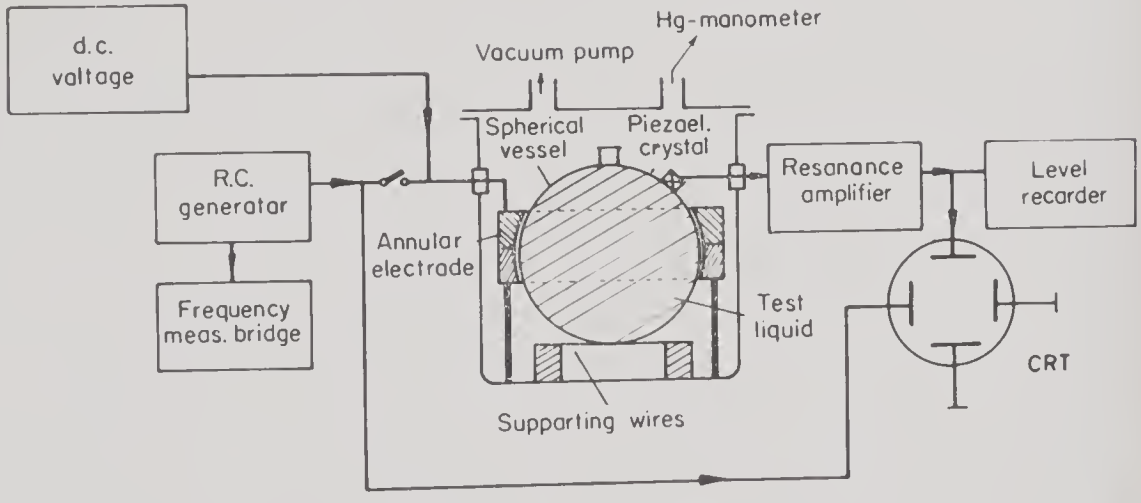

Fig. III.20. Spherical resonator method.

In *spherical resonators*, very low wall and friction losses may be realized by the use of symmetrical radial pulsation vibrations. The excitation of such vibration modes is readily obtained by applying a broad band of frequencies (e.g., as obtained from a noise generator) with a piezoelectric transducer fixed at the wall of the spherical vessel. A short time after excitation has been stopped, the other undesired vibrational modes will have died away (8–11). Tamm and Kurtze (12) excited such vibration modes by electrostatic forces, using an annular electrode to surround the resonating spherical container (Figure III.20). For observation of the decaying vibration, small piezoelectric transducers fixed at the resonator walls are used.

For minimum loss, the vessel (usually fused quartz) is supported by a structure of thin steel wires. The vessel should have a very good spherical symmetry and constant wall thickness. A volume of approximately 10

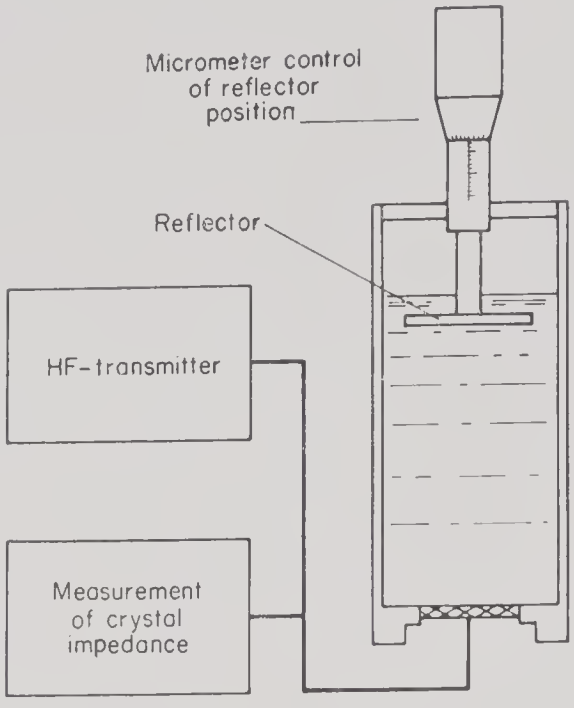

Fig. III.21. Acoustical interferometer.

l. has been used; it is usually quite difficult to measure at the lowest resonance mode of the vessel because of an inhomogeneous wall thickness and symmetry deviations. For accurate measurements of sound absorption at low frequencies, relatively large amounts of liquid are necessary in most cases. If smaller spheres are used (13), very high precision work is required.

Cylindrical resonators have been used for the determination of sound absorption and dispersion in gases (14). Longitudinal and radial vibration modes may be superposed, and a quite complicated resonance spectrum of the resonator will result.

The decay time of the resonating structure is usually the most accurately measurable quantity. Compared to the measurement of the shape of the resonance curve, the stability requirements for the exciting electrical oscillator are less severe; it must only remain tuned to the resonance peak during the observation of a few excitation and decay cycles. It is also unnecessary to measure small frequency deviations close to resonance. If the losses are great, however, it may be easier to determine the half-width of the resonance curve. From the time constant of vibrational decay T_d or from the decay rate $1/T_d = (1/t) \ln (p_0/p_t)$ the attenuation constant $\alpha = 1/\mathbf{v}T_d$ ($\mathbf{v}$ = sound velocity) or the energy absorption per wavelength $\mu = 2\alpha\lambda = 4\pi(1/\omega T_d)$ can readily be determined.

(2) Intermediate frequency region: stationary waves (50 kc.–2 Mc.). The *acoustic interferometer* is similar to a cylindrical resonator: the distance between a transmitting crystal and a reflecting surface can be varied and

accurately measured. The exciting crystal current is measured as a function of the distance of the reflecting plate. At half-wave intervals, sharp dips can be observed in the exciting current, showing that a high mechanical impedance is coupled into the crystal by the standing-wave system between the crystal and the reflector. Absorption data can be obtained from the dip width, whereas the wavelength is measured from the position of the dips (15–21) (Figure III.21). In the interferometer, the cylindrical walls can be moved away from the sound beam so that radial vibration modes do not restrict the number of longitudinal modes that may be observed. A large frequency region may therefore be covered by the acoustical interferometer. Measurements are possible to several megacycles, with a corresponding wavelength of a few tenths of a millimeter (22). A slight curvature of the wavefront may occur, however, depending on the radius of the transmitting and reflecting surfaces (23). The resonance positions of the reflector will not be exactly equidistant and the accuracy of wavelength measurements may suffer. A theoretical treatment of the interferometer has been given by Hubbard (17). [For further literature see ref. (3).]

At higher frequencies, the resonator methods become impractical, because the single normal modes of oscillation become less and less distinct. It is then difficult to get separate excitation of one of these modes of vibration (in a vessel of appropriate dimensions) that also maintains the condition of low losses. Measurement of the decay time of a superposition of vibration modes centered at the desired frequency is then more advisable.

Such a method [first suggested for liquids by Meyer and Skudrzyk (24)] is realized in a measurement of *reverberation* time (25–27). A great number of vibrational modes are simultaneously excited by pulsed high-frequency or noise bands. The vessel containing the solution should, in this case, have a very low symmetry, so that every vibration is reflected on the walls of the container with as many different angles as possible. This requirement is necessary in order to obtain equal reflection loss for every vibration present in the measured frequency band, so that equal decay times for the different vibrational modes are realized. The reverberating vessel may be a tilted cylinder (27), hanging on metal wires (to prevent energy loss in the supporting structure), and having thin aluminum walls that follow the movements of the vibrating liquid. Reflection will then take place, in effect, at the outer boundary (metal-air), giving lower friction loss. One of two piezoelectric transducers, fixed on the wall of the vessel, is used for excitation with short pulses of high frequency. The reverberation-time constant is determined directly on a cathode-ray oscillograph after amplification and frequency conversion. The rate of decay may be directly obtained from the slope of a straight line displayed on the cathode-ray

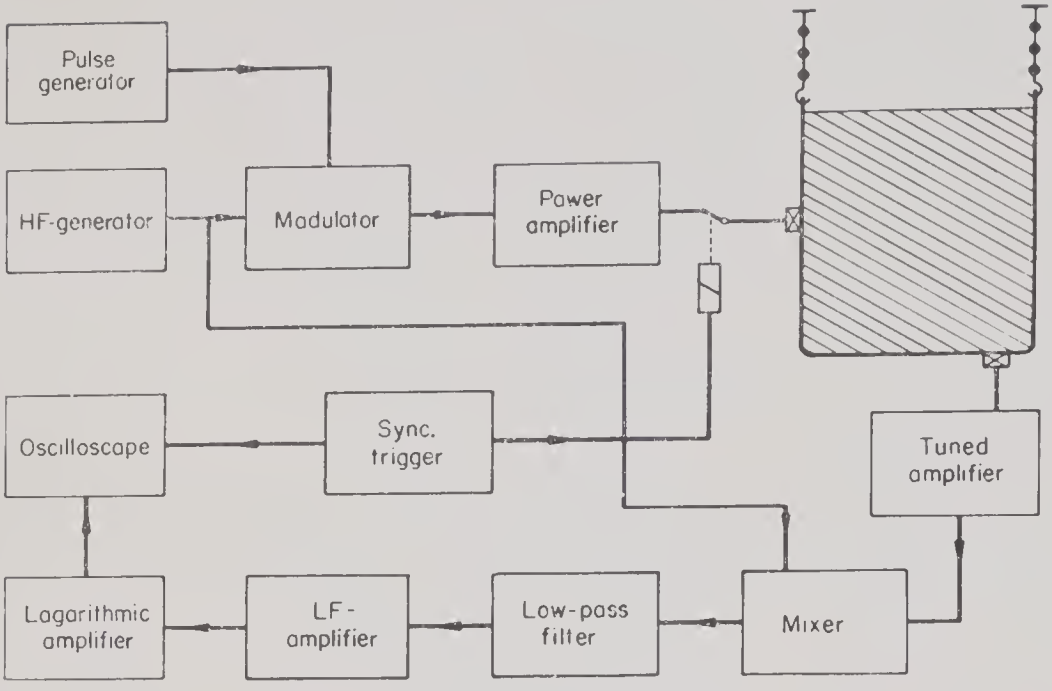

Fig. III.22. Reverberation method.

oscillograph, if a logarithmic ordinate measure is used (amplifier with logarithmic response) (Figure III.22).

(3) High-frequency region: progressive waves (greater than 1 Mc). For high frequencies, the absorption generally becomes so great that it is possible to measure directly the attenuation of the propagated sound wave. Such a measurement may be carried out with an *optical method* based on an effect discovered independently by Debye and Sears (28a), and Lucas and Biquard (28b): the progressive sound wave creates regions of compression and dilatation which alternate at distances of one-half wavelength. For a parallel light beam, these regions act like a diffraction grating. From the spacing of diffraction orders, the wavelength can be determined. Alternatively, the light intensity in the diffraction orders can be used for a determination of sound intensity, because an increase in the intensity of the sound wave forces more and more light from the zero-diffraction order into the higher orders. The first-order diffraction can be separated by a slit, and, as long as higher orders are sufficiently weak, the photometrically measured light intensity is directly proportional to the sound-pressure level (29). The light beam and the slit may be moved away from the sound transmitter so that the pressure level can be measured very accurately as a function of distance from the transmitter surface, giving the attenuation constant directly (Figure III.23).

The measurements may be carried out using a continuous sound wave (30a). However, for an accurate amplification of the photometrically measured light intensity (avoiding dark-current effects of the photocell

or photomultiplier and amplifier drift), it is preferable to have a pulsed-light signal. It is possible to use a rotating shutter to chop the light beam, but in most cases it is easier to use a periodically pulsed excitation of the transmitting crystal (square-wave modulation of the excitation oscillator). The photocell signal can then be amplified by a tuned amplifier and, after rectification, recorded by a logarithmic pen recorder (30b).

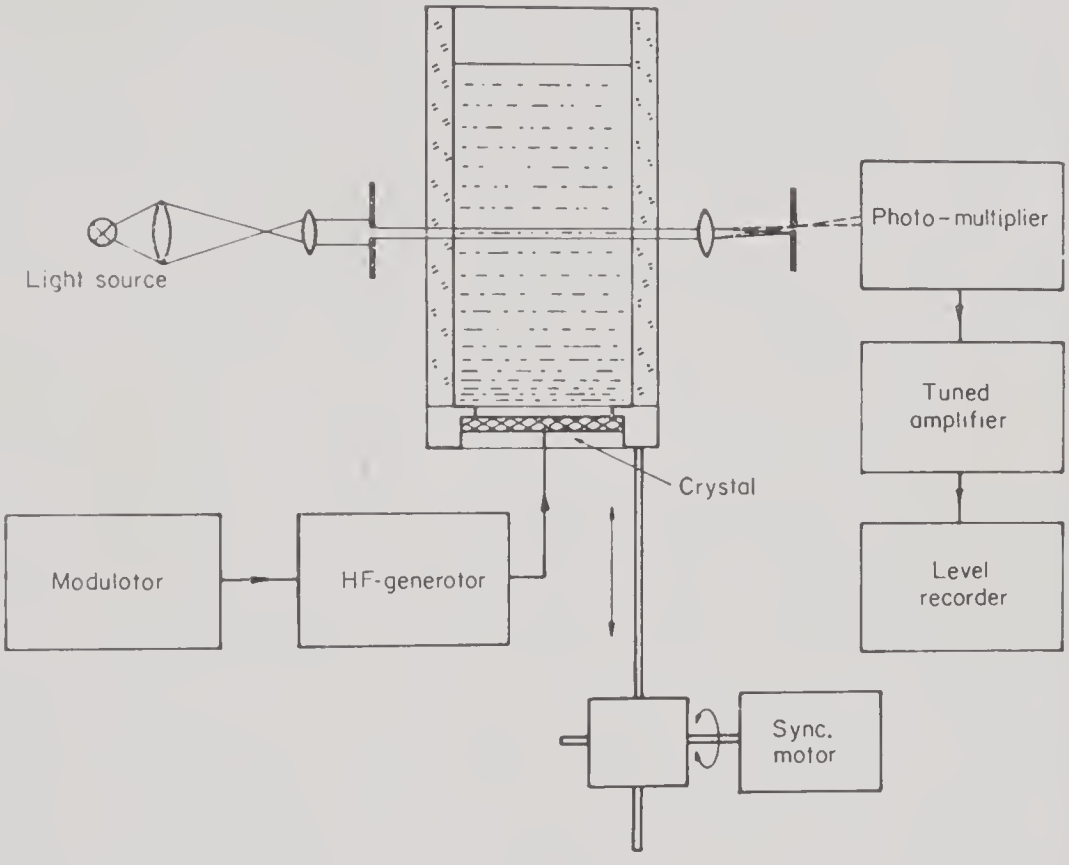

Fig. III.23. Optical method (Debye-Sears effect) for sound-absorption measurement.

A related optical method, known as the method of isochromates, has also been used for the study of ultrasonic absorption in liquids (31). The intensity distribution of the diffracted light over different diffraction orders varies with the wavelength of the light. On using a white light source, a color picture of the sound field is obtained; lines of equal sound intensity are then represented by lines of equal color (isochromates). Absorption coefficients may be determined by measuring the distance of a given color from the transmitting crystal as a function of radiated power.

For very high frequencies (greater than 100 Mc.), the sound intensity required for a sufficiently bright diffraction pattern becomes prohibitively high; at the same time, large attenuation takes place in very short distances, and optical measurements become very difficult.

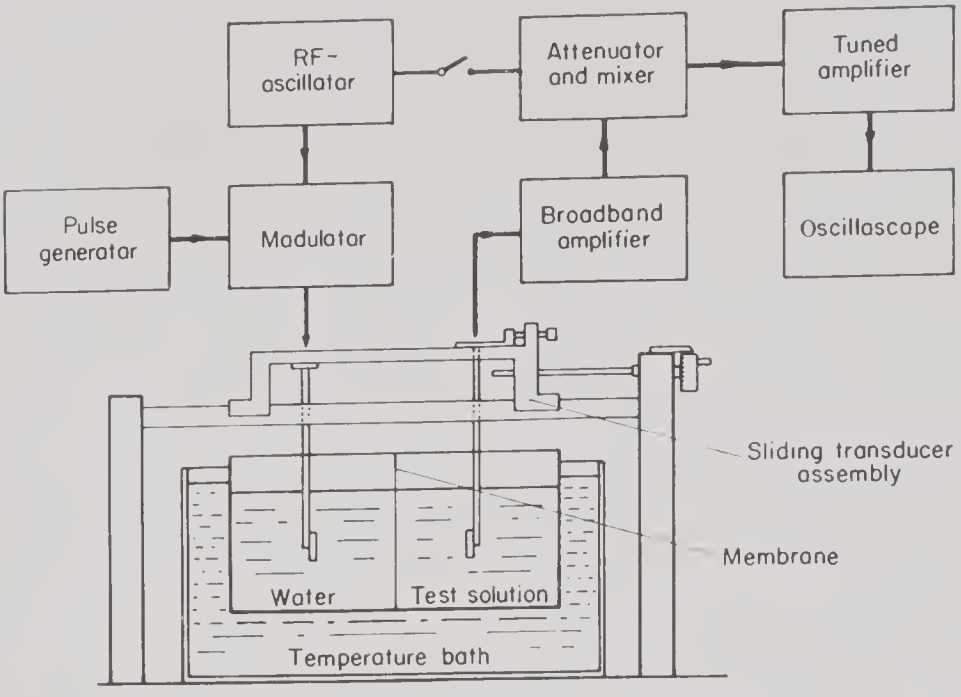

Fig. III.24. Differential method for measuring sound absorption and dispersion.

Direct measurement of *radiation pressure* as a function of distance from the sound transmitter will also give a measure of sound absorption in a progressive wave (32,33). The forces to be measured, however, are very small, and the disturbances introduced in the sound field by the measuring device should not be neglected. The latter difficulty is not present in the optical method. Because of sound absorption, there is a *gradient of radiation pressure,* which, in turn, will cause a steady flow of liquid away from the sound source. In the steady state, of course, this flow must be compensated by recirculation toward the sound source in regions outside the propagating sound beam. Hall and Lamb (34) studied sound absorption between 100 kc. and 1.5 Mc. from such second-order phenomena (acoustic streaming).

Dispersion measurements in continuous progressive waves are related to a *measurement of phase.* Fox and Marion (35) compared the sound velocities of two different but harmonically related frequencies, which were simultaneously transmitted in the medium, by measuring the relative phase of both frequencies as a function of distance from the transmitter. Since very high accuracy is possible in phase measurements, the limiting factor for detection of a sound dispersion is the curvature of the wavefront. A comparison method has been used by Carstensen (36): The total constant distance between a transmitting and a receiving transducer is separated by a (sound-transparent) membrane in two compartments containing the solution and the solvent, respectively. Direct phase comparison between transmitter and receiver voltage as a function of relative path length in

the two media gives a measure for the difference in sound speed (Figure III.24).

In this connection, the "spectraphone" method, developed by the Russian school (37), should be mentioned. The procedure consists of an excitation of sound waves by the input of energy from modulated light. A modulated beam of infrared light passes through the system; a portion of its energy is taken up by absorption in vibrational degrees of freedom and is converted into translational and rotational energy, thus producing detectable pressure oscillations. The finite time of energy transfer produces a phase shift between modulated light and pressure, which can be measured very accurately. Relaxation times down to microseconds can be determined. These time constants, however, are related to the process of energy transfer and not to real chemical relaxation. Furthermore, the method is restricted to studies in gases.

For the very high frequency region (greater than 100 Mc.), *pulse techniques* have been developed (38–43). A quartz transmitter radiates pulses of the desired frequency into the liquid. They travel a variable distance through the liquid and are then received by a second quartz crystal. The measured amplitude, as a function of distance, yields the attenuation. Distances down to a few tenths of a millimeter have to be used, as the attenuation in the liquid is exceedingly high (for pure water it is about 24 neper/cm. at 300 Mc.). To avoid electrical cross-talking at such distances,

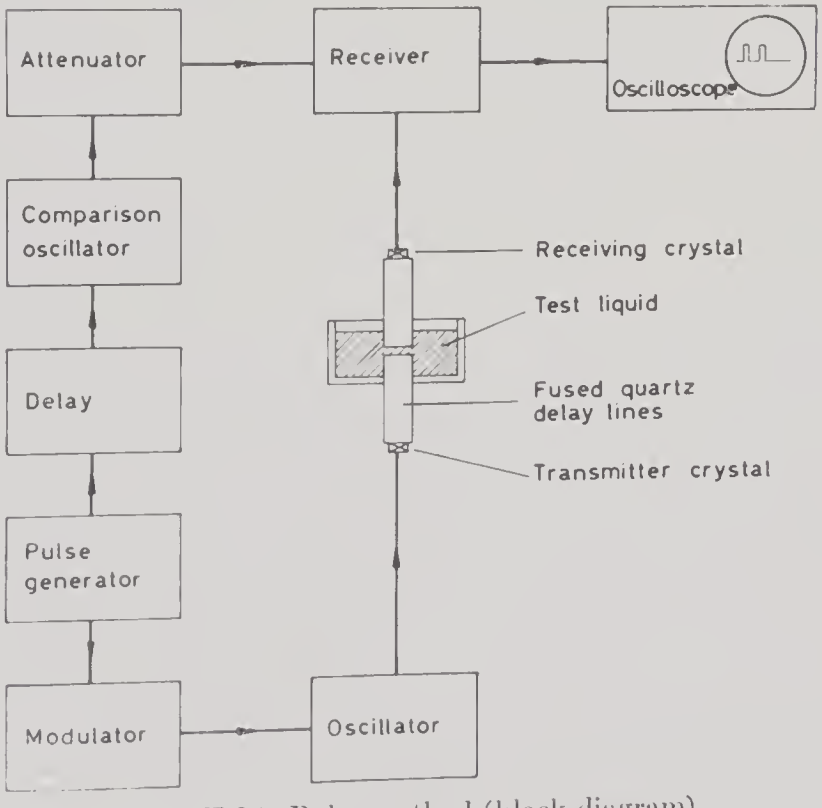

Fig. III.25. Pulse method (block diagram).

fused quartz rods are used between the liquid and the transmitting or the receiving transducer. These rods act as acoustical delay lines, so that the stray electric impulses have decayed at the moment the acoustical impulse is received. The quartz rods must have optically flat surfaces, and they must be mounted exactly parallel. Amplitude is measured by comparison of the heights of the received and the transmitted pulses, which have passed a calibrated attenuator (Figure III.25). It is also possible to use a single quartz crystal as transmitter and receiver in combination with a reflecting surface (*echo method*). Sound velocity measurements can be made using similar apparatus if the delay time between transmitted and received impulse is accurately determined.

Very accurate determinations of this type have been accomplished recently by the use of the "sing-around system" (44). In this method, the transmitting crystal is excited with a very short single pulse (approximating the form of a δ-function), yielding a damped wave train (of the eigenfrequencies of the crystal), which traverses the sample. At the receiver, one of the multiply reflected echoes is selected by appropriate timing gates and is used for retriggering the transmitter crystal, a process which may be repeated indefinitely. The time required for an electronically counted number of "sing-around" cycles is measured. Then the electronic delay must be subtracted from the total delay to obtain the acoustical travel time, which, at a given distance, is characteristic of the sound velocity. Relative accuracies (of velocity changes in solids at low temperatures) of one part in 10^7 have been reported (44b). It should be mentioned that the electronic equipment required for such accurate measurements is fairly involved.

The time range of chemical relaxation phenomena that may be continuously covered by the different sound techniques described above (*cf.* Table III.1), extends from a few hundred cycles per second to 500 Mc. (τ between 10^{-3} and 2×10^{-10} sec.). A special technique, recently described by Boemmel and Dransfeld (45) even allows the excitation of sound waves in the ultra-high-frequency range (10,000 Mc.). A cylindrical quartz crystal is mounted with one side in a resonating cavity that is excited with electromagnetic waves. The attenuation of the sound wave is very high in the crystal itself, and depends strongly on temperature. Such high frequencies are becoming available for the study of acoustical phenomena; nevertheless, considerable difficulties are to be expected for applications to chemical rate processes in liquids.

The sensitivity of the acoustical methods for the investigation of chemical relaxation is not very high; appreciable concentrations of the reacting components are required (at least 0.001M, preferably 0.01 or 0.1M solutions are to be used).

TABLE III.1
Experimental Methods for Acoustical Investigation of Relaxation

Technique	Absorption measured from	Frequency range	Dispersion measured from
Stationary waves			
Tuning fork	Decay time (7)	100 c.p.s. ...	
Spherical resonator	Decay time (12)	5–50 kc.	Harmonic resonance frequencies
Reverberation	Decay time (12)	50 kc.–1 Mc.	
Interferometer	Sharpness of resonance curve (18)	50 kc.–2 Mc.	Wavelength
Progressive waves			
Continuous plane waves	Light diffraction (12, 31)	2–100 Mc.	Phase shift (35, 36)
	Radiation pressure (32)	5–50 Mc.	
	Radiation pressure gradients (34) (acoustic streaming)	100 kc.–10 Mc.	
Impulse methods	Attenuation (43)	1–300 Mc.	Delay time (44)

Acoustical measurements of chemical relaxation of gaseous reaction equilibria are very difficult because of the extreme conditions under which appreciable dissociation occurs. Nevertheless, a great number of physical relaxation phenomena in gases (relaxation of vibrational and rotational energy transfer, etc.) have been observed. The transient methods which usually involve greater amplitudes of the equilibrium displacement and sensitive selective measuring methods are better adjusted to these systems (shock-wave methods, etc.).

B. EVALUATION AND INTERPRETATION OF SOUND ABSORPTION DATA

The sound intensity is proportional to the square of the effective amplitude of pressure or of particle velocity at a given point in the sound field. It is defined as the time average of energy flux through unit area normal to sound propagation and is given by energy density $\times$ sound velocity. Therefore, the acoustical intensity level, expressed by $\ln (I_1/I_2)$ (i.e., the logarithmic ratio of intensities) at two points in the sound field is equal to twice the acoustical pressure level, $\ln (p_1/p_2)$ (provided the acoustical impedances at both points are the same). The energy absorption coefficient is then characterized by 2α, as shown in Section II.3.E.

The acoustical intensity level can be measured directly by the radiation pressures at two distances from the sound transmitter, whereas optical or piezoelectric methods give information about the pressure levels. Some

authors express the acoustical level (logarithmic measure for the ratio of two quantities) in nepers when the quantities are scalar amplitude values, whereas the measure decibel (db) is defined for power ratios (intensities):

Intensity level (Power level)	$= \log_{10} (I_1/I_2)$ db $(= 20 \log_{10} (p_1/p_2)$ db)
Pressure level (Amplitude level)	$= \ln (p_1/p_2)$ neper $(= {}^1/_2 \ln (I_1/I_2)$ neper)

One neper is equivalent to 8.686 decibels.

Another (dimensionless) quantity is the (coefficient of) "absorption per wavelength" $\mathfrak{u} = 2\alpha\lambda$. From comparison measurements with the pure solvent or a reference solution, the measured quantities α or $\mathfrak{u}$ can be split into a residual and a chemical part. Often, the residual part is taken equal to the value of α or $\mathfrak{u}$ in the pure solvent or the reference solution. This procedure is not quite correct, since the residual absorption may change in the presence of the solute (solvent structure change, further relaxation phenomena, etc.). It is better to determine the single parts of α or $\mathfrak{u}$ from accurate absorption measurements in a wide frequency range. It is very practical then to plot the quantity α/ν^2 or α/ω^2 (or its logarithm) against log ω as shown in Figure III.26. Discrete relaxation phenomena are then characterized by discrete steps; the residual part can thus be determined directly from experimental values.

For a physical interpretation, it may be practical to relate the chemical excess absorption to the single molecule of solute and to define a (chemical) absorption "cross section" Q by

$$Q = 2\alpha_{\text{chem}}/(N_A\, c_i^0) \qquad \text{cm.}^2\text{/molecule} \qquad \text{(III.2.4)}$$

with N_A: Avogadro's number, c_i^0: total number of solute moles (unreacted) per cubic centimeter of solution. This quantity can be interpreted physically as a surface normal to the plane-wave field, through which power is transmitted just equal to that absorbed by a single molecule.

The quantity $[Q\lambda]$ has the dimension of volume per molecule; it represents a volume in the sound field containing an energy equal to that absorbed by a single molecule during one period. This "absorption volume," like the coefficient $\mathfrak{u}$, has its maximum value for $\omega \approx 1/\tau$, as was shown in Section II.3.E.

For an easy interpretation of chemical relaxation phenomena, $\mathfrak{u}$ or $[Q\lambda]$ is plotted against frequency (ν or ω) on a log-log scale. The relaxation time τ is found from the position of $[Q\lambda]_{\max}$. The absolute value of $[Q\lambda]_{\max}$ allows the determination of ΔV or ΔH if a complete analysis of the reaction mechanism is possible. Measurement of the temperature dependence of $[Q\lambda]_{\max}$ will give further indications of the validity of the as-

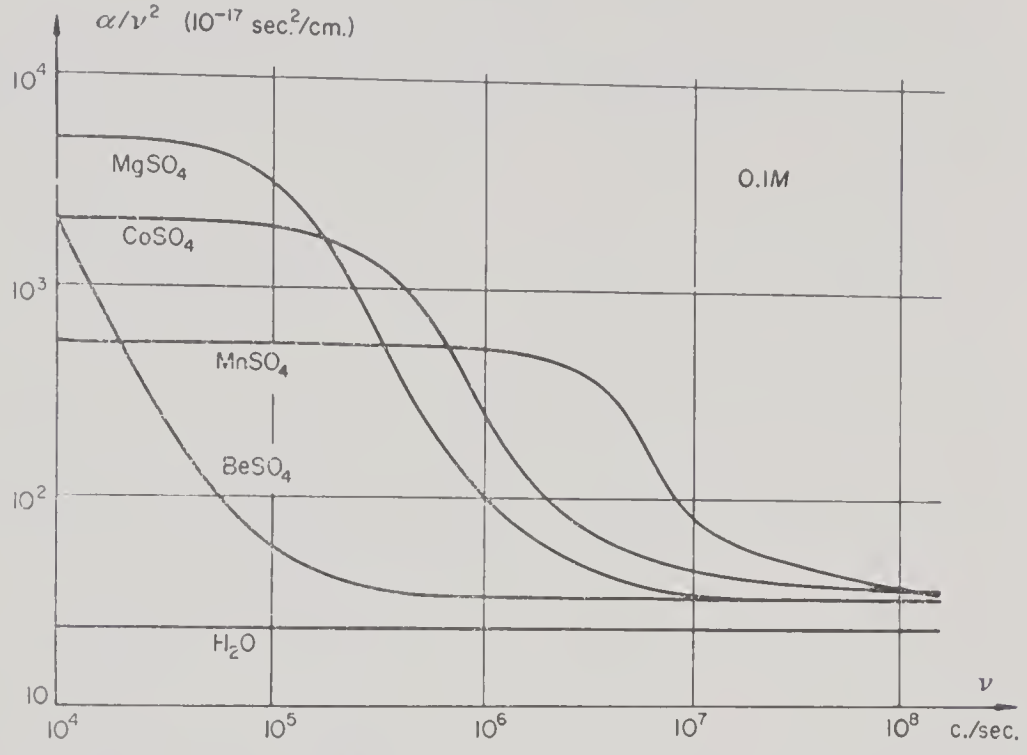

Fig. III.26. Sound absorption (α/ν^2) for different aqueous electrolyte solutions.

sumptions made in the evaluation of reaction enthalpy, volume, and equilibrium constant, if the latter quantities are not directly measurable by other methods (46).

Dispersion measurements yield the residual and the (chemical) excess parts of sound velocity (or compressibility) directly, if they are carried out over a sufficiently wide frequency range. Absorption measurements are usually the more sensitive ones. This fact is a result of the form of frequency terms occurring in the absorption coefficient α (or μ) and phase velocity v_{re} (*cf.* Section II.3.E). A small chemical contribution to the compressibility can become predominant for α (or μ) at $\omega \lesssim 1/\tau_{chem}$, provided that relaxation for the residual part occurs at much higher frequencies. In contrast, the relative contribution of the chemical term to v_{re} is always (appreciably) smaller than that of the residual term. Since this usually is very small, good temperature stabilization will be required for dispersion measurements because sound velocity is dependent on temperature and corresponding density changes.

Survey on Acoustical Measurements. Measurements of sound absorption and dispersion in fluids are quite numerous. However, applications to genuine chemical relaxation and analyses of the reaction mechanism involved are still very scarce. Following the scope of this chapter, we can refer only to these applications. Other applications, especially studies of energy transfer between translational, rotational, and vibrational degrees

of freedom of molecules in the gaseous state, or investigations of structural phenomena in liquids (such as molecular interactions, cluster formation, etc.), are excellently reviewed in a monograph by Herzfeld and Litovitz (*cf.* General References p. 900), which has recently appeared. [For other review articles see Kneser (6), Davies and Lamb (46), Verma (48), Sette (47), and, also, ref. (49).]

On considering chemical applications, the classic example of the NO_2–N_2O_4 gas equilibrium [which about 50 years ago led Nernst (50) and Einstein (51) to the first consideration of sound dispersion in connection with chemical relaxation] could not be studied by sound absorption techniques until recently (52,53). These measurements reconfirm previous data that have been obtained by shock-wave (54) and impact-tube (55) experiments (see transient methods, Section III.1.D).

Further chemical relaxation studies by sound absorption techniques have been carried out in liquids. A serious restriction is the requirement of a relatively high concentration of reactants. This difficulty does not occur if studies are made with pure liquids, although the interpretation may then become less straightforward, since an important parameter, the concentration, cannot be varied.

Studies of rotational isomerism, initiated and promoted primarily by Lamb and co-workers, proved to be one of the most fruitful applications [for survey see ref. (46)]. Although it may be a question of definition to call two isomers "chemically" different species, the transformations appear phenomenologically as typical chemical (first-order) reactions. An example of such studies is shown in Fig. III.27(a), where the absorption coefficient per wavelength, measured in pure triethylamine at different temperatures (56), is plotted against frequency. The typical frequency dependence with a maximum at $\omega = 2\pi\nu = \tau_{PS}^{-1}\,[1 - \bar{\kappa}_S^{ch}/\bar{\kappa}_S]^{-1/2}$, as predicted by theory (46) (full lines), is reproduced by the experimental values. The evaluation of measurements follows from Section II.3.E, where only a finite ΔH has to be considered ($\Delta V = 0$). Since the equilibrium constant cannot be obtained from a variation in concentration, the study of temperature dependence (in order to obtain ΔH) is very important in these cases. The relaxation frequency for first-order transformations gives only the sum of the rate constants of the forward and reverse reactions (*cf.* Table II.1); a separate determination of both rate constants requires the knowledge of the equilibrium constant. Here, the temperature dependence will also yield additional information. Many other examples of rotational isomerism have been studied. They include unsaturated aldehydes and ketones (57), esters (58,59), cyclohexane derivatives (59–61), substituted carbohydrates (62,63) (with three alternative states), and other systems [see ref. (64)]. One can also mention the studies of molecular association in

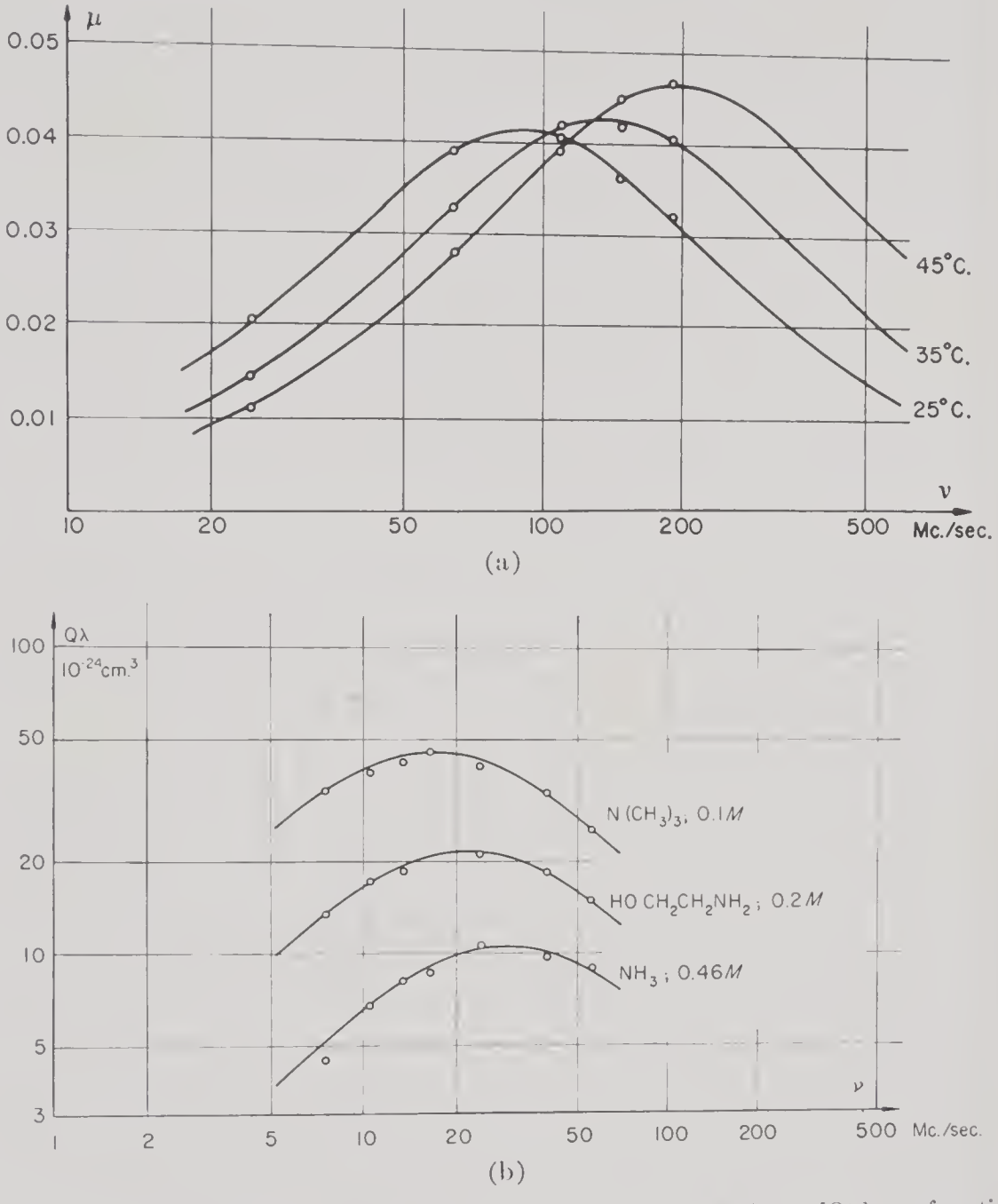

Fig. III.27. Examples for measured sound-absorption curves (μ or $[Q\lambda]$ as a function of frequency ν: (a) triethylamine (pure liquid) (60); (b) amines in aqueous solution (73), (74).

pure liquids exhibiting hydrogen bonding (65–57). The interpretation, here again, is complicated by the fact that no variation of concentration is possible in pure liquids, although even for a study of a higher-order reaction, such as association, the concentration dependence would yield valuable information [see also the studies of two-component mixtures (68)]. In some cases, where association is strong enough as in the case of dimerization of carboxylic acids, studies could be performed in more dilute solutions using nonpolar liquids as solvents (69,70). These studies gave definite

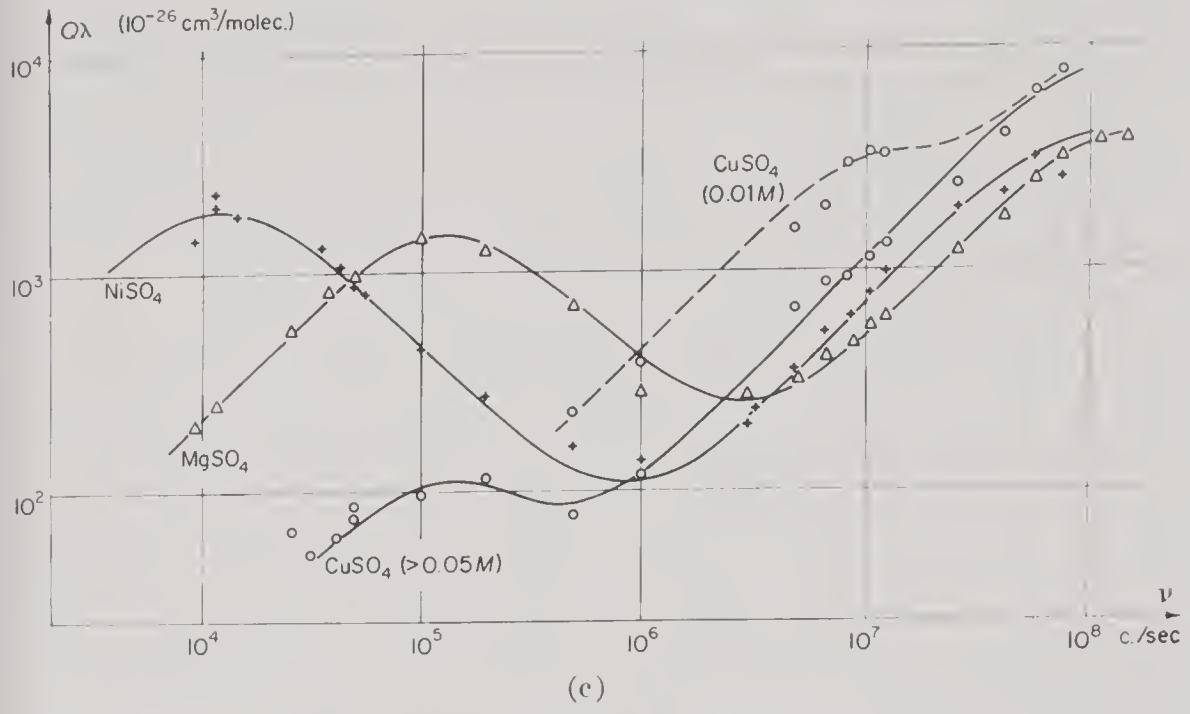

(c)

Fig. III.27 (*continued*). (c) $NiSO_4$, $MgSO_4$, and $CuSO_4$ in aqueous solution (42).

results about the kinetics of dimerization. Measurements can even be made at one frequency (71,72), if concentration and temperature are varied. In such a determination, however, the reaction must be represented by a (known) one-step mechanism. Studies of frequency dependence, in any case, are superior, at least for kinetic applications.

A number of real chemical reactions, that is, chemical transformations with changes in the composition of molecules, have been studied in aqueous solutions. The excess sound absorption in aqueous systems, which is a result of chemical relaxation, is primarily determined by a finite ΔV for the reaction system. (This statement does not mean that the heat of reaction ΔH is zero, but that the pressure change is not accompanied by an appreciable temperature change, owing to the small value of the coefficient of expansion α_P (density anomaly).) Reactions involving a neutralization of electric charges are accompanied by appreciable changes in solvent structure (solvation) and therefore fulfill the condition of appreciable volume change. One of the first systems that could be studied and interpreted quantitatively (since all equilibrium parameters of the chemical system were known) was the base equilibrium of NH_3 in aqueous solution (73,42). The experimental values of absorption per wavelength as a function of ω are represented in Figure III. 27b [see ref. (73,42); remeasured values according to ref. (74)]. They can be quantitatively interpreted using the known values of $K_0' = 1.75 \times 10^{-5}$ mole $l.^{-1}$ (dissociation constant) and $\Delta V = V_{NH_3 \cdot H_2O} - V_{NH_4^+} - V_{OH^-}) = 28$ cm.^{3}/mole, and yield $k_r =$

3.4×10^{10} l. mole^{-1} sec.$^{-1}$ (rate constant of recombination). Measurements of the pressure dependence of μ (75) reconfirmed these results. A number of other acids and bases have been studied in the same way, giving interesting results about protolytic, hydrolytic (74), as well as inter- and intra-molecular proton transfer processes (76,77) in solutions. In combination with other relaxation measurements, as described in Section III.1, they yield a detailed picture of the mechanism of protolysis and hydrolysis in aqueous systems.

Other applications have been made to the study of metal-complex formation in aqueous solution. The interpretation of early sound absorption measurements in aqueous solutions (78) was hindered by the fact that studies were made only over limited frequency ranges. Later, when measurements were extended over a wide frequency range (e.g., 10^4 to 3×10^8 c.p.s.) (8–10,42), a detailed picture of the mechanisms involved could be obtained. The chemical nature of the processes causing the sound absorption in solutions of 2:2 electrolytes [compare the example in Figure III.-27.c)] was soon recognized (79–83,9), but a quantitative description required the application of the theory of coupled reaction mechanisms as outlined in Section II.1.C [see also the expression for μ given in Section II.3.E Equation II.3.93ff) (84,85)]. (Practically none of the previous investigations were undertaken with the aim of studying chemical kinetics.) The kinetic analysis yielded the rate constants for the single steps of substitution of water molecules from different coordination spheres of the metal ion, so that—in combination with other relaxation studies—a detailed picture of the general mechanism of metal-complex formation could be obtained (86). For applications to the analysis of ionic interactions in electrolyte solutions see refs. (84,85). Some values of rate constants of these and other reactions are listed in Section IV.

C. ELECTRICAL METHODS (HIGH-FIELD TECHNIQUES)

Apart from pressure and temperature, which can be periodically changed in a sound field, electric and magnetic field strengths are parameters that can easily be varied in a periodic way. Chemical equilibria will depend directly upon the electric field strength, if the reaction partners and the reaction products have different effective dipole moments (i.e., if $\Sigma \nu_i \mathbf{P}_i^2 \neq 0$, $\mathbf{P}_i$ = permanent electric moment of species i) or if the reaction proceeds with a production or neutralization of charged particles (dissociation field effect). Magnetic fields will influence chemical equilibria if the reaction involves a corresponding difference in magnetic moments of reactants and products (e.g., reactions between free radicals or other paramagnetic species), although the effects to be expected are extremely small.

As in the case of sound waves, temperature and pressure oscillations will also exist in a medium subjected to adiabatically and isochorically varying electric or magnetic fields, provided the temperature or pressure dependence of the total dielectric constant or magnetic permeability does not vanish. Reaction systems that are not directly influenced by static, electric, or magnetic fields can therefore, in principle, be disturbed by temperature changes accompanying dynamically varying fields, as shown in Section II.3.C.

By analogy to sound absorption, methods for studying chemical relaxation phenomena induced by electric or magnetic fields could be based on the measurement of excess energy dissipation in the system when the thermodynamic forcing parameter and its conjugated system parameter are out of phase. On the other hand, any system variable that is related to a chemical reaction induced by a periodically changing forcing variable, may be used for a determination of the transfer function.

Ionic Equilibria. Relaxation of the second Wien effect has been studied using transient methods (*cf.* Section III.1.D). A stationary method has been proposed by Pearson (87). Since the equilibrium shift induced by the electric field in an ionic equilibrium depends upon the absolute value of the field density, the periodic change in ionization does not have the same frequency as the applied alternating field.

For a binary monovalent electrolyte equilibrium of the form $A^+ + B^- \rightleftharpoons AB$, subjected to a sinusoidally varying field intensity, $E = E_0 \sin \omega_0 t$, the corresponding relative increase in ionization can be described by a constant term, augmented by a sum of harmonically related periodic oscillations:

$$\frac{\delta\alpha}{\alpha} = \frac{1-\alpha}{2-\alpha}\,\frac{4\pi e_0^3}{2\epsilon\epsilon_0 k^2 T^2}\,\frac{2\mathbf{E}_0}{\pi}\left[1 - \sum_{n=1}^{n=\infty}\frac{2\cos(2n\ \omega_0 t - \varphi_n)}{4n^2-1}\right] \qquad \text{(III.2.5)}$$

where φ_n expresses the phase shift introduced by the transfer function $\mathfrak{S}_n$ for each of the harmonic frequencies $2n\ \omega_0$:

$$\mathfrak{S}_n = (\cos\varphi_n - j\sin\varphi_n)\rho_n$$
$$= \{1/[1 + (2n\omega_0)^2\tau^2]\} - j\{2n\omega_0\tau/[1 + (2n\omega_0)^2\tau^2]\} \qquad \text{(II.2.6)}$$

This derivation is based on a first-order approximation of Onsager's theory of the dissociation field effect (see Equation II.3.41), neglecting the influence of ionic atmosphere effects. The phase shifts between the applied electric field and the harmonically related components of the oscillating ionization lead to an absorption of energy from the field.

Unfortunately, there is always a large dissipation of energy as a result of the Ohmic conductance of a system containing ionized species. With

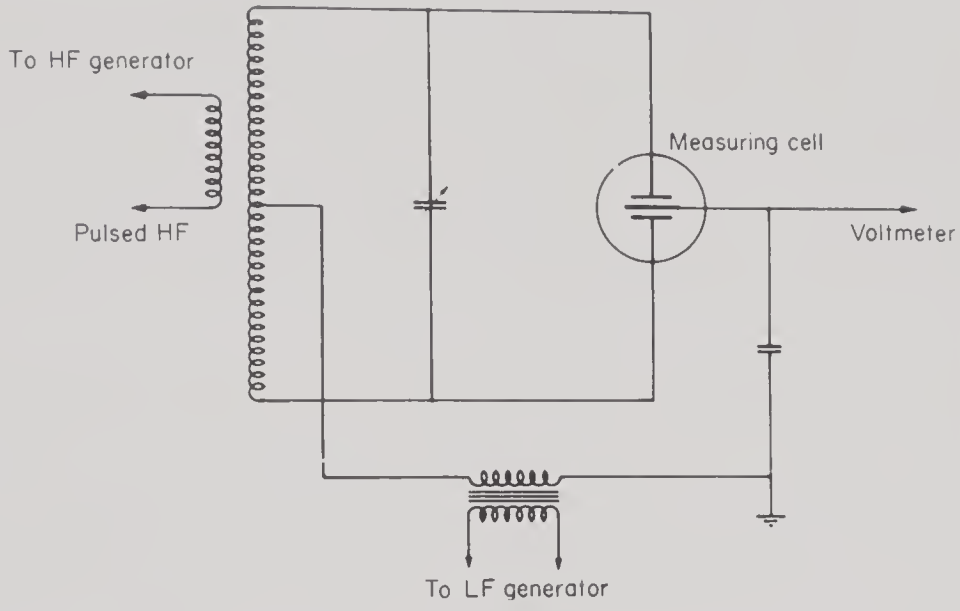

Fig. III.28. Modulation method for measuring the dissociation field effect.

present techniques, it seems very hard to detect the excess power loss or to measure the corresponding dispersion in the total Ohmic resistance with sufficient accuracy in the frequency range of interest. The expected excess loss will amount to much less than $^1/_{100}$ of the loss from conduction; if the measurements are carried out at relatively low field intensities, the presence of ionic atmosphere effects (which disturbs the linear field dependence, compare the discussion of Equation II.3.41) will again invalidate the above approximation and will lead to still smaller effects.†

A different technique (89) for a stationary measurement of the dissociation field effect and its dispersion is based on the fact that the relation between ionization and applied electric field contains the *absolute* value of the electric field strength.

An external electric field that is periodically switched on and off will therefore modulate the ionization (and, as a consequence, the electrical conductance of the system) with the switching repetition frequency, regardless of whether the switched electric field has a constant direction or an alternating one. Repetitive pulses of a high-frequency alternating high voltage can therefore be used to modulate the conductance of a solution between two electrodes. The impressed modulation can be detected by simultaneously applying an alternating voltage (carrier) to the same or to other electrodes; sum and difference frequencies between the modulation and the carrier frequencies are then generated. A schematic arrangement is given in Figure III.28; this circuit acts in somewhat the same way as a balanced (phase-sensitive) modulator. If the modulation and the

† A technique described by Gilkerson (88) for improving the sensitivity of Pearson's method is founded on incorrect equations and does not represent any progress.

carrier frequencies are the same, a d.c. component results, which charges the capacitor "C." Dispersion of the dissociation field effect because of relaxation will lower the modulation efficiency. The effective value of conductance variation will become lower as the switching period becomes smaller and approaches the relaxation time. With decreasing modulation efficiency, the charge on the capacitor C will also decrease. Because of the inherent property of frequency conversion, such methods allow an accurate determination of small effects.

It should be noted that the dependence of the dissociation field effect upon the absolute value of the external field as described in Equation (II.3.41) is based upon Onsager's treatment of the stationary equilibrium, which does not include the consideration of time-dependent effects. A theoretical treatment involving frequency dependence has not yet been given. It is to be expected that deviations from Onsager's equation will occur when the frequency of the applied external field approaches the reciprocal relaxation time of the ionic atmosphere. This limits the applicability of the methods described here, since the dissociation field effect will effectively vanish for such high frequencies. The application of the method, however, may be straight-forward if reactions with time lags appreciably larger than the ionic atmosphere relaxation time are involved. Any method which involves the application of high fields to conducting systems should be analysed with respect to thermal effects because of heat dissipation, which also will introduce conductivity changes. Repetitive or stationary field methods will in general be applicable only to (nonaqueous) systems with low conductivity.

Dipolar Equilibria. It has been shown in Section II.3 that chemical equilibria, in which partial molar polarizations are different on both sides of the reaction equation, depend upon the square of the electric field.

Therefore, for any effect to be measurable, a very high field should be applied. For an observation of the dispersion of such effects, however, it will not be necessary to use alternating fields of high intensities. If a small alternating field $\delta\mathbf{E}$ is superimposed on a high field $\mathbf{E}_0$ of constant direction, the resulting equilibrium shift is given by a constant term, proportional to $\mathbf{E}_0^2$, which is augmented by a periodically varying term, proportional to $\mathbf{E}_0\delta\mathbf{E}$. For given and constant $\mathbf{E}_0$ ($\gg \delta\mathbf{E}$) one obtains a linear relationship between $\xi(t)$ and $\delta\mathbf{E}(t)$ corresponding to a periodic change in the total number of dipolar species present in the system. The part of these dipoles that is oriented in the field is again proportional to the total field, so that the linear relationship between $\mathbf{D}^*(t)$ and $\delta\mathbf{E}(t)$ depends on the (constant) factor $\mathbf{E}_0^2$, as might be expected, since this relation describes a contribution to the dynamic permittivity which should not depend upon the sign of $\mathbf{E}_0$, provided that $\mathbf{E}_0$ and $\delta\mathbf{E}$ have the same absolute direction.

The contribution to the dynamic permittivity $\epsilon_{S,V}$ is finite, if ΔD^*, ΔH, or ΔV have finite values. The latter two quantities are only effective if finite (and appreciable) temperature and pressure dependences of the total dielectric constant are also present (90).

The situation is now completely analogous to the case of sound absorption. Instead of a complex compressibility, one obtains a complex adiabatic, isochoric dielectric constant, owing to relaxing chemical contributions. Relaxation times can be measured from the dispersion in the real part of $\epsilon_{S,V}(\mathbf{E}_0)$ as well as from energy loss as a result of the imaginary part, corresponding to the phase shift between field strength and polarization. It must be emphasized that this situation holds only in the presence of a constant field $\mathbf{E}_0$, which should be quite high in order to produce measurable effects. If this condition is fulfilled, however, all linear relationships, which have been derived previously, will hold for any small superimposed disturbance of this field (*cf.* Section II.3.C).

The dispersion in the real part will be very small and will, in general, be difficult to measure. Such measurements can, in principle, be carried out using the frequency-beat method for the comparison of the resonance frequency of a tuned circuit containing the system under test, with a known and constant frequency of a quartz oscillator. This method has been used for the determination of the (static) field dependence of the dielectric constant in nonreacting systems (91). No relaxation measurements have been reported as yet.

Energy absorption as a result of the imaginary part may be easier to detect. Energy loss in a capacitor is characterized by the loss factor tan δ_l; the angle δ_l is equal to the complement of the phase angle between the alternating voltage appearing at the condenser plates and the alternating current flowing at any instant.

Contributing to the electric losses are the finite Ohmic conductivity σ_{el} of the system, the dielectric loss from dispersion of orientational polarization (dielectric relaxation), and finally the chemical relaxation phenomena described here. The latter are only present at very high field strengths of the alternating or of a superimposed constant field. We shall consider only the case of a superimposed constant field, which is most easily realized experimentally and which gives rise to linear equations describing the losses measured with a small alternating voltage.

Let us consider a solution of a reacting dipolar species in a nonpolar solvent. For simplicity, we shall assume that the orientational relaxation can be described by a simple mechanism involving a single relaxation time τ_d, which is much shorter than the relaxation time τ_c of the discrete one-step chemical mechanism. The condition $\tau_d \ll \tau_c$ implies that, during chemical transformation, the orientation equilibrium is always established and

that in the orientation relaxation range the system is at constant composition.

The adiabatic-isochoric dielectric constant of the medium as a function of frequency for a given constant field $\mathbf{E}_0$ can then be written:

$$\epsilon_{S,V}(\mathbf{E}_0) = \epsilon_\infty + [\epsilon_{\text{orient}}/(1 + j\omega\tau_d)] + [\delta\epsilon_{\text{chem}}/(1 + j\omega\tau_c)] \qquad \text{(III.2.7)}$$

(If τ_d and τ_c are of the same order of magnitude, such a separation is no longer possible; instead, a treatment by use of new normal coordinates (as outlined in Section II) is required.) The term ϵ_∞ is the dielectric constant at sufficiently high frequencies that orientational polarization is negligible (ϵ_∞ primarily refers to the nonpolar solvent and is approximately given by n^2 (n = refractive index); it also includes contributions from atomic polarization). The term ϵ_{orient} represents the total contribution to ϵ because of orientation (at $\mathbf{E}_0$), but at constant composition. Finally, $\delta\epsilon_{\text{chem}}$ is the total contribution because of chemical reaction (change of composition with $\delta\mathbf{E}$ at $\mathbf{E}_0$) as derived in Equation (II.3.68).

This last term vanishes for $\mathbf{E}_0 = 0$, whereas the second term depends only slightly on $\mathbf{E}_0$ for field densities that can be experimentally realized.

The alternating current density $\delta\mathbf{i}$ corresponding to an alternating field $\delta\mathbf{E}$ of the frequency ω is given by

$$\delta\mathbf{i} = \chi\delta\mathbf{E} = [\sigma_{el} + j\omega\epsilon_0\epsilon_{S,V}(\mathbf{E}_0)]\,\delta\mathbf{E} \qquad \text{(III.2.8)}$$

with $\epsilon_0 = 8.86 \times 10^{-14}$ amp. sec. v.$^{-1}$ cm.$^{-1}$; σ_{el} = Ohmic conductivity; χ is the complex "admittivity." Combining (III.2.7) and (III.2.8) one obtains for $\omega \ll 1/\tau_d$:

$$\chi = \sigma_{el} + \omega^2\epsilon_0 \left\{ \tau_d\epsilon_{\text{orient}} + [\delta\epsilon_{\text{chem}}/(1 + \omega^2\tau_c^2)]\tau_c \right\}$$

$$+ j\omega\epsilon_0 \left\{ \epsilon_\infty + \epsilon_{\text{orient}} + [\delta\epsilon_{\text{chem}}/(1 + \omega^2\tau_c^2)] \right\} \qquad \text{(III.2.9)}$$

The loss factor is given by the ratio of the real to the imaginary part of the admittivity.

$$\tan\delta_l = \frac{\sigma_{el} + \omega^2\,\epsilon_0 \left\{ \tau_d\epsilon_{\text{orient}} + \tau_c\,[\delta\epsilon_{\text{chem}}/(1 + \omega^2\tau_c^2)] \right\}}{\omega\epsilon_0 \left\{ \epsilon_\infty + \epsilon_{\text{orient}} + [\delta\epsilon_{\text{chem}}/(1 + \omega^2\,\tau_c^2)] \right\}} \qquad \text{(III.2.10)}$$

From measurements of the loss factor with and without a superimposed constant field, the contribution of chemical relaxation can be determined if the losses resulting from circuit properties, Ohmic conductivity, and relaxing orientational polarization remain small enough. It is to be noted that

the Ohmic conductivity may itself become a function of the applied constant field, and this effect may be appreciable in media with a low dielectric constant (dissociation field effect).

However, the excess Ohmic loss factor at high values of the constant field is a linear function of the frequency of the alternating field, so that the chemical effect may still be separated, if the measurements cover a sufficiently wide frequency range in the relaxation region [*cf.* Equation (III.2.10)].

A detailed description of experimental methods for the measurement of electric losses will not be given here, because applications to the observation of chemical relaxation phenomena have barely started, and the experimental techniques (related to those commonly known for the determination of dielectric losses) are being developed and adapted now to the specific requirements of such studies [*cf.* ref. (90)].

In the lower radio-frequency region (about 20 or 30 Mc.) impedance bridges of the Schering type or derived from twin-T networks could be used, in principle. For higher frequencies, the loss factor may be obtained from the resonance sharpness or the decay time of tuned circuits or resonators. At still higher frequencies, the determination of the wave parameters of coaxial line elements or waveguides containing the dielectric system may be practical. Measurements of loss as a function of the constant superposed field and over a sufficiently wide frequency range should be made for an unambiguous interpretation of the data obtained. The expected effects are rather small and very accurate instrumentation together with a thorough investigation and elimination of possible error sources will therefore be necessary.

A different class of experimental methods, not based on the determination of energy loss, may take advantage of the full nonlinear relationship between chemical equilibrium and total field, if "modulation" techniques are used, similar to that proposed for the measurement of the dissociation field effect. For equilibria depending upon the electric field strength (dipole equilibria or temperature-dependent equilibria in a medium with temperature-dependent dielectric constant) the permittivity can be varied by an alternating or periodically switched field of sufficient amplitude. The modulation frequency will be the second harmonic of the frequency of an alternating field, or it may be the "pulse repetition frequency" and its harmonics for a repetitively switched high-frequency or direct-current field. Simultaneous application of other fields (carrier), together with well-known filtering techniques for the desired carrier side bands that occur in nonlinear systems, may result in a number of very sensitive methods for the investigation of some very fast chemical processes to which little consideration has been given before.

The detection of similar effects resulting from magnetic fields seems too difficult at present, as the relative changes in the magnetic permeability, owing to chemical effects, are about three orders of magnitude smaller than the changes in the permittivity. This situation is due to the small magnetic moments of single particles as compared to the electric moments obtainable by charge separation in a single molecule. The large value of magnetic permeability in the case of ferromagnetic substances is not a property of single atoms or molecules, but is a cooperative phenomenon (domain orientation). If magnetic techniques should ever become sensitive enough for such studies, a treatment similar to that described for the electric analogue may be applicable.

References

1. F. V. Hunt, *Propagation of Sound in Fluids* in *American Institute of Physics Handbook*, McGraw-Hill, New York, 1957, pp. 3–25 ff.
2. W. P. Mason, *Piezoelectric Crystals and Their Application to Ultrasonics*, Van Nostrand, New York, 1950.
3. L. Bergmann, *Der Ultraschall*, S. Hirzel Verlag, Stuttgart, 1954.
4. J. Matauschek, *Einführung in die Ultraschalltechnik*, Verlag Technik, Berlin, 1957.
5. K. Tamm, in *Encyclopedia of Physics*, Vol. 11/I, Springer Verlag, Berlin, 1961; *cf.* also K. Tamm, *Z. Elektrochem.*, **64**, 73 (1960).
6. H. O. Kneser, *Ergeb. exakt. Naturwiss.*, **22**, 121 (1949).
7. J. H. Andreae, C. Jupp, and D. G. Vincent, *J. Acoust. Soc. Am.*, **32**, 406 (1960).
8. R. W. Leonard, *J. Acoust. Soc. Am.*, **20**, 224 (1948)
9. O. B. Wilson and R. W. Leonard, *J. Acoust. Soc. Am.*, **26**, 223 (1954).
10. O. B. Wilson, *Phys. Rev.*, **81**, 657 (1951).
11. C. J. Moen, *J. Acoust. Soc. Am.*, **23**, 62 (1951).
12. G. Kurtze and K. Tamm, *Acustica*, **3**, 33 (1953).
13. J. H. Andreae, *Z. Elektrochem.*, **64**, 86 (1960).
14. H. Knötzel, *Akust. Z.*, **5**, 245 (1940); *Ann. phys.*, **2**, 393 (1948).
15. G. W. Pierce, *Proc. Am. Acad. Boston*, **60**, 271 (1925).
16. W. H. Pielemeyer, *Phys. Rev.*, **34**, 1184 (1929).
17. J. C. Hubbard, *Phys. Rev.*, **35**, 1442 (1930); **41**, 523 (1932); **46**, 525 (1934).
18. F. E. Fox, *Phys. Rev.*, **52**, 973 (1937).
19. D. Tabuchi, *Mem. Inst. Sci. and Ind. Research*, Osaka Univ., **11**, 37 (1954); **12**, 111 (1955).
20. J. L. Hunter, *J. Acoust. Soc. Am.*, **22**, 243 (1950).
21. J. L. Hunter and F. E. Fox, *J. Acoust. Soc. Am.*, **22**, 238 (1950).
22. F. E. Fox and G. D. Rock, *Proc. I.R.E.*, **30**, 29 (1942).
23. E. Grossman, *J. Acoust. Soc. Am.*, **6**, 106 (1934).
24. E. Skudrzyk, *Österr. Ingr.-Arch.*, **4**, 408 (1950).
25. C. E. Mulders, *Appl. Sci. Research*, **131**, 341 (1949).
26. J. Karpovitch, *J. Acoust. Soc. Am.*, **26**, 819 (1955).
27. K. Tamm, *Nachr. Akad. Wiss. Göttingen, Math.-Physik. Kl.*, **10**, 81 (1952).
28. (a) P. Debye and F. W. Sears, *Proc. Natl. Acad. Sci. Wash.*, **18**, 410 (1932); (b) R. Lucas and P. Biquard, *Compt. rend.*, **194**, 2132 (1932).

29. C. V. Raman and N. S. Nath, *Proc. Indian Acad. Sci.*, A3, 75 (1936).

30. (a) Ch. J. Burton, *J. Acoust. Soc. Am.*, 20, 186 (1948); (b) G. Kurtze, *Nachr. Akad. Wiss. Göttingen, math.-Physik. Kl.*, 10, (1952).

31. E. Schreuer and K. Osterhammel, *Naturwissenschaften*, 29, 44 (1941). M. Kamura *J. Acoust. Soc. Am.*, 27, 5 (1956).

32. E. T. Y. Hsu, *J. Acoust. Soc. Am.*, 17, 127 (1945).

33. T. Beyer and M. C. Smith, *J. Acoust. Soc. Am.*, 18, 424 (1946).

34. J. E. Piercy and J. Lamb, *Proc. Roy. Soc.* (*London*), A226, 43 (1954). D. N. Hall and J. Lamb, *Proc. Phys. Soc.* (*London*), 73, 354 (1959).

35. F. E. Fox and Th. M. Marion, *J. Acoust. Soc. Am.*, 25, 661 (1953).

36. E. L. Carstensen, *J. Acoust. Soc. Am.*, 26, 858, 862 (1954).

37. G. Govelik, *C. R. Acad. Sci. U.R.S.S.*, 54, 779 (1946). P. V. Slobodskaya, *Izvest. Akad. Nauk. S.S.S.R. Ser. Fiz.*, 12, 656 (1948); *cf.* also T. L. Cottrell, *Trans. Faraday Soc.*, 46, 1025 (1950); M. E. Jacox and S. H. Bauer, J. Phys. Chem., 61, 833 (1957).

38. J. R. Pellmann and K. J. Galt, *J. Acoust. Soc. Am.*, 18, 251 (1946); *J. Chem. Phys.*, 14, 608 (1948).

39. R. A. Rapuano, *Phys. Rev.*, 72, 78 (1947).

40. J. M. M. Pinkerton, *Proc. Phys. Soc.* (*London*), B62, 286 (1949).

41. T. A. Litovitz, *J. Acoust. Soc. Am.*, 23, 75 (1951).

42. K. Tamm., G. Kurtze, and R. Kaiser, *Acustica*, 4, 380 (1954).

43. J. H. Andreae, R. Bass, E. L. Heasell, and J. Lamb, *Acustica*, 8, 131 (1958).

44 (a) N. P. Cedrone and D. R. Curran, *J. Acoust. Soc. Am.*, 26, 963 (1954). (b) R. L. Forgacs, *Electronics* (47), 33, 98 (1960).

45. H.E. Boemmel and K. Dransfeld, *Physic. Rev. Letters*, *1/7*, 234 (1958).

46. R. O. Davies and J. Lamb, *Quart. Revs.* (*London*), 11, 134 (1957).

47. D. Sette, *Nuovo Cimento*, 1, 800 (1955).

48. G. S. Verma, *J. Chem. Phys.*, 29, 1186 (1958).

49. *Encyclopedia of Physics*, Vol. 11/I edited by S. Flügge, Springer, Berlin, 1961.

50. F. Keutel, Dissertation, Berlin, 1910.

51. A. Einstein, *Sitzber. preuss. Akad. Wiss. Physik-math. Kl.*, 380 (1920).

52. G. Sessler, Paper presented at the third International Congress on Acoustics, Stuttgart, 1959.

53. H. Bauer and H. O. Kneser, Paper presented at the third International Congress on Acoustics, Stuttgart, 1959.

54. D. Britton, N. Davidson, and G. Schott, *Discussions Faraday Soc.*, 17, 58 (1954).

56. S. H. Bauer and M. R. Gustavson, *Discussions Faraday Soc.*, 17, 69 (1954).

57. M. S. de Groot and J. Lamb, *Trans. Faraday Soc.*, 51, 1676 (1955); *Nature*, 177, 1231 (1956); *Proc. Roy. Soc.* (*London*), A242, 36 (1957).

58. J. M. M. Pinkerton, *Koninkl. Vlaam. Acad. Wetenschap.*, Colloq. Ultrasonore Trillingen, Brussels 1951, p. 177; D. H. A. Huddart, Thesis, London, 1950; P. Biquard, *Ann. Phys.*, 6, 195 (1936); L. N. Liebermann, *Phys. Rev.*, 75, 1415 (1949); 76, 440 (1949).

59. J. Karpovich, *J. Chem. Phys.*, 22, 1767 (1954).

60. J. Lamb and J. Sherwood, *Trans. Faraday Soc.*, 51, 1674 (1955). E. L. Heasell and J. Lamb, *Proc. Phys. Soc.* (*London*), B69, 869 (1956).

61. R. Clausnitzer and H. O. Kneser, International Commission on Acoustics, 2nd Congress, 1956, Paper I.B.2.

62. J. M. Young and A. A. Petrauskas, *J. Chem. Phys.*, 25, 943 (1956); J. H. Chen and A. A. Petrauskas, *ibid.*, 30, 304 (1959).

63. J. C. McCoubrey and A. R. Ubbelohde, *Quart. Revs.* (London), **5**, 364 (1951).
64. J. Lamb, *Z. Elektrochem.*, **64**, 135 (1960).
65. E. Freedman, *J. Chem. Phys.*, **21**, 1784 (1953).
66. J. Lamb and J. M. M. Pinkerton, *Proc. Roy. Soc.* (*London*), **A199**, 114 (1949); J. Lamb and D. H. A. Huddart, *Trans. Faraday Soc.*, **46**, 540 (1950).
67. D. Tabuchi, *Z. Elektrochem.*, **64**, 141 (1960).
68. R. N. Barfield and W. G. Schneider, *J. Chem. Phys.*, **31**, 488 (1959).
69. W. Maier, *Z. Elektrochem.*, **64**, 132 (1960).
70. J. E. Piercy and J. Lamb, *Trans. Faraday Soc.*, **52**, 930 (1956).
71. A. Mez and W. Maier, *Z. Naturforsch.*, **10a**, 997 (1955).
72. W. Maier and H. D. Rudolph, *Z. physik. Chem. N.F.*, **10**, 83 (1957).
73. M. Eigen, *Z. physik. Chem., N.F.*, **1**, 176 (1954).
74. M. Eigen and G. Schwarz (to be published).
75. E. H. Carnevale and T. A. Litovitz, *J. Acoust. Soc. Am.*, **30**, 610 (1958).
76. M. Eigen, K. Tamm, and K. Tjaden (to be published).
77. M. Eigen and G. Maass (to be published).
78. J. Claeys, J. Errera, and H. Sack, *Compt. rend.*, **202**, 1493 (1936); *Trans. Faraday Soc.*, **33**, 136 (1937); P. Bazulin, *C. R. Acad. Sci. U.R.R.S.*, **19**, 153 (1938); *J. Exptl. Theoret. Phys.* (*U.S.S.R.*), **9**, 1147 (1939); W. Buss, *Ann. Phys. Lpz.*, **33**, 143 (1938); W. Rüfer, *Ann. Phys. Lpz.*, **41**, 301 (1942); C. E. Mulders, *Appl. Sci. Research*, **B1**, 341 (1949); *Nature*, **164**, 347 (1949); *Diss. Delft* (1950); R. E. Barrett, F. L. McNamara, and R. T. Beyer, *J. Acoust. Soc. Am.*, **23**, 629 (1951); **26**, 966 (1954) [*cf.* also ref. (33)]; A. van Itterbeek and L. Verhaegen, *Koninkl. Vlaam. Acad. Wetenschap.*, Colloq. Ultrasonore Trillingen, Brussels 1951, p. 220.
79. M. Eigen, G. Kurtze, and K. Tamm, *Z. Elektrochem.*, **57**, 103 (1953).
80. L. Liebermann, *J. Acoust. Soc. Am.*, **20**, 868 (1948); *Phys. Rev.*, **76**, 1520 (1949).
81. D. A. Bies, *J. Chem. Phys.*, **23**, 428 (1955).
82. M. Manes, *J. Chem. Phys.*, **21**, 1791 (1953).
83. F. H. Fisher, *J. Acoust. Soc. Am.*, **30**, 441 (1958).
84. M. Eigen, *Discussions Faraday Soc.*, **24**, 24 (1957).
85. M. Eigen and K. Tamm, *Z. Electrochem.*, **66**, 93 (1962).
86. M. Eigen, *Z. Elektrochem.*, **64**, 115 (1960).
87. R. G. Pearson, *Discussions Faraday Soc.*, **17**, 187 (1954).
88. W. R. Gilkerson, *J. Chem. Phys.*, **27**, 914 (1957).
89. L. De Maeyer (to be published).
90. K. Bergmann, M. Eigen, and L. De Maeyer (to be published).
91. A. Piekara and A. Chetkowski, *J. Chem. Phys.*, **25**, 794 (1956); see also A. Piekara and S. Kielich, *ibid.*, **29**, 1297 (1958).

IV. SURVEY ON RESULTS AND CONCLUSIONS

It may be of interest at the end of this chapter, concerned primarily with techniques, to include a brief survey on available results. It is not intended, however, to give a discussion of any specific reaction mechanism, which can be found elsewhere (1). Only rate constants are quoted, although the more interesting information is involved in the analysis of the reaction mechanisms. The survey, furthermore, must be incomplete in view of the fact that most of the relaxation techniques for reaction rate studies have been developed quite recently and that many such studies are now in progress.

The most familiar type of elementary chemical transformation is the (quasi-)bimolecular† reaction. Many fundamental transformations in solution, such as ionic recombination, complex formation, dimerization, substitution, electron or proton transfer, belong to this type.

The maximum speed of the reaction between two separate partners in solution is limited by the rate of diffusive encounters, which can be expressed by a second-order rate constant [k_{12} in scheme (II.1.25)]. According to Debye (2), this rate constant is given by

$$k_{12} = (4\pi N_A z_A z_B e_0^2/\epsilon kT)\,(D_A + D_B)/[\exp(z_A z_B e_0^2/\epsilon r_D kT) - 1] \quad \text{(IV.1)}$$

N_A = Avogadro's number, z_A, z_B = valence (note that z has the sign of the charge), e g , for A^+ and B^-: $z_A z_B = -1$), D_i = diffusion coefficients, ϵ = electric permittivity of the solvent, r_D = reaction distance (closest approach at which a spontaneous reaction occurs), e_0 = elementary charge, and k = Boltzmann's constant. If all quantities are expressed in c.g.s. units, k_{12} would have the dimension cm.^{3} mole^{-1} sec.$^{-1}$ which can be easily converted to the usual dimension M^{-1} sec.$^{-1}$ by multiplying by 10^{-3}.* For z_A and/or $z_B \to 0$, k_{12} becomes identical with an expression first derived by v. Smoluchowsky (3): $k_{12} = 4\pi N_A r_D (D_A + D_B)$; for $r_D \to$ zero (but finite and negative $z_A z_B$) k_{12} is given by $4\pi N_A z_A z_B e_0^2 (D_A + D_B)/\epsilon kT$, an expression derived by Langevin (4) and Onsager (5). Expression (IV.1) holds only for diffusion-controlled reactions at concentrations low enough to permit a stationary treatment of the diffusion problem (6–8) and the neglect of ionic atmosphere effects. At higher concentrations of charged reaction partners, interference with relaxation of the ionic atmosphere complicates the treatment. Furthermore, it is supposed that the shape of the partners is spherical and "r_D" (the reaction distance) is large enough (e.g., for $z_i = 1$: $r_D \gtrsim 5$ A) to allow the use of the macroscopic dielectric constant. Deviations from these conditions may be corrected by the introduction of "steric" factors.

If the recombination is diffusion controlled, the rate constant of the reverse reaction (though of first order) must again contain the sum of diffusion coefficients, since the equilibrium constant is independent of diffusion rates. The rate constant of this diffusive reverse process is given [under the suppositions of the validity of Equation (IV.1)] by (9)

$$k_{21} = (3 z_A z_B e_o^2/\epsilon kT r_D^3)\,\{(D_A + D_B)/[1 - \exp(-z_A z_B e_0^2/\epsilon r_D kT)]\} \quad \text{(IV.2)}$$

† The molecularity here is related to the principal reaction partners and does not take into consideration the presence of solvent molecules (which might be very important for the particular mechanism).

* If the electrostatic terms are expressed in v.-amp.-sec. units, ϵ has to be replaced by $4\pi\epsilon_0\epsilon$.

According to the scheme (II.1.25) the total reaction can be expressed as a one-step transformation, if the concentration of AB is small with respect to the concentrations of C and A or B. The condition for a diffusion-controlled recombination is then given by $k_{21} << k_{23}$. Thus, the over-all rates can be expressed by $\vec{k} = k_{12}$ and $\overleftarrow{k} = k_{21}\, k_{32}/k_{23}$. It is important to note that k_{12} represents an upper limit of $\vec{k}$. Even for the very highly mobile H^+ and OH^- ions in aqueous solutions this limit can hardly exceed the order of magnitude of $10^{11} M^{-1}$ sec.$^{-1}$ For other (less mobile) reaction partners, the limit is usually lower, depending on conditions of steric and electrostatic interaction. If experiments lead to values above this limit—and there is quite a bit of such data in the literature, derived from indirect methods—the interpretation (e.g., the assumed mechanism) cannot be correct.

Typical diffusion-controlled reactions are recombination processes involving the solvent ions H^+ and OH^- in aqueous solution. Data obtained by means of relaxation methods are quoted in Tables IV.1(a)–(d). The high rates of these processes result from the anomalous mechanism of solvent ion mobility. The proton and hydroxyl ion (defect proton) can, without hindrance, penetrate the coordination spheres of counter ions, provided that a direct H-bond connection between the reacting partners exists. The high speed of such proton transfer processes (reaching frequency numbers of 10^{13} to 10^{14} sec.$^{-1}$) has been directly demonstrated by measurements in the H-bond lattice of ice crystals (10). Differences in the rate constants given in Tables IV.1(a) and (b) can be quantitatively explained by the specific conditions of electrostatic interaction (charge type, ionic strength) and steric behavior (reaction site, etc.). The activation energies are generally of the order of magnitude to be expected for a diffusion-controlled process (2–4 kcal./mole).

There is, however, a number of protolytic reactions whose rates remain considerably below the diffusion controlled limit. Electrostatic effects (repulsion between equally charged partners) are generally not of great influence as is shown by the first examples in Table IV.1(c). However, an accumulation of charges may perturb the H-bond structure so drastically that the proton at the reacting site is not bridged any more with the solvent structure. This effect reduces greatly the recombination rates as the examples of nitrilotriacetic acid, EDTA, etc., in Table IV.1(c) show. The effect becomes still more apparent if the reacting proton is involved in an internal hydrogen bond [*cf.* salicylic acid, maleic acid, dimethylanthranilic acid, etc., in Table IV.1(c)]. This effect is strongest if a planar six-membered ring chelate is formed by the internal H-bond (as in the cases of salicylic acid, azo dyes with hydroxo groups in ortho position to the azo

TABLE IV.1(a)
Recombination and Dissociation Rates in Acid Equilibria

Reaction	Conditions[a]	k_R M^{-1} sec.$^{-1}$	k_D sec.$^{-1}$	Method[b] (references)
$H^+ + HO^- \rightleftharpoons H_2O$	298°K. $I \approx 0$	1.4×10^{11}	2.5×10^{-5}	E (11)
$D^+ + DO^- \rightleftharpoons D_2O$	298°K. $I \approx 0$	8.4×10^{10}	2.5×10^{-6}	T (65)
$H^+ + F^- \rightleftharpoons HF$	298°K. $I \approx 0$	1.0×10^{11}	7×10^{7}	E-disp. (12)
$H^+ + SO_4^{2-} \rightleftharpoons HSO_4^-$	293°K. $I \approx 0.1$	$\sim 1.0 \times 10^{11}$	$\sim 1.0 \times 10^{9}$	Sound (13)
$H^+ + HS^- \rightleftharpoons H_2S$	298°K. $I \approx 0$	7.5×10^{10}	4.3×10^{3}	E-disp. (12)
$H^+ + HCO_3^- \rightleftharpoons H_2CO_3$	298°K. $I \approx 0$	4.7×10^{10}	$\sim 8 \times 10^{6}$	E-disp. (14)
$H^+ + HCOO^- \rightleftharpoons HCOOH$	298°K. $I \approx 0$	$\sim 5 \times 10^{10}$	$\sim 8.6 \times 10^{6}$	E-disp. (16)
$H^+ + CH_3COO^- \rightleftharpoons CH_3COOH$	298°K. $I \approx 0$	4.5×10^{10}	7.8×10^{5}	E-disp. (17)
$H^+ + C_2H_5COO^- \rightleftharpoons C_2H_5COOH$	298°K. $I \approx 0$	4.3×10^{10}	5.7×10^{5}	E-disp. (16)
$H^+ + C_6H_5COO^- \rightleftharpoons C_6H_5COOH$	298°K. $I \approx 0$	3.5×10^{10}	2.2×10^{6}	E-disp. (61)
$H^+ + o\text{-}H_2NC_6H_4COO^- \rightleftharpoons$ *o*-aminobenzoic acid	298°K. $I \approx 0$	$\sim 5 \times 10^{10}$	6×10^{5}	E-disp. (61)
$H^+ + m\text{-}(NO_2)C_6H_4O^- \rightleftharpoons$ *m*-nitrophenol	298°K. $I \approx 0$	4.2×10^{10}	1.9×10^{2}	E-disp. (12)
$H^+ + p\text{-}(NO_2)C_6H_4O^- \rightleftharpoons$ *p*-nitrophenol	298°K. $I \approx 0$	3.6×10^{10}	2.6×10^{3}	E-disp. (12)
$H^+ + C_3N_2H_4 \rightleftharpoons C_3N_2H_5^+$ (imidazole)	286°K. $I \approx 0.1$ (KNO_3)	1.5×10^{10}	1.5×10^{3}	T (18)
$H^+ + PR^{--} \rightleftharpoons HPR^-$ (phenol red)	286°K. $I \approx 0.1$ (KNO_3)	$(3 \pm 2) \times 10^{10}$	6×10^{2}	T (20)
$H^+ + CPR^{--} \rightleftharpoons HCPR^-$ (chlorphenol red)	286°K. $I \approx 0.1$ (KNO_3)	2.3×10^{10}	1.9×10^{4}	T (20)
$H^+ + C_{16}H_6(SO_3)_3O^{4-} \rightleftharpoons$ 3-oxypyrene-5,8,10-trisulfonate	298°K.	2.7×10^{10}	1.4×10^{3}	R (21)

[a] I = Ionic strength [M], k_R = rate constant of recombination; k_D = rate constant of dissociation.

[b] Methods: E = electric field (square pulse); P = pressure jump; T = temperature jump; E-disp. = electric field (amplitude dispersion); sound = sound absorption and dispersion; R = radiation method.

TABLE IV.1(b)
Recombination and Dissociation Rates in Base Equilibria

Reaction	Conditions[a]	k_R M^{-1} sec.$^{-1}$	k_D sec.$^{-1}$	Method[b] (references)
$OH^- + NH_4^+ \rightleftharpoons NH_3 + H_2O$	295°K. $I \approx 0$	3.4×10^{10}	6×10^5	Sound E-disp. (9, 17, 22)
$OH^- + (CH_3)NH_3^+ \rightleftharpoons (CH_3)NH_2 + H_2O$	293°K. $I \approx 0$	3.7×10^{10}	1.6×10^7	Sound (22)
$OH^- + (CH_3)_2NH_2^+ \rightleftharpoons (CH_3)_2NH + H_2O$	293°K. $I \approx 0$	3.1×10^{10}	1.9×10^7	Sound (22)
$OH^- + (CH_3)_3NH^+ \rightleftharpoons (CH_3)_3N + H_2O$	293°K. $I \approx 0$	2.1×10^{10}	1.4×10^6	Sound, E-disp. (16,22)
$OH^- + C_3N_2H_5^+ \rightleftharpoons C_3N_2H_4 + H_2O$ (imidazole)	298°K. $I \approx 0$	2.5×10^{10}	2.5×10^3	E-disp. (18)
$OH^- + {}^+H_3N\,CH_2\,COO^- \rightleftharpoons H_2NCH_2COO^- + H_2O$ (glycine)	295°K. $I \approx 0.5$	1.4×10^{10}	8.4×10^5	Sound (22,23)
$OH^- + {}^+H_2(CH_3)NCH_2COO^- \rightleftharpoons H(CH_3)NCH_2COO^- + H_2O$ (sarcosine)	295°K. $I \approx 0.25$	1.1×10^{10}	1.8×10^6	Sound (22,23)
$OH^- + {}^+H(CH_3)_2NCH_2COO^- \rightleftharpoons (CH_3)_2NCH_2COO^- + H_2O$ (dimethylglycine)	295°K. $I \approx 0.25$	7.3×10^9	6.5×10^5	Sound (22,23)
$OH^- + HCO_3^- \rightleftharpoons CO_3^{2-} + H_2O$	293°K. $I \approx 1$ (Na_2CO_3)	$\sim 6 \times 10^9$	—	Sound (22)
$OH^- + HCrO_4^- \rightleftharpoons CrO_4^{2-} + H_2O$	293°K. $I \approx 0.2$	$\sim 6 \times 10^9$	—	Sound (22)
$OH^- + C_5H_{12}N^+ \rightleftharpoons C_5H_{11}N + H_2O$ (piperidine)	298°K. $I \approx 0$	2.2×10^{10}	3×10^7	Sound (23)
$OH^- + C_5H_5N_5 \rightleftharpoons C_5H_4N_5^- + H_2O$ (adenine)	298°K. $I \approx 0$	1×10^{10}	6.3×10^5	Sound (23)
$OH^- + C_6H_5OH \rightleftharpoons C_6H_5O^- + H_2O$ (phenol)	298°K. $I \approx 0$	$\sim 1.4 \times 10^{10}$	$\sim 1.3 \times 10^6$	Sound (23)

group, etc.). In these cases recombination can occur only after the H bonds have dissociated.

Another case of slower protolytic reaction is represented by pseudo acids. An example of this type which is representative of a number of organic reactions involving carbanion formation (such as keto enol tautomerization, halogenation of ketonic substances, condensation reactions, etc.) is shown in Table IV.1(d). The keto form reacts considerably slower than the

TABLE IV.1(c)
Charge and H-bond Influence in Protolytic Reactions

Reaction	Conditions	k_R M^{-1} sec.$^{-1}$	k_D sec.$^{-1}$	Method (reference)
$H^+ + [(H_2NC_2H_4)_3 \cdot NH_3]^{3+} \rightleftharpoons$ triethylenetetrammonium	298°K. $I \approx 0$	5.6×10^9	2.7×10^6	Sound (23)
$H^+ + [Co(NH_3)_5OH]^{2+} \rightleftharpoons [Co(NH_3)_5OH_2]^{3+}$	298°K. $I = 0.1$	4.8×10^9	3.4×10^3	T (19)
$H^+ + [Pt(en)_3{}^a]^{3+} \rightleftharpoons [Pt(en)_3]^{4+}$	298°K. $I = 0.1$	1.7×10^9	8.5×10^2	T (19)
$OH^- + HPO_4^{2-} \rightleftharpoons PO_4^{3-} + H_2O$	298°K. $I = 0.1$	$\sim 2 \times 10^9$	$(\sim 2 \times 10^7)$	Sound (22)
$OH^- + HATP^{3-} \rightleftharpoons ATP^{4-} + H_2O$ (adenosine-5′-triphosphate)	298°K. $I = 0.1$	1.2×10^9	5.2×10^1	T (19)
$OH^- + HP_2O_7^{3-} \rightleftharpoons P_2O_7^{4-} + H_2O$	298°K. $I = 0.1$	4.7×10^8	1.8×10^3	T (19)
$OH^- + HEDTA^{3-} \rightleftharpoons EDTA^{4-} + H_2O$ (ethylene diaminotetraacetate)	298°K. $I = 0.1$	3.8×10^7	1.1×10^4	T (19)
$OH^- + HNTA^{2-} \rightleftharpoons NTA^{3-} + H_2O$ (nitrilotriacetate)	298°K. $I = 0.1$	1.3×10^7	1.3×10^3	T (19)
$OH^- + HOOC(CH):(CH)\text{-}COO^- \rightleftharpoons$ maleate ion	298°K. $I = 0.1$	3×10^8	7,8	T (19)
$OH^- + p\text{-}NH_2 \cdot C_6H_3(OH)\text{-}COO^- \rightleftharpoons p$-aminosalicylate ion[b]	298°K. $I \approx 1.0$	3×10^7 [1.5×10^7]	–	Sound (24)
$OH^- + o\text{-}N(CH_3)_2 \cdot C_6H_4 \cdot\text{-}COOH \rightleftharpoons o$-dimethylaminobenzoate ion	298°K. $I = 0.1$	1.2×10^7	4.8×10^1	T (19,61)

[a] In $Pt(en)_3{}^{3+}$ 1 en (= ethylenediamine) deprotonated; in $Pt(en)_3{}^{4+}$ all ligands (en) neutral.

[b] The value in brackets refers to alizarine-R (where the reacting group also is salicylate) at $I = 0.1$ and pH $\approx$ 12 (PAS: $I = 1.0$, pH 13–14)

enol form (note, however, the relatively slow proton transfer from enol to OH^-, which is hindered by an internal H bond), although in both processes direct proton transfer occurs. In this sense all protolytic reactions of Table IV.1 are only special examples of the more general type of proton transfer process shown below in Table IV.3(b).

Generally, the protolytic and hydrolytic reactions are characterized by a coupled-reaction mechanism. Even in a simple system like an acid in aqueous solution, the reaction may consist of either a direct recombination between the proton and the conjugate base, or by hydrolysis, i.e., by direct

TABLE IV.1(d)
Protolysis and Hydrolysis of Acetylacetone

Reaction	Conditions	k_R M^{-1} sec.$^{-1}$	k_D sec.$^{-1}$	Method (reference)
$H^+ + [CH_3COCHCOCH_3]^- \rightleftharpoons CH_3COCH{:}COHCH_3$ (enol)	298°K. $I = 0.1$	3×10^{10}	1.7×10^2	E, T (61,19)
$H^+ + [CH_3COCHCOCH_3]^- \rightleftharpoons CH_3COCH_2COCH_3$ (ketone)	298°K. $I = 0.1$	1.2×10^7	1.4×10^{-2}	T, flow (19)
$OH^- + CH_3COCH{:}COHCH_3 \rightleftharpoons [CH_3COCHCOCH_3]^- + H_2O$	288°K. $I = 0.1$	1.6×10^7	28	T (19)
$OH^- + CH_3COCH_2COCH_3 \rightleftharpoons [CH_3COCHCOCH_3]^- + H_2O$	298°K. $I = 0.1$	4×10^4	3.5×10^{-1}	T (19)

reaction of the conjugate base with a water molecule yielding the acid and an OH^- ion [*cf.* imidazole around pH 7, Tables IV.1(a) and (b)]. The connection between both mechanisms is provided by the neutralization reaction $H^+ + OH^- \rightleftharpoons H_2O$, which was found to be the fastest bimolecular reaction of this charge type. A knowledge of this rate constant (determined separately in pure water) is required for a complete analysis of the general acid-base mechanism.

The protolytic reactions are sometimes followed by slower transformations, such as dehydration. As examples the rate constants of hydrolysis of halogens as well as of some dehydration/hydration reactions are quoted in Tables IV.2(a) and (b). The data in Table IV.2(b) may be compared with those obtained by other (e.g., flow) methods (28,29).

TABLE IV.2(a)
Hydrolysis of Halogens
$X_2 + H_2O \rightleftharpoons XOH + X^- + H^+$

X_2	Conditions	$\vec{k}$ sec.$^{-1}$	$\overleftarrow{k}$ M^{-2} sec.$^{-1}$	Method (reference)
Cl_2	293°K. $I = 0.1$	11.0	1.8×10^4	T (62)
Br_2	293°K. $I = 0.1$	110.	1.6×10^{10}	T (62)
I_2	293°K. $I = 0.1$	3.0	4.4×10^{12}	T (62)

TABLE IV.2(b)
Hydration/Hydrolysis Reactions

Reaction	Conditions	$\vec{k}$ sec.$^{-1}$	$\overleftarrow{k}$ sec.$^{-1}$ (M^{-1} sec.$^{-1}$)	Method (reference)
$CO_2 + H_2O \rightleftharpoons H_2CO_3$[a]	298°K. $I = 0.1$	4.3×10^{-2}	15 [5.6×10^4]	P,T (14,26) (*cf.* also refs. 27–29)
$SO_2 + H_2O \rightleftharpoons H_2SO_3$[a]	293°K. $I = 0.1$	3.4×10^6	6.3×10^7 [2×10^8]	Sound (63)
$CH_3 \cdot CO \cdot CO_2H + H_2O \rightleftharpoons CH_3 \cdot C(OH)_2 \cdot CO_2H$	298°K. $I = 0.1$	5.3×10^{-1}	2.2×10^{-1}	P, T (64)

[a] The rate constants are formally attributed to these reaction steps. The equilibrium may actually be established via: $XO_2 + H_2O \rightleftharpoons HXO_3^- + H^+$. The values in brackets refer to such a mechanism. For rate constants of the alternative reactions $HXO_3^- + H^+ \rightleftharpoons H_2XO_3$ and $HXO_3^- + OH^- \rightleftharpoons XO_3^{2-} + H_2O$ *cf.* Table IV.1. (a), (b).

The direct exchange of protons between different acid and base molecules [*cf.* Table IV.3(a)] is also a very rapid process, which may be diffusion controlled, if the proton donor is a stronger acid than the protonated acceptor. The rates are smaller than in the case of simple protolytic reactions [transfer from H_3O^+ to acceptor, *cf.* Table IV.1(a)], owing to the smaller diffusion coefficients of acid and base molecules and to steric factors. Although, in some cases, the rates remain below the upper limit to be expected for a diffusion controlled mechanism, they exceed the dissociation rates of the acid molecules by many orders of magnitude, indicating a direct transfer mechanism (for which, again, H bonds are very important).

A number of individual influences become apparent especially if the pK's of donor and acceptor are nearly equivalent. Here transfer processes in H bonds of the type NH...N and especially SH...S are generally slower than those of the type OH...O, OH...N. Also resonance stabilization of an acid or base with respect to its conjugate causes some reduction of rate if the pK's are nearly equal. All these influences are extreme in the case of C acids, which are therefore often called "pseudo" acids. Detailed studies of these processes (23), of which only a few examples are shown in Table IV.3(b), contribute to a better understanding of the mechanism of general acid base catalysis.

Table IV.3(c) shows some examples of intramolecular proton transfer. These processes demonstrate the possibility of fast, direct proton transfer between amino-acid residues of proteins.

TABLE IV.3(a)
Intermolecular Proton Transfer

Reaction[a]	Conditions	$\vec{k}$ M^{-1} sec.$^{-1}$	k M^{-1} sec.$^{-1}$	Method (reference)
$HCPR^- + Im \rightleftharpoons CPR^{2-} + {}^+HIm$	286°K. $I = 0.1$	9×10^8	1.2×10^8	T (18)
$PR^{2-} + HATP^{3-} \rightleftharpoons HPR^- + ATP^{4-}$	286°K. $I = 0.1$	7×10^8	4.5×10^7	T (25)
$PR^{2-} + HADP^{2-} \rightleftharpoons HPR^- + ADP^{3-}$	286°K. $I = 0.1$	7×10^8	3.3×10^7	T (20)
$HCPR^- + ATP^{4-} \rightleftharpoons CPR^{2-} + HATP^{3-}$	286°K. $I = 0.1$	2×10^8	8×10^7	T (25)
$HCPR^- + ADP^{3-} \rightleftharpoons CPR^{2-} + HADP^{2-}$	286°K. $I = 0.1$	2×10^8	1×10^8	T (20)
$PR^{2-} + (Ca)HATP^- \rightleftharpoons$ $HPR^- + (Ca)ATP^{2-}$	286°K. $I = 0.1$	$\sim 10^9$	$\sim 10^6$	T (25)

[a] Im = imidazole; PR = phenol red; CPR = chlorphenol red; ATP = adenosine-5′-triphosphate; ADP = adenosine-5′-diphosphate ($I = 0.1M$ KNO_3).

The quantitative understanding of phenomena like acid-base catalysis, buffer action, enzymatic hydrolysis, etc., requires the knowledge of the elementary processes involved. The data quoted in Tables IV.1–IV.3 will be of help in the analysis of these and other more complicated reaction mechanisms.

Studies of electron exchange (redox) reactions by relaxation techniques are still at their very beginning, although some examples studied have proved the applicability of the methods to this particular reaction type. The example quoted in Table IV.4 demonstrates the principal possibilities of getting information about important elementary steps in these reactions. The electron exchange between quinone and hydroquinone anions, i.e., the formation of semiquinone radicals, is a quite rapid process. Nevertheless, a specific spatial position for both reaction partners is required to allow fast electron transfer, as may be seen from a comparison with the corresponding rates for duro-compounds [*cf.* Porter *et al.* (32)]. Other studies of this type are under way, and more results may be expected in the future.

The behavior of H^+ and OH^- in recombination reactions, as discussed above, is uniquely a result of their properties as solvent ions. Ordinary ionic recombination processes in solution (e.g., the formation of aquo complexes) should be much slower, owing to the fact that ions are solvated and solvent molecules from coordination spheres have to be substituted in the process of complex formation. In many cases, substitution of solvent mole-

TABLE IV.3(b)
Intermolecular Proton Transfer
($XH + Y \rightleftharpoons X + HY$)

Reaction	Condition	$\vec{k}$ M^{-1} sec.$^{-1}$	$\overleftarrow{k}$ M^{-1} sec.$^{-1}$	Method (reference)
1. Acetic acid	293°K. $I \rightarrow 0$			
+ *m*-chloroaniline		1.1×10^8	3.0×10^9	Sound (23)
+ formate		4.6×10^7	4.6×10^8	
+ aniline		2.4×10^8	3.5×10^8	
+ imidazole		1.2×10^9	6.3×10^6	
+ hydrazine		2.2×10^9	9.5×10^5	
2. Phenol	293°K. $I \rightarrow 0$			
+ imidazole		8.5×10^6	9.9×10^9	Sound (23)
+ hydrazine		6.2×10^7	4.4×10^9	
+ ammonia		2.8×10^8	1.4×10^9	
+ propylamine		6.6×10^8	1.6×10^8	
+ piperidine		9.0×10^8	6.4×10^7	
3. Thioglycol [$HS(CH_2)_2OH$]	293°K $I \rightarrow 0$			
+ imidazole		1.4×10^6	5×10^8	Sound (23)
+ hydrazine		5.2×10^6	1.3×10^8	
+ dimethylamine		2.4×10^7	8.6×10^5	
4. Acetylacetone (keto)	298°K. $I = 0.1$			
+ acetate		2.5	4.3×10^4	T (19)
+ imidazole		9.0	1×10^3	
+ phenolate		5.5×10^3	6.2×10^2	
+ glucose anion		2×10^4	10	

TABLE IV.3(c)
Intramolecular Proton Transfer in Amino Acids

Reaction	Conditions	Exchange rate $1/\tau$ sec.$^{-1}$	Method (reference)
$HSCH_2CH_2NH_2 \rightleftharpoons {}^-SCH_2CH_2NH_3{}^+$	293°K. $I \approx 0$	2×10^7	Sound (24)
$H_2NC_6H_4COOH \rightleftharpoons {}^+H_3NC_6H_4COO^-$	293°K. $I \approx 0$	2.5×10^7	Sound (24)
o-Aminobenzoic acid	293°K. $I \approx 0$	1.7×10^7	Sound (24)
m-Aminobenzoic acid	293°K. $I \approx 0$	2.5×10^7	Sound (24)
p-Aminobenzoic acid			

TABLE IV.4
Electron Transfer Reactions (in Quinone Systems)

Reaction[a]	Conditions	$\vec{k}$ M^{-1} sec.$^{-1}$	$\overleftarrow{k}$ M^{-1} sec.$^{-1}$	Method (reference)
(1) $Q + Q^{2-} \rightleftharpoons 2Q^{-}$	284°K.	2.6×10^{8}	7×10^{7}	T (station) (30)
(2) $Q + HQ^{-} \rightleftharpoons Q^{-} + HQ^{\cdot}$	aqueous soln. $I = 0.1$ pH > 10	$< 7 \times 10^{6}$	—	T (station) (30)
(3)[b] $Q + OH^{-} \rightarrow R^{2-}$	295°K.	2.3	—	flow (31)
(4) $DQ + DQ^{2-} \rightleftharpoons 2DQ^{-}$	291°K. water/ethanol $I \approx 0.65$	5.9×10^{6}	4.6×10^{6}	flash (32)

[a] Q = benzoquinone, Q^{2-} = anion of hydroquinone, Q^{-} = semiquinone, DQ = duroquinone, etc., R^{2-} = oxyhydroquinone. T (station) indicates, that reactions (1) and (2) have been studied in the stationary state (by means of the temperature-jump method).

[b] Q disappears according to reaction (3). Example (4) (studied by flash photolysis) is given for comparison.

TABLE IV.5
Metal-Complex Formation

Reaction[a]	Conditions	k_R M^{-1} sec.$^{-1}$	k_D sec.$^{-1}$	Method (reference)
$Mg^{2+} + ADP^{3-} \rightleftharpoons MgADP^{-}$	298°K. $I = 0.1$	3.0×10^{6}	2.5×10^{3}	T (20)
$Mg^{2+} + HADP^{2-} \rightleftharpoons MgHADP$	298°K. $I = 0.1$	1.0×10^{6}	3×10^{4}	T (20)
$Mg^{2+} + ATP^{4-} \rightleftharpoons MgATP^{2-}$	298°K. $I = 0.1$	1.2×10^{7}	1.2×10^{3}	T (25)
$Mg^{2+} + HATP^{3-} \rightleftharpoons MgHATP^{-}$	298°K. $I = 0.1$	3×10^{6}	3×10^{4}	T (25)
$Ca^{2+} + ADP^{3-} \rightleftharpoons CaADP^{-}$	298°K. $I = 0.1$	$\geqslant 2.5 \times 10^{8}$	$\geqslant 3.5 \times 10^{5}$	T (20)
$Ca^{2+} + ATP^{4-} \rightleftharpoons CaATP^{2-}$	298°K. $I = 0.1$	$\geqslant 1 \times 10^{9}$	$\geqslant 2 \times 10^{5}$	T (25)
$Mg^{2+} + MgF^{4-} \rightleftharpoons Mg_2F^{2-}$	298°K. $I = 0.1$	1.6×10^{6}	10	T (33)
$Ca^{2+} + HF^{5-} \rightleftharpoons CaHF^{3-}$	298°K. $I = 0.1$	7×10^{8}	90	T (33)

[a] ADP, ATP *cf.* Table IV.(3a). F = metal phthalein (= phenolphthalein with methylene-iminodiacetate substituents in *o*-position to phenolic oxygens) (34).

TABLE IV.6
Substitution in Inner-Sphere Aquo Complexes

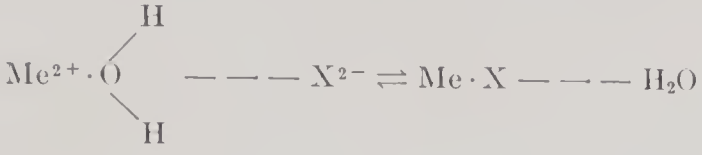

Metal ion, ligand	Conditions	$\vec{k}$[a] sec.$^{-1}$	$\overleftarrow{k}$ sec.$^{-1}$	$H^{\#}$[b] kcal./mole	Method (reference)
Be^{2+}, SO_4^{2-}	293°K. $I \approx 0.1$	1×10^2	1.3×10^3	—	T, P, Sound (15,36–38)
Mg^{2+}, SO_4^{2-}	293°K. $I \approx 0.1$	1×10^5	8×10^5	6.5	Sound (13,15,38)
Mg^{2+}, $S_2O_3^{2-}$	293°K. $I \approx 0.1$	1×10^5	1.3×10^6	—	Sound (15,38)
Mg^{2+}, CrO_4^{2-}	293°K. $I \approx 0.1$	1×10^5	1×10^6	—	Sound (15,38)
Ca^{2+}, CrO_4^{2-}	293°K. $I \approx 0.1$	$>5 \times 10^7$	1.5×10^8	—	Sound (15,38,23)
Mn^{2+}, SO_4^{2-}	293°K. $I \approx 0.1$	3×10^6	1.5×10^7	~6	Sound (13,15,38)
Fe^{2+}, SO_4^{2-}	293°K. $I \approx 0.1$	$\sim 10^6$	$\sim 10^7$	—	Sound (23)
Co^{2+}, SO_4^{2-}	293°K. $I \approx 0.1$	3×10^5	2.5×10^6	6.0	Sound (13,15,38)
Ni^{2+}, SO_4^{2-}	293°K. $I \approx 0.1$	1×10^4	1×10^5	7.8	Sound (13,15,38)
Cu^{2+}, SO_4^{2-}	293°K. $I \approx 0.1$	$>5 \times 10^7$	$>10^8$	—	Sound (15)
Al^{3+}, SO_4^{2-}	298°K. $I \approx 0.7$	~1	4	—	P (39)
Fe^{3+}, SO_4^{2-}	298°K. $I \approx 0.1$	5×10^2[c]	~10		P (39)
Zn^{2+}, SO_4^{2-}	298°K. $I \approx 0.1$	3×10^7	1.9×10^8		Sound (23)

[a] k values are fairly independent of ionic strength (tested for $I = 0.01$ to 0.5 $[M]$), error limits of activation energies ± 1 kcal./mole.

[b] Apparent activation energies (from plot of $\log \nu_{max}/T$ against $1/T$).

[c] Estimated from over-all rates.

cules in metal-ion coordination spheres turned out to be the rate-limiting step for the total reaction, even if chelation with a multivalent ligand is involved. Examples are quoted in Table IV.5. The rates of recombination for a given charge type are strongly dependent on the metal ion, but less dependent on the ligand. (The stability of the complex is expressed primarily in the dissociation rate.) Therefore, the rates are usually much

TABLE IV.7
Formation of Binuclear Aquo Complexes

Reaction	Conditions[a]	$\vec{k}$ M^{-1} sec.$^{-1}$	k sec.$^{-1}$	Method (reference)
$FeOH^{2+} + FeOH^{2+} \rightleftharpoons (FeOH)_2^{4+}$	298°K. $I = 0.5$	60 ± 20	0.12 ± 0.04	P (37,39)
$FeOH^{2+} + FeCl^{2+} \rightleftharpoons (FeOH \cdot FeCl)^{4+}$	298°K. $I = 0.5$	2.5 ± 8	—	P (37,39)
$FeOH^{2+} + FeBr^{2+} \rightleftharpoons (FeOH \cdot FeBr)^{4+}$	298°K. $I = 0.5$	33 ± 7	—	P (39)
$FeOH^{2+} + FeSCN^{2+} \rightleftharpoons (FeOH \cdot FeSCN)^{4+}$	298°K. $I = 0.5$	27 ± 4	—	P (39)
$FeOH^{2+} + FeSO_4^{+} \rightleftharpoons (FeOH \cdot FeSO_4)^{3+}$	298°K. $I = 0.5$	50 ± 20	—	P (39)

[a] These reactions are catalyzed by hydroxyl ions. The data given in Table VII correspond to the uncatalyzed reaction (extrapolated to low pH values). Similar reactions of $BeOH^+$ have been studied (36), but the interpretation of the relaxation times in terms of rate constants is complicated by the presence of a greater variety of hydroxo-complexes.

more characteristic of the metal ion than are the stability constants [compare the difference of Ca^{++} and Mg^{++} in ATP complexes, which is of interest for the metal-activated enzymatic transformations of these compounds (35)].

Generally, it is possible to distinguish between two types of complex formation reactions. In the first type, the rate of water substitution is rate limiting. The rate of complex formation for a given metal ion is fairly independent of the incoming ligand, apart from electrostatic influences of different charge types and steric factors, which, however, can be estimated. In the second type, the rate of substitution is slower than the rate of hydrolysis, so that, before substitution of H_2O occurs, a hydroxo compound is formed which then determines the further reaction. In this type, the rate is strongly dependent on the base strength of the ligand. Thus a ligand, which is a good proton acceptor, will accelerate the hydrolysis. Substitution in the coordination spheres of metal ions like Fe^{3+} belongs to the second type, whereas substitution involving the alkaline earth and most divalent transition metal ions is characteristic of the first type. The elementary step of H_2O substitution can be directly studied for these ions (38). Some results are shown in Table IV.6. The substitution of outer-sphere water molecules could also be measured. The rate constants of substitution were, in all cases, of the order of magnitude of 10^9 sec.$^{-1}$ (Al^{3+}, 10^8 sec.$^{-1}$) and quite unspecific for the metal ion (activation energies of 2–4 kcal. mole^{-1}). The inner-sphere substitution rate, on the other

hand, is very specific for the metal ion and shows influences or size, coordination number (deviation from simple ion dipole interaction even for ions with noble gas electron configuration because of dipole-dipole interaction) and specific influences (crystal field stabilization for Ni^{2+}, square planar configuration of Cu^{2+}). The rates turned out to be characteristic also for stronger complexes with chelating species such as EDTA or similar compounds. The results were checked by different methods, so that the identification of the different processes is quite unambiguous. For ions like Fe^{3+}, Al^{3+}, or Be^{2+}, the relaxation spectra are more complicated because of the presence of higher nuclear complexes. Solutions of $BeSO_4$, even in the acidic range (e.g., pH 2–5) exhibit six different relaxation times between 0.1 and 10^{-9} sec. (36), of which only four could be interpreted unequivocally. A quantitative analysis of reaction rates of binuclear complexes was possible for some Fe^{3+} complexes, as shown in Table IV.7.

Among other studies in aqueous solutions, we may mention investigations with solutions of polyelectrolytes [such as polyphosphate (40), polystyrene sulfonate (41), polyacrylate (41), polyvinyl compounds (41), and nucleic acids (42)]. The relaxation times for univalent counter-ion association have been found to be of the order of about 10^{-6} to 10^{-7} sec. at concentrations around 10^{-3} to 10^{-4} M (related to the monomer). An interpretation in terms of rate constants would be difficult due to the multiplicity of simultaneous rate processes.

Studies of the rate of structural transformations of polypeptides and proteins (e.g., helix-random-coil transformation) as well as investigations of more complicated biochemical reactions (enzyme catalysis, antibody-hapten reaction) by means of transient (relaxation) methods are still at a very early stage. Preliminary results indicate that the described techniques are useful for such studies, allowing an identification of the fast elementary processes involved in such reactions (35).

Tables IV.8–IV.10, finally, present some results on reactions in nonaqueous solvents or pure liquids. The dimerization reactions involving formation of two H bonds (Table IV.8) are almost diffusion controlled. The values for benzoic acid in CCl_4 correspond quantitatively to these expectations. The (very approximate) estimations for acetic acid certainly set an upper limit for rate constants of this reaction type. The values for benzoic acid in toluene seem to indicate some interaction of the benzene rings lowering the rate of dimerization via H bonds (47)

The results quoted in Tables IV.9 and IV.10 are more specifically related to structural transformation than to chemical change. However, such a classification may be a question of definition, since the different molecular configurations have at least a finite lifetime and differ in their energy states. The *cis-trans* isomerism is usually related to rotation

TABLE IV.8

Dimerization: $2RCOOH \leftrightharpoons$ 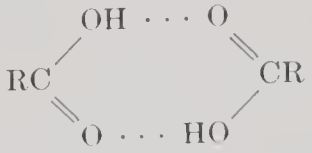

Solvent[a]	Conditions	k_R M^{-1} sec.$^{-1}$	$H_R^{\#}$ (kcal./mole dimer)	k_D sec.$^{-1}$	$H_D^{\#}$ (kcal./mole dimer)	Method (reference)
(a) CCl_4	298°K.	4.7×10^9	2.86 ± 0.6	7.4×10^5	13.3 ± 1.3	Sound
	conc. <3 mole %	5.2×10^9	3.3 ± 1.0	7.2×10^5	13.8 ± 2.1	(43,44,45)
(b) Toluene	298°K. conc. <3 mole %	$1.6 \cdot 10^9$	3.0 ± 0.2	3.7×10^6	8.7 ± 0.7	Sound (43,44)
(c) Chlorobenzene	298°K. conc. <2 mole %	$\sim 10^{10}$ [b]	—	$\sim 6 \times 10^7$ [b]	—	Sound (46)

[a] R for (a) and (b) is C_6H_5—; for (c) is CH_3—.

[b] Estimation from experimental data: $\nu_{max} = 50$–70 Mc. sec.$^{-1}$ for $n_x^0/n_S = 0.8$ mole % [using the K value given in ref. (46)] n_x^0 = total mole number of solute, n_S = mole number of solvent.

around double bonds. Such a process is generally quite slow. In contrast, rotation around single bonds is very rapid but in many cases not completely free. Planar configurations of the molecule may be stabilized in structures exhibiting resonance [compare the esters in Table IV.9(d) or the unsaturated aldehydes and ketones in Table IV.9(e)]. The different mechanisms to which the results in Table IV.9 refer are represented in Figure IV.1. Relaxation frequencies ($\omega_{max} = 1/\tau$) rather than rate constants are reported in this case. If these are attributed to rate constants, a possible multiple population of states of equal energy (*cf.* case a) must be considered. Of special interest are the energy values, which are also included in the table as far as available. [For a more detailed discussion, see ref. (59).] The nature of the solvent can influence the different rate parameters of rotational isomerism, if the transformations include changes of electrical moments. This influence is demonstrated in Table IV.10. The effects of the nonpolar (*n*-hexane) and the polar solvent (acetone) are opposite. In the case of crotonaldehyde, the parameters are almost independent of the solvent, since the steric hindrance is predominant in this case.

The relative error for the data presented in Tables IV.1–IV.10 is, in the

TABLE IV.9
Rotational Isomerism (Pure Liquids)

System	Conditions, °K.	$\omega_{max} = 1/\tau$, sec.$^{-1}$	$H_1^{\#}$ kcal./mole trans ↓ gauche	$H_2^{\#}$ kcal./mole gauche ↓ trans	Method (reference)
(a) Substituted hydrocarbons					Sound
1,1,2-Trichloroethane	243 (233)	—	7.9	5.8	(48)
1,1,2-Tribromoethane	—	—	8.0	6.4	(48)
1-Bromopropane	243 (223–298)	—	4.9	3.6	(48)
1,2-Dichloropropane	—	—	5.8	4.7	(48)
1,2-Dibromopropane	—	—	5.8	4.9	(48)
Sym. tetrabromoethane	—	—	5.2	4.3	(48)
2-Methylbutane	200 (180–220)	5×10^7	5.6	4.7	(49)
2,3-Dimethylbutane	200 (150–260)	—	3.8	2.8	(50)
2-Methylpentane	200 (150–260)	—	4.8	3.9	(50)
3-Methylpentane	200 (150–260)	—	5.0	4.1	(50)
(b) Substituted amines					Sound
Triethylamine	298 (298–343)	5.6×10^8 ($\approx k_{21}$)	—	6.8	(51)
(c) Alicylic compounds					Sound
Methylcyclohexane	289	8.8×10^5	—	—	(52)
Ethylcyclohexane	289	3.8×10^5	—	—	(52)
trans-1,2-dimethylcyclohexane	289	7.5×10^5	—	—	(52)
trans-1,4-dimethylcyclohexane	289	9.4×10^5	—	—	(52)
Cyclohexanol	305	1.4×10^6	—	—	(53)
Cyclohexylamine	292	7×10^5	—	—	(53)
Dicyclohexylamine	292	$\sim 1.4 \times 10^6$	—	—	(53)
o-Methylcyclohexane	291	$\sim 1.4 \times 10^6$	—	—	(53)
trans-4-methylcyclohexanol	291	$\sim 1.4 \times 10^6$	—	—	(53)
Cyclohexene	309	5×10^5	—	—	(53)

best cases, within 5–10%. Some less accurate determinations have been included as well. Where only orders of magnitude are safe, the rate constants are designated by the symbol "∼." Since most of the methods have been established only recently, there will be some improvement of results in the future. However, the principal conclusions should be quite reliable. Satisfactory internal agreement was found where the same system

TABLE IV.9 (*continued*)

System	Conditions, °K.	$\omega_{max} = 1/\tau$ sec.$^{-1}$	$H_1^{\#}$ kcal./mole	$H_2^{\#}$ kcal./mole	Method (reference)
					Sound
(d) Esters					
Methylformate	298	2.2×10^6	—	—	(53)
Ethylformate[b]	298	2.5×10^6	—	—	(53,54)
Methylacetate	293	4.3×10^7	—	—	(53,55)
Ethylacetate	293	7.4×10^7	—	5.7	(53,56)
(e) Aldehydes, ketones, and vinyl ethers			*trans* ↓ *cis*	*cis* ↓ *trans*	Sound
Acrolein	298 (248–298)	1.1×10^9	7.1	5.0	(57–59)
Crotonaldehyde	298 (273–323)	1.9×10^8	7.4	5.5	(57–59)
Cinnamaldehyde	298 (298–348)	9.8×10^7	7.1	5.6	(57–59)
Methacrolein	298 (248–298)	1.1×10^9	8.4	5.3	(58)
Furacrolein	333 (333–373)	8.5×10^7	6.3	5.1	(58)
2-Ethyl-3-propylacrolein	298	1.55×10^8	—	—	(58)
Hexyl cinnamic aldehyde	298	1.15×10^8	—	—	(58)
Tiophene-2-aldehyde	348	4.2×10^7	—	—	(58)
Propionaldehyde	248	3.0×10^9	—	—	(58)
n-Butyraldehyde	248	1.0×10^9	—	—	(58)
Methyl vinyl ketone	248	5.1×10^8	—	—	(58)
Methyl isopropenyl ketone	273	3.7×10^8	—	—	(58)
Furfural acetone	323	6.1×10^7	—	—	(58)
Methyl vinyl ether	248	1.4×10^9	—	—	(58)
Ethyl vinyl ether	248	1.3×10^9	—	—	(58)
2-Chloroethyl vinyl ether	248	1.9×10^9	—		(58)

[a] See also reference (45).
[b] See Table IV.10.

could be studied by various methods [e.g., NH_3 in Table IV.1(b), Be^{2+} in Table IV.6]. The upper limit for the rates of (bimolecular) second-order processes was discussed at the beginning of this section. It turned out that, in principle, the rate constants of these (and of higher-order) processes are detectable by relaxation methods. The corresponding upper limit for the rates of first-order (intramolecular) transformations still lies beyond the experimental range. If the transformation involves mass transfer, this limit should be of the order of 10^{11} to 10^{13} sec.$^{-1}$. If the transformation involves only changes in the electronic configurations (e.g., the transformation between two tautomeric states, such as the quinone-lactone con-

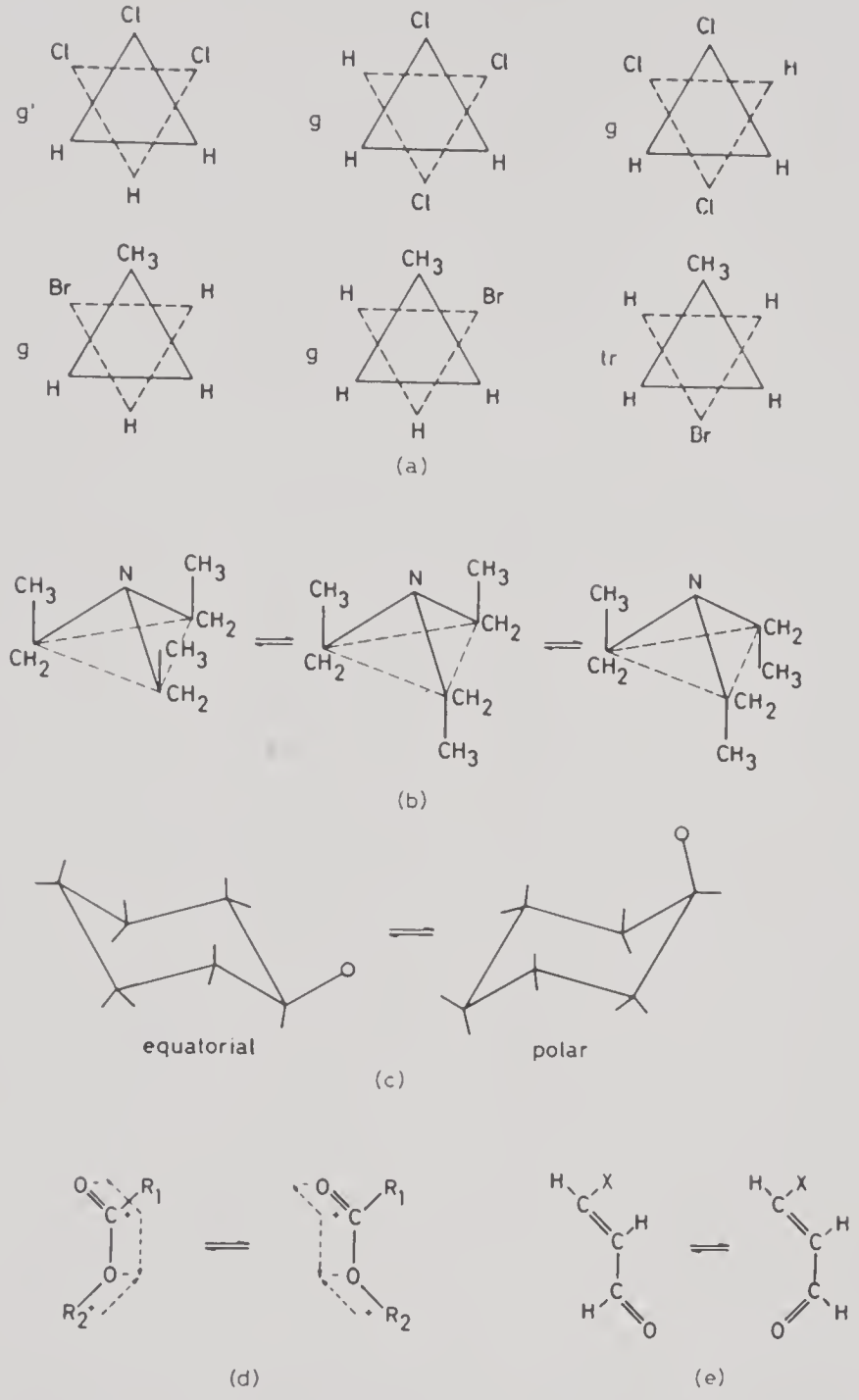

Fig. IV.1. Mechanisms of rotational isomerism (*cf.* Table IV.9). (a) Substituted hydrocarbons (examples: 1,1,2-trichloroethane, 1-bromopropane). The positions of g (gauche) are of equal energy, differing from g′ or tr (trans); (b) substituted amines; (c) alicyclic compounds (alternate chair forms; the "chair-boat" transformation is much more rapid; $\nu_{max} > 200$ Mc./sec.); (d) esters (*cf.* the compensation of electrical moments); (e) aldehydes.

figuration of phenolphthalein) the rate may be high but remains, in any case, considerably below the electronic resonance frequencies ($\sim 10^{15}$ sec.$^{-1}$) due to Franck-Condon restrictions. However, there will not be too many problems of real chemical transformation in this time range, prob-

TABLE IV.10
Rotational Isomerism of Ethyl Formate in Different Solvents

Solvent	Conditions, °K.	$\omega_{max} = 1/\tau$ sec.$^{-1}$	Method (reference)
100% Ethyl formate[a]	298	8.5×10^5	Sound (60)
50% *n*-Hexane	298	$\sim 1.1 \times 10^6$	Sound (60)
100% *n*-Hexane (extrapolated)	298	$\sim 1.3 \times 10^6$	Sound (60)
50% Acetone	298	$\sim 7.4 \times 10^5$	Sound (60)
100% Acetone (extrapolated)	298	$\sim 5.3 \times 10^5$	Sound (60)

[a] This (more recent) value differs from that given in Table IV.9.

ably less than in the range of 1 to some 10^{-11} sec., which is presently accessible for chemical rate studies.

The authors are indebted to Dr. K. Kustin, Dr. R. Mills and Dr. G. Maass for having read the manuscript and having made valuable suggestions.

References

1. M. Eigen, *Chemische Relaxation*, edited by Dr. D. Steinkopff, Darmstadt (in preparation).
2. P. Debye, *Trans. Electrochem. Soc.*, **82**, 265 (1942).
3. M. v. Smoluchowsky, *Physik. Z.*, **17**, 557, 585 (1916).
4. P. Langevin, *Ann. chim. et phys.*, **28**, 433 (1903).
5. L. Onsager, *J. Chem. Phys.*, **2**, 599 (1934).
6. E. W. Montroll, *J. Chem. Phys.*, **14**, 202 (1946).
7. R. M. Noyes, *J. Am. Chem. Soc.*, **79**, 551 (1957).
8. A. Weller, *Z. physik. Chem. N.F.*, **13**, 335 (1957).
9. M. Eigen, *Z. physik. Chem. N.F.*, **1**, 176 (1954).
10. M. Eigen and L. De Maeyer, *Proc. Roy. Soc. (London)*, **A247**, 505 (1958).
11. M. Eigen and L. De Maeyer, *Z. Elektrochem.*, **59**, 986 (1955).
12. M. Eigen and K. Kustin, *J. Am. Chem. Soc.*, **82**, 5952 (1960).
13. M. Eigen, G. Kurtze, and K. Tamm, *Z. Elektrochem.*, **57**, 103 (1953).
14. M. Eigen, K. Kustin, and R. Munson, *Z. physik. Chem. N. F.*, (in preparation).
15. M. Eigen and K. Tamm, *Z. Elektrochem.*, **66**, 93, 107 (1962).
16. M. Eigen, A. Wittig, J. Johnson, and K. Kustin (unpublished data).
17. M. Eigen and J. Schoen, *Z. Elektrochem.*, **59**, 483 (1955).
18. M. Eigen, G. G. Hammes, and K. Kustin, *J. Am. Chem. Soc.*, **82**, 3482 (1960).
19. M. Eigen and W. Kruse (unpublished data).
20. M. Eigen and G. G. Hammes, *J. Am. Chem. Soc.*, **82**, 5951 (1960).

21. K. Breitschwerdt and A. Weller, *Z. Elektrochem.*, **64**, 395 (1960).
22. M. Eigen and G. Schwarz, *Z. physik. Chem. N. F.*, (in preparation).
23. M. Eigen and G. Maass (unpublished data).
24. M. Eigen, K. Tamm, and K. Tjaden, (to be published).
25. H. Diebler, M. Eigen, and G. G. Hammes, *Z. Naturforsch.*, **15b**, 554 (1960).
26. S. Ljunggren and O. Lamm, *Acta chem. Scand.*, **12**, 1834 (1958).
27. K. F. Wissburn, D. M. French, and A. Patterson, Jr., *J. Phys. Chem.*, **58**, 693 (1954).
28. F. J. W. Roughton, *J. Am. Chem. Soc.*, **63**, 2930 (1941); B. R. W. Pinsent, L. Pearson, and F. J. W. Roughton, *Trans. Faraday Soc.*, **52**, 1594 (1956).
29. J. Meir and G. Schwarzenbach, *Helv. Chim. Acta*, **40**, 907 (1957).
30. H. Diebler, M. Eigen, and P. Matthies, *Z. Naturforsch.*, **16b**, 629 (1962).
31. P. Matthies, Dissertation, Göttingen, 1961.
32. K. Bridge and G. Porter, *Proc. Roy. Soc.* (*London*), **A244**, 259, 276 (1958).
33. G. Czerlinski, H. Diebler, and M. Eigen, *Z. physik. Chem. N.F.*, **19**, 246 (1959).
34. G. Schwarzenbach, *Die komplexometrische Titration*, edited by F. Enke, Stuttgart, 1957.
35. M. Eigen and G. G. Hammes, *Advances in Enzymology*, **25** (1963).
36. H. Diebler and M. Eigen, *Z. physik. Chem. N.F.*, **20**, 299 (1959).
37. H. Wendt and H. Strehlow, *Z. Elektrochem.*, **64**, 131 (1960).
38. M. Eigen, *Z. Elektrochem.*, **64**, 115 (1960).
39. H. Wendt, Dissertation, Göttingen, 1960.
40. M. Eigen and G. Schwarz, *J. Coll. Sci.*, **12**, 181 (1957); *cf.* also *Electrolytes*, Pergamon Press, New York, 1962).
41. K. F. Wissbrunn and A. Patterson, Jr., *J. Polymer Sci.*, **33**, 235, 249 (1958).
42. M. Eigen, N. Ise, and G. Schwarz (in preparation).
43. W. Maier, *Z. Elektrochem.*, **64**, 132 (1960).
44. W. Maier, L. Borucki, B. Dischler, and H. Rieseberg (to be published).
45. W. Maier and H. D. Rudolph, *Z. physik. Chem. N. F.*, **10**, 83 (1957).
46. J. E. Piercy and J. Lamb, *Trans. Faraday Soc.*, **52**, 930 (1956).
47. A. Weller, *Z. Elektrochem.*, **64**, 145, 198 (1960).
48. J. Lamb, *Z. Elektrochem.*, **64**, 135 (1960).
49. J. M. Young and A. A. Petrauskas, *J. Chem. Phys.*, **25**, 943 (1956).
50. J. H. Chen and A. A. Petrauskas, *J. Chem. Phys.*, **30**, 304 (1959).
51. E. L. Heasell and J. Lamb, *Proc. Roy. Soc.* (*London*), **A237**, 233 (1956).
52. J. Lamb and J. Sherwood, *Trans. Faraday Soc.*, **51**, 1674 (1955).
53. J. Karpovich, *J. Chem. Phys.*, **22**, 1767 (1954).
54. L. N. Liebermann, *Phys. Rev.*, **75**, 1415 (1949).
55. P. Biquard, *Ann. Phys.*, **6**, 195 (1936).
56. J. M. M. Pinkerton, Ultrasonics Conference, Brussels, 1951 (pg. 117, *Med. Vlaamsche Akad. Wet.*).
57. M. S. de Groot and J. Lamb, *Trans. Faraday Soc.*, **51**, 1676 (1955).
58. M. S. de Groot and J. Lamb, *Proc. Roy. Soc.* (*London*), **A242**, 36 (1957).
59. R. O. Davies and J. Lamb, *Quart. Revs.*, **11**, No. 2, 134 (1957).
60. D. N. Hall and J. Lamb, *Trans. Faraday Soc.*, **55**, 784 (1959).
61. M. Eigen and E. Eyring, *J. Am. Chem. Soc.* (in press).
62. M. Eigen and K. Kustin, *J. Am. Chem. Soc.* **84**, 1355 (1962).
63. M. Eigen, K. Kustin, and G. Maass, *Z. physik. Chem. N.F.*, **30**, 130 (1961).
64. M. Eigen, K. Kustin, and H. Strehlow, *Z. physik. Chem. N.F.*, **31**, 140 (1962).
65. G. Ertl and H. Gerischer, *Z. Elektrochem.*, **66**, 560 (1962).

APPENDIX

List of Symbols

A	affinity
A_1, A^+, B_1, AB, etc.	symbols for chemical species
A', A'', A_{ik}	general constants [Equation (II.3.92)] and amplitude factors
A	matrix of rate coefficients
a	activity
a_{ik}	matrix element (rate equations)
B	matrix of rate coefficients (diagonalized)
B_i, B_i''	general constants, Equation (II.3.92)
b	parameter in Onsager's treatment of the dissociation field effect
b	damping constant
b_{ik}	matrix element (transformed rate equations)
C	electric capacitance
C_P, C_V	heat capacities
c_i	general concentration variable (if not specified); volume concentration (if specified)
$\bar{c}_i$	equilibrium concentration
c_P, c_V	specific heats
ch	index of chemical part (of derived thermodynamic functions; ∞ = index of residual part)
$\mathfrak{D}$	differential operator d/dt
D*	electric derived vector, conjugate to **E**
D_A, D_B	diffusion coefficients
d, ∂	differential symbols
db	decibel
E	electric field strength vector
$\mathfrak{E}$	unit matrix
E	symbol for enzyme
e_0	elementary charge
F	Helmholtz free energy
$F(j\omega)$	Fourier transformed function
F	Faraday number
f	general function
f_i, (f)	activity coefficient (mean)
G	Gibbs free energy
G^*	function analogous to G (inclusion of term **ED***)
g	proportionality factor

H	enthalpy
$H^{\#}$	apparent activation energy, obtained from a plot of log ν/T against $1/T$ (*cf.* tables)
h	Planck's constant
I	light intensity, sound intensity
$\mathbf{I}$	electric current
I	ionic strength (given in molar concentration)
Im (im)	symbol for imaginary part of function
$\mathbf{i}$	current density (electric flux)
i, k, etc.	general index for component or state
J	Massieu function
j	imaginary number
K_0	equilibrium constant (conventionally defined for $\Sigma A \rightleftharpoons \Sigma B$ as $\Pi a_B/\Pi a_A$
K'_0	inverse of K
K	equilibrium function
k	rate constant
k	constant in rate equation (II.3.72)
$\mathbf{k}$	Boltzmann constant
L	inductance
l	length
$\mathbf{M}$, $\mathbf{M}^{-1}$	transformation matrices
M	molecular weight
Me	symbol for metal (ion)
m_{ik}, m'_{ik}	matrix elements
m	mass
m_i	molality concentration (moles/1000 g. solvent)
N_A	Avogadro's number
n	mole number (n_0 related to the initial state)
P	pressure
p_1	pressure (incremental value)
$\mathbf{p}$	dipole moment
p	complex exponent
Q	sound absorption cross section (per molecule)
q	area
$\mathbf{R}$	gas constant
R	Ohmic resistance
Re (re)	symbol for "real" part of function
r_D	(diffusive) reaction distance
r	index for reference state
S	entropy

s	index for sample system
s	"condensation" [Equation (II.3.78)]
T	temperature (absolute)
T_d, T_B, T_F	decay times
t	time
U	(internal) energy
U	voltage
u	particle velocity
u_i	electric mobilities
V	volume
v	sound velocity (complex)
v_{re}	phase velocity of sound
X	vector formed of components x_i
x	space coordinate
x_i, $(\bar{x}_o)$	small displacement of concentration (δc_i)
Y	Planck's function
Y	vector formed of components y_i
y_i, $(\bar{y}_i)$	small displacement of concentration (normal variable)
Z_i	general thermodynamic variable
z	valency
α	degree of dissociation
$\mathfrak{a}$	attenuation constant (sound absorption)
α_P	coefficient of thermal expansion (isobaric)
β	degree of transformation
β_{VE}	isochoric temperature coefficient of $\mathbf{D}^*$
Γ	function of equilibrium constant [defined by Equation (II.3.10)]
Γ^*	generalized function Γ (inclusion of activity coefficients)
γ_i	mole fraction
γ	ratio of specific heats c_P/c_V
Δ	symbols for reaction quantities; ΔH, ΔV, $\Delta\mathbf{D}^*$, (operator $(\partial/\partial\xi)$ at constant intensive variables. For a reaction system $\Sigma A \rightleftharpoons \Sigma B$, $\Delta H = \Sigma H_B - \Sigma H_A$)
δ	small displacement
δ_l	loss angle
ϑ	integral boundary
ϑ	centigrade temperature
Θ	impulse duration

ϵ, ϵ_{SV}, etc.	electric permittivity (dielectric constant)
ϵ_0	influence constant
ϵ_i', ϵ_i''	molar extinction coefficients (of component i) (ϵ_i'' decadic)
η	shear viscosity
η_b	bulk or volume viscosity
η'	dilatational viscosity
κ_T, κ_S	compressibilities
λ	(sound) wave length
λ_E, λ_F	(light) wave length (extinction and fluorescence)
λ_h	coefficient of heat conduction
$\mathfrak{u}$	coefficient of (sound) absorption per wave length (related to energy absorption)
μ_i	chemical potential (of component i)
ν	frequency (sound)
ν_E, ν_F	frequency (light extinction and fluorescence)
ν_i	stoichiometric coefficients
ξ	extent of reaction
Π	symbol of product
Πk	sum of products [Equation (II.1.27)]
ρ	density
ρ	factor (effective amplitude ratio)
Σ	symbol for sum
$\mathfrak{S}$	(complex) transfer function
σ_{el}	electrical conductivity
τ, τ_i, τ_{SP}, etc.	relaxation times
φ	phase angle
χ	complex electrical admittivity
ω	circular frequency $2\pi\nu$

CHAPTER XIX

FLASH PHOTOLYSIS

GEORGE PORTER, *The University, Sheffield, England*

I. Introduction 1056
II. The Experimental Method 1058
1. The Photolysis Flash 1059
2. Spectroscopic Recording Apparatus 1060
3. Flash Spectroscopy 1060
4. Kinetic Spectrophotometry 1061
5. Triggering and Synchronization 1061
III. Description of a Standard Flash Photolysis Equipment 1062
1. Construction of Flash Lamps 1063
2. Reaction Vessel and Reflector 1063
3. Electrical Supplies for Flash Lamps 1066
4. Monitoring Source 1067
5. Monochromator and Detector 1068
6. Additional Apparatus for Flash Spectroscopy 1070
7. Trigger and Delay Circuits 1070
8. Summary of Characteristics 1072
IV. Preliminary Flash Spectrographic Investigation 1072
1. The Extent of Permanent Reaction 1073
2. The Spectra of Transient Intermediates 1074
3. Lifetime and Kinetics of Transient Intermediates 1075
V. Measurement of Absorption Spectra 1075
1. Use of Constant γ plates 1076
2. Plate Calibration by Standard Density Wedge 1077
VI. Determination of Absolute Concentrations and Extinction Coefficients 1077
VII. Kinetic Investigations by the Spectrophotometric Method 1080
1. Relation between Intensity and Oscillograph Deflection 1082
2. Response Time of the Detector Circuits 1082
3. Validity of Beer's Law 1082
VIII. Thermal Effects Following Flash Photolysis 1084
1. Utilization of the Thermal Effect 1086
IX. Other Flash Photolysis Arrangements 1087
1. Higher Flash Energies 1087
2. Lower Flash Duration 1087
3. Other Modifications 1088
X. Examples of Kinetic Studies by Flash Photolysis 1088
XI. The Triplet States of Organic Molecules in Solution 1089
XII. Photochemistry of Quinones and Dyes and the Reactions of Semiquinones 1094
Postscript 1102
References 1104

I. INTRODUCTION

Two experimental problems arise in connection with the direct investigation of a very fast reaction. First, the reaction must be initiated in a time which is short in comparison with the overall reaction time, and in a manner which ensures homogeneity of reaction throughout the volume of reaction mixture which is studied kinetically. Second, some significant parameter of the reacting system must be recorded after initiation in such a manner that useful information regarding the mechanism and kinetics of the reaction can be derived therefrom. The second problem has been solved to a considerable extent by modern advances in the high speed electronic recording of many types of physical change, but the rapid homogeneous initiation of chemical reaction presents many difficulties.

There are several general methods of bringing about a chemical reaction, e.g., by mixing the reactants, by heating the reaction mixture, or by subjecting the reaction mixture to radiation or electrical discharge. For very fast reactions, some of the methods have fundamental limitations. The mixing of two reactants is a powerful technique which has been discussed elsewhere in this volume. With most liquids it can be brought about in a time of about 1 millisecond, but rather longer is required for viscous liquids and, usually, for gases; the method is, of course, in appropriate for solids.

Initiation of chemical change by heating a reaction mixture in the conventional way is a very slow process. In a gas at atmospheric pressure and in a vessel 1 or 2 cm. in diameter, the time taken for a temperature change at the wall of the vessel to be equilibrated through the gas is of the order of seconds and the time is, of course, much longer in liquids. However, there are newer methods (e.g., relaxation methods, which are described elsewhere in this volume) where such difficulties do not exist. The shock tube technique, for example, now makes it possible to raise the temperature of a gas by many hundreds of degrees in a time of the order of microseconds, and provides a powerful approach to the study of thermal dissociation in the gas phase. The accuracy is, however, usually found to be considerably lower than that attainable by means of the techniques discussed in this chapter.

The initiation of reaction by irradiation is less common for preparative chemistry than either of the two general methods discussed above, but it has proved to be a most powerful method for the study of chemical mechanism and of the transient intermediates of chemical change. In particular, the photochemical study of gas reactions has provided some of the most detailed information yet available about elementary chemical processes. It is therefore fortunate that photochemical initiation of reaction is the

most convenient method of bringing about a large extent of reaction in a short interval of time in a homogeneous system by the method of flash photolysis (44). It is probable that other pulsed irradiation techniques employing, for example, pulses of X-rays or electrons, will also prove valuable, particularly for the study of the primary processes of radiation chemistry.

Flash photolysis is a method whereby a nonequilibrium situation can be created in a reaction system in a short interval of time. It provides a general means of preparing unstable intermediates in concentrations higher than can be obtained by other methods. It is applicable to gases, liquids, and solids, and to the whole available temperature range. The nonequilibrium situation created by the flash can be made homogeneous throughout a reaction vessel of any required shape and dimensions. In conjunction with physical methods of observation the concentration of intermediates can be directly measured as a function of time and their physical and chemical properties determined.

Like the photochemical method itself, flash photolysis is of very general applicability and, with an appropriate choice of reacting system, most types of chemical change can be initiated and most classes of chemical intermediate can be prepared. On the other hand photochemical techniques are rather specific and, by a suitable choice of wavelength, the primary process can often be very clearly defined.

In the flash photolysis technique a reactant is irradiated with an intense flash of visible or ultraviolet light. The intensity must be sufficient to produce a measurable change in chemical composition, but of short duration compared with that of the ensuing reactions which are to be studied. In practice, although the times vary considerably from one system to another, the flash duration is typically of the order of microseconds. Most applications of the method so far have been associated with subsequent studies of the chemical change by absorption spectroscopy in the visible or ultraviolet regions. This may be carried out by a second flash technique known as flash spectroscopy (44) or by photoelectric recording.

In view of the high energies, and the consequently rather elaborate equipment which are sometimes used, it may be supposed that the technique is a rather specialized one which cannot readily be adopted in some laboratories and it is important that this impression should be corrected. Most recent kinetic investigations, on a wide variety of systems including excited state spectra and kinetics, free radical spectra and kinetics in gases, liquids, and solids, and the recombination of atoms, have employed one or two flash lamps with a total energy of 500 j. or less per flash. Except for the oscillograph and spectrograph, which are standard equipment, such an apparatus can be constructed at very little cost and occupies only a few

square feet of bench space. If required, the noise of the flash can be almost completely suppressed by a simple enclosure and there are no special hazards except those connected with the use of voltages of the order of 10 kilovolts, which are now quite common in standard laboratory equipment.

II. THE EXPERIMENTAL METHOD

A typical flash photolysis arrangement consists of three parts:

1. A photolysis flash for producing a short pulse of light of very high intensity along with associated energy storage units—usually condensers—and equipment for charging and initiating the discharge (triggering).

2. A reaction vessel with associated thermostats and filters, and a reflector to condense light from the photolysis flash.

3. Some arrangement for physical detection and estimation of transient intermediates. Most usually absorption spectroscopy is the method adopted and the two principal techniques are as follows. (*a*) A second spectroflash, of short duration, timed to fire at any required interval afert the photolysis flash, and a spectrograph. The spectroflash gives essentially continuous light which records the absorption spectra of reaction intermediates photographically in a single flash of a few microseconds duration. (*b*) A monochromatic source (e.g., a tungsten lamp and monochromator), the light from which is collimated and passed through the reaction vessel, an electronic detector and a rapid recorder (e.g., photomultiplier cell and oscillograph).

The general arrangement of these components is illustrated in Figure 1.

The original flash photolysis apparatus (44) employed a condenser bank of 10,000 j. and had a flash duration of several milliseconds. The synchronization was effected by a rotating mechanical shutter, in order to

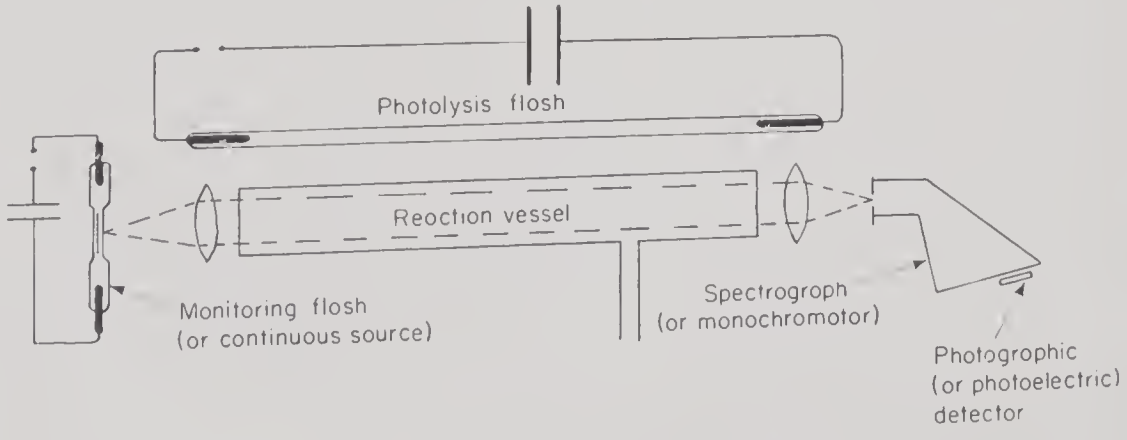

Fig. 1. Schematic diagram illustrating the principle of the flash photolysis technique.

eliminate the scattered light from the photolysis flash, and recording was photographic. The efficiency of light absorption by this equipment was surprisingly high; 16% of the total energy stored in the condenser was absorbed in the region between 2,000 and 4,000 A. The reaction vessel was 1 meter long and the high efficiency of light production resulted in almost complete destruction of substances like acetone and NO_2 in the gas phase. Most subsequent work has utilized smaller energies, of the order of several hundred joules, although some work with still higher energies, up to 500,000 j. is in progress (9).

The most suitable arrangement of a flash photolysis equipment depends to a large extent on the particular application for which it is intended. The main possibilities are outlined below.

1. The Photolysis Flash

This is almost invariably an electronic flash produced by the discharge of a condenser through a quartz tube filled with a rare gas, sometimes with hydrogen added. Other sources, e.g., the spark (29) and the exploding wire (40) have also been used. These are far less satisfactory for most applications although spark sources have some useful features, e.g., short duration and a line spectrum.

The ideal flash photolysis source, in all applications, is one with the minimum duration and highest intensity. In practice, increasing the energy of the flash increases the duration and a compromise is usually necessary. At one extreme, when duration is not of great importance, very high energies can be dissipated. A single lamp, 1 meter in length, will dissipate up to 10,000 j. per flash and higher energies can be obtained by using a number of synchronized lamps, each with its own condenser bank. The duration of such flashes will be several milliseconds and they are therefore useful only for the relatively small number of transients whose lifetimes fall in this range. At the other extreme, flashes of a few millimicroseconds duration are available, with energies of microjoules per flash (30,58). This energy is usually too small to produce a measurable photochemical effect, though such sources prove useful in studies of the radiative lifetime of excited states (60).

The most useful range in flash photolysis work at present is intermediate between these extremes and flash durations (measured at half peak light) nearly always lie between 1 and 100 microseconds with energies per flash of 20–2,000 j. These figures do not imply a direct proportionality between energy and duration since many other factors are important. Roughly, for a given energy per flash in this range, duration increases with capacity and tube length but depends little on voltage.

The light emitted by electronic flash tubes of this kind consists of a continuum on which are superposed the broadened atomic spectral lines of the rare gas. It extends well into the infrared and vacuum ultraviolet regions if quartz absorption is eliminated by using a transparent window.

2. Spectroscopic Recording Apparatus

As already stated, the absorption spectrum may be investigated in two ways and a single experiment may be used either to record the whole range of wavelengths at a single time or alternatively a single wavelength over all times. We may call the first approach flash spectroscopy and the second kinetic spectrophotometry.

Each has its advantages and disadvantages. For exploratory work on a system where the spectra of the transients are unknown or uncertain, it is advisable to record the spectra photographically over the whole spectral range of interest. For vapor phase studies, where simple intermediates having fine structure are likely to appear, photographic recording is almost essential.

Very short lived species, which are present only in a photostationary state during the flash, can often be detected by flash spectroscopy when photoelectric methods would be unsuitable owing to interference by scattered light from the photolysis flash. On the other hand the spectrophotometric method is somewhat simpler, no delay unit is required and, if the absorption spectra are reasonably extended, simple filters are sufficient to isolate the required wavelength. It is also far more accurate for kinetic work, once the intermediates have been identified, and far less tedious since the whole kinetic record of concentration versus time is obtained in a single experiment.

3. Flash Spectroscopy

The flash source used for this purpose may be similar to the photolysis flash but viewed end-on through a suitable window. Alternatively a small quartz capillary whose dimensions are comparable with those of the spectrographic slit may be used. A single flash of energy 100 j. is sufficient to give an adequate record throughout the visible and quartz ultraviolet region at moderately high dispersion (e.g., with the Hilger medium or large quartz spectrographs) in 15 μseconds.

Interference between the two flashes is slight and shutter mechanisms are unnecessary unless the system is fluorescent. Scattered light from the photolysis flash can be reduced below detection level by simple collimation and tests have shown that even when the photolysis and spectroscopic

flashes are of equal energy, the geometry of the arrangement is such that the relative contribution of the spectroscopic flash to the photochemical change is negligible.

4. Kinetic Spectrophotometry

Except for reactions of long duration (several milliseconds at least), it is not feasible to use a scanning spectrophotometer, since the band width necessary to give adequate definition and scanning speed results in an unacceptable signal/noise ratio. If it is required to record a spectrum spectrophotometrically, it is therefore usual to scan the spectrum point by point. For any given conditions the signal/noise ratio is proportional to the square root of the intensity of the monitoring beam and it is advisable that the monitoring source lamp should be as intense as possible. In addition, however, short time stability of this source is important, especially for small absorption changes, and d.c. sources are of course essential. For many purposes a tungsten filament lamp (12–48 w.), operated from batteries, is very satisfactory. In the ultraviolet region, and when much higher intensities are required, a d.c. xenon arc lamp is suitable.

The beams must be very accurately collimated in order to reduce the scattered light from the photolysis flash. The filters or monochromator and the photomultiplier, cathode follower, amplifiers, and oscillograph are standard equipment and require no comment at this point.

5. Triggering and Synchronization

There are two methods of ensuring that the flash lamps do not fire during the charging of the condensers, but fire reproducibly at the required time. The first is to fill the lamps with a gas at a pressure high enough to prevent breakdown at the operating voltage but low enough for the discharge to take place when a trigger pulse is applied to a third electrode. This is a simple method and it ensures that the energy is all dissipated in the flash lamp itself. It is perfectly satisfactory if the flashing of the lamp is the master operation, which initiates the other operations. It is less satisfactory when lamps have to be fired at a definite time, e.g., the spectroscopic flash or several photolysis flash lamps in parallel, since when high energies are discharged through these lamps their triggering characteristics become erratic. A second difficulty is that the pressure of gas required to hold off the discharge may be high enough to explode the lamp if a high energy of discharge is used.

The alternative method is to use a hold-off gap which may be a thyratron or similar valve or a spark-gap. The energy lost in such a gap is not

serious and the system is far more reliable, at high energies, than the internal trigger electrode. Delays between flashes are best introduced by an electronic delay unit although, for times greater than a few milliseconds, a mechanical delay is quite satisfactory.

III. DESCRIPTION OF A STANDARD FLASH PHOTOLYSIS EQUIPMENT

Every design of apparatus is a compromise and the wide range of energies and other factors which have been used in flash photolysis apparatus have been indicated. For practical purposes it will be useful if one type of equipment is now described in detail. This apparatus has been found to be generally useful for a variety of kinetic studies, and, although inexpensive

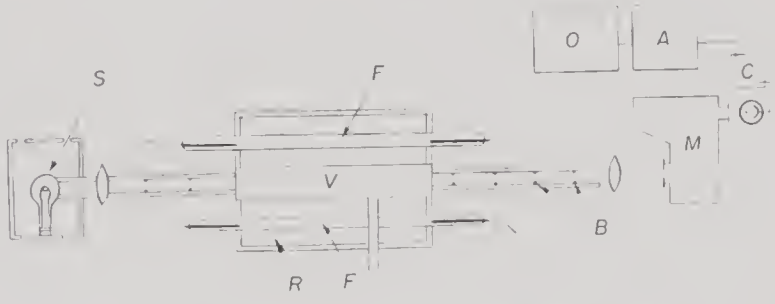

Fig. 2. Arrangement of apparatus with photoelectric recording. *S*, continuous source; *V*, reaction vessel; *F*, photolysis flash; *R*, reflector; *B*, light baffles; *M*, monochromator; *C*, cathode followers; *A*, d.c. amplifiers; *O*, oscillograph and camera.

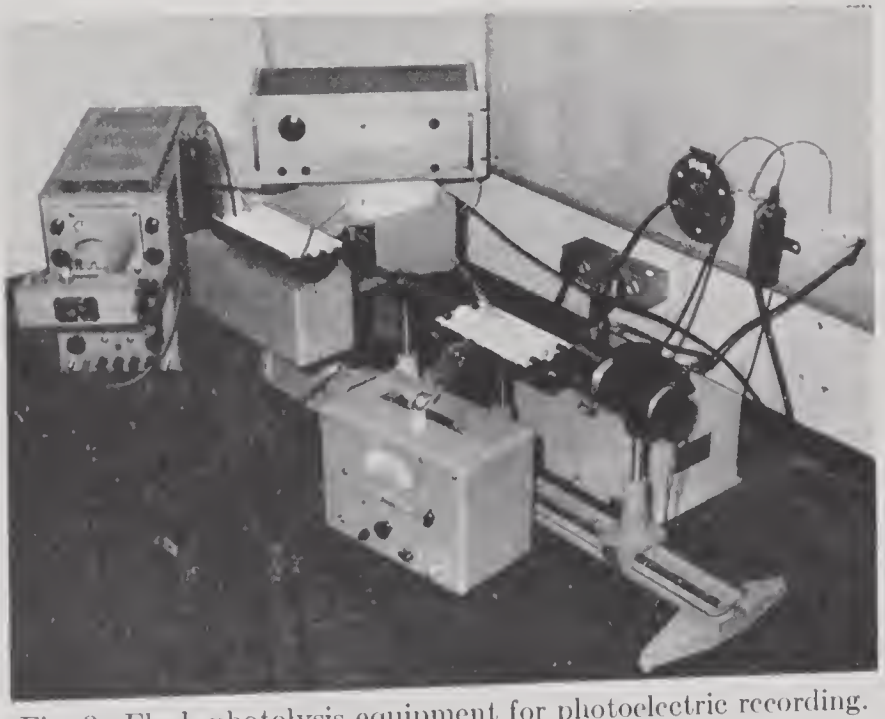

Fig. 3. Flash photolysis equipment for photoelectric recording.

and simple to construct, it provides a useful compromise between flash duration and energy and the necessary sensitivity and stability for quantitative work.

The complete apparatus includes facilities both for flash spectroscopy, using photographic recording, and for kinetic spectrophotometry. As already explained, for the full study of a new system it is advisable to use both methods but, since it is rather more simple and is quite sufficient once the spectra of the intermediates are known, the latter will be described first.

The complete arrangement for flash photolysis and spectrophotometric recording is shown in Figure 2. The reaction vessel and two flash lamps are 20 cm. in length, and these, as well as the monitoring light source, monochromator and photocell are rigidly mounted on an optical bench. A photograph of a typical apparatus is shown in Figure 3.

1. Construction of Flash Lamps

These are quartz tubes, 11 mm. in internal diameter, with an electrode sealed into each end. The separation between tips of the electrodes is the same as the length of the reaction vessel, viz., 20 cm. The electrodes are of 3 mm. tungsten or molybdenum rod and are sealed into the quartz by means of a standard lead seal. These seals are commercially available and have been found more satisfactory than metal (e.g., molybdenum) foil seals, being very resistant to thermal shock. A side arm is attached to the tube for evacuation and filling.

The lamp is thoroughly evacuated and gently flamed under vacuum and then filled with pure krypton (argon and xenon are also satisfactory) to a pressure of 100 mm. It should then be flashed, without sealing, under operating conditions (see later) about twenty times to outgas the electrodes and again evacuated. It is then filled again with inert gas at 100 mm. pressure and sealed off close to the main tube. Such a lamp will be satisfactory for many thousand flashes. If the outgassing is inadequate it will still be satisfactory for a limited period but will require reevacuation and filling after fewer flashes.

2. Reaction Vessel and Reflector

The reaction vessel is a quartz cylinder (or may be of glass if only the visible and near ultraviolet regions are of interest), 15 mm. in internal diameter and 20 cm. in length, with flat plates sealed onto either end and with a suitable side tube for evacuation, filling, and outgassing of solutions (Fig. 4). It is very important that the end windows be as nearly optically

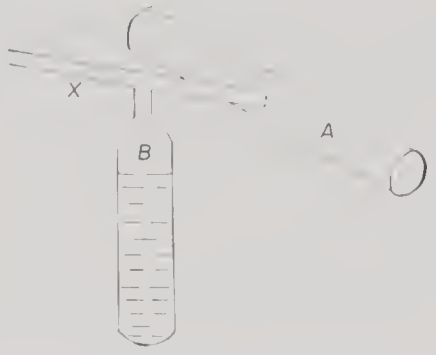

Fig. 4. Reaction vessel for study of outgassed solutions.

flat and transparent as possible since reflection and scattering of the flash by these windows presents a serious problem in many investigations where the light scattered in this way may be comparable with, or greater than, the light received by the photocell from the monitoring beam.

The reaction vessel is mounted rigidly in a cylindrical reflector which also serves to support the two flash lamps and which is itself mounted on the optical bench. The design of this reflector is shown in Figure 5. It is in two parts, with the upper half easily removable for inspection and change of reaction vessel, and is made from a cylinder of aluminum 10 cm. in diameter. The inner surface of the reflector is coated with magnesium oxide, which has a very high total albedo through the whole of the visible and quartz ultraviolet region of the spectrum. The coating of magnesium oxide is formed by condensing the smoke from burning magnesium ribbon onto the surface of the reflector; it breaks off rather easily and must be replaced from time to time.

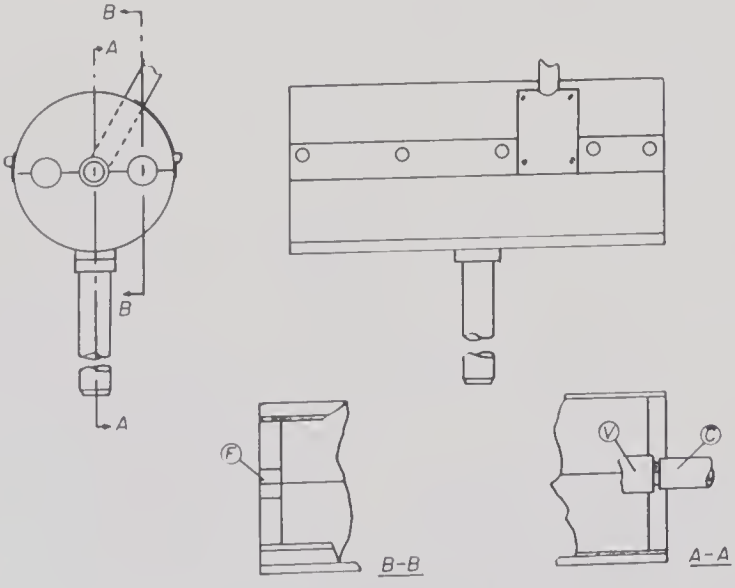

Fig. 5. Reflector and mount for reaction vessel and flash lamps. *F*, flash tube support; *V*, reaction vessel; *C*, collimating tube.

The lamps are placed on the reflector so that the tips of the electrodes are adjacent to the windows of the reaction vessel and the connecting leads project outside the reflector. It is advisable to cover these, and all other high voltage leads and connections, with tubing of an insulating material. In addition to the slots at the end of the reflector, which accommodate the lamps and the reaction vessel, there is a slot in the middle of the cylinder, cut between the upper and lower halves, to allow projection of the side arm of the reaction vessel, and of any ancillary equipment which may be connected to it. For gas phase studies this may be connected permanently with the vacuum line. For most work in solution it will be connected to a tap or will be sealed off. Nearly all work involving transient intermediates such as free radicals or excited states in solution is carried out after the solution has been thoroughly outgassed. The solution is outgassed by successively freezing the solution, evacuating the cell, and remelting. Since freezing is liable to crack the vessel it should not be carried out in the reaction vessel itself but in the separate chamber B (Fig. 4). When outgassing is complete the liquid is again frozen in vessel B, the assembly is sealed at X and the solution, after melting, is poured into the reaction vessel A for investigation.

If accurate temperature control is required, or if it is required to vary the temperature of the reaction mixture, either of two procedures may be used. The first, is to regulate the temperature of the whole reflector assembly, either by enclosing it in a furnace or, more simply, by placing an air heater at the bottom of the reflector. If temperatures greatly in excess of room temperature are to be used it will be necessary to have double windows on the reaction vessel with an evacuated space between them. The flash lamps change their characteristics very little with temperature and may be operated without difficulty to at least 300°C.

An arrangement which gives better uniformity of temperature in the reaction vessel is shown in Figure 6. The reaction vessel has double windows and is totally enclosed in an outer jacket, the whole being constructed of glass or quartz. The outer jacket is filled with a transparent liquid

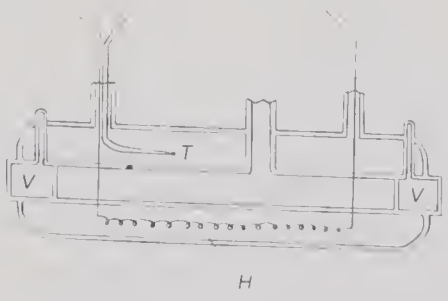

Fig. 6. Reaction vessel with outer jacket for temperature control. V, evacuated cells; H, heater element; T, thermocouple.

which is either heated in an external thermostat and pumped through the vessel, or is heated *in situ* by an electric element immersed in the liquid. Suitable liquids for the heating jacket are (*a*) silicone oil, a typical sample of which has over 90% transmission above 3,500 A. and may be used up to temperatures of at least 250°C. for long periods, and to higher temperatures if air is excluded, (*b*) ethylene glycol, commercial grades of which usually have over 90% transmission above 2,900 A., can be used below 2,400 A. after further purification and are useful for temperatures up to about 140°C.

This type of jacketed vessel is also useful for filtering the radiation from the photolysis flash. Ethylene glycol is a solvent for both inorganic ions and organic dyestuffs, and filter solutions for various wavelength ranges are described in the literature, e.g., Bowen (3). In using such a filter for flash photolysis work, it must be remembered that, even when there is no permanent photochemical change, many colored solutions, particularly organic dyes, are temporarily bleached during the flash and a separate flash photolysis investigation with the filter solution in the reaction vessel should be carried out before it is adopted for this purpose.

3. Electrical Supplies for Flash Lamps

The method, which may be applied to any number of flash lamps, is to use a single charging unit for all condensers, a single spark gap to ensure simultaneity of firing but a separate condenser for each flash tube in order to keep total flash duration to a minimum. The wiring diagram of this arrangement is shown in Figure 7. Apart from the main charging unit for the power condensers it includes a small spark coil for triggering the gap, a condenser which is discharged across the primary of this coil, and a charging unit for the condenser. Whatever the ancillary apparatus, the firing of the photolysis flash lamps is made the master operation and all other operations are timed from this. It is therefore only necessary to have a button switch in the trigger circuit to initiate the sequence.

The high frequency chokes in the charging circuit enable a single power unit to be used for charging all lamp circuits but isolate the circuits from each other during the discharge. All leads, and particularly those associated with the trigger spark, should be well screened to prevent interference with the detector circuits. The spark gap operates in air, consists of two electrodes with spherical ends of tungsten or similar metal and is enclosed in a lucite box to decrease the noise which arises mainly from this gap. The distance between the ends of the electrodes is typically 3 mm. and is adjustable. The trigger spark is brought to a copper tip which terminates a few mm. from one electrode.

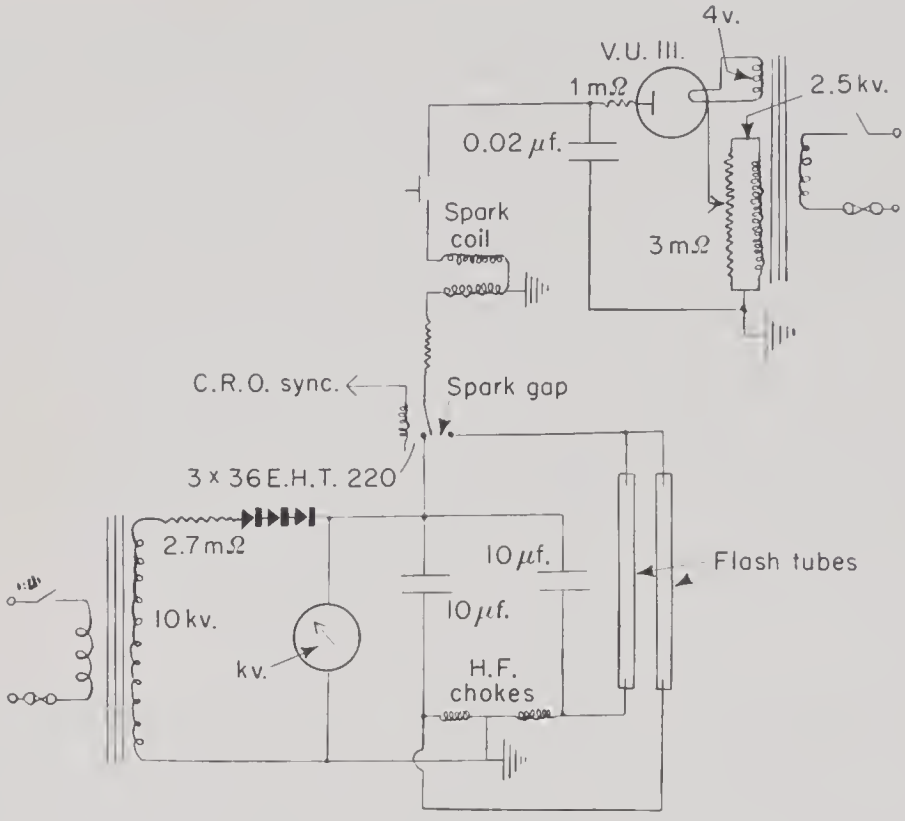

Fig. 7. Charging and trigger circuits for photolysis flash lamps.

If ordinary condensers, of the type supplied for power rectification, are used for the flash lamps, a half peak duration of approximately 20 μsec. may be expected. This may be somewhat reduced by the use of special low inductance condensers but only if the length of the connecting leads between lamps and condensers is reduced to a minimum.

4. Monitoring Source

The light source used for monitoring must be as intense and as free from fluctuations as possible. The requirement for a high intensity arises first because the signal from the monitoring source should be as great as possible compared with the scattered light from the flash and second, because, for a given detector, the signal to noise ratio is proportional to the square root of the signal intensity. Constancy of signal over short time intervals is required to prevent distortion of the trace and over longer periods to prevent change in the position of zero calibrations. Slow drift over times longer than a few seconds is less important.

The most satisfactory way of obtaining the required constancy of supply is to use storage batteries but these should be of sufficient capacity to prevent significant drift of voltage during the experiment. For the visible region a simple source, which is satisfactory for many purposes, is a stand-

ard tungsten filament lamp of the automobile headlamp type, e.g., 6 v. 24 w. For intensities approximately one hundred times greater, or if ultraviolet monitoring is required, a high pressure d.c. arc is necessary, e.g., a xenon arc lamp rated at 375 w. and 25 amp.

Apart from fluctuations in power supply a principal source of inconstancy of the above sources over short time intervals is caused by refractive index changes in the air flowing past the lamp. The envelope of the lamp runs very hot and both the above types are air cooled. The turbulent currents of cooling air may cause fluctuations of several per cent in the monitoring beam intensity. A flow of cooling air over the lamp envelope is essential, but fluctuations in the monitoring beam may be reduced by enclosing this beam in a glass or quartz tube the end of which fits closely to the lamp envelope (Fig. 5).

5. Monochromator and Detector

After passing through the reaction vessel the monitoring beam passes to a monochromator and then on to a photomultiplier cell. The signal from the photomultiplier passes through a cathode follower and amplifier to the oscilloscope. A suitable monochromator is the Hilger D247, although an instrument of smaller aperture would be no disadvantage. The light from the monitoring source is made parallel by means of a lens approximately 10 mm. in aperture and of 12 cm. focal length. A second similar lens condenses the parallel beam onto the entrance slit of the monochromator. Between the lenses and the faces of the reaction vessel the light beam is further collimated by means of blackened tubes, 12 mm. in internal diameter, inside which are placed a number of washer-shaped baffles the inner holes of which are approximately 7 mm. in diameter. These two collimating tubes should be at least 20 cm. in length and are an important part of the optical arrangement. They must ensure that the only light viewed by the detector is that which has passed along the axis of the reaction vessel and that no part of the wall of the reaction tube is directly visible at the slit of the monochromator. Without this precaution it will be found that the peak scattered light from the photolysis flash may be many times that from the monitoring beam and, since measurements cannot be made until the scattered light is nearly zero, the shortest time of observation for a given flash duration may be determined mainly by the intensity of scattered light.

The photomultiplier cell is fixed to the exit slit of the monochromator. Low dark current and high sensitivity are not essential requirements and suitable cells are the 931A or 27M1 for the visible and near ultraviolet regions and the 1P28 or 27M3 for wavelengths down to 2,300 A. Very im-

portant is the stability of the power supply which must be quite free from a.c. ripple and other fluctuations. A battery of dry cells satisfies these requirements but the long term drift is a disadvantage. Commercial 1,000 volt units giving less than 0.1% variation for 10% change in mains voltage are available, and if the full signal deflection does not exceed one C.R.T. screen diameter these are satisfactory. For higher sensitivities extra smoothing units must be incorporated.

The detector circuits are d.c. coupled so that calibration traces with zero and full light can readily be recorded and so that the question as to whether there is any permanent change, accompanied by return to a different zero position, can be continuously checked. The cathode follower forms part of the photomultiplier assembly which is connected to the monochromator. The output from the cathode follower passes to a d.c. amplifier

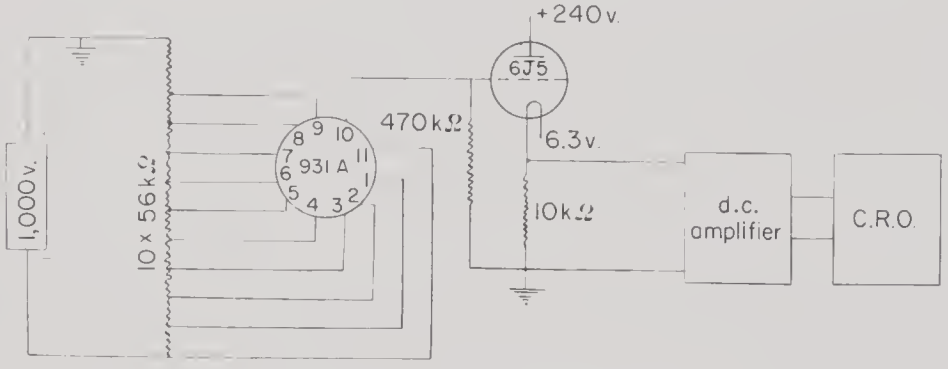

Fig. 8. Photomultiplier and cathode follower circuits.

which should have a band width of at least 200 kc./sec. and a gain sufficient to give a sensitivity on the oscilloscope of at least 1 cm./v. The photomultiplier is operated at considerably less than maximum voltage so that the d.c. coupled cathode follower is operated on a linear part of its characteristic and this is the reason for the subsequent stage of amplification. The electrical diagram of the detector and recording circuits is given in Figure 8.

The only requirement of the oscilloscope is that linear time bases, having adequate writing speeds with the camera employed, should be available at scanning speeds up to 10 μsec./cm. A calibration oscillator is also required, which should have been counted against a standard. The time calibration may be introduced as a separate oscillatory trace or as "bright up" marks on the record itself. Since single-sweep operation is used, the shutter of the recording camera is opened before the flash and no special synchronization is required. The oscilloscope time base is conveniently triggered by coupling the "sync" lead loosely to the spark gap connections.

6. Additional Apparatus for Flash Spectroscopy

For this purpose the monochromator, photoelectric detector, and continuous monitoring source are not required but the photolysis flash lamps, with their electrical units, and the reaction vessel as well as the rest of the optical arrangement are unchanged. The monitoring source is replaced by a "spectroflash" lamp filled with krypton at 10 cm. of Hg, the design of which is shown in Figure 9. It is mounted parallel to the slit of the spectrograph and the purpose of the capillary tube is to increase the current density and so to increase the intensity of the continuum relative to that of the emission lines. Although this results in the appearance of a few absorption lines of silicon, the spectrum is more suitable for spectroscopic

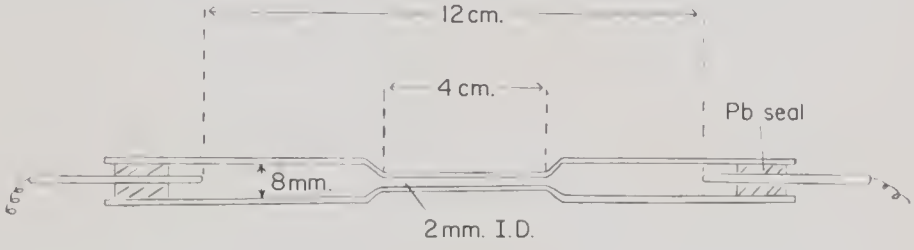

Fig. 9. Source for flash spectroscopy.

purposes than that of the wider tube flash lamp. The charging, power, and trigger circuits are identical with those of the photolysis flash lamps except that a smaller capacity condenser is used. A 4 μf. condenser, operated at 10 kv., is sufficient to produce an intense continuous record with standard (e.g., Selochrome) photographic plates at a dispersion of 10 A./mm. with a slit width of 0.05 mm. in a single flash with an effective duration of 20 μsec.

The spectrograph is a prism instrument of small or medium dispersion. This is adequate for all work in solution and for all gas phase work except that concerned with simple molecules having fine rotational structure, i.e., mainly diatomic and triatomic radicals. For such work a Littrow type instrument is useful but, for the highest sensitivity, the high resolution of a large grating instrument is necessary.

7. Trigger and Delay Circuits

The photolysis flash is fired manually as before, and is the master operation. Light from this flash is passed to a photocell and cathode follower, and then to a delay unit the last thyratron of which is in series with the primary of a pulse transformer and a condenser. When the thyratron fires, the high voltage pulse from the transformer secondary triggers the

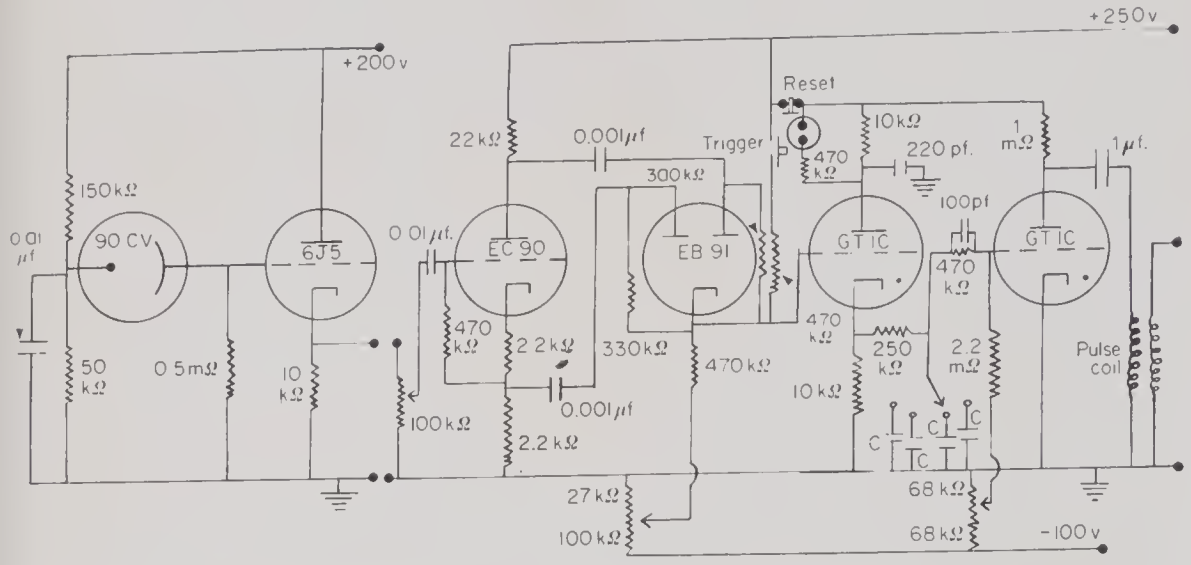

Fig 10. Photocell and delay units. Values of condensers C, in pf, are calculated from the formula $t \approx 0.03(C + 100)$ μsec.

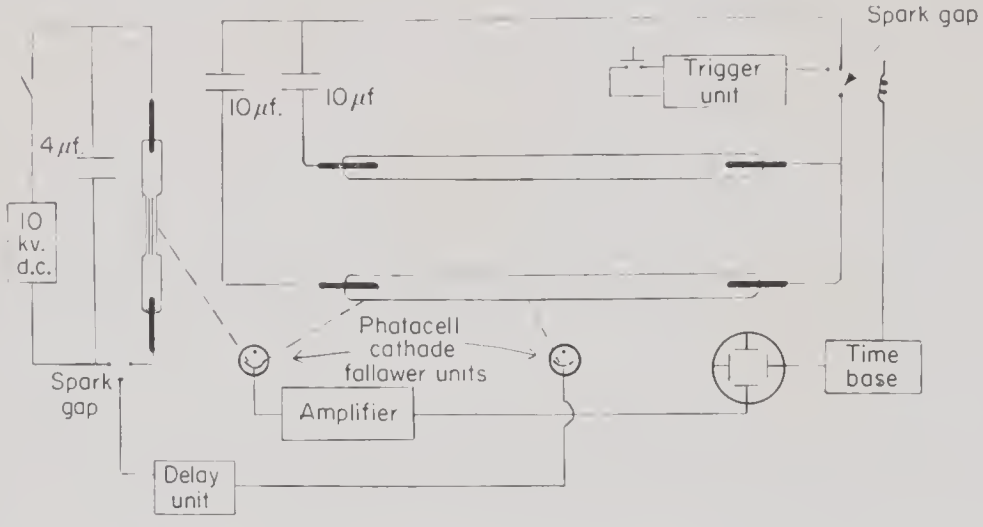

Fig. 11. Electrical arrangement for synchronized flash photolysis and flash spectroscopy.

spark gap which is in series with the spectroscopic flash lamp. The wiring diagram of the delay unit designed by Lintin and Wooding, and of the photocell circuit are shown in Figure 10 and the block diagram of the whole trigger arrangement is given in Figure 11. The components given in Figure 10 may be chosen to give any required CR values in the time range of μ seconds to seconds and the exact delay times should be checked by direct calibration. For accurate work the delay should be recorded for each experiment since it may vary somewhat with the condition of the lamps and other electrical components. For this purpose a second photocell, of the type used in the trigger circuits, is arranged so that approximately equal energies are received from the photolysis and spectroscopic flash lamps and the output is measured directly on an oscilloscope.

8. Summary of Characteristics

Typical operating characteristics of the standard apparatus are as follows:

Photolysis flash

Capacity	10 μF./lamp
Voltage (max.)	10 kv.
Energy/flash (max.)	1,000 j.
Rise time	1 μsec.
Flash duration to 50% peak	20 μsec.
Flash duration to 1% peak	250 μsec.
Quanta/flash in range 200–400 mμ	10^{20} quanta
Average intensity over 25 μsec. (200–400 mμ)	6.6 Einstein/sec.
Ratio scattered light/monitoring signal (unfiltered)	0.5 for 24 w. tungsten lamp at 5,000 A.
	0.1 for 375 w. Xe arc at 4,000 A.
Spectrum	Continuum plus line spectrum from quartz limit at 200 mμ to above 700 mμ

Spectroscopic flash

Capacity	4 μf.
Voltage	10 kv.
Energy/flash	200 j.

Spectral characteristics similar to photolysis flash but with higher continuum/line ratio.

IV. PRELIMINARY FLASH SPECTROGRAPHIC INVESTIGATION

It is useful to obtain some idea of the intensity of the photolysis flash by study of the decomposition of a standard actinometer solution. For this purpose uranyl oxalate or ferrioxalate solutions are suitable and it has been established in both cases that the quantum yield is unchanged at the high intensities of flash photolysis (6,41). Uranyl oxalate begins to absorb at 4,000 A. and its spectrum extends to the quartz absorption limit at about 2,000 A. With a solution 0.001M in oxalate, decompositions of the order of 6% are obtained with a flash energy of 1,000 j. This corresponds to an output, in the region of 2,000–4,000 A. of approximately 10^{20} quanta/flash. (Very rough estimates of quantum yield in a flash photolysis reaction have been determined in this way but an entirely different arrangement involving collimation of the photolysis source would be necessary for accurate quantum yield determinations.)

Unless a previous study of the system has been carried out it will usually be necessary to begin with a spectroscopic investigation using the flash photographic recording apparatus. The system to be investigated is introduced to the reaction vessel and, if liquid, it is thoroughly outgassed. The slit of the spectrograph is opened, the spectroflash power unit only is charged, and a record taken of the absorption spectrum of the reaction mixture before photolysis. The plate position is now changed, both power units are charged, the delay is set to approximately 20 μsec. and a second record taken. Next, the first experiment with the spectroflash alone is repeated. Now a series of spectra are recorded at different delay times and in a random order and finally the spectroflash alone is again recorded. It is advisable also to record the scattered light from the photoflash alone. Examples of flash photographic records are shown in Figures 14, 19, and 20.

The principal information derived from such records is as follows:

1. The Extent of Permanent Reaction

Comparison of the first record before photolysis, with those of the spectroflash alone after one photolysis flash, and also at the end of the experiment, may show a decrease in absorption of the reactant or additional absorption due to permanent products. If these are extensive the interpretation of the records is made more difficult but the random order in which the spectra were taken makes it possible to separate, at least qualitatively, changes which correlate with the delay time from those which correlate with the extent of photolysis, i.e.,with permanent changes in composition before flashing. For further, more accurate, work it will usually be necessary to reduce the amount of permanent change by reducing the intensity of the photolysis flash or by alteration of other conditions such as concentration. If these methods are not sufficient it will be necessary to resort to the more tedious procedure of replacing the reaction mixture after each flash and the investigation should be transferred to the photoelectric apparatus as soon as possible.

Fortunately, in practice, it is found that many reactions can be studied without causing appreciable permanent change in one flash. Many are "relaxation" systems, i.e., reactions in which the dark reaction following photolysis restores the original reactants. In others it is often the case that the extinction coefficients of the intermediates are so high that they may be readily studied when their concentration is very small compared with that of the reactants so that the extent of permanent reaction has no significant effect on composition.

2. The Spectra of Transient Intermediates

Absorption spectra which are not present in the records before or after the experiment, but only at relatively short delay times, must be attributed to transient changes in composition. Similarly, if the absorption by the parent substance is less at short delay times than before or after the experiment, it follows that part of the reactant has been converted temporarily into some other substance.

The identification of the intermediates responsible for any new absorption spectra often calls for much ingenuity if the spectra are not already known. Very rapid progress in the recording and assignment of free radical absorption spectra is being made at the present time and, as the number of known spectra increases, the problem of identifying the unknown becomes progressively easier.

In an isothermal system (see later) the only common transient intermediates are free radicals and excited states. Some useful sources of information on spectra of these intermediates are mentioned in the following sections.

A. GAS PHASE

1. "The identification of molecular spectra," by Pearse and Gaydon. (43).

This forms a very useful starting point and lists simple molecular spectra in order of wavelength and in alphabetical order of species.

2. References to simple polyatomic radicals occurring during flash photolysis. HS_2 (45), NH_2 (61), CHO (18), HNO (11), NCO (20), C_3 (37,10), CH_3 (19).

3. Aromatic radicals such as benzyl, anilino, phenoxy, etc., in the gas phase (50).

4. Triplet states of aromatic molecules in the gas phase (51).

5. Vibrationally excited gaseous molecules (33).

B. LIQUID PHASE

Far less information is available concerning condensed phases, and until quite recently the only spectra known were of substances which could be obtained in thermodynamic equilibria such as triphenylmethyl. A number of unstable aromatic radicals and excited states have recently been reported, both by flash spectroscopic methods and by radical stabilisation at low temperatures.

1. Aromatic radicals, in solution (53).

2. Aromatic radicals, mainly derivatives of benzyl, anilino and phenoxy, in rigid solvents (35,54).
3. Semiquinone radicals and radical ions (4).
4. Ketyl radicals and radical ions (59).
5. Triplet states of organic molecules in solution (52,55).

In using data obtained under different conditions it should be remembered that absorption spectra usually shift to longer wavelengths in passing from the gas phase to solution and from fluid to rigid solvents.

If the spectrum is unknown, assignments must be made on the basis of what is already known of the reaction and of the spectra of related substances and also on information derived by subsequent kinetic studies of the behavior of the transient spectrum under various conditions. Only with simple molecules in the gas phase is it possible to assign an unknown spectrum purely on spectroscopic grounds.

3. Lifetime and Kinetics of Transient Intermediates

In most cases these are more conveniently studied by means of the photoelectric technique but a preliminary photographic investigation is often valuable. If more than one intermediate is present, or if the intermediate has a fine structure, as have most simple radicals in the gas phase, the flash photographic method becomes almost essential. Although plate densitometry measurements are far less accurate than direct spectrophotometry, density measurements can, with care, be made accurate enough to distinguish between pure second and first order kinetics and to give rate constants to an accuracy of about 20%. The most complete investigation carried out in this way is that of the ClO radical and the photochemical reaction between chlorine and oxygen (46,47,24).

V. MEASUREMENT OF ABSORPTION SPECTRA

One of the most difficult problems associated with the spectroscopic investigation of transient substances is that neither their concentration nor their absolute extinction coefficients are known so that, if the reaction order in the intermediate is higher than first, absolute rate constants are also unobtainable. Extinction curves of the spectrum on a relative basis are readily obtained by plate photometry and from these, or from photoelectric measurements, the kinetics of the reaction can be investigated. Once this has been done it is often possible to determine the absolute concentration of the intermediate under some particular conditions and this allows all the data, including extinction coefficients and rate constants, to be put into absolute terms.

Assuming the validity of Beer's law, which is discussed later, we have

$$\log I_0/I_t = \epsilon_\lambda c_t l$$

where I_0 is the light intensity falling on the photographic plate with no absorbing species in the reaction vessel, I_t is the intensity at the same wavelength and at time t when absorbing substance is present, ϵ_λ is its molar decadic extinction coefficient at this wavelength, c_t its concentration in moles per liter and l is the length of the reaction vessel.

Now the total light of wavelength λ falling on the photographic plate during a single flash from the spectroflash is $\int_0^\infty I_\lambda dt$ and this must be related to the density D of the plate image and to the extinction of the solution. This may be done in two ways:

1. Use of Constant γ Plates

For two exposures, E_0 and E_t,

$$E_0/E_t = \int_0^\infty I_0 dt / \int_0^\infty I_t dt$$

and since the ratio of the transmitted light through two different solutions is independent of incident intensity

$$E_0/E_t = I_0/I_t$$

at all times during the exposure provided these are short compared with the reaction time. The density of a photographic image D is approximately related to exposure by the expression

$$D = \gamma \log E + \text{const}$$

where γ is a constant.

Then

$$D_0 - D_t = \gamma \log E_0/E_t = \gamma \log I_0/I_t$$

If I_0 and I_t are the light intensities transmitted by the solution before photolysis and at time t after photolysis, then $\log I_0/I_t$ is the optical density of the transient at time t and

$$D_0 - D_t = \gamma \epsilon_\lambda c_t l$$

where c_t is the concentration of transient at time t.

The densities D, of the photographic image are related to microdensitometer readings, R, as follows:

$$D_0 = \log R_p/R_0 \text{ and } D_t = \log R_p/R_t$$

where R_p, R_0, and R_t are the microdensitometer readings on the unexposed

plate, the spectrum before photolysis, and the spectrum at time t respectively.

Then

$$D_0 - D_t = \log R_t/R_0 = \gamma \epsilon_\lambda c_t l$$

so that the product $\epsilon_\lambda c_t$ is determined from the two densitometer readings R_t and R_0 if γ is known.

2. Plate Calibration by Standard Density Wedge

A step wedge, having about seven narrow steps of varying density in the range required (e.g., 0.2–1.4) and of total height equal to the slit height, is interposed in the light beam at the spectrographic slit and an exposure made of the spectroflash alone. The wedge is then removed and other records made in the usual way. The plate is developed with all possible precautions to ensure even development, and positions near the edge of the plate, where sensitivity is most likely to vary, are avoided. Microdensitometer readings are taken, at the required wavelength, of all step density wedge records and of each record of the transient. A graph is constructed of microdensitometer reading versus wedge density and from this the densities of the reaction mixture are read off directly from the respective microdensitometer readings. These densities are equal to $\epsilon_\lambda c_t l$ for the transient at the wavelength studied.

This method is more reliable than method 1, but not necessarily more accurate and is certainly more time consuming since each plate must be separately calibrated and measured. The usual procedure is to check the constant γ method, under standard processing conditions by means of the density wedge, once or twice for each batch of plates, when it will usually be found sufficiently reliable to dispense with the density calibration for the majority of runs. If a complete record of all wavelengths is required it will be necessary to carry out the check calibration at a number of wavelengths through the required range.

We now have optical densities of the transient spectrum over a range of wavelengths from which values of $\epsilon_\lambda c_t$ are obtained since the cell length is known. A plot of $\epsilon_\lambda c_t$ versus λ gives the true relative extinction curve of the transient spectrum since, for any single exposure, c_t is constant. To convert this to absolute extinction coefficients c_t must be determined.

VI. DETERMINATION OF ABSOLUTE CONCENTRATIONS AND EXTINCTION COEFFICIENTS

The absolute concentration of a transient species whose extinction coefficient is unknown may, in principle be determined by one of two meth-

ods: (*a*) analysis, by conventional methods, of the concentration of products produced by the flash; (*b*) spectroscopic determination of the concentration of all other intermediates at the same time as the absorption of the transient species is determined. Both methods imply a complete knowledge of the reaction mechanism; it is therefore usually necessary to carry out a rather complete investigation of the kinetics in relative terms before the final determination of absolute concentrations, and each system presents its own problems.

The simplest situation occurs where the parent molecule and the transient are the principle species present. This case is not uncommon and, if the proportion of reactant converted is measurable, the determination of absolute concentrations is straightforward once the kinetic scheme has been established. One simple and important example of this situation is the conversion of a molecule into a metastable, e.g., a triplet, state. Quite often only the ground state and the triplet state of the molecule are present and there is no overall chemical change. Depletion of the ground state then gives a direct measure of the concentration in the triplet state and the method has been used to determine absolute extinction coefficients of the triplet state absorption spectra of a number of aromatic hydrocarbons (see Fig. 15). The maximum conversion to the triplet state, immediately after the flash, was 10% or greater in these determinations.

A second example, this time in the gas phase, is that of the extinction coefficient of ClO. In the main part of the work, which was concerned with the photochemical reaction between chlorine and oxygen the percentage depletion of chlorine was very small and could not be determined, although the kinetics were fully elucidated in terms of extinction coefficients (46). The absolute extinction coefficients were then determined from a system which, although less interesting in itself, made possible the direct determination of the extinction coefficient of ClO. This was the photolysis of ClO_2, which is converted almost completely to ClO in a single flash. Since the decay of ClO is relatively slow, the only chlorine containing species immediately after the flash are ClO_2 and ClO and the concentration of ClO is therefore directly determined from the depletion in ClO_2 concentration. This enabled all rate constants to be expressed in absolute terms (24).

A difficulty arises in the determination of the extinction coefficient of a transient, whose spectrum is unknown, by measurement of the depletion of the parent molecule. Suppose that only the reactant and the transient whose extinction coefficient is to be determined are present. Then, at a given wavelength and time, the optical density of the reaction mixture is given by

$$d = \epsilon_r c_r l + \epsilon_t c_t l$$

where r and t refer to reactant and transient respectively. If these are the only species present, and c_0 is the initial concentration of reactant

$$d = \epsilon_r c_r l + \epsilon_t (c_0 - c_r) l$$

in which there are two unknown terms, ϵ_t and c_r. In spite of this both may usually be evaluated by using one of the following methods:

(*A*) At some wavelength where $\epsilon_r \neq 0$ a spectrum is obtained where $d = 0$. Then $c_r = 0$ and at all wavelengths $d = \epsilon_t c_0 l$. If d is not equal to zero but is small, the inequality $c_t < c_0$ enables a useful lower limiting value of ϵ_t to be determined.

(*B*) Over a range of wavelengths ϵ_r changes very considerably, probably showing complex band structure, but ϵ_r is proportional to d over this range. It follows that ϵ_t is proportional to ϵ_r over the whole range or that ϵ_t is zero. The former condition, implying identical spectra of reactant and transient, is usually sufficiently improbable to be ignored and the absorption in this region can then be assigned to the reactant from which its concentration, and consequently that of the transient can be deduced. From the optical densities of absorption by the transient at other wavelengths its absolute extinction coefficients are now determinable.

A second case which allows absolute concentrations to be determined occurs when an intermediate, whose extinction coefficient is known, converts quantitatively into one whose extinction coefficient is unknown. This situation arises mainly when the form of the intermediate first produced is not the equilibrium one under the ambient conditions. A common and important example is that of acid-base equilibria. It happens, not infrequently, that the unprotonated form of a free radical is sufficiently stable to be prepared in detectable equilibrium concentrations. If, then, the acid radical is produced photochemically under such conditions of hydrogen-ion concentration that it rapidly reverts to the radical ion, the extinction coefficient of the neutral radical may be derived from that of the radical ion. There are already several examples of this situation and one, that of the semiquinone radicals and radical ions, is discussed later.

Methods based on analysis of the final products have not yet been used for the determination of absolute concentrations of intermediates. They are, in principle, as powerful as the methods discussed above but either a considerable extent of reaction or sensitive methods of analysis are necessary. The increasing availability of the latter will probably emphasize the importance of this method.

VII. KINETIC INVESTIGATIONS BY THE SPECTROPHOTOMETRIC METHOD

The advantages of the spectrophotometric method for detailed kinetic studies have already been indicated. Even before the transient spectra have been assigned it may be necessary to resort to kinetic spectrophotometry in order that the mechanism of the change can be elucidated as a preliminary to the assignment of the spectra. Once the principal kinetic features of the reaction are known, greater accuracy is always available if the measurements are repeated with spectrophotometric apparatus.

Preliminary studies by the method described will have determined the wavelengths of interest and positions are chosen for spectrophotometric study which are as far as possible separated from the absorption of other species whose concentration is varying. If there are n species, with overlapping spectra, whose concentrations vary, then it will be necessary to investigate the kinetics at n wavelengths. This will result in n simultaneous equations which can be solved to give the concentration of each species at all times once the individual extinction coefficients are known.

The procedure for a kinetic investigation is as follows. The required wavelength is set on the monochromator and the slit width is chosen to be the maximum one available which still ensures the validity of Beer's law (see later). The monitoring source and detector are switched on and allowed to attain steady conditions. The photographic record on each frame includes three separate traces which are illustrated in Figure 12. First the scan is triggered with the slit closed (trace *a*), second with slit open and monitoring light on (trace *b*) and third the photolysis flash is triggered and the absorption by the transient recorded (trace *c*). If very short times, comparable with the duration of the flash, are used, it is also necessary to record, on the same trace, the scattered light from the photolysis flash with the monitoring light off (trace *d*). Typical traces of this kind are shown in Figures 16, 21, 22, and 24.

If the transient absorbs only a small fraction of the light it will be necessary to amplify the oscilloscope signal for greater accuracy in which case the "light off" trace will not appear on the screen. In this case the "light off" trace is recorded by reducing the gain of the detector circuits by a constant factor. This may be achieved by a calibrated attenuator, often incorporated in the oscilloscope itself, or by an external voltage divider circuit.

The oscillograph traces are recorded on 35 mm. film and for measurement these are projected onto graph paper and traced or they may be enlarged photographically, a graph paper grid being superposed on the record during enlargement. If time traces are obtained from separate traces

care must be taken that the optical arrangement of the enlarger is unchanged. The data required from these traces are optical densities of the reaction vessel, referred to the unflashed reaction mixture as zero, as a function of time.

If oscilloscope response is proportional to light intensity

$$I_0 = k(\text{"light on" deflection} - \text{"light off" deflection}) = kx_0$$
$$I = k(\text{"transient deflection"} - \text{"light off" deflection}) = kx$$

where k is a constant which depends on detector sensitivity and which need not be evaluated. Since $\log I_0/I = \log x_0/x = \epsilon_\lambda c_t l$, relative or absolute concentrations can be determined as a function of time, and the order and rate of the transient reactions determined.

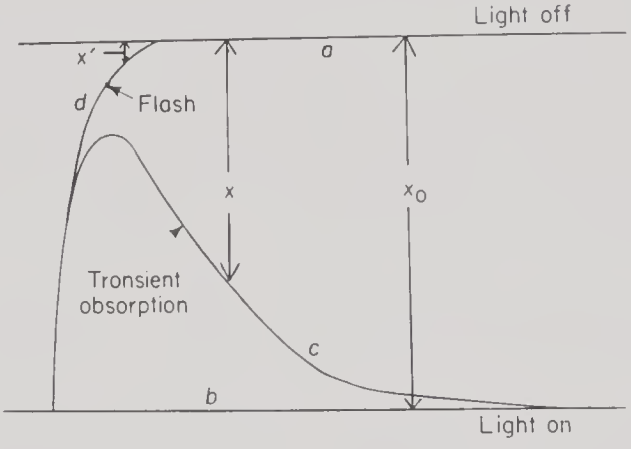

Fig. 12. Record of oscillograph traces. For explanation see text.

If the duration of the flash is comparable with the lifetime of the transient the values of x should be corrected by subtracting x', the deflection caused by scattered light from the flash. This method is only justified when the integrated light from the flash in the region studied is negligible compared with total integrated intensity.

The interpretation of kinetic data obtained in this way is carried out in the conventional manner and the principles and methods of kinetic analysis have been fully treated in Volume III, Part I. There are, however, several conditions which must be established before the concentration measurements obtained from decay curves following flash photolysis can be considered reliable.

The determination of both relative and absolute concentrations of intermediates by the method outlined above depends on the following three conditions being satisfied; (*a*) the oscillograph deflection is proportional to light intensity; (*b*) the response time of detector circuits is less than the shortest reaction times; (*c*) Beer's law is obeyed.

1. Relation between Intensity and Oscillograph Deflection

The detecting system includes the photomultipler, cathode follower, amplifier, and oscilloscope, and the most satisfactory way of establishing its linearity of static response is by direct calibration of the overall system. This is readily carried out by the use of a number of filters or density wedges, the optical densities of which are measured directly on a spectrophotometer at the wavelengths required. Any type of filter may be employed for the purpose and, if these are not available, solutions of various concentrations which absorb in the required region may be introduced directly into the reaction vessel.

If the response is not linear a calibration curve must be constructed but it will facilitate further work if the causes of nonlinearity are investigated. One of the most likely causes is the photomultiplier, which is normally operated at rather low voltages and consequently low sensitivity, particularly with the more intense monitoring sources. Better linearity may be achieved by strapping the last few stages together, and with this modification it will usually be found that overall response is linear within the accuracy of measurement of the deflections.

2. Response Time of the Detector Circuits

The linearity tested in the last section is purely static and it must also be established that response is linear during the short times employed in recording the transient. The circuit described should produce no distortion of transients which decay to $1/e$ or less of their original value in times of 10 μsec. or more but, since this value is dependent on connecting leads and impedances introduced in the construction of the components, it should always be checked. Again the simplest and most reliable method of checking response time is by direct study of the complete equipment. The scattered light from the flash itself is usually a sufficient test since the decay time of the flash is always less than that of the shortest transient which can be usefully investigated.

3. Validity of Beer's Law

All spectrophotometric studies must utilise some relation between optical density and the product ecl, and since the relation cannot usually be directly tested on the spectrum of a transient product it is necessary to assume the validity of Beer's law:

$$\text{Optical density} \equiv \log I_0/I = \epsilon_\lambda cl$$

For a single substance this relationship is always exactly true at any single wavelength. Deviations may arise for either of the following reasons:

1. Absorption at the single wavelength investigated results from more than one species. This effect is well known in conventional spectrophotometry, particularly as a result of association, which may result in absorption by the monomer at low concentrations and dimer or higher polymers at higher concentrations. It is rarely of importance in the study of transients, which are nearly always at sufficiently low concentrations to ensure that no association takes place and for which association would, in any case, almost invariably result in deactivation or reaction. Changes of this kind form part of the kinetic study and are not deviations from Beer's law.

2. The wavelength interval studied is finite and the extinction coefficient changes significantly over this interval.

This may cause very serious apparent deviations from Beer's law. Suppose the light entering the detector is composed of two wavelength intervals $\delta\lambda_1$ and $\delta\lambda_2$ and that the corresponding extinction coefficients at these wavelengths are ϵ_1 and ϵ_2. Then, if the intervals are small, Beer's law will be valid for each and

$$\log I_{0(1)}/I_{(1)} = \epsilon_1 cl$$

and

$$\log I_{0(2)}/I_{(2)} = \epsilon_2 cl$$

Suppose the light intensity from the source, in interval $\delta\lambda_2$ is x times that in interval $\delta\lambda_1$. Then

$$I_{0(2)} \equiv xI_{0(1)}$$

The observed light is the sum of that from the two wavelengths and the apparent optical density d_{app} is given by

$$d_{\text{app}} = \log [I_{0(1)}(1 + x)/(I_{(1)} + I_{(2)})]$$

Substituting the above equations in the expression for optical density we find

$$d_{\text{app}} = \log [(1 + x)/\exp(-\epsilon_1 cl) + x \exp(-\epsilon_2 cl)]$$

Beer's law is only valid if this term is proportional to concentration. This is true if either

1. x is zero or very large. This corresponds to the use of monochromatic light.

or

2. $\epsilon_1 = \epsilon_2$

It will be noted that, provided the extinction coefficient is constant, there is no necessity for uniform intensity of the monitoring source over the wavelength interval investigated.

Spectra having fine rotational structure are quite unsuitable for measurements of relative concentration unless some independent method of calibration can be used. One method which has proved useful is the two path method which uses the principle that, when optical densities in two reaction vessels of different length are equal for the same wavelength and absorbing substance then

$$l_1 c_1 = l_2 c_2$$

where the figures 1 and 2 now refer to the two path lengths. Since the lengths are known, the ratio of concentrations can be determined.

Usually in the gas phase, and quite generally in solution, the spectrum of the intermediate has a constancy of extinction coefficient over a sufficient wavelength interval for the application of Beer's law to be valid. In this case a suitably broad band is chosen and the validity of the law is established in the following way: the narrowest practicable slit width is used and the absorption of the transient is recorded at different wavelengths through the band. If identical results are obtained over a relatively wide interval it may safely be assumed that Beer's law is valid. The range over which the absorption is constant indicates the maximum slit-width which it is permissable to use and a further check may be obtained by establishing that the form of the decay curve is unchanged as the slit width is varied.

If the species being studied is stable under certain conditions a direct calibration can be carried out and absolute concentration measurements can then be made even when the departure from Beer's law is considerable.

VIII. THERMAL EFFECTS FOLLOWING FLASH PHOTOLYSIS

The production of a high concentration of reactive intermediates in a short interval of time is followed by the liberation of a considerable heat of reaction. Furthermore, the quantum yield is rarely unity and the excess light energy will usually be liberated as heat. Except in gases at very low pressures, or when the reaction time is several milliseconds or more, the change proceeds nearly adiabatically and the heat liberated results in a rise in temperature of the reaction mixture. This effect may be utilised for the thermal initiation of reaction but it often presents a serious difficulty which is associated with all studies of fast reactions. It is, fortunately, never important in solution reactions when spectroscopic methods are used and can usually be made insignificant in gas reactions as well.

Some idea of the magnitude of the thermal effect is indicated by the following consideration. Suppose that 1% of the molecules in a gas mix-

ture absorb radiation of wavelength 3,000 A. and that this energy is liberated as heat in a time which is short compared with the time of thermal conduction to the wall of the vessel. Assuming a specific heat of the gas of 5 cal. per mole, the temperature rise will be 190°C. Much higher proportions of the molecules may absorb light and much higher temperature rises are common in flash photolysis reactions in the gas phase.

The temperature rise may disturb the reaction and the kinetic investigation in a number of ways, e.g., by affecting the rates of reaction and by changing the spectral distribution and extinction coefficients. The temperature rise has, however, the even more important though less obvious effect of creating an uneven concentration distribution in the reaction cell. Suppose a gas, initially at 300°K. is suddenly brought to $(x + 300)$°K. by flash heating, while the reaction vessel remains at the original temperature. Immediately, the gas adjacent to the walls of the vessel will begin to cool and, in order to equalize the pressure throughout the vessel, gas will flow from the hot interior towards the walls. This process will continue until cooling reaches the center of the vessel, after which the gas flow will be reversed. At the peak, just before the gas at the center of the vessel begins to cool, the concentration along the axis of a cylindrical reaction vessel may be very significantly less than the average concentration. Since the monitoring light beam is collimated so as to pass down the axis of the vessel the measured concentration of all species will be lower than the true one and the apparent variation with time may be very different from that which would be observed in a homogeneous reacting system. In extreme cases the record may indicate extensive dissociation of the parent substance when no chemical change has taken place and the only effect recorded is that caused by the thermal concentration gradient.

Although approximate calculations of the type indicated above should always be carried out for gaseous systems in order to estimate whether thermal effects are significant, and more detailed calculations have been made (8,5), it is rarely feasible to treat the effect quantitatively with sufficient accuracy since concentration, specific heat, coefficient of thermal conductivity, extinction coefficients, and reaction rate are functions of temperature. It is therefore necessary to reduce thermal effects to insignificant proportions. In practice this means that if an accuracy of 1% is to be attained in the measurement of concentration the temperature rise, if the original temperature is near 20°C., should be less than 5°C. If the concentration of an intermediate is small and is estimated by difference from the decrease in concentration of the parent molecule, a higher absolute accuracy of concentration measurement is required and the temperature rise must be correspondingly less (compare, for example, the recombination of atoms (8).

The only method by which the temperature rise can be reduced, assuming that the concentration of intermediate, and hence the extent of photolysis, is inviolate, is by the addition of inert gas in order to increase the thermal capacity of the system. This is a simple and completely effective expedient which also has the advantage of reducing other sources of inhomogeneity caused by diffusion to and reaction at the walls of the vessel.

1. Utilization of the Thermal Effect

There are few methods by which the temperature of a volume of gas may be raised homogeneously in a short interval of time, the main ones being by adiabatic compression and by shock waves. The very considerable rapid temperature rise produced by flash photolysis is therefore useful in the study of thermally initiated rapid reactions. Applications to the study of relaxation processes and energy transfer should prove valuable, but at the present time the main application has been to the study of explosive combustion.

It is now known that the reactions which occur during combustion of a fuel such as a hydrocarbon, in a flame or explosion, are very different from those which take place during slow combustion occurring at a measurable rate at lower temperatures. Since an explosive combustion process may be complete in a time of one millisecond or less it is clear that, if it is to be studied as a homogeneous reaction, it must be initiated homogeneously throughout the reaction mixture in a time which is much shorter than this. If the combustible mixture absorbs light, the flash will result in the liberation of heat, and generally also of free radicals and, if the irradiation is uniform and the absorption by the gas is not too high, the effect will be homogeneous throughout the reaction mixture. The explosion chains will then begin uniformally at a very large number of points in the vessel and the effects observed will be rate determined by the chemical reactions rather than by diffusion and flame propagation. If the reaction mixture does not itself absorb light it is necessary to add a small proportion of some other gas to initiate the explosion.

The method has been used to study the explosive combustion of hydrogen–oxygen (36) and hydrocarbon–oxygen (37) mixtures, the photochemical initiator being nitrogen dioxide which is itself completely destroyed during the flash. The homogeneity of reaction and the long path length (1 meter) resulted in the observation, for the first time in absorption, of the spectra of several radicals which had long been known in the emission spectra of flames, e.g., C_2, CH, and NH. The kinetics of such systems are intrinsically very complex but direct studies of this kind allow useful conclusions to be reached concerning the order of appearance of radicals and the times of

reaction. More detailed studies, at high dispersion, should give information about the temperature and in particular about lack of thermal equilibrium. The method has already been useful in providing a partial elucidation of the mechanism of carbon formation (22,48).

IX. OTHER FLASH PHOTOLYSIS ARRANGEMENTS

It is not possible, in the compass of this chapter, to discuss the numerous variations on the basic apparatus which has been described. It may be useful, however, to indicate some of the principal modifications which have been described in the literature.

1. Higher Flash Energies

The original photolysis apparatus employed an energy of 10,000 j. and a single lamp, but the author's experience has been that lower energies are more frequently required, partly because of the requirement for shorter flash duration and partly because a very high degree of permanent change and the possibility of two quantum processes are always to be avoided. Equipment employing very high energies per flash, without proportionately long flash durations, the most recent of which employs an energy of $^1/_2$ megajoule, has been described by Claesson and his collaborators (9).

If higher energies than those available in the standard apparatus described above are required they may be attained (*a*) by increasing the energy per lamp, or (*b*) by increasing the number of lamps. The energy per lamp is best increased by increasing the voltage, but at 20 kv. and 10 μf. (2,000 j.) per lamp the discharge becomes violent enough to decompose the silica tube and frequent refilling of the lamps is necessary. There is no limit, apart from geometrical and economic ones, to the number of lamps which can be used.

2. Lower Flash Duration

With lamps of the length and energy described the flash duration may be reduced by about a factor of two by the use of special low in inductance condensers and special attention to reduction of the impedence of circuits. Further reduction in duration is only possible by reduction of capacity or of tube length. Linschitz and his colleagues (23) have used an arrangement employing the commercial "arditron lamp" which is 4 cm. between electrodes and has a half peak duration of 2 μsec. Four lamps were employed in parallel and, although no hold-off gap was employed and each lamp was

triggered separately, firing was simultaneous to within 0.2 μsec. These lamps have a maximum rating of 36 j. per flash and, having a glass envelope, are limited to the spectral region above 3,500 A. They also have a relatively long "tail" which makes their effective flash duration much longer than half peak duration.

If very small energies and electrode separations are used flash durations of the order of millimicroseconds may be attained (30,58). Energies available in this range (microjoules) are much too low to produce a measurable photochemical effect but they have been used in the related field of fluorescence lifetime determinations (60).

3. Other Modifications

Strong and Willard have described an arrangement employing four flash lamps with common gas connection but separate electrodes (63). Herzberg and Ramsay have used high dispersion grating spectrographs and have applied the multiple pass method of White to obtain increased absorption (65). Herzberg has recorded spectra in the vacuum ultraviolet region of radicals produced by flash photolysis in the quartz ultraviolet (19,64). Nelson and Ramsay have attempted to use sapphire flash lamps in order to extend the spectrum of the flash into the vacuum ultraviolet (34). Porter and Wooding have used quartz packed flash tubes to reduce the intensity of the "tail" of the flash (56). McClure and Hanst (32) and Morantz and Porter (4) have used vessels which allow solutions to be flashed at liquid nitrogen temperatures. Bridge and Porter have recorded transients simultaneously at two wavelengths by use of a multiple photocell attachment to the plate holder of a spectrograph (4). Mechanical trigger and shutter mechanisms which allow the scattered light from the photolysis flash to be completely eliminated have been described (44). Filters have been used, both to isolate regions of the photolysis flash spectrum, and to replace the monochromator in the monitoring beam (8). Spark gaps have been replaced by hydrogen thyratrons in the main flash circuit (17). Emission spectra have been used to supplement the information derived from absorption spectra following flash initiated reactions (38).

X. EXAMPLES OF KINETIC STUDIES BY FLASH PHOTOLYSIS

Some of the systems which have been studied kinetically by flash photolysis methods are as follows:

Gas reactions	Reference
1. Chlorine–oxygen and reactions of ClO.	46,47
2. Chlorine dioxide decomposition.	24,12
3. Hydrogen–oxygen explosions.	36
4. Hydrocarbon–oxygen explosions.	37
5. Hydrogen sulfide–oxygen explosions.	39
6. Effect of lead tetraethyl on hydrocarbon–oxygen explosions.	13
7. Formation and deactivation of vibrationally excited oxygen.	33
8. Recombination of iodine atoms.	7,8,31,62,63,5
9. Recombination of bromine atoms.	63
10. Aromatic radicals, e.g., benzyl.	51
11. Triplet states of naphthalene, anthracene etc.	50
12. Photochemistry of aliphatic aldehydes and ketones.	21,22

Solution reactions	
1. Triplet states of aromatic molecules.	49,52,55
2. Kinetics of triplet state quenching.	57,28
3. Photochemistry of chlorophyl.	25,26,1,27,23
4. Aromatic hydrocarbon radicals, e.g., benzyl.	53
5. Haemoglobin–ligand reactions.	14,15
6. Semiquinone radicals and radical ions.	4
7. The methylene blue–ferrous ion system.	42
8. The radical-ions I_2^-, Br_2^-, and Cl_2^-.	17
9. Ketyl radicals.	59
10. Ovalbumin and its constituents.	16

In addition there has been extensive work on free radical spectra obtained by flash photolysis methods, particularly on the simple radicals such as NH_2, CHO, and CH_3, but no kinetic studies of these have been reported. Much of the kinetic work on the systems mentioned above is very preliminary and rapid progress is to be expected in the elucidation of these and similar reactions by flash techniques during the next few years.

As examples of the technique two studies of organic chemical systems in solution will be described, each of which involves the use of both flash photographic and spectrophotometric recording.

XI. THE TRIPLET STATES OF ORGANIC MOLECULES IN SOLUTION

The discovery of the triplet states of organic molecules by phosphorescence studies in rigid media, and early work on their emission spectra and radiative behavior has been fully reviewed elsewhere. These triplet or "biradical" states play a very important part in photochemical reactions and probably determine the course of certain thermal reactions as well.

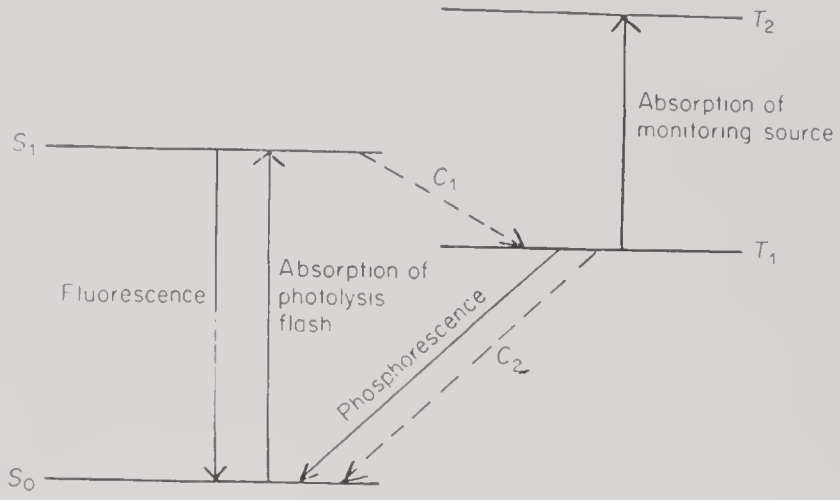

Fig. 13. Transitions between singlet and triplet states.

The phenomenon of phosphorescence which has been mainly used for their characterization is, however, almost exclusively associated with solids and very viscous liquids and therefore cannot be used to study the chemical reactivity and properties of triplet states in ordinary solutions or in the gas phase.

Since no phosphorescence is observed in solution it must be concluded either that the triplet state is not formed under these conditions or that it is very rapidly deactivated in a time which is short compared with the radiative lifetimes which usually lie in the range 10^{-3}–10 seconds. It was shown by Porter and Windsor (49) that triplet states are as readily formed in solution as in solids and rigid media, and that their lifetimes under these conditions, although shorter than the radiative lifetime, are usually not shorter than 10^{-5} second and therefore lie within the resolving time of flash photolysis techniques.

The principle of the study of triplet state kinetics by flash photolysis is as follows. Owing to the weakness of singlet-triplet absorption spectra, the triplet state cannot be significantly populated by direct optical excitation from the ground state. The flash therefore elevates the molecule in the first place to an upper singlet state from which there is, in a large number of molecules, a high probability of radiationless conversion to the lowest triplet state by process c_1 of Figure 13. Before the molecule reverts to the ground state the triplet state is observed by means of the second spectroscopic flash which raises the molecule to an upper triplet state, T_2, and records a triplet-triplet absorption spectrum which is not forbidden by spin conservation rules and is usually at least as intense as the first singlet-singlet transition. One of the first records of this type to be obtained was the triplet state of anthracene in hexane solution and is shown in Figure 14. The spectrum taken before the photolysis flash shows only the singlet

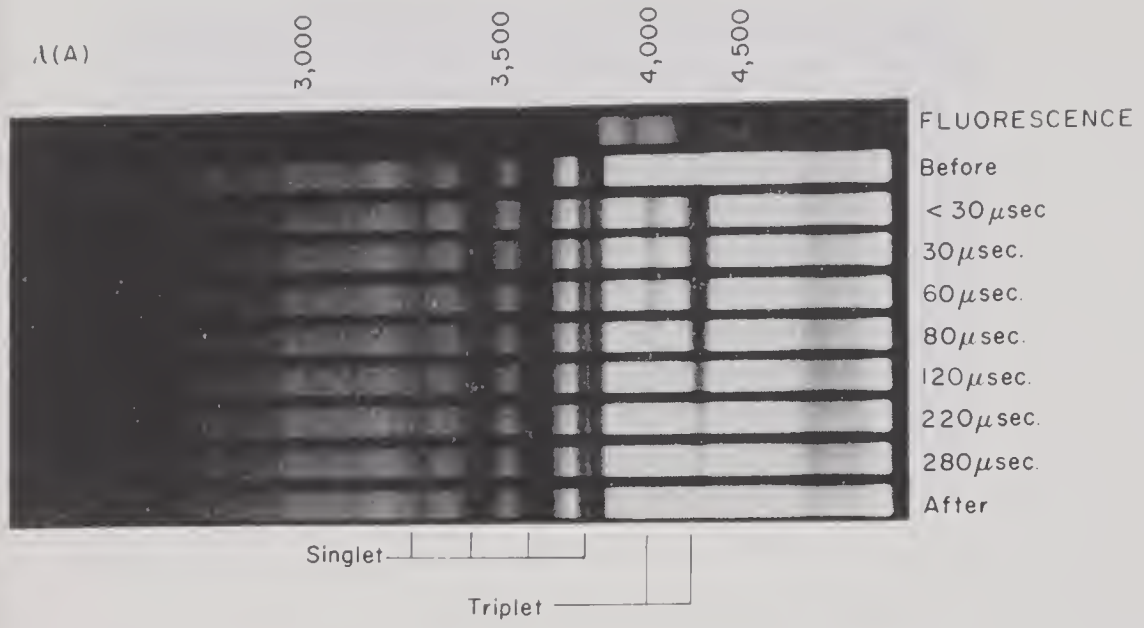

Fig. 14. Flash photolysis of anthracene in hexane solution.

absorption spectrum of anthracene in hexane at a concentration of $10^{-4}M$, and is recorded with the spectroflash alone. Above this is a record obtained with the photolysis flash alone showing only the fluorescence of the anthracene solution. Subsequent records were obtained with both flashes at varying time delays and show that immediately after the flash the concentration of anthracene in the ground state is reduced (by about 20% in this example) and that a new band system appears at longer wavelengths as well as further continuous absorption at shorter wavelengths. These new absorption spectra decay with a half-life of the order of 100 μsec. and the final record, taken with the spectroflash alone at the end of the experiment,

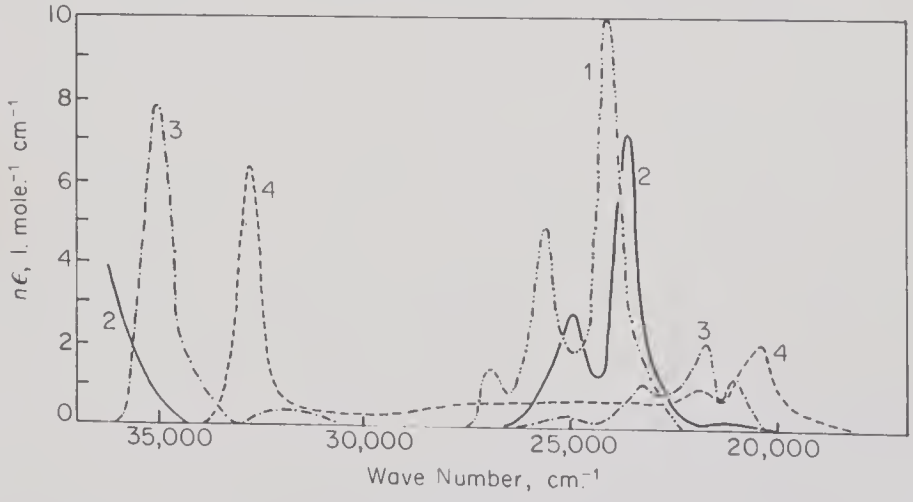

Fig. 15. Absolute extinction coefficients of triplet-triplet transitions measured from flash spectra. 1. Naphthalene, $n = 10^{-3}$; 2. anthracene, $n = 10^{-4}$; 3. naphthacene $n = 10^{-5}$; 4. pentacene, $n = 10^{-5}$.

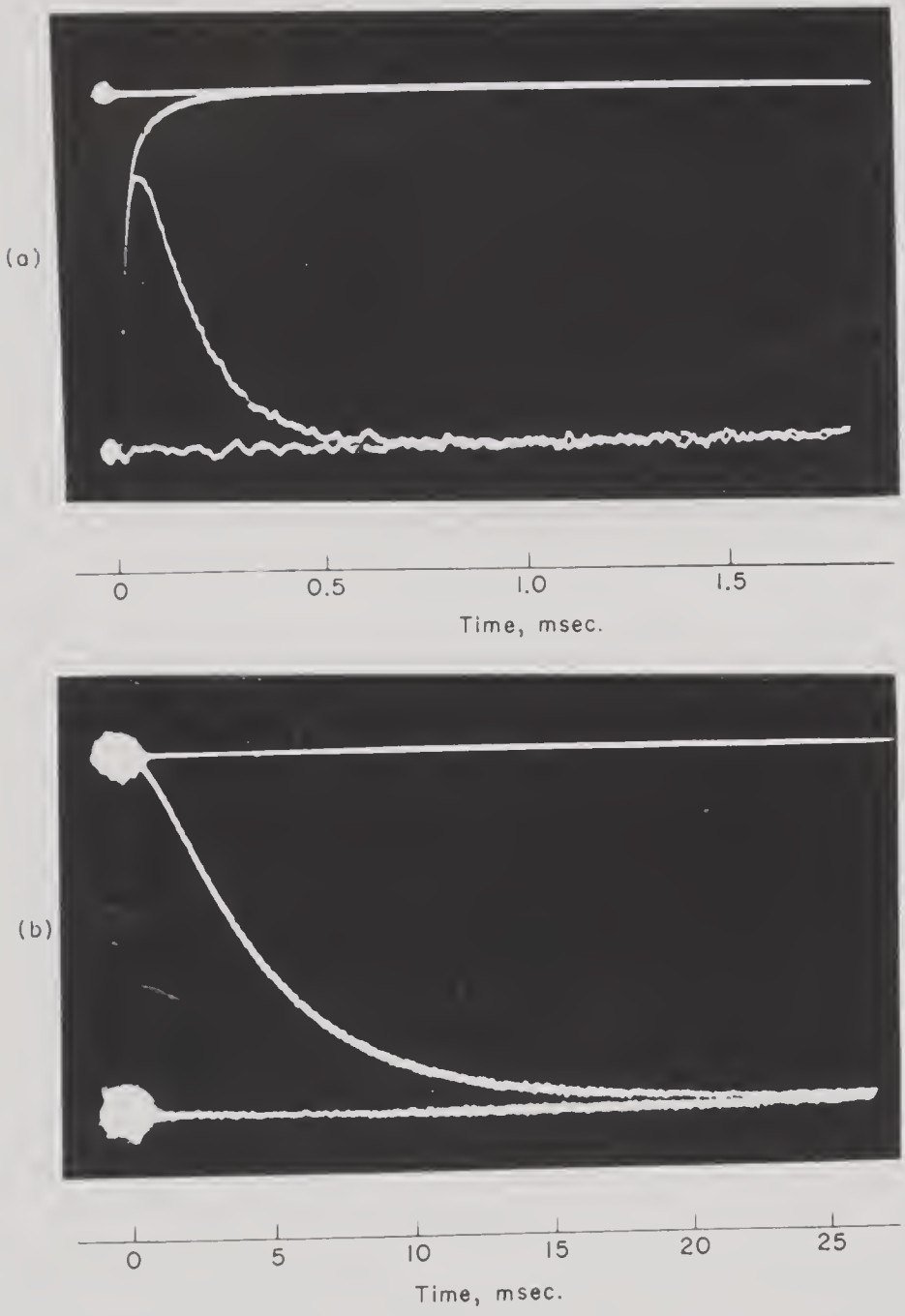

Fig. 16. Oscillographic records of the decay of triplet naphthalene in (a) hexane (b) viscous paraffin.

shows no overall change. Each flash therefore converts approximately 20% of the anthracene to its triplet state, which is observed by means of its own absorption spectrum and which returns in a short but measurable time to the ground state.

This phenomenon has been observed with a wide variety of aromatic molecules, and a few aliphatic ones, in many different solvents as well as in the gas phase. The rate of the radiationless return to the ground state of anthracene by process c_2 is characteristic of most other triplet molecules

so far observed in solution provided no chemical reaction takes place. From the photographic records extinction curves have been determined, and, in a number of cases, absolute extinction coefficients and concentrations have been measured from the depletion of the ground state (55). Typical triplet-triplet extinction curves obtained in this way are shown in Figure 15.

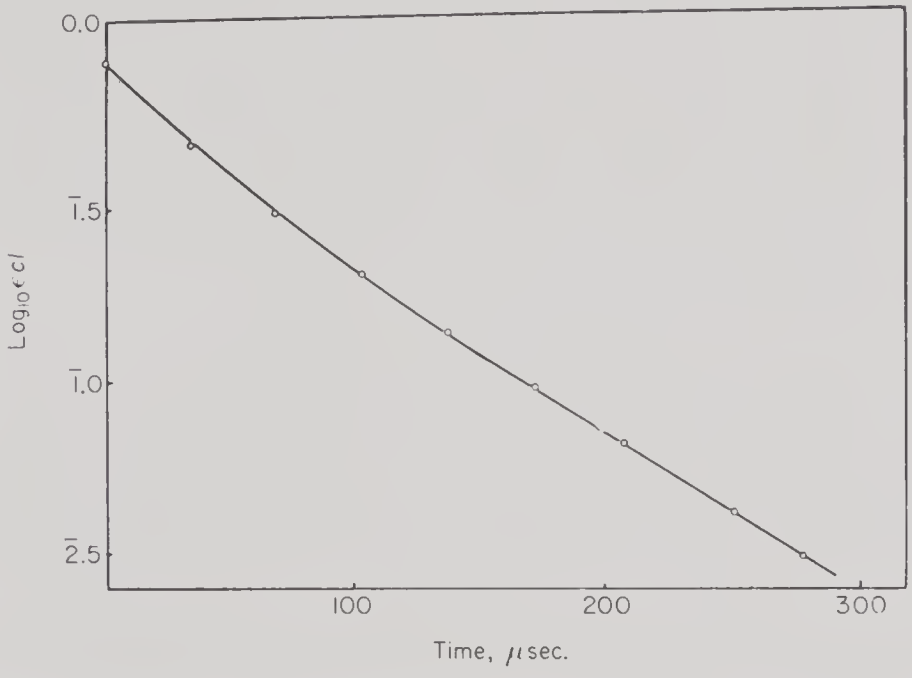

Fig. 17. First-order plot derived from record of Figure 16(a). Time zero is 150 μsec. after the flash peak.

For more detailed studies of the kinetics of triplet decay the spectrophotometric method was used (57). Typical oscillograph traces of the decay of triplet naphthalene in hexane and liquid paraffin solvents are shown in Figure 16. The lowest trace is obtained with monitoring source on before the flash, the highest trace with source off and the intermediate trace, showing the transient formation and decay, is recorded immediately after the flash. The scattered light from the flash is also shown in the hexane trace and was rather high in these experiments since the monitoring source employed was a 24 w. tungsten lamp whose intensity at 4,100 A., the wavelength of the triplet absorption, is quite low.

The first-order plot, derived by measurement of the first of these traces, in the manner described, is shown in Figure 17. It is not exactly linear and the deviation from linearity is caused by a contribution from the second-order reaction which was not detectable by flash photographic methods. By analysis of these traces both first- and second-order rate constants have been determined.

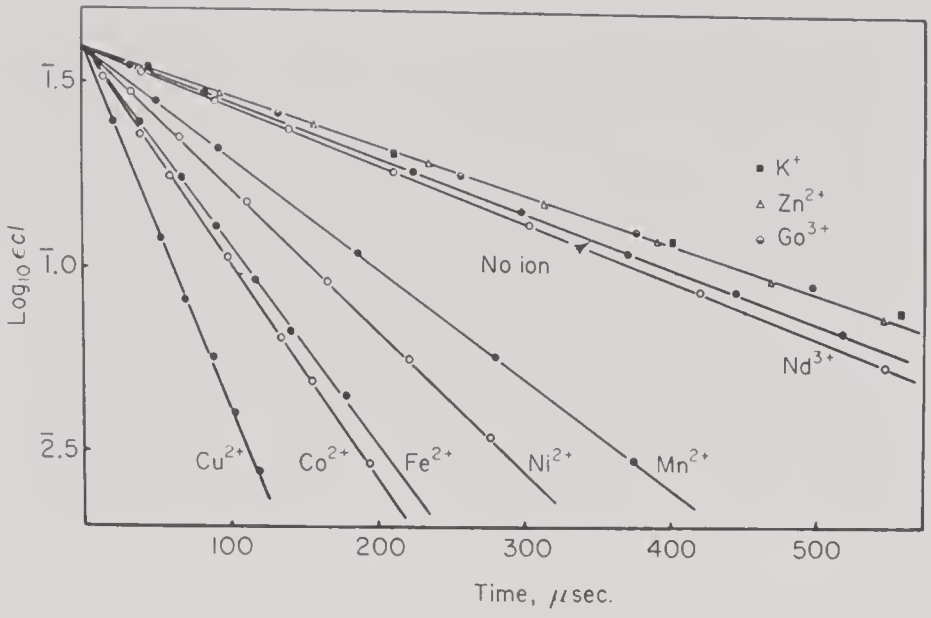

Fig. 18. Decay curves of triplet naphthalene showing quenching by ions in glycol solution.

The kinetics of reaction of the triplet state with other substances may be studied by adding these to the solution at a concentration sufficient to increase the rate by a measurable amount without reducing the lifetime beyond the resolving time of the apparatus. First-order plots showing the quenching of triplet states by paramagnetic ions (57) are shown in Figure 18. For the values of rate constants and their interpretations the original papers should be consulted.

XII. PHOTOCHEMISTRY OF QUINONES AND DYES AND THE REACTIONS OF SEMIQUINONES

Many substances, of which quinones and related dyes are typical, are converted by the absorption of light into a state which is capable of reaction with the solvent and which, in the presence of oxygen, is capable of photosensitizing the oxidation of the solvent. Previous work, based on studies of the overall kinetics of the reactions and analysis of the final products (2) had indicated that semiquinones were intermediates in the change which proceeded by the following mechanism:

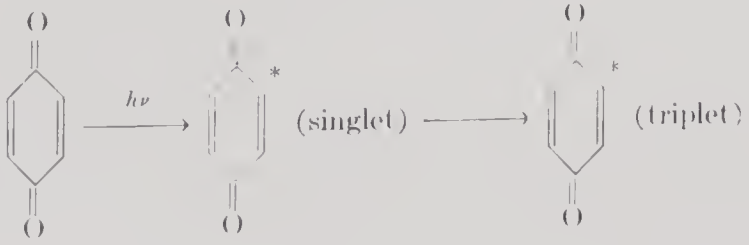

(1)

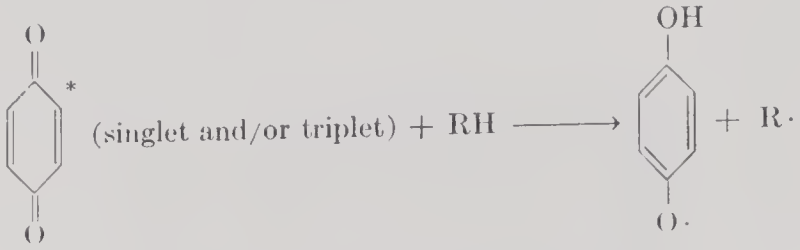

(2)

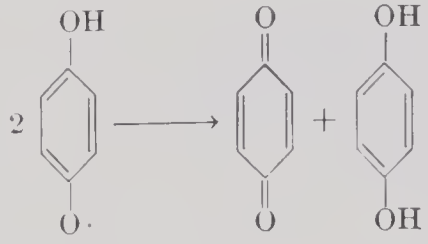

(3)

and, in the presence of oxygen,

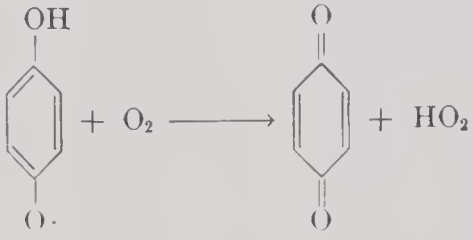

(4)

and

$$R + O_2 \longrightarrow RO_2 \longrightarrow \text{oxidation products} \qquad (5)$$

In addition we shall expect the equilibrium

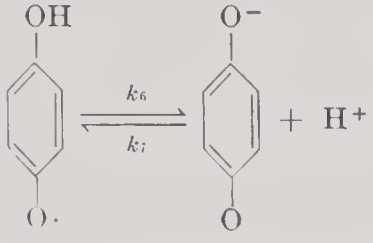

(6 and 7)

and there is the possibility that reaction 2 should be replaced by

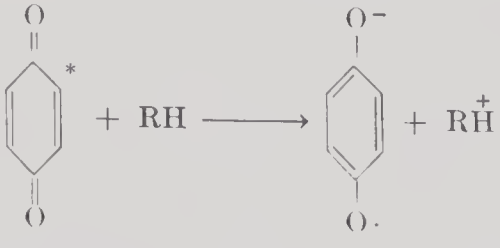

(8)

$$RH^+ \longrightarrow R + H^+ \qquad (9)$$

In the absence of oxygen three transient products of the quinone are therefore to be expected, viz., the triplet state (the upper singlet has a maximum life of 10^{-6} second and will not therefore be observed) the semiquinone neutral radical and the semiquinone radical ion.

Fig. 19. Flash spectroscopic records of duroquinone photolysis in viscous paraffin.

In their preliminary studies of the flash photolysis of quinones Bridge and Porter (4) found that several transient spectra were observed following irradiation of quinones in organic solutions and that, in the case of the anthraquinones, there was a clear correlation between the intensity of these transients and the photosensitizing power of the quinone. Since the principal problems of interest were concerned with the primary processes before oxygen entered into the reaction most studies were carried out in the absence of oxygen. In order to simplify the system further a quinone was sought which did not undergo appreciable permanent change in the course of several flashes but showed strong transients. For these, and other reasons, duroquinone was eventually chosen for detailed study.

The transient spectra observed after flash photolysis of duroquinone in hydrocarbon , alcohol, and other organic solvents were intense but very complex. It was clear that more than one transient was involved and that the absorption changed, not only with solvent, but also with time and with

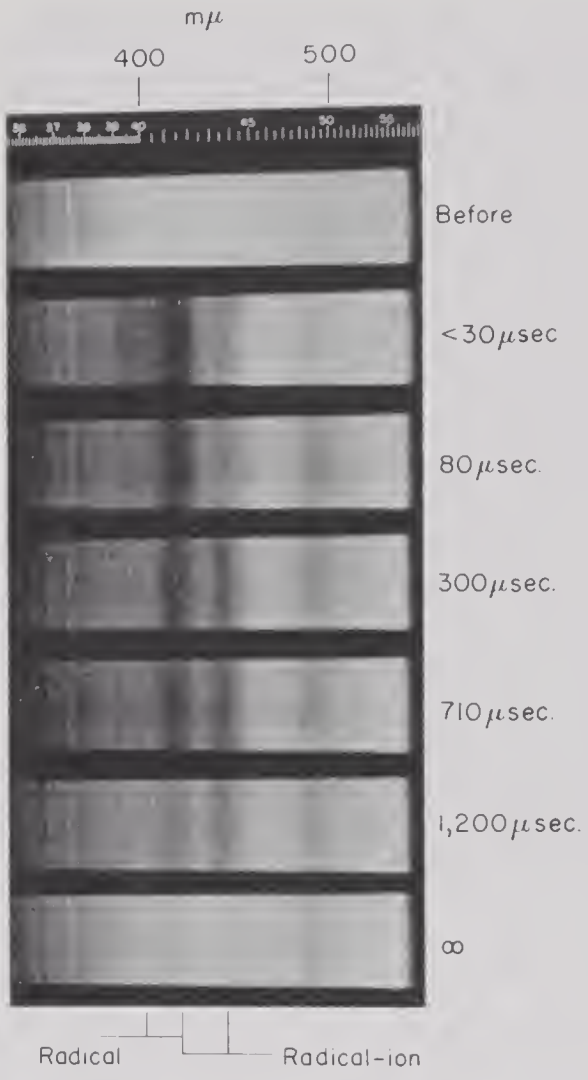

Fig. 20. Flash spectroscopic records of duroquinone photolysis in 96% ethanol.

pH. The spectra of the transients overlapped to a considerable extent and it was also clear that there were significant wavelength shifts from solvent to solvent even for a single transient. A detailed study, using mixed solvents and covering a wide pH range, eventually showed that all transient spectra could be interpreted in terms of three intermediates, which is just the number to be expected on the basis of the mechanism outlined above. Typical photographic records of these transients, which illustrate the considerable changes from one solvent to another and the changes with time, are shown in Figures 19 and 20.

The three transients had long wavelength maxima centered near 410, 430, and 490 mμ respectively. The assignment of these spectra was effected as follows:

1. The relative intensities of the 410 and 430 mμ transients were clearly related to pH. Only the 410 mμ peak appeared in strongly acid solutions and only the 430 mμ transient in strongly alkaline solutions. This indi-

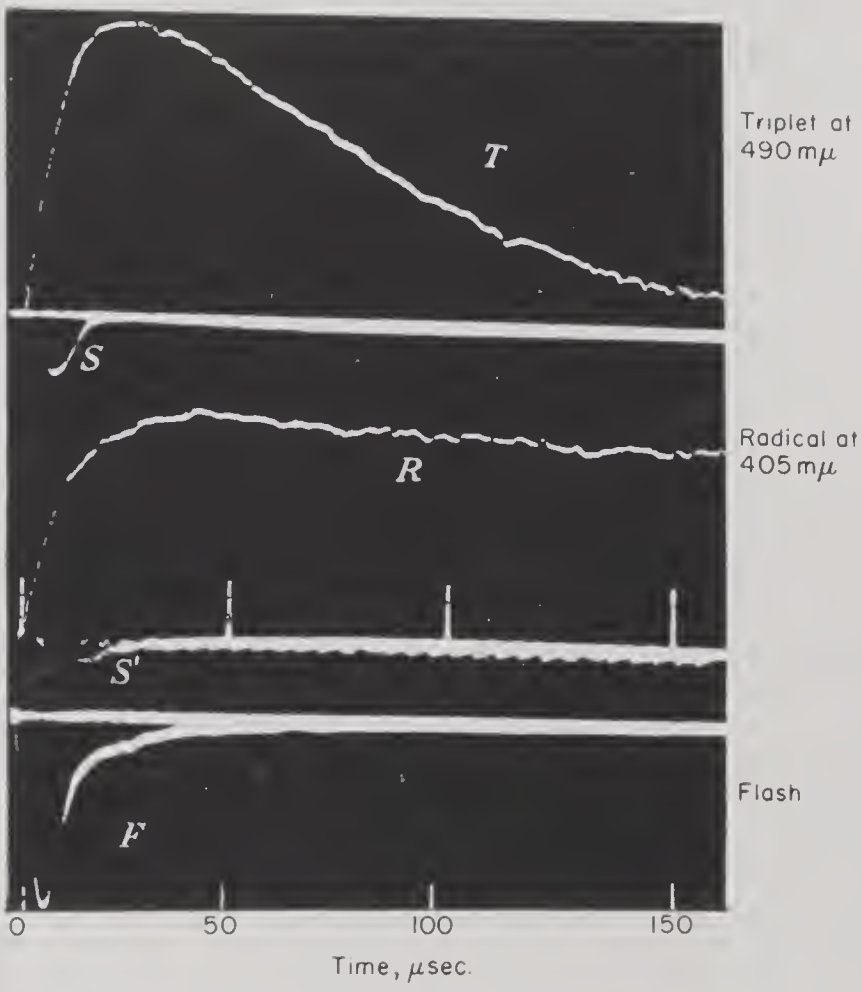

Fig. 21. Oscillographic records of duroquinone transients in viscous paraffin. T, triplet; R, durosemiquinone radical; F, flash profile; S and S', scattered light from photolysis flash.

cated that these two transients were the acid and base of a single species which strongly suggested their assignment to the semiquinone radical and radical-ion respectively.

2. The 430 mμ transient was quite stable for many minutes in alkaline solutions and its spectrum was identical with the durosemiquinone ion already studied by earlier workers under equilibrium conditions.

3. If the 410 and 430 mμ bands are assigned to the two radicals the remaining band at 490 mμ was very probably the triplet state. Some support for this view was obtained from the fact that its lifetime and behavior in viscous solvents were characteristic of triplet states previously investigated. Confirmation was sought by a study of the solution in rigid media at low temperatures under which conditions the behavior of triplet states and of radicals is quite distinct. Although the lifetime of triplet states may be prolonged in rigid solvents it can never exceed the radiative lifetime which is, at the most, of the order of seconds. On the other hand the formation of radicals is somewhat restricted, and, if formed at all, they

are trapped permanently in the matrix. The flash photolysis of duroquinone in a rigid paraffin solution at −78°C. showed only the 490 mμ band with a lifetime which was prolonged compared with that at room temperature but still less than one second. This behavior is characteristic of all known triplet states and uncharacteristic of any known radical.

The transient spectra having been assigned the second stage of the investigation was a kinetic study of all three species by spectrophotometric methods. Typical decay curves of the triplet and radical in liquid paraffin

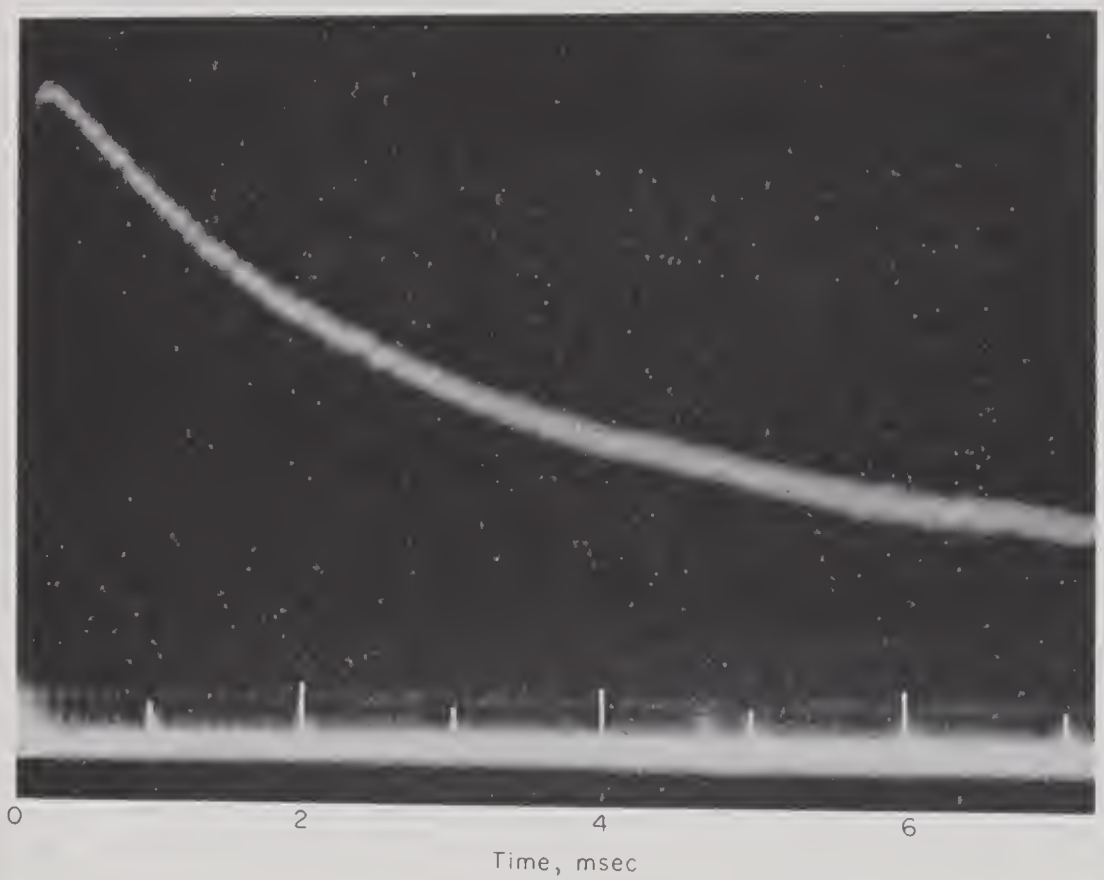

Fig. 22. Decay of durosemiquinone in viscous paraffin.

are shown in Figures 21 and 22, and kinetic plots of these two decays are given in Figure 23. As expected the decay of the triplet is first order and that of the radical second order in accordance with the scheme of reaction already given. Further kinetic investigations confirmed this scheme and gave additional support to the assignments of the transient spectra which had been made on other grounds. Absolute rate constants of each of the elementary steps in the reaction were derived and, in particular, it was possible to answer the two questions regarding mechanism which have been mentioned, viz., the relative importance of singlet and triplet excited states in the primary act and the role of hydrogen versus electron abstraction.

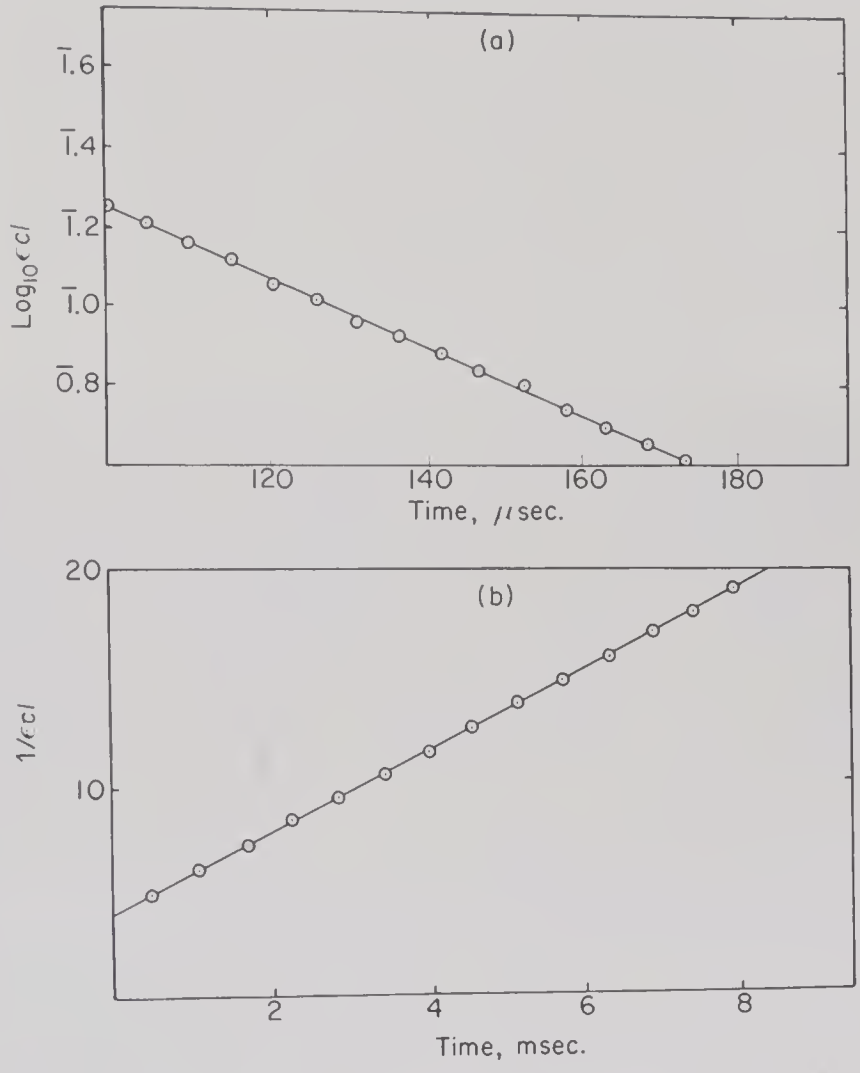

Fig. 23. Plots of data from Figures 21 and 22 showing (a) first-order decay of the triplet (b) second-order decay of the radical.

The findings on these two points were as follows:

1. The decay of the radicals was very slow compared with both the decay of the triplet and the duration of the flash. The growth of the radical was, however, quite rapid compared with the rate of decay of the triplet indicating that the triplet did not give rise to the radical. Detailed investigation showed that

$$[\mathrm{R}]_t = \text{constant} \times \int_0^t I_t dt$$

where $[\mathrm{R}]_t$ is the concentration of radical at time t, and I_t is the intensity of flash at time t, the integral being evaluated directly from the recorded trace of the flash. This shows that the radical is formed in a time which is short compared with the lifetime of the triplet, and even compared with the duration of the flash, and that it cannot be formed from the triplet state in a significant amount. It was concluded that the radical is formed by reaction of the excited singlet state whose lifetime is 2×10^{-6} second.

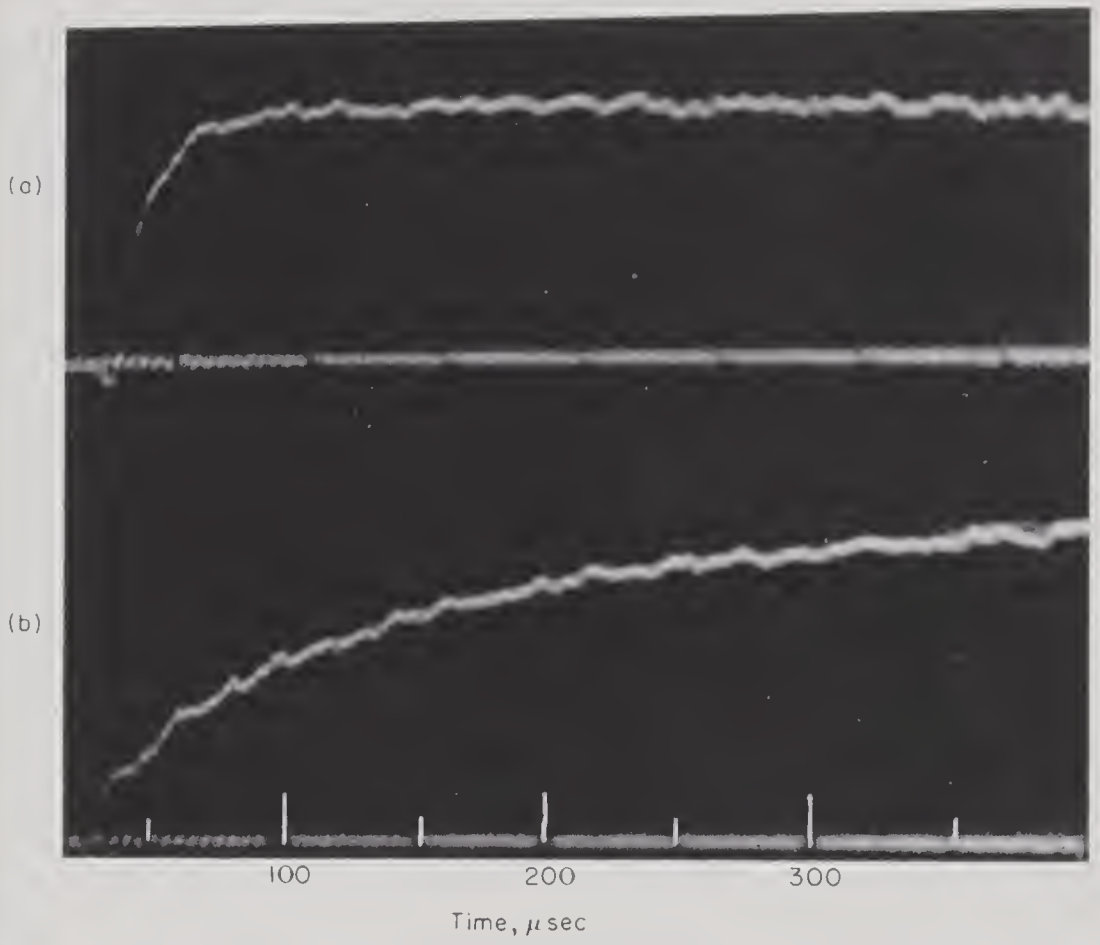

Fig. 24. Oscillographic traces of durosemiquinone radical (a) and radical-ion (b) in ethanol showing growth of radical-ion after photolysis.

2. Although only the radical is observed in strong acids and only the radical ion in strong alkaline solutions both are observed together in the range of pH 7. Quantitative study of the variation of relative concentration with pH allows the pK of the equilibrium 6–7 to be determined. More interesting still is the fact that, in ethanol solutions containing only 4% water, the equilibrium between the acid and base is not immediately established and the relative proportions of acid and base change after the flash. This is seen clearly in the photographic record of Figure 20 and also in the photometric traces of Figure 24 which record the radical and radical ion simultaneously. The concentration of radical ion immediately after the flash is seen to be nearly zero and to increase, with a simultaneous disappearance of the neutral radical. It follows that the primary reaction of the excited state of the quinone with the alcohol is hydrogen abstraction rather than electron transfer, even when the equilibrium form of the radical is the unprotonated one. The dissociation of the acid is directly observed and absolute rate constants have been derived. Since the constant of the acid-base equilibrium has already been measured the rate of the recombination of cation and proton is also obtained.

The system just described is one of the most complex which has yet been elucidated by direct flash photolysis methods and provides a useful example of the power of the method when applied to organic mechanism. Questions such as the role of hydrogen abstraction versus electron transfer in oxidation are of fundamental importance and are still controversial and the overall kinetic mechanism can always be equally well satisfied by both. Only direct observation of the intermediates themselves will allow an unequivocal decision to be made regarding their relative importance in any particular reaction.

The assignment of the unknown spectra to the various intermediates presented considerable difficulties in the quinone system just described and the example is probably typical of most organic systems. It is to be expected, however, that further investigations of similar reactions will present fewer difficulties partly because the kinetic experience gained in one reaction can often be carried over to another but particularly because the recording and assignment of the spectra of organic free radicals and excited states in solution is proceeding quite rapidly and it is probable that, in a few more years, most of the common types of intermediate spectra will be known.

POSTSCRIPT

The above chapter was completed in 1958 and the last four years have been a period of great activity in this field. The basic flash apparatus, described in section III is, however, unaffected by recent developments and is still the best general purpose arrangement, at least for preliminary investigations.

Some of the techniques referred to in the introduction have now been developed and, in particular, pulse radiolysis employing electron pulses of energy 2–10 j. and duration 1μsec. have been used to study the primary products of radiation chemical processes in liquid systems, [McCarthy, R. L., and Maclachlan, A., *Trans. Faraday Soc.*, **56**, 1187 (1960)].

The relation between flash energy and flash duration and the consequent limitations of the flash photolysis method have been discussed by Porter [*Z. Electrochem.*, **64**, 59 (1960)]. It is shown that the method should be applicable to all transients which disappear by bimolecular processes. Marginal improvements in flash duration have been obtained by the increasing availability of low-inductance condensers, by greater attention to the design of low-inductance circuits, and by the addition of small amounts of molecular gases to the normal inert gas filling of the flash lamps [Gover, T. A., and Porter, G., *Proc. Roy. Soc.* (*London*), **A262**, 476 (1961)]. Flash

photolysis studies have been successfully extended into the vacuum ultraviolet region [Black, G., and Porter, G., *Proc. Roy. Soc.* (*London*), **A266,** 185 (1961)]. The flash-heating effect, described in Section VIII, has been applied to heterogeneous systems and to the production of free radical spectra pyrolysis [Nelson, L. S., and Lundbergh, J. L., *J. Phys. Chem.*, **63,** 433 (1959), and Kuebler, N. A., and Nelson, L. S., *J. Opt. Soc. Am.*, **51,** 1411 (1961)]. The development of the optical maser has greatly increased the available intensity of flash sources and the maser's application to flash photolysis is being investigated. At present it is not suitable for general use owing to its low total energy output and its limited spectral range. The application of pulse-sampling techniques to flash photolysis has been described by Witt [*Z. Physik. Chem.* (Frankfurt), **20,** 193 (1959)]. A combination of flash photolysis and shock-tube techniques has been described by Burns and Hornig [*Can. J. Chem.*, **38,** 1702 (1960)].

Of the numerous new applications of flash photolysis techniques, mention should be made of the studies of nonequilibrium vibrationally excited molecules by Norrish and his collaborators [e.g., Basco, N., Callear, A. B., and Norrish, R. G. W., *Proc. Roy. Soc.* (*London*), **A260,** 459 (1960) and *Discussions Faraday Soc.* (1962)]; the detection of transient charge-transfer complexes of atoms [Rand, S. L., and Strong, R. L., *J. Am. Chem. Soc.*, **82,** 5 (1960), Gover, T. A., and Porter, G., *Proc. Roy. Soc.* (*London*), **A262,** 476 (1961)]; and the study of chloroplast suspensions by Witt and his collaborators [e.g., Rumberg, B., Müller, A., and Witt, H. T., *Nature* **194,** 854 (1962)].

Studies of the triplet states of organic molecules, referred to in Section XI, have been greatly extended. The spectra of acidic and basic forms have been distinguished and pK's measured [Jackson, G., and Porter, G., *Proc. Roy. Soc.* (*London*), **A260,** 13 (1961)]. Quenching by paramagnetic substances [Porter, G., and Wright, M. R., *Discussions Faraday Soc.*, **27,** 18 (1959); Linschitz, H., and Pekkarinen, *J. Am. Chem. Soc.*, **82,** 2411 (1960)] and by energy transfer [Porter, G., and Wilkinson, F., *Proc. Roy. Soc.* (*London*), **A264,** 1 (1961)] have been investigated. Much attention has been paid to the influence of viscosity on triplet state lifetimes [Jackson, G., and Livingston, R., *J. Chem. Phys.*, **35,** 2182 (1961); Hoffman, M. Z., and Porter, G., *Proc. Roy. Soc.* (*London*), **A268,** 46 (1962); Porter, G., and Stief, L. J., *Nature*, **195,** 991 (1962)].

Many new transient spectra have been described; Herzberg, after many years of searching, has obtained the spectrum of methylene [*Proc. Roy. Soc.* (*London*), **A262,** 291 (1961)]. Other simple radical spectra described recently are NCS [Holland, R., Style, D. W. G., Dixon, R. N., and Ramsay, D. A., *Nature*, **182,** 336 (1958)], BO_2 [Johns, J. W. C., *Can. J. Phys.*, **39,** 1738 (1961)], and CF_2 [Mann, D. E. and Thrush, B. A., *J. Chem. Phys.*, **33,** 1732

(1960)]. The spectra of nearly 100 aromatic free radicals have now been characterised by Porter and his co-workers [Land, E. J., Porter, G., and Strachan, E., *Trans. Faraday Soc.*, **57**, 1885 (1961); Land, E. J., and Porter, G., *J. Chem. Soc.*, **1961**, 3540, and later papers in *Trans. Faraday Soc.*]. These studies also included determinations of acidity constants of the free radicals and preliminary kinetic investigations.

Of the many kinetic studies by flash photolysis, reference will be made only to those dealing with organic molecules in solution. These include studies of the effect of oxygen and metal ions on kinetics of semiquinone radicals [Bridge, N. K., and Reed, M., *Trans. Faraday Soc.*, **56**, 1796 (1960)]; the reaction of ketyl radicals [Porter, G., and Wilkinson, F., *Trans. Faraday Soc.*, **57**, 1686 (1961)], photoionization and recombination kinetics of alkali metals and aromatic negative ions [Linshitz, H., and Eloranta, J., *Z. Electrochem.*, **64**, 169 (1960)]; the photoreduction of methylene blue [Parker, C. A., *J. Phys. Chem.*, **63**, 26 (1959)]; and thionine [Hatchard, G. C., and Parker, C. A., *Trans. Faraday Soc.*, **57**, 1093 (1961); the photodecomposition of complex oxalates [Parker, C. A., and Hatchard, C. G., *J. Chem. Phys.*, **63**, 22 (1959)]; the photochemistry of the visual pigments [Abrahamson, E. W., Marquisee, J., Cavuzzi, P., and Roubie, J., *Z. Elektrochem.*, **64**, 177 (1960)]; and further studies of the reactions of haem compounds [Gibson, Q., *Progr. Reaction Kinetics*, Volume II (1962)].

References

1. E. W. Abrahamson and H. Linschitz, *J. Chem. Phys.*, **23**, 2198 (1955).
2. J. L. Bolland and H. R. Cooper, *Proc. Roy. Soc.* (*London*), **A225**, 405 (1954).
3. E. J. Bowen, *Chemical Aspects of Light*, 2nd ed. rev., Oxford Univ. Press, London, 1946.
4. N. K. Bridge and G. Porter, *Proc. Roy. Soc.* (*London*), **A244**, 259, 276 (1958).
5. D. L. Bunker and N. Davidson, *J. Am. Chem. Soc.*, **80**, 5085, 5090 (1958).
6. M. I. Christie and G. Porter, *Proc. Roy. Soc.* (*London*), **A212**, 390, 398 (1952).
7. M. I. Christie, R. G. W. Norrish, and G. Porter, *Proc. Roy. Soc.* (*London*), **A216**, 152 (1952).
8. M. I. Christie, A. J. Harrison, R. G. W. Norrish, and G. Porter, *Proc. Roy. Soc.* (*London*), **A231**, 446 (1955).
9. S. Claesson and L. Lindquist, *Arkiv Kemi*, **11**, 535, 561 (1957), **12**, 1 (1958); private communication.
10. K. Clusius and A. E. Douglas, *Can. J. Phys.*, **32**, 319 (1954).
11. F. W. Dalby, *Can. J. Phys.*, **36**, 1336 (1958).
12. F. H. C. Edgecombe, R. G. W. Norrish, and B. A. Thrush, *Proc. Roy. Soc.* (*London*), **A243**, 24 (1957).
13. K. H. L. Erhard and R. G. W. Norrish, *Proc. Roy. Soc.* (*London*), **A234**, 178 (1956).
14. Q. H. Gibson, *J. Physiol.*, **134**, 112 (1956).
15. Q. H. Gibson, *Progr. Biophys. Biophys. Chem.*, **9**, 1 (1959).

16. L. I. Grossweiner and M. S. Matheson, *J. Chem. Phys.*, **23**, 2443 (1955).
17. L. I. Grossweiner and M. S. Matheson, *J. Phys. Chem.*, **61**, 1089 (1957).
18. G. Herzberg and D. A. Ramsay, *Proc. Roy. Soc. (London)*, **A233**, 34 (1955).
19. G. Herzberg and J. Shoosmith, *Can. J. Phys.*, **34**, 523 (1956).
20. R. Holland, D. W. G. Style, R. N. Dixon, and D. A. Ramsay, *Nature*, **182**, 336 (1958).
21. M. A. Khan, R. G. W. Norrish, and G. Porter, *Proc. Roy. Soc. (London)*, **A219**, 312 (1953).
22. K. Knox, R. G. W. Norrish, and G. Porter, *J. Chem. Soc.*, **1952**, 1477.
23. H. Linschitz and K. Sarkanan, *J. Am. Chem. Soc.*, **80**, 4826 (1958).
24. F. J. Lipscomb, R. G. W. Norrish, and G. Porter, *Nature*, **174**, 785 (1954); F. J. Lipscomb, R. G. W. Norrish, and B. A. Thrush, *Proc. Roy. Soc. (London)*, **A233**, 455 (1956).
25. R. Livingston and V. A. Ryan, *J. Am. Chem. Soc.*, **75**, 2176 (1953).
26. R. Livingston, G. Porter, and M. W. Windsor, *Nature*, **173**, 485 (1954).
27. R. Livingston, *J. Am. Chem. Soc.*, **77**, 2179 (1955).
28. R. Livingston and D. W. Tanner, *Trans. Faraday Soc.*, **54**, 765 (1958).
29. G. J. Mains, J. L. Roebber, and G. J. Rollefson, *J. Phys. Chem.*, **59**, 733 (1955).
30. J. H. Malmberg, *Rev. Sci. Inst.*, **28**, 1027 (1957).
31. R. Marshall and N. Davidson, *J. Chem. Phys.*, **21**, 659 (1953).
32. D. S. McClure and P. L. Hanst, *J. Chem. Phys.*, **23**, 1772 (1955).
33. W. D. McGrath and R. G. W. Norrish, *Proc. Roy. Soc. (London)*, **A242**, 265 (1957).
34. L. S. Nelson and D. A. Ramsay, *J. Chem. Phys.*, **25**, 372 (1956).
35. I. Norman and G. Porter, *Proc. Roy. Soc. (London)*, **A230**, 399 (1955).
36. R. G. W. Norrish and G. Porter, *Proc. Roy. Soc. (London)*, **A210**, 439 (1952).
37. R. G. W. Norrish, G. Porter, and B. A. Thrush, *Proc. Roy. Soc. (London)*, **A227**, 423 (1955).
38. R. G. W. Norrish, G. Porter, and B. A. Thrush, *Symp. Combust., 5th, Pittsburgh, 1954*, 651 (1955).
39. R. G. W. Norrish and A. P. Zeelenberg, *Proc. Roy. Soc. (London)*, **A240**, 293 (1957).
40. G. K. Oster and R. A. Marcus, *J. Chem. Phys.*, **27**, 189 (1957).
41. C. A. Parker and C. G. Hatchard, *Proc. Roy. Soc. (London)*, **A235**, 518 (1956).
42. C. A. Parker, *Nature*, **182**, 245 (1958).
43. R. W. B. Pearse and A. G. Gaydon, *The Identification of Molecular Spectra*, Chapman and Hall, London, 1950.
44. G. Porter, *Proc. Roy. Soc. (London)*, **A200**, 284 (1950).
45. G. Porter, *Discussions Faraday Soc.*, **9**, 60 (1950).
46. G. Porter and F. J. Wright, *Discussions Faraday Soc.*, **14**, 23 (1952).
47. G. Porter and F. J. Wright, *Z. Elektrochem.*, **56**, 782 (1952).
48. G. Porter, *Symp. Combust., 4th, Cambridge, Mass., 1952*, 248 (1953).
49. G. Porter and M. W. Windsor, *Discussions Faraday Soc.*, **17**, 178 (1954).
50. G. Porter and F. J. Wright, *Trans. Faraday Soc.*, **51**, 395 (1955).
51. G. Porter and F. J. Wright, *Trans. Faraday Soc.*, **51**, 393 (1955).
52. G. Porter and M. W. Windsor, *Mol. Spectr., Rept. Conf., London, 1954*, 6 (1955); *Discussions Faraday Soc.*, **17**, 178 (1954).
53. G. Porter and M. W. Windsor, *Nature*, **180**, 187 (1957).
54. G. Porter and E. Strachan, *Trans. Faraday Soc.*, **54**, 1595 (1958).
55. G. Porter and M. W. Windsor, *Proc. Roy. Soc. (London)*, **A245**, 238 (1958).
56. G. Porter and E. R. Wooding, *4th International Congress on High Speed Photography*, Cologne, 1958.

57. G. Porter and M. R. Wright, *J. Chim. Phys.*, **55**, 705 (1958).
58. G. Porter and E. R. Wooding, *J. Sci. Inst.*, Vol. 36, 147 (1959).
59. G Porter and F. Wilkinson, *Trans. Faraday Soc.*, **57**, 1686 (1961).
60. E. Rabinowitch, *J. Chim. Phys.*, **55**, 927 (1958).
61. D. A. Ramsay, *J. Chem. Phys.*, 25, 188 (1956).
62. K. E. Russel and J. Simons, *Proc. Roy. Soc.* (*London*), **A217**, 271 (1953).
63. R. L. Strong, J. C. W. Chien, P. E. Graf, and J. W. Willard, *J. Chem. Phys.*, 26, 1287 (1957).
64. B. A. Thrush, *Proc. Roy. Soc.* (*London*), **A243**, 555 (1958).
65. J. U. White, *J. Opt. Soc. Am.*, **32**, 285 (1942).

CHAPTER XX

DETERMINATION OF ACTIVE INTERMEDIATES IN REACTIONS

G. M. Burnett, *University of Aberdeen, Scotland*

Sir H. W. Melville, *Department of Scientific and Industrial Research, London*

I. General Considerations 1107
II. Initiation 1109
III. Lifetime of Reaction Chains 1110
IV. Intermittent Illumination 1111
1. Simple Theory 1111
2. Modification Allowing for Constant Dark Rate 1117
3. General Theory for Simultaneous First- and Second-Order Terminations 1118
4. Nonuniformity of Radical Generation 1122
5. "Square Wave" Light Pulses 1124
V. Experimental Methods 1127
VI The Nonstationary State 1130
1. Introduction 1130
2. Theory of Nonstationary State 1131
3. Application to Gas Phase Reactions 1132
4. Oxidation by Gaseous Oxygen 1133
References 1136

I. GENERAL CONSIDERATIONS

In the kinetic analysis of reactions which proceed through the intermediary of atoms or free radicals, use has been made of the principle of the stationary state, described in other chapters of this volume. From the standpoint of such chain reactions, there are three elementary reactions—initiation, propagation, and termination. In order to evaluate the concentration of the intermediary active species or the rate constants of the individual chemical processes involved, it is necessary to carry out three experimental determinations. These determinations are (*a*) overall rate of reaction, (*b*) rate of initiation, (*c*) lifetime of the radical chain. The first two may be considered as relatively easily accessible by conventional methods, so that this section will be mostly concerned with the determination of lifetimes. It might be well to mention that direct estimation of the

concentration of intermediates of atomic or free radical character is not yet possible although the rapid advances of the techniques of flash spectroscopy and electron paramagnetic resonance make it reasonably likely that this goal will be reached in the foreseeable future.

In order to show clearly how the methods are used, it is convenient to postulate a generalized mechanism for the interaction of two molecules A_2 and B_2:

$$A_2 \longrightarrow 2A \qquad (k_1) \qquad \text{(i)}$$

$$A + B_2 \longrightarrow AB + B \qquad (k_2) \qquad \text{(ii)}$$

$$B + A_2 \longrightarrow AB + A \qquad (k_3) \qquad \text{(iii)}$$

$$2A \longrightarrow A_2 \qquad (k_4) \qquad \text{(iv)}$$

$$2B \longrightarrow B_2 \qquad (k_5) \qquad \text{(v)}$$

$$A + B \longrightarrow AB \qquad (k_6) \qquad \text{(vi)}$$

$$A + X \longrightarrow AX \qquad (k_7) \qquad \text{(vii)}$$

$$B + X \longrightarrow BX \qquad (k_8) \qquad \text{(viii)}$$

Here we have all the possibilities. It is assumed that A can combine with B as well as with A, and similarly B can react with either A or B. Also we suppose that the atoms or radicals A and B can react with molecules X added to the system and that the entities—which must be radicals—that emerge from this collision disappear by processes which do not interfere with the overall course of the reaction. In gas reactions, but less likely in liquid reactions, the walls of the vessel may remove A or B, the rate of removal being governed by the rate at which the active centers reach the walls. The initiation process has been written in its simplest form but it may be more complex and may, therefore, lead to complication of the kinetic expressions. This raises problems which are outside the scope of this chapter, since special methods would have to be evolved to deal with each case.

If stationary state conditions have been set up, then the rate of production of A (and of B) will be precisely equal to their rate of removal by all processes. Suppose in the first place that X is absent, then there will be three possible cases, the rate of the second reaction ($A + B_2$) will be greater than, equal to, or less than the rate of the third reaction ($B + A_2$). If the third reaction is slower then it follows that (B) > (A) providing k_4, k_5, k_6 are of comparable value. The rate of removal of A_2 is then simply

$$-d(A_2)/dt = k_3(B)(A_2) \qquad (1)$$

Provided the chain cycle occurs many times before the removal of B, the concentration of B is

$$(B) = [k_1(A_2)/k_5]^{1/2} \tag{2}$$

Substituting in Equation (1)

$$-d(A_2)/dt = k_3(k_1/k_5)^{1/2}(A_2)^{3/2} \tag{3}$$

Similarly if the reaction B + A_2 is faster than the other step of the cycle, (A) > (B), and following the same reasoning

$$(A) = [k_1(A_2)/k_4]^{1/2} \tag{4}$$

and

$$-d(A_2)/dt = k_2(k_1/k_4)^{1/2}(A_2)^{1/2}(B_2) \tag{5}$$

When the rates and hence the concentrations of A and B are comparable, the kinetic expressions become very complex and are useless for experimental application. Even the simple expressions (3) and (5) show that measurement of overall rate and rate of initiation ($k_1(A_2)$) would not allow us to separate k_2 and k_4 or k_3 and k_5.

If X is present in such amount as to allow reactions (vii) and (viii) to predominate there are the following possibilities

$$-d(A_2)/dt = k_1k_2k_7^{-1}(B_2)(X)^{-1} \tag{6}$$

$$-d(A_2)/dt = k_1k_3k_8^{-1}(A_2)(X)^{-1} \tag{6a}$$

depending upon whether A or B is removed. Kinetically the necessary discrimination can be readily achieved.

II. INITIATION

The rate of chain initiation can be determined in a number of ways, but, in general, certain assumptions have to be made which are difficult, if not impossible, to substantiate directly. In this section we will deal with methods which are generally applicable to all chain processes. Special methods peculiar to polymer systems are discussed in Chapter XXI.

Many reactions are completely suppressed by the addition of small quantities of specific inhibitors (1–6). If we can assume that the complete suppression of reaction arises from the interaction of the inhibitor with either A or B before the propagation cycle can commence, it follows that the length of the inhibition period gives a direct measure of the rate of removal of the inhibitor and hence of the rate of production of A or B. A point

still to be settled is whether one or two radicals are removed by a molecular inhibitor, e.g., *p*-benzoquinone, but it is usually safe to assume that two radicals react (7). There is some chemical evidence to support this in that diethers have been identified in the reaction products of the interaction of free radicals with quinones (8).

Usually the addition of a foreign molecular material will lead to a diminution in the rate of reaction, defined as retardation. As far as the mechanism of this type of reaction is concerned it appears that the reaction between the propagating species and retarder molecule does not come about until an appreciable number of propagation cycles have been completed. If, however, it can be arranged that the chains are stopped wholly by X but are still long, the rate of uptake of X will be equal to the rate of generation of either A or B. Frequently addition of very small amounts of retarder gives a pronounced reduction of rate and it is not then possible to follow the disappearance of X by conventional analytical means. A less direct method is to observe the course of reaction against time and from a plot of rate against time it is possible to deduce the rate of initiation. Indeed under the experimental conditions laid down above the reciprocal rate is a linear function of time and the rate of initiation, R_i, can be found from the simple relationship

$$\text{slope/intercept} = R_i/(\mathrm{X})_0 \tag{7}$$

where $(\mathrm{X})_0$ is the initial concentration of retarder. Applications of this type of analysis are to be found in fundamental studies on oxidation (9,10). A critique of various methods of dealing with retardation data has been given by Cowley and Burnett (11) in which some rarer phenomena are also discussed.

Procedures such as these, despite the assumptions which are necessary, are the only ones which will give a precise measure of initiation rate for all types of chain reactions. Other possible methods include measurement of light absorption coupled with the assumption of a primary quantum efficiency but this, at best, is extremely approximate. When a free radical producing initiator is employed, it has often been assumed that the rate of decomposition of the initiator will give a measure of the rate of chain initiation. This is true only if each of the radical fragments starts a chain. It is becoming increasingly apparent that such a situation is exceptional (12).

III. LIFETIME OF REACTION CHAINS

As has been mentioned, in order to disentangle the rate constants for propagation and termination it is necessary to evaluate the lifetime of the reaction chain. This quantity we define as

$$\tau = \frac{\text{stationary concentration of radicals}}{\text{rate of removal of radicals}}$$

$$= (\mathrm{A})/k_4(\mathrm{A})^2 = [k_4(\mathrm{A})]^{-1} \tag{8}$$

But, according to the scheme of Section I, $k_4(\mathrm{A}_2) = k_4(\mathrm{A})^2$, so Equation (8) becomes

$$\tau = [k_1 k_4(\mathrm{A}_2)]^{-1/2} \tag{9}$$

If then k_1 has been calculated from measurement of the rate of initiation it follows that k_4 can be evaluated (and also k_5 and k_6 under suitable experimental conditions). Consequently it is of prime importance that suitable precise methods for the measurement of lifetime should be available since only in this way can the precise details of the characteristics of complex chain processes be appreciated.

Obviously the most direct method would be to measure the actual concentration of active intermediary or its variation with time during the build up to the stationary concentration. So far, the first of these alternatives has proved to be impracticable, but recently methods have been developed which enable one to follow the growth or decay of the chain process. These methods are discussed in Section VI. The only essential for the application of these techniques is that we must have an easily controllable means of chain initiation and therefore the only practicable method is photochemical or radiochemical. While this might be thought to be restrictive, it can usually be arranged experimentally that thermal and photochemical processes follow the same path. In any event, it is usually true that small differences in the methods of initiation have a negligible effect on the course and characteristics of the chain process which is governed predominantly by the propagation and termination processes.

IV. INTERMITTENT ILLUMINATION

1. Simple Theory

If photochemical initiation methods are assumed to be used, when light is switched on the concentration of free radicals does not immediately attain the stationary state value but builds up in the manner shown in Figure 1 (slow). The horizontal part of the curve, corresponding to steady state, is achieved in a time somewhat greater than the lifetime of the active entity. For long chains, the rate of reaction is sensibly proportional to the concentration of active species, and therefore the extent of reaction to the product of concentration and time. Since both of these quantities are necessarily

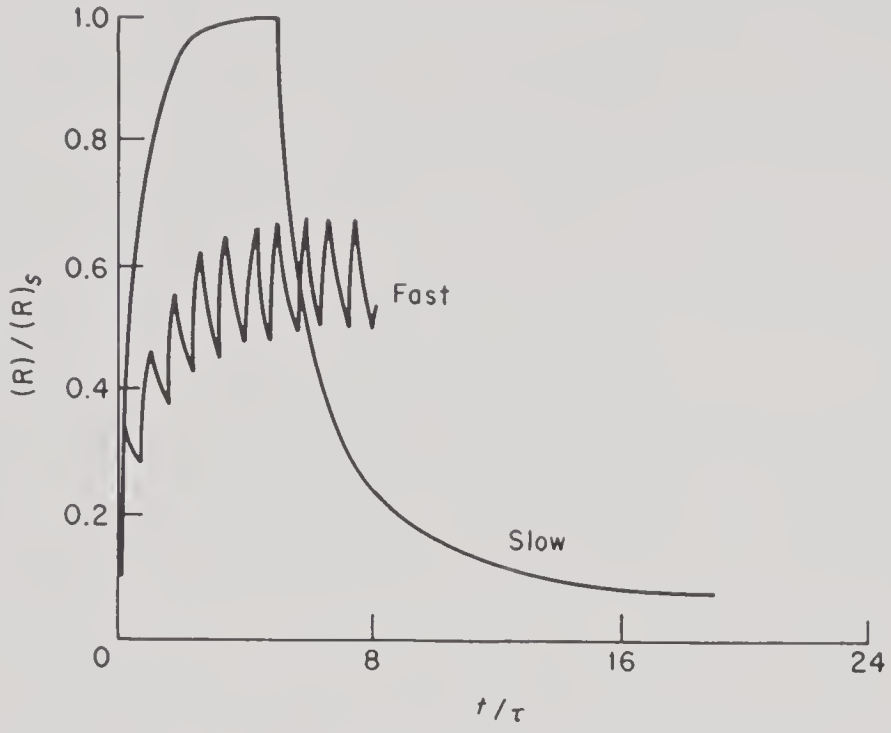

Fig. 1. Build up and decay of radical concentration during intermittent illumination.

very small, the problem resolves itself to finding methods of measuring very small amounts of reaction in extremely short intervals of time.

While the problem stated above has been substantially solved, historically the solution was achieved in a different way. The dependence of the rate of reaction on the initiation rate gives very definite information as to the nature of the termination step as will be seen from Equations (3), (5), and (6). These show that if termination is by destruction of two active species the reaction rate is proportional to the square root of initiation rate. Early in the development of photochemistry and photography a standard technique for altering the intensity of light was to rotate a slotted disc between the light source and the reaction system; the aperture of the disc was known so that the diminution in light intensity could be calculated. While a linear dependence of reaction rate on light intensity always gave a rate simply proportional to the aperture of the disc, this was not true when the square root law was obeyed (13). The theory was later worked out by Chapman (14) who was able to show that the method made it possible to evaluate the life time of the active species. This was first used to measure the life time of radicals in polymerization (15,16,17). Since these early beginnings the technique has become so widely used (18–23) that it is pertinent to sketch the theory and certain developments.

The simplest case to be considered is that for which the square root dependence holds, although, as is shown in Section IV.3, the method has general applicability to all reactions for which the rate is proportional to a

power of the light intensity less than unity. If we consider the ideal case, for which the ratio of dark to light periods is r, the rate of reaction for high speeds of sector rotation is

$$R_f = K[I/(r + 1)]^{1/2}$$

For very low speeds of rotation, the situation is equivalent to that of having the reaction taking place for $(r + 1)^{-1}$ of the time, so:

$$R_s = KI^{1/2}/(r + 1)$$

and thus

$$R_f/R_s = (r + 1)^{1/2}$$

In these expressions I is the intensity of illumination and K, a proportionality constant.

To develop the theory let us consider the simple reaction

$$C + h\nu \longrightarrow R \qquad (\text{rate} = R_i)$$

$$C + R \longrightarrow R \qquad (\text{rate} = k_p(C)(R))$$

$$R + R \longrightarrow \text{inactive products} \qquad (\text{rate} = k_t(R)^2)$$

where C is a molecule, R denotes similar radicals participating in the reaction, and k_p and k_t, the velocity constants for propagation and termination. When steady state conditions obtain, the concentration of radicals $(R)_s$, is easily shown to be

$$(R)_s = (R_i/k_t)^{1/2} \tag{10}$$

During the light flash the concentration of radicals is governed by

$$d(R)/dt = R_i - k_t(R)^2 \tag{11}$$

whence

$$(R) = (R)_s \tanh [(k_t R_i)^{1/2} t + C] \tag{12}$$

If λ is the duration of the light flash the average concentration of radicals is:

$$\bar{R}_t = (\lambda)^{-1} \int_0^{\lambda} (R)dt = (2k_t\lambda)^{-1} \ln \left\{ \frac{1 - [(R)_1/(R)_s]^2}{1 - [(R)_2/(R)_s]^2} \right\} \tag{13}$$

During the dark period

$$d(R)/dt = -k_t(R)^2$$

whence

$$(R)^{-1} = k_t t + C' \tag{14}$$

or using the conditions that at $t = 0$, $(R) = (R)_2$, $t = r\lambda$, $(R) = (R)_1$

$$(R)_1^{-1} - (R)_2^{-1} = rk_t\lambda \tag{15}$$

so that the mean concentration of radicals during the dark period is:

$$\bar{R}_d = (r\lambda)^{-1}\int_0^{r\lambda} R\, dt = (rk_t\lambda)^{-1} \ln [(R)_2/(R)_1] \tag{16}$$

The average radical concentration over the whole cycle is

$$\bar{R}_0 = (r + 1)^{-1}(\bar{R}_l + r\bar{R}_d) \tag{17}$$

or, on substitution of (13) and (16)

$$\bar{R}_0 = \frac{1}{2(r + 1)\lambda k_t}\left\{\ln \frac{1 - [(R)_1/(R)_s]^2}{1 - [(R)_2/(R)_s]^2} + \ln [(R)_2^2/(R)_1^2]\right\} \tag{18}$$

We now define a dimensionless parameter, m, as

$$m = \tanh^{-1}[(R)_2/(R)_s] - \tanh^{-1}[(R)_1/(R)_s] = k_t\lambda(R)_s = (R_ik_t)^{1/2}\lambda \tag{19}$$

Casting this in logarithmic form enables us to substitute for the first term in the bracket of Equation (18) whence substituting for $(R)_1$ using Equation (15)

$$\frac{\bar{R}_0}{(R)_s} = (r + 1)^{-1}\left\{1 + m^{-1} \ln \left[1 + \frac{rm}{1 + (R)_s/(R)_2}\right]\right\} \tag{20}$$

Also from Equations (15) and (19) we can show

$$\tanh^{-1} [(R)_2/(R)_s] - \tanh^{-1}\{[(R)_2/(R)_s]/[rm(R)_2/(R)_s + 1]\} = m \tag{21}$$

Converting this to exponential form and solving we obtain

$$\frac{(R)_2}{(R)_s} = \frac{rm \tanh m + [r^2m^2 \tanh^2 m + 4(rm + \tanh m) \tanh m]^{1/2}}{2(rm + \tanh m)} \tag{22}$$

Substitution of Equation (22) in (20) will yield $\bar{R}_0/(R)_s$ in terms of r and m only. If one can assume that the chains are long (and this is usually so), then to a good approximation the rate of reaction is proportional to radical concentration. Consequently we may replace $\bar{R}_0/(R)_s$ by the ratio of the average rate under intermittent illumination and the steady state rate.

Figure 1 shows the build up and decay of radical concentration during flashing cycles at low and high sector speeds. It will be seen that in the latter case the radical concentration oscillates about a mean position determined by the sector ratio. Figure 2 gives the values of $(R)_1/(R)_s$; $(R)_2/(R)_s$ and $\bar{R}_0/(R)_s$ as function of log m for $r = 3$ while Figure 3 shows the completed curves. In order that the relevant master curve should be

TABLE I. Values of $R_0/(R)_s$ as Function of m for Various Values of r

m	$r = 1$	$r = 2$	$r = 3$	$r = 4$	$r = 5$
Small	0.707	0.577	0.500	0.447	0.408
0.10	0.707	0.577	0.499	0.446	0.407
0.20	0.707	0.576	0.498	0.445	0.406
0.30	0.706	0.574	0.496	0.442	0.403
0.40	0.705	0.572	0.493	0.438	0.399
0.50	0.704	0.569	0.489	0.433	0.393
0.60	0.702	0.566	0.484	0.429	0.387
0.70	0.701	0.562	0.480	0.423	0.381
0.80	0.699	0.558	0.476	0.418	0.375
0.90	0.697	0.555	0.471	0.412	0.369
1.00	0.695	0.552	0.467	0.407	0.363
1.50	0.684	0.533	0.443	0.381	0.336
2.00	0.672	0.515	0.422	0.360	0.315
2.50	0.662	0.500	0.406	0.343	0.298
3.00	0.653	0.487	0.392	0.330	0.286
3.50	0.645	0.477	0.381	0.319	0.278
4.00	0.637	0.467	0.372	0.310	0.267
4.50	0.631	0.460	0.361	0.302	0.259
5.00	0.625	0.453	0.357	0.296	0.253
5.50	0.620	0.447	0.351	0.290	0.248
6.00	0.616	0.442	0.346	0.286	0.244
6.50	0.611	0.437	0.341	0.281	0.240
7.00	0.607	0.432	0.337	0.277	0.236
7.50	0.604	0.429	0.334	0.274	0.233
8.00	0.601	0.425	0.330	0.271	0.230
8.50	0.598	0.422	0.327	0.268	0.228
9.00	0.595	0.419	0.324	0.265	0.225
9.50	0.592	0.416	0.322	0.263	0.223
10	0.590	0.413	0.319	0.261	0.221
15	0.571	0.395	0.303	0.246	0.207
20	0.560	0.384	0.293	0.237	0.199
25	0.552	0.377	0.287	0.232	0.194
30	0.546	0.372	0.282	0.227	0.191
35	0.542	0.368	0.278	0.224	0.188
40	0.538	0.364	0.276	0.222	0.186
45	0.535	0.362	0.274	0.220	0.184
50	0.533	0.360	0.272	0.218	0.183
60	0.529	0.356	0.269	0.216	0.181
70	0.526	0.354	0.267	0.214	0.179
80	0.523	0.352	0.265	0.213	0.178
90	0.521	0.350	0.264	0.212	0.177
100	0.520	0.349	0.263	0.211	0.176
200	0.512	0.342	0.257	0.206	0.172
300	0.508	0.340	0.255	0.204	0.170
400	0.507	0.338	0.254	0.2033	0.1695
500	0.5065	0.3375	0.2533	0.2028	0.1690
600	0.5048	0.3369	0.2528	0.2024	0.1687
700	0.5042	0.3364	0.2525	0.2021	0.1684
800	0.5037	0.3361	0.2522	0.2018	0.1682
900	0.5034	0.3358	0.2520	0.2016	0.1680
1000	0.5031	0.3356	0.2518	0.2015	0.1679
High	0.5000	0.3333	0.2500	0.2000	0.1667

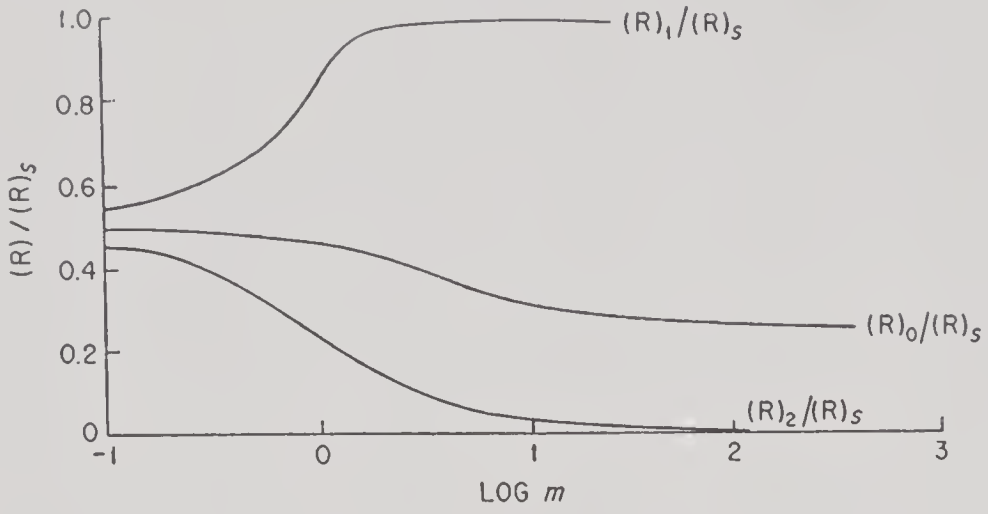

Fig. 2. $R_0/(R)_s$, $(R)_1/(R)_s$, and $(R)_2/(R)_s$ as functions of m for $r = 3$.

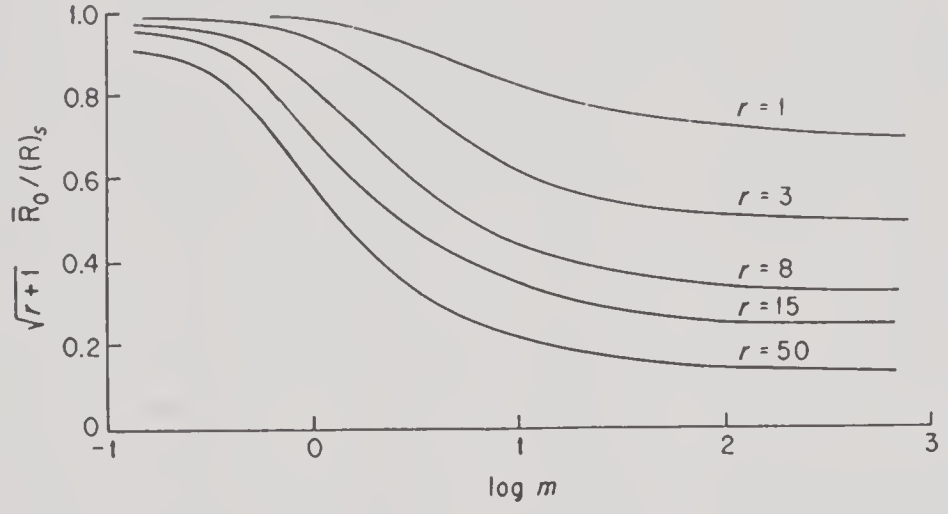

Fig. 3. Completed sector curves normalized to unity for various values of r.

available to all wishing to use the technique, the data are set out in Table I.

It is evident that experimental evaluation of the ratio of rates under intermittent and steady illumination will give a value for m either from a master curve or by interpolation in the tables, and consequently a relationship between m and the lifetime is required for evaluation of the latter quantity.

The definition of the lifetime, τ, given in Equation (9) is, in the symbols of this section,

$$\tau = (k_t R_i)^{-1/2} \tag{23}$$

which gives, using Equation (19),

$$m = \lambda/\tau \qquad \text{or} \qquad \tau = \lambda/m \tag{24}$$

2. Modification Allowing for Constant Dark Rate (20,24)

The analysis presented in Section IV.1 makes several implicit assumptions: (*1*) the reaction is free from any dark (thermal) rate; (*2*) generation of active centers is uniform throughout the reaction system; and (*3*) the flash of light has a "square wave form." By careful design of the apparatus and working conditions the last two assumptions may be realized, but it is not always possible to eliminate a thermal reaction, neglect of which can lead to erroneous results.

The generation of radicals in a dark reaction can be assumed to take place at a rate $n\mathrm{R}_i$ where R_i is, as before, the rate of photoinitiation. Then the radical concentrations during the light flash and dark period are governed by:

$$\text{light:} \quad d(\mathrm{R})/dt = (n+1)\mathrm{R}_i - k_t(\mathrm{R})^2 \tag{25}$$

$$\text{dark:} \quad d(\mathrm{R})/dt = n\mathrm{R}_i - k_t(\mathrm{R})^2 \tag{26}$$

Proceeding as in Section IV.1 we have

$$\bar{\mathrm{R}}_l = -(2k_t\lambda)^{-1} \ln \left\{ \frac{1 - [(\mathrm{R})_2/(\mathrm{R})_s]^2}{1 - [(\mathrm{R})_1/(\mathrm{R})_s]^2} \right\} \tag{27}$$

and

$$\bar{\mathrm{R}}_d = -(2k_t r\lambda)^{-1} \ln \left\{ \frac{1 - [(\mathrm{R})_2/(\mathrm{R})_s]^2[n/(n+1)]}{1 - [(\mathrm{R})_1/(\mathrm{R})_s]^2[n/(n+1)]} \right\} \tag{28}$$

We now require to define two dimensionless parameters m and m', m being as Equation (19) with $(n+1)\mathrm{R}_i$ in place of R_i and

$$m' = \tanh^{-1}\{[(n+1)/n]^{1/2}[(\mathrm{R})_2/(\mathrm{R})_s]\} - \tanh^{-1}\{[(n+1)/n]^{1/2}[(\mathrm{R})_1/(\mathrm{R})_s]\} = mr[n/(n+1)]^{1/2} \tag{29}$$

Using these definitions and replacing $[n/(n+1)]^{1/2}$ by z we get

$$\frac{\bar{\mathrm{R}}_0}{(\mathrm{R})_s} = (r+1)^{-1} \left\{ 1 + rz + m^{-1} \ln \left[\frac{1 + (\mathrm{R})_1/(\mathrm{R})_s}{1 + (\mathrm{R})_2/(\mathrm{R})_s} \right] \left[\frac{1 + z^{-1}(\mathrm{R})_2/(\mathrm{R})_s}{1 + z^{-1}(\mathrm{R})_1/(\mathrm{R})_s} \right] \right\} \tag{30}$$

Integrating Equation (25) and inserting boundary conditions gives

$$\frac{(\mathrm{R})_2}{(\mathrm{R})_s} = \frac{[(\mathrm{R})_1/(\mathrm{R})_s] + \tanh m}{1 + [(\mathrm{R})_1/(\mathrm{R})_s] \tanh m} \tag{31}$$

and similarly from Equation (26)

$$[(\mathrm{R})_2/(\mathrm{R})_s]\{z^{-2}[(\mathrm{R})_1/(\mathrm{R})_s] \tanh zrm - z^{-1}\} = \tanh zrm - z^{-1}[(\mathrm{R})_1/(\mathrm{R})_s]$$

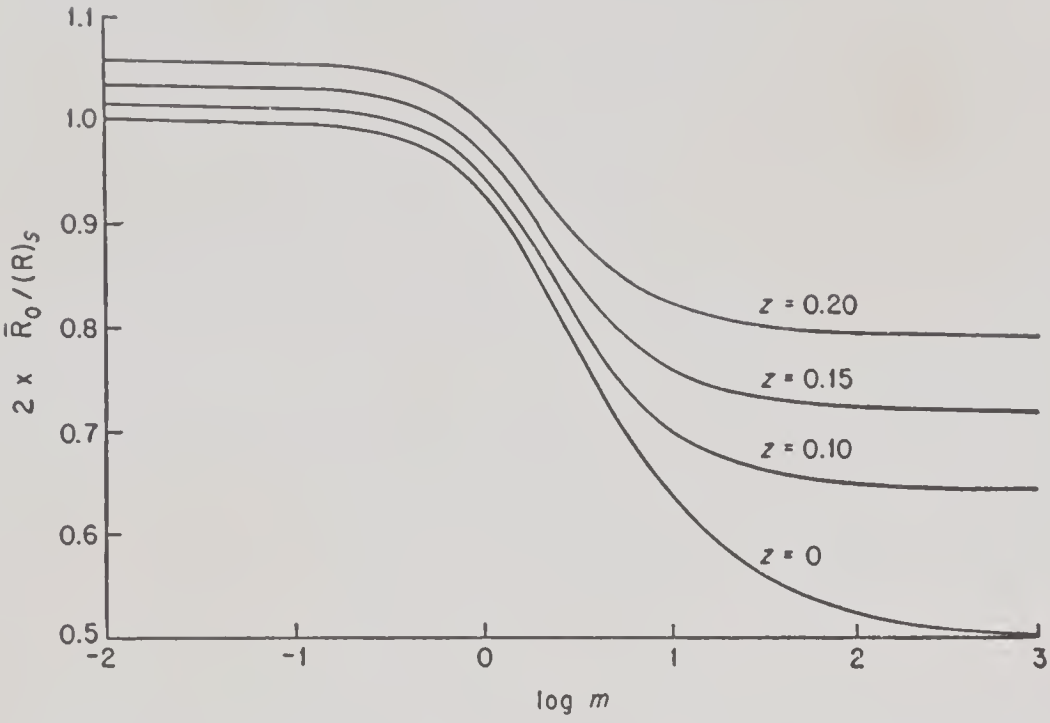

Fig. 4. Sector curves for simultaneous dark reaction for $r = 3$ and various values of z

Substitution for $(R)_2/(R)_s$ from Equation (31) leads to a quadratic in $(R)_1/(R)_s$ whose solution enables Equation (30) to be expressed in terms of z, r, and m only and m can be shown to have its former significance. Further one can show that the ratio of thermal rate, R_{th}, to photochemical rate, R_{ph}, is

$$R_{th}/R_{ph} = [n/(n+1)]^{1/2} = z \tag{32}$$

Figure 4 shows a selection of curves demonstrating the effect of increasing z on the rate under intermittent illumination. It is unlikely that neglect of the thermal rate will be significant in the estimation of lifetime provided $z < 0.05$ but this statement can be true only if the rate ratio lies close to the point of inflection of the curve.

3. General Theory for Simultaneous First- and Second-Order Terminations

For any chain reaction which shows the reaction rate to be proportional to some power of the initiation rate less than unity, intermittent illumination gives a variation in the reaction rate as the sector speed is altered. The analysis is necessarily complex and that followed in this section is a development (25) of earlier work (26). An exponent of the initiation rate lying between 0.5 and 1 is achieved if both first- and second-order termination operates as in the extended scheme

$C + h\nu \longrightarrow$	radical products	rate $= R_i$
$C + R \longrightarrow$	R	rate $= k_p(C)(R)$
$2R \longrightarrow$	inactive products	rate $= k_t(R)^2$
$R \longrightarrow$	inactive products	rate $= k_x(R)$

In the steady state, therefore,

$$R_i - k_t(R)_s^2 - k_x(R)_s = 0$$

whence

$$(R)_s = -(k_x/2k_t) + [(k_x^2 + 4k_tR_i)/4k_t^2]^{1/2} = \alpha - \beta \tag{33}$$

where

$$\alpha = (k_x^2 + 4k_tR_i)^{1/2}/2k_t \qquad \beta = k_x/2k_t \tag{34}$$

Equation (33) may be further simplified by writing $\beta/\alpha = \gamma$ to give

$$(R)_s = \beta(\gamma^{-1} - 1) \tag{33a}$$

During the light flash, the equation governing radical concentration is

$$d(R)/dt = R_i - k_t(R)^2 - k_x(R) \tag{34}$$

which integrates to give

$$\tanh^{-1}\{[(R) + \beta]/\alpha\} = k_t t + C' \tag{35a}$$

or

$$[(R) + \beta]/\alpha = p + \gamma = \tanh(\alpha k_t t + C') \tag{35b}$$

where $(R)/\alpha = p$.

Also, since $(R) = (R)_i$ at $t = 0$,

$$C' = \tanh^{-1}(p_1 + \gamma) \tag{36}$$

$$\bar{R}_l = -\beta + (k_t\lambda)^{-1} \ln [\cosh \alpha k_t\lambda(1 + \tanh \alpha k_t\lambda \tanh C')]$$

which using Equation (36) reduces to

$$\bar{R}_l = -\beta + \beta(\gamma m)^{-1} \ln \{\cosh m [1 + (p_1 + \gamma) \tanh m]\} \tag{37}$$

where

$$m = \alpha k_t\lambda \tag{38}$$

In the same way for the dark period

$$d(R)/dt = -k_t(R)^2 - k_x(R)$$

from which

$$(R) = 2\beta[\exp\{2\beta k_t t + C''\} - 1]^{-1} \tag{39}$$

As before $\bar{R}_d$ can be shown to be

$$\bar{R}_d = (rm\lambda)^{-1} \ln [(p_2 + 2\gamma)/(p_1 + 2\gamma)] \tag{40}$$

Combination of Equations (37) and (40) gives the average radical concentration over the cycle as

$$\bar{R}_0 = (r+1)^{-1}\{-\beta + \beta(\gamma m)^{-1} \ln [\cosh m\,(1 + (p_1 + \gamma)\tanh m)] + \beta(\gamma m)^{-1} \ln [(p_2 + 2\gamma)/(p_1 + 2\gamma)]\} \quad (41)$$

or using Equation (33a):

$$\bar{R}_0/(R)_s = (r+1)^{-1}(\gamma^{-1} - 1)^{-1}\{-1 + (\gamma m)^{-1} \ln [\cosh m\,(1 + (p_1 + \gamma)\tanh m]\,[(p_1 + 2\gamma)/(p_2 + 2\gamma)]\} \quad (42)$$

Substituting the conditions $(R) = (R)_1$ when $t = 0$; $(R) = (R)_2$ at $t = \lambda$ in Equation (35a) followed by elimination of C', gives

$$\tanh^{-1}(p_2 + \gamma) - \tanh^{-1}(p_1 + \gamma) = m$$

or

$$(p_2 + \gamma) = (p_1 + \gamma + \tanh m)/1 + (p_1 + \gamma)\tanh m \quad (43)$$

Similarly since $(R) = (R)_2$ when $t = 0$, $(R) = (R)_1$ when $t = r\lambda$, elimination of C'' from (39) gives

$$p_2(p_1 + 2\gamma)/p_1(p_2 + 2\gamma) = \exp\{2\gamma rm\} \quad (44)$$

Solving Equations (43) and (44) gives

$$p_1 = [a - (a^2 - 4bc)^{1/2}]/2b$$

$$p_2 = \frac{2\gamma \exp\{2\gamma rm\}\,[a + (a^2 - 4bc)^{1/2}]}{1 - \exp\{2\gamma rm\}\,[a + (a^2 - 4bc)^{1/2}] + 4\gamma b} \quad (45)$$

where:

$$a = -\tanh m\,(1 - 3\gamma^2) - 2\gamma + \exp\{2\gamma rm\}\,[(1 + \gamma^2)\tanh m + 2\gamma]$$

$$b = -1 + \gamma \tanh m + \exp\{2\gamma rm\}(1 + \gamma \tanh m)$$

$$c = 2\gamma(1 - \gamma^2)\tanh m.$$

Substitution in Equation (41) gives $\bar{R}_0/(R)_s$ in terms only of r, m, and γ.

For a very fast rotating sector the radical concentration is as Equation (33) with $R_i(r+1)^{-1}$ in place of R_i:

$$(R) = -\beta + [k_x^2 + 4k_t R_i(r+1)^{-1}]^{1/2}/2k_t = -\beta + \{(r+1)^{-1}(r\beta^2 + \alpha^2)\}^{1/2} \quad (46)$$

Hence

$$R_\infty/(R)_s = [-1 + \{(r+1)^{-1}(r + \gamma^{-2})\}^{1/2}]/(\gamma^{-1} - 1) \quad (47)$$

Thus experimental measurement of $R_\infty/(R)_s$ will give a measure of γ. Table II gives $R\infty/(R)_s$ for various γ and r which is useful in the application of the technique.

TABLE II

$R_\infty/(R)_s$ as a Function of γ for Various Values of r

γ	$r = 1$	$r = 2$	$r = 3$	$r = 4$	$r = 5$
0	0.7071	0.5773	0.5000	0.4472	0.4082
0.05	.6922	.5566	.4757	.4204	.3798
0.10	.6784	.5368	.4527	.3957	.3537
0.15	.6647	.5179	.4313	.3728	.3301
0.20	.6526	.5000	.4115	.3521	.3090
0.25	.6385	.4832	.3932	.3333	.2903
0.30	.6260	.4674	.3764	.3164	.2737
0.35	.6142	.4526	.3611	.3014	.2591
0.40	.6027	.4390	.3471	.2879	.2462
0.45	.5975	.4260	.3344	.2757	.2348
0.50	.5812	.4142	.3229	.2649	.2288
0.55	.5767	.4031	.3124	.2552	.2158
0.60	.5615	.3928	.3028	.2464	.2078
0.65	.5526	.3834	.2940	.2385	.2007
0.70	.5437	.3747	.2860	.2314	.1943
0.75	.5356	.3664	.2787	.2249	.1885
0.80	.5275	.3590	.2720	.2190	.1833
0.85	.5200	.3520	.2659	.2136	.1785
0.90	.5130	.3451	.2600	.2087	.1742
0.95	.5060	.3392	.2550	.2042	.1703
1.00	.5000	.3333	.2500	.2000	.1667

Provided γ is known measurement of $\bar{R}_0/(R)_s$ can give m utilizing data such as those shown in Table III. Thus since $m = \alpha k_t \lambda$ we have a measure of αk_t. Now

$$\alpha k_t = (k_x^2 + 4k_t R_i)^{1/2}/2 = m/\lambda = \xi \tag{48}$$

and

$$\gamma = \beta/\alpha = k_x/(k_x^2 + 4k_t R_i)^{1/2} \tag{49}$$

whence

$$2\gamma\xi = k_x \tag{50}$$

Also squaring (48) we have

$$\xi^2 = k_t R_i + k_x^2/4 \tag{51}$$

so a plot of ξ^2 against R_i gives a straight line of slope k_t and intercept $k_x^2/4$, so that both k_t and k_x may be evaluated.

TABLE III

Values of $R_0/(R)_s$ as a Function of m for Various Values of γ ($r = 3$)

m	0.0	0.1	0.2	0.3	0.4	0.5
0.1	0.499	0.451	0.411	0.376	0.346	0.321
0.2	0.498	0.450	0.409	0.375	0.346	0.320
0.3	0.496	0.449	0.407	0.372	0.343	0.319
0.4	0.493	0.445	0.404	0.369	0.341	0.318
0.5	0.489	0.441	0.400	0.366	0.338	0.315
0.6	0.484	0.435	0.396	0.361	0.335	0.312
0.7	0.480	0.429	0.392	0.356	0.332	0.308
0.8	0.476	0.423	0.386	0.352	0.327	0.305
0.9	0.471	0.417	0.381	0.348	0.323	0.302
1.0	0.467	0.411	0.376	0.344	0.320	0.293
2.0	0.422	0.360	0.333	0.307	0.291	0.279
3.0	0.392	0.340	0.307	0.291	0.281	0.270
4.0	0.372	0.320	0.293	0.281	0.276	0.265
5.0	0.357	0.310	0.286	0.276	0.272	0.262
6.0	0.346	0.300	0.280	0.272	0.268	0.259
7.0	0.337	0.292	0.278	0.268	0.265	—
8.0	0.330	0.288	0.274	0.265	0.263	—
9.0	0.324	0.284	0.271	0.263	0.261	—
10.0	0.319	0.281	0.269	0.261	—	—
20.0	0.293	0.265	0.258	—	—	—
40.0	0.276	—	—	—	—	—
60.0	0.269	—	—	—	—	—
80.0	0.265	—	—	—	—	—
100.0	0.263	—	—	—	—	—

To facilitate the evaluation of m, Table III gives $\bar{R}_0/(R)_s$ as a function of m for various values of γ for $r = 3$. It will be noted from this table that as the value of γ increases, i.e., when the proportion of first order termination becomes relatively great the utility of the method is much reduced as the difference between the limiting values of the ratio becomes small.

4. Nonuniformity of Radical Generation

Since the absorption of light by a medium follows an exponential law it is evident that as the extinction coefficient increases there will be a greater tendency for light to be preferentially absorbed at the fact of the reaction vessel nearer the lamp. This means that the volume in which the reaction takes place will be less than the total volume of the reactant. In general if

$$I/I_0 = 10^{-\epsilon cd}$$

where the symbols have their usual significance, the value of ϵ should not exceed 0.01 to ensure that in a depth of 3 cm. not more than 10% of the

incident light is adsorbed. Under conditions of weak absorption the tacit assumption regarding uniform generation of centers is valid.

Two simple experimental tests may be applied to show that the radicals are generated uniformly. In the first test the two reaction vessels used are so designed as to give very different light paths. If absorption is slight the rate of reaction will be independent of the vessel size but if absorption is high the rate of reaction in the smaller vessel will apparently be greater than in the larger. This is essentially a qualitative test although a rough measure of the effective volume can be deduced from the measurements. A quantitative method has been evolved which is quite simple to apply (27). The reaction system is irradiated first by one lamp and then by two identical lamps operating on opposite sides of the vessel. If absorption is small, then effectively the intensity of illumination is doubled so that with two lamps the rate is $\sqrt{2}$ times that with one lamp. If absorption is confined to only a very small skin, then when two lamps are used two reactions occur independently in the same vessel, so that the rate with two lamps is twice that with one.

The situation can be analysed very simply in the following way. We assume that the position of a radical alters little during its life time. In liquids it is almost certain that diffusion movement will be slight but should convection occur this assumption might become invalid. At any point in the reaction vessel of length d, the total radiation from two identical source operating on either side of the vessel is

$$I_x = I_0[\exp\{-kx\} + \exp\{-k(d - x)\}]$$

where x is the distance from one lamp. For a single lamp

$$I_x = I_0 \exp\{-kx\}$$

Since the concentration of radicals is proportional to the square root of the light intensities the total concentration of radicals for one lamp is:

$$(\mathrm{R})_{\mathrm{I}} = KI_0^{1/2} \int_0^d \exp\{-kx/2\}\,dx$$

and for both lamps:

$$(\mathrm{R})_{\mathrm{II}} = KI_0^{1/2} \int_0^d [\exp\{-kx\} + \exp\{-k(d - x)\}]^{1/2}dx$$

Figure 5 shows a series of curves for various values of d.

Now if the rate of reaction for one lamp is v_1 and for both lamps v_2 it can be shown that the extent to which the two beams cross, i.e., the amount of interference between the reaction zones is

$$Z = (2v_1 - v_2)/0.414\,v_2$$

Figure 6 shows a plot of the interference against effective reaction volume. From this figure the necessary corrections to rate data may be carried out.

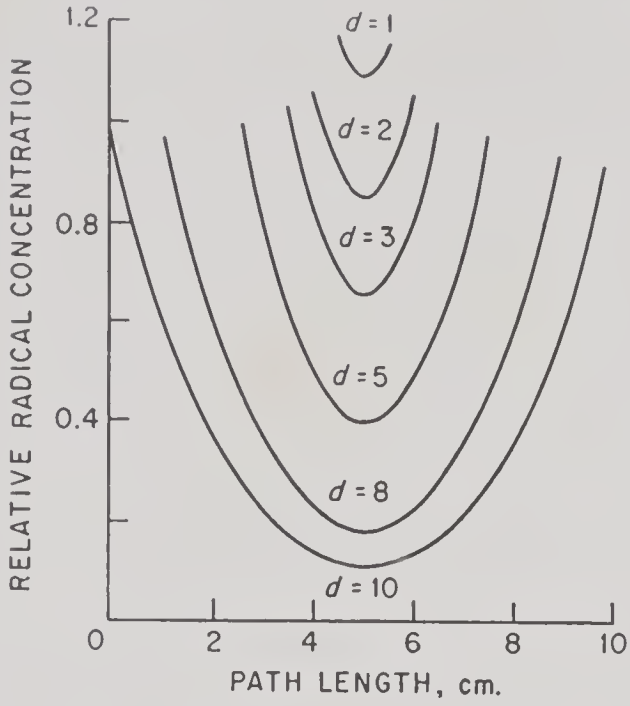

Fig. 5. Radical concentration for two light sources for various path lengths ($k = 1$).

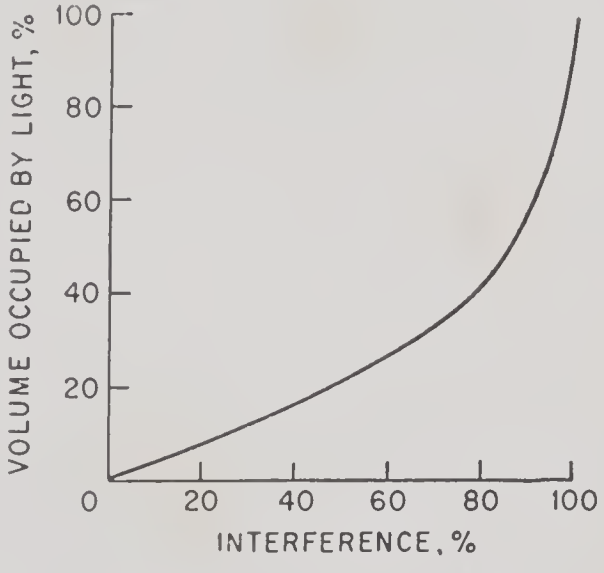

Fig. 6. Relationship between interference and effective volume within which reaction takes place.

A more elegant theory has been worked out in considerable detail for the reaction between chlorine and carbon monoxide sensitized by light of 3,650 A. (28). The data in this paper relate to the correction of the sector theory for $r = 3$ using a reaction mixture containing 300 mm. chlorine at 25°C. in a cell 20 mm. deep and is, therefore, of only limited applicability.

5. "Square Wave" Light Pulses

It is much more convenient to design an apparatus to give instantaneous switching from light to dark and vice versa. If however this is not possible

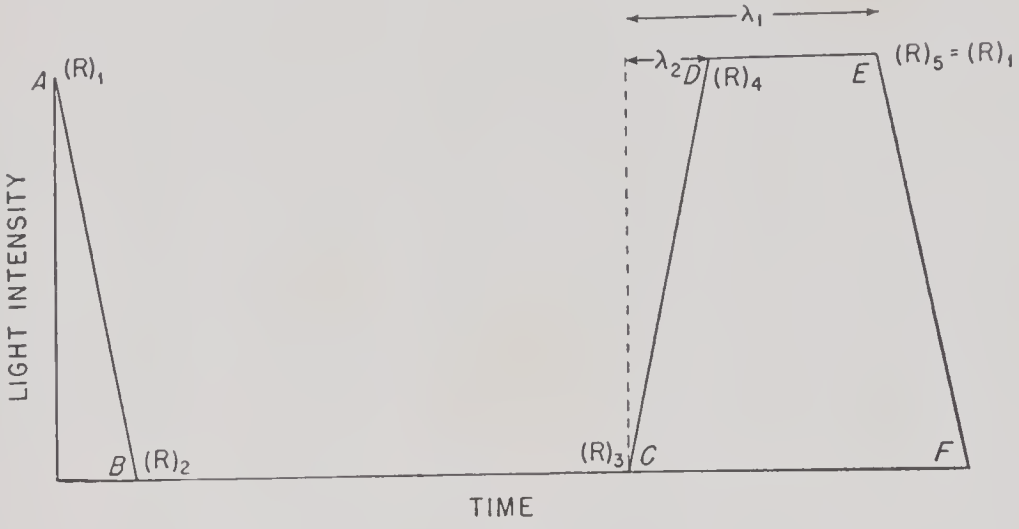

Fig. 7. "Trapezoidal" light flash.

it is necessary for allowance to be made for the build up and decay of the light intensity. The analysis has been set out by Burns & Dainton (28). Assuming the build up to full intensity is linear we can adopt the wave form of Figure 7 as being applicable. Then the following equations have to be considered:

$$d(\mathrm{R})/dt = [\mathrm{R}_i(\lambda_2 - t)/\lambda_2] - k_t(\mathrm{R})^2 \qquad \text{(from A to B)} \qquad (52)$$

$$d(\mathrm{R})/dt = -k_t(\mathrm{R})^2 \qquad \text{(from B to C)} \qquad (53)$$

$$d(\mathrm{R})/dt = \mathrm{R}_i t/\lambda_2 - k_t(\mathrm{R})^2 \qquad \text{(from C to D)} \qquad (54)$$

$$d(\mathrm{R})/dt = R_i - k_t(\mathrm{R})^2 \qquad \text{(from D to E)} \qquad (55)$$

Equations (53) and (55) have already been dealt with. To solve Equations (52) and (54) it is necessary to substitute $k_t(\mathrm{R}) = x^{-1}(dx/dt)$ when the solution for x is a power series in t. The mean values of the radical concentrations which are found by graphical integration or direct calculation are:

$$(\mathrm{R})_2/(\mathrm{R})_s = \{\Sigma_1 + [(\mathrm{R})_1/(\mathrm{R})_s]\Sigma_3\}/\{\Sigma_2 + [(\mathrm{R})_1/(\mathrm{R})_s]\Sigma_4\} \qquad (56)$$

$$(\mathrm{R})_3/(\mathrm{R})_s = [(\mathrm{R})_s/(\mathrm{R})_2 + rm - a]^{-1} \qquad (57)$$

$$(\mathrm{R})_4/(\mathrm{R})_s = \{\Sigma_1 + [(\mathrm{R})_3/(\mathrm{R})_s]\Sigma_3\}/\{\Sigma_2 + [(\mathrm{R})_3/(\mathrm{R})_s]\Sigma_4\} \qquad (58)$$

$$(\mathrm{R})_f/(\mathrm{R})_s = (\mathrm{R})_1(\mathrm{R})_s = \tanh\{(m - a) + \tanh^{-1}[(\mathrm{R})_4/(\mathrm{R})_s]\} \qquad (59)$$

where $a = m/f$ and $f = \lambda/\lambda_2$ in which λ_2 is the time of traverse.

$$\Sigma_1 = a/2 + a^3/(2\cdot3\cdot5) + a^5/(2\cdot3\cdot5\cdot6\cdot8) + a^7/(2\cdot3\cdot5\cdot6\cdot8\cdot9\cdot11) + \ldots$$

$$\Sigma_2 = 1 + a^2/3 + a^4/(3\cdot4\cdot6) + a^6/(3\cdot4\cdot6\cdot7\cdot9) + \ldots$$

$$\Sigma_3 = 1 + a^2/2\cdot3 + a^4/(2\cdot3\cdot5\cdot6) + a^6/(2\cdot3\cdot5\cdot6\cdot8\cdot9) + \ldots$$

$$\Sigma_4 = a + a^3/(3\cdot4) + a^5/(3\cdot4\cdot6\cdot7) + a^7/(3\cdot4\cdot6\cdot7\cdot9\cdot10) + \ldots$$

TABLE IV

Radical Concentrations Calculated for Trapezoidal Light Pulses

m	λ_1/λ_2	a	$(R)_1/(R)_s$	$(R)_2/(R)_s$	$(R)_3/(R)_s$	$(R)_4/(R)_s$	$(R)_5/(R)_s$
1	40	0.025	0.8466	0.8406	0.2401	0.2511	0.8430
1	20	0.05	0.8466	0.8353	0.2411	0.2630	0.8297
1	10	0.10	0.8466	0.8248	0.2432	0.2865	0.8270
4	40	0.10	1.0000	0.9531	0.07723	0.1263	0.9994
4	20	0.20	1.0000	0.9119	0.07754	0.1750	0.9993
4	10	0.40	1.0000	0.8429	0.07820	0.2688	0.9991
10	40	0.25	1.0000	0.8929	0.03239	0.1557	1.0000
10	20	0.50	1.0000	0.8131	0.03254	0.2735	1.0000
10	10	1.00	1.0000	0.7014	0.03287	0.4787	1.0000
40	40	1.00	1.0000	0.7014	0.00830	0.4615	1.0000
40	20	2.00	1.0000	0.5752	0.00835	0.7352	1.0000
40	10	4.00	1.0000	0.4592	0.00846	0.9134	1.0000

TABLE V

Areas under the Various Sections of the Curve for Trapezoidal Light Pulses

m	λ_1/λ_2	A − B	B − C	C − D	D − E	Sum	Ideal	Error
1	40	0.0211	1.2532	0.0061	0.5872	1.8676	1.8652	0.0034
1	20	0.0421	1.2427	0.0124	0.5742	1.8714	1.8652	0.0062
1	10	0.0835	1.2213	0.0257	0.5460	1.8765	1.8652	0.0113
4	40	0.0976	2.5133	0.0094	3.3267	5.9470	5.9456	0.0014
4	20	0.1909	2.4652	0.0221	3.2690	5.9472	5.9456	0.0016
4	10	0.3659	2.3775	0.0568	3.1459	5.9461	5.9456	0.0005
10	40	0.2359	3.3175	0.0183	9.2014	12.7727	12.7726	0.0001
10	20	0.4487	3.2189	0.0567	9.0485	12.7728	12.7726	0.0002
10	10	0.8252	3.0621	0.1890	8.6972	12.7726	12.7726	0.0000
40	40	0.8252	4.4372	0.1667	38.6867	44.1158	44.1109	0.0049
40	20	1.4572	4.2330	0.5787	37.9383	44.2072	44.1109	0.0963
40	10	2.4820	3.9946	0.7128	35.9557	44.1451	44.1109	0.0342

The areas under the curves for the various regions are:

(A-B) estimated using Simpson's rule

(B-C) $k^{-1} \ln [(R)_2/(R)_s]$

(C-D) $k^{-1} \ln [\Sigma_3 + (R)_3/(R)_s \Sigma_4]$

(D-E) $k^{-1} \ln \{\cosh (m - a) + [(R)_4/(R)_s] \sinh (m - a)\}$

It will be noted from the data of Tables IV and V that there is a compensation over the periods of high sector speeds but that the effect of deviation from square wave form is more marked at low speeds.

V. EXPERIMENTAL METHODS

The range of lifetimes which may be encountered in practice but is also subject to the experimental conditions as is obvious from Equation (23). For the application of intermittent illumination this fact is not of prime importance although it will govern the precise form of the experimental arrangement. The apparatus suitable for lifetimes less than 2 seconds or so will be described first. For these a rotating slotted disc suffices to produce a range of flashing lines essential for a complete analysis of the reaction.

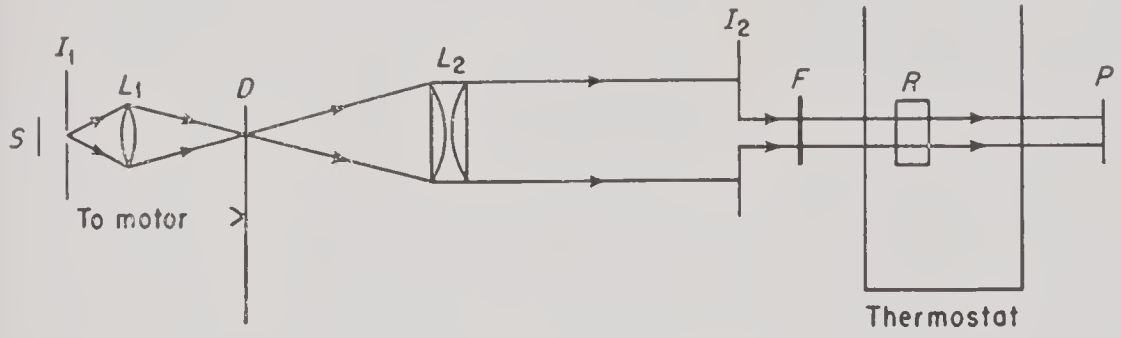

Fig. 8. Experimental arrangement using rotating sector.

Figure 8 shows an arrangement by which the main assumptions of the theoretical section regarding "squareness" of waveform and uniformity of the illumination over the beam are met. The light source, S, must be small so that it is most convenient to use a compact source mercury arc lamp. Commercial lamps of this type usually have an arc length of 2–3 mm. and about 2 mm. (maximum) breadth. The light from this source is brought to a focus by means of the lens, L_1, in such a manner as to produce an image with a minimum dimension of the order of 0.1 mm. The function of the iris, I_1, is to cut down parasitic light which would tend to enlarge the image. The sector disc, D, is placed at the focal position and is arranged to cut the smallest dimension of the image. The light is then condensed by lens, L_2, and the dimensions of the beam defined by iris, I_2. After passing through a filter (if required) the light falls on the reaction system in a suitable thermostat. It is convenient to mount a photocell behind the reaction vessel for the purpose of monitoring the light beam.

Some parts of this system require consideration in greater detail. The light source must be capable of giving a steady output, so that it is essential to shield from draft and to use a constant electrical supply. Several circuits have been devised to give a stability of about 1%; those employing a transducer seem to be the most successful. The lenses in ultraviolet work at short wavelengths must be fused quartz, but if wavelengths above,

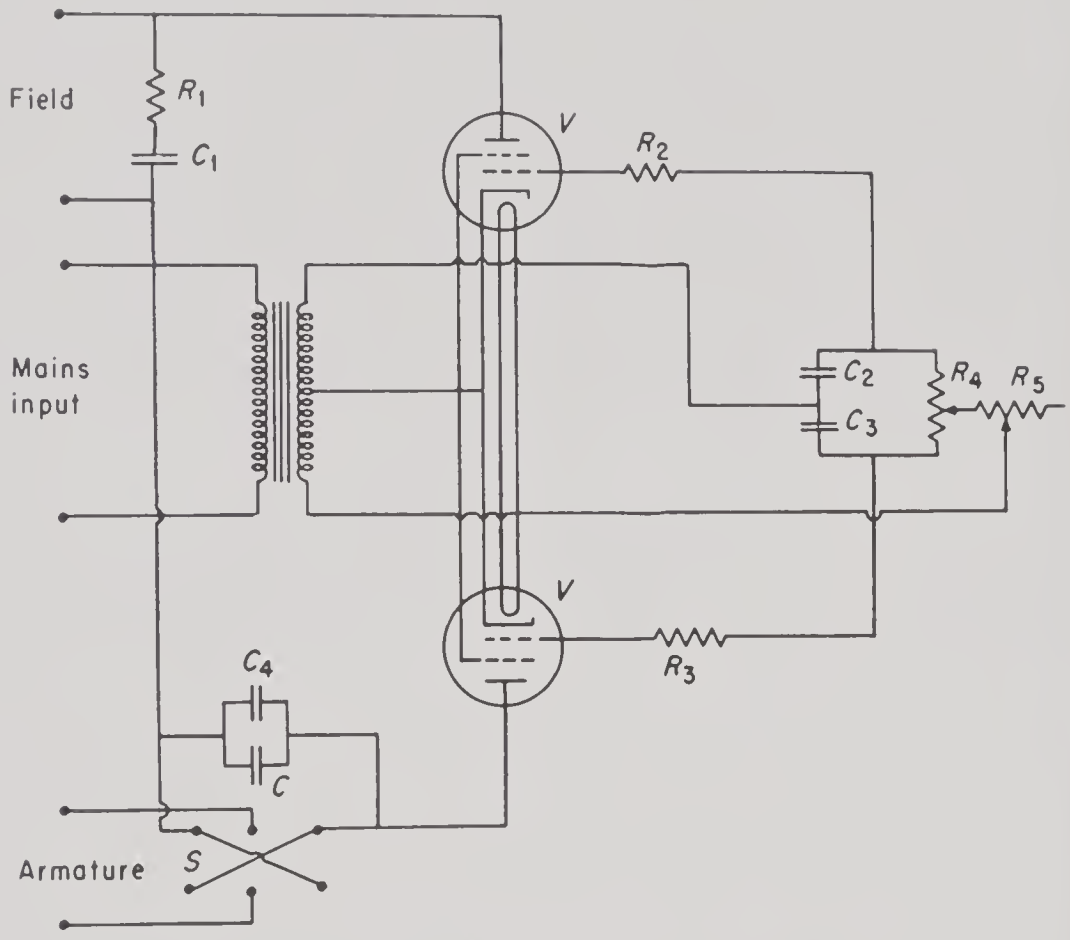

Fig. 9. Motor control circuit.

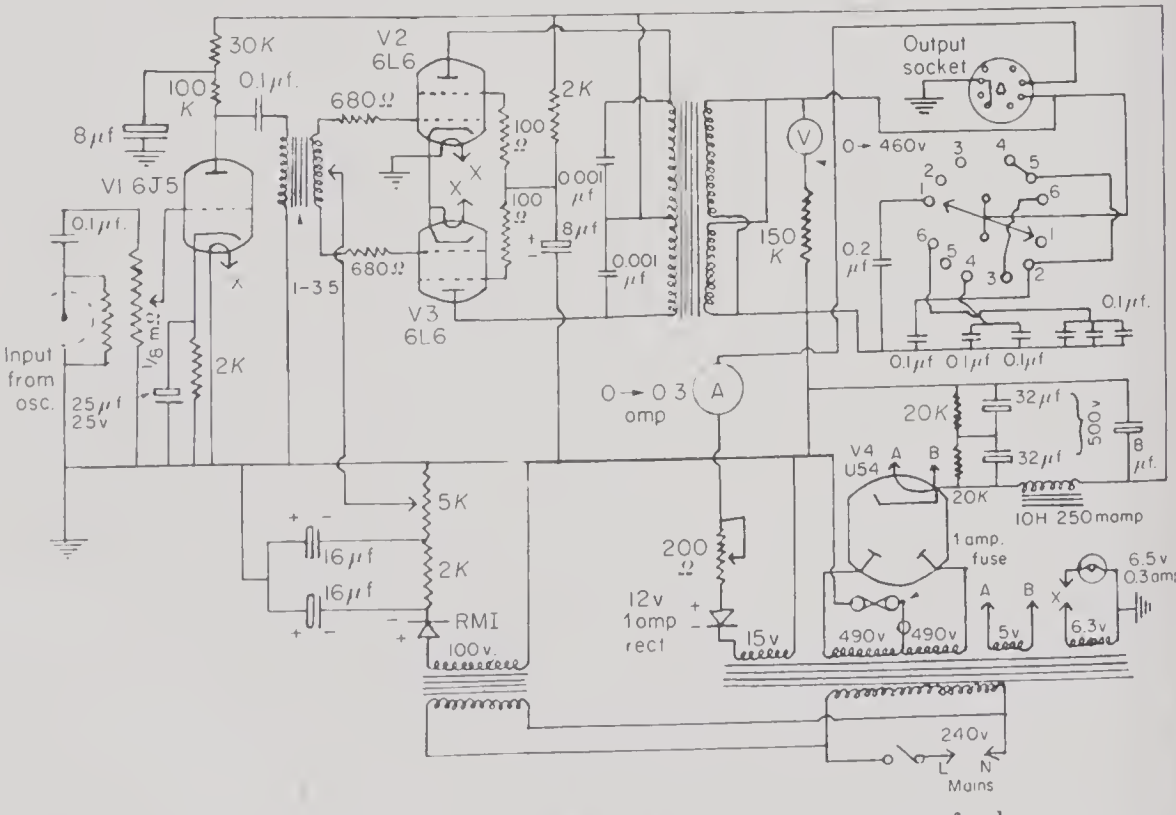

Fig. 10. Wide band amplifier suitable for phonic motor feed.

say, 3,000 A. are being used it is possible to replace quartz by a hard glass or by some transparent plastics, e.g., Lucite (Perspex).

The major problem in the design of the apparatus is the production of the light pulses. This requires that the sector be driven at a constant speed and be free from any internal instability. It would be best to use a solid, transparent disc with the sectors blacked out, but this obviously raises difficulties in the choice of a suitable material transparent to the light used: some plastic materials would probably be suitable. More generally a metal disc is used from which sectors are cut. Under these circumstances the perimeter ought to be weighted in order to achieve smooth rotation. The choice of the ratio, r, is also worthy of close consideration. Differentiation of Equation (20) with respect to r shows that the slope of the central portion of the curve increases with r making it easier to differentiate between two relatively close flashing times. The disadvantage of using high values of r is obvious in that the overall rate of reaction is very much reduced; thus, some compromise is necessary in order to achieve a reasonable rate coupled with a convenient slope of the central section. If dark reaction is appreciable, then it has greater importance as r increases as will be seen from Equation (30). As a general principle, values of r greater than 3 are unnecessary.

Since the duration of the light flash must be stable throughout a run and also be variable with fairly wide limits, it is necessary to pay particular attention to the control of the motor driving the sector disc. Figure 9 shows a motor control circuit designed to give motor speeds controlled to within 2% over a 20-fold range. More recently special synchronous motors capable of locking to feed frequencies between 50 and 2,000 cycles have become available. This automatically gives a 40-fold speed range which may be increased by the use of suitable gear train. The use of such phonic motors involves the design of stable oscillators and wide band amplifiers: a suitable circuit for the latter is shown in Figure 10.

It is necessary to measure the duration of the light flash. This is a relatively simple procedure and a number of methods have been used, e.g., by stroboscope or tachometer. With the advent of electronic scaling units designed for high speed counting, signals from a photocell mounted as in Figure 8 could be used to evaluate the speed of rotation of the disc and hence the duration of the flash.

If the lifetime becomes longer than say 5 seconds it is no longer possible to use the simple rotating disc device described above mainly because of inherent mechanical deficiencies. For excessively long exposures it is probably most convenient to use a manual technique, timing the exposure by means of a stop watch, but such a method is tedious and places an undesirable strain on the operator. Probably the best method would be an

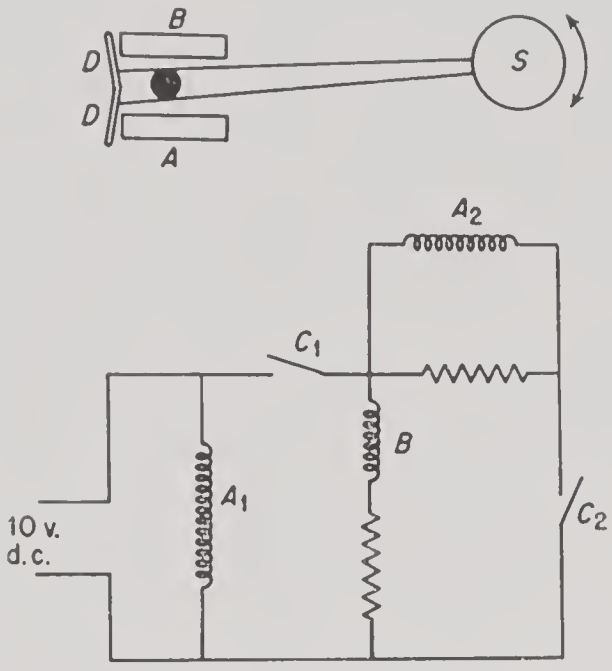

Fig. 11. Shutter arrangement for intermittent illumination.

adaptation of the standard "maltese cross" device of cinema photography. In such a system the motor would have to drive a series of cams which may be changed as required and actuate a relay so that the disc rotates by a series of flicks. In this way the sector cuts through the light source at high speed and so retains the square wave pulse. In a similar way use could be made of focal plane shutters operated magnetically. A suitable arrangement is shown in Figure 11.

VI. THE NONSTATIONARY STATE

1. Introduction

As a consequence of their nature, chain reactions require a finite time in which to achieve their maximum (steady state) rate. Under normal conditions it is not possible to detect these small natural induction periods because of the experimental difficulty of achieving simultaneously high resolution in time and high sensitivity in detection of reaction. Once these two conditions have been met by the design of very specialized equipment, the detection of the induction period and indeed the analysis of the reaction course during short intervals of time has been found to be possible.

The first demonstration of the time-lag just mentioned is due to Weigert and Kellermann (29) who, using a spark of controllable discharge time, were able to show that the steady state of the hydrogen-chlorine reaction

did not occur until between 0.01 and 0.025 second after the commencement of initiation. This experiment afforded good supporting evidence for the theory but did not give the possibility of measurement of the induction period with any degree of precision. Semenov (30) carried through a formal analysis of the phenomenon which was used semiquantitatively by Kowalsky (31) in an investigation of the reaction between hydrogen and oxygen. Pressure changes were recorded on a moving down recorder with considerable accuracy, over a period of about 0.3 second. Recently considerable activity in this type of precision measurement has been undertaken more particularly in the fields of oxidation (32–35) and polymerization (36–48), with evidence of a new approach to purely gas phase reactions (49).

In this chapter we will deal specifically with oxidation and gas phase processes, while polymerization will be dealt with in more detail in Chapter XXI.

2. Theory of Nonstationary State (36)

To obtain a clearer idea of the various principles involved in the experimental techniques a short account of a simple analysis will be given. In the first instance it is assumed that termination of chains is bimolecular so that during the initial stages we have as before:

$$d(\mathrm{R})/dt = \mathrm{R}_i - k_t(\mathrm{R})^2$$

which on integration yields

$$(\mathrm{R}) = (\mathrm{R})_s \tanh (t/\tau)$$

where $(\mathrm{R})_s$ is steady state concentration of active species (i.e., $(\mathrm{R})_s = (\mathrm{R}_i/k_t)^{1/2}$), τ is the average chain life time ($\tau = (k_t\mathrm{R}_i)^{-1/2}$). For small amount of change, such as would obtain during the nonstationary part of the reaction, the fraction F of conversion is given by

$$F = k_p k_t^{-1} \ln [\cosh (t/\tau)] \tag{60}$$

whence for $\tau \ll t$,

$$F = k_p k_t^{-1} (t/\tau - \ln 2) \tag{61}$$

This predicts a linear plot of F against t for a given value of R_i. The intercept of the line on the time axis is a measure of $\tau \ln 2$ whence both τ and $k_p k_t^{-1}$ are accessible.

As we have already seen in Section IV.3 the usefulness of the rotating sector method diminishes as the amount of linear (first-order) termination increases, and it should be in such circumstances that the importance of the

nonstationary state approach ought to be greatest. Suppose the termination step to be

$$\mathrm{R} + \mathrm{X} \rightarrow \text{inactive products} \qquad k_t'$$

Then by the same type of analysis as above it can be shown that

$$F = [(k_p \mathrm{R}_i/k_t'(X)t - k_p \mathrm{R}_i/k_t'^2(X)^2][1 - \exp\{-k_t'(X)t\}] \qquad (62)$$

After the source of initiation has been removed the reaction proceeds at a decreasing rate. The relevant equations governing the diminution in rate are:

$$\text{mutual termination:} \qquad d(\mathrm{R})/dt = -k_t(\mathrm{R})^2$$

$$\text{linear termination:} \qquad d(\mathrm{R})/dt = -k_t(\mathrm{R})(X)$$

Solution of these equations is most clearly expressed in terms of the rate of reaction, i.e.,

$$\text{mutual termination:} \qquad r_t^{-1} - r_s^{-1} = k_p k_t^{-1}(\mathrm{A})^{-1}t \qquad (63)$$

$$\text{linear termination:} \qquad \ln r_t = \ln [k_p/k_t'(\mathrm{A})] - k_t(X)t \qquad (64)$$

where (A) is the initial concentration of the reactant. From (64) it is obvious that $\ln r_t$ is a linear function of t where r_t is the rate at time t after switching off the light. The slope of this line is $k_t'(X)$ so that the rate constant k_t' is easily determined as is k_p from measurement of the appropriate intercept.

3. Application to Gas Phase Reactions

Except for the early investigations of Kowalsky which have already been mentioned the activity in this field has been limited. This may in part be because many simpler gas phase reactions do not involve very long reaction chains and so very stringent demands are imposed on the performance of the detection apparatus. Moseley and Robb have ingeniously circumvented these difficulties and produced an elegant system with the required performance.

In essence the apparatus consists of a thin steel diaphragm, 0.001 in. in thickness, which will respond to pressure changes by alteration in shape. The extent of movement of the center of the circular diaphragm was determined by the change in capacity of the condenser formed between the diaphragm and a small probe, $^1/_{16}$ in. in diameter. Using a diaphragm 4 cm. in diameter a pressure change of 10^{-4} mm. produces a displacement of about 10^{-3} mm. at the center of the diaphragm, which is well within the range of detection. Capacity changes were measured using 100 Mc./

second oscillations, using standard tuned circuit technique. By using cathode ray oscilloscope display the response of the apparatus was better than 10^{-3} second.

One of the major difficulties in this type of work lies in the dissipation of the heat of reaction. It is usually, if not always, impossible to remove the heat sufficiently quickly so that inevitably the pressure change due to the evolution of heat is added to that due to the reaction. In the cases investigated the pressure change due to the temperature change was found to be about seven times greater than that due to reaction. It is therefore necessary to work under adiabatic conditions and measure the induction of the temperature rise and by making allowance for the pressure changes due to reaction the true induction period and reaction rate may be determined. Using these methods Moseley and Robb have determined the rate constant for the recombination of methyl radicals generated by the photolysis of acetone. The value of the rate constant was found to be $3.8 \pm 1.2 \times 10^{10}$ l. mole^{-1} sec.$^{-1}$ which is in reasonable agreement with the values given by Gomer and Kistiakowsky (50) and Durham and Steacie (51).

4. Oxidation by Gaseous Oxygen

Oxidation of olefins and aldehydes in the liquid phase by gaseous oxygen follows this reaction scheme:

Let RH represent the olefin or aldehyde. The initial step is the production of the radical R· the subsequent reactions being

$$\mathrm{R}\cdot + \mathrm{O_2} \longrightarrow \mathrm{RO_2}\cdot \qquad k_2$$

$$\mathrm{RO_2}\cdot + \mathrm{RH} \longrightarrow \mathrm{RO_2H} + \mathrm{R}\cdot \qquad k_3$$

$$\left.\begin{array}{l} 2\mathrm{R}\cdot \\ \mathrm{RO_2}\cdot + \mathrm{R}\cdot \\ 2\mathrm{RO_2}\cdot \end{array}\right\} \longrightarrow \text{inactive products} \qquad \begin{array}{l} k_4 \\ k_5 \\ k_6 \end{array}$$

Using the usual stationary state approximation the rate of hydroperoxide production, which is essentially the rate of oxygen uptake since the reaction chains are sufficiently long, is

$$d(\mathrm{RO_2H})/dt = k_3(\mathrm{RH})(\mathrm{O_2})R_i^{1/2}\{k_2^{-2}k_3^{2}k_4(\mathrm{RH})^2 + 2k_2^{-1}k_3k_5(\mathrm{RH})(\mathrm{O_2}) + k_6(\mathrm{O_2})^2\}^{-1/2} \qquad (65)$$

At high oxygen pressures the equation reduces to

$$d(\mathrm{RO_2H})/dt = k_3k_6^{-1/2}(\mathrm{RH})\mathrm{R}_i^{1/2} = r \qquad (66)$$

while at low pressures

$$d(\mathrm{RO_2H})/dt = k_2k_i^{-1/2}(\mathrm{O_2})\mathrm{R}_i^{1/2} \qquad (67)$$

In the former case the rotating sector technique has been successfully applied but in the low pressure region (Equation 67) this has not been found possible. Two different methods of approach have been adopted of which the simpler is due to Bateman and Gee (35) while Bamford and Dewar's method is the simpler in principle for their investigations in polymerization (see Chapter XXI).

As has been stated in Section VI.2, the rate of reaction diminishes relatively slowly after photoinitiation is stopped, and this may be followed in terms of the oxygen absorption. Bateman and Gee define a quantity, I_d, the photochemical after effect, as

$$I_d = (r - r_D)dt \tag{68}$$

where r_D is the steady dark rate. Now if the rate of thermal initiation is R_{iD}, adaptation of Equation (66) gives

$$r_D = k_3 k_s^{-1/2}(\mathrm{RH})R_{iD}^{1/2} \tag{69}$$

The overall rate at any instant can be written as

$$r = k_3(\mathrm{RO_2}\cdot)(\mathrm{RH}) \tag{70}$$

while during the after effect

$$d(\mathrm{RO_2}\cdot)/dt = (dr/dt)k_3^{-1}(\mathrm{RH})^{-1} = R_{iD} - k_6(\mathrm{RO_2}\cdot)^2 \tag{71}$$

Combination of Equations (69–71) yields

$$dr/dt = k_3^{-1}k_6(\mathrm{RH})^{-1}(r_D^2 - r^2) \tag{72}$$

whence

$$I_d = \int_{r_L}^{r_D} [(r - r_D)/(dr/dt)]dr = k_3 k_6^{-1}(\mathrm{RH}) \ln [(r_L + r_D)/2r_D] \tag{73}$$

In the same way a growth intercept may be defined as

$$I' = k_3 k_6^{-1}(\mathrm{RH}) \ln [2r_L/(r_L + r_D)] \tag{74}$$

In the very important low pressure region the dark reaction rate is

$$r_D = k_2 k_4^{-1/2}(\mathrm{O_2})R_{iD}^{1/2}$$

and the overall rate is essentially

$$r = k_2(\mathrm{R}\cdot)(\mathrm{O_2})$$

In this instance the very low oxygen pressures used means that it is no longer possible to consider the oxygen pressure as remaining constant even during the nonstationary stage of the reaction. Indeed both (R·) and

(O_2) will change so that a new variable $x = r/(O_2) = k_2(R\cdot)$ is introduced, whence

$$dx/dt = k_4k_2^{-1}(x^2 - x_D^2)$$

for the decay reaction.

The variation of oxygen pressure with time however is not nearly so simple in either case, since it is found that the measurement of the intercepts is influenced by two main factors to a greater or less extent. Use is made of the disappearance of oxygen as a measure of the rate of reaction but this is only true if the concentration of oxygen in solution remains constant. In general the concentration of oxygen in the stationary state, C, will be less than that associated with a quiescent system saturated with oxygen, C_0. If ΔC is a measure of the differences and provided the solution obeys Henry's law, the rate of solution is k_sC_0, where k_s is a factor dependent upon the rate of shaking. Oxygen will be lost from solution partly by reaction and partly by evaporation (rate $= k_sC$) whence

$$r = k_s\Delta C \tag{75}$$

During the nonstationary stage the oxygen concentration in solution will change and it is evident from (75) that during the change from dark to light reaction the concentration will decrease by $(r_L - r_D)/k_s$. Hence if I_d' and I_ϱ' are the measured intercepts it is convenient to use the difference to give a diminution in error, i.e.,

$$I_d' - I_\varrho' = k_3k_6^{-1}(RH) \ln [(r_L + r_D)/4r_Lr_D] \tag{76}$$

In similar manner at low pressure the oxygen uptake is given by

$$d(O_2)/dt = k_sC_0 - (O_2)(k_s + x) \tag{77}$$

The equations given for low pressure reaction are not readily handled but may be expressed as a summation whereby k_4/k_2 is expressed as a function of $(I_d - I_\varrho)$.

The technique has been applied with some success to the oxidation of ethyl linoleate and digeranyl (52) to give a good evaluation of all the rate constants for the oxidation process. The velocity constants for oxidation at 25°C. are as follows.

	$10^6\,k_2$	k_3	$10^6\,k_4$	$10^6\,k_5$	$10^6\,k_6$
Ethyl linoleate	9	10	20	50	30
Digeranyl	1	3	0.9	9	9

Two interesting points emerge from these figures. In the first instance the value of k_2, i.e., the addition of oxygen to the radical R·, is very large

compared with the hydrogen abstraction process k_3. The magnitude of k_3 largely determines the oxidizability of the hydrocarbon. Secondly, the high value of k_4 in the case of ethyl linoleate is surprising since it might have been expected that high k_3 would be associated with low k_4 although it is obvious that steric and other effects must play a considerable part in determining the reactivity. It is probably also noteworthy that as in copolymerization processes the rate constant for interaction of unlike radicals is usually greater than those for the radical interaction.

References

1. S. Foord, *J. Chem. Soc. London*, 1940, 48.
2. G. M. Burnett and H. W. Melville, *Proc. Roy. Soc. London*, A189, 456 (1947).
3. W. Kern and K. Feuerstein, *J. prakt. Chem.*, 158, 186 (1941).
4. H. W. Melville and W. F. Watson, *Trans. Faraday Soc.*, 44, 886 (1948).
5. J. C. Bevington, *J. Chem. Soc.*, 1956, 3506.
6. R. N. Haward, private communication on the use of furfurylidene maleonitrile.
7. F. R. Mayo and R. A. Gregg, *J. Am. Chem. Soc.*, 70, 1284 (1948).
8. P. D. Bartlett, G. S. Hammond, and H. Kwart, *Discussions Faraday Soc.*, 2, 342 (1947).
9. H. R. Cooper and H. W. Melville, *J. Chem. Soc. London*, 1951, 1993.
10. T. A. Ingles and H. W. Melville, *Proc. Roy. Soc. London*, A218, 163 (1953).
11. P. R. Cowley and G. M. Burnett, *Trans. Faraday Soc.*, 49, 1409 (1953).
12. See, for example, J. C. Bevington, J. H. Bradbury, and G. M. Burnett, *J. Polymer Sci.*, 12, 449 (1954).
13. A. Berthou and H. Bellenot, *Helv. Chim. Acta*, 7, 307 (1924).
14. D. L. Chapman, F. Briers, and E. Walters, *J. Chem. Soc. London*, 1926, 562.
15. H. W. Melville, *Proc. Roy. Soc. London*, A163, 151 (1937).
16. T. T. Jones and H. W. Melville, *ibid.*, A175, 392 (1940).
17. H. W. Melville, Tilden Lecture, *J. Chem. Soc. London*, 1941, 414.
18. G. M. Burnett and H. W. Melville, (a) *Nature*, 156, 661 (1945); (b) *Proc. Roy. Soc. London*, A189, 456 (1947).
19. B. D. Bartlett and C. G. Swain, *J. Am. Chem. Soc.*, 67, 2273 (1945); 68, 2381 (1946).
20. L. Bateman and G. Gee, *Proc. Roy. Soc. London*, A195, 391 (1948).
21. J. L. Bolland, *Quart. Rev. London*, 3, 1 (1949). (Review of oxidation processes.)
22. G. M. Burnett, *ibid.*, 4, 292 (1950). (Review of polymerization processes.)
23. G. M. Burnett and H. W. Melville, *Chem. Revs.*, 54, 225 (1954).
24. M. S. Matheson, E. B. Bevilacqua, E. E. Auer, and E. J. Hart, *J. Am. Chem. Soc.*, 71, 497 (1948).
25. G. M. Burnett and W. W. Wright, *Proc. Roy. Soc. London*, A221, 37 (1954).
26. (a) D. L. Chapman and F. Briers, *J. Chem. Soc. London*, 1928, 1802; (b) O. K. Rice, *J. Chem. Phys.*, 10, 440 (1942).
27. G. M. Burnett, H. W. Melville, and L. Valentine, *Trans. Faraday Soc.*, 45, 960 (1949).
28. W. G. Burns and F. S. Dainton, *Trans. Faraday Soc.*, 46, 411 (1950).
29. F. Weigert and K. Kellermann, *Z. physik. Chem.*, 107, 1 (1923).
30. N. Semenov, *Chemical Kinetics and Chain Reactions*, Chapter II, Clarendon Press, Oxford, 1935.

31. A. Kowalsky, *Physik. Z. Sowjetunion*, **4**, 723 (1933).
32. C. H. Bamford and M. J. S. Dewar, *Proc. Roy. Soc. London*, **A198**, 252 (1949).
33. L. Bateman and G. Gee, *Trans. Faraday Soc.*, **47**, 155 (1951).
34. L. Bateman, J. L. Bolland, and G. Gee, *Trans. Faraday Soc.*, **47**, 274 (1951).
35. L. Bateman, G. Gee, A. L. Morris, and W. F. Watson, *Discussions Faraday Soc.*, **10**, 250 (1951).
36. G. M. Burnett, *Trans. Faraday Soc.*, **46**, 772 (1950).
37. W. H. Stockmayer, *J. Chem. Phys.*, **12**, 143 (1944).
38. D. W. E. Axford, *Proc. Roy. Soc. London*, **A197**, 374 (1949).
39. C. H. Bamford and M. J. S. Dewar, *Nature*, **158**, 380 (1946).
40. C. H. Bamford and M. J. S. Dewar, *Discussions Faraday Soc.*, **2**, 314 (1947).
41. C. H. Bamford and M. J. S. Dewar, *Proc. Roy. Soc. London*, **A192**, 309 (1948).
42. C. H. Bamford and M. J. S. Dewar, *Proc. Roy. Soc. London*, **A197**, 356 (1949).
43. G. Dixon-Lewis, *Proc. Roy. Soc. London*, **A198**, 510 (1949).
44. N. Grassie and H. W. Melville, *Proc. Roy. Soc. London*, **A207**, 285 (1951).
45. T. G. Majury and H. W. Melville, *Proc. Roy. Soc. London*, **A205**, 309 (1951).
46. W. I. Bengough and H. W. Melville, *Proc. Roy. Soc. London*, **A230**, 429 (1955).
47. S. Fujii, *Bull. Chem. Soc. Japan*, **27**, 238 (1954).
48. H. Mayama, *ibid.*, **29**, 711 (1956).
49. F. R. Moseley and J. C. Robb, *Proc. Roy. Soc. London*, in press.
50. R. Gomer and G. B. Kistiakowsky, *J. Chem. Phys.*, **19**, 85 (1951).
51. R. W. Durham and E. W. R. Steacie, *J. Chem. Phys.*, **20**, 582 (1952).
52. L. Bateman, G. Gee, A. L. Morris, and W. F. Watson, *Discussions Faraday Soc.*, **10**, 250 (1951).

CHAPTER XXI

Polymerization and Polymer Reactions

G. M. BURNETT, *University of Aberdeen, Scotland*

I. Introduction 1140
II. Isolation and Purification of Polymers 1141
1. Precipitation 1141
2. Fractionation of High Polymers 1142
3. Chromatographic Procedures 1144
4. Fractional Solution or Extraction 1145
5. "Crystallization" Chromatography 1145
6. Paper Strip Chromatography 1146
7. Separation of Mixed Polymers 1146
8. Drying of Polymers 1148
III. Condensation Polymerization 1149
1. General Principles 1149
2. Production of Polymers 1150
3. Factors Influencing Reaction Velocity 1151
4. Products of Condensation Polymerization 1152
5. Kinetics of Simple Condensation Polymerization 1153
6. Treatment of Data 1155
7. Interchange Reactions 1156
8. Three Dimensional Polymers 1157
IV. Radical Addition Polymerization 1160
1. Nature of the Reaction 1160
2. Measurement of Reaction Rate 1163
3. Initiation Reaction 1167
4. Termination Mechanism 1172
5. Transfer Mechanism 1173
6. Rate Constants for Homopolymerization 1175
V. Copolymerization 1181
1. Copolymer Composition Equation 1181
2. Determination of Monomer Reactivity Ratios 1184
3. Rates of Reaction 1186
4. Block and Graft Copolymers 1189
VI. Emulsion Polymerization 1193
1. Qualitative Theory 1193
2. Quantitative Theory 1195
3. Experimental Investigations 1196
VII. Ionic Polymerization 1197
1. Carbonium Ion Reactions 1197
2. Anionic Polymerization 1200
3. "Living" Polymers 1201
4. Ionic Copolymerization 1203

VIII. Stereospecific Polymerization 1204
1. Tacticity 1204
2. Catalytic Systems 1205
3. Experimental Techniques 1207
4. Allied Reactions 1208
5. Reaction of Polar Monomers 1210
IX. Degradation of Polymers 1210
1. Hydrolytic Degradation 1210
2. Thermal Degradation 1214
3. Photochemical Degradation 1216
4. Mechanical Degradation 1217
5. Oxidative Degradation 1218
References 1220

I. INTRODUCTION

Any attempt to establish the mechanism of a polymerization reaction, in which a high polymer containing many monomeric units is produced, requires, in general, the application of techniques specially designed for the problem in hand.

To clarify the situation it is best to commence by defining the various types of polymerization processes which are well established. There are two main classes of polymerization, i.e., condensation reactions which are essentially stepwise in character and are repetitive simple organic condensation processes; addition polymerization involving unsaturated monomers which proceed by a chain mechanism in which the chain carrier can be either an ion or a free radical. In order to elucidate a mechanism completely it is necessary to study not only the kinetic characteristics of the process but also to examine the product more particularly with regard to its molecular weight.

High polymers are notoriously ill-defined compounds when compared with simple substances. The molecules in any given specimen vary over a wide range of sizes; they frequently have some elements of irregularity in their structure produced by minor reactions. Of recent years, the most marked change in approach to the study of large molecules and their production has been a tendency towards higher precision more particularly in the definition of the structure of the molecules.

As far as this chapter is concerned, the techniques dealing with the study of reactions involving the creation and destruction of polymeric molecules will be considered in some detail. The third possible type of reaction, i.e., intermolecular processes involving large molecules, has been but little studied and indeed it is doubtful if any comprehensible results would be obtained in view of the complexity of such reactions involving, as they

must, the participation of many hundreds of functional groups attached to one and the same molecule. Also in contrast to simple molecules it is not possible to avoid environmental changes by working at high dilution since the multiplicity of substituents will always be constrained in such a way as to remain in the same locality giving rise therefore to high local concentrations. This point may well be of importance in interpreting the phenomenon of branched chain polymers.

II. ISOLATION AND PURIFICATION OF POLYMERS

1. Precipitation

Polymeric molecules possessing more than a few monomer units are characterized by having a negligible vapor pressure and no (or little) tendency to separate from solution in a crystalline form. For these reasons the standard techniques of purification used by the organic chemist are denied to the high polymer chemist. The problem is to separate substances not attached to the polymer, and at the same time it is frequently desirable to be able to retain the low molecular weight fraction of the polymeric material.

The most widely used technique of isolation has involved the precipitation of the polymer by pouring a solution of it into a liquid which will mix with the polymer solvent but is not a solvent for the polymer. It is naturally necessary to choose as precipitant a liquid which will dissolve all the impurities expected in the polymer. This procedure can be affected by (*a*) the concentration of polymer solution, (*b*) the rate and method of mixing, and (*c*) the temperature of precipitation.

If polymer solutions are too concentrated the polymer comes down as a gummy material partly due to lack of efficient mixing of solution and precipitant and partly to a natural tendency for the polymer to retain quantities of solvent. On the other hand if the polymer solution is too dilute, the precipitate may be so finely divided as to make handling very awkward. The optimum conditions are difficult, if not impossible, to predict and must be reached by trial. Good stirring is always essential in successful separation and is all the more necessary for polymers with low softening points, e.g., polyvinyl acetate. A procedure especially applicable to this polymer involves its precipitation from toluene solution added slowly to cooled *n*-hexane with violent stirring (1). The material so produced is light and fibrous in appearance and readily goes into solution in suitable solvents.

Repeated cycles of precipitation are effective in obtaining polymer almost completely free from small molecules. Kern and Kammerer (2)

showed that *p*-bromobenzoyl peroxide could be removed from polymethyl methacrylate by precipitating twelve times with carbon disulfide from toluene solution. High temperature precipitation is more effective when impurities are likely to be adsorbed tenaciously (3). In some instances it is essential that the polymer is freed from even small amounts of the initiator used in polymerization (see Section IV.3). It has been found that with 2,2′-azoisobutyronitrile, the unused initiator can be effectively removed by leaching the polymer with boiling water (4). Using isotopically labelled initiator, the efficacy of the procedure can be stringently tested. Table I affords a demonstration of the validity of the technique, when applied to an artificial mixture of initiator and polymer. A similar type of test was applied to the standard precipitation method with the same kind of result (5).

TABLE I
Extraction of 2,2′-Azoisobutyronitrile with Boiling Water

No. of extractions	Radioactive count rate per min.	Mole initiator ÷ mole polymer
0	37,900[a]	0.125
10	341	1.13×10^{-3}
20	156	5.15×10^{-4}

[a] After one precipitation with methanol from benzene followed by freeze drying the benzene solution.

Normally, low molecular weight material is the most soluble and consequently might be lost in the separation procedure. For many purposes it is essential that such losses should be avoided; this may however be achieved by careful selection of precipitant. For example, Schulz and Husemann (6) demonstrated that polystyrene is completely precipitated from toluene solution by methanol. This was verified by the fact that above a certain volume of methanol further additions gave no increase in the weight of polymer recovered.

2. Fractionation of High Polymers (7)

It is occasionally necessary to prepare samples of polymer of more uniform molecular size than would be obtained from a reaction. This is normally accomplished by a rather hazardous procedure of fractional precipitation followed by a refractionation of the cuts so obtained. In essence the principle of the process is that the least soluble high molecular weight material will be ejected from solution first—to be followed by the lower

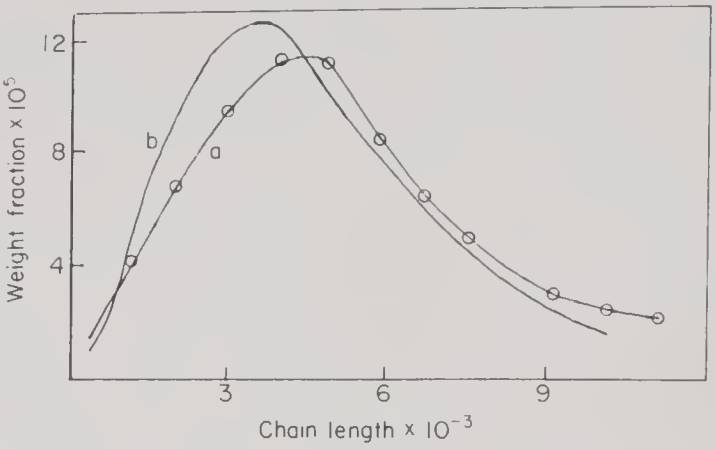

Fig. 1. Differential molecular weight distribution for polymethyl methacrylate determined by precipitation. (a) experimental, (b) theoretical.

molecular weight polymer. By careful working reasonably good cuts with sharp distribution can be obtained but the procedure is of necessity somewhat laborious.

The usual type of method is to add precipitant to the stirred polymer solution until a slight turbidity is obtained. The practice, in order to achieve equilibrium between the two phases, is to warm the solution to homogeneity and allow precipitation to occur gradually on slow cooling of the system to the temperature of the fractionating bath. The solution is stirred slowly during this process but, when complete, stirring is discontinued and the precipitated phase is allowed to settle over a period of up to 24 hours; the supernatant liquid is removed and the process repeated.

In fact, the process which has been described essentially effects the separation into two liquid layers, the one relatively rich in polymer being described as the precipitate. It is inescapably true that all species irrespective of molecular weight are soluble in the two phases, but it turns out that the smaller molecules have about the same concentration in the two phases. Thus in order to achieve the most nearly ideal separation the original solution must be kept very dilute and the ratio of the volumes of supernatant to precipitated phases at least as great as ten. Any one of the fractions obtained may be subjected to refractionation along the lines suggested.

Figure 1 shows results obtained from the fractionation of polymethyl methacrylate by such a procedure (8). It will be noted that the agreement with theory is reasonably good, but it is comparatively rare that such a state of affairs is found.

If the polymer can occur in crystalline form it is preferable to adopt conditions which will allow the polymer to separate as a totally amorphous liquid. This is extremely difficult, if not impossible to achieve. If

crystallization takes place then it is likely that the rate of crystallization will play a dominant part in the separation process. Fractional precipitation of crystalline polymers such as cellulose acetate, nitrocellulose, high melting polyamides, and polyvinylide chloride is extremely inefficient and may produce anomalies such as middle cuts having higher molecular weight than the initial fractions (9).

A method which is based essentially on the fractional precipitation procedure is turbidimetric titration of very dilute solution of polymer (0.01 g./100 ml. or less). The precipitant is added slowly with constant stirring at a fixed temperature, and the turbidity due to precipitation is measured by the diminution in the intensity of transmitted light. An empirical correlation between the concentration of precipitant and molecular weight of polymer fraction must first be established. The experimental curve can be converted to an integral (cumulative) distribution curve from which the differential distribution can be found. This method was originally suggested by Morey and Tamblyn (10) and has been successfully applied to polyvinyl acetate (11), nitrocellulose (12), and polymethyl methacrylate (13).

3. Chromatographic Procedures (14)

The theories of chromatographic separation need not concern us here and are, in any event, available in extended form in a companion volume (15). The great advantage of the method lies in its high selectivity enabling separation of very closely allied materials to be effected with ease. This selectivity emboldened polymer chemists, as early as 1936, to use the technique for fractionation purposes (16) but their efforts met with little success and the method was abandoned. However, in an elegant series of researches, Claesson (17) was successful in applying frontal analysis methods to achieve a fractionation of nitrocellulose from acetone, synthetic rubbers from benzene, and polyvinyl acetate from acetone.

In his experiments Claesson did not achieve 100% recovery of his polymer from activated carbon columns, but in 1952 Williams (18,19) showed that nylon could be recovered entirely from celite columns using formic acid. As a result it became possible to make use of elution or displacement chromatography. It was also demonstrated that, in the same solvent, molecules of differing molecular weights traversed the column at different rates—the small molecules travelling more rapidly. Since nylon could be fractionated by precipitation from formic acid solution with water, it was likely that gradient elution would achieve still better separation with an increasing gradient of formic acid in water. The technique was moderately successful in separating two samples of average molecular weights

35,000 and 15,000, but partial hydrolysis tended to produce both small and intermediate size molecules. Successful separation of low molecular weight silicones was achieved from animal charcoal columns using a gradient of diethyl ether in methanol.

4. Fractional Solution or Extraction

As we have already seen the very small solubility difference between molecules of the same species but of differing size may be utilized in the fractional precipitation of polymers. In like manner these same small differences make it possible to carry out fractionation by extraction. The genesis of the modern methods lies in the work of Desreux (20,21). The method is to pack a column with celite or fine sand on which the polymer has been precipitated, and to extract by continuously varying solvent mixtures. This is not a chromatographic procedure but it does yield fractions of high homogeneity and is claimed to be superior to fractional precipitation. Fuchs (22) utilized essentially the same technique but deposited the polymer in a thin film on metal foil.

5. "Crystallization" Chromatography

This type of separation procedure bears several experimental similarities to the methods of Desreux and Fuchs, but differs from them in that the latter are essentially one stage procedures carried out under nonequilibrium conditions. This new method, due to Baker and Williams (23), uses a column packed with a completely inert supporting material (usually glass beads of about 0.1 mm. diameter) on which the material under study can "crystallize." The column is fitted with a jacket so arranged that the top of the column is held at a higher temperature than the foot. As with gradient elution, a progressively improved solvent is passed down the column, which then virtually consists of a series of filter beds at different temperatures. It is easy to see that a simple substance will travel down such a column in a series of transfers between precipitated phase and saturated solution and will emerge in saturated solution at the foot of the column. In this way a polymer would be subjected to a vast number of fractional precipitations so that one might reasonably expect efficient separation.

Figure 2 shows the results obtained with polystyrene, in which comparison is made with the theoretical distribution calculated from the kinetic data for the polymerization. Fractionation was carried out with a solvent gradient of methyl ethyl ketone in ethanol and a temperature gradient of 60–10°C. The claims that the method gives much superior fractionation

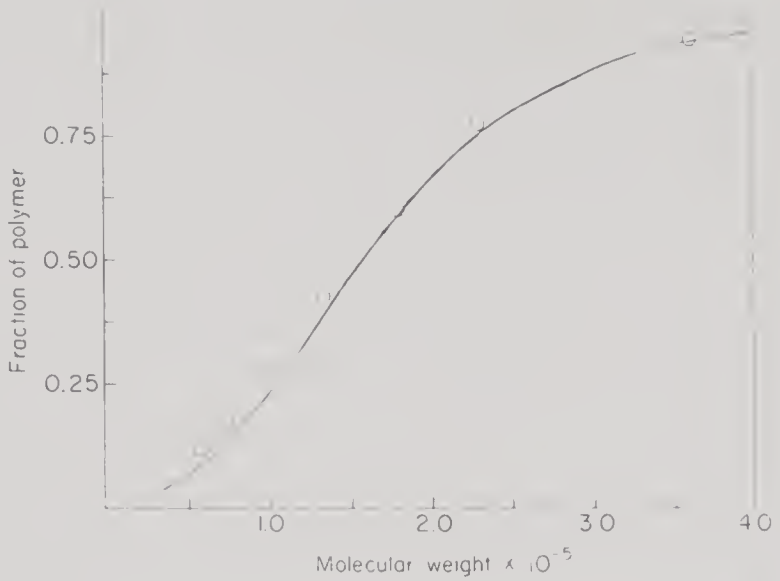

Fig. 2. Molecular weight distribution of polystyrene from "crystallization" chromatography (23). Solid line denotes the theoretical curve.

to fractional extraction and also greater homogeneity of fractions than batch precipitations appear to be totally vindicated. The degree of homogeneity found is independent of the source of the polymer

6. Paper Strip Chromatography

Little use has been made of paper strip chromatography although some work on separation of polymer types has been reported (24,25). Caplan (14) has been able to achieve moderate separation of molecular sizes. In this instance the polymer used was polysarcasine dimethylamide. This material is known to have a very sharp—near Poisson—distribution (26) and it has been shown that three polymers of average molecular weights 12,000, 5,000, and 1,500 may readily be separated. The polymer was prepared from monomer labelled with C^{14} which enabled the paper strip to be scanned radiometrically.

7. Separation of Mixed Polymers

Growth of interest in the preparation and properties of graft and block copolymers has posed a considerable problem in the separation of the desired material from other polymers (homopolymers) formed during the preparation. In the past, the main concern has been to remove small molecules from the polymer for which, as we have seen, a number of possible techniques is available.

The new situation has been met in part at least by adaptation of the procedures described in the preceding sections.

Conventional fractional precipitation and solution procedures have been used with limited success (27,28). Indeed the solution technique was a failure because of the ease with which dried down dispersions of certain polymers were redispersed in extracting solvents or mixtures of solvents.

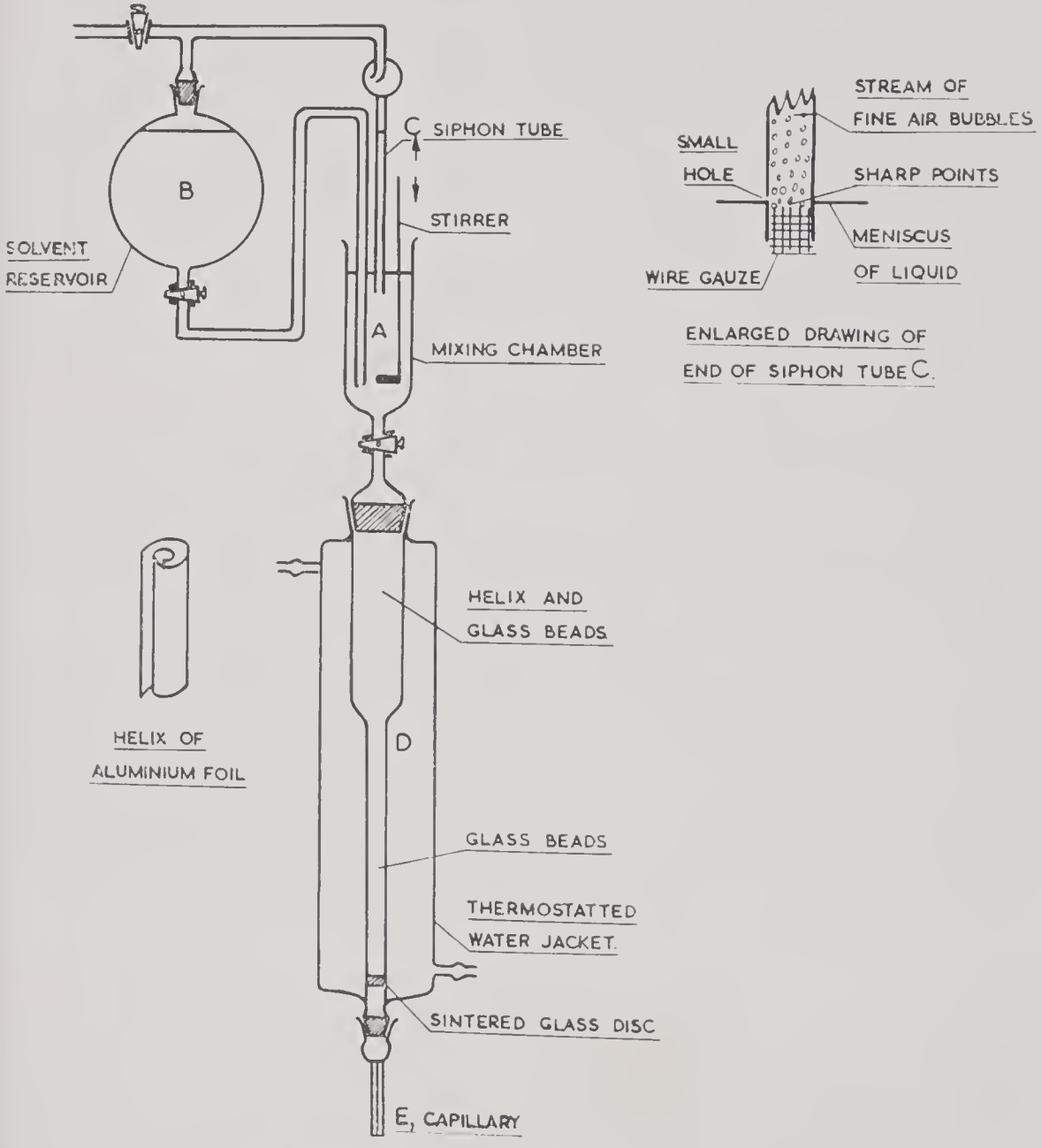

Fig. 3. Apparatus for separation of mixed polymers (30).

Turbidimetric titration procedures were introduced into this field by Melville and Stead (29) who showed the utility of the method in demonstrating the presence of block or graft copolymer in a given mixture. This method is not, however, suitable for the preparation of samples of any size.

Most success in this latter problem has been gained by Hartley (30) using a modification of Baker and William's method (23). The apparatus shown in Figure 3 was designed to separate graft copolymers of vinyl acetate and vinyl alcohol and does not have the temperature gradient jacket advocated by Williams. The reason is that it is likely that the polymers used would have a negative temperature coefficient of solution as is the case for 80–85% hydrolysed polyvinyl acetate (31).

Referring to Figure 3, *A* and *B* are parts of a siphon system which automatically provide an exponential solvent gradient (water and ethanol). Near the end of the siphon tube *C* there is a small hole adjusted to be in the meniscus of the liquid in the mixing vessel. When the siphon operates, air is drawn into tube *C* through this hole and is broken into a stream of fine bubbles by the wire gauze plug in the bottom of the tube. This ensures a steady flow of air up tube *C* when the siphon is working, and, in turn, a steady flow of solvent into the mixing vessel in which a constant level is maintained.

The main fractionating column, *D*, is 40 cm. long and 2 cm. in diameter opening at the top to a tube 3 cm. in diameter and 20 cm. long; a sintered glass disc was sealed into the bottom of the narrow tube. The whole column was jacketed and maintained at 20°C. A fine bore glass tube was connected by a ground glass joint to the bottom of the column. Fractions were collected in an automatic collector.

The column was packed with fine glass beads. Polymer was deposited on a 19 cm. square sheet of aluminum foil wound to a cylindrical helix. The coated helix was introduced into the upper part of the fractionating column which was already filled with water and partly packed. More glass beads were added to complete the packing in and around the helix. After connection of the gradient portion of the apparatus, the fractionation was allowed to proceed. Reasonably good separation was obtained.

8. Drying of Polymers

The polymers which are obtained in a stage of reasonable purity by any of the foregoing methods are usually wet and the removal of the last traces of solvent and/or precipitant is frequently extremely difficult. The conventional method of heating under reduced pressure does not always lead to weight constancy in a reasonable time or else gives a flattening of the composition-time plot before quantitative recovery of the solvent has been achieved. This is all the more noticeable when the molecular weight of the evaporating material increases, owing to the low diffusion rate through the polymeric material. Displacement of such materials can be accelerated by swelling and drying cycles using solvents of lower molecular weight.

The time required for drying can be minimized by reducing the particle size of the solid materials. If the materials are brittle, milling or grinding is effective, but if the amount of liquid held is appreciable such treatment alone will not be effective. In this case grinding with a little solid carbon dioxide can be useful. At the same time excessive grinding or milling should be avoided in view of the possibility of degradation.

A method of quite general applicability is that of freeze drying, usually of a solution of polymer in benzene. The solution is frozen at about 0°C. and the benzene sublimed under high vacuum into a liquid air trap (32,33). This gives a porous mass which does not collapse if held at low temperatures during the sublimation. The method is obviously applicable to other solvents having a high vapor pressure over the solid form.

III. CONDENSATION POLYMERIZATION

1. General Principles

Condensation polymerization occurs between monomeric molecules possessing at least two functional groups which may undergo simple organic condensation reactions usually with elimination of water. The reactions are therefore stepwise in character and do not involve the formation of transient intermediates. The molecular weight of the product increases during the reaction and theoretically becomes infinite when no further functional groups remain.

The chemistry of condensation polymers was studied extensively by Carothers in a series of investigations between 1929 and 1936 (34). The kinetics of the formation, interaction and degradation of these polymers has been the subject of much work more particularly by Flory (35–38), thereby putting the whole subject on a firm quantitative basis.

It is convenient to group this type of polymerization into three classes depending on the structure of the monomeric units involved:

Class 1. The two (different) functional groups reside on the same monomeric molecule as typified by ω-hydroxy acids such as ω-hydroxyhendecanoic acid, $HO\cdot(CH_2)_9COOH$ investigated by Carothers and van Natta (39). For the general case the reaction proceeds as follows:

$$2HO—R—COOH \longrightarrow HORCO\cdot O—R—COOH + H_2O$$

$$HO—R—(COOR)_nCOOH + HORCOOH \longrightarrow$$

$$HO—R(COOR)_{n+1}COOH + H_2O$$

It is also possible for two polymeric molecules to interact thus:

$$HOR(COOR)_mCOOH + HOR(COOR)_nCOOH \longrightarrow HOR(COOR)_{m+n+1}COOH + H_2O$$

At each stage it will be noted that the bifunctionality is maintained.

Class 2. In this class—the largest—the polyfunctionality is divided between two monomeric molecules, e.g., dibasic acids, dihydric alcohols, diamines and the like. Important members of the class are polyesters, polyamides, phenol- and urea-formaldehydes, polyurethanes, silicones, etc. A common example is the condensation of adipic acid and hexamethylene diamine to give nylon:

$$HOOC\cdot(CH_2)_4COOH + H_2N(CH_2)_6NH_2 \longrightarrow HOOC(CH_2)_4CO\cdot NH(CH_2)_6NH_2 + H_2O$$

By this reaction the dimeric molecule is formally identical with the monomers of class 1 but may also condense with further acid or amine molecules at the reactive ends. If the functionality of either molecule exceeds two then space networks will be built up. Such polymers typified by the bakelite series are insoluble and infusible.

Class 3. Polymers in this group are formed by ring opening followed by addition of other cyclic monomers to one or both ends of the opened molecules. These reactions differ from the previous ones in that frequently no small molecule is eliminated. An example in this class is the polymerization of ϵ-caprolactone (40)

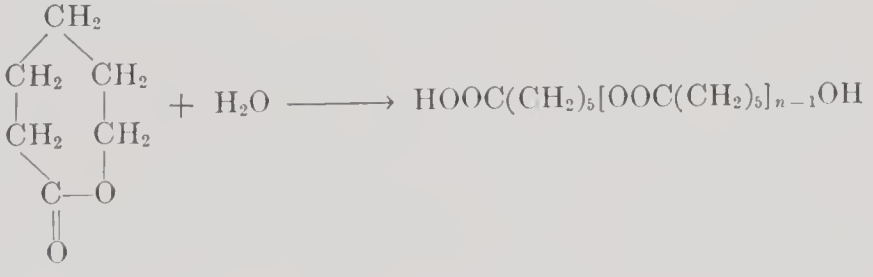

$$+ H_2O \longrightarrow HOOC(CH_2)_5[OOC(CH_2)_5]_{n-1}OH$$

A more important example of commercial significance is the polymerization of the corresponding lactam (41), giving a polyamide.

2. Production of Polymers

Inspection of class 2 reactions shows that the necessary stoichiometric requirement is that an equivalence of reactants is required in order to obtain polymers of any size. Frequently it is the practice to prepare and isolate the dimer of the first step illustrated above and use this material for subsequent polymerization. Thus for dibasic acid–diamine condensa-

tions, the salt may be prepared by reacting amine and acid in water solution and crystallizing out the requisite material.

In practice several factors operate to prevent the chain length of the final polymer reaching infinite values. In the first place the exact equivalence required is rarely achieved and consequently sooner or later all chain ends are identical. Another important side reaction is that of intramolecular cyclization which tends to remove active groupings. This latter problem has been carefully analyzed by Stockmayer (42). Furthermore, since many of the reactions are reversible, chain lengths tend to be limited. In many cases the equilibrium may be shifted in such a way as to favor the formation of polymer. This is particularly easy if one of the products of reaction is volatile, e.g., water or ammonia. Thus, polyesterification and polyamidation reactions are usually carried out at elevated temperatures either under vacuum or with an inert gas flow (43) to remove water. Even if all of these conditions are met it must be remembered that at high conversions the concentration of functional groups is so low that the absolute rate of reaction becomes vanishingly small—a feature which is of increasing importance as the order of reaction becomes greater (35b). It is also not impossible that the rate of reaction will be reduced by the high viscosity of the medium in the later stages of reaction.

Class 3 reactions differ from the others in that polymerization is brought about by the introduction of small quantities of a material containing a group similar to that obtained on opening the ring. In such a system the end group reacts with the ring, producing from it another similar group capable of reacting with a further ring, i.e.,

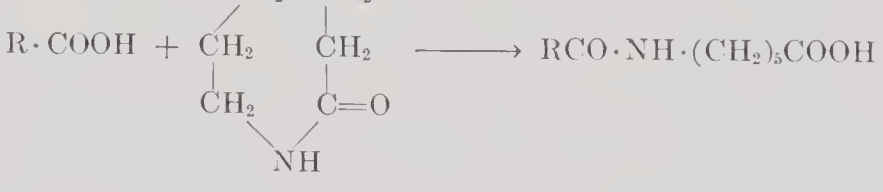

If in such systems this process is faster than any possible interchange processes then the distribution obtained is much sharper than would be the case for classes 1 and 2 (35c).

3. Factors Influencing Reaction Velocity

As has been stated polymerization of this type proceeds by successive condensations, but unlike simple condensation processes (e.g., between monobasic acid and monohydric alcohol) the product of reaction can itself take part in further reaction. If it were necessary to introduce a new rate constant for each successive step it is quite easy to see that the mathe-

matical analysis would soon be impossible. It turns out however (35b,43–45) that after only one or two additions the rate constant for the condensation process becomes independent of the size of the reacting molecules and hence the analysis of the reaction is indeed possible. This assumption has good experimental backing in that it is known from an examination of the rates of reaction of a series of homologues that after 8 or 10 carbon atoms the effect of molecular size on the reactivity of a functional group is negligible.

The effect of viscosity on the rate of reaction has been shown to be of little or no significance at any stage of reaction. Most probably this is due to the high activation energy of the process which would render it almost impossible for the reaction to become diffusion controlled.

4. Products of Condensation Polymerization

In the formation of polymer by progressive reaction of equal amounts of two bifunctional molecules, the degree of polymerization, $\overline{DP}_n$, is measured by the number of linkages formed by reaction of end groups. One end group of each type is destroyed for each link so formed and, assuming that the other condensation product, e.g., water, is eliminated the total number of molecules in the system is reduced by one. If there are N_0 of each type of group then there will originally be N_0 molecules in the system. When a fraction, p, of the groups have reacted, the number of molecules remaining in the system will be $(1 - p)N_0$ whence

$$\overline{DP}_n = (1 - p)^{-1} \tag{1}$$

Any desired degree of polymerization can therefore be achieved by simply stopping the reaction at the required degree of conversion but, of course, subsequent operations will be likely to produce further reaction. Therefore, it is usual to add "molecular weight" stabilizers which may be either monofunctional compounds or, in the case of class 2, an excess of one of the reactants.

Consider the condensation

$$\text{A—A} + \text{B—B} \longrightarrow \text{A—AB—B}$$

which contains an excess of the first type of molecule. If N_A and N_B are the numbers of A and B groups originally present, the total number of molecules is $(N_A + N_B)/2$. If a fraction p of the B groups react then number of molecules remaining must be

$$(N_A + N_B)/2 - pN_B$$

since the removal of one B group corresponds to a reduction of one in the number of molecules present. This leads us to:

$$\overline{DP}_n = (N_A + N_B)/[(N_A + N_B) - 2pN_B] \tag{2}$$

so that when all the B groups are consumed, i.e., when $p = 1$

$$\overline{DP}_n = (N_A + N_B)/(N_A - N_B) \tag{3}$$

If by the other method there are equal numbers of A and B groups but a monofunctional stabilizer is added, the following analysis is necessary. Let there be S_A monofunctional molecules, then initially there are $N_A + S_A$ molecules present. After a conversion p there will be $N_A(1 - p) + S_A$ so that when $p = 1$ $\overline{DP}$ is given by

$$\overline{DP}_n = (N_A + S_A)/S_A \tag{4}$$

Table II shows the significance of the addition of monofunctional groups and also draws attention to the need for stoichiometric balance.

TABLE II
Effect of Addition of Monofunctional Molecules and Stoichiometry on $\overline{DP}_n$

S_A/N_A	0.001	0.01	0.1
$\overline{DP}_n$ (from Eq. (4))	1,000	101	11
N_A/N_B	1.001	1.01	1.1
$\overline{DP}_n$ (from Eq. (2))	2,001	201	21

5. Kinetics of Simple Condensation Polymerization

Nearly all the quantitative data pertaining to kinetics of condensation reactions are based on end group analysis (46). If one assumes that the rate constant remains independent of the size of molecule to which the reacting group is attached, then, if our polyreaction is bimolecular, i.e.,

$$A—(AB)_n—B + A—(AB)_m—B \longrightarrow A—(AB)_{m+n+1}—B$$

the rate expression will take the form

$$-d(1 - a)A_0/dt = k(1 - a)(1 - b)A_0B_0 \tag{5}$$

where a and b are the fractions of A and B ends which have been consumed, while A_0 and B_0 are the initial concentrations. In cases of practical interest $a = b = p$, the necessary criterion for the formation of big molecules. Equation (5) then becomes

$$-A_0d(1 - p)/dt = k(1 - p)^2A_0^2 \tag{6}$$

which gives on integration

$$(1 - p)^{-1} = kA_0t + 1 \tag{7}$$

We have already seen that the left hand side is a measure of the DP of the polymer at conversion p so that a plot of $\overline{DP}_n$ against t should be linear if the reaction follows the course suggested with the limitations on k already mentioned. Flory (35b) investigated the degree of polymerization, DP, as a function of time for the interaction of diethylene glycol and adipic acid at 109°C. using p-toluenesulfonic acid as catalyst. Figure 4 shows that in the later stages of reaction k is indubitably constant but at low values of p there is a drift from constancy as one might have expected from the foregoing discussion.

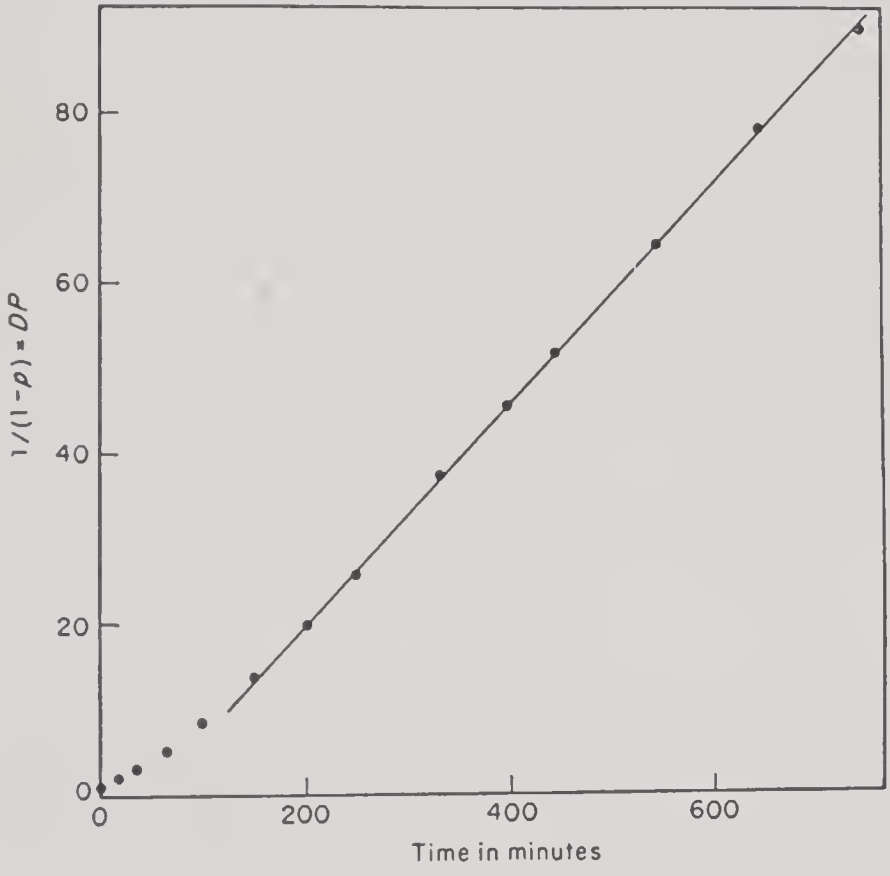

Fig. 4. Reaction rate of diethylene glycol-adipic acid condensation at 109°C. catalyzed by p-toluenesulfonic acid.

Other condensations obeying different rate expressions have also been studied and confirm still further Flory's generalizations. Some condensations involve reactions between groups which are dissimilar in the monomeric species. Thus in glycerol there are two primary and one secondary hydroxyl groups and it has been shown that the condensation rate constant involving the secondary hydroxyl differs substantially from that for the primary groups. However, investigation of systems such as these is fraught with the further difficulty of gelation.

6. Treatment of Data

Most methods of attack on the problems associated with condensation reactions are indirect. This may have been activated by the statistical approach which has characterized all the theoretical investigations. This gave expressions for distribution of sizes and, in some instances, for complexity of molecules, and average molecular weights. Direct correlation between rates of reaction, degree of conversion, and time appears to have been neglected.

Also at the time in question no really reliable method of fractionation was available so that the theories were tested by recourse to average molecular weight determinations. Even these were to some extent based on empirical measurements such as measurement of viscosities of concentrated reacting mixtures (47) and of cloud points (48).

It is now possible to check with greater precision on the number and weight average molecular weights owing to the development of more exact methods of measurement of these quantities of osmometry and light scattering. Stockmayer (49) has shown that, for class 1 and 2 polymerizations, the following relationships hold (if one neglects intramolecular reactions (i.e., cyclization)):

$$\overline{\mathrm{DP}}_n = 2/(2 - pf) \tag{8}$$

$$\overline{\mathrm{DP}}_w = (1 + p)/[1 - (f - 1)p] \tag{9}$$

where f is the number of functional groups per monomer molecule and p is the reacted fraction of those groups. When $f = 2$ we have the simplest case and the equations become

$$\overline{\mathrm{DP}}_n = 1/(1 - p) \tag{8a}$$

$$\overline{\mathrm{DP}}_w = (1 + p)/(1 - p) \tag{9a}$$

where $\overline{\mathrm{DP}}_w$ is the weight average degree of polymerization. If the bimolecular rate expression (Equation (7)) is generalized to take into account cases of $f > 2$, p may be defined in terms of the velocity constant, k, as

$$p = fNkt/(1 + fNkt) \tag{10}$$

where N is the initial concentration of monomer molecules. For class 2 the monomer unit is given by the combination of reactants giving the simplest repeating unit in the polymer. Substitution of Equations (8) and (9) in (10) gives

$$\overline{\mathrm{DP}}_n = (2 + 2\,fNkt)/[2 + (2f - f^2)Nkt] \tag{11}$$

$$\overline{\mathrm{DP}}_w = (1 + 2\,fNkt)/[1 + (2f - f^2)Nkt] \tag{12}$$

It has been suggested (50,51) that these expressions can be used to evaluate the rate constant, k. If $\overline{DP}_n$ or $\overline{DP}_w$ is measured as a function of time, values of k and f in either (11) or (12) may be selected to give the best fit to the experimental curve. Fractional values of f would indicate that part of the reaction is intramolecular or that all functional groups do not behave alike.

Class 3 reactions can be treated in a similar manner. For example, polymerization of a cyclic monomer (M) initially opened by a small quantity of reagent (C) may occur according to:

$$M + C \longrightarrow CM$$

$$CM + M \longrightarrow CM_2$$

$$CM_n + M \longrightarrow CM_{n+1}$$

As usual, we consider all the rate constants equivalent, and find

$$-d(M)/dt = k(M)\sum_{n \geqq 1} CM_n \tag{13}$$

However it is easy to show $\sum CM_n = C_0$ where C_0 is the initial number of catalyst molecules, whence

$$-d(M)/dt = kMC_0$$

and if M_0 is the initial number of monomer molecules:

$$M/M_0 = \exp\{-C_0kt\} \tag{14}$$

The number of molecules converted to polymer at time t is $(M_0 - M)$ and the number of polymer molecules is C_0 so that

$$\overline{DP}_n = (M_0 - M)/C_0 = (1 - M/M_0)M_0/C_0$$

$$= [1 - \exp\{-C_0kt\}]M_0/C_0 \tag{15}$$

These equations may be used to evaluate k from changes in M or $\overline{DP}_n$ with time. While it is usually most convenient to employ end group methods for classes 1 and 2, the most convenient measurement for class 3 is the concentration of unchanged monomer; Majury (52), for example, has used a dilatometric procedure to follow the polymerization of caprolactam.

7. Interchange Reactions

Interchange reactions, such as those involving low molecular weight alcohols and esters, are well known and the same sort of behavior involving

a terminal hydroxyl group and an ester linkage in a polyester is also possible.

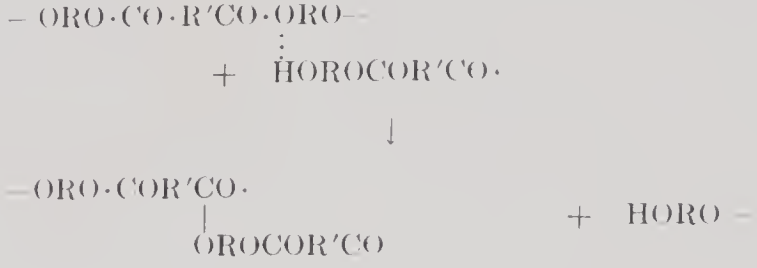

Similar interchanges with carboxyl ends are also known, but occur only very slowly.

Reactions of this type involving polyesters do not bring about any alteration in the number of molecules in the system and consequently the number average degree of polymerization remains unchanged. At the same time a change in the distribution may conceivably occur and with it a concomitant change in the weight average quantity. This may be demonstrated in the following manner. If we consider three molecules of chain length 100, 400, and 1,000 units and ester interchange gives three new molecules of lengths 300, 500, and 700; the $\overline{DP}_n$ for each group is 500. The corresponding weight averages are 780 and 553 respectively. Thus any method of measuring the weight average may be used to follow changes occurring in distribution on mixing two polyester samples of differing average molecular weight. This has been carried out by Flory who showed that the approach to equilibrium distribution could be predicted using the same assumptions as made in the previous treatment of condensation reactions (35).

8. Three Dimensional Polymers

As has already been mentioned the use of monomers possessing more than two functional groups will lead to the formation of very large molecular networks. Characteristic of these cross-linked molecules is their infusibility and insolubility so that the polymerizing system will contain a certain amount of gel. It has been found that the appearance of the insoluble gel phase is sudden; broadly speaking experiment and theory are substantially in agreement regarding the point of formation.

If condensation is occurring between a difunctional molecule A—A to which a trifunctional compound 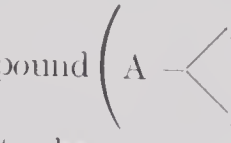 has been added and a difunctional monomer of opposite character, B—B, then molecules of the type

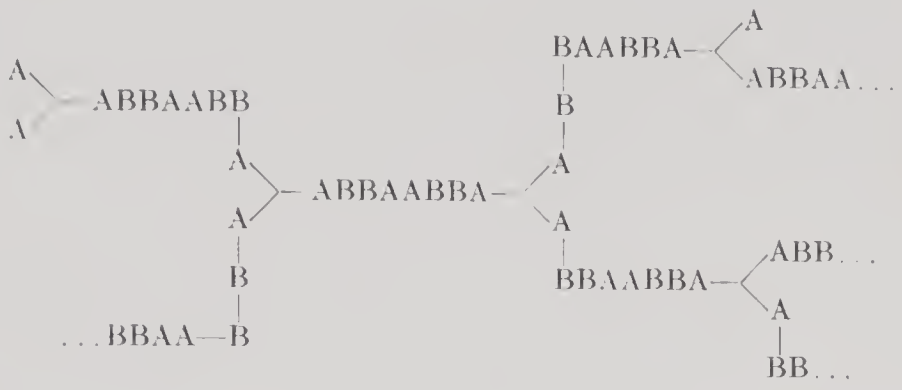

will be formed. It is important to note that the addition of each trifunctional molecule increases the functionality of the polymer molecule. Thus sooner or later these molecules will grow further at the expense of small molecules of lower functionality. It is also true that with highly branched species the opportunity for interaction of two functional groups on the same polymer (intramolecular reaction) must become of considerable importance. Unfortunately it is impossible, so far, to make any headway in the mathematical assessment of this kind of side reaction. Consequently all mathematical treatments of branching assume the absence of intramolecular reactions so that one must expect some discrepancy between theory and practice. The importance of intramolecular processes has been demonstrated conclusively in the condensation of glycerol with dibasic acids (53).

Any given molecule such as that illustrated above may be regarded as a system of chains connected through polyfunctional, or branch, units. We must determine first the branching coefficient, α, which can be defined as the probability that a given functional group of a branch unit leads via a chain to another branch unit.

The formation of chains of the type defined above may be written as

$$A\!-\!A + A\!<\!\begin{matrix}A\\A\end{matrix} + B\!-\!B \longrightarrow \!-\!A\!-\![B\!-\!BA\!-\!A]_i B\!-\!BA\!-$$

where i may have any integral value or zero. Other chains will be formed, one or both ends of which have unreacted terminal groups. As usual, we assume equal reactivities of all A and all B groups, so that the probability that the first A group shown in the above chain has reacted is p_A, the fraction of A groups reacted; similarly the probability that the next B group has reacted will be p_B. Let ρ represent the ratio of A's belonging to branch units to the total A's in the mixture. Then the probability that a B group has reacted with a branch unit is ρp_B and with a conventional difunctional unit, $p_B(1 - \rho)$. Thus the probability that any given branch point is connected through a sequence of i units to a second branch point is given by

$$p_A[p_B(1 - \rho)p_A]^i p_B\rho \tag{16}$$

The probability, α, that a chain ends in a branch unit irrespective of i is

$$\alpha = \sum_{i=0}^{\infty} p_A p_B \rho [p_A p_B (1 - \rho)]^i$$

$$= p_A p_B \rho / [1 - p_A p_B (1 - \rho)] \tag{17}$$

If the ratio of A to B groups initially present is r, then $p_A = r p_B$ and (17) become

$$\alpha = r p_B^2 \rho / [1 - r p_B^2 (1 - \rho)]$$

or

$$\alpha = p_A^2 \rho / [r - p_A^2 (1 - \rho)] \tag{17b}$$

In applying these equations r and ρ are fixed by the mixture originally used, and either unreacted A or B groups determined analytically so that α is accessible. Flory (54) has pointed out several important particular cases which render experimental study somewhat easier.

The critical value of α at which the formation of an infinite network occurs can be deduced in the following way. Consider first that the branching unit is trifunctional, when each chain ending in a branch point will be succeeded by two chains. If each of these end in a branch point four more chains are produced and so on. If $\alpha < 1/2$ there is a less than even chance that a chain will end in a branch point so that branching cannot continue indefinitely since eventually termination of chains will outweigh branching. Obviously if $\alpha > 1/2$ there is a better than even chance that each chain leads to a branch unit and consequently infinite branching becomes possible. Thus the critical value of α will be 0.5. It is easy to generalize the above statements to include f functional units ($f > 2$). Using the same argument it can be shown that

$$\alpha_c = 1/(f - 1) \tag{18}$$

Kienle and Petke (55) investigated reactions between glycerol and a number of dibasic acids and were able to show $\alpha_c = 0.58$ on the assumption that all the hydroxyl groups were equally reactive. Allowing for a different reactivity of the secondary group has the effect of reducing the observed α_c but a divergence from the calculated value remains. An elegant investigation by Flory (35f) of the gel points for varying quantities of tricarballylic acid added to glycol dibasic acid mixtures, revealed similar results as shown in Table III. The gel point was determined experi-

TABLE III
Polymerization of Glycol and Dibasic Acid in Presence of Tricarballylic Acid

Dibasic acid	p	r	α_c
Adipic	1.000	0.293	0.59
	0.800	0.375	0.58
Succinic	1.000	1.194	0.59
	1.002	0.404	0.58

mentally by the loss in fluidity of the reaction system as observed by the failure of bubbles to rise in the mixture. The number average degree of polymerization at the gel point is not exceptionally large which shows that many molecules are still present. This does not exclude the formation of very large molecules beyond that point.

The discrepancy between observed and theoretical α_c can be explained by the neglect of intramolecular reactions. This has been demonstrated in an investigation of the condensation of adipic acid and pentaerythritol ($f = 4$)(56). In this instance $\alpha = p^2$ and $\alpha_c = {}^1/_3$ so $p_c = 0.577$. The observed result gave $p_c = 0.63$. It was argued that if the reaction were carried out at infinite concentration no intramolecular reaction would be possible. Therefore p_c was determined in the presence of varying amounts of diluent and plotted against $1/c$. On extrapolation to $1/c = 0$, the intercept gave the value of p_c at infinite concentration as 0.578 which is in remarkably good agreement with theory. This result obviously justifies the fact that disregard of intramolecular reactions leads to the observed discrepancies quoted above.

Numerous theoretical investigations of the molecular weight distributions in the post gel reaction have been reported and are excellently developed by Flory (57) but experimental verification is so far lacking.

IV. RADICAL ADDITION POLYMERIZATION

1. Nature of the Reaction

Unlike the condensation polymerization processes discussed in Section III, addition polymerization proceeds by a chain reaction involving either free radical or ionic intermediaries; in this section the former will be treated. For free radical polymerization the monomer is a substituted ethylene molecule during the polymerization of which double bonds are destroyed as the monomers link up and, unlike class 1 and 2 condensations, no small molecules are produced. The reaction chain length is very long (usually greater than 1,000).

The evidence deciding the mechanism of the reaction is contained in the work of Dostal, Mark, Melville, and others in the period from 1925–1940 (58). Being a chain reaction the overall picture is much the same as that given in Chapter XVIII, in that basically there are three reaction steps affecting the rate, viz., initiation, propagation and termination. The main difference lies in the fact that the propagation cycle required say in oxidation processes is replaced by a single reaction. Addition of a molecule to an active free radical simply increases the length of the chain involved but does not alter the character of the radical in the least. Thus schematically we have:

Initiation

Production of active free radicals R· by some convenient process

$$R\cdot + CH_2{=}CHX \longrightarrow R\cdot CH_2\cdot \dot{C}HX \text{ rate } = R_i$$

Propagation

$$R\cdot CH_2\cdot \dot{C}HX + CH_2{=}CHX \longrightarrow R\cdot CH_2\cdot CHX\cdot CH_2\cdot \dot{C}HX$$

$$R(CH_2CHX)_rCH_2\dot{C}HX + CH_2{=}CHX \longrightarrow R(CH_2CHX)_{r+1}CH_2\dot{C}HX$$

Termination

$$R(CH_2CHX)_sCH_2\dot{C}HX + R(CH_2CHX)_mCH_2\dot{C}HX \longrightarrow R(CH_2CHX)_sCH_2CHX\cdot CHX\cdot CH_2(CHX\cdot CH_2)_mR\cdot$$

or

$$R(CH_2CHX)_sCH_2CH_2X + R(CH_2CHX)_mCH{=}CHX$$

Since the process is a chain reaction it follows that large polymer molecules are present in the system from the start of the reaction. Indeed even in the early stages the reaction mixture consists almost wholly of monomer and very large molecules. This is in marked contrast to condensation processes in which the production of very large molecules depends on being able to carry the reaction to high conversion. Secondly it will be noted that the interaction of two active species results in the formation of inactive polymeric molecules which usually will not take any further part in the reaction; in condensation reactions, condensation of two large molecules possessing the required functional groups gives a new molecule still capable of undergoing a similar reaction.

It will also be noted that the first type of termination reaction gives rise to an irregularity in the polymer chain at the point of junction. This is not detectable by present methods but may be important in the degradation properties of the polymer.

As well as the three basic reactions given above, there are other possible side reactions even in homopolymerization, i.e., bulk polymerization of

pure monomer. It is always possible for a radical to achieve saturation by abstracting a suitable atom (usually hydrogen) from a molecule. This can be written as

$$R(CH_2CHX)_rCH_2\dot{C}HX + CH_2{=}CHX \longrightarrow R(CH_2CHX)_rCH_2CH_2X + \dot{C}H{=}CHX$$

The new small radical is usually active enough to bring about a repropagation of the chain so that the rate of the reaction is not affected. On the other hand, reactions such as these bring about a reduction in the potential molecular weight of the polymer formed, i.e., the average number of monomer units in polymer molecules will be less than the kinetic chain length defined as the number of monomer molecules reacting from initiation to final destruction of radicals by a termination process.

A second type of transfer involving inactive polymer molecules is also possible. In this, the growing radical abstracts an atom from the polymer molecule creating a new radical on which polymerization occurs. It is not difficult to see that such abstraction may occur anywhere on the polymer chain so that the new growth will form a branch to the original molecule. This type of reaction is unlikely to be of very great moment at low conversions, but could have an over-riding influence at high conversions when it could replace the more usual monomer transfer process.

On the basis of the mechanism which has been suggested above, a kinetic analysis can readily be carried out. As for condensation reactions, we will assume (not without justification) that the rate constants are independent of the size of reactants. Then we have, applying normal stationary state kinetics,

$$\text{rate} = -d(M)/dt = k_p(P)(M) = k_p k_t^{-1/2} R_i^{1/2}(M) \tag{19}$$

where k_p and k_t are the rate constants for propagation and termination respectively (P) is the total radical concentration irrespective of size and (M) is the monomer concentration.

The degree of polymerization, $\overline{DP}_n$, may be defined by

$$\overline{DP}_n = \text{rate of polymerization} \div \text{rate of formation of polymer molecules} \tag{20}$$

If there is no transfer, polymer molecules are formed only in the termination processes. By definition k_t is the rate constant for the radical destruction reaction, i.e., $-d(P)/dt = k_t(P)^2$ so that for the combination reaction, rate of polymer formation is one half the rate of radical disappearance while for disproportionation the two rates are equal. Consequently,

$$\text{Rate of formation of polymer molecules} = ak_t(P)^2 \tag{21}$$

where $a = {}^1/_2$ or 1. On substitution of (19) and (21) in (20)

$$\overline{\mathrm{DP}}_n = k_p(P)(M)/ak_t(P)^2$$

But $(P) = (R_i/k_t)^{1/2}$, so

$$\overline{\mathrm{DP}}_n = k_p(M)/aR_i^{1/2}k_t^{1/2} \tag{22}$$

If $a = 1$, Equation (22) gives the kinetic chain length also.

The interference of a transfer reaction to monomer gives an additional reaction producing polymer molecules at a rate $= k_f(P)(M)$, where k_f is the rate constant for the transfer step. Making the necessary substitutions in Equation (20) yields:

$$\overline{\mathrm{DP}}_n = k_p(P)(M)/[k_f(P)(M) + ak_t(P)^2] \tag{23}$$

or more conveniently,

$$\overline{\mathrm{DP}}_n{}^{-1} = k_f/k_p + ak_t^{1/2}R_i^{1/2}/k_p(M) \tag{23a}$$

Substituting for R_i in terms of the rate given by (19) Equation (23a) becomes

$$\overline{\mathrm{DP}}_n{}^{-1} = k_f/k_p + ak_t[-d(M)/dt]/k_p^2(M) \tag{23b}$$

Thus we have a linear relationship between the rate and the reciprocal of the average degree of polymerization from which the ratios k_f/k_p and ak_f/k_p^2 may be found. Departures from this linear plot can usually be ascribed to the presence of impurities or to a transfer reaction involving a molecule of initiator.

2. Measurement of Reaction Rate

Most, if not all, radical addition polymerizations are affected by the presence of oxygen so that it is necessary to operate under high vacuum conditions, in order to obtain reasonable reproducibility. Such a statement also implies that all materials have to be rigorously purified and free from dissolved air. This latter object can be achieved by liquid air freezing of monomer purified by a standard procedure of distillation (preferably in an atmosphere of nitrogen or carbon dioxide). The frozen monomer is subjected to strong pumping before being isolated from the remainder of the apparatus. When the monomer is allowed to thaw out, dissolved gas is released; the freezing-pumping-thawing cycle is repeated until no more gas is found. Before use, it is now common practice to prepolymerize the monomer to 2–3% conversion using mercury arc illumination. Such a procedure destroys any adventitious impurities present in the monomer which may then be distilled to the reaction vessel into which initiator if

required has already been introduced. To test for reproducibility, duplicates are usually run from the same initial batch of monomer.

To follow the reaction, it is most convenient to measure some change in a physical property so that measurement is continuous and can be carried out without opening the reaction system.

Early methods such as removal of monomer by distillation, precipitation, and weighing of dried polymer and titrimetric determination of the reduction in unsaturation by Wijs solution or bromine are all extremely laborious, and time consuming, giving results of rather low accuracy.

Many systems of measurement depending on changes in physical properties have been used and will be described in detail.

Absorption Spectra. Changes both in ultraviolet (59, 60) and infrared (61) absorption spectra frequently arise, but it has not been found convenient to make the method generally useful.

Diamagnetic Susceptibility. For any simple addition reaction between two molecules, the molecular susceptibility of the dimer, χ_D is given by $\chi_D = 2\chi_M + \lambda$ where χ_M is the molecular susceptibility of the monomer and λ is a constant arising from differences in the bonding before and after reaction. For polymerization of n molecules $\chi_P = n\chi_M + (n - 1)\lambda$, in which χ_P is the susceptibility of the polymer. We can now write $\chi_P = \chi_{Mn}$, where M is the molecular weight of the monomer so that

$$\chi = [n\chi_M + \lambda(n - 1)]/nM \tag{24}$$

In (24) n is simply the number of molecules which have polymerized; the degree of polymerization is immaterial.

This technique was employed by Farquharson (62,63) in a study of the polymerization of 2,3-dimethylbutadiene. At intervals the reaction mixture was cooled to room temperature and the susceptibility measured using a Gouy balance. The results agree well with those determined by other methods (64). Since the method measures the mass susceptibility no account need be taken of the density changes accompanying the reaction. For complete comversion a change in susceptibility of about 25% occurs.

Refractive Index. Increases in refractive index occur during polymerization but, even although these increases are quite substantial, little use has been made of the method largely because of the difficulty encountered in designing suitable equipment for measuring refractive index changes in a closed system.

Melville and Watson (65) have devised a method designed to give continuous observation on a single sample, by confining the monomer in a cylindrical tube so that the specimen functioned as a cylindrical lens in an optical system. The position of the image of a fine thread focussed by this lens depends critically on the refractive index of the lens material. The

choice of thermostat liquid is critical in determining the sensitivity of the equipment. In view of the fact that refractive index is relatively sensitive to temperature it is doubtful if a system such as this could be operated at high conversions when non-isothemal tendencies would appear.

An ingenious application of the principles of Pfund's oblique line refractometer (66) has been made by Naylor and Billmeyer (67) to the study of methyl methacrylate polymerization. Essentially the apparatus consists of a series of oblique slots arranged behind cylindrical reaction tubes and illuminated. As the refractive index of the polymerizing system alters the angle of the slot viewed through the tube varies; total change is about 83°C. The system is convenient in that a number of runs can be carried out simultaneously and a photographic record is easily made. While no very great accuracy is claimed for the procedure, it appears that potentially it is a precise method in view of the high variation in angle. As with other refractive index methods great attention has to be paid to the nature of the liquid bath used, since the change in oblique line angle depends on the refractive index of both bath and tube material.

Density. Dilatometry gives the most convenient method of rate measurement for liquid phase polymerization. This arises in part, at least, from the high sensitivity of the technique which results from the large difference in density between polymer and monomer; also it has been demonstrated that there is a linear relationship between the densities of monomer–polymer mixtures and their composition (68).

Some difficulties arise in estimating the theoretical contraction for a given conversion in that the appropriate polymer density is that in solution which may be appreciably different from the bulk value. If the polymer precipitates from the medium it will in all likelihood be swollen to a greater or less extent and this excludes any accurate knowledge of the density. Consequently calibration of the dilatometric procedure by gravimetric estimation of polymer is necessary.

Table IV gives an indication of the sensitivity of the method for a num-

TABLE IV

Theoretical Contractions for Monomers at 100% Polymer Conversion at 60°C. (69)

Monomer	Monomer density	Polymer density	% contraction for complete reaction
Acrylonitrile	0.762	1.19	36.1
Methacrylonitrile	0.758	1.153	34.25
Methyl acrylate	0.900	1.191	24.3
Vinyl acetate	0.890	1.160	23.2
Styrene	0.869	1.041	16.4

ber of polymer–monomer systems at 60°C. The coefficient of expansion of polymer is usually very much smaller than that of the monomer so that the difference between polymer and monomer densities increases with temperature rendering the dilatometric procedure more sensitive at higher temperatures.

The usual type of dilatometer consists of a small bulb of 1–2 ml. capacity fused to a length of precision bore capillary tube. The dilatometer is usually connected to some vessel in which the outgassing procedure is carried out. Before sealing off the dilatometer the liquid level must be adjusted so as to reach a convenient height at the working temperature. Alteration in the volume of the contents is measured by means of a cathetometer normally reading to 0.02 mm. or better. Since it is evident that such dilatometers will also act as thermometers thermostatting of the reaction system is critical.

With simple dilatometers of the type described, bulk reactions can be followed to about 20% conversion; with solutions, suspensions, and emulsions higher conversions may be reached without loss in precision. The limitation of working range is set partly by the increasing viscosity of the reaction medium which has the effect of distorting the liquid meniscus, and partly by the difficulty in dissipating the heat of reaction. In extreme cases this will bring about local boiling and the appearance of slow holes in the reacting mass.

In order to obviate this difficulty special designs of dilatometer must be used. The first most important modification in this respect was due to Schulz and Harborth (70) in whose design the monomer was confined in a short cylindrical tube behind mercury. Changes in volume were recorded by movement of the mercury meniscus in a suitable capillary. This to some extent allowed better conduction of the heat from the reaction zone and completely eliminated the difficulties associated with distortion of the

Fig. 5. Mushroom head dilatometer suitable for vacuum operation. The dilatometer is connected to high vacuum apparatus at A and after filling is sealed off at the constriction.

meniscus. A great improvement may be effected by expanding the tube containing the monomer to such an extent that a sample of 1–2 ml. monomer appears as a film only 1 mm. or so thick. The great advantage for dissipation of heat is obvious. A design suitable for use under vacuum is shown in Figure 5 (71). With mushroom head instruments it is possible to obtain reliable information on the course of reaction up to complete conversion.

Isothermal Calorimetry. Provided the heat of polymerization is known, a reasonably accurate measure of the course of reaction can be obtained by use of an isothermal calorimeter (72). Essentially polymerization is carried out in a small sealed tube immersed in a liquid heat in equilibrium with its own vapor at its boiling point. Under these conditions heat released from the reacting system will bring about the evaporation of the surrounding liquid. The loss in weight of the assembly will be a measure of the extent of polymerization.

This apparatus, while primarily designed to measure heats of polymerization of unsaturated monomers has been used to follow the course of methyl methacrylate polymerization, with results very much in accord with those determined by more conventional methods (72). Heats of polymerization for a number of monomers are set out in Table V.

TABLE V
Heats of Polymerization of Some Esters of Methacrylic Acid (72,73)

Monomeric ester	$-\Delta H$, kcal./mole
Methyl	13.0 ± 0.2
n-Butyl	13.5 ± 0.2
Cyclohexyl	12.2 ± 0.2
Benzyl	13.4 ± 0.2
Phenyl	12.3 ± 0.2

More specialized methods of following polymerization reactions which have been designed primarily to give very high sensitivity will be described later (Section 6).

3. Initiation Reaction

A. TYPES OF INITIATORS

The primary function of the initiation process is to provide an adequate supply of free radicals to the reacting system. This can be accomplished by a variety of methods of which the most important from the extent of usage are thermal, photochemical and the addition of initiators which on heating give rise to free radicals by simple scission.

Several monomers undergo purely thermal polymerization although at temperatures below about 100°C., this is virtually negligible for styrene, methyl methacrylate, and vinyl acetate. Almost all monomers can be polymerized by using radiation in the near u.v. ($\lambda > 3{,}500$ A.). The mechanism of this procedure is rather vague. It has been suggested that the first step is the excitation of π electrons into a free state to give a free diradical. This mechanism was shown to be unlikely on theoretical grounds because the close proximity of two active centers would give rise to high local concentrations of radicals with a concomitant high probability of termination by radicals on the same molecule. This has been virtually proved in a large number of cases in which the creation of diradicals from suitable initiators has been attempted. Such experiments give either no polymer or polymer whose molecular weight versus rate characteristics are identical with those for monoradical initiation (75,76). Presumably under such conditions any free diradicals formed undergo some rearrangement and scission to give two monoradicals.

In view of these results, therefore, it would appear that diradical initiation is impossible in both thermal and photochemical initiation and one should consider scission of the molecule as being the primary process.

Free radical producing compounds have been very widely used as initiators. The main classes are peroxides, azo compounds, and oxidation-reduction systems. Of the peroxides, that most commonly used is benzoyl peroxide, $C_6H_5CO \cdot O \cdot O \cdot OC \cdot C_6C_5$, which decomposes thermally to give two benzoyloxy radicals which, in turn, can lose CO_2 to give phenyl radicals, thus

$$C_6H_5 \cdot CO \cdot O \cdot O \cdot OC \cdot C_6H_5 \longrightarrow 2C_6H_5CO \cdot O \cdot \longrightarrow 2C_6H_5 \cdot + 2CO_2$$

Either of the radicals, benzoyloxy or phenyl, will be capable of initiating polymerization and it has been shown that this indeed happens. This can be admirably demonstrated by using peroxide labelled with C^{14}, giving a very sensitive method of analysis. It has been found that if the radioisotope is present in the ring the activity of the polymer is reduced on hydrolysis while if C^{14} is in carbonyl group all activity is lost on the same treatment (77,78).

Peroxides generally show some tendency to undergo side reactions with other radicals in the system. Consequently the order of decomposition is not quite unity, and their use in quantitative kinetic work is rendered more difficult (79–82).

Azo compounds were introduced as polymerization initiators by Lewis and Matheson (83) in 1949. These compounds possessing the general form, $R \cdot N{:}N \cdot R$, decompose unimolecularly with the elimination of nitro-

gen

$$R\cdot N{:}N\cdot R \longrightarrow 2R\cdot + N_2\cdot$$

They are not subject to any side reactions as far as is known and apparently decompose at the same rate independent of the solvent used (84). At the same time not all of the radicals produced are capable of initiating polymerization (85–88) but this is likely to be due to a "cage effect" giving dimerization of the radicals formed initially, i.e.,

$$2R \longrightarrow R{-}R\cdot$$

A process, known as reduction activation, discovered fortuitiously in 1942 has proved an extremely valuable method of initiating reactions. Essentially this involves an electron transfer process followed by scission to give, normally, one free radical. Typical of all reactions of this type is the decomposition of hydrogen peroxide by ferrous ion which, according to the Haber-Weiss mechanism (89), follows

$$H_2O_2 + Fe^{2+} \longrightarrow Fe^{3+} + OH^- + HO\cdot$$

$$HO\cdot + H_2O_2 \longrightarrow H_2O + HO_2\cdot$$

$$HO_2\cdot + H_2O_2 \longrightarrow H_2O + O_2 + HO\cdot$$

$$HO\cdot + Fe^{2+} \longrightarrow Fe^{3+} + OH^-$$

This mechanism postulates the production of free hydroxyl radicals in the first step and this has been amply verified by Evans (90). Other systems operating in similar manner include alkali peroxides, ceric sulfate, sodium hypochlorite with sulfite (91) and persulfate with a variety of reducing agents (92). Extension to purely organic systems has also been successful (93,94). In emulsion polymerization a great deal of work has been carried out by the Kolthoff school (95).

B. RATE OF INITIATION

As with all chain reactions, the overall rate expression involves at least two rate constants and the initiation rate. It is impossible to derive the rate constants separately so the rate of initiation cannot be deduced from the overall rate. It is therefore necessary to devise methods for the determination of the rate of the initiation process. This is essential for the determination of rate constants for the various steps of the reaction.

Until the discovery and wide use of suitable radioactive isotopes, rates of initiation depended on somewhat indirect measurements, the interpretation of which depended on assumptions whose validity could not always be assured. Chief among these methods was the use of inhibitors or retarders. Inhibitors have the property of completely suppressing all reac-

tion until they are consumed, at which point the reaction proceeds at its uninhibited rate. From the time required for the reaction to start, and the quantity of inhibitor used, the rate of consumption can be evaluated. It now becomes necessary to assume a mechanism for the inhibition process in order to decide whether an inhibitor molecule stops one or more reaction chains. Unless the precise chemistry of this step is known, this will give rise to considerable uncertainty but one normally supposes a molecular species will be capable of stopping two chains. Indeed there is some proof that this is so, in specific cases (96). More recently stable free radicals, e.g., 1,1-diphenyl-2-picrylhydrazyl have found extensive use as inhibitors on the assumption that only one chain is cut off per radical used. Some doubts have been cast on the validity of this suggestion. In any event, the use of more potent inhibitors may defeat its own purpose when initiation is brought about by a free radical producing agent. It could happen that the inhibitor functions by reaction with free radicals produced by decomposition of the initiator, in which case measurement of the rate of production of free radicals would result. Unless the efficiency of initiation was unity, this would not give the rate of chain initiation.

Alternatively, retarders may be used which only diminish the rate of reaction. By this means the last difficulty is avoided in that the reaction chain must have developed to some extent before being terminated. Again one has to decide the ratio of chains stopped to molecules of retarder used with introduction of the same kind of uncertainty as before. In this type of process the typical curve describing the course of reaction exhibits an "ankle" which is more pronounced as the effectiveness of the retarder increases. Following this ankle a relatively linear plot of the reaction course is obtained. It is common practice to extrapolate the linear portion to the time axis and treat the intercept as the time taken for complete consumption of the retarder (this virtually assumes the retarder to act as an inhibitor). Melville and Cooper (97) have shown that a plot of the reciprocal rate against time is linear for a substantial period. The ratio of the intercept (on reciprocal rate axis) to slope is a measure of the initiation rate divided by the initial concentration of retarder. The merits of the various methods of treating data have been reviewed theoretically (98) and suggest the final procedure to be the most reliable, within the limits of precision imposed by assumption of mechanism.

The absolute method of measurement of initiation rate, which depends solely on the assumption (wholly justifiable) that radical fragments add to monomer, has been devised by Bevington *et al.* (99) using initiator labelled with C^{14}. If we consider azoisobutyronitrile, $(CH_3)_2C(CN)\cdot N{=}N\cdot C(CN)(CH_3)_2$, as initiator, the radicals resulting from decomposition are 2-cyano-2-propyl which add to monomer. If one of the four carbon atoms

is radioactive any polymer formed will have the effect of diluting the radioactivity and essentially the problem reduces to measurement of the extent of dilution.

The activities of the initiator A_i and polymer A_p are inversely proportional to the number of carbon atoms in each species, i.e.,
A_i/A_p = no. of C atoms in polymer ÷ no. of C atoms in initial fragment
For the azo initiation under consideration

$$A_i/A_p = (4 + \nu n)/4 \approx \nu n/4 \text{ (for large } n) \tag{25}$$

where n is the number of C atoms in monomer and ν the average number of monomeric units associated with each fragment, i.e., kinetic chain length. A_i and A_p may be measured by standard techniques and η is known so that ν may be found. Now the kinetic chain length, ν, is defined as

$$\nu = \text{rate of reaction/rate of initiation} = R_p/R_i \tag{26}$$

whence substituting the approximate Equation (25) for ν,

$$R_i = R_p A_p/4A_i \tag{27a}$$

or, more precisely, and generally

$$R_i = R_p A_p n/n'(A_i - A_p) \tag{27b}$$

where n' is the number of C atoms in the initiator fragment.

The method, on theoretical grounds, is absolutely precise and gives a true measure of the kinetic chain length. No allowance has to be made for transfer, method of termination, branching, or efficiency of the initiator. Indeed the latter quantity may readily be derived from experimental data in the following way. If the rate constant for the decomposition of the initiator is k_d, the rate of production of radicals is $2k_d$(init.) so that the efficiency e is

$$e = R_i/2k_d(\text{init.}) \tag{28}$$

where (init.) is initiator concentration.

Estimation of activity has usually been carried out by oxidation of the carbon containing compounds to CO_2 by wet combustion (100,101) and using standard gas counting techniques on the CO_2 suitably diluted with CS_2 (102). Gas counting in this way offers several definite advantages over solid counting with an end-window counter in that the geometry of the system is constant, there are no self-absorption corrections and the efficiency is increased by some 50-fold so that much smaller quantities of expensive radioactive material are required.

4. Termination Mechanism

Usually radical chains are terminated by interaction of two radicals to give either one or two inactive molecules. There are one or two instances in the literature for which this mechanism does not hold. Thus the rate of polymerization of allyl compounds is proportional to the rate of initiation so that only one radical takes part in the termination process (103). In any event the polymers produced in such reactions are very small ($\overline{DP}_n$ = 10–15) so strictly do not come within the scope of this chapter.

The precise mechanism of the termination step is of some importance in that interpretation of rate versus molecular weight relationships depends on this knowledge. Many attempts have been made to elucidate the mechanism of which the earlier have already been adequately reviewed (104). More recently new and more sensitive techniques have been brought to bear on the problem and it now appears that there is a reasonably well defined answer in the case of certain monomers but is is equally certain that there is no general solution and that each must be treated on its merit. Melville (105) has used radioactive labelling in order to achieve an answer. If the reaction is carried out at sufficiently low temperature or sufficiently high rate than it is possible to discount the effect of chain transfer and one can assume that all molecules of the polymer possess one or two initiator fragments depending on their mode of formation. The method is essentially a development of that already described for rate of initiation measurements (Section IV.3.B). Under the conditions of no transfer the kinetic chain length is either equal to, or $^1/_2$, of the number average molecular weight depending on whether disproportionation or combination is operative. By this method it has been demonstrated that for styrene the termination is by combination, while for methyl methacrylate there is both combination and disproportionation, the latter becoming more important as the temperature of reaction increases (105).

A second ingenious method is to use as initiator an azo compound possessing a functional group such as carboxyl or hydroxyl, e.g., $(CH_3)_2C(COOH)N{=}N\cdot C(COOH)(CH_3)_2$ (106). Using such an initiator under nontransfer conditions polymer molecules will have one or two carboxyl groups depending on the mode of formation. If such a polymer is heated with a dihydric alcohol in the presence of a suitable catalyst condensation will occur. For two carboxyls per molecule the reaction will be the same as for polycondensation processes (Section III), and the molecular weight will increase many fold. If on the other hand there is only one carboxyl per molecule the increase will be by a factor of 2. Using such a method Melville's results are substantiated and it appears that disproportionation also operates with vinyl acetate. If transfer occurs neither of these proc-

esses gives a reasonable answer. The second has the advantage that if the molecular weight does increase more than two fold, there can be no argument as to the occurrence of combination; if there is only a two fold increase it is possible to interpret the results in two ways.

Ideally if initiation by diradicals can be achieved, the problem is simple in that with combination the DP is independent of overall rate and with disproportionation the DP varies inversely. As has already been stated (Section IV-3.A) initiation by diradicals produces no polymer. It is, however, possible to simulate the diradical system by using a dihydroperoxide with ferrous ions (107). Provided the initiator is substantially exhausted during the reaction, the DP is independent of rate in the case of styrene over quite a wide range. The beauty of the method lies in the fact that measurement of absolute molecular weights are unnecessary since one merely has to decide whether or not variation takes place.

5. Transfer Mechanism

It is generally thought that the mechanism of transfer reactions involves the abstraction of a hydrogen or other atom from a monomer or solvent molecule to give a free radical, capable of repropagating the chain. An extreme case of this is found in the addition of CCl_3Br to unsaturated molecules, e.g., cyclohexene, stoichiometrically described by

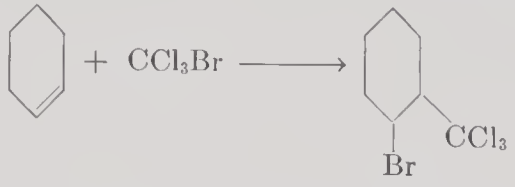

but whose mechanism is known to be a free radical one involving the creation of trichloromethyl radicals (108,109). The steps are then

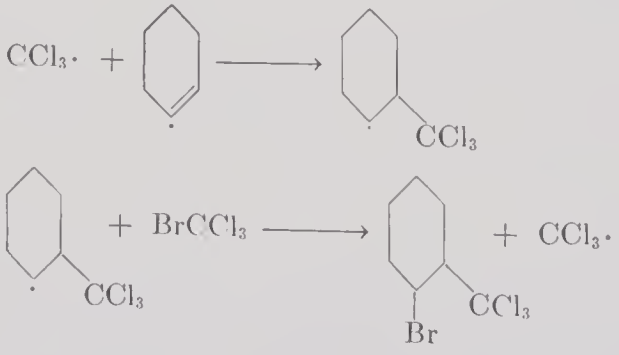

Although this may be true in most cases it should be remembered that stability could be achieved by the radical by donation of a suitable atom to an unsaturated monomer. This is true for the simple dimerization of methallyl chloride (110) which proceeds by the mechanism

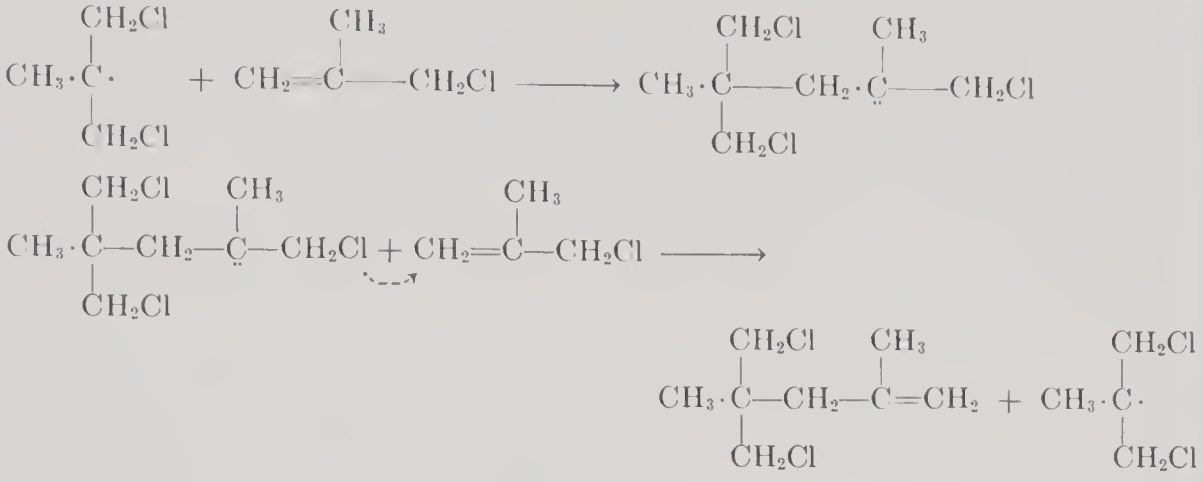

Interaction of small radicals with aromatic molecules usually yields addition products. In polymerization this fact has for long been disregarded, but recently evidence has accumulated to show that the simple "extraction" mechanism is unlikely to be true. It has been shown that polymerization of vinyl acetate in benzene gives a polymer with many (10–15) benzene molecules incorporated in the chain (111). This has been found to be true also for methyl methacrylate (112). Another almost inexplicable fact is that, when polymerized in chlorobenzene solution, polystyrene so formed contains no chlorine even though molecular weight measurements would suggest the contrary (113,114). This has been verified using radioactive labelling of bromobenzene (115), in which experiments apparently no aromatic fragments are incorporated in the chain. Mayo (116) explains this in the following way:

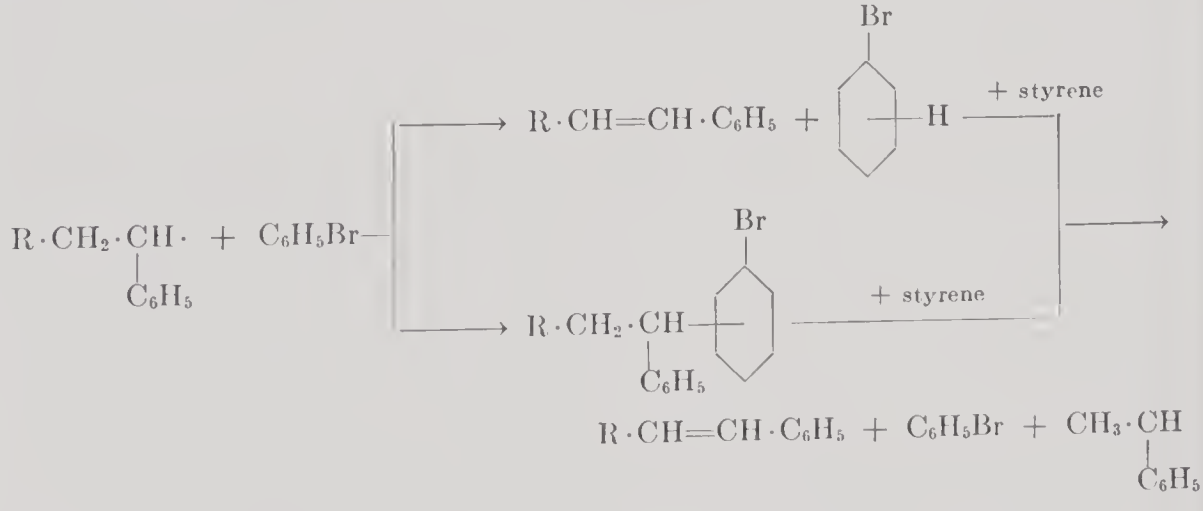

The first of these processes involving the surrender of a hydrogen atom by the growing radical and the subsequent abstraction of a monomer appears to be the more likely. A similar type of reaction has been recorded by Ford and Mackay (117) in the decomposition of 2-thenoyl peroxide in halogenobenzenes when the main product is phenyl thiophenate with displacement of halogen presumably as hydride.

It is, therefore, obvious that the mechanism of transfer reactions is by no means well authenticated or understood. With saturated nonaromatic solvents, however, it is inescapable that the first mechanism is operative. In general terms we may write

$$P_n\cdot + XS \longrightarrow P_nX + S\cdot$$

$$S\cdot + M \longrightarrow SP_1 \text{ etc.} \qquad k_f'$$

A reaction such as this produces dead polymer so by analogy with Equation (23a) the degree of polymerization is given by

$$\overline{DP}_n^{-1} = k_f/k_p + k_f'(XS)/k_p(M) + ak_t^{1/2}R_i^{1/2}/k_p(M) \qquad (29)$$

In the case of the thermal polymerization of styrene $R_i = k_1(M)^2$ so that (29) becomes

$$\overline{DP}_n^{-1} = k^2/k_p + ak_t^{1/2}k_1^{1/2}/k_p + k_f'(XS)/k_p(M) \qquad (29a)$$

i.e., there is a linear relationship between $\overline{DP}_n^{-1}$ and the molar ratio of solvent to monomer. This equation has been extensively used to determine the ratio k_f'/k_p (118).

The general mechanism given above does not take into account the fact that the radicals derived from the solvent might interact either with polymeric radicals or other solvent radicals to bring about chain termination. The effect on this on the molecular weight will not be likely to be a first order effect but it will alter rate of reaction very considerably. Indeed an hypothesis such as this gives a plausible explanation for much of the early discrepancies in results obtained in solution (119–122).

6. Rate Constants for Homopolymerization

The main method which has been used for the determination of propagation and termination rate constants, is that of intermittent illumination (123–137); the theory and technique has already been dealt with in Chapter XX. In almost all these studies the rate of initiation was determined by inhibitor retarder methods. Occasionally an alternative procedure adopted, in particular, by Melville and Valentine (130) was used. This method makes use of the fact that the kinetic chain has a material existence as one or more macromolecules. Measurement of the number average chain length by osmometry or some such method will give a relationship between chain length and rate which according to Equation (23b) is

$$\overline{DP}_n^{-1} = k_f/k_p + ak_t[-d(M)/dt]/k_p^2(M)^2$$

Plotting $\overline{\mathrm{DP}}_n^{-1}$ against rate, $-d(\mathrm{M})/dt$, gives a straight line of slope $a_p k_t/k_p^2(\mathrm{M})^2$ and intercept on the $\overline{\mathrm{DP}}_n^{-1}$ axis of k_f/k_p. Again by definition, the lifetime of the radical chain is given by

$$\tau = (k_t R_i)^{-1/2}$$

or

$$\tau^{-1} = k_t[-d(\mathrm{M})/dt]/k_p(\mathrm{M}) \tag{30}$$

Thus there is again a linear relationship between the reciprocal lifetime and rate, the slope of the line being $k_t/k_p(\mathrm{M})$. In this way it is possible to obtain the ratios k_t/k_p^2 and k_t/k_p provided a is known and so k_p, k_t, and then k_f may be determined separately. The uncertainty in the method relates to the value of a for which separate experiments are required.

Melville and Valentine's data give a good illustration of this procedure. In a particular series of experiments using styrene under intermittent illumination with a sector for which $\tau = 1$ (see Chapter XX for definition) the results shown in Table VI were obtained. Table VII gives data

TABLE VI
Lifetimes as a Function of Rate in Styrene Polymerization

Rate $\times 10^5$, mole l.$^{-1}$ sec.$^{-1}$	τ, sec.	τ^{-1}
2.45	1.89	0.53
2.90	1.68	0.595
2.98	1.74	0.575
4.10	1.54	0.650
4.10	1.48	0.675

TABLE VII
DP_n of Polystyrene as a Function of Rate

Rate $\times 10^5$, mole l.$^{-1}$ sec.$^{-1}$	$\overline{DP}_n$	$\overline{DP}_n^{-1} \times 10^4$
2.27	798	12.53
3.04	615	16.26
3.40	566	17.67
4.00	460	21.74

on molecular weight measurements for a similar series of runs. Plotting each of these series of data in the manner suggested above gives $k_t/k_p(\mathrm{M}) = 2.33 \times 10^4$ from lifetime data and $ak_t/k_p^2(\mathrm{M})^2 = 52.4$, $k_f/k_p = 3.2 \times 10^{-5}$ from Table VII. The molar concentration of styrene was 8.71 moles per liter so we have

$$ak_t/k_p^2 = 3.98 \times 10^3 \text{ liters}^{-1} \text{ mole second} \qquad k_t/k_p = 2.03 \times 10^5$$

If, as was assumed by the authors, disproportionation is the effective termination process, division of the second quantity by the first yields $k_p = 51.0$ liters mole^{-1} second^{-1} and thus $k_t = 10.4 \times 10^6$ liters mole^{-1} second^{-1} and $k_f = 1.6 \times 10^{-3}$ liters mole^{-1} second^{-1}. Subsequently it has been shown that combination is operative in which case $a = 0.5$ which has the effect of reducing the k_p and k_t values and increasing k_f by a factor of 2, i.e., the correct values in the light of additional experiment are

$$k_p = 25.5 \text{ liters mole}^{-1} \text{ second}^{-1}$$

$$k_t = 5.2 \times 10^6 \text{ liters mole}^{-1} \text{ second}^{-1}$$

$$k_f = 3.3 \times 10^{-3} \text{ liters mole}^{-1} \text{ second}^{-1}$$

The nonstationary state method can also be conveniently applied to polymerizing systems with the same reservations as we have already made. Direct measurement of the natural induction and decay periods of polymerizing systems have been made using a number of changes in physical properties, e.g., dielectric constant (139,140), refractive index (141), and temperature (142). The latter arises from the discovery, in attempting to apply the other methods directly, that the rise in temperature due to the heat evolved produces greater changes than those resulting from the formation of polymers.

The apparatus for the dielectric method consisted of a 50 Mc. per second signal generator used to feed two arms of a bridge circuit, the feeds being identical in amplitude but of opposing phase. Two tuned circuits are in the arms of the bridge, these being arranged to resonate at the generator frequency. The outputs of the circuits are fed to a suitable receiver so that any difference arising from a chemical change occurring in one circuit gives rise to a difference signal which can be amplified and recorded. Figure 6 gives a schematic diagram of the apparatus used. The tuned circuits used were of the conventional capacity-inductance type. The condenser

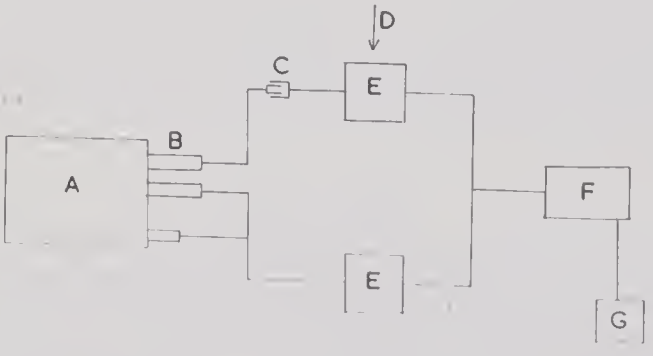

Fig. 6. Schematic diagram of dielectric constant apparatus (140). A, signal generator; B, attenuators; C, phase shifter; D, light source; E, tuned circuits; F, receiver; G, recorder.

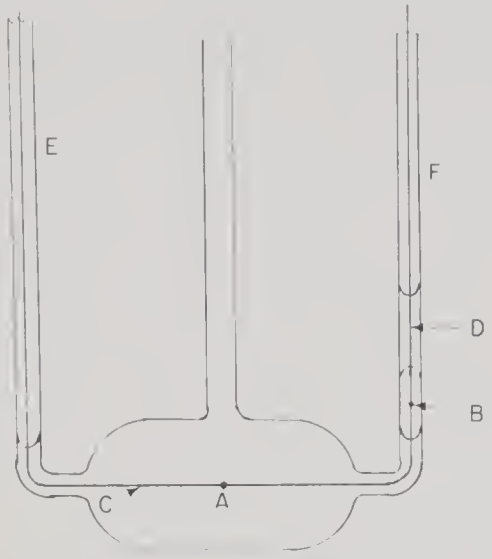

Fig. 7. Thermometric apparatus for nonstationary state measurements (142).

consisted of two parallel metal plates between which the monomer, contained in a parallel face silica vessel, was placed. On illuminating one of the reaction vessels, polymerization occurred which increased the dielectric constant of the medium as the polymer formed, but produced a reduction as heat is evolved and the temperature increased. The latter effect is approximately three times greater than the former.

Tests of the instrument show that the sensitivity is adequate for the study of the nonstationary phase, but the following limitations are apparent: (*1*) overall rate of reaction must be greater than 10^{-6} parts per second so that capacity changes due to reaction will exceed 10^{-7} parts per second, i.e., exceed the drift rate; (*2*) kinetic lifetime must be short and certainly not greater than one second; (*3*) quantum efficiency should be reasonably high.

The overall increase in refractive index for a number of monomers is about 0.15 for complete conversion. In order to utilize this physical change in nonstationary state experiments it is necessary to estimate conversion accurately to about 1 part in 10^6, or a refractive index change of 1 part in 10^7. This lies within the precision of an interferometer. A change in refractive index $d\mu$ is related to the number of interference fringes passing a given point by

$$d\mu = n\lambda/l$$

where λ is the wavelength of light used and l, the length of the light path. Thus for a change of 0.15 in μ for light of wavelength 5,461 A. (green mercury line) in 25 cm. tubes

$$n = ld\mu/\lambda = 7 \times 10^4$$

and a shift of one fringe would correspond to a conversion of 1 part in 6×10^6. Hence to achieve the required sensitivity a shift of 0.1 fringes has to be estimated. This is not very easy since fringes are necessarily diffuse, but it was found to be possible.

In operation it was found convenient to fill both tubes with the monomer under investigation but to one tube a quantity of inhibitor was added so that it could act as a reference tube. After checking the drift of fringes which is likely to be due to slow thermal polymerization both tubes were illuminated simultaneously and the movement of fringes observed either visually or by motion photography.

The simplest method so far devised for following the initial period of polymer reactions is a simple thermometric device in which the rise in temperature is measured using a simple thermocouple (142). The reaction vessel shown in Figure 7 consists of a dilatometer of about 15 ml. capacity made of soft glass with a copper/constantan thermocouple, *A*, sealed into the bulb and a balancing thermocouple, *B*, sealed in a glass tube just outside the dilatometer. The wires *C* and *D* are soldered to screened leads which are connected to the input terminals of a low impedance d.c. amplifier; the leads are covered with rubber tubing which is slipped over the side tubes *E* and *F*. The output of the amplifier is fed to a pen recorder or photographic recorder through a suitable switching arrangement.

Runs were carried out in a thermostat controlled to within ± 0.01°C. but the temperature difference recorded between the thermocouples for a static system was never greater than 0.001°C. which is the minimum error. Noise level in the amplifier gave rise to a temperature error of about 0.00014°C. An ordinary pen recorder has a response time of about 0.5 sec. for full scale deflection. In order to improve the resolution in time photographic recording of the reflected spot from a galvanometer (response time 0.025 second) was employed. The recording was achieved on a large drum camera whose speed was arranged so that 5 in. of paper corresponded to 1 second. In this way accurate records were obtained from which very precise lifetime data could be obtained.

This method cannot be claimed to be as sensitive as either of the methods previously described either in measurement of conversion (i.e., temperature

TABLE VIII
Comparison of Sensitivity of Nonstationary State Apparatus

Method	Refractive index	Dielectric constant	Thermocouple
Sensitivity in time, sec.	2×10^{-2}	10^{-4}	10^{-1}
Sensitivity in temperature, °C.	10^{-4}	10^{-5}	2×10^{-4}

change) or in time resolution (see Table VIII) but it has several advantages. In the first place it is cheaper and much simpler in operation. It can be used to investigate polymerizations at high conversion and to demonstrate variations in lifetime with conversion up to about 100% conversion. It is possible to thermostat the system so that a study of the effect of temperature becomes possible with additional information on activation energies and so on. The results of these investigations have been admirably summarized by Melville (143).

Finally, we consider a method of extreme experimental elegance devised originally by Bamford and Dewar (144). The technique involves the use of viscosity measurements in a suspended level vacuum viscometer to follow the early stages of reaction. Obviously this method requires that the molecular weight remains constant, which further enforces the limitation of low conversion. Essentially three quantities are measured (*1*) rate of change of viscosity at very low conversions, (*2*) molecular weight of the product, (*3*) increase in viscosity during photochemical after-effect. Thus the first requirement is an accurate knowledge of the relationship between the specific viscosity at infinite dilution, η_{sp}, and the molecular weight. This can be expressed as

$$\eta_{sp}/c = K'(M_0\overline{\mathrm{DP}}_n)^{\alpha} \tag{31}$$

where c is concentration expressed as moles of monomer units per unit volume, K' and α are constants, M_0 is molecular weight of monomer and $\overline{\mathrm{DP}}_n$, the number average degree of polymerization. Basing their arguments on a scheme which allows for diradical initiation and disproportionation, Bamford and Dewar (144) show that for thermal polymerization

$$d\eta_{sp}/dt = K'M_0(\mathrm{M})^2k_0^{1/2(1-\alpha)}/(k_p^2/k_t)^{1/2(1-\alpha)}(\beta + 2^{\alpha}\omega)/(\beta + 1)^{1+\alpha} \tag{32}$$

where k' is the rate constant for thermal initiation, $\beta = (k_ik_t)^{-1/2}k_f$; $\omega = (2 + \alpha)/2^{1+\alpha}$. The corresponding equation for a photoinitiated polymerization is:

$$d\eta_{sp}/dt = K'M_0(\mathrm{M})^2(k_p^2/k_t)^{1/2(1+\alpha)}k_i^{1/2(1-\alpha)}[\xi(\beta + 2^{\alpha}\xi)/(\beta + \xi)^{1+\alpha}] \tag{33}$$

where $\xi = (1 + AI)^{1/2}$ in which A is a constant and I the relative light intensity. The DP_n of the thermal polymer is

$$\overline{\mathrm{DP}}_n = 2k_p(k_ik_t)^{-1/2}(2\beta + 1) \tag{34}$$

The additional relationship is provided by study of the photochemical after effect. The mathematical relationships here are very complex. The reader is referred to the original (144) or to an extended version (145).

Experimentally, the measurements are relatively simple and require no elaborate equipment. As far as the after-effect is concerned the

following method was adopted. If monomer is irradiated for a time t_1 seconds, and the total increase in viscosity is measured after a further time, t_2 seconds, the total change may be expressed as

$$\delta\eta = at_1 + bt_2 + \Delta\eta_I^{t_2} - \Delta'\eta_I^{t_1}$$

where a and b are the photochemical and thermal rates respectively, $\Delta\eta_I^{t_2}$ is the after-effect and $\Delta'\eta_I^{t_1}$ the pre-effect (i.e., the viscosity change during the build up to steady state). Plotting $(\xi\eta - bt_2)$ against t_1 gives a straight line from which a and $(\Delta\eta_I^{t_2} - \Delta'\eta_I^{t_1})$ may be found. It is not easy to separate pre- and after-effects but at high light intensities the latter is only a small fraction of the measured quantity and can readily be allowed for provided t_1 is always long enough for the steady state to be closely approximated. In practice t_2 is always great enough for the rate to have returned to the thermal value so that the quantity $(\Delta\eta_I^{\infty} - \Delta'\eta_I^{\infty})$ is measured.

The method has been successfully applied to styrene (146), methyl methacrylate (147), *p*-methoxyl styrene (148), and vinyl acetate (149). In theory, the analysis can be extended to copolymerization but no experimental details are available (150).

V. COPOLYMERIZATION

1. Copolymer Composition Equation

It has been known for a long time that a mixture of two or more vinyl monomers will polymerize to give a high molecular weight product in whose chain molecules all the monomeric units are represented. Further, the relative amounts of monomer incorporated in polymer is usually different from the composition of the monomer mixture. Despite the long history of production of copolymers, fundamental studies date only from about 1944. The stumbling block to earlier progress was a failure to grasp the mechanism of the propagation step.

In a copolymerization involving n monomers there will be n^2 possible propagation steps, i.e., for two monomers, four propagation steps, thus

$$\mathrm{P}\cdot + \mathrm{A} \longrightarrow \mathrm{P}\cdot \qquad \text{rate} = k_{p,\,aa}(\mathrm{P})(\mathrm{A})$$

$$\mathrm{P}\cdot + \mathrm{B} \longrightarrow \mathrm{Q}\cdot \qquad \text{rate} = k_{p,\,ab}(\mathrm{P})(\mathrm{B})$$

$$\mathrm{Q}\cdot + \mathrm{A} \longrightarrow \mathrm{P}\cdot \qquad \text{rate} = k_{p,\,ba}(\mathrm{Q})(\mathrm{A})$$

$$\mathrm{Q}\cdot + \mathrm{B} \longrightarrow \mathrm{Q}\cdot \qquad \text{rate} = k_{p,\,bb}(\mathrm{Q})(\mathrm{B})$$

where A and B are the monomers and P· and Q· growing radicals ending in A and B monomeric units respectively. In the steady state with long chains the consumption of monomer is wholly by the above reactions and their relative rates consequently govern the composition of the copolymer. This was first realized in 1944 and brought about the formulation of the so called copolymer composition equation (151–153). The rates of disappearance of the respective monomers are

$$-d(\mathrm{A})/dt = [k_{p,\,aa}(\mathrm{P}) + k_{p,\,ba}(\mathrm{Q})](\mathrm{A})$$

$$-d(\mathrm{B})/dt = [k_{p,\,ab}(\mathrm{P}) + k_{p,\,bb}(\mathrm{Q})](\mathrm{B})$$

thus we can write

$$d(\mathrm{A})/d(\mathrm{B}) = (\mathrm{A})[k_{p,\,aa}(\mathrm{P}) + k_{p,\,ba}(\mathrm{Q})]/(\mathrm{B})[k_{p,\,ab}(\mathrm{P}) + k_{p,\,bb}(\mathrm{Q})] \quad (36)$$

giving the relative rates if incorporation of A and B in the growing chain. If a stationary state is to exist then it follows that the rate of conversion of P radicals to the Q type must equal the rate of conversion of Q to P, i.e.,

$$k_{p,\,ab}(\mathrm{P})(\mathrm{B}) = k_{p,\,ba}(\mathrm{Q})(\mathrm{A}) \quad (37)$$

Thus, we can substitute for (Q) in Equation (36) to obtain

$$d(\mathrm{A})/d(\mathrm{B}) = [k_{p,\,aa} + k_{p,\,ab}](\mathrm{A})/[k_{p,\,ab} + k_{p,\,bb}k_{p,\,ab}(\mathrm{B})/k_{p,\,ba}(\mathrm{A})](\mathrm{B})$$

which can readily be reduced to

$$d(\mathrm{A})/d(\mathrm{B}) = (\mathrm{A})[k_{p,\,aa}/k_{p,\,ab}](\mathrm{A}) + (\mathrm{B})]/(\mathrm{B})[(\mathrm{A}) + (k_{p,\,bb}/k_{p,\,ba})(\mathrm{B})]$$

by multiplying through by $(\mathrm{A})/k_{p,\,ab}$. Now we define

$$r_1 = k_{p,\,aa}/k_{p,\,ab}$$

$$r_2 = k_{p,\,bb}/k_{p,\,ba} \quad (38)$$

in which r_1 and r_2 are termed the monomer activity ratios and the equation

$$d(\mathrm{A})/d(\mathrm{B}) = (\mathrm{A})/(\mathrm{B})[r_1(\mathrm{A}) + (\mathrm{B})]/[(\mathrm{A}) + r_2(\mathrm{B})] \quad (39)$$

the copolymer composition equation which will define the instantaneous composition. Equation (39) may be integrated to give the overall copolymer composition for finite conversion thus:

$$r_2 = \frac{\ln(\mathrm{B})_0/(\mathrm{B}) - (1/p)\ln\{1 - p[(\mathrm{A})/(\mathrm{B})]\}/\{1 - p[(\mathrm{A})_0/(\mathrm{B})_0]\}}{\ln(\mathrm{A})_0/(\mathrm{A}) + \ln\{1 - p[(\mathrm{A})/(\mathrm{B})]\}/\{1 - p[(\mathrm{A})_0/(\mathrm{B})_0]\}} \quad (40)$$

in which $(\mathrm{A})_0$ and $(\mathrm{B})_0$ are the initial concentrations of the monomers and

$$p = (1 - r_1)/(1 - r_2) \quad (41)$$

The copolymer composition equation can be derived on purely statistical considerations without having recourse to the steady state assumption (154).

Data from copolymerization experiments afford a means of comparing the rates of reaction of monomers with free radicals, since the quantities measured arise from differences given by competing reactions and are accordingly sensitive to small variations in rate. Referring to the definition of monomer reactivity rates we have

$$k_{p,\,ab} = k_{p,\,aa}/r_1 \tag{42}$$

where $k_{p,\,ab}$ defines the rate of addition of a radical with A type end group to a B molecule. Thus, measurement of r_1 for the copolymerization of monomer A with a series of different monomers B_1, B_2, . . . B_n, we have

$$k_{p,\,ab1} = k_{p,\,aa}/r_{11} \qquad k_{p,\,ab2} = k_{p,\,aa}/r_{12} \qquad k_{p,\,abn} = k_{p,\,aa}/r_{1n}$$

For comparative purposes $k_{p,\,aa}$ may be set equal to unity when the reactivities of the individual monomers become the reciprocals of the reactivity ratios.

It is also quite evident that, if the absolute rate constant $k_{p,\,aa}$, is known from studies of homopolymerization, the absolute value of $k_{p,\,ab}$ may be obtained by evaluation of r_1 (155).

The values of r_1 and r_2 are frequently used as a measure of the tendency of a system to alternate, i.e., the tendency of P· to react with B and Q· with A. Thus it is evident that if r_1 is less than unity B will add to P· faster than will A, so that with comparable concentrations of monomer, the appearance of the sequence A—B in the polymer becomes greater. It can be demonstrated that the smaller the value of the product r_1/r_2 the greater is the tendency to alternation (156).

In general it is found that monomer reactivity ratios are remarkably insensitive to reaction media (157,158) and rate of reaction (157), but are affected a little by temperature (157,159). The insensitivity to medium gives confirmation to the radical mechanism and demonstrates conclusively that there is little or no polar effect. The above treatment may be extended to systems of several monomers (160,161).

Copolymers may be formed between monomers one or both of which do not undergo homopolymerization, e.g., styrene and maleic anhydride (162) or maleic anhydride and stilbene (163). More curiously, copolymers have been prepared between vinyl monomers and nonethylenic molecules such as oxygen (164) and sulfur dioxide (165).

2. Determination of Monomer Reactivity Ratios

When only small conversions are considered it is possible to determine monomer reactivity ratios by direct application of Equation (39). Most conveniently this equation is solved for r_2 to give

$$r_2 = [(A)/(B)]\{d(B)/d(A)[1 + (A)/(B)r_1] - 1\} \quad (43)$$

Experimentally one can measure the reed ratio (A)/(B) and the polymer composition which at low conversion may be taken as $d(A)/d(B)$. With a knowledge of these quantities the straight line represented by Equation (43)

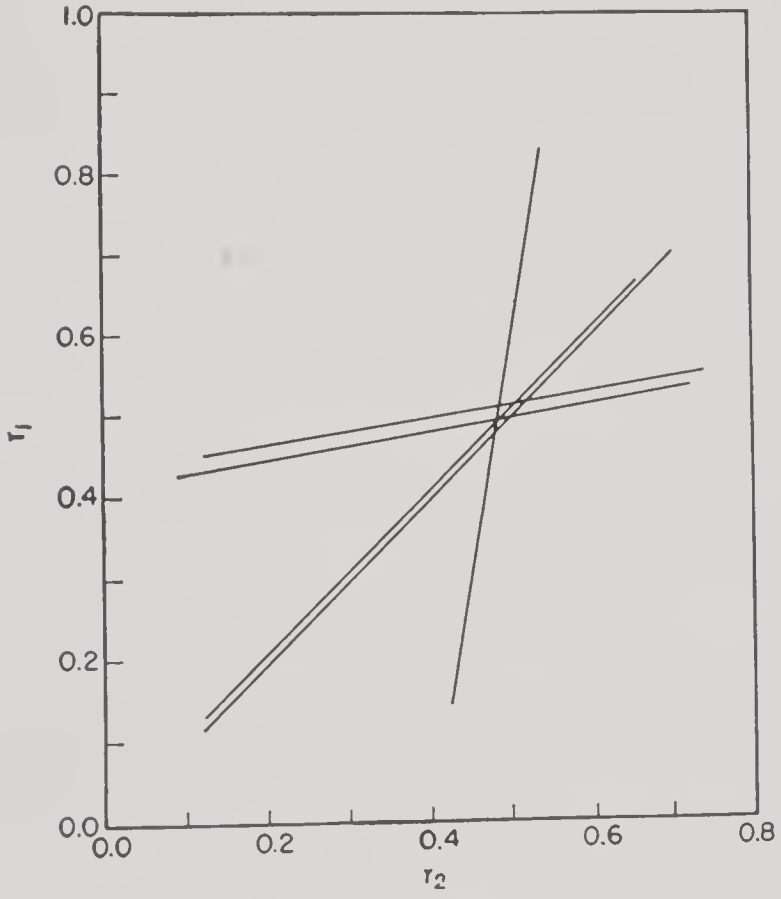

Fig. 8. Plots of r_1 versus r_2 for data derived from styrene–methyl methacrylate copolymerization.

can be plotted. Repetition of the procedure for various feeds gives a number of straight lines which should intersect in a point defining r_1 and r_2 for the system.

An illustration of the application of the method is shown in Figure 8 (151). It will be seen that the lines do not pass through a single point but define a small area from which the precision of the measurements may be deduced. Strictly speaking, Equation (43) can be applied only to small conversions (say 1%) but somewhat higher conversions may be tolerated

using the average value of the feed. Even this refinement soon brakes down and certainly above 20% conversion it is necessary to use the integrated expression (40).

The greatest errors are introduced in the analysis of the product to determine the proportion of monomers incorporated in the polymer. The preparation of the sample and its isolation is carried out using methods described in Section I. Copolymer composition is determined by standard analytical procedures in the main although occasionally difficulties are encountered, as in the Kjeldahl estimation of nitrogen which almost invariably gives low results (157,158,166). Analysis for characteristic groups can be used with advantage, e.g., acetoxy in vinyl acetate, and similarly with characteristic atoms, e.g., oxygen in copolymers of hydrocarbon monomer and an ester (167). Purely physical methods such as refractive index (168,169), and ultraviolet (170) and infrared (171) absorption have also found some application. Potentially the most powerful and sensitive method is the use of a monomer containing a radioactive atom, but only one instance of this technique is recorded (172).

Monomer reactivity ratios for a very large number of copolymer systems have been evaluated and most of these have been drawn together in tabulated form (173). Efforts have been made to systematize the results from reactivity ratio studies in the hope that values could be calculated for monomer pairs without the necessity of specific investigation of each pair. The most significant of these attempts, whose aim is to provide a numerical basis of classification, is due to Alfrey and Price (174,175,176). According to this treatment, the rate constants for propagation reactions are written in the form:

$$k_{p,\,aa} = \alpha_{aa} \exp\{-\Delta F_{aa}/RT\} = \alpha_{aa} \exp\{-(p_a + q_a + \epsilon_a^2/rD)/RT\}$$

$$k_{p,\,ab} = \alpha_{ab} \exp\{-\Delta F_{ab}/RT\} = \alpha_{ab} \exp\{-(p_a + q_b + \epsilon_a\epsilon_b/rD)/RT\}$$

where ΔF_{aa} and ΔF_{ab} are the free energies of activation for P + A and P + B reactions respectively, and the α terms are related to the frequency factors; p_a is related to the radical reactivity and q's to the ease of addition of radical to the monomeric molecules. The factors ϵ_a^2/rD and $\epsilon_a\epsilon_b/rD$ are intended to express the interaction of charge associated with the radical and double bond, r being the separation in the transition state and D, the effective dielectric constant; these factors are influenced to a great extent by substituents on the molecules. The monomer reactivity ratio can now be expressed as:

$$r_1 = \alpha_{aa} \exp\{-(p_a + q_a + {}_a\epsilon^2/rD)/RT\}/\alpha_{ab} \exp\{-(p_a + q_b + \epsilon_a\epsilon_b/rD)/RT\} \quad (44)$$

If there are no abnormal steric factors $\alpha_{aa} \approx \alpha_{ab}$ and (44) becomes

$$r_1 = [\exp\{-q_a/RT\}/\exp\{-q_b/RT\}] \exp\{-\epsilon_a(\epsilon_a - \epsilon_b)/rDRT\} \quad (45)$$

which is usually written in the form

$$r_1 = (Q_a/Q_b) \exp\{-e_a(\epsilon_a - e_b)\} \quad (46)$$

The parameters Q and e are characteristic of each monomer and so in an ideal system it would be possible to calculate reactivity ratios from established Q and e values. It has been found that this situation does not obtain in any great measure and the whole method must be considered as only semiquantitative. At the same time it does provide a fairly reliable guide to possible reactivity ratios for monomer pairs not directly investigated. The assumptions do reveal some weaknesses in the method in that no provision is made for differing electrostatic effects between the radical and molecule form of a monomeric unit. Any modification to allow for possible differences of this nature is, however, likely to complicate matters still further and to make reasonable correlation even more difficult (177).

3. Rates of Reaction

Studies of copolymer composition and the concomitant evaluation of monomer reactivity ratios gives very considerable information on reactions between radicals and unsaturated molecules, but cannot cope with the more interesting and difficult problem of interradical processes. Copolymerization affords a convenient method of making at least a limited attack on this problem in that the termination reaction in a binary copolymerization involves not only interaction of like radicals but also quite probably interaction of unlike radicals. Indeed we have as possible termination steps:

$$\left.\begin{array}{l} 2\mathrm{P}\cdot \\ 2\mathrm{Q}\cdot \\ \mathrm{P}\cdot + \mathrm{Q}\cdot \end{array}\right\} \longrightarrow \text{Inactive products} \quad \begin{array}{l} \text{rate} = k_{t,\,aa}(\mathrm{P})^2 \\ \text{rate} = k_{t,\,bb}(\mathrm{Q})^2 \\ \text{rate} = k_{t,\,ab}(\mathrm{P})(\mathrm{Q}) \end{array}$$

On carrying out the usual stationary state kinetic analysis one obtains the following expression for the reaction rate (178)

$$-d[(\mathrm{A}) + (\mathrm{B})]/dt = [r_1(\mathrm{A})^2 + 2(\mathrm{A})(\mathrm{B}) + r_2(\mathrm{B})^2]R_i^{1/2}[r_1^2\delta_a^2(\mathrm{A})^2 + 2\phi r_1 r_2 \delta_a \delta_b(\mathrm{A})(\mathrm{B}) + r_2^2\delta_b^2(\mathrm{B})^2]^{-1/2} \quad (47)$$

in which symbols have their usual significance and in addition

$$\delta_a^2 = k_{t,\,aa}/k_{p,\,aa}^2 \qquad \delta_b^2 = k_{t,\,bb}/k_{p,\,aa} \qquad \phi = k_{t,\,ab}(k_{t,\,aa}k_{t,\,bb})^{-1/2}$$

The new quantity ϕ is in effect a measure of the preference for reaction between like radicals.

When one of the monomers, say B, does not polymerize a new analysis has to be carried through since it is not sufficient merely to eliminate terms involving ($r_2 = 0$) from Equation (47). The correct expression is

$$-d[(A) + (B)]/dt = (A)[r_1(A) + 2(B)]R_i^{1/2}[r_1^2\delta_a^2(A)^2 + 2\phi r_1\delta_a\xi(A)(B) + \xi^2(B)^2]^{-1/2} \quad (48)$$

in which $\xi^2 = k_{t,\,bb}/k^2_{p,\,ba}$.

A similar expression applies to systems in which neither monomer polymerizes alone, i.e.,

$$-d[(A) + (B)]/dt = 2(A)(B)R_i^{1/2}[\xi_a^2(A)^2 + 2\phi\xi_a\xi_b(A)(B) + \xi_b^2(B)^2]^{-1/2} \quad (49)$$

where the ξ has the same form as previously.

Generalized treatments of the rate equations for systems of many monomers can be worked out but are of doubtful utility (180).

The usual methods for following the rate of reaction have been used in assessing rates of copolymerization, but it is obviously necessary to use average values of physical properties of the monomer and polymer if techniques such as dilatometry are used (181,182). In order to achieve a satisfactory evaluation of the ϕ factor it is necessary to evaluate the rate of initiation, which can be troublesome. In almost all cases so far studied it is found that the rate of reaction as a function of monomer composition passes through a minimum. With the styrene and methyl methacrylate system the addition of small amounts of styrene depresses the rate of reaction very markedly but after a relatively rapid drop, the rate slowly increases as the amount of styrene is further increased (182,183). On the whole, the minima observed experimentally are rather broad and their position cannot be sufficiently accurately determined to allow estimation of ϕ, as has been suggested by Palit (184). In all the systems studied ϕ is

TABLE IX
Interaction of Unlike Radicals

Monomer system	ϕ	Refs.
Styrene–*p*-methoxystyrene	1	185
Styrene–methyl methacrylate	6–20	182,183
Styrene–butyl acrylate	7–150	167,181
Styrene–methyl acrylate	20–90	183
Styrene–*m*-vinyl phenol	*ca.* 1	186
Styrene–diethyl fumarate	6	187
Methyl methacrylate–vinyl acetate	450	188
p-Methoxy styrene–methyl methacrylate	*ca.* 24	185

found to be greater than unity as is shown in Table IX. In this table the values given as ranges are intended to indicate that there is a trend in the value of ϕ which apparently increases as the proportion of the first monomer increases.

The variation in ϕ with monomer feed is indeed perplexing and various explanations have been put forward, none of which seem to account adequately for the magnitude of the effect in certain systems. Burnett and Loan (189) suggested that the increase in ϕ with increasing styrene content could be interpreted as implying a transfer reaction involving the aromatic nucleus which could then act as a chain breaking radical. This appears logical on the lines of their investigation of polymerization in aromatic solvents. If such a transfer reaction does occur and the radicals are capable of stopping chains the effect increases with styrene concentration. Further the neglect of such side processes invalidates Equation (47) in the denominator of which there would be further terms involving the styrene concentration. To test this hypothesis the experiments with the vinyl acetate–methyl methacrylate system (188) were carried out, when it was found that no such trend occurred.

The one universal discovery was the fact that ϕ is generally greater than and is certainly never less than unity. This is in line with results for other free radical processes, e.g., oxidation (see Chapter XX).

Very occasionally the rate of copolymerization exceeds the homopolymerization rate so that the rate versus composition curve passes through a maximum (172,187,190). It has recently been shown that this is explicable provided both reactivity ratios are less than 2. Indeed for the systems described experimentally one has always been zero, i.e., one nonpolymerizable monomer. The condition is not necessary and sufficient, as high ϕ values for example may cause the maximum to disappear but as one might expect in such systems the rate then decreases as the proportion of nonpolymerizable monomer increases (191).

The data on reaction rates are really too scanty to allow generalizations to be made but a scheme reminiscent of the Alfrey-Price system of Section V.2. has been suggested by Melville (181). It is suggested that the termination constants may be expressed as

$$k_{t,\,aa} = \mathrm{A}_{aa}\mathrm{P}_a{}^2 \exp\left\{-e_a{}^2\right\}$$
$$k_{t,\,ab} = \mathrm{A}_{ab}\mathrm{P}_a\mathrm{P}_b \exp\left\{-e_a e_b\right\}$$

with a similar expression for $k_{t,\,bb}$. Substituting these in the definition of ϕ gives

$$\phi_2 = (\mathrm{A}_{ab}{}^2/\mathrm{A}_{aa}\mathrm{A}_{bb}) \exp\left\{e_a{}^2 - 2e_a e_b + e_b{}^2\right\}$$
$$= (\mathrm{A}_{ab}{}^2/\mathrm{A}_{aa}\mathrm{A}_{bb})(r_1 r_2)^{-1}$$

The correlation between ϕ and r_1r_2 is shown in Table X in which average values of ϕ have been adopted. It will be seen that the agreement is quite good and is altogether in line with the general idea of radical reactivity.

TABLE X
Correlation Between ϕ and r_1r_2

System	r_1r_2	ϕ
Styrene–*p*-methoxystyrene	0.95	1
Styrene–methyl methacrylate	0.26	14
p-Methoxystyrene–methyl methacrylate	0.09	24
Styrene–methyl acrylate	0.19	50
Styrene–butyl acrylate	0.07	150
Styrene–diethyl fumarate	0.028	6

4. Block and Graft Copolymers

A. SYNTHESIS OF BLOCK COPOLYMERS

Copolymers prepared by allowing a mixture of suitable monomers to polymerize together will have a more or less random arrangement of monomeric units in the chain, with certain modifications introduced by the tendency of the monomers to alternate. It is possible to conceive another type of copolymer in which there are long sequences of monomeric units of the same type. The properties of such copolymers might be of considerable importance; more particularly as fiber forming materials. It has been shown that silk fibroin has just such a structure (192,193). Edgar and Hill (194) have shown that the product of condensation of polyethylene glycol and terephthalic acid is superior in some respects to the similar polymer obtained from ethylene glycol and terephthalic acid. The former will possess long sequences of methylene groups and so could be classified as similar to the copolymers envisaged above. Long sequence copolymers based on cellulose (195) have been produced but the production of purely synthetic material is of recent interest. Mark (196) gave such products the name of "macromolecules of long range periodicity" but it is now generally agreed that despite some ambiguity the name of "block copolymers" should be adopted.

In this section we will be concerned with the synthesis of block copolymers by free radical mechanisms. The early work of Bolland and Melville (197) contained a technique by which block copolymers may well have arisen. In the vapor phase both methyl methacrylate and chloroprene gave the appearance of polymerizing by means of free radicals of exceptionally long life. If therefore a layer of polymethyl methacrylate is laid

down on the walls of a reaction vessel under conditions when long life radicals are formed, it is possible to pump off the methacrylate vapor and replace it by chloroprene which then polymerizes spontaneously. It seems highly probable therefore that long sequences of methacrylate and chloroprene units succeeded one another. No test of the polymer formed was ever carried out.

From purely radical standpoint the simplest method would apparently be to cause the scission of a polymer molecule in the presence of a foreign monomer. It would be expected that, given favorable conditions for addition, the radicals formed in the scission process would initiate the polymerization of the monomer to building up a block copolymer. This was attempted without success using ultrasonic irradiation to give the chain rupturing reaction (198). Since these early experiments, claims have been made that all types of shear processes may be used to bring about break down of a number of polymers and that the fragments are capable of initiating polymerization (199). It is certainly true that if rubber is masticated in the presence of a monomer such as methyl methacrylate block copolymers are formed (200).

The same end may be achieved in another way. If a mixture of two polymers is subjected to high shear either by milling or by ultrasonic irradiation of a suitable solution, the fragments resulting from scission may recombine to give block copolymers.

Some systems have been investigated by a method which involves the creation of a barrier between two monomers. If one monomer is water soluble and the other insoluble then it is possible to prepare an emulsion in which the extended phase is a solution of the one monomer in water, in which the second monomer is dispersed as an emulsion. Using a water soluble initiator such as potassium persulfate one would expect polymerization of the soluble monomer to proceed until the growing radical penetrated a micelle, when addition of the second monomer would occur. This was attempted by Melville and Dunn (201) with somewhat inconclusive results.

A second method utilizing emulsions appears to be more promising. In this one monomer is polymerized in emulsion to about 80% conversion using γ-radiation for initiation. It is necessary to irradiate only until the steady state is reached after which the reaction is nonterminating. After about 80% conversion a second emulsified monomer is added to the original emulsion and polymerization is known to continue until most of this added material has been consumed (202).

If a monomer is flowing rapidly through a capillary tube and is subjected to intense illumination at a point in its path, a very large concentration of free radicals is created in the tube. By arranging that the time of flow

between the point of illumination and the exit from the tube is short compared with the lifetime of the radicals, the greater proportion of radicals will leave the tube and may be dispersed in a second monomer thereby giving rise to block copolymers (203).

These methods are not, however, too convenient in application and it has been shown to be more expedient to form polymers with suitable end groups which may be reacted together to give rise to block copolymers. This can be accomplished for example, by carrying out polymerization in the presence of carbon tetrabromide or trichlorobromomethane, transfer reactions will ensure that almost all the polymer molecules produced will have terminal CBr_3 or CCl_3 groups. This polymer is isolated and dissolved in a second monomer and irradiated with light of requisite energy to cause scission of the CBr bond. This will give rise to a polymeric radical and a bromine atom both of which may initiate polymerization to give a block copolymer and a homopolymer of the second monomer (204).

A similar method has been worked out by Bamford and White (205) who use a tertiary amine as a chain transfer agent. If relatively high amine to monomer ratios are used almost all the polymeric molecules produced bear tertiary amine end groups. This polymer is isolated and dissolved in a second monomer as in the previous method. On polymerizing this monomer transfer occurs preferentially at the terminal group of the added polymer and so block copolymers are formed. The mechanism of the reaction, by means of which copolymers of methyl methacrylate and acrylonitrile were prepared, is given for the first polymer as:

$$P_n\cdot + \dot{R}CH_2\cdot N\cdot R'R'' \longrightarrow P_nH + R\dot{C}H\cdot N\cdot R'R''$$

$$R\dot{C}H\cdot N\cdot R'R'' + CH_2{=}CHX \longrightarrow R\cdot CH(NR'R'')\cdot CH_2\cdot \dot{C}HX \text{ etc.}$$

so that the first polymer has the structure

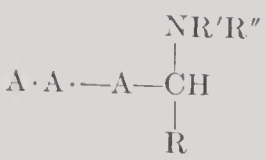

Transfer in the second monomer is thought to involve the other methylenic hydrogen of the group already participating in the reaction so that the block copolymer has the structure

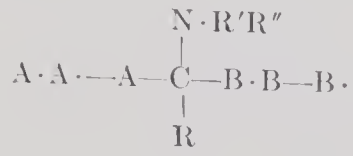

To obviate the difficulty of separating fairly large quantities of homopolymer, one can make use of dihydroperoxides in the following way. A monomer is polymerized using dihydroperoxide as initiator, the reaction being taken to a stage such that about half the hydroperoxy groups are destroyed. The polymer is then isolated and dissolved in a second monomer along with a source of ferrous ion. The resulting reduction activation process will give only polymeric radicals from which block copolymer will result. A little homopolymer will also be formed as a result of transfer reactions but this will not be so serious as in the previous case (206,207,208). This peroxide in conjunction with complexed iron(II) has been used to produce block copolymers of styrene and butadiene (209).

Probably the simplest method of chemical production of block copolymers is to condense together homopolymers with suitable functional end groups. At the same time, straightforward esterification between a carboxyl and hydroxyl ended polymer is unlikely to be successful because of the exceptionally low concentration of the participating species. This would however give the cleanest product if it could be operated. Usually polymers are prepared with like ends, say hydroxyl groups, which can be linked together by reaction with diisocyanates (210) or dicarboxylic acids. The latter are used in considerable excess in order to achieve a reasonable rate of reaction. This can be varied by using carboxylic end groups on the polymer and condensing with a suitable diol (211). In either of these cases molecules of the same polymer can undergo linkage which will mean that the block copolymer is in admixture with both homopolymers.

B. SYNTHESIS OF GRAFT POLYMERS

Graft copolymers may be defined as polymers in which branches are formed by different monomeric units from the main chain, i.e., they would have the general structure

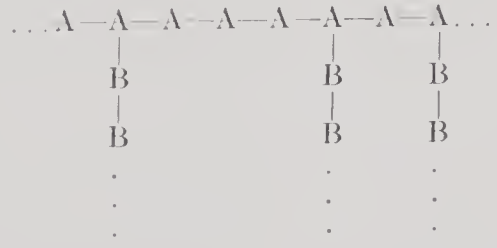

Synthesis is much more readily accomplished than for block copolymers, since polymerization in the presence of a suitable polymer will give the possibility of transfer to the polymer with growth occurring to give branches of the second polymer. This method was introduced by Smets (212) and has proved most successful. As with all reactions of this kind the chain length of the branches are subject to a distribution in lengths. In order to

achieve more uniform branch lengths Peaker (213) has used a condensation process which has proved successful with partially hydrolyzed polyvinyl acetate (essentially a copolymer of vinyl acetate and vinyl alcohol). Any hydroxyl end group polymer may be grafted to this main chain using diisocyanate or dicarboxylic acid as described above. Since one can fractionate the second polymer first a much more regular branch length is obtained.

Grafting of synthetic polymers such as polymethyl methacrylate or polystyrene to natural macromolecules such as rubber or cellulose is likely to be of some technical importance; such rubber products are available commercially on a limited scale. The fundamental work behind this type of graft reduction was carried out in 1954. To test the efficacy of the procedure the polymerization of a number of monomers in the presence of dihydromyrcene (2,6-dimethylocta-2,6-diene), a diisoprene system was investigated. It was found that both the rate and molecular weight were reduced (214). It seems reasonable to suppose that rubber would act as a macromolecular transfer agent, but this was not wholly realized. Using benzoyl peroxide as initiator for the rubber–methyl methacrylate system it was found that graft copolymers were formed but that this did not happen on replacing the peroxide by an azo initiator. When grafting does take place numerous short side chains are formed (215).

An ingenious special case of graft polymer formation has been elaborated by Guillet and Norrish (216) who photolyzed polymethyl vinyl ketone using light of sufficient energy to bring about ketonic fission. Since each monomeric unit has such a pendant ketonic group fission will give free radicals which are capable of bringing about polymerization with the formation of graft molecules.

C. PURIFICATION OF BLOCK AND GRAFT COPOLYMERS

Purification techniques which have been applied include fractional precipitation and chromatographic procedures such as those detailed previously. The problem is much more complicated than purification of a homopolymer and it is doubtful if a reasonably pure sample of block copolymer has yet been obtained. The solution of this problem is of great importance if studies on the properties of block copolymers are to be successful or meaningful.

VI. EMULSION POLYMERIZATION

1. Qualitative Theory

Many vinyl monomers can be polymerized at relatively high rates in an aqueous medium containing an emulsifier and a water soluble initiator.

Although the rate of reaction is high, the molecular weight of the product is much higher than would be obtained at comparable rates in bulk. A typical simple "recipe" would consist of 100 parts of monomer, 180 parts of water, 2 to 5 parts of a fatty acid soap, and 0.1 to 0.5 parts of potassium persulfate. Various other water soluble initiators may be used, as can cationic soaps such as dodecylamine hydrochloride.

When soap is added to water in excess of a critical concentration micellar aggregates are formed (217) which may contain 50 to 100 or more soap molecules depending on the size of the soap molecule. The precise structure of the micelle is not too clear, there being both lamellar and spherical configurations suggested.

The solubility of a monomer in water is increased considerably by the presence of soap micelles (218,219). X-ray and light scattering measurements reveal that the micelles increase in size when monomer is added showing that solubilized monomer is present in the micelles. Only a small part of the monomer is so accommodated, the remainder being present as droplets which are stabilized by some of the soap. The most important feature of this picture is the micellar soap which presents a greater surface than the droplets although very much less in volume.

Before one can make an attack on the kinetic features of the reaction it is necessary to inquire into the locus of the polymerization reaction. From a survey of much experimental evidence, Harkins (218) concluded that there are two principal loci of polymerization, one operating at the outset and the second later in the reaction when the character of the emulsion has altered. The micelles in which the monomer is relatively more abundant provide the most likely environment for initiation by radicals generated in the surrounding medium. As polymerization proceeds in the micelle more monomer is supplied to it from the external phase. Soon the polymer chain exceeds the size of the original micelle before termination is effected by a second radical. When this stage is reached the micelle is replaced by a polymer or latex particle. The soap is acquired by these polymer particles and so the soap concentration falls below the critical value and micelles cease to exist. Further polymerization occurs exclusively in the latex particles. It is not surprising that this occurs since the larger surface area of the latex particles make them more efficient in radical capture than the larger (in volume) monomer droplets. Monomer consumption within the latex particles is made up by diffusion from the droplets which serve as reservoirs supplying monomer to the polymer. At an advanced stage in the reaction (probably around 50% conversion) the excess of monomer in the droplets is exhausted and consequently the concentration of monomer in the latex diminishes as does the reaction rate.

2. Quantitative Theory

Several early attempts to place the foregoing qualitative theory on a quantitative basis gave expressions which could not be successfully applied to experiment because of their complexity. The problem was solved to a very good approximation by Haward (220) and Smith and Ewart (221). The latter theory will be developed briefly.

Under normal conditions the rate of generation of radicals is about 10^{13}/ml./second and the number of latex particles is about 10^{14}/ml. so that if all initiator radicals enter latex particles, any given particle will acquire a radical once in 10 seconds. The diffusion current, I, into a spherical particle of radius r is $I = 4\pi rD\ \Delta C$ where D is the diffusion constant and ΔC is the difference in concentration between the surface of the particle (taken to be zero) and far from it. If the latter is taken as the equilibrium concentration in the aqueous phase, $(\mathrm{R})_{aq}$ we have

$$(\mathrm{R})_{aq} = I/4\pi rD$$

Taking $D = 10^{-5}$ cm.^{2} second^{-1}, $r = 5 \times 10^{-6}$ cm. and I we know is 10^{-1} per second $(\mathrm{R})_{aq} \approx 10^8$ radicals per ml. Since the rate of generation is 10^{13}/ml./second the average time spent in the aqueous phase is about 10^{-5} second. The radical concentration is such that the rate of destruction of radicals in the aqueous phase cannot exceed 10^3/ml./second so that virtually all radicals generated enter latex particles. Furthermore the time spent by a radical in the aqueous phase is too short for addition of monomer to take place.

Within a particle of volume, v, containing n radicals the rate of termination r_t is

$$r_t = 2k_t n(n - 1)/v$$

Now k_t in units of ml. molecule^{-1} second^{-1} is about 5×10^{-16} and the volume about 5×10^{-16} ml. whence $2k_t/v = 2 \times 10^2$ per second. If the particle contains only 2 radicals termination will occur within $r_t^{-1} = v/4k_t = 2.5 \times 10^{-3}$ seconds. This is very much shorter than the time interval between captures and so we may consider that to a good approximation a particle will contain zero or one radical. Thus polymerization within the latex particles proceeds in bursts separated by equal periods during which the particle is dormant. It can also be shown that diffusion is adequate to maintain the observed rate of reaction.

Smith and Ewart (221) showed that the rate of reaction in the steady state, i.e., when the supply of monomer from droplets is still adequate to maintain the rate, is

$$r_p = k_p(N/2)(\mathrm{M})$$

expressed as rate per milliliter of water, where N is the number of particles per milliliter and (M) is the concentration within the particles. Thus the rate depends primarily on the number of latex particles and is independent of both the rate of generation of radicals and the size of particle, providing this is not so great as to render the above analysis invalid.

3. Experimental Investigations

To test the theory just put forward it is necessary to measure the reaction rate, the number of latex particles, and the concentration of monomer within the particles. None of these quantities is easily determined. Standard rate measurement using say dilatometry is difficult since the reaction mixture is virtually opaque and distortion of the meniscus can arise without being observable, and retention of emulsion character is usually impossible without stirring. Nevertheless this method has been successfully employed (222,223) provided modifications of the bulk technique are made, such as suitable coating of the capillary preferably with a silicone (223). The normal procedure is to use small bottles sealed by rubber or polyisoprene stoppers. Samples can be withdrawn through the stoppers by means of a hypodermic syringe, the caps being self-sealing. The bottles are tumbled end over end in order to preserve the emulsion. Using the latter system it is almost impossible to free the emulsion mixture from dissolved air although sealing off under nitrogen helps to reduce the effects. Using dilatometric procedures Burnett and Lehrle (223) were able to carry out a thorough out-gassing routine.

Estimation of the particle number has usually been carried out by electron microscopy (224,225) or by a soap titration procedure based on electron microscope calibration (226,227). Smith (224) measured the volume of the latex particles from estimation of diameters on electron micrographs. The particles were metal shadowed and apparently uncorrected for thickness of metal and expansion under electron bombardment. Burnett and Lehrle compared this procedure with that of making a count of the number of particles in a small volume of diluted latex. When care is taken to make the necessary corrections good agreement between the two methods is obtained. A further technique utilizing light-scattering data has been described and again gives results in accord with the previous measurements (228).

The usual method of estimation of the concentration of monomer in the latex particle is to allow a given volume of monomer to come to equilibrium with a known weight of latex suspended in water. The diminution in volume of monomer gives the amount necessary to saturate the latex from which the concentration in the particle is determined. This gives

a static equilibrium value which is likely to be higher than the dynamic value obtaining during the reaction. This problem has been studied by Burnett and Lehrle (225) who find that it is possible to estimate the concentration by careful determination of the course of reaction. At the point at which the reaction rate starts to decrease, all the unconverted monomer is present in the latex particles. Since this is a known quantity the concentration per particle can be assessed if the size (or number) of the particles is known.

The complexity of the measurements which are required to determine the propagation rate constant are such that wide variations in values quoted are to be expected. This is found to be so, and in general they are much higher than the bulk values (229) except for the final results of Burnett and Lehrle based on three differing methods for determination of N.

VII. IONIC POLYMERIZATION

1. Carbonium Ion Reactions

Substituents on vinyl type monomers must have the effect of altering the polarity of the double bond so that it is more or less inclined to release electrons, i.e., the bond possesses a more or less basic character. As this basic character increases it is feasible that an electron acceptor (e.g., a Lewis acid) will be able to initiate a chain polymerization in which the chain carrier is a carbonium ion. This type of reaction has been known for over 100 years (230), but the unravelling of the mechanism is of relatively recent origin. Suitable catalysts to promote this type of reaction include BF_3, $AlCl_3$, $AlBr_3$, $TiCl_4$, $SnCl_4$, some activated clays, iodine, and sulfuric acid.

The reactions are difficult to study in that rate measurements are frequently almost impossible to achieve with any precision, since the operational temperature is usually low (*ca.* $-70°$C.) and the reaction extremely fast. Conventional steady state methods of experimentation and of kinetic analysis are therefore out of the question. Adiabatic methods have been employed to measure the rise in temperature resulting from the release of energy during polymerization (231,232).

As far as the mechanism of these reactions is concerned, it is certain that a chain process is operative. The evidence for the cationic nature of the chain carrier is: (*1*) the pronounced effect of polar solvents; (*2*) the cationic nature of the catalyst or, in the instance of covalent catalysts, the necessity for a cocatalyst; (*3*) inhibition by amines and anions (233,234). One of the earliest proposed mechanisms has been elaborated by Price

(235,236) to account for the polymerization of styrene by stannic chloride (237). The propagating species is supposed to have the form $Cl_4\bar{S}n[CH_2\cdot\overset{+}{C}HPh]_nCH_2\cdot\overset{+}{C}HPh$ but these intermediates have been criticized as improbable. In any event, the mechanism gives no explanation of cocatalysts so often essential in ionic polymerizations, but the mechanism has been invoked to explain the polymerization of styrene and α-methyl styrene by aluminum chloride in carbon tetrachloride where no cocatalysis by water or hydrogen chloride has been found (238,239).

The discovery of water cocatalysis made it possible to formulate a carbonium ion mechanism for polymerization (240) similar to that postulated by Whitmore for Friedel-Crafts reactions; thus for isobutene catalyzed by BF_3,

Complex formation: $BF_3 + ROH \longrightarrow BF_3\cdot ROH \rightleftharpoons F_3\bar{B}OR + H^+$

Initiation: $H^+ + CH_2{:}CH(CH_3)_2 \longrightarrow (CH_3)_3C^+$

Propagation: $(CH_3)_3C^+ + CH_2{:}C(CH_3)_2 \longrightarrow (CH_3)_3C\cdot CH_2\cdot\overset{+}{C}(CH_3)_2$

Termination: $\sim\!\!\sim\overset{+}{C}H_2\cdot C(CH_3)_2 \longrightarrow \sim\!\!\sim CH{=}C(CH_3)_2 + H^+$

or $\sim\!\!\sim CH_2-C\begin{matrix}\diagup\ CH_3\\ \\ \diagdown\!\!\diagdown\ CH_2\end{matrix} + H^+$

As well as initiation by protons in the manner just indicated, initiations by carbonium ions must also occur. This is typified by polymerization of vinyl octyl ether by triphenylmethyl chloride in ionizing solvents (240) and the incorporation of alkyl end groups in polymers prepared in solution in alkyl halides (241). In summary, initiation appears to come about in two ways which can be generalized as follows,

for acid catalysts (HA):

$$HA + CH_2.CHX \longrightarrow CH_3\cdot\overset{+}{C}HX + A^-$$

for Friedel-Crafts catalysts (MY_n):

$$MY_n\cdot AB + CH_2{:}CHX \longrightarrow A\overset{+}{C}H_2CHX + MY_nB$$

where AB is a potentially ionizable compound whose dissociation is enhanced on complexing with the Friedel-Crafts halide.

In the foregoing, it should be noted that the isolated ion notation is used for convenience. It is most probable that ion pairs rather than the free ions are involved.

As far as the kinetics of the reactions are concerned, for many systems the overall rate appears to be governed by

$$\text{rate} = k(\text{M})^2(\text{C}) \text{ or } k(\text{M})^2(\text{C}_o)$$

where k is a composite constant, and (C) and (C_o) the catalyst and co-catalyst concentrations respectively. This suggests initiation is a bi-molecular process (first order in in both monomer and catalyst complex) and termination is a unimolecular process. These relationships presuppose a steady state reaction which is frequently manifestly untrue (242).

Polymerization of vinyl ethers by iodine give quite different kinetics which can be explained if initiation takes place via an iodine cation formed by $2I_2 \rightarrow I^+ + I_3^-$. If this reaction is slow, a stationary concentration of cations is established and initiation is effectively independent of monomer concentration (240). The full reaction scheme is

$$2I_2 \longrightarrow I^+ + I_3^- \qquad k_1$$

$$(I)^+(I_3)^- + M \longrightarrow (IM)^+(I_3)^- \qquad k_2'$$

$$\left.\begin{aligned}(IM)^+(I_3)^- + M &\longrightarrow (IM_2)^+(I_3)^- \\ (IM_{n-1})^+(I_3)^- + M &\longrightarrow (IM_n)^+(I_3)^-\end{aligned}\right\} \qquad k_2$$

$$(IM_n)^+(I_3)^- \longrightarrow IM_n + (H)^+(I_3)^- \qquad k_3$$

$$(IM_n)^+(I_3)^- + M \longrightarrow IM_n + (M)^+(I_3)^- \qquad k_4$$

from which steady state analysis gives

$$\text{rate} = (k_1k_2/k_3)(I_2)^2(M)$$

$$\overline{DP}_n = k_2(M)/[k_3 + k_4(M)]$$

This rate equation has been substantiated. The measured degree of polymerization is virtually independent of monomer concentration which is true if $k_4(M) \gg k_3$, i.e., if transfer is very important. Some complications arise in that vinyl ethers tend to form an inactive complex with iodine thereby reducing its effective concentration. This gives a maximum in the rate versus monomer concentration curve at high values of (M) (243).

Polar solvents, particularly halogeno- and nitro- compounds, produce marked acceleration of cationic polymerization. Two effects have to be distinguished, first solvent cocatalysis and secondly the general effect of the polarity of the solvent on the ionic processes involved. This can be discussed in terms of the effect of dielectric constant on the simple ionic reactions (233,244,245). Since data of sufficient precision are too scanty it is not possible to evolve a quantitative theory, but qualitatively it is clear that the dielectric and dipolar properties of the medium will influence

the energies of charge separation. As the dielectric constant D is increased the rate of reaction is also increased but the degree of polymerization is only moderately affected. From this it would appear that the initiation process is most influenced. This is well illustrated in the systems, octyl vinyl ether–iodine in hexane and in ethylene dichloride, and styrene–stannic chloride in carbon tetrachloride and in ethyl chloride. In both instances the rate is greater in the solvent of greater dielectric constant despite the fact that under these conditions the activation energy is also greater. This is indicative of an increase in the concentration of ions or ion pairs capable of initiation.

For a given system it is frequently difficult to separate the two solvent effects, especially when the details of initiation are obscure, as with nitro compounds. In many halogenated solvents both effects are present. With stannic chloride, carbon tetrachloride (D = 2) does not act as a co-catalyst since this is only possible if the solvent is sufficiently polar, e.g., ethyl chloride (D = 5) or ethylene dichloride (D = 10).

Without the complication of cocatalysis, the purely polar effect is seen in the polymerization of styrene by hydrogen chloride and hydrogen bromide (246). In solvents of low dielectric constant, e.g., CCl_4, $CHCl_3$, and $C_2H_4Br_2$ no polymerization is observed at 25°C. but in CH_2Cl_2, $C_2H_4Cl_2$, $C_2H_5NO_2$, and CH_3NO_2 whose dielectric constants range from 8.9 to 39, rapid polymerization results along with addition to the double bond.

2. Anionic Polymerization

Monomers with electronegative substituents are readily susceptible to polymerization by a chain mechanism involving carbanions. Beaman (247) has shown sodium in liquid ammonia to be particular effective. The polymerization of methacrylonitrile is effected by Grignard reagents and triphenylmethyl sodium (247). Acrylonitrile (248) and methyl methacrylate (247) were polymerized by sodium in liquid ammonia, and styrene gives some low polymer under the same conditions. Butadiene and isoprene polymerize readily in the presence of metallic sodium at ordinary temperatures but the reaction rate is only moderate (249–252). Alkali metal alkyls are used in polymerization of diolefins (249,251,252) while styrene is converted to low polymers by the amide ion (253,254).

The nature of the propagating species is decided on the following evidence: (*1*) the nature of the catalyst; (*2*) the intense colors which frequently develop during the reaction; (*3*) the inhibition of sodium catalyzed polymerization by carbon dioxide (252) and the failure of *tert*-butylcatechol to act similarly (253); (*4*) the conversion of triphenylmethane to triphenylmethyl sodium in the reaction zone during isoprene

polymerization initiated by metallic sodium (252); (*5*) the structure of diene polymers differ from those produced by cationic or radical mechanisms; and (*6*) copolymerization ratio (Section VII.4).

The only reaction of this type which has been extensively studied from a kinetic point of view is the polymerization of styrene by potassamide in liquid ammonia (254). The polymer contains one amino group per polymer molecule and there is no consumption of potassamide. It is concluded that chains are initiated by the amide ion, NH_2^-, and terminated by proton transfer from the solvent ammonia, according to the scheme

$$\text{Initiation: } NH_2^- + CH_2{:}CHPh \longrightarrow NH_2 \cdot CH_2 \cdot \bar{C}HPh$$

$$\text{Propagation: } NH_2(CH_2 \cdot CHPh)_n CH_2 \cdot \bar{C}HPh + CH_2{:}CHPh \longrightarrow$$
$$NH_2 \cdot (CH_2CHPh)_{n+1}CH_2CHPh$$

$$\text{Termination: } \sim\!\!\sim\bar{C}HPh + NH_3 \longrightarrow \sim\!\!\sim CH_2Ph + NH_2^-$$

From such a scheme the following relationship holds

$$\text{rate} = k(NH_2^-)(\textit{styrene})^2$$

and

$$\overline{DP}_n = k'(\textit{styrene})$$

in agreement with experiment.

Detailed kinetic examination of sodium catalyzed polymerization is hampered by the heterogeneous nature of the reaction; for example, a swollen gel grows out from the sodium surface in pure liquid butadiene (255).

3. "Living" Polymers

As was pointed out in the previous section, termination of polymerization initiated by anions results from proton donation from the solvent, so that one might reasonably expect that in nonproton donating solvents such as tetrahydrofuran no termination step would be possible, and polymerization could occur to an unlimited degree. It has been established that conjugated hydrocarbons such as styrene, butadiene, and isoprene can be polymerized either pure or in tetrahydrofuran solution using the ionic "salts" of aromatic hydrocarbons as initiators (257). The mechanism of the reaction was been elucidated by Szwarc and his co-workers (258) along the lines of an electron transfer process, similar to that already described by Scott

(259). The latter showed that in the presence of phenanthrene the naphthalene ion transferred an electron according to

$$\text{naphthalene}^- + \text{phenanthrene} \rightleftharpoons \text{phenanthrene}^- + \text{naphthalene}$$

In the case of styrene the structure of the ionic entity could be either

$$:\bar{C}HPh\cdot CH_2\cdot \qquad \text{or} \qquad \cdot CHPh\cdot \bar{C}H_2:$$

which on addition of monomer will give

$$:\bar{C}HPh\cdot CH_2\cdot CHPh\cdot CH_2\cdot \qquad \text{or} \qquad :\bar{C}HPhCH_2\cdot CH_2\cdot CHPh$$

These structures represent radical ions but the radicals dimerize rapidly so that polymerization proceeds substantially by the ionic mechanism.

Reaction is extremely rapid taking only a few seconds to effect total conversion. With styrene the reaction is characterized by a color change as the green naphthalene$^-$ ion is replaced by bright red benzyl$^-$ ion. As well as the monomers already named it has been found possible to initiate the polymerization of methyl methacrylate by this mechanism (260). In this instance the color of the system is completely destroyed since the monomer appears to be capable of terminating the chains by killing the propagating ion. It is suggested that an intramolecular mechanism of the type

is operative.

The fact that the polymer from methyl methacrylate is dead in contrast to the "living" polymer from styrene is easily demonstrated by adding methyl methacrylate monomer to a sample of styrene previously polymerized by Na^+ (naphthalene)$^-$. Polymerization of the methacrylate is instantaneous with elimination of the red color. The reverse experiment gives no polymerization of monomeric styrene.

The activity of the styrene polymer can be destroyed by any proton donating system, e.g., water, alcohol, etc. The polymer produced in these reactions is essentially monodisperse with a degree of polymerization given by the ratio (monomer)/(catalyst/2). This has been verified in detail as it has been shown that molecular weight is independent of monomer concentration (provided the monomer to catalyst ratio is constant) and of temperature (261).

4. Ionic Copolymerization

A. RANDOM COPOLYMERS

Copolymerization can be brought about by both carbonium ion and carbanion initiation processes, both monomers being incorporated in the polymer chain. These reactions have not yet been investigated in any detail beyond the determination of monomer reactivity ratios along the lines already described (Section V.2). In contrast to the radical initiated process there is some evidence that the reactivity ratios are subject to variation with solvent or initiator system. Thus Landler (262) finds the reactivity ratios for vinyl acetate, methyl acrylate, and methyl methacrylate with styrene substantially higher in benzene or nitrobenzene solution than in the absence of solvent (263).

There appears to be considerable confusion with regard to variations arising from the use of different catalysts. Thus Florin (264,265) finds for the copolymerization of styrene and 3,4-dichlorostyrene in carbon tetrachloride, r_1 is 2.8 using $AlCl_3$ catalyst and 7.2 with $TiCl_4$, but the variation is smaller in nitrobenzene solution (266). Overberger (267) has examined the styrene-*o*-chlorostyrene system in detail using a variety of catalysts but finds variation in the reactivity ratios only if the reaction ceases to be homogeneous.

One notable feature of the results is that there is apparently little or no tendency to alternation in this reaction (i.e., $r_1r_2 \approx 1$ in all cases). The order of carbonium ion reactivity relative to styrene has been set up by Pepper (263).

Some carbanion reactivity ratios have been tested (263) but are too few to allow firm general conclusions to be drawn. Differences from carbonium ion and radical results underline the differing mechanisms. Two cases of alternation have been reported, vinyl acetate–styrene (262) ($r_1r_2 = 0.001$) and acrylonitrile–butyl vinyl sulfone (266) ($r_1r_2 = 0.22$).

B. BLOCK COPOLYMERS

Little activity in this field has been reported although it is evident that living polymer technique can readily be applied at least in a limited field. Szwarc (260) has already demonstrated the possibility of applications along these lines and there is little doubt that further extension can be undertaken. Using the living polymer technique it should be possible to prepare a polymer containing several different blocks or alternating blocks of monomeric units. No report of such polymers is known.

VIII. STEREOSPECIFIC POLYMERIZATION

1. Tacticity

It has usually been acknowledged that polymeric molecules prepared by radical or ionic mechanisms have a limited regularity of structure in that the monomeric units are connected in either head-to-tail or head-to-head, tail-to-tail array. The substituents, on the other hand take up completely random configuration. Within recent years new catalysts have been formed which not only initiate polymerization but also exert a directing influence on the propagation reaction. Most such catalysts appear to operate heterogeneously, the polymerization being initiated at sites on the surface. In this way polymers of well defined stereochemical structure have been prepared. Before discussing polymers of this type, it is necessary to consider the stereochemical features of long chain polymers.

In vinyl polymers $(CH_2CHX)_n$ in which the structural unit contains a single substituent, structural studies have revealed that the common and preferred structure is a head-to-tail one, thus:

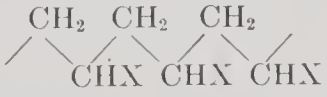

In such an arrangement each alternate carbon atom can be regarded as an asymmetric center having four differing substituents. However, two of the substituents differ only in the length of the chain and the immediate environment of the centers is so similar that the resulting optical activity of any center is too small for measurement. Further there will be sequences of + and − centers of varying length, the net effect of which is a vanish-

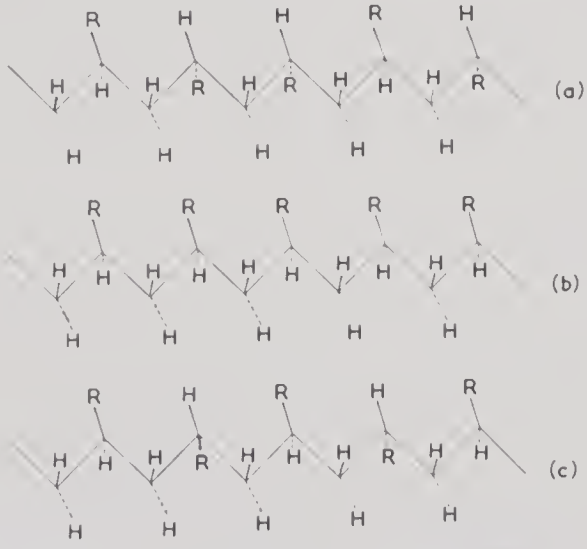

Fig. 9. Possible structures of linear polymers from CH_2—CHR. (a) atactic, (b) isotactic, (c) syndiotactic.

ingly small activity. The relative configurations of these tertiary carbon atoms affects the regularity along the length of the chin (Fig. 9a). If the side chains are placed all on one side of the backbone then a regular stereochemical pattern results (Fig. 9b), which would also be true if monomer units were joined in alternate + and − configurations (Fig. 9c).

Although other more complex arrangements can be envisaged these appear to be the most commonly encountered. Natta has proposed the nomenclature atactic, isotactic, and syndiotactic to cover the three cases exemplified in Figure 9.

With diene monomers such as butadiene, $CH_2{:}CH\cdot CH{:}CH_2$, or isoprene, $CH_2{:}C(CH_3)\cdot CH{:}CH_2$, further forms are possible. Usually both 1,2 and 1,4 additions occur in a random manner to give complex structures. Also 1,4 additions can give rise to either a cis or trans isomer

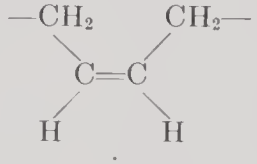

cis

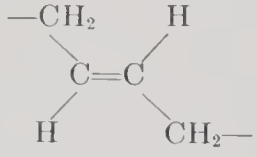

trans

This situation is precisely that encountered in nature in that Hevea rubber is a polyisoprene with a cis-1,4 structure and gutta-percha (balata) has the trans configuration. As well as the 1,4 arrangements it is possible to have 1,2 additions in which the vinyl group acts in the same way as the general substituent in Figure 9; i.e., atactic, isotactic, and syndiotactic polymers are all possible.

The structure of these polymers has been determined largely by X-ray study of the crystalline polymers (269). It is found that the chain is helocoidal with differing numbers of monomer units per turn; the number is governed primarily by the shape and size of the side groups and the ability of the molecules to pack into a crystal. These features are the determining factors in the melting point and other physical properties of the polymer.

2. Catalytic Systems

The most significant development in this field was the discovery that ethylene could be polymerized at normal pressures and room temperature at a high rate by catalysts formed by interaction of aluminum alkyls and certain metal halides (270). The principal combinations which have been described, and on which almost all kinetic work have been studied, is triethyl aluminum and titanium tetrachloride or trichloride although chlorides of most of the transition metals, e.g., V, Cr, or Zr and organometallic compounds based on Li, Be, Mg, Zn, Tl, and In have also found some appli-

cation. Ziegler was successful in showing that, in the presence of trialkyl aluminum, titanium tetrachloride was reduced to a mixture of $TiCl_3$ and $TiCl_2$ probably by the following stages:

$$AlR_3 + TiCl_4 \longrightarrow AlR_2Cl + TiCl_3R$$

$$AlR_2Cl + TiCl_4 \longrightarrow AlRCl_2 + TiCl_2R_2$$

$$RTiCl_3 \longrightarrow TiCl_3 + R\cdot$$

$$TiCl_3 + AlR_3 \longrightarrow AlR_2Cl + TiCl_2R$$

$$RTiCl_2 \longrightarrow TiCl_2 + R\cdot$$

Natta's school (271–275) favors preparation of the catalyst from solid titanium trichloride, which is insoluble in *n*-heptane, the usual solvent, with a little trialkyl aluminum. It appears from the literature that several factors are of importance in the preparation of the catalyst. Titanium trichloride occurs in three modifications of which the best is Natta's so called α (violet) modification which apparently has a layer lattice structure (276). The catalyst system forms a solid phase the particle size and dispersion of which plays an important but rather ill defined role in governing the crystalline (isotactic)/amorphous ratio.

The mechanism of these reactions is a matter of some conjecture but there is no doubt that both components of the catalyst system are essential for the production of isotactic polymer. There seems to be little doubt that in an inert solvent the catalyst system is the solid titanium trichloride on the surface of which the metal alkyl is adsorbed or complexed, most likely the latter. The structure of this complex is not known but is presumed to be similar to that of dimeric aluminum chloride. Detailed study shows that the aluminum-carbon bond is involved in the reaction, this being activated by the presence of the metal halide. (It may be true that tracer evidence on this point is misleading in that Ti-carbon bonds might be present in the complex.) The highly polarized metal-alkyl bond so formed gives complex with olefin directly or after sorption on the surface. The olefin thus is polarized and inserts itself between the metal and the alkyl—or attached polymer chain. Schematically this would give, for propene,

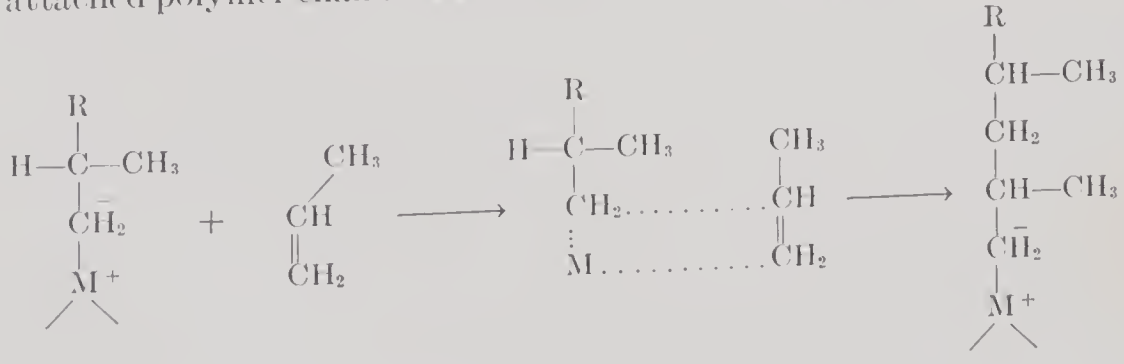

The process repeats by successive insertion at the metal-carbon bond until growth ceases by transfer or a hydride ion to the metal atom giving a terminal double bond to each polymer molecule, thus:

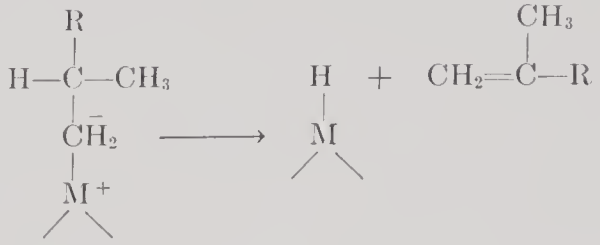

This mechanism is by no means fully confirmed experimentally but does agree with certain observations in that there is usually about one double bond per polymer molecule and that the alkyl group of the aluminum appears in the polymer chain.

The stereospecificity of the process is taken to arise from the dual effect of attachment of the growing chain to a single site at the surface together with the stereochemical configuration at that site. This imposes certain restrictions on the rotational freedom of the monomer molecule, thereby limiting its orientation on approach.

Such rate measurements which exist on this type of reaction show that the rate is usually proportional to titanium concentration (276–8) and occasionally shows a slight dependence on aluminum (279) but usually to a very low power. It is universally agreed that the rate is proportional to monomer concentration.

3. Experimental Techniques

Experimentally these reactions are difficult to study from a kinetic point of view since it appears essential to keep the catalyst in dispersion. With gaseous monomers such as ethylene and propylene the course of reaction is conveniently followed by pressure changes and the catalyst system is kept in suspension by vigorous stirring. With liquid monomers such as styrene this is not so easy to achieve. It is possible to employ dilatometry provided that the composition of the polymer produced does not vary. This has been shown to be the case over quite high conversion ranges (up to 60%) (280).

A convenient dilatometric procedure is as follows. The dilatometer bulb of some 10 ml. capacity has a flat bottom (Fig. 10) and is provided with a glass covered magnetic stirrer. Precision bore tube (2 mm. bore) is used to measure contraction. The dilatometer filling apparatus is shown in Figure 11. The required quantity of $TiCl_3$ is introduced into a weighed tube in a dry box in which air has been replaced by pure nitrogen. The tube is stoppered and reweighed. The dilatometer filler is evacuated

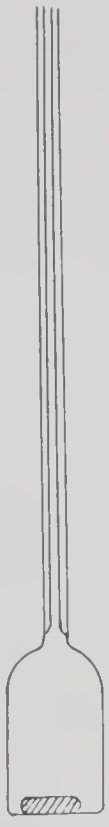

Fig. 10. Dilatometer for following polymerization using heterogeneous catalyst.

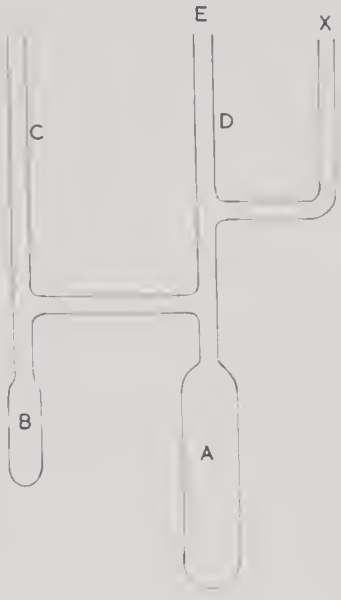

Fig. 11. Filling apparatus for use with dilatometer of Figure 10. Dilatometer attached at X.

through *E* and filled with dry nitrogen. The $TiCl_3$ is rapidly transferred from the weighing tube to bulb *B*, and the filler is quickly sealed at *C*, and rapidly pumped out on the high vacuum line. The required weight of alkyl aluminum is distilled into bulb *A* from a weighing tube, followed by the solvent (*n*-heptane) in known volume. Finally, purified and prepolymerized monomer is distilled into *A* from a graduated tube and the apparatus is sealed off at *D*. The contents of bulb *A* are allowed to melt, mixed with the solid in bulb *B* and transferred to the dilatometer which is sealed off, care being taken throughout the operation that the catalyst is uniformly dispersed through the liquid. The dilatometer is transferred to the thermostat and stirring commenced immediately. By working to a strictly timed routine of this nature adequate reproducibility is achieved.

4. Allied Reactions

Before the discovery of isotactic polymers Morton (281) had used the so-called "Alfin" catalyst system to polymerize butadiene and obtained a product with a high concentration (*ca.* 75%) of *trans*-1,4-linkage. The catalyst is prepared by treating sodium isopropoxide in a hydrocarbon

solvent with allyl chloride. More recently, it is claimed that this catalyst gives isotactic polystyrene in the liquid phase (282). Some soluble catalysts formed by reacting titanates, $Ti(OR)_4$ (275) or titanium cyclopentadiene chloride (284) with aluminum alkyl have been found capable of polymerizing ethylene at low pressure giving an atactic product. At the same time they appear to give rise to a mixture of atactic, isotactic, and syndiotactic diolefin polymers (283).

A similar reaction from the point of view of the mechanism is the formation of polyalkylidines, $(CHR)_n$, by polymerization of diazoalkanes using boron compounds as catalysts. The precise mechanism has been worked out by Bawn (284) and it bears many features reminiscent of the Ziegler-Natta mechanism discussed above. Using boron trifluoride the initial step is the formation of a complex between the diazo compound and the fluoride, thus

$$BF_3 + CHRN_2 \longrightarrow F_3\bar{B}\cdot CHRN^+{\equiv}N$$

The zwitterion so formed loses nitrogen and undergoes a rearrangement by migration of a fluorine atom:

$$F_3\bar{B}\cdot CHR\cdot N^+{\equiv}N \longrightarrow F_3\bar{B}\cdot\overset{+}{C}HR + N_2 \longrightarrow F_2B\cdot CHR\cdot F$$

This new compound reacts with a further diazo molecule with a similar rearrangement according to the scheme

$$F_2B\cdot CHRF + CHRN_2 \longrightarrow F_2\bar{B}\cdot\underset{\underset{CHRN_2}{|\ \ +}}{CHRF} \xrightarrow[\text{rearrange}]{-N_2} F_2B\cdot CHR\cdot CNRF\cdot$$

Polymerization proceeds in this way until all the monomer is consumed to termination intervenes in the form of a hydrogen ion transfer. The high polymer formed by this process has a terminal group similar to that of the initiator so that the polymer itself can function as a catalyst for the further polymerization of diazoalkanes. It is evident that this type of reaction is well adapted to the production of block copolymers of the type $(CHR)_m(CHR')_n$ by use of the corresponding diazo compounds.

Gold salts also effect the polymerization of diazoalkanes with the production of crystalline polymers, the yield being small. It is not unlikely that a similar mechanism operates with the formation of a gold alkyl (285).

Other types of catalytic systems are also known to produce isotactic but kinetic data are lacking for these systems. Notable among them is the catalyst used by the Phillips Petroleum Company which consists of an activated chromium oxide on a silica support.

Polymerization of dienes to polymers or regular structure appears to be easier to achieve in most cases than for simple vinyl hydrocarbons. The systems mentioned above are applicable but stereospecificity can be achieved by alkali metals notably lithium or the alkyls of alkali metals. Thus it is possible to prepare a *cis*-1,4 polyisoprene which is identical structurally with natural rubber using a dispersion of 0.1 parts of lithium metal in 100 parts of isoprene (286). Ziegler catalysts give much the same product (287). It is difficult to see a link between the metal catalyzed reaction and that requiring mixed catalysts except by the prior formation of a metal alkyl.

5. Reaction of Polar Monomers

Ziegler type catalysts have not been found to be effective in producing crystalline polymers from polar monomers such as vinyl acetate or methyl acrylate. However, Schildknecht (288) showed that a crystalline polymer was obtained from isobutyl vinyl ether using boro trifluoride–ether complex as catalyst at low temperature. Using higher temperatures the product was rubbery. The reaction proceeds heterogeneously at low temperature.

Recently a crystalline polymer of methyl methacrylate has been successfully prepared using lithium 9-fluorenyl as catalyst (289).

IX. DEGRADATION OF POLYMERS

1. Hydrolytic Degradation

This section is concerned with the ways in which polymeric molecules are broken down to give smaller molecules. This decrease in molecular weight of the product leads to losses in other physical properties, notably in mechanical strength, and the phenomenon is therefore worthy of close attention. By degradation is meant a process which results in lower molecular weight and it will be used in that sense here. A different but closely allied phenomenon is that of depolymerization which is in essence the reverse of addition polymerization and as far as is known is confined to that class of polymer.

Cellulose and its derivatives are subject to hydrolysis (290) during which main chain links are destroyed, and the DP of the material falls as the

reducing power rises. The cellulose molecule is bound together by acetal linkages which are very susceptible to acid attack. For this reason acid hydrolysis has been extensively studied and this has been a powerful weapon in the development of an understanding of the structure of the cellulose molecule as well as the fiber structure of the polymer.

The addition of a water molecule to the cellulose chain produces a rupture of the chain with the formation of a degraded product with greater reducing power than the original, as will be seen from the following formalized reaction scheme:

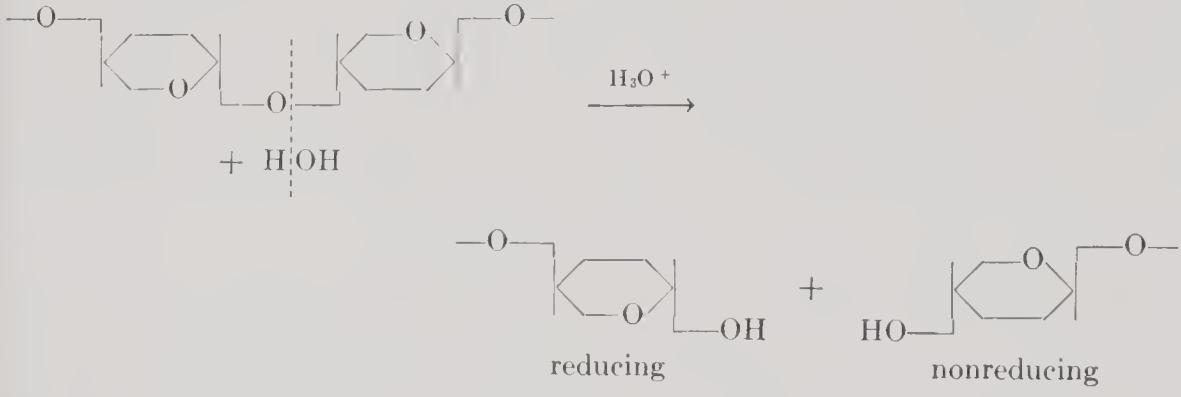

As written this suggests a typical prototropic catalysis as has been well substantiated by experiment. In the years before the war a large body of evidence had established, at least qualitatively, the nature of the reaction (291,292) although precise data on which a quantitative theory could be built was not available until later (293). On the whole the literature presents a somewhat confusing picture, due in large measure to the reactions being carried through in a heterogeneous system in which the ability of reagents to penetrate the network of crystalline, mesomorphous, and amorphous regions of the cellulose fiber constituted the main rate determining feature. This situation is now well appreciated and fundamental studies on homogeneous systems have been prosecuted vigorously.

Two main experimental methods have been utilized to study this degradation, viz., end group determination and dilute solution viscosity measurements. The former method has the advantage that it yields a good direct measure of the number of chains present but is, at the same time, relatively insensitive with high molecular weight material. Viscosity determinations must be linked to true molecular weight measurements by a calibration procedure usually involving osmometry. This technique does, however, offer successful investigation at high molecular weights and has the advantage of being rapid and is applicable to the degrading system without disturbing it.

The pioneering work of Kuhn (294,295), Mark (296), and Freudenberg (297–299) established that the activation energy was about 28 kcal./mole

and the rate of cleavage was probably a function of the distance of the bond from the chain end.

Many attempts were made to derive mathematical expressions to cope with the experimental results but most of these proved to be too complex to be subject to experimental use (300). Approximations must therefore be introduced in order to progress and this has been achieved by proposing that all links are equally susceptible to hydrolysis. The structure of cellulose is usually accepted to be linear with repeating anhydroglucopyranose units joined through β-glucosidic links. Some exception to this simple picture has been taken and the existence of certain weak links has been postulated (301–5). If one supposes that there are occasional 1,5-semiacetal crossbonds joining chains laterally, at regular intervals, then hydrolysis might be expected to occur preferentially at these bonds leaving the normal 1,4-glucoside links relatively unaffected. The outcome of such a hypothesis would be that initially a rapid decrease in DP would occur followed by a levelling off to a limiting value.

Experiments in homogeneous media tend to disprove this theory. The rate of change of intrinsic viscosity, $[\eta]$, with time does not serve as a measure of the number of chain breaks. On the other hand the change in the reciprocal, i.e., the intrinsic fluidity, $[\phi]$, can be so related. The validity for this statement may be proved as follows. Assume a sample of cellulose contains n moles of glucosidic links per liter. After hydrolysis for a time, t, q such links have been broken and $(n - q)$ remain. The fraction of links remaining is then $(1 - q/n)$.

If the further assumption is made that the rate of hydrolysis is proportional only to the concentration of unbroken links and that the concentration of acid is always very large, then the rate of cleavage is given by

$$dq/dt = k(1 - q/n) \tag{50}$$

Since when $t = 0$, $q = 0$, integration of (50) yields

$$-n^{-1}[\ln (1 - q/n)] = kt \tag{51}$$

when $n \gg q$ Equation (51) approximates to

$$q = nkt = k'r \tag{52}$$

which is certainly true in the early stages.

For a given weight of polymer, W, the number of breaks, q, is equal to the increase in the number of molecules, thus

$$q = N_s - N_0 = \Delta N = \Delta(W/\bar{M})_n \tag{53}$$

where N_0 and N_s are respectively the number of molecules originally present and after scission, and $\bar{M}_n$ is the number average molecular weight. For a

randomly degraded polymer the number average molecular weight is very nearly half the weight average value (306). Also for cellulose and cellulose derivatives the viscosity measurement is very nearly proportional to the weight average molecular weight, i.e.,

$$\bar{M}_w = K[\eta] \tag{54}$$

whence substitution in Equation (53) leads to

$$q = \Delta(2W/K\ [\eta]) \tag{55}$$

By definition $1/[\eta] = [\phi]$ so

$$q = \Delta(2W[\phi]/K) = K'\Delta[\phi] \tag{56}$$

Substituting Equation (56) in (52) gives

$$[\phi] = (k'/K')t \tag{57}$$

If, therefore, the boundary assumptions are correct the change in intrinsic fluidity is a linear function of time and the slope gives a measure of the rate of degradation. If a limiting DP is approached the rate of reaction should decrease to near zero. Plotting previous data in this way has revealed no change in the slope of the line even after 50 hours hydrolysis (307), and this may arise from the fact that the logarithmic approximation in the above analysis ceases to be valid.

Extensive revaluation of much early data leads to the conclusion that there is no unassailable experimental evidence in favor of the weak link theory (308).

The heterogeneous hydrolytic reaction in which acid interacts with cellulose as a solid phase is technically important but experimentation is difficult with the result that a rather confused picture still exists. Early experiments provided data applicable only over limited ranges (309,310). From more recent kinetic measurements it would appear that the course of reaction is adequately interpreted by the postulation of two concurrent first-order processes within the crystalline and amorphous regions of the fibers (311,312). Somewhat at variance with this view is the assertion by Meller (313) that the rate controlling step is zero order, this being due to diffusion control although the high activation energy recorded (28–29 kcal./mol.) scarcely supports this view.

Only condensation polymers are likely to undergo hydrolytic degradation although little work has been done in this field. Flory (314) studied the degradation of polyesters brought about by ester exchange with small quantities of alcohol or glycol. The experimental technique used was novel in that the reaction was followed using melt viscosity measure-

ments. Melt viscosity can be related to weight average molecular weight by an empirical formula.

2. Thermal Degradation

The study of thermal degradation particularly of addition polymers was for long held back because of attempts to fit the random scission theories to the process. The divergencies from theory have been listed by Jellinek (315) as (*a*) degradation slows down or stops completely when smaller chain lengths have been reached; (*b*) distribution of sizes in degraded material is much sharper than would be predicted; (*c*) the amount of monomer produced is much greater than expected.

Identification of the products of thermal degradation has been carried out by mass spectrographic examination of polymer pyrolyzed in vacuum (316,317). Monomer production varies from about 10% for styrene–maleic anhydride copolymers to nearly 100% for polymethyl methacrylate (318). With most polymers one also obtains gaseous products, a liquid fraction, a wax, and a harder solid.

Kinetic methods have been applied to the study of these processes, but of necessity interpretation of results on a purely quantitative basis has been difficult. The main experimental methods used have been a direct measurement of weight loss and a flow technique. In the former a weighed quantity of polymer is contained in a small silica bucket suspended from a silica spiral. The whole assembly is maintained under high vacuum conditions to prevent oxidative degradation. The bucket and its contents are heated electrically and the loss in weight recorded by contraction of the spiral. The method is a simple one in principle but its operation is exacting. In the flow method first used by Grassie and Melville (318) powdered polymer mixed with powdered copper is heated in a shallow tray. The monomer evolved is pumped off to a liquid air trap passing along a tube in which a Pirani gauge is mounted. The rate of flow of the monomer is recorded by pressure changes on the gauge. This method is relatively simple to operate and can be made to give automatic records. It does measure only the evolution of volatile material which may place a limitation on its utility. In conjunction with molecular weight measurements however this experimental procedure is very useful.

Theoretical investigation has lagged considerably behind the experimental work. Early work mainly by Simha (319), Jellinek (320), and Tobolsky (321), gave too complicated expressions for useful application. More recently Simha, Blatz, and Wall (322) have presented a relatively simple analysis which appears to be amenable to experimental verification. Basically, the assumed mechanism is that the initial step is the scission of

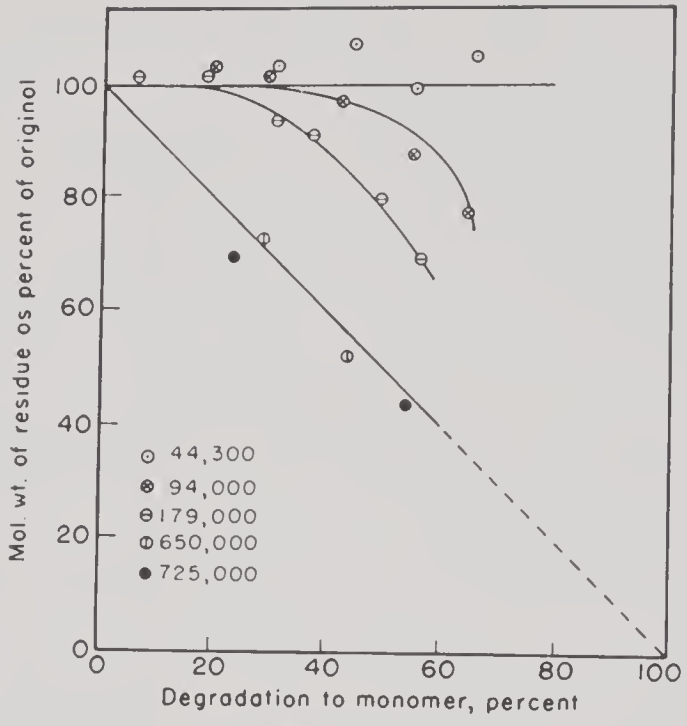

Fig. 12. Variation of molecular weight during thermal degradation.

the long chain molecule to give two free radicals which rapidly lose monomeric units. Termination of this reverse polymerization is brought about by interaction of radicals and two possible transfer reactions are envisaged. Somewhat different results arise for random initial breaking of the chain and for breaking at the ends. The chief drawback to the original treatment lies in the assumption of a uniform polymer sample. However, it has been found possible to make the required modifications to achieve a more general solution (323). A similar analysis has been presented by Gordon (324).

The most extensively studied polymer has been polymethyl methacrylate which depolymerizes almost exclusively to monomer. The proof of the radical nature of the process lies in the inhibition of the reaction by the incorporation of 1,4-diaminoanthraquinone in the melt.

The molecular weight of the residue was measured at intervals throughout the reaction. High initial molecular weight samples showed a steady diminution in molecular weight throughout the reaction while low initial molecular weight material revealed only slight or no such variation (Fig. 12). The near constancy of molecular weight in the latter case suggests that initiation occurs by scission of a terminal bond followed by stripping of monomer units from the macro radical until the whole polymeric molecule has disappeared. The decrease in the case of high molecular weight material is usually symptomatic of stepwise degradation but can be interpreted on the radical mechanism if transfer or termination with a second

radical occurs. In this way the large radical initially produced would eventually give rise to a smaller macromolecule.

It has also been demonstrated that very frequently the nature of the end group of the polymer chain affects the rate of depolymerization. Thus differences in reaction rate can arise which depend on the method of production of the polymer sample.

Weak link hypotheses have frequently been suggested as explaining the initiation step (325,326). Such weak links can arise in a variety of ways but most readily by addition of a monomeric unit in the wrong direction during polymerization, i.e., a head-to-head link in a predominantly head-to-tail structure. Some mechanism of this type seems to operate in the case of styrene degradation (327).

The degradation of polyvinyl esters is much more complex, e.g., vinyl chloride and acetate polymers. In both cases a polyene structure appears to be formed by the loss of either hydrochloric or acetic acid. Grassie (328) has made a study of the reaction in the case of the acetate and postulates a nonchain process. Most recent information on polyvinyl chloride suggests that bases accelerate the loss of HCl (329). These authors suggest that the reaction falls into three parts: (*1*) relatively slow initiation process; (*2*) relatively fast attack by base at allylic positions on the chain; (*3*) relatively slow termination reaction due to dissipation of base at cross-links.

3. Photochemical Degradation

In many respects photochemical degradation processes parallel the thermal degradations very closely. Using very similar techniques to those described previously, Melville and Cowley (30) carried out a thorough investigation of the photodegradation of polymethyl methacrylate. Breakdown of polymer molecules occurs at measurable rates above 130°C. using mercury resonance radiation (2,537 A.) giving mainly monomeric products. Other polymers do not depolymerize so readily, e.g., polystyrene.

The intensity exponent varies considerably but is predominantly 0.5 indicating initial destruction of free radicals. With low molecular weight material the value can be considerably in excess of this figure. This is interpreted as being due to physical removal of the small radicals which kinetically is the same as linear termination. This is further supported by the increase in exponent at higher temperature under which conditions the tendency towards volatilization of small radicals would increase.

Melville and Cowley also investigated the effects of diffusion on the various processes. At low temperatures one might reasonably expect that monomer is only slowly removed from the system and has an opportunity to repolymerize. There are indications that this is so.

The rate of depolymerization is also affected to some extent by the nature of the end groups but this is not so pronounced as in the thermal reaction.

Photochemical data on other polymer systems are extremely scanty. Since most work has been carried out in air, it is not improbable that most, if not all, the degradation noted is due to oxidative processes. The combined action of air and light is of technical importance in assessing the durability of polymers.

4. Mechanical Degradation

When polymer solutions or occasionally the solid polymers are subjected to high shearing forces, degradation frequently results. High shearing is encountered in ultrasonic irradiation, milling, high speed flow, and even vigorous stirring.

Both natural and synthetic polymers have been degraded by ultrasonic irradiation of suitable solutions. Of the synthetic polymers those most investigated include polystyrene, polyacrylic and polyvinyl esters (331–334). In the field of natural polymers cellulose and its derivatives have claimed considerable attention (335–337). The usual method of following the course of reaction is by measurement of the viscosity changes, most conveniently by using a viscometer designed as reaction vessel.

The early experimental results of Schmid bore remarkable resemblance to those obtained in hydrolytic degradation in that there is an apparent limiting DP below which further degradation cannot take place. Much the same remarks apply to this phenomenon as in the previous case and indeed plots of change in intrinsic fluidity against time show good linear character (338).

While there was general agreement as to the nature of the initial step adequate proof has been obtained only very recently. Early attempts to trap the proposed radicals using iodine and benzoquinone were unsuccessful. Henglein (339) has shown that using 1,1-diphenyl-2-picrylhydrazyl, two retarder radicals are removed per bond broken. This is in surprisingly good agreement with theory, and more than adequately verifies the free radical hypothesis.

A second importance piece of information is the formation of block copolymers by irradiating a polymer in solution in a second monomer. Henglein (340) has demonstrated the formation of such copolymers* by irradiation of polyacrylamide in the presence of acrylonitrile. Such a reaction must result from the prior formation of free radicals which act as initiators for the formation of new polymer chains.

* The paper describes the polymers as graft copolymers but it is obvious from the mode of formation that the correct designation is block copolymers.

As well as the ultrasonic methods, high shearing forces occur in the milling of solid polymers. Watson has investigated the milling of rubber and finds considerable degradation even in the absence of air when free radical capturing agents such as DPPH are present. In their absence there is apparently no degradation. This is interpreted in the following way. Rubber molecules undergo scission to radicals in each case, but in nitrogen atmosphere and in the absence of radical acceptors the radicals so formed merely recombine. With oxygen or radical acceptors this reaction is not possible and consequently the chains remain ruptured (341,342).

High rates of shear can be attained in specially designed viscometers and the degradation of long chain molecules has been investigated in this manner. It appears likely that some of the energy affecting the individual inter- and intramolecular motions constituting the overall shear process is stored temporarily as potential energy in the bonds during the times required for the individual motions. If sufficient potential energy is introduced into the bond in excess of the thermal energy, bond rupture may occur (343).

5. Oxidative Degradation

Many polymers degrade in the absence of air at elevated temperatures or under conditions of mechanical stress. In the presence of oxygen degradation at much lower temperatures is observed. Oxidation has long been recognized as the primary cause of the ageing of rubber and the tendering of cellulose. Oxidative changes of this type are of very great commercial importance.

The chemistry of rubber oxidation reveals that the oxygen attack occurs at carbon atoms adjacent to double bonds, giving rise to hydroperoxides in the first instance (344). The subsequent breakdown of these hydroperoxides gives rise to chain scission or aggregation. The formation of hydroperoxides is also recognized as an essential step in the oxidation of saturated hydrocarbons (345–347). The first stage in the oxidation of 1,3-dimethylcyclopentane is the formation of a hydroperoxide whose subsequent decomposition can be shown to give rise to the known products of oxidation (346).

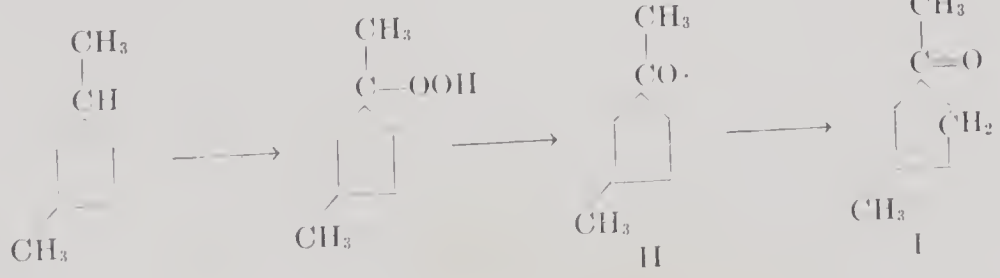

Radical I may either abstract a hydrogen atom or dimerize. The mono- and diketones so formed have been isolated and identified (347). Radical II can also undergo a hydrogen abstraction reaction yielding a tertiary alcohol (347).

The kinetics of olefin oxidation have been extensively studied more particularly by Gee and co-workers. The mechanism of the reaction is now well established as outlined in Chapter XX. In the more complex polyolefin systems the secondary reactions following oxidation can be divided into two types, viz., aggregative and disaggregative (348,349). Aggregative reactions are those which bring about molecular weight increase by further polymerization, branching, or cross linking. Disaggregative reactions result from depolymerization and chain scission and lead to a decrease in molecular weight. Cyclization may also occur. The main reactions are:

Aggregative

$$2R\cdot \longrightarrow R{-}R$$

$$R\cdot + RO_2\cdot \longrightarrow RO_2R$$

$$RO_2\cdot + RO_2\cdot \longrightarrow RO_2R + O_2$$

$$R\cdot + C{=}C \longrightarrow RC{-}C\cdot$$

$$RO_2\cdot + C{=}C \longrightarrow RO_2C{-}O\cdot$$

Disaggregative

$$\sim\!\!\sim CH_2CHXCH_2\dot{C}XCH_2CHX\sim\!\!\sim \longrightarrow \sim\!\!\sim CH_2CHX + CH_2{=}CXCH_2CHX\sim\!\!\sim$$

$$\sim\!\!\sim CH_2CHXCH_2CHXCH_2\dot{C}HX \longrightarrow \sim\!\!\sim CH_2CHXCH_2\dot{C}HX + CH_2{=}CHX$$

$$\sim\!\!\sim CH_2CHXCH_2CHXOOCH_2CHX\sim\!\!\sim \longrightarrow \sim\!\!\sim CH_2CHXCH_2CHXO\cdot + \cdot OCH_2CHX\sim\!\!\sim$$

$$\sim\!\!\sim CH_2CHXCH_2CHXO\cdot \longrightarrow \sim\!\!\sim CH_2CHXCH_2\cdot + CHXO$$

$$\sim\!\!\sim CH_2CHXCH_2CHX(OOH)CH_2CHX\sim\!\!\sim \longrightarrow \sim\!\!\sim CH_2CHXCH_2CXO\cdot + HO\cdot + \cdot CHXCH_2\sim\!\!\sim$$

$$\sim\!\!\sim CH_2CHXCH_2CHXCH_2CHX\sim\!\!\sim \longrightarrow \sim\!\!\sim CH_2CHXCH_2CHX\cdot + \cdot CH_2CHX\sim\!\!\sim$$

where R· denotes radicals formed in the scission process and $RO_2\cdot$ R radicals which have reacted with oxygen. Scission and crosslinking occur simultaneously but the effects can be easily separated experimentally. Thus in solution radicals are usually sufficiently dispersed so that disaggregative reactions predominate.

The oxidation of cellulosic materials is not so complex in many ways in that the main effect is a disaggregative one leading to the familiar "tendering" phenomenon. Model compounds such as alcohols and ethers have been studied in an attempt to elucidate the mechanism of the process. In

neither case is the Bolland-Gee mechanism fully applicable since the reaction does not proceed by a chain process. Boland and Cooper (350,351) suggest the following mechanism for the photooxidation of ethanol sensitized by an anthraquinone dye, Q. The absorption of light by the dye creates an excited state in which the molecule abstracts a hydrogen atom from the α carbon giving a free radical from the alcohol and a semiquinone free radical. The proposed mechanism is:

$$Q + h\nu \longrightarrow Q^*$$

$$Q^* + CH_3CH_2OH \longrightarrow QH + CH_3\dot{C}HOH$$

$$CH_3\dot{C}HOH + O_2 \longrightarrow CH_3{-}\underset{\displaystyle OH}{\overset{\displaystyle H}{\overset{|}{\underset{|}{C}}}}{-}O_2\cdot$$

$$2CH_3{-}\underset{\displaystyle OH}{\overset{\displaystyle H}{\overset{|}{\underset{|}{C}}}}{-}O_2\cdot \longrightarrow 2CH_3COOH + H_2O_2$$

$$CH_3{-}\underset{\displaystyle OH}{\overset{\displaystyle H}{\overset{|}{\underset{|}{C}}}}{-}O_2\cdot + HO_2\cdot \longrightarrow CH_3CHO + H_2O_2 + O_2$$

$$QH + O_2 \longrightarrow HO_2\cdot + Q$$

With ethers, the main products of reaction are esters and ketones. The extension of this mechanism to cellulose oxidation is self-evident.

A similar type of mechanism has been found for the photooxidation of amines sensitized in the same way. *N*-substituted amides are more susceptible to oxidation, the main products being hydrogen peroxide, an aldehyde from the nitrogen substituent, and an isocyanate (at least as an intermediary) (352). Such oxidations are obviously related to the degradation of nylon.

References

1. T. Alfrey and M. Berdick, *J. Polymer Sci.*, **3**, 899 (1949).
2. W. Kern and H. Kammerer, *Makromol. Chem.*, **2**, 127 (1948).
3. H. Mark, *Anal. Chem.*, **20**, 104 (1948).
4. J. C. Bevington, J. H. Bradbury, and G. M. Burnett, *J. Polymer Sci.*, **12**, 469 (1954).
5. J. C. Bevington, H. W. Melville, and R. P. Taylor, *J. Polymer Sci.*, **12**, 449 (1954).
6. G. V. Schulz and E. Husemann, *Z. physik. Chem.*, **B34**, 187 (1936).
7. For a review of precipitation methods in particular see L. H. Cragg and H. Hammerschlag, *Chem. Rev.*, **39**, 79 (1946); P. J. Flory, *Principles of Polymer Chemistry*, Cornell University Press, Ithaca, New York, 1953, Chapters VIII-3 and XIII.

8. J. H. Baxendale, S. Bywater, and M. G. Evans, *Trans. Faraday Soc.*, **42**, 675 (1946).

9. D. R. Morey and J. W. Tamblyn, *J. Phys. Chem.*, **50**, 12 (1946).

10. D. R. Morey and J. W. Tamblyn, *J. Appl. Phys.*, **16**, 419 (1945).

11. D. R. Morey, E. H. Taylor, and G. P. Waugh, *J. Colloid Sci.*, **6**, 470 (1951).

12. A. Oth, *Bull. soc. chim. Belges*, **58**, 285 (1949).

13. I. Harris and R. G. J. Miller, *J. Polymer Sci.*, **7**, 377 (1951).

14. For excellent reviews of such methods see S. R. Caplan, *Symposium on Techniques of Polymer Science*, Reports of the Royal Institute of Chemistry, London, No. 5, 1956; S. R. Caplan and M. A. Young, *Proceedings of the Second International Congress on Surface Activity*, Vol. 3, Butterworths, London, 1957, p. 516.

15. H. G. Cassidy, *Technique of Organic Chemistry*, Vol. V, Interscience, New York–London, 1951.

16. H Mark and G. Saito, *Monatsh.*, **68**, 237 (1936); G. R. Levi and A. Giera, *Gazz. chim. ital.*, **67**, 719 (1937); Y. Landler, *Compt. rend.*, **225**, 334 (1947); B. V. Losikov, N. I. Kaverina, and A. A. Fedyantseva, *Khim. i Tekhnol. Topliva*, **No. 3**, 51 (1956).

17. S. Claesson, *Arkiv. Kemi*, **26A**, 25 (1949); *Discussions Faraday Soc.*, **7**, 221 (1949).

18. R. J. P. Williams, *Analyst*, **77**, 905 (1952).

19. D. W. Bannister, C. S. G. Phillips, and R. J. P. Williams, *Anal. Chem.*, **26**, 1451 (1954).

20. V. Desreux, *Rec. trav. chim.*, **68**, 789 (1950).

21. V. Desreux and M. C. Spiegels, *Bull. soc. chim. Belges*, **59**, 476 (1950).

22. C. Fuchs, *Makromol. Chem.*, **5**, 245 (1950); **7**, 259 (1952).

23. C. A. Baker and R. J. P. Williams, *J. Chem. Soc. (London)*, **1956**, 2352.

24. C. W. Ayers, *Analyst*, **78**, 382 (1953).

25. E. D. Bernal, *Rev. plasticos (Madrid)*, **6**, 268 (1955).

26. D. G. H. Ballard and C. H. Bamford, *Proc. Roy. Soc. (London)*, **223A**, 495 (1954).

27. J. A. Blanchette and L. E. Nielson, *J. Polymer Sci.*, **20**, 317 (1956).

28. G. Smets and M. Claesson, *J. Polymer Sci.*, **8**, 289 (1952).

29. H. W. Melville and B. D. Stead, *J. Polymer Sci.*, **16**, 505 (1955).

30. F. D. Hartley, *J. Polymer Sci.*, **34**, 397 (1959).

31. F. F. Nord, M. Bier, and S. N. Timasheff, *J. Am. Chem. Soc.*, **73**, 289 (1951).

32. F. M. Lewis and F. R. Mayo, *Ind. Eng. Chem., Anal. Ed.*, **17**, 134 (1945).

33. A. Goldberg, *Ind. Eng. Chem.*, **39**, 1570 (1947).

34. H. Mark and G. S. Whitby, eds., *Collected Papers of W. H. Carothers*, Interscience, New York–London, 1940.

35. P. J. Flory, (a) *J. Am. Chem. Soc.*, **58**, 1877 (1936); (b) **61**, 3334 (1939); (c) **62**, 1057 (1940); (d) **62**, 1561 (1940); (e) **62**, 2261 (1940); (f) **63**, 3083 (1941); (g) **63**, 3091 (1941); (h) **63**, 3097 (1941);(i) **64**, 2205 (1942).

36. P. J. Flory, *J. Phys. Chem.*, **46**, 132 (1942).

37. P. J. Flory, *J. Chem. Phys.*, **12**, 425 (1944).

38. P. J. Flory, *Chem. Revs.*, **39**, 137 (1946).

39. W. H. Carothers and F. van Natta, *J. Am. Chem. Soc.*, **55**, 4714 (1933).

40. F. van Natta, J. Hill, and W. H. Carothers, *J. Am. Chem. Soc.*, **56**, 455 (1934).

41. See for example, O. Wichterle, *J. Polymer Sci.*, **34**, 309 (1959).

42. W. H. Stoekmayer and H. Jacobsen, *J. Chem. Phys.*, **18**, 1600 (1950).

43. S. Rafikov and V. Korshak, *Doklady Akad. Nauk, USSR*, **64**, 211 (1949).

44. G. Chelenkov, S. Rafikov, and V. Korshak, *Doklady Akad. Nauk, USSR*, **64**, 353 (1949).

45. W. Baker, C. Fuller, and J. Heiss, *J. Am. Chem. Soc.*, **63**, 2142 (1941).
46. P. J. Flory in *High Molecular Weight Compounds*, R. Burk and O. Grummett, eds., Interscience, New York–London, 1949.
47. L. Anderson and J. Porter, *Ind. Eng. Chem.*, **41**, 741 (1949).
48. S. Finn and L. Rogers, *J. Soc. Chem. Ind. (London)*, **67**, 51 (1948).
49. W. H. Stockmayer, *J. Chem. Phys.*, **11**, 45 (1943).
50. M. Bechtold, *J. Polymer Sci.*, **4**, 219 (1949).
51. G. Ostrer, *J. Colloid Sci.*, **2**, 291 (1947).
52. T. G. Majury, private communication.
53. R. H. Kienle, P. A. van der Meulen, and F. E. Petke, *J. Am. Chem. Soc.*, **61**, 2258, 2268 (1939).
54. P. J. Flory, *Principles of Polymer Chemistry*, Cornell University Press, Ithaca, New York, 1953, Chapter IX-1a.
55. R. H. Kienle and F. E. Petke, *J. Am. Chem. Soc.*, **62**, 1053 (1940); **63**, 481 (1941).
56. W. H. Stockmayer and L. L. Weill, cited in *Advancing Fronts of Chemistry*, S. B. Twiss, ed., Reinhold, New York, 1945, Chapter 6.
57. P. J. Flory, *Principles of Polymer Chemistry*, Cornell University Press, Ithaca, N. Y., 1953, Chapter IX-2 and IX-3.
58. P. J. Flory, *ibid.*, Chapter I, and G. M. Burnett, *Mechanism of Polymer Reactions*, Interscience, New York–London, 1954.
59. J. W. Goodeve, *Trans. Faraday Soc.*, **34**, 1239 (1938).
60. J. S. Owens, *Ind. Eng. Chem.*, **11**, 643 (1939).
61. E. L. Kropa and R. B. Barnes, *Am. Chem. Soc. Meeting*, 1941.
62. J. Farquharson, *Trans. Faraday Soc.*, **32**, 219 (1936).
63. J. Farquharson, *Trans. Faraday Soc.*, **33**, 824 (1937).
64. S. V. Lebedov, *J. Soc. phys. chim. russe*, **45**, 1313 (1933).
65. H. W. Melville and W. F. Watson, *Trans. Faraday Soc.*, **44**, 68 (1948).
66. A. H. Pfund, *J. Opt. Soc. Am.*, **30**, 410 (1940).
67. M. A. Naylor and F. W. Billmeyer, *J. Am. Chem. Soc.*, **75**, 2181 (1953).
68. H. W. Starkweather and G. B. Taylor, *J. Am. Chem. Soc.*, **52**, 4708 (1930).
69. A. D. Jenkins in *Symposium on Techniques of Polymer Science*, Report of Royal Institute of Chemistry, London, No. 5, (1956).
70. G. V. Schulz and G. Harborth, *Angew. Chem.*, **59**, 90 (1947).
71. G. M. Burnett and G. L. Duncan, unpublished data.
72. L. K. J. Tong and W. O. Kenyon, *J. Am. Chem. Soc.*, **67**, 1278 (1945).
73. L. K. J. Tong and W. O. Kenyon, *J. Am. Chem. Soc.*, **68**, 1355 (1946).
74. R. N. Haward, *Trans. Faraday Soc.*, **46**, 204 (1950).
75. A. V. Tobolsky, *Ann. Rev. Phys. Chem.*, **7**, 167 (1956).
76. G. M. Burnett and A. N. Wright, unpublished data.
77. M. M. Koton, *Doklady Akad. Nauk, USSR*, **96**, 85 (1954); *Chem. Abstracts*, **48**, 10374f (1954).
78. J. C. Bevington and C. S. Brooks, *J. Polymer Sci.*, **22**, 257 (1956).
79. D. J. Brown, *J. Am. Chem. Soc.*, **62**, 2657 (1940).
80. K. Nozaki and P. D. Bartlett, *J. Am. Chem. Soc.*, **68**, 1686 (1946).
81. B. Barnett and W. E. Vaughan, *J. Phys. Chem.*, **51**, 926, 942 (1947).
82. W. E. Cass, *J. Am. Chem. Soc.*, **68**, 1976 (1946); **69**, 500 (1947).
83. F. M. Lewis and M. S. Matheson, *J. Am. Chem. Soc.*, **71**, 747 (1949).
84. C. E. H. Bawn and S. F. Mellish, *Trans. Faraday Soc.*, **47**, 1216 (1951).
85. L. M. Arnett, *J. Am. Chem. Soc.*, **74**, 2027 (1952).
86. L. M. Arnett and J. H. Peterson, *J. Am. Chem. Soc.*, **74**, 2031 (1952).

87. J. C. Bevington, *Proc. Roy. Soc.*, (*London*), **A239**, 420 (1957).
88. G. M. Burnett and A. C. Gowan, unpublished data.
89. F. Haber and J. Weiss, *Naturwissenschaften*, **20**, 948 (1932); *Proc. Roy. Soc.* (*London*), **A147**, 332 (1934).
90. M. G. Evans, J. H. Baxendale, and G. S. Park, *Trans. Faraday Soc.*, **42**, 155 (1946).
91. R. G. R. Bacon, *Trans. Faraday Soc.*, **42**, 140 (1946).
92. L. B. Morgan, *Trans. Faraday Soc.*, **42**, 169 (1946).
93. W. Kern, *Makromol. Chem.*, **1**, 199 (1948).
94. R. G. R. Bacon, *Quart. Rev.*, **9**, 287 (1955).
95. I. M. Kolthoff *et al.*, *Emulsion Polymerization*, Interscience, New York–London, 1955.
96. See, for example, T. A. Ingles and H. W. Melville, *Proc. Roy. Soc.* (*London*), **A218**, 163, 175 (1953).
97. H. R. Cooper and H. W. Melville, *J. Chem. Soc.* (*London*), **1951**, 1984.
98. P. R. E. J. Cowley and G. M. Burnett, *Trans. Faraday Soc.*, **49**, 1409 (1953).
99. J. C. Bevington, J. H. Bradbury, and G. M. Burnett, *J. Polymer Sci.*, **12**, 469 (1954).
100. D. D. van Slyke *et al.*, *J. Biol. Chem.*, **136**, 509 (1940); **191**, 299 (1951); **192**, 769 (1951).
101. R. F. Glascock, *Isotopic Gas Analysis for Biochemists*, Academic Press, New York, 1954, p. 99.
102. S. C. Brown and W. W. Miller, *Rev. Sci. Instr.*, **18**, 496 (1947).
103. P. D. Bartlett and R. Altschul, *J. Am. Chem. Soc.*, **67**, 816 (1945).
104. See G. M. Burnett, *Mechanism of Polymer Reactions*, Interscience, New York–London, 1954, p. 67 *et seq.*
105. H. W. Melville, J. C. Bevington, and R. P. Taylor, *J. Polymer Sci.*, **12**, 449 (1954).
106. C. H. Bamford and A. D. Jenkins, *Nature* (*London*), **176**, 78 (1955).
107. G. M. Burnett and A. M. North, unpublished data.
108. M. S. Kharasch *et al.*, *J. Am. Chem. Soc.*, **69**, 1105 (1947); *J. Org. Chem.*, **14**, 79, 239, 537 (1949).
109. H. W. Melville, J. C. Robb, and R. C. Tutton, *Discussions Faraday Soc.*, **10**, 154 (1951); **14**, 150 (1953).
110. F. R. Mayo, K. E. Wilzbach, and R. van Meter, *J. Am. Chem. Soc.*, **70**, 4069 (1948).
111. W. H. Stockmayer and L. H. Peebles, *J. Am. Chem. Soc.*, **75**, 2278 (1953).
112. D. B. Anderson and G. M. Burnett, unpublished data.
113. J. W. Breitenbach, *Naturwissenschaften*, **29**, 708 (1941); *Makromol. Chem.*, **8**, 147 (1952).
114. J. W. Breitenbach and H. Karlinger, *Monatsh.*, **82**, 245 (1951).
115. D. B. Anderson and G. M. Burnett, unpublished data.
116. F. R. Mayo, *J. Am. Chem. Soc.*, **75**, 6133 (1953).
117. M. C. Ford and D. Mackay, *J. Chem. Soc.* (*London*), **1957**, 4620.
118. F. R. Mayo, *J. Am. Chem. Soc.*, **65**, 2324 (1943).
119. A. Conix and G. Smets, *J. Polymer Sci.*, **10**, 525 (1953).
120. G. M. Burnett and L. D. Loan, *Trans. Faraday Soc.*, **51**, 214, 219, 226 (1955).
121. P. W. Allan, F. M. Merrett, and J. Scanlan, *Trans. Faraday Soc.*, **51**, 95 (1955).
122. A. D. Jenkins, *Trans. Faraday Soc.*, in press.
123. G. M. Burnett and H. W. Melville, *Nature* (*London*), **156**, 661 (1945); *Proc. Roy. Soc.* (*London*), **A189**, 456 (1947). Vinyl acetate.

124. P. D. Bartlett and C. G. Swain, *J. Am. Chem. Soc.*, **67**, 2273 (1945); **68**, 2381 (1946).

125. P. D. Bartlett, H. S. Broadbent, and K. Kwart, *J. Am. Chem. Soc.*, **72**, 1060 (1956). Vinyl acetate.

126. M. S. Matheson, E. B. Bevilacqua, E. E. Auer, and E. J. Hart, *J. Am. Chem. Soc.*, **71**, 497 (1949). Methyl methacrylate.

127. M. S. Matheson, E. B. Bevilacqua, E. E. Auer, and E. J. Hart, *J. Am. Chem. Soc.*, **73**, 1700 (1951). Styrene.

128. M. S. Matheson, E. B. Bevilacqua, E. E. Auer, and E. J. Hart, *J. Am. Chem. Soc.*, **71**, 2610 (1949). Vinyl acetate.

129. H. W. Melville and H. M. Mackay, *Trans. Faraday Soc.*, **45**, 332 (1949). Methyl methacrylate.

130. H. W. Melville and L. Valentine, *Trans. Faraday Soc.*, **46**, 210 (1950). Styrene.

131. N. Grassie and E. Vance, *Trans. Faraday Soc.*, **52**, 727 (1956). Methacrylonitrile.

132. G. M. Burnett and W. W. Wright, *Proc. Roy. Soc.* (*London*), **A221**, 41 (1954). Vinyl chloride.

133. B. R. Chinmayanandam and H. W. Melville, *Trans. Faraday Soc.*, **50**, 73 (1954). Methyl methacrylate.

134. M. S. Matheson, E. B. Bevilacqua, E. E. Auer, and E. J. Hart, *J. Am. Chem. Soc.*, **73**, 5395 (1951). Methyl acrylate.

135. H. W. Melville and A. F. Bickel, *Trans. Faraday Soc.*, **45**, 1049 (1949). *n*-Butyl acrylate.

136. G. M. Burnett, P. Evans, and H. W. Melville, *Trans. Faraday Soc.*, **49**, 1096 (1953). *n*-Butyl methacrylate.

137. G. M. Burnett, P. Evans, and H. W. Melville, *Trans. Faraday Soc.*, **49**, 1105 (1953). *n*-Propyl methacrylate.

138. C. H. Bamford, A. D. Jenkins, and R. Johnston, cited by A. D. Jenkins in *Symposium on Techniques in Polymer Seience*, Royal Institute of Chemistry, London, No. 5 (1956).

139. C. M. Burrell, T. G. Majury, and H. W. Melville, *Proc. Roy. Soc.* (*London*), **A205**, 309 (1951).

140. T. G. Majury and H. W. Melville, *Proc. Roy. Soc.* (*London*), **A205**, 318 (1951).

141. N. Grassie and H. W. Melville, *Proc. Roy. Soc.* (*London*), **A207**, 285 (1951).

142. W. I. Bengough and H. W. Melville, *Proc. Roy. Soc.* (*London*), **A225**, 330 (1954); **A230**, 429 (1955).

143. H. W. Melville, *Z. Elektrochem.*, **60**, 276 (1957).

144. C. H. Bamford and M. J. S. Dewar, *Proc. Roy. Soc.* (*London*), **A193**, 309, 329 (1948).

145. G. M. Burnett, *Mechanism of Polymer Reactions*, Interscience, New York–London, 1954, p. 210 *et seq.*

146. C. H. Bamford and M. J. S. Dewar, *Proc. Roy. Soc.* (*London*), **A193**, 309 (1948).

147. C. H. Bamford and M. J. S. Dewar, *Proc. Roy. Soc.* (*London*), **A197**, 374 (1949).

148. R. W. E. Axford, *Proc. Roy. Soc.* (*London*), **A197**, 374 (1949).

149. G. Dixon-Lewis, *ibid.*, **A198**, 410 (1949).

150. C. H. Bamford and M. J. S. Dewar, *J. Chem. Phys.*, **17**, 1188 (1949).

151. F. M. Lewis and F. R. Mayo, *J. Am. Chem. Soc.*, **66**, 1594 (1944).

152. T. Alfrey and G. Goldfinger, *J. Chem. Phys.*, **12**, 205 (1944).

153. F. T. Wall, *J. Am. Chem. Soc.*, **66**, 2050 (1944).

154. G. Goldfinger and T. Kane, *J. Polymer Sci.*, **3**, 462 (1948).

155. H. W. Melville and L. Valentine, *Proc. Roy. Soc.* (*London*), **A200**, 337 (1950).

156. F. M. Lewis, F. R. Mayo, and C. Walling, *J. Am. Chem. Soc.*, **70**, 1529 (1948).
157. F. M. Lewis, C. Walling, W. Cummings, E. R. Briggs, and F. R. Mayo, *J. Am. Chem. Soc.*, **70**, 1519 (1948).
158. K. Nozaki, *J. Polymer Res.*, **1**, 455 (1956).
159. G. Goldfinger and M. Steidlitz, *J. Polymer Sci.*, **3**, 786 (1948).
160. C. Walling and E. R. Briggs, *J. Am. Chem. Soc.*, **67**, 1774 (1945).
161. T. Alfrey and G. Goldfinger, *J. Chem. Phys.*, **12**, 322 (1944).
162. A. Voss and E. Dickhauser, German patent 540,101 (1930).
163. T. Wagner-Jauregg, *Ber.*, **63**, 3213 (1930).
164. F. Bovey and I. M. Kolthoff, *J. Am. Chem. Soc.*, **69**, 2143 (1947).
165. G. Ibing and W. Schacht, *Ber.*, **B77**, 542 (1944).
166. C. Walling, E. R. Briggs, K. B. Wolfstirn, and F. R. Mayo, *J. Am. Chem. Soc.*, **70**, 1537 (1948).
167. E. J. Arlman and H. W. Melville, *Proc. Roy. Soc. (London)*, **B203**, 301 (1950).
168. K. R. Hennery-Logan and R. V. V. Nichols, quoted by F. R. Mayo and C. Walling, *Chem. Revs.*, **46**, 191 (1950).
169. F. M. Lewis, C. Walling, W. Cummings, E. R. Briggs, and W. J. Wenisch, *J. Am. Chem. Soc.*, **70**, 1527 (1948).
170. R. Simha and L. A. Wall, *J. Research Natl. Bur. Standards*, **41**, 521 (1948).
171. C. S. Marvel, G. E. Inskeep, R. Deanen, D. Hein, P. V. Smith, J. D. Young, A. E. Juve, C. H. Schroeder, and M. M. Goft, *Ind. Eng. Chem.*, **40**, 2371 (1948).
172. D. C. Blackley and H. W. Melville, *Makromol. Chem.*, Standinger Festband, 1956, p. 16.
173. F. R. Mayo and C. Walling, *Chem. Revs.*, **46**, 191 (1950); G. M. Burnett, *Mechanism of Polymer Reactions*, Interscience, New York–London, 1954, p. 257 *et. seq.*; T. Alfrey, J. H. Bohrer, and H. Mark, *Copolymerization*, Interscience, New York–London, 1955.
174. T. Alfrey and C. C. Price, *J. Polymer Sci.*, **2**, 101 (1947).
175. C. C. Price, *Discussions Faraday Soc.*, **2**, 304 (1947).
176. C. C. Price, *J. Polymer Sci.*, **3**, 772 (1948).
177. L. A. Wall, *J. Polymer Sci.*, **2**, 542 (1947).
178. H. W. Melville, B. Noble, and W. F. Watson, *J. Polymer Sci.*, **2**, 229 (1947).
179. G. M. Burnett, *Mechanism of Polymer Reactions*, Interscience, New York–London, 1954, p. 121.
180. G. M. Burnett, *loc. cit.*, p. 123; D. C. Blackley, H. W. Melville, and L. Valentine, *Proc. Roy. Soc. (London)*, **A227**, 10 (1954).
181. E. J. Arlman, H. W. Melville, and L. Valentine, *Rev. trav. chim., Pays-Bas*, **68**, 945 (1949).
182. H. W. Melville and L. Valentine, *Proc. Roy. Soc. (London)*, **A200**, 353 (1950).
183. C. Walling, *J. Am. Chem. Soc.*, **71**, 1930 (1948).
184. S. R. Palit, *Trans. Faraday Soc.*, **51**, 1129 (1955).
185. E. P. Bonsall, H. W. Melville, and L. Valentine, *J. Polymer Sci.*, **7**, 39 (1952).
186. E. P. Bonsall, H. W. Melville, and L. Valentine, *Trans. Faraday Soc.*, **48**, 763 (1952).
187. C. Walling and E. A. McElhill, *J. Am. Chem. Soc.*, **73**, 2819 (1951).
188. G. M. Burnett and H. R. Gersmann, *J. Polymer Sci.*, **28**, 655 (1958).
189. G. M. Burnett and L. D. Loan, *Trans. Faraday Soc.*, **51**, 219 (1955).
190. W. Cooper *et al.*, *Proc. of Third Rubber Tech. Conf.*, Heffer, Cambridge, 1954, p. 150.
191. G. M. Burnett, *J. Polymer Sci.*, **28**, 642 (1958).
192. D. Coleman and F. O. Howitt, *Proc. Roy. Soc. (London)*, **A190**, 145 (1949).

193. B. Drucker and S. G. Smith, *Nature, London*, **165**, 196 (1950).
194. O. B. Edgar and R. Hill, *J. Polymer Sci.*, **8**, 1 (1952).
195. W. E. Roseveare, R. C. Walker, and J. N. Wilson, *Textile Research J.*, **18**, 114 (1948).
196. H. Mark, *Research*, **4**, 167 (1951).
197. J. L. Bolland and H. W. Melville, *Proc. Rubber Technology Conference, (London)*, 1938, Heffer, Cambridge, p. 239; *Ost. Chem.-Ztg.*, **42**, 201 (1939).
198. H. W. Melville and A. J. R. Murray, *Trans. Faraday Soc.*, **46**, 996 (1950).
199. British Patent, 679,562 (1952).
200. W. F. Watson and M. Pike, *J. Polymer Sci.*, **9**, 229 (1952).
201. A. S. Dunn and H. W. Melville, *Nature*, **169**, 699 (1952). See also R. Hart and A. de Pauw, *Simposio Internazionale di Chemica Macromoleculare*, 1956, p. 265.
202. P. E. M. Allen, M. Downer, and G. M. Burnett, unpublished data.
203. J. A. Hicks and H. W. Melville, *J. Polymer Sci.*, **12**, 461 (1954).
204. A. S. Dunn, H. W. Melville, and D. B. Stead, *Trans. Faraday Soc.*, **50**, 279 (1954).
205. C. H. Bamford and E. F. T. White, *Trans. Faraday Soc.*, **52**, 716 (1956).
206. P. E. M. Allen, J. M. Downer, G. W. Hastings, H. W. Melville, P. Molyneux, and J. R. Urwin, *Nature, (London)*, **977**, 910 (1956).
207. J. R. Urwin, *J. Polymer Sci.*, **27**, 580 (1958).
208. G. M. Burnett, P. Meares, and C. Paton, unpublished data.
209. R. J. Orr and H. L. Williams, *J. Am. Chem. Soc.*, **79**, 3137 (1957).
210. F. Dalton, Ph.D. Thesis (Birmingham), 1956.
211. C. H. Bamford and A. D. Jenkins, *Nature (London)*, **176**, 78 (1955).
212. G. Smets and M. Claeson, *J. Polymer Sci.*, **9**, 289 (1952).
213. F. W. Peaker and R. L. Vale, *J. Polymer Sci.*, **30**, 29 (1958).
214. J. Scanlan, *Trans. Faraday Soc.*, **50**, 756 (1954).
215. F. M. Merrett, *Trans. Faraday Soc.*, **50**, 759 (1954).
216. J. E. Guillet and R. G. W. Norrish, *Simposio Internazionale di Chemica Macromoleculare*, 1956, p. 250.
217. J. W. McBain in *Advances in Colloid Science, Vol. I*, Interscience, New York–London, 1942, p. 124; G. S. Hartley, *Aqueous Solutions of Paraffin Chain Salts*, Hermann and Cie, Paris, 1936.
218. W. D. Harkins, *J. Am. Chem. Soc.*, **69**, 1428 (1947).
219. H. B. Klevens, *Chem. Revs.*, **47**, 1 (1950).
220. R. N. Haward, *J. Polymer Sci.*, **4**, 273 (1949).
221. W. V. Smith and R. H. Ewart, *J. Chem. Phys.*, **16**, 592 (1948).
222. J. Bakker, *Philips Research Repts.*, **7**, 344 (1952).
223. G. M. Burnett and R. S. Lehrle, in press.
224. W. V. Smith, *J. Am. Chem. Soc.*, **70**, 3695 (1948).
225. G. M. Burnett and R. S. Lehrle, in press.
226. M. Morton, P. P. Salatiello, and H. Landfield, *J. Polymer Sci.*, **8**, 111, 215, 279 (1952).
227. S. H. Maron, M. E. Elder, and I. N. Ulevitch, *J. Colloid Sci.*, **9**, 89 (1954).
228. G. M. Burnett, R. S. Lehrle, D. W. Ovenall, and F. W. Peaker, *J. Polymer Sci.*, **29**, 417 (1958).
229. G. M. Burnett, *Mechanism of Polymer Reactions*, Interscience, New York–London, 1954.
230. A. Deville, *Ann. Chim.*, **75**, 66 (1839).
231. K. E. Russell and R. G. W. Norrish, *Nature*, **160**, 543 (1949); *Trans. Faraday Soc.*, **48**, 91 (1952).
232. P. H. Plesch, *J. Chem. Soc. (London)*, **1947**, 868.

233. J. George, H. Wechsler, and H. Mark, *J. Am. Chem. Soc.*, **72**, 3891 (1950).
234. J. George and H. Wechsler, *J. Polymer Sci.*, **6**, 725 (1951).
235. C. C. Price and J. M. Ciskowski, *Ann. N. Y. Acad. Sci.*, **44**, 368 (1938).
236. C. C. Price, *Reactions at Carbon-Carbon Double Bonds*, Interscience, New York–London, 1946.
237. G. Williams, *J. Chem. Soc.* (*London*), **1950**, 775.
238. I. Clark, in P. H. Plesch, ed., *Cationic Polymerization*, Heffer, Cambridge, 1953, p. 99.
239. D. O. Jordon and A. R. Mathieson, *J. Chem. Soc.* (*London*), **1952**, 2354, 2358, 2363.
240. D. D. Eley and A. W. Richards, *Trans. Faraday Soc.*, **45**, 425 (1949).
241. P. H. Plesch, *J. Chem. Soc.* (*London*), **1953**, 1653.
242. See D. C. Pepper, *Quart. Rev.* (*London*), **8**, 88 (1954).
243. D. D. Eley and J. Saunders, *J. Chem. Soc.* (*London*), **1952**, 4167.
244. D. C. Pepper, *Nature* (*London*), **158**, 789 (1946).
245. D. C. Pepper, *Trans. Faraday Soc.*, **45**, 397 (1949).
246. D. C. Pepper and D. Somerfield, in P. H. Plesch, ed., *Cationic Polymerization*, Heffer, Cambridge, 1953, p. 75.
247. R. G. Beaman, *J. Am. Chem. Soc.*, **70**, 3115 (1948).
248. F. C. Foster, *J. Am. Chem. Soc.*, **74**, 2299 (1952).
249. L. Küchler, *Polymerizationskinetik*, Springer-Verlag, Berlin, 1951, p. 246.
250. K. Zielger *et al.*, *Ann.*, **511**, 13, 45, 64 (1934).
251. J. L. Bolland, *Proc. Roy. Soc.* (*London*), **A178**, 24 (1941).
252. R. E. Robertson and L. Marion, *Can. J. Research*, **26B**, 657 (1948).
253. J. J. Sanderson and C. R. Hauser, *J. Am. Chem. Soc.*, **71**, 1595 (1949).
254. W. C. E. Higginson and N. S. Wooding, *J. Chem. Soc.* (*London*), **1952**, 760.
255. A. Abkin and S. Medvedev, *Trans. Faraday Soc.*, **32**, 286 (1936); *J. Phys. Chem.* (*U.S.S.R.*), **13**, 705 (1939).
256. O. Mamontova, A. Abkin, and S. Medvedev, *Acta Physicochim.* (*U.R.S.S.*), **12**, 269 (1940).
257. N. D. Scott, U. S. Patent, 2,181,771 (1939).
258. M. Szwarc, M. Levy, and R. Milkovich, *J. Am. Chem. Soc.*, **78**, 2656 (1956).
259. N. D. Scott, J. F. Walker, and V. L. Hansley, *J. Am. Chem. Soc.*, **58**, 2442 (1936).
260. A. Rembaum and M. Szwarc, *J. Polymer Sci.*, **22**, 189 (1956).
261. R. Waack, A. Renbaum, J. D. Coombes, and M. Szwarc, *J. Am. Chem. Soc.*, **79**, 2026 (1957).
262. Y. Landler, *Compt. rend.*, **230**, 539 (1950); *J. Polymer Sci.*, **8**, 64 (1952).
263. D. C. Pepper, *Quart. Rev.* (*London*), **8**, 88 (1954). (See Table IV of this paper for reactivity ratios in cationic polymerization.)
264. R. E. Florin, *J. Am. Chem. Soc.*, **71**, 1867 (1949).
265. R. E. Florin, *J. Am. Chem. Soc.*, **73**, 4468 (1951).
266. R. E. Florin, *Intern. Congr. Pure Appl. Chem.*, 1951.
267. C. G. Overberger, R. J. Ehrig, and D. Tanner, *J. Am. Chem. Soc.*, **76**, 772 (1954).
268. F. C. Foster, *J. Am. Chem. Soc.*, **74**, 2299 (1952).
269. See, for example, G. Natta, *Chimie e industrie* (*Milan*), **37**, 888 (1955).
270. K. Ziegler, *Angew Chem.*, **67**, 541 (1955).
271. G. Natta, P. Pino, G. Mazzanti, P. Corradini, and U. Giannini, *Atti accad. nazl. Lincei, Rend., Classe sci. fis. mat. e nat.*, **19**, 397 (1955).
272. G. Natta, P. Corridini, and I. W. Bassi, *ibid.*, 404.
273. M. Reding, *J. Polymer Sci.*, **21**, 547 (1956).

274. G. Natta and P. Corridini, *Angew. Chem.*, **68**, 615 (1956); *Atti accad. nazl. Lincei Rend., Classe sci. fis. mat. e nat.*, **20**, 560 (1956).
275. G. Natta, P. Pino, U. Giannini, E. Mantica, and M. Peraldo, *Chimie e industrie*, **39**, 19 (1957).
276. G. Natta, *J. Polymer Sci.*, **34**, 21 (1959).
277. G. Natta, I. Pasquon, and E. Giachett, *Angew. Chem.*, **69**, 213 (1957).
278. G. M. Burnett and P. J. T. Tait, *J. Polymer Sci.*, **34**, 46 (1959).
279. K. Vesely, *J. Polymer Sci.*, **34**, 46 (1959).
280. G. M. Burnett and P. J. T. Tait, *Polymer*, **1**, 151 (1960).
281. A. A. Morton, *Ind. Eng. Chem.*, **42**, 1488 (1950).
282. J. R. L. Williams, J. van der Berg, W. J. Dulmage, and K. R. Dunham, *J. Am. Chem. Soc.*, **78**, 1260 (1956).
283. See C. E. H. Bawn, *Proc. Chem. Soc. (London)*, **1958**, 138; C. E. H. Bawn and R. Symcox, *J. Polymer Sci.*, **34**, 139 (1959).
284. C. E. H. Bawn, A. Ledwith, and P. Matthies, *J. Polymer Sci.*, **34**, 93 (1959).
285. C. E. H. Bawn, and A. Ledwith, *Chem. and Ind. (London)*, **1957**, 1180.
286. F. W. Stavely *et al.*, *Ind. Eng. Chem.*, **48**, 778 (1956).
287. S. E. Horne, J. P. Kiehl, J. J. Shipman, V. L. Folt, C. F. Gibbs, E. A. Wilson, E. B. Newton, and M. A. Reinhart, *Ind. Eng. Chem.*, **48**, 748 (1956).
288. C. E. Schildknecht, S. T. Cross, H. R. Davidson, J. M. Lambert, and A. O. Zoss, *Ind. Eng. Chem.*, **40**, 2104 (1948).
289. T. G Fox *et al.*, *J. Am. Chem. Soc.*, **80**, 1768 (1958).
290. For a review of cellulose degradation see L. F. McBurney in E. Ott and H. M. Spurlin, eds., *Cellulose and Cellulose Derivatives*, Part I, Interscience, New York–London, 1954, p. 99 *et seq.*
291. K. Freudenberg and W. Kuhn, *Ber.*, **65B**, 484 (1932).
292. G. V. Schulz and H. J. Lohmann, *J. prakt. Chem.*, **157**, 238 (1941).
293. G. C. Gibbons, *J. Textile Inst.*, **43**, T25 (1952).
294. W. Kuhn, *Ber.*, **63B**, 1503 (1930).
295. W. Kuhn, *Z. physik. Chem.*, **B159**, 368 (1932).
296. H. Mark, K. H. Meyer, and H. Hopff, *Ber.*, **62B**, 1103 (1929).
297. K. Freudenberg, W. Kuhn, W. Dürr, F. Bolz, and G. Steinbrunn, *Ber.*, **63B**, 1510 (1930).
298. K. Freudenberg and E. Braun, *Ann.*, **460**, 288 (1928).
299. K. Freudenberg and G. Blomquist, *Ber.*, **68B**, 2070 (1935).
300. G. Beall and L. Jorgensen, *Textile Research J.*, **21**, 203 (1951).
301. L. A. Heller and E. Pacsu, *ibid.*, **16**, 490 (1946).
302. E. Pacsu, *Fortschr. Chem. org. Naturstoffe*, **5**, 129 (1948).
303. G. V. Schulz, E. Husemann, and H. J. Lohmann, *Z. physik. Chem.*, **B52**, 23 (1942).
304. E. Husemann and A. Carnap, *Makromol Chem.*, **1**, 140 (1947).
305. G. V. Schulz, *J. Polymer Sci.*, **3**, 365 (1948).
306. P. J. Flory, *J. Am. Chem. Soc.*, **58**, 1877 (1936).
307. L. F. McBurney, in E. Ott and H. M. Spurlin, eds., *Cellulose and Cellulose Derivatives*, Part I, Interscience, New York–London, 1954, p. 112–114.
308. L. Jorgensen, *Studies on the Partial Hydrolysis of Cellulose*, Emil Mostue, Oslo, 1950.
309. C. Birtwell, D. A. Clibbens, and A. Geake, *J. Textile Research*, **17**, 1451 (1926).
310. F. H. Yorston, *Quart. Rev., Forest Products Laboratory of Canada*, **No. 13**, 16 (1933).
311. H. J. Philip, M. L. Nelson, and H. M. Ziifle, *J. Textile Research*, **17**, 585 (1947).

312. M. L. Nelson and C. M. Conrad, *ibid.*, **18**, 149 (1948).
313. A. Meller, *J. Polymer Sci.*, **4**, 619 (1949).
314. P. J. Flory, *J. Am. Chem. Soc.*, **62**, 2255 (1940).
315. H. G. H. Jellinek, *Trans. Faraday Soc.*, **40** 266 (1944).
316. S. L. Madorsky and S. Straus, *J. Research Natl. Bur. Standards*, **40**, 417 (1948).
317. S. L. Madorsky, S. Straus, D. Thompson, and L. Williamson, *ibid.*, **42**, 499 (1949).
318. N. Grassie and H. W. Melville, *Proc. Roy. Soc. (London)*, **A199**, No. 1, 14 (1949).
319. R. Simha, *J. Appl. Phys.*, **12**, 569 (1941); R. Simha and E. Montroll, *J. Chem. Phys.*, **8**, 721 (1940).
320. H. H. G. Jellinek, *Trans. Faraday Soc.*, **44**, 345 (1948).
321. P. J. Blatz and A. V. Tobolsky, *J. Phys. Chem.*, **49**, 77 (1945).
322. R. Simha, P. J. Blatz, and L. A. Wall, *J. Polymer Sci.*, **5**, 615 (1950).
323. R. Simha, *Trans. Faraday Soc.*, **54**, 1345 (1958).
324. M. Gordon, *Trans. Faraday Soc.*, **53**, 1662 (1957).
325. H. H. G. Jellinek, *J. Polymer Sci.*, **3**, 850 (1948).
326. H. H. G. Jellinek, *ibid.*, **4**, 1 (1949).
327. N. Grassie and W. W. Kerr, *Trans. Faraday Soc.*, **53**, 234 (1957).
328. N. Grassie, *ibid.*, **48**, 379 (1952).
329. J. E. Campbell and W. H. Ramscher, *J. Polymer Sci.*, **18**, 461 (1955).
330. H. W. Melville and P. R. E. J. Cowley, *Proc. Roy. Soc. (London)*, **A221**, 320 (1952).
331. G. Schmid and O. Rommel, *Z. Elektrochem.*, **49**, 659 (1943).
332. G. Schmid and O. Rommel, *Z. physik. Chem.*, **185A**, 97 (1939).
333. G. Schmid and E. Bentenmuller, *Z. Elektrochem.*, **49**, 325 (1943).
334. H. W. Melville and A. J. R. Murray, *Trans. Faraday Soc.*, **46**, 996 (1950).
335. St. A. Buckingham, *Paper Ind.*, **18**, 749 (1936).
336. S. Ono, *Rev. Phys. Chem. (Japan)*, **14**, 25 (1940).
337. A. Szalay, *Z. physik. Chem.*, **164A**, 234 (1933).
338. G. Hastings, *Thesis (Birmingham)*, 1956.
339. A. Henglein, *Makromol Chem.*, **15**, 188 (1955).
340. A. Henglein, *Makromol Chem.*, **14**, 128 (1954).
341. M. Pike and W. F. Watson, *J. Polymer Sci.*, **9**, 225 (1952).
342. G. Ayrey, C. G. Moore, and W. F. Watson, *ibid.*, **19**, 1 (1956).
343. A. B. Bestul, *J. Chem. Phys.*, **24**, 1196 (1956).
344. See J. L. Bolland, *Quart. Rev. (London)*, **3**, 1 (1949).
345. F. F. Rust and W. E. Vaughan, U. S. Patents 2,396,206 and 2,396,217.
346. P. George and A. D. Walsh, *Trans. Faraday Soc.*, **42**, 94 (1946).
347. G. Chavanne and O. Miller, *Bull. soc. chim. (Belg.)*, **40**, 611 (1931).
348. D. Spence and J. D. Ferry, *J. Am. Chem. Soc.*, **59**, 1648 (1937).
349. H. Stevens, *ibid.*, **64**, 135 (1945).
350. J. L. Bolland and H. R. Cooper, *Nature*, **172**, 423 (1953).
351. J. L. Bolland and H. R. Cooper, *Proc. Roy. Soc. (London)*, **A225**, 405 (1954).
352. G. M. Burnett and A. C. Flett, unpublished data.

CHAPTER XXII

ENZYMIC REACTIONS

FRANK M. HUENNEKENS, *University of Washington**
BRITTON CHANCE, *University of Pennsylvania*

Part 1. Measurement of Enzyme Reactions and General Theory of Enzyme Kinetics.
FRANK M. HUENNEKENS 1232
I. Introduction 1232
1. Biological Reactions 1232
2. General Characteristics of Enzymic Reactions 1233
II. Measurement of the Rate of Enzymic Reactions 1236
1. Discontinuous Methods 1236
2. Continuous Methods 1238
III. Enzyme Kinetics 1243
1. General Considerations 1243
2. Effect of Enzyme Concentration 1246
3. Effect of Substrate Concentration 1248
4. Effect of Inhibitors 1278
5. Effect of pH 1287
6. Effect of Temperature 1292
7. Effect of Pressure 1301
References 1303
General References 1313
Part 2. Enzyme Kinetics in the Transient State. BRITTON CHANCE 1314
I. Introduction 1314
1. An Extension of the Theory of Michaelis and Menten 1317
2. Experimental Methods 1321
II. The Peroxidatic Reaction of Catalase 1323
1. Measurements of the Over-all Reaction 1324
2. Kinetics and Spectra of the Enzyme–Substrate Compound 1325
3. Order of the Reactions 1327
4. The Ternary Complex of Enzyme, Substrate, and Donor 1330
5. Effect of pH upon the Reaction Velocity Constants for Catalase Activity 1330
6. Reaction of Peroxide Complex of Bacterial Catalase with Donors 1332
III. The Catalase Reaction 1332
1. Reaction of Catalase Methyl Hydrogen Peroxide with Hydrogen Peroxide 1332
2. A Mechanism for Catalase Action 1333
3. Experimental Studies of the Over-all Reaction of Catalase 1335
4. Spectroscopic Studies of the Catalase–Hydrogen Peroxide Complex 1336
5. Measurement of k, for Reaction of Catalase and Hydrogen Peroxide 1338
IV. The Peroxidatic Reactions of the Catalase–Hydrogen Peroxide Complex 1339

* Present address: Scripps Clinic and Research Foundation, La Jolla, California.

1. The Fate of Hydrogen Peroxide 1339
2. Spontaneous Decomposition 1340
3. Donor Specificity 1341
4. Coupled Oxidations 1342
5. Effect of pH 1342
6. The Ternary Complex of Enzyme, Substrate, and Donor 1343
V. The Peroxidases 1343
1. Introduction 1343
2. Spectroscopic Data 1344
3. Kinetics of Formation of Primary Complexes 1346
4. Transition from Primary to Secondary Complexes 1346
5. Acceleration of the Transition from Primary to Secondary Complexes 1349
6. The Second-Order Reaction of Complex I with the Donor Molecule 1350
7. The Second-Order Reaction of Complex II with the Donor Molecule 1351
8. Relative Activities of Hydrogen and Alkyl Hydrogen Peroxide Complexes of Peroxidase 1352
9. Donor Specificity of Peroxidases 1353
VI. Summary 1354
References 1357
General References 1359

Part 1. MEASUREMENT OF ENZYME REACTIONS AND GENERAL THEORY OF ENZYME KINETICS

I. INTRODUCTION

1. Biological Reactions

Kinetic studies of biological systems have encompassed a wide variety of rate processes occurring in living organisms, or in systems derived from the living organisms. While some difficulty is encountered in providing a truly rigorous definition (1,2) of the term "living," it is sufficient for the present purpose to state that living systems: (*a*) are represented by cellular forms containing, *inter alia*, certain indispensable substances such as proteins, nucleic acids, and "energy-rich" phosphate esters (e.g., adenosine triphosphate) (3); and (*b*) exhibit the phenomena of growth, reproduction, adaptation, and irritability.

There has been a growing realization in recent years (see, for example, Green's review (4)) that even the most complex biological reactions are controlled at the molecular level by a specialized group of proteins, the enzymes, which have remarkable catalytic powers. Descriptions of the multitude of known enzymes may be found in various texts on enzymology

(5–8). The present discussion will be concerned chiefly with the techniques for measurement of *individual* enzyme-catalyzed reactions, and with the general theory of enzyme kinetics. Complex biological processes involving a multiplicity of enzymic steps, such as the growth of bacteria (9), the labeling of metabolic pools by radioactive tracers (10,11), the transport of substances across membranes (12), or the transmission of nerve impulses (12) are not treated here since the kinetics of these, and other systems, have been covered in previous reviews (13–18).

2. General Characteristics of Enzymic Reactions

In 1926, J. B. Sumner (19) isolated from a plant tissue the first crystalline enzyme, urease:

$$CO(NH_2)_2 + H_2O \xrightarrow{\text{urease}} CO_2 + 2NH_3 \qquad (1)$$

Subsequently, biochemists have systematically isolated and characterized a large number of other enzymes from animal, plant, and microbial sources and have used these enzymes to reconstruct cellular metabolic sequences. Although crystallinity per se is not an absolute proof for the homogeneity of proteins (20,21), it remains as a desirable goal in the purification of a protein. Dixon and Webb (22) have listed over one hundred enzymes which have already been obtained in crystalline form. Most of the known enzymes, however, have only been partially purified and certain enzymes still have not been solubilized from the particulate fractions (e.g., mitochondria, microsomes, nuclei, chloroplasts, grana) of the cell in which they reside. The conventional methods (23) of protein purification require that the material be soluble, but recently Green and his colleagues (24) have devised new techniques for purifying particulate enzymes without solubilization.

Although instances have been recorded where the kinetic properties of an enzyme have been altered as a result of purification or detachment from particulate matter (e.g., malic dehydrogenase (25)) it is apparent that metabolic or kinetic studies are more apt to be reliable when highly purified enzymes are used. On the other hand, valid studies have been made, and will continue to be made, with partially purified systems under those fortunate circumstances where competing reactions or destructive effects upon the enzyme or the substrate are minimal.

The catalytic efficiency of enzymes is readily demonstrated in those instances where the reaction can also be catalyzed by chemical agents. The rate constant is larger, often by several orders of magnitude, for the enzyme-catalyzed reaction as contrasted to the noncatalyzed reaction or the chemically-catalyzed reaction (26). More expressive, however, than the

rate constant is the designation of an enzyme activity by its turnover number, i.e., the number of molecules of substrate transformed into product each minute by one molecule of enzyme acting under optimal conditions. Turnover numbers usually range from 10^2 to 10^4 for most enzymes, but may even rise to 10^6 as in the case of the decomposition of hydrogen peroxide by catalase:

$$H_2O_2 \xrightarrow{\text{catalase}} H_2O + {}^1/_2O_2 \qquad (2)$$

The oxidation of succinic acid provides another example of the ability of enzymes to implement otherwise difficult reactions. In the chemical laboratory, succinic acid is slowly converted to fumaric acid in the presence of strong oxidizing agents at elevated temperatures. Succinic dehydrogenase, on the other hand, carries out the same reaction with facility at neutral pH and room temperature, and only a relatively weak oxidant, flavin-adenine-dinucleotide, is required as a coenzyme:

$$\text{Succinate} + \text{FAD} \xrightarrow[\text{dehydrogenase}]{\text{succinic}} \text{fumarate} + \text{FADH}_2 \qquad (3)$$

The following abbreviations are used: FAD, $FADH_2$, oxidized and reduced flavin-adenine-dinucleotide; DPN, DPNH, TPN, TPNH, oxidized and reduced di- and triphosphopyridine nucleotide; AMP, ADP, and ATP, adenosine mono-, di-, and triphosphate; P_i, inorganic phosphate; PP, pyrophosphate; CoA, coenzyme A.

Detailed kinetic measurements of various enzymes have contributed to an increased understanding of the *mechanism* of enzyme action (27–29). Enzymes behave like "polyfunctional catalysts," i.e., the active centers appear to contain more than one reactive group and these groups work cooperatively through their spatial orientation to achieve effects not possible to the groups acting separately (30,31). Polyfunctional catalysis is explicit in the mechanism of Figure 1.1, suggested by Swain and Brown (30) to account for the ability of 2-hydroxypyridine to catalyze the mutarotation of glucose at a rate several orders of magnitude higher than that of phenol or pyridine alone or admixed. The extension of this principle to an enzymic reaction is illustrated by the proposed mechanism (32) for fumarase, as shown in Figure 1.2.

Enzymic reactions may be divided into three broad categories (33,34) depending upon the number of substrates involved (the reactions may be reversible or irreversible):

$$A + B \rightleftharpoons C + D \qquad \text{Type I}$$

$$A + B \rightleftharpoons C \qquad \text{Type II}$$

$$A \rightleftharpoons B \qquad \text{Type III}$$

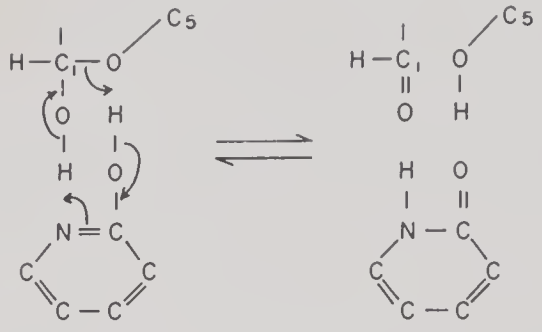

Fig. 1.1. Mechanism of polyfunctional catalysis (30).

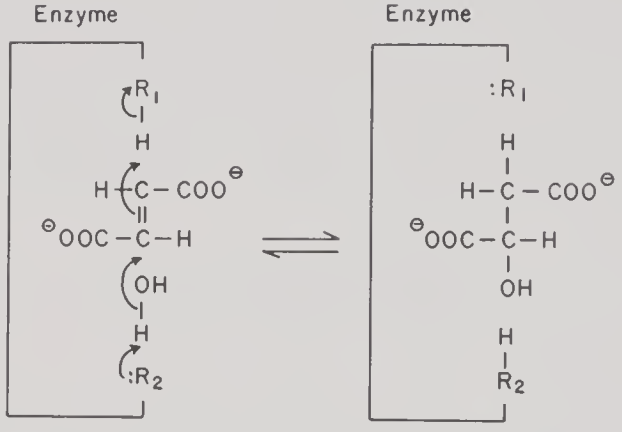

Fig. 1.2. Mechanism of the fumarase-catalyzed reaction (32).

Reactions of Type I are the most numerous and include those catalyzed by the hydrolytic enzymes, transferases, and oxido-reductases. Neglecting the enzyme, these reactions will ordinarily be bimolecular except when one of the substrates is water, whereupon the system becomes pseudo-monomolecular. Type II reactions involve decarboxylases, hydrases, etc. and are bimolecular if studied from left to right, or monomolecular if studied in the reverse direction. Finally, the Type III reactions, represented by isomerases and racemases, are monomolecular in either direction. Reactions of the type: Acetate + ATP + CoA $\rightleftharpoons$ acetylCoA + AMP + PP can be considered formally, and in some instances have been shown experimentally, to be composed of two separate bimolecular reactions (35).

It is clear, then, that enzymic reactions are readily studied by the usual methods of chemical kinetics except for the reservations that the catalyst (enzyme), and in some instances even the substrates, are sometimes not available in pure form, and that the catalyst is usually destroyed by exposure to temperatures above 30 to 40°C. and to pH regions removed from neutrality. Section II of this part summarizes the commonly used experimental methods for carrying out kinetic studies on enzyme-catalyzed reactions, while the final section (III) discusses the theory and treatment of the rate data obtained from the measurement of enzymic reactions.

II. MEASUREMENT OF THE RATE OF ENZYMIC REACTIONS

The usual rationale for the measurement of ordinary chemical reactions applies as well to enzymic reactions. For a typical reaction,

$$A + B \xrightarrow{\text{enzyme}} C + D \tag{4}$$

the stoichiometry demands that, at any time during the reaction, both A and B must have decreased by the same amount, and C and D must have increased by this amount. Deviations from this equivalence indicate the presence of side reactions. In most kinetic studies it has been customary to follow the change in concentration of only one of the substances, and to assume that the "blank" or "control" determinations (i.e., complete systems minus one component) will detect, and correct for, any side reactions.

1. Discontinuous Methods

A. CHEMICAL ANALYSIS

In any *discontinuous* method of measurement, samples are withdrawn periodically from the reaction vessel and analyzed separately, perhaps even at a later time. The reaction in the aliquot can be stopped by the addition of a deproteinizing agent (trichloroacetic acid, ethanol, etc.), by heating the solution, or even by dilution with a large volume of water or buffer. In the above procedures, the time for inactivating the enzyme must be short compared to the time of reaction and, where multiple reactions are being studied, the enzymes must not be inactivated at different rates. The inactivation process must neither destroy labile intermediates nor give rise to substances which interfere with the subsequent analyses.

The reactant or product whose concentration changes are being followed may be quantitated by conventional titrimetric or colorimetric determinations, such as inorganic phosphate by the molybdate method, or α-amino acids by the reaction with ninhydrin. Neurath and Schwert (36) have described a variety of methods, in addition to the ninhydrin reaction, for tracing the action of proteolytic enzymes. Analytical techniques for most of the substances encountered in enzymic reactions may be found, for example, in the definitive compendium, *Methods in Enzymology* (37).

Although widely used in enzymic studies, the discontinuous assay method suffers from the obvious defect that a point-by-point analysis may overlook unexpected deviations and, furthermore, the method is unsuitable for short time intervals (<15 sec.) where the time of sampling itself is of the order of seconds.

B. RADIOACTIVE TRACERS

An important extension of the analytical method has been provided through the availability of radioactive tracers. Owing to the sensitivity of detecting and counting isotopic samples, small quantities of a substance may be estimated when the more gross analytical tools are inapplicable (38). Much of the present-day knowledge of intermediary metabolism is referable to the use of tracers to establish the pertinent chemical sequences.

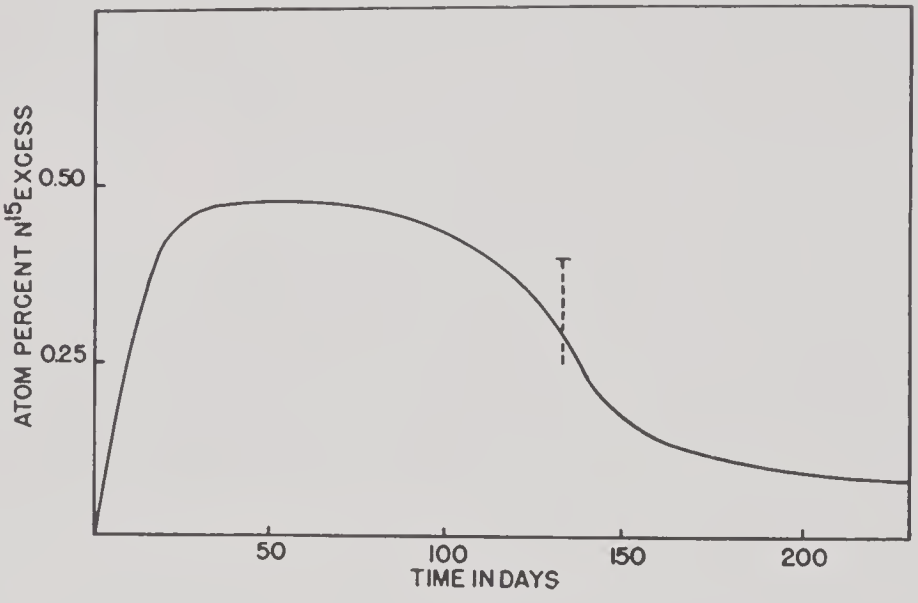

Fig. 1.3. Specific activity of N^{15}-labeled hemin (41).

Although equally valid and applicable, less use has been made of tracers to study the *rate* of biological reactions. Branson (39) has discussed the possibilities of using integral equations to describe metabolizing systems with special reference to tracer problems. Despite the restrictions upon the type and strength of radiation which enzymes and biological systems can endure, as well as the more obvious considerations (half-life, dilution effects, etc.) in tracer work, certain physiological processes including the rate of regeneration, or turnover, of many diverse compounds (40) have been investigated successfully by this method.

One process which illustrates the power of tracer methods and which will serve as an example of the general procedure is the classic determination by Shemin and Rittenberg (41) of the life-span of the red blood cell. When N^{15}-labeled glycine is fed to a man, various metabolically active substances become labeled if glycine is a precursor in their formation. With such compounds the N^{15} content rises to a maximum within a day or two after termination of the feeding and thereafter declines exponentially. This has been demonstrated with liver and plasma proteins (42) and indi-

cates a dynamic state in which the substance is being continuously synthesized and degraded. Such behavior, however, was not manifested in the case of hemin from red blood cells. Instead, the specific activity curve for hemin (see Fig. 1.3) rose for about 20 days, remained more or less level for about 70 days, and then declined in a sigmoid curve. Hemin is not, therefore, in a state of constant dynamic equilibrium, and the incorporation of N^{15} into this compound occurs only during the formation of the red blood cell. The labeled hemin then remains with the cell until disintegration, whereupon it is largely excreted as bile pigment and not incorporated into newly formed red blood cells. Mathematical analysis of the data in the figure yielded the value of about 127 days for the average life span (T) of the human red cell.

2. Continuous Methods

In the continuous methods of analysis, the reaction mixture is essentially undisturbed during the measurement. Changes in some physical property (light absorption, pressure, pH, etc.) of the solution are measured and may be transmitted as a signal to a recording device in order to obtain a continuous record of the course of the reaction. It is apparent, too, that continuous methods can be used to record concentration changes occurring during very short time intervals.

A. SPECTROPHOTOMETRY

In many instances where a substrate or product of the enzymic reaction absorbs light, it has been possible to follow the reaction by means of absorption spectrophotometry. Pioneering in this area, Warburg (43) and von Euler (44) were among the first investigators to take advantage of the observation that the reduced form of the coenzyme, diphosphopyridine nucleotide, absorbed light at 340 mμ and realized this could be used as the basis of a spectrophotometric method for following the action of the pyridinoprotein dehydrogenases (45),

$$AH_2 + DPN^+ \overset{\text{dehydrogenase}}{\rightleftharpoons} A + DPNH + H^+ \qquad (5)$$

where AH_2 and A are the reduced and oxidized forms, respectively, of the substrate. Further development of this technique (see, for example, the review by Ochoa (46)), included its extension to the assay of other enzymic reactions which may be coupled to the pyridinoprotein dehydrogenases,

$$\text{D-Alanine} + O_2 \xrightarrow{\text{D-amino acid oxidase}} \text{pyruvate} + NH_3 + H_2O \qquad (6)$$

$$\text{pyruvate} + DPNH + H^+ \xrightarrow{\text{lactic dehydrogenase}} \text{lactate} + DPN^+ \qquad (7)$$

Other typical examples, selected from a variety of enzymic reactions which are amenable to the spectrophotometric approach, include:

$$\text{DPNH} + 2\ (\text{cytochrome } c)_{ox} \xrightarrow{\substack{\text{cytochrome} \\ c\ \text{reductase}}} \underset{(550\ \text{m}\mu)}{\text{DPN} + \text{H}^+ + 2\ (\text{cytochrome } c)_{red}} \quad (8)$$

$$\text{Malate} \underset{}{\overset{\text{fumarase}}{\rightleftharpoons}} \underset{(300\ \text{m}\mu)}{\text{fumarate}} \quad (9)$$

$$\text{Acetate} + \text{ATP} + \text{CoA} \overset{\substack{\text{acetate-} \\ \text{activating} \\ \text{enzyme}}}{\rightleftharpoons} \underset{(236\ \text{m}\mu)}{\text{acetyl} + \text{CoA} + \text{AMP} + \text{PP}} \quad (10)$$

$$\text{Xanthine} + \text{O}_2 \xrightarrow{\substack{\text{xanthine} \\ \text{oxidase}}} \underset{(290\ \text{m}\mu)}{\text{uric acid} + \text{H}_2\text{O}_2} \quad (11)$$

$$\underset{(450\ \text{m}\mu)}{\text{Alanine} + \text{FAD}} \xrightarrow{\substack{\text{L-amino acid} \\ \text{oxidase}}} \text{pyruvate} + \text{NH}_3 + \text{FADH}_2 \quad (12)$$

The wavelength of maximum absorption (~pH 7) of the component customarily measured is given in parentheses.

If the molal extinction coefficient at a particular wavelength of one component of the reaction (or for the *difference* in coefficient between reactant and product) is sufficiently high ($>10^6$ cm.^{2} mole^{-1}) the reaction can be followed spectrophotometrically. Since proteins and nucleic acids have their maximum absorption in the region of 260 to 280 mμ, enzyme reactions are ordinarily not followed in this region unless a highly purified protein is being used.

The theory and instrumentation of absorption spectrophotometry, with special reference to the ultraviolet and visible regions, is presented in several excellent reviews (47–50). A number of sensitive, compact, and adaptable instruments (for example, the Beckman Spectrophotometer, Model DU) for measuring absorption spectra are commercially available. Kinetic studies, such as those illustrated by Equations (8–12) are usually carried out by measuring the change in optical density at a single wavelength and for this purpose even simple colorimeters may be substituted for spectrophotometers. Temperature control compartments have been built to keep the reaction mixtures in the cuvettes at a constant temperature (51–53) while micro- or macrocuvettes can be purchased to suit the peculiar requirements of the problem. Cuvettes which may be evacuated and stirred under vacuum have been applied to the study of anaerobic

reactions (54,55). Use of a spring-driven plunger device (56) enables a reactant or enzyme to be added to a cuvette and mixed with the other components in a very short time interval (<1 sec.) without removing the cuvette from the instrument. Recording spectrophotometers are especially suited for kinetic studies. The Cary instrument, for example, uses a motor-driven prism to scan the spectrum at a predetermined rate, while the signal corresponding to light absorption is transmitted continuously to the recorder (47). For kinetic studies, the instrument is set at one wavelength whereupon the recorder pen traces the continuous decline or build-up of a particular component.

The utility of recording spectrographic equipment with a rapid time response for the study of the hemoglobin–oxygen interaction was recognized in 1923 by Hartridge and Roughton (57). Later, Millikan (58) and Chance (59–64) refined their procedures and applied them with conspicuous success to the study of enzyme kinetics, especially the heme-containing enzymes (65,66). For the measurement of rapid reactions (67) the "stopped flow" or "continuous flow" methods are employed. In the former method, the reactants are mixed during a very brief time interval and the subsequent change in concentration of one reactant is recorded with a rapidly responding spectrophotometer. For "continuous flow" studies, the reactants are mixed and injected through a tube at a constant velocity. The concentration of one reactant at a particular point along the tube is measured by an ordinary spectrophotometer and by varying the flow rate, other concentrations can be achieved at the point of analysis. One particular instrument, designed by Chance (61), records small concentration changes at time intervals as low as 1 millisec. and uses only 0.1 ml. of solution. Further information on these techniques may be found in Part 2 of this chapter.

Prior to the advent of spectrophotometry, Thunberg tubes were used for studying certain oxido-reduction reactions in the absence of oxygen. For a substance whose enzymic oxidation can be coupled to the reduction of a chromophoric, artificial electron acceptor (e.g., methylene blue):

$$\underset{}{AH_2} + \underset{\text{(colored)}}{\text{dye}} \rightarrow A + \underset{\text{(colorless)}}{\text{reduced dye}} \qquad (13)$$

the reaction may be followed visually by observing the bleaching of the dye. Since many dyes in their reduced form are sensitive to reoxidation by oxygen, the Thunberg tube (see Fig. IX,1.9, Ref. 13) is designed to permit the tube contents to be evacuated before the dye is mixed with the other components. Usually, the time for complete decolorization of the dye is determined visually and since the rate of decolorization is usually linear until nearly all of the dye is reduced, a semiquantitative comparison

can be made between the reciprocals of bleaching time of separate experiments.

B. MANOMETRY (68–70)

Since a number of enzymic reactions involve the uptake or evolution of a gas (e.g., O_2, CO_2, H_2, N_2), manometric instruments have been devised for measuring the rate of gas exchange between the atmosphere and the solution.

Unfortunately, the enzymic oxidation of most substrates proceeds via a number of electron carriers and coenzymes (the "electron transport sequence") before oxygen, as the terminal electron acceptor, is reduced to water. Thus, the oxidation of a substrate is not a simple bimolecular reaction:

$$AH_2 + {}^1/_2O_2 \rightarrow A + H_2O \qquad (14)$$

and the interpretation of the kinetics of oxygen uptake becomes complex owing to the multiple steps involved (71,72). The problem is further complicated by the fact that the enzymic apparatus for these oxidations is housed in a particulate unit derived from the mitochondrial fraction of the cell, and considerable information remains to be collected concerning the amount, molecular weight, turnover number, and other kinetic characteristics for most of the enzymes and carriers participating in the electron transfer sequence (see Green (72a) for a review of this field).

A few soluble, highly purified enzymes have been studied in which oxygen is reduced to hydrogen peroxide or water with only a single enzyme-bound coenzyme (shown in parenthesis in the equation below) intervening in the flow of electrons from substrate to oxygen, e.g.,

$$\text{Ascorbic acid} + {}^1/_2O_2 \xrightarrow[(Cu^{2+})]{\text{ascorbic acid oxidase}} \text{dehydroascorbic acid} + H_2O \qquad (15)$$

$$\text{D-Alanine} + O_2 \xrightarrow[(FAD)]{\text{D-amino acid oxidase}} \text{pyruvate} + NH_3 + H_2O_2 \qquad (16)$$

Diaphorase-like enzymes, which link reduced pyridine nucleotides to oxygen, as shown in the equation below (the arrows indicate the transfer of electrons),

$$AH_2 \xrightarrow{\text{dehydrogenase}} DPN \xrightarrow{\text{diaphorase}} FAD \xrightarrow{\text{diaphorase}} \text{dye} \xrightarrow{\text{chemical}} O_2 \qquad (17)$$

can be used in conjunction with the pyridinoprotein dehydrogenases to permit the latter enzymes to be assayed manometrically; this may be necessary if the dehydrogenase is present in a turbid preparation which is unsuitable for spectrophotometric measurement.

Manometry can be applied, as well, to reactions involving gases other than oxygen. The fixation of H_2 or N_2 by microorganisms has been extensively studied by this technique (68). In carboxylation or decarboxylation reactions, e.g.,

$$CO_2 + \text{pyruvate} \xrightarrow[\text{decarboxylase}]{\text{oxalacetic}} \text{oxalacetate} \tag{18}$$

$$\text{Histidine} \xrightarrow[\text{decarboxylase}]{\text{histidine}} \text{histamine} + CO_2 \tag{19}$$

the uptake or evolution of CO_2 from solutions containing bicarbonate is readily measured. CO_2 production from HCO_3^- buffers can also be used to measure reactions where there is net acid production e.g.,

$$\text{Methylglyoxal} \xrightarrow{\text{glyoxalase}} \text{lactic acid} \tag{20}$$

$$\text{Sarcosine} + 2Fe(CN)_6^{3-} \xrightarrow[\text{dehydrogenase}]{\text{sarcosine}} HCHO + \text{glycine} + 2Fe(CN)_6^{4-} + 2H^+ \tag{21}$$

The most universally used of the manometric instruments is the constant volume respirometer (see Fig. IX.1.1, Ref. 13) which was adapted by Warburg (73) from a similar instrument, the "blood-gas manometer" of Barcroft and Haldane (74). The theory and operation of many different types of manometers have been described in detail elsewhere (68–70). Micromanometric techniques have been used to measure accurately the respiration of single cells (75–78).

Polarographic methods are ideally suited in principle for continuously measuring concentration changes in oxidizable or reducible substances. The dropping mercury electrode (reviewed by Muller (79) and by Kolthoff and Lingane (80)) has been used in biological systems (81) to measure oxygen uptake during the photosynthesis and respiration. An improvement in this technique involves the use of the stationary platinum electrode for measuring changes in oxygen tension in solution. With open vessels, the method is unsuited for reactions where the rate of oxygen uptake is low since oxygen from the air slowly re-equilibrates with the solution. Despite this limitation, instruments of this latter type (64,82–84) are becoming increasingly more popular and may partially replace manometers for oxygen uptake measurements.

C. ELECTRODE METHODS

Glass electrodes (reviewed by Michaelis (85)) can be used to follow reactions involving changes in pH, i.e., reactions where acid is liberated or consumed. It is not desirable, however, in enzymic reactions to allow the pH to change continuously in an unbuffered medium since this may result in a

decreased activity of the enzyme as the pH moves away from its optimum (see Section III.5). The enzyme may even be denatured if the pH is allowed to drift several units away from neutrality. An automatic titrator (86), which continuously adds base or acid and keeps the pH at a constant value as the reaction proceeds, overcomes the above difficulties. Instruments of this type have been used principally for following the course of reactions catalyzed by proteolytic enzymes or esterases, e.g.,

$$\mathrm{RC(=O)OR' + H_2O \xrightarrow{esterase} RCOO^- + H^+ + R'OH} \qquad (22)$$

D. OTHER METHODS

At the present time enzymologists are beginning to utilize more advanced techniques in an effort to gain further insight into the mechanism of enzymic reactions. The fact that many biological compounds exhibit optical rotation due to asymmetric centers provides a means, in principle, for measuring the rates of many enzymic reactions in a thermostatted polarimeter (87). Magnetometric methods have already been applied to the study of peroxidase (88), and the ability of the electron spin resonance technique to detect valence changes has been applied to otherwise unexplorable facets of photosynthesis (89); these methods will undoubtedly receive more widespread attention in the future.

III. ENZYME KINETICS

1. General Considerations

The basic premise underlying the kinetic theory of enzymic reactions is that the following minimal sequence of events occurs: (*1*) reversible combination of enzyme (E) and substrate (S) into an enzyme–substrate (ES) complex; (*2*) transformation of the substrate into product (P); and (*3*) expulsion of the product from the enzyme. This sequence may be formulated in one of two ways depending upon whether or not an enzyme–product (EP) complex is considered to exist.

$$\mathrm{E + S \rightleftharpoons ES \rightarrow E + P} \qquad (23)$$

$$\mathrm{E + S \rightleftharpoons ES \rightarrow EP \rightarrow E + P} \qquad (24)$$

In most instances, the ES complex is probably composed of one molecule of substrate bound at the active site of one molecule of enzyme: however, examples of multivalency (i.e., two or more molecules of substrate bound

independently to a single molecule of enzyme) have also been described (90–92). Measurements of "steady state" kinetics (see below) rarely yield any decisive information concerning the composition of the ES complex. Similarly, very little is known about the mode of binding between the substrate and enzyme in the ES complex except that it is probably due to a combination of ionic and van der Waals' forces in most systems (see Lumry (93) and Linderstrøm-Lang and Schellman (94) for comprehensive discussions of the forces involved in E–S interaction). However, in certain reactions, e.g., the chymotrypsin-catalyzed hydrolysis of *p*-nitrophenyl acetate (95–99), a relatively stable, covalent bond between the enzyme and one of the products is formed during the overall reaction.

According to the principle of microscopic reversibility (100), the enzyme *must* catalyze a reaction in both the forward and reverse direction (101) provided that the reaction is thermodynamically reversible. In some instances, e.g., the hexokinase reaction:

$$\text{Glucose} + \text{ATP} \xrightarrow{\text{hexokinase}} \text{glucose-6-phosphate} + \text{ADP} \qquad (25)$$

the equilibrium lies so far to the right that sensitive tracer techniques are required to demonstrate the reversibility (102).

It should be noted that only the most elementary type of enzymic reaction is depicted above in Equations (23) and (24), namely a uni-directional reaction involving only a single substrate. This prototype is illustrated by the hydrolysis of a model peptide by a proteolytic enzyme:

$$\mathrm{RC(=O)\text{-}NHR' + H_2O \rightarrow RC(=O)OH + R'NH_2} \qquad (26)$$

where the dashed line indicates the site of bond cleavage. A second substrate, water, also participates in the reaction as shown in the equation, but since it is present in great excess and at virtually a constant concentration the reaction may be considered kinetically to be pseudo-monomolecular with respect to substrate.

Among the few apparent exceptions to the general rule (34), that enzymic reactions involve *two* substrates, are the following isomerization reactions:

$$\text{Uridine diphosphoglucose} \overset{\text{epimerase}}{\rightleftharpoons} \text{uridine diphosphogalactose} \qquad (27)$$

$$\text{L-Alanine} \overset{\text{alanine racemase}}{\rightleftharpoons} \text{D-alanine} \qquad (28)$$

$$\text{Methylglyoxal} \xrightarrow{\text{glyoxalase}} \text{lactate} \qquad (29)$$

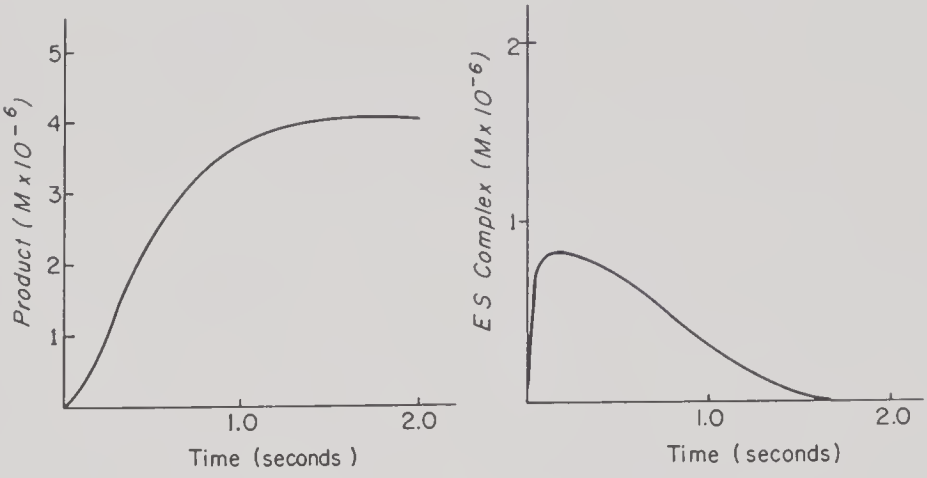

Fig. 1.4. Concentrations of P and ES during an enzymic reaction (104).

In each instance, however, the reaction is probably more complex than indicated, owing to the involvement of coenzymes.

The participation of water has been studied with the hydrolytic enzyme fructo-furanosidase (103) where it was found that the presence of excess sucrose or alcohol inhibited the enzyme, presumably due to a decrease in the effective concentration of water.

Although the elementary formulation in Equations (23) and (24) is applicable only to the hydrolytic enzymes, it provides a simple and useful model for illustrating many of the features of enzyme kinetics (Sections III.3.A–D). More complex enzymic reactions, which involve two substrates, and which may be either reversible or irreversible, are treated in subsequent sections (III.3.E and F).

The mechanism in Equation (23) may be examined further with regard to the time sequence of events. When the enzyme and substrate are mixed, combination occurs rapidly and the concentration of free enzyme decreases as the concentration of ES increases. This is followed by the conversion of ES to EP (or to E + P) or the dissociation of ES into E + S. A steady state level of ES is then reached where the rate of formation of ES is just balanced by its rate of disappearance (i.e., $d(\mathrm{ES})/dt = 0$). At the steady state, the overall conversion of S to P proceeds at a uniform rate until the concentration of substrate has become too low to saturate the enzyme, whereupon the concentration of ES will decrease and approach zero. The changes in P and ES, during the course of a typical enzymic reaction, are depicted in Figure 1.4, taken from the data of Chance (104).

"Transient state kinetics" pertains to the events which occur while the concentration of ES is approaching toward, or receding from, its maximal value. Since the time interval is usually very short, i.e., less than 1 sec., for the transient phases of an enzymic reaction, a special apparatus with a

fast time response is required for the continuous analysis of the reaction mixture. In Part 2 of this Chapter (see also Ref. 67), Chance describes such equipment and illustrates its use to obtain values for the individual rate constants involved in the formation and breakdown of the ES complex, and to obtain information about the number and composition of the ES complexes.

On the other hand, technical limitations prevent most investigators from studying enzyme kinetics in the more informative "transient state" range and require instead that measurements be carried out during the "steady state" phase. The great bulk of kinetic measurements have been carried out in this manner, and while the data are most useful for defining the optimal assay conditions for the enzyme, considerable insight into the mechanism of enzyme action has accumulated from the results of these investigations.

Part 1 of this Chapter deals primarily with the "steady state" kinetics of enzymic reactions. This approach examines the overall velocity of an enzymic reaction by measuring the rate of disappearance of substrate or the appearance of product. The experimentally controlled variables such as enzyme concentration, substrate concentration, inhibitor concentration, pH, ionic strength, temperature, and pressure are altered one at a time, and the effect of this alteration upon the velocity is measured. Various mechanisms, which lead to a rate expression for velocity in terms of the variables, may then be tested for their conformity to the experimental results.

2. Effect of Enzyme Concentration

As described in Sections III.3.A and E, virtually all of the mechanisms for different types of enzymic reactions lead to a rate law where the velocity is proportional to the first power of enzyme concentration, i.e.,

$$v = k(\mathrm{E}) \tag{30}$$

In the ideal case, a straight line relationship is obtained when velocity is plotted against enzyme concentration (Fig. 1.5A). This situation is encountered in studies of most purified enzymes and even with a number of crude systems. It forms the basis for the assumption, invoked during enzyme purification, that the number of "units" of enzyme is directly proportional to the observed activity.

A number of deviations from the ideal case (summarized by Dixon and Webb (105)) have been reported. For example, the curve may be linear at low levels of enzyme concentration, but then level off at a finite value of E (Fig. 1.5B). This effect is usually due to some parameter other than en-

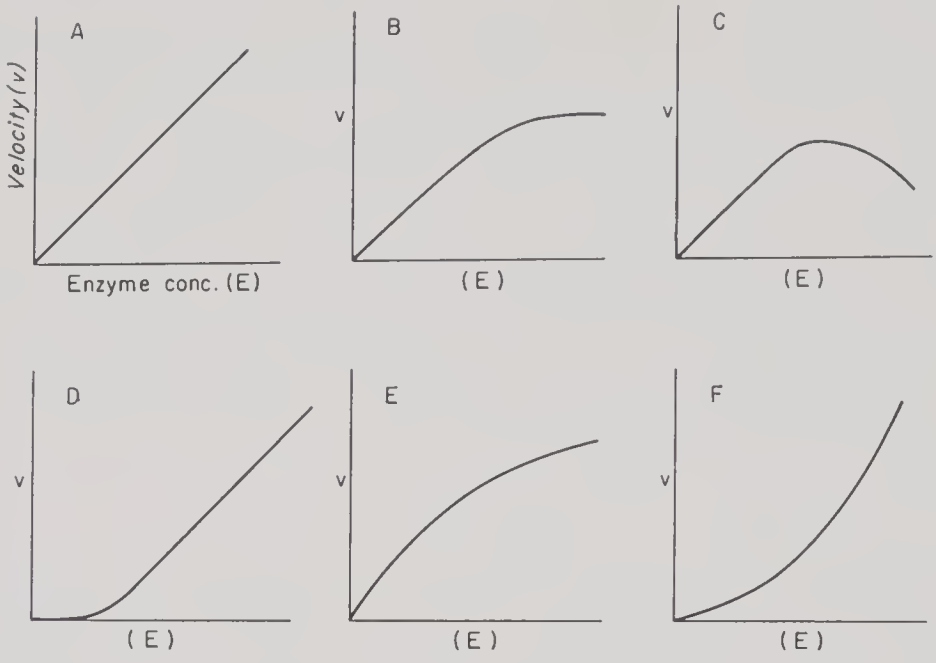

Fig. 1.5. Velocity as a function of enzyme concentration (105).

zyme concentration (e.g., solubility of the gas during a manometric experiment, limiting amount of a second enzyme used in the assay, or exhaustion of the substrate) becoming the rate-limiting factor. An even more exaggerated example of this phenomenon is shown in Figure 1.5C, where the plateau is followed by an inhibition at higher concentrations of the enzyme. This point is illustrated by an assay (106) for lactic dehydrogenase (Equation 31), where the primary reaction was coupled with diaphorase (Equations 32 and 33).

$$\text{Lactate} + \text{DPN}^+ \rightleftharpoons \text{pyruvate} + \text{DPNH} + \text{H}^+ \qquad (31)$$

$$\text{DPNH} + \text{H}^+ + \text{dye} \rightarrow \text{DPN}^+ + \text{reduced dye} \qquad (32)$$

$$\text{Reduced dye} + \text{O}_2 \rightarrow \text{dye} + \text{H}_2\text{O}_2 \qquad (33)$$

The affinity of the dehydrogenase for DPNH is so high than an excess of the enzyme effectively prevents the DPNH from reacting with diaphorase. High concentrations of enzyme are known to shift the equilibrium of a reaction owing to selective binding of a reactant or a product. This phenomenon has been demonstrated with alcohol dehydrogenase (107), creatine kinase (108), and the sulfate-activating enzyme (109).

In a third type of deviation, shown in curve D, the expected straight line relationship is preceded by a "lag phase" in terms of enzyme added. A reasonable explanation for this effect is that some inhibitory substance (e.g., a metal ion) has been introduced inadvertently with one of the reagents into the reaction mixture where it inactivates an increment of enzyme.

Finally, the remaining two cases, curves E and F, may be considered together. The former situation is encountered when an inhibitor is introduced simultaneously with the enzyme, so that at higher concentrations of enzyme, more of the enzyme will be in the inactive form (Equation 34). This effect, which causes the curve to be concave downward, has been observed with trypsin containing trypsin inhibitor (110). Conversely, in curve F, the enzyme contains a dissociable activator, so that the concentration of *active* enzyme increases non-linearly as the amount of enzyme preparation is increased. Data giving this type of v versus E curve have been reported for arylsulfatase (111) and for the proteolytic enzymes, ficin and papain (112).

$$E + I \rightleftharpoons EI \tag{34}$$

Downward curvature of v versus E plots has also been reported (113) for the action of several proteolytic enzymes acting upon protein substrates. These curves may be fitted by a function (114,115) involving a fractional power of E, e.g.,

$$v = f(E)^{1/2} \text{ or } v = f(E)^{2/3} \tag{35}$$

Since proteolytic enzymes give satisfactory straight line plots of v versus E when acting upon low molecular weight model peptides, it has been suggested that the above deviations are caused by the multiplicity of susceptible bonds in the protein substrates and by the inaccessibility of these bonds to the enzyme (116).

3. Effect of Substrate Concentration

A. THE MICHAELIS-MENTEN EQUATION

Early observations on the rates of enzyme-catalyzed reactions disclosed two fundamental features: (*1*) at a constant initial substrate concentration the rate is proportional to the enzyme concentration over a wide range; and (*2*) at a constant enzyme concentration the rate increases with the concentration of the substrate (following a curve which is the section of a rectangular hyperbola) and eventually levels off asymptotically. Michaelis and Menten (117) extended the earlier work of Henri (118) and Brown (119) and suggested a mathematical formulation of the above observations. The resulting equation, now a cornerstone of enzyme chemistry, rightly bears their names.

The Michaelis-Menten derivation assumes that the enzyme and substrate combine to form a transient intermediate, the enzyme–substrate complex, which then breaks down to the products of the reaction. Let E, S, ES,

and P represent the enzyme, substrate, enzyme–substrate complex, and reaction products, respectively. Furthermore, let:

(e) = total concentration of enzyme
(p) = concentration of the enzyme–substrate complex
$(e - p)$ = concentration of the free enzyme
(x) = concentration of the free substrate (equal to the total concentration of substrate if the amount of enzyme is small)
k_1, k_2, k_3 = rate constants for the corresponding steps shown below.

Then, the sequence may be written as follows:

$$\underset{(e-p)}{\mathrm{E}} + \underset{(x)}{\mathrm{S}} \underset{k_2}{\overset{k_1}{\rightleftharpoons}} \underset{(p)}{\mathrm{ES}} \xrightarrow{k_3} \mathrm{E} + \mathrm{P} \tag{36}$$

The same mechanism is also applicable when ES reacts with an excess of a second substrate (S′) in order to break down into E + P (see Section III.3.E).

The relationship between E, S, and ES may be related by a dissociation constant, K_s, if it is assumed that breakdown of ES into E + P does not affect the equilibrium. In terms of the rate constants, this assumption implies that $k_2 \gg k_3$. Then,

$$K_s = (e - p)(x)/(p) \tag{37}$$

Rearranging,

$$(p) = (e)(x)/[K_s + (x)] \tag{38}$$

The rate of the overall reaction, v, will be determined by the rate of the slow step, namely the breakdown of ES:

$$v = k_3(p) \tag{39}$$

Substituting the value for (p) from Equation (38) in Equation (39)

$$v = k_3(e)(x)/[K_s + (x)] \tag{40}$$

When (x) is very large compared to K_s, v becomes $V_{\max.}$ and Equation (40) reduces to:

$$v = V_{\max.} = k_3(e) \tag{41}$$

Rewriting Equation (40) to include $V_{\max.}$:

$$v = V_{\max.}\,(x)/[K_s + (x)] \tag{42}$$

Equation (42) is the customary form of the Michaelis-Menten rate equation.

Dixon and Webb (120) have recast Equation (42) into the descriptive form:

$$\phi = \sigma/(1 + \sigma) \tag{42a}$$

where σ = relative substrate concentration = x/K_m, and ϕ = relative velocity = $v/V_{max.}$. It should be noted that the ratio $v/V_{max.}$ can also be expressed in terms of the amount of enzyme existing in the ES complex, i.e., $v/V_{max.} = (p)/(e)$ (combining Equations (39) and (41)).

More generalized forms of the original Michaelis-Menten derivation were subsequently proposed by Van Slyke and Cullen (121), Briggs and Haldane (122), and Chance (104). Briggs and Haldane pointed out that the rate-determining step for the overall reaction would not be the rate of breakdown of ES unless the substrate concentration is high or the enzyme–substrate affinity is high. Furthermore, they presented the following generalized derivation, based upon the "steady state" concentration of ES:

Using the symbols and mechanism of Equation (36), the rate of formation of the intermediate complex is:

$$dp/dt = k_1(e - p)(x) - (k_2 + k_3)(p) \tag{43}$$

and the rate of disappearance of the substrate is:

$$-dx/dt = k_1(x)(e - p) - k_2(p) \tag{44}$$

Combining Equations (43) and (44) yields the interesting relationship:

$$-d(p + x)/dt = k_3(p) \tag{45}$$

In other words, the over-all velocity, v (equal to $k_3(p)$ by Equation (39)), will equal the sum of the rates of disappearance of substrate in the forms of x and p. Equations such as (43) and (44) have been solved explicitly with the aid of a differential analyzer (123). Plots from Chance's paper (123) showing solutions for these equations are discussed by Alberty (124).

The Briggs-Haldane derivation simplifies the above problem, however, by the assumption of steady state conditions where the concentration of the enzyme–substrate complex is constant, i.e., $dp/dt = 0$. Chance (104,123) has shown that this assumption is valid both for the initial part of the reaction and for any subsequent portions provided that the velocity is a linear function of time.

From Equation (43), setting $dp/dt = 0$,

$$(p) = \frac{(e)(x)}{[(k_2 + k_3)/k_1] + (x)} \tag{46}$$

The term in the denominator containing the rate constants is replaced by a single constant, K_m, usually referred to as the "Michaelis constant" and defined as:

$$K_m = (k_2 + k_3)/k_1 \tag{47}$$

Equation (46) is rewritten to include K_m:

$$(p) = (e)(x)/[K_m + (x)] \tag{48}$$

The remainder of the derivation follows Equations (39) to (41), and leads to Equation (49), which is identical to Equation (42) except for the difference between K_m and K_s.

$$v = V_{\max.}(x)/[K_m + (x)] \tag{49}$$

Hereafter in this article, Equation (49) will be considered as the Michaelis-Menten equation and K_m, the Michaelis constant, will be assumed to consist of the three rate constants (as defined in Equation 47), unless otherwise indicated.

The same rate equations (Equations 42 or 49) can be derived by mechanisms other than the Michaelis-Menten formulation (Equation 36). For example, King (125) and Medwedew (126) have suggested the following mechanism, not involving an ES complex,

$$\mathrm{E'} + \mathrm{S} \xrightarrow{k_1} \mathrm{E} + \mathrm{P} \tag{50a}$$

$$\mathrm{E'} \underset{k_3}{\overset{k_2}{\rightleftharpoons}} \mathrm{E} \tag{50b}$$

where E′ is a catalytically inactive form of the enzyme. The same result is also achieved by a mechanism (120) where the ES complex does not yield product:

$$\mathrm{E} + \mathrm{S} \underset{k_2}{\overset{k_1}{\rightleftharpoons}} \mathrm{ES} \tag{51a}$$

$$\mathrm{E} + \mathrm{S} \xrightarrow{k_3} \mathrm{E} + \mathrm{P} \tag{51b}$$

Rate equations of the Michaelis-Menten form have also been obtained by mechanisms involving a chain reaction (116) or action at a distance (127).

B. DETERMINATION OF K_m AND $V_{\max.}$

The kinetic data relating velocity as a function of substrate concentration may be plotted in several different ways in order to determine the values of K_m and $V_{\max.}$, the two constants in Equation (49). It should be noted

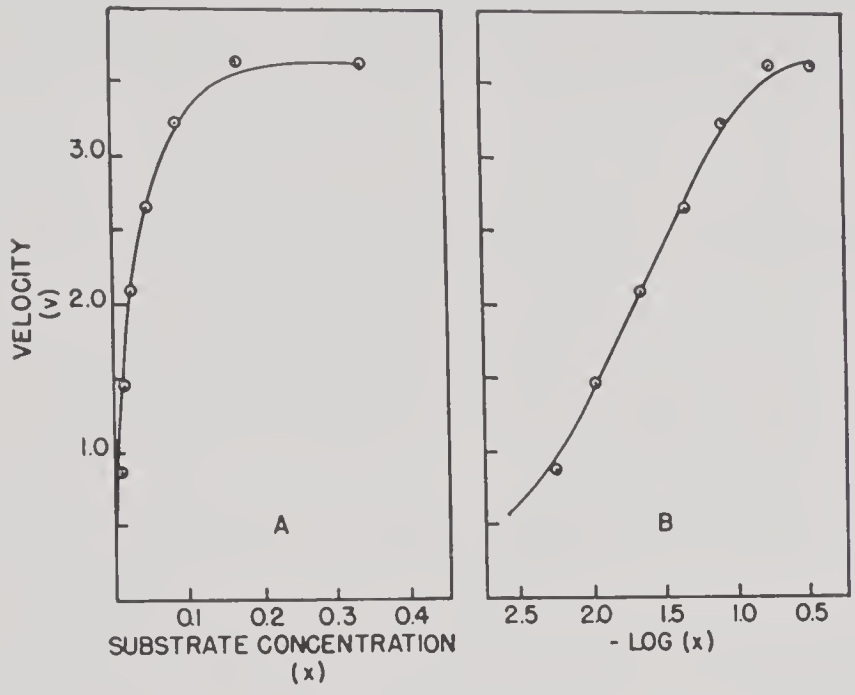

Fig. 1.6. Velocity as a function of substrate concentration (curve A) and logarithm of substrate concentration (curve B) for the hydrolysis of sucrose by sucrase (117). Velocity is expressed in arbitrary units of change in optical rotation (degrees per minute).

that in all of these methods K_m is an *experimentally determined* value (in units of concentration), and, as such, provides no information about the composition of K_m in terms of the individual rate constants.

In the most simple treatment of Equation (49), the velocity, v, may be plotted directly against substrate concentration, x, to yield the expected hyperbolic curve. Figure 1.6A shows a v versus x plot from the original data of Michaelis and Menten (117) on the enzyme-catalyzed hydrolysis of sucrose. From an inspection of Equation (49), it is evident that when $v = V_{\text{max.}}/2$, K_m will be equal to (x). From the curve it is estimated that when $v = V_{\text{max.}}/2 = 1.85$, $(x) = K_m = 1.50 \times 10^{-2}M$. The uncertainty in determining the plateau of the curve makes uncertain the value of $V_{\text{max.}}$, and the steep slope of the ascending portion of the curve makes it difficult to obtain an accurate value for K_m. By the same token, plotting v against $\log x$ (Fig. 1.6B) will yield $\log K_m = \log x$ when $v = V_{\text{max.}}/2$, but the same uncertainties obtain.

The difficulty in fitting a hyperbolic curve to the experimental points is readily apparent; contrarily, if the theoretical curve were linear, the points could be fitted by the method of "least squares" (128). Lineweaver and Burk (129) pointed out that Equation (49) may be recast into the linear form:

$$1/v = (K_m/V_{\text{max.}})[1/(x)] + 1/V_{\text{max.}} \tag{52}$$

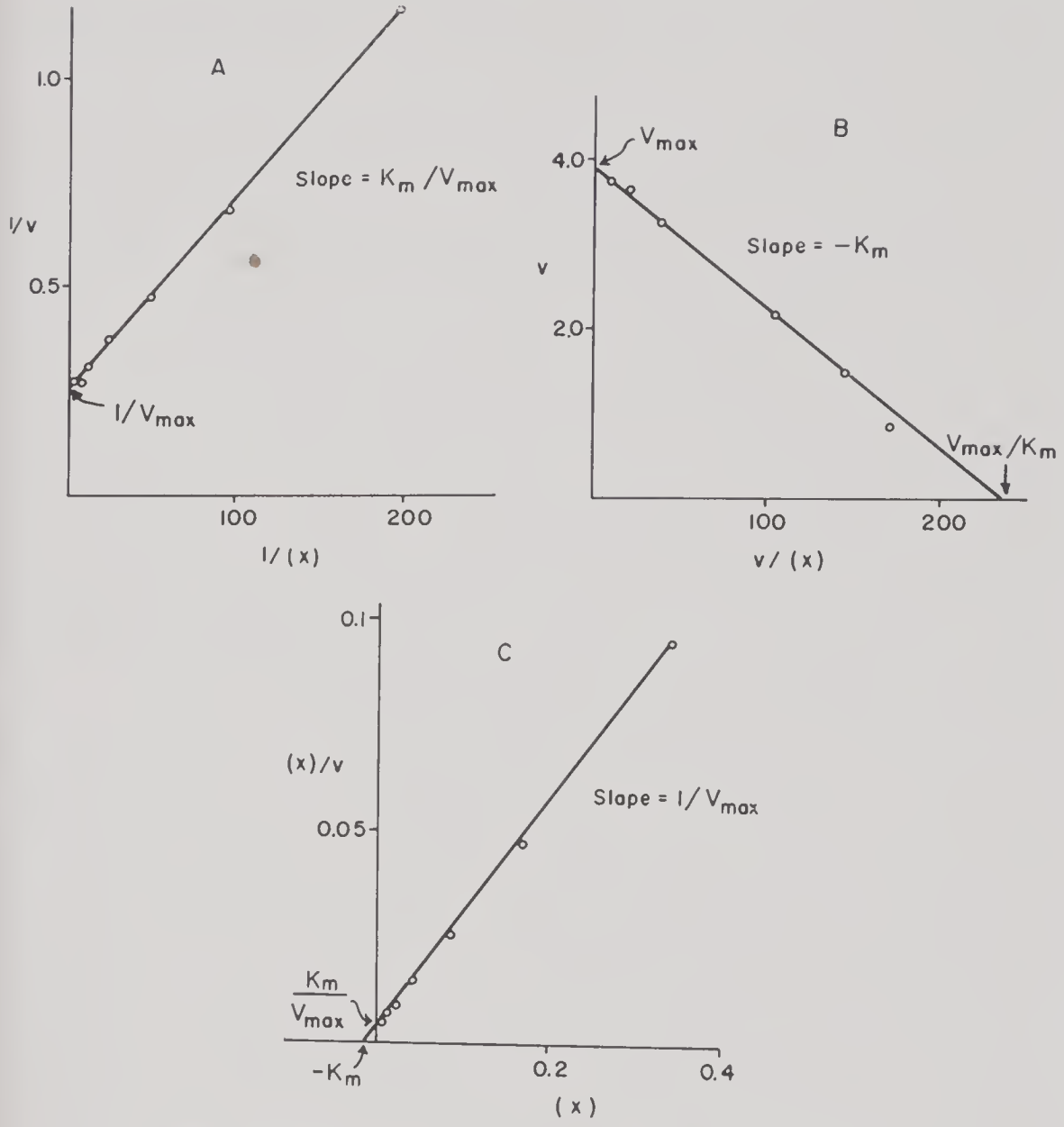

Fig. 1.7. Linear plots of velocity–substrate concentration relationships. Curve A, $1/v$ versus $1/x$ (Lineweaver-Burk (129)). Curve B, v versus v/x (131); Curve C, x/v versus x (132).

By plotting $1/v$ against $1/(x)$, a straight line is obtained with the slope $K_m/V_{max.}$ and the intercept $1/V_{max.}$. The data of Figure 1.6 have been replotted in Figure 1.7A according to the Lineweaver-Burk equation. $1/V_{max.}$ is the intercept on the $1/v$ axis and is equal to 2.55×10^{-1}. The slope of the curve is 4.23×10^{-3} and, since the slope $= K_m/V_{max.}$, K_m is calculated to be $1.66 \times 10^{-2} M$. As pointed out by Dixon (130), the curve can also be extended to intercept the x axis at a point equal to $-1/K_m$. It will be noted that this type of reciprocal plot emphasizes points where the substrate concentration is small, i.e., $1/(x)$ large. This is advantageous

if the enzyme is inactivated at high substrate concentrations, but suffers in that some uncertainty may attend measurements made at low concentrations of substrate.

Two other methods have also been proposed for expressing in a linear form the velocity data for an enzymic reaction: (*1*) plotting v versus v/x, where the slope is $-K_m$ and the intercepts are $V_{max.}$ and $V_{max.}/K_m$, respectively (131); and (*2*) plotting x/v versus x where the slope is $1/V_{max.}$ and the intercepts are $K_m/V_{max.}$ and $-K_m$, respectively (132). These plots are illustrated in Figures 1.7B and C.

All of these methods for the determination of K_m values have found wide application in contemporary enzymology, and the evaluation of K_m for the substrate (or for the coenzyme) has become virtually obligatory in the description of a new enzyme. In the limiting case where $K_m = k_2/k_1$ and K_m is a measure of the enzyme–substrate affinity, it is not surprising to find similar K_m values for a series of homologous substrates with a given enzyme or for the substrates of a particular class of enzymes. Similarity in K_m values under these circumstances is probably a reflection of the fact that only a limited number of different reactive groups on the enzyme surface are available for interaction with the substrate.

In general, the *ratio* of the Michaelis constants of an enzyme with two substrates may be readily computed from the directly measured K_m values for each substrate. In certain instances when a manometric method may be required for the assay, it may be unsuited for measuring velocities at low initial substrate concentrations since, owing to the finite equilibration period, the reaction may be nearly complete before any readings are taken. Some uncertainty, therefore, is possible in the experimental values of K_m. To meet this specific problem, Thorn (133) proposed a method for calculating the *ratio* of the K_m values for two substrates which utilizes data from a system where the enzyme is functioning at nearly maximal velocity.

The rate equation for a single substrate (Equation 49) can be expanded to include a second substrate as follows:

$$v = V_{max.}(x)/\{(x) + K_m[1 + (x')/K'_m]\} \tag{53}$$

where (x') and K'_m are the concentration and Michaelis constant, respectively, of the second substrate (Section III.3.E). A similar equation is obtained when (x') is a competitive inhibitor (Section III.4.A). Similarly, the velocity due to the second substrate is given by

$$v' = V'_{max.}(x')/\{(x') + K'_m[1 + (x)/K_m]\} \tag{54}$$

The total observed velocity V_t of the reaction is the sum of Equations (53) and (54):

$$V_t = V_{max.}(x)/\{(x) + K_m[1 + (x')/K'_m]\} + V'_{max.}(x')/\{(x') + K'_m[1 + (x)/K_m]\} \quad (55)$$

Foster and Niemann (134) have derived similar equations and demonstrated their applicability for the competitive hydrolysis of acetyl-L-tryptophanamide and acetyl-L-tyrosinamide by chymotrypsin. The values of K_m and k_3 (Sections III.3, B and D) were determined experimentally for two different ratios of the competing substrates and found to be in agreement with the corresponding values calculated from

$$(K_m)_t = x + x'/(x/K_m + x'/K'_m) \quad (56)$$

and

$$(k_3)_t = (k_3x/K_m + k'_3x'/K'_m)/(x/K_m + x'/K'_m) \quad (57)$$

The individual values K'_m, K_m, k'_3, and k_3 were determined independently with each substrate.

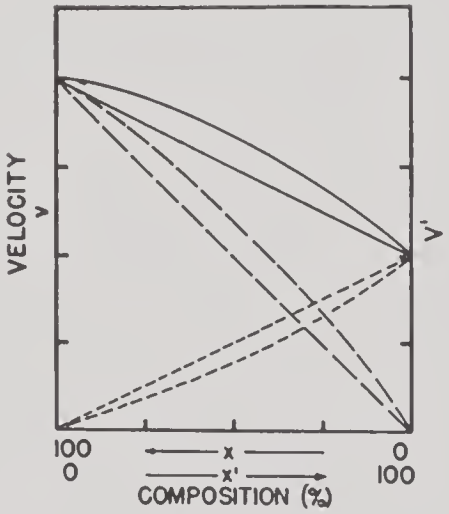

Fig. 1.8. Hypothetical plot of velocity as a function of relative amounts of two substrates (133). The curves are represented by the following symbols: v (— —); v' (- - -); v_t (——).

In the most general case (133) of Equation (55), where the substrate concentrations are not equal, the plot of the reaction velocities v, v', and v_t', against the composition of the mixture has the form shown in Figure 1.8. When it is assumed that $K_m < K'_m$ and $V_{max.} > V'_{max.}$, the curved lines in the plot are obtained. When $K_m = K'_m$ the straight lines are obtained, and Equation (55) reduces to:

$$v_t = [V_{max.}(x) + V'_{max.}(x')]/[K_m + (x_t)] \quad (58)$$

With mixtures of succinic acid (x) and tetradeuterosuccinic acid (x'), Thorn obtained a series of points when v_t was plotted against composition. The curved line which best fitted the data was obtained by using the value $K'_m/K_m = 1.45$ in Equation (55). Employing the less accurate, but conventional methods, K'_m and K_m were found to be $2.2 \times 10^{-3}M$ and $1.2 \times 10^{-3}M$, respectively, giving a ratio of 1.83.

Whittaker and Adams (135,136) have proposed a variation of the above method. If the concentrations of the two substrates are equal, $(x) = (x') = (s)$, Equation (55) reduces to:

$$v_t = [V_{\text{max.}}/K_m + V'_{\text{max.}}/K'_m]/[1/K_m + 1/K'_m + 1/(s)] \qquad (59)$$

The maximum velocity for the mixture $V_{(\text{max.})t}$ results when (s) is large:

$$V_{(\text{max.})t} = [V_{\text{max.}}/K_m + V'_{\text{max.}}/K'_m]/[1/K_m + 1/K'_m] \qquad (60)$$

which can be rearranged to:

$$K_m/K'_m = [V_{\text{max.}} - V_{(\text{max.})t}]/[V_{(\text{max.})t} - V'_{\text{max.}}] \qquad (61)$$

In practice, the maximum velocities, $V_{\text{max.}}$, $V'_{\text{max.}}$, and $V_{(\text{max.})t}$ are measured separately for (x), (x'), and $(x + x')$, where $(x) = (x')$, each under conditions of excess substrate and a constant amount of enzyme.

C. DETERMINATION OF RATE CONSTANTS

Although the composite constant (either K_m or K_s) in Equations (42) or (49) can be determined with facility by the methods just described, the individual rate constants in even the most simple enzyme mechanism (Equation 36) are more difficult to evaluate. It is evident that k_1 and k_2 will become more accessible if conditions can be arranged to prevent the further breakdown of the ES complex, thus isolating the equilibrium $K_s = k_2/k_1$. Then, if a sensitive technique is available, the equilibrium constant, K_s, can be measured by "titrating" the enzyme with substrate, and if either one of the rate constants can also be measured directly, the other constant is readily calculated.

For peroxidase (Equation 62), the enzyme–H_2O_2 complex has a different

$$AH_2 + H_2O_2 \xrightarrow{\text{peroxidase}} A + 2H_2O \qquad (62)$$

absorption spectrum than that of the free enzyme (104). In the absence of the cosubstrate (AH_2), only the first step of the mechanism is possible. (Actually, the complex designated here is only one of four possible complexes which may be formed between peroxidase and H_2O_2 (137,138); the multiplicity of ES complexes does not affect the present discussion.)

$$E + H_2O_2 \underset{k_2}{\overset{k_1}{\rightleftharpoons}} E\text{–}H_2O_2 \tag{63}$$

$$E\text{–}H_2O_2 + AH_2 \xrightarrow{k_3} E + A + 2H_2O \tag{64}$$

By spectrophotometric measurements Chance (104) obtained values of 2×10^{-8} mole liter^{-1} and 1.2×10^{7} liter mole^{-1} sec.$^{-1}$ for K_s and k_1, respectively; k_2 is, therefore, 0.2 sec.$^{-1}$.

In the presence of a cosubstrate (AH_2), such as the reduced form of the dye, malachite green, the over-all velocity o fthe reaction will be given by the equation:

$$v = k_3(E\text{–}H_2O_2)(AH_2) \tag{65}$$

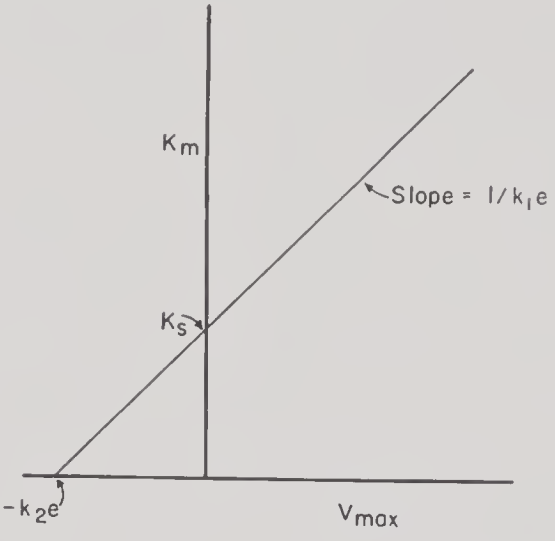

Fig. 1.9. Plot of K_m versus $V_{max.}$ for different concentrations of the second substrate (139).

and by measuring v and the concentration of ($E\text{–}H_2O_2$) under steady state conditions, rather than equilibrium conditions, a value of 1.8×10^5 moles^{-1} sec.$^{-1}$ was obtained for k_3. (For comparison with the other rate constants, k_3 should include the concentration of the second substrate, i.e., $k_3' = k_3(AH_2)$. In these terms, a typical value for k_3' is 4.5 sec.$^{-1}$.)

It is apparent that many other reactions, where the concentration of a second reactant (other than water) may be used to control breakdown of the ES complex, are also susceptible to analysis in terms of individual rate constants. Slater and Bonner (139) drew attention to the interesting relationship which may be derived from Equation (47), since $K_s = k_2/k_1$:

$$K_m = K_s + k_3/k_1 \tag{66}$$

or,

$$K_m = K_s + k_3e/k_1e \tag{67}$$

and, since $V_{max.} = k_3e$:

$$K_m = K_s + \frac{V_{max.}}{k_1 e} \tag{68}$$

When K_m is plotted versus $V_{max.}$ for different concentrations of the second substrate, a straight line is obtained (Fig. 1.9). When $V_{max.} = 0$, the y-intercept equals K_s, and when $K_m = 0$, the x-intercept is $-k_2e$. In order to obtain an absolute value of k_2 the enzyme concentration in molal units must also be known.

This treatment is not applicable to mechanisms more complex than those described by the simple Michaelis-Menten or Briggs-Haldane formulations. Thus, in the case of certain flavoprotein systems (139) where the plot passes through the origin, the apparent conclusion that $k_2 = 0$ is not valid (139,140), since it is quite possible that the actual mechanism is more complex and involves a dissociation of the product from the enzyme (E) prior to reoxidation of the enzyme-bound flavin, viz.

$$\begin{aligned} \text{E—F} + \text{AH}_2 &\rightleftharpoons \text{AH}_2\text{—E—F} \\ \text{AH}_2\text{—E—F} &\rightleftharpoons \text{A—E—FH}_2 \\ \text{A—E—FH}_2 &\rightleftharpoons \text{E—FH}_2 + \text{A} \\ \text{E—FH}_2 + \text{O}_2 &\rightarrow \text{E—F} + \text{H}_2\text{O}_2 \end{aligned} \tag{69}$$

(F, FH_2, A, and AH_2 are the oxidized and reduced forms, respectively, of the flavin and the substrate).

Roughton and Gutfreund (142,143) have devised another method for evaluating rate constants based upon the rate of appearance of product during the very early phase ("pre-steady state") of the reaction when the concentration of the ES complex is still increasing. In the mechanism shown in Equation (36), p and z may be used to designate the concentration of the ES complex and product, respectively. Then, from Equation (39):

$$v = dz/dt = k_3p \tag{70}$$

or taking the second derivative

$$d^2z/dt^2 = k_3\, dp/dt \tag{71}$$

and substituting the expression for dp/dt from Equation (43) in Equation (71)

$$d^2z/dt^2 + dz/dt[k_1(x) + k_2 + k_3] - k_1k_3(c)(x) = 0 \tag{72}$$

Equation (73) represents a solution to this equation, which is valid for the early portion of the reaction when x is not appreciably different from x_0.

$$z = z_0 + k_3(x_0)\,et/[(x_0) + (k_2 + k_3)/k_1] + k_1k_3(x_0)e/[k_1(x_0) + k_2 + k_3]^2\left\{\epsilon^{-[k_1(x_0) + k_2 + k_3]t} - 1\right\} \quad (73)$$

z_0 is the *initial* concentration of product and z_0 will usually not have a finite value at the beginning of the reaction unless it represents a reaction product like H^+. Gutfreund (144) measured the kinetics of the proteolytic enzymes trypsin, chymotrypsin, and ficin on synthetic substrates where H^+ production is a direct measure of product formation (86). By neglecting terms which are small at low values of t,

$$z - z_0 = k_1k_3e(x_0)t^2/2 \quad (74)$$

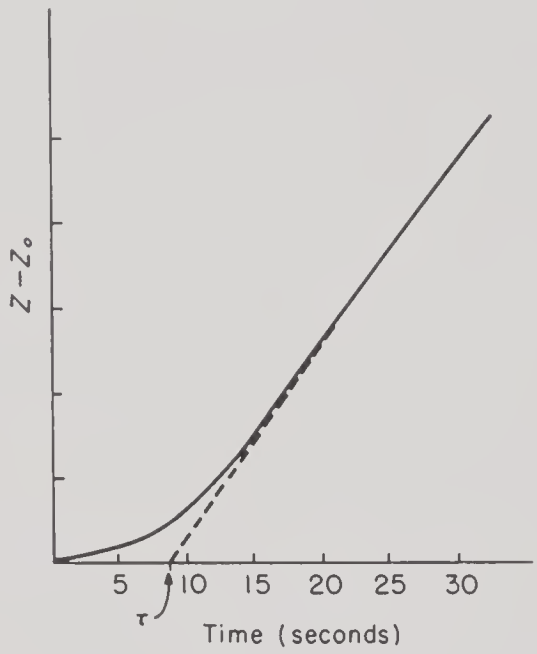

Fig. 1.10. Graphical determination of k_1 (144).

Thus, by measuring z as a function of time, it is possible to obtain a value for k_1k_3e. Since k_3 can be determined independently from Equation (41), k_1 is immediately evaluated. Knowing k_1 and k_3, k_2 is calculated from Equation (47) after K_m has been measured directly.

Gutfreund (144) later treated the complex Equation (73) in an alternate manner. If the experimental values of $(z - z_0)$, are plotted versus t, the curved line at low values of t merges into a straight line at higher values of t (see Fig. 1.10). Under the latter conditions (t large), the exponential term in Equation (73) vanishes and,

$$z - z_0 = k_3(x_0)et/[(x_0) + K_m] - k_3(x_0)e/k_1[(x_0) + K_m]^2 \quad (75)$$

If $(x_0) \gg K_m$, this equation reduces to:

$$z - z_0 = k_3et - k_3e/k_1(x_0) \quad (76)$$

When $z - z_0 = 0$, the intercept on the x-axis, τ, equals $1/k_1(x_0)$, and from a determination of τ, k_1 may be calculated.

It should be re-emphasized that conventional kinetic methods, even with enzymes obeying the most simple mechanism (Equation 36), yield only the values for K_m (or K_s) and $V_{max.}$ (Section III.3.B). From $V_{max.}$, the rate constant, k_3, can be calculated directly from Equation (41) provided that the enzyme concentration is known. In certain favorable cases where k_2 is known or assumed to be small relative to k_3, k_1 can also be determined from $K_m = k_3/k_1$. (If k_2 is negligible, any factor which changes $V_{max.}$ should also change K_m proportionately since each of these parameters is directly proportional to k_3 under these circumstances. Lumry *et al.* (145) have shown that changes in the structure of the substrate, pH, or D_2O concentration do produce identical changes in K_m and $V_{max.}$ for carboxypeptidase.) Otherwise, neither k_1 nor k_2 will be readily accessible unless measuring devices with a short time response can be applied to investigate the "pre-steady state" phase of the reaction. On the other hand, only one of these two constants needs to be measured directly since the other can be calculated from the expression for K_m or K_s.

Attempts have been made to approximate the values for the rate constants from steady state measurements coupled with assumptions about the relative magnitudes of k_2 and k_3. Thus, in earlier formulations (146) of the simple rate equation it was assumed that $k_2 \gg k_3$ whereupon $K_m = K_s = k_2/k_1$. From Gutfreund's (143,144) values of the rate constants, it can be seen that this limiting assumption is apparently valid for several of the proteolytic enzymes. In most systems, however, k_3 is of sufficient magnitude that the equilibrium is affected by the breakdown of the complex into the products. Pursuing this point further, k_3 may be much larger than k_2, whereupon $K_m = k_3/k_1$ as first considered by Van Slyke and Cullen (121).

At one time it was thought that the affinities of a *pair* of substrates for either of the proteolytic enzymes, chymotrypsin (147) and carboxypeptidase (148), could be expressed in terms of inequalities. Given that $(K_m)_1 > (K_m)_2$, two separate cases were considered (36): if $(k_3)_1 < (k_3)_2$, then $(k_2/k_1)_1 < (k_2/k_1)_2$; but if $(k_3)_1 > (k_3)_2$, the case is indeterminate. Later, a more detailed analysis (149) showed that both cases are actually indeterminate.

Extensive measurements in Niemann's laboratory of K_m and k_3 for the hydrolysis of various substrates by α-chymotrypsin has revealed that in almost all cases K_m is approximately equal to the dissociation constant (K_s) for the ES complex. Table I.1 shows the kinetic constants for a series of *N*-acetyl-L-tyrosine substrates. Although k_3 varies over a 50-fold range, the value for K_m remains approximately constant and is of the same order of magnitude as the inhibition constant (K_I) for the D-enantiomorphs. Thus, the ratio $K_m = (k_2 + k_3)/k_1$ is independent of k_3 and must be ap-

TABLE I.1
Hydrolysis of *N*-Acetyl Amino Acid Esters by α-Chymotrypsin (From Neurath and Hartley (150))

Acetyl tyrosine—*X* *X*	L-Substrate K_m, $M \times 10^3$	L-Substrate k_2, sec.$^{-1}$	D-Inhibitor, $M \times 10^3$	Reference
$-NHNH_2$	22	0.05	7.5	151,152
$-NH_2$	33	0.17	12.	153
$-NHCH_2CONH_2$	23	0.50	—	152
$-NHOH$	43	2.20	7.5	152,154

proximately equal to $k_2/k_1 = K_s$. A similar situation has been observed when the acyl group is varied in a series of *N*-acyl-L-tyrosinamides (153). Other proofs that K_m is approximately equal to K_s for the chymotrypsin system have been deduced from the effect of buffer (155), salts (156), sucrose (157), organic solvents (158), and pH (159,160) on the kinetic constants.

D. EVALUATION OF DATA FOR THE VELOCITY OF AN ENZYMIC REACTION

Kinetics of a Typical Proteolytic Enzyme: Carboxypeptidase. In order to illustrate the utility of the simple Michaelis-Menten equation, especially with regard to the manner of determining the velocity, and to contrast the treatment of enzyme-catalyzed reactions with ordinary chemical kinetics, the data from a typical problem (161) will be discussed in some detail. The proteolytic enzyme, carboxypeptidase, catalyzes the hydrolysis of a synthetic peptide substrate such as carbobenzoxyglycyl-DL-phenylalanine (DL-CGP) into its products, carbobenzoxyglycine and DL-phenylalanine: the dashed line shows the site of bond cleavage.

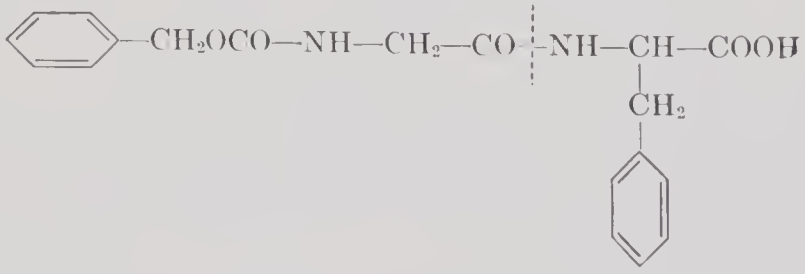

In order to follow the course of this proteolytic reaction, the substrate in a phosphate buffer at pH 7.5 is thermostatted at 25°C. and the reaction is started by adding a solution of enzyme. At various time intervals aliquots are withdrawn, the reaction is stopped, and the concentration of product is estimated as liberated α-amino groups by a colorimetric ninhydrin reaction (162). The results may be plotted as disappearance of

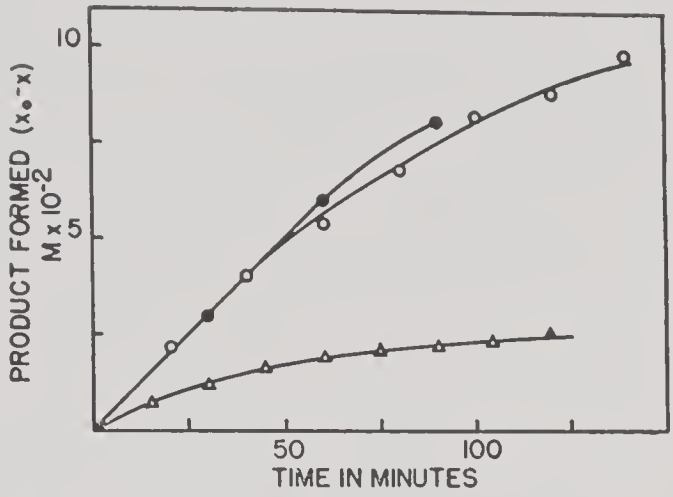

Fig. 1.11. Hydrolysis of carbobenzoxyglycyl-DL-phenylalanine (DL-CGP) by carboxypeptidase (161). The curves represent the following initial substrate concentrations (with respect to the L-isomer): black circles, 0.0753*M*; white circles, 0.0548*M*; triangles, 0.0128*M*.

substrate or, as in Figure 1.11, appearance of a product against time for several initial substrate concentrations.

In the original investigation (161) it was shown that the hydrolyses of DL-CGP and L-CGP follow the same initial rate curves, and, on the basis of this finding, DL-CGP was used routinely as the substrate. Recently, Niemann and his colleagues (134,163,164) have made a careful study of the chymotrypsin-catalyzed hydrolysis of acetyl-L-tryptophanamide, nicotinyl-L-tryptophanamide, and acetyl-L-tyrosinamide, and have shown that each of these reactions is inhibited by the D-antipode of the substrate and also by one of the products, the acylated α-amino acid. Thus, the use of DL-substrates, and the measurement of rates over a period of time when appreciable amounts of the products have accumulated, would appear to require justification for each of the proteolytic enzymes. For the example cited here, i.e., the splitting of DL-CGP by carboxypeptidase, the lack of inhibition by D-isomer was discussed above. With regard to inhibition by the reaction product, Neurath and DeMaria (165) have shown that L-phenylalanine produces only a small inhibition ($K'_m \approx 1.5 \times 10^{-2}$).

Order of Reaction. If a simple proteolytic reaction of this type conforms to first-order kinetics with respect to the substrate, the system should be described by the equation:

$$k = (1/t)\ 2.3\ \log\ (x_0/x) \tag{77}$$

where k is the first-order rate constant, and x_0 and x represent the initial concentration of substrate and the concentration at time t.

A plot of log (x_0/x) against t should give a straight line with slope equal to $k/2.3$ and k should be independent of initial substrate concentration.

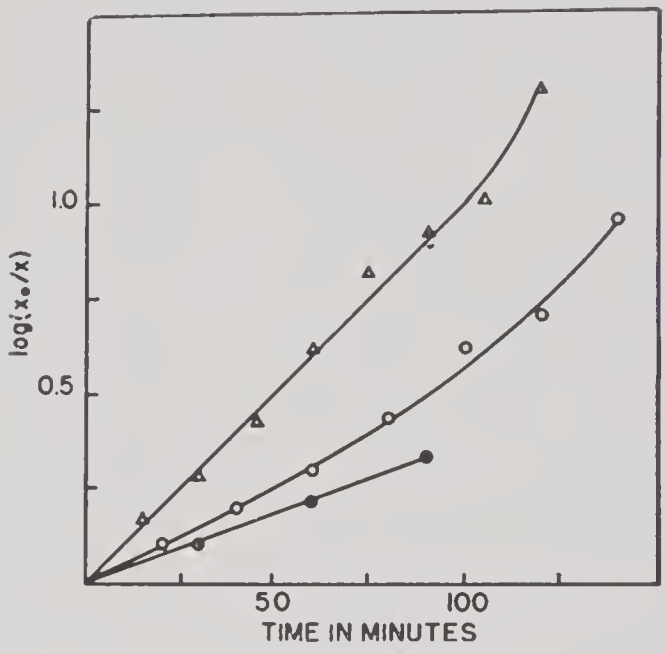

Fig. 1.12. First-order plot for hydrolysis of DL-CGP by carboxypeptidase; data and symbols as in Figure 1.11.

The data in Figure 1.11 are replotted in Figure 1.12 according to the conventional first-order equation (77). It is seen that, as the reaction nears completion, the curves deviate from linearity and that the first-order rate constant, determined from the linear portion of the curves, increases with decreasing substrate concentration. These anomalies are not unexpected in view of the fact that the Michaelis-Menten formulation contains three rate constants and it is undoubtedly an oversimplification to assume that the entire process can be described in terms of a single first-order constant.

If $K_m \ll x$ in Equation (49), the rate becomes independent of x, the substrate concentration, and first order with respect to the enzyme concentration (148,155). Conversely, when $K_m \gg x$, the equation is first order with respect to both enzyme and substrate concentration, or second order over-all. It has been shown in the case of the trypsin-catalyzed hydrolysis of α-benzoyl-L-arginamide hydrochloride (166) that the apparent first-order reaction constant decreases progressively if the enzyme is allowed to stand in solution for progressively longer periods of time before adding the substrate. Confirming the results of Kunitz and Northrop (167), this effect was attributed to the spontaneous autolysis of the enzyme which took the form of a second-order reaction between the enzyme (active trypsin) and a substrate (reversibly denatured trypsin). By testing the data of the *inactivation* process according to the equation:

$$k'' = 1/t(1/A - 1/A_0) \tag{78}$$

where A_0 is the initial activity of the enzyme and A the fraction of the

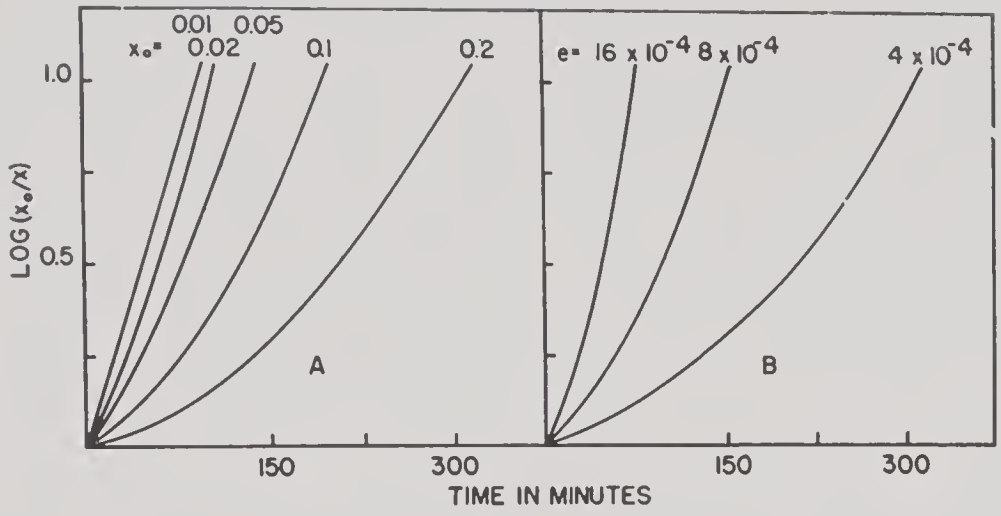

Fig. 1.13. Integrated Michaelis-Menten equation for a hypothetical reaction (161). Assumed values for (A): $K_m = 3 \times 10^{-2}$, $k_3 = 2$, $e = 4 \times 10^{-4}$, and $x_0 = 0.2$ to $0.1M$, as indicated. Values for (B): $K_m = 3 \times 10^{-2}$, $k_3 = 2$, $x_0 = 0.2$, and $e = 4 \times 10^{-4}$ to 16×10^{-4}, as indicated.

activity remaining at time t, a second-order constant, k'', was obtained which did not vary over the course of the inactivation reaction.

In addition to the restrictions imposed by substrate concentration, the order of the reaction is occasionally altered owing to inhibition by the reaction product, α-benzoyl L-arginine in the case of the trypsin-catalyzed hydrolysis of α-benzoyl-L-arginamide (168,169) and ammonium ion in the hydrolysis of urea (170–172), or by the substrate itself, in the case of carboxypeptidase by hippuryl-β-phenyllactate (148), acetylcholine esterase by acetylcholine (173,174) and urease by urea (159). The urease–urea reaction serves to illustrate the formidable difficulties which are apt to be encountered in even a simple enzymic reaction. The enzyme is inhibited by one of the products (NH_4^+), by an excess of the substrate, and also by Na^+ (171). The inhibition by Na^+ (and, to a lesser extent, by K^+) was initially attributed to the anionic partner, phosphate ion (175).

The Integrated Michaelis-Menten Equation; Evaluation of k_3. As described briefly in the preceding section, the *order* of an enzymic reaction may change during the course of the reaction for any one of several reasons. This problem was first treated by Bodansky in his classical work on the hydrolysis of β-glycerophosphate by bone phosphatase (176). For many enzymic studies, however, the initial velocity is measured over a short time interval where the order of reaction is constant.

If the velocity decreases during the course of an enzymic reaction only because the decreasing substrate concentration lowers the degree of saturation of the enzyme, it is still possible to utilize the Michaelis-Menten equation, provided that it is converted to an integrated form. This

derivation, anticipated by the early work of Henri (118), has been developed and used in a number of investigations (161,163,177–180).

Writing Equation (40) in terms of K_m:

$$v = -dx/dt = k_3(e)(x)/(x + K_m) \tag{79}$$

integration and rearrangement gives the useful relationship:

$$k_3(e) = (1/t)[2.3\ K_m \log\ (x_0/x) - (x_0 - x)] \tag{80}$$

If the total concentration of the enzyme, e, is assumed to remain constant throughout the course of the reaction, k_3e may be replaced by k', another rate constant:

$$k' = (1/t)[2.3\ K_m \log\ (x_0/x) - (x_0 - x)] \tag{81}$$

Comparison of Equation (81) with (77) reveals that the correct rate law is far more complex than the simple first-order formulation. The relative magnitudes of the two terms in the right-hand member of Equation (81) will control the order of the reaction. Thus, first-order kinetics will result when the first term predominates by virtue of K_m being large, i.e., $(k_2 - k_3) \gg k_1$, or x small, and zero-order kinetics when the second term predominates, i.e., K_m small and x large. Controlling the order of the reaction by means of the initial substrate concentration is generally feasible except when high substrate concentrations are limited by the availability or solubility of the substrate and low concentrations are limited by the sensitivity of the analytical method.

The integrated Michaelis-Menten equation (81) has been illustrated in a novel manner by Elkins-Kaufman and Neurath (161) with a plot of a hypothetical enzymic reaction (Fig. 1.13A). The data are plotted in the conventional first-order form with the assumed values of $K_m = 3 \times 10^{-2}$, $k_3 = 2$, $e = 4 \times 10^{-4}$ mg. of enzyme nitrogen per milliliter, and $x_0 = 0.2$ to $0.01M$. At low initial substrate concentrations the curves obey first-order kinetics and the slopes converge to a maximum value of 1.16×10^{-2} as predicted by the equation, i.e., $k_3(e)/2.3\ K_m$. At higher initial substrate concentrations, however, the zero-order term of Equation (81) predominates. In this case, the curves are concave upward with low initial slopes which, as the concentration decreases, again approach the limiting slope. It can be shown, furthermore, that the curvature in the case of the highest concentration is not due to the long time required for the reaction to reach completion. If the enzyme concentration is increased, holding the initial substrate concentration constant, the initial slope increases proportionally but the curvature remains (see Fig. 1.13B).

A "two-phase" equation similar to Equation (81) was derived by Van Slyke and Cullen (121):

$$t = (2.3/k_1) \log (x_0/x) + (1/k_3)(x_0 - x) \tag{82}$$

for the more restricted case where $e = 1$ and $k_3 \gg k_2$.

The integrated form of the Michaelis-Menten equation (81) contains the constant, k_3, which is independent of time, substrate concentration, and enzyme concentration. The data (161) for the hydrolysis of DL-CGP by carboxypeptidase can be used to demonstrate the determination of k_3 from Equation (81) and this value may be compared with the result of an independent method for evaluating this constant. In order for the various

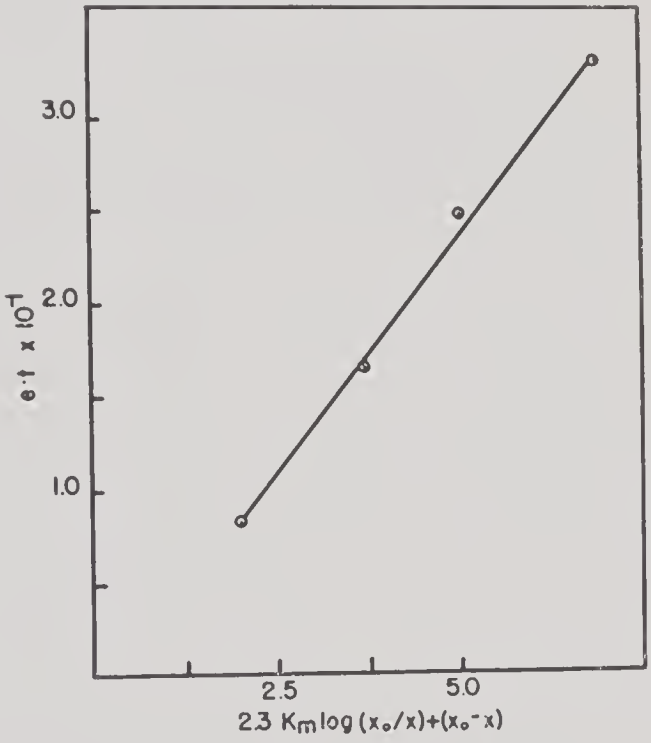

Fig. 1.14. Determination of k_3 from a plot of equation (81) (Ref. 161).

equations to be dimensionally correct, the following self-consistent units must be maintained: x, moles liter^{-1}, e, mg. of nitrogen per ml.; v, $V_{max.}$, moles liter^{-1} min.$^{-1}$; K_m, moles liter^{-1}; k_1, min.$^{-1}$ (mg. of nitrogen per ml.)$^{-1}$; k_2, k_3, moles liter^{-1} min.$^{-1}$ (mg. of nitrogen per ml.)$^{-1}$.

Knowing K_m, the right-hand member of Equation (81) is plotted against $e \times t$, whereupon k_3 is equal to the slope of the resulting straight line. (The Lineweaver-Burk plot (Equation 52) for the hydrolysis of DL-CGP by carboxypeptidase yields $K_m = 3.3 \times 10^{-2}$ and $V_{max.} = 8.0 \times 10^{-4}$ for a concentration of enzyme $e = 4.0 \times 10^{-4}$ mg. N/ml. (In view of the later findings of Neurath and DeMaria (165) the numerical value of K_m used here may be slightly in error.) The value determined from Figure 1.14 is 1.96. From the known value of $V_{max.}$, k_3 may be determined directly from Equation (41). $V_{max.}$ is given in the original article (161) as 2.4×10^{-2},

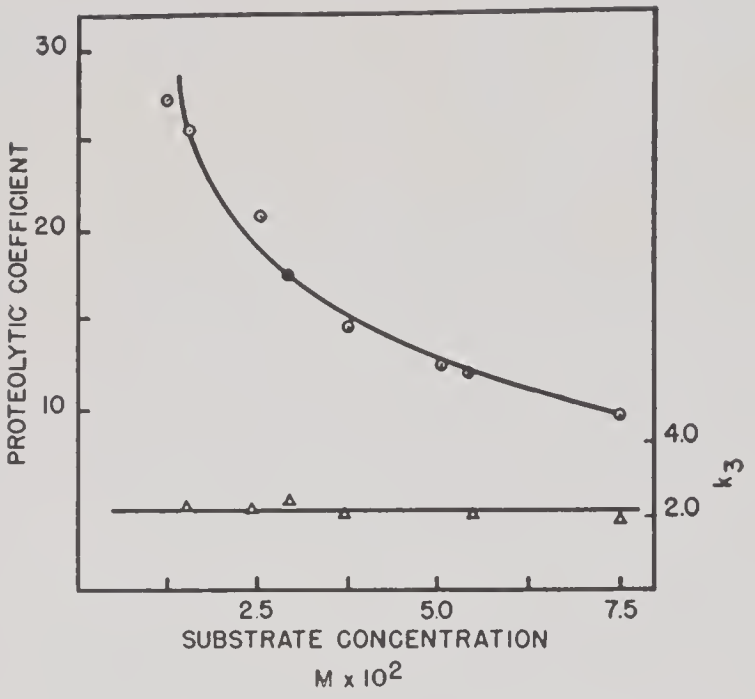

Fig. 1.15. Proteolytic coefficient (circle) and k_3 (triangle) for hydrolysis of DL-CGP by carboxypeptidase (161). Substrate concentration given for the L-isomer.

but this is actually the velocity over a 30 minute period. Therefore, $V_{max.} = 8.0 \times 10^{-4}$ mole liter^{-1} min.$^{-1}$ and $k_3 = 2.00$.

Proteolytic Coefficient. Much of the early kinetic work on proteolytic enzymes was reported in terms of the *proteolytic coefficient*, which was defined as the first-order rate constant in decimal logarithms obtained at unit enzyme concentration (milligrams of enzyme nitrogen per milliliter) and at an arbitrary initial substrate concentration (usually $0.05M$). Early workers (181,182) assumed first-order kinetics for proteolytic enzymes, and defined the proteolytic coefficient, C, as:

$$C = k'/e = (1/t) \log (x_0/x)/e \tag{83}$$

If the integrated Michaelis-Menten equation (81) is assumed to contain only the first-order term:

$$k_3/2.3K_m = (1/t) \log (x_0/x)e \tag{84}$$

combining Equations (84) and (83) yields an equation for the proteolytic coefficient:

$$C = k_3/2.3K_m \tag{85}$$

Elkins-Kaufman and Neurath (161) determined the proteolytic coefficient for carboxypeptidase at different initial concentrations of substrate, DL-CGP (see Fig. 1.15). There is a threefold variation in C as the initial substrate concentration is varied from 0.0125 to $0.075M$. In agreement

with previous workers, however, the authors (161) found that, at a constant substrate concentration, the proteolytic coefficient is independent of enzyme concentration. It is readily apparent from the above theoretical considerations and from the illustrative example that the use of proteolytic coefficients to compare the activity of an enzyme with respect to several substrates, or several enzymes with respect to the same substrate, is highly questionable. The validity of this concept only in systems showing first-order kinetics serves to limit its general utility. As seen in Figure 1.15, the proteolytic coefficient increases as the initial substrate concentration decreases until a limiting value is reached when true first-order kinetics are obtained. The variation in the proteolytic coefficient is in marked contrast to the constancy of k_3, shown also in Figure 1.15.

E. EXTENSIONS OF THE MICHAELIS-MENTEN FORMULATION

One Substrate. The simple Michaelis-Menten equation, discussed in the previous section (III.3.A), represents the proteotype of enzymic reactions involving a single substrate. A number of examples have been encountered (146,183,184), however, where the experimental kinetics have required more complex mechanisms leading to correspondingly more complex functions for $V_{max.}$ and K_m in terms of the rate constants. Both real and hypothetical extensions of the Michaelis-Menten mechanism for one substrate have been described in detail elsewhere (185–187). Several of the more important examples are summarized in Table I.2, and it should be noted that in all instances the derivation of the rate equation from the mechanism follows the rationale of Equations (37) through (44). Not shown in the Table are two special situations: (*a*) two substrates competing for the same enzyme; and (*b*) two enzymes competing for the same substrate. The former case has been described previously in Equation (53).

It should be noted that example 2 in Table I.2 treats a reversible reaction. Even if the equilibrium constant for the reaction is near unity, the *initial* velocities may be measured in either direction provided that the time interval is kept short. K_m and $V_{max.}$ values for either substrates or products may be determined in the usual manner (Section III.3.B). It was first pointed out by Haldane (146), and later by other authors (196,197) that the *kinetically determined* K_m and $V_{max.}$ values are related to the *thermodynamic* equilibrium constant ($K_{eq.}$) by the following equation:

$$K_{eq.} = V_f(K_m)_r/V_r(K_m)_f \tag{86}$$

where the subscripts f and r apply to the forward and reverse direction and where only *one* substrate and *one* product are involved. From Equation

(86) and the expressions for $V_{max.}$ and K_m in Table I.2, it is readily shown that for example 3 (two symmetrical ES complexes):

$$K = k_1k_3k_5/k_2k_4k_6 \tag{87}$$

More complex relationships exist for the various mechanisms of two-substrate reactions (198,199). Agreement between the equilibrium constant calculated from kinetic data and the measured equilibrium constant has been obtained with DPN-synthetase (197), alcohol dehydrogenase (200), and fumarase (201–203).

Two Substrates (or Substrate and Coenzyme). When two substrates, or a substrate and a coenzyme, are involved in an enzymic reaction, the concentration of each must be considered in the mechanism and in the derived rate equation. The simplest mechanism (104) assumes that only one of the substrates (S) forms a complex with the enzyme, and that interaction of this ES complex with the second substrate (S′) leads to the formation of free enzyme and the products, P and P′:

$$\underset{(x)}{\mathrm{E} + \mathrm{S}} \overset{k_1}{\underset{k_2}{\rightleftharpoons}} \mathrm{ES} \tag{88}$$

$$\underset{(x')}{\mathrm{ES} + \mathrm{S}'} \overset{k_3}{\rightarrow} \mathrm{E} + \mathrm{P} + \mathrm{P}' \tag{89}$$

Treatment of the mechanism in the usual manner leads to the steady state equation:

$$v = k_3(\mathrm{E})_0(x')/\{1 + [k_2 + k_3(x')]/k_1(x)\} \tag{90}$$

Comparison of this equation with Equation (49) reveals that $V_{max.} = k_3(\mathrm{E})_0(x')$ and $K_m = [k_2 + k_3(x')]/k_1$, i.e., both terms involve the concentration of (x'). The over-all kinetics of peroxidase (104) are represented by Equation (90).

If two binary complexes, ES and EP, appear in the mechanism (200), rate constants must be assigned for all of the reversible steps.

$$\underset{(x)}{\mathrm{E} + \mathrm{S}} \overset{k_1}{\underset{k_2}{\rightleftharpoons}} \mathrm{ES} \tag{91}$$

$$\underset{(x')}{\mathrm{ES} + \mathrm{S}'} \overset{k_3}{\underset{k_4}{\rightleftharpoons}} \underset{(z')}{\mathrm{EP} + \mathrm{P}'} \tag{92}$$

$$\mathrm{EP} \overset{k_5}{\underset{k_6}{\rightleftharpoons}} \underset{(z)}{\mathrm{E} + \mathrm{P}} \tag{93}$$

TABLE I.2
Extensions of the Michaelis-Menten Formulation for One Substrate (After Alberty (185))

Mechanism	Expressions for $V_{max.}$ and K_m (to be substituted in Equation (49))	Ref.
1. A series of ES complexes[a]		188
$E + S \underset{k_2}{\overset{k_1}{\rightleftharpoons}} ES \xrightarrow{k_3} ES' \xrightarrow{k_4} ES'' \xrightarrow{k_5} E + P$	$V_{max.} = (E_0)/(1/k_3 + 1/k_4 + 1/k_5)$	
	$K_m = (k_2 + k_3)/[k_1k_3(1/k_3 + 1/k_4 + 1/k_5)]$	
2. Reversible Reaction with one ES Complex	For the forward reaction, $(V_{max.})_f$ and $(K_m)_f$, are given by the previous Equations (41) and (47), while for the reverse reaction:	185
$E + S \underset{k_2}{\overset{k_1}{\rightleftharpoons}} ES \underset{k_4}{\overset{k_3}{\rightleftharpoons}} E + P$	$(V_{max.})_r = k_2(E)_0$	
	$(K_m)_r = (k_2 + k_3)/k_4$	
3. Reversible reaction with two symmetrica ES complexes		146, 189, 190
$E + \underset{(x)}{S} \underset{k_2}{\overset{k_1}{\rightleftharpoons}} ES \underset{k_4}{\overset{k_3}{\rightleftharpoons}} EP \underset{k_6}{\overset{k_5}{\rightleftharpoons}} E + \underset{(z)}{P}$	$v_f = (V_{max.})_f/[1 + (K_m)_f/(x)]$ $\quad v_r = (V_{max.})_r/[1 + (K_m)_r/(z)]$	
	$(V_{max.})_f = k_3k_5(E)_0/(k_3 + k_4 + k_5)$ $\quad (V_{max.})_r = k_2k_4(E)_0/(k_2 + k_3 + k_4)$	
	$(K_m)_f = \dfrac{(k_2k_5 + k_2k_4 + k_3k_4 + k_3k_5)}{k_1(k_3 + k_4 + k_5)}$ $\quad (K_m)_r = \dfrac{k_2k_5 + k_2k_4 + k_3k_4 + k_3k_5}{k_6(k_2 + k_3 + k_4)}$	

4. Substrate inhibition[b] or activation[c] (If $k_8 < k_3$, inhibition will result at high substrate concentrations; if $k_8 > k_3$, there will be activation)

$$E + S \underset{(x)}{\overset{k_1}{\rightleftharpoons}} ES \xrightarrow{k_3} E + P$$
$$k_2$$

$$E + S \underset{k_5}{\overset{k_4}{\rightleftharpoons}} SE$$

$$SE + S \underset{k_7}{\overset{k_6}{\rightleftharpoons}} SES \xrightarrow{k_8} SE + P$$

$$SE + S \underset{k_7}{\overset{k_6}{\rightleftharpoons}} SES \xrightarrow{k_8} SE + P$$

(SE is a form of enzyme–substrate complex that does *not* break down to yield E + products)

The steady state velocity is given by:

$$v = \frac{[(V_{max.})_2 + (V_{max.})_1 k_2]/[1 - (V_{max.})_1/(V_{max.})_2](x)}{1 + k^2/[1 - (V_{max.})_1/(V_{max.})_2](x) + k_1 k_2/[1 - (V_{max.})_1/(V_{max.})_2](x)^2}$$

191–194

$$(V_{max.})_1 = k_3(E)_0/[1 + (K_m)_{ES}/(K_m)_{St.}] \qquad (V_{max.})_2 = k_8(E)_0$$

where $(V_{max.})_1$ and $(V_{max.})_2$ are maximum velocities at low and high substrate concentration

$$k_1 = (K_m)_{ES}/[1 + (K_m)_{ES}/(K_m)_{SE}] \qquad k_2 = (K_m)_{SE}(K)_{SES}(1 - k_3/k_6)/[(K_m)_{ES} + 1/(K_m)_{SE}]$$

$$(K_m)_{ES} = (k_2 + k_3)/k_1, \; (K_m)_{SE} = k_5/k_4, \; (K_m)_{SES} = (k_7 + k_8)/k_6$$

[a] Where a series of enzyme–substrate compounds are encountered, as for example in the case of peroxidase and catalase, the "Michaelis complex" may be defined as the catalytically active complex (65).

[b] See also Section III.4.A.

[c] Since fumarase is activated by a wide variety of anions (195), it is probably that the substrates themselves, being anions, are also activators.

During the initial phase of the reaction in the forward direction, the concentration of P and P′ may be considered to be zero. The following relationships are then obtained:

$$v = (V_{max.})_f/[1 + (K_m)_s/(x) + (K_m)_{s'}/(x') + (K_m)_{ss'}/(x)(x')] \quad (94)$$

If S′ = 0, Equation (94) reduces to the expression for V_f in example 3 of Table I.2. The same rate equation is also obtained if a single ternary complex (204) is formed:

$$E + S \rightleftharpoons ES \quad (91a)$$

$$ES + S' \rightleftharpoons ESS' \rightleftharpoons EP + P' \quad (92a)$$

$$EP \rightleftharpoons E + P \quad (93a)$$

$$(V_{max.})_f = k_5(E)_0 \quad (95)$$

$$(K_m)_s = k_5/k_1 \quad (96)$$

$$(K_m)_{s'} = k_5/k_3 \quad (97)$$

$$(K_m)_{ss'} = k_2k_5/k_1k_3 \quad (98)$$

The symmetrical relationships are obtained for the reverse reaction:

$$v = (V_{max.})_r/[1 + (K_m)_p/(z) + (K_m)_{p'}/(z') + (K_m)_{pp'}/(z)(z')] \quad (94')$$

$$(V_{max.})_r = k_2(E)_0 \quad (95')$$

$$(K_m)_p = k_2/k_6 \quad (96')$$

$$(K_m)_{p'} = k_2/k_4 \quad (97')$$

$$(K_m)_{pp'} = k_2k_5/k_4k_6 \quad (98')$$

Here it is seen that the equation for velocity, v, in either direction is independent in the numerator of the concentration of either substrate, in contrast to the previously derived Equation (49). Likewise, the K_m value for either of the substrates (or products) may be determined experimentally in the usual manner, but from the above equations it is apparent that the K_m values cannot be interpreted as simple dissociation constants. A more complete discussion of this type of mechanism will be found in Section III.3.F.

The most general mechanism for two-substrate reactions involves the random formation of two ternary complexes (205,206):

$$E + S \rightleftharpoons ES \quad (99)$$

$$E + S' \rightleftharpoons ES' \quad (100)$$

$$ES + S' \rightleftharpoons ESS' \quad (101)$$

$$ES' + S \rightleftharpoons ESS' \quad (102)$$

The stepwise breakdown of ESS′ into products is omitted here to conserve space and the reverse reaction is neglected. A discussion of this mechanism (207), and its application to the activation of pyruvic kinase by K^+, has been presented by Kachmar and Boyer (208). Yeast alcohol dehydrogenase (209) and creatine kinase (210) also conform to this type of mechanism.

The above complex situation is simplified somewhat if it is assumed that the rate-determining step involves conversion of ESS′ into an enzyme–product complex, EPP′. Under these conditions the rate expression assumes the form of Equation (94). The coefficients for the steady state rate equation have been given for the case where ESS′ dissociates directly into products (211). Further simplification is introduced if it is assumed that the affinity of the enzyme for one substrate is not influenced by the presence of the second substrate, i.e., that the equilibrium constants are equal for reactions (99) and (102) and equal for (100) and (101). Under these conditions the rate equation becomes:

$$v = V_{\text{max.}}/[1 + K_m/(x)][1 + K_m'/(x')] \qquad (103)$$

This equation has also been derived by other investigators (184,212,213) for the simple case where two substrates are bound independently at separate sites on the enzyme. Florini and Vestling (214) and Frieden (215) have suggested graphical methods for determining the values of the dissociation constants (K_m and K_m') for two-substrate systems.

F. KINETICS OF A TYPICAL TWO-SUBSTRATE REACTION: ALCOHOL DEHYDROGENASE

One of the most well-documented studies of two-substrate systems in the field of enzyme kinetics is provided by the definitive work of Theorell and his colleagues (107,200,216,217) on the alcohol dehydrogenase system (*cf.* Equation 104):

$$\text{Ethanol} + \text{DPN}^+ \rightleftharpoons \text{acetaldehyde} + \text{DPNH} + \text{H}^+ \qquad (104)$$

Crystalline alcohol dehydrogenase (mol. wt. = 84,000) from horse liver was used for these studies. The turnover number is 140 for this enzyme. A crystalline alcohol dehydrogenase has also been obtained from baker's yeast. The yeast enzyme, however, contains 4 moles of bound Zn^{2+} per mole of enzyme, whereas the liver enzyme contains only 1 mole of bound Zn^{2+} (218). The function of Zn^{2+} in the enzymic reaction is not yet well understood.

The equilibrium constant (107,219) for reaction (104) is $\sim 1 \times 10^{-11}$; at pH 7 this value is reduced to $\sim 10^{-4}$. When reaction (104) is studied

TABLE I.3
Values[a] of K_m and $V_{max.}$ for the Alcohol Dehydrogenase System (107)

Substrate	pH	K_m, moles liter^{-1} $\times$ 10^{-6}	$V_{max.}$, moles liter^{-1}sec.$^{-1}$
DPN	10.0	17	2.6
DPNH	7.0	17	43
Ethanol	6.8	1,200	1.2
	9.8	2,000	3.1
Acetaldehyde	7.0	120	50

[a] These values were determined before the effect of buffer ions upon the constants was fully appreciated (*cf.* Ref. 216, pp. 303 *et seq.*, for a discussion of this point).

from left to right, the unfavorable equilibrium can be shifted by changing the pH to *ca.* 9 to 9.5, or by adding semicarbazide to "trap" the aldehyde.

Measurements of pyridine nucleotide-linked reactions customarily make use of the fact that DPNH, but not DPN, absorbs light at 340 mμ (see Section II.2.A). The initial kinetic studies by Theorell and Bonnichsen (107) were carried out in the conventional manner by measuring the *initial velocity* of the reaction in either direction as a function of concentration of DPN, DPNH, ethanol, and acetaldehyde. Experimental values of K_m and $V_{max.}$ were obtained in each instance (see Table I.3), but it was apparent from the mechanism that K_m for each substance would be a complex function of the separate rate constants (see Section III.3.E).

It became possible to approach this problem in more detail following the observation that the binding of DPNH by the enzyme produced a shift in spectrum of the pyridine nucleotide from 340 to 325 mμ (Fig. 1.16). A sulfhydryl group on the protein is probably involved in binding the coenzyme as shown by the fact that addition of *p*-chloromercuribenzoate to the E–DPNH complex causes the spectrum to revert back to that of free DPNH. A direct "titration" of the enzyme by successive additions of DPNH revealed that 2 moles of DPNH were bound per mole of enzyme in the pH range 7 to 9, while at pH 10 approximately 1 mole was bound. Evidence for enzyme–DPNH interaction, as signalled by a shift in absorption spectrum of the latter substance, has also been observed with lactic dehydrogenase (220) and with respiring yeast (221); the spectral shift is not seen, however, with yeast alcohol dehydrogenase, 3-phosphoglyceraldehyde dehydrogenase, or glutamic dehydrogenase (220). Likewise, the binding of flavin mononucleotide by the "old yellow enzyme" (a TPNH diaphorase) has been demonstrated both spectrophotometrically and fluorimetrically (222).

DPN is also bound to the enzyme as discussed below, but no shift in the DPN spectrum ($\lambda_{max.}$ at 260 mμ) occurs upon binding. Since DPNH is

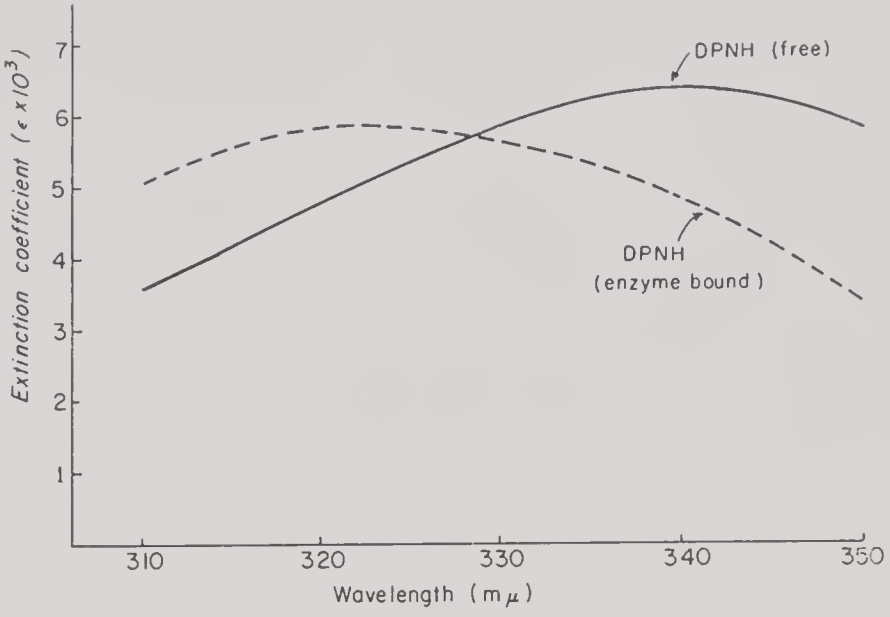

Fig. 1.16. Absorption spectra of free and enzyme-bound DPNH (107).

bound more strongly than DPN to the enzyme (see rate constants below), the over-all equilibrium of reaction (104) can be varied appreciably in the presence of large amounts of enzyme. Thus, the equilibrium constant, K, for the reaction is *ca.* 100 times larger in the pH range 6 to 8 and 20 times larger at pH 9 when the amount of enzyme exceeds the amount of substrates. Dixon and Webb (223) have shown by recalculation of the data that the earlier value (107) of $K = 200$ is too high.

Theorell and Chance (200) suggested the following mechanism for the alcohol dehydrogenase reaction, and made detailed kinetic measurements in order to determine the individual rate constants:

$$\mathrm{E} + \mathrm{DPNH} \underset{k_2}{\overset{k_1}{\rightleftharpoons}} \mathrm{E{-}DPNH} \tag{105}$$

$$\mathrm{E{-}DPNH} + \mathrm{H^+} + \mathrm{ald.} \underset{k_6}{\overset{k_4}{\rightleftharpoons}} \mathrm{E{-}DPN} + \mathrm{alc.} \tag{106}$$

$$\mathrm{E{-}DPN} \underset{k_5}{\overset{k_3}{\rightleftharpoons}} \mathrm{E} + \mathrm{DPN} \tag{107}$$

This mechanism, which treats reaction (104) in reverse, assumes that only *one* product, the pyridine nucleotide, dissociates in a rate-limiting manner from the enzyme. E, ald., and alc. represent enzyme, aldehyde, and alcohol, respectively. It should be noted that the numbering of the rate constants in Equations (105) through (107) follows the original derivation (200,216).

From the spectra of DPNH and E—DPNH (*cf.* Fig. 1.16) it was seen that the largest *difference* in absorption occurs at 310 and 350 mμ. There was, however, no single wavelength where the formation of E—DPNH could be recorded without changes in the concentration of free DPNH being superimposed. Careful scrutiny of the DPNH spectrum showed that the ϵ value is *equal* at 328 and 354 mμ. A recording spectrophotometer was devised to measure only the *difference* in absorption at these two wavelengths; any changes in DPNH concentration are thereby rejected and only changes in E—DPNH concentration are recorded (a diagram of this instrument is shown on p. 1129 of Ref. 200). As a check, the optical density at 328 mμ was also recorded. Since 328 mμ is the isobestic point for DPNH and E—DPNH, the optical density at this wavelength did not change during the interconversion of these two species.

With this more sensitive technique the titration of enzyme by DPNH was reinvestigated using smaller quantities (1 to 3 μmoles) of the reactants. The binding of 2 moles of DPNH by 1 mole of enzyme was confirmed. At pH 7.0 the *dissociation* constant for E–DPNH was found to be 10^{-7} *M*. The rate constant for combination, k_1, was measured directly by means of a special rapid-flow apparatus and found to be 4×10^6 liter mole^{-1} sec.$^{-1}$. This value, combined with the above dissociation constant, yields a computed value of k_2 equal to 0.4 sec.$^{-1}$.

It is more difficult to measure directly the rate of reaction (104), since it is extremely rapid unless the acetaldehyde concentration is kept low. Fortunately, formaldehyde reacts at a much slower rate, and this substrate can be used over a wide range of concentration to study the aldehyde-dependent decomposition of the E–DPNH complex. From these data, k_4 was estimated (200,216) to be 3.4×10^{12} M^{-2} sec.$^{-1}$ for acetaldehyde and about two orders of magnitude smaller for HCHO. In the earlier publication (200), the value reported for k_4 was actually that for $k_4(H^+)$. k_6 is more difficult to determine, but since at pH 7.0 the equilibrium of reaction (104) lies well to the left, it is apparent that $k_6 \ll k_4$. A value of *ca.* 10^4 has been estimated for k_6.

If the Michaelis constant for one of the substrates $(K_m)_1$, is defined in the usual way as the substrate concentration which gives one-half the maximal velocity in the presence of an excess of the other substrate, the numerical values are those shown in Table I.2. But how is a given K_m, which has an experimentally determined numerical value, to be interpreted in terms of the individual rate constants? For the mechanism explicit in Equations (105) through (107), it can be shown that K_m for DPNH is equal to the ratio k_3/k_1. This ratio obviously does not represent a true "dissociation constant" but, strangely enough, is composed of constants related to the

affinities of E with DPNH and DPN. At low aldehyde concentration, K_m for DPNH is more complex, i.e.,

$$K_m = (k_2 + k_4[\text{ald.}])/k_1 \tag{108}$$

Studies of the reverse reaction are hampered by the fact that there is no direct method for measuring the concentration of the E–DPN complex as distinguished from free DPN. Approximate values of the rate constants may be estimated, however, by indirect methods. Thus, from the above relationship that K_m for DPNH is equal to k_3/k_1, and from the previously determined values for K_m (Table I.3) and k_1, k_3 is found to be 68 sec.$^{-1}$. The dissociation constant for E–DPN is about 100-fold larger than that for E–DPNH, or $K \approx 10^{-5}$ for E–DPN. This figure, in conjunction with the previously calculated value of k_3, permits the assignment of an approximate value of 7×10^6 M^{-1} sec.$^{-1}$ to k_5.

The accuracy of the above determined rate constants may be checked by utilizing the relationship between the over-all equilibrium constant for reaction (104) and the rate constants, *viz.*

$$K_{\text{equil.}} = \frac{(\text{product of rate constants})_{\text{forward}}}{(\text{product of rate constants})_{\text{reverse}}} \tag{109}$$

or

$$K_{\text{equil.}} = k_2k_5k_6/k_1k_3k_4 \tag{110}$$

Substituting the above values for the rate constants, $K_{\text{equil.}}$ is calculated to be *ca.* 3×10^{-11}. Since the measured value of $K_{\text{equil.}}$ is 1×10^{-11} (107, 219), the agreement is very good in view of the number of terms involved in the ratio. Later measurements by Theorell and his colleagues (217), using more sensitive fluorimetric techniques for DPNH and E–DPNH (224), have provided more accurate values for the individual rate constants and even better agreement between the calculated and measured values of $K_{\text{equil.}}$ for the over-all reaction. Dalziel and Theorell (225) have also considered in detail the effect of pH and of various anions upon the rate constants.

Of interest is the fact that *yeast* alcohol dehydrogenase follows a different mechanism (226) than that presented in Equations (105) through (107) for the liver enzyme. It has been postulated that with the yeast enzyme a ternary complex, substrate–enzyme–coenzyme, is formed and that the rate-limiting step is an internal oxido-reduction between the two reactants.

4. Effect of Inhibitors

In view of the fact that most enzymes exhibit a high degree of substrate specificity, it is not surprising that other substances, containing chemical

groups similar to those in the substrate, may interfere with the enzyme-catalyzed reaction by competition at the "active center" of the enzyme. Likewise, the presence of reactive groups (—SH, —NH_2, —COOH, imidazole, etc.) at, or near, the "active center" renders the enzyme susceptible to attack by agents capable of binding to these groups. Inhibition of an enzyme by an analogue of the substrate or by a binding agent can often be used advantageously to gain valuable information regarding the nature of the enzyme-catalyzed reaction or the topology of the "active center." An outstanding example of this approach is the work of Wilson and Nachmansohn with acetyl cholinesterase (194,227,228). Furthermore, an entire area of pharmacology is concerned with the search for new drugs which selectively depress an unwanted metabolic process without, at the same time, being harmful to normal processes (229–232).

Numerous studies have been made of the effects of inhibitors on enzyme systems and the corresponding treatment of the kinetics of inhibition in terms of the Michaelis-Menten equation. The two most common types of inhibition have been called *competitive* and *noncompetitive*. In the former, the inhibitor competes with the substrate for the "active site" on the enzyme, and the degree of inhibition will thus depend upon the relative concentrations of both substrate and inhibitor. In the noncompetitive inhibition, the inhibitor interferes by attacking the protein at a site not occupied by the substrate or, if attacking at the substrate site, in such a manner that it is not displaced by the substrate. This type of inhibition, of course, is independent of the substrate concentration.

A. COMPETITIVE INHIBITOIN

Following the formulation given previously in Section III.3.A, competitive inhibition is treated as follows. (Dixon and Webb (233) have also derived equations for "partial" competitive inhibition where the inhibitor affects the affinity of the enzyme for the substrate, although the inhibitor and substrate react at different sites.) In addition to the other symbols, let:

x' = concentration of the inhibitor
p' = concentration of the inhibitor–enzyme complex
v', $V'_{max.}$ = velocity and maximum velocity in the presence of the inhibitor
$K'_m = k'_2/k'_1$

Since there is no breakdown of the enzyme–inhibitor complex into products, and hence no k'_3, K'_m is truly an equilibrium constant as represented above. It is, therefore, correct to compare the affinities of an enzyme for two competitive inhibitors by means of their respective K'_m

values, but incorrect to compare the affinity of an enzyme for its substrate and an inhibitor by comparing values of K_m and K'_m.

The over-all reaction may be written (with the concentrations underneath each substance):

$$\begin{array}{ccccc} \mathrm{E} & + \mathrm{S} & \overset{k_1}{\rightleftharpoons} & \mathrm{ES} & \overset{k_3}{\rightarrow} \mathrm{Q} \\ (e - p - p') & (x) & \overset{k_2}{} & (p) & \end{array} \tag{111}$$

and:

$$\begin{array}{ccccc} \mathrm{E} & + \mathrm{S}' & \overset{k'_1}{\rightleftharpoons} & \mathrm{ES}' & \\ (e - p - p') & (x') & \overset{k'_2}{} & (p') & \end{array} \tag{112}$$

Following the derivation given previously (Equations 36 to 49), the over-all velocity, v', is given by the equation:

$$v' = k_3 K'_m(e)(x)/[K_m K'_m + K_m(x') + K'_m(x)] \tag{113}$$

The maximum velocity, $V'_{\mathrm{max.}}$, will again be obtained when all of the enzyme is bound in the form of the enzyme–substrate complex, i.e., when $e = p$. Therefore, substituting Equation (41) in Equation (113) and rearranging yields:

$$v' = V'_{\mathrm{max.}}(x)/[x + K_m(1 + x'/K'_m)] \tag{114}$$

Or, recasting the equation into the Lineweaver-Burk form:

$$\frac{1}{v'} = \frac{K_m}{V'_{\mathrm{max.}}}\left(1 + \frac{x'}{K'_m}\right)\cdot\frac{1}{(x)} + \frac{1}{V'_{\mathrm{max.}}} \tag{115}$$

Comparison of Equation (115) with Equation (52) for the uninhibited reaction shows that the slope of the Lineweaver-Burk plot has been increased by the quantity $K_m x'/K'_m$ without any concomitant change in intercept, and that $V'_{\mathrm{max.}}$ is the maximum velocity in the presence or absence of the inhibitor. Competitive inhibitors increase the value of K_m without affecting $V_{\mathrm{max.}}$, while, as shown below, noncompetitive inhibitors decrease $V_{\mathrm{max.}}$ without affecting K_m.

Similarly, the integrated Michaelis-Menten equation for competitive inhibition (Equation 116) is changed from Equation (80) only to the extent that K_m is replaced by $K_m(1 + x'/K'_m)$:

$$k_3 et = 2.3\, K_m(1 + x'/K'_m)\log(x_0/x) + (x_0 - x) \tag{116}$$

In the event that the competitive inhibitor (x') is one of the reaction products, and hence is being generated at the same velocity as the substrate disappears (234), the corresponding equation is:

$$k_3 et = 2.3\, K_m(1 + x_0/K'_m)\log(x_0/x) + (1 - K_m/K'_m)(x_0 - x) \tag{117}$$

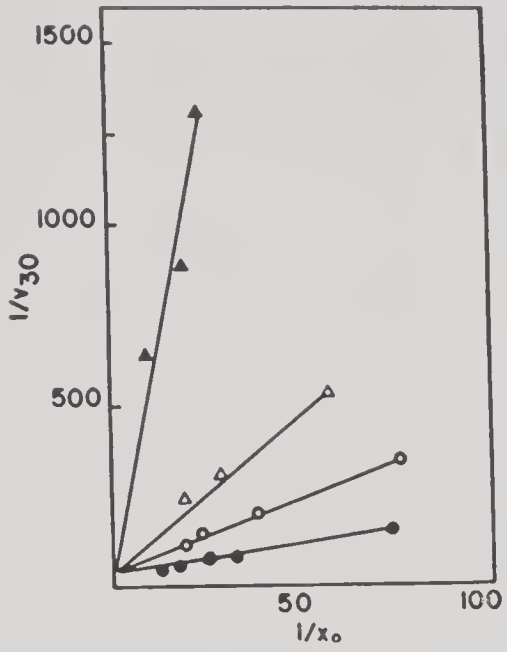

Fig. 1.17. Competitive inhibition of the hydrolysis of DL-CGP by carboxypeptidase (234). Velocity is expressed per thirty minute period. The curves are defined by the following symbols: black circle, no inhibitor; white circle, $2 \times 10^{-3}M$ phenyl butyrate; white triangle, $2 \times 10^{-3}M$ phenyl acetate; black triangle, $2 \times 10^{-3}M$ phenyl propionate.

It is apparent from Equations (116) and (117) that the generation of a competitive inhibitor during the course of the reaction will cause an enhancement of the first-order term at the expense of the zero-order term.

Examples of competitive inhibition are too numerous to cite in detail. Figure 1.17, replotted from the data of Elkins-Kaufman and Neurath (234) for the inhibition of carboxypeptidase, may be used as an illustration. Since K_m is known to be 3.7×10^{-2} for L-CGP in the noninhibited reaction (161), the value of K'_m for a particular inhibitor can be obtained from the slope of the curve. In the case of inhibition by phenyl acetate, it is seen that $V_{\max.} = 8.33 \times 10^{-4}$ and the slope = 270. Since:

$$\text{Slope} = (K_m/V_{\max.})(1 - x'/K'_m) \tag{118}$$

the above values may be substituted and K'_m determined to be 3.93×10^{-4}.

B. NONCOMPETITIVE INHIBITION

For the treatment of noncompetitive inhibition the same symbols are used as with competitive inhibition with one addition, p'', which represents the inactive enzyme–substrate–inhibitor complex. The pertinent equations are:

$$\underset{(e - p - p' - p'')}{\text{E}} + \underset{(x)}{\text{S}} \overset{k_1}{\underset{k_2}{\rightleftharpoons}} \underset{(p)}{\text{ES}} \xrightarrow{k_3} \text{Q} \tag{119}$$

$$\underset{(c-p-p'-p'')}{\mathrm{E}} + \underset{(x')}{\mathrm{S}'} \overset{k'_1}{\underset{k'_2}{\rightleftharpoons}} \underset{(p')}{\mathrm{ES}'} \tag{120}$$

$$\underset{(p)}{\mathrm{ES}} + \underset{(x')}{\mathrm{S}'} \overset{k''_1}{\underset{k''_2}{\rightleftharpoons}} \underset{(p'')}{\mathrm{ESS}'} \tag{121}$$

The assumption is again made that:

$$K''_m = k''_2/k''_1 = K'_m = k'_2/k'_1 \tag{122}$$

The formation of an ESS′ complex was not invoked in the case of competitive inhibition where both substrate and inhibitor compete for the same site on the enzyme. In the present case of noncompetitive inhibition the ESS′ complex may also be formed by the reaction:

$$\mathrm{ES}' + \mathrm{S} \rightleftharpoons \mathrm{ESS}' \tag{123}$$

but this route is not unique, and the constants subsequently drop out of the derivation. A special type of noncompetitive inhibition is found in the case where the substrate can be bound at two sites, only one of which is catalytically active. This is illustrated by example 4 in Table I.2, where the mechanism is similar to that in Equations (119) through (121) except for the assumption that SES, the inactive complex, may break down usefully to give SE (inactive) and products.

By the same manipulations which led to Equations (49), (52), (114), and (115), the following expressions are obtained for noncompetitive inhibition:

$$v' = V'_{\mathrm{max.}}(x)K'_m/[K'_m + (x')][(x) + K_m + V'_{\mathrm{max.}}] \tag{124}$$

$$1/v' = [1 + (x')/K'_m][1/V'_{\mathrm{max.}} + K_m/V'_{\mathrm{max.}} \times 1/(x)] \tag{125}$$

Comparison of Equation (125) with (52) shows that noncompetitive inhibition increases *both* the slope and the intercept by the factor $(1 + (x')/K'_m)$.

In several instances, e.g., the inhibition of carboxypeptidase by various organic acid anions (234), urease by ammonium ion (172), arginase by monoamino acids (235), galactosidase by alkali metal ions (236), and dihydrofolic reductase by the folic acid antagonists, aminopterin and amethopterin (237), the inhibition is nearly, but not exactly, noncompetitive since the slope and intercept do not change by identical amounts.

A classical example (238) of noncompetitive inhibition is demonstrated (Fig. 1.18) by the effect of carbon monoxide upon nitrogen fixation in *Azotobacter*. Both the slope and the intercept of the uninhibited line increase by the factor of 1.5 in the presence of the inhibitor, carbon monoxide. The increase in intercept ($V'_{\mathrm{max.}} < V_{\mathrm{max.}}$) thus distinguishes noncompetitive from competitive inhibition.

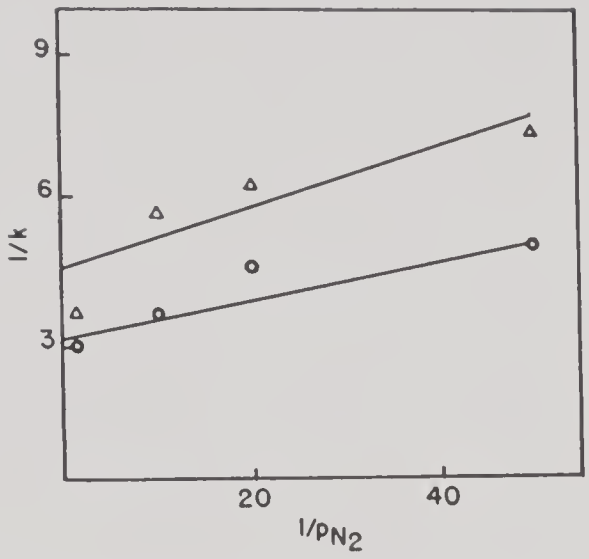

Fig. 1.18. Noncompetitive inhibition of nitrogen fixation in *Azotobacter* by carbon monoxide (238). The reciprocal of the rate is plotted against the reciprocal of the partial pressure of nitrogen. The curves are defined by the following symbols: circle, no inhibitor; triangle, 0.3% carbon monoxide.

Another means of distinguishing the two principal types of inhibition has been suggested by Wilson (239) using the function v/v', where v and v' are the velocities of the noninhibited and inhibited reactions, respectively. Kistiakowsky and Shaw (240) have used a slightly different function $\phi = (v - v')/v'$, where ϕ is defined as the *inhibition index*, to describe the various types of inhibition. For competivive inhibition:

$$v/v' = 1 + (K_m/K'_m)[x'/(K_m + x)] \tag{126}$$

and for noncompetitive inhibition:

$$v/v' = 1 + (x'/K'_m) \tag{127}$$

By plotting v/v' against x', different curves are obtained for each type of inhibition, in accord with the above equations. In the noncompetitive inhibition of nitrogen fixation in *Azotobacter* by carbon monoxide, Ebersole *et al.* (238) have shown that the conventional plot of the data according to equation (127) results in a curve which is concave upward. This was interpreted to mean that n molecules of inhibitor combine with one molecule of enzyme with the resulting change in equation:

$$v/v' = 1 + [(x')^n/K'_m] \tag{128}$$

For the case mentioned above, the data were replotted as log $(v/v' - 1)$ against log (x') and a straight line was obtained with a slope n equal to 2.

Equations (126) and (127) have been used in a slightly different form by

Hunter and Downs (235). If α is defined as the fractional activity, i.e., v'/v, these equations may be rearranged to:

$$(x')[\alpha/(1 - \alpha)] = K'_m(x)/K_m - K'_m \tag{126'}$$

$$(x')[\alpha/(1 - \alpha)] = K'_m \tag{127'}$$

By plotting $(x')\alpha/(1 - \alpha)$ against (x) one obtains, for competitive inhibition, a straight line with slope K'_m/K_m and intercept K'_m; and, for noncompetitive inhibition, a straight line of zero slope and intercept K'_m. Graphic representations of Equations (126′) and (127′) and a comprehensive survey of the applications of inhibitor studies to the field of chemotherapy are provided in Chapter IV of the text by Work and Work (230).

C. GENERALIZED TREATMENT OF STRAUS AND GOLDSTEIN

In the preceding derivations for the Michaelis-Menten equation and for both competitive and noncompetitive inhibition, it was assumed that the concentration of the enzyme is very much smaller than that of the substrate. While this is true for most *in vitro* experiments, it may not be entirely valid for certain *in vivo* systems, where the specific localization of the enzyme in a subcellular region may lead to its effective concentration being high.

Straus and Goldstein (241,242) (and later Myers (243)) have examined this problem in detail and have derived a more generalized set of equations where it is no longer assumed that the concentration of free substrate equals the total substrate concentration. Thus,

$$\underset{(e-p)}{\mathrm{E}} + \underset{(x-p)}{\mathrm{S}} \overset{k_1}{\underset{k_2}{\rightleftharpoons}} \underset{(p)}{\mathrm{ES}} \rightarrow \mathrm{E} + \mathrm{Q} \tag{129}$$

and the Michaelis constant is defined as:

$$K_m = (e - p)(x - p)/p \tag{130}$$

It will be noted that the effect on K_m of the breakdown of ES into products, Q, is neglected in this case (see Section III.3.A).

Let a, the fractional activity, be defined as:

$$a = p/e = v/V_{\max.} \tag{131}$$

so that:

$$e - p = e(1 - a) \tag{132}$$

and:

$$x - p = x - ae \tag{133}$$

Substituting these latter values in Equation (130) and solving for x:

$$x = K_m[a/(1 - a)] + ae \tag{134}$$

Straus and Goldstein stressed that the importance of (e) could only be assessed by comparison with K_m. Accordingly, they introduced the concept of the *specific concentration*, e^*, which is defined as e/K_m. Dividing equation (134) by K_m and introducing $x^* = x/K_m$:

$$x^* = a/(1 - a) + ae^* \tag{135}$$

When e^* is small, Equation (135) reduces to the usual Michaelis-Menten equation.

The case of noncompetitive inhibition is treated in a similar manner. The amounts of free enzyme, substrate and inhibitor are given by ($e - p - p' - p''$), and ($x' - p' - p''$). The assumption is made that the concentration of substrate is high enough to saturate the free enzyme and, therefore:

$$a = (e - p - p')/e \tag{136}$$

Similarly, it can be shown that:

$$p' = (1 - a)e/K_m \tag{137}$$

The usual equilibrium expression is set up:

$$K'_m = (e - p - p')(x' - p')/p' \tag{138}$$

Solving Equation (136) for p and substituting that and p' from Equation (137) into (138) yields (solving for x'):

$$x' = [(1 - a)/a]K'_m + (1 - a)e \tag{139}$$

and, dividing through by K'_m:

$$x'^* = (1 - a)/a + e^*(1 - a) \tag{140}$$

For Equation (140) the first term in the right-hand member represents free inhibitor and the second term the combined inhibitor. Three "zones of behavior" are used to describe noncompetitive inhibition depending on whether the first, second, or both terms are used in Equation (140). In zone A all the inhibitor is free so that: $x'^* = (1 - a)/a$. In zone C all the inhibitor is combined: $x'^* = e^*(1 - a)$. Zone B includes that region where both terms are used and its boundaries may be established by a graphic method based on the permissible error in a. For the particular system chosen by Straus and Goldstein, a was set at 0.01 and zone B included the region $0.1 < e'^* < 100$.

The formulation for competitive inhibition is more complex, since zone

behavior will obtain for both substrate and inhibitor. By a rather laborious calculation it can be shown that:

$$x'^* = \{(x^* - ae^*)[(1 - a)/a] - 1\} + \{(1 - a)[1 + 1/(x^* - ae^*)]\} \tag{141}$$

This expression may be simplified by neglecting the amount of free enzyme which is usually small when both p and p' are present:

$$x'^* = (x^* - ae^*)[(1 - a)/a] + (1 - a)e^* \tag{142}$$

For the use of these equations with the data of the cholinesterase–physostigmine–acetylcholine system, the reader should consult the original papers of Straus and Goldstein (241,242). In addition, their data permitted them to calculate the rate constants for the combination and dissociation of acetylcholine with cholinesterase (and hence K_m), as well as the corresponding constants for physostigmine with cholinesterese (and K'_m).

Other results of their observations which bear on enzyme kinetics in general may be summarized as follows: (*1*) Most enzyme systems fall into zone A since K_m is usually greater than 10^{-5}. When $K_m < 10^{-5}$, e would have to be larger than 10^{-4} moles/liter to shift the system to zones B or C. (*2*) Competitive inhibition cannot exist in zone C. (*3*) The number of molecules of inhibitor combined with the enzyme may be determined from the "dose-effect" curves. (*4*) Inhibition depends markedly on the concentration of the substrate; hence it is difficult to compare *in vitro* with *in vivo* experiments where the substrate concentrations may be of different orders of magnitude. (*5*) Dilution effects on isolated enzyme systems may cause a decrease in inhibition above that predicted by the dilution ratio.

Ackermann and Potter (244) and Bain (245) have emphasized further the idea that the assumptions in the usual Michaelis-Menten formulation may not be valid in certain instances in which the equations were derived from the premise that the enzyme and inhibitor formed a reversible complex. If, on the other hand, the dissociation constant for enzyme and inhibitor, K'_m, is extremely small, the complex will approach irreversibility. In this event, the calculation of K'_m is meaningless and the concentration of the enzyme cannot be ignored since the degree of inhibition will depend upon the amounts of both enzyme and inhibitor. Taking into account the above effects, Ackermann and Potter have derived the following equation (expressed in the symbols previously used in this chapter):

$$v = -k_3\left[\frac{K'_m(x)}{2K_m} + \frac{(x')}{2} - \frac{(e)}{2}\right] \pm k_3\left[\left\{\frac{K'_m(x)}{2K_m} + \frac{(x')}{2} - \frac{(e)}{2}\right\}^2 + \frac{K'_m(x)(e)}{K_m}\right]^{1/2} \tag{143}$$

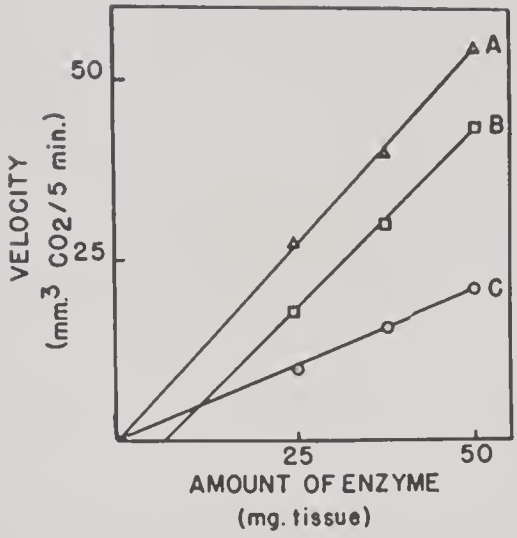

Fig. 1.19. Irreversible inhibition of cholinesterase (245). The curves are defined by the following symbols: A = control, no inhibitor; B = $2.5 \times 10^{-9}M$ TEPP; C = $1.0 \times 10^{-6}M$ physostigmine.

With no inhibitor present ($K'_m = 0, x' = 0$) the equation reduces to:

$$v = k_3(e) \tag{144}$$

and if the velocity is plotted against the enzyme concentration, a straight line through the origin will result with a slope equal to k_3 (curve A of Fig. 1.19). When the enzyme and inhibitor are tightly bound ($K'_m \rightarrow 0$, but x' finite) Equation (143) reduces to:

$$v = k_3[(e) - (x')] \tag{145}$$

In this event, the curve (B) will be parallel to that obtained with no inhibitor present and will have the same slope, k_3, but with an intercept on the enzyme axis, indicating the amount of enzyme "titrated" by the inhibitor. These effects are shown in Figure 1.19 taken from the data of Bain for the inhibition of cholinesterase by tetraethylpyrophosphate (TEPP). For comparative purposes, the effect of a normal, competitive inhibitor, physostigmine, is shown as curve C. Ackermann and Potter have observed similar effects in the succinoxidase system where malonate and itaconate exhibit normal competitive inhibition, while quinone and copper ion inhibit by combining with, and irreversibly inactivating, the enzyme.

D. OTHER TYPES OF INHIBITION

In addition to the well-defined examples of competitive and noncompetitive inhibition, other less frequently encountered types have also been described. General mechanisms for the various types of inhibition have been presented by Alberty (246) and Ogston (247).

"Partially competitive" inhibition refers to the situation where the inhibitor combines with a site adjacent to the substrate site in such a way as to interfere with enzyme–substrate interaction. Other mixtures of competitive and noncompetitive inhibition have also been treated theoretically (92,248,249).

"Apparent competitive" inhibition (207) occurs when the binding of the inhibitor has no effect on the rate of breakdown of ESS′; in this instance $V_{max.}$ is independent of (S′) while K_m is a nonlinear function of (S′).

The term "uncompetitive inhibition" was originally applied to the case where the reciprocal plots in the presence of different amounts of inhibitor are all straight lines parallel to that obtained in the absence of inhibitor. This type of behavior was attributed (238) to a combination of the inhibitor solely with the ES complex but an alternate explanation (250) is that the inhibitor affects only k_3 in the case where $K_m = k_3/k_1$. Thus, the inhibitor produces the same proportional changes in $V_{max.}$ and K_m.

5. Effect of pH

Because it involves a readily controlled experimental variable, the effect of pH upon rate is included routinely in the description of most enzymes. The customary bell-shaped curve, obtained by plotting velocity as a function of pH, defines the permissible pH range where the reaction occurs at a measurable rate. Analysis of pH curves also may provide an indication of the prototropic groups at the "active site" of the enzyme. Theoretical interpretations to account for the observed effects of pH upon enzymic reactions have been presented in several extensive reviews (251–256).

It is apparent that the pH may affect enzymic reactions by influencing: (*1*) ionization of the enzyme, specifically at the "active site"; (*2*) ionization of the substrate or coenzyme; and (*3*) the equilibrium between active and inactive enzyme. For most investigations, however, the latter two effects may be neglected since in the narrow pH range usually selected, the substrate (or coenzyme) assumes only one ionic form and there is little denaturation or pH-inactivation of the enzyme.

Ionization of the enzyme cannot be expected to be understood in any detail until the amino acid composition and sequence in the protein is known, yet it is interesting to note that as early as 1911, Michaelis and Davidsohn (257) suggested that the pH optimum curves, available then for only a few enzymes, were referable to ionization of groups on the enzyme surface. They were incorrect, however, in their assumption that the pH optimum corresponded to the isoelectric point of the enzyme. Haldane (146) later pointed out that the isoelectric point of many enzymes could not be correlated with their pH optima, and it is more probable.

therefore, that the ionization of only a few key groups on the enzyme is necessary for the activity.

A simplified, and remarkably fruitful, treatment for pH effects on enzyme kinetics assumes that there are two key ionizing groups on the enzyme (254). In the neutral pH range proteins have a large number of prototropic groups but it is assumed in this treatment that only two of these groups at the "active site" will directly affect the velocity of the reaction.

$$\underset{\text{inactive}}{\text{E}} \overset{\text{H}^+}{\rightleftharpoons} \underset{\text{active}}{\text{EH}} \overset{\text{H}^+}{\rightleftharpoons} \underset{\text{inactive}}{\text{EH}_2} \tag{146}$$

The further assumption is made that the enzyme–substrate complex will not break down into enzyme and product unless one of the groups is protonated and the other group is proton-free (i.e., the EH form is the enzymatically active form of the protein). Laidler (258,259) has discussed alternate mechanisms where either ES or EH_2S may break down to yield product.

When these pH considerations are superimposed upon the usual formulation of enzyme kinetics, the following interrelationships are obtained (254):

$$\begin{array}{ccccc} \text{E} & & \text{ES} & & \\ \Big\uparrow\Big\downarrow (K_b)_{\text{E}} & & \Big\uparrow\Big\downarrow (K_b)_{\text{ES}} & & \\ \text{S} + \text{EH} & \underset{k_2}{\overset{k_1}{\rightleftharpoons}} & \text{EHS} & \xrightarrow{k_3} & \text{EH} + \text{P} \\ \Big\uparrow\Big\downarrow (K_a)_{\text{E}} & & \Big\uparrow\Big\downarrow (K_a)_{\text{ES}} & & \\ \text{EH}_2 & & \text{EH}_2\text{S} & & \end{array} \tag{147}$$

where the K's are *dissociation* constants:

$$\begin{aligned} (K_a)_{\text{E}} &= (\text{H}^+)(\text{EH})/(\text{EH}_2) & (K_b)_{\text{E}} &= (\text{H}^+)(\text{E})/(\text{EH}) \\ (K_a)_{\text{ES}} &= (\text{H}^+)(\text{EHS})/(\text{EHS}) & (K_b)_{\text{ES}} &= (\text{H}^+)(\text{ES})/(\text{EHS}) \end{aligned} \tag{148}$$

The dashed arrows represent the various dissociations of the free enzyme and the enzyme–substrate complex. Treatment of this mechanism in the usual manner yields a pH-dependent form of the Michaelis-Menten equation:

$$V_{\max.} = k_3(\text{E})_0/[1 + (\text{H}^+)/(K_a)_{\text{ES}} + (K_b)_{\text{ES}}/(H^+)] \tag{149}$$

$$K_m = \left(\frac{k_2 + k_3}{k_1}\right)\left(\frac{1 + \text{H}^+/(K_a)_{\text{E}} + (K_b)_{\text{E}}/(\text{H}^+)}{1 + (\text{H}^+)/(K_a)_{\text{ES}} + (K_b)_{\text{ES}}/(\text{H}^+)}\right) \tag{150}$$

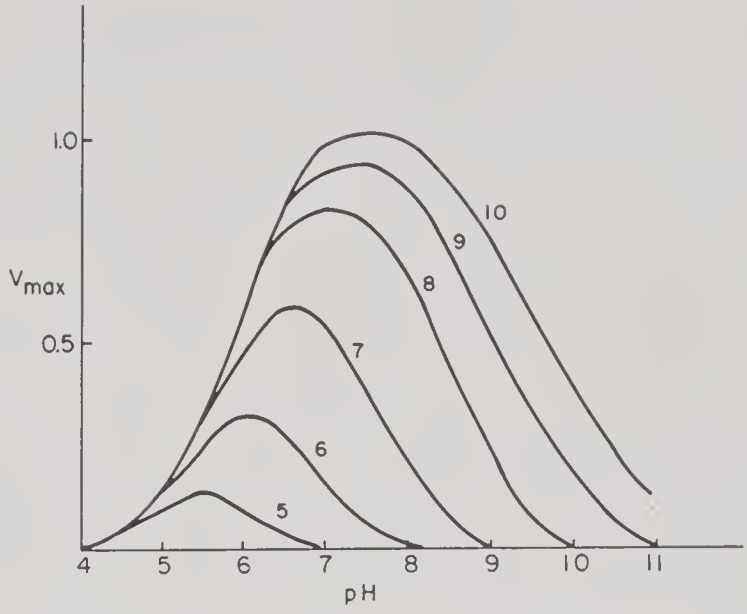

Fig. 1.20. Variation of $V_{max.}$ with pH (254).

Equation (150) has also been derived by Waley (260) and by Friedenwald and Maengwyn-Davies (248); the latter authors also have suggested that the constants, $(K_a)_{ES}$ and $(K_b)_{ES}$, may be evaluated by plotting $1/V_{max.}$ versus $((H^+)_0/(H^+) + (H^+)/(H^+)_0)$ where $(H^+)_0$ represents the hydrogen ion concentration at the optimum pH. Other graphical methods have also been suggested for obtaining the values of the ionization constants (252,255).

If it is found experimentally that $V_{max.}$ varies with pH under conditions of high substrate concentration so that the enzyme is always saturated, the effect of pH must be concerned with the rate-limiting step, i.e. the breakdown of the ES complex. Thus, the enzyme–substrate complex must ionize or its breakdown must be controlled by acid-base catalysis. There is, as yet, no known precedent to support the latter assumption. At lower substrate concentrations, the pH dependence of the velocity, v, is controlled by the ionization of the free enzyme.

Alberty has also presented Equation (149) in a visual fashion (Fig. 1.20). If $k_3(E)_0$ and $(K_a)_{ES}$ are chosen arbitrarily to be 1 and 10^{-6}, respectively, the pH versus $V_{max.}$ curves may be constructed for different values of $(K_b)_{ES}$. In each case, the pH maximum falls at the arithmetic mean of the two pK values. It is evident also that $V_{max.}$ will be 1 only when all of the enzyme–substrate complex is in the EHS form (*cf.* Equations 146 and 147). This favorable condition can occur only if the pK's are at least *three* units apart; if the pK values are closer, the overlap will cause one group to assume an unfavorable ionic form before the other group is entirely in its favorable form. When the pK's are more than 3 units apart, the values can be read

directly from the curve at the points corresponding to $V_{max.}/2$. Even when the pK's are not separated by 3 units, they may still be determined (261) from the hydrogen ion concentrations, $(H^+)_a$ and $(H^+)_b$, corresponding to the two values of $V_{max.}/2$ by the following equations:

$$(K_a)_{ES} = (H^+)_a + (H^+)_b - 4[(H^+)_a(H^+)_b]^{1/2} \quad (151)$$

$$(K_b)_{ES} = (H^+)_a(H^+)_b/(K_a)_{ES} \quad (152)$$

If Equation (149) is divided by Equation (150), a useful relationship is obtained:

$$V_{max.}/K_m = [k_1k_3(E)_0/(k_2 + k_3)]/[1 + (H^+)/(K_a)_E + (K_b)_E/H^+] \quad (153)$$

If $V_{max.}/K_m$ is plotted versus pH, a bell-shaped curve is obtained from which $(K_a)_E$ and $(K_a)_E$, the ionization constants of the free enzyme, may be calculated (251) by the preceding equations (Equations 151 and 152).

Measurements which report the effect of pH on K_m and $V_{max.}$ separately have been obtained only in relatively few cases. In addition to the fumarase-catalyzed reaction (262), which is discussed in detail below, the data for cholinesterase and xanthine oxidase have been treated by Dixon (251) and by Laidler (252), while Smith *et al.* (263) have analyzed their own kinetic data for papain by similar methods. The effect of pH on the K_m alone has been measured for histidine α-deaminase (180), alkaline phosphatase (264), β-fructofuranosidase (265), and arylsulfatase (266); interpretations of these data have been presented by Dixon (251,255).

The theoretical treatment becomes more complex in the case of a reversible reaction where pH affects to a different extent the ability of the enzyme to catalyze the forward and reverse reactions. An example of this occurrence is provided by the enzyme fumarase (Equation 154), which has been extensively studied by Alberty and his colleagues (253,254). The following mechanism has been suggested:

$$\underset{(F)}{\text{Fumarate}} + H_2O \rightleftharpoons \underset{(M)}{\text{malate}} \quad (154)$$

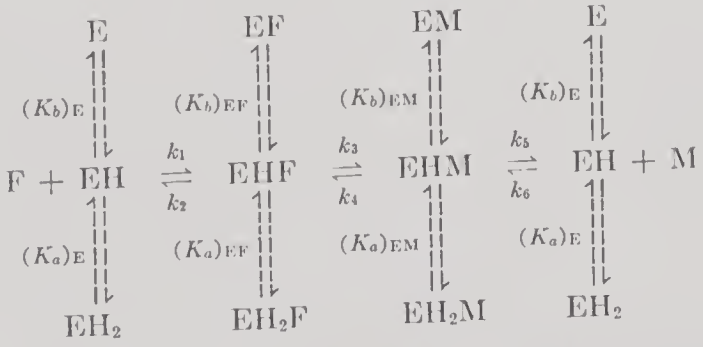

(155)

where (F) and (M) refer to fumarate and malate, respectively, and the dashed arrows represent dissociations of the various enzyme–substrate

complexes. By this generalized treatment, the acid dissociation constants of the two types of enzyme–substrate complex are assumed to differ from each other and to differ from that of the free enzyme.

For the forward reaction, the maximal velocity $(V_{max.})_f$ and the Michaelis constant $(K_m)_f$ are both functions of pH:

$$(V_{max.})_f = \{k_3k_5(E)_0/[k_3 + k_4 + k_5]\}/[1 + (H^+)/(K_a)_{EF} + (K_b)_{EF}/(H^+)] \quad (156)$$

$$(K_m)_f = \frac{(k_2k_5 + k_2k_4 + k_3k_5)(1 + H^+/(K_a)_E + (K_b)_E/(H^+))}{k_1(k_3 + k_4 + k_5)(1 + (H^+)/(K_a)_{EF} + (K_b)_{EF}/(H^+))} \quad (157)$$

The pK values for the various dissociation constants (101) are summarized in Table I.4. It has been suggested that the two prototropic groups at

TABLE I.4
pK Values for Fumarase (101,189,262)

$(pK_a)_E = 6.2$	$(pK_b)_E = 6.8$
$(pK_a)_{EF} = 5.3$[a]	$(pK_b)_{EF} = 7.3$[a]
$(pK_a)_{EM} = 6.6$[a]	$(pK_b)_{EM} = 8.4$[a]

[a] Dixon and Webb, Ref. 7, pp. 137–138, have replotted the primary data and obtained the following values: $(pK_a)_{EF} = 5.7$, $(pK_b)_{EM} = 7.7$; $(pK_a)_{EF} \approx 7$, $(pK_b)_{EM} \approx 9$.

the "active site" of the enzyme are both imidazole residues. The ionization constants for each of the two groups on the enzyme differ appreciably when fumarate and malate are bound. At a given pH, therefore, the enzyme–substrate complex will contain a different number of protons than the free substrate and enzyme, i.e., protons are taken up or liberated by the formation of the E–S complex.

The above interrelationship between the ionization of the two groups at the "active site" and the ability of the enzyme to bind substrate (and the converse relationship in which the binding of substrate alters the pK values of the two groups) is similar to the well-known example of hemoglobin where the ionization of two imidazole groups determines the oxygen-binding capacity of the protein. Wyman (267) has used the phrase "linked functions" to characterize the interdependence of protein, substrate, and (H^+) in the latter example.

Alberty (268) has offered an interesting explanation for the experimental finding that *two* ionizing groups are essential for catalytic activity of fumarase, and that only one of them must be protonated. As shown earlier in Figure 1.2, the double bond of fumarate may be considered to be polarized under the influence of the enzyme, so that the protonated group

donates an H^+ as the basic group accepts a proton from water, thus making available an OH^- ion to complete the reaction.

It is anticipated that other extensive studies on the effect of pH on the kinetic constants of various enzymes will shed more light on the nature of the ionizing groups comprising the "active centers." Edsall (269) has listed a range of values for the pK's and heats of ionization of the common ionizing groups in proteins.

6. Effect of Temperature

A. COLLISION THEORY

As early as 1895 Tammann (270) had observed that enzyme-catalyzed reactions, unlike chemical reactions, are influenced in two ways by temperature. A rise in temperature of 10°C. will usually double or triple the rate of the reaction, but at the same time, the protein portion of the enzyme may undergo thermal denaturation. The range of temperatures, in which one of these processes can be studied to the exclusion of the other, differ for each enzyme. In some instances both reactions may be studied simultaneously (see Section III.6.B), although in most of the following examples kinetic studies have been carried out in a temperature range below the region of thermal denaturation.

As a first approximation, the Arrhenius equation (271):

$$k = PZ \exp \{-E/RT\} \tag{158}$$

can be employed to describe the effect of temperature upon biological reactions. The symbols have the following meanings for bimolecular reactions: k is the specific rate constant, P is a steric factor, Z is the collision frequency, E is the energy of activation, R is the gas constant, and T is the absolute temperature. (This treatment assumes that the reaction involves the enzyme and only one substrate.) When this equation was applied to many biological systems, it was found that the experimental rate was much slower than that predicted by the simplified Arrhenius equation with the P term omitted. The assumption was then made that in the case of enzymes or other large molecules, every energetically effective collision might not result in reaction because the collision did not occur at an "active center" of the large molecule. P was defined, therefore, as a steric factor ($P < 1$).

Equation (158) can be rewritten in the following manner:

$$\log k = -(E/2.3R)(1/T + C) \tag{159}$$

where C represents a function of the product, PZ. After k for a particular reaction has been measured at several temperatures, a plot of $\log k$ against

$1/T$ is fitted to the best straight line by the least squares method, and the slope of the line is $-E/2.3R$.

Measured in temperature ranges where the thermal denaturation of the proteins was insignificant, the activation energies have been determined for a number of enzyme-catalyzed reactions. These values have been compiled in several extensive reviews (13,16,272–274). In many instances the Arrhenius plots (log k versus $1/T$) appear to consist of two linear segments with different slopes, rather than a single straight line with a constant slope. Nonlinear plots are usually concave downward (*e.g.*, urease (171, 275,276)), although in one instance, fumarase (in alkaline solution only) (277), the plot is concave upward. A break in the Arrhenius plot has been interpreted to mean that a change occurs in the nature of the reaction at a certain "critical temperature" (275,278–280). Kistiakowsky and Lumry (281) offered the following objections to the two-segment plots: (*1*) in ordinary chemical kinetics curvatures (<100 cal. deg.$^{-1}$) are commonly encountered but such sharp breaks imply a phase transition of a reactant; (*2*) at best, rate measurements are only accurate enough to establish that the straight segments are joined by a curved segment over a range of several degrees; (*3*) if the curvature were so limited to a few degrees the activation energies would have to differ by several hundred thousand calories; (*4*) even if the enzyme exists in two catalytically active forms in equilibrium with each other, two straight segments joined by a curved line over several degrees would again imply $\Delta H \approx 200{,}000$ cal. mole^{-1} and $\Delta S \approx 700$ cal. mole^{-1} deg.$^{-1}$ for the equilibrium reaction. In agreement with a similar suggestion by Morales (282), these authors have proposed that the Arrhenius plots of enzymic reactions are more accurately interpreted in terms of the enzyme existing in equilibrium between two forms, active and inactive. The inactive form may result from thermal denaturation or from the combination with inhibitors. At low temperatures, or in the absence of an inhibitor, the reaction will be characterized by the true activation energy, E, whereas, at higher temperatures or in the presence of an inhibitor, the observed activation energy will be modified to $(E - \Delta H)$ where ΔH is the heat of reaction for the equilibrium between the active and inactive forms. This hypothesis predicts either a straight-line plot or a gradually curving plot with a lower activation energy at higher temperatures. A careful investigation of the urease-catalyzed reaction (281) showed that, in the absence of sulfite ion, the Arrhenius plot is a straight line between 5 and 20°C. with an activation energy of 8,830 cal. mole^{-1}. In the presence of sulfite ion, however, the apparent activation energy rises to about 15,000 cal. mole^{-1} near 5°C., and the heat of the reaction for the inhibition by sulfite is about $-29{,}000$ cal. mole^{-1}.

B. TRANSITION STATE THEORY

In enzyme kinetics and in chemical kinetics, obvious discrepancies appeared in the application of collision theory to the various problems. The transition state theory was developed in order to provide a more rational interpretation of thermal data and its widespread utility has been amply documented (283,284).

Transition state theory has been successful in predicting the absolute reaction rates for certain simple chemical reactions, but the complexity of enzymic reactions has limited its utility in this field. The theory provides, however, reasonable thermodynamic constants for an enzymic process where the rate constant is known and it is able, moreover, to explain satisfactorily the effects of pressure and temperature upon enzymic reactions. More recently, Eyring and his colleagues (12,285) have extended this formulation to such complex processes as the conduction of impulses in nerve tissue, the transfer of substances across a membrane, and other complex physiological processes.

The basic equation of the transition state theory takes the equivalent forms:

$$k = (k'T/h) \exp\left\{-\Delta F^{\ddagger}/RT\right\} = (k'T/h) \exp\left\{-\Delta H^{\ddagger}/RT\right\} \exp\left\{\Delta S^{\ddagger}/R\right\} \quad (160)$$

where k is the rate constant, k' the Boltzmann constant, h the Planck constant, T the absolute temperature, R the gas constant and $\Delta F^{\ddagger}$, $\Delta H^{\ddagger}$, and $\Delta S^{\ddagger}$ the free energy, heat, and entropy of activation, respectively. The energy of activation term in the collision theory (*cf.* Equation 158) is replaced by a *free energy* of activation which, in turn, may be subdivided into terms containing the heat and entropy of activation. Since the experimental energy of activation, E, is related to the heat of activation as follows:

$$E = \Delta H^{\ddagger} + RT \quad (161)$$

the right-hand member of Equation (160) may be altered to contain the energy of activation:

$$k = (ek'T/h) \exp\left\{-E/RT\right\} \exp\left\{\Delta S^{\ddagger}/R\right\} \quad (162)$$

For a typical biochemical reaction, carried out at 38°C., $k'T/h$ in the above equations, has the value 6.47×10^{12} sec.$^{-1}$. Under most experimental conditions, i.e., $T \approx 20$ to 30°C., E will be larger than $\Delta H^{\ddagger}$ by about 600 cal./mole. Employing the above equations, LuValle and Goddard (286) have made a series of interesting calculations concerning the limits of these quantities in biological processes. For a hypothetical reaction where the

entropy of activation is zero and the reaction is monomolecular with a half-life of about one minute, $\Delta F\ddagger$ will be of the order of 21 kcal. mole^{-1} (about 22 kcal. mole^{-1} for E).

Thermal Denaturation of Proteins. One of the first applications of the transition state theory to biochemistry was in connection with the kinetics of protein denaturation (15,287–289). This type of reaction may be represented by the equation:

$$S \rightleftharpoons S^* \rightleftharpoons P \tag{163}$$

where S is the native protein, P the denatured product, and S* the transition state complex. In general, P represents an *irreversibly* denatured protein which is incapable of returning to the native state. Having determined the rate for irreversible denaturation of a protein as a function of temperature, a plot of log k versus $1/T$ yields the energy of activation, E, which is converted to $\Delta H\ddagger$ by Equation (161). $\Delta S\ddagger$ is calculated from Equation (160) and $\Delta F\ddagger$ from the familiar thermodynamic equation:

$$\Delta F\ddagger = \Delta H\ddagger - T\Delta S\ddagger \tag{164}$$

Table I.5 is a compilation of data for the unimolecular thermal denaturation of a number of proteins and enzymes. It is interesting to note that $\Delta F\ddagger$ is nearly constant for a number of these reactions; larger values of $\Delta H\ddagger$ are compensated for by larger values of $\Delta S\ddagger$. Experimentally, denaturation of all the proteins listed takes place at a comparable rate, a fact not readily apparent from an inspection of the $\Delta H\ddagger$ (or $\Delta E\ddagger$) values and the collision theory formulation.

TABLE I.5
Thermodynamic Values for the Thermal Denaturation of Proteins

Protein	Temp., °C.	$\Delta F\ddagger$, kcal. mole^{-1}	$\Delta H\ddagger$, kcal. mole^{-1}	$\Delta S\ddagger$, cal. mole^{-1} deg.$^{-1}$	Ref.
Insulin	80	27.20	35.60	23.8	290
Trypsin	50	25.70	40.00	44.7	291
Emulsin	60	23.20	45.00	65.3	270
Solanain	60	25.10	61.30	109	292
Hemoglobin	60.5	24.70	75.60	153	293
Leucosin	55	23.62	84.30	175	294
Invertase	50	25.50	110.40	263	294
Egg albumin	65	25.40	132.00	316	293
Vibriolysin	50	22.70	128.00	326	295
Tetanolysin	50	24.35	172.60	459	295
Hemolysin	50	24.60	198.00	537	295

An even more convincing demonstration of the power of the transition state theory was given by Stearn (15) using various data on the *reversible* thermal inactivation of trypsin. Such a reaction may be represented by the equilibrium between S, S*, and P (Equation 163), where ΔF (and similarly, ΔH and ΔS) refers to the over-all equilibrium, $\Delta F_1\ddagger$ to the forward direction (inactivation), and $\Delta F_2\ddagger$ to the reverse direction (reactivation). Mirsky and Anson (296) measured the equilibrium between native and denaturated trypsin in the temperature range 40 to 50°C. At 50°C. k was found to be 7.20 and hence, $\Delta F = 1{,}269$ cal. mole^{-1}. ΔH was measured by these same authors and found to be 67,000 cal. mole^{-1}. ΔS is, therefore, calculated to be 213.1 cal. mole^{-1}. Pace (291) measured the energy of activation for the forward reaction and found $E_1 = 40{,}800$ cal. mole^{-1}, which corresponds to $\Delta H_1\ddagger = 40{,}160$ cal. mole^{-1}. The rate constant for the forward action, k_1 is known to be 2.83×10^{-5}. From Equation (160) $\Delta F_1\ddagger$ is calculated to be 25,700 cal. mole^{-1} and $\Delta S_1\ddagger$ to be 44.7 cal. mole^{-1} deg.$^{-1}$. The corresponding thermodynamic values for the reverse reaction are readily determined by the simple relationship:

$$\Delta F = \Delta F_1\ddagger - \Delta F_2\ddagger \tag{165}$$

Thus, $\Delta F_2\ddagger = 27{,}000$ cal. mole^{-1}, $\Delta H_2\ddagger = -27{,}400$ cal. mole^{-1}, and $\Delta S_2\ddagger = -168.4$ cal. mole^{-1} deg.$^{-1}$. In terms of the collision theory, it would be difficult to explain the large negative value of $\Delta H_2\ddagger$, for this would predict a very fast rate for the reverse reaction. On the other hand, no difficulty is encountered in the interpretation by the transition state theory. The large negative $\Delta H_2\ddagger$ is balanced by an equally large loss in entropy so that $\Delta F_2\ddagger$ is of the same order of magnitude as $\Delta F_1\ddagger$ and the rates are nearly equal for the reaction in either direction. From Equation (162) and the above values, k_2 is calculated to be 4.3×10^{-6}; in good agreement, the value of k_2 obtained from K and k_1 is 3.9×10^{-6}.

A thorough study of the experimental techniques and a detailed analysis of the data for the reversible thermal denaturation of proteins has been given by Kunitz (297) for crystalline soy bean trypsin inhibitor and by Eisenberg and Schwert (298) for chymotrypsinogen. A summary of the thermodynamic values for this example and the preceding investigation is given in Table I.6.

Stearn (15) has discussed the implications of the large positive entropy changes associated with protein denaturation. Since no chemical decomposition takes place, it is suggested that many weak hydrogen bonds are broken during the denaturation. During the first phase of the denaturation, relatively few bonds are broken with little change in configuration and only small increases in entropy. This loosening process continues until the molecule is so weakened that the breaking of a few additional bonds

TABLE I.6
Thermodynamic Values for the Reversible Thermal Denaturation of Proteins

Value	Trypsin (289,291,296)	Chymotrypsinogen (298)	Crystalline soy bean trypsin inhibitor (297)
ΔF, kcal. mole^{-1}	−1.269	−1.440	−0.950
ΔH, kcal. mole^{-1}	67.000	99.600	57.300
ΔS, kcal. mole^{-1} deg.$^{-1}$	213.1	316	180
$\Delta F_1\ddagger$	25.700	19.850	24.600
$\Delta H_1\ddagger$	40.160	84.550	55.354
$\Delta S_1\ddagger$	44.7	202	95.4
$\Delta F_2\ddagger$	27.000	21.300	25.500
$\Delta H_2\ddagger$	−27.400	−15.700	−1.946
$\Delta S_2\ddagger$	−168.4	−116	−85
Temperature	50	47.2	50
pH	—	2.0	3.0

results in the collapse of the structure accompanied by a large increase in entropy. Stearn has made an ingenious calculation of the entropy of activation for these processes. Assuming that each bond broken involves a ΔH of 5,000 cal. and a ΔS of 12 cal. deg.$^{-1}$, the experimentally determined $\Delta H\ddagger$ is divided by 5,000 cal. to give a measure of the number of bonds broken. This value, multiplied by 12 cal. deg.$^{-1}$, yields a calculated value of $\Delta S\ddagger$, which is in good agreement with the experimentally determined value, especially in those cases where the number of bonds broken is large.

Caution must be exercised, however, in the interpretation of entropy values since their validity is dependent upon the correct formulation of the standard state of all reactants. In this respect, the difficulty centers principally about the standard state of the enzyme (15,36,281,299,300), which depends upon a knowledge of the exact molecular weight, the number of binding sites for the substrate, and the ionic species present.

Enzymic Reactions. The success of the transition state theory in interpreting the effects of temperature upon simple chemical reactions, including protein denaturation, has led to attempts to extrapolate the theory to enzyme-catalyzed reactions. There is little difficulty, of course, in measuring the variation of velocity of an enzymic reaction as a function of temperature, but analysis of the data in terms of the usual rate constants, k_1, k_2, and k_3, and the Michaelis constant, K_m, can only be accomplished in special instances.

Addition of the transient state theory to the simple Michaelis-Menten formulation may be represented as follows:

$$\mathrm{E} + \mathrm{S} \rightleftharpoons (\mathrm{ES})_1{}^* \rightleftharpoons (\mathrm{ES}) \rightleftharpoons (\mathrm{ES})_2{}^* \rightarrow \mathrm{E} + \mathrm{P} \qquad (166)$$

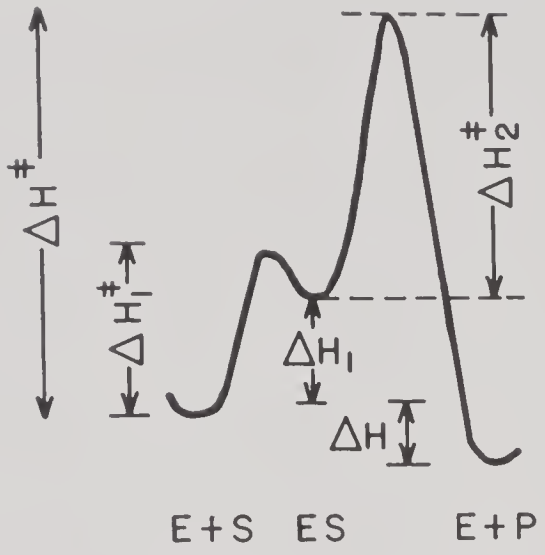

Fig. 1.21. Energy profile showing relation of ΔH, $\Delta H_2\ddagger$, and $\Delta H\ddagger$ as a function of extent of reaction (300).

where E, S, and ES, and P are the enzyme, substrate, enzyme–substrate complex, and product, respectively, and $(ES)_1{}^*$ and $(ES)_2{}^*$ are the transition state complexes interposed upon each part of the reaction. These relationships may be depicted by means of an energy profile diagram (Fig. 1.21). The additional step, $ES \rightleftharpoons (ES)_2{}^* \rightleftharpoons EP \rightleftharpoons (EP)^* \rightarrow E + P$, and the expanded formulation to include a reversible reaction (274) are both neglected here for simplicity.

As described earlier in this section, the initial velocities of a number of enzymic reactions have been measured over a limited temperature range, where protein denaturation is not encountered, and the results plotted as log v versus $1/T$ in order to obtain E, and hence ΔH. To understand the significance of the experimental ΔH value in terms of Figure 1.21, it is necessary to have information about the relative order of magnitude of the principal rate constants, and to carry out measurements of the effect of temperature on K_m and $V_{max.}$. Gibson (301) and Dixon and Webb (302) have discussed some of the experimental pitfalls that may prevent the true value of K_m or $V_{max.}$ from being obtained as the temperature is varied.

If $K_m = k_2/k_1$, the temperature measurements are being made on a true equilibrium from which the Arrhenius plot yields ΔH, ΔF_1, can be calculated from the equilibrium constant, K_m, and ΔS, from Equation (164). These thermodynamic values are for the *over-all* reaction involving combination of enzyme with substrate, and yield no information about the nature of $\Delta H_1\ddagger$, $\Delta F_1\ddagger$, or $\Delta S_1\ddagger$.

When $K_m = k_3/k_1$, a plot of log K_m versus $1/T$ will give the *difference* between the heats of activation of the processes of breakdown and formation of the ES complex, i.e., $\Delta H_2\ddagger - \Delta H_1\ddagger$. Since $V_{max.} = k_3 e$, the effect

TABLE I.7
Heat and Entropy of Activation for Enzymic Reactions (from Laidler (306))

Enzyme	Substrate	Thermodynamic values, kcal./mole				Ref.
		$\Delta H_1‡$ or ΔH_1	$\Delta S_1‡$ or ΔS_1	$\Delta H_2‡$	$\Delta S_2‡$	
Pepsin	Carbobenzoxy-L-glutamyl-L-tyrosine ethyl ester	23.1	14.1	20.7	−6.5	299
Pepsin	Carbobenzoxy-L-glutamyl-L-tyrosine	20.2	2.6	17.2	−21.8	299
Trypsin	Benzoyl-L-arginamide			14.9	−8.2	307
Trypsin	Benzoyl-L-arginine ester			11.2	−16.5	169
Trypsin	Sturin			11.8	−6.7	307
Trypsin	Chymotrypsinogen	16.3	8.5			307
Chymotrypsin	Methyl hydrocinnamate	11.5	−23.2	16.8	−11.8	308
Chymotrypsin	Methyl-DL-α-chloro-β-phenylpropionate	6.9	−33.0	15.4	−13.2	308
Chymotrypsin	Methyl-L-β-phenyllactate	3.1	−47.2	11.1	−23.4	308
Chymotrypsin	Acetyl-L-tyrosine ethyl ester			11.5	−10.7	308
Chymotrypsin	Benzoyl-L-tyrosine ethyl ester	0.8	−38.5	9.2	−21.4	309
Chymotrypsin	Benzoyl-L-phenylalanine ethyl ester			12.5	−11.0	308
Chymotrypsin	Benzoyl-tyrosyl-glycyl-amide			11.5	−19.8	307
Chymotrypsin	Benzoyl-L-tyrosinamide	3.7	−43.0	14.6	−13.0	309
Carboxypeptidase	Carbobenzoxyglycyl-L-tryptophan	9.9	−8.5	9.9	−19.8	145
Carboxypeptidase	Carbobenzoxyglycyl-L-phenylalanine	9.6	−8.5	9.6	−18.5	145
Carboxypeptidase	Carbobenzoxyglycyl-L-leucine	11.0	−7.5	8.6	−20.0	145
Adenosine triphosphatase (ATP-ase)	ATP	21.0	44.0	13.0	−8.0	310
Urease	Urea	6.8	−6.8	9.7	−7.2	311

of temperature on $V_{max.}$ yields a value for $\Delta H_2‡$, provided that the *molal* concentration of enzyme, e, is known. Knowing $\Delta H_2‡$, $\Delta H_1‡$ can be obtained from the above considerations. $\Delta H_1‡$ can also be determined by measurements at low substrate concentration when $v = k_3e/K_m = k_1e$. Using rapid flow techniques, Bonnichsen *et al.* (303) have studied the effect of temperature on the direct combination of H_2O_2 and catalase, and have found the value of $E = 1.7$ kcal./mole for the plot of log k versus $1/T$.

The corresponding value of $\Delta H_1\ddagger$ is 1.1 kcal./mole, which demonstrates the power of the enzyme to reduce the activation energy below 17 kcal./mole for the uncatalyzed reaction (304,305).

Previously, the extreme cases where K_m is a function of only two rate constants have been considered. If K_m is a function of all three constants, plots of log K_m versus $1/T$ yield a "ΔH" value which is a composite of ΔH, $\Delta H_1\ddagger$, and $\Delta H_2\ddagger$.

Laidler (306) has prepared a summary of thermodynamic values (heat content and entropy changes) for various enzymic reactions. These data are reproduced in Table I.7 except that ΔH, rather than E, values are given. When the substrate concentration is high, the *breakdown* of the enzyme–substrate complex is rate limiting and the Arrhenius plot yields unequivocally $\Delta H_2\ddagger$. All of the $\Delta H_2\ddagger$ values are positive while the $\Delta S_2\ddagger$ values are negative. Laidler (306) has pointed out that the negative entropy values may be explained by assuming an increase in polarity during the formation of $(ES)_2$* from ES with the concomitant increase in binding of the solvent.

It is more difficult to obtain unequivocal thermodynamic values for the *formation* of the ES complex. At low substrate concentrations the plot of log K_m versus $1/T$ will yield $\Delta H_1\ddagger$ provided that $k_3 \gg k_2$. These conditions are probably fulfilled for the values in Table I.7 where $\Delta S_2\ddagger$ is negative. When the entropy value is positive, it probably represents ΔS_1 for the reversible formation of ES (i.e., in this case $k_2 \gg k_3$ and $K_m = k_2/k_1$.

It is of interest to note that the value of $\Delta H\ddagger$ (the heat of activation for the over-all reaction) for the urease–urea reaction is considerably lower (12.5 kcal./mole) than that for the acid-catalyzed reaction (24.5 kcal./mole)

TABLE I.8
Comparison of Chemical and Enzymic Catalysts

Substrate	Catalyst	$\Delta H\ddagger$ kcal. mole^{-1}	Reference
Hydrogen peroxide	None	17.0–18.0	304,305,312
	I^-	13.5	312,313
	Platinum	11.7	314
	Fe^{2+}	10.1	315
	Catalase	1.7	303
Sucrose	H^+	25.6	14
	Sucrase	11.0	316
Carbonic acid	None	20.5	286
	Carbonic anhydrase	11.7	317
Urea	H^+	24.5	300
	Urease	12.5	300

under similar conditions (300). These data afford another example of the repeatedly observed phenomenon (see Table I.8) that enzyme catalysis is always more efficient than chemical catalysis of the same reaction, i.e., by lowering the activation energy, the rate is increased.

7. Effect of Pressure

Another striking proof of the validity of the transition state theory is furnished by the response of reaction rates to pressure (12). From the original formulation it is readily seen that, at constant pressure, the equivalence:

$$\Delta F = \Delta H - T\Delta S = \Delta E + P\Delta V - T\Delta S \tag{167}$$

leads to the introduction of volume and pressure terms into equations for the transition state theory. Let:

(E_0) = concentration of the total enzyme
(E_d) = concentration of the denatured enzyme
(E_n) = concentration of the native enzyme
(x) = concentration of the substrate
C = k'/h (see Equation (160) for these symbols)
T = absolute temperature
k_1, $\Delta H\ddagger$, and $\Delta S\ddagger$ = rate, heat of activation and entropy of activation for the enzyme-catalyzed reaction
K, ΔH, and ΔS = equilibrium constant, heat, and entropy for the equilibrium: $(E_n \rightleftharpoons (E_d))$

Then:

$$k_1 = CT(E_n)(x) \exp\left\{-\Delta E\ddagger/RT\right\} \exp\left\{-P\Delta V\ddagger/RT\right\} \exp\left\{\Delta S\ddagger/R\right\} \tag{168}$$

$$k = \exp\left\{-\Delta E\ddagger/RT\right\} \exp\left\{-P\Delta V\ddagger/RT\right\} \exp\left\{\Delta S\ddagger/R\right\} \tag{169}$$

$$k_1 = \frac{C'T \exp\left\{-\Delta E\ddagger/RT\right\} \exp\left\{P\Delta V\ddagger/RT\right\}}{1 + \exp\left\{-\Delta E/RT\right\} \exp\left\{P\Delta V/RT\right\} \exp\left\{\Delta S/R\right\}} \tag{170}$$

For reactions involving simple chemical species the expected volume changes are not large (*ca.* 2 to 15 ml.). For larger molecules, however, the volume changes are larger and the effect of pressure more pronounced. A volume increase of 50 ml./mole was observed by Campbell and Johnson (319,320) for the effect of pressure on a rabbit serum antigen–antibody reaction. As Stearn (15) has pointed out, temperature effects rarely lead to a change in the sign of $\Delta H\ddagger$ since, if the reaction proceeds at a measureable rate, $\Delta F\ddagger$ will be positive and only rarely will $\Delta S\ddagger$ overcome the effect of $\Delta H\ddagger$. On the other hand $P\Delta V\ddagger$ may increase or decrease without changing the sign of $\Delta F\ddagger$.

The activation and denaturation of the native enzyme molecule, as well as the action of certain inhibitors, are believed to cause an *increase* in the volume of the enzyme. Such a view requires that the enzyme must unfold and expose a larger surface. It was first predicted and then verified experimentally by Johnson and his colleagues (320,325) that increased pressure, tending to oppose the volume increase, should reverse the above processes. Considering first the effect of temperature, it would follow that at low temperatures increased pressure should *decrease* the reaction rate by opposing the activation process. At high temperatures the effect of pressure would be to *increase* the reaction rate by opposing the denaturation process and helping to maintain the native enzyme. Typical results verifying this hypothesis are illustrated in Figure 1.22, where the luminescence of bacteria is utilized as a measure of reaction rate and the effects of pressures up to several hundred atmospheres have been observed (325).

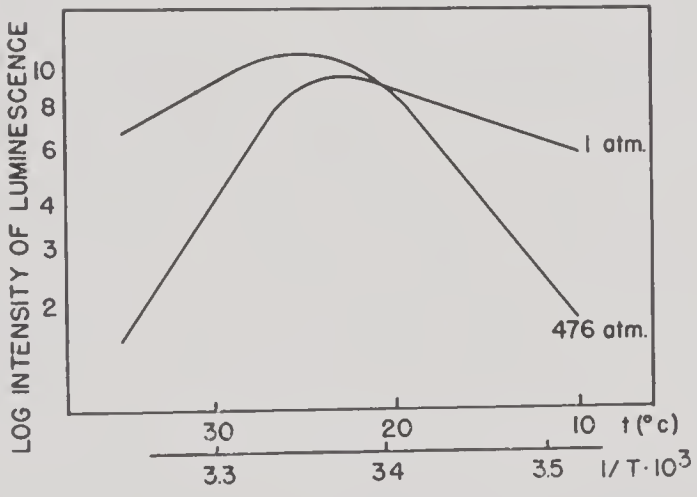

Fig. 1.22. Effect of pressure and temperature on luminescence intensity of *Vibrio phosphorescens* (325).

The action of certain inhibitors may also be reversed by pressure changes. Lipid-soluble substances, e.g., ethyl alcohol, chloroform, novocaine, and phenyl carbamate, reduce the intensity of light emitted by luminescent bacteria (324). By increasing the pressure, the volume increase associated with the enzyme–inhibitor combination may be repressed and the normal luminescence restored. Other substances such as sulfanilamide also decrease the luminescence, but in a different manner, since the application of pressure does not reverse the inhibition.

The effect of pressure on single enzymes has been noted by a number of investigators, notably Curl and Jansen (326) working with trypsin, chymotrypsin, pepsin, and chymotrypsinogen. In agreement with the conclusions expressed above, these authors found that the effect of pressure (P)

on trypsin and chymotrypsin could be expressed by the following diagram:

$$E_i \overset{P}{\leftarrow} E_a \underset{(OH^-)}{\overset{P \text{ or } (H^+)}{\rightleftharpoons}} E_r \qquad (171)$$

The equilibrium between the active (E_a) and reversibly inactive (E_r) form of the enzyme is controlled by pH, the optimum activity occurring just in the alkaline region. If the active form is slightly unfolded, pressure will tend to shift the equilibrium to the inactive form. Some observed irreversible inactivation (E_i) made it necessary to assume a second unidirectional pathway of pressure inactivation.

As in the preceding section which treated the effect of temperature on enzymic reactions, the observed effect of pressure on rate may be interpreted in terms of $\Delta V\ddagger$ for the over-all process, or $\Delta V_2\ddagger$ for the reaction carried out at high substrate concentrations. Values of these thermodynamic constants for certain enzymic reactions are summarized in Table I.9; in certain instances assignments of the volume change as $\Delta V\ddagger$ or $\Delta V_2\ddagger$ had been made by Laidler after an examination of the data.

TABLE I.9
Volume Changes for Enzyme-Catalyzed Reactions

Enzyme	Substrate	$\Delta V\ddagger$	$\Delta V_2\ddagger$	Reference
Luciferase	Luciferin	11.6		318,323,327
Invertase	Sucrose		−8	328
Salivary amylase	Starch		−22	318,329
Pancreatic amylase	Starch		−28	318,329
Pancreatic lipase	Tributyrin	13		318,329
Pepsin	Gelatin	22		318,329
Chymotrypsin	Casein	−13.8		330
	Tyrosine ethyl ester		−13.5	330
Trypsin	β-Lactoglobulin	−36		330
	Benzoyl-L-arginamide		0	330
	Benzoyl-L-arginine isopropyl ester		0	330
	L-Arginine methyl ester		−5.5	330
Adenosine triphosphatase (ATP-ase)	ATP	8 to 23[a]	−32 to −25[a]	331

[a] Depending on KCl concentration.

References

1. N. W. Pirie, in J. Needham and D. E. Green, eds., *Perspectives in Biochemistry*, Cambridge University Press, 1937, pp. 11–22.

2. E. Schrödinger, *What Is Life*, Macmillan, New York, 1946.

3. F. M. Huennekens and H. R. Whiteley, in M. Florkin and H. Mason, eds., *Comparative Biochemistry*, Vol. 1, Academic Press, New York, 1960, pp. 107–180.

4. D. E. Green, in D. E. Green, ed., *Currents in Biochemical Research*, Interscience, New York, 1946, pp. 149–164.

5. J. B. Neilands and P. K. Stumpf, *Outlines of Enzyme Chemistry*, 2nd ed., Wiley, New York, 1958.

6. A. H. Mehler, *Introduction to Enzymology*, Academic Press, New York, 1957.

7. M. Dixon and E. C. Webb, *Enzymes*, Academic Press, New York, 1958.

8. P. D. Boyer, H. Lardy, and K. Myrbäck, *The Enzymes*, 2nd ed., Vol. 1, Academic Press, New York, 1959.

9. C. N. Hinshelwood, *The Chemical Kinetics of the Bacterial Cell*, Oxford, Clarendon Press, 1946.

10. M. Kamen, *Radioactive Tracers in Biology*, Academic Press, New York, 1947.

11. H. G. Bray and K. White, *Kinetics and Thermodynamics in Biochemistry*, Academic Press, New York, 1957, pp. 187–203.

12. F. H. Johnson, H. Eyring, and M. J. Polissar, *The Kinetic Basis of Molecular Biology*, Wiley, New York, 1954.

13. F. M. Huennekens, in S. L. Friess and A. Weissberger, eds., *Investigation of Rates and Mechanisms of Reactions* (*Technique of Organic Chemistry*, Vol. VIII), Interscience, New York, 1953, pp. 535–627.

14. P. Wilson, in H. A. Lardy, ed., *Respiratory Enzymes*, Burgess, Minneapolis, 1944, pp. 16–57.

15. A. E. Stearn, in F. F. Nord, ed., *Advances in Enzymology*, Vol. IX, Interscience, New York, 1949, pp. 25–74.

16. I. W. Sizer, in F. F. Nord and C. H. Werkman, eds., *Advances in Enzymology*, Vol. III, Interscience, New York, 1943, pp. 35–62.

17. N. Rashevsky, *Mathematical Biophysics*, University of Chicago Press, Chicago, 1948.

18. H. G. Bray and K. White, *Kinetics and Thermodynamics in Biochemistry*, Academic Press, New York, 1957, pp. 295–335.

19. J. B. Sumner, *J. Biol. Chem.*, **69**, 435 (1926).

20. R. L. Baldwin, L. J. Gosting, J. W. Williams, and R. A. Alberty, *The Physical Chemistry of Enzymes, Discussions Faraday Soc.*, **No. 20**, 13–23 (1955).

21. J. F. Taylor in H. Neurath and K. Bailey, eds., *The Proteins*, Vol. 1, Part 1, Academic Press, New York, 1953, pp. 1–85.

22. M. Dixon and E. C. Webb, *Enzymes*, Academic Press, New York, 1958, p. xix.

23. S. Schwimmer and A. B. Pardee, in F. F. Nord, ed., *Advances in Enzymology*, Vol. XIV, Interscience, New York, 1953, p. 375.

24. D. E. Green in *The Harvey Lectures*, Academic Press, New York, 1958, pp. 177–227.

25. F. M. Huennekens, *J. Exptl. Cell Research*, **2**, 115 (1951).

26. F. M. Huennekens, in S. L. Friess and A. Weissberger, eds., *Investigation of Rates and Mechanisms of Reactions* (*Technique of Organic Chemistry*, Vol. VIII), Interscience, New York, 1953, Table IX,1.8, p. 610.

27. W. D. McElroy and B. Glass, eds., *The Mechanism of Enzyme Action*, The Johns Hopkins Press, Baltimore, 1954.

28. M. Dixon and E. C. Webb, *Enzymes*, Academic Press, New York, 1958, Chap. VII, p. 299.

29. Symposium on Enzyme Reaction Mechanisms, *J. Cellular Comp. Physiol.*, **54**, Supplement 1 (1959).

30. C. G. Swain and J. F. Brown, *J. Am. Chem. Soc.*, **74**, 2534, 2538 (1952).
31. P. D. Bartlett, in A. R. Todd, ed., *Perspectives in Organic Chemistry*, Interscience, New York, 1956, p. 22.
32. R. A. Alberty, *J. Cellular Comp. Physiol.*, **46**, Supplement 1, 245 (1956).
33. O. Hoffmann-Osterhof, in F. F. Nord, ed., *Advances in Enzymology*, Vol. XIV, Interscience, New York, 1953, p. 219.
34. F. M. Huennekens and H. R. Mahler, in preparation.
35. P. Berg, *J. Am. Chem. Soc.*, **77**, 3163 (1955).
36. H. Neurath and G. W. Schwert, *Chem. Revs.*, **46**, 69 (1950).
37. S. P. Colowick and N. O. Kaplan, *Methods in Enzymology*, Vols. I–IV, Academic Press, New York, 1955–1957.
38. P. R. O'Connor, in S. L. Friess and A. Weissberger, eds., *Investigation of Rates and Mechanisms of Reactions*, (*Technique of Organic Chemistry*, Vol. VIII), Interscience, New York, 1953, Chap. III, Part 1, pp. 69–99.
39. H. Branson, *Cold Spring Harbor Symposia Quant. Biol.*, **13**, 35 (1948).
40. G. Hevesy, *Radioactive Indicators*, Interscience, New York, 1948, Chap. VIII.
41. D. Shemin and D. Rittenberg, *J. Biol. Chem.*, **166**, 627 (1946).
42. D. Shemin and D. Rittenberg, *J. Biol. Chem.*, **153**, 401 (1944).
43. O. Warburg and W. Christian, *Biochem. Z.*, **303**, 40 (1939).
44. E. Adler, H. von Euler, G. Gunther, and M. Plass, *Biochem. J.*, **33**, 1028 (1939).
45. F. Schlenk, in J. B. Sumner and K. Myrbäck, eds., *The Enzymes*, Vol. II, Part 1, Academic Press, New York, 1951, pp. 250–315.
46. S. Ochoa, in F. F. Nord, ed., *Advances in Enzymology*, Vol. XV, Interscience, New York, 1954, pp. 183–270.
47. H. J. Harley and S. E. Wiberley, *Instrumental Analysis*, Wiley, New York, 1954, pp. 3–62.
48. W. West, in A. Weissberger, ed., *Physical Methods of Organic Chemistry*, Vol. I, Part 3, Chapter XXVIII Interscience, New York, 1960, pp. 1799–1958.
49. C. F. Hiskey, in G. Oster and A. W. Pollister, *Physical Techniques in Biological Research*, Vol. 1, 1955, Academie Press, New York, pp. 74–130.
50. J. F. Scott, in G. Oster and A. W. Pollister, *Physical Techniques in Biological Research*, Vol. 1, Aeademie Prsse, New York, pp. 131–203.
51. P. H. Bell and C. R. Stryker, *Science*, **105**, 415 (1947).
52. M. Calvin and G. D. Dorough, *J. Am. Chem. Soc.*, **70**, 699 (1948).
53. K. S. Gibson, *Natl. Bur. Standards (U.S.)* Circ. No. 484.
54. F. M. Huennekens and M. Calvin, *J. Am. Chem. Soc.*, **71**, 4024 (1949).
55. S. F. Velick and P. Strittmatter, *J. Biol. Chem.*, **221**, 265 (1956).
56. G. H. Dixon and H. Neurath, unpublished results; *cf.* E. S. Awad, Ph.D. Thesis of Washington, 1959, Fig. 6, p. 50.
57. H. Hartridge and F. J. W. Roughton, *Proc. Roy. Soc. London*, **A104**, 376 (1923).
58. G. A. Millikan, *Proc. Roy. Soc. London*, **A155**, 277 (1936).
59. B. Chance, *J. Franklin Inst.*, **229**, 455 (1940).
60. B. Chance, E. N. Harvey, F. Johnson, and G. A. Milliken, *J. Cellular Comp. Physiol.*, **15**, 195 (1940).
61. B. Chance, *Rev. Sci. Instr.*, **13**, 158 (1942); **18**, 601 (1947).
62. B. Chance and V. Legallais, *Rev. Sci. Instr.*, **22**, 627 (1951).
63. B. Chance, *The Harvey Lectures*, **1953–54**, Academic Press, New York, 1955, pp. 145–175.
64. B. Chance, *Proc. I.R.E.*, **47**, 1821 (1959).
65. B. Chance, in E. S. G. Barron, ed., *Modern Trends in Physiology and Biochemistry*, Academie Press New York. 1952 p. 25.

66. B. Chance, in A. Weissberger and S. L. Friess, eds., *Investigation of Rates and Mechanism of Reaction*, (*Technique of Organic Chemistry, Vol. VIII*), Interscience, New York, 1395, pp. 627–667.

67. F. J. W. Roughton and B. Chance, in A. Weissberger and S. L. Freiss, eds., *Investigation of Rates and Mechanism of Reaction*, Interscience, New York, 1953, pp. 669–709.

68. W. W. Umbreit, R. H. Burris, and J. F. Stauffer, eds., *Manometric Techniques and Tissue Metabolism*, Burgess, Minneapolis, 1949.

69. M. Dixon, *Manometric Methods*, Cambridge University, Press, Cambridge, 1934.

70. F. M. Huennekens, in S. L. Friess and A. Weissberger, eds., *Investigation of Rates and Mechanisms of Reactions*, (*Technique of Organic Chemistry*, Vol. VIII), Interscience, New York, 1953, pp. 538–554.

71. B. Chance and G. R. Williams, in F. F. Nord, ed., *Advances in Enzymology*, Vol. XVII, Interscience, New York, 1956, pp. 65–134.

72. D. E. Green, in F. F. Nord, ed., *Advances in Enzymology*, Vol. XXI, Interscience, New York, 1959, pp. 73–130.

72a. D. E. Green, "Structure and Function of Subcellular Particles," Plenary Address, *5th Intern. Congr. Biochem.*, (Moscow, Aug. 1961), Pergamon Press, London, 1962.

73. O. Warburg, *Uber den Stoffwechsel der Tumoren*, Springer, Berlin, 1926.

74. J. Barcroft and J. S. Haldane, *J. Physiol.*, **28**, (1902).

75. K. Linderstrøm-Lang, *Nature*, **140**, 108 (1937).

76. C. L. Claff and T. N. Tahmisian, *J. Biol. Chem.*, **179**, 577 (1949).

77. D. Glick, *Techniques of Histo- and Cytochemistry*, Interscience, New York, 1949, pp. 342–393.

78. H. Holter, K. Linderstrøm-Lang, and E. Zeuthen, in G. Oster and A. W. Pollister, *Physical Techniques in Biological Research*, Vol. III, Academic Press, New York, 1956, pp. 578–626.

79. O. H. Muller in A. Weissberger, ed., *Physical Methods of Organic Chemistry*, (Technique of Organic Chemistry, Vol. 1, Part 2), Interscience, New York, 1949, pp. 1785–1885.

80. I. M. Kolthoff and J. J. Lingane, *Polarography*, Interscience, New York, 1941.

81. W. W. Umbreit, R. H. Burris, and J. F. Stauffer, eds., *Manometric Techniques and Tissue Metabolism*, Burgess, Minneapolis, 1949, pp. 89–92.

82. P. W. Davies and F. Brink, Jr., *Rev. Sci. Instr.*, **13**, 524 (1942).

83. E. D. Harris and A. J. Lindsay, *Nature*, **162**, 413 (1948).

84. B. Chance, *Federation Proc.*, **16**, 671 (1957).

85. L. Michaelis, in A. Weissberger, ed., *Physical Methods of Organic Chemistry*, Vol. II, Interscience, New York, 1946, pp. 1051–1114.

86. C. F. Jacobsen, J. Leonis, K. Linderstrøm-Lang, and M. Ottesen, in D. Glick, ed., *Methods of Biochemical Analysis*, Vol. IV, Interscience, New York, 1957, pp. 171–210.

87. W. Heller, in A. Weissberger, ed., *Physical Methods of Organic Chemistry*, Vol. II, Interscience, New York, 1946, pp. 869–988.

88. H. Theorell and A. Ehrenberg, *Arch. Biochem. Biophys.*, **41**, 442 (1952).

89. M. Calvin, *Rev. Mod. Phys.*, **31**, 157 (1959).

90. E. A. Moelwyn-Hughes, in J. B. Sumner and K. Myrback, eds., *The Enzymes*, Vol. 1, Part I, Academic Press, New York, 1950, p. 28.

91. G. B. Kistiakowsky and A. J. Rosenberg, *J. Am. Chem. Soc.*, **74**, 5020 (1952).

92. J. Botts and M. Morales, *Trans. Faraday Soc.*, **49**, 696 (1953).

93. R. Lumry, in P. D. Boyer, H. Lardy, and K. Myrback, eds., *The Enzymes*, 2nd ed., Vol. 1, Academic Press, New York, 1959, pp. 171–173.

94. K. J. Linderstrøm-Lang and J. A. Schellman, in P. D. Boyer, H. Lardy, and K. Myrbäck, eds., *The Enzymes*, 2nd ed., Vol. 1, Academic Press, New York, 1959, pp. 467–479.
95. A. K. Balls and H. N. Wood, *J. Biol. Chem.*, **219**, 245 (1956).
96. G. H. Dixon, W. J. Dreyer, and H. Neurath, *J. Am. Chem. Soc.*, **78**, 4810 (1956).
97. G. H. Dixon and H. Neurath, *J. Am. Chem. Soc.*, **79**, 4558 (1957).
98. G. H. Dixon and H. Neurath, *J. Biol. Chem.*, **225**, 1049 (1957).
99. C. E. McDonald and A. K. Balls, *J. Biol. Chem.*, **227**, 727 (1957).
100. E. D. Eastman and G. K. Rollefson, *Physical Chemistry*, McGraw-Hill, New York, 1947, pp. 396–398.
101. R. A. Alberty, in F. F. Nord, ed., *Advances in Enzymology*, Vol. XVII, Interscience, New York, 1956, pp. 34–35.
102. E. A. Robbins and P. D. Boyer, *J. Biol. Chem.*, **224**, 121 (1957).
103. J. M. Nelson and M. P. Schubert, *J. Am. Chem. Soc.*, **50**, 2188 (1928).
104. B. Chance, *J. Biol. Chem.*, **151**, 553 (1943).
105. M. Dixon and E. C. Webb, *Enzymes*, Academic Press, New York, 1958, pp. 64–73.
106. F. B. Straub, *Enzymologia*, **9**, 143 (1940).
107. H. Theorell and R. Bonnichsen, *Acta Chem. Scand.*, **5**, 1105 (1951).
108. L. Noda, S. A. Kuby, and H. A. Lardy, *J. Biol. Chem.*, **210**, 83 (1954).
109. P. W. Robbins and F. Lipmann, *J. Biol. Chem.*, **233**, 686 (1958).
110. J. H. Northrop, M. Kunitz, and R. M. Herriott, *Crystalline Enzymes*, 2nd ed., Columbia University Press, New York, 1948.
111. E. C. Webb, unpublished observations, cited in Ref. 7, p. 71.
112. G. W. Irving, J. S. Fruton, and M. Bergmann, *J. Biol. Chem.*, **138**, 231 (1941).
113. B. S. Miller and J. A. Johnson, *Arch. Biochem. Biophys.*, **32**, 200 (1951).
114. E. Schutz, *Z. Physiol. Chem.*, **9**, 571 (1885).
115. J. Schutz, *Z. Physiol. Chem.*, **30**, 1 (1900).
116. E. A. Moelwyn-Hughes, *Ergebn. Enzymforsch.*, **6**, 23 (1937).
117. L. Michaelis and M. Menten, *Biochem. Z.*, **49**, 333 (1913).
118. W. Henri, *Compt. rend.*, **135**, 916 (1902); see also *Lois generales de l'action des diastases*, Hermann, Paris, 1903.
119. A. J. Brown, *Trans. Chem. Soc.*, **81**, 373 (1902).
120. M. Dixon and E. C. Webb, *Enzymes*, Academic Press, New York, 1958, p. 76.
121. D. D. Van Slyke and G. E. Cullen, *J. Biol. Chem.*, **19**, 141, 211 (1914).
122. G. E. Briggs and J. B. S. Haldane, *Biochem. J.*, **19**, 338 (1925).
123. B. Chance, *Science*, **109**, 204 (1949).
124. R. A. Alberty, in F. F. Nord, ed., *Advances in Enzymology*, Vol. XVII, Interscience, New York, 1956, pp. 5–6.
125. E. L. King, quoted in Alberty (Ref. 97, p. 10).
126. G. Medwedew, *Enzymologia*, **2**, 1, 31, 53 (1937).
127. G. Weber, "The Physical Chemistry of Enzymes," *Discussions Faraday Soc.*, No. 20, 156 (1955).
128. R. Livingston, in A. Weissberger, ed., *Investigation of Rates and Mechanisms of Reactions*, (*Technique of Organic Chemistry*, Vol. VIII), Interscience, New York, 1953, p. 191.
129. H. Lineweaver and D. Burk, *J. Am. Chem. Soc.*, **56**, 658 (1934).
130. M. Dixon, *Biochem. J.*, **55**, 170 (1953).
131. G. S. Eadie, *J. Biol. Chem.*, **146**, 85 (1942).
132. B. J. H. Hofstee, *Science*, **116**, 24 (1949).
133. M. B. Thorn, *Nature*, **164**, 24 (1949).

134. R. J. Foster and C. Niemann, *J. Am. Chem. Soc.*, **73**, 1552 (1951).
135. V. P. Whittaker and D. H. Adams, *Nature*, **164**, 315 (1949).
136. D. H. Adams and V. P. Whittaker, *Biochem. Biophys. Acta*, **4**, 543 (1950).
137. B. Chance, *Arch. Biochem. Biophys.*, **41**, 415 (1952).
138. B. Chance and R. R. Ferguson, in W. D. Elroy and B. Glass, eds., *Mechanism of Enzyme Action*, Johns Hopkins Press, Baltimore, 1954, p. 399.
139. E. C. Slater, and W. D. Bonner, *Biochem. J.*, **52**, 185 (1952).
140. E. C. Slater, "The Physical Chemistry of Enzymes," *Discussions Faraday Soc.*, **No. 20**, 231, 308 (1955).
141. M. Dixon, "The Physical Chemistry of Enzymes," *Discussions Faraday Soc.*, **No. 20**, 23, 301 (1955); *ibid.*, p. 308.
142. F. J. Roughton, "The Study of Fast Reactions," *Discussions Faraday Soc.*, **No. 17**, 116 (1954).
143. H. Gutfreund, "The Study of Fast Reactions," *Discussions Faraday Soc.*, **No. 17**, 220 (1954).
144. H. Gutfreund, "The Physical Chemistry of Enzymes," *Discussions Faraday Soc.*, **No. 20**, 167 (1955).
145. R. Lumry, E. L. Smith, and R. R. Glatnz, *J. Am. Chem. Soc.*, **73**, 4330 (1951).
146. J. B. S. Haldane, *Enzymes*, Longman, Green, London, 1930.
147. J. E. Snoke and H. Neurath, *Arch. Biochem.*, **21**, 351 (1949).
148. J. E. Snoke and H. Neurath, *J. Biol. Chem.*, **181**, 789 (1949).
149. D. S. Hogness and C. Niemann, *J. Am. Chem. Soc.*, **74**, 3183 (1952).
150. H. Neurath and B. Hartley, *J. Cellular Comp. Physiol.*, **54**, Supplement, 180 (1959).
151. R. Lutwack, H. F. Mower, and C. Niemann, *J. Am. Chem. Soc.*, **79**, 5690 (1957).
152. R. J. Foster and C. Niemann, *J. Am. Chem. Soc.*, **77**, 1886, 3370 (1955).
153. D. T. Manning and C. Niemann, *J. Am. Chem. Soc.*, **80**, 1478 (1958).
154. R. J. Foster, H. J. Shine, and C. Niemann, *J. Am. Chem. Soc.*, **77**, 2378 (1955).
155. R. J. Kerr and C. Niemann, *J. Am. Chem. Soc.*, **80**, 1469 (1958).
156. R. B. Martin and C. Niemann, *J. Am. Chem. Soc.*, **80**, 1481 (1958).
157. H. J. Shine and C. Niemann, *J. Am. Chem. Soc.*, **78**, 1872 (1956).
158. T. H. Applewhite, R. B. Martin, and C. Niemann, *J. Am. Chem. Soc.*, **80**, 1457 (1958).
159. B. R. Hammond and H. Gutfreund, *Biochem. J.*, **61**, 187 (1955).
160. L. W. Cunningham and C. S. Brown, *J. Biol. Chem.*, **221**, 287 (1956).
161. E. Elkins-Kaufman and H. Neurath, *J. Biol. Chem.*, **175**, 893 (1948).
162. G. W. Schwert, *J. Biol. Chem.*, **174**, 411 (1948).
163. H. T. Huang and C. Niemann, *J. Am. Chem. Soc.*, **73**, 1541, 1555 (1951).
164. D. W. Thomas, R. V. MacAllister, and C. Niemann, *J. Am. Chem. Soc.*, **73**, 1548 (1951).
165. H. Neurath and G. DeMaria, *J. Biol. Chem.*, **186**, 653 (1950).
166. G. W. Schwert, H. Neurath, S. Kaufman, and J. E. Snoke, *J. Biol. Chem.*, **172**, 221 (1948).
167. M. Kunitz and J. H. Northrop, *J. Gen. Physiol.*, **17**, 591 (1933).
168. K. M. Harmon and C. Niemann, *J. Biol. Chem.*, **178**, 743 (1949).
169. G. W. Schwert and M. A. Eisenberg, *J. Biol. Chem.*, **179**, 665 (1949).
170. K. J. Laidler and J. P. Hoare, *J. Am. Chem. Soc.*, **71**, 2699 (1949).
171. G. D. Fasmann and C. Niemann, *J. Am. Chem. Soc.*, **73**, 1646 (1951).
172. J. P. Hoare and K. J. Laidler, *J. Am. Chem. Soc.*, **72**, 2487 (1950).
173. K-B. Augustinsson, *Arch. Biochem.*, **23**, 111 (1949).
174. K-B. Augustinsson and D. Nachmansohn, *Science*, **110**, 99 (1949).

175. K. M. Harmon and C. Niemann, *J. Biol. Chem.*, **177**, 601 (1949).
176. O. Bodansky, *J. Biol. Chem.*, **120**, 555 (1937).
177. T. H. Applewhite and C. Niemann, *J. Am. Chem. Soc.*, **77**, 4923 (1955).
178. R. J. Foster and C. Niemann, *Proc. Natl. Acad. Sci., U.S.*, **39**, 999 (1953).
179. M. L. Sweat, L. T. Samuels, and R. Lumry, *J. Biol. Chem.*, **185**, 75 (1950).
180. A. C. Walker and C. L. A. Schmidt, *Arch. Biochem.*, **5**, 445 (1944).
181. M. Bergmann, in F. F. Nord and C. H. Werkman, eds., *Advances in Enzymology*, Vol. II, Interscience, New York, 1942, pp. 49–67.
182. M. Bergmann and J. S. Fruton, in F. F. Nord and C. H. Werkman, eds., *Advances in Enzymology*, Vol. I, 1941, pp. 63–96.
183. I. M. Socquet and K. J. Laidler, *Arch. Biochem. Biophys.*, **25**, 171 (1950).
184. G. W. Schwert and M. T. Hakala, *Arch. Biochem. Biophys.*, **38**, 55 (1952).
185. R. A. Alberty, in F. F. Nord, ed., *Advances in Enzymology*, Vol. XVII, Interscience, New York, 1956, pp. 8–13.
186. M. Dixon and E. C. Webb, *Enzymes*, Academic Press, New York, 1957, pp. 91–96.
187. J. Z. Hearon, S. A. Bernhard, S. L. Friess, D. J. Botts, and M. F. Morales, in P. D. Boyer, H. Lardy, and K. Myrback, eds., *The Enzymes*, 2nd ed., Vol. 1, Academic Press, New York, 1959, pp. 50–155.
188. J. Z. Hearon, *Physiol. Revs.*, **32**, 499 (1952).
189. C. Frieden and R. A. Alberty, *J. Biol. Chem.*, **212**, 859 (1955).
190. V. Massey, *Biochem. J.*, **53**, 67 (1953).
191. R. A. Alberty and R. M. Bock, *Proc. Natl. Acad. Sci. U.S.*, **39**, 895 (1953).
192. T. L. Hill, *J. Am. Chem. Soc.*, **74**, 4710 (1952).
193. D. R. P. Murray, *Biochem. J.*, **24**, 1890 (1930).
194. I. B. Wilson, in W. D. McElroy and B. Glass, eds., *The Mechanism of Enzyme Action*, Johns Hopkins Press, Baltimore, 1954, pp. 642–657.
195. V. Massey, *Biochem. J.*, **53**, 67 (1953).
196. H. Friedrich-Freksa, *Z. Naturforsch.*, **6b**, 397 (1951).
197. B. L. Horecker and J. Gergeley, quoted in A. Kornberg, *J. Biol. Chem.*, **182**, 779(1950).
198. R. A. Alberty, in F. F. Nord, ed., *Advances in Enzymology*, Vol. XVII, Interscience, New York, 1956, pp. 35–37.
199. M. Dixon and E. C. Webb, *Enzymes*, Academic Press, New York, 1957, pp. 117–118.
200. H. Theorell and B. Chance, *Acta. Chem. Scand.*, **5**, 1127 (1951).
201. R. A. Alberty, V. Massey, C. Frieden, and A. R. Fuhlbrigge, *J. Am. Chem. Soc.*, **76**, 2485 (1954).
202. R. M. Boek and R. A. Alberty, *J. Am. Chem. Soc.*, **75**, 1921 (1953).
203. C. Frieden and R. A. Alberty, *J. Biol. Chem.*, **212**, 859 (1955).
204. R. A. Alberty, *J. Am. Chem. Soc.*, **75**, 1928 (1953).
205. M. Dixon and E. C. Webb, *Enzymes*, Academic Press, New York, 1958, pp. 78–81.
206. R. A. Alberty, in F. F. Nord, ed., *Advances in Enzymology*, Vol. XVII, Interscience, New York, 1956, pp. 17–19.
207. H. Segal, J. F. Kachmar, and P. D. Boyer, *Enzymologia*, **15**, 187 (1952).
208. J. F. Kachmar and P. D. Boyer, *J. Biol. Chem.*, **200**, 669 (1953).
209. E. Negelein and H. J. Wulff, *Biochem. Z.*, **293**, 351 (1937).
210. S. A. Kuby, L. Noda, and H. A. Lardy, *J. Biol. Chem.*, **210**, 65 (1954).
211. L. L. Ingraham and B. Makower, *J. Phys. Chem.*, **58**, 226 (1954).
212. K. J. Laidler and I. M. Socquet, *J. Phys. Colloid Chem.*, **54**, 519, 530 (1950).
213. J. E. LuValle and D. R. Goddard, *Quart. Rev. Biol.*, **23**, 197 (1948).

214. J. R. Florini and C. S. Vestling, *Biochim. Biophys. Acta*, **25**, 575 (1957).
215. C. Frieden, *J. Am. Chem. Soc.*, **79**, 1894 (1957).
216. H. Theorell, in D. E. Green, ed., *Currents in Biochemical Research*, Interscience, New York, 1956, p. 293.
217. H. Theorell, in F. F. Nord, ed., *Advances in Enzymology*, Vol. XX, Interscience, New York, 1958, p. 31.
218. B. L. Vallee, *Physiol. Revs.*, **39**, 443 (1959).
219. E. Racker, *J. Biol. Chem.*, **184**, 313 (1950).
220. B. Chance and J. B. Neilands, *J. Biol. Chem.*, **199**, 383 (1952).
221. B. Chance, *Nature*, **169**, 215 (1952).
222. H. Theorell and A. P. Nygaard, *Acta. Chem. Scand.*, **8**, 877 (1954).
223. M. Dixon and E. C. Webb, *Enzymes*, Academic Press, New York, 1958, pp. 113–117.
224. H. Theorell, A. P. Nygaard, and R. Bonnichsen, *Acta. Chem. Scand.*, **9**, 1148 (1955).
225. K. Dalziel and H. Theorell, *Biochem. J.*, **66**, 34P, (1957).
226. A. P. Nygaard and H. Theorell, *Acta. Chem. Scand.*, **9**, 1300 (1955).
227. D. Nachmansohn and I. B. Wilson, in F. F. Nord, ed., *Advances in Enzymology*, Vol. XII, 259 (1951).
228. I. B. Wilson in "The Physical Chemistry of Enzymes," *Discussions Faraday Soc.*, **No. 20**, 119 (1955).
229. W. D. McElroy, *Quart. Rev. Biol.*, **22**, 25 (1947).
230. T. S. Work and E. Work, *The Basis of Chemotherapy*, Interscience, New York, 1948.
231. D. W. Woolley, *A Study of Antimetabolites*, Wiley, New York, 1952.
232. L. Massart, in J. B. Sumner and K. Myrbäck, eds., *The Enzymes*, Vol. I, Part 1, Academic Press, New York, 1950, pp. 307–42.
233. M. Dixon and E. C. Webb, *Enzymes*, Academic Press, New York, 1958, pp. 174–176.
234. E. Elkins-Kaufman and H. Neurath, *J. Biol. Chem.*, **178**, 645 (1949).
235. A. Hunter and C. E. Downs, *J. Biol. Chem.*, **157**, 427 (1945).
236. J. Lederberg, *J. Bact.*, **60**, 381 (1950).
237. M. J. Osborn, M. Freeman, and F. M. Huennekens, *Proc. Soc. Exptl. Biol. Med.*, **97**, 429 (1958).
238. E. R. Ebersole, C. Guttentag, and P. W. Wilson, *Arch. Biochem.*, **3**, 399 (1944).
239. P. Wilson, in H. A. Lardy, ed., *Respiratory Enzymes*, Burgess, Minneapolis, 1944, p. 24.
240. G. B. Kistiakowsky and W. H. R. Shaw, *J. Am. Chem. Soc.*, **75**, 866 (1953).
241. O. H. Straus and A. Goldstein, *J. Gen. Physiol.*, **26**, 559 (1943).
242. A. Goldstein, *J. Gen. Physiol.*, **27**, 529 (1944).
243. D. K. Myers, *Biochem. J.*, **52**, 46 (1952).
244. W. W. Ackermann and V. R. Potter, *Proc. Soc. Exptl. Biol. Med.*, **72**, 1 (1949).
245. J. A. Bain, *Prod. Soc. Exptl. Biol. Med.*, **72**, 9 (1949).
246. R. A. Alberty in F. F. Nord, ed., *Advances in Enzymology*, Vol. XVII, Interscience, New York, 1956, pp. 19–25.
247. A. G. Ogston in "The Physical Chemistry of Enzymes," *Discussions Faraday Soc.*, 161 (1955).
248. J. S. Friedenwald and G. D. Maengwyn-Davies in W. D. McElroy and B. Glass, eds., *The Mechanism of Enzyme Action*, Johns Hopkins Press, Baltimore, 1954, p. 154.
249. M. Dixon and E. C. Webb, *Enzymes*, Academic Press, New York, 1958, pp. 174–179.

250. K. S. Dodgson, B. Spencer, and K. Williams, *Nature*, **177**, 432 (1956).
251. M. Dixon, *Biochem. J.*, **55**, 161 (1953).
252. K. J. Laidler, *Trans. Faraday Soe.*, **51**, 550 (1955).
253. R. A. Alberty, *J. Cell. Comp. Physiol.*, **47**, Supplement 1, 245 (1956).
254. R. A. Alberty, in F. F. Nord, ed., *Advances in Enzymology*, Vol. XVII, Interscience, New York, 1956, pp. 26–34.
255. M. Dixon and E. C. Webb, *Enzymes*, Academic Press, New York, 1958, pp. 120–150.
256. K. J. Laidler, *The Chemical Kinetics of Enzyme Action*, Clarendon Press, Oxford, 1958, pp. 117–162.
257. L. Michaelis and H. Davidsohn, *Biochem. Z.*, **35**, 386 (1911).
258. K. J. Laidler, *Trans. Faraday Soc.*, **51**, 528 (1955).
259. K. J. Laidler, *Trans. Faraday Soc.*, **51**, 540 (1955).
260. S. G. Waley, *Biochim. Biophys. Acta*, **10**, 27 (1953).
261. R. A. Alberty and V. Massey, *Biochem. Biophys. Acta*, **13**, 347 (1954).
262. V. Massey and R. A. Alberty, *Biochim. Biophys. Acta*, **13**, 354 (1954).
263. E. L. Smith, B. L. Finkle, and A. Stockell, "The Physical Chemistry of Enzymes," *Discussions Faraday Soc.*, **No. 20**.
264. R. K. Morton, *Biochem. J.*, **65**, 674 (1957).
265. K. Josephson, *Z. Physiol. Chem.*, **134**, 50 (1924).
266. K. S. Dodgson, B. Spencer, and K. Williams, *Biochem. J.*, **61**, 374 (1955).
267. J. Wyman, *Advances in Protein Chem.*, **4**, 407 (1948).
268. R. A. Alberty, in F. F. Nord, ed., *Advances in Enzymology*, Vol. XVII, Interscience, New York, 1956, pp. 49–54.
269. E. J. Cohn and J. T. Edsall, *Proteins, Amino Acids and Peptides*, Rheinhold, New York, 1943, p. 445.
270. G. Tammann, *Z. Physik. Chem.*, **8**, 426 (1895).
271. S. Arrhenius, *Z. Physik. Chem.*, **4**, 226 (1889).
272. F. M. Huennekens, in S. L. Friess and A. Weissberger, eds., *Investigation of Rates and Mechanisms of Reactions* (*Technique of Organic Chemistry*, Vol. VIII), Interscience, New York, 1953, pp. 598–602.
273. K. J. Laidler, *The Chemical Kinetics of Enzyme Action*, Clarendon Press, Oxford, 1958, pp. 194–209.
274. M. Dixon and E. C. Webb, *Enzymes*, Academic Press, New York, 1958, pp. 150–170.
275. I. W. Sizer, *J. Gen. Physiol.*, **22**, 719 (1939).
276. I. W. Sizer, *J. Biol. Chem.*, **132**, 209 (1940).
277. V. Massey, *Biochem. J.*, **53**, 72 (1953).
278. W. J. Crozier, *J. Gen. Physiol.*, **7**, 189 (1924).
279. W. J. Crozier, H. Federight, and T. B. Stier, *J. Gen. Physiol.*, **7**, 123, 137, 151, 429, 565, 571, 699, 705 (1924).
280. I. W. Sizer, *J. Gen. Physiol.*, **21**, 695 (1938).
281. G. B. Kistiakowsky and R. Lumry, *J. Am. Chem. Soc.*, **71**, 2006 (1949).
282. M. F. Morales, *J. Cellular Comp. Physiol.*, **30**, 303 (1947).
283. R. Livingston, in S. L. Friess and A. Weissberger, eds., *Investigation of Rates and Mechanisms of Reactions*, (*Technique of Organic Chemistry*, Vol. VIII), Interscience, New York, 1953, pp. 1–36.
284. S. Glasstone, K. Laidler, and H. Eyring, *The Theory of Rate Processes*, McGraw-Hill, New York, 1941.
285. H. Eyring, R. Lumry, and J. W. Woodbury, *Record of Chemical Progress*, 1949, p. 100.

286. J. E. LuValle and D. R. Goddard, *Quart. Rev. Biol.*, **23**, 197 (1948).
287. H. Eyring and A. E. Stearn, *Chem. Revs.*, **24**, 253 (1939).
288. A. E. Stearn and H. Eyring, *Chem. Revs.*, **29**, 509 (1941).
289. A. E. Stearn, in F. F. Nord and R. Wiedenhagen, eds., *Ergenbnisse der Enzymforschung*, Vol. VII, Akadem, Verlagsgesellschaft, Leipzig, 1938, p 1.
290. T. D. Gerlough and R. W. Bates, *J. Pharmacol.*, **45**, 19 (1932).
291. J. Pace, *Biochem. J.*, **24**, 606 (1930).
292. W. Kauzmann, A. M. Chase, and E. H. Brigham, *Arch. Biochem.*, **24**, 281 (1949).
293. P. S. Lewis, *Biochem. J.*, **20**, 965, 978 (1926).
294. H. von Euler and I. Laurin, *Z. physiol. Chem.*, **108**, 64 (1919); **110**, 55 (1920).
295. L. W. Famulener and T. Madsen, *Biochem. Z.*, **11**, 186 (1908).
296. A. E. Mirsky and M. L. Anson, *J. Gen. Physiol.*, **17**, 393 (1934).
297. M. Kunitz, *J. Gen. Physiol.*, **32**, 241 (1948).
298. M. A. Eisenberg and G. W. Schwert, *J. Gen. Physiol.*, **34**, 583 (1951).
299. E. J. Casey and K. J. Laidler, *J. Am. Chem. Soc.*, **72**, 2159 (1950).
300. K. J. Laidler and J. P. Hoare, *J. Am. Chem. Soc.*, **72**, 2489 (1950).
301. K. D. Gibson, *Biochim. Biophys. Acta*, **10**, 221 (1953).
302. M. Dixon and E. C. Webb, *Enzymes*, Academic Press, New York, 1958, pp. 161–162.
303. R. Bonnichsen, B. Chance, and H. Theorell, *Acta. Chem. Scand.*, **1**, 685 (1947).
304. J. Williams, *Trans. Faraday Soc.*, **24**, 245 (1928).
305. C. Pana, *Trans. Faraday Soc.*, **24**, 486 (1928).
306. K. J. Laidler, *The Chemical Kinetics of Enzyme Action*, Clarendon Press, Oxford, 1958, pp. 198 and 202.
307. J. A. V. Butler, *J. Am. Chem. Soc.*, **63**, 2971 (1941).
308. J. E. Snoke and H. Neurath, *J. Biol. Chem.*, **182**, 577 (1950).
309. S. Kaufman, H. Neurath, and G. W. Schwert, *J. Biol. Chem.*, **177**, 792 (1949).
310. L. Oullet, K. J. Laidler, and M. F. Morales, *Arch. Biochem. Biophys.*, **39**, 37 (1952).
311. M. C. Wall and K. J. Laidler, *Arch. Biochem. Biophys.*, **43**, 299 (1953).
312. E. A. Moelwyn-Hughes, *The Kinetics of Reaction in Solution*, Oxford University Press, 1933.
313. J. H. Walton, *Z. phys. Chem.*, **47**, 185 (1904).
314. G. Bredig and R. M. von Berneck, *Z. phys. Chem.*, **31**, 258 (1899).
315. J. H. Baxendale, M. G. Evans, and G. S. Park, *Trans. Faraday Soc.*, **42**, 155 (1946).
316. I. W. Sizer and E. S. Josephson, *Food Research*, **7**, 201 (1942).
317. M. Kiese, *Biochem. Z.*, **307**, 400 (1941).
318. K. J. Laidler, *The Chemical Kinetics of Enzyme Action*, Clarendon Press, Oxford, 1958, pp. 210–225.
319. D. H. Campbell and F. H. Johnson, *J. Am. Chem. Soc.*, **68**, 725 (1946).
320. F. H. Johnson and D. H. Campbell, *J. Biol. Chem.*, **163**, 689 (1946).
321. F. H. Johnson, H. Eyring, and R. W. Williams, *J. Cellular Comp. Physiol.*, **20**, 247 (1942).
322. F. H. Johnson and I. Lewin, *J. Cellular Comp. Physiol.*, **28**, 1, 23, 47, 77 (1946).
323. D. E. Brown, F. H. Johnson, and D. Marsland, *J. Cellular Comp. Physiol.*, **20**, 151 (1942).
324. F. H. Johnson, D. E. Brown, and D. Marsland, *J. Cellular Comp. Physiol.*, **20**, 269 (1942).
325. F. H. Johnson, D. E. Brown, and D. Marsland, *Science*, **95**, 200 (1942).
326. A. L. Curl and E. F. Jansen, *J. Biol. Chem.*, **184**, 45 (1950); **185**, 713 (1950).

327. H. Eyring and J. L. Magee, *J. Cell. Comp. Physiol.*, **20**, 169 (1942).
328. H. Eyring, F. H. Johnson, and R. L. Gensler, *J. Phys. Colloid Chem.*, **50**, 453 (1946).
329. J. Benthaus, *Biochem. Z.*, **311**, 108 (1941–42).
330. H. Werbin and A. D. McLaren, *Arch. Biochem. Biophys.*, **31**, 285 (1951); **32**, 325 (1951).
331. K. J. Laidler and A. J. Beardell, *Arch. Biochem. Biophys.*, **55**, 138 (1955).

General References

Alberty, R. A., "Enzyme Kinetics," in F. F. Nord, ed., *Advances in Enzymology*, Vol. XVII, Interscience, New York, 1956, pp. 1–64.

Alberty, R. A., "Symposium on Structure of Enzymes and Proteins," *J. Cellular Comp. Physiol.*, **47**, Supplement 1, 245–281 (1956).

Alberty, R. A., "The Rate Equation for an Enzymic Reaction," in P. D. Boyer, H. Lardy, and K. Myrbäck, *The Enzymes*, Vol. 1, Academic Press, New York, 1959, pp. 1–48.

Alberty, R. A., "Enzyme Kinetics," in D. E. Green, ed., *Currents in Biochemical Research*, Interscience, New York, 1956, pp. 560–484.

Bray, H. G., and K. White, *Kinetics and Thermodynamics in Biochemistry*, Academic Press, New York, 1957.

Bull, H. B., "The Enzyme–Substrate Complex as an Intermediate in Enzyme-Catalyzed Reactions," in W. D. McElroy and B. Glass, eds., *The Mechanism of Enzyme Action*, Johns Hopkins Press, Baltimore, 1954, pp. 123–135.

Chance, B., "Biological Reactions, Part 2, Reaction Kinetics of Enzyme–Substrate Compounds," in S. L. Friess and A. Weissberger, eds., *Investigation of Rates and Mechanisms of Reactions* (*Technique of Organic Chemistry*, Vol. VIII), Interscience, New York, 1953, pp. 535–627.

Dixon, M., and E. C. Webb, *Enzymes*, Academic Press, New York, 1958, Chap. 2, pp. 8–34 and Chap. 4, pp. 62–181.

Eyring, H., R. Lumry, and J. D. Spikes, "Kinetic and Thermodynamic Aspects of Enzyme–Catalyzed Reactions," in W. D. McElroy and B. Glass, eds., *The Mechanism of Enzyme Action*, Johns Hopkins Press, Baltimore, 1954, pp. 123–135.

Friedenwald, J. S., and G. D. Maengwyn-Davies, "Elementary Kinetic Theory of Enzymatic Activity," in W. D. McElroy and B. Glass, eds., *The Mechanism of Enzyme Action*, Johns Hopkins Press, Baltimore, 1954, pp. 123–135.

Green, N. M., and H. Neurath, "Proteolytic Enzymes," in H. Neurath and K. Bailey, eds., *The Proteins*, Vol. II, Part B, Academic Press, New York, 1954, pp. 1057–1198.

Hearon, J. Z., S. A. Bernhard, S. L. Friess, D. J. Botts, and M. F. Morales, "Enzyme Kinetics," in P. D. Boyer, H. Lardy, and K. Myrbäek, *The Enzymes*, Vol. 1, Academic Press, New York, 1959, pp. 1–48.

Huennekens, F. M., "Biological Reactions, Part 1, Measurement and General Theory," in S. L. Friess and A. Weissberger, eds., *Investigation of Rates and Mechanisms of Reactions*, (*Technique of Organic Chemistry*, Vol. III), Interscience, New York, 1953, pp. 535–627.

Johnson, F. H., H. Eyring, and M. J. Polissar, *The Kinetic Basis of Molecular Biology*, Wiley, New York, 1954.

Laidler, K. J., *The Chemical Kinetics of Enzyme Action*, Clarendon Press, Oxford, 1958.

Neurath, H., and G. W. Schwert, "The Mode of Action of the Crystalline Pancreatic Proteolytic Enzymes," *Chem. Revs.*, **46**, 69 (1950).

Reiner, J. M., *Behavior of Enzyme Systems*, Burgess, Minneapolis, 1959.

Segal, H. L., "The Development of Enzyme Kinetics," in P. D. Boyer, H. Lardy, and K. Myrbäck, *The Enzymes*, Vol. 1, Academic Press, New York, 1959, pp. 1–48.

Sizer, I. W., "Effect of Temperature on Enzyme Kinetics," in F. F. Nord and C. H. Werkman, eds., *Advances in Enzymology*, Vol. II, Interscience, New York, 1943, pp. 35–62.

Stearn, A. E., "Kinetics of Biological Reactions with Special Reference to Enzymic Processes," in F. F. Nord, ed., *Advances in Enzymology*, Vol. IX. Interscience, New York, 1949, pp. 25–74.

Wilson, P. W., in H. A. Lardy, ed., *Respiratory Enzymes*, Burgess, Minneapolis, 1949, pp. 16–57.

Part 2. ENZYME KINETICS IN THE TRANSIENT STATE

I. INTRODUCTION

The observation of the kinetics of the enzyme–substrate complex itself provides a new approach to the study of enzymic reactions. This approach has been emphasized in recent work with a number of techniques: spectrophotometric, fluorometric, and electron spin resonance (1–1c). Since the emphasis here is on method of approach rather than encyclopedic scope, we shall draw upon examples from the author's experimental experience to illustrate studies of enzyme kinetics in the transition state. Thus we shall omit from this section important work on the "active site" of enzymes in which the structure of the site is not yet known. This section will demonstrate the application of direct studies of the kinetics of formation and disappearance of enzyme–substrate complexes, in particular those of the hemoproteins catalase and peroxidase, to elucidate the mechanism of enzyme action. By stressing the kinetic approach to enzyme mechanisms of hemoproteins we necessarily de-emphasize the important chemical studies of Keilin and Hartree and of Theorell as well as work on reaction kinetics in the steady state (*cf.* Part 1 of this chapter and General References). However such an approach is appropriate here as an illustration of the application of rapid reaction techniques described in Chapter XIV.

A first step toward understanding the mode of action of biocatalysts was made by those workers who recognized and demonstrated by indirect kinetic methods the existence of intermediate compounds of the catalyst and its substrate. Michaelis and Menten (2), following the work of Henri (3), derived a mathematical expression for such an intermediate compound and verified the fact that the theory conformed to the experimental data on invertase. The work of many others on the over-all kinetics of enzyme

action was reviewed and evaluated in detail by Haldane (4). The studies of the over-all reaction kinetics then reached the point of diminishing returns for, although many kinetic data fitted the theory of Michaelis, no direct evidence for an intermediate compound had yet been obtained.

It was in 1936 that Stern (5) observed that the brown color of a catalase solution changed to a red color upon the addition of ethyl hydrogen peroxide. And shortly thereafter, Keilin and Mann (6) discovered that the brown color of a horse-radish peroxidase solution changed to red upon the addition of hydrogen peroxide. Most important, Keilin and Mann showed that the red color disappeared upon the addition of a reducing substrate. Thus, Keilin and Mann provided for the first time qualitative evidence for the combination of an enzyme with its substrate to form an enzyme–substrate complex which was capable of reacting with a donor or reducing substrate and thereby opened the era of studies of enzyme mechanism by means of the enzyme–substrate complexes. Theorell (7) and his coworkers made quantitative studies possible by their crystallizations and detailed studies of peroxidases and catalases.

It was some time, however, before an apparatus could be developed that was capable of measuring the kinetics of enzyme–substrate compounds—their lifetimes are too short to permit the use of ordinary spectrophotometers. Closely following the developments of Roughton and Millikan (8) on the rapid flow method, Chance (9) made significant improvements in the fluid economy and spectrophotometric sensitivity and, in 1940 (10), was able to make direct measurements of the kinetics of the red enzyme–substrate complex of Keilin and Mann in the presence of leucomalachite green; in 1943 (11), he was able to prove that the reaction kinetics of this complex were in excellent agreement with mathematical solutions of the equations representing the Michaelis theory. The interpretation of Chance's results was rendered dubious by Theorell's (12) discovery in 1941 that the red compound of Keilin and Mann is preceded by a labile green compound. However, Chance (13) later found that the transition from the green to the red complex is very rapid in the presence of a donor and that the reaction of the red complex with the donor is the rate-determining step in the peroxidase kinetics. Thereby the earlier studies were substantiated.

The kinetic data available at this point showed the time sequence of the formation of the green compound, its conversion into the red compound, and the subsequent decomposition of the latter into the free enzyme. As discussed below, the integral of the trace for the green intermediate was found to correspond very closely to the observed curve for the formation of the red intermediate, leading to the conclusion that the pathway between the two intermediates was a compulsory one. Since peroxide has two oxidizing equivalents, the sequential formation of the green and red

intermediates in the decomposition of peroxide by peroxidase furnished the first direct application of Michaelis' views on compulsory univalent oxidation-reduction reactions to enzyme–substrate complexes themselves (14), and provided experimental foundation for the more detailed views of LuValle and Goddard (15).

Further evidence of the one-step nature of the green-red intermediate interconversion was provided by a limited proportionality between the rate of formation of the red compound and the concentration of ascorbate (13). However, George's direct measurement of a 1:1 stoichiometry of the reaction of the red complex with ferrocyanide showed the formation of the free enzyme from this intermediate to be a one-electron change (16) and thus provided a direct and convincing proof.

On the basis of these views, it is reasonable to expect that the products of the reaction of the hydrogen donor with the green and red complexes would be free radicals; indeed labile colored oxidation products have been observed in the presence of these intermediates (B. Chance, unpublished data). A more direct method of determining the presence of free radical oxidation products in such systems is electron spin resonance which has been applied to peroxidase (17) and to laccase (18).

The development of ideas on the participation of enzyme–substrate compounds in the action of catalase on hydrogen peroxide was impeded by difficulties encountered in observing the green intermediate. Although catalase had been purified and crystallized for some years (19), no evidence of a color change upon the addition of hydrogen peroxide could be observed by ordinary techniques (20,21). However, many workers concluded, on the basis of the kinetics of the over-all reaction of catalase and hydrogen peroxide, that such a complex of catalase and hydrogen peroxide might exist (22,23). In 1947, Chance demonstrated by means of spectrophotometric time resolution the existence of this postulated complex and elucidated the mechanism of catalase action (24). Interestingly, however, this complex did not exhibit the properties predicted by earlier workers. Instead it appeared to be analogous to the peroxidase intermediate (24) with one exception: a kinetic complication introduced by the fact that the enzyme participates in a consecutive reaction with two molecules of substrate, a feature unique among hemoproteins. Studies of the interaction of aminotriazol with the green intermediate reported recently by Margoliash and his co-workers (25–27) provide some insight as to its nature. Chance and Schonbaum have obtained preliminary evidence that the structure of the green complex retains the elements of peroxide (28). Brill and Williams have greatly enlarged upon the earlier suggestion (28a) that the peroxide bound to the iron interacts with the methine bridges of the porphyrin. Under certain conditions, however, a red complex is formed and can be

shown to oxidize hydroquinones with a relatively slow activity and nitrite with a high activity (29).

In the following presentation a detailed discussion will be presented of the background leading to conclusions concerning the nature and action of enzyme intermediates in catalases and peroxidases. The procedure here is basic to that which is being taken up actively in connection with a large number of other enzymes in which the intermediate compounds may be less readily detected. Instead of presenting all the data available on enzyme mechanisms, it is preferred here to give a detailed discussion of the procedure leading to a careful consideration of intermediates in the catalase and peroxidase reactions. It is in this way that the development of a logical approach to the mechanism of enzyme action based upon studies of the actual intermediates compounds can be evolved and ultimately applied to other enzyme systems.

This section of Chapter XXII embraces the early work on the kinetics of the "over-all" activity of catalase and peroxidase and then considers the more recent work on the mechanism of these reactions based upon direct studies of the kinetics of the enzyme–substrate complexes. The general conclusion is that those explanations of enzymic action based solely upon the kinetics of the over-all reaction are generally inadequate and that full explanations require direct studies of the reaction kinetics of the enzyme–substrate complexes themselves. It must, however, be emphasized that even direct studies are limited to those intermediates that can be detected by physical methods and shed no light on those which do not exist in measurable concentrations.

Through the kinetic study of these enzyme–substrate complexes, the sequence of action of the enzyme with the various substrates can be determined under appropriate conditions (11,30). Also the separate velocity constants for the combination of the enzyme and substrate and for the reaction of the enzyme-substrate complex and the donor molecule may be evaluated. In this way the study of the enzyme specificity has been placed on a quantitative basis. In addition, some data have been obtained on the relation between the kinetics and activity of enzyme–substrate compounds and the chemical linkages between the iron porphyrin prosthetic group and the protein moiety of catalases and peroxidases. Other approaches to the study of enzymes are described in Part 1 of this chapter and elsewhere (31,32).

1. An Extension of the Theory of Michaelis and Menten

A. ONE-ENZYME, ONE-INTERMEDIATE SYSTEM

Since in these studies the kinetics of the enzyme–substrate complexes are recorded directly, solutions of the equations representing the Michaelis

theory are required not only for the over-all reaction but also for the kinetics of the intermediate complex. The classic equations of Michaelis and Menten in which the enzyme–substrate complex breaks down "spontaneously" into free enzyme and reaction products in a first-order reaction have been fully analyzed in Part 1 of this chapter. The enzyme–substrate compounds of catalases and peroxidases, however, react in a second-order manner with the donor molecule. Thus, the equations of Michaelis and Menten are suitably extended as follows:

For the case of a single intermediate complex of enzyme and substrate, as in the case of the green catalase–alkyl hydrogen peroxide complex which reacts with alcohols, etc., the reactions are represented by the following equations, where e is the initial enzyme concentration, p_1 is the concentration of the intermediate complex, x_0 the initial substrate concentration, a_0 the initial donor concentration, and x and a are their respective values at any time. The values of the concentrations are written underneath the symbols in the equations:

$$\underset{e-p_1}{\mathrm{E}} + \underset{x}{\mathrm{S}} \underset{k_2}{\overset{k_1}{\rightleftharpoons}} \underset{p_1}{[\mathrm{ES}]_1} \tag{1}$$

$$\underset{p_1}{[\mathrm{ES}]_1} + \underset{a}{\mathrm{AH_2}} \xrightarrow{k_4} \mathrm{E} + \mathrm{SH_2} + \mathrm{A} \tag{2}$$

The usual equations for the over-all reactions (disappearance of substrate or disappearance of donor) are:

$$-dx/dt = k_1x(e - p_1) - k_2p_1 \tag{3}$$

$$-da/dt = k_4ap_1 \tag{4}$$

It can be demonstrated that the substrate disappears at the same rate as the donor if the equation for the kinetics of the enzyme–substrate complex is written in the following form:

$$dp_1/dt = k_1x(e - p_1) - (k_2 + k_4a)p_1 \tag{5}$$

Upon addition of Equations (3), (4), and (5), the relation:

$$(dp_1/dt) + (dx/dt) - (da/dt) = 0 \tag{6}$$

is obtained. For the conditions of the steady state ($dp_1/dt = 0$) or for the related condition $dx/dt \gg dp_1/dt$, then:

$$dx/dt = da/dt \tag{7}$$

Thus the rates of disappearance of substrate and donor are identical, and therefore identical values of the activity will be obtained.

The values of k_1 and k_4 of Equations (3), (4), and (5) can be computed from the values of dx/dt or da/dt. The Michaelis constant, or substrate concentration which gives half maximal activity (K_m), is readily derived from Equation (5) by setting $dp_1/dt = 0$ and solving for p_1/e.

$$p_1/e = x/(x + K_m) \tag{8}$$

where:

$$K_m = (k_2 + k_4a)/k_1 \tag{9}$$

It is seen that K_m is directly proportional to the donor concentration when $k_4a \gg k_2$.

When $x \gg (k_2 + k_4a)/k_1$, $p_1 = e$, and k_4 is measured directly from Equation (4):

$$k_1 = \frac{1}{ea}\left(-\frac{da}{dt}\right) = \frac{1}{ea}\left(-\frac{dx}{dt}\right) \tag{10}$$

And when $x \ll (k_2 + k_4a)/k_1$, $p_1 \ll e$, and k_1 is measured directly from Equation (3) if it is assumed that $k_1x \gg k_2$:

$$k_4 = \frac{1}{ex}\left(\frac{dx}{dt}\right) = \frac{1}{ex}\left(\frac{da}{dt}\right) \tag{11}$$

Actually, it is very difficult to determine, by studies of the over-all reactions of peroxidases (or catalases), when the inequality $x \gg (k_2 + k_4a)/k_1$ obtains since k_2, k_4, and k_1 are not known and the inequality can only be satisfied by "saturation" of the enzyme with substrate ($p_1 \rightarrow e$). Frequently no simple saturation curve is obtained, only bell-shaped maxima caused by enzyme inactivation which do not truly indicate whether a true "saturation" has been obtained (see especially Mann (33)).

In the mechanism represented by Equations (1) and (2), a true "saturation" with respect to the donor does not occur since no complex of enzyme, substrate, and donor is postulated. A "pseudo saturation" effect does occur if the substrate concentration is maintained constant and the donor concentration is varied. By combining Equations (4), (7), (8), and (9):

$$\frac{dx}{dt} = \frac{da}{dt} = -k_4ap_1 = -k_4a\,\frac{ex}{x + K_m} = \frac{-k_4ae}{1 + [(k_2 + k_4a)/k_1x]} \tag{12}$$

$$\frac{dx}{dt} = \frac{da}{dt} = -\frac{e}{(1/k_4a) + (1/k_1x)} \tag{13}$$

when $k_4a \gg k_2$.

The rate of the over-all reaction becomes independent of the donor concentration when $k_4a \gg k_1x$. Such a "pseudo saturation" effect could, of course, be easily mistaken for a true saturation effect unless both substrate and donor concentrations were varied (see Mann (33)).

A procedure for determining k_1 and k_4 by a variation of the relative values of k_4a and k_1x of Equation (13) has been described (34) and values of k_1 agreeing to within 10% of those obtained by direct kinetic records (see below) are obtained. The values of k_4 differed by ~20%. It is clear, however, that the experimental design would have been very difficult had the values of k_1 and k_4 not already been known from studies of the kinetics of formation and decomposition of the enzyme–substrate complex.

In summary, it is theoretically possible to determine k_1 and k_4 (but not k_2) from studies of the over-all reactions of catalases and peroxidases. However, the practical difficulty arises in the evaluation of the saturation of the enzyme with substrate without increasing the latter to such an extent that enzyme inactivation obscures the true saturation.

For this reason, direct spectroscopic measurements of the kinetics of the enzyme–substrate complex are much more reliable because the quantity p_1/e is measured directly and k_4 or k_1 can be readily calculated from Equation (10) or (11). Actually this is seldom as convenient as are direct measurements of k_1 from the kinetics of formation of the enzyme–substrate complex immediately after the addition of substrate. From Equation (5):

$$k_1 = [1/(e - p_1)x](dp_1/dt) \tag{14}$$

for small p_1. Equations (3), (4), and (5) show no obvious solution for k_4 based directly upon the kinetics of the enzyme–substrate complex. However, with the following manipulations, k_4 can be measured directly from the kinetics of the enzyme–substrate complex alone. Upon addition of Equations (3) and (5):

$$dp_1/dt + dx/dt = -k_4ap_1 \tag{15}$$

and upon integration between 0 and t:

$$x = x_0 - p_1 - k_4a_0\int_0^t p_1dt + c \tag{16}$$

for a constant value of $a = a_0$.

The definite integral is obtained by integrating between the limits $t = 0$ when $x = x_0$ and $p_1 = 0$, and $t = \infty$ when $x = 0$, $p_1 = 0$. Thus:

$$k_4a_0\int_0^\infty p_1dt = x_0 - x - p_1 \Big]_{\substack{x = 0,\ p_1 = 0 \\ x = x_0,\ p_1 = 0}} \tag{17}$$

and then:

$$k_4 = x_0/a_0\int_0^\infty p_1dt \tag{18}$$

Thus k_4 is measured directly by dividing the ratio of the initial substrate and donor concentrations by the area under the curve for the kinetics of the enzyme–substrate complex. It has been found (11) that this area

may be simply evaluated from the product of the maximum values of p_1, $p_{1(\text{max.})}$, and $t_{1/2\,\text{off}}$; the time from $t = 0$ until $p_{1(\text{max.})}$ falls to $p_{1(\text{max.})}/2$. Thus k_4 is readily evaluated by the following useful equation:

$$k_4 = x_0/a_0 p_{1(\text{max.})} t_{1/2\,\text{off}} \tag{19}$$

The effect of k_2 on the accuracy of Equation (19) is discussed elsewhere (see Chapter VII and Ref. 30) and the appropriate equation for large values of k_2 gives the correction terms in brackets:

$$k_4 = \frac{x_0}{a_0 p_{1(\text{max.})} t_{1/2\,\text{off}}} \left[1 - \frac{(1 - a)k_2}{k_1 x_0 + k_4 a_0 + k_2} \right] \tag{20}$$

Computer studies of kinetic curves suggest that a value of $a = {}^1/_2$ will give agreement to about 10%.

By a combination of measurements of the kinetics of the over-all reaction where dx/dt or da/dt is measured and the kinetics of the enzyme–substrate complex where p_1 is measured, Equation (10) may be used without reservation in the following form:

$$k_4 = (1/p_1 a)\,(-\,da/dt) = (1/p_1 a)\,(-\,dx/dt) \tag{21}$$

The foregoing analysis shows that the two important reaction velocity constants k_1 and k_4 may be measured. These quantities are absolute measures of enzymic activity.

B. A FIGURE OF MERIT FOR ENZYMIC ACTIVITY

A single number representing the figure of merit for an enzyme following this mechanism may be defined as either k_1 or k_4, but the total merit of an enzyme might well be defined as the product of the values of k_1 and k_4 obtained with the most active substrates. It has been useful, however, to define activity in terms of the value of k_4, the velocity constant for the reaction of the enzyme–substrate complex with the donor molecule, and this procedure is used here.

Enzyme specificity is quantitatively defined by the relative values of k_1 or k_4 for a series of substrates or donors.

Much of the work described in this part of Chapter XXII is concerned with quantitative studies of the activity and specificity of various catalases and peroxidases under different experimental conditions. In this way a systematic study of the essential characteristics of enzymic activity may be made.

2. Experimental Methods

Only a brief summary of methods is given here, since these matters are presented in Chapter XIV and involve considerable physical and electronic

detail well beyond the scope of this chapter. The following methods have given fruitful results.

A. ORDINARY SPECTROPHOTOMETRIC METHODS

These are extremely useful for studies of the over-all reaction; for example, in the measurement of peroxidase activity by the rate of formation of tetraguaiacol from guaiacol (34,35) at 470 mμ or malachite green from leuco-malachite green at 610 mμ. Various other leuco dyes are also suitable (36). Spectrophotometers suitable for the ultraviolet region are useful for measuring the oxidation of donors such as ascorbic acid or dihydroxymaleic acid at 270 mμ (37,38).

The over-all reactions of both catalases and peroxidases may be measured in terms of the rate of disappearance of peroxide (dx/dt) at 230 mμ (39,40). This method is especially convenient for the measurement of catalase activity where colored oxidation products of the donor are not formed.

B. RAPID, SENSITIVE SPECTROPHOTOMETRIC METHODS

Because of the intense absorption bands of the catalases and peroxidases in the region 370–450 mμ, spectrophotometric methods are quite suitable for studies of their enzyme–substrate complexes. But with catalases, and especially with peroxidases, the half-times, $t_{1/2\,\mathrm{off}}$, of the reactions are too short to be measured by spectrophotometers of ordinary sensitivity and speed of response. For this reason, two specialized forms of the flow method of Hartridge and Roughton have been developed for studies of enzyme–substrate complexes and are termed the "accelerated" and "stopped" flow methods (9). The salient features of these methods are high spectrophotometric sensitivity, rapid response speed, and high fluid economy. In addition, the absorption spectra of unstable enzyme–substrate complexes may be readily measured. A particular apparatus covers a wavelength range of 360 to 630 mμ, a time range of 1 to 20 millisec. and 4 millisec. to 10 min., and a concentration range from 5×10^{-7} to $1 \times 10^{-5} M$ hematin iron catalase or peroxidase. A complete kinetic curve is obtained from 0.1 cc. of the enzyme solution (41). (A detailed description of this apparatus and its use is presented in Chapter XIV.)

C. POLAROGRAPHIC METHODS

The dropping mercury electrode is quite suitable for measuring the rate of disappearance of hydrogen peroxide (42). The method is at present unsuitable for use with flowing liquids and therefore the stationary platinum microelectrode (42) has been used for measuring the rate of disappearance

of hydrogen peroxide in conjunction with the rapid spectrophotometric method.

D. pH METHODS

The over-all reaction of catalase may be measured by means of the change in pH caused by the oxidation of formate. Spectrophotometric methods using a suitable indicator, for example, bromothymol blue, are convenient and sensitive (see Chapter XIV).

E. MAGNETOMETRIC METHODS

Kinetic studies of peroxidase reactions can be carried out by means of sensitive magnetometric methods developed by Theorell and Ehrenberg (43). Unfortunately, this technique suffers from two disadvantages: the time from mixing to the first reading is ~2 min., and a high concentration of enzyme (300 μM) is required. Considerable reduction of these values has been obtained in this laboratory by means of an improved Rankine balance (44); with this adaptation, 10^{-5} to $10^{-4}M$ solutions are studied with a response time of almost 0.05 sec.

F. ELECTRON-SPIN RESONANCE METHODS

The combination of rapid flow apparatus with electron-spin resonance measurements is now available (44a,44b). The concentration limits are $\sim 10^{-6}M$ and time limits ~10 millisec.

G. TEMPERATURE-JUMP METHODS

These are applied to especially rapid reactions, particularly those that may be observed fluorometrically (44c).

II. THE PEROXIDATIC REACTIONS OF CATALASE

A peroxidatic reaction is defined as the reaction of a hemoprotein with a peroxide molecule and a donor molecule in which the donor is oxidized and no oxygen is evolved.

The oxidation of alcohols and related substances in the presence of catalases and methyl or ethyl hydrogen peroxides (CH_3OOH or C_2H_5OOH) is presented first because the kinetics of the enzyme–substrate complex accurately follow the simple mechanism of Equations (1) and (2) over a reasonable range of experimental conditions.

The actual mechanism of this reaction remained obscure for some years in spite of the considerable work done by Stern and Keilin and Hartree, which is summarized briefly:

In 1936 Keilin and Hartree (45) showed that catalase oxidizes ethyl alcohol to acetaldehyde in the presence of ethyl hydrogen peroxide. However, they attributed the oxidation reaction to hydrogen peroxide derived from the decomposition of ethyl hydrogen peroxide and did not recognize the substituted peroxide as a substrate for catalase.

Also in 1936, Stern (5) discovered that catalase, like ferrihemoglobin (46), forms a red compound with ethyl hydrogen peroxide and concluded that this complex was the active enzyme–substrate compound in the formation of acetaldehyde from ethyl hydrogen peroxide. Contrary to the conclusions of Keilin and Hartree (45), Stern did not consider that alcohol participated in this reaction.

In 1949, Chance (39) showed Stern's red compound to be preceded by a labile green compound responsible for the catalytic effect which Stern observed. Actually Stern himself saw this green compound, but attributed it to "concomitant pigments" of the enzyme solution. Chance showed the green and red complexes to be in reversible equilibrium and the latter to be an inhibitor of the enzymic activity (47). He also showed that alcohol reacts with the green intermediate and that the reaction of catalase, ethyl hydrogen peroxide, and alcohol follows a simple peroxidatic mechanism involving the green enzyme–substrate complex only, as indicated in Equations (1) and (2) (47). With dilute substrate and excess donor, negligible amounts of the red complex are formed.

The decomposition of the red complex by the action of phenols, reported by George (48) and more recently in greater detail by Nicholls (49), does not appear to be involved in the oxidation of alcohols by the green catalase complex.

1. Measurements of the Over-all Reaction

The disappearance of alkyl hydrogen peroxide (dx/dt) in the presence of catalase and alcohol can readily be measured in the ordinary spectrophotometer at 250 mμ, as shown in Figure 2.1 (39). The disappearance of alcohol (da/dt) is difficult to measure, but, if formate is used as a donor, the change in pH caused by the disappearance of formate is readily measured spectrophotometrically by using an indicator. However, it is not possible to evaluate k_4 from these data alone, and the value of p_1 is not known. The value of p_1 is most conveniently measured spectrophotometrically from the kinetics of the green enzyme–substrate complex.

Agner and Theorell (50) have shown that the formate inhibits catalase

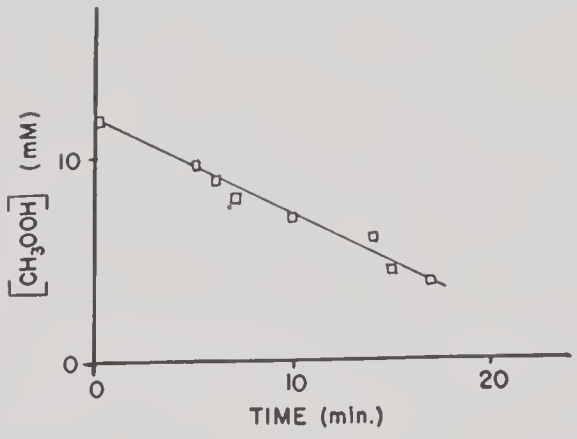

Fig. 2.1. The measurement of the zero order over-all reaction in the system catalase–methyl hydrogen peroxide by optical measurements of the rate of disappearance of substrate (Expt. 158–4).

activity. These experiments may be carried out at such low concentrations of formate that negligible inhibition occurs at the value of pH used.

2. Kinetics and Spectra of the Enzyme–Substrate Compound

The spectrum of the green enzyme–substrate intermediate can be obtained by the flow method or, at 4°C., by the rapid recording spectrophotometer (51) (at which low temperature the intermediate is sufficiently stable to permit recording with this instrument). Spectra representing the free enzyme and complexes I, II, and III are illustrated by Figure 2.2 for both the Soret and the visible regions. These spectroscopic data (51,52) show the difference between the extinction coefficients of the free catalase and the green primary (I) enzyme–substrate complex to be maximal at 405 mμ. Thus, this is a suitable wave length for measuring the reaction kinetics of complex I. A record (47) of the formation and disappearance of complex I is shown in Figure 2.3. This record is measured in the rapid spectrophotometric apparatus and may be explained in the following manner.

In this form of the rapid flow method, the enzyme and substrate are drawn up into two separate 1 cc. syringes, and, through suitable connections, can be manually discharged into a small mixing chamber and caused to flow very rapidly down a 1 mm. bore observation tube. Several discharges can be made before the 1 cc. syringes are emptied, so that the experiment may be repeated several times. At 0.3–1.0 cm. from the mixing chamber, monochromatic light of a wavelength of 405 mμ passes through the observation tube and onto a photocell connected to a sensitive amplifier and to two recorders, one a rapid oscillograph recorder and the other a slower pen-and-paper recorder (41). Thus, small changes in optical density

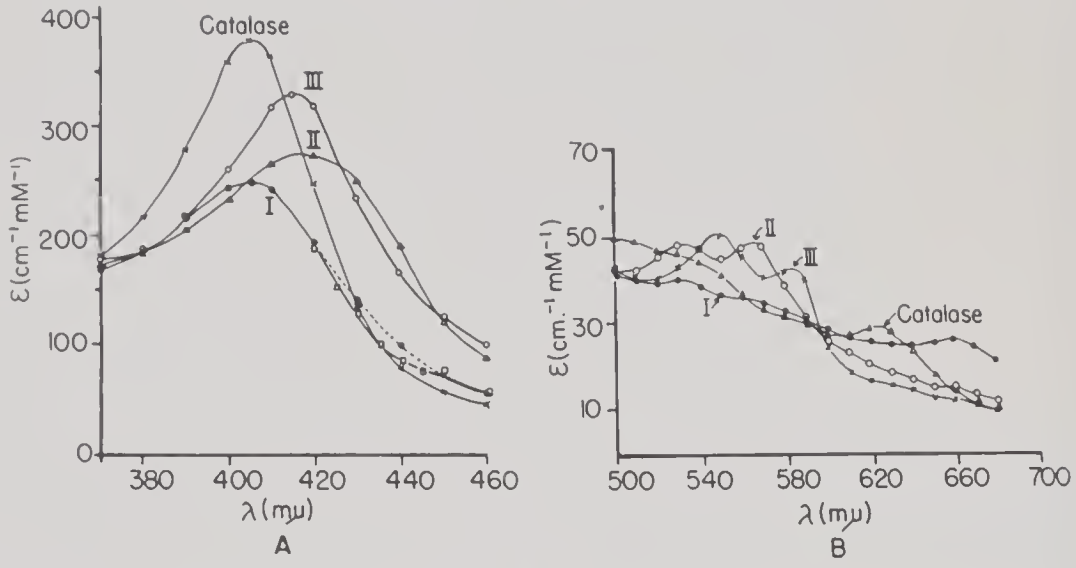

Fig. 2.2. The Soret (left) and visible (right) bands of the primary (I), secondary (II), and tertiary (III) catalase complexes as obtained with methyl hydrogen peroxide as substrate. Curve (I) was obtained with a 5-fold ratio of substrate to enzyme concentration; curve (II) with a very large excess of substrate; and curve (III) by means of the addition of hydrogen peroxide to (II) (Expt. 847d) (Ref. 51).

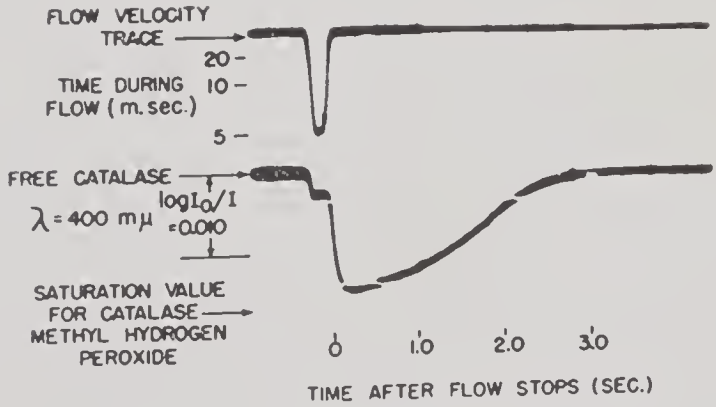

Fig. 2.3. Measurement of kinetics of the formation and disappearance of the primary catalase–methyl hydrogen peroxide complex in the presence of ethanol by the accelerated and stopped-flow methods (Expt. 468).

caused by the formation of complex I are automatically recorded on slow and fast time scales.

The time interval between mixing and observation is measured by the quotient of the distance from the mixing to the observation point and the flow velocity. The former is about 1 cm. and the latter is automatically registered by a separate oscillograph trace, the upper one in Figure 2.3. The appropriate time scale is marked vertically in Figure 2.3. This flow velocity trace shows that the discharge of the syringes lasts only about 0.3 sec. and in that short time the kinetics of the formation of complex I are measured. After the flow stops, the course of the reaction is measured

directly as a function of time, indicated by the horizontal scale of Figure 2.3. Thus, two methods are combined to cover the very rapid formation of complex I and its much slower disappearance. These methods are termed the "accelerated" and "stopped" flow methods.

The record begins with the observation tube filled with the end products of the previous discharge of the syringes, free catalase. When the flow is started, as indicated by the top trace, the optical density decreases due to the partial formation of complex I, as would be expected from the spectroscopic data of Figure 2.2, since a wavelength of 405 mμ is used. The total optical density change is not, however, measured at the high flow velocities; insufficient time is permitted for the reaction of enzyme and substrate to go to completion. The value of k_1 is measured directly from this curve and is computed according to Equation (14). As the flow velocity falls to zero, longer times are measured, the reaction of enzyme and substrate goes to completion, and the total density change of Figure 2.2 is measured since sufficient substrate is present to saturate the enzyme. The reaction of complex I with the donor now proceeds according to the steady state solution of Equations (3), (4), and (5) with a constant concentration of the enzyme–substrate complex. The steady state continues for several seconds and then terminates as the substrate is exhausted. The concentration of the enzyme–substrate complex then falls to zero, as indicated by the rise of the trace. The value of k_4 is then computed directly from the ink recording by means of Equation (19).

Thus, it is possible to measure directly the values of k_1 and k_4 for the reaction of catalase with methyl hydrogen peroxide and catalase–methyl hydrogen peroxide I with ethanol. The advantage of this method over the classical measurement of the over-all reaction should be made obvious by this demonstration. However, independent controls are required to insure that the enzyme actually follows the mechanism represented by Equations (1) and (2).

3. Order of the Reactions

In order to prove that the reactions occur according to the mechanism of Equations (1) and (2), it is necessary to demonstrate that the value of dp_1/dt increases with x according to Equation (14). This has been done by measuring dp_1/dt with several different initial values of x, as shown in Figure 2.4, in which both methyl and ethyl hydrogen peroxides have been used as substrates (47). In this figure the values of k_1[ROOH] have been computed for the various values of [ROOH]. The straight lines verify that the first-order velocity constant for the reaction of enzyme and substrate increases linearly with the substrate concentration over a wide range.

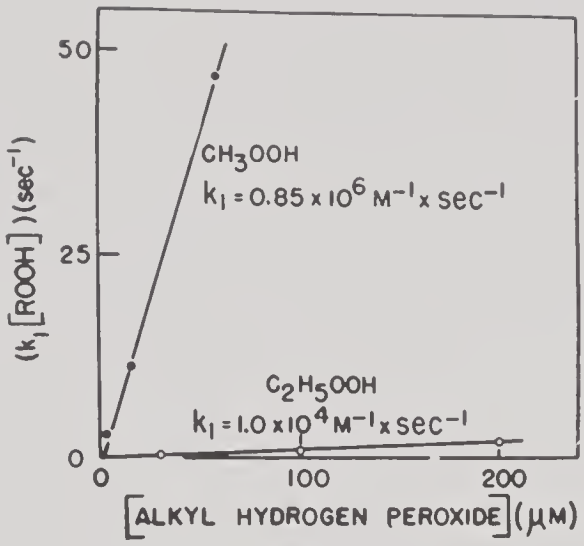

Fig. 2.4. Experimental evidence showing that the first-order velocity constant for the reaction of catalase and alkyl hydrogen peroxides increases linearly with the concentration of alkyl hydrogen peroxide (Expt. 91e, 120b).

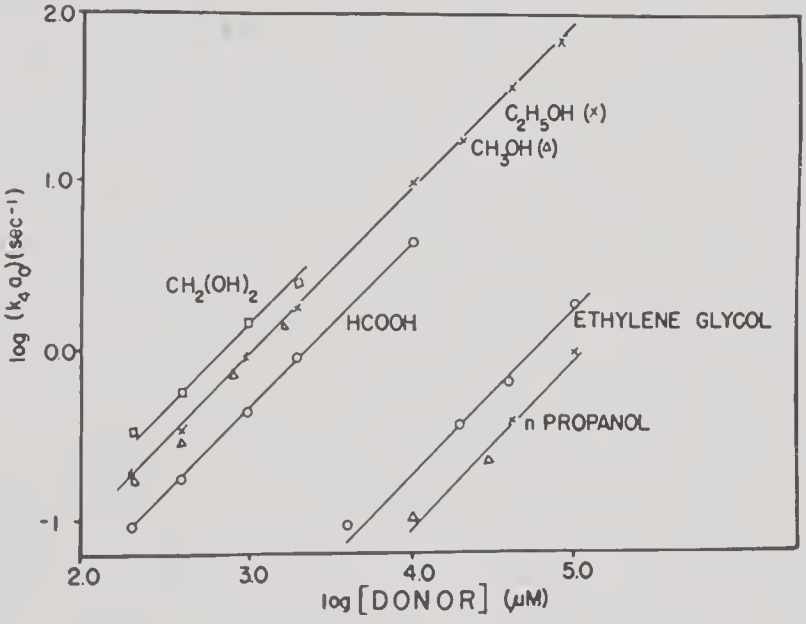

Fig. 2.5. Experimental evidence showing the increase of the first-order velocity constant for the reaction of mammalian catalase–ethyl hydrogen peroxide complex with increasing concentration of various donor molecules. The values of k_4 are: methylene glycol, 1200; ethanol and methanol, 910; formate, 450; ethylene glycol, 17; and *n*-propanol, 10 M^{-1} sec.$^{-1}$ at pH = 7.0 (Expt. 374, 375d).

Other data show that the reaction is also first order with respect to the enzyme as required by Equation (1). The large difference in the slopes of the two curves clearly shows that catalase combines more rapidly with the smaller methyl hydrogen peroxide molecule than with the larger ethyl hydrogen peroxide molecule. The order of the reaction of the primary catalase–methyl hydrogen peroxide complex with alcohols and related

substances is given in Figure 2.5. The data are presented in the same way as in Figure 2.4; the values of k_4 are computed according to Equation (19) by means of experiments similar to that of Figure 2.3, but with various types of donor (a_0). The product k_4a_0 is then plotted against a_0 on logarithmic coordinates. The 45° straight lines clearly indicate that the reaction of complex I with the various donor molecules is second order, as required by Equation (19).

The data of Figures 2.4 and 2.5 permit quantitative evaluation of the substrate and donor specificities of catalase. The outstanding feature of the reaction kinetics obtained with alcohols is the large magnitude of k_1 compared with the value of k_4; the velocity constant for the combination of the enzyme with the substrate is much greater than the velocity constant for the reaction of the enzyme–substrate complex with these donors. Direct reaction of peroxide with catalase apparently occurs more rapidly than does the reaction of the alcohol molecule with the catalase–peroxide complex. In the case of formate, the free acid is the reactive species (53) and the value of k_4, calculated on the basis of the free formic acid concentration, is thus much larger and comparable to k_1. A second feature of some interest is the great decrease in the velocity constants for the reaction of the enzyme with substrates or donors of increasing sizes (for donors larger than ethanol). This effect may be attributed to steric effects in the reaction of catalase with the substrate and donor. Apparently the heme of catalase may not be readily accessible to large molecules, possibly because it is "hidden" by the protein component of the enzyme. Other approaches to this question are afforded by proton relaxation times (54) and ultimately by the determination of the structure of the protein in the vicinity of the heme (55,56).

It is also possible to make some general rules concerning the substrate and donor specificities of catalase on the basis of these data. (*1*) The substrate molecule may be an unsubstituted or a monosubstituted peroxide; disubstituted peroxides do not react with catalase (Stern (20)). Thus, one hydrogen atom must be free on the peroxide group. (*2*) The nature of the donor molecule can be fairly accurately defined. Whereas formaldehyde (as methylene glycol) and formic acid are readily oxidized, acetaldehyde and acetic acid react at a scarcely measurable rate, the difference being in excess of 1,000-fold. The chief structural difference between these substrates is that the latter two lack a hydrogen atom attached to the carbonyl group. Thus, since catalase has a general specificity for alcohols, the groups required of the donor molecule are a hydrogen atom and a hydroxyl group attached to the same carbon atom. Other data show that the same groups may be attached to nitrogen as in nitrites or oxygen as in hydrogen peroxide. An equation for such an oxidation may be written:

$$\mathrm{Cat(OOR)_4 + 4CH_3OH \xrightarrow{k_4} Cat(OH)_4 + 4HCHO + 4ROH} \quad (21)$$

$Cat(OOR)_4$ represents the enzyme–substrate complex with one peroxide molecule attached to each one of the four independent catalase hematins. Thus, the action of catalase may be generally described as that of a dehydrogenase which removes two hydrogen atoms from the donor molecule.

4. The Ternary Complex of Enzyme, Substrate, and Donor

There is considerable interest in the possibility that the enzyme–substrate compound combines with the donor molecule to form a distinct complex which then breaks down into the free enzyme and the reaction products (see LuValle and Goddard (15)). The existence of such a complex would be demonstrated by nonconstancy in the value of k_4 at high donor concentrations. The methods suitable for demonstrating a complex of this kind were enumerated and discussed earlier. The measurement of the over-all reaction is not only faulty for the reasons previously mentioned, but suffers from the additional disadvantage that high donor concentrations require correspondingly high substrate concentrations—which may lead to enzyme inactivation (see Mann (33)). The latter effect may be falsely attributed to the formation of such a ternary complex. For this reason most of the studies have been carried out by means of measurements of the kinetics of enzyme–substrate complexes. In the case of catalase methyl hydrogen peroxide the constancy of k_4 has been demonstrated from 0.2 to 80 mM ethanol (57). Furthermore, no measurable spectroscopic shift occurs upon the addition of donor to the enzyme–substrate complex. Thus, there is no positive evidence for a ternary complex of enzyme, substrate, and donor. Nevertheless, its existence has not been disproved; its lifetime may be too short to permit detection by available methods or no shift of the spectrum may occur upon combination of the enzyme–substrate complex with the donor.

5. Effect of pH upon the Reaction Velocity Constants for Catalase Activity

The effect of pH upon enzyme activity was studied previously by measurements of the over-all activity of the enzyme and it was difficult to attribute changes in over-all activity specifically to a change in the particular reaction velocity constants for the enzyme mechanism. In the catalase system it is possible to measure independently the two principal velocity constants of the enzyme activity, k_1 and k_4 of Equations (1) and (2). The curve of Figure 2.6 shows that k_1 is fairly constant from pH 2.2 to 11 (53). The effect of pH upon k_4 is more readily measured when hydrogen peroxide

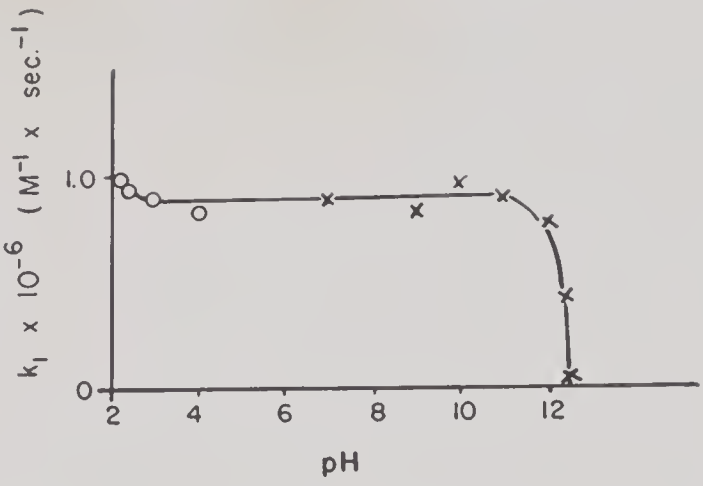

Fig. 2.6. Illustrating the small effect of pH upon the second-order velocity constant for the combination of catalase and methyl hydrogen peroxide (k_1) (Expt. 337d, 403) (Ref. 53).

is the substrate and the data are given later in Figure 2.14. Thus both k_1 and k_4 are only slightly affected by pH over a wide range.

Beyond these values of pH, the catalase protein is unstable and it is therefore not possible, on the basis of these studies of the effect of pH upon k_1 and k_4, to attribute catalase activity to anything less general than the integrity of the protein component.

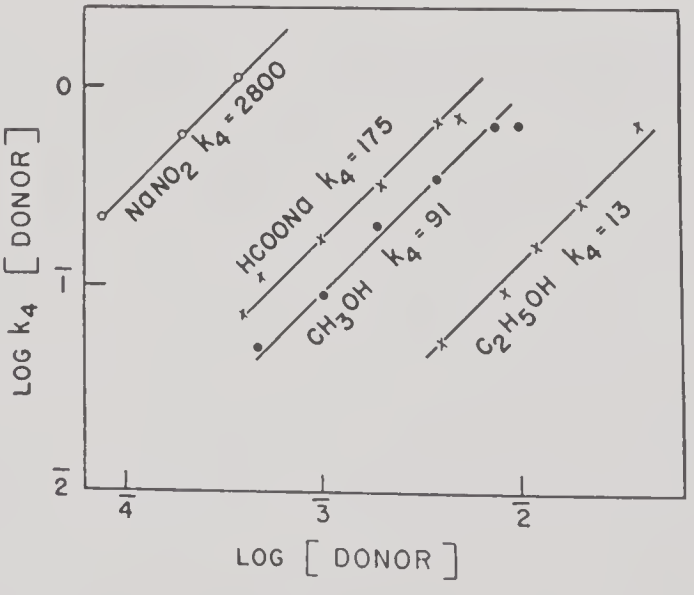

Fig. 2.7. Illustrating the increase of the pseudo-first-order velocity constant for the reaction of the primary bacterial catalase–methyl hydrogen peroxide complex with the various concentrations of donors (59). The straight lines at 45° indicate a second-order reaction, and their position gives the value of k_4. The values of k_4 are in units of M^{-1} sec.$^{-1}$ at pH = 7.0 (Expt. 411).

6. Reaction of Peroxide Complex of Bacterial Catalase with Donors

Bacterial catalase, prepared from *Micrococcus lysodeikticus* by the method of Herbert and Pinsent (58) forms complexes with methyl or ethyl hydrogen peroxide which are spectroscopically almost identical with those of mammalian catalase (59). The bacterial catalase complexes also oxidize alcohols, formate, and methylene glycol (formaldehyde in dilute aqueous solutions). The reactive species in the case of formate and nitrate are the free acids, and thus the values of k_4 computed on the basis of the free acid concentration are considerably larger for these two substances.

The values of k_4 decrease much more rapidly with the size of the alcohol molecule (see Fig. 2.7) than in the case of mammalian catalase and it is suggested that the hemes of bacterial catalase are "buried" in the protein molecule to a greater extent than are the hemes of mammalian catalases.

III. THE CATALATIC REACTION

A "catalatic" reaction is defined as the reaction of a hemoprotein with hydrogen peroxide giving oxygen and water.

1. Reaction of Catalase Methyl Hydrogen Peroxide with Hydrogen Peroxide

If hydrogen peroxide is added to catalase, water and oxygen are evolved in a very rapid reaction. This is defined as the "catalatic" function of catalase, as distinguished from the peroxidatic function described above. One of the few incisive experiments on the mechanism of this catalatic function is provided by experiments on the peroxidative activity of the primary catalase alkyl hydrogen peroxide complex in the presence of hydrogen peroxide (60). (The alkyl hydrogen peroxides are not decomposed into alcohol and oxygen by dilute solutions of catalase.) If hydrogen peroxide is added to the primary catalase methyl hydrogen peroxide complex, the latter disappears momentarily while the hydrogen peroxide is being decomposed, and then reappears when the hydrogen peroxide has been decomposed. This suggests that hydrogen peroxide may react with alkyl hydrogen peroxide groups bound to catalase hematin.

A more dramatic demonstration of this reaction is afforded when the hydrogen peroxide is formed continuously and at a low concentration by the reaction of glucose and oxygen, catalyzed by the glucose oxidase system (61). The left-hand record of Figure 2.8 is similar to that of Figure 2.3, although the values of the concentrations employed are not identical.

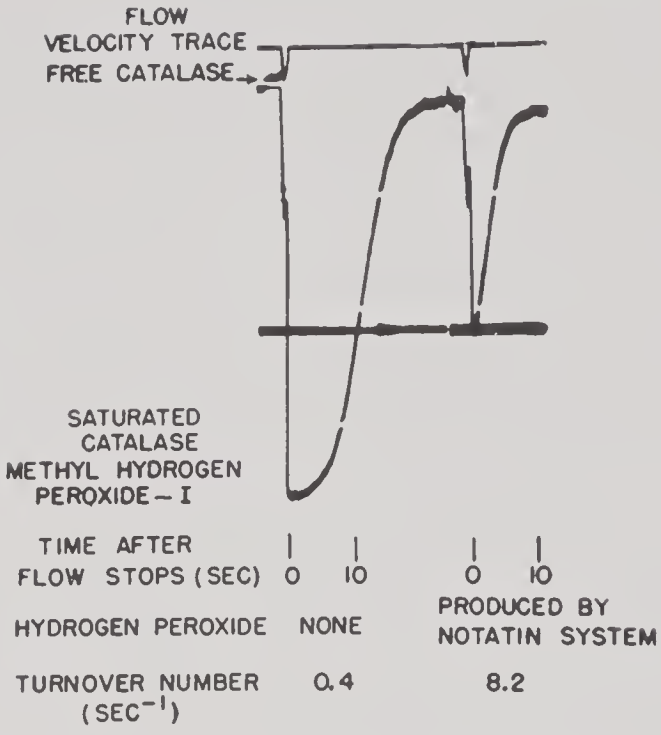

Fig. 2.8. Illustrating the reaction of the primary catalase-methyl hydrogen peroxide complex with hydrogen peroxide as donor (40). In the left-hand curve hydrogen peroxide is absent; the "cycle" is terminated in a reasonable time by the presence of some ethanol. In the right-hand curve hydrogen peroxide is continuously generated by the system notatin, glucose and oxygen. The rapid reaction of hydrogen peroxide with the primary complex is indicated by the large decrease in the cycle time and in the maximum concentration of the enzyme-substrate complex (Expt. 245) (Ref. 40).

However, the typical cycle of the appearance and disappearance of complex I in the presence of ethanol is clearly demonstrated. In the right-hand curve, very dilute hydrogen peroxide is present, but its rapid reaction with complex I is indicated by the dramatic decrease in $p_{1\max.}$ and $t_{1/2\text{off}}$ of the cycle. A value of k_4 for the reaction of hydrogen peroxide and complex I is computed to be of the order of magnitude of 10^7 M^{-1} sec.$^{-1}$—much larger than any value of k_4 found for ethanol.

2. A Mechanism for Catalase Action

This experiment suggests that hydrogen peroxide would also act as a donor toward a catalase–hydrogen peroxide complex, and accordingly a mechanism for the catalytic activity of this enzyme may be written:

$$\mathrm{E} + \mathrm{S} \underset{k_2}{\overset{k_1}{\rightleftharpoons}} \mathrm{ES} \tag{22}$$

$$\mathrm{ES} + \mathrm{S} \xrightarrow{k_4} \mathrm{E} + \mathrm{P} \tag{23}$$

These equations are, in fact, identical to Equations (1) and (2) except that S replaces AH_2 in Equation (2). The equation for the over-all reaction (disappearance of hydrogen peroxide) is written in the following manner, using the same symbols as in Equations (3) and (4):

$$dx/dt = -k_1x(e - p_1) - k_4xp_1 + k_2p_1 \tag{24}$$

or:

$$dx/dt = -k_1x[e - (1 - k_4/k_1)p_1] + k_2p_1 \tag{25}$$

This equation has the same general form as equation (3); the over-all rate for a given enzyme depends upon x and $(e - p_1)$.

If, however, the differential equation for p_1 is written:

$$dp_1/dt = k_1x(e - p_1) - (k_2 + k_4x)p_1 \tag{26}$$

and solved for p_1/e for the condition $dp_1/dt = 0$:

$$\frac{p_1}{e} = \frac{1}{k_4/k_1 + 1 + k_2/k_1x} \tag{27}$$

For the condition $k_1x \gg k_2$(or $x \gg k_2/k_1$):

$$\frac{p_1}{e} = \frac{1}{k_4/k_1 + 1} \tag{28}$$

Here is indeed a striking difference between the peroxidatic and catalatic mechanisms. For in the peroxidatic mechanism p_1/e is a function of x until $x \gg (k_2 + k_4a)/k_1$ (see Equations 8 and 9), while in the catalatic mechanism, p_1/e is a function of x only until $x \gg k_2/k_1$. Experience with peroxidase shows that k_2/k_1 may be a very small number ($<10^{-6}$) and, therefore, Equation (28) would be expected to be valid over the available experimental range over which x can now be measured. In this case, p_1/e is constant, and, according to Equation (25), the rate of the over-all reaction (dx/dt) is directly proportional to the product of the enzyme (e) and substrate (x) concentrations, as shown by substituting for p_1 its steady-state value given by Equation (28) (Ref. 62):

$$\frac{dx}{dt} = -k_1xe\left[1 - \frac{1 - (k_4/k_1)}{1 + (k_4/k_1)}\right] + \frac{k_2e}{1 + (k_4/k_1)} \tag{29}$$

If k_2 is negligible—actually $(2k_4/k_1)x \gg k_2$—Equation (29) simplifies to:

$$\frac{dx}{dt} = -k_1xe\left[1 - \frac{1 - (k_4/k_1)}{1 + (k_4/k_1)}\right] \tag{30}$$

and is readily integrated and simplified:

$$k_1'' = \frac{2}{1/k_4 + 1/k_1} = \frac{1}{et}\ln\frac{x_0}{x} \tag{31}$$

where x_0 is the initial hydrogen peroxide concentration. Catalase activity may then be evaluated directly as k''_1. Thus, the hydrogen peroxide should always disappear in a first-order reaction of rate proportional to the catalase concentration.

By substituting the value of k_4 of Equation (28) in Equation (31) we may calculate k_1 from k''_1:

$$k''_1 = 2k_1[1 - (p_1/e)] \tag{31a}$$

However, we usually use catalase molarity to calculate k'_1, while the iron molarity is used to calculate k_1 (catalase has four iron atoms). Thus, in the experimental units:

$$k'_1 = 8k_1[1 - (p_1/e)] \tag{31b}$$

The simple Equation (14) for calculating k_1 does not apply to the consecutive reaction mechanism for catalase action; the following equation is correct (62):

$$k_1 = [1.1p_{1\,\max.}\,(dp_1/dt)]/[ex_0(p_{1\,\max.} - p_1)] \tag{31c}$$

where $p_{1\max.}$ is the maximum value of p_1 obtained with the given value of x_0. The factor 1.1 is an empirical constant which corrects for the use of x_0 instead of the value of x at t.

3. Experimental Studies of the Over-all Reaction of Catalase

In the very considerable literature on catalase activity, many authors observed that the velocity constant for the over-all reaction, k'_1, decreases at higher values of the hydrogen peroxide concentration and interpreted this decrease to be caused by the saturation of a hypothetical enzyme–substrate complex with a Michaelis constant of about $0.03M$. However, Millikan showed in 1940 (see Bonnichsen, Chance, and Theorell (63)) that a constant of $0.03M$ did not exist when concentrated catalase was used. The platinum microelectrode technique (63) of Chance and a rapid titration method (63) have confirmed that catalase activity (k'_1) is constant over a very wide range of hydrogen peroxide concentrations, as shown by Figure 2.9, in which the linear relationship between k'_1x and x is shown by curve A. If, however, more dilute enzyme is used as in curve B, catalase inactivation occurs; this inactivation was erroneously interpreted previously as indicating a Michaelis constant (22,23).

By use of a "quenching" method (see p. 799) Ogura (64) found catalase activity to increase linearly with the peroxide concentration up to about $0.5M$ H_2O_2. Thereafter a definite saturation effect was found with a "K_m" value of $1.1M$. It is proposed that a ternary intermediate, ESS,

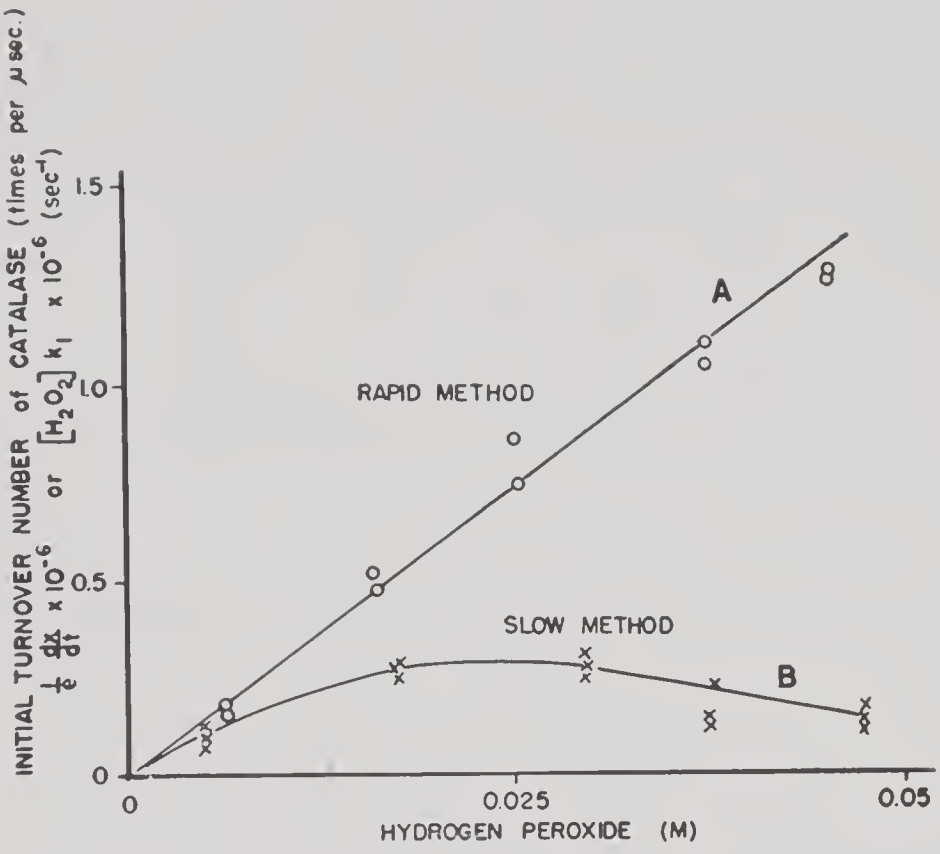

Fig. 2.9. Curve A illustrates the linear increase in the turnover number of catalase with increasing hydrogen peroxide concentration; this is in accordance with the mechanism represented by equations (22) and (23). Curve B illustrates that if more dilute catalase is used and longer reaction times are involved, catalase becomes inactivated and a nonlinear relation is obtained. This nonlinear relation was previously attributed to the existence of a "Michaelis constant" for catalase activity (Expt. 95b) (Ref. 63).

is formed and limits the activity at very high concentrations of hydrogen peroxide ($1.5M$).

4. Spectroscopic Studies of the Catalase–Hydrogen Peroxide Complex

In spite of the efforts of a number of investigators (20,21) the existence of the catalase–hydrogen peroxide complex was not demonstrated until the improved rapid spectrophotometric technique (24) of Chance was employed (see Chapter XIV). A glance at Equation (28) reveals why some experimental difficulty might be anticipated: the largest value of the saturation of the enzyme with the substrate (p_1/e) is determined by k_4/k_1. If k_4/k_1 were 100, only 1% of the enzyme would even be found in the complex. Actually, the ratio k_4/k_1 is not so large (see later), but is about 3 for mammalian catalase, so that p_1/e reaches a value of only about 25%. Thus, the "saturated" catalase–hydrogen peroxide complex contains about 75% of free catalase and only about 25% of the complex; its spectroscopic detection is, therefore, rather difficult without special apparatus.

The spectrum of such an unstable complex can actually be measured in the rapid flow apparatus by measuring the deflections obtained for the formation of the catalase–hydrogen peroxide complex at a variety of wavelengths. By applying suitable corrections, these deflections can be converted into changes in the extinction coefficient; from the latter the absolute absorption spectrum of the catalase–hydrogen peroxide complex is obtained, as shown in Figure 2.10 (24). Since the spectrum of the catalase–hydrogen peroxide complex shown in Figure 2.10 resembles that of free catalase much more closely than does the spectrum shown in Figure 2.2, we have reason to believe that the value of p_1/e is indeed less than 1. Figure 2.2 shows that the peaks in the absorption spectra of catalase and catalase–

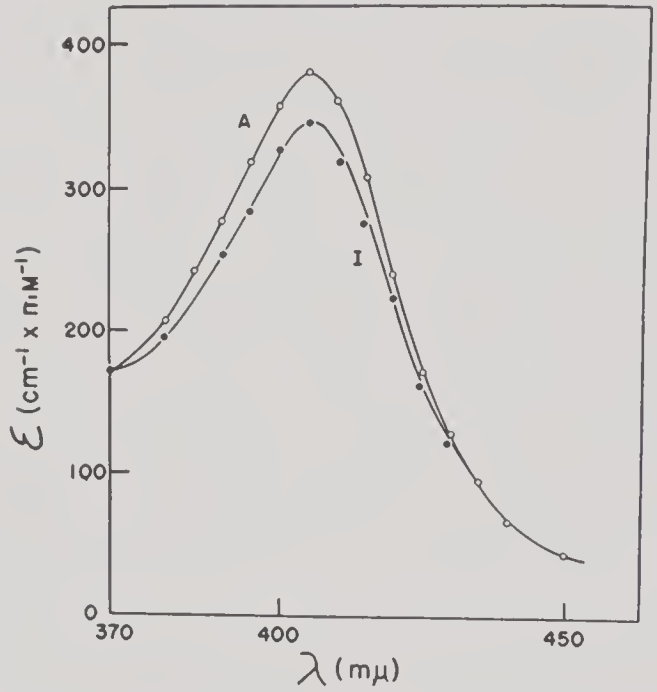

Fig. 2.10. Soret band for horse-blood catalase (A) and the primary catalase-hydrogen peroxide complex (I) as measured in the rapid flow apparatus (24).

methyl hydrogen peroxide I lie at approximately the same wavelength, and it is, therefore, justifiable to make a calculation of the value of p_1/e directly from the ratio of the decrease in the extinction coefficient at 405 mμ measured from Figure 2.10 and from Figure 2.2. This ratio is, in fact, 45/140 or approximately $^1/_3$, and this is the value of p_1/e for this catalase.

A verification of the spectroscopic data of the rapid flow apparatus is readily obtained in the ordinary spectrophotometer if the hydrogen peroxide is continuously supplied, for example, by the oxidation of glucose in the presence of notatin (61). A further verification of the value of p_1/e is given by direct measurements of the reaction of the catalase–hydrogen peroxide complex with cyanide (65). Such experiments show that free

mammalian catalase binds approximately 33% more cyanide than does the catalase–hydrogen peroxide complex.

The mean values for p_1/e are (from spectroscopic data) $(1.3 \pm 0.1)/4$ and (from the cyanide data) $(1.2 \pm 0.1)/4$ for erythrocyte catalase. For bacterial catalase the value is found to be 1.7/4 (59).

Since this catalase–hydrogen peroxide complex is a mixture of three parts of free catalase and one part of peroxide compound, it is difficult to observe the latter by visual spectroscopy. Definite evidence has, however, been obtained that the visible spectrum of the hydrogen peroxide compound is similar to that of the alkyl hydrogen peroxide complex: they both have an absorption band at 650–655 mμ.

Catalase also forms a secondary complex with hydrogen peroxide which has clearly visible absorption bands at 536 and 572 mμ (40). These bands are in the same position as those of the secondary alkyl hydrogen peroxide complex and these compounds are of presumably identical nature. Keilin and Hartree recently revised these band-positions to 536 and 568 mμ and added those of a third complex (66) of which the Soret band can be seen at 416 mμ in Figure 2.2.

5. Measurement of k_1 for Reaction of Catalase and Hydrogen Peroxide

By means of the rapid flow method, the value of k_1 can be determined directly by using a reasonable excess of substrate—in order that the forward reaction should be in excess of any reasonable value of the back reaction—and by measuring at the earliest possible time after mixing in order to avoid errors caused by the reaction of the catalase–hydrogen peroxide complex with a second molecule of hydrogen peroxide according to Equation (21). The formation of this complex has been found to proceed so rapidly that it has not always been possible to fulfill the latter condition; however, Equation (31c) corrects for this effect. An illustration of a typical measurement is given in Figure 2.11. In this case the reaction is roughly 50% complete at a time after mixing of less than 5 millisec. Data similar to these give an average value of $k_1 \approx 0.5 \times 10^7\ M^{-1}$ sec.$^{-1}$, as calculated from Equation (31c) (62).

Similar measurements of the value of k_1 for the combination of bacterial catalase and hydrogen peroxide give $2 \times 10^7\ M^{-1}$ sec.$^{-1}$ (59,62). From these values of k_1 and p_1/e it is possible to compute k_4 by means of Equation (28). In the case of both erythrocyte and bacterial catalase, k_4 is approximately equal to $1.7 \times 10^7\ M^{-1}$ sec.$^{-1}$ (62).

The quantity k'_1 can also be measured directly from the rate of disappearance of hydrogen peroxide (see Equation 29 and 31c), values of 3.5×10^7 and $4.9 \times 10^7\ M^{-1}$ sec.$^{-1}$ have been obtained for erythrocyte (63) and

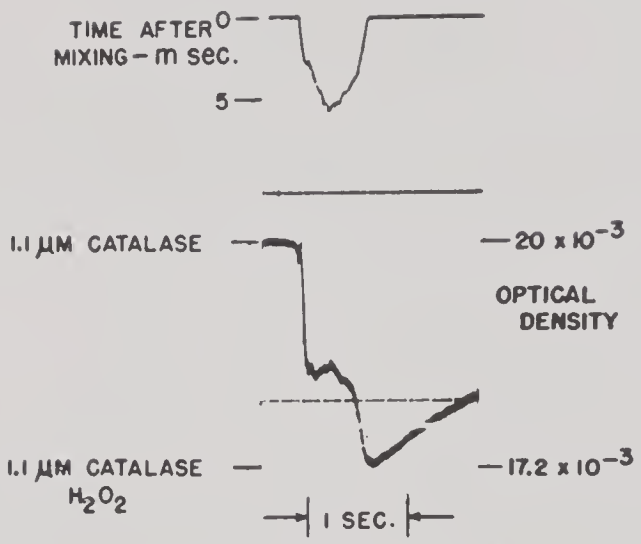

Fig. 2.11. The kinetics of formation of the primary compound of catalase and hydrogen peroxide as measured by the accelerated flow method (24). The reaction is more than half complete at the shortest time measured (5 milliseconds) (Expt. 69).

bacterial catalase (59), respectively. However, these values are based on the molar catalase concentration used in the experiment and are appropriately converted to values of k_1 by Equation (31b), giving values of 0.6 and $1.1 \times 10^7\ M^{-1}$ sec.$^{-1}$, respectively, in rather good agreement with the values of k_1 computed from direct kinetic studies of the catalase–hydrogen peroxide complex (0.5 and $2 \times 10^7\ M^{-1}$ sec.$^{-1}$, respectively). The reaction mechanism based upon consecutive reactions of hydrogen peroxide with catalase and with catalase–hydrogen peroxide provides a satisfactory explanation of catalase activity.

IV. THE PEROXIDATIC REACTIONS OF THE CATALASE–HYDROGEN PEROXIDE COMPLEX

1. The Fate of Hydrogen Peroxide

The nature of the reaction kinetics of catalase and hydrogen peroxide is such that the concentration of the catalase–hydrogen peroxide complex does not fall abruptly to zero as soon as the hydrogen peroxide has been decomposed. It can be demonstrated experimentally that the catalase–hydrogen peroxide complex persists for a considerable time after the hydrogen peroxide concentration has been reduced to a very low value. For example in Figure 2.12 the kinetics of disappearance of both the hydrogen peroxide and the catalase–hydrogen peroxide complex have been measured under the same conditions. The latter is registered as the top trace. The abrupt downward deflection indicates the formation of the complex and the

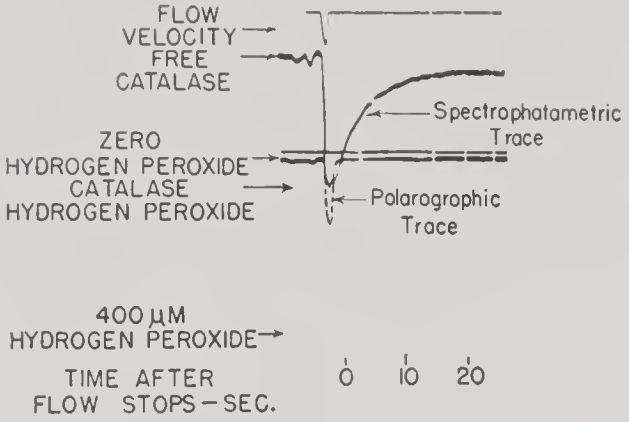

Fig. 2.12. Simultaneous polarographic (dotted trace) and spectrophotometric (solid trace) measurements (24) of the kinetics of hydrogen peroxide disappearance and of the formation and disappearance of the catalase-hydrogen peroxide complex as measured by the accelerated and stopped flow methods. The abrupt rise in the polarographic trace to zero hydrogen peroxide concentration immediately after stopping the flow indicates that the "catalatic" reaction is essentially complete long before the catalase-hydrogen peroxide complex begins to decompose (Expt. 118a).

slow exponential rise of a half-period of roughly 8 sec. indicates its disappearance. On the bottom trace the kinetics of hydrogen peroxide disappearance have been recorded by means of the platinum microelectrode; these kinetics are relatively more rapid. In fact, the abrupt rise of the platinum microelectrode trace toward zero hydrogen peroxide in the first few tenths of a second after the flow has stopped indicates that nearly all the hydrogen peroxide is decomposed in the first few moments of the reaction under these experimental conditions. Thus, the catalase–hydrogen peroxide complex decomposes essentially in the absence of free hydrogen peroxide. It is, therefore, possible to measure the reaction of this complex with donor molecules such as alcohol without interference from the catalatic activity. The experimental conditions under which the time separation of the catalatic and peroxidatic reactions is adequate for obtaining accurate results have been specified (67).

2. Spontaneous Decomposition

As the alcohol concentration is reduced to zero, it is found that the velocity constant for the disappearance of the catalase–hydrogen peroxide complex does not fall to zero. There appears to be a "spontaneous" breakdown of the catalase–hydrogen peroxide complex, which occurs in the apparent absence of donors. The velocity constant for this reaction is 0.02 sec.$^{-1}$ for the case of erythrocyte and liver catalases (24). In the case of bacterial catalase this "spontaneous" reaction proceeds somewhat more slowly; values of 0.0035 sec.$^{-1}$ have been observed (63).

3. Donor Specificity

The catalase–hydrogen peroxide complex reacts rapidly with donors of the type which are found to react with the primary alkyl hydrogen peroxide complexes. In fact, the reaction velocity constants (k_4) are generally identical; k_4 is valued according to this equation:

$$ES + AH_2 \overset{k_4}{\rightleftharpoons} E + SH_2 + A \tag{32}$$

which is formally identical with Equation (2); there is a second-order reaction of the catalase–hydrogen peroxide with the donor molecule. Actually, Equation (32) is not a sequence in the cyclic operation of the enzyme as is Equation (2); there is no free hydrogen peroxide in solution and hence there is no turnover in this reaction.

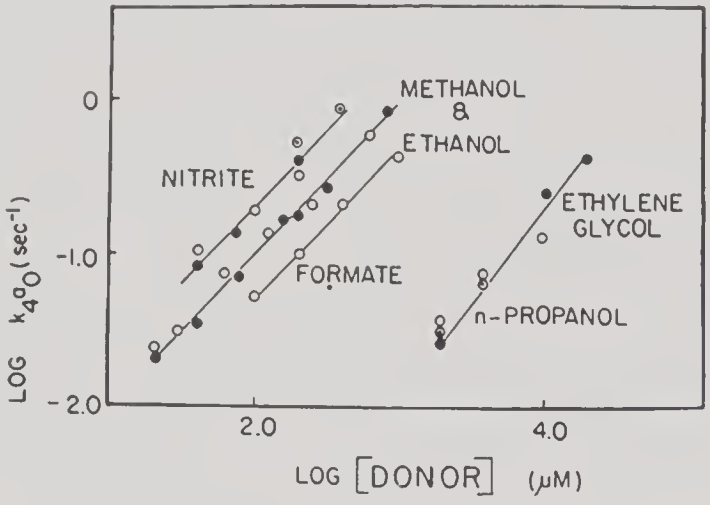

Fig. 2.13. Illustrating the increase of the first-order velocity constant for the reaction of the primary catalase-hydrogen peroxide complex with the concentration of various donors. The values of k_4 are: nitrite, 2000; methanol and ethanol, 1000; formate, 500; ethylene glycol and *n*-propyl alcohol, 27 M^{-1} sec^{-1} at pH 7.0 (Expt. 70, 71, 372, 373) (Ref. 24).

The straight lines representing the data of Figure 2.13 show that the first-order velocity constant for the reaction of the primary complex with donors increases linearly with donor concentration. Data on the variation of enzyme concentration show that the reaction is of the second order as required by Equation (32). The position of the lines represents the values of k_4 with the various donors. It is seen that the donor specificity of the catalase–hydrogen peroxide complex is nearly identical with that of the primary catalase alkyl hydrogen peroxide complexes. There are, however, two differences: (*1*) the former reacts smoothly with nitrite (68), and (*2*) the latter reacts smoothly with methylene glycol. Certain side processes

occur in the reactions of the former with methylene glycol, and the latter with nitrite. Nitrite is found to accelerate the formation of complex II (29). However, the same definition of specificity given earlier for the primary catalase–alkyl hydrogen peroxide complexes pertains here.

4. Coupled Oxidations

The reaction represented by Equation (30) occurs in the coupled oxidations of Keilin and Hartree (45,69). However, in coupled oxidations catalase is continuously supplied with hydrogen peroxide and considerable turnover of the substrate and the donor occurs. The particular conditions necessary for an efficient coupled oxidation (one in which all the hydrogen peroxide is utilized in the oxidation of the donor) have been specified (40) and require that the steady-state concentration of hydrogen peroxide and of the catalase–hydrogen peroxide complex be small (40).

5. Effect of pH

With alkyl hydrogen peroxides as substrates, the rapid increase in the rate of formation of the inactive secondary complex in acid solutions makes it difficult to obtain accurate values of k_4. However, the amount of the secondary catalase–hydrogen peroxide complex which forms under the experimental conditions illustrated in Figure 2.12 is very small, even at values of pH as low as 3.5. The data of Figure 2.14 clearly show that the activity of the catalase–hydrogen peroxide complex is quite independent of pH between 4 and 10. The lack of a pronounced effect of pH upon this reaction is remarkable and certainly indicates that hydrogen or hydroxyl ions are not reaction products. This independence also suggests that any

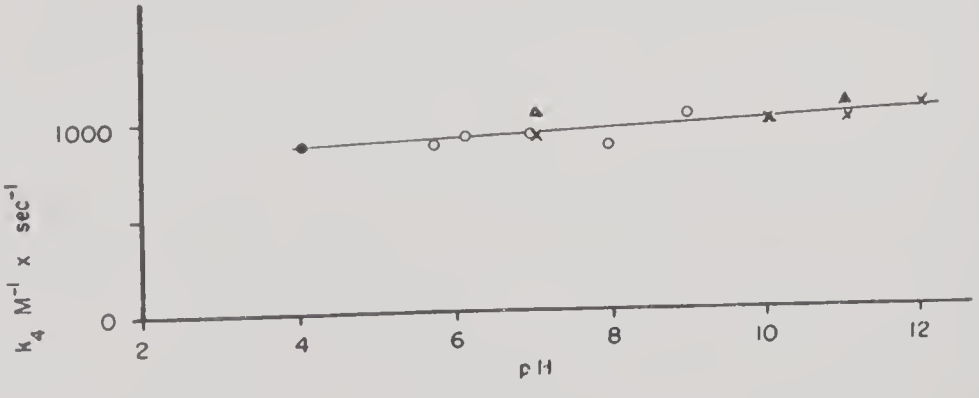

Fig. 2.14. Effect of pH upon the velocity of the reaction of catalase hydrogen peroxide with ethanol. The almost complete independence of the values of k_4 and pH suggests that hydrogen and hydroxyl ions are not involved in the reaction of the catalase–hydrogen peroxide complex and the donor molecule (Expt. 337b, 402a,d, 470) (Ref. 53).

changes in catalase-heme linkages occurring within this pH range are not effective in altering the value of k_4.

6. The Ternary Complex of Enzyme, Substrate, and Donor

Curvature in the relation between the first-order reaction velocity constant and the donor concentration has been observed at high donor concentrations in the case of the reaction of catalase–hydrogen peroxide and ethanol and has been attributed to a ternary complex (24), but this curvature is due to inadequate separation between the catalytic and peroxidatic reactions and not to the formation of a ternary complex (57). In addition, no nonlinearity has been found in the relation between the increase in the turnover number of the primary catalase–alkyl hydrogen peroxide complexes and the donor concentration. In fact, in this case turnover numbers of 80 sec.$^{-1}$ have been obtained, for which the value of k_4 is identical with that obtained for smaller donor concentrations (see Section IV.3). Most striking, however, are the extremely high turnover numbers which are obtained for the reaction of the catalase–hydrogen peroxide complex with hydrogen peroxide. As mentioned above, there is considerable evidence for a ternary complex that becomes rate limiting in the breakdown of hydrogen peroxide at concentrations of 1 to 5M H_2O_2. Such an intermediate has a half-life of 2×10^{-8} sec. at 25°C. An analogous ternary complex of such a short half-life could not be demonstrated with alcohols, etc., because of the lower values of k_4 (70). Thus, the ternary complex need only be considered at very high catalase turnover numbers.

V. THE PEROXIDASES

1. Introduction

Although a discussion of the reaction kinetics of the peroxidases might seem more logically to precede that of the catalases, it has been deferred to this point because of their apparently greater complexity. Whereas the activity of catalases toward alcohols, etc., involves only one type of peroxide complex, that of horse-radish peroxidase and lactoperoxidase involves two types of peroxide complexes; actually these two enzymes form a variety of complexes, designated: (I) green; (II) pale red; (III) bright red; and (IV) light green. The kinetics of enzyme–substrate compounds of catalase are distinguished from those of horse-radish peroxidase and lactoperoxidase by the fact that the former require only the green compound (I) whereas the latter require both the green and the pale red com-

plexes (I) and (II) (13,71), (III) and (IV) still being apparently unnecessary. Under the usual experimental conditions for the catalytic function of peroxidase, the values of the various velocity constants involved in the reaction kinetics have such values that the pale red complex (II) is the Michaelis or rate-limiting enzyme–substrate compound in peroxidase action. During the catalytic function of catalases a green enzyme–substrate compound is seen, whereas during the catalytic function of peroxidases a pale red enzyme–substrate compound is seen. The kinetics of both enzyme–substrate compounds follow a mathematical solution of an extension of the theory of Michaelis over a wide range of experimental conditions and with a considerable degree of accuracy.

2. Spectroscopic Data

The spectra of the free enzymes and their primary and secondary hydrogen peroxide compounds are given in Figures 2.15 and 2.16 for both horse-radish peroxidase (72) and lactoperoxidase (71). Complex II of horse-radish peroxidase was first identified by Keilin and Mann who used

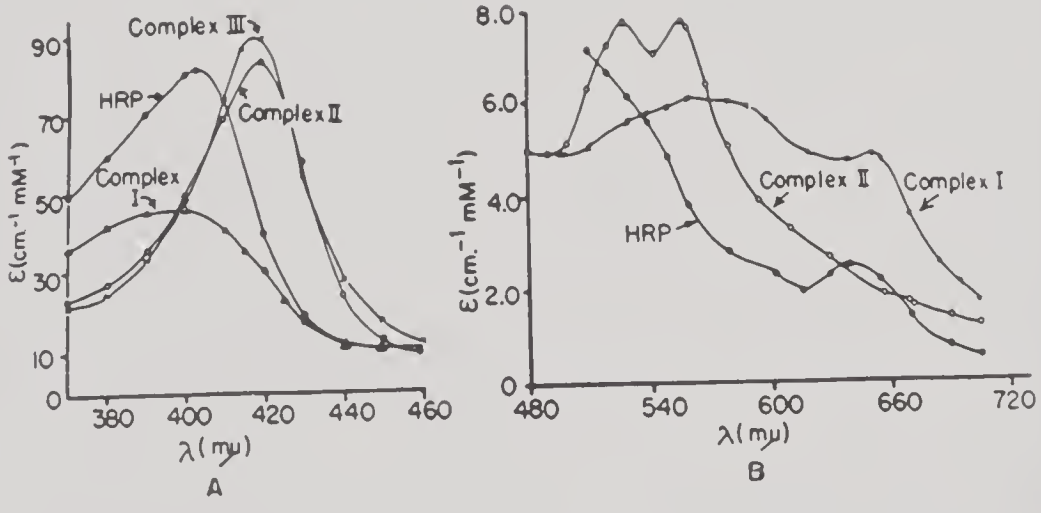

Fig. 2.15. Soret (left) and visible (right) bands of free peroxidase (HRP) and peroxidase combined with hydrogen peroxide to form the primary (I), secondary (II), and tertiary (III) complexes (51). The similarity between curve I of the left-hand portion of this figure and curve I of Figure 2.2 should be noted (Expt. 839d,e, 960b).

visual spectroscopy (6). Complex I of horse-radish peroxidase and complex II of lactoperoxidase were discovered by Theorell (12,73). The absorption spectra of the secondary complexes of both enzymes can be measured in the ordinary spectrophotometer (71,72), but the spectra of the primary compounds can only be determined by means of special devices such as the rapid flow apparatus, since their lifetimes are too short for measure-

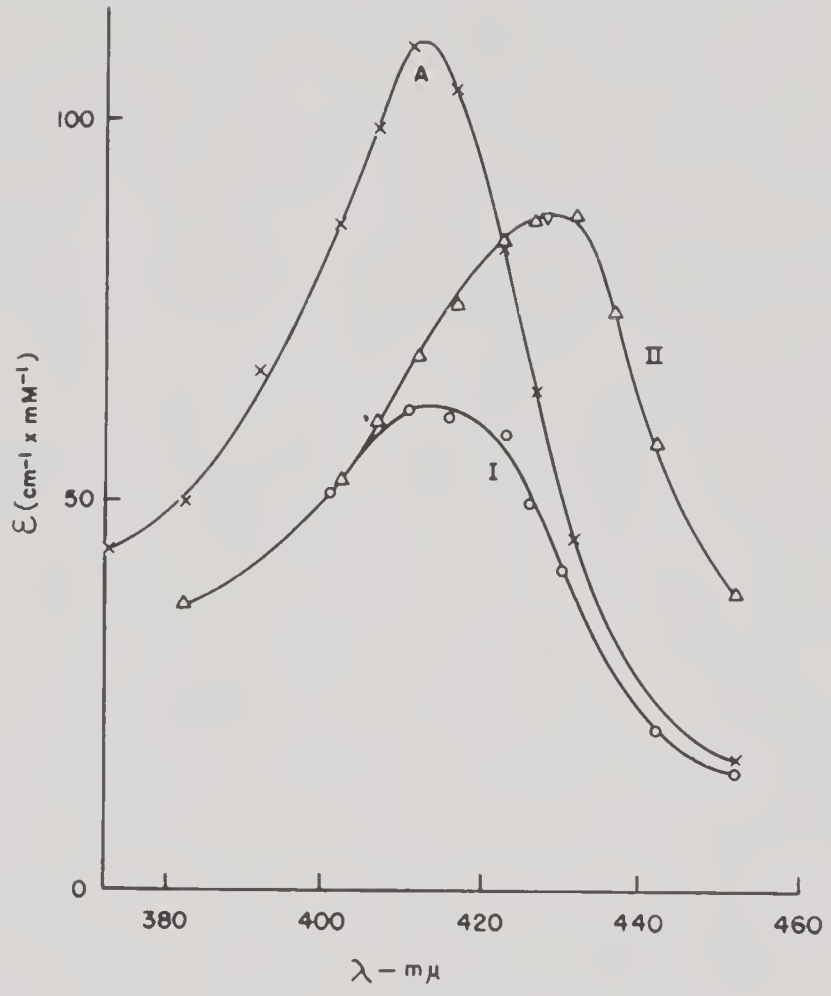

Fig. 2.16. Soret bands of free lactoperoxidase and lactoperoxidase combined with hydrogen peroxide to form the primary (I) and secondary (II) compounds (Expt. 278b-I) (Ref. 71).

ments by ordinary spectrophotometric means (71,72). Considerable progress has more recently been made on stabilization of the primary intermediate so that the spectra can be plotted with a rapid recording spectrophotometer. Such stabilization of the intermediate is due to pretreatment of the enzyme with excess peroxide in order to deplete the enzyme of endogenous donor (51). It has also been found that chromatography of the enzyme will give material which shows a highyl stable primary intermediate (74). Experiments with such material have greatly improved the definition obtainable in recording the bands of the primary intermediate in the visible region of the spectrum and such data are included in Figure 2.15. It has also been found that these two enzymes form identical complexes with the substituted hydrogen peroxides (methyl or ethyl hydrogen peroxide). Compounds with various oxidizing agents that are closely related to complex II have recently been described by George (16). Preliminary evidence has been obtained that verdoperoxidase forms both

primary and secondary compounds having spectra analogous to those shown in Figures 2.15 and 2.16 (75).

After long exposure to hydrogen peroxide or methyl hydrogen peroxide (72), a peroxidase complex (IV) with a relatively intense band at 675 mμ is formed and, at the same time, the intensity of the Soret band is greatly diminished. The color of this compound is bright green. It is suggested that this compound is related to the green oxidation products of hemoglobin and catalase, studied by Lemberg and his associates (see "General References").

A general remark may be made on the similarity of the Soret bands of the primary complexes of mammalian catalase, bacterial catalase, horseradish peroxidase, and lactoperoxidase. In these four cases the spectrum of the primary compound is distinguished by the fact that its intensity is considerably less than that of free enzyme, although the wavelength of maximum absorption is shifted very little. This type of spectrum differs markedly from that found for any other known compound of these hemoproteins; even the green azide or fluoride compounds differ significantly—their Soret bands are of equal or greater intensity compared with those of the free enzyme. Quantitatively, the decrease in the intensity of the Soret band of these hemoproteins on forming their primary complexes is very similar, lying between 35 and 48 cm.$^{-1}$ M^{-1} per hematin iron group bound to peroxide for all four enzymes.

The dissimilarity between these spectra and those of other compounds of these hemoproteins and their resemblance to the spectra of the oxidation products of these hemoproteins led us to suggest in 1949 (65) that the porphyrin ring is actually oxidized in a reversible manner on formation of the primary complex, by electron transfer from the iron peroxide complex, and is then reduced on reaction with the reducing substrate or donor. George's data (16) support this idea, but the actual configuration of the primary complexes has not yet been established (76,76a).

3. Kinetics of Formation of Primary Complexes

In the absence of a donor the kinetics of formation of the primary complexes of horse-radish peroxidase and lactoperoxidase may be studied before significant conversion to the secondary complex has occurred. A typical record illustrating the measurement of the second-order velocity constant for the formation of the primary complex of horse-radish peroxidase and methyl hydrogen peroxide is illustrated in Figure 2.17. In the left-hand record dilute peroxide is used and the reaction is sufficiently slow that it proceeds to a negligible extent before the flow has stopped; the complete kinetics, indicated by the downward sweep of the oscillograph trace,

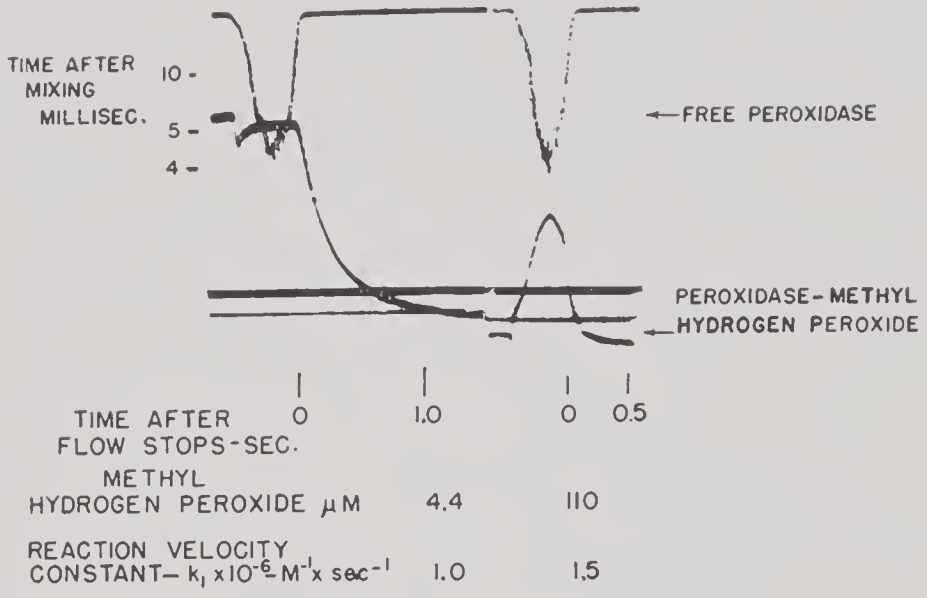

Fig. 2.17. Illustrating the use of the stopped flow method (left) and the accelerated flow method (right) in the measurement of the kinetics of the reaction of horse-radish peroxidase and methyl hydrogen peroxide (Expt. 173a) (Ref. 13).

are readily measured by the stopped flow method. In the right-hand record, a much higher concentration of peroxide is used, and the reaction is measured by means of the accelerated flow method; the time after mixing is measured directly from the scale appended to the left-hand edge of the record. A good indication of the second-order mechanism for the combination of enzyme and substrate is indicated by the relatively good agreement of the two values of k_1 obtained over this wide range of peroxide concentrations.

Figure 2.18 illustrates typical data on the combination of horse-radish peroxidase with hydrogen peroxide, methyl hydrogen peroxide, and ethyl hydrogen peroxide. The linear increase in the first-order constant for the combination reaction with increasing initial peroxide concentration verifies that these reactions are second order as required by Equation (1).

4. Transition from Primary to Secondary Complexes

The lowest curve of Figure 2.18 represents the effect of peroxide concentration upon the kinetics of formation of the secondary compounds. For peroxide concentrations above a few micromoles per liter, the conversion of the primary compound into the secondary compound is quite independent of the peroxide concentration and under these conditions may be considered a first-order reaction. This may be regarded as preliminary evidence that the secondary compound is not formed directly from peroxidase but from the primary complex.

Detailed proof of this supposition is given in Figure 2.19, where, by choosing appropriate wavelengths, it has been possible to measure the rate of formation and disappearance of the primary complex at 410 mμ, and the slower appearance of the secondary complex at 427 mμ, and the sum of both complexes at 395 mμ. Reference to the data of Figure 2.15 indicates that these are the appropriate wavelengths for such recordings. A study of the relationship between the curve for complex I at 410 mμ and complex II at 427 mμ clearly indicates that the secondary complex is formed from the primary complex. Mathematical support for this statement is furnished by the dotted curve which represents the area under the curve at 410 mμ. The curve representing the increase of this area as a function of time is seen to agree reasonably well with the experimental curve measured at 427 mμ. This result shows that the primary to secondary conversion in peroxidase is a compulsory pathway and that one-electron steps are involved.

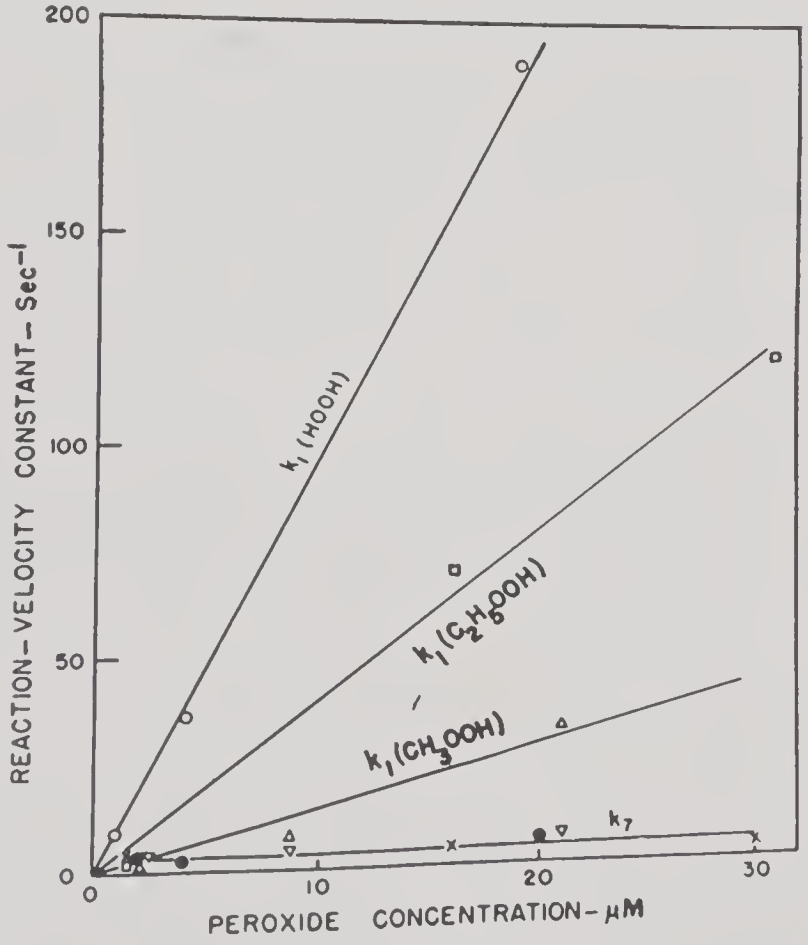

Fig. 2.18. Illustrating the linear increase of the first-order velocity constant for the formation of complex I of horse-radish peroxidase with peroxidase concentration (13). The bottom curve illustrates that the speed of transition from the primary to the secondary complex is independent of the peroxide concentration in the absence of a donor (Expt. 163a).

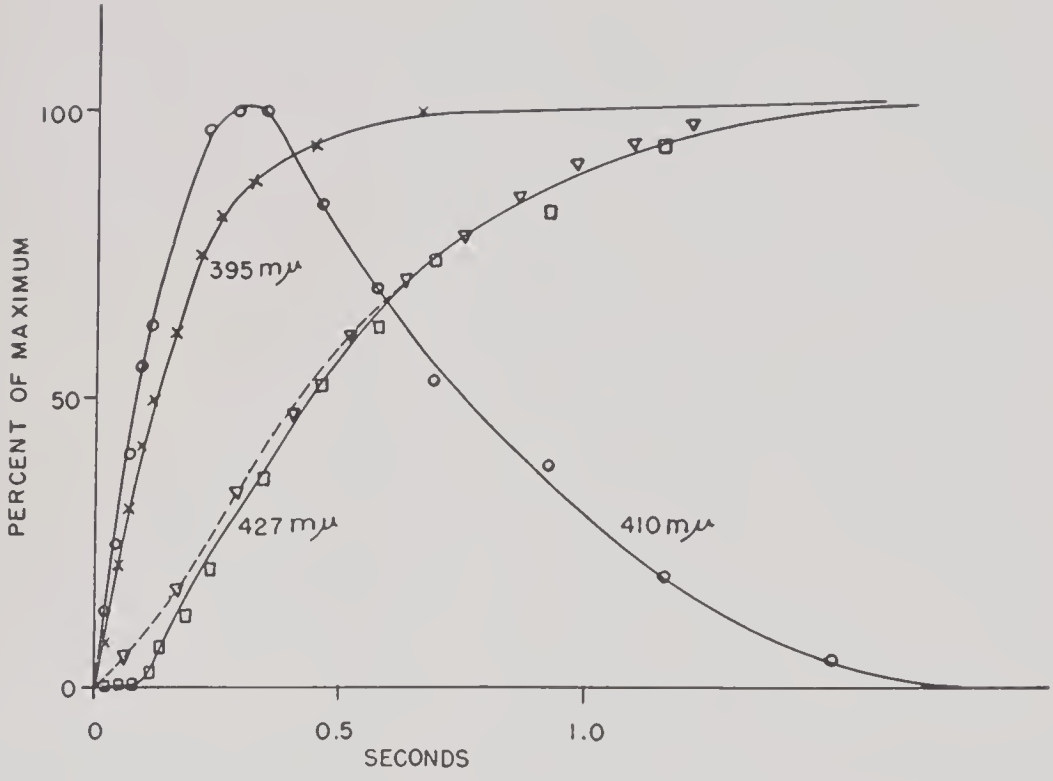

Fig. 2.19. A detailed study (13) of the kinetics of formation and disappearance of the primary complex of peroxidase and hydrogen peroxide and its conversion into the secondary complex. The data at 410 mμ represent complex I; at 427 mμ they represent complex II. The broken curve represents the area under the curve obtained at 410 mμ. These data indicate that the primary compound is transformed into the secondary compound (Expt. 301).

5. Acceleration of the Transition from Primary to Secondary Complexes

In the records thus far shown, the transition from the primary to the secondary complex requires a relatively long time, approximately one second, as shown by Figure 2.19. Since the values of the turnover numbers of peroxidases may reach several hundred times per second in the presence of donor, some mechanism must be present to speed up this transition during catalytic activity for this enzyme. Studies of the kinetics of the primary to secondary shift with the rapid flow method clearly show an acceleration of this reaction in the presence of a donor in the case of both horse-radish peroxidase and lactoperoxidase. Figure 2.20 illustrates how the rapid flow method may be used for demonstrating this effect by measurement of the effect of donor concentration upon the kinetics of formation of complex II in the presence of two concentrations of ascorbic acid. The upper record of Figure 2.20 shows that the formation of complex II is about 25% complete at the fastest value of flow velocity employed, whereas in the lower record, in which 200 μM ascorbic acid is employed, the formation of complex II is 50% complete during the flow. Since the only

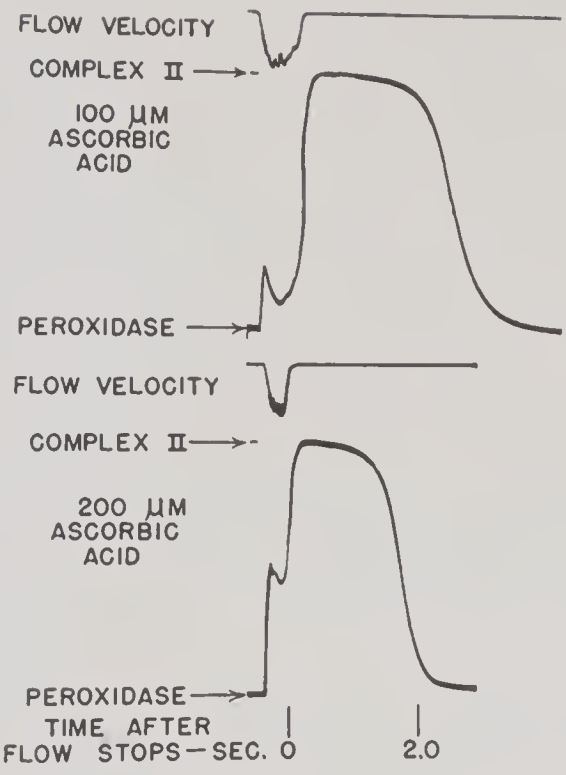

Fig. 2.20. Experimental evidence (13) that an increase in donor concentration increases the speed of transition from the primary to the secondary horse-radish peroxidase–hydrogen peroxide complex (Expt. 165b).

difference in the experimental conditions of these two records is the ascorbic acid concentration, the transition from complex I to complex II must have been accelerated by the increase in the donor concentration.

This increase in the speed of transition from complex I to complex II is apparently caused by all donors with which horse-radish peroxidase and lactoperoxidase peroxides react. Quantitative data are difficult to obtain over a wide range of experimental conditions but, under all experimental conditions so far studied directly by means of the rapid flow apparatus, the speed of transition from complex I to complex II is sufficiently great that complex II is the only one of the two enzyme–substrate complexes detectable during catalytic activity; a steady state concentration of complex I is usually negligible. For this reason, previous studies of the kinetics of horse-radish peroxidase based upon complex II are verified (77).

6. The Second-Order Reaction of Complex I with the Donor Molecule

By taking advantage of the relatively high stability of complex I, as formed from the peroxide-pretreated enzyme, it has been possible to determine the second-order velocity constant for the reaction of complex I with the donor molecule to form complex II (72). Figure 2.21 shows the

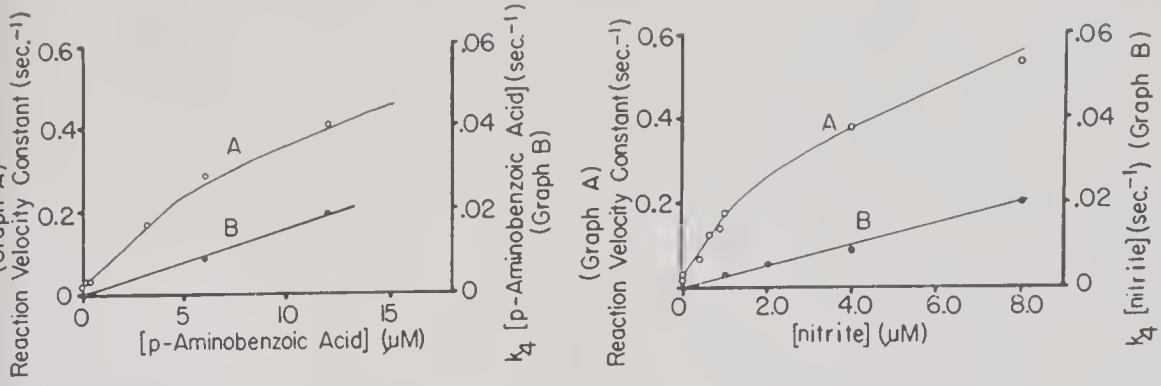

Fig. 2.21. Experimental data illustrating a second-order reaction of complex I and the donor molecule to form complex II. Graphs A represent the effect of donor concentration on the speed of formation of complex II; the circles represent experimental results and the solid lines are obtained from an electronic analogue computer solution based upon the second-order reaction mechanism. Both the points and the lines of Graphs B are experimental and are determined from the kinetics of formation and disappearance of complex II as calculated according to Equation (19) (Expts. S51a, AC-641) (Ref. 72).

variation of the speed of formation of complex II with the increase of concentration of two donors, *p*-aminobenzoic acid (left) and nitrite (right). At lower concentrations of the donor, the reaction velocity increases linearly with the donor concentration; at higher concentrations, the rate of formation of the primary intermediate becomes rate limiting and deviations from linearity are observed. Curve B of this figure is discussed in the next section.

Curves A are not drawn to follow the experimental points but are obtained from independent electronic analogue computer studies of the reaction mechanism which take into account the second order reaction of complex I with the donor molecule to form complex II. Thus, the compulsory nature of the transition from complex I to complex II is verified in the presence of an excess of donor molecules.

7. The Second-Order Reaction of Complex II with the Donor Molecule

The linear relation between the value of $k_4 a_0$ (Equation (19) for complex II) and the value of a_0 (ascorbic acid) is verified for three types of donor molecule in graph B of Figure 2.21 and in Figure 2.22. These values are computed directly from the "cycles" of complex II for Equation (19). Figure 2.21 shows this linear relation to obtain for *p*-aminobenzoic acid and for nitrite over a reasonable range of concentrations. Studies over a much wider range are obtained with ascorbic acid as donor. In the lower ranges of ascorbic acid concentration, the results are corrected for the blank or spontaneous rate of decomposition of complex II (Fig. 2.22).

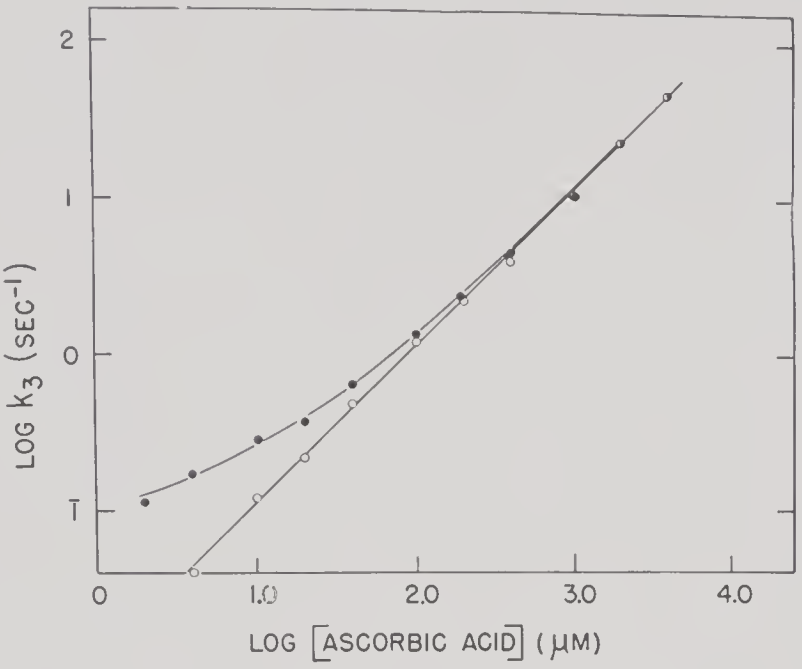

Fig. 2.22. Illustrating the second-order reaction of complex II and ascorbic acid over a wide range: $k_3 = k_4 a_0$ is computed from equation (19) by direct measurements of cycles of complex II. The experimental data (solid circles) are corrected for a blank rate to give the open circles (Expt. 368) (Ref. 78).

The straight line of 45° slope shows the linear increase of reaction velocity with the increase in concentration of the donor molecule. Since these reactions appear to be second order over as wide a range of donor concentration as can be used experimentally, we find no reason to postulate a further intermediate in the reaction of complex II with the donor, i.e., a ternary complex of enzyme–substrate intermediate and donor. On the basis of the results of such studies with catalase, such an intermediate might have an extremely short life and would therefore be difficult to demonstrate experimentally.

8. Relative Activities of Hydrogen and Alkyl Hydrogen Peroxide Complexes of Peroxidase

Although peroxidases combine with the substituted peroxides more slowly than with hydrogen peroxide (see Fig. 2.18), experimental data (78) show that the reactivities of the secondary complexes toward donors, in the case of horse-radish peroxidase, is independent of whether the alkyl group or a hydrogen atom is present on the peroxide molecule. Figure 2.23 illustrates the constancy of k_4 for the reactions of the three different enzyme–substrate compounds with ascorbic acid. Although in each record of Figure 2.23 the saturation of the enzyme with substrate and the duration of the cycles differs, the values of k_4 shown by the figure are nearly

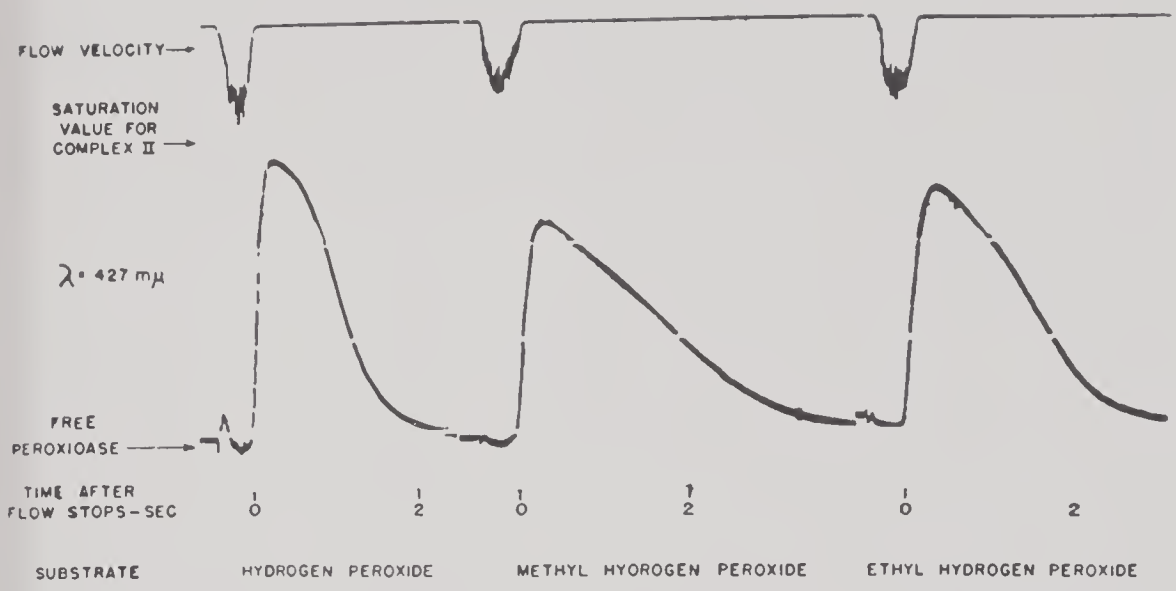

Fig. 2.23. The reaction kinetics of the secondary complex of horse-radish peroxidase with hydrogen peroxide, methyl hydrogen peroxide, or ethyl hydrogen peroxide in the presence of the same concentration of ascorbic acid. The values of k_4 calculated according to equation (19) are 2800, 2800, and 2200 M^{-1} sec.$^{-1}$, respectively. Thus the reactivity of complex II toward ascorbic acid is very nearly independent of the substituent attached to the peroxide group (Expt. 175).

identical. This has been found to be substantially true for the reactions of the catalase–peroxide complexes. With lactoperoxidase there is some decrease in activity when alkyl hydrogen peroxides are used.

The fact that the three different peroxide molecules should form intermediates of identical reactivity with the donor molecule has suggested to George (see General References) that the configuration of complex II does not involve the substituted portions of the peroxide molecule. For this reason, he has suggested that the intermediates be called compounds rather than complexes. An experimental determination of the step in the enzyme–substrate interaction at which the alkoxy portions of the substitute of peroxide are released is a topic on which no direct experimental data are available at the present time and thus an objective evaluation of George's interesting suggestion must await further experiments.

9. Donor Specificity of Peroxidases

The activities of the secondary complexes of peroxidases toward various donors has been quantitatively evaluated in terms of k_4, the velocity constant for the reaction of complex II with the donor. A survey of the values of k_4 for a large number of donors shows that this value can rise to one considerably in excess of the velocity constant for the combination of peroxidase and hydrogen peroxide: values approaching 10^8 M^{-1} sec.$^{-1}$ have

been obtained. On the other hand, the blank rate is so small when using the kinetics of complex II as a measure of the value of k_4 that significant measurements of k_4 have been obtained when its value is considerably less than 100 M^{-1} sec.$^{-1}$. These quantitative data verify the general rules established by Balls and Hale (79) that phenols, amines, and aminophenols react most rapidly with complex II.

The activity of the peroxidases is probably not limited to aromatic compounds but includes a class of substances containing the enediol group, such as reductone, ascorbic acid, and dihydroxymaleic acid.

The specificity of peroxidase appears to be much broader than that of catalase. However, it must be pointed out that we are here comparing the properties of catalase complex I with those of peroxidase complex II. Under such conditions we find that the steric effects demonstrated in the reaction of catalase I with alcohols of increasing chain lengths are not found in the case of peroxidases for which the reaction of complex II with large donor molecules can proceed quite rapidly; *p*-hydroxydiphenyl reacts more rapidly than hydroquinone or phenol. The properties of catalase complex II in its reaction with the quinones and related compounds appear to show some similarities to those of peroxidase complex II (49).

VI. SUMMARY

Kinetic data on intermediates in enzyme action show clearly how the mechanism of the enzyme action can be deduced from the reaction kinetics; the perplexing problems of enzyme mechanisms are readily illuminated by these techniques, for example, how the green and red intermediates of peroxidase participate in the over-all activity, or the mechanism by which catalase decomposes hydrogen peroxide by consecutive reactions of hydrogen peroxide and catalase and with the catalase–hydrogen peroxide complex. In fact, there are a few conclusions that can be drawn from these data that are useful concepts for the consideration of enzyme action in general.

These direct studies of the nature of enzyme–substrate compounds of peroxidases and catalases prove that the ideas of Henri and of Michaelis and Menten are correct; the rates of these reactions are governed by the concentrations of the active enzyme–substrate compounds. The reaction mechanisms, however, are rather different from those of invertase and the proteolytic enzymes on which many of the classical studies were based (for summaries see Lineweaver and Burk (80)). The kinetics of the peroxidases and catalases involve the consecutive reactions of the substrate and

the donor molecule with the enzyme and with the enzyme–substrate complex:

$$E + S \underset{k_2}{\overset{k_1}{\rightleftharpoons}} ES \tag{33}$$

$$ES + AH_2 \overset{k_4}{\rightleftharpoons} E + SH_2 + A \tag{34}$$

The Michaelis constant K_m for such a system is not a true constant; it is proportional to the donor concentration, $K_m = (k_4[A] + k_2)/k_1$.

No experimental evidence has been obtained for the reaction:

$$ES + AH_2 \rightleftharpoons ESAH_2 \tag{35}$$

and therefore there is no Michaelis constant for the donor. It follows that there are no "optimum conditions" for enzymic activity; the activity or turnover number increases linearly with the donor concentration provided only that the substrate concentration is sufficient, that is:

$$[S] \gg (k_4[A] + k_2)/k_1$$

Thus, "optimum" activity would be found at infinite substrate and donor concentrations. Surely, deviations from these simple kinetics occur at very high substrate and donor concentrations, but the nature of such deviations can be explained on the basis that the enzyme is being inactivated—that the concentration of E is being reduced and not that $ESAH_2$ is being formed.

The decomposition of hydrogen peroxide by mammalian and bacterial catalases is a peroxidatic reaction in which S and AH_2 are the same substance, hydrogen peroxide. In this case activities, or turnover numbers, of ten million times per second have been measured without any deviations from the general mechanism of Equations (1) and (2).

There is no single reaction velocity constant which specifies the activity of a peroxidase or a catalase (for which S and A are different molecules); both k_1 and k_4 must be specified. The relative values of k_1 and k_4 for various substrates and donors are the enzyme specificity. The donor specificity of horse-radish peroxidase has been found to vary over a range of four million to one.

The only substances which have yet been found to react with catalase complex I at considerable values of k_4 are substances with a hydrogen atom and a hydroxyl group attached to carbon (as in alcohols and formate), nitrogen (as in nitrites), and oxygen (as in hydrogen peroxide). Many substances react with peroxidase complexes I and II—aromatic and aliphatic organic compounds, as well as some inorganic ones. Phenols,

amines, and aminophenols give by far the larger values of k_4, although fairly rapid reactions occur with aliphatic enediols.

The values of k_4 for the reaction of the horse-radish peroxidase–peroxide complexes do not appear to be affected by the size of the donor molecule; this is in accord with the supposition that the hemes of horse-radish peroxidase lie exposed on the surface of the protein: the heme is readily split off in a reversible fashion (81). On the other hand, the values of k_4 for the reaction of the bacterial and erythrocyte catalases with donor decrease markedly with increasing size of the donor molecule. This agrees with the supposition that the hemes of these catalases are "buried" within the protein molecule. As yet, no catalase has been reversibly split into hemes and protein. This limited accessibility of the catalase hematins greatly restricts the number of donors for which k_4 has a measurable value.

Studies of the effect of pH upon k_1 and k_4 show, in general, negligible effect in the range 4 to 10. Therefore, hydrogen or hydroxyl ions do not appear or disappear in Equations (1) and (2). As yet, clear-cut evidence for the effect of the dissociation of heme-linked groups on k_1 and k_4 is lacking (82).

As the details of the enzymic reaction mechanism become unravelled to a greater extent, the number of intermediates involved in the reaction likewise increases. As stated above, bimolecular reaction with only the substrate was sufficient to explain the mechanism considered by Henry (3) and by Michaelis and Menten (2). Equation (34) above emphasizes the importance of the donor reaction. The observation in peroxidase that both the green and the red compounds participate in a compulsory reaction sequence and that the transition between the two is pseudo-first order with respect to the donor concentration leads us to elaborate on Equations (33) and (34) for the particular case of peroxidase, as follows:

$$\text{HRP} + \text{H}_2\text{O}_2 \underset{k_2 = 0.5 \text{ sec.}^{-1}}{\overset{k_1 = 0.9 \times 10^7 \, M^{-1} \text{ sec.}^{-1}}{\longrightarrow}} \text{HRP-I} + \text{H}_2\text{O}_2 \qquad (36)$$

$$\text{HRP-I} + \text{AH}_2 \xrightarrow{k_7 = 2 \times 10^7 \, M^{-1} \text{ sec.}^{-1}} \text{HRP-II} + \text{AH}^\circ \qquad (37)$$

$$\text{HRP-II} + \text{AH}_2 \xrightarrow{k_4 = 2.4 \times 10^5 \, M^{-1} \text{ sec.}^{-1}} \text{HRP} + \text{AH}^\circ \qquad (38)$$

Velocity constants for a particular donor molecule (*p*-aminobenzoic acid) show that the first two steps are very rapid relative to the last step which will be rate limiting under usual conditions of enzyme activity. In view of the fact that the two steps from complex I to complex II and from complex II to the free enzyme can represent at most a one electron transition, it is apparent that electrons must be donated from the oxidizable substrate one at a time. This we find in peroxidase an example of

Michaelis's compulsory univalent oxidation-reduction reaction (83). It is not clear why the two intermediate steps can readily be observed in peroxidase but not in the oxidation of alcohols by catalase complex I. It may be that peroxidase complex I can accept only one of the two electrons from the donor and that the latter must be replaced by a fresh molecule before further reduction of the enzyme can occur. This latter suggestion is in accord with the observation of small concentrations of free radicals in peroxidase-catalyzed reactions (84) and in laccase oxidation (85).

The reactions of catalase and peroxidase have served as sound models for the critical evaluation of various reaction mechanisms in biological oxidation-reduction reactions. It is of great interest to consider further refinements of the mechanisms of these reactions and to apply the results thereby obtained to oxidation reactions involving molecular oxygen.

References

1. H. Theorell, *Advances in Enzymol.*, **21**, 31 (1958).
1a. V. Massey, Q. H. Gibson, and C. Veeger, *Biochem. J.*, **77**, 341 (1960).
1b. B. Commoner and T. C. Hollocher, Jr., *Proc. Natl. Acad. Sci. U. S.*, **46**, 404 (1960).
1c. T. C. Hollocher, Jr., and B. Commoner, *Proc. Natl. Acad. Sci. U. S.*, **46**, 416 (1960).
2. L. Michaelis and M. L. Menten, *Biochem. Z.*, **49**, 333 (1913).
3. V. Henri, *Lois generales de l'action des diastases*, Hermann, Paris, 1903.
4. J. B. S. Haldane, *Enzymes*, Longmans Green, London, 1931.
5. K. G. Stern, *J. Biol. Chem.*, **114**, 473 (1936).
6. D. Keilin and T. Mann, *Proc. Roy. Soc. London*, **B122**, 119 (1937).
7. H. Theorell, *Arkiv. Kemi Mineral. Geol.*, **A16**, No. 2 (1942).
8. F. J. W. Roughton and G. A. Millikan, *Proc. Roy. Soc. London*, **A155**, 258 (1936).
9. B. Chance, *J. Franklin Inst.*, **228**, 459 (1940).
10. B. Chance, J. G. Brainerd, F. A. Cajori, and G. A. Millikan, *Science*, **92**, 455 (1940).
11. B. Chance, *J. Biol. Chem.*, **151**, 553 (1943).
12. H. Theorell, *Enzymologia*, **12**, 250 (1941).
13. B. Chance, *Arch. Biochem.*, **22**, 224 (1949).
14. L. Michaelis, *Ann. N. Y. Acad. Sci.*, **40**, 39 (1940).
15. J. E. LuValle and D. R. Goddard, *Quarterly Rev. Biol.*, **23**, 197 (1948).
16. P. George, *Nature*, **169**, 612 (1952).
17. L. H. Piette, I. Yamazaki, and H. S. Mason, *Free Radicals Biol. Systems, Proc. Symp., Stanford, Calif., 1960*, 195 (1961).
18. T. Nakamura, *Free Radicals Biol. Systems, Proc. Symp., Stanford, Calif., 1960*, 169 (1961).
19. J. D. Sumner and A. L. Dounce, *J. Biol. Chem.*, **121**, 417 (1937).
20. K. G. Stern, *J. Gen. Physiol.*, **20**, 631 (1937).
21. D. Keilin and E. F. Hartree, *Biochem. J.*, **39**, 148 (1945).
22. H. von Euler and K. Josephson, *Ann.*, **452**, 158 (1927).
23. K. G. Stern, *Z. physiol. Chem.*, **209**, 176 (1932).
24. B. Chance, *Acta Chem. Scand.*, **1**, 236 (1947).

25. E. Margoliash and A. Novogrodsky, *Biochem. J.*, **68**, 468 (1958).
26. E. Margoliash, A. Novogrodsky, and A. Schejter, *Biochem. J.*, **74**, 339 (1960).
27. E. Margoliash and A. Schejter, *Biochem. J.*, **74**, 349 (1960).
28. B. Chance and G. R. Schonbaum, in *Haematin Enzymes, A Symposium of the International Union of Biochemistry (Canberra, 1959)*, Pergamon Press, Oxford, 1961, p. 255. See also *J. Biol. Chem.*, **237**, 2391 (1962).
28a. B. Chance, *J. Biol. Chem.*, **179**, 1336 (1949).
29. D. Keilin and P. Nicholls, *Biochim. et Biophys. Acta*, **29**, 302 (1958).
30. J. Higgins, Ph.D. thesis, University of Pennsylvania, 1959.
31. M. Dixon and E. C. Webb, *Enzymes*, Academic Press, New York, 1958.
32. P. D. Boyer, H. Lardy, and K. Myrbäck, *The Enzymes*, 2nd ed., Academic Press, New York, 1959.
33. P. J. G. Mann, *Biochem. J.*, **24**, 918 (1931).
34. B. Chance and A. C. Maehly, in *Methods in Enzymology*, Vol. 2, Academic Press, New York, 1955, p. 771.
35. A. C. Maehly and B. Chance, *Methods Biochem. Anal.*, **1**, 412 (1954).
36. M. G. Schmidt, W. B. Robinson, and E. Stotz, *J. Biol. Chem.*, **179**, 881 (1949).
37. B. Chance, *Arch. Biochem.*, **24**, 389 (1949).
38. B. Chance, *J. Biol. Chem.*, **197**, 577 (1952).
39. B. Chance, *J. Biol. Chem.*, **180**, 865 (1949).
40. B. Chance, *Biochem. J.*, **46**, 387 (1950).
41. B. Chance, *Rev. Sci. Instr.*, **18**, 601 (1947).
42. I. M. Kolthoff and J. J. Lingane, *Polarography*, Interscience, New York, 1941; 2nd ed., 1952.
43. H. Theorell and A. Ehrenberg, *Arch. Biochem. Biophys.*, **41**, 442 (1952).
44. A. Brill, H. den Hartog, and V. Legallais, *Rev. Sci. Instr.*, **29**, 383 (1958).
44a. B. Chance, V. Legallais, and L. Bicking, *Free Radicals Biol. Systems, Proc. Symp., Stanford, Calif., 1960*, 101 (1961).
44b. I. Yamazaki, H. S. Mason, and L. Piette, *J. Biol. Chem.*, **235**, 2444 (1960).
44c. G. Czerlinski, in preparation.
45. D. Keilin and E. F. Hartree, *Proc. Roy. Soc. London*, **B119**, 141 (1936).
46. D. Keilin and E. F. Hartree, *Proc. Roy. Soc. London*, **B117**, 1 (1935).
47. B. Chance, *J. Biol. Chem.*, **179**, 1341 (1949).
48. P. George, *Biochem. J.*, **52**, xix (1952).
49. P. Nicholls, Ph.D. thesis, University of Cambridge, 1959.
50. K. Agner and H. Theorell, *Arch. Biochem.*, **10**, 321 (1946).
51. B. Chance, *Arch. Biochem. Biophys.*, **41**, 404 (1952).
52. B. Chance, *J. Biol. Chem.*, **179**, 1331 (1949).
53. B. Chance, *J. Biol. Chem.*, **194**, 471 (1952).
54. H. Kon and N. Davidson, *J. Mol. Biol.*, **1**, 190 (1959).
55. M. F. Perutz, M. G. Rossman, A. F. Cullis, H. Muirhead, G. Will, and A. C. T. North, *Nature*, **185**, 416 (1960).
56. J. C. Kendrew, R. E. Dickerson, B. E. Strandberg, R. G. Hart, D. R. Davies, D. C. Phillips, and V. C. Shore, *Nature*, **185**, 422 (1960).
57. B. Chance, *J. Biol. Chem.*, **182**, 643 (1950).
58. D. Herbert and J. Pinsent, *Biochem. J.*, **43**, 193 (1948).
59. B. Chance and D. Herbert, *Biochem. J.*, **46**, 402 (1950).
60. B. Chance, *J. Biol. Chem.*, **180**, 947 (1949).
61. D. Keilin and E. F. Hartree, *Biochem. J.*, **42**, 221 (1948).
62. B. Chance, D. S. Greenstein, and F. J. W. Roughton, *Arch. Biochem. Biophys.*, **37**, 301 (1952).

63. R. K. Bonnichsen, B. Chance, and H. Theorell, *Acta Chem. Scand.*, **1**, 685 (1947).
64. Y. Ogura, *Arch. Biochem.*, **27**, 288 (1955).
65. B. Chance, *J. Biol. Chem.*, **179**, 1311 (1949).
66. D. Keilin and E. F. Hartree, *Biochem. J.*, **49**, 88 (1951).
67. B. Chance, *J. Biol. Chem.*, **182**, 643 (1950).
68. L. A. Heppel and V. T. Porterfield, *J. Biol. Chem.*, **178**, 549 (1949).
69. D. Keilin and E. F. Hartree, *Biochem. J.*, **39**, 293 (1945).
70. B. Chance, in *Currents in Biochemical Research*, Interscience, New York, 1956, p. 308.
71. B. Chance, *J. Am. Chem. Soc.*, **72**, 1577 (1950).
72. B. Chance, *Arch. Biochem.*, **21**, 416 (1949).
73. H. Theorell and A. Akeson, *Arkiv. Kemi Mineral. Geol.*, **B17**, No. 7 (1943).
74. K. G. Paul, personal communication.
75. B. Chance, unpublished data.
76. B. Chance, in *Haematin Enzymes, A Symposium of the International Union of Biochemistry, (Canberra, 1959)*, Pergamon Press, Oxford, 1961, p. 254.
76a. A. S. Brill and R. J. P. Williams, *Biochem. J.*, **78**, 253 (1961).
77. B. Chance, *Arch. Biochem. Biophys.*, **37**, 235 (1952).
78. B. Chance, *Arch. Biochem.*, **24**, 380 (1949).
79. A. K. Balls and W. S. Hale, *J. Biol. Chem.*, **107**, 767 (1934).
80. H. Lineweaver and D. Burk, *J. Am. Chem. Soc.*, **55**, 658 (1934).
81. H. Theorell, *Arkiv. Kemi Mineral. Geol.*, **B14**, No. 20 (1940).
82. B. Chance, *Arch. Biochem. Biophys.*, **40**, 153 (1952).
83. L. Michaelis, *Chem. Revs.*, **16**, 243 (1935).
84. I. Yamazaki, H. S. Mason, and L. Piette, *Federation Proc.*, **19**, 33 (1960).
85. T. Nakamura, *Federation Proc.*, **19**, 26 (1960).

General References

Chance, B., "Enzyme-Substrate Compounds," in *Advances in Enzymology*, Vol. XII, F. F. Nord, ed., Interscience, New York, 1951, p. 153.

Chance, B., "Enzyme-Substrate Compounds and Electron Transfer," in *Currents in Biochemical Research*, D. E. Green, ed., Interscience, New York, 1956, p. 308.

Chance, B., "The Identification of Enzyme-Substrate Compounds," in *Modern Trends in Biochemistry and Physiology*, E. S. G. Barron, ed., Academic Press, New York, 1952.

Chance, B., and Smith, L., "Biological Oxidations," *Ann. Rev. Biochem.*, **21**, 687 (1952).

Falk, J. E., Lemberg, R., and Morton, R. K., eds., *Haematin Enzymes, A Symposium of the International Union of Biochemistry* (Canberra, 1959), Pergamon Press, Oxford, 1961.

George, P., "On the Nature of Hemoprotein Reactions," in *Currents in Biochemical Research*, D. E. Green, ed., Interscience, New York, 1956, p. 338.

George, P., "The Specific Reaction of Iron in Some Hemoproteins," in *Advances in Catalysis*, Vol. IV, Academic Press, 1953, p. 367.

Keilin, D., and Hartree, E. F., "Purification of Horse-Radish Peroxidase and Comparison of Its Properties with Those of Catalase and Methemoglobin," *Biochem. J.*, **49**, 88 (1951).

Lemberg, R., and Legge, J. W., *Hematin Compounds and Bile Pigments, Their Constitution, Metabolism, and Function*, Interscience, New York, 1949.

Nicholls, P., and Schonbaum, G., in *The Enzymes*, 2nd ed., P. D. Boyer, H. Lardy, and K. Myrbäck, eds., Academic Press, New York, in press.

Theorell, H., "Heme-Linked Groups and Mode of Action of Some Hemoproteins," in *Advances in Enzymology*, Vol. VII, F. F. Nord, ed., Interscience, New York, 1947, p. 265.

Wyman, Jr., Jeffries, "Heme Proteins," in *Advances in Protein Chemistry*, Vol. IV, Academic Press, New York, 1948.

CHAPTER XXIII

Thermodynamics and Reaction Mechanism

MAURICE M. KREEVOY, *University of Minnesota*

I. Statistical Thermodynamics 1361
1. The Reason Why 1361
2. Equilibrium Constant in Terms of Partition Functions 1361
3. Partition-Function Formulas 1364
4. Rate Constant in Terms of Partition Functions 1371
5. Complex and Reversible Reactions 1371
6. The Brønsted Rate Law 1374
7. The Effect of Pressure 1374
8. Some Qualifications 1375
II. Applications 1375
1. To Gas-Phase Equilibria 1375
2. To Gas-Phase Rates 1376
3. Entropies of Reaction in Solution 1380
4. Activation Energy and Energy of Reaction 1392
5. The Behavior of Activity Coefficients—The Hammett Acidity Function and Related Functions 1399
III. Conclusion 1403
References 1402
General References 1460

I. STATISTICAL THERMODYNAMICS

1. The Reason Why

The debt owed by the chemical kineticist to statistical thermodynamics is enormous. This is particularly true of the organic kineticist, as he almost always deals with complex reactions of large complex molecules in nonideal condensed phases. Treatment of such reactions by collision theory is usually unilluminating.

Statistical thermodynamics, in which the author includes the transition state theory of reaction rates, has offered the most useful alternatives (1).

2. Equilibrium Constant in Terms of Partition Functions

Although many derivations of equilibrium constants in terms of partition functions are available in standard texts (2), the author will take

this opportunity to present still another. The equilibrium (1) will be considered, in which A and B are isomeric molecules.

$$A \rightleftharpoons B \tag{1}$$

For any system of electrons and nuclei (considered single particles for purposes of the present discussion) in space, there is a corresponding energy which is a function of the position and momentum of each particle. (Each molecule is considered a system in this discussion.) If a very large number of such systems is to be considered and if equilibrium has been attained, the number of systems N in a particular state i having a particular set of positions and momenta, is given by the Boltzmann expression, shown in Equation (2)

$$N = \alpha \exp(-\epsilon_i/kT) \tag{2}$$

In Equation (2), α is a proportionality factor with which we need not be concerned, k is the Boltzmann constant, ϵ_i is the energy relative to some arbitrary standard, and T is the absolute temperature. (For purposes of the present discussion, it is assumed that the energy of each system is very nearly independent of the positions of all other systems, so that the position of the nuclei only needs to be specified with respect to some arbitrary reference point within each system.) It is apparent from the exponential form of Equation (2) that only those states having ϵ_i close (by comparison with kT) to the lowest attainable value of ϵ_i, ϵ_0, will be heavily populated. Experience has shown that there are usually a number of states having particularly low energies. These are the states that resemble the equilibrium configurations of stable molecules. In the present case, we have assumed that there are two groups of such states. For each of these groups there is a single state having the lowest energy within that group. These two states have quite different arrangements of the nuclei, so that to pass from one to the other a system must pass through one or more high energy states. About each of the lowest energy states a number of other states are grouped, with nuclear arrangements only slightly different from, and energies only slightly higher than, the two lowest energy states. One of these groups we consider characteristic of the molecule A and the other, characteristic of the molecule B. We shall ignore high energy states for the moment. If a large number of these systems has been allowed to come to equilibrium, N_A of them will be molecules of A, and N_B will be molecules of B. Equation (3) follows from the Boltzmann expression.

$$N_A = \alpha \sum_i^A \exp(-\epsilon_i/kT) \tag{3}$$

The starting point for the energies ϵ_i is perfectly arbitrary, and it is both convenient and conventional to consider that A molecules would have zero energy if their nuclei had no momentum and were occupying positions of minimum potential energy. The same convention is applied to B molecules. In the general case, the potential energy minimum associated with the arrangement that we have called B will not be the same as that associated with A, and, for purposes of argument, it will be assumed higher by an amount $\Delta\epsilon_0$. The energy levels ${\epsilon'}_i^{\mathrm{B}}$ of the various B states will then be given by Equation (4).

$$ {\epsilon'}_i^{\mathrm{B}} = \Delta\epsilon_0 + \epsilon_i^{\mathrm{B}} \tag{4} $$

In Equation (4), ${\epsilon'}_i^{\mathrm{B}}$ is the energy level if zero is assigned as the energy of the most stable arrangement of all, i.e., with the particles arranged as an A molecule and no momentum associated with the nuclei. Equation (5) follows directly from these definitions.

$$ \begin{aligned} N_{\mathrm{B}} &= \alpha \sum_i^{\mathrm{B}} \exp\left\{-(\Delta\epsilon_0 + \epsilon_i^{\mathrm{B}})/kT\right\} \\ &= \alpha \exp\left(-\Delta\epsilon_0/kT\right) \sum_i^{\mathrm{B}} \exp\left(-\epsilon_i^{\mathrm{B}}/kT\right) \end{aligned} \tag{5} $$

The assumption (made above), that the potential energy of each molecule (system) could be specified by indicating the coordinates of the particles with respect to some internal reference point, is equivalent to assuming that both A and B are perfect gases. The thermodynamic equilibrium constant K for Equation (1) is given by Equation (6).

$$ \begin{aligned} K &= N_{\mathrm{B}}/N_{\mathrm{a}} \\ &= e^{-\Delta\epsilon_0/kT} \frac{\sum_i^{\mathrm{B}} \exp\left(-\epsilon_i^{\mathrm{B}}/kT\right)}{\sum_i^{\mathrm{A}} \exp\left(-\epsilon_i^{\mathrm{A}}/kT\right)} \end{aligned} \tag{6} $$

By a simple conversion of units, $\Delta\epsilon_0/kT$ becomes $\Delta E_0/RT$, ΔE_0 will be recognized as the potential energy of reaction (1) and the two summations are the *partition functions* f of B and A. Straightforward application of thermodynamics then gives the standard free energy, entropy, and enthalpy of reaction (1).

$$ \begin{aligned} \Delta F^\circ &= -RT \ln K \\ &= \Delta E_0 - RT \ln (f_{\mathrm{B}}/f_{\mathrm{A}}) \end{aligned} \tag{7} $$

$$ \begin{aligned} \Delta H^\circ &= RT^2(d/dT)(\ln K) \\ &= \Delta E_0 + RT^2(d/dT)\left[\ln (f_{\mathrm{B}}/f_{\mathrm{A}})\right] \end{aligned} \tag{8} $$

$$ \begin{aligned} \Delta S^\circ &= (\Delta H^\circ - \Delta F^\circ)/T \\ &= R \ln (f_{\mathrm{B}}/f_{\mathrm{A}}) + RT(d/dT)\left[\ln (f_{\mathrm{B}}/f_{\mathrm{A}})\right] \end{aligned} \tag{9} $$

3. Partition Function Formulas

The motions of the nuclei within a molecule are very minute compared to the motions of the molecule as a whole. The translational energy of a molecule may be calculated by considering that the whole molecule is a single mass point. Quantum mechanics gives the energy levels shown by Equation (10) for a particle in a three-dimensional box (3).

$$\epsilon = h^2/8m[(n_x^2/a^2) + (n_y^2/b^2) + (n_z^2/c^2)] \tag{10}$$

In Equation (10), m is the mass of the particle; h is Planck's constant; a, b, and c are the dimensions of a rectangular box; n_x, n_y, and n_z are integral quantum numbers. The important thing to note about Equation (10) is that, for any reasonable sized box, the energy levels are extremely close together, even for fairly high quantum numbers. For example, for a molecule of mol. wt. 60 in a container with $a = 1$ cm., the change in ϵ on going from $n_x = 100$ to $n_x = 101$ is $\sim 10^{-29}$ ergs/molecule or $\sim 1.4 \times 10^{-16}$ kcal./mole.

For a fairly good approximation, we may also consider that the rotational motions of a molecule are independent of its internal motions. Unfortunately, quantum mechanics does not give us an analytical function for the rotational energy levels of the general polyatomic molecule (4); to get some idea of their spacing, we may examine the rotational energy levels ϵ_n of a heteronuclear diatomic molecule. These are given by Equation (11) in which I is the rotational moment of

$$\epsilon_n = (h^2/8\pi^2 I)n\ (n + 1) \tag{11}$$

inertia and n is the rotational quantum number (5). With a moment of inertia of about 10^{-38} gm. cm.^{2} (typical for a molecule of molecular weight around 60), $\epsilon_{101} - \epsilon_{100}$ is $\sim 3.5 \times 10^{-14}$ ergs/molecule or ~ 0.5 kcal./mole; $\epsilon_2 - \epsilon_1$ is $\sim 10^{-2}$ kcal./mole. These spacings are still fairly small, but they are much larger than those for translation.

If we consider a particle (atomic nucleus) that is not part of a molecule, it is obvious that any motion it may execute can be considered some linear combination of motions along its three cartesian coordinates. These are then called its *normal modes*. To the approximation that translational and rotational motions are independent of internal vibrations, there are three normal translational modes and three normal rotational modes for the general polyatomic molecule. For the n-atomic molecule there remain $3n - 6$ normal internal or vibrational modes, because no normal modes are lost in the formation of a molecule. If the molecule has only two normal rotational modes (a diatomic or linear polyatomic molecule), it will then have one more normal internal mode. The number of normal modes

of a particular type is equal to the number of degrees of freedom of that type.

For a complex organic molecule, some of these normal modes can be easily located to a good approximation by inspection. For example, the motion of a hydrogen atom along a C—H bond, toward and away from the carbon atom to which it is bonded, will very nearly be a normal mode in any molecule containing a C—H bond. Other normal modes, particularly those involving the motions of the heavier atoms of a molecule, will be very complex indeed, particularly when the molecule has little or no symmetry. Any motion of a molecule can be described as some linear combination of these normal modes.

The normal motion of a group of atoms is mathematically equivalent to the motion of a mass point along a single coordinate under the influence of an appropriate potential function. For example, a heteronuclear diatomic molecule has a single normal internal mode which consists of the atoms moving toward and away from each other. The reduced mass μ for this motion is given by Equation (12)

$$\mu = m_1 m_2/(m_1 + m_2) \tag{12}$$

in which m_1 and m_2 are the masses of the atoms. The force F tending to restore the atoms to their equilibrium positions can be expressed as a power series in x, the distance by which the bond is stretched beyond its equilibrium length.

$$F = -(ax + bx^2 + \ldots) \tag{13}$$

(The negative sign appears because the force is always in the opposite direction from the displacement.) Since the force is the negative derivative of the potential energy ϵ, $d\epsilon/dx$ is given by Equation (14),

$$d\epsilon/dx = ax + bx^2 + \ldots \tag{14}$$

and ϵ is given by Equation (15).

$$\epsilon = ax^2 + bx^3 + \ldots \tag{15}$$

The displacements involved are small, so all higher terms in Equation (15) are customarily neglected (6) for all but the most precise work. Equations (14) and (15) are identical with the equations governing the potential energy of a point of mass μ moving along a straight line if the force tending to restore it to its equilibrium position is given by Equation (13), with x its distance from the equilibrium position in the positive direction. If all the higher terms in Equation (15) are neglected, such a mass point will be a harmonic oscillator and the constant a can be equated to a force constant k.

The permitted energy levels of a quantum mechanical harmonic oscillator are given by Equation (16) (ref. 7).

$$\epsilon_n = (h/2\pi)(k/\mu)^{1/2}(n + {}^1/_2) \tag{16}$$

The force constant is not readily evaluated from first principles, and the reduced mass can also be hard to come by if the normal mode is a complicated one. Fortunately, the whole quantity $(1/2\pi)(k/\mu)^{1/2}$ can be equated to a fundamental vibrational frequency ν which can be obtained by an appropriate analysis of the molecule's infrared spectrum or estimated by analogy. Fundamental vibrational frequencies of organic molecules usually range between $\sim$200 cm.$^{-1}$ and $\sim$4000 cm^{-1}. With the former value of ν, $\epsilon_2 - \epsilon_1$ is 0.572 kcal./mole, whereas, with the latter, it is 11.44 kcal./mole. It is apparent that even the lower value is of the order of magnitude of RT around room temperature so that the population in higher vibrational levels is small. Figure 1 shows a vibrational energy level and some of its associated rotational and translational levels.

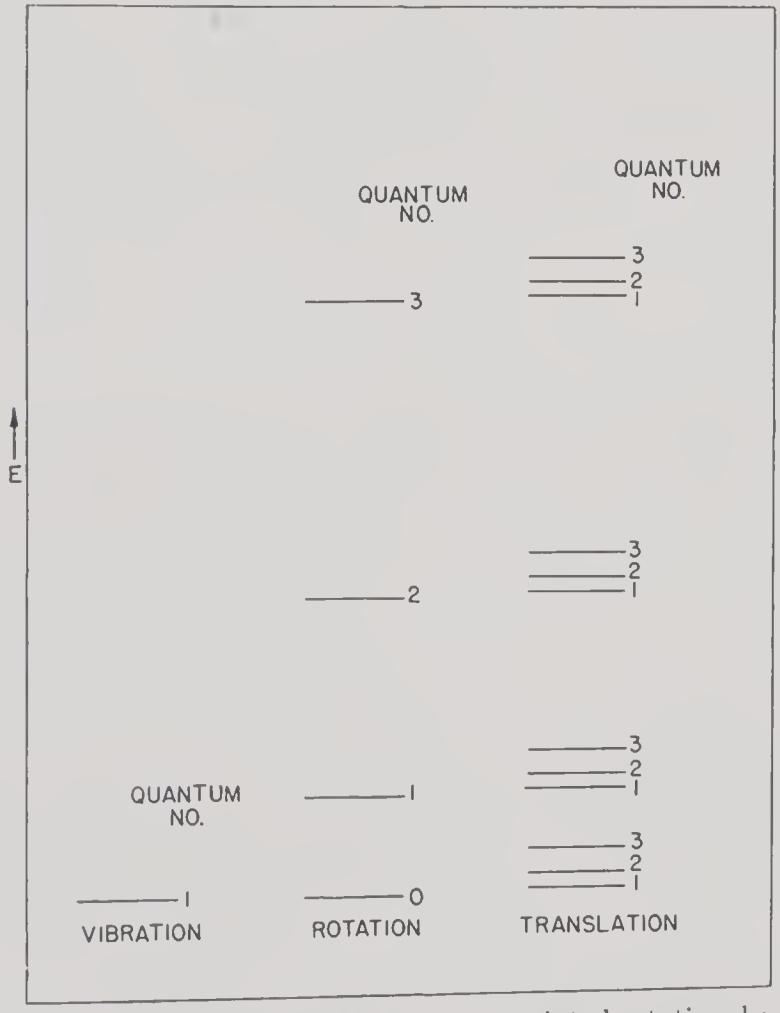

Fig. 1. A single vibrational energy level and its associated rotational and translational energy levels. The rotational energy levels are compressed relative to the translational levels so that several rotational levels can be shown.

The energy required to lift an electron from the highest filled energy level to the lowest unfilled level is so high that, at ordinary temperatures and in the absence of excitation by ultraviolet or visible light, only the lowest possible electronic energy levels are populated. The change in electronic energy accompanying reaction (1) is included in $\Delta\epsilon_0$, and we may omit further discussion of the electrons.

It has already been assumed that translation, rotation, and internal vibration are independent motions. With that assumption, the total energy of a molecule such as A may be written as the sum of its translational, rotational, and vibrational energy.

$$\epsilon_i = \epsilon^j_{\text{vib}} + \epsilon^k_{\text{rot}} + \epsilon^l_{\text{trans}} \tag{17}$$

The superscripts j, k, and l in Equation (17) denote the quantum numbers of the vibrational, rotational, and translational states. Equation (17) and the definition of f lead directly to Equations (18–20).

$$\begin{aligned} f = \sum_1^l \exp\{-(\epsilon^1_{\text{vib}} + \epsilon^1_{\text{rot}} + \epsilon^l_{\text{trans}})/kT\} + \\ \sum_1^l \exp\{-(\epsilon^1_{\text{vib}} + \epsilon^2_{\text{rot}} + \epsilon^l_{\text{trans}})/kT\} + \ldots \\ + \sum_1^l \exp\{-(\epsilon^2_{\text{vib}} + \epsilon^1_{\text{rot}} + \epsilon^l_{\text{trans}})/kT\} + \ldots \end{aligned} \tag{18}$$

$$\begin{aligned} f = \exp\{-(\epsilon^1_{\text{vib}} + \epsilon^1_{\text{rot}})/kT\} \sum_1^l \exp(-\epsilon^l_{\text{trans}}/kT) + \\ \exp\{-(\epsilon^1_{\text{vib}} + \epsilon^2_{\text{rot}})/kT\} \sum_1^l \exp(-\epsilon^l_{\text{trans}}/kT) + \ldots \\ + \exp\{-(\epsilon^2_{\text{vib}} + \epsilon^1_{\text{rot}})/kT\} \sum_1^l \exp(-\epsilon^l_{\text{trans}}/kT) + \ldots \end{aligned} \tag{19}$$

$$\begin{aligned} f = \sum_1^l \exp(-\epsilon^l_{\text{trans}}/kT)\,[\exp\{-(\epsilon^1_{\text{vib}} + \epsilon^1_{\text{rot}})/kT\} + \\ \exp\{-(\epsilon^1_{\text{vib}} + \epsilon^2_{\text{rot}})/kT\} + \ldots + \exp\{-(\epsilon^2_{\text{vib}} + \epsilon^1_{\text{rot}})/kT\} + \ldots] \end{aligned} \tag{20}$$

The quantity $\sum_1^l \exp(-\epsilon^l_{\text{trans}}/kT)$, which has been separated out, is called the *translational partition function* f_{trans}. In a similar way, the rotational and vibrational partition functions can be taken out of Equation (20) so that the partition function is given by Equation (21).

$$f = f_{\text{trans}} \times f_{\text{rot}} \times f_{\text{vib}} \tag{21}$$

Translational energy levels are so closely spaced that the summation in f_{trans} can be replaced with an integration, which leads (8) to Equation (22).

$$f_{\text{trans}} = (2\pi mkT)^{3/2}(V/h^3) \tag{22}$$

The f_{trans} given by Equation (22) is that for a *single molecule* contained in a volume V, and k is Boltzmann's constant. If one cc. is inserted for V in Equation (22) and the resulting partition function is used together with related expressions given below to calculate standard thermodynamic properties via Equations (6–9), the standard state referred to will be the perfect gas at a concentration of one molecule per cc. ΔF° and ΔS° can then be converted to the values appropriate to a more convenient standard state in the usual way.

Replacing the summation in f_{rot} by an integration is less justified because the energy levels are more widely separated; this seems to be the only reasonably simple way to evaluate f_{rot}. In the general case of a polyatomic molecule, Equation (23) is obtained (9).

$$f_{rot} = (8\pi^2/\sigma h^3)(I_1 I_2 I_3)^{1/2}(2\pi kT)^{3/2} \tag{23}$$

I_n are the three rotational moments of inertia, and σ is the symmetry number of A. For a diatomic or a linear polyatomic molecule, we have seen that there are only two rotational degrees of freedom and only one rotational moment of inertia. For this case, Equation (23) should be replaced by Equation (24).

$$f_{rot} = (8\pi^2 IkT/\sigma h^2) \tag{24}$$

In estimating σ, the molecule is assumed rigid in its most stable configuration, and rotation about its three principal axes of rotation is visualized. The number of times the original structure can be reproduced by interchanging identical atoms in the molecule is σ. No single configuration is to be counted more than once. For example, acetylene has a symmetry number of 2, and benzene has $\sigma = 12$. Monodeuterobenzene, however, has a symmetry number of 2. All linear saturated hydrocarbon molecules larger than ethane have symmetry number of 2. Some interesting predictions can be made on the basis of symmetry numbers (10).

The vibrational partition function f_{vib} must be evaluated directly from the quantum mechanically permitted energy levels because these levels are much too widely spaced to permit the summation to be replaced with an integration. The summation is very easily evaluated for a harmonic oscillator, however. Before this is done, it should be noted that the lowest permitted vibrational energy level is substantially different from zero. This occurs because the Heisenberg uncertainty principle will not permit us simultaneously to know both the position and momentum of any particle with complete certainty. If a harmonic oscillator were permitted to have zero energy, this principle would be violated because the mass point would occupy its equilibrium position and have zero momentum. Instead, the lowest permitted energy level of a harmonic oscillator is $^1/_2 h\nu$. With this

in mind and substituting ν for $(1/2\pi)(k/\mu)^{1/2}$, Equation (16) can be rewritten as Equation (25).

$$\epsilon_n = nh\nu + {}^1/_2h\nu \tag{25}$$

The vibrational partition function for a single degree of freedom is then given by Equation (26).

$$\begin{aligned} f_{\text{vib}} &= \sum_1^n e^{-(nh\nu+{}^1/_2h\nu)/kT} \\ &= e^{-{}^1/_2h\nu/kT} \sum_1^n e^{-nh\nu/kT} \end{aligned} \tag{26}$$

Very frequently the zero point energy term is separated and combined with $\Delta\epsilon_0$. Alternately, Equation (6) can be rewritten

$$\begin{aligned} K &= \exp(-\Delta\epsilon_0/kT) \times \exp(-{}^1/_2 \sum^{\text{B}} h\nu/kT) \times \\ &\qquad \exp({}^1/_2 \sum^{\text{A}} h\nu/kT) \times (f_{\text{B}}/f_{\text{A}}) \\ &= \exp(-\Delta\epsilon_0/kT) \times \exp(-\Delta\epsilon_z/kT) \times (f_{\text{B}}/f_{\text{A}}) \end{aligned} \tag{27}$$

where f_{vib} for a single degree of freedom has been redefined by Equation (28)

$$f_{\text{vib}} \equiv \sum_1^n e^{-nh\nu/kT} \tag{28}$$

and $\Delta\epsilon_z$ has been defined as ${}^1/_2\sum^{\text{B}}h\nu - {}^1/_2\sum^{\text{A}}h\nu$. Equations (7–9) must, of course, be altered accordingly. This latter practice points up the importance of zero point vibrational energy and is very useful in dealing with isotope effects.

With f_{vib} for a single vibrational degree of freedom defined by Equation (28), the vibrational partition function for a polyatomic molecule is given by Equation (29), with the product taken over all s vibrational degrees of freedom (11).

$$f_{\text{vib}} = \prod_s \frac{1}{1 - e^{-h\nu_s/kT}} \tag{29}$$

There is one type of pseudo-vibrational motion for which Equation (29) does not give a suitable partition function and which must be considered separately. This is internal rotation, either free, as in dimethylacetylene, or hindered, as in ethane. The partition function for internal rotation $f_{\text{i.r.}}$ can be separated in the same way as f_{trans}, f_{rot}, and f_{vib}, so that $f = f_{\text{trans}} \times f_{\text{rot}} \times f_{\text{vib}} \times f_{\text{i.r.}}$. In Equation (29), s is reduced by one for every

degree of internal rotational freedom. (One in both ethane and dimethylacetylene, two in the xylenes.)

For free internal rotation, $f_{\text{i.r.}}$ is given by Equation (30) (ref. 12) where $\sigma_{\text{i.r.}}$

$$f_{\text{i.r.}} = (8\pi^3 I_{\text{i.r.}} kT)^{1/2}/\sigma_{\text{i.r.}} h \tag{30}$$

is the symmetry number for internal rotation, and $I_{\text{i.r.}}$ is the reduced moment of inertia for internal rotation. For restricted internal rotation in which the barrier to rotation is less than ~20 kcal./mole, no explicit formula can be given. Fortunately, numerical values of the partition function for this case have been tabulated (13,14). If the barrier to internal rotation is higher than ~20 kcal./mole, the rotation approaches a torsional oscillation at ordinary temperatures and can be treated as a vibration.

The derivatives of the natural logarithms of the partition functions with respect to temperature are required for entropy calculations.

(For three degrees of rotational freedom.)

$$(-d/dT) \ln f_{\text{trans}} = 3/2T \tag{22a}$$

$$(d/dT) \ln f_{\text{rot}} = 3/2T \tag{23a}$$

(For one degree of vibrational freedom.)

$$(d/dT) \ln f_{\text{vib}} = (h\nu/kT^2) \times 1/(h\nu/e^{kT} - 1) \tag{29a}$$

(For one degree of free internal rotation.)

$$(d/dT) \ln f_{\text{i.r.}} = 1/2T \tag{30a}$$

It is apparent from the definition that the partition function for a particular type of motion will be large if there are many low-lying energy levels, because it will then be a sum of many terms $e^{-\epsilon/kT}$, each of which approaches unity as ϵ approaches zero. Partition functions for translation are accordingly very large, whereas those for vibration may approach unity for simple molecules. Partition functions for rotation (both internal and external) have intermediate values.

If the starting material A in Equation (1) is actually two molecules C and D, $f_{\text{A}} = f_{\text{C}} \times f_{\text{D}}$. The same is true of the product. Since $f_{\text{C}} \times f_{\text{D}}$ will involve two partition functions for three degrees of translational freedom, it is plain that the partition function for two molecules will almost always be much larger than that for the single molecule in which they have somehow been joined.

4. Rate Constants in Terms of Partition Functions

The transition state theory of reaction rates is discussed elsewhere in this volume (15). In terms of the foregoing discussion, the rate constant k_r is given by Equation (31) for reactions not involving metastable intermediates. In Equation (31), k is Planck's constant, h is Boltzmann's constant, and the

$$k_r = (\kappa kT/h) \exp(-\Delta\epsilon_0/kT) \times \exp(-\Delta\epsilon_z/kT) \times f_{\ddagger}/f_s \qquad (31)$$

transmission coefficient κ can usually be taken as unity. The partition function of the starting materials is f_s, but $f_{\ddagger}$ is *not* the partition function of the transition state (16). In the derivation of Equation (31), certain terms have been removed from the transition state partition function in order to cancel undesired terms in the pre-exponential factor, so that $f_{\ddagger}$ is the partition function of a molecule with one less degree of freedom than the transition state. The degree of freedom that is missing is that along the reaction coordinate. On the other hand, the zero-point vibrational energy along the reaction coordinate has not been removed from $\Delta\epsilon_z$. It can be seen that the equilibrium constant $K^{\ddagger}$, defined by Equation (32), is a somewhat strange one and should be approached with due caution.

$$K^{\ddagger} \equiv \exp(-\Delta\epsilon_0/kT) \times \exp(-\Delta\epsilon_z/kT) \times f_{\ddagger}/f_s$$

$$K^{\ddagger} = k_r \frac{h}{\kappa kT} \qquad (32)$$

The standard free energy $\Delta F^{\ddagger}$, standard enthalpy $\Delta H^{\ddagger}$, and standard entropy of activation bear the same relation to $K^{\ddagger}$ that the same quantities of reaction bear to an ordinary equilibrium constant, and they can be obtained from Equations (7–9) in terms of partition functions by appropriate substitution. The thermodynamic quantities of activation for a reaction in solution are given by Equations (33–35) in terms of the rate constant.

$$\Delta F^{\ddagger} = -RT \ln(k_r h/\kappa kT) \qquad (33)$$

$$\Delta H^{\ddagger} = RT - RT^2(d/dT) \ln k_r \qquad (34)$$

$$\Delta S^{\ddagger} = (\Delta H^{\ddagger} - \Delta F^{\ddagger})/T \qquad (35)$$

5. Complex and Reversible Reactions

Many reactions do not proceed directly from starting materials to products but, rather, go through one or more metastable intermediates. In

general, the effect of such intermediates on the reaction rate is predictable. Several specific cases will be considered.

A. There are two transition states along the reaction coordinate; the intermediate occurring between them is metastable; each step is of the first order; the over-all reaction is not appreciably reversible. The reaction scheme is shown in Equations (36) and (37).

$$\mathrm{A} \underset{k_{-1}}{\overset{k_1}{\rightleftharpoons}} \mathrm{B} \tag{36}$$

$$\mathrm{B} \xrightarrow{k_2} \mathrm{C} \tag{37}$$

Using the steady-state approximation, the concentration of B is given by Equation (38) (18).

$$\begin{aligned} d(\mathrm{B})/dt &= 0 = k_1(\mathrm{A}) - k_{-1}(\mathrm{B}) - k_2(\mathrm{B}) \\ (\mathrm{B}) &= k_1(\mathrm{A})/(k_{-1} + k_2) \end{aligned} \tag{38}$$

Since

$$d(\mathrm{C})/dt = k_2(\mathrm{B}) \tag{39}$$

then

$$d(\mathrm{C})/dt = \frac{k_1 k_2}{k_{-1} + k_2}(\mathrm{A}) \tag{40}$$

and k_r, the measured first-order rate constant, is given by Equation (41).

$$k_r = k_1 k_2/(k_{-1} + k_2) \tag{41}$$

The measured "enthalpy" and "free energy" of activation defined by Equations (33) and (34) are given in terms of the corresponding quantities for single steps in Equations (42) and (43).

$$\Delta F^{\ddagger} = -RT \ln \frac{\exp(-\Delta F_1{}^{\ddagger}/RT) \exp(-\Delta F_2{}^{\ddagger}/RT)}{\exp(-\Delta F_{-1}{}^{\ddagger}/RT) + \exp(-\Delta F_2{}^{\ddagger}/RT)} \tag{42}$$

$$\Delta H^{\ddagger} = \Delta H_1{}^{\ddagger} + \Delta H_2{}^{\ddagger} - \frac{k_{-1}\Delta H_{-1}{}^{\ddagger} + k_2 \Delta H_2{}^{\ddagger}}{k_{-1} + k_2} \tag{43}$$

If k_{-1} is comparable but unequal to k_2, it is quite obvious that none of the over-all thermodynamic quantities of activation have any simple significance, and there is no "rate-determining step" in the usual sense of that term. In this situation, $\Delta H^{\ddagger}$ and $\Delta S^{\ddagger}$ may be temperature dependent, but there are a large number of special cases in which they will be constant or nearly so. In addition to cases B and C, $\Delta H^{\ddagger}$ will be constant if $k_2 \gg k_{-1}$ and also if $\Delta H_{-1}{}^{\ddagger} = \Delta H_2{}^{\ddagger}$. An approach to one or several of

these conditions may make $\Delta H^{\ddagger}$ approximately constant. The finding that $\Delta H^{\ddagger}$ is not a function of temperature therefore does not preclude a multi-step reaction (19).

B. If k_{-1} exactly equals k_2, $\Delta F_{-1}{}^{\ddagger}$ is exactly equal to $\Delta F_2{}^{\ddagger}$, and Equations (41–43) become Equations (44–46). There is still no step that would be recognized as "rate-determining."

$$k_r = k_1/2 \tag{44}$$

$$\Delta F^{\ddagger} = \Delta F_1{}^{\ddagger} + RT \ln 2 \tag{45}$$

$$\Delta H^{\ddagger} = \Delta H_1{}^{\ddagger} + [(\Delta H_2{}^{\ddagger} - \Delta H_{-1}{}^{\ddagger})/2] \tag{46}$$

C. If k_{-1} is much larger than k_2, $\Delta F_2{}^{\ddagger}$ must be correspondingly larger than $\Delta F_{-1}{}^{\ddagger}$. In that case, Equations (42) and (43) reduce to Equations (47) and (48).

$$\Delta F^{\ddagger} = \Delta F_1{}^{\ddagger} - \Delta F_{-1}{}^{\ddagger} + \Delta F_2{}^{\ddagger} \tag{47}$$

and

$$\Delta H^{\ddagger} = \Delta H_1{}^{\ddagger} - \Delta H_{-1}{}^{\ddagger} + \Delta H_2{}^{\ddagger} \tag{48}$$

It is clear from Equations (47) and (48) that the rate and all the thermodynamic properties of activation are completely determined by the properties of the starting state along with the corresponding properties of the *second* transition state. This is true even though the free energy required to reach the second transition state from the intermediate B may be *less* than the free energy required to reach the first transition state from A. Under these conditions, reaction (37) may be considered the rate-determining step for the over-all reaction.

The presence and structure of intermediates is of interest even if they do not directly influence the rate of reaction. If they can be detected and identified, they limit the structures that must be considered for the over-all transition state. Conversely, the structure of the over-all transition state, if known, may require that one or more metastable intermediates precede it along the reaction coordinate.

The problem of multiple barriers of approximately equal height has been discussed in connection with ester, amide, and anhydride hydrolysis by Bender and co-workers (19a) and in connection with enzyme reactions by Lumry (19b). The special problem of multiple small barriers has been discussed by Giddings and Eyring (19c), who have introduced some useful simplifying approximations.

In principle, all nonphotochemical reactions are reversible under the conditions of the forward reaction, because no state of finite energy has $N = 0$ in Equation (2). Since the energy of a state completely governs its

equilibrium concentration regardless of its mode of formation, the reverse reaction will always retrace the steps of the forward reaction (20,21) (again with the possible exception of photochemical reactions). This principle is called the principle of microscopic reversibility or, sometimes, the principle of detailed balance.

In practice it is often difficult or impossible to study a given reaction in both the forward and reverse directions, so it is a helpful consequence of this principle that the mechanism of the reverse reaction must be a detailed reversal of the mechanism of the forward reaction. The enthalpy, free energy, and entropy of activation for the reverse reaction are given by the corresponding quantities for the over-all reaction.

6. The Brønsted Rate Law

The "rate constant," defined by Equation (31), will not be truly constant under any change in conditions that alters ΔE_0, ΔE_z, or the partition functions. For reactions in solution, this means that k_r will be altered by every change in medium. This difficulty antedates Equation (31). A useful formalization has been suggested by Brønsted (22) and is given in Equation (49).

$$k_r = k_r^0(\pi\alpha_x/\alpha_\ddagger) \tag{49}$$

In terms of modern rate theory, $\alpha_\ddagger$ is the thermodynamic activity coefficient of the transition state, and $\pi\alpha_x$ is the product of the activity coefficients of all the reactants. The rate constant under some set of standard conditions, usually infinite dilution in a solvent, is k_r^0.

Equation (49) is readily derived if the transition state is considered to be in equilibrium with the reactants, since its concentration will then be governed by its thermodynamic activity. The rate of the reaction is a function of the transition state "concentration" only, so $\alpha_\ddagger$ does not cancel out. Equation (48) can be useful in determination of mechanism because under some conditions the effect of medium changes on activity coefficients can be correlated with structure.

Although this derivation seems essentially to be correct, it should be borne in mind that the "concentration" involved is that of the hypothetical species whose partition function is $f_\ddagger$.

7. The Effect of Pressure

The derivative of a rate constant with respect to pressure is given by Equation (50), which is obtained from Equation (33) and the thermodynamic identities (23a).

$$d\ (\ln k)/dp = -(\Delta V^\ddagger/RT) \tag{50}$$

The quantity $\Delta V^{\ddagger}$ is the change in volume accompanying the conversion of one mole of starting material to one mole of transition state. It can be determined experimentally by studying the effect of pressure on the rate constant. Simple consideration of the compression that takes place upon making a bimolecular transition state out of two separate molecules leads to the conclusion that $\Delta V^{\ddagger}$ should be about -5 to -10 cc. for such reactions (23a,23b). On the other hand, $\Delta V^{\ddagger}$ should be much smaller and probably positive for unimolecular reactions (23b). These conclusions are not reliable if a change in the number or charge type of ions accompanies the reaction, because of the probable change in solvent volume.

It has been suggested that the sign and magnitude of $\Delta V^{\ddagger}$ can be used to distinguish between a rate-determining step involving covalent bond formation between a protonated substrate and a solvent molecule and a rate-determining step not involving covalent bond formation (23b).

8. Some Qualifications

The foregoing is all derived for highly simplified cases. The author believes that the results are essentially correct, however, and that the methods by which they were obtained are more illuminating than more rigorous ones. The results have considerably more generality than would be supposed from the assumptions by which they were obtained, and they will be frequently be used in situations for which they were not derived.

II. APPLICATIONS

1. To Gas-Phase Equilibria

In principle, all the quantities in Equation (27) can be calculated if the structures of A and B are known. In practice, $\Delta\epsilon_0$ is calculable only for the very simplest of reactions at the present time. The vibrational partition functions and $\Delta\epsilon_z$ are also very difficult to evaluate from first principles, but few chemists will object to taking these from spectroscopic data. The other partition functions can all be evaluated, for molecules in the gas phase, from the formulas given above.

Given the partition functions but lacking $\Delta\epsilon_0$, ΔS_0 can still be calculated. If the structure of A were known and that of B were in doubt, a fairly good check on the postulated structure could be obtained by calculating ΔS_0 and comparing it with the experimental value, as the partition functions are sensitive functions of structure. This type of work has provided values for the barriers to internal rotation in saturated hydrocarbons, (24) and compelling evidence that cyclopentane is nonplanar (25). It is usually

more convenient and less ambiguous, however, to determine the structure of stable molecules by physical methods.

2. To Gas-Phase Rates

The problem of the kineticist may be rather arbitrarily divided into two parts. The first—and historically the first to be recognized—is the determination of the form of the rate law. From this, the rate-determining step can frequently be identified, and some information can be obtained about fast steps which may precede the rate-determining step. Information to be obtained from the form of the rate law is discussed elsewhere in this volume (26). The second problem of the kineticist is to determine, with as much detail as possible, the structure of all states that are significant to the progress of the reaction and, especially, the structure of the transition state. In this task, no direct physical measurements can be brought into play because the transition state, *by definition*, is too short-lived for such measurements to be made (27). The only thing that the kineticist can actually *measure* is the reaction *rate*. Fortunately, by measuring the rate under a variety of conditions, any thermodynamic property of activation that seems useful can be evaluated with the aid of the transition-state theory of reaction rates (28). These thermodynamic properties can then be compared with those calculated from partition functions and estimates of $\Delta\epsilon_0$. The agreement of calculated and observed properties provides the *only* available test of postulated transition-state structures. The two problems are closely related because the information obtained from the rate law can be used to limit the number of transition-state structures that must be tested; the transition-state structure, once established, may provide convincing evidence for or against rapid reactions preceding or following the rate-determining step.

For reactions in the homogeneous gas phase, the best test of transition-state structure is probably a comparison of calculated and observed entropies of activation, avoiding the difficult and uncertain estimation of $\Delta\epsilon_0$. Several examples of such tests are provided. The Diels-Alder reaction, shown in Equation (51), for the general case, has been studied in the homogeneous gas phase in both the forward and reverse direction (29,30). Two reaction paths suggest themselves—one a direct addition, in which both

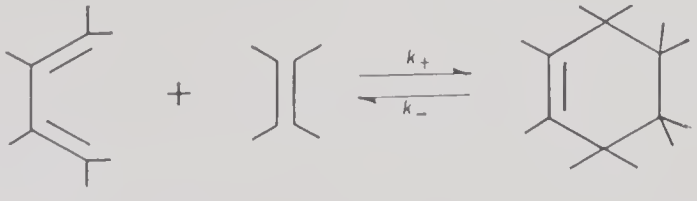

(51)

new bonds are formed in the same step and more or less simultaneously, and the other, a two-step process involving a diradical intermediate, as shown in Equation (52a) and (52b). In the latter, either step may be rate-determining. The transition state will be cyclic, fairly rigid, and geometrically very similar to the product if the one-step mechanism is correct or if the two-step mechanism is correct with the second step rate-determining. On the other hand, if Equation (52a) represents the rate-

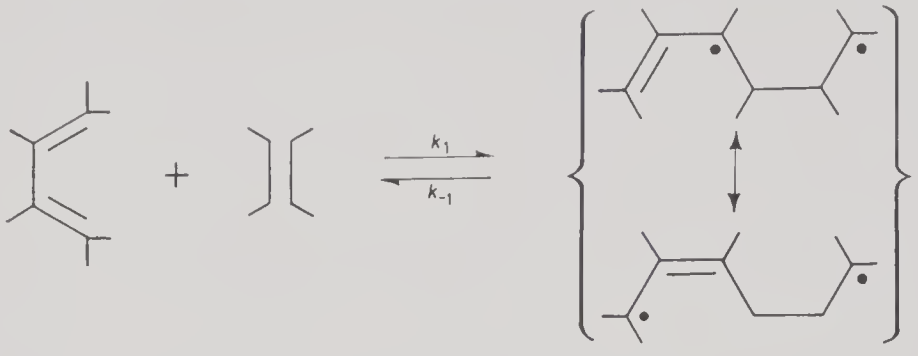

(52a)

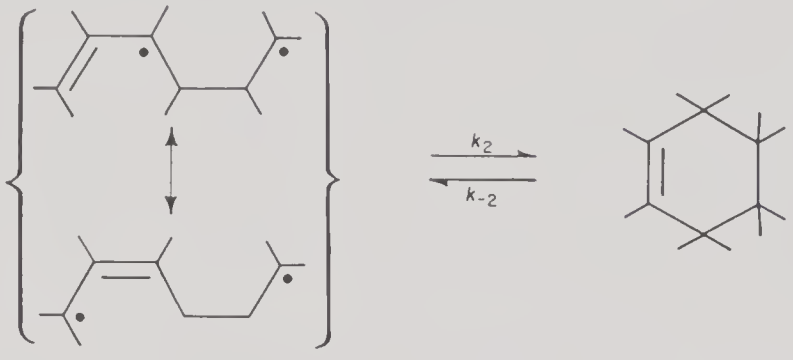

(52b)

determining step, the transition state would probably resemble the intermediate shown. Calculation of the entropy of activation for the dimerization of butadiene has not yielded conclusive results (30,31,32) because the rotational moments of inertia and many of the vibrational frequencies of the suggested transition states were not known with sufficient assurance. On the other hand, one can quite straightforwardly predict a small negative entropy of activation (owing to a loss of a carbon-carbon stretching frequency) for the reverse reaction if the transition state resembles the product. If the carbon-carbon single bond stretching frequency is $\sim$1000 cm.$^{-1}$, the predicted entropy of activation would be ~ -1 cal./mole deg. If the transition state resembled the diradical, a substantial positive entropy of activation would be expected. The entropies of activation for the dissociation of dicyclopentadiene and 3,6-endomethylene-1,2,3,6-tetrahydrobenzaldehyde have been measured (29). They are 0 and -3 cal./

mole deg., effectively eliminating any transition state resembling the diradical intermediate from consideration. It seems intuitively unlikely that Equation (52b) is the rate-determining step because it probably has a nearly zero potential energy of activation. (It is not altogether inconceivable that Equation (52b) represents the rate-determining step, however, because it certainly would have a negative entropy of activation and, therefore, a finite and positive free energy of activation.) It has also been impossible chemically to detect any diradical in simple, gas-phase, Diels-Alder reactions (32). It seems very likely, then, that no diradical is involved as a discreet intermediate.

It is not required, however, that the two new bonds be formed with complete synchronization. Therefore, one of the new bonds may be weaker than the other in the transition state, particularly when more complicated reactants are involved. Evidence has recently been presented suggesting that this is the case, in at least some Diels-Alder reactions (33). The foregoing also has no bearing on the role of a relatively stable charge transfer complex that may be formed by the reactants prior to the rate-determining step. Such a complex would have no effect on the thermodynamics of activation unless a substantial fraction of the starting material were complexed.

Another gas-phase organic reaction for which the entropy of activation may be illuminating is the first-order *cis-trans* isomerization of olefins (34). Table I shows the entropies of activation for all the examples of this reaction that have been studied in the gas phase.

TABLE I
Gas-Phase *Cis-Trans* Isomerizations

Starting isomer	$\Delta S^{\ddagger}$
cis-Ethylene-d_2	+1
cis-2-Butene	−3
cis-Stilbene	−4
cis-β-Cyanostyrene	−9
cis-Methylcinnamate	−14
Dimethylmaleate	−39
Dimethylcitraconate	−39

These reactions have been divided into two categories. In the first category, which contains most of the known examples of this reaction, the entropies of activation lie between −14 cal./mole deg. and +1 cal./mole deg. A small negative entropy of activation would be expected for this reaction if it involved only the thermal rupture of a carbon-carbon π-bond. It would arise from the loss of the torsional oscillation frequency (which

becomes the reaction coordinate) and from the loss of some freedom by the substituents. The entropies of activation in first category fit these expectations nicely.

There are only two known examples of the second category at present—both diesters. These have entropies of activation close to −40 cal./mole deg. It is difficult to reconcile such an entropy of activation with the simple mechanism suggested above. Another possible reaction mechanism is shown in Equations (53–55). The arrows represent the electron spins, and the intermediate in which they are parallel is the first electronically

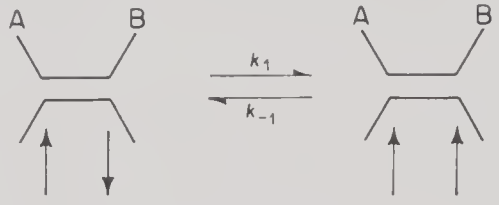

(53)

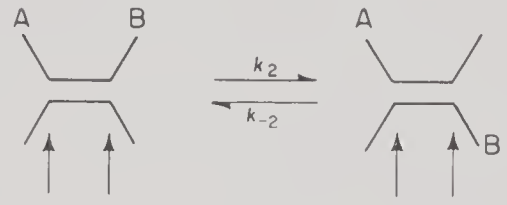

(54)

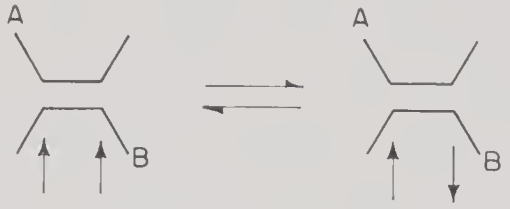

(55)

excited state of the substituted ethylene. Reaction (54) would have an energy and free energy of activation of very nearly zero because the two electrons in p orbitals with parallel spins, if anything, seek a configuration of *minimum* overlap. Only a very small fraction of the molecules possessing the excitation energy reach the excited state, however, because such a transition, involving a change in multiplicity, is quantum mechanically "forbidden." The result is that κ, which is assumed to be near unity for most reactions, is very much less than unity for this reaction if the foregoing mechanism is utilized. Because κ was assumed to be unity in calculating $\Delta F^{\ddagger}$ via Equation (33), a quantity $R \ln \kappa$ has been added to $\Delta S^{\ddagger}$ calculated via Equation (35). This is a substantial negative number when κ is much less than unity, as in the present case. Equations (53–55), therefore,

account for isomerization with a relatively low energy of activation but a large, negative, entropy of activation, and they are thought to represent the mechanism of choice for those isomerizations which display these characteristics.

Both of the examples discussed above involve first-order reactions. Entropies of activation can also be estimated for reactions of other orders in favorable cases. It should be borne in mind, however, that the numerical value of $\Delta S^{\ddagger}$ obtained depends on the standard state chosen for any but first-order reactions. This caution also applies when entropies of activation are being compared with measured entropies of reaction.

Future work of this type will be facilitated by the increasing availability of infrared spectroscopic data (35) and the assignment of group frequencies (36).

Directly calculated, and experimental values of $\Delta\epsilon_0$ have also been compared in an effort to support suggested transition state structures (37). In a few cases, it may be possible to eliminate certain transition states because the energy required to form them is clearly too great; for the most part, the approximations required to calculate $\Delta\epsilon_0$ directly make such comparisons unreliable. More empirical comparisons are described below.

3. Entropies of Reactions in Solution

Most of the reactions in which organic chemists are interested take place in highly nonideal solutions rather than in the gas phase. Equations (6–9) and (31) are applicable to such reactions, as is the partition function formula for vibration, provided that the fundamental vibrational frequencies appropriate to the solution are used. (These are frequently not too different from those for the vapor phase.) Partition functions for internal rotations will also be the same in solution as in the vapor phase, provided that the barrier to rotation is not changed. (It may be changed by hydrogen bonding, for example.) The partition functions for rotation and (especially) for translation, however, must be replaced by complex expressions that take account of the structure of the solvent as well as of the solute. This cannot yet be done to a satisfactory degree of reliability for systems in which organic chemists are interested. In spite of this, the behavior of the partition functions, and even of $\Delta\epsilon_0$ as various conditions are changed, can be qualitatively predicted if the nature of the solvent and the structure of the solute are known. Whenever possible, such predictions should be verified with data pertaining to equilibria among molecules of known structure.

If the perfect gas, A, dissolves in some liquid to give an infinitely dilute solution, the equilibrium constant K is given by Equation (56), where N

$$\begin{aligned} K &= N_{\text{sol}}/N_{\text{gas}} \\ &= \exp\,(-\Delta E_0/RT) \times \exp\,(-\Delta E_z/RT)\,[f_{\text{sol}}/(f_{\text{gas}} \times f_{\text{liq}})] \end{aligned} \qquad (56)$$

is the number of molecules of A per unit volume. In general, solute and solvent molecules will attract each other, owing to van der Waals' attractions. These are generally fairly small. If the solvent and solute molecules both have either permanent or induced dipoles, there will be attraction because of dipole-dipole forces. In the extreme case of hydrogen-bonding solutes and solvents, these may rise to ΔE_0 terms as large as $\sim$10 kcal./mole. If the solvent is polar or polarizable and the solute is ionic, ion-dipole forces come into play that may give rise to ΔE_0 terms as large as $\sim$100 kcal./mole. It is not possible to consider the partition function of a single molecule in the liquid state as was done for the gas phase, because the translational and rotational energy levels of each molecule depend on the proximity, orientation, and energy of its neighbors. The quantities f_{liq} and f_{sol} are, nevertheless, still summations over exp $(-\epsilon_i/kT)$ terms. The more restricted the motions of molecules, the further apart these energy levels will be spaced, and the smaller the partition function will be.

Ion-dipole forces, dipole-dipole forces, and even van der Waals' forces, depend to varying extents on the orientation of solvent to solute molecules and consequently restrict the motions of both. The predicted result of this is that $f_{\text{sol}}/f_{\text{gas}} \times f_{\text{liq}}$ should usually be smaller than unity and should rapidly become smaller still as the solute becomes more polar (or ionic). (An exception to this would be the case in which a pure liquid is highly oriented, such as water, and the introduction of solute breaks down the structure of the liquid.) According to Equation (9), then, the introduction of a polar solute or an ionic species into a polar or polarizable solvent should give rise to a substantial negative entropy if the same units of concentration are used for both phases. The total process of orienting solvent must be a favorable one in terms of ΔF, however, as otherwise the orientation would not take place.

The behavior of ΔS^0, ΔH^0, ΔF^0, and K as a function of solvent polarity can all be roughly predicted for a reaction producing ions. If the reaction shown in Equation (57) proceeds in a nonpolar solvent such as benzene, the solvent

$$\text{A} + \text{B} \rightleftharpoons \text{A}^{\oplus} + \text{B}^{\ominus} \tag{57}$$

molecules acquire induced dipoles, and ion-dipole forces will restrict the movements of many benzene molecules. Furthermore, since the dielectric constant of a liquid such as benzene is small, the lines of force will go far out into the solvent, and a great many benzene molecules will be involved. This is graphically illustrated by the ability of small concentrations of ionic materials to gel hydrocarbon solvents (napalm). In these gels, *all* the solvent molecules are immobilized. The partition function for the ionic solution f_{+-} should, therefore, be much smaller than the partition

function of the starting state f_{AB}, and reaction (57) should be accompanied by a large negative ΔS^0. As the solvent becomes more polar, its dielectric constant increases, reducing the volume encompassed by the lines of force and thereby reducing the number of solvent molecules that are immobilized. At the same time, ΔE_0 is drastically reduced because the work required to separate charges is inversely proportional to the dielectric constant of the medium. The first effect will give rise to a sharp increase in f_{+-}, so that the magnitude of the negative ΔS^0 will be decreased. Both effects will give rise to a more negative ΔF°. Since ΔF° and $T\Delta S^\circ$ are both changing in the same sense, the change in ΔH^0 must be smaller than the change in ΔF^0, and, in practice, it is frequently smaller than the change in $T\Delta S^0$, also. Calculations based on these ideas have been made, taking the distance between the positive and the negative charge as one angstrom in the starting state and as infinity in the products, and neglecting all other effects (38). The values of ΔF^0, ΔH^0, and ΔS^0 obtained for a variety of solvents are shown in Table II.

TABLE II
Calculated Electrostatic Effects in Various Solvents (38)[1]

Solvent	Dielectric constant, 20°	ΔF_0, kcal./mole	ΔS_0, cal./mole deg.	ΔH_0, kcal./mole
Vacuum	1.0	312	0	312
Hexane	1.9	164	−117	130
Carbon tetrachloride	2.25	139	−117	104
Benzene	2.3	135	−119	100
Chloroform	4.5	69	−231	2
Chlorobenzene	6.65	47	−136	7.2
Ethyl bromide	9.35	33	−164	−15
Acetone	20.0	15.6	−72	−5.5
Ethyl alcohol	25.0	12.5	−75	−9.5
Methyl alcohol	32.5	9.6	−52	−5.6
Nitrobenzene	35.8	8.7	−45	−4.6
Water	80.0	3.9	−18	−1.5

[1] Reprinted with permission from A. A. Frost and R. G. Pearson, *Kinetics and Mechanism*, Wiley, New York, 1953.

These general principles have been verified by studies of the thermodynamic properties of ionization in pure and mixed solvents. Ionization of neutral acids in aqueous solution gives rise to entropies of around −20 to −30 cal./mole deg. (39). Ion-pair dissociations of the type shown in Equation (58) have entropies ranging between −30 and −36 cal./mole deg. in ethylene chloride and ethylidene chloride (40).

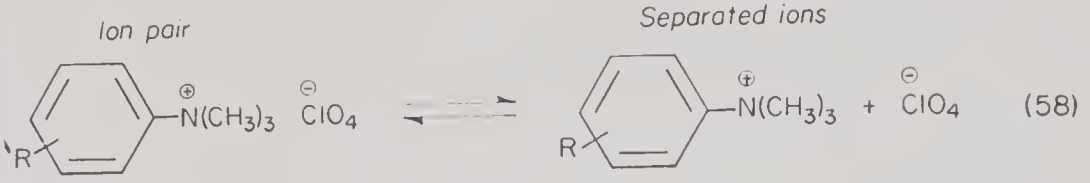

Ion-pair dissociations for tetra-*n*-alkylammonium picrates in ethylene chloride, ethylidene chloride, and propylene chloride have entropies of activation ranging from −24 cal./mole deg. to −40 cal./mole deg. (41). The ions involved in these dissociations must surely be quite effective in immobilizing solvent molecules, even in the ion-pair state. The negative entropies of dissociation must arise from the fact that even *more* solvent molecules are immobilized by the free ions.

It seems significant that, in this last reaction, the largest negative entropy (−40 cal./mole deg.) is for tetramethylammonium picrate and the values increase steadily to −24 cal./mole deg. for tetra-*n*-butylammonium picrate. The larger alkyl groups apparently reduce the number of solvent molecules immobilized by the positive charge (by preventing their approach) (41).

It is also noteworthy that all the dissociations give rise to two species in the place of one. In the gas phase, this would mean three degrees of translational freedom and three degrees of rotational freedom in the products that were not present in the starting materials, and the reactions would certainly be accompanied by a very substantial *positive* entropy. The results quoted above indicate that this positive contribution is smaller than the large negative entropy effects accompanying the immobilization of solvent.

As predicted above, ΔS^0 for ionization reactions rapidly takes on larger negative values as the solvent becomes less polar, whereas the changes in ΔH^0 are much smaller. Table III gives the ΔH^0 and $T\Delta S^0$ for dissociation of formic acid in water and in dioxane–water mixtures. The thermodynamic properties of ionization behave similarly for water and other simple carboxylic acids (42). Other equilibrium data in general accord with the foregoing principles could easily be collected.

Entropies of activation for reactions in solution can often provide convincing evidence about the structure of the transition state. A few examples will be discussed.

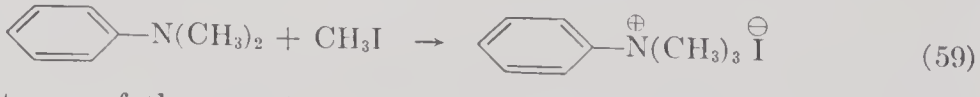

A. The entropy of the reaction shown in Equation (59) is −37.1 cal./mole deg. in nitrobenzene solution. The entropy of activation for the same reaction is −36.1 cal./mole deg., providing strong evidence that the transition state closely resembles the products (43). Since it is highly unlikely that the transition state resembles the separated ions and because it has

TABLE III
Enthalpies and Entropies of Ionization for Formic Acid
in Dioxane-Water Mixtures at 25°[1]

Dioxane, %	$\Delta H°$, kcal./mole	$T\Delta S°$, kcal./mole
0	−0.02	−5.1
20	−0.35	−6.0
45	−1.06	−8.0
70	−1.47	−11.0
82	−3.67	−16.1

[1] These values were calculated from parameters given by H. S. Harned and B. B. Owen, *The Physical Chemistry of Electrolytic Solutions*, Reinhold, New York, 1958, p. 759, except that the values for 82% dioxane were calculated from the data of S. S. Danyluk, H. Taniguchi, and G. J. Janz, *J. Phys. Chem. 61*, 1679 (1957).

been noted that the dissociation of ion pairs involves a considerable negative entropy, these results also strongly suggest that the product of reaction (59) exists principally as an ion pair under the conditions of the measurement of ΔS^0.

B. The acid cleavage of methylmercuric iodide has an entropy of activation of −23 cal./mole deg. (44). (The original paper contains a numerical error.) This was an important part of the evidence for a transition state in which the carbon-mercury bond is almost completely ionized while the new carbon-hydrogen bond is just beginning to form (44). The new charge centers in the transition state would immobilize a good deal of water, and this effect was used to explain the major part of the negative entropy of activation.

C. The entropy of reaction (60) has been determined in aqueous solution at 25° along with the entropies of activation in both directions (45a).

$$(CH_3)_2C{=}CH_2 + H_2O \overset{H^\oplus}{\rightleftharpoons} (CH_3)_3COH \qquad (60)$$

The entropy of reaction is −22 cal./mole deg., $\Delta S^\ddagger$ (forward) is −3 cal./mole deg., and $\Delta S^\ddagger$ (backward) is 19 cal./mole deg. The originally postulated reaction mechanism (45) is given in Equations (61–64).

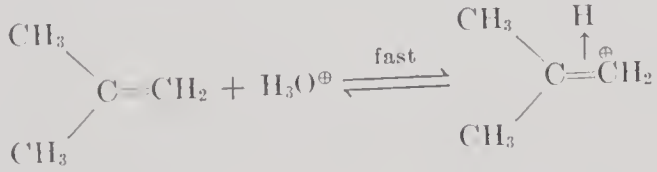

(61)

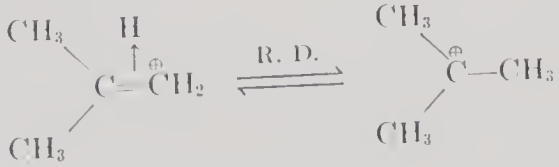

(62)

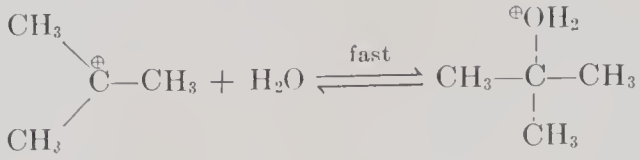

(63)

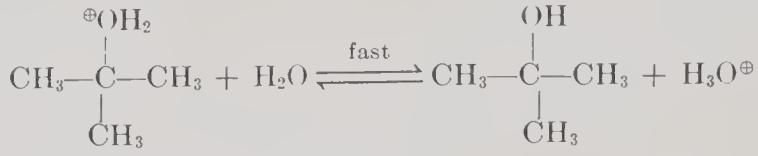

(64)

The substantial negative entropy of reaction is probably attributable to two sources: the loss of whatever translational and rotational freedom is associated with a water molecule in liquid water, and the reduction in mobility of the surrounding water molecules on going from isobutene to the more polar *t*-butyl alcohol. The entropy of liquid water at 25° is 16.7 cal./mole deg. The elements of water retain some freedom in *t*-butyl alcohol to which not more than about 4 cal./mole deg. may be assigned, as shown by the following calculations:

It seems quite likely that the *internal* motions of a molecule in solution are not too different from those in the gas phase, so Equations (29) and (30) are still useful here. The elements of water will have nine degrees of freedom in *tert*-butyl alcohol—eight vibrations and one internal rotation. The internal rotation is actually somewhat hindered, but it can be treated as free without introducing too much error. Equations (9) and (30) give $R \ln \{(8\pi^3 I_{i.r.} kT)^{1/2}/\sigma_{i.r.} h\} + {}^1/_2 R$ as the entropy contribution from a single degree of free internal rotation. Substitution of the numerical values gives 2.4 cal./mole deg. Of the eight vibrations, the C—H and OH stretching vibrations have frequencies around 3,000 cm.$^{-1}$ or higher and make no significant contribution to the entropy near room temperature. The two C—H bending frequencies and the O—H bending frequency were assumed to be 1,400 cm.$^{-1}$; the C—O stretching frequency was assumed to be 1,000 cm.,$^{-1}$ and the two C—O bending frequencies were rather arbitrarily assigned the value 500 cm.$^{-1}$ (46, 47). Substitution in Equations (9) and (29) gives 1.4 cal./mole deg. as the contribution of these eight vibrational degrees of freedom to the entropy of *tert*-butyl alcohol. Computation is greatly facilitated by the use of Table 5 in the Appendix of Dole's *Introduction to Statistical Thermodynamics* (48).

The elements of isobutene move more freely in *t*-butyl alcohol than in the parent molecule (principally because the barrier to rotation about the carbon-carbon double bond is drastically reduced on going to the alcohol). Assuming that the oscillation had a frequency of 200 cm.$^{-1}$ and that the rotation is free, this results in an entropy change of 1.3 cal./mole deg. The greater solvation of the alcohol must, then, account for about 10 cal./mole deg. (22 − 17 + 4 + 1), which is not unreasonable. On going from isobutene to the transition state, no change in the number of species or in the charge types is involved. The hydrocarbon cation is undoubtedly somewhat less effective than the hydronium ion in immobilizing water molecules, but the water molecule, which has been freed in the first step, is more effective than isobutene, so the net result is an entropy not far from

zero. On the other hand, if the transition state is produced from *t*-butyl alcohol via the path shown, the water molecule has already been liberated giving rise to about 13 cal./mole deg. of entropy. If the alcohol molecule, which has been consumed, were less effective in immobilizing solvent than the water molecule that has been produced, that part of the transformation would give rise to n cal./mole deg. of entropy (n being negative). Since the hydrocarbon cation is somewhat less effective in immobilizing water than the hydronium ion, a positive entropy results here with a value given by $19 - 13 - n$. Any value of n between -2 cal./mole deg. and -6 cal./mole deg. would be reasonable. Thus the postulated mechanism is consistent with the observed entropies.

Taft now suggests that the intermediate "carbonium ion" is not truly "free," but rather is weakly bound to a water molecule (45b). Water molecules are not truly "free" in liquid water either, however, so that such a water molecule probably resembles an unperturbed water molecule in the bulk of the solvent more than it does the "water molecule" in *tert*-butyl alcohol. If this is true, the foregoing discussion remains essentially correct.

D. Bartlett and Hiatt (49) have studied the thermal decomposition of *tert*-butyl peresters. The primary decomposition products include considerable quantities of CO_2. It was found that the entropy of activation for the reaction becomes increasingly more negative in the series $CH_3COOOC_4H_9$, $(C_6H_5)CH_2COOOC_4H_9$, $(C_6H_5)_2CHCOOOC_4H_9$, and related series. In the series cited, the introduction of the first phenyl group gives rise to a reduction in the entropy of activation by 13 cal./mole deg., whereas the second gives rise to a reduction of 5 cal./mole deg. The introduction of phenyl groups is simultaneously accompanied by large reductions in the enthalpy of activation. The authors interpret these changes to mean that the carbon dioxide is produced in the rate-determining step in the case of the phenyl and diphenyl peresters but not in the case of the unsubstituted perester. The two mechanisms are shown in Equations (65–67). The transition state for reaction (67) is shown in Figure 2. It is severely re-

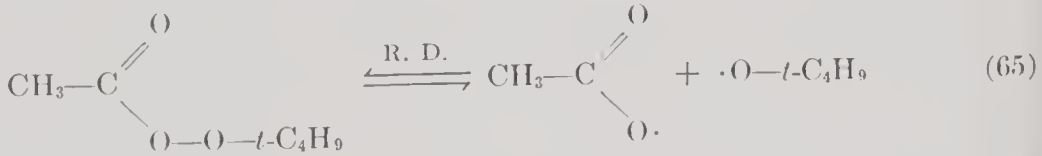

(65)

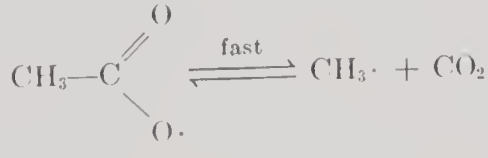

(66)

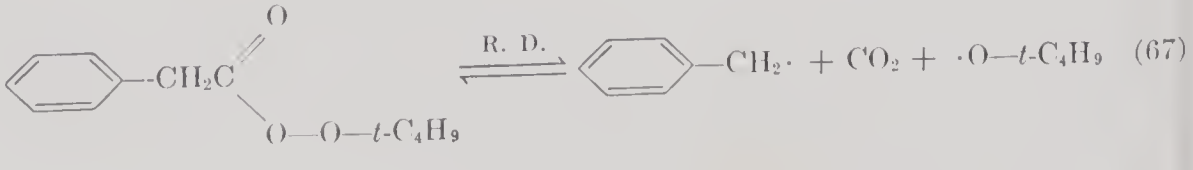

(67)

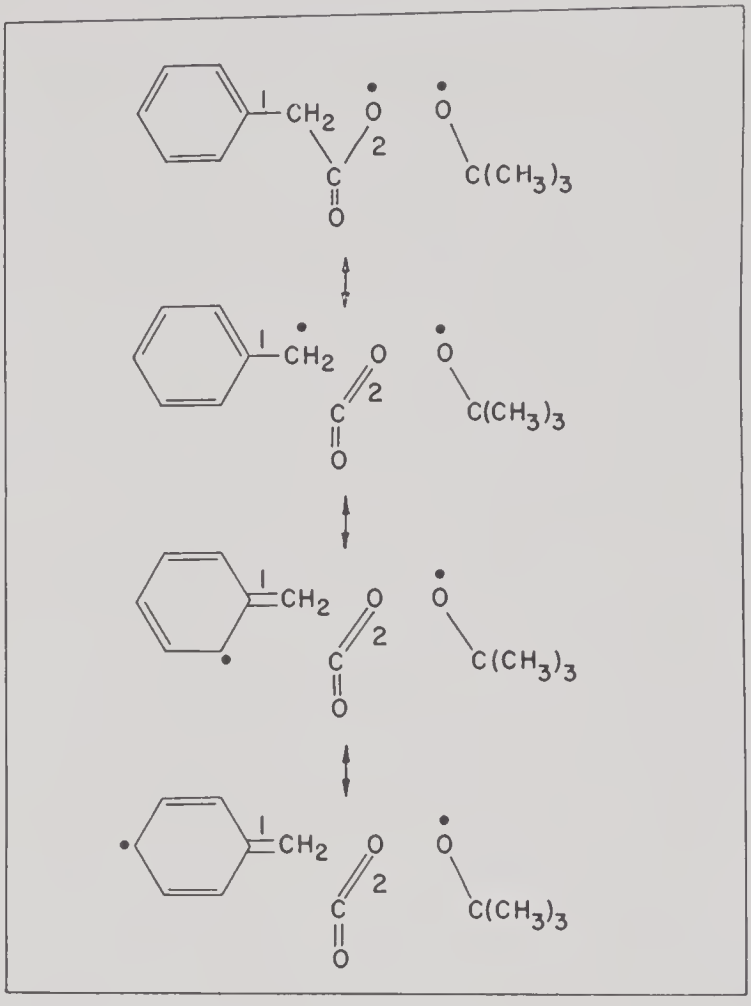

Fig. 2. Transition state resonance hybrid for the thermal cleavage of *t*-butyl phenylperacetate showing the bonds about which rotation becomes hindered.

stricted in its rotation about bonds 1 and 2 by the steric requirements of resonance. Assuming that the rotation of the phenyl group was free in the starting material and is converted to a torsional oscillation with fundamental vibrational frequency of 200 cm.$^{-1}$, the restriction of rotation about bond 1 would reduce the transition state entropy by about 6 cal./mole deg. The reduction in entropy as a result of the loss in rotation about bond 2 is harder to estimate because the geometry is uncertain. If the reasonable approximations are made that the masses of the alkoxyl group and the phenyl group are localized 2 A. off the rotational axis and the methylene group and the carbonyl oxygen are both localized 1 A. off the rotational axis, the entropy associated with free rotation about bond 2 is $\sim$10 cal./mole deg. If this (nearly) free rotation is converted to a torsional oscillation with fundamental frequency of $\sim$200 cm.$^{-1}$ in the transition state, there would be a net loss of about 7.5 cal./mole deg. associated with the "freezing" of rotation about bond 2. If another phenyl group is present and is similarly immobilized, another 6 cal./mole deg. loss in entropy is to

be anticipated. [These results were all calculated in a straightforward manner from Equations (9, 29, and 30).] The observed results are in better agreement with those estimates than they have any real right to be!

A number of semiempirical generalizations have been made about entropies of activation. Price and Hammett (50) have suggested that the rotational freedom of complex molecules will be reduced if polar molecules or transition states are produced from them. From this it would be predicted that entropies of reaction (or activation) would become more negative with increasing molecular complexity if a polar or ionic molecule (or transition state) is produced from one less polar. This generalization is nicely borne out by entropies of activation for semicarbazone formation (50), entropies of activation for olefin hydration (45), entropies of activation for the reaction of substituted pyridines with methyl iodide (51), and entropies of activation for the reaction of alkyldimethylsilanes with base (52). On the other hand, the entropies of ion-pair dissociation, discussed above, become less negative with increasing molecular complexity. One possible cause of the difference is the nature of the solvent, which is much less polar for the ion-pair dissociations. A less polar solvent emphasizes the role of the *solvent* in determining entropies of reaction or activation because the lines of force go further out into space. Another possible cause of the difference is that, in the former cases, the structure is being altered on one side of the functional group only. The solvent can still approach as close as before on three sides of the charge center. In the case of the ion-pair dissociations, the structure is simultaneously being ramified on all sides of the charge center, and a comparable increase in molecular complexity may result in a much more effective exclusion of solvent. In any event, this example shows that the Price and Hammett generalization, like the other principles under discussion here, must be applied with care. Neither molecular structure nor reaction conditions can be safely ignored.

Another generalization for relative entropies of activation is the strain-entropy rule. Taft (53) has suggested that "If a group such as H (or CH_3) be replaced by a group with many more internal degrees of freedom, and if the activation process is such that these groups are compressed..., then the activation process will also be accompanied by a greater loss of internal motions." In other words, it is held that a transition state sterically more crowded than the starting state can also give rise to a trend toward more negative entropies with increasing molecular complexity. If there is such a trend, it is often hard to distinguish its cause, and the same results cited above to support the Price and Hammett principle are also consistent with Taft's strain-entropy rule (54). The value of the strain-entropy rule, if it is correct, is that heats and free energies in a particular reaction series can be considered free of steric effects if no such trend

TABLE IV

Entropy of Activation and Transition State Structure[1]

Reaction	Transition state	$\Delta S^{\ddagger}$, cal./mole deg.
$(CH_3)_2C{=}CH_2 + H_2O \longrightarrow (CH_3)_3COH$	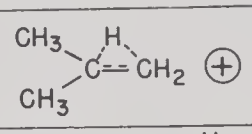	-2^{45}
$CH_2(OC_2H_5)_2 + H_2O \longrightarrow CH_2{=}O + 2C_2H_5OH$	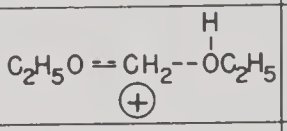	$+7^{55}$
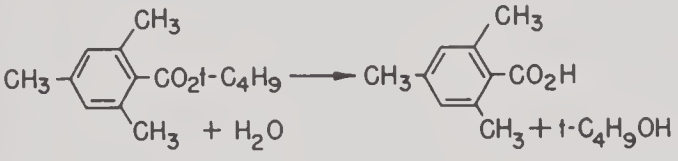	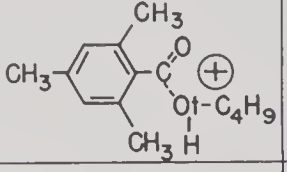	$+9^{55}$
$(CH_3)_2C(O)CH_2 + H_2O \longrightarrow (CH_3)_2C(OH)CH_2OH$	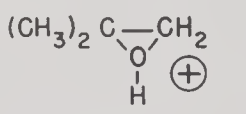	-4^{55}
$CH_3CO_2CH_3 + H_2O \longrightarrow CH_3CO_2H + CH_3OH$	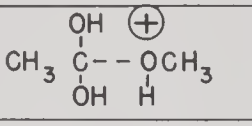	-21^{55}
$(CH_3)_2C{=}CHCHO + H_2O \longrightarrow (CH_3)_2C(OH)CH_2CHO$	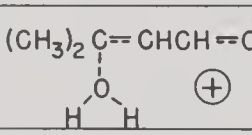	-23^{45}
$2CH_3HgI + H_3O^{\oplus} \longrightarrow CH_4 + CH_3Hg^{\oplus} + HgI_2 + H_2O$	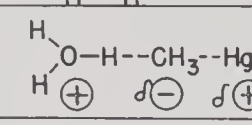	-29^{44}

[1] The exact structure of this transition state is not known, but there is independent evidence that a water molecule is firmly bound to the substrate in the transition state (ref. 45).

in entropies were observed. Here, as elsewhere, a good deal more data on well-understood rates and equilibria would be very desirable.

For many acid-catalyzed organic reactions, it is of interest to determine whether a water molecule, in addition to the proton, is firmly bound to the substrate in the transition state. Long, Pritchard, and Stafford (55), amplifying a suggestion of Taft and coworkers (45), have shown that a substantial negative entropy of activation, usually in excess of 20 cal./mole deg., accompanies many reactions in the transition states for which a water molecule is so bound. On the other hand, if the transition state consists simply of the substrate plus a proton, the entropy of activation may be either positive or negative and is numerically small. Long and coworkers (55) suggest that binding a water molecule to a protonated organic substrate is accompanied by a decrease of 20–30 cal./mole deg. in entropy.

Table IV shows the transition states for a number of reactions and their entropies of activation. These data and others cited by Long (55) bear out the generalization nicely.

The origin of the Long generalization seems quite plain. If a proton is transferred from a hydronium ion to an organic substrate, the solvent becomes somewhat less restricted because the resultant ion is larger and therefore less effectively solvated. On the other hand, the internal mobility of the substrate is reduced by the charge and the solvent. Also, the water molecule that is released is more effective in immobilizing other water molecules than most neutral substrates. These effects approximately cancel each other with the result that the entropy of activation is small and may be of either sign. When a water molecule is added to a protonated organic substrate, most of its entropy is immediately lost. In addition, the two hydrogens of the water molecule usually take on substantial positive charges; since they are usually quite exposed, they are very effective in immobilizing solvent. Each of these effects apparently gives rise to a negative entropy of from 10 to 15 cal./mole deg. Whalley (23b) has pointed out the possibility that some reactions involving an attack by solvent on the protonated substrate in the rate-determining step may have a positive or a very small negative entropy of activation. Such reactions will undoubtedly be found in cases where the transition state resembles the separated molecules closely, but the Long generalization will probably be right far more often then not.

A good deal of effort has been devoted by organic kineticists to the study of the effect of solvent on reactivity. Examples of this are the work of Norris and Prentiss on the reaction of pyridine with methyl iodide (56), that of von Halban on the decomposition of triethylsulfonium bromide (57), and that of Tommila (58), Swain (59), Winstein (60), and their students, on solvolysis reactions. The variation in rate, and, therefore, in free energy of activation, is about what one would expect from the discussion given above. Although there are certain exceptions, when a more polar transition state is produced from a less polar starting state, the reaction is generally accelerated by making the solvent more polar (56,58–60). The converse seems true when the transition state is less polar than the starting state (57).

The variations in $\Delta H^{\pm}$ and $\Delta S^{\pm}$ with solvent composition are very complex (58,60). If one steps back and looks from some distance at changes in $\Delta S^{\pm}$ with solvent composition, they are about as one would expect. The entropy of activation for reactions in which the transition state is more polar than the starting state usually becomes more negative as the solvent becomes less polar. Closer examination of plots of $\Delta S^{\pm}$ vs. solvent composition frequently reveals several maxima and minima, however.

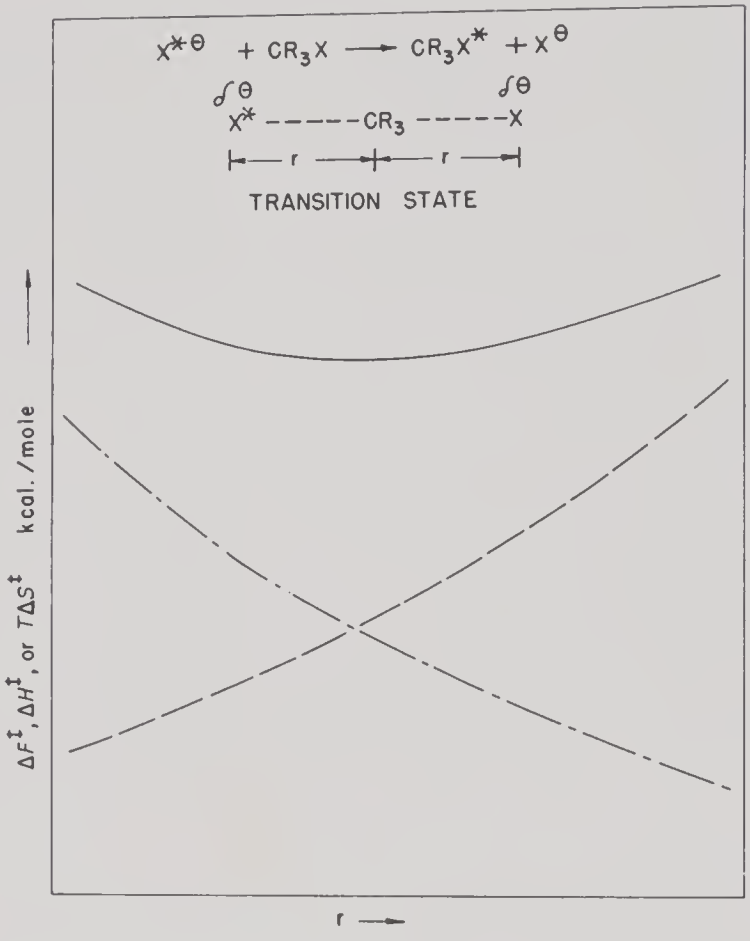

Fig. 3. Variation in $\Delta F\ddagger$, $\Delta S\ddagger$ and $-T\Delta S\ddagger$, with the C–X distance in the transition state shown. $\Delta F\ddagger$ is ——, $\Delta H\ddagger$ is - - - - -, and $-T\Delta S\ddagger$ is —·—·—·—. A slight change in conditions could bring about a considerable change in r_{C-X} without changing $\Delta F\ddagger$ very much, because the curve of $\Delta F\ddagger$ vs. r_{C-X} is rather flat. Both $-T\Delta S\ddagger$ and $\Delta H\ddagger$ would be changed profoundly, however.

Changes in heats of activation are similarly complicated, and both are much more complicated and larger than changes in free energies of activation. It is not surprising that this should be so. Figure 3 shows a purely hypothetical but reasonable variation in $\Delta F^{\pm}$, $\Delta H^{\pm}$, and $\Delta S^{\pm}$ with charge separation for a hypothetical transition state. It is plain that large variations in $\Delta H^{\pm}$ and $\Delta S^{\pm}$ may accompany small changes in $\Delta F^{\pm}$ because nature will select just such a transition state that $\partial(\Delta F^{\pm})/\partial f_s$ equals zero, where f_s is any function of the transition state structure. No such "variation principle" applies to $\Delta S^{\pm}$ or $\Delta H^{\pm}$. These complex plots of $\Delta H^{\pm}$ and $\Delta S^{\pm}$ vs. solvent composition provide a very exacting test of our knowledge of transition state structure and its variation with solvent composition. So far our knowledge has failed this test.

It is, of course, necessary to have reliable entropies of activation before any attempt at interpretation can be made. In the past, the implications of this in terms of the required accuracy of rate constants and the required

temperature range have not always been fully realized. For example, around room temperature, a probable error of as little as 1% in rate constants leads to a probable error of ±1 cal./mole deg. in the entropy of activation, if this is determined from rates at two temperatures 10° apart (61). Such accuracy is uncommon in the measurement of the rates of organic reactions. A probable error of 15% in the rates at each temperature would lead to a probable error of 13 cal./mole deg. in the entropy of activation and will usually make it completely valueless. It is, of course, also not possible to determine whether $\Delta H^{\ddagger}$ and $\Delta S^{\ddagger}$ are constant unless rates are measured at more than two temperatures.

In most cases, it seems necessary that entropies of activation be derived from rates at no less than four temperatures spread over at least a 20°-temperature range before they can be considered very significant. An even larger range of temperatures is desirable, particularly if the rate constants are not known with great accuracy. Equation (68), in which T_0 and k_0 are taken as arbitrary parameters, gives the Eyring heat of activation in a form convenient for least-squares calculation. From the heat of activation the entropy of activation can be derived via Equations (33–35).

$$\ln (k_T/T) = -\Delta H^{\ddagger}/RT + [\Delta H^{\ddagger}/RT_0 - \ln (T_0/k_0)] \qquad (68)$$

4. Activation Energy and Energy of Reaction

Examination of Equations (7–9) shows that two types of quantities determine entropy, heat, and free energy of reaction. These are the potential energy of reaction and the partition functions. A third quantity, zero-point vibrational energy, has also been more or less arbitrarily separated. The foregoing section has been largely concerned with the testing of postulated transition states by comparison of estimated and observed entropies of activation (or changes in entropies of activation with structure or solvent). Postulated transition state structures (and, in principle, also the structure of stable molecules) can also be tested by comparison of measured and estimated heats or free energies of activation. These, however, involve the potential energy and zero-point vibrational energy terms, as well as the partition functions, whereas the entropy involves only the last. In favorable cases, entropies can be calculated from nonkinetic data, and zero-point vibrational energy changes can also be estimated. Potential energy changes can, at present, be estimated with sufficient reliability to provide a check for a postulated transition-state structure for only a very few reactions of interest to organic chemists. Undaunted, organic chemists have built up an extensive, empirical body of quantitative and qualitative correlations of potential energy (relative rates) with structure, and these provide perhaps the most common method of testing postu-

lated transition-state structures. Some of these are time-honored and used almost without thought. For example, no modern chemist would seriously consider the possibility that the first step in the hydration of ethylene oxide is a dissociation into an oxygen atom and ethylene. The reaction is known to proceed at a reasonable rate at about room temperature, and the dissociation into ethylene plus an oxygen atom is thought to require a very large input of potential energy. The idea that the simultaneous rupture of more than one covalent bond requires a large input of potential energy (and is therefore unlikely at moderate temperatures) has been called the "principle of minimum structural change" (62). These correlations will not be discussed in detail in this chapter—they are discussed elsewhere in this volume (63). In the following paragraphs some of the assumptions implicit in their use will be discussed.

It is frequently assumed, implicitly or explicitly, that a free energy or heat of reaction (or activation) is a measure of the potential energy of reaction (or activation). Equations (7) and (8) become Equations (69) and (70) after separation of the change in zero-point vibration energy, ΔE_z, from the partition functions. If the energy level spacings in B are identical with

$$\Delta F^0 = \Delta E_0 + \Delta E_z - RT \ln (f_B/f_A) \tag{69}$$

$$\Delta H^0 = \Delta E_0 + \Delta E_z + RT^2(d/dT)[\ln (f_B/f_A)] \tag{70}$$

those in A, f_B will equal f_A and both $\ln (f_B/f_A)$, and its derivative with respect to temperature will be identically zero. Since zero-point vibrational energies are determined by the same vibrational frequencies which determine the energy-level spacings, ΔE_z must also be identically zero if f_B equals f_A. It follows, then, that ΔF^0 and ΔH^0 both equal ΔE_0 when f_B equals f_A. Equation (9) shows that ΔS^0 equals zero when f_B equals f_A, and this can be used as an indication that the identification of ΔF° or ΔH^0 with ΔE_0 is permissible (64).

Fortunately, it is only relative free energies for a series of homologous reactions that are wanted in most cases. In that case, Equations (71–74) show that it is necessary only that the entropies of reaction (or activation) remain the same throughout the series in order that changes in ΔF^0 or ΔH^0 be interpretable in terms of potential energy changes.

$$\mathrm{RX + Y \rightarrow RY + X} \tag{71}$$

$$\mathrm{R^0X + Y \rightarrow R^0Y + X} \tag{72}$$

$$\mathrm{RX + R^0Y \rightarrow RY + R^0X} \tag{73}$$

$$\Delta S_{73}{}^0 = \Delta S_{71}{}^0 - \Delta S_{72}{}^0 \tag{74}$$

R = the general substituent
$\mathrm{R^0}$ = some standard substituent

The entire foregoing argument is not rigorous for most organic reaction series because the higher vibrational frequencies, which contribute a large part of the zero-point vibrational energy, are not appreciably excited at the temperatures at which these reactions are carried out. As a consequence, their contribution to the partition functions is unity, regardless of the exact value of their frequencies or their contributions to ΔE_z. Fortunately, most such vibrational frequencies are approximately characteristic of a particular bond type, and it will be noted that the same number of each type of bond appears on both sides of the arrow in Equation (73).

In many reaction series that follow the Hammett equation, entropies of activation or reaction are constant within their probable error. The use of the Hammett equation to correlate rate and equilibrium constants has been justified by the assumption that changes caused by *m*- and *p*-substitution in the benzene ring are largely potential energy changes (65). There are, however, a number of reaction series in which the Hammett equation is obeyed with good precision in spite of the fact that ΔS^0 is not constant. The prime example of these is the ionization of substituted benzoic acids, which originally provided the substituent parameters for the Hammett equation. This result seems best explained in the following fashion: The observed entropy changes are a consequence of variations in the degree of immobilization of water by the organic ions. These variations are a simple function of the charge delocalization into the substituted benzene ring. Potential energy effects on the ionization constants are due to these same delocalizations. As a result, the changes in ln (f_B/f_A) are proportional to the changes in ΔE_0. Changes in ΔE_z would also tend to parallel changes in ΔE_0 because these changes would also be a result of the immobilization of water. In some such cases, ΔF^0 seems to be a better measure of ΔE_0 than is ΔH^0, apparently because ln (f_B/f_A) is better behaved than its derivative with respect to temperature (66). In all such cases, independent verification is necessary before either ΔH^0 or ΔF^0 can be identified with ΔE_0. Justification frequently takes the form that variations in ΔF^0 and/or ΔH^0 can be nicely explained in terms of known or suspected potential energy effects.

It is not uncommon to see the energy of a transition state identified with the energy of a starting material or product. For example, "reaction *x* doesn't proceed because A (a product) is sterically hindered" or "reaction *y* is rapid because it produces a product that is highly resonance stabilized." It is of interest to examine the validity of such identifications.

Hammond (67) has offered the following postulate to determine whether the starting state, or the product, or neither is a good model for the transition state of a particular reaction [cf. Lumry and Eyring (68)]: "If two states . . . occur consecutively during a reaction process and have nearly

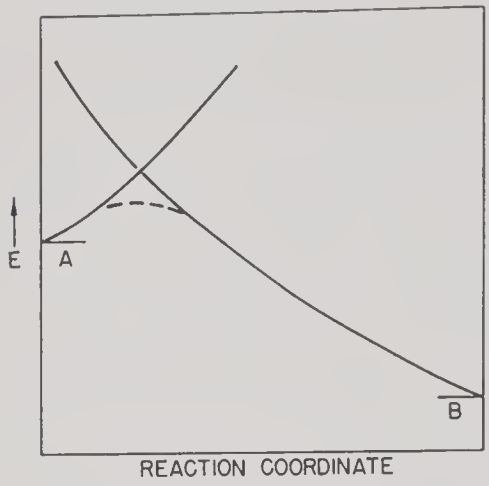

Fig. 4. The exothermic reaction A→B. The solid line leading to state B is the energy the system would have if the bonds were arranged as they are in B. The solid line leading to the state A is the energy the system would have if the bonds were arranged as they are in A. The dotted line is the energy of the ground state of the real system (a resonance hybrid, A→B). It is plain that the transition state will occur at a position on the reaction coordinate close to the state that it resembles energetically in most cases. Exceptions may occur if the differenee in energy between A and B is not great and/or if the solid curves are very different in shape.

the same energy content, their interconversion will involve only a small reorganization of the molecular structures." In other words, a transition state will resemble a particular stable molecule or intermediate if it occurs just before or just after that molecule or intermediate in the reaction path and has a similar energy. The general correctness of such a postulate can be seen from Figure 4.

Hammond's principle is probably reflected by the behavior of acid-catalyzed acetal and ketal hydrolysis rates (69,70). The mechanism of acid-catalyzed acetal and ketal hydrolysis seems quite well established (70) and is shown in Equations (75–77). The transition state must be

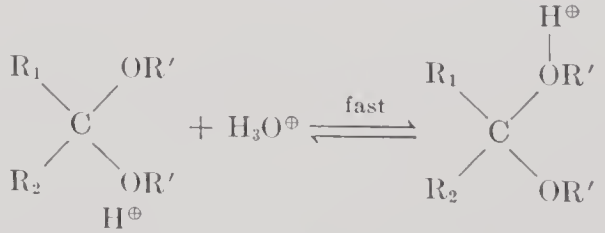

(75)

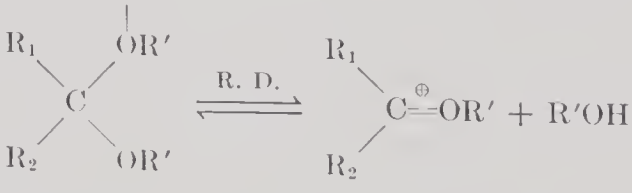

(76)

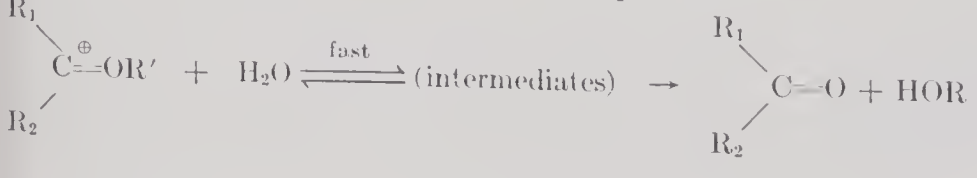

(77)

intermediate between the two high-energy intermediates shown in Equation (76). As long as R_1 and R_2 have no π-orbitals conjugated with the functional group, the product of the rate-determining step is apparently less stable than the protonated substrate. The transition state resembles that product in that it is strongly stabilized by the introduction of α,β-unsaturation in R_1 and R_2. (A species resembling $R_1R_2C{=}{=}OR^{\oplus}$ would be so stabilized; a species resembling the protonated substrate would not.) After the transition state—and presumably the closely related product—has been stabilized to the extent of about 7 kcal./mole, in this fashion, the product of the rate-determining step apparently becomes more stable than the protonated substrate because further stabilization of the transition state by conjugation is not possible. The transition state now resembles the protonated substrate.

It is worth noting that a transition state can also resemble a state that does not lie along the reaction path at all. This is illustrated by the base-induced elimination from 1-bromo-2-aryl ethanes, shown in reaction (78).

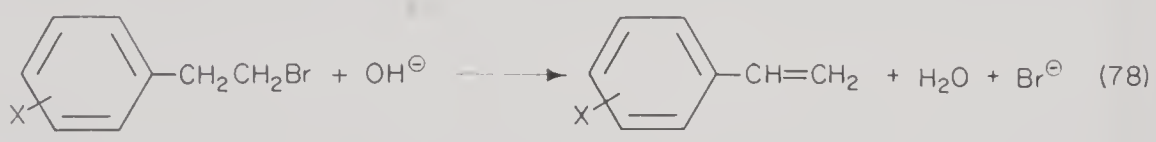

(78)

The effect of the group X on the rate is about what would be expected if the transition state resembled the ion I (72) but isotopic studies (73,74) have

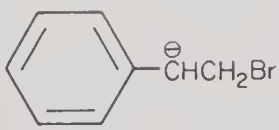

I

shown that such an ion is not an intermediate—that the products are probably produced directly from the starting materials. The energetics of the situation are shown in Figure 5.

Another question worth discussing may be phrased as follows: Does the fact that a bond is inappreciably made or broken in a transition state *necessarily imply* that it is unmade or unbroken in the product of that transition state? If the words "necessarily imply" are replaced by "strongly suggest," the statement seems true, but there may be exceptions. The acid-catalyzed hydration of epoxides has been extensively studied by Long and Pritchard (75a–e). The evidence seems to point to a prototropic equilibrium followed by a rate-determining step for which the transition state closely resembles the protonated substrate. It might be concluded

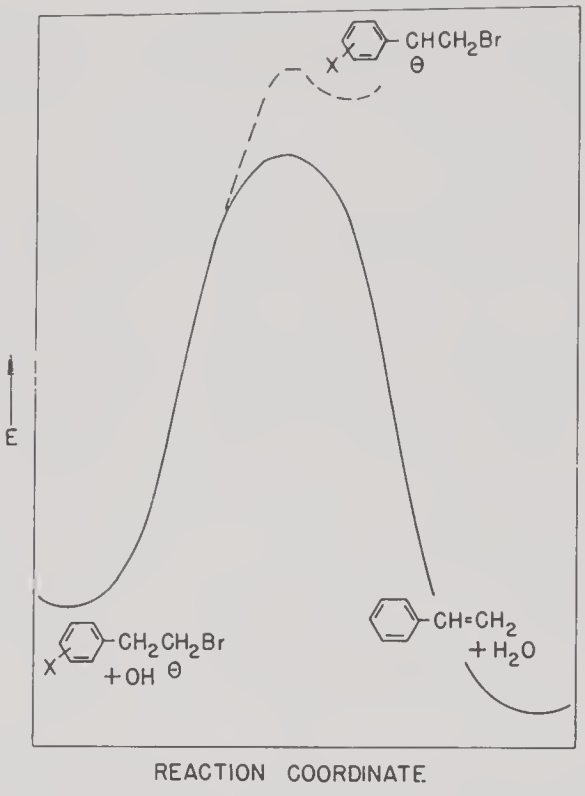

Fig. 5. Reaction coordinate for Reaction (77) (solid line) with the energy of the state $H_2O + I$ and configurations leading to that state superimposed (broken line). This figure shows how the transition state for Reaction (78) may resemble the later state without the anion actually being an intermediate in the reaction.

from this that the product of the rate-determining step must be the carbonium ion; in the specific case of ethylene oxide, this is $HOCH_2CH_2^+$.

The evidence that the transition state resembles the protonated substrate rather than the carbonium ion is: (a) The rates of reaction for monosubstituted ethylene oxides $CH_2\text{—}CHX$ can all be correlated by a single Taft-

Hammett plot regardless of whether X is more or less electron-supplying than a hydrogen atom. If X is more electron-supplying than a hydrogen atom, the carbonium ion will have the structure $HOCH_2\overset{\oplus}{C}H\text{—}X$, whereas, if it is less electron-supplying, it will be $HOCHXCH_2^{\oplus}$. The only likely *symmetrical* transition state is one resembling the protonated substrate; (b) The reaction of ethylene oxide is less than a power of ten faster than that of trimethylene oxide. The mechanisms of the two reactions have been shown to be analogous (75d). If the carbon-oxygen bond were significantly broken, the latter would be many powers of ten slower than the former because of the greater strain inherent in the three-membered ring and removed in the product ion; (c) The Taft-Hammett parameter ρ^*, which is a measure of the electron deficiency at the carbon to which X

is attached, is 1.6, whereas values between 3 and 4 are usually found when the carbon atom carries a unit positive charge; (d) The reaction shows no obvious Baker-Nathan effect.

If the rate-determining step is the conversion of the protonated substrate to the carbonium ion, the Hammond principle then requires that the latter be much more stable than the former. It has already been indicated, however, that a protonated acetal or ketal, II, is much *more* stable than the carbonium ion, III ↔ IV, plus R′OH, as long as R_1 and R_2 do not strongly favor the carbonium ion. Since the acetal or ketal carbonium ion probably derives ~28 kcal./mole of stabilization from resonance of the type III ↔ IV (this is a very crude and probably conservative estimated obtained by

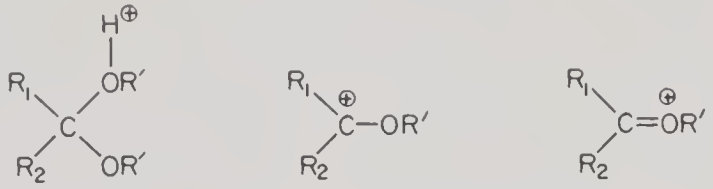

II III IV

an L.C.A.O.-M.O. calculation with the Coulomb integral for oxygen set equal to that for carbon, and the carbon-oxygen resonance integral set equal to 14 kcal./mole) and is, nevertheless, *less* stable than the protonated acetal or ketal, it seems quite unlikely that carbonium ions derived from protonated epoxides are *more* stable than the protonated epoxides. The most reasonable rate-determining step, therefore, seems to be that shown in Equation (79), in spite of the fact that the water molecule apparently is

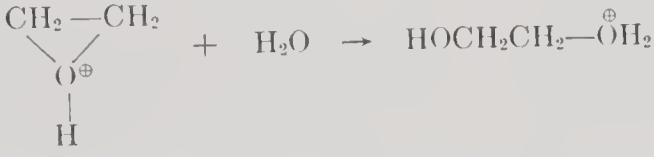

(79)

only very weakly bound to the substrate in the transition state. This view has recently been directly supported by the finding of a negative volume of activation (75f), but, by almost all criteria, this transition state seems to resemble the protonated substrate so closely that it does not give information about the product of the rate-determining step.

Most reactions of interest to the organic chemist involve over-all activation free energies of at least 15 kcal./mole in both directions. From this and the Hammond principle, it follows that neither the starting material nor the ultimate product is likely to be a good model for the transition state. Unstable intermediates frequently are such models, and much insight into the structure of the transition state can sometimes be gained by comparing its behavior with that expected for certain hypothetical intermediates. In addition, *certain aspects* of the activation process may resemble equilibria.

For example, the change to which a molecular acid is subjected when it acts as a catalyst in general acid-catalyzed reactions frequently resembles the change it undergoes on ionization. The Brønsted catalysis law is the result (76).

It is interesting that a particular species is not rigorously excluded as a reaction intermediate simply because its free energy of formation from the starting materials is higher than the free energy of activation as defined by Equation (33). The reason is that $f_{\pm}$, which is used in the calculation of $K^{\pm}$ and $\Delta F^{\pm}$, lacks a degree of freedom—the degree along the reaction coordinate—that the true transition state possesses. In practice, this means that a possible intermediate must have a free energy of formation from the starting materials perhaps 5 kcal./mole in excess of the measured free energy of activation before it can be excluded on these grounds.

5. The Behavior of Activity Coefficients—The Hammett Acidity Function and Related Functions

Changes in activity coefficients result both from changes in potential energy and changes in partition functions. In spite of this, activity coefficients can be estimated for a number of structural types in a variety of nonideal solutions. It is plain that such estimates can be combined with Equation (49) to give rate constants that, in one way or another, can be compared with measured values. If the agreement is not good, either the postulated transition-state structure (or, in a few cases, the structure of the starting materials) is incorrect, or the method of estimating its activity coefficient is incorrect.

The first applications of this method antedate the transition state theory of reaction rates. The Debye-Hückel theory gives the activity coefficients of ions as a function of ionic strength in dilute salt solutions (77). If the charge on the transition state is postulated, the variation in rate constant with ionic strength can be predicted. An example of this is the reaction of ammonium cyanate to give urea (78). The starting material is known to be predominantly in the form of ammonium ions and cyanate ions. Equation (49) and the Debye-Hückel theory give the proper dependence of rate on ionic strength, if the transition state is assumed to be neutral.

It is important to note that *no* information about the path by which the reactants reached the transition state has been obtained. In fact, the mechanism probably involves the mobile equilibrium

$$NH_4^{\oplus} + CNO^{\ominus} \rightleftharpoons NH_3 + HCNO \qquad (80)$$

followed by a rate-determining reaction of the neutral molecules (78).

A more recent and more empirical method of estimating activity coef-

ficient ratios is provided by the Hammett acidity function H_0 and related functions (79). Briefly, Hammett and coworkers found that, in aqueous mineral acid, the activity coefficient ratio $\alpha_{H^\oplus}\alpha_{B^\oplus}/\alpha_{BH^\oplus}$ was independent of the structure of the neutral base B as long as the protonated base $BH^\oplus$ differed from the base only by the addition of a proton. (The activity coefficient of the proton $\alpha_{H^\oplus}$ can be a real quantity even if the concentration of protons in solution is vanishingly small.) This allowed them to define a function H_0 by Equation (81),

$$H_0 \equiv -\log \left\{ (H^\oplus)(\alpha_{H^\oplus}\alpha_B)/\alpha_{BH^\oplus} \right\} \tag{81}$$

where $(H^\oplus)$ is the stoichiometric acid concentration. It will be noted that H_0 becomes identical with pH in the limit of infinitely dilute solutions.

The thermodynamic definition of the ionization constant K of B in a real solution is given by Equation (82),

$$K = \frac{(BH^\oplus)}{(B)(H^\oplus)} \times \frac{\alpha_{BH^\oplus}}{\alpha_B \alpha_{H^\oplus}} \tag{82}$$

so values of H_0 can be obtained from Equation (83) by measuring ratios of protonated to unprotonated bases in various solutions. In practice, most of the

$$H_0 = \log K + \log \left[(B)/(BH^\oplus) \right] \tag{83}$$

measurements have been made spectrophotometrically. The thermodynamic ionization constants were either determined directly in very dilute solutions or (more frequently) by reference to solutions of known H_0. The values of H_0 so obtained are approximately independent of the nature and structure of the base and have been extensively tabulated (79a).

If the transition state for an acid-catalyzed reaction differs from the substrate by the addition of a proton and nothing more, $\alpha_{BH^\oplus}$ can be identified with $\alpha_\ddagger$ and $\alpha_{H^\oplus}\alpha_B = \pi\alpha_r$ in Equation (49). The rate constant in a moderately concentrated mineral-acid solution is then given by Equation (84). In practice, such reactions are studied under conditions in which the acid

$$\log \left\{ k_r(H^\oplus) \right\} = \log k_r^0 - H_0 \tag{84}$$

concentration does not change during the course of the reaction, but the substrate is consumed. Since Equation (85) gives the rate law, $k_r(H^\oplus)$ is identical

$$-d(S)/dt = k_r(H^\oplus)(S) \tag{85}$$

with the measured first-order rate constant. For reactions to which this technique is applied, k_r^0 is frequently not available, so the quantity log

$\{k_r(H^{\oplus})\} + H_0$ is examined for a variety of acid concentrations. If it does not change by more than 0.2–0.3 in the range 1–5M acid, the results are usually thought to be consistent with a transition state differing from the substrate only by the addition of a proton.

It was originally thought that Equation (84) would fail if the transition state did not bear the same general sort of relation to the starting state that a protonated indicator bears to the unprotonated indicator. Equation (86) was thought to govern the behavior of the activity coefficients if

$$(H_2O)\alpha_{H_2O}\alpha_{H^{\oplus}}\alpha_S/\alpha_{\pm} \sim 1 \tag{86}$$

was thought to govern the behavior of the activity coefficients if a discreet water molecule, in addition to the proton, is strongly bonded to the substrate in the transition state (79b). In that case $k_r \sim k_r^0$. In Equation (86), (H_2O) is the mole fraction of water, and α_{H_2O} is its activity coefficient referred to pure water. Values of H_0 diverge strikingly from $-\log (H^{\oplus})$ in the region 1–5M acid. This provided the first and most widely used means for determining the role of solvent molecules in acid-catalyzed reactions. Two examples of its use are provided by the acid-catalyzed hydration of olefins and the acid cleavage of methyl mercuric iodide. The mechanism of the former reaction was thought to be that shown in Equations (61–64). The postulated transition state must clearly have the character of a protonated substrate, so this mechanism predicts that $\log \{k_r(H^{\oplus})\} + H_0$ should be a constant. The fact that this sum *is* a constant played an important role in assigning the mechanism shown (45). In the postulated mechanism for the acid cleavage of methyl mercuric iodide, also discussed above, the water molecule is firmly bound to the substrate through the proton that is being transferred. Here it would be predicted that k_r would be a constant. The fact that it is nearly constant up to 5M perchloric and sulfuric acids was one of the important pieces of evidence for this mechanism (44).

If we extend this reasoning, the ionization of alcohols according to Equation (87) should also fail to follow H_0. This reaction has been extensively studied by Deno and his students (80). They have defined the function H_R [*cf.* Gold's J_0 (81)]

$$ROH + H^{\oplus} \rightleftharpoons R^{\oplus} + H_2O \tag{87}$$

Equation by 88. They measured H_R in the manner outlined above for H_0 and found

$$H_R \equiv -\log \frac{(H^{\oplus})\ \alpha_{H^{\oplus}}\alpha_{ROH}}{(H_2O)\ \alpha_{H_2O}\alpha_{R^{\oplus}}} \tag{88}$$

that it also was approximately independent of the alcohol structure (over a rather limited range of alcohol structures) and was even more widely divergent from $-\log(H^{\oplus})$ than was H_0. The equilibrium constant for reaction (87) is given by Equation (89), where K_n is the equilibrium constant for

$$K = K_{90}K_{91}K_{92} \tag{89}$$

$$ROH + H^{\oplus} \rightleftharpoons ROH_2^{\oplus} \tag{90}$$

$$ROH_2^{\oplus} \rightleftharpoons R' + H^{\oplus} + H_2O \tag{91}$$

$$R' + H^{\oplus} \rightleftharpoons R^{\oplus} \tag{92}$$

reaction n. The species R′ would be an olefin if ROH were an ordinary aliphatic alcohol. Most of Deno's alcohols were triarylcarbinals, so R′ does not correspond to a stable molecule, but the thermodynamic argument is not impaired.

Since ROH and R′ can both be considered neutral bases, K_{90}, K_{91}, and K_{92} are given by Equation (93–95) if Equations (81) and (86) apply to these systems. Combination of Equations (88) and (89) with (93–95) gives

$$\log K_{90} = H_0 + \log\{(ROH_2^{\oplus})/(ROH)\} \tag{93}$$

$$\log K_{91} = H_0 + \log\{(R^{\oplus})/(R')\} \tag{94}$$

$$\log K_{92} = \log(H^{\oplus}) + \log\{(R')/(ROH_2^{\oplus})\} \tag{95}$$

Equation (96) (ref. 81).

$$H_R = 2H_0 + \log(H^{\oplus}) \tag{96}$$

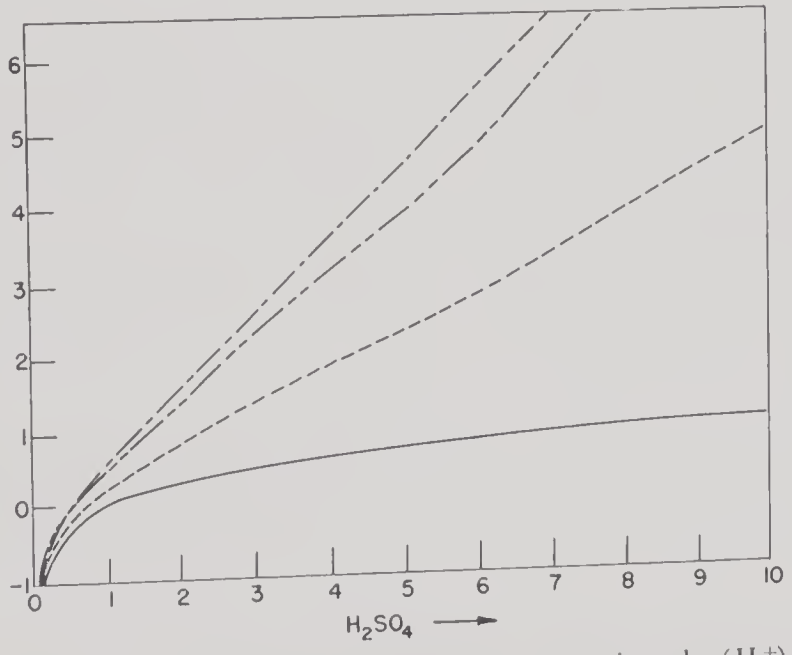

Fig. 6. Acidity functions in aqueous sulfuric acid. —— is $-\log(H^+)$; - - - - is H_0; — - — - is C_0; — - - — - - is $2H_0 + \log(H^{\oplus})$.

Figure 6 shows $-\log(H^{\oplus})$, H_0, H_R, and the quantity $2H_0 + \log (H^{\oplus})$ for aqueous sulfuric-acid solutions. Considering the various approximations involved, the correspondence between H_R and the quantity $2H_0 + \log (H^{\oplus})$ seems entirely satisfactory. The agreement between H_R and $2H_0 + \log (H^{\oplus})$ is less adequate for nitric and perchloric-acid solutions but is still moderately satisfactory (80b). Clearly, H_R can be used in about the same way as H_0 and $\log (H^{\oplus})$ in determining transition-state structure.

In the last few years, however, these criteria of mechanism have been shown to be unreliable because Equation (84) is apparently more general than was originally thought. For example, rates of both olefin hydration and alcohol dehydration are governed (45b) by Equation (84), although it is plain that the transition state cannot simultaneously be a protonated alcohol and a protonated olefin. In the ethylene oxide hydration discussed above, rates are also governed by Equation (84), in spite of the fact that a water molecule apparently attacks the protonated substrate in the rate-determining step.

A number of new ways of using acidity-function correlations have been suggested (80,82), but none of them seem well established as yet. It seems safe to say that rates of reactions involving transition states that closely resemble a protonated substrate will follow H_0; those involving a nearly intact hydronium ion in the transition state will follow $\log (H^{\oplus})$. Prediction of the behavior of other types of reaction rates awaits the development of new theory, or the accumulation of more data on reactions of known mechanism, or both.

III. CONCLUSION

In conclusion, the only perfectly general thing that can be said about the methods of determining mechanism outlined in this chapter is that none of them is completely reliable. For this reason, it is desirable that mechanistic problems be "solved" in as many ways as possible, so that more confidence may be placed both in the solution and the methods that were used to reach it.

Acknowledgments

The author is grateful to the Graduate School of the University of Minnesota for support while this chapter was being prepared; and to Miss Ruth Judd, who did the typing.

References

1. R. S. Livingston, this volume, Chapter 2.
2. See, for example, M. Dole, *Introduction to Statistical Thermodynamics*, Prentice-Hall, New York, 1954, Chapt. 7.

3. H. Eyring, J. Walter, and G. E. Kimball, *Quantum Chemistry*, Wiley, New York, 1944, p. 72.

4. G. Herzberg, *Infrared and Raman Spectra of Polyatomic Molecules*, Van Nostrand, New York, 1945, p. 44.

5. H. Eyring, J. Walter, and G. E. Kimball, *loc. cit.*, p. 74.

6. G. Herzberg, *Molecular Spectra and Molecular Structure*, Van Nostrand, New York, 1950, pp. 74, 468.

7. H. Eyring, J. Walter, and G. E. Kimball, *loc. cit.*, p. 77.

8. M. Dole, *loc. cit.*, pp. 105–108.

9. M. Dole, *loc. cit.*, pp. 108–113.

10. W. Benson, *J. Am. Chem. Soc.*, **80**, 5151 (1958).

11. M. Dole, *loc. cit.*, p. 114.

12. *Ibid.*, p. 171.

13. K. S. Pitzer and W. D. Gwinn, *J. Chem. Phys.*, **10**, 428 (1942).

14. J. C. M. Li and K. S. Pitzer, *J. Phys. Chem.*, **60**, 466 (1956).

15. R. S. Livingston, this volume, Chapter 2.

16. S. Glasstone, K. Laidler, and H. Eyring, *The Theory of Rate Processes*, McGraw-Hill, New York, 1941, pp. 10–14, 184.

17. *Ibid.*, pp. 99–100, 200.

18. A. A. Frost and R. G. Pearson, *Kinetics and Mechanism*, Wiley, New York, 1953, p. 151.

19. (a) M. L. Bender, R. D. Ginger, and J. P. Unic, *J. Am. Chem. Soc.*, **80**, 1044 (1958); (b) R. Lumry in H. Lardy, P. Boyar, and K. Myrbäch, *The Enzymes*, Academic, New York, 1958, Chapt. 4; (c) J. C. Giddings and H. Eyring, *J. Phys. Chem.*, **62**, 305 (1958).

20. A. A. Frost and R. G. Pearson, *loc. cit.*, p. 202.

21. P. D. Bartlett in H. Gilman, *Organic Chemistry*, Vol. III, Wiley, New York, 1953, p. 9.

22. J. N. Brønsted, *Z. physik. Chem.*, **102**, 169 (1922).

23. (a) S. Glasstone, K. Laidler, and H. Eyring, *loc. cit.*, p. 470; (b) E. Whalley, *Trans. Faraday Soc.*, **55**, 798 (1959).

24. W. G. Dauben and K. S. Pitzer, in M. S. Newman, *Steric Effects in Organic Chemistry*, Wiley, New York, 1956, p. 54.

25. *Ibid.*, p. 35.

26. J. F. Bunnett, this volume, Chapter 6.

27. R. S. Livingston, this volume, Chapter 2.

28. S. Glasstone, K. Laidler, and H. Eyring, *loc. cit.*, p. 195.

29. G. B. Kistiakowsky and J. R. Lacher, *J. Am. Chem. Soc.*, **58**, 123 (1936).

30. G. B. Kistiakowsky and W. W. Ransom, *J. Chem. Phys.*, **7**, 725 (1939).

31. S. Glasstone, K. Laidler, and H. Eyring, *loc. cit.*, p. 271.

32. A. Wassermann, *J. Chem. Soc.*, **1942**, 613.

33. (a) R. B. Woodward and T. J. Katz, *Tetrahedron*, **5**, 70 (1959); (b) M. J. S. Dewar, *Tetrahedron Letters*, No. 4, 16 (1959); (c) R. B. Woodward and T. J. Katz, *Tetrahedron Letters*, No. 5, 19 (1959).

34. (a) J. L. Magee, W. Shand, and H. Eyring, *J. Am. Chem. Soc.*, **63**, 677 (1941); (b) B. S. Rabinovitch and K.-W. Michel, *J. Am. Chem. Soc.*, **81**, 5065 (1959); (c) J. E. Douglas, B. S. Rabinovitch, and F. S. Looney, *J. Chem. Phys.*, **23**, 315 (1955).

35. L. J. Bellamy, *The Infrared Spectra of Complex Molecules*, Wiley, New York, 1954.

36. W. T. King, Characteristic Group Vibrations, Ph.D. Thesis, University of Minnesota, 1956.

37. S. Glasstone, K. Laidler, and H. Eyring, *loc. cit.*, ch. 5.
38. A. A. Frost and R. G. Pearson, *loc. cit.*, pp. 124–127.
39. *Ibid.*, p. 123.
40. J. T. Denison and J. B. Ramsey, *J. Am. Chem. Soc.*, **77**, 2615 (1955).
41. K. H. Stern and A. E. Martell, *J. Am. Chem. Soc.*, **77**, 1983 (1955).
42. H. S. Harned and B. B. Owen, *The Physical Chemistry of Electrolytic Solutions*, Reinhold, New York, 1958, p. 759.
43. S. Glasstone, K. Laidler, and H. Eyring, *loc. cit.*, p. 418.
44. M. M. Kreevoy, *J. Am. Chem. Soc.*, **79**, 5928 (1957).
45. (a) R. W. Taft, Jr., E. L. Purlee, P. Riesz, and C. A. DeFazio, *J. Am. Chem. Soc.*, **77**, 1584 (1955); (b) R. H. Boyd, R. W. Taft, Jr., A. P. Wolf, and D. R. Christman, *J. Am. Chem. Soc.*, **82**, 4729 (1960).
46. L. J. Bellamy, *loc. cit.*, p. 108.
47. W. T. King, *loc. cit.*, p. 134.
48. M. Dole, *loc. cit.*, p. 233.
49. P. D. Bartlett and R. R. Hiatt, *J. Am. Chem. Soc.*, **80**, 1398 (1958).
50. F. P. Price, Jr., and L. P. Hammett, *J. Am. Chem. Soc.*, **63**, 2387 (1941).
51. H. C. Brown and A. Cohn, *J. Am. Chem. Soc.*, **77**, 1715 (1955).
52. Data of L. H. Sommer and W. P. Barrie, Jr., cited by R. W. Taft, Jr., in M. S. Newman, *Steric Effects in Organic Chemistry*, Wiley, New York, 1956, p. 655.
53. R. W. Taft, Jr., *J. Am. Chem. Soc.*, **75**, 4534 (1953).
54. R. W. Taft in M. S. Newman, ed., *Steric Effects in Organic Chemistry*, Wiley, New York, 1956, p. 655.
55. F. A. Long, J. G. Pritchard, and F. E. Stafford, *J. Am. Chem. Soc.*, 79, 2362 (1957).
56. J. F. Norris and S. W. Prentiss, *J. Am. Chem. Soc.*, **50**, 3042 (1928).
57. H. von Halban, *Z. physik. Chem.*, **67**, 129 (1909).
58. E. Tommila, *Suomen Kemistilehti*, **29a**, 205 (1956); references to other work by Tommila and his students can be found in this paper.
59. C. G. Swain, R. B. Mosely, and D. E. Bown, *J. Am. Chem. Soc.*, **77**, 3731 (1955); references to other work by Swain and his students can be found in this paper.
60. (a) A. H. Fainberg and S. Winstein, *J. Am. Chem. Soc.*, **79**, 1608 (1957); (b) S. Winstein and A. H. Fainberg, *J. Am. Chem. Soc.*, **79**, 5937 (1957); references to other work by Winstein and his students can be found in these papers.
61. E. L. Purlee, R. W. Taft, Jr., and C. A. DeFazio, *J. Am. Chem. Soc.*, **77**, 837 (1955).
62. G. W. Wheland, *Advanced Organic Chemistry*, Wiley, New York, 1946, p. 95.
63. J. F. Bunnett, this volume, Chapter 6.
64. L. P. Hammett, *Physical Organic Chemistry*, McGraw-Hill, New York, 1940, p. 78.
65. *Ibid.*, p. 206.
66. L. P. Hammett, *Introduction to the Study of Physical Chemistry*, McGraw-Hill, New York, 1952, pp. 161–163.
67. G. S. Hammond, *J. Am. Chem. Soc.*, **77**, 334 (1955).
68. R. Lumry and H. Eyring in W. D. McElroy and B. Glass, *Mechanisms of Enzyme Action*, Johns Hopkins, Baltimore, 1954, p. 123.
69. M. M. Kreevoy and R. W. Taft, Jr., *J. Am. Chem. Soc.*, **79**, 4016 (1957).
70. M. M. Kreevoy, *Tetrahedron*, **5**, 233 (1959).
71. M. M. Kreevoy and R. W. Taft, Jr., *J. Am. Chem. Soc.*, **77**, 3146 (1955).
72. W. H. Saunders, Jr., and R. A. Williams, *J. Am. Chem. Soc.*, **79**, 3712 (1957).

73. P. S. Skell and C. R. Hauser, *J. Am. Chem. Soc.*, **67**, 1661 (1945).

74. V. J. Shiner and M. L. Smith, *J. Am. Chem. Soc.*, **80**, 4095 (1958).

75. (a) F. A. Long and J. G. Pritchard, *J. Am. Chem. Soc.*, **78**, 2663 (1956); (b) J. G. Pritchard and F. A. Long, *J. Am. Chem. Soc.*, **78**, 2667 (1956); (c) J. G. Pritchard and F. A. Long, *J. Am. Chem. Soc.*, **78**, 6008 (1956); (d) J. G. Pritchard and F. A. Long, *J. Am. Chem. Soc.*, **80**, 4162 (1958); (e) F. A. Long, J. G. Pritchard, and F. E. Stafford, *J. Am. Chem. Soc.*, **79**, 2362 (1957); (f) J. Koskikallio and E. Whalley, *Trans. Faraday Soc.*, **55**, 798 (1959).

76. R. P. Bell, *Acid-Base Catalysis*, Oxford at the Clarendon Press, 1941, p. 82.

77. A. A. Frost and R. G. Pearson, *loc. cit.*, p. 138.

78. *Ibid.*, p. 257.

79. (a) M. A. Paul and F. A. Long, *Chem. Revs.*, **57**, 1 (1957); (b) F. A. Long and M. A. Paul, *Chem. Revs.*, **57**, 935 (1957).

80. (a) N. C. Deno and C. Perizzolo, *J. Am. Chem. Soc.*, **79**, 1345 (1957); (b) N. C. Deno, H. E. Berkheimer, W. L. Evans, and H. J. Peterson, *J. Am. Chem. Soc.*, **81**, 2344 (1959); reference to other work by Deno and his students can be found in these papers.

81. V. Gold, *J. Chem. Soc.*, **1955**, 1263; reference to other work by Gold and co-workers can be found in this paper.

82. J. F. Bunnett, *J. Am. Chem. Soc.*, **82**, 499 (1960).

General References

Dole, M., *Introduction to Statistical Thermodynamics*, Prentice-Hall, New York, 1954.

Frost, A. A., and R. G. Pearson, *Kinetics and Mechanism*, Wiley, New York, 1953.

Glasstone, S. K., Laidler, and H. Eyring, *The Theory of Rate Processes*, McGraw-Hill, New York, 1941.

Hammett, L. P., *Physical Organic Chemistry*, McGraw-Hill, New York, 1940.

CHAPTER XXIV

The Product Criterion of Mechanism

EDWARD S. LEWIS, *William M. Rice University*
CHARLES E. BOOZER, *Emory University*

I. Introduction 1407
II. Application to Ionic Reactions 1410
1. The Elimination Reaction 1410
2. Aromatic Substitution 1413
III. Application to Divalent Carbon Intermediates 1416
IV. Application to Free-Radical Intermediates 1417
1. Applicability 1417
2. Reaction of Hydrocarbons with Oxygen 1418
3. The Decomposition of Acyl and Aroyl Peroxides 1421
4. Effects of Solvents in the Photochlorination of Hydrocarbons 1423
References 1424

I. INTRODUCTION

Before one can consider problems of reaction mechanism, it is imperative that some information on the nature of the process under consideration be available. Usually, when questions of mechanism arise, the information will consist of a knowledge of the identity of the important reagents and products. Here, we shall be concerned primarily with this common case and the information that can be gained from a quantitative study of the important products and sometimes also of the minor ones. Nevertheless, it should be kept in mind that a reaction is sometimes detected because of the occurrence of an observable change, even though the exact nature of the reagents or the products may be unknown. In such cases, it is sometimes fruitful to consider possible reaction mechanisms, in spite of the paucity of information.

An example of this situation is the deterioration of rubber, which is a conspicuous process involving chemical reactions even though the structure and compositions of both the reagents and the products were initially quite obscure. The suggestion that the reaction was oxidation and that the mechanism was similar to the autoxidation of simpler hydrocarbons (and therefore susceptible to inhibition by the same antioxidants) was patently very useful.

The identification of the substances involved, however, yields far more useful information. An example showing the advance possible after the identification of a key product is again the autoxidation reaction. The isolation of a hydroperoxide as the principal primary product of the oxidation of hydrocarbons led rapidly to the presently accepted free-radical chain mechanism. The study of the reaction rate, or of the more stable final products of the reaction, would have led to this mechanism only with great difficulty.

The reactions we shall consider at greater length will be those for which the general nature of the products is already known. Those features of a mechanism that are studied by relating the stereochemistry of the products to that of the reagent or by observing the fate of isotopically tagged atoms in a reagent will not be discussed here, since they are covered in other chapters of this volume (1,2).

When a chemist is faced with the problem of preparing a substance by a single reaction, it is not necessary that he know more than the yield of the desired substance and the nature of by-products which may interfere with the isolation or purification of the main product. In mechanistic studies, it is helpful to know the identities of as many of the products as possible, both major and minor, and the yields of each. The formation of a particular set of compounds does not lead unequivocally to a mechanism (even in the restricted sense of a series of intermediates), but a proposed mechanism must account for all the observed products. There is, then, a reasonably good analogy between a fairly complex mixture of products and a complicated rate law; neither leads directly to a mechanism, but both must be fitted by an acceptable mechanism. It is in just such cases that the combination of a kinetic study and a thorough product study is the most powerful general approach to the determination of the mechanism. It should be remembered that side reactions of unrelated mechanisms may obscure both the kinetic and the product distribution pictures; the separation of unrelated reactions is not a serious problem very often.

Once the qualitative composition of the product mixture is established, much can be gained by a quantitative determination of each of the observed products. This is generally an analytical problem of major dimensions. In this chapter we have selected examples yielding various types of useful mechanistic information and illustrating some of the analytical methods. No attempt has been made to collect all cases of the use of product analysis to illuminate a mechanism, since every study has used the product analysis to at least some extent.

The quantitative interpretation of the product yields is sometimes quite straightforward. Consider the two final products B_1 and B_2 resulting from two different reactions of substance A, which may be either a reagent

or an intermediate, with some of the other reagents present (C, D, . . .), as shown by reactions (1) and (2).

$$A + C + D + \ldots \rightarrow B_1 \quad (1)$$

$$A + C + D + \ldots \rightarrow B_2 \quad (2)$$

Let us make the simplifying assumption that the rates of formation of the two products are given by Equations (3) and (4), in which the concentration

$$d(B_1)/dt = k_1 f_1[(A), (C), (D), \ldots] \quad (3)$$

$$d(B_2)/dt = k_2 f_2[(A), (C), (D), \ldots] \quad (4)$$

functions $f_1[(A), \ldots]$ and f_2 are not necessarily simple products, since reactions (1) and (2) do not have to be simple one-step processes. The factorability of the rate expression into a rate constant k and a function of concentrations f is not always possible, of course; it is done here for simplification and because it is generally possible. The relative rates of formation of B_1 and B_2 are then given by Equation (5).

$$d(B_1)/d(B_2) = k_1 f_1/k_2 f_2 \quad (5)$$

The integration of this equation is possible if the ratio f_1/f_2 is known. A frequent case that is particularly simple occurs when $f_1 = f_2$. In this case the right-hand side of Equation (5) is a constant, and it suffices to determine the ultimate yields of the products, which may be called Y_1 and Y_2; the ratio of the rate constants is then given by Equation (6).

$$Y_1/Y_2 = k_1/k_2 \quad (6)$$

An example is the case in which B_1 and B_2 are isomeric substances produced by the attack of the same reagents at two nonequivalent positions on the same molecule. A complicated kinetic law can be simplified experimentally by choosing the conditions in such a way that one or more concentrations do not change significantly in the course of a run. Similarly, it is often possible to reduce Equation (5) to a form similar to Equation (6), except that the right-hand side of the equation would include a number of concentrations that did not change during the run, although they might be varied at will in successive experiments. The most common way to achieve the near constancy of a reagent during a run is to have a very large excess of it. An alternative method, applicable to reactions which proceed at a slow rate in comparison to the analysis used or to those reactions which may be quenched in any manner, is to allow the reaction to proceed to only a small extent. This method is especially popular in gas-phase reactions where the presence of a large solvent excess does not interfere with an analysis for a minor component of the mixture. When the reaction is carried to only a few per cent completion and there are no undetected unstable interme-

diates, it is possible to use Equation (5) directly in the differential form, using the initial concentrations of the added reagents in the functions f.

By using the above methods, it can be seen that it is, in principle, possible to determine simultaneously the ratio of the rate constants and the ratio of the concentration dependences for any two alternate fates of reagent A. The above treatment is valid even when there are multiple routes for the reagent. When reagent A in these reactions is an unstable intermediate that cannot be isolated, such as a free radical or a carbonium ion, these yield determinations constitute the only practical approach to the problem of relative rates. If the experiments on yield determinations include a study of temperature variation, so that k_1/k_2 is known at several temperatures, one can calculate the difference in activation energies and the ratio of the pre-exponential factors from the Arrhenius equation. The first is given by the slope of a plot of ln k_1/k_2 vs. $1/RT$; the second is the antilogarithm of the intercept of this line on the $1/RT$ axis. The corresponding terms of the Eyring equation can, of course, also be calculated. The individual activation parameters, like the individual rate constants themselves, cannot be calculated from the yield data alone. It often happens that a rate constant has been determined by independent experiments involving time measurements; these data can then be combined with the relative rate data from yield measurements to get a complete kinetic description.

The treatment above is rigorous (except for the factoring of the rate expression, which is not essential to most of the arguments), but, when the reactions are reversible, the kinetic laws are complicated, and the relative yields approach those predicted by thermodynamic considerations alone. When the reverse reactions are sufficiently fast, the relative rates drop out, and the reaction is said to be equilibrium controlled. The sulfonation of naphthalene is an interesting example of a reaction in which the isomer distribution is determined by relative rates at low temperatures but is equilibrium controlled at higher temperatures (3).

II. APPLICATIONS TO IONIC REACTIONS

1. The Elimination Reaction

The reactions of alkyl halides and analogous substances to yield olefins are examples of reactions both with and without unstable intermediates which can yield more than one product. The understanding of the various mechanisms has been greatly helped by product analysis.

The so-called E_2 reaction goes without the intermediacy of unstable molecules. When a typical secondary alkyl halide undergoes this reac-

tion, there are two different olefins that can be produced by the elimination of the two (nonequivalent) β-hydrogens. There is, of course, a greater number of different olefins produced when stereoisomers are considered and when a tertiary halide is used. Much of our present information on these processes has been based on studies of the distribution of the various possible olefins and also the distribution of the olefins and the substitution products.

One of the first results obtained long before the kinetically distinguishable paths had been identified pertained to the direction of the elimination. Saytzeff, in 1875, showed that the product of elimination from an alkyl halide was the most highly substituted olefins (4). In the apparently related elimination from quaternary ammonium hydroxides, Hofmann devised the rule now named after him, which predicts the loss of the hydrogen from the least highly substituted position (5). These rules amount to a prediction of the relative rates of elimination in the various possible directions. It was realized much later that the reactions did not follow a single path, but that the rules did correctly predict the predominant olefin. Thus the thermal decomposition of *sec*-butyldimethylsulfonium ethoxide gave 57.7% total olefins, of which 74% was 1-butene, and 26% was a mixture of stereoisometric 2-butenes (6). The analysis for total olefins was done by conventional bromometric titration; the composition of the olefins mixture was estimated from the density of a purified sample of, the dibromide and from the rate of reaction of the dibromide with iodide ion. A quantitative distillation confirmed the results, but neither method distinguished well between *cis*- and *trans*-2-butenes, although it was suggested that the amount of the former was small. The substitution product was not identified; presumably, it was mostly methylethyl ether. In this study, the total rate of base consumption was also measured, so it was possible to calculate a rate constant for the formation of each product.

Extensions of this general method have yielded much of our present knowledge concerning the elimination reaction, and a variety of constantly improving analytical techniques have been employed. These studies have not only been concerned with the range of applicability and sources of the Hofmann and the Saytzeff rules, but have also dealt with problems of solvent effects (7), temperature (8), stereochemistry (9), and steric effects (10). The last studies, by H. C. Brown and co-workers, at first used the refractive index as an olefin analysis and, in other cases, the more general and refined method of infrared spectrometry. The above work pertained both to the one-step E_2 reaction and to the E_1 reaction involving the intermediate carbonium ion.

The carbonium ion intermediate in the E_1 reaction is presumably the same as that in the S_N1 reaction. A most convincing demonstration of the

accuracy of this presumption by product study has been presented by Ingold and co-workers (11). If the solvolysis products of the compound RX are completely determined in the second step of the reaction, which is the reaction of the R^+ ion, the nature of X should have no effect on the relative rates of reaction of R^+ with the solvent in the various possible ways. Thus the fraction of elimination should be independent of X. The system covered most thoroughly was the solvolysis of tertiary halides in aqueous ethanol, and the olefin yield was determined. As an example, the solvolyses of tertiary amyl chloride, bromide, and iodide in 80% ethanol yielded 33.3, 26.2, and 26.0% olefins, respectively. Considering a factor of over one hundred in reaction rates, this variation in product composition is very small; it was therefore concluded that the carbonium ion was the same intermediate in all the reactions. The small residual variation in product composition showed that the leaving group was not entirely absent in the transition state of the product-determining steps. Earlier, a "shielding effect" by the leaving group had been used to account for the incomplete racemization in the S_N1 process, so that no new concepts had to be introduced to accommodate the minor but detectable role of the leaving group in the E_1 reaction. It is also possible that the halide ions play a small role in removing the β-hydrogen after they have become completely separated from the carbonium ion. In this work, advantage was taken of the obvious principle that an intermediate must show the same reactivity in any reaction no matter what the source of this intermediate. This principle and the product-analysis method of applying it are powerful tools for the study of reactions for which intermediates are proposed. When applicable, it is the most convincing argument to demonstrate the identity of the intermediates in two different reactions. If it can be shown that the reactivities of two intermediates are very nearly the same in two different reactions, one can conclude with rather less rigor that the two intermediates are very nearly identical.

Olefin-forming eliminations also occur in certain gas-phase pyrolyses, and some of those which are not of a free-radical character will be discussed here, even though they are probably not ionic in character either. The present discussion illustrates both the extent of mechanistic information that can be obtained from observations of products and the importance of the choice of analytical method.

The pyrolysis of esters of carboxylic acids, like that of xanthates, is believed to pass through a cyclic transition state in which the β-hydrogen becomes partially bonded to the acid fragment, as the bond to carbon is being broken. This conclusion was derived from stereochemical considerations and appears very solidly founded. It was reported, (12) that the pyrolysis of methylisopropylcarbinyl acetate yielded pure 3-methyl-1-

butene, the Hofmann rule product, rather than the more stable 2-methyl-2-butene. The purity of the product was believed to have been well demonstrated by fractional distillation, refractive index, and even infrared spectra. This specificity, which was extraordinary in view of the high temperature of the pyrolysis, led to a description of the transition state in which the electron availability at the C-H bond was the controlling factor (13). This was contrasted to the unimolecular pyrolysis of alkyl bromides, in which the electronic environment of the C-Br bond was the more important. Alternately, it was suggested that the transition state had very little contribution from olefin-like structures (14). In a different system, Depuy and Leary (15) showed that, in a system devoid of complicating steric effects, the more stable olefin was produced. They pyrolyzed 1-phenyl-3-*p*-anisyl-2-propyl acetate; hydrogen bromide was then added to the resulting olefins, and a measurement of the solvolysis rate allowed a straightforward analysis, since the compound with the bromine next to the *p*-anisyl group reacted far more rapidly than its isomer. The preponderance of the olefin conjugated to the *p*-anisyl group cast suspicion on the general applicability of the Hofmann rule to these reactions, and several reinvestigations of the product distribution in aliphatic esters appeared. By using the very powerful analytical tool of gas chromatography, it was shown that the original results were in error; in fact, the olefins are found in amounts approximating those predicted on a statistical basis alone, so that it is not necessary to look for any explanation involving large activation energy differences (16,17). It is now seen that the factors in ester pyrolysis are both the olefin stability and steric or statistical effects. The same factors have been shown to apply to the pyrolysis of xanthate esters (18).

It now appears that the application of gas-phase chromatography will become increasingly more important in the study of the elimination reaction, since the analysis of isomeric olefins was previously the limiting factor in restricting the application of product analysis to this reaction. We shall see that it has now been applied fruitfully to a variety of reactions yielding volatile products.

2. Aromatic Substitution

One of the earliest considerations of organic reaction mechanisms was in the field of aromatic substitution. It was realized at an early date that orientation rules existed (19) and that the same rules applied to nitration, sulfonation, acylation, and halogenation. The similarity of the orientations was recognized as indicating a similarity of the mechanisms, and this idea has more recently been extended to suggest that a reaction which does not follow the ordinary orientation rules has an entirely different mecha-

nism. Thus the Gomberg arylation of nitrobenzene gives substantial yields of the corresponding *p*-arylnitrobenzene, and this has been taken as evidence that there are intermediate free radicals which attack the aromatic system (20). Similarly, the amination of quinoline with sodium amide gives a product with substitution in the heterocyclic ring, in contrast to the position of substitution by the conventional reagents. It has been concluded that this reaction therefore involves nucleophilic attack, rather than the more common electrophilic attack (21).

The clear statement that the orientation rules were a consequence of different rates of attack at the different positions in the same aromatic molecule was due to Holleman. He also established quantitatively the yields of *ortho*-, *meta*-, and *para*-disubstituted benzenes from the nitration, halogenation, and other attacks on many monosubstituted benzenes (22). Holleman also studied the temperature effect on the isomer distribution and provided the first reliable data which could be used to calculate the activation parameter differences. The methods for the analysis of the mixtures of isomers that Holleman and co-workers used included the measurement of physical properties, such as the melting point, of the mixtures. These methods, although sensitive, are subject to gross errors from contamination with unexpected foreign substances; they will not be described here since many newer and more reliable methods are now available. One can not help but admire the perseverance and skill of these investigators, which enabled them to use these difficult methods and obtain results that are still quantitatively useful.

An example of the newer techniques is found in the study of the mercuration of toluene (23). The analysis of the mixture of mercurated toluenes was accomplished by the quantitative conversion of the mercurials to the corresponding bromo compounds with radioactive bromine. Then equal-weight samples of each of the isomeric nonradioactive bromotoluenes were added to equal separate aliquots of the mixture, and the concentrated bromotoluene in each was oxidized (in less than quantitative yield) to the corresponding bromobenzoic acid, which could be purified to constant activity by recrystallization. The ratios of the specific activities of the isomeric acids were then the ratios of the yields of the corresponding mercurated toluenes. Since the counting rates of neither the bromine nor the undiluted bromotoluenes were reported, the absolute yields were not determined as they would have been in a more conventional isotopic dilution analysis. The accuracy of the relative yields by this method was believed to be better than 2%. The results confirmed the authors' suggestion that the cationic mercuric ion in the presence of perchlorate ion was more susceptible to orientational effects than the neutral and covalent mercuric acetate.

Another example of isotopic dilution analysis applied to aromatic substitution was the determination of the isomer distribution in the nitration of the halobenzenes (24). This study, which was designed to find deviations in the effect of substituents on the relative rates of nitration from those predicted by the Hammett equation, also succeeded, and the previously overlooked small amount of *meta*-nitration was found. Radioactivity was introduced as chlorine, bromine, or iodine in the starting halobenzene. Since no suitable fluorine isotope exists, the substitution pattern of fluorobenzene was not studied.

Infrared analysis has also been applied to the problem of isomeric mixtures from aromatic substitution. The nitration of 2,5-dichloronitrobenzene was studied in an effort to understand the apparently anomalously large extent of nitration *ortho* to the nitro group (25). The authors did indeed find a large amount of *ortho*-nitration product, which they attributed to an electrostatic interaction between the entering nitronium ion and the negative end of the dipole of the nitro group, which finds itself in close proximity to the *ortho* position. Elsewhere, Hammond (26) points out that infrared methods are not always suitable for the analysis of mixtures and illustrates some of the problems involved.

Apparently, the first deliberate effort to use product distribution to obtain relative rates of substitution of two different aromatic substances by product analysis was that of Wibaut (27), who nitrated a mixture of large excesses of chlorobenzene and toluene and found that the product contained far more nitrotoluene than nitrochlorobenzene. He was thus able to show that the rate of nitration of toluene was much greater than that of chlorobenzene, but was unable to estimate the ratio of the rate constants with any precision, since the experiments gave rather variable results. He attributed the difficulty to the heterogeneity of the system.

The first quantitatively successful determination of relative rates of nitration by this competitive method was that of Ingold and Shaw (28), who worked in a homogeneous system containing acetic anhydride. They were able to establish the relative reactivities of benzene, fluorobenzene, chlorobenzene, and bromobenzene toward nitration. They estimated the *o*- and *p*-nitrohalobenzenes by determining the amount of base required to hydrolyze the compounds. The results of this and of subsequent work on other compounds by this competitive method have been summarized (29). In this same reference, Ingold has also given the relative rates at the different positions of various monosubstituted benzenes, as calculated from a combination of the competitive results and the isomer distributions. The particular applicability of the competitive method became clear when it was established that the direct rate measurements were confused by the fact that the rate-determining step in nitration often did not involve the

aromatic substance at all. The contribution of these relative reactivities and isomer distributions to the study of the mechanism can hardly be overestimated. The main details that were left unresolved by these studies centered about the nature of the attacking group; these have, of course, been resolved in the case of nitration and halogenation by direct rate measurements.

III. APPLICATION TO DIVALENT CARBON INTERMEDIATES

The intermediacy of divalent carbon compounds in organic reactions, although old in concept, has been demonstrated convincingly only recently, especially by the work of Hine (30). One of the most convincing parts of his evidence was that the products of the alkaline hydrolysis of chloroform are carbon monoxide and formate ion, but in the presence of thiophenoxide ion (which does not change the rate) the product is mostly phenyl thioorthoformate. This observation, which demonstrates a reactive intermediate, coupled with certain kinetic evidence, led to the conclusion that carbon dichloride is the reactive intermediate; the further conclusion can then be drawn that carbon dichloride reacts more rapidly with thiophenoxide than it does with hydroxide.

The unsubstituted methylene species, or carbene, was shown to be an intermediate of interest to organic chemists from experiments in which diazomethane is subjected to photolysis in the presence of organic substances. The studies of this intermediate have been limited essentially to measurements of the relative rates of its possible reactions by product analysis. Doering and co-workers have studied the reactions of the unsubstituted carbene (as they have named it) from diazomethane, with pentane, 2,3-dimethylbutane, and cyclohexene (31). They found very small differences among the rates of attack at the different bonds to hydrogen in these molecules. The relative rates were determined by analysis of the product mixtures by gas chromatography, coupled in one case with infrared analysis of two substances which were not resolved by the column used.

The highly indiscriminate behavior of carbene has been the subject of controversy, since it appears that the photolysis of ketene gives a carbene which is more discriminating than that from diazomethane (32). Since new bonds result from the reactions of carbene, its reactions are highly exothermic, and part of the discrepancy is accounted for by variations in the extent of rearrangement of vibrationally excited states of the initially formed product before it is collisionally deactivated. The variation of product composition with pressure of inert gases led Frey and Kistiakowsky (33) to conclude that the methylene from ketene photolysis is itself in an

excited state, and shows more selectivity after collision deactivation. They also suggested, from spectroscopic evidence, that the carbene from diazomethane may have even more excess energy; if this is so, it would explain the very low selectivity observed by Doering and co-workers.

The excess energy problem may be largely avoided by the use of less violent syntheses. The preparation of carbenes by the action of bases on haloforms by an alpha-elimination reaction appears suitable. In fact, dichlorocarbene does appear to be more selective than the unsubstituted carbene, presumably both because the substitution stabilizes the molecule and because it is produced in temperature equilibrium with its surroundings. Dichlorocarbene will react with olefins to produce cyclopropane derivatives but does not attack carbon-hydrogen bonds (34). The relative rates of reaction of dibromocarbene with different olefins have been determined by mixing two olefins with bromoform and potassium *tert*-butoxide and estimating the relative yields of the corresponding dibromocyclopropanes by fractional distillation (35). The olefin reactivities paralleled the relative reactivities of the same olefins toward bromine and peracids. Vapor-phase chromatography was used for the analysis in a similar study on the reactivity of dichlorocarbene with olefins (36). Skell and Garner concluded from these reactivities and from their earlier demonstration that the reaction with 2-butene is a stereospecific *cis* addition (37), and that the reaction is essentially an electrophilic attack analogous to bromination or epoxidation. It was also suggested that these results implied an electron-paired structure for the carbene, a point of some controversy (38).

The chemistry of these interesting intermediates has therefore been attacked with a fair degree of success, resulting in the elucidation of several features of the reaction mechanism. The evidence cited has been based almost exclusively on the analysis of the product mixtures, since the reactions of the carbenes themselves are much too fast to study by normal kinetic methods.

IV. APPLICATION TO FREE-RADICAL INTERMEDIATES

1. Applicability

Free-radical reactions, especially chain reactions, often lend themselves to study by product analysis even better than ionic and molecular reactions. A chain reaction can be broken down into the three phases: (1) initiation, (2) propagation, and (3) termination. The mechanism of the process can only be described sketchily until something is known about all three

phases. The problem of initiation is most often simplified through the use of a known convenient source of free radicals like 2,2′-azobis(2-methylpropionitrile) (ABN), acetyl peroxide, or photolysis. This avoids the complication of initiation by adventitious impurities. Analysis for initiator fragments in the products has often been useful in determining the efficiency of the initiator, and in confirming its identity. When the kinetic chain is long, the major portion of the products comes from the propagation step, the nature of which can often be elucidated merely by identifying the products. In vinyl polymerization much has been learned about structure and reactivity relationships of the intermediate radicals with the monomer by determining the proportions of two competing monomers in the product. Chain transfer by solvents has been studied by finding solvent fragments in the products. The termination reaction products are present in very small quantities, when the kinetic chain is long, and are found only when sensitive detection methods are available or when the chain length is made short to increase the proportion of termination-to-propagation products.

The specific examples chosen for the more detailed discussion of the application of product determination to mechanism studied are not intended to be comprehensive, but are representative examples of a few of the applications. Photochemical reactions are purposely omitted here because of the thorough coverage in another volume of this series (39). Comprehensive discussions of general aspects of free-radical reactions may be found in the general references listed at the end of this chapter.

2. Reaction of Hydrocarbons with Oxygen

The reaction of organic substances with oxygen has been the subject of much interest and very much confusion. Information is gradually accumulating from controlled reactions so that now many of these reactions are no longer a mystery. The structure of the hydroperoxide isolated from the reaction between cyclohexene and oxygen was correctly identified as 3-cyclohexenyl hydroperoxide by Criegee in 1935 (40). Many similar hydroperoxides were soon recognized, and a radical chain process leading to their formation was demonstrated. The rates of oxidation are independent of the oxygen pressure over the range 200–700 mm., indicating that oxygen occurs only in a very rapid step, that all carbon radicals are trapped by oxygen, and that only peroxy radicals are involved in the termination reaction. The use of azobisisobutyronitrile ABN as the initiator, together with the observed hydroperoxide formation and kinetics, lead (41) reasonably to the following sequence where R· represents both the initiating cyanoisopropyl radical and the hydrocarbon radical:

$$\begin{aligned} &\text{ABN} \rightarrow (CH_3)_2CCN \quad (R\cdot) \\ &R\cdot + O_2 \rightarrow ROO\cdot \\ &ROO\cdot + RH \rightarrow ROOH + R\cdot \\ &2ROO\cdot \rightarrow \text{nonradical products} \end{aligned}$$

Under conditions of short chain length, Russell was able to identify one of the products from the oxidation of ethylbenzene as acetophenone. Identification was made by infrared spectroscopy. Assuming that this is a termination product, the suggested termination mechanism is then:

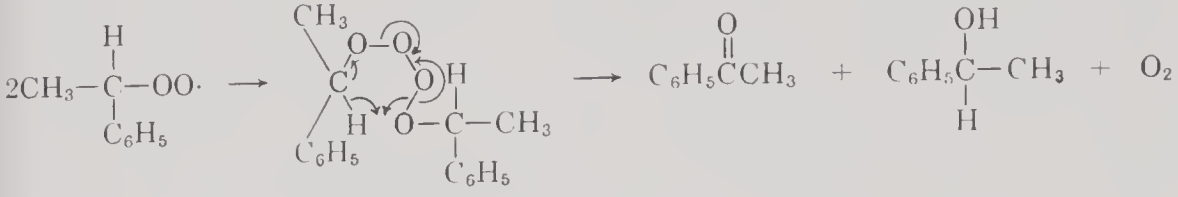

This mechanism is further supported by deuterium-isotope effect measurements and quantitative considerations based on kinetic data. Careful consideration was necessary to eliminate the possibility that the acetophenone came from the decomposition of the hydroperoxide, especially in view of the fact that the 1-phenylethanol, postulated as the other product of the above reaction, was not detected (42). Further confirmation of the termination was made by studying the termination step alone. Isobutyryl peroxide was decomposed in the presence of oxygen to produce isopropylperoxy radicals (43). Since this is not a chain reaction, the final products would then be the result of the same reaction as those of the termination step in the autoxidation of propane. A combination of distillation, infrared, and vapor-phase chromatography confirmed that the products contained isopropyl alcohol and acetone, perhaps by the mechanism shown below.

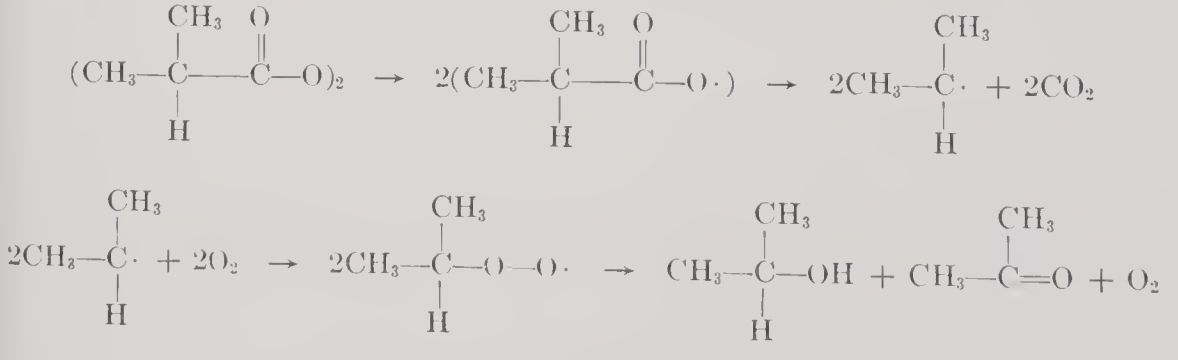

Another type of reaction of oxygen with carbon radicals has been discussed by Mayo, Miller, and Russell (44–47) in a recent series of papers. Compounds containing a terminal olefin group were found to give products other than hydroperoxides when subjected to reaction with oxygen in the presence of free-radical initiators. In several cases, good yields of poly-

peroxides insoluble in methanol could be isolated. For these cases, the propagation step can reasonably be written as:

$$R_2C{=}CH_2 + R'O_2\cdot \rightarrow R'O_2CH_2CR_2\cdot$$
$$R'O_2CH_2CR_2\cdot + O_2 \rightarrow R'O_2CH_2CR_2O_2\cdot \ (=R'O_2\cdot)$$

The reaction is far from being this simple, however. For example, styrene forms, in addition to considerable quantities of benzaldehyde, formaldehyde and styrene oxide. The yields are sensitive to oxygen pressure. Maximum yields of these other products were obtained at low oxygen pressures. This one observation alone leads to the suggestion that the radicals responsible for the low-molecular-weight products were those trapped by oxygen and were therefore not $R'O_2\cdot$. The depolymerization reaction shown below was used to explain the epoxide formation.

$$R_2CCH_2O_2(CR_2CH_2O_2)_nR' \rightarrow R_2C\!\!-\!\!\!\diagdown\!\!\diagup\!\!-CH_2 + \cdot O(CR_2CH_2O_2)_nR'$$
$$\qquad\qquad\qquad\qquad\qquad\qquad\qquad\qquad\qquad\qquad\quad O$$

The presence of alkoxy radicals formed by the above and other reactions is the source of the difference between this and ordinary autoxidations, which is necessary to explain the extra products. If the alkoxy radical adds to a monomer, the result will be an ether linkage that could block the depolymerization reaction. Also, the alkoxy radical could react by a new one-step depolymerization process to produce some of the observed products:

$$R'OOCH_2\overset{\displaystyle R}{\underset{\displaystyle R}{\overset{|}{\underset{|}{C}}}}\!\!-O\cdot \rightarrow R'O\cdot + CH_2O + R_2C{=}O$$

The identical products would be formed by the following two-step sequence, if the second reaction were very fast:

$$R'OOCH_2\overset{\displaystyle R}{\underset{\displaystyle R}{\overset{|}{\underset{|}{C}}}}\!\!-O\cdot \rightarrow R'OOCH_2\cdot + R_2C{=}O$$

$$R'OOCH_2\cdot \rightarrow R'O\cdot + CH_2O$$

Benzaldehyde is formed even at high oxygen pressures. The following reaction of the $R'O_2\cdot$ radical was proposed to account for this observation:

$$R'O_2\cdot + H_2C{=}\overset{\displaystyle R}{\underset{\displaystyle R}{\overset{|}{\underset{|}{C}}}} \rightarrow R'\cdot + CH_2O + R_2C{=}O$$

The effect of structure on the products is also very important. As an example, it was found that α-methylstyrene, as well as other disubstituted terminal olefins, yield a greater proportion of cleavage products at all

oxygen pressures. This is understandable if we consider that these monomers form more stable radicals when they are attacked. The stable radicals then have more time to depolymerize before reacting with oxygen or other monomers.

3. The Decomposition of Acyl and Aroyl Peroxides

Based on product study alone, Szwarc and Smid (48) were able to compare and contrast the decomposition of aliphatic acyl peroxides and benzoyl peroxide. Propionyl peroxide, decomposed in acetic acid, does not lead to the formation of methane. If attack on the acetic acid acidic hydrogen occurred, the following sequence should result:

$$\begin{aligned} CH_3CH_2\cdot + CH_3COOH &\rightarrow CH_3COO\cdot + C_2H_6 \\ CH_3COO\cdot &\rightarrow CH_3\cdot + CO_2 \quad \text{etc.} \end{aligned}$$

It had already been established that methyl radicals from acetyl peroxide would form methane under the same condition. The high CO_2 yields, as well as thermochemical arguments, led to the suggestion that the dissociation of RCOO· radicals to R· + CO_2 is a rapid exothermic reaction. The yields were determined by a combination of manometric and gas-absorption techniques.

In contrast to the above, the decomposition of benzoyl peroxide in acetic or propionic acid does yield methane or ethane, respectively, showing that some of the radicals attack the OH bond. Yields of methane and ethane were on the order of 6%. Even more striking are the results obtained by decomposing benzoyl peroxide in trifluoroacetic acid with isooctane as a hydrogen donor for the CF_3· radicals. In contrast to the decomposition in pure trifluoroacetic acid, fluoroform is formed in amounts up to 70% of the products. Under the same conditions, propionyl peroxide decomposition did not lead to the formation of any fluoroform. No fluoroform was formed from trifluoroacetic acid and benzoyl peroxide in the absence of isooctane, presumably because the CF_3· radicals could not abstract the acidic hydrogen from trifluoroacetic acid. That the CF_3· radical was being formed was established by the use of scavengers, such as benzoquinone or iodine, to lower the fluoroform yield and, in the latter case, produce CF_3I.

The different behavior of benzoyloxy and propionyloxy radicals remains to be explained. One obvious explanation is that there are different types of radicals reacting. The benzoyloxy radical is known to enter into several reactions before decarboxylation (49), whereas acyloxy radicals have not been known to react as such but always given products from the hydrocarbon radicals (except in cases of induced decomposition). Szwarc (50) has concluded from thermodynamic considerations that the decarboxylation is essentially instantaneous. The specific ability of an oxygen

radical to remove the acidic hydrogen from carboxylic acids is probably a result of a hydrogen-bond intermediate. The stronger trifluoroacetic acid forms a stronger hydrogen bond and increases the importance of the hydrogen-bonded intermediate.

A noted example of the use of product analysis to study a reaction is found in the work of Pausacker on the arylation by aromatic peroxides and the reactions of aroyl peroxides. One is especially impressed with the careful and near-quantitative separation of the products by conventional chemical means.

The arylation of *p*-dichlorobenzene with benzoyl peroxide, iodosobenzene dibenzoate, lead tetrabenzoate, and that of diphenyl with benzoyl peroxide are chosen as examples for discussion here (51). It had been shown earlier that variable yields of products other than phenylated compounds may be formed from aromatic compounds and either benzoyl peroxide or iodosobenzene dibenzoate. *p*-Dichlorobenzene was chosen, as it can give only a single arylated derivative.

Carbon dioxide from the reaction was trapped, and the mixture was separated by alkali treatment into a benzoic acid fraction (acid I), a fraction saponifiable to benzoic acid (acid II), and a neutral fraction. The neutral fraction contained 2,5-dichlorodiphenyl and higher boiling materials in all cases.

The sum of the yields of benzoic acid (I and II) and carbon dioxide was very nearly two moles per mole of benzoyl peroxide, showing that there was very little loss in the separation. The yield of 2,5-dichlorodiphenyl was usually equal to or less than the yield of acid I. On this basis, they proposed the following mechanism, reactions (1) and (2):

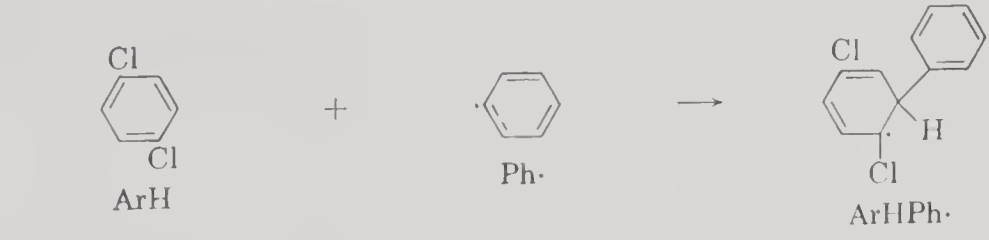

(1)

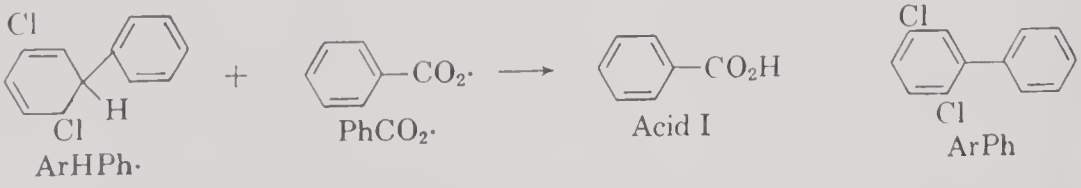

(2)

At more elevated temperatures, the yield of acid I dropped below that of the diphenyl ArPh, so that an alternate mechanism must exist for the loss of the hydrogen atom from the intermediate ArHPh·. They propose that the original peroxide is the hydrogen acceptor and that the eventual product is benzoic anhydride, which is then found as acid II.

The remaining products can be accounted for on the basis of some further reactions. An alternate path for the radical ArHPh· is disproportionation by reaction (3).

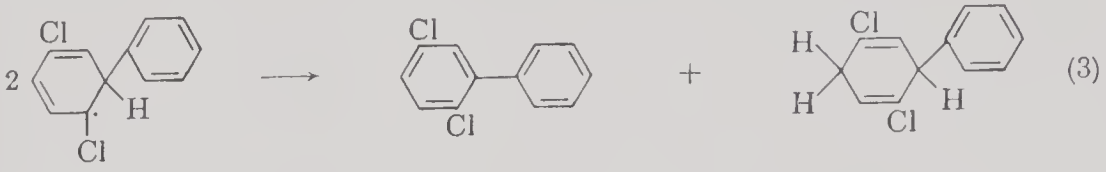

(3)

The diene product shown, or its *ortho*-quinonoid isomers, could be expected to phenylate more readily than the *para*-dichlorobenzene, and the resulting new free radical could dimerize or disproportionate itself and ultimately yield even more highly phenylated products.

This proposed reaction course is supported by the observation that the yield of high-boiling material increases as the yield of acid I decreased with increasing temperature, showing that the high-boiling material and acid I were alternate fates of a single intermediate. The fact that the quantity and elemental composition of the high-boiling material was entirely in keeping with the proposed mechanism is not a strong confirmation of the mechanism, since it merely represents all otherwise unaccounted residues. This observation is, however, a tribute to the quantitative nature of the product isolations and demonstrates convincingly that analysis by ordinary chemical separations and isolations need not be suspect.

The study of reaction mechanisms by these methods has been exploited by Pausacker and co-workers to an impressive extent. Other recent papers using these techniques, which in turn give reference to their earlier work, include a study of the reactions of benzoyl peroxide with some inorganic acid chlorides (52), a study of the arylation of pyridine and quinoline with benzoyl peroxide (53), the reaction of benzoyl peroxide with ferrocene (54), and many further studies on the reactions of the somewhat analogous iodosobenzene dibenzoate (55).

4. Effects of Solvents in the Photochlorination of Hydrocarbons

A very interesting investigation of the effects of solvent on free-radical photochlorination has been made by Russell (56). Product analysis and interpretation were simplified by using 2,3-dimethylbutane as the substrate, since only two monochloro derivatives could be formed. It was found that there could be readily separated and quantitatively determined by means of gas chromatography. The relative reactivities of the tertiary and the primary hydrogen atoms were calculated from the mole ratio of the two products after multiplying the yield of the tertiary compound by a statistical factor of six, since there are six times as many primary as tertiary

hydrogens. The chlorination in most aliphatic solvents produces approximately 60% of 1-chloro-2,3-dimethylbutane (*prim*-RCl) and 40% of 2-chloro-2,3-dimethylbutane (*tert*-RCl), giving, therefore, a relative reactivity of 4.0.

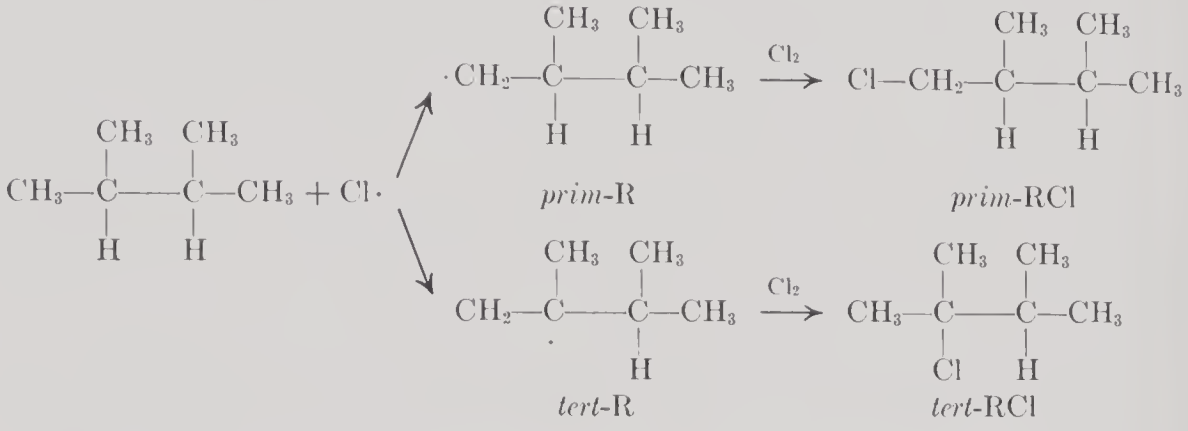

In 4.0*M* nitrobenzene, this ratio increases to 4.9, in chlorobenzene to 10.2, in benzene to 14.6, in *tert*-butylbenzene to 24, and in 1-chloronaphthalene to 33. It is clear that the same reagents are not present in each solvent, and, since no strong interaction of the hydrocarbon with the aromatic solvents is to be expected, one is led to a complex of the chlorine atom with the solvent as a reasonable source of the variation in reactivity. A large number of other solvents was studied and it was found that the increasing specificity for the tertiary hydrogen was best correlated with the relative basicities of the aromatic solvents. A π-complex is therefore suggested, which lowers the reactivity and increases the selectivity of the chlorine radicals. A very striking exception to the usual inertness of the aliphatic solvents is found in carbon disulfide, which changes the reactivity ratio to about 25 under the same conditions as those used in obtaining the values given above, and to 225 at the 12*M* level at 25°C. The ratio decreases considerably with increasing temperature.

References

1. S. L. Friess, this volume, Chapter XXVII.
2. W. Saunders, this volume, Chapter XXVI.
3. C. M. Suter and A. M. Weston, in R. Adams, ed., *Organic Reactions*, Vol. III, Wiley, New York, 1945, p. 141.
4. A. Saytzeff, *Ann.*, **179**, 296 (1875).
5. A. W. Hofmann, *ibid.*, **78**, 253 (1851).
6. E. D. Hughes, C. K. Ingold, G. A. Maw, and L. I. Woolf, *J. Chem. Soc.*, 1948, 2077.
7. K. A. Cooper, M. L. Dhar, E. D. Hughes, C. K. Ingold, B. J. McNulty, and L. I. Woolf, *ibid.*, 1948, 2043.
8. K. A. Cooper, E. D. Hughes, C. K. Ingold, G. A. Maw, and B. J. McNulty, *ibid.*, 1948, 2049.

9. W. Hückel, W. Tappe, and G. Legutke, *Ann.*, **543**, 191 (1940).
10. H. C. Brown and I. Moritani, *J. Am. Chem. Soc.*, **77**, 3607, 3623 (1955); H. C. Brown and M. Nakagawa, *ibid.*, **77**, 3610, 3614 (1955); H. C. Brown and Y. Okamoto, *ibid.*, **77**, 3619 (1955).
11. C. K. Ingold, *Structure and Mechanism in Organic Chemistry*, Cornell University Press, Ithaca, 1953, p. 426.
12. W. J. Bailey and C. King, *J. Am. Chem. Soc.*, **77**, 75 (1955).
13. A. Maccoll, *J. Chem. Soc.*, **1958**, 3398.
14. E. S. Lewis and M. C. R. Symons, *Quart. Revs.*, **12**, 230 (1958).
15. C. H. Depuy and R. E. Leary, *J. Am. Chem. Soc.*, **79**, 3705 (1957).
16. D. H. Freemsdorf, C. H. Collins, G. S. Hammond, and C. H. Depuy, *ibid.*, **81**, 643 (1959)
17. W. J. Bailey and W. F. Hale, *ibid.*, **81**, 647 (1959).
18. R. A. Benkeser and J. J. Hazdra, *ibid.*, **81**, 228 (1959).
19. W. Körner, *Gazz. chim. ital.*, **4**, 305, 446 (1874); H. Hübner, *Ber.*, **9**, 873 (1875); E. Nölting, *ibid.*, **9**, 1797 (1876).
20. W. A. Waters, *Chemistry of Free Radicals*, Oxford University Press, London, 1946, p. 154.
21. M. T. Leffler, in R. Adams, ed., *Organic Reactions*, Vol. III, Wiley, New York, 1945, p. 91.
22. A. Holleman, *Die Direkte Einführung von Substituenten in den Benzolkern*, Veit, Leipzig, 1910; *Chem. Revs.*, **1**, 187 (1925).
23. W. J. Klapproth and F. H. Westheimer, *J. Am. Chem. Soc.*, **72**, 4461 (1950).
24. J. D. Roberts, J. K. Sanford, F. L. J. Sixma, H. Cerfontain, and R. Zagt, *ibid.*, **76**, 4525 (1954).
25. G. S. Hammond, F. J. Modic, and R. M. Hedges, *ibid.*, **75**, 1388 (1973).
26. J. S. Fritz and G. S. Hammond, *Quantitative Organic Analysis*, Wiley, New York, 1957.
27. J. P. Wibaut, *Rec. trav. chim.*, **34**, 241 (1921).
28. C. K. Ingold and F. R. Shaw, *J. Chem. Soc.*, **1927**, 2918.
29. C. K. Ingold, *Structure and Mechanism in Organic Chemistry*, Cornell University Press, Ithaca, 1953, p. 246.
30. J. Hine, *J. Am. Chem. Soc.*, **72**, 2438 (1950).
31. W. v. E. Doering, R. G. Buttery, R. G. Laughlin, and N. Chaudhuri, *ibid.*, **78**, 3224 (1956).
32. H. M. Frey, *ibid.*, **79**, 1259 (1957); J. H. Knox and A. F. Trotman-Dickenson, *Chem. & Ind.*, **1957**, 731, 1039.
33. H. M. Frey and G. B. Kistiakowsky, *J. Am. Chem. Soc.*, **79**, 6376 (1957).
34. W. v. E. Doering and A. K. Hoffmon, *ibid.*, **76**, 6162 (1954).
35. P. S. Skell and A. Y. Garner, *ibid.*, **78**, 5430 (1956).
36. W. v. E. Doering and W. A. Henderson, *ibid.*, **80**, 5274 (1958).
37. P. S. Skell and A. Y. Garner, *ibid.*, **78**, 3409 (1956).
38. P. S. Skell and R. C. Woodworth, *ibid.*, **78**, 4496 (1956).
39. A. Weissberger, ed., *Technique of Organic Chemistry*, 2nd ed., Vol. II, "Catalytic, Photochemical, Electrolytic Reactions," Interscience, New York, 1956.
40. R. Criegee, *Ann.*, **522**, 75 (1935).
41. L. Bateman, *Quart. Revs.*, **8**, 147 (1954).
42. G. A. Russell, *J. Am. Chem. Soc.*, **79**, 3871 (1957).
43. C. E. Boozer, C. B. Love, Jr., and J. M. Motes, unpublished work.
44. F. R. Mayo, *J. Am. Chem. Soc.*, **80**, 2465 (1958).
45. F. R. Mayo and A. A. Miller, *ibid.*, **80**, 2380 (1958).

46. F. R. Mayo, *ibid.*, **80**, 2497 (1958).
47. F. R. Mayo, A. A. Miller, and G. A. Russell, *ibid.*, **80**, 2500 (1958).
48. M. Szwarc and J. Smid, *J. Chem. Phys.*, **27**, 421 (1957).
49. G. S. Hammond and L. M. Soffer, *J. Am. Chem. Soc.*, **72**, 4711 (1950).
50. L. Jaffe, E. J. Prosen, and M. Szwarc, *J. Chem. Phys.*, **27**, 416 (1957).
51. M. Karelsky and K. Pausacker, *Australian J. Chem.*, **11**, 39 (1958).
52. M. Karelsky and K. H Pausacker, *ibid.*, **11**, 336 (1958).
53. K. H. Pausacker, *ibid.*, **11**, 200 (1958).
54. K. H. Pausacker, *ibid.*, **11**, 509 (1958).
55. L. K. Dyall and K. H. Pausacker, *ibid.*, **11**, 491 (1958).
56. G. A. Russell, *J. Am. Chem. Soc.*, **80**, 4987, 4997, 5002 (1958).

CHAPTER XXV

Evidence for the Formation of Intermediates in Organic Chemical Reactions

MYRON L. BENDER, *Northwestern University**

I. Introduction 1428
1. The Importance of Intermediates in Mechanistic Studies 1428
2. Classification of Intermediates 1429
3. Reactive Intermediates That Have Been Characterized 1432
4. Transition States and Intermediates 1435
II. Detection of Intermediates by Isolation 1439
III. Detection of Transient Intermediates by Physical Properties 1442
IV. Evidence for Intermediate Formation from Chemical Properties 1446
1. Kinetics 1446
A. Kinetic Form 1446
B. Entropies of Activation 1452
C. Solvent and Salt Effects 1452
D. Catalysis and Inhibition 1457
E. The Hammett Acidity Function 1460
2. The Effect of Structure on Reactivity as a Criterion of Intermediate Formation 1463
A. Structural Effects of the Organic Molecule 1463
B. Kinetic Isotope Effects 1472
C. The Element Effect 1475
3. Chemical Consequences Diagnostic of Intermediate Formation 1475
A. Products as a Criterion of Intermediate Formation 1475
(1) Statistical Product Distributions 1476
(2) Multiple Products 1477
(3) Constant Ratios of Products 1479
(4) The Rate-Product Criterion 1480
(5) Diagnostic or Trapping Reactions 1480
(6) Rearrangements 1484
B. Stereochemistry as a Criterion of Intermediate Formation 1486
C. Isotopic Investigations as Criteria of Intermediate Formation 1492
(1) Isotopic Tracer Methods 1492
(2) Isotopic Exchange Methods 1499
V. Conclusions 1503
References 1508
General References 1517

* This chapter was written while the author was on the faculty of the Illinois Institute of Technology.

I. INTRODUCTION

1. The Importance of Intermediates in Mechanistic Studies

As organic chemistry has come of age, a considerable effort has been expended in the elucidation of the mechanisms of organic chemical reactions. These investigations, in general, have started with the isolation of products of the reaction and then have proceeded to investigations of the kinetics of the process, the effect of structure on reactivity, and the effect of various external factors, such as temperature, catalysts and solvent, on reactivity. It became evident early that many processes whose stoichiometry seemed straightforward did not, in fact, proceed by a single stage but rather through a series of steps (1).

Such a stepwise mechanism implies the presence of a reactive intermediate. A mechanism of a reaction has been defined as a collision-by-collision account of a chemical reaction, and must therefore include a description of all intermediates as well as a description of all transition states in the process. The description of a mechanism must therefore include the knowledge of the factors affecting the free energies of the intermediates as well as the transition states.

It has not been possible to approach the problem of the description of the transition state of a reaction in any experimental fashion as yet. However, it has been possible to describe reactive intermediates in a number of chemical reactions, sometimes with direct experimental evidence and sometimes with indirect experimental evidence of varying degrees of pertinence. For this reason it is often desirable to describe the mechanism of a chemical reaction in terms of (*1*) the intermediates which occur and (*2*) the rate-determining steps of the process (*2*). In many instances it is possible to describe an important transition state in terms of the known properties of a reactive intermediate, because of the structural similarity of the two species.

An intermediate has been defined as a minimum in a plot of standard free energy vs. reaction coordinate. Not every chemical reaction involves an intermediate; however, the history of the study of reaction mechanisms has shown that many complex chemical reactions have been successfully analyzed in terms of a series of simple reactions, which necessarily involve the formation of a series of reactive intermediates between the reactants and the products of the reaction. For this reason a good deal of attention has been devoted to acquiring evidence for the formation of intermediates in chemical reactions. For example, it is possible to describe, with a good deal of assurance, the mechanism of the hydrogen ion-catalyzed esterification of acetic acid with ethanol, as shown in Figure 1.

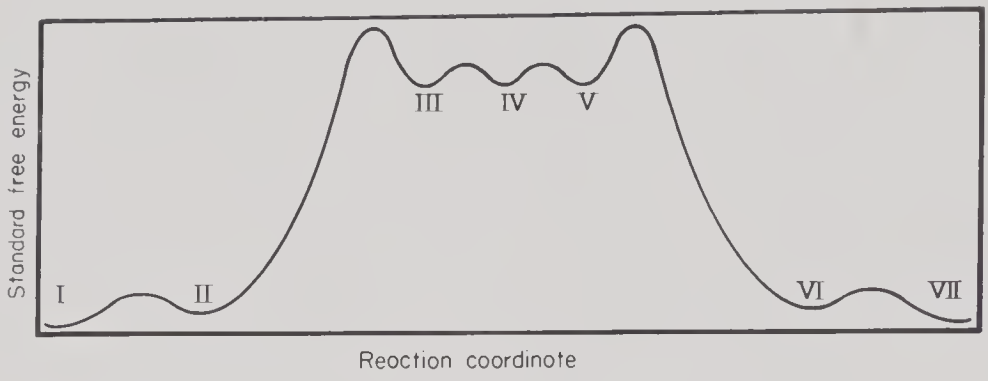

Fig. 1. Standard free energy vs. reaction coordinate for the acid-catalyzed esterification of acetic acid and ethyl alcohol.

The numbers in Figure 1 correspond to the various reactants, intermediates, and products (I–VII) in this relatively simple process. This stepwise behavior exemplifies the importance of intermediates in even relatively

$$\underset{(I)}{CH_3CO_2H} + C_2H_5OH_2^+ \rightleftarrows \underset{(II)}{CH_3CO_2H_2^+} + C_2H_5OH \rightleftarrows$$

$$\underset{(III)}{CH_3C(\overset{+}{\overset{|}{H}}OH)_2OC_2H_5} \rightleftarrows \underset{(IV)}{CH_3C(OH)_2OC_2H_5} \rightleftarrows$$

$$\underset{(V)}{CH_3C(OH)(OH_2^+)(OC_2H_5)} \rightleftarrows \underset{(VI)}{CH_3C(=OH^+)OC_2H_5} + H_2O \rightleftarrows \underset{(VII)}{CH_3CO_2C_2H_5} + H_3O^+$$

simple reactions, and, therefore, points to the importance of the consideration of intermediates in reaction processes.

In this discussion, an attempt will be made to maintain an operational approach to the postulation of intermediates and to assess the relative importance of various kinds of evidence for intermediate formation.

2. Classification of Intermediates

Intermediates may be classified from a kinetic viewpoint. The reaction sequence

$$A \underset{k_2}{\overset{k_1}{\rightleftarrows}} B \xrightarrow{k_3} C \qquad (1)$$

is the most common form encountered in organic chemistry. It is possible to treat the kinetics of this process by the steady-state approximation: $dB/dt = k_1A - k_2B - k_3B = 0$. It can then be shown that

$$dA/dt = dC/dt = [k_1k_3/(k_2 + k_3)]A = [k_1/((k_2/k_3) + 1)]A \qquad (2)$$

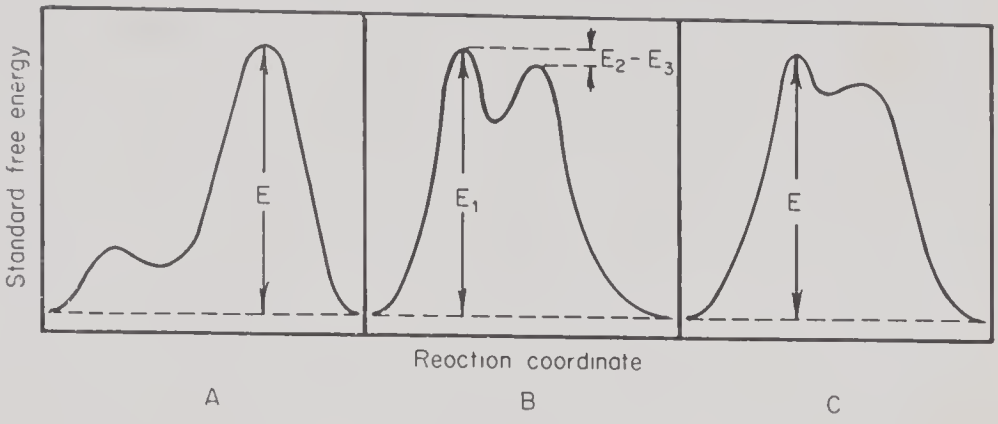

Fig. 2. Plot of standard free energy vs. reaction coordinate for: A, a reaction involving a pre-equilibrium; B, a reaction involving an unstable intermediate ($k_3 \cong k_2$); C, a reaction involving an unstable intermediate ($k_3 \gg k_2$). It is assumed that the ground states of reactant and product have identical standard free energies.

If k_3 and k_2 are of comparable magnitude, Equation (2) cannot be simplified; the over-all rate is affected by both the rate of bond-making (k_1) and by the partitioning of the intermediate (k_2/k_3). This intermediate has been classified as a van't Hoff intermediate (3). If k_2 is large compared to k_3, a pre-equilibrium occurs followed by a rate-determining step. This situation leads to $-d\mathrm{A}/dt = d\mathrm{C}/dt = k_3K\mathrm{A}$, where $K = k_1/k_2$. In this case the intermediate is classified as an Arrhenius intermediate. If, on the other hand, k_3 is much larger than k_2, a situation prevails in which k_1 is the rate constant of the slow step of the reaction, which is also completely rate-determining.

It is possible to construct standard free energy vs. reaction coordinate diagrams for these processes. A reaction involving an intermediate formed in a pre-equilibrium (an Arrhenius intermediate) would follow the plot of Figure 2A. Other reactions involving an intermediate are shown in Figures 2B and 2C (in the former k_2 and k_3 are of comparable magnitude, and in the latter $k_3 \gg k_2$).

In case A, the activation energy of the over-all reaction, the energy difference between the starting material and the transition state, can be identified in a straightforward manner with the sum of the energy of the preequilibrium and the activation energy of step 3. There are innumerable examples of case A involving, for example, a host of hydronium and hydroxide-catalyzed reactions.

Case B is exemplified by a large number of reactions including the unimolecular solvolysis of RX, the hydrolysis of carboxylic acid derivatives, and aromatic substitution reactions. In B, the activation energy of the first step is sometimes measured directly, as in reactions proceeding through carbonium-ion intermediates. In one reaction of this kind, it has been

possible to measure the difference in activation energies of the partitioning of the carbonium ion intermediate between two nucleophiles, water and azide ion. It was found that $\Delta E_{\text{azide}} - \Delta E_{\text{water}} = 4$ kcal./mole for the *p,p'*-dimethylbenzhydryl cation in 90% aqueous acetone (4).

On the other hand, one sometimes measures the activation energy of the over-all process in case B which has no precise physical meaning. An example of such a situation is in the basic hydrolysis of esters or amides. By means of an isotopic exchange technique to be described later, it is possible to determine E_1 and $(E_3 - E_2)$, defined in Figure 2B (5). In the alkaline hydrolysis of benzamide, it is calculated that $\Delta E_{\text{hydrolysis}} = 14.8$, $E_1 = 17.2$, and $(E_3 - E_2) = -3.2$ kcal./mole. Furthermore, it was shown that the over-all activation energy ($\Delta E_{\text{hydrolysis}}$) should not generally show a temperature independence, since the rate constant for the reaction (Eq. 2) is complex. However, in the benzamide hydrolysis and in the ethyl benzoate hydrolysis as well as in many other organic reactions involving intermediates, it is possible that temperature-independent behavior of the over-all activation energy will be observed if the over-all activation process is primarily determined by step 1; this implies that the effect of temperature on steps 2 and 3 is small and constant.

Case C is exemplified by the halogenation of acetone and the aldol condensation of acetaldehyde. The least amount of information on intermediate behavior is available for this extreme case, although the evidence for intermediate formation, as will be discussed later, is convincing.

The elegant formulation of Christiansen allows one to treat kinetically a series of consecutive reactions involving any number of unstable intermediates, and thus to extend the simple treatment given above to more complicated cases (6).

Another classification of reactive intermediates depends on the chemical structure of the species. Organic compounds containing both tetracovalent carbon and di- or trivalent carbon have been recognized as intermediates in chemical reactions. A number of organic substances of usually stable existence have been recognized as reactive intermediates in certain reactions. In such cases, it is quite often possible to gather direct evidence of their formation. This is not to say that such substances are to be equated with substances colloquially called "synthetic intermediates," which are not intermediates in the sense discussed here, but rather chemical compounds of particularly wide synthetic utility. A number of organic compounds of normal valence but not recognized as unstable compounds have been postulated as intermediates in chemical reactions. Their formation often cannot be directly observed, and, thus, reliance on indirect evidence is usually necessary for the postulation of their occurrence. In addition to intermediates of normal valency, a number of intermediates containing

other than normal valency have been postulated. Some examples of these are carbonium ions, carbanions, free radicals, and carbene intermediates, which have been especially popular with organic chemists. One is again forced to rely on indirect measurements in order to make a case for these intermediates.

3. Reactive Intermediates That Have Been Characterized

A number of species related to the unstable intermediates mentioned above have been prepared, and identified, sometimes under rather special conditions. Many chemists have utilized stable analogs of reactive intermediates as evidence from which they have extrapolated to the reactive species. Although this extrapolation may be open to question in certain instances, it is comforting to know that there are stable carbonium ions, carbanions, free radicals, and addition compounds. Examples of stable carbonium ions, carbanions, and free radicals are extensively discussed by Leffler (7). It should be pointed out that the free energy of a series of intermediates varies in a continuous fashion and that the extrapolation the investigator must make from the hypothetical reaction intermediates to the real intermediate of some stability is in the optimum case across a continuum.

Since the pioneer work of Gomberg (8), on the synthesis of the free radical triphenylmethyl, a large number of stable free radicals has been prepared. These radicals frequently exist in equilibrium with the corresponding dimeric covalent compounds. A good deal of work has been carried out to determine the equilibrium between radicals and covalent compounds by means of spectroscopy (9), molecular-weight determination (10), and more recently by paramagnetic susceptibility measurements (11) and paramagnetic resonance (electron spin resonance)(12). Of these methods, the last two have proved to be the most reliable and sensitive experimental methods for the determination of the free-radical nature of stable as well as transient substances (see later). A number of substances has been shown to exist entirely in the free-radical form even in the solid state, mainly through measurements of paramagnetic susceptibility and electron spin resonance (12). Some of these extremely stable radicals are pentaphenylcyclopentadienyl, tris(*p*-phenylphenyl)methyl, 1,1-diphenyl-2-picrylhydrazyl (VIII), α,γ-bisdiphenylene-β-phenylallyl, and a phenoxy radical isolated from the oxidation of 3,3′,5,5′-tetra-*tert*-butyl-4,4′-dihydroxydiphenylmethane (IX) (13).

The multitude of stable, solid free radicals is not reflected in a corresponding number of isolatable carbonium ions. Certain triphenylmethane dyes such as crystal violet, malachite green, pararosaniline, and others

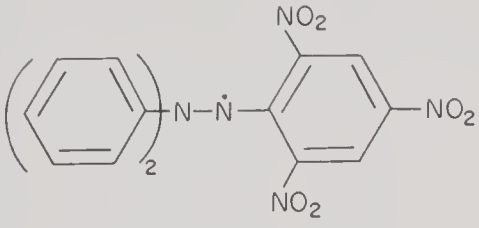

(VIII)

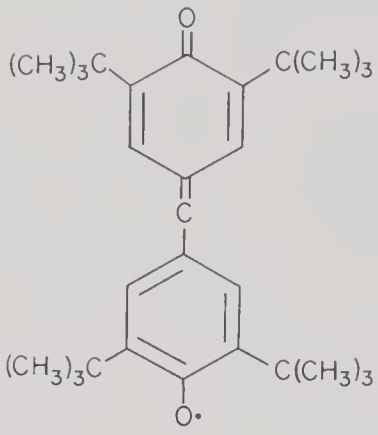

(IX)

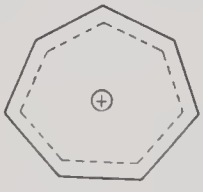

(X)

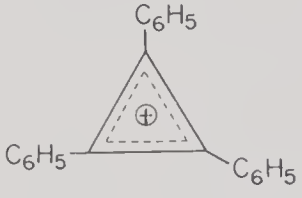

(XI)

can be considered highly stabilized carbonium ion salts, although the charge distribution of their resonance hybrids indicates that they are closer to ammonium salts than carbonium salts. Cycloheptatrienylium (tropylium) bromide (X) (14) and *S*-triphenylcyclopropenyl picrate (XI) (15) are two examples of isolable ionic compounds in which the cationic charge is associated only with carbon atoms. The cations in these two systems are especially stable because of the high degree of resonance stabilization possible. A number of cationic alkylbenzene tetrafluoroborate complexes of the general structure $ArH_2^+BF_4^-$, $ArHC_2H_5^+BF_4^-$, and $ArHCHO^+BF_4^-$ have been synthesized and isolated at low temperature in crystalline form. These carbonium ion salts have utilized the aromatics toluene, *m*-xylene, mesitylene (XII), and isodurene (16). Finally, the formation of a stable non-classical carbonium ion in 60% sulfuric acid has been reported (XIII) (16a).

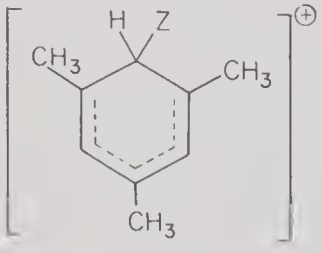

(XII)

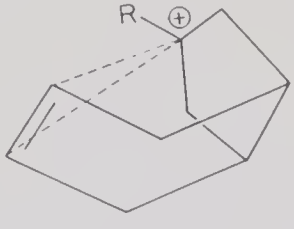

(XIII)

These are a number of examples of stable organometallic compounds that have a carbanionic character to a greater or lesser extent. Methyl sodium

and ethyl sodium are presumably ionic, whereas alkyl lithium compounds have properties associated with a covalent carbon-metal bond. Compounds such as triphenylmethyl sodium are strong electrolytes in liquid ammonia. A discussion of the ionic character of organometallic compounds is given by Leffler (17).

Carbonium ions and carbanions have been studied extensively in solvents that stabilize organic cations or anions. The ionization of triphenylmethyl chloride in liquid sulfur dioxide to triphenylmethyl carbonium ion and chloride ion via the corresponding ion pair has been extensively studied by conductivity (18) and spectrophotometric measurements (18). The formation of triarylcarbonium ions has further been studied in other solvents using spectrophotometric measurements of the equilibria (19). Conductometric measurements have also been made, of solutions of sodium triphenylmethyl in liquid ammonia and in pyridine, which indicate the presence of the ionic species, triphenylmethide ion (20). Evidence has been given recently for the anion of fluoradene (indeno[1,2,3-*jk*]fluorene), which has been shown to be of comparable basicity to the phenoxide ion (21).

The equilibria involving the ionization of organic compounds to produce carbanions and enolate ions have been discussed in great detail (22). The ionization constants for the protonation of organic compounds in sulfuric acid have been determined, usually spectroscopically, for ketones, carboxylic acids, and amides (23). Measurements of the solubility of hydrogen chloride in dilute solutions of aromatic compounds in *n*-heptane has led to a scale of the relative degree of protonation of aromatic hydrocarbons (24). Conductivity measurements of aromatic hydrocarbon solutions in anhydrous hydrogen fluoride has given equilibrium constants for the protonation of a large number of aromatic hydrocarbons in this solvent (25). Because of the enormous spread in the equilibrium constants in the latter system compared to the very small spread in the Henry's law constants in the former system, the protonated species in hydrogen fluoride are usually referred to as sigma complexes. In these complexes a covalent bond is formed between the proton and a specific carbon atom of the ring, whereas the protonated species in the former system are referred to as pi-complexes, in which the proton interacts with the pi-electron cloud of the ring (24). Knowledge of the prototropic equilibrium constants of organic compounds described above permits the calculation of the equilibrium concentration of possible intermediate species, both cationic and anionic, in various reactions.

Quantitative measurements have also been made on equilibria involving the direct formation of carbonium ions. These measurements have involved the ionization of triarylmethyl chlorides to the corresponding car-

bonium-ion pair in sulfur dioxide solution (26), the ionization of diarylmethyl carbinols to the carbonium ion in sulfuric acid solution (27), and the equilibrium between diarylolefins and diarylalkyl cations (27a).

In addition to these quantitative measurements, a number of qualitative observations indicates that cationic organic species exist under special circumstances. From cryoscopic measurements in 100% sulfuric acid, it is possible to determine the number of particles formed from an organic solute dissolved in this medium. The fate of a large number of organic molecules in sulfuric acid solution has been investigated in this fashion (28). In particular, it is possible to determine which oxy compounds exist as the protonated oxy compound in 100% sulfuric acid (a van't Hoff i factor of 2) and which exist as the corresponding carbonium ion (a van't Hoff i factor of 4 in general).

Prototropic equilibria leading to anionic or cationic intermediates can be detected by the broadening of the proton magnetic resonance peak caused by exchange of a proton of an organic compound with protons of the solvent. Such equilibria can further be followed by exchange between the proton of the organic compound and deuterium oxide solvent, determined experimentally by proton magnetic resonance or infrared spectroscopy. These techniques were used, for example, to demonstrate the ionization of the proton at carbon 2 of thiazolium salts, leading to a carbanion which has been postulated as the active intermediate in the enzymatic reactions of thiamine pyrophosphate (28a).

Another group of organic compounds which may function as reactive intermediates are addition compounds. A host of addition compounds of widely varying types can exist (29). Some examples of stable addition compounds, which are pertinent to a discussion of reactive intermediates, are the addition compounds of Lewis acids and various organic compounds (30,31), the addition compounds of nucleophiles to negatively substituted aromatic compounds (32,33), the addition compounds of alkyl-substituted aromatic compounds with BF_3 and HF or RF mentioned earlier (16), and the addition compounds of water, alcohols, or amines to the carbonyl group of aldehydes, ketones, esters, and amides (34).

4. Transition States and Intermediates

An intermediate can be defined as a minimum in a plot of standard free energy vs. reaction coordinate and a transition state a maximum in such a plot. The simplest reaction containing one intermediate would then necessarily contain two transition states. The terms transition state and intermediate have been used synonomously by some authors to indicate some hypothetical structure that occurs between reactant and product. The

definitions given above unambiguously distinguish the two terms. This does not preclude a close structural resemblance between reactive intermediates and transition states in many instances. It also does not preclude the possibility of a continuous change from a single transition state to an intermediate in a series of related reactions; that is, the relative stability of an intermediate, defined as the free-energy difference between the intermediate valley and the lowest transition state, may vary over a wide range.

The similarity between an intermediate and a transition state will generally be most marked when only a small molar free energy difference exists between the two, that is, when the intermediate is highly unstable. In these circumstances it is reasonable to extrapolate from intermediate to transition state or vice versa. This type of mental scaffolding has proved to be of great value when considering the effect of structure on reactivity, as will be discussed in more detail later. The above statement of similarity of intermediate and transition states is a restatement of a postulate enunciated by Hammond (35): "If two states, as for example, a transition state and an unstable intermediate, occur consecutively during a reaction process and have nearly the same energy content, their interconversion will involve only a small reorganization of the molecular structure." It should be kept in mind that this reorganization must encompass both steric and electronic changes that may occur to differing extents. An important consequence of this postulate, with regard to a discussion of intermediates, is that, in highly exothermic steps (where intermediates are usually not formed), it is expected that the transition states will closely resemble reactants. However, in endothermic steps leading to intermediates, the intermediates will provide the best models for the transition states (35). A corollary of this argument is that the reaction of a high energy intermediate to give products will pass through a transition state resembling the high energy intermediate. In such cases it is possible that the reaction governed, as it must be, by structural considerations in the high energy intermediate, may lead to a thermodynamically unstable product.

According to these ideas, it is therefore reasonable to expect, as has been borne out by experiment, that structural variations in free radical, carbonium ion or carbanion intermediates, which effect a decrease in the free energies of dissociation, will be reflected nearly quantitatively in increased rates of production of the intermediates (35). This relationship will hold in the general case only if the structure of the reactive intermediate is similar to the transition state. In the particular case of carbonium ion reactions, the enthalpies and entropies of formation of alkyl carbonium ions in solution have been calculated from the corresponding quantities for gaseous ions and the enthalpies and entropies of solution. These values

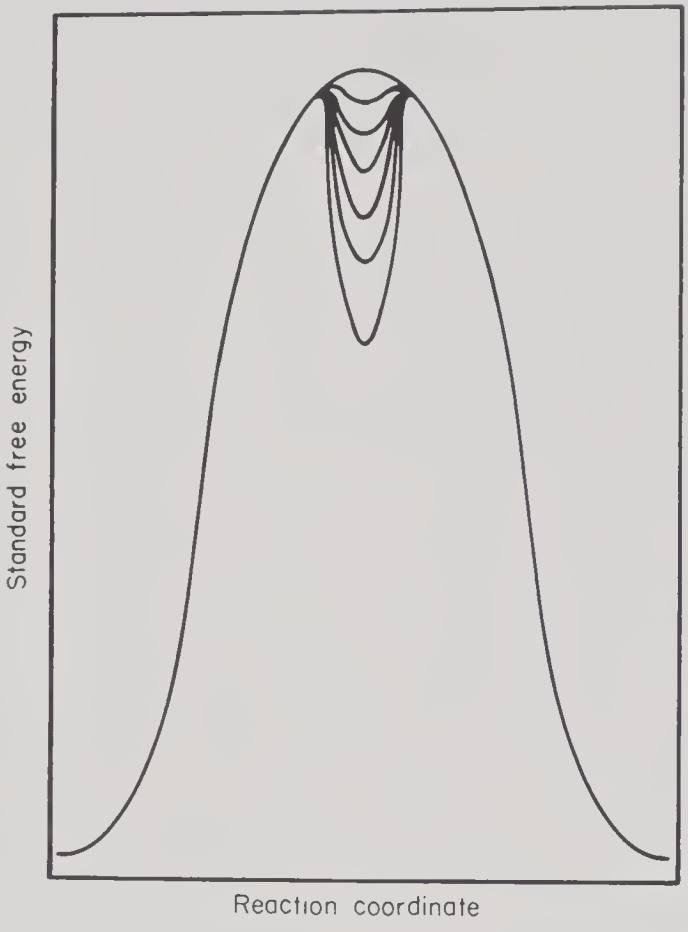

Fig. 3. A continuum of intermediates leading to a single transition state.

were then used to evaluate the activation parameters for the hydrolysis of alkyl halides, the hydration of isobutene and the dehydration of *tert*-butyl alcohol. The rates of reaction calculated in this way were found to be in fortuitously close agreement with published experimental data (36). Direct experimental tests of the relationship between the equilibrium formation of carbonium ions and the rates of reactions involving carbonium ion intermediates will be discussed later.

In recent years considerable attention has been devoted to the problem of "borderline mechanisms," which revolve about the point of a continuum between a reaction possessing only a single transition state (for example, the S_N2 reaction) and a reaction possessing a reactive intermediate (for example, the S_N1 reaction). The problem may be exemplified by the solvolysis of benzyl chloride. It has been postulated that, in this reaction, which exhibits the characteristics of both an S_N2 reaction and an S_N1 reaction, the mechanism might involve: (*1*) a bimolecular transition state, in which the transition state is a resonance hybrid with a contribution from a canonical structure in which a positive charge resides on carbon; (*2*) a continuous spectrum of such transition states, with variable contribution from the

structure containing positive carbon; or (*3*) the concurrence of the two extreme forms of the S_N1 and S_N2 mechanism (37). It is fairly generally agreed now that possibility (*3*) must not be operative (37,38), and possibility (*1*) or (*2*) must be operative, for certain systems at least (37,39). If one then extrapolates to include the extreme cases of the hybrid transition state, it appears that a continuum must exist between a reaction involving a transition state and one involving an intermediate (which, of course, must be preceded by a transition state), as was pointed out by Ingold long ago (40–43).

A continuum between a reaction involving only a single transition state and one involving an intermediate ultimately depends on a continuum in the relative stability of a series of intermediates. In principle, there appears to be no reason to question the occurrence of intermediates of any degree of stability, as illustrated in Figure 3. Only in circumstances where the half-life of an intermediate is a matter of minutes have intermediates been isolated directly from reaction mixtures without tampering with the chemistry of the system. One can calculate what minimum free energy difference must exist between intermediate and transition state for isolation of this sort. Approximate calculation of the half-life of a model bimolecular reaction at room temperature leads to the conclusion that an activation energy of at least 15 kcal./mole must exist for the compound to be isolable.*

It is conceivable that many intermediates will occur having activation energies and, therefore, half-lives less than those calculated above as a minimum for isolation. One must, therefore, be reconciled to the fact that many intermediates will never be isolated directly from a reaction mixture. Certainly the best evidence for intermediate formation is isolation from the reaction mixture. But, in addition to frontal assault, a wide range of indirect experimental approaches has been developed in order to provide evidence for intermediate formation. A number of these approaches are semidirect in that they attempt to measure, by physical means, some property of the postulated intermediate directly in the reaction mixture. Thus, a large number of spectroscopic investigations, including ultraviolet absorption, infrared absorption, paramagnetic resonance absorption, and electron spin resonance as well as paramagnetic susceptibility have indicated that intermediates are present in certain reactions.

In addition to measurements of intermediates via their physical properties, a large number of completely indirect methods have been devised to

* The rate equation was taken from Frost and Pearson (44) for a bimolecular reaction of diatomic molecules, $K_r \cong 10^{-10} \exp(-E_0/RT)$. The concentrations of the species were assumed to be $0.1M$. Under these conditions, a half-life of approximately 20 sec. is calculated.

furnish evidence for intermediate formation. As is the case with all mechanistic approaches, these methods must not be used singly but rather in a complementary fashion in order to build a case for an unstable intermediate. The first of these indirect methods is the use of analogy or extrapolation from stable species. Kinetic evidence has been utilized in a variety of ways to provide proof for intermediate formation. The effect of structure on reactivity has been utilized as a criterion of intermediate formation. Finally, chemical consequences that are diagnostic of intermediate formation have been utilized as a criterion of intermediate formation, including product formation, stereochemistry, rearrangements, and isotopic investigations. Each of these topics will be discussed at length.

II. DETECTION OF INTERMEDIATES BY ISOLATION

As was pointed out earlier, an intermediate must have a sufficiently long half-life if isolation is to be within the realm of possibility. In many cases, the half-life of an intermediate may be lengthened by suitable adjustment of its environment. The control necessary to inhibit the reaction of intermediates to give products may involve physical control such as temperature or the use of a viscous matrix, or it may involve chemical control such as manipulation of the pH or the solvent.

The technique of lowering the temperature of a reaction in order to observe or isolate an intermediate has been successfully used in a large number of instances. Probably the most elegant of these procedures have involved trapping free-radical intermediates in a solid matrix at very low temperatures, from liquid nitrogen down to liquid helium temperatures. Entrapment of radicals in a solid solution of a hydrocarbon or other glass effectively prevents recombination of radicals. When the matrix is allowed to melt, the radicals disappear by recombination or other reactions, and occasionally with explosive violence (45). The entrapment of radicals in a rigid matrix may be considered a form of isolation of these intermediate species. Although the radicals in this form are not in the pure state, they are of the same order of stability as a pure material and have been investigated by a number of physical means such as paramagnetic susceptibility studies (46), spectroscopic examination, both ultraviolet (47) and infrared (48), and electron spin resonance (49). Two approaches have been used to prepare stable solid solutions of radicals. One is photolysis of the substrate, which has been previously imbedded in the solid matrix (50). It is postulated that absorption of energy by the substrate molecule is accompanied by absorption of the excess energy by the immediate surroundings, leading to the diffusion of the radicals that have been formed into the softened matrix

in the immediate vicinity. The medium then prevents further diffusion and, therefore, reaction (51). The other method for producing radicals trapped in a solid matrix utilizes reaction in the gas phase (irradiation, electrical discharge, or thermal treatment) followed by immediate condensation of the reaction products on a surface cooled by liquid nitrogen. It has been possible to stabilize radicals in rigid media at ordinary temperature. For example, it has been possible to prepare solid solutions of triphenylmethyl in triphenylamine which are stable in air for many months (52). Furthermore, paramagnetic resonance absorption has indicated the presence of radicals in gelatinized partially polymerized samples of vinyl monomers, in coal, and in irradiated polymethyl methacrylate, all of which can be considered examples of entrapment of radicals in a solid matrix (53,54).

By the use of these methods, it has been possible to stabilize and detect such radicals as diphenylnitrogen (50), iodine atom (51), the imine radical (46,55), dimethylamino radical (45), hydroperoxy radical (49), ethanol radicals (which are formed from the reaction of HO_2 radicals and ethanol solvent in the solid phase) (47), and methyl radical (48).

The stabilization of unstable species in rigid media offers a fruitful approach for the detection of intermediates other than free radicals. This technique has been utilized for the detection of free radicals almost exclusively because of the experimental ease with which radicals are formed and stabilized in a solid matrix. But it is certainly conceivable that methods for the production of ions could be developed in conjunction with stabilization in solid solution. Triphenylnitrogen cation has been obtained in solid solution by photolysis of triphenylamine (50). This photolytic oxidation process could conceivably be extended to the production of other unstable ionic species in rigid medium.

The reaction of oxygen with organometallic compounds clearly points out the utility of lower temperature in the isolation of an intermediate in an organic reaction (56). It is well known that the rapid reaction of aliphatic Grignard reagents with molecular oxygen yields alcohols. However, when aliphatic Grignard reagents are added slowly to oxygen-saturated solvents at about $-70°$, organic hydroperoxides can be isolated in good yield. It was shown further that the magnesium salt of *tert*-butyl hydroperoxide reacts with an equivalent of *tert*-butylmagnesium chloride to give a 70% yield of *tert*-butyl alcohol after hydrolysis. This is a complete confirmation of the intermediacy of the hydroperoxide in the oxidation of a Grignard reagent.

By limiting one reagent in a reaction, it is sometimes possible to isolate an intermediate. For example, in the Darzen's condensation of a ketone and a halide, it was possible to convert only a small fraction of the starting

materials into condensation products and to isolate the intermediate halohydrin by restricting the amount of base present (57). This reaction is a specific example of a general method for isolation of intermediates based on the hypothesis that the further reaction of the intermediate occurs by a bimolecular process. Restriction of the reagent that reacts with the intermediate should decrease the rate of that reaction and make it possible to isolate the intermediate.

Inhibition of further reaction has been a highly fruitful method for the isolation of reactive intermediates. In a general sense, inhibition of further reaction must occur any time a reactive intermediate is isolated. In certain instances no positive steps are taken to prevent further reaction of the intermediate. In other cases, the temperature is lowered or reagents are limited, as stated above. Finally, chemical reagents may be added to the reaction mixture to inhibit further reaction, without perturbing the intermediate itself.

There are many examples of inhibition of reactions leading to the isolation of intermediates, both in organic chemistry and in biochemistry. In the oxynitration of benzene to picric acid using nitric acid and mercuric nitrate, inhibition of the reaction with urea led to the isolation of phenylmercuric nitrate as an intermediate (58). The urea destroyed the dinitrogen tetroxide in the reaction mixture and thus prevented its reaction with the phenylmercuric nitrate intermediate.

Variation of the hydrogen ion concentration has been effectively used to isolate the acetylchymotrypsin intermediate in the reaction of *p*-nitrophenyl acetate and α-chymotrypsin. In this instance, the hydrogen ion can be considered the inhibitor, since the first step in the stepwise chymotrypsin-catalyzed hydrolysis of *p*-nitrophenyl acetate is found to have a hydrogen ion dependence different from that of the second step (59).

Biochemists investigating metabolic pathways, which commonly contain a large number of intermediates between reactants and products, have successfully utilized inhibition (or blocking) of reactions by specific chemical reagents in order to observe intermediates. The addition of fluoride ion, for example, led to the accumulation of D-phosphoglyceric acid in the the glycolysis of fructose-1,6-diphosphate. This result is understandable in the light of the strong inhibition by fluoride ion of the enzyme enolase (a magnesium-containing enzyme), which ordinarily carries out the next step in the glycolytic sequence (60).

Hereditary inability to metabolize certain intermediate compounds has been the basis for a technique for biochemical genetics, which has provided a powerful approach to the detection of metabolic intermediates. Thus, in certain artificially induced mutant strains of the mold *Neurospora crassa*, it has been shown that 3-hydroxyanthranilic acid is an intermediate in the

normal pathway for the synthesis of nicotinic acid from tryptophan, since the mutant strain is capable of reaction only to the intermediate stage, whereas the normal strain is capable of reaction to the product (61,62).

III. DETECTION OF TRANSIENT INTERMEDIATES BY PHYSICAL PROPERTIES

In recent years, with the advent of extremely sensitive instruments for the measurement of physical properties coupled with rapid recording devices, it has been possible to detect transient intermediates with greater facility. As pointed out in Section I,3, spectrophotometry, in the ultraviolet and visible regions, in particular, and physical measurements associated with free radicals, such as electron spin resonance and paramagnetic susceptibility, have proved to be of great value. A few recent and representative examples will be described here without an attempt to treat the problem exhaustively.

The ultraviolet and visible regions of the spectrum have been utilized more fruitfully than the infrared region for the detection of transient intermediates. This follows, since the extinction coefficients associated with electronic transitions occurring in the ultraviolet and visible regions are much greater than those associated with vibrational or rotational transitions occurring in the infrared. Accordingly, in using the ultraviolet or visible region of the spectrum, it is possible to detect concentrations of species as low as $10^{-6}M$. With fluorescence measurements it is possible to detect species at even lower concentrations.

The formation and reaction of a transient intermediate may then be qualitatively detected or quantitatively fitted in the kinetics of a reaction scheme by observation of the appearance and disappearance of an absorption at a characteristic wavelength, or vice versa. In this way, a number of intermediates in liquid phase reaction shown in Figure 4 have been detected: A, the metallic enolate intermediate in the metal-ion-catalyzed decarboxylation of dimethyloxaloacetic acid (65); B, the trianisylmethyl carbonium ion pair intermediate in the reaction of trianisylmethyl chloride with pyrrole in benzene (66); C, spiro[2.5]octa-1,4-dien-3-one in the reaction of 2-*p*-hydroxyphenyl-1-ethyl bromide with base (67); D, the cyclic intermediate between periodic acid and a 1,2-glycol in the periodic acid oxidation of glycols (68); E, the dienone intermediate in the bromodesulfonation of an aromatic sulfonate (68); F, the acetylimidazole intermediate in the imidazole-catalyzed hydrolysis of *p*-nitrophenyl acetate (70); and G, the addition intermediate of hydroxylamine and ketones in the oximation of ketones (71).

Spectroscopic evidence of a special kind of intermediate, a charge transfer complex, merits special attention. Such complexes involving aromatic

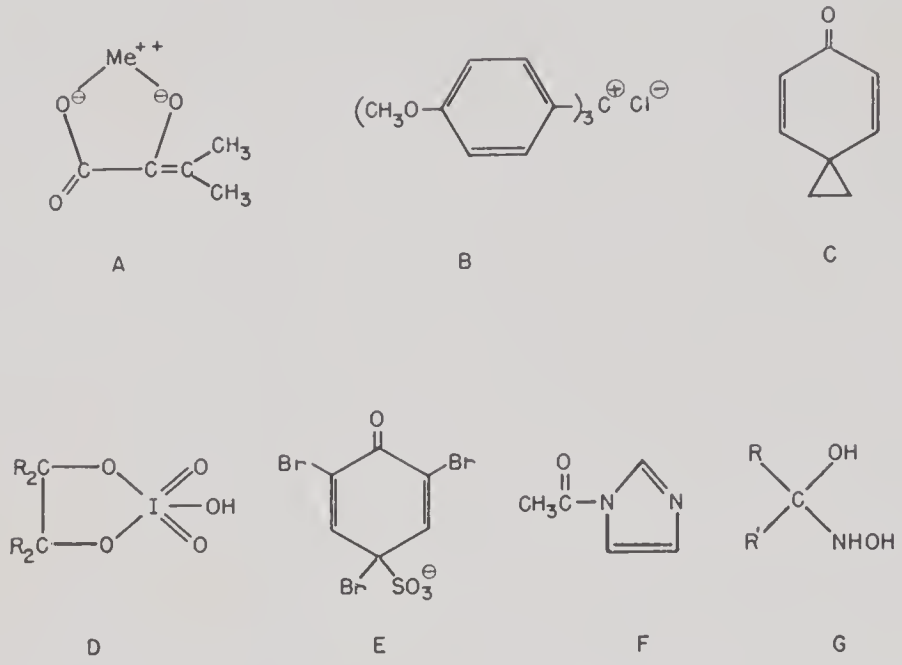

Fig. 4. Some reactive intermediates detected spectrophotometrically in organic reactions.

acceptors and/or donors have been extensively observed through the appearance of new ultraviolet or visible absorption bands (72). It has been suggested in several instances that these complexes serve as intermediates in chemical reactions, such as aromatic substitution, and in enzymatic catalysis (73).

The most convincing spectroscopic demonstration of the presence of an intermediate is that case in which the spectrophotometric determination of the appearance and disappearance of the intermediate is accompanied by an independent kinetic determination of the disappearance of reactant and the appearance of product. For a completely definitive test, all the kinetic data must fit the rate equations for a consecutive reaction.

Chance (74) has extended the usefulness of spectrophotometric detection of intermediates to the study of enzyme-substrate complexes in which the half-lives of the reactions involving unstable intermediates are of the order of seconds rather than minutes or hours. By utilizing forms of the flow method of Hartridge and Roughton (75), called accelerated- and stopped-flow methods, together with highly sensitive and rapid spectrophotometric detection, Chance has been able to measure the kinetics of formation and disappearance of a number of intermediates in the reactions of catalase and peroxidase (74).

It has been mentioned above that infrared absorption spectroscopy has not been utilized for the detection of reactive intermediates because of the insensitivity of such measurements. In a few isolated cases where rather large (equilibrium) concentrations of intermediates have been

formed, it is possible to use infrared or Raman spectroscopic evidence. This approach has been successfully used in the identification of the nitronium ion as the nitrating species in aromatic nitration in sulfuric acid solution (76,77), and in the detection of the addition intermediate in the oximation of ketones (71).

Electron spin resonance (paramagnetic resonance absorption) has been previously mentioned as a powerful experimental approach to the detection of free-radical intermediates trapped in a rigid medium at low temperature or in a semirigid partial vinyl polymerizate. This technique has also been utilized for the detection of semiquinone radical intermediates in various reactions, such as the reduction of quinones by glucose in alkaline alcoholic solutions (Eq. 3), the air oxidation of hydroquinone in alkaline alcoholic solution, and the one-electron reduction of nitrogen compounds such as riboflavin (78). The electron spin resonance method is inherently more sensitive than magnetic susceptibility and potentiometric methods for the detection of free-radical intermediates (see later). Therefore, electron spin resonance holds promise for the detection of free-radical intermediates and the elucidation of the kinetics of radical reactions.

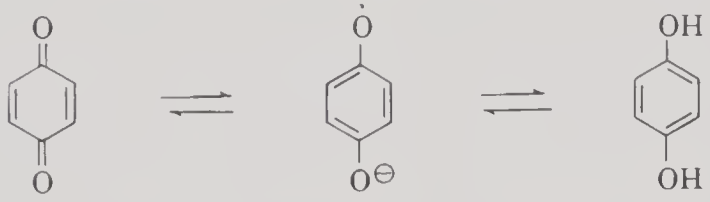

(3)

Paramagnetic susceptibility measurements, which are in a sense parallel to electron spin resonance since they both depend on the presence of an unpaired electron in the molecule, have been applied to the detection of a number of short-lived free-radical intermediates, in oxidation-reduction reactions as well as in photolytic reactions. Michaelis applied paramagnetic susceptibility measurements to the determination of the free-radical semiquinone intermediates in certain oxidation-reduction systems. He was able to show that the maximum amount of the radical arises at 50% reduction in the reduction of phenanthrenequinone-3-sulfonate by glucose (79) and that, in the reduction of duroquinone, the maximum stoichiometric percentage of the durosemiquinone radical formed at pH 13 is about 50% (80). The most successful method employed measurements of the change in magnetic susceptibility during a slowly progressing reduction (81). The paramagnetism resulting from the radical Wurster's blue in the partial oxidation of tetramethyl-*p*-phenylenediamine was also observed (82). Magnetic susceptibility measurements on *p*-dimethylaminobenzenediazonium chloride during the irradiation of this compound by ultraviolet light have indicated the presence of free-radical intermediates up to a

concentration of $1 \times 10^{-3}M$ (83). An aryl radical can then be postulated as an intermediate in this photodecomposition:

$$\begin{aligned} ArN_2^+Cl^- &\rightarrow Ar\cdot + N_2 + Cl\cdot \\ Ar\cdot + Cl\cdot &\rightarrow ArCl \end{aligned} \qquad (4)$$

Historically speaking, potentiometry and not paramagnetic susceptibility provided the first evidence for the formation of semiquinone radical intermediates in the reduction of quinones. Michaelis was able to demonstrate by potentiometric titration that the two-electron reduction must occur in two discrete one-electron transfers. This behavior is reflected in the step-wise nature of the titration curves, the slopes of these curves and their symmetry about the inflection points (84). Numerous examples were investigated by Michaelis and co-workers indicating the step-wise nature of the reduction of various quinones and of the oxidation of hydroquinones and of phenylene diamine derivatives, which lead to Wurster's salts as intermediates. Since polarographic reduction gives a direct indication of one-electron or two-electron transfers and also indicates the number of discrete steps in a reduction process, an exact parallel would be expected to exist between potentiometric titration data and polarographic data for the same system. This is indeed the case, as was shown in the two-step reduction of α-oxyphenazine. The two methods yield similar two-step curves and also illustrate the symmetry of the curves around the midpoint of the waves (85).

In the final analysis, a discussion of the detection of transient intermediates by physical properties is intimately tied to the study of fast reactions (86). In Chapters XIV through XX, a number of powerful approaches to the study of rapid reactions are discussed in detail. In certain instances, explicit reference has been given in these chapters to the detection of transient intermediates in fast reactions. In other instances, it is reasonable to suppose that some of the same techniques used for the determination of the disappearance of reactants or appearance of products in rapid reactions can be applied to the detection of transient intermediates.

There are a number of ingenious approaches that have been utilized for the production of a sufficient quantity of a reactive intermediate for a sufficiently long period of time so that some aspect of its physical properties can be measured. The experimental difficulties encountered in extreme cases are threefold: the necessity for rapid homogeneous initiation of the reaction, the necessity for isothermal conditions, and the necessity of a highly sensitive and rapid method of detection (87). If one wishes to perturb a gas phase reaction, a sink, usually a liquid nitrogen trap, can be introduced to collect the reactive intermediate for a leisurely inspection of physical properties. However, if one does not wish to perturb the reaction,

grave difficulties are often met, principally because the concentrations of transient intermediates are often so low that the intermediate cannot be detected. One method that has overcome the difficulty of the short time available for measurement is the flow technique, in which the system is made time invariant (Chapter XIV). A second method including sector and allied techniques, modulates the source of initiation at a frequency comparable with the rate of reaction investigated (Chapter XX). When the reaction can be initiated photochemically by the flash technique, the concentration of intermediates can become so high that the concentration of a variety of radicals and ions can be determined by flash spectrophotometry (Chapter XIX). Another general method of approach consists of introducing a sample of a reaction mixture into the ionization chamber of a mass spectrometer, where the presence of radicals can often be detected and their nature determined by the fact that the ionization potentials of radicals are rather smaller than those of the molecules from which they are derived (88). Finally, by measurements of the chemical relaxation of a system at equilibrium, which has been perturbed by an extremely rapid variation of pressure, electrical field density, or temperature, it is possible to detect intermediates in ionic processes not accessible by other approaches (Chapter XVIII).

IV. EVIDENCE FOR INTERMEDIATE FORMATION FROM CHEMICAL PROPERTIES

The detection of intermediates by isolation and by means of specific physical properties are direct approaches to the problem of intermediate formation. The rest of this chapter is devoted to a discussion of indirect (chemical) evidence for intermediate formation. Indirect arguments for intermediate formation have been known to give what later proved to be incorrect conclusions or to give ambiguous conclusions. The "definitive" experiment usually does not exist in this realm of mechanistic investigation, except to rule out certain possibilities. A body of self-consistent but indirect arguments, based on a number of experiments none of which is definitive in its own right, is the usual basis for mechanistic conclusions. This includes conclusions regarding the formation of intermediates in chemical reactions. It is within this framework that the evidence for intermediate formation from chemical properties will be discussed.

1. Kinetics

A. KINETIC FORM

Arguments based on kinetic considerations, whether these arguments are directed to molecularity of a chemical reaction, to intermediate formation,

or to other mechanistic considerations, are of necessity indirect arguments. This is not to say that kinetic arguments cannot be powerful or useful, but caution must be exercised in using kinetic arguments, as well as all other indirect arguments, for intermediate formation.

Nonkinetic, rather than kinetic, arguments must be used to distinguish which of several intermediate species in equilibrium with one another are involved in a rate determining process. The reason for this failure of kinetics to distinguish between species in equilibrium with one another is that kinetic order, in general, can only reflect what is in the transition state and can neither specify the pathway by which the transition state is formed nor specify the structural features of the transition state. The celebrated case of the ammonium cyanate–urea conversion is an example of the confusion that may arise in such a situation. In this instance, monumental confusion arose as to whether ammonium ion and cyanate ion reacted to form urea or whether it was ammonia and cyanic acid (89).

Another limitation in the use of kinetic arguments to deduce the formation of intermediates in chemical reactions is evident in studies of the oxidation of 1,2-diols by periodic acid. In the original kinetic analysis of this system, it was stated that the kinetic form required that the glycol and periodic acid rapidly formed an intermediate of some kind, which then reacted in a rate-determining process to give the products of the reaction (96). It was subsequently pointed out that this mechanism is kinetically indistinguishable from one in which the intermediate serves merely as a storehouse for the reactants; that is, the intermediate is a blind alley (91). Furthermore, another possible mechanism exists involving both a real intermediate leading to products and a blind-alley intermediate. This confusion reflected the fact that the intermediate was formed much more rapidly than its breakdown; the confusion was lifted when a system was investigated in which the intermediate was formed at a rate comparable with that of its breakdown (92). In this case, the kinetic analysis is consistent only with the interpretation that the intermediate is a necessary precursor of the products.

The kinetic order of a reaction can imply the presence of an intermediate in the reaction. This is particularly true when the kinetic order of the reaction differs from the stoichiometry of the reaction. A classical example of this phenomenon was discovered by Lapworth (93) in the alkaline bromination of acetone. Although the stoichiometric equation requires one mole of acetone, one mole of base, and one mole of bromine, the kinetics indicate dependence solely on acetone and base concentrations and independence of the bromine concentration. Reconciliation of this dilemma leads to the postulation of the rate-determining formation of an enolate

ion intermediate, followed by a fast reaction of the intermediate with bromine to form the products of the reaction.

$$\begin{aligned} &CH_3\overset{\overset{O}{\|}}{C}CH_3 + B \rightleftharpoons CH_3\overset{\overset{O}{\|}}{C}CH_2^{\ominus} + BH^{\oplus} \\ &CH_3\overset{\overset{O}{\|}}{C}CH_2^{\ominus} + Br_2 \rightarrow CH_3\overset{\overset{O}{\|}}{C}CH_2Br + Br^{\ominus} \end{aligned} \qquad (5)$$

The base-catalyzed aldolization of acetaldehyde involves a similar disparity between stoichiometry (second order in acetaldehyde) and kinetics (first order in acetaldehyde). On the basis of this evidence, the rate-determining formation of an enolate ion intermediate has been postulated (94).

$$\begin{aligned} &CH_3\overset{\overset{O}{\|}}{C}H + B \rightleftharpoons {}^{\ominus}CH_2\overset{\overset{O}{\|}}{C}H + BH^{\oplus} \\ &{}^{\ominus}CH_2\overset{\overset{O}{\|}}{C}H + CH_3\overset{\overset{O}{\|}}{C}H \rightleftharpoons CH_3\overset{\overset{O^{\ominus}}{|}}{C}H{-}CH_2{-}\overset{\overset{O}{\|}}{C}H \\ &CH_3\overset{\overset{O^{\ominus}}{|}}{C}HCH_2\overset{\overset{O}{\|}}{C}H + BH^{+} \rightleftharpoons CH_3\overset{\overset{OH}{|}}{C}HCH_2\overset{\overset{O}{\|}}{C}H + B \end{aligned} \qquad (6)$$

The postulation of intermediate formation to explain the discrepancy between kinetic order and stoichiometry of a reaction has been extensively applied to organic systems and, in particular, has been developed by Ingold to a high degree in his investigations of the substitution reactions at a saturated carbon atom. The general principle was enunciated by Ingold with the following analogy (95): "If two horses nibble the same haystack, neither interferes with the meal of the other because there is plenty of haystack; but if the two are jointly hand-fed, one straw at a time (from a limited source), then what one gets the other must go without. In the first case, the feeding rates are additive; in the second, they are complementary. That is the whole principle. So, for example, when we examine the solvolysis of benzhydryl bromide in an aqueous medium, with added azide ions as competitor, the rates will tell us whether the water and azide ions are simultaneously attacking the 'haystack' of plentifully available benzhydryl bromide molecules, as in mechanism S_N2, or whether they are competing for the 'straw ration' of carbonium ions, formed one at a time, as in mechanism S_N1" (95).

Kinetic evidence of this kind for the formation of carbonium ion intermediates in displacement reactions at a saturated carbon atom has been well documented (96,97). For example, the rate of the displacement reaction of triphenylmethyl halide in polar solvents is independent of the concen-

tration, or even of the nature, of the entering substituent, although certain anions such as the azide ion can divert the product from triphenylcarbinol

$$(C_6H_5)_3CX \underset{k_2}{\overset{k_1}{\rightleftharpoons}} (C_6H_5)_3C^{\oplus} + X^{\ominus} \begin{cases} \xrightarrow[H_2O]{k_3} (C_6H_5)_3COH + H^+ \\ \xrightarrow[N_3^-]{k_4} (C_6H_5)_3CN_3 \end{cases} \tag{7}$$

(with no azide ion present) to a 90% yield of trityl azide (with $1.3 \times 10^{-3} M$ sodium azide) (106). If one considers the rigorous treatment given earlier (see Section I.2) of the steady-state kinetics of the reaction of an unstable intermediate, it is obvious that the above kinetic picture is oversimplified, since steps 2 and 3 will contribute in general to the over-all rate constant

$$-dRX/dt = k_1/[k_2X^-/(k_3 + 1)]RX$$

Steps 2 and 3 must contribute, in this instance, since it has been shown that there is a relatively large difference in activation energy between the water and the azide ion partitioning of the carbonium ion intermediate (Section I.2) and since k_2/k_3 has been shown to be equal to or greater than one from salt effect data for a large number of tertiary halides. (See Section IV.1.C.) Therefore, the generalization that steps other than the formation of a reactive intermediate will have no effect whatsoever on the over-all kinetics of a process must be used with caution.

The identity of rates of a number of different reactions of a given substance have also been utilized as an argument for the occurrence of a common intermediate in many reactions.

When an enolate ion is formed in the rate-determining step of a reaction, the addition of any reagent, which combines with this highly reactive intermediate, apparently has no effect whatsoever on the over-all kinetics of the reaction. It was shown, for example, that, in the halogenation of acetone, the rates of bromination, iodination, and chlorination were the same (98). Identity of rates, furthermore, is found in the halogenation, deuterium exchange, and racemization reactions of ketones. The rate constant for the acid-catalyzed iodination of phenyl *sec*-butyl ketone is equal within experimental error to the rate constant for racemization of the optically active ketone under the same conditions (99). It is reasonable that both reactions involve the rate-controlling formation of an enol intermediate, which, having a plane of symmetry, is as likely upon ketonization to give the *d*-isomer as the *l*. Furthermore, the rate of the acetate ion-catalyzed bromination of the same ketone was found to be equal to the rate of racemization under the same conditions (100). Furthermore, it has been demonstrated that the rates of the deuteroxide ion-catalyzed racemization

and deuterium exchange are identical (101). In these base-catalyzed reactions, it is probable that the intermediate is the enolate anion. In these cases, steps 2 and 3 apparently contribute nothing to the over-all kinetics, which leads to the conclusion that $k_3(X_2) \gg k_2\ (BH^+)$ in the steady-state treatment of this process. It is conceivable, however, that reaction conditions can be found in which this inequality does not hold.

The decarboxylation of β-keto acids, such as acetoacetic acid and the brominative decarboxylation of these compounds, occur at the same rate (102). It is, therefore, concluded that a common enol intermediate is formed in each of these reactions. The same phenomenon has been noted in the decarboxylation of nitroacetic acid and α-nitroisobutyric acid (103).

A somewhat similar situation occurs in the simultaneous hydrolysis and isotopic oxygen exchange of esters (104). In this instance, the rates of the two processes are not identical but are quite similar (usually within an order of magnitude). It was suggested that a common intermediate, the hydrate of the ester, is partitioned to give hydrolysis products or isotopically exchanged reactant. Although the slow step of the reaction is the formation of the intermediate, steps 2 and 3 involving the partitioning of the intermediate must contribute to the rate to a small extent, as opposed to the case of enolate-ion formation where various reactions of the intermediate apparently have no kinetic effect on the over-all reaction.

In enzymatically catalyzed reactions, an apparent discrepancy ordinarily occurs between the kinetic results and the law of mass action. That is, when the substrate concentration is sufficiently low, the velocity of the reaction is proportional to the substrate concentration, but, when the substrate concentration is sufficiently high, the velocity is independent of the substrate concentration. This anomaly, like the anomaly between kinetic order and stoichiometry, has been reconciled by assuming the formation of an enzyme-substrate complex as an intermediate stage in the reaction (105–107). If one is able to observe not only the steady state of the enzymatic process but also the pre-steady-state portion of the reaction, it is possible to gather information concerning the formation of an intermediate (beyond the enzyme-substrate complex). A demonstration of this method of intermediate determination has been given, for example, in the reaction of chymotrypsin and *p*-nitrophenyl acetate using a spectrophotometric technique with a stopped-flow apparatus (108). Observation of both the presteady state and the steady-state portions of a reaction is good evidence for intermediate formation.

An intermediate in equilibrium with the reactant is often encountered in organic reactions and can be kinetically treated with certainty. An example of such a system is the acid hydrolysis of amides, which is postulated to proceed through the protonated amide as intermediate.

$$RCONH_2 + H^+ \rightleftharpoons RC(OH)=NH_2^+ \xrightarrow[k_2]{H_2O} \text{hydrolysis products} \qquad (8)$$

The kinetics of this system have been extensively studied. In dilute acid solution the rate of hydrolysis is proportional to the hydronium ion concentration. The most significant feature of the kinetics, however, is that a rate maximum has been found to occur in the hydrolysis of a number of aliphatic and aromatic amides in strong acid (109–112). The concentration of sulfuric acid for maximum rate varies from about 2.5 to 5M, solutions in which amides would be expected to be appreciably protonated. The hypothesis of the protonated amide as intermediate effectively accounts for all the experimental facts. Below the concentration for maximum rate, the effect of increasing acid strength is chiefly to increase the concentration of the protonated intermediate; above the concentration for maximum rate, the effect is chiefly to decrease the concentration or activity of the water (111). The work of Edward (113) has shown that this hypothesis can account quantitatively for the changes in rate of hydrolysis with acid concentration. It was shown that the experimental rate constant k_{obs} was related to the second-order rate constant k_2 by the expression

$$k_{obs} = k_2 (H_3O^+)/(K + h_0) \qquad (9)$$

where K is the equilibrium constant for the dissociation of protonated amide and h_0 is the Hammett acidity function. For very weak bases, such as esters, $K \ll h_0$ in the range of acid concentration of 2–5M sulfuric acid and so Equation (9) simplifies to

$$k_{obs} = k_2 (H_3O^+)/K \qquad (10)$$

This gives the linear dependence of the experimental first-order constant on the concentration of hydronium ion which has been found for the hydrolysis of esters in strong acid solution (114). However, when $K \ll h_0$, Equation (9) simplifies to

$$k_{obs} = k_2 (H_3O^+)/h_0 \qquad (11)$$

Since h_0 increases with concentration much more rapidly than (H_3O^+) when mineral acid concentrations exceed about 2M, k_{obs} will decrease in high acid concentrations. When $K \ll h_0$, ionization to the protonated amide will be substantially complete; the decrease in rate of hydrolysis can then be regarded as a result of the decreasing availability of water, since $(H_2O) = K_W(H_3O^+)/h_0$, where K_W is the equilibrium constant for the reaction $H_3O^+ \rightleftharpoons H_2O + H^+$.

B. ENTROPIES OF ACTIVATION

Another kinetic criterion for intermediate formation is concerned with entropies of activation. Taft (115) has suggested that hydrolytic reactions proceeding by A-1 mechanisms (with carbonium ion or acylium ion intermediates) should have more positive entropies of activation than those involving A-2 mechanisms, since the latter mechanisms involve more constraint on the reaction system in the transition state, owing to the orientation and participation of a specific water molecule from the solvent. Long *et al.* (116) have calculated entropies of activation from available data for several acid-catalyzed reactions for which the mechanisms are quite well known and showed that the entropies of activation fall into two distinct groups separated by some 25–30 entropy units, corresponding to the two types of mechanism. The criterion that the hydrolytic reactions of compounds that form carbonium ion or acylium ion intermediates have positive entropies of activation, which are far different from those of the hydrolytic reactions of compounds that do not form such intermediates, appears to be a fairly general one.

C. SOLVENT AND SALT EFFECTS

The effect of solvent on the rates of reaction is often striking. Whereas a number of equations have been proposed for the quantitative correlation of the rates of reactions with the nature of the solvent, none appears to have complete generality (117). However, the theory of Hughes and Ingold (118), although not entirely general, has been useful in considering the qualitative effect of solvent on reaction rate. According to this theory, an increase in the ion-solvating power of the medium will accelerate the creation and concentration of charges and inhibit their destruction and diffusion. This qualitative rule does not specifically apply to intermediates but rather to the change of charge between the ground state and the transition state. It has, however, been used within limits to specify, for example, whether a carbonium ion intermediate is formed in a reaction. That is, the reaction of a molecule RX to form a carbonium ion intermediate would be expected to proceed through a transition state with considerable separation of charge and thus be accelerated to a very considerable extent by increased solvent polarity. This is not an unambiguous argument, since it is also possible that the same effect of increased solvent polarity could be caused by the reaction of a solvent (neutral) molecule with RX, which would also proceed through a transition state with a separation of charge. In spite of this ambiguity, the use of a variation in solvent polarity coupled with a variation in the nucleophile has been a powerful method of changing from a reaction in which a carbonium ion intermediate (an

S_N1 reaction) is formed to one in which no intermediate is formed (S_N2 reaction). An example of this change is shown in the reaction of benzyl chloride, which, with iodide ion in acetone solution, gives a cleanly second-order reaction (119), presumably proceeding through a single transition state and which, in its solvolysis in the ionizing solvent (50% acetone–50% water), proceeds through a carbonium ion (120).

The quantitative evaluation of salt effects on rates of reaction has been of considerable use as a criterion of intermediate formation. One of the instances in which kinetic salt effects has added considerably to knowledge of intermediate formation is in the heterolytic reactions of alkyl halides, postulated to proceed through carbonium ions (S_N1 reactions). The deviations from simple first-order kinetics in some solvolysis reactions have provided some of the first compelling evidence for carbonium ion-intermediate formation in these reactions.

The hydrolysis of *tert*-butyl bromide in 90% acetone-water exhibits good first-order kinetics in dilute solution (less than $0.02M$), whereas in more concentrated solutions, such as $0.1M$, it shows first-order rate constants that increase as the reaction proceeds (121). This result was explained on the basis of carbonium-ion-intermediate formation by attributing the increase in rate to an increase in ionic strength as the reaction proceeds. The effect of ionic strength on the rate of reaction should follow Equation (12)

$$\log k/k_0 = 2Z_A Z_B \alpha(\mu)^{1/2} \tag{12}$$

on the basis of the Debye-Hückel theory and the transition state theory (122).

On the other hand, the solvolysis of *p,p'*-dimethylbenzhydryl chloride in the same solvent exhibits exactly the opposite phenomenon, the first-order rate constant decreasing during the reaction (123). This fact was ascribed to the recombination of the carbonium ion intermediate with the chloride ions formed during the reaction. In the early part of the reaction, essentially no carbonium ions combine with chloride ion, since the concentration of chloride ion is too low, but, in later stages of the reaction, recombination of the carbonium ion intermediate and chloride ion becomes, important. This reversion to reactants (according to a mass law effect) slows the overall reaction in spite of the increase in ionic strength, which tends to accelerate the formation of carbonium ion.

Salt effects and mass-law effects in a reaction involving a carbonium ion intermediate are illustrated by the solvolysis of *p,p'*-dimethylbenzhydryl chloride in 85% acetone-water in the presence of a number of different ionic species as shown in Table I (123).

TABLE I

Relative Rates of Hydrolysis of *p,p'*-Dimethylbenzhydryl Chloride with Added Salt

0.051*N* salt added	Relative rate	Explanation
No salt	1.00	
Lithium bromide	1.46	Primary salt effect (ionic strength). Although the anions of these salts might combine with the carbonium ion, the products formed are more reactive than RCl, and rapidly reform the carbonium ion. Therefore, the total effect is an ionic strength effect.
Tetramethylammonium nitrate	1.53	
Lithium chloride	0.49	Mass-law effect (two-thirds of the carbonium ions combine with chloride ion to regenerate the starting material).
Sodium azide	1.50	Primary salt effect (ionic strength). Although the rate is not affected by azide ion, the product is 64% RN_3.

A complete kinetic analysis can be made for the solvolysis of an alkyl chloride in the presence of only chloride ion (124). For the reaction

$$RCl \underset{k_2}{\overset{k_1}{\rightleftharpoons}} R^+ + Cl^- \xrightarrow{k_3} \text{products} \tag{13}$$

it can be shown that the rate of the reaction is a function of the partitioning of the intermediate, $\alpha = k_2/k_3$.

$$\text{Rate} = k_1(RCl)/(\alpha(Cl^-) + 1) \tag{14}$$

Values for α, corresponding to the partitioning of the intermediate, have been obtained using the above equation (and taking into account ionic-strength effects). The results shown in Table II indicate an increase in α with the presumed increase in stability of the carbonium ion, which is consistent with the selectivity-reactivity relationship enunciated for other systems (125). Thus there is partitioning by the carbonium ion intermediate between chloride ion and water, as well as between azide ion and

TABLE II

The Partitioning of the Intermediate Carbonium Ion in Some Solvolysis Reactions (126)

Alkyl halide	α (k_2/k_3)
Triphenylmethyl chloride	400
p,p'-Dimethylbenzhydryl chloride	68–69
p-Methylbenzhydryl chloride	28–35
p-tert-Butylbenzhydryl chloride	20–43
Benzhydryl chloride	10–16
Benzhydryl bromide	50–70
tert-Butyl bromide	1–2

water. In the latter partitioning, it was shown that there exists an activation-energy difference of about 4 kcal./mole in the two processes. One might, therefore, expect, that in the former process, an activation-energy difference of the same order of magnitude would occur. It would be predicted that activation energies of such magnitude would be reflected in the over-all rate of solvolysis. So far, this has not been demonstrated.

The reduction in rate via the mass-law effect is one of a number of phenomena which may be described as the partitioning of an intermediate. Added substances may affect the rate of a reaction by causing the intermediate to revert to reactant or may affect the products without affecting the rate. These occurrences are important arguments in the establishment of a basis for intermediate formation. Similar evidence for the partitioning of intermediates will appear in a number of different forms throughout this discussion.

A further confirmation of the presence of a carbonium ion intermediate is seen in the hydrolysis of triphenylmethyl chloride in 75% dioxane-water in the presence of azide ion. In this system, the carbonium ion can be partitioned in two ways to produce products: (*1*) reaction with water to produce alcohol and (*2*) reaction with azide ion to produce alkylazide. Increasing the ionic strength should have different effects on these two reactions. It was found that the mole per cent of alcohol in the product increased from 20.2 to 41 when the lithium perchlorate concentration was increased from zero to 0.0892*M* (127). Thus an effect of an intermediate on partitioning again increases the confidence with which we can postulate the existence of the intermediate.

In addition to these "normal" salt effects, more subtle effects have recently been noted in a number of organic reactions. These effects have been associated with ion-pair formation.

The acetolysis of α,α-dimethylallyl chloride has been shown to involve simultaneous acetolysis and rearrangement to γ,γ-dimethylallyl chloride (128). The external chloride ion has no effect on the rate, indicating that the rearrangement is not due to reversion of free carbonium ions to allylic chloride. Furthermore, the alcoholysis of α,α-dimethylallyl chloride occurs at the same rate as the acetolysis without any concurrent isomerization. These facts can be understood on the basis that a common intermediate, an ion pair of the allylic carbonium ion and the chloride, occurs for both acetolysis and isomerization of the tertiary chloride.

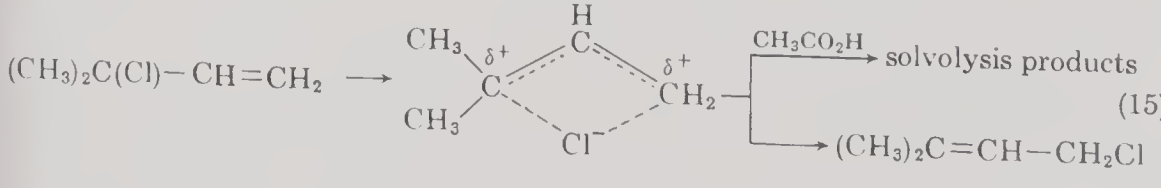

(15)

As a consequence of this investigation and others to be discussed later, Winstein and co-workers (129) have elaborated the kinetic scheme of the S_N1 reaction of Hughes and Ingold to recognize explicitly ion-pair intermediates as well as the dissociated form of the carbonium ion.

$$\begin{array}{ccccccc} & & \text{internal ion pair} & & \text{external ion pair} & & \text{dissociated ions} \\ RX & \rightleftharpoons & R^+X^- & \rightleftharpoons & R^+//X^- & \rightleftharpoons & R^+ + X^- \\ & & & & \downarrow & & \downarrow \\ & & & & \text{product} & & \text{product} \end{array} \qquad (16)$$

An ion pair is necessary to explain "internal return" such as mentioned above, the mechanism and stereochemistry of solvolysis to be discussed later, as well as the conductivity of solutions of triarylmethyl chlorides. To explain certain ionic strength phenomena, it is necessary to consider two ion-pair stages in the process of ionization and dissociation leading from RX to R^+.

Striking salt effects on the rates of acetolysis of a number of benzenesulfonates, which yield carbonium ions with bridged structures, have been observed (130). For example, the acetolysis of neophyl and *p*-methoxyneophyl halides and arylsulfonates (131) exhibit a first-order titrimetric solvolysis rate constant, which is affected by various salts only in a "normal" linear manner. The experimental rate constants are equal to the ionization rate constants k_1, since the acetolysis proceeds predominantly by way of an anchimerically assisted ionization involving aryl participation. The salt effects observed for these compounds, therefore, involve effects on the ionization rate only. In this instance, any ion-pair return would give rise to a tertiary derivative that will survive only briefly and will therefore not affect the rate. On the other hand, in the acetolysis of *o*- and *p*-anisylethyl-*p*-toluenesulfonates (132), lithium perchlorate produces both a very steep rise in the first-order rate constant below 0.01*M* salt (a "special" salt effect) and a subsequent small, linear increase in the rate constant at higher salt concentrations (a "normal" salt effect). The former designation refers to a very steep rise in titrimetric rate constant from the base value, owing to low salt concentration. The latter refers to the linear increase in rate constant at somewhat higher salt concentrations. The normal salt effect in these systems is approximately equal to that observed with the neophyl analogs, and is again presumed to be a salt effect on ionization. The origin of the special salt effect of lithium perchlorate is presumed to be concerned with suppression of the ion-pair return, which is possible in these systems but not in the neophyl analogs.

Special salt effects were observed in a number of other similar systems. In the acetolysis of cholesteryl-*p*-toluenesulfonate and bromobenzenesul-

fonate and 2-(2,4-dimethoxyphenyl)ethylbromobenzenesulfonate (133), the special salt effects are especially striking. Whereas normal salt effects are specific with regard to the nature of the salts, there is no specificity in the magnitude of special salt effects. These results support the view that special salt effects are concerned with reduction of ion-pair return.

The most definitive work on the special salt effects, as related to ion-pair intermediates in solvolysis reactions, is concerned with the acetolysis of *threo*-3-*p*-anisyl-2-butylarenesulfonates (134). The ionization of these substances, which is exclusively anchimerically assisted, gives rise to an internally compensated bridged cation from which a racemic product results. Polarimetric rate constants therefore represent ionization (k_1), whereas titrimetric rate constants can be considerably smaller if ion-pair return accompanies solvolysis. The lithium perchlorate salt effect on the former rate constant shows a normal linear pattern; its effect on the latter rate constant shows a combination of the steep special salt effect and the more shallow normal linear pattern. From these data on the same substance, it is again concluded that special salt effects are not concerned with ionization, but with reduction of ion-pair return. The most striking aspect of these results is that the special salt effect only partly closes the gap between polarimetric and titrimetric rate constants for acetolysis, indicating that ion-pair return is only partially eliminated by the special salt effect. To explain these data and other data indicating that ion-pair return is important in certain systems, such as the acetolysis of norbornyl compounds where special salt effects are absent, it is postulated that two discrete carbonium ion-pair intermediates exist in solvolysis reactions, intimate and solvent-separated ion pairs. The solvent-separated ion pair is postulated to be much more reactive toward added lithium perchlorate than the intimate ion pair. If so, lithium perchlorate would be expected to trap the solvent-separated ion pair while still permitting return from the intimate ion pair, namely *internal* return. Thus the special salt effect in the present case is postulated to be concerned with elimination of *external* ion-pair return.

The salt effects described above are further, highly refined examples of evidence concerning the partitioning of intermediates under varying reaction conditions. It is repeated again that much of the indirect chemical evidence concerning intermediate formation is dependent on this concept.

D. CATALYSIS AND INHIBITION

The influence of catalysts on reactions is often attributed to the formation of reactive intermediates by the action of the catalyst on the reactant. This hypothesis is often reversed to claim that the influence of a particular

catalyst on a reaction is evidence for the formation of a particular reactive intermediate. This reasoning, which may appear to be circuitous, has validity because of the strong network of interconnecting pieces of evidence in certain systems. It is often generalized that ionic catalysts form ionic intermediates and that free-radical catalysts form free-radical intermediates. This is usually true, although there are exceptions to both of these statements, as has been pointed out by Leffler (135).

Some of the most clear-cut cases of the use of evidence of catalytic activity to postulate intermediates in a reaction have been brought to light in the realm of free-radical chemistry. For example, in the study of the kinetics of benzoyl peroxide decomposition in solution, it was found that the reaction was induced by triphenylmethyl and diphenylnitrogen, two known free-radical species, and furthermore was inhibited by oxygen, hydroquinone, *tert*-butylcatechol, dinitrobenzene, and picric acid, which are known scavengers of stable free radicals (136). On the basis of this evidence and of kinetic evidence which indicates mixed first- and three-halves order kinetics, it was postulated that the decomposition produces benzoyloxy free-radical intermediates in the following series of steps in both spontaneous and induced decomposition:

$$\begin{aligned} (\phi CO_2)_2 &\rightarrow 2\phi CO_2\cdot \\ 2\phi CO_2\cdot &\rightarrow CO_2 + \phi CO_2\phi \\ \phi CO_2\cdot + (\phi CO_2)_2 &\rightarrow CO_2 + \phi CO_2\phi + \phi CO_2\cdot \end{aligned} \qquad (17)$$

Once it is shown that stable free-radical species can induce the decomposition of peroxides, it is then possible to argue cogently that other reactions initiated by the decomposition of peroxides also proceed through free-radical intermediates. For example, the classical studies on the anti-Markovnikov addition of hydrogen bromide to olefins showed conclusively that the reaction is accelerated by peroxides and eliminated by inhibitors, such as hydroquinone and diphenylamine, which react with peroxides (137,138).

A host of reactions have been shown to be accelerated or decelerated by stable free radicals (for example, triphenylmethyl, nitric oxide, and oxygen); by substances which are known to decompose into free-radical species (such as alkyl peroxides, acyl peroxides, azobisalkylnitriles, tetraethyllead, and diazo compounds); by substances which are known to react with stable free radicals (such as iodine, oxygen, olefins, polynitro aromatic compounds, quinones and hydroquinones, phenols, and aromatic amines); by metallic ions and metals that engage in one-electron transfer reactions (for example, silver ion and ferrous or ferric ion); and, finally, by light energy, heat energy, or irradiation. There is presumptive evidence that such reactions proceed via free-radical intermediates.

Photochemical and thermal reactions probably deserve additional comment. The generalization that one can make about most photochemical reactions is that they are not very polar and often involve free-radical intermediates. However, it is conceivable that molecular reactions without the formation of free-radical intermediates may occur. The same possibility may transpire in thermal reactions (138). One diagnostic criterion that has been used to distinguish between intermediate formation and non-intermediate formation in thermal reactions and especially in photochemical reactions is the presence or absence of a chain reaction. If a chain reaction does occur, it is mandatory that some highly reactive species propagate the chain (disregarding the possibility of thermal chains). The reasoning behind this argument is that the activation energy associated with the various propagation steps, including the regeneration of the reactive species, must be very small compared to the activation energy for the initiation step in order for quantum yields (the ratio of propagation steps to initiation steps) to be much greater than unity, as they must be in chain reactions. It is often possible to corroborate the free-radical character of light-initiated reactions by demonstrating the initiation of these reactions by known free radicals or by substances known to decompose into free radicals. For example, it has been shown that the halogenation of alkanes is initiated by a quantum of light and, further, is initiated by the addition of hexaphenylethane (which dissociates to triphenylmethyl free radical), as well as by the addition of tetraethyllead at elevated temperature (139). Furthermore, the autooxidation of benzaldehyde was shown to be initiated by both a quantum of light (with a quantum yield of approximately ten thousand) and also by hexaphenylethane (140).

Returning to our circuitous reasoning, we can again say that any substance that is capable of initiating a known free-radical chain, such as a free-radical polymerization, is capable of forming an intermediate itself. This is an attractive approach, since the sensitivity of this method is high. Of course, it must be kept in mind that, in the case of polymerization, the chain reaction can be initiated by known electrophiles and nucleophiles. In these cases, the chain-propagating species would presumably be electrophilic and nucleophilic, respectively (141).

When dealing with carbonium ions, it is possible to prepare stable species by a number of methods including the reactions of alcohols with strong mineral acid, the reactions of olefins with strong mineral acid, the reactions of alkyl halides with electrophilic reagents such as silver ion, mercuric ion, hydrogen halides or metal halides, and the reactions of amines with nitrous acid. (See Section I.3.) Therefore, when these various reagents, all of which can be considered electrophilic reagents, are utilized to catalyze a reaction in which it is not possible to isolate any intermediate, it is still

reasonable to assume that the catalytic activity of these reagents is concerned with the formation of unstable carbonium ion intermediates.

A similar argument may be advanced with regard to the production of carbanion intermediates. It is known, for example, that it is possible to produce stable carbanions by the action of strong bases on suitable organic molecules. The action of basic or nucleophilic catalysts in systems where intermediates are not isolable can be presumed to occur via carbanion intermediates. The arguments given above depend on the rankest kind of circumstantial evidence. No investigator would presume that such evidence is definitive but would strive to supplement it by independent evidence of other kinds.

General basic catalysis of a number of reactions, including aromatic nucleophilic substitution, aromatic electrophilic substitution, and hydrolysis of anilides, has provided convincing evidence for intermediate formation. In the best documented case, an example of aromatic nucleophilic substitution, it was found that the reaction of *N*-methylaniline with 2,4-dinitrofluorobenzene was linearly dependent on potassium acetate concentration. The acetate ion-catalyzed reaction was shown to be an example of general basic catalysis (142). A similar, although not definitive, result was obtained in the reaction of 2,4-dinitrochlorobenzene with *n*-butylamine and sodium hydroxide, in which the kinetic results suggested that the reaction with the amine is subject to catalysis by hydroxide ion (143). In electrophilic aromatic substitution, involving the reaction of a diazonium ion with a phenol derivative, general basic catalysis has also been observed (144). Finally, in the alkaline hydrolysis of anilides, a term which is second order in hydroxide ion has been found, which is again interpretable in terms of a general basic catalysis, although certainly not proven (145). In these three reactions, the demonstration of general basic catalysis is readily interpretable in terms of a reaction involving an addition intermediate, although it is not inconsistent with any form of a one-step mechanism for the displacement reaction.

E. THE HAMMETT ACIDITY FUNCTION

Catalysis by strong acids has produced arguments for intermediate formation, especially through the use of the Hammett acidity function.

A characteristic feature of the H_0 acidity scale of Hammett (146a) is that, with increasing acid concentration, H_0 grows increasingly larger than C_{H^+}. An opportunity is thus afforded to test whether certain acid-catalyzed reactions, whose specific rates are known to increase much faster than C_{H^+} at high acid concentrations, are in fact more closely correlated with the acidity function H_0. Many such correlations have indeed been found, exhibiting linear relationships between the log of the rate constant

and $-H_0$ with a slope approximating unity. Hammett has pointed out that this correlation is to be expected if the hydrolysis mechanism involves a first-order rate-determining reaction of the conjugate acid of the substrate.

$$\begin{aligned} S + BH^+ &\rightleftharpoons SH^+ + B \\ SH^+ &\xrightarrow{\text{slow}} X^+ \\ X^+ + H_2O &\rightarrow \text{products} + H^+ \end{aligned} \tag{18}$$

Applying the Brønsted equation for the effects of changes in the medium to the rate-determining step, it is possible to show that

$$\log k_1 = -H_0 + \log (f_{BH^+} f_S)/(f_B f_{\pm}) + \text{constant}$$

The observed linear correlation between $\log k_1$ and $-H_0$ follows if the activity coefficient ratio remains constant with changing medium. This is quite plausible if $f_{\pm}$ can be assumed to vary with changes in the medium in essentially the same way as f_{SH^+}, the activity coefficient of the conjugate acid of S. Such an assumption is *a priori* reasonable, since the transition state differs from SH^+ only in displacement along the reaction coordinate. The alternative mechanism, in which the nucleophile H_2O participates in the rate-determining step

$$\begin{aligned} S + H_3O^+ &\rightleftharpoons SH^+ + H_2O \\ SH^+ + H_2O &\rightarrow \text{products} + H^+ \end{aligned} \tag{19}$$

leads to a kinetic expression which predicts that

$$\log k_1 = \log C_{H_3O^+} + \log (f_S f_{H^+} a_{H_2O})/f_{\pm} + \text{constant} \tag{20}$$

This leads to a linear relationship between the logarithm of the first-order rate constant and the log of the concentration of the hydrogen ion, if one assumes that the activity coefficient term is unity.

Using this criterion of mechanism, it has been shown that a number of the reactions of organic compounds in strong acid follow the first of these linear correlations, namely, a linear relationship between the logarithm of the rate constant and $-H_0$. This then implies that an intermediate X^+ exists transiently in such reactions. Although the kinetics indicate nothing about what the intermediate X^+ might be, it is usually possible, on the basis of structural concepts, to specify what form the intermediate X^+ takes.

A comprehensive review of the application of the H_0 acidity function to kinetics and mechanisms of acid catalysis has summarized the information on intermediate formation in such systems (146b). Some examples of reactions whose rate constants follow the acidity function H_0 are shown

in Table III together with the postulated structure of the intermediate X^+ formed in the reaction.

TABLE III
Intermediates Postulated on the Correlation of log k_1 with the Acidity Function H_0

Reaction	Postulated structure of the intermediate X^+
Hydrolysis of methyl mesitoate	$[Ar—C{=}O]^+$
Hydrolysis of alkoxymethyl acetate	$—[CH_2{=}OR]^+$
Hydrolysis of β-propiolactone	$[R—C{=}O]^+$
Depolymerization of trioxane	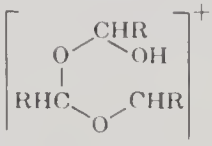
Hydrolysis of propylene oxide	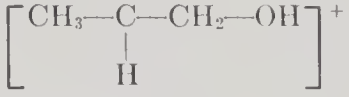
Hydrolysis of acetic anhydride	$[CH_3C{=}O]^+$
Hydrolysis of methylal	$[ROCH_2]^+$
Pinacol rearrangement	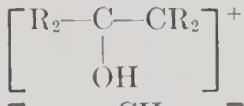
Hydration of isobutylene	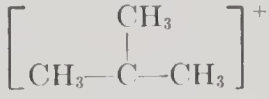
Aromatic hydrogen-isotope exchange	Sigma complex of proton and aromatic

An important by-product of the study of the dependence of the rate on the acidity function H_0 with regard to intermediate formation has arisen in the last two cases shown in Table III. The hydration of isobutylene is a specific hydronium ion-catalyzed reaction, implying protonation in a fast preequilibrium followed by a rate-determining step. This preequilibrium cannot involve the reversible formation of a carbonium ion for the recovered olefin after 50% reaction in deuterium oxide shows no deuterium exchange, nor does the recovered 2-methyl-1-butene, after 50% hydration, show any isomerization to 2-methyl-2-butene. Therefore, the preequilibrium required by specific hydronium ion catalysis must involve a species other than a carbonium ion. Since the rate of the hydration of isobutylene depends on H_0 and since structural evidence indicates the formation of a carbonium ion intermediate, it was postulated that a protonated isobutylene is transformed into carbonium ion in the rate-determining process. It was further postulated that the protonated substrate is the pi-complex of the proton and the olefin in which the proton interacts with the pi-cloud of the olefin (147). Recently, it was demonstrated that not only the hydration of isoolefins but also the dehydration of the corresponding alcohols exhibit a rate dependency on H_0. This result leads to the paradox

that the Zucker-Hammett hypothesis (Eq. 18) ascribes two different compositions [(alcohol + proton) or (olefin + proton)] to the same transition state and, therefore, casts doubt on the utility of the hypothesis (147a). However, in the hydration of isobutylene, all evidence indicates that both a pi-complex and a carbonium ion are formed as intermediates, including catalytic evidence, the nonexchange of reactants, and the effect of structure on reactivity (vide infra).

In the aromatic hydrogen isotope exchange (the last entry in Table III), the dependence of rate on the acidity function H_0 has been demonstrated with a number of aromatic compounds in a number of strong acid solutions. The mechanism proposed, on the basis of this evidence, involves the preequilibrium formation of a pi-complex composed of proton and aromatic, followed by a rate-determining reaction to a sigma complex of the proton and aromatic. Since the exchange reaction is symmetrical, these reactions must be followed by further (fast) transformations to a new pi-complex and finally to exchanged aromatic (148). This process implies specific hydronium ion catalysis, as was found in the isobutylene hydration. However, in the only case thus far amenable to investigation (involving 2,4,6-trimethoxybenzene-*1-t*), general acid catalysis was found, which, although compatible with a mechanism involving a sigma complex, is not compatible with the preequilibrium formation of a pi-complex, nor is it compatible with an H_0 rate dependency (148a).

The conflicting evidence and the doubts, which have been raised recently in connection with the strict validity of the original hypothesis concerning the correlation between rate and the Hammett acidity function, somewhat diminish its value as a diagnostic criterion (149). For this reason, evidence based on the acidity function should probably be used only as corroborative evidence for intermediate formation and not as direct or sole evidence.

2. The Effect of Structure on Reactivity as a Criterion of Intermediate Formation

A. STRUCTURAL EFFECTS OF THE ORGANIC MOLECULE

Intermediate formation depends generally on rather stringent structural requirements, both steric and electronic, of the reactant species that produce such intermediates. It is, therefore, desirable to consider the structure of an intermediate in order to ascertain what structural features in a reactant molecule would lead to its formation. Knowledge of the effect of structural features on reactivity can then provide evidence, although indirect, for the formation of intermediates in chemical reactions. If we focus attention on carbonium ion intermediates as an example, for the most extensive reactivity studies have been carried out on these systems, we

find that the transition state of the reaction resembles the intermediate rather closely. Of course, relative reactivity is related to the difference in free energies of the ground state and the transition state of the reaction. But, since the transition state usually closely approximates the carbonium ion intermediate, the same structural changes that will affect the free energy of the carbonium ion will have a similar effect on the free-energy content of the transition state leading to the carbonium ion. In such systems, the relative stability of the carbonium ion intermediate should be reflected in the relative rates of reaction.

A direct experimental demonstration of the parallelism between the rates of reactions presumed to proceed through carbonium ion intermediates and the stability of carbonium ions has been given for a series of diarylmethyl cations (150). This was done by the determination of the pK_{R^+} values for the equilibrium in Eq. (21) using the acidity function H_R, followed by com-

$$R^+ + H_2O \rightleftharpoons ROH + H^+ \tag{21}$$

parison of the relative pK_{R^+} values with the log of the relative rate constants of the alcoholysis of the corresponding diarylchloromethanes. The parallel between rate and equilibrium data involving triarylmethyl carbonium ions has been formalized by Brown by testing the adherence of such systems to a Hammett-type relationship. It was found that three related systems involving triarylmethyl carbonium ions fit such a relationship: an equilibrium involving carbonium ion formation from triarylcarbinols in aqueous sulfuric acid, an equilibrium involving ionization of triarylcarbinyl chlorides to ion pairs in sulfur dioxide, and a solvolytic reaction of triarylcarbinyl chlorides in 40% ethanol–60% ethyl ether (151). A similar correlation has been shown to exist between the ionization constants producing carbanions and the rate constants of reactions which are presumed to proceed through carbanion intermediates (152). Finally, a logarithmic relationship exists between the rates and equilibrium constants for the dissociation of hexaphenylethane in a series of solvents (152a). These relationships involve the logs of the equilibrium and rate constants, relationships which are equivalent to linear relationships between the free energy of the equilibrium and the free energy of activation (153). These demonstrations serve as an important bridge between the observations of stable ions, which have been discussed previously, and the use of relative reactivity data as a criterion for intermediate formation.

The carbonium ion intermediate and the transition state leading to it differ from the reactant in several ways. First, there is a much larger partial positive charge on the carbon atom at which displacement occurs. Second, the three groups attached to this carbon atom assume a more nearly coplanar configuration, leading to approximately sp^2 hybridization in the

carbonium ion. Relative reactivity data, therefore, which reflect changes from normal covalent (sp^3) bonding, can be cited as evidence for carbonium ion intermediate formation. For example, atoms or groups that supply electrons to an electron-deficient carbon atom would be expected to stabilize the carbonium ion and thus enhance the reaction. There are numerous examples of this behavior. The replacement of the α-hydrogen atoms of an alkyl halide by saturated alkyl groups causes a large increase in solvolytic reactivity; the relative rates of formolysis of alkyl bromides at 100° are: *tert*-butyl, 10^8; isopropyl, 44.7; ethyl, 1.71; and methyl, 1.00 (154).

It is not clear that the above effects are caused solely by electron release to the carbonium ion center. It is, therefore, profitable to consider the effects of *meta*- or *para*-substituents on reactivity on an aromatic ring or on the side chain of the ring in which cationic intermediates are formed. The Hammett equation has provided the most successful approach to the quantitative treatment of such effects of structure on reactivity (155,156) dealing originally with side chain reactions on the benzene ring. A large number of such measurements has been made, and attempts have been made to correlate relative reactivity with the Hammett sigma constants for the particular substituents. Serious deviations involving *p*-alkyl and *p*-alkoxyl substituents have been noted in a number of these attempts. It has been pointed out that these groups, through resonance interaction with the electron deficient transition state, would be able to stabilize the transition state for a reaction at the para position more than would be expected from the value of the Hammett *sigma* constant for the substituents (157,158). A new set of constants for para substituents ($sigma^+$) has been calculated from the solvolysis data of the substituted phenyldimethylcarbinyl chlorides. These substituent constants correlate a large number of reactions presumably involving electron-deficient transition states, leading to the following *rho* values: solvolysis of phenyldimethylcarbinyl chlorides, −4.63; nitration of monosubstituted benzenes in nitromethane or acetic anhydride, −6.53; halogenation of monosubstituted benzenes by bromine or chlorine in acetic acid, −11.35; protonolysis of phenyltrimethylsilanes by perchloric acid, −4.59; and brominolysis of substituted phenylboronic acids, −4.30 (159,151). These very large Hammett *rho* constants indicate great electron demand in the transition states of these reactions. Those substituents which would show greatest resonance interaction with such a transition state have the greatest positive deviations in the normal Hammett treatment. These facts point to the possibility of cationic intermediates in these reactions.

It is probably an oversimplification to state that substitution reactions involving variations in the organic moiety (the B moiety of the reaction $A + BC \rightarrow AB + C$) leading to large negative *rho* values involve cationic

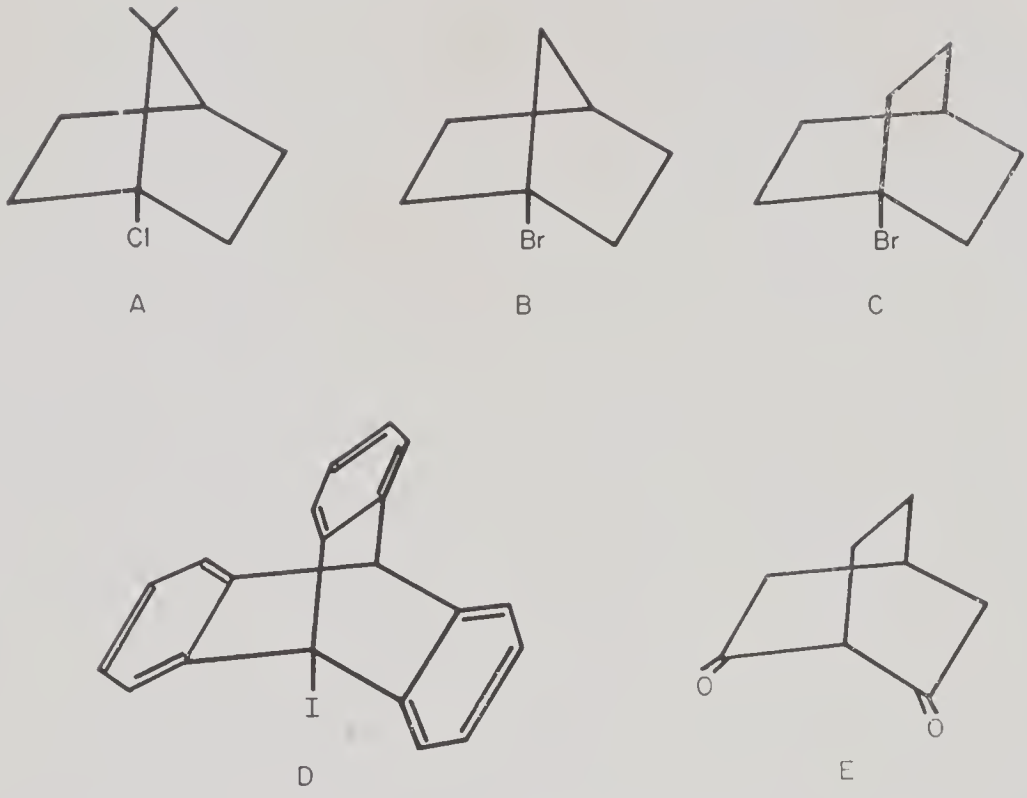

A B C D E

Fig. 5. Rigid bicyclic systems that have been utilized to test intermediate formation in various reactions: A, apocamphyl chloride; B, 1-bromobicyclo[2.2.1]heptane; C, 1-bromobicyclo[2.2.2]octane; D, 1-iodotryptycene; E, bicyclo[2.2.2]octanedione.

intermediates. However, this generalization seems to hold for all data now available (156). Furthermore, the converse of this generalization also seems to hold: that substitution reactions involving variations in the organic moiety leading to a large positive *rho* value involve anionic intermediates (156,160,161). It is difficult to set limits for such a crude generalization; it will arbitrarily be stated that the magnitude of *rho* is large if it is greater than 2.0.

The replacement of α-hydrogen atoms by phenyl radicals increases the solvolytic reactivity of alkyl chlorides. For example, it has been estimated that, in 80% acetone, triphenylmethyl chloride hydrolyzes about 10^6 times as rapidly as benzhydryl chloride, which in turn reacts about 10^3 times as rapidly as α-phenylethyl chloride (162). Likewise, a rate enhancement of 10^{14} is found in the ethanolysis of chlorodimethyl ether, relative to that of methyl chloride (163). These results can be most readily explained by assuming the enhanced reactivity is related to enhanced resonance stabilization of an intermediate carbonium ion. For similar reasons, allylic and benzylic halides display considerably increased solvolytic reactivity.

Similar examples can be found in reactions where one is led to postulate free-radical intermediates. For example, the thermal decompositions

of a series of *tert*-butyl peresters, $RC(O)OOC(CH_3)_3$, occur at rates that are widely different and that are parallel to the stability of the free radical R. The change in R from methyl to diphenylmethyl leads to a rate enhancement of over 10^4 (164). These data and others led to the postulation of a concerted decomposition of the perester to alkyl radical, carbon dioxide, and *tert*-butoxy radical in which the resonance stabilization of the diphenylmethyl or other alkyl radicals contributes substantially to lowering the energy level of the transition state.

The structural requirement that the carbon atom undergoing covalent change must assume an sp^2 hybridized state when proceeding through a carbonium ion intermediate has led to significant studies concerning intermediate formation. Reactions postulated to proceed through such intermediates would be expected to occur with great difficulty at the bridgehead of a bicyclic system having extreme structural rigidity. It was shown that the reaction of apocamphyl chloride (Fig. 5A) with alcoholic silver nitrate, a reagent that ordinarily leads to ready carbonium ion formation with halides, gives essentially no reaction upon being refluxed for 48 hours (165). The low reactivity can be explained by saying that the carbonium ion formed at a bridgehead would be highly strained relative to the expected coplanar (sp^2 hybridization) configuration of a normal carbonium ion intermediate. It was further found that 1-bromobicyclo[2.2.1]heptane (Fig. 5B) yields the corresponding alcohol only upon treatment with aqueous silver nitrate at 150° for 2 days, whereas the corresponding bicyclo[2.2.2]octane (Fig. 5C) derivative reacts at room temperature in 4 hours. Although the latter compound is about 10^6 less reactive than a typical tertiary alkyl bromide, it is much more reactive than the former bridgehead compound, a fact that is attributed to the possibility of spreading the strain required to approach planarity over a large number of bonds (166). The compound 1-iodotryptycene (Fig. 5D) is about 10^9 slower than the bicyclo[2.2.2]octane compound described above. This has led to the conclusion that benzene rings fused on the bridges of a bicyclo[2.2.2]octane have a strongly deactivating influence on the carbon-halogen bond at position 1(167).

The compound bicyclo[2.2.2]octane-2,6-dione (Fig. 5E), unlike typical β-diketones, shows little tendency to form an enol, giving no interaction with ferric chloride or cupric ion. Furthermore, it does not dissolve in aqueous alkali, indicating that it is unable to form a resonance-stabilized carbanion (168), presumably because of the rigid non-coplanar system. The thermal decomposition of diapocamphyl peroxide in a similar fashion, was found to be unusually slow. However, it did react in carbon tetrachloride solution to give products, including apocamphyl chloride, which indicates that the noncoplanar 1-apocamphyl radical can be formed (169).

The decomposition of ditriptoyl peroxide in benzene, furthermore, gives a significant yield of triptycene, which must arise from an abstraction reaction of the triptycyl radical (167). Although free radicals can be formed at a bridgehead, their formation is undoubtedly slower than at a corresponding open chain position as has been shown in the methyl abstraction reaction (169a). These investigations of carbonium ions, carbanions, and radicals formed at the bridgeheads of rigid systems then provide evidence consistent with the stereochemical picture of the postulated intermediates in the various systems.

Other steric effects can be explained in a straightforward fashion by the postulation of carbonium ion intermediates. The bulk of the three α-alkyl groups in a tertiary halide or alcohol has been shown to increase the reactivity of these compounds significantly. This type of steric acceleration has been postulated to be a result of relief of steric strain between large alkyl groups upon transformation to a carbonium ion intermediate, since an increase (from about 109.5 to about 120°) in the angle between the alkyl groups would accompany this transformation (170–172).

Extensive investigations of the effect of ring size on the relative reactivity of cycloalkyl halides, or *p*-toluenesulfonates, and cyclic ketones have brought to light significant correlations between relative reactivity and the changes that would be expected in reactions in going from a four-coordinate ground state to a three-coordinate (sp^2) transition state (or intermediate) and vice versa (173). Cyclopropyl and cyclobutyl derivatives are the least reactive of the halides or tosylates in solvolytic reactions, with the cyclopropyl derivative being the extreme in unreactivity. The reactivities of small ring compounds can be explained in terms of strain arising from the distortion of bond angles, if one assumes that a carbonium ion intermediate is formed in the reaction (174). For example, the internal angles of the cyclopropyl compound are assumed to be 60° in the ground state, corresponding to an angle strain of 49.5° from the optimum value of 109.5° for a tetrahedral carbon atom. The formation of a carbonium ion with optimum bond angles of 120° would increase this strain and is, hence, not a favored process. Ionization to a carbonium ion intermediate should be strongly favored in the 5- and 7-ring systems, which are strained in the ground state, owing to bond opposition forces, but ionization should not be favored in the stable, unstrained cyclohexyl derivatives. Indeed, in the cyclohexylcarbonium ion, there will be introduced two partial oppositions, so that a cyclohexyl derivative should have less tendency toward ionization in comparison with an open-chain derivative (175). The medium rings (8–11 members) are strongly strained, owing to bond opposition forces, with some contribution from atom compression. Here also the internal strain should be partially relieved by a decrease in the number of bonds. Finally,

the large rings should approach those of the open-chain compounds. This picture of the differences between a tetracovalent reactant and a tricovalent transition state (or intermediate) is fully consistent with the known reactivity data and, further, is consistent with equilibrium constants for the formation of cyclic cyanohydrins (sp^3) from the corresponding ketones (sp^2)(176,177).

In summary, it can be stated that knowledge of the steric and electronic effects in the ground state and the transition state of a reaction, coupled with the hypothesis that the transition state resembles the intermediate in many processes, enables one to use relative reactivity data as circumstantial evidence for intermediate formation. It is fitting that this section be ended with a note of caution. Cognizance must be taken of the fact that the transition state can also resemble an intermediate state that does not lie along the reaction path. This concept is illustrated in the elimination reaction of 1-bromo-2-arylethanes.

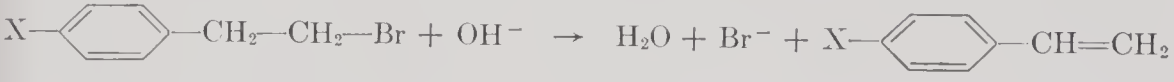

The effect of the substituent on the rate (178) is approximately what one would expect ($p > +2$) if the transition state resembled the possible intermediate

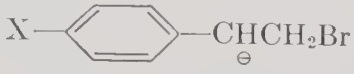

However, both deuterium exchange (179) and kinetic isotope effect studies (180) indicate that such an ion is not an intermediate, but rather that the loss of a proton and bromide ion constitute a concerted process.

Special effects of structure on reactivity have been found in a number of solvolytic reactions in which the molecules contain, in addition to the group being displaced, a second, "neighboring" group on the adjacent carbon atom (181). Ordinarily these solvolytic reactions would be expected to proceed through carbonium ion intermediates, but in these special instances bridged ions may be formed directly as intermediates, as shown in Equation 22.

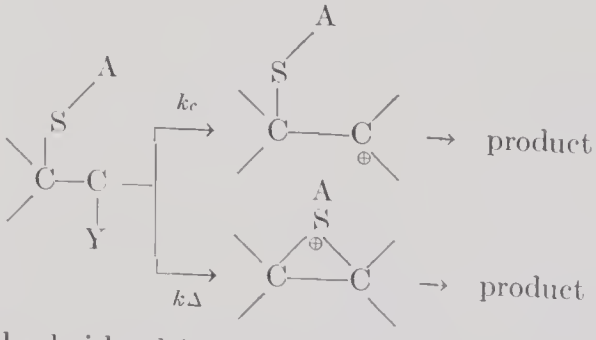

(22)

The formation of the bridged ion via a neighboring group participation of the intramolecular nucleophilic group SA should lead to an enhanced rate,

The nucleophilic driving force of the neighboring group may be expressed in terms of k_Δ/k_c, the ratio of the rate of the neighboring group displacement to that of direct carbonium ion formation. Using the relationship,

$$k_\Delta = k_{obs} - k_c$$

knowing the observed rate constant, and making an approximation for k_c, based on the dipole-dipole interaction between the group SA and the incipient carbonium ion, calculations were made (see Table IV) indicating large effects of the β-substituents on the rate, through the formation of cyclic intermediates. These large rate enhancements have been termed anchimeric assistance and are good evidence for the formation of bridged ions as intermediates in solvolytic reactions.

TABLE IV

Effects of β-Substituents on Rates of Neighboring Group Displacements and Carbonium Ion Formation of Substituted Ethyl Compounds (181)

β-Substituent	k_Δ/k_c
O^-	10^4
SCH_2CH_2OH	10^9
NH_2	10^5
I	2×10^6
Br	2×10^3
OH	10

Neighboring group participation, with consequent enhancement of reactivity, is not restricted to reactions at a saturated carbon atom, but also has been observed in homolytic bond cleavage. The rate constant for the decomposition of *tert*-butyl-*o*-methylthioperbenzoate is 2×10^4 larger than that of *tert*-butyl perbenzoate indicating the participation of the methylthio group in the bond rupture and the formation of a cyclic intermediate involving the sulfur atom (162). Furthermore, neighboring group participation has been found in the hydrolytic reactions of carboxylic acid and phosphoric acid derivatives. For example, high reactivity in the hydrolysis of aspirin, compared to phenyl acetate, as well as the effect of pH on the rate constant, has been explained by the participation of neighboring carboxylate ion leading to an anhydride, salicoyl acetyl anhydride, as intermediate in this reaction (Eq. 23) (183). Anhydride intermediates

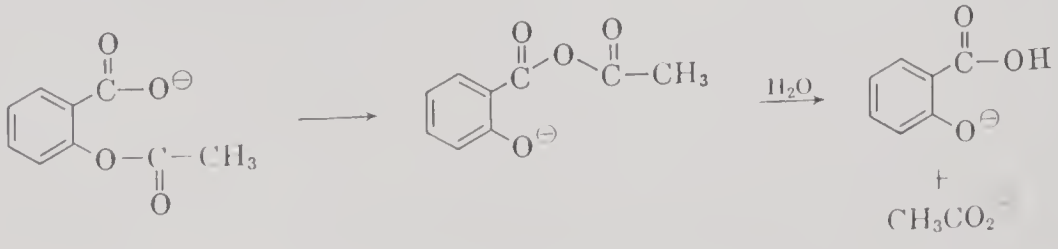

(23)

have also been postulated to explain the extremely high solvolysis rates of a copolymer of acrylic acid and *p*-nitrophenyl methacrylate (184) and of phthalamic acid (185).

Special effects of structure on reactivity have also been found in rearrangement reactions. A number of these reactions, which follow first-order kinetics, have been proved to be unexpectedly fast in solvents facilitating ionization to a carbonium ion. For example, the formolysis of 2,2,2-triphenylethyl chloride (186) and the acetolysis of 2,2,2-triphenylethyl tosylate (187) have been shown to be 6×10^4 and 7.7×10^3 faster than the reactions of the corresponding neopentyl derivatives. When corrected for the expected inductive effect of a phenyl group on an ionization process, the rates of these solvolysis reactions are 10^6 to 10^7 faster than the neopentyl derivatives. These large rate enhancements have been explained by the presence of a driving force resulting from participation of the phenyl groups in the ionization process, leading to a bridged carbonium ion intermediate of the form:

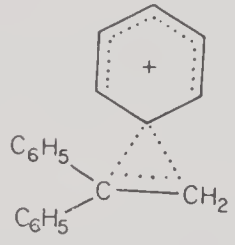

(XIV)

The generation of the bridged ion in preference to the classical ion would be expected if the nonclassical ion were the more stable. In such a case, the transition state for the formation of the bridged ion would be similarly stabilized by the incipient formation of the bridge in an analogous fashion to neighboring group participation.

A number of striking effects of structure on reactivity have been found in systems where a double bond is situated in the neighborhood of a group that can ionize to produce a carbonium ion. The acetolysis of *anti*-norborn-7-enyl-*p*-toluenesulfonate (Fig. 6A) is 10^{11} times more rapid than that of the 7-norbornyl analog (188). The phenomenon has been attributed to the stabilization of the incipient cationic center at C-7 by the pi-orbital of the double bond, leading to the formation of the intermediate ion (Fig. 6B). The stabilization of this ion by electron delocalization (189) is analogous to that predicted theoretically for the cyclopropenyl cation, a derivative of which was recently synthesized (Fig. 6C) (190). There are many other examples of marked rate effects on structure, which have led to the postulation of nonclassical ions. The examples given above, which involve participation of the pi-electron clouds of phenyl groups and double bonds in

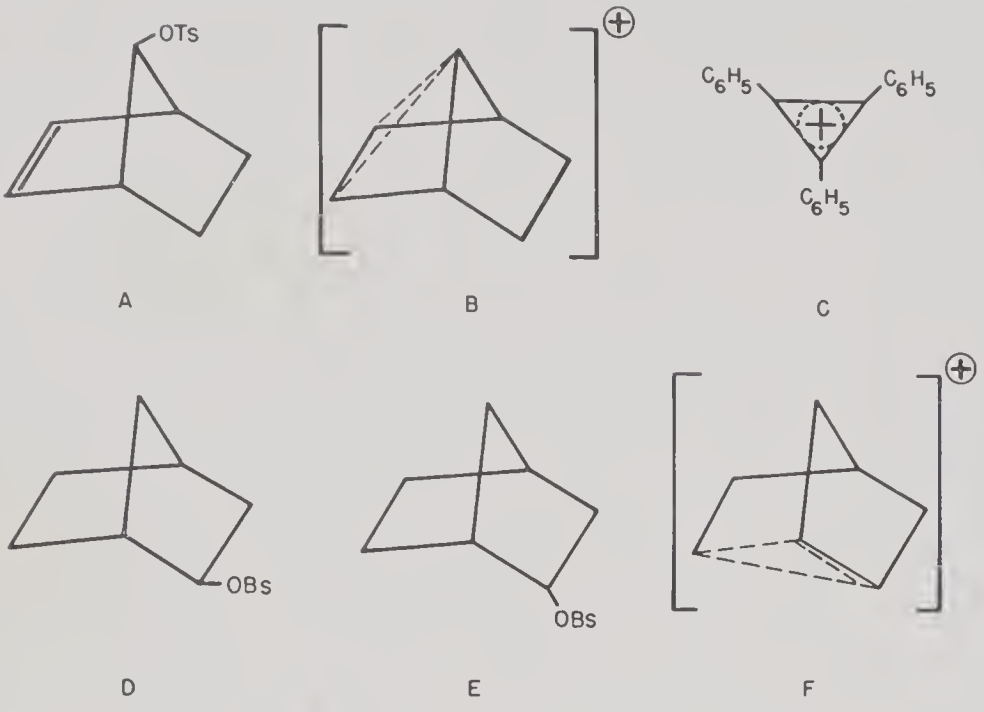

Fig. 6. A, *anti*-norborn-7-enyl *p*-toluenesulfonate; B, intermediate in the solvolysis of A; C, triphenylcyclopropenyl cation; D, *exo*-norbornyl *p*-bromobenzenesulfonate; E, *endo*-norbornyl *p*-bromobenzenesulfonate; F, intermediate in the solvolysis of *exo*-norbornyl *p*-bromobenzenesulfonate.

the ionization of a compound, give the largest rate enhancements. The acetolysis of *exo*-norbornyl-*p*-bromobenzenesulfonate (Fig. 6D) occurs about 350 times faster than the acetolysis of the corresponding *endo*-isomer (Fig. 6E) or than the cyclohexyl derivative. This significant, although relatively minor, rate enhancement has been attributed to the participation of a saturated carbon atom in the ionization process (191). It is postulated that the geometry is proper for the delocalization of sigma electrons in the rate-determining ionization to produce the bridged ion (Fig. 6F). In this system, the stereochemistry of the products (see later) can be explained by either the formation of the bridged ion (Fig 6F) or by a rapid tautomeric equilibrium between two carbonium ions. The latter possibility can be ruled out by the rate enhancement noted here, which would not be expected if a classical carbonium ion were first formed in a rate-determining step.

B. KINETIC ISOTOPE EFFECTS

The discovery that two bonds involving different isotopes of the same element are broken at different rates has proven to be of importance in the study of reaction mechanisms. The pioneering work in this field gave evidence for the identity of the covalent bond broken in the rate-determin-

ing step of a reaction.* More recently, kinetic isotope effects have been used to elucidate more subtle aspects of mechanism, including evidence for intermediate formation.

Deuterium and tritium kinetic isotope effects have provided information concerning the formation of intermediates in aromatic substitution reactions. No hydrogen isotope effects have been found for the nitration of benzene, bromobenzene, naphthalene, or nitrobenzene, nor for the bromination of benzene and the azo coupling of 1-naphthol-4-sulfonic acid. On the other hand, hydrogen isotope effects have been found in aromatic sulfonation, cyclodehydration of 2-anilinopent-2-en-4-one, the reactions of some diazonium ions upon 2-naphthol-6,8-disulfonic acid, the iodination of phenol, the bromination of dimethylaniline, and acid-catalyzed cyclizations of 2-carboxybiphenyl (193,194). In cases where no hydrogen isotope effect occurred, it was postulated that the lack of a hydrogen isotope effect was due to the fact that the electrophilic aromatic substitution reaction occurred with the formation of an intermediate having the structure (XV)

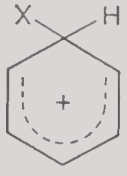

(XV)

and, further, that the formation of this intermediate and not the breakdown of the intermediate to products was the slow step. This argument has been criticized on the basis that the experimental results can be explained by a one-step mechanism whose transition state involves very little stretching of the carbon-hydrogen bond (and consequently very little hydrogen isotope effect) (195). It is significant that the reactions exhibiting a hydrogen isotope effect are those in which the greatest stabilization of an intermediate is possible, leading to an activation process that could discriminate between hydrogen and deuterium. Specifically, those cases that show the greatest hydrogen isotope effect, the iodination of phenol (196), the bromination of dimethylaniline, and the reactions of diazonium ions with hindered 2-naphthol-6,8-disulfonic acid (197), involve compounds that should be able to form stable dienone-like intermediates. It is therefore reasonable to say that, at present, the hydrogen kinetic isotope effect data (in electrophilic aromatic substitution) are consistent with the formation of reactive intermediates of the general structure shown above.

The effect of substituting deuterium oxide for water on the rates of or-

* For example, the study of the chromic acid oxidation of 2-propanol-*2-d* indicated that the secondary hydrogen (or deuteron) was removed in the rate-determining step (192).

ganic reactions has provided evidence for intermediate formation. The fact that the chlorination of phenol is faster in deuterium oxide than in water has been given as evidence for the formation of the chloronium ion (and not the protonated form of hypochlorous acid) as the intermediate in the chlorination in aqueous medium (198). The deuterium oxide solvent isotope effect on the rate of hydration of olefins has been given as evidence for the equilibrium formation of the protonated form of the olefin in this reaction, as opposed to a rate-determining proton transfer in the hydration (199). This intermediate is designated as a pi-complex of olefin and a proton. This isotopic evidence for intermediate formation corroborates the evidence based on a correlation of rate with the acidity constant H_0, mentioned earlier.

In addition to kinetic isotope effects in which a hydrogen or deuterium atom plays a direct role in the chemical reaction, there are instances in which indirect hydrogen isotope effects have been observed, as for example in the decomposition of *sec*-alkyl chlorosulfites (200) and the solvolysis of *tert*-amyl chlorides (201). In both of these cases, as well as in a number of subsequent reactions, it has been found that compounds containing deuterium atoms on the carbon atom adjacent to that holding a replaceable group react at rates 15–100% slower than the corresponding hydrogen compounds, depending on the number of deuterium atoms in the molecule. This unusual indirect isotope effect has been attributed to the weakening of the carbon-hydrogen (or carbon-deuterium) bonds in these positions in the transition step of the reaction. This weakening in the transition state has generally been attributed to hyperconjugation of these hydrogen atoms with an electron-deficient carbon atom in the transition state. The effect of deuterium substitution in a methyl group, para to a reaction at a benzylic position, substantiates the hyperconjugative nature of this isotope effect (202,203).

However, the kinetic isotope effects resulting from isotopic substitution of hydrogen in the methyl group of toluene are of the order of 3% or less in nitration, mercuration, and bromination reactions (204). Since one would expect hyperconjugation to be of paramount importance in aromatic substitution reactions, it is difficult to reconcile these results with the argument that the large secondary isotope effects in solvolysis are due to hyperconjugation. On the other hand, the effect of deuterium substitution on the α-carbon atom of ketals leads to significant isotope effects, which are in general agreement with the postulation of hyperconjugative stabilization of the transition state in these reactions obtained by other methods (205). Although there is still controversy concerning the origin of this isotope effect, there appears to be general agreement concerning the hypothesis that an electron-deficient atom such as that present in a carbonium

ion is a necessary, although not a sufficient, condition for the appearance of these indirect kinetic isotope effects.

More recently, hydrogen isotope effects have been observed in substitution processes in which deuterium is substituted for hydrogen in the carbon atom containing the replaceable group (206–209). These studies show that a deuterium atom in an alpha position slows the rate appreciably in reactions which may be classified as S_N1 processes and does not affect the rate in reactions which may be classified as S_N2 processes. These results have been explained (209) on the basis of the variable steric hindrance to the out-of-plane bending mode of the carbon-hydrogen bond in the transition state. In an S_N1 reaction, the hindrance would be least operative; in an S_N2 reaction containing a pentavalent transition state, the hindrance would be most effective. This criterion for carbonium-ion-intermediate formation may prove to be of value in future investigations, although it is obviously limited to the investigation of primary and secondary compounds.

C. THE ELEMENT EFFECT

Using arguments similar to those advanced with respect to the hydrogen isotope effects in aromatic electrophilic substitution, the absence of an "element" effect has been shown to be of value as a criterion for intermediate formation in aromatic nucleophilic substitution (210). In the reaction of 1-substituted 2,4-dinitrobenzenes with piperidine in methanol, three substituents, fluorine, nitro, and *p*-toluenesulfonoxy, were displaced very rapidly, whereas six substituents were displaced more slowly with remarkably little variation in rate among the six. Since displacement of these six substituents involved the breaking of bonds between carbon and five other elements, this result indicates that bond-breaking has not made significant progress in the rate-determining transition states of these reactions. These facts are most easily interpreted in terms of a rate-determining formation of an addition intermediate of the type (XVI):

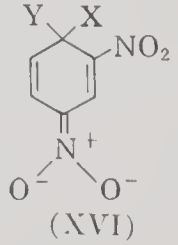

(XVI)

3. Chemical Consequences Diagnostic of Intermediate Formation

A. PRODUCTS AS A CRITERION OF INTERMEDIATE FORMATION

The products of reaction have long been used as a criterion for intermediate formation in a reaction. More precisely, it is often stated that the

products can be explained on the basis of the formation of a certain intermediate. This type of argument can be based on the flimsiest of reasoning, or, on the other hand, it can prove of great value in postulating an intermediate. The immediate circumstances surrounding the reaction and the isolation of products are of importance, and for this reason it will be desirable to consider some particular cases.

A reactant may give a product with the occurrence of no rearrangement or by-products. When the postulate of "least structural change" is followed, the organic chemist will not be forced and will therefore not seek to postulate an intermediate in the process. On the other hand, a reactant may give two or more products; these multiple products may be produced in different yields under differing conditions; one product may be formed where two might have been predicted; the same ratio of products may be formed starting with different reactants; added reagents may divert the production of normal products to abnormal products; deep-seated rearrangements or stereochemical changes may occur; and the reactant may initiate wholely new reactions. In such cases, the organic chemist has been forced to devise schemes involving intermediates in order to explain the path of the reaction.

Many generalizations have been enunciated on the basis of observations such as those described above. For example, the generalization that reactions proceeding with the formation of free-radical intermediates give complex products has been of some value as a diagnostic tool. To explain the acid-catalyzed polymerization of olefins (211) and, later, the Wagner-Meerwein rearrangements of various alkyl derivatives, the concept of the carbonium ion intermediate was first widely enunciated. Furthermore, a number of empirical rules, such as the Markovnikov rule for the addition of unsymmetrical addends to olefins, have in recent years been couched in terms of the formation of an unstable intermediate, as has the anti-Markovnikov rule, in turn. It is sometimes not clear which of these formulations in the cause of the postulation of intermediate formation and which is the effect of other evidence for intermediate formation or the effect of the general vogue of intermediate formation. An attempt will be made here to separate real diagnostic material for intermediate formation from the morass of speculation that has occurred in this area.

(1) **Statistical Product Distributions.** It was mentioned above that certain reactions are known to give a complex mixture of products. This result could be a result of the fact that the activation energies associated with reactions of high energy intermediates are very small. This argument could, of course, apply to high energy intermediates of any structure. In the extreme case, it would be expected that a high energy intermediate would give a statistical distribution of products formed from a series of completely random interactions.

Such a result is found in the reactions of carbene produced by the photolysis of diazomethane, with the hydrocarbons pentane and 2,3-dimethylbutane (212). The distribution of products resulting from the insertion of the carbene into a carbon-hydrogen bond of pentane, for example, corresponds very closely to the statistical distribution of hexane isomers shown in Equation (24).

$$CH_3CH_2CH_2CH_2CH_3 + CH_2 \rightarrow$$

$$CH_3CH_2CH_2CH_2CH_2CH_3 + CH_3\underset{\displaystyle CH_3}{\underset{|}{C}}HCH_2CH_2CH_3 + CH_3CH_2\underset{\displaystyle CH_3}{\underset{|}{C}}HCH_2CH_3 \quad (24)$$

Statistical distribution	50	33.3	16.7
Distribution at 15°	49	34	17

In recent years, a selectivity-reactivity relationship has been expressed in quantitative fashion for the reactions associated with aromatic electrophilic substitution (213). Specifically, a linear relationship has been shown to exist between the log of the *para* partial rate factors, taken as a measure of the activity (actually the inverse of the activity) of the reactions, and the log of the *para* to *meta* partial rate factors, taken as a measure of the selectivity of the reactions. Thus far, all electrophilic reactions of toluene for which accurate data are available follow this relationship. One would expect that the greater the "activity" of the reactive intermediate the more closely a statistical distribution of isomers would be approximated and vice versa. This hypothesis has been shown to hold quantitatively. Although not giving direct evidence for intermediate formation, these data can be correlated with the expected stabilities of the reactive cationic intermediates in aromatic electrophilic substitution.

(2) **Multiple Products.** Let us consider a reaction leading to two or more products. Such a process could conceivably proceed through the requisite number of parallel paths or, alternately, it could proceed initially through one pathway to a reactive intermediate whose partitioning could lead to more than one product. Therefore, the formation of multiple products is not a sufficient condition for postulation of intermediate formation.

A situation in which the product distribution can be varied from one corresponding to thermodynamic equilibrium to one corresponding to kinetic control of product formation leads to a strong argument for intermediate formation. The theoretical considerations leading to this possibility have been discussed previously (35) and state essentially that the reaction of a high energy intermediate to give products will pass through a transition state resembling the high energy intermediate. Kinetically controlled products will therefore be expected in such a system; that is, the charge distribution in the intermediate will determine the product distribution. The product distribution can then be, and has been observed to be, dif-

ferent from a thermodynamic distribution when conditions in the reaction prevent the attainment of thermodynamic equilibrium. On the other hand, the product distribution would be expected to, and has been observed to, correspond to a thermodynamic distribution when reaction conditions facilitate the attainment of thermodynamic equilibrium. There are many examples of these phenomena in the reactions of allylic compounds and systems leading to allylic intermediates. For example, the addition of chlorine to butadiene gives a mixture of 66% 1,2-dichloro-3-butene and 33% 1,4-dichloro-2-butene (214), whereas the equilibrium mixture of these two isomers contains 70% of the 1,4 isomer (215). A clear example of both kinetic and thermodynamic control of products is seen in the acetolysis of cinnamyl chloride, which gives, after limited reaction, a mixture of cinnamyl and phenylvinylcarbinyl acetates but, on prolonged reaction, leads solely to cinnamyl acetate, the thermodynamically stable product (216).

$$C_6H_5CH{=}CH{-}CH_2Cl \xrightarrow{HOAc} C_6H_5\overset{\delta+}{C}H{\cdots}CH{\cdots}\overset{\delta+}{C}H_2 \longrightarrow \begin{cases} C_6H_5CH{=}CH{-}CH_2OAc \\ C_6H_5CH(OAc){-}CH{=}CH_2 \end{cases} \quad (25)$$

The fact that the carbonium ion intermediates in these reactions appear to combine with anions in such a way that the less stable isomer is formed more rapidly has been enunciated as a general rule (217). However, it is difficult to conceive that the vagaries of charge distribution will necessarily result in such a distribution of charge in the intermediate that the reaction with an anion will always lead to the thermodynamically unstable isomer. It must be admitted, however, that there are many examples conforming to this generalization involving both cationic and anionic intermediates (218).

A similar situation has been postulated for the base-catalyzed reactions of methyl ketones in which a proton can be removed from either of two different carbon atoms adjacent to the carbonyl group. Alkyl methyl ketones lose a primary proton in base-catalyzed iodination, aldol condensation, Claisen condensation, and carboxylation reactions but lose a secondary proton in the base-catalyzed reaction with dimethyl sulfate. The difference has been attributed (219) to the fact that, in the former reactions, which are all fast reactions, kinetic control of intermediate formation occurs; that is, the faster rate of removal of the primary proton determines the ultimate product. On the other hand, the latter reaction, a slow reaction, forms that intermediate ion which is the most stable, the secondary enolate ion.

An important example of differing product distributions under differing reaction conditions, leading to a thermodynamic distribution of products in one instance and a "nonthermodynamic" distribution under other con-

ditions, occurs in the isomerization of methylbenzenes with hydrogen fluoride and boron trifluoride (220). When roughly one-tenth mole of BF_3 is used per mole of a xylene, approximately 60% *m*-xylene is formed irrespective of which xylene is used as reactant. On the other hand, when approximately 3 moles of BF_3 is used per mole of xylene, 100% *m*-xylene is formed. The thermodynamic equilibrium composition of *m*-xylene, determined in the gaseous phase, is 57%, which is in good agreement with the former figure, indicating that, under the first set of isomerizing conditions, thermodynamic equilibrium is attained. The 100% yield of *m*-xylene, produced with an excess of boron trifluoride, is explained by postulating the formation of an intermediate (XVII) from xylene, hydrogen fluoride, and boron trifluoride:

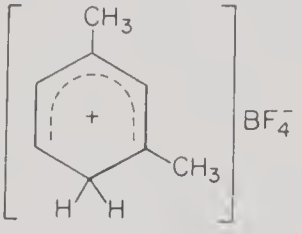

(XVII)

This intermediate would be soluble in the acid phase of this two-phase reaction system and would thereby be in equilibrium among the various isomeric salts. This equilibrium of xylene salts would be expected to be different from the gas-phase equilibrium of the parent xylene compounds, and, indeed, it appears that the former equilibrium contains essentially 100% of the ionic compound illustrated above.

The examples of multiple-product formation, which are dependent on a competition between thermodynamic and kinetic control or between two kinds of thermodynamic control, are fairly persuasive arguments for intermediate formation. In most cases given above, there is partitioning of an intermediate in one fashion or another. A necessary condition for acceptance of these examples of multiple-product formation as evidence for intermediate formation is that the partitioning follows predictable rules of chemical behavior.

(3) Constant Ratios of Products. A convincing argument for intermediate formation based on product identification is illustrated by the data of the solvolysis of *tert*-alkyl halides, carboxylates, and dimethylsulfonium salts. In general, it can be said that the ratio of olefin formation to substitution product is constant in the unimolecular solvolysis of corresponding *tert*-alkyl derivatives, including chlorides, bromides, benzoates, mesitoates, and dimethylsulfonium salts, whereas the rates of the various reactions are quite different, as seen in Table V. Since the elimination fraction is

TABLE V
Fraction of Elimination in the Solvolysis of Some *tert*-Alkyl Derivatives in 80% Ethanol

Compound	Temperature, °C.	Fraction elimination
Chloride (221)	50	0.403
Dimethylsulfonium salt (221)	50	0.478
Benzoate (222)	49	0.38, 0.40

independent of the leaving group in these reactions, whereas this is distinctly not the case in known bimolecular nucleophilic reactions leading to elimination (223), the conclusion is reached that a common intermediate is formed in each of these reactions; this intermediate must, of course, be partitioned in identical fashion in each case.

A similar argument has been made in the Friedel-Crafts benzoylation of toluene (224). In this reaction, the relative rates of reaction utilizing various metallic chlorides varied over five powers of ten. However, the isomer distribution in all cases was closely similar. It was therefore concluded that identical partitioning of a common reaction intermediate, a benzoyl acylium ion, determines the common product formation, whereas the differences in reaction rates are due to differing rates of formation of the intermediates.

(4) **The Rate-Product Criterion.** The solvolysis of *p,p'*-dimethylbenzhydryl chloride in 85% aqueous acetone, a reaction that has been discussed earlier from the point of view of salt effects on the kinetics of the reaction, illustrates an important point with regard to product formation as a criterion for intermediate formation. In the presence of 0.051*N* sodium azide, the rate of the reaction is unaffected (except for a normal ionic strength effect), but the product changes from pure alcohol to 60% alkyl azide. The existence of a direct, additional mode of reaction of the alkyl chloride leading to the alkyl azide should cause a corresponding increase in the rate of reaction of the alkyl chloride. The fact that an appreciable amount of the azide is formed with no effect on the rate is strong evidence for the partitioning of an unstable intermediate. This "rate-product" criterion for intermediate formation is a classical contribution of Ingold and is the progenitor of many variants in arguments described here for postulating intermediate formation. This criterion for intermediate formation is intimately related to the evidence obtained in cases in which the stoichiometry and kinetic order of a reaction differ from one another, a situation discussed extensively in Section IV.1.A.

(5) **Diagnostic or Trapping Reactions.** Diagnostic reactions are useful in demonstrating the existence of a reactive intermediate. The specific nature of the diagnostic reaction for the species in question must, of course,

be demonstrated. This can sometimes be done through the reactions of known, stable analogs of the reactive species under consideration.

The classic work by Paneth in the removal of lead mirrors by gaseous free radicals (224a) such as methyl, ethyl, or benzyl radicals is an example of a diagnostic reaction. The reaction

$$4R\cdot + Pb \rightleftharpoons R_4Pb \qquad (26)$$

is a specific process, which offers convincing, although circumstantial, evidence for the formation of alkyl free radicals in the thermal decomposition of organometallic compounds. The mirror-trapping method has been used for the detection of a large number of free-radical intermediates in the gas phase, produced by the thermal decomposition of such organic compounds as hydrocarbons, alcohols, aldehydes, ketones, ethers, and diazomethane (225).

The reaction with lead and other metallic mirrors is probably the only general method for the trapping of free-radical intermediates in the gas phase. Other methods are more specific. For example in the vapor phase decomposition of di-*tert*-butyl peroxide, the first-order kinetics and activation energy are consistent with a rate-determining scission of the oxygen-oxygen bond. This hypothesis was put on firm ground by the trapping of the free radical intermediate, *tert*-butoxy radical as *tert*-butyl alcohol (Eq. 27) upon the introduction of a hydrogen donor, isopropylbenzene

$$2(CH_3)_3CO\cdot + 2C_6H_5CH(CH_3)_2 \rightarrow 2(CH_3)_3COH + [C_6H_5C(CH_3)_2]_2 \qquad (27)$$

(226). The products isolated in this instance are of course different from the products normally obtained in the process without the addition of a hydrogen donor:

$$\begin{aligned} (CH_3)_3CO\cdot &\rightarrow (CH_3)_2C{=}O + CH_3\cdot \\ 2CH_3\cdot &\rightarrow CH_3CH_3 \end{aligned} \qquad (28)$$

Although the principal products of decomposition are acetone and ethane, evidence for methyl radical formation was obtained by the isolation of some methane and of methyl ethyl ketone, which can be formed by the reaction of methyl radical with acetone to form acetonyl radical, which can then combine with methyl radical. More direct evidence for the formation of methyl radical was obtained by trapping the methyl radical with nitric oxide, leading to formaldoxime, isolated and characterized as the trimer hydrochloride. Thus the two reactive intermediates in this decomposition were trapped by reasonably specific reactions of the intermediates.

A number of "oxy" free-radical intermediates have been trapped by reactions with 2,4,6-trisubstituted phenols. For example, the benzoyloxy radical was trapped as the dienone derivative (Eq. 29) (227). In addition,

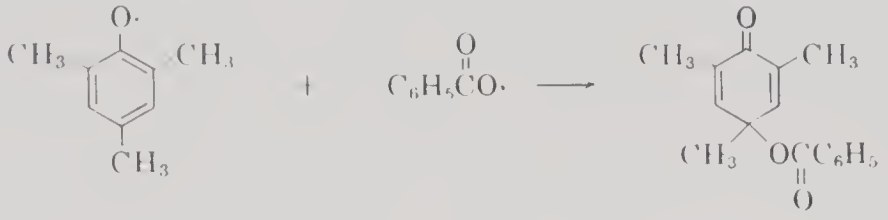

(29)

the *tert*-butylperoxy radical, the hydroperoxy radical (228), and the peroxy radical in the autoxidation of cumene (229) were trapped in a similar fashion by reaction with 4-methyl-2,6-di-*tert*-butylphenol. The reactions above proceed presumably through phenoxy radicals. Reactions of phenols as antioxidants are thus seen to be related to the trapping of the chain carrier, the alkylperoxy radical.

Radical scavengers other than phenols are frequently utilized for the trapping of free-radical species in solution. An important study of the decomposition of benzoyl peroxide in the presence of iodine indicated that the primary dissociation product is the benzoyloxy free radical since essentially 100% of the starting material is recovered as benzoic acid in moist carbon tetrachloride (230) without the interceptor, iodine, influencing the rate or kinetic form of the decomposition:

$$(C_6H_5CO_2)_2 \xrightarrow{\text{slow}} 2C_6H_5CO_2\cdot$$

$$2C_6H_5CO_2\cdot + I_2 \xrightarrow{\text{fast}} 2C_6H_5CO_2I$$

$$C_6H_5CO_2I + H_2O \xrightarrow{\text{fast}} C_6H_5CO_2H + HOI \qquad (30)$$

In studying the thermal decomposition of azo-bis-isobutyronitrile, a number of radical scavengers such as 1-butanethiol, iodine, oxygen, and 2,2-diphenylpicrylhydrazyl were utilized as radical scavengers. It was possible to carry out quantitative efficiency measurements with the last three scavengers. It was demonstrated that an appreciable fraction of the pairs of radicals produced in the thermal decomposition reaction react with each other before they diffuse apart, thus leading to incomplete capture of the radicals (231). In conclusion, it can be said that there is a fairly wide range of radical scavengers or trapping agents that can be utilized to detect free-radical intermediates.

Although trapping reactions have been particularly successful in dealing with free-radical intermediates, there are also examples of the trapping of ionic intermediate species; a few illustrative cases will be cited. It has been postulated that the addition of bromine to an olefin consists of the addition of a bromine cation in the rate-controlling step to yield an intermediate ion. It would be expected that this intermediate would then rapidly react with any available nucleophilic reagent, as has been found in

the reaction of ethylene with bromine in aqueous solution in the presence of sodium chloride or of sodium nitrate (232).

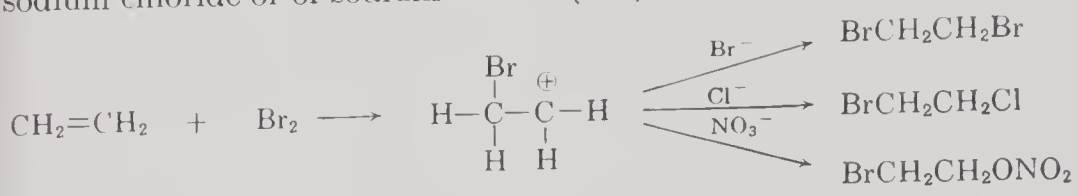

(31)

In the oxynitration of benzene in the presence of mercuric nitrate, the postulated benzenediazonium ion was trapped by means of its facile reaction with *N*,*N*-dimethylaniline, producing an easily detectable azo dye (56).

The formation of *cis*-cyclohexeneacetoxonium ion in the solvolysis of *trans*-2-acetoxycyclohexyl-*p*-toluenesulfonate in ethanol solution (Eq. 32) has been postulated on the basis of stereochemical evidence to be discussed later. Its existence is corroborated by its trapping as *cis*-cyclohexeneethyl orthoacetate in the absence of other nucleophiles such as water or acetate ion which lead to ring opening (233). This diversionary reaction has also been accomplished in the reaction of the ketene acetal of *cis*-1,2-cyclohexanediol (234).

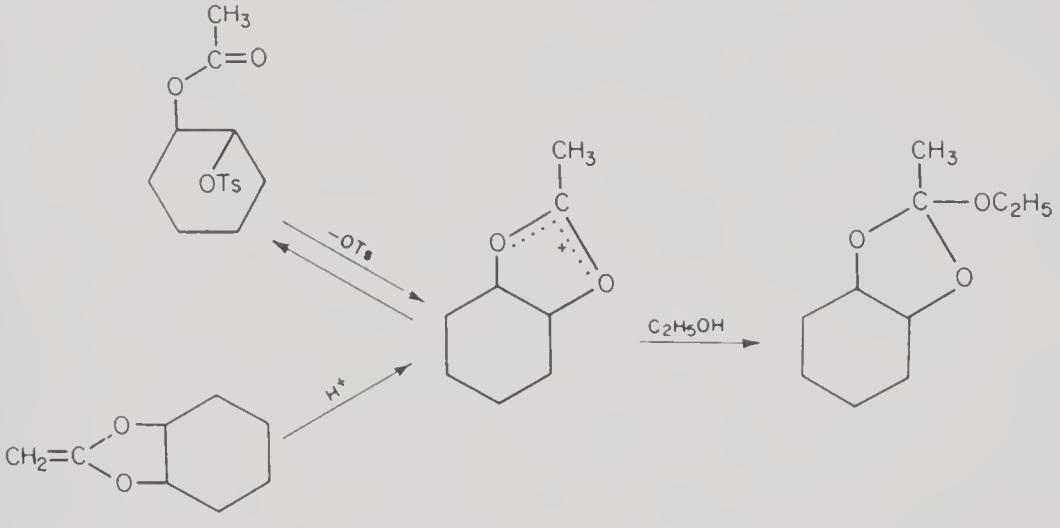

(32)

Evidence that the decarboxylation of quinaldinic acid involves an α-quinolyl carbanion comes from the observation that the decarboxylation in the presence of aldehydes and ketones produce α-quinolylcarbinols (235).

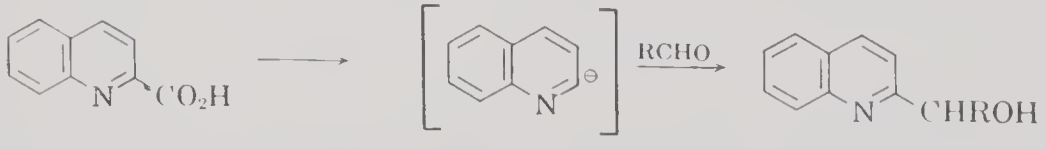

(33)

The proposed intermediate in the *p*-Claisen rearrangement, a dienone derivative in which the allyl group is attached to the *ortho* position, has been successfully captured by the dienophile maleic anhydride (238).

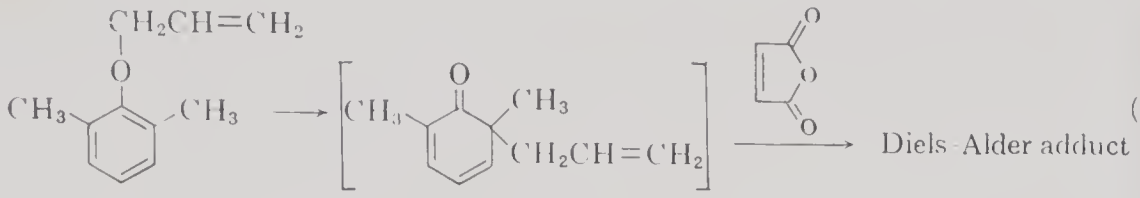

(34)

The diversion of a reactive intermediate by the trapping reactions described above is not the only type of diagnostic reaction that can be utilized for postulation of intermediate formation. For example, the initiation of other reactions has often been utilized as a criterion for intermediate formation. The polymerization reaction, in particular, has been used as such a diagnostic aid. It is known that polymerization can be brought about by nucleophilic, electrophilic, and radical species. Furthermore, copolymerization can distinguish among free-radical, electrophilic, or nucleophilic species in the polymerization of a mixture of styrene and methyl methacrylate: free radicals form a 50-50 copolymer of the two monomers; electrophilic species form polystyrene; and nucleophilic species form polymethyl methacrylate (237,238). The most important attribute of the polymerization reaction is its chain character, which makes polymerization an extremely sensitive criterion for the presence of reactive species capable of initiation.

(6) **Rearrangements.** Rearrangement of an organic compound involving the movement of alkyl groups or double bonds and possibly other substituents implies that some deep-seated electronic movements have also taken place. In order that these electronic changes occur, it is usually postulated that the normal covalent linkages of the organic molecule are markedly perturbed, facilitating the subsequent movement of electrons and groups. This description of rearrangement reactions implies that intermediates of other than normal valence may be involved or that charge delocalization may occur in an intermediate. Such a hypothesis has been proved to be true in a number of rearrangements investigated in detail.

A large majority of the rearrangements involving shifts in the carbon skeleton (so-called 1,2-shifts) have been explained on the basis of the formation of carbonium ion intermediates (239). The pinacol rearrangement and related reactions, the retropinacol rearrangement, the Demjanov rearrangement, the Hofmann rearrangement, the Lossen rearrangement, the Curtius rearrangement, the Wolff rearrangement, and the benzilic acid rearrangement are all explicable in terms of the intermediacy of a species containing an electron deficient atom (Eq. 35) (240). The postulation of such an intermediate is consistent with all the pertinent facts of these rearrangement reactions, including the specific effects of catalysts, the effect of solvent, and the effect of the leaving group. Although these rearrangements offer no conclusive proof of the intermediacy of a species containing

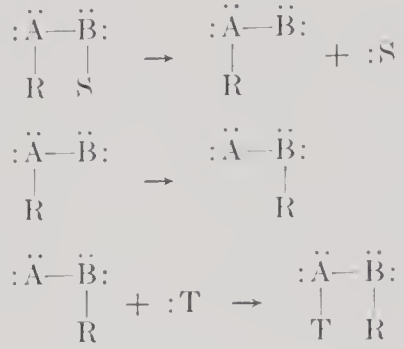

(35)

electron-deficient atoms, hypothesis of their formation in rearrangement reactions correlates and systematizes a rather large amount of material. In addition to the above rearrangements, the isomerization of paraffins such as butane in the presence of aluminum chloride catalyst has been postulated to proceed through carbonium ion intermediates on the basis that traces of olefins or their equivalent are necessary for reaction (241). On the basis of isotopic tracer evidence, to be discussed later, this picture may be an oversimplified version of the process.

Rearrangements resembling 1,2-shifts have also been noted in reactions involving carbanion (242) and free-radical (243) intermediates. The rearrangements per se again do not appear to offer any direct evidence for intermediate formation. But, again, one may say that the formation of rearranged products is adequately explained by the postulation of these reactive intermediates.

Charge delocalization often has straightforward chemical consequences. For example, the distribution of the charge between positions 1 and 3 in an allylic carbonium ion intermediate suggests that ionic recombination may involve either of these positions and, in a substituted allyl ion, may lead either to a product with the original position of the double bond or to a rearranged product. This approach is important in the detection of a rearranged reactant as well as a rearranged product. Each case has been discussed in another section.

Evidence for the formation of cyclic onium ions has been adduced from the products of some reactions of derivatives of mustard gas and nitrogen mustards. For example, the reaction of ethyl-1-hydroxy-2-propyl sulfide with hydrochloric acid yields a rearranged chloride (244).

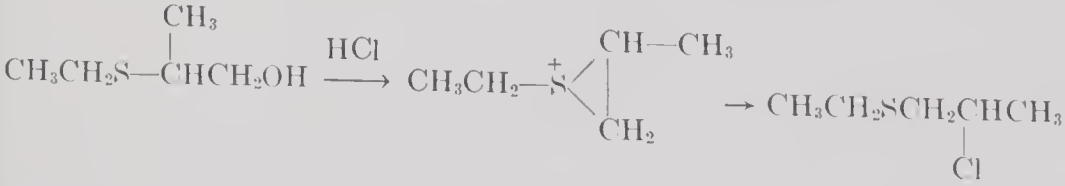

(36)

Likewise, the hydrolysis of *N*,*N*-diethylamino-2-chloropropane has been found to lead to a rearranged product (245). The postulation of sulfonium

ion and immonium ion intermediates in these rarrangement processes provides the simplest explanation for the products obtained in these cases.

In the reactions of α- or β-bromonaphthalene with sodium amide in the presence of piperidine, a mixture of both α- and β-naphthylpiperidines are obtained. Whereas a straightforward nucleophilic substitution process might explain the formation of the normal isomer, the additional formation of a rearranged isomer in each case leads to the postulation of an intermediate that is symmetrical with respect to the α- and β-positions (246).

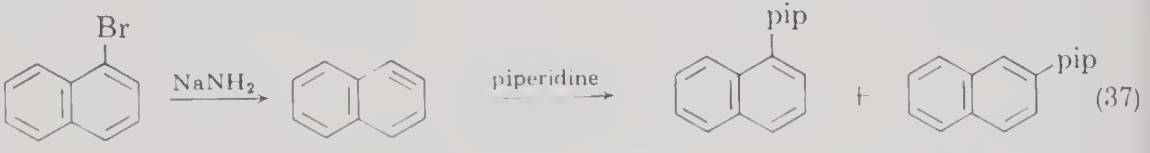

(37)

Such intermediates have been referred to as benzyne intermediates and will be discussed in more detail in Section IV.3.C.1.

A few examples have been given above of reactions yielding rearranged products, which have been explained on the basis of the formation of reactive intermediates. Numerous other examples could also have been cited. However, these examples should suffice to illustrate the general method of approach as well as the limited amount of information that can be obtained in this fashion. It is probably fair to say that any information on intermediates gleaned from the formation of rearranged products will, at best, exhibit consistency and, at the worst, lead to folly.

B. STEREOCHEMISTRY AS A CRITERION OF INTERMEDIATE FORMATION

The determination of the stereochemical changes that occur in both the reactants and products of a reaction has been of major importance as evidence for intermediate formation, particularly in carbonium ion reactions. Earlier, it was stated that a carbonium ion intermediate would be expected to assume a planar configuration. If such is the case, an optically active compound in which a single asymmetric carbon atom becomes a carbonium ion must produce racemic products, in contrast to a displacement reaction, which proceeds with inversion of configuration. This prediction has been borne out by the racemization of the hydrogen phthalate of *p*-methoxybenzhydrol in a number of solvents and in some solvolyses of esters of arylmethylcarbinols (247). However, the more usual experiments of this nature, involving the solvolysis of such materials as optically active 2-octyl bromide (248), α-phenethyl chloride (249), and hydrogen 2,4-dimethylhexyl-4-phthalate (250) yield partial racemization of variable amounts. The lack of complete racemization in these reactions has been explained (251) by the hypothesis that carbonium ions may react with the solvent before the departing halide ion is more than a few molecular diameters away

and will, therefore, be less likely to react at the front side because of the steric hindrance produced by the anion (the "shielding effect"). Shielding of the leaving group has also been couched in terms of the production of an ion pair. The results have alternately been explained in terms of two intermediates, each involving a "pentacovalent carbonium ion," in which both lobes of the p orbital of the carbonium ion overlap with orbitals of two nucleophiles. Each of these bonds is rather weak and should be considered, at best, as a half bond. The three remaining bonds are formed from sp^2 hybrid orbitals of the central carbon atom (250,251). One such intermediate, leading to inversion, will involve the leaving group in one of the split p orbitals and the solvent in the other split p orbital. The other intermediate, leading to racemization, will involve two solvent molecules in each of the two split p orbitals—a symmetrical configuration. There is a good deal of controversy concerning the details of this and allied subjects, including the occurrence of mixed versus intermediate mechanisms. (See Section I.4.) Consideration of these arguments is beyond the scope of this article. However, it can be said that much of the argument lacks operational definition and suffers from semantic difficulties. Certainly new kinds of evidence for intermediate formation for application in this particular area are badly needed. However, the explanation of any racemization must be associated with a symmetric intermediate of some variety, as noted above. Assuming no racemization of either reactants or products, it is probably justified to conclude that racemization during a reaction is evidence for (a trigonal or trigonal bipyramid) intermediate formation. However, the converse, no racemization, does not preclude the possibility of intermediate formation (252).

The stereochemistry of displacement reactions involving participation of neighboring groups has led to the postulation of cyclic intermediates in a number of solvolytic reactions. The symmetry characteristics of cyclic intermediates have led to the design of a number of very informative stereochemical experiments. Historically, the reactions of optically active α-bromopropionic acid and its derivatives are of interest. It was found that, in dilute alkaline solution in methanol, the solvolysis of the α-bromopropionate anion is first order, and the α-methoxypropionate anion formed has the same configuration as the starting material. Both the stereochemical and kinetic results are in direct contrast to reactions occurring in strong base or with the corresponding ester (253). The hydrolysis of this anion gave similar results. The results have been explained by the nucleophilic displacement of the bromide ion by the carboxylate anion of the same molecule, with the formation of a reactive α-lactone intermediate, which may then undergo a second nucleophilic displacement by solvent to give the final product with over-all retention of configuration (254).

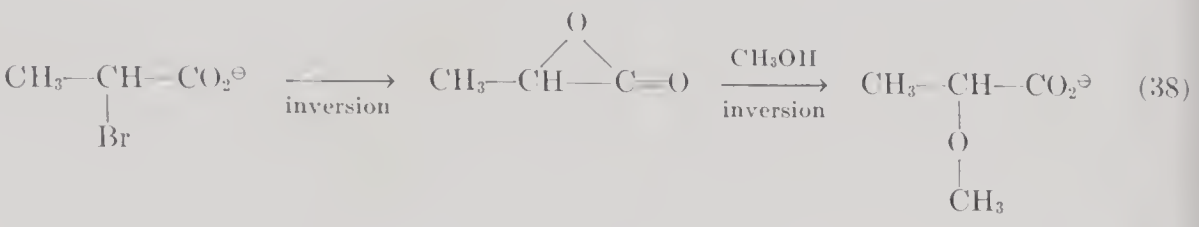

(38)

Addition of bromine to maleic acid yields the racemic dibromide (Eq. 39), whereas addition to fumaric acid gives the meso compound. These stereospecific addition reactions cannot result from simultaneous addition of two bromine atoms. The results have been explained on the basis that the intermediate cationic species is not a free carbonium ion but is rather a stereospecific bromonium ion intermediate (255). Not only does the formation of this intermediate satisfy the requirement of a stereospecific addition but it also satisfies the requirement of trans-addition, since the opening of the brominium ion ring by nucleophilic bromide ion will result in inversion. Conclusive stereochemical evidence for bromonium ion intermediates has been obtained in the reactions of fuming hydrobromic acid with optically active *erythro*-3-bromo-2-butanol and *threo*-3-bromo-2-butanol. The former compound yielded *meso*-2,3-dibromobutane, whereas the latter compound gave *dl*-2,3-dibromobutane (256). These stereospecific displacement reactions, which occur with over-all retention of configuration involving the two asymmetric centers, can be explained on the basis of inversion of configuration in both the formation and rupture of bromonium ion intermediates of the type shown in Equation (39). Of the numerous in-

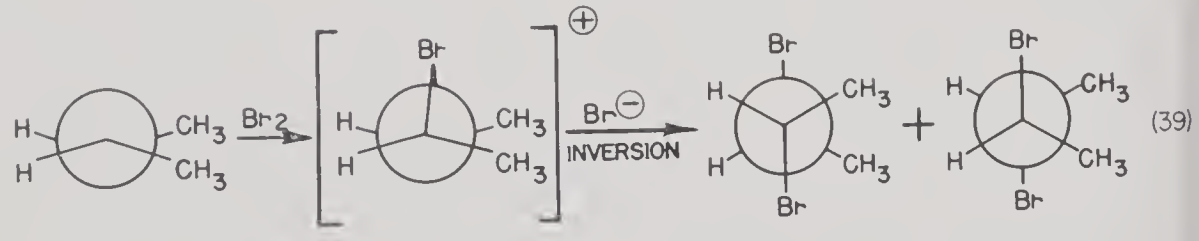

(39)

vestigations of this nature involving cyclohexyl derivatives, a typical example involves the solvolysis of *trans*-2-iodocyclohexyl-*p*-bromobenzenesulfonate, which, on the basis of over-all retention of configuration (as well as relative reactivity), has been postulated to proceed via an iodonium ion intermediate (257).

Stereochemical evidence points to the participation of neighboring aromatic groups in displacement reactions in a manner analogous to that described for the carboxylate group and halogen groups. The solvolysis of the stereoisomers of 3-phenyl-2-butyl tosylate illustrate the approach. Optically active *threo*-tosylate on acetolysis yields racemic *threo*-acetate (Eq. 40), whereas an active *erythro* form yields the acetate of the same active

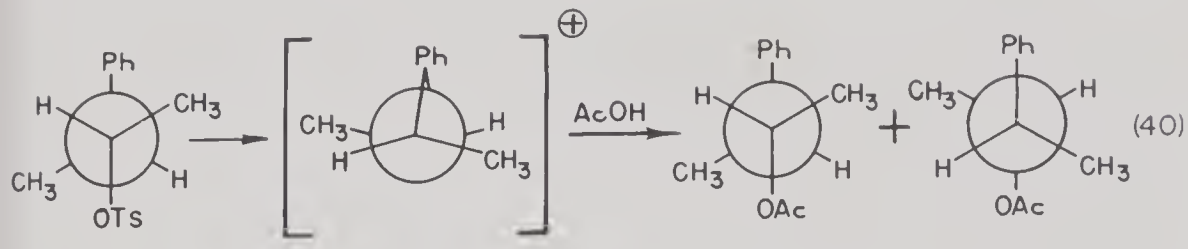

(40)

erythro-alcohol (Eq. 41) (258). Thus both reactions proceed with retention of configuration, but only in the *erythro* case is optical activity preserved.

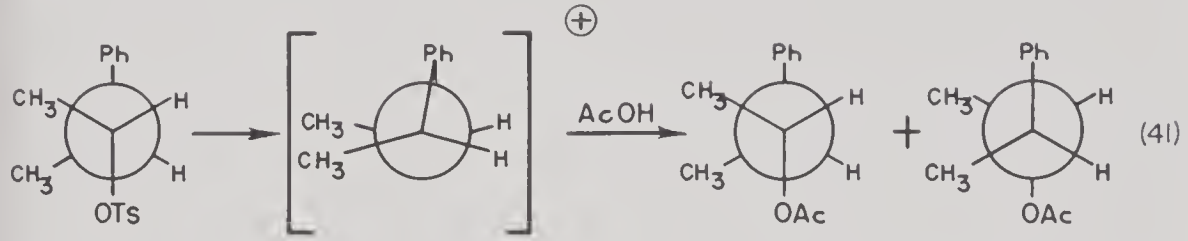

(41)

These results are interpreted in terms of the intermediate formation of phenonium ions as shown in the above sequences. The *threo*-compound yields a phenonium ion possessing a plane of symmetry, and reaction at either of the central carbon atoms then gives the *threo* acetate, but with loss of optical activity. No such plane of symmetry exists in the case of the *erythro* ion, and attack at either carbon atom yields the same optical enantiomer. A mechanism involving a rapid tautomeric equilibrium between two enantiomorphic 3-phenyl-2-butyl carbonium ions (Eq. 42) cannot be ruled out absolutely in the *threo* case (and also in other reactions

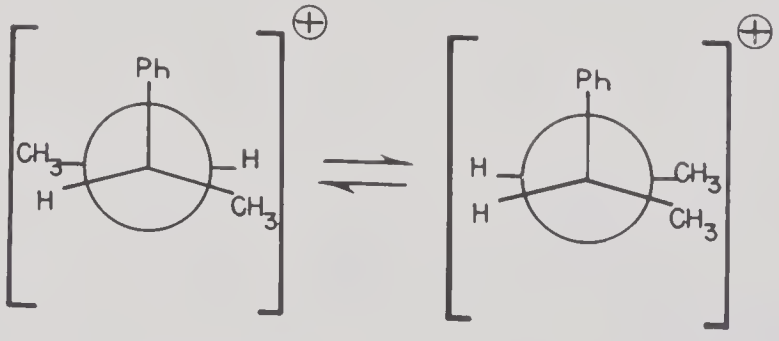

(42)

previously postulated to proceed through cyclic onium intermediates on the basis of the formation of *dl* mixtures). However, the relative reactivity data discussed previously provides evidence of anchimeric or synartetic assistance in reactions of other compounds involving phenyl groups, supporting the concept of phenonium ion intermediates.

Convincing stereochemical evidence for the participation of a saturated hydrocarbon radical in a nucleophilic displacement reaction on carbon is observed in the acetolysis of optically active *exo*-norbornyl-*p*-bromobenzenesulfonate, which yields racemic *exo*-norbornyl acetate (259). This

observation, in conjunction with the relative rate data discussed earlier, can be explained in terms of a bridged ion intermediate (Fig. 6F).

Ion-pair intermediates in solvolysis reactions have previously been postulated on the basis of salt effects. Evidence has also been advanced for the postulation of ion-pair intermediates on the basis of a disparity in the rates of racemization and product formation of optically active materials whose reactions involve nonclassical cationic intermediates. For example, in the solvolysis of optically active 3-phenyl-2-butyl-*p*-toluenesulfonate, both the polarimetric and titrimetric rate constants exhibit good first-order behavior, but the polarimetric racemization rate constant exceeds the titrimetric (product formation) rate constant by factors of 2.5 and 1.18 in ethanol and formic acid, respectively. The disparity in the two rate constants could possibly be explained by the incursion of a second simultaneous process, such as attack by *p*-tohuenesulfonate ion, but this was shown not to occur. Therefore, it was suggested that, for both processes, racemization and solvolysis, a common intermediate is involved, namely, a racemic ion pair, which can revert to the starting materials or can react with solvent to produce the solvolysis products (260). Likewise, during the solvolysis of optically active *exo*-norbornyl brosylate, the rate of loss of optical activity exceeded the rate of formation of *p*-bromobenzenesulfonic acid (a product) although both rates were accurately of first order (261). The results are again interpretable in terms of the formation of an initial intermediate ion pair. The values for the rate ratio k_2/k_3 at 25° (again a measure of the partitioning of an intermediate) are given for various solvents: acetic acid, 2.46; ethanol, 1.94; 75% aqueous acetone, 0.40 (244). Similar results have been obtained in the reactions of allylic systems. In the solvolysis of

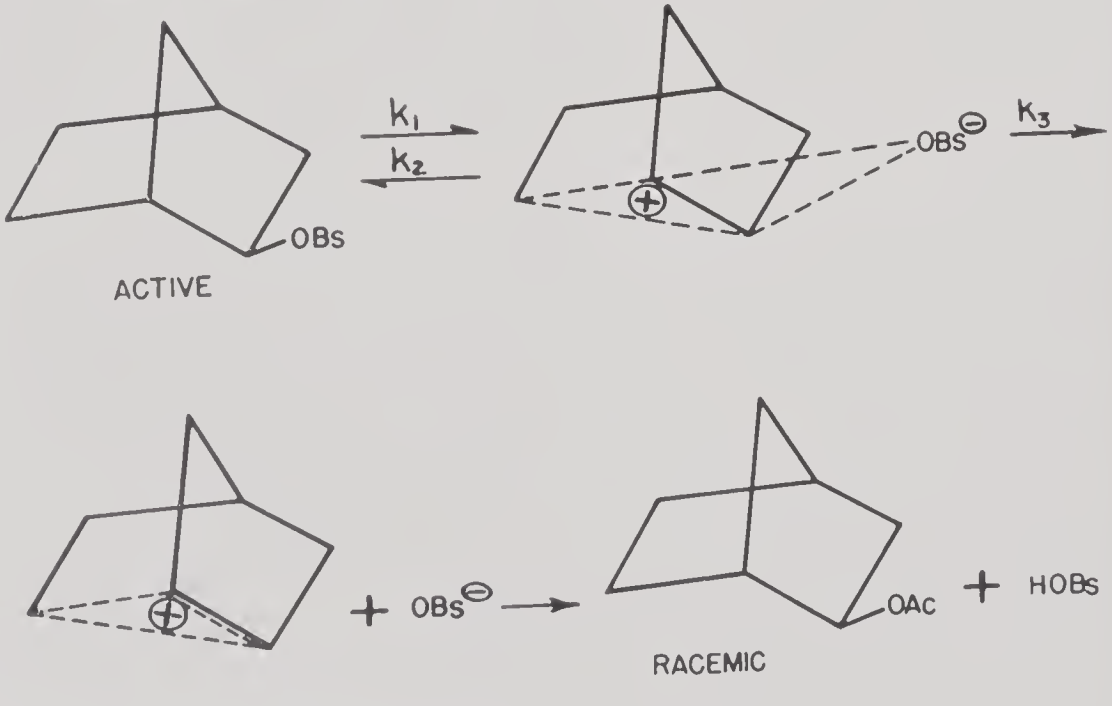

(43)

cis- or *trans*-3-chloro-5-methylcyclohexene in both ethanol and acetic acid, the same binary mixture of *cis*- and *trans*-solvolysis products is obtained. This result indicates a common (carbonium ion) intermediate for the solvolytic process. In these solvolyses it was further shown that the rate of loss of optical activity exceeds the rate of solvolysis, and, by isolation of the reactant after 0.7 life of racemization, it was shown that the racemization occurs without *cis-trans* isomerism. These facts, together with the negligible effect of chloride ion on the ratio of the polarimetric and titrimetric rate constants have led to the postulation of a second intermediate in the reaction scheme, a stereospecific ion pair (262) resulting in an over-all scheme involving two intermediates, one a stereospecific ion pair and the other a dissociated carbonium ion salt.

Other intermediates, which are predicted to assume a trigonal structure with sp^2 hybridization, would also be expected to lose optical activity originally present in the reactants. The chlorination of optically active 1-chloro-2-methylbutane was found to result in racemic 1,2-dichloro-2-methylbutane, pointing to the intermediate formation of a symmetrical free radical in this chain reaction (263). The results of this reaction also preclude the direct formation of the product by a free-radical displacement on carbon (Eq. 44). Likewise, it was found that the decarbonylation of optically active methylethylisobutylacetaldehyde in the presence of *tert*-

$$\mathrm{CH_3{-}CH_2{-}\underset{\displaystyle CH_3}{\underset{|}{C}}HCH_2Cl + Cl\cdot \rightarrow HCl + CH_3CH_2{-}\underset{\displaystyle CH_3}{\underset{|}{\overset{\displaystyle \cdot}{C}}}{-}CH_2Cl}$$

not

$$\mathrm{CH_3CH_2{-}\underset{\displaystyle CH_3}{\underset{|}{C}}HCH_2Cl + Cl\cdot \rightarrow CH_3CH_2{-}\underset{\displaystyle Cl}{\underset{|}{\overset{\displaystyle CH_3}{\overset{|}{C}}}}{-}CH_2Cl + H\cdot} \qquad (44)$$

butyl peroxide yielded racemic 2,4-dimethylhexane, again indicating the presence of a racemic intermediate free radical (264).

Comparable experiments to determine the possible loss of optical activity in reactions presumed to involve carbanion intermediates have also been carried out. It was shown, for example, that optically active phenyl *sec*-butyl ketone undergoes racemization and bromination at the same rate in the presence of acetate ion (265). This result provides good evidence for the formation of an enolate ion intermediate, since it has been shown that comparable anions, such as anions of *sec*-nitroparaffins are racemic (266). Carbanion intermediates have been shown, however, to retain their optically active configuration; the *trans*-butenyl anion exhibits 91% retention at $-15°$; the 2-octyl anion exhibits 20% retention at $-70°$; a cyclopropyl anion exhibits 60% retention at 6° (226a).

In the simple Wurtz reaction involving metallic sodium and an alkyl halide, presumably an alkyl sodium intermediate is formed first and subsequently reacts with additional alkyl halide to yield the coupled product. The mode of formation of the alkyl sodium is not entirely clear, but there is little doubt that the over-all reaction proceeds predominantly by way of a displacement reaction involving an alkyl sodium intermediate, since it has been shown that the Wurtz reactions of optically active α-phenylethyl chloride (267) and 2-chlorobutane (268) give optically active hydrocarbon coupling products. Furthermore, it has been shown that the simple Wurtz reaction, involving sodium and 2-chlorooctane, involves an inversion of configuration of the carbon atom bearing the chlorine (269). These pieces of stereochemical evidence indicate that the Wurtz reaction does not proceed through the coupling of any (free radical) intermediates, which would be expected to yield a racemic product, but rather through the formation of an alkyl sodium intermediate, followed by a nucleophilic displacement of optically inactive alkyl sodium intermediate on the second molecule of optically active alkyl halide.

$$\begin{aligned} 2\mathrm{Na} + \mathrm{RX} &\rightarrow \mathrm{RNa} + \mathrm{NaX} \\ \mathrm{RNa} + \mathrm{RX} &\rightarrow \mathrm{R{-}R} + \mathrm{NaX} \end{aligned} \tag{45}$$

C. ISOTOPIC INVESTIGATIONS AS CRITERIA OF INTERMEDIATE FORMATION

(1) **Isotopic Tracer Methods.** The use of isotopic tracers has given new degrees of freedom to the investigation of structural changes that occur during a reaction process. In recent years, a multitude of investigations using both stable and radioactive isotopic tracers have elucidated various aspects of mechanism, including the question of intermediate formation. In some investigations it has been of interest to determine the fate of the isotopic tracer in the reactant as the reaction proceeds, as well as to determine the fate of the tracer in the products. Isotopes of carbon, oxygen, and hydrogen have been most commonly used in these studies. Some of the important approaches that have been successfully used to gain evidence for intermediate formation via isotopic tracers will be presented (270).

A great deal of work has been carried out with carbon isotopes, both with the stable carbon-13 and the weak beta emitter, carbon-14, mostly pointed toward the elucidation of carbonium ion intermediates. The isomerization of carbon-13-labeled *n*-butane over a water-promoted solid aluminum bromide catalyst gave a distribution of products in which carbon-13 was statistically distributed between the 1 and 2 positions of both the isobutane and the *n*-butane; that is, the ratio of butane-*1*-C^{13} to butane-*2*-C^{13} was 1:1, and the ratio of methylpropane-*1*-C^{13} to methylpropane-*2*-C^{13} was 3:1. When the reaction was stopped before thermodynamic equilibrium

between the butane isomers was achieved, the statistical distribution of carbon-13 in the isobutane was still observed (271). These observations are completely incompatible with observations on the rearrangement of 2-methyl-2-chlorobutane-*1*-C^{14} and similar compounds with aluminum halide in the liquid phase (272). Under the latter conditions, an equilibrium distribution of the isotope between the 1- and 4-positions was obtained with only a trace appearing at the 2- or 3-position. The latter results are explicable on the basis of the formation of carbonium ion intermediates, for it might be expected that the *tert*-amyl carbonium ion formed in the reaction would equilibrate.

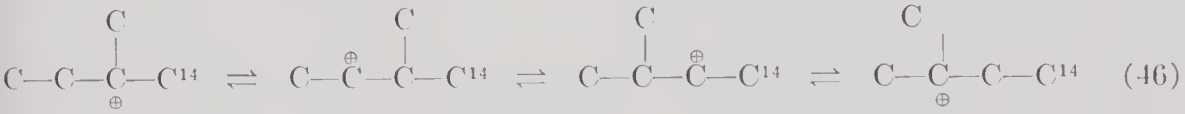

(46)

On the other hand, the statistical distribution of the isotopic tracer between the various positions obtained in the former experiment cannot be explained in a straightforward manner, since it necessitates the breaking of the rules of the relative stability of carbonium ions. The statistical distribution might suggest that an intermediate or transition state is formed in which all carbons in the butane are equivalent to one another, but this is pure conjecture. It is conceivable that the difference between the two sets of reaction conditions might lead to different isotopic results, with the movement of the tracer in the former case greater than in the latter, because of the greater severity of conditions in the former case.

As indicated in the section on stereochemistry, certain intermediates such as nonclassical carbonium ions may have different symmetry characteristics from those of the corresponding classical structures. As a consequence, positions which are nonequivalent in the starting molecule or even in the classical carbonium ion intermediate may become equivalent in the nonclassical ion intermediate, leading to a distribution of an isotopic tracer among several positions in the product.

Isotopic tracer evidence in the acetolysis of *exo*-norbornyl-*p*-bromobenzenesulfonate has required that the non-classical structure of the carbonium ion intermediate (XVIII), suggested before on the basis of the relative rate of the reaction and the stereochemical consequences of the reaction, be modified. The nonclassical carbonium ion intermediate (XVIII) implies the equivalence of positions 1 and 2 and of positions 3 and 7. A reaction utilizing a compound labeled with carbon-14 at positions 2 and 3 thus predicts a product in which the isotopic tracer is equally distributed in positions 1, 2, 3, and 7. Upon degradation of the product, carbon-14 was found in positions 1, 2, 3, 7, and, in addition, 15% of the total radioactivity was found in positions 5 and 6 (273). The isotopic distribution in the products

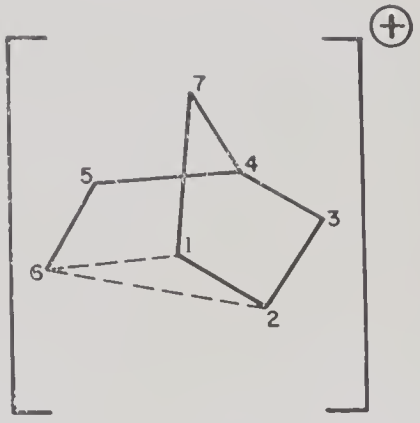

(XVIII)

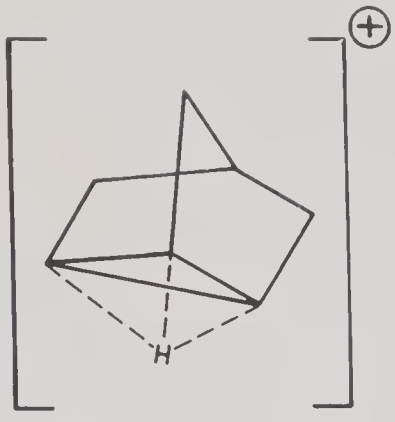

(XIX)

can be explained by the formation of an intermediate (XIX), which processes a higher degree of symmetry than (XVIII). The formation of intermediate (XIX) implies the shift of a hydrogen from position 2, which may accompany the formation of the intermediate (XVIII) or which may follow it. A possible pitfall in this argument, as in other arguments based on symmetry considerations, is that the structure possessing the complete symmetry requirements of the system, whether determined by stereochemical evidence or isotopic tracer evidence, may be either a transition state or an intermediate. That is, the equilibrium position of the hydrogen in intermediate (XIX) could alternately be explained, and has been explained, by an equilibrium mixture of nonclassical carbonium ions of the type (XVIII). These alternative explanations differ essentially in the question of whether the form bearing the highest requirement of symmetry be a transition state or a n intermediate in the over-all process. This problem is a difficult and fundamental one in a number of situations and will be discussed in detail later.

Cyclopropylmethyl derivatives undergo solvolysis very rapidly and lead to a mixture of products, including allylcarbinyl, cyclopropylcarbinyl, and cyclobutyl derivatives (274,275). Deamination of cyclopropylcarbinylamine gave the corresponding three alcohols. Deamination of cyclopropylcarbinyl-C^{14} amine gave a cyclobutanol in which the three methylene carbon atoms had equivalent amounts of carbon-14 activity. This isotopic distribution, coupled with the enhanced rate of reaction, strongly suggests the following nonclassical carbonium ion intermediate (XX) in this solvolysis.

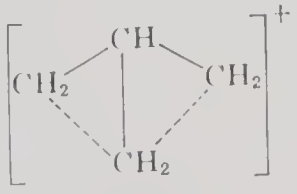

(XX)

From isotopic tracer work, there appears no clear-cut positive evidence, and in some instances clear-cut negative evidence, as to the formation of nonclassical ions in the rearrangements of "simple" aliphatic compounds. The deamination of a number of 2-substituted-ethylamine-*1*-C^{14} molecules, in which the substituents were hydrogen, methyl, and various phenyl groups, led to carbon-14 in the 2-position of the product, indicating the occurrence of some rearrangement in all cases (276,277). However, in no case did the isotopic distribution between the 1- and 2-positions suggest the formation of a completely symmetrical intermediate that could be partitioned equally in each direction. The various possible bridged carbonium ions, here involving a hydrogen, methyl, or phenyl bridge, must be rejected as intermediates. For even in cases where completely symmetrical distribution of the isotopic tracer occurs, the occurrence of an intermediate of the required symmetry is not mandatory. In the present cases, where symmetrical distribution of the isotopic tracer is far from being achieved, there is little reason for the postulation of a bridged intermediate.

Carbon-14 tracer experiments have indicated that the bridged phenonium intermediate is not always formed in the rearrangement of phenyl groups. In the solvolysis of 1,2,2-triphenylethyl derivatives, labeled with carbon-14 in the 1-phenyl group, the distribution of carbon-14 in the product indicated a random distribution of the isotopic tracer among all three phenyl groups. A 50-50 distribution of the carbon-14 tracer would have been expected between the two halves of the ethyl group if a phenonium (bridged) intermediate were formed. Therefore, one is forced to explain the results in terms of the equilibration of open-chain (classical) carbonium ions (278). On the other hand, the deamination of 2-amino-3-phenylbutane-*1*-C^{14} yielded a phenyl migration product 3-phenyl-2-butanol-*1,4*-C^{14}_2, in which the carbon-14 was equally distributed between the 1- and 4-positions, as would be predicted by the intermediacy of a phenonium ion (279). The difference in these two systems may be rationalized by saying that, in the former system, the open carbonium ions are stabilized via their benzylic character, whereas, in the latter system, the phenonium ion is stable relative to the open phenylethyl carbonium ions.

The Favorskii reaction of an α-haloketone with alkoxide ion to yield a (rearranged) ester was investigated with the aid of carbon-14 in the position to which the halogen was attached. In the final product, this position is radiochemically equivalent to another one, which was the α' position of the original ketone. This result may be most readily explained by the postulation of a cyclopropanone intermediate, which has the proper symmetry characteristics (280).

A striking isotopic tracer result is seen in the reaction of chlorobenzene-*1*-C^{14} with potassium amide in liquid ammonia which produces aniline-*1*-C^{14}

and aniline-*2*-C^{14} in equal amounts (281). This result implies that an intermediate is formed, in which positions 1 and 2 are equivalent to each other. The kinetic isotope effect for the *ortho* hydrogen shows k_H/k_D to be equal to 5.7, indicating a cleavage of the *ortho* carbon-hydrogen bond in the rate determining step. These two pieces of information supply good evidence for the intermediate formation of an electrically neutral benzyne intermediate.

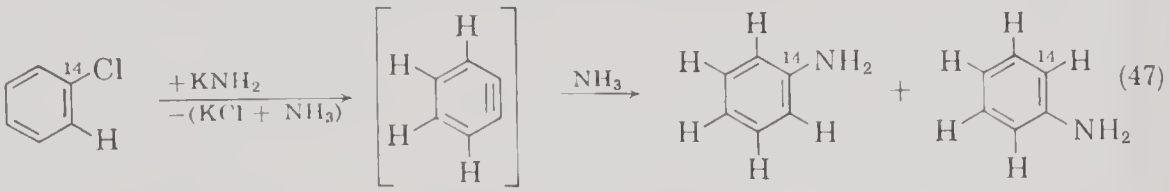

In a similar fashion, it has been shown that cyclohexyne is an intermediate in the coupling of phenyl lithium with 1-chlorocyclohexene labeled with carbon-14 in the 2- and 6-positions (282). It should be pointed out that product analysis of the reaction of bromonaphthalenes with a strong base has indicated the presence of the benzyne intermediate, without the use of isotopic tracer methods (269). In the latter case, the asymmetry of the naphthalene nucleus served the same purpose as the isotopic tracer in the benzene series. There does not seem to be any important reason for using an isotopic tracer in a situation such as that above in which structural asymmetry can be provided without influencing the reaction. In other systems, the use of an isotopic tracer is an absolute necessity.

Another example of the postulation of an intermediate on the basis of the distribution of an isotope among potentially equivalent positions is seen in the reaction of methyl benzoate-*carbonyl*-O^{18} and α-phenylethyldimethylamine (282a). Oxygen-18 was distributed equally in the two oxygen atoms of the product of this reaction, α-phenylethyl benzoate, indicating that the two oxygen atoms of the original ester had become equivalent to one another during the reaction. The formation of a benzoate ion intermediate satisfies this requirement.

Isotopic criteria have been used for the postulation of ion pairs as intermediates in various reactions. For example, the reaction of benzoic anhydride-*carbonyl*-O^{18} with aniline in ether solution yielded benzoic acid and benzanilide with a statistical oxygen-18 composition. This result indicated that the oxygen-18 in the anhydride, originally in the carbonyl position only, had been completely equilibrated among all three oxygen atoms of the anhydride. The complete scrambling of the oxygen atoms in the anhydride can be most easily explained by the formation of an ion-pair intermediate (XXII), following the formation of an addition intermediate (XXI), since the ion pair necessitates an equilibration of the carbonyl and alkoxyl oxygens of the original anhydride (283).

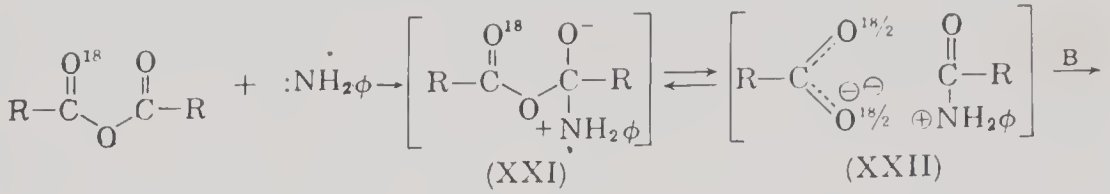

(XXI) (XXII)

$$RC(=O)NH\phi + RCO_2^- + BH^+ \qquad (48)$$

In the isomerization of 9-decalyl perbenzoate-*carbonyl-O*^{18} to the corresponding acylal, it was observed that the oxygen-18 remained as carbonyl oxygen (284). In the isomerization of 2-phenyl-1-propylbromobenzenesulfonate and 2-anisyl-1-propyltoluenesulfonate during acetolysis, two different tracer results were obtained. In the former case, the alkyl oxygen atom in the rearranged ester is 57% the original alkyl oxygen in the corresponding alcohol and 43% one of the other oxygen atoms. With the 2-anisyl-1-propyl ester, the three oxygen atoms of the toluenesulfonate group have become equivalent in the rearranged ester (285). All three reactions are presumed to involve ionization to an ion pair. The differences in oxygen-18 results have been explained on the basis of the nature and behavior of the ion pairs in the several cases. In the perbenzoate case, it is suggested that the ion-pair intermediate has a preferred orientation (with respect to oxygen atoms), which accounts for the isotopic tracer results. The difference in the oxygen-18 results with the arenesulfonates is consistent with the fact that some specific orientation of oxygen atoms is observed in the isomerization in which intimate ion-pair formation occurs (the 2-phenyl-1-propyl system), but complete equilibration of oxygen atoms occurs in that isomerization in which external ion-pair formation also occurs, (the 2-anisyl-1-propyl analog) (286).

Oxygen-18 tracer studies have been utilized to provide evidence for anhydride intermediates in various general modes of catalysis of ester and amide hydrolysis. Equation (49) illustrates a double-label experiment, in

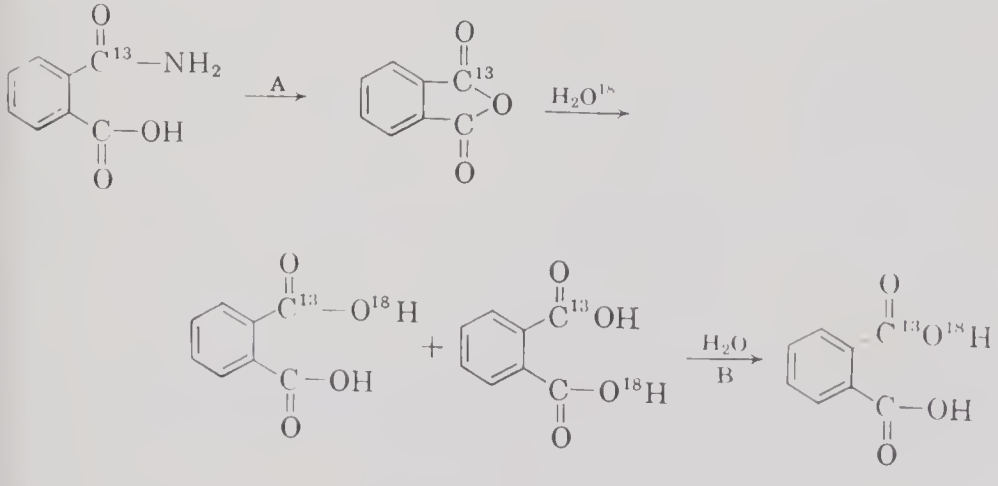

(49)

which a C^{13}-labeled amide was treated with O^{18}-labeled water. If the water (H_2O^{18}) attacks the phthalamic acid amide group directly, as in an ordinary amide hydrolysis (Path B), all the oxygen-18 would occupy the carboxylic group labeled with carbon-13. If, on the other hand, the water attacks the symmetrical phthalic anhydride intermediate, the oxygen-18 atoms will be equally divided between the two carboxylic acid groups as shown in Path A, leading to a different distribution of carbon dioxide isotopes on decarboxylation, which was found experimentally (287). In the hydrolysis of aspirin in H_2O^{18} (Eq. 23), the hypothetical mixed anhydride should cleave to the extent of 6% at the ring carbonyl position (calculated from the relative reactivities of ethyl acetate and ethyl salicylate). Oxygen-18 was found in the salicylic acid product, corresponding to 6% cleavage at this position (288). In the reaction of acetate-O^{18} ion and 2,4-dinitrophenyl benzoate, the hypothetical mixed anhydride acetylbenzoyl anhydride should cleave at the acetyl carbonyl position to the extent of 94% (calculated from the reactivities of the corresponding esters). Oxygen-18 was found in the benzoic acid, corresponding to about 75% cleavage at the position noted (289). This indirect tracer evidence for the formation of anhydride intermediates again depends on observations deduced from the symmetry properties of the postulated intermediate.

There are innumerable examples of the use of isotopic tracer experiments as evidence for intermediate formation in biochemical systems. Such systems encompass various intermediary metabolic cycles, the biogenesis of alkaloids, and other naturally occurring substances and the photosynthetic cycle. Some of the more elegant methods of approach have been developed in the investigations of Calvin on the path of carbon in photosynthesis (290). Investigations have been made of the radiocarbon uptake of the algae *Chlorella* and *Scenedesmus* in the presence of carbon dioxide-C^{14}. By the use of a combination of tracer studies and paper chromatography–radioautography, a large number of compounds have been identified as products of carbon assimilation during short periods of photosynthesis (one minute or less) using $C^{14}O_2$. A number of compounds including amino acids, carboxylic acids, hexose and triose phosphates, phosphoglyceric acid, etc., known in the field of intermediary metabolism, were identified, as well as two heretofore unknown sugar phosphates, ribulose diphosphate and sedoheptulose monophosphate. By varying the time of exposure of the plant to $C^{14}O_2$, by varying the external conditions such as temperature and carbon dioxide pressure, and by the use of chemical inhibitors, a pattern of carbon fixation was determined in terms of the distribution of C^{14} among compounds and among carbon atoms within each compound. From this data, a photosynthetic carbon reduction cycle has been proposed by Calvin, involving about 12 intermediate compounds and as many en-

zymatic reactions. The carbon-14 in this work was used as a tracer in the sense described in the rest of this section and also as a tagging agent to assist in the isolation or identification of intermediates, a widely applicable and powerful approach.

(2) **Isotopic Exchange Methods.** Throughout this work, a recurrent theme has been emphasized: that indirect evidence for intermediate formation can be obtained from experiments designed to observe the partitioning of intermediates. A successful method for observing such a partitioning is to observe the isotopic exchange reactions (with the solvent or with added ions) that may accompany a main reaction process. Isotopic exchange occurring concurrently with the formation of reaction products could *a priori* occur by a separate parallel reaction path, in which case its occurrence would have no bearing on intermediate formation, or it could occur by the partitioning of an intermediate formed in the reaction. The equivalence of the rates of isotopic exchange and product formation can be used to argue for the partitioning of an intermediate, for it would be fortuitous if the two processes of exchange and product formation would occur by separate paths and still yield the same rate. Furthermore, it is easy to explain equivalent rates of exchange and product formation on the basis of a common rate-determining formation of an intermediate, which is then partitioned in fast steps. Ordinarily, complete equivalence of the rates of exchange and product formation is not found. Practically all variations have been encountered, from reactions in which exchange is infinitely faster than product formation to the other extreme. In the real cases, therefore, chemical arguments must be advanced in conjunction with the exchange data in order to make a reasonable case for intermediate formation. Isotopic exchange reactions that have proved to be of importance as criteria for intermediate formation have involved oxygen exchange, deuterium exchange, and, to a minor, extent anionic exchange.

The alkaline hydrolysis of simple esters such as ethyl benzoate is a second-order reaction and exhibits acyl-oxygen fission. On the basis of this information, two possible mechanisms can be postulated, one, an S_N2 displacement of the alkoxyl group by the hydroxyl ion, and the other, a mechanism involving the formation of an unstable addition intermediate as shown in Equation (50). The presence of an intermediate in the hy-

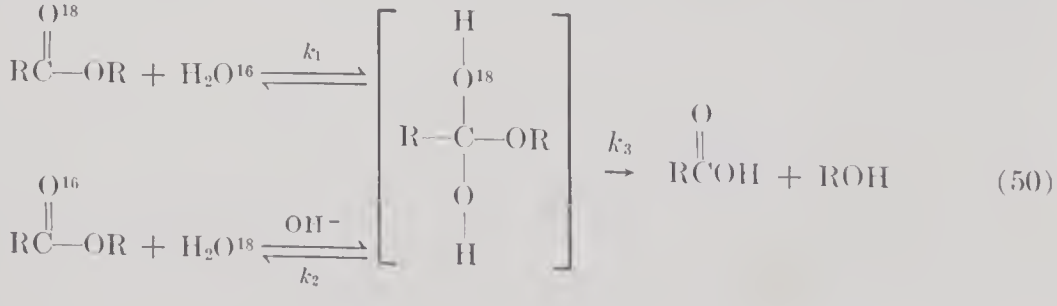

(50)

drolysis reaction can be deduced from observation of concurrent isotopic oxygen exchange and hydrolysis of the ester (291). On the other hand, no isotopic oxygen exchange will be expected to occur if a nucleophilic displacement (S_N2) reaction is operative, for the labeled carbonyl oxygen atom is not a participant in any reversible step. Concurrent carbonyl oxygen exchange and hydrolysis have been demonstrated for the hydrolyses of a number of benzoate esters (290), benzamide (292,293), benzoic anhydride (293), and certain substituted benzoyl chlorides (293). In general, the rate constants of concurrent hydrolyses (k_h) and exchange (k_e) do not differ from one another by more than a factor of ten, although in no case are the rate constants of isotopic exchange and hydrolysis equal. On the basis of the above scheme, it can be shown that $k_h/k_{ex} = 2k_3/k_2$, which indicates that the partitioning of the intermediate is a direct function of the relative rate constants of hydrolysis and exchange. It can be seen from Table VI that the relative amount of hydrolysis to exchange increases as the stability of the leaving group X increases (measured in terms of its basicity).

TABLE VI
Partitioning of the Intermediate in the Hydrolysis of Carboxylic Acid Derivatives from Oxygen Exchange Data[a]

Reaction	Leaving group	k_h/k_{ex}	k_3/k_2
Benzamide + OH^-	NH_2^-	0.53[b]	0.27
Ethyl benzoate + OH^-	$OC_2H_5^-$	11.3	5.7
Benzoic anhydride + H_2O	$O_2CC_6H_5^-$	20[c]	10
Benzoyl chloride + H_2O	Cl^-	25[c]	12.5
Ethyl benzoate + H_3O^+	C_2H_5OH	5.3	2.7
Benzamide + H_3O^+	NH_3	∞(>374)	∞(>187)

[a] In aqueous solution at 25° unless noted.
[b] 40°.
[c] 75% dioxane-water.

This is the expected behavior on the basis that hydrolyses proceed through addition intermediates of the form $RC(OH)_2X$ in which partitioning of the intermediate can lead either to exchange by loss of OH^- or to hydrolysis by loss of X^-. Thus, the relative ability of X^- to leave the addition compound compared to OH^-, reflected in the ratios of k_h/k_{ex}, follows the sequence (293)

$$X = Cl > OCOC_6H_5 > OR > NH_2$$

a sequence similar to that of the case of ionization of a group from a saturated carbon atom.

The values of k_h/k_{ex} for acidic and basic catalysis of the hydrolysis of ethyl benzoate differ by a factor of approximately two (294). In view of

the fact that the rates of hydrolysis differ by a factor of roughly 10^4, the argument for a common intermediate, the unionized hydrate of the ester in these two cases, is particularly strong.

Oxygen exchange has also been utilized to investigate the formation of intermediates in the pinacol-pinacolone rearrangement by the similar technique of the isotopic analysis of the reactant after partial reaction. It was found that oxygen exchange did indeed occur, indicating the formation of a carbonium ion intermediate that could either revert to reactant or proceed with rearrangement of a methyl group. It was further noted that approximately 70% of the carbonium ions originally formed returned to the reactant, pinacol (295), at low concentrations of acid. The rate of isotopic exchange of *tert*-butyl alcohol with H_2O^{18} in acidic solution exceeds the rate of dehydration, indicating a slow formation of a carbonium ion which can be partitioned in two ways (295a).

When oxygen exchange reactions accompany product formation, the generalization can be made that a reactant unsymmetrical with respect to oxygen atoms must proceed through an intermediate that is symmetrical with respect to oxygen atoms. Two different cases have been illustrated above, one involving the formation of an intermediate containing two equivalent oxygen atoms (ester hydrolysis), and the other involving the formation of an intermediate containing no oxygen atoms (alcohol reactions). Either intermediate contains the requisite symmetry for oxygen exchange.

Deuterium exchange has been utilized in a fashion somewhat similar to oxygen exchange to investigate the possibility of intermediate formation. In reactions run in deuterated solvents, principally deuterium oxide or deuteroethanol, either the reactant or the product has been analyzed for the incorporation of a deuterium atom during the reaction process. Evidence for the formation of carbanion intermediates in a number of processes has been obtained by the observation of deuterium exchange during the process. The isomerization of the β,γ-unsaturated nitrile (Eq. 51) by

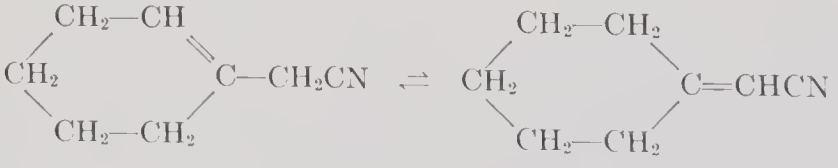

(51)

sodium deuteroxide in deuteroethanol is accompanied by deuterium exchange of the reactant with the solvent at a rate vastly in excess of the rate at which it isomerizes (296). The deuterium exchange can be explained by the formation of a resonance-stabilized intermediate anion which may combine with a hydrogen ion to form either reactant or product. Deuterium exchange has provided important evidence for intermediate formation in the reactions of phenyl *sec*-butyl ketone. The rates of the deuter-

oxide-catalyzed racemization and deuterium exchange of this compound are identical (297). The equivalence of these rates, together with the equivalence of the rates of racemization and bromination of this ketone, are strong evidence for the formation of enolate ion intermediates in the rate-determining steps of these three reactions.

Evidence for the formation of a carbanion intermediate in the elimination reaction of β-benzenehexachloride with sodium ethoxide in deuteroethanol was found on the basis that unreacted starting material isolated after about 50% completion contained a small amount of deuterium (298). From the exchange data, it was calculated that the carbanion intermediate reverted to reactant once out of the 150 times that it proceeded to the elimination product.

The fact that chloroform undergoes a base-catalyzed deuterium exchange very much faster than basic hydrolysis has been used as evidence for the relatively rapid formation of the trichloromethyl anion intermediate in the hydrolysis of chloroform (299).

The aldol condensation of acetaldehyde was originally reported to give no concurrent deuterium exchange when carried out in deuterium oxide (300). It has now been shown, by working at high concentrations of acetaldehyde, that there is indeed deuterium exchange of acetaldehyde accompanying its aldol condensation (301). Furthermore, it is possible to calculate from the deuterium exchange data that the partitioning of the enolate anion of acetaldehyde to reactants relative to products is 1:50.

Anionic exchange has been used in the investigation of intermediate formation in carbonium ion reactions. It was found that halide exchange occurred at the same rate (zero order in salt) between triphenylmethyl chloride and either a radiochloride or a fluoride quaternary ammonium salt in benzene solution (302). This is a variant of the kinetic argument for the formation of a carbonium ion intermediate, described previously.

The exchange between *p*-toluenesulfonate and *p*-bromobenzenesulfonate groups has been observed in a number of solvolytic reactions. This exchange has been postulated to proceed through a solvent-separated ion pair or through a dissociated carbonium ion. Information from these exchange reactions has been correlated with data on common ion rate depression resulting in a description of the spectrum of intermediates present in the solvolysis of a series of substrates (303). (See Section IV.1.D.) The occurrence of an exchange reaction involving an ion Y^- similar to X^- has been utilized as evidence for carbonium ion formation; conversely, the lack of such an exchange reaction has been used as evidence against carbonium ion formation. The negative evidence, according to Winstein (303), is evidence that return from an external carbonium ion pair does not occur. The positive evidence indicates that either dissociated car-

bonium ions or external carbonium ion pairs occur. This situation could be clarified by a quantitative determination of exchange reactions in systems involving carbonium ions, as has been done in other exchange systems involving oxygen-18 and deuterium, mentioned above.

In the examples given above, which are but a few investigations employing isotopic exchange, the amount of exchange relative to that of product formation varies over wide limits. In some cases, exchange of the reactant is far more rapid than product formation; in other cases exchange is exactly equal to product formation; and in still other cases it is much slower than product formation.

The case in which the rate of exchange is exactly equal to the rate of product formation is probably the most interesting one to consider. In the deuterium exchange of ketones, the equivalence of this rate to the rate of product formation leads to the conclusion that the reaction of the enolate ion intermediate to form reactants or products occurs either with equal activation energies in either direction or with little activation energy in either direction, relative to the activation energy of enolate formation.

In cases where the rate of exchange does not equal the rate of product formation, the possibility exists that two separate reactions produce exchange and product formation. For example, when exchange is far more rapid than the over-all reaction, the intermediate being observed may be a blind-alley intermediate. Ambiguities such as this can be minimized by the determination of the effect of structure on the relative rate of exchange, as well as the effect of solvent, of temperature, and other external factors on the relative rate of exchange. In favorable cases where the effects of these factors can be reasonably explained in terms of intermediate formation, such as in ester hydrolysis, it is possible to postulate the formation of an intermediate.

V. CONCLUSIONS

Many organic reaction mechanisms in the older literature were postulated to involve a series of intermediates on the basis of speculation and consistency with the major products of a reaction. In this chapter an attempt has been made to present those direct and indirect experimental methods now available for detection of intermediate formation. The importance of a knowledge of intermediate formation for the elucidation of reaction mechanisms is an acknowledged fact. The future will provide a more quantitative approach to the problem of intermediate formation, more sensitive instruments for the detection of highly reactive intermediates, and the increased use of these methods of physical organic chemistry in the area complicated biochemical problems.

Addendum

The two years since this chapter was first written have witnessed continued interest in the subject of intermediates in organic reactions. Novel methods have been utilized in the isolation of reactive intermediates, transient intermediates have been detected by the use of new physicochemical properties and further evidence has been found for intermediate formation by the use of various chemical properties. An exhaustive survey of the advances that have occurred in the last two years will not be attempted, but a few of the highlights will be mentioned.

It has been postulated for some time that aromatic nucleophilic substitution reactions of activated halides, for example, *p*-nitrofluorobenzene, proceed through the addition of the nucleophile to the benzene ring with the formation of an addition intermediate. By the simple expedient of carryout the reaction of *p*-nitrofluorobenzene with azide ion in the aprotic solvent dimethylformamide instead of the usual protic solvent, it was possible to demonstrate the intermediate in this reaction (304,305). When both reactants were consumed, neither of the products was formed, but a new species with $\lambda_{max} = 397$ mμ was observed. When this solution was poured into excess water, the product *p*-nitrophenylazide was precipitated in quantitative yield. It was therefore concluded that a stable intermediate complex (XXIII) is formed which liberates fluoride ion only when a protic solvent is available to solvate the fluoride ion. The reason for the formation

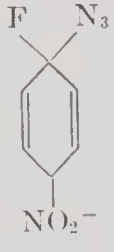

(XXIII)

of a stable intermediate under these conditions is that the aprotic solvent stabilizes the intermediate and destabilizes the product all at the same time because of the striking solvation changes from protic to aprotic solvents.

The transformation of pyruvate to acetaldehyde and/or acetoin is catalyzed by the enzyme carboxylase which contains thiamine pyrophosphate as a cofactor. In these enzymic transformations it has been abundantly shown that adducts of pyruvate with thiamine pyrophosphate and of acetaldehyde with thiamine pyrophosphate occur as intermediates. Both "active pyruvate," XXIV and "active acetaldehyde," XXV have been isolated from the enzyme carboxylase. The former was isolated from a reacting system after a few seconds of reaction.

The latter compound, however, exists naturally in certain carboxylase preparations (306,307).

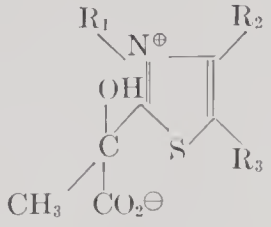

(XXIV)

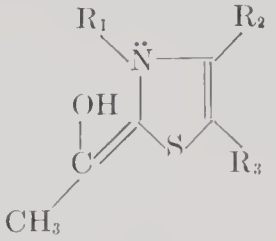

(XXV)

Increasing emphasis is being placed on the detection of transient intermediates by physicochemical methods. Ultraviolet spectroscopy, optical rotation, electron spin resonance and fluorescence measurements are being increasingly used for this purpose. The latter two methods, fluorescence and electron spin resonance measurements are particularly suited for the detection of transient intermediates at extremely low concentrations because of the high sensitivity of these methods.

It is now possible to utilize electron spin resonance techniques to study free radical formation and decay in the photolysis of organic molecules. Electron spin resonance responds only to systems containing unpaired electrons such as free radicals. Direct ultraviolet irradiation of an organic material may be conducted in the microwave cavity of an electron spin resonance spectrometer and simultaneously one may measure the steady-state concentration of the free radical intermediates formed. The steady-state free radical intermediates can then be identified from their characteristic hyperfine patterns and their measured rates of decay. In the photolysis of alkyl hydroperoxides such identification has been made (308).

Benzyne has been postulated as the intermediate in the nucleophilic substitution reactions of unactivated halobenzenes, on the basis of product analyses and isotopic tracer experiments. More recently it has been possible to prepare this intermediate by flash photolysis of benzenediazonium-2-carboxylate (XXVI) and to identify the species by its ultraviolet spectrum. The over-all reaction leads to nitrogen, carbon dioxide and bi-

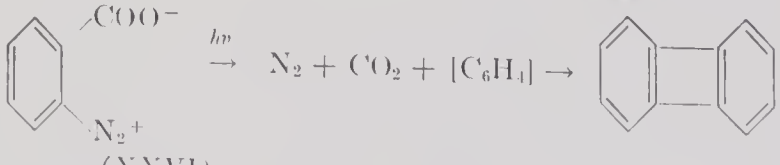

(XXVI) (52)

phenylene. By determining the spectrum approximately 10 μsec. after flash irradiation it is possible to obtain the spectrum of a transient intermediate with a broad maximum between 238.5 and 241.5 mμ and considerable end absorption, which can be identified as the benzyne intermediate (309).

Fluorimetric measurements have provided the means for the observation of the binary and ternary complex intermediates formed between a number of dehydrogenase enzymes, their respective substrates and reduced diphosphopyridine nucleotide (DPNH). The latter compound exhibits a fluorescence spectrum which is perturbed on binding with a dehydrogenase enzyme. Furthermore, this binary complex is further perturbed by the additional binding of the substrate to be reduced. A number of such systems have been investigated in detail such as the trio, yeast alcohol dehydrogenase, ethyl alcohol and DPNH, and the trio, malic dehydrogenase, malic acid and DPNH (310).

In the basic hydrolysis of succinamide it is possible to observe spectrophotometrically the formation and decomposition of the succinimide intermediate formed in this reaction. Furthermore, the kinetics of formation and decomposition of this intermediate can be correlated with the kinetics of the overall reaction (311). An imide intermediate has also been observed by means of optical rotation studies in the hydrolysis of a related succinic acid derivative (312).

There have been many examples in the past few years of reactions in which intermediates have been postulated on the basis of chemical consequences. In fact, these studies have been so numerous that only a few examples may be mentioned here.

Stereochemistry of the products and the relative reactivity of a reaction series have been used to distinguish between carbenes (divalent carbon species in the singlet state) and methylenes (divalent carbon species in the triplet state). The former species appear to give stereospecific *cis*-addition to a double bond and lead to a reactivity sequence with substituted olefins similar to that found with the heterolytic addition of bromine. On the other hand methylenes do not give stereospecific addition and lead to a reactivity sequence with substituted olefins similar to that found in homolytic addition. On the basis of these criteria it is therefore possible to distinguish between carbenes and methylenes. The species ϕ_2C: (313), CH_2: produced from the photosensitized decomposition of diazomethane (314) and HC≡CH: have been shown on this basis to be triplets.

The solvolysis of *cis*- and *trans*-3-bicyclo[3.1.0]hexyl tosylates has been shown to give rise to a non-classical cationic intermediate. The acetolysis of the *cis*-compound leads to the *cis*-acetate while the acetolysis of the *trans*-compound leads to a mixture of 66% *cis*-acetate and 33% olefin. Since the *cis*-compound is 35 times more reactive than the *trans*-compound, it appears that the ionization of the *cis*-compound is anchimerically accelerated. A special salt effect is noted with the *cis*-compound, which is diagnostic of ion pair formation of a stabilized intermediate (which evidently reacts stereospecifically with solvent). When the group R is a deuterium atom, the deuterium is found in the product in positions 1, 3, and 5 of the

cyclohexane ring, with twice as much deuterium in the cyclopropane ring as in the original position. The stereospecificity, kinetic data, lack of olefin formation and deuterium scrambling of the *cis*-compound are consistent with the mechanism shown in Equation (53) involving a tris-homocyclopropenyl cation (315).

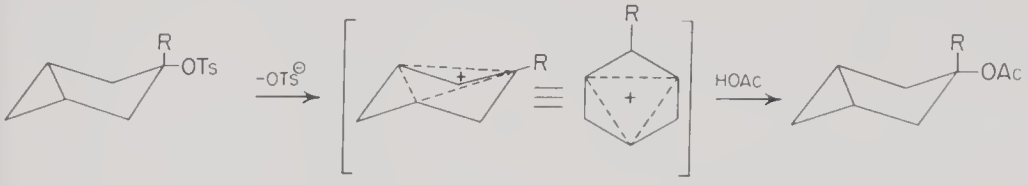

(53)

O-Acetyl-4-hydroxymethylimidazole undergoes hydroxide ion-catalyzed hydrolysis about 10^5 times faster than expected of a simple aliphatic ester. Furthermore alkyl-oxygen fission was found and the hydrolysis was shown to be a general base-catalyzed reaction. These facts may be rationalized on the basis of a mechanism involving the postulation of the unsaturated intermediate shown in Equation (54) (316).

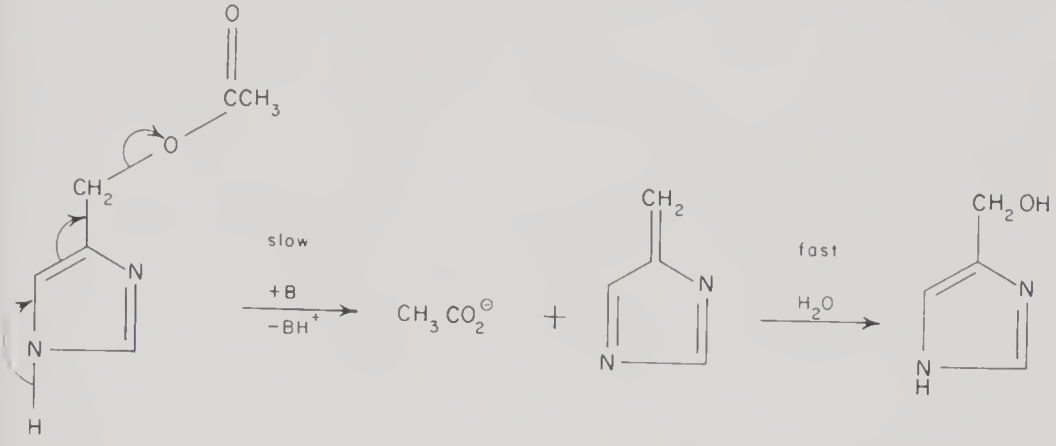

(54)

The concept of nonclassical cationical intermediates, as described in this chapter, has been criticized by H. C. Brown (318,319). He has reinterpretated the data on which such intermediates have been postulated, pointing out that some of the supposed examples of anchimeric assistance can be explained on the basis of the relief of steric strain, and that the stereochemical, isotopic tracer, and optical properties of the products, as well as rearrangements, can be explained in terms of the products expected from a rapidly equilibrating mixture of the corresponding classical cations. This view defines the non-classical cationic species as a transition state rather than an intermediate, a question that has been specifically considered in the discussion of the intermediate in the acetolysis of exo-norbornyl-*p*-bromobenzenesulfonate (see page 1493). Considerable controversy surrounds this subject at the moment: the explanation of all data in terms of classical cationic intermediates is not accepted by all. Philosophically it may be argued that one should not invoke non-classical

cationic intermediates unless it is impossible to explain the data in terms of (mixtures of) classical cations. On the other hand, the conceptual utility of non-classical ions cannot be overlooked. It may be predicted that this controversy will lead to definitive experiments probing the structure of cationic intermediates in a number of reactions discussed in this chapter. One such experiment indicates that the 1,2-dianisylnorbornyl cation exists as a mixture of equilibrating ions, and not as a non-classic cation (320).

References

1. A. Lapworth, *J. Chem. Soc.*, **1904**, 30.
2. C. G. Swain and E. E. Pegues, *J. Am. Chem. Soc.*, **80**, 812 (1958).
3. A. Skrabal, *Homogenkinetik*, T. Steinkopff, Dresden, 1941, pp. 38–43.
4. A. R. Hawdon, E. D. Hughes, and C. K. Ingold, *J. Chem. Soc.*, **1952**, 2499.
5. M. L. Bender, R. D. Ginger, and J. P. Unik, *J. Am. Chem. Soc.*, **80**, 1044 (1958).
6. J. A. Christiansen, *Z. physik. Chem.*, **33B**, 145 (1936); **37B**, 374 (1937).
7. J. E. Leffler, *The Reactive Intermediates of Organic Chemistry*, Interscience, New York, 1956.
8. M. Gomberg, *Ber.*, **33**, 3150 (1900); *J. Am. Chem. Soc.*, **22**, 757 (1900).
9. J. Piccard, *Ann.*, **381**, 347 (1911); K. Ziegler and L. Ewald, *ibid.*, **473**, 163 (1929).
10. M. Gomberg and L. H. Cone, *Ber.*, **37**, 2037 (1904); W. Schlenk, T. Weickel, and A. Herzenstein, *Ann.*, **372**, 1 (1910); M. Gomberg and C. S. Schoepfle, *J. Am. Chem. Soc.*, **39**, 1652 (1917); **41**, 1655 (1919).
11. N. W. Taylor, *ibid.*, **48**, 854 (1926); E. Müller, I. Müller-Rodloff, and W. Bunge, *Ann.*, **520**, 235 (1935); M. F. Roy and C. S. Marvel, *J. Am. Chem. Soc.*, **59**, 2622 (1937); P. W. Selwood and R. M. Dobres, *ibid.*, **72**, 3860 (1950).
12. C. A. Hutchison, Jr., A. Kowalsky, R. C. Pastor, and G. W. Wheland, *J. Chem. Phys.*, **20**, 1485 (1952); D. H. Whiffen, *Quart. Revs.*, **12**, 250 (1958).
13. E. Müller and I. Müller-Rodloff, *Ber.*, **69B**, 665 (1936); G. H. Coppinger, *J. Am. Chem. Soc.*, **79**, 501 (1957).
14. W. von E. Doering and L. H. Knox, *ibid.*, **76**, 3203 (1954).
15. R. Breslow, *ibid.*, **79**, 5318 (1957).
16. G. A. Olah and S. J. Kuhn, *ibid.*, **80**, 6535 (1958); **80**, 6541 (1958); G. A. Olah, A. E. Pavlath, and J. A. Olah, *ibid.*, **80**, 6540 (1958).
16a. G. Leal and R. Petit, *ibid.*, **81**, 3160 (1959).
17. Ref. 7, pp. 174–180.
18. P. Walden, *Ber.*, **35**, 2018 (1902); M. Gomberg, *Ber.*, **35**, 2403 (1902); K. Ziegler and H. Wollschitt, *Ann.*, **479**, 90 (1930); K. Ziegler and W. Mathes, *ibid.*, **479**, 111 (1930); N. N. Lichtin and P. D. Bartlett, *J. Am. Chem. Soc.*, **73**, 5530 (1951); N. N. Lichtin and H. Glazer, *ibid.*, **73**, 5537 (1951).
18a. Y. Pocker, *Proc. Chem. Soc.*, **1959**, 386.
19. A. G. Evans, I. H. McEwan, and J. H. Thomas, *J. Chem. Soc.*, **1957**, 4644; J. W. Bayles, A. G. Evans, and J. R. Jones, *ibid.*, **1955**, 206; **1957**, 1020.
20. K. Ziegler and H. Wollschitt, *Ann.*, **479**, 123 (1930); C. A. Kraus and R. Rosen, *J. Am. Chem. Soc.*, **47**, 2739 (1925).
21. H. Rapoport and G. Smolinsky, *ibid.*, **80**, 2910 (1958).
22. J. B. Conant and G. W. Wheland, *ibid.*, **54**, 1212 (1932); R. G. Pearson and R. L. Dillon, *ibid.*, **75**, 2439 (1953).
23. R. Stewart and K. Yates, *ibid.*, **80**, 6355 (1958); L. A. Flexser, L. P. Hammett,

and A. Dingwall, *ibid.*, **57**, 2103 (1935); L. A. Flexser and L. P. Hammett, *ibid.*, **60**, 885 (1938); L. Zucker and L. P. Hammett, *ibid.*, **61**, 2785 (1939); J. T. Edward and S. C. R. Meacock, *J. Chem. Soc.*, **1957**, 2000.

24. H. C. Brown and J. D. Brady, *J. Am. Chem. Soc.*, **74**, 3570 (1952).

25. M. Kilpatrick and F. E. Luborsky, *ibid.*, **75**, 577 (1953).

26. N. Lichtin, quoted by H. C. Brown and Y. Okamoto, *ibid.*, **80**, 4986 (1958).

27. N. C. Deno and A. Schriesheim, *ibid.*, **77**, 3051 (1955).

27a. N. C. Deno, P. T. Groves, and G. Saines, *ibid.*, **81**, 5790 (1959).

28. L. P. Hammett, *Physical Organic Chemistry*, McGraw-Hill, New York, 1940, p. 45; R. J. Gillespie and J. A. Leisten, *Quart. Revs.*, **8**, 40 (1954).

28a. R. Breslow, *J. Am. Chem. Soc.*, **79**, 1762 (1957); **80**, 3719 (1958).

29. P. Pfeiffer, *Organische Molekülverbindungen*, F. Enke, Stuttgart, 1922.

30. E. Krause and P. Dittmar, *Ber.*, **63B**, 2401 (1930).

31. H. C. Brown and W. J. Wallace, *J. Am. Chem. Soc.*, **75**, 6265, 6268, 6279 (1953); H. C. Brown, L. P. Eddy, and R. Wong, *ibid.*, **75**, 6275 (1953); H. C. Brown and M. Grayson, *ibid.*, **75**, 6285 (1953); H. C. Brown and K. L. Nelson, *ibid.*, **75**, 6292 (1953).

32. J. D. Farr, C. C. Bard, and G. W. Wheland, *ibid.*, **71**, 2013 (1949).

33. J. Meisenheimer, *Ann.*, **323**, 205 (1902).

34. R. Bieber and G. Trumpler, *Helv. Chim. Acta*, **30**, 1860 (1947); R. P. Bell and J. C. Clunie, *Trans. Faraday Soc.*, **48**, 439 (1952); F. Swarts, *Bull. soc. chim. Belgique*, **35**, 414 (1926); M. L. Bender, *J. Am. Chem. Soc.*, **75**, 5986 (1953); O. H. Wheeler, *ibid.*, **79**, 4191 (1957); W. P. Jencks, *ibid.*, **81**, 475 (1959).

35. G. S. Hammond, *ibid.*, **77**, 334 (1955).

36. J. L. Franklin, *Trans. Faraday Soc.*, **48**, 443 (1952).

37. B. Bensley and G. Kohnstam, *J. Chem. Soc.*, **1957**, 4747.

38. See, however, V. Gold, *ibid.*, **1956**, 4633.

39. M. L. Bird, E. D. Hughes, and C. K. Ingold, *ibid.*, **1954**, 634.

40. E. D. Hughes, C. K. Ingold, and U. G. Shapiro, *ibid.*, **1936**, 225.

41. M. L. Dhar, E. D. Hughes, and C. K. Ingold, *ibid.*, **1948**, 2058.

42. See C. G. Swain, *J. Am. Chem. Soc.*, **70**, 1119 (1948) and the following papers for a discussion on the relationship of cationic solvation and nucleophilic attack, as applied to borderline mechanisms.

43. See S. Winstein, E. Grunwald, and H. W. Jones, *ibid.*, **73**, 2700 (1951) for the relationship of solvent effects on solvolysis rates as applied to borderline mechanisms.

44. A. A. Frost and R. G. Pearson, *Kinetics and Mechanism*, Wiley, New York, 1953, p. 91.

45. F. O. Rice and C. J. Grelecki, *J. Am. Chem. Soc.*, **79**, 2679 (1957).

46. F. O. Rice and M. Freamo, *ibid.*, **73**, 5529 (1951).

47. M. C. R. Symons and M. Townsend, *J. Chem. Phys.*, **25**, 1299 (1956); R. G. Sowden and N. Davidson, *J. Am. Chem. Soc.*, **78**, 1291 (1956).

48. I. L. Mador, *J. Chem. Phys.*, **22**, 1617 (1954).

49. R. L. Livingston, J. Ghormley, and H. Zeldes, *ibid.*, **24**, 483 (1956); J. F. Gibson, D. J. E. Ingram, M. C. R. Symons, and M. G. Townsend, *Trans. Faraday Soc.*, **53**, 914 (1957).

50. G. N. Lewis and D. Lipkin, *J. Am. Chem. Soc.*, **64**, 2801 (1942).

51. I. Norman and G. Porter, *Nature*, **174**, 508 (1954).

52. F. C. Adam and S. I. Weissman, *J. Am. Chem. Soc.*, **80**, 2057 (1958).

53. G. K. Fraenkel, J. M. Hirshon, and C. Walling, *ibid.*, **76**, 3606 (1954).

54. J. Uebersfeld, A. Etienne, and J. Combrisson, *Nature*, **174**, 614 (1954); E. E. Schneider, *Disc. Faraday Soc.*, No. **19**, 158 (1955).

55. F. O. Rice and C. Grelecki, *J. Am. Chem. Soc.*, **79**, 1880 (1957).

56. C. Walling and S. A. Buckler, *ibid.*, **75**, 4372 (1953); C. Walling and S. A. Buckler, *ibid.*, **77**, 6032 (1955).

57. M. Ballester and D. Pérez-Blanco, *J. Org. Chem.*, **23**, 652 (1958).

58. F. H. Westheimer, E. Segel, and R. Schramm, *J. Am. Chem. Soc.*, **69**, 773 (1947).

59. A. K. Balls and H. N. Wood, *J. Biol. Chem.*, **219**, 245 (1956).

60. J. S. Fruton and S. Simmonds, *General Biochemistry*, Wiley, New York, 1953, pp. 428–433.

61. G. W. Beadle, *Chem. Revs.*, **37**, 15 (1945).

62. R. P. Wagner and H. K. Mitchell, *Genetics and Metabolism*, Wiley, New York, 1955.

63. *Cf.* Section I.3.

64. *Cf.* Section I.3.

65. R. Steinberger and F. H. Westheimer, *J. Am. Chem. Soc.*, **73**, 429 (1951).

66. C. G. Swain, L. E. Kaiser, and T. E. C. Knee, *ibid.*, **77**, 4681 (1955).

67. S. Winstein and R. Baird, *ibid.*, **79**, 756 (1957).

68. G. J. Buist, C. A. Bunton, and J. H. Miles, *J. Chem. Soc.*, **1957**, 4575.

69. L. G. Cannell, *J. Am. Chem. Soc.*, **79**, 2927, 2932 (1957).

70. M. L. Bender and B. W. Turnquest, *ibid.*, **79**, 1626 (1957).

71. W. P. Jencks, *ibid.*, **81**, 475 (1959).

72. R. S. Mulliken, *J. Phys. Chem.*, **56**, 801 (1952); L. J. Andrews, *Chem. Revs.*, **54**, 713 (1954).

73. P. W. Robertson, J. E. Allan, K. N. Haldane, and M. G. Simmers, *J. Chem. Soc.*, **1949**, 933; E. M. Kosower, *J. Am. Chem. Soc.*, **78**, 3497 (1956).

74. B. Chance, Chapter XXII, this volume.

75. F. J. W. Roughton and B. Chance, Chapter XIV, this volume.

76. C. K. Ingold, D. J. Millen, and H. G. Poole, *J. Chem. Soc.*, **1950**, 2576.

77. D. J. Millen, *ibid.*, **1950**, 2589, 2600, 2606.

78. B. Venkataraman and G. K. Fraenkel, *J. Chem. Phys.*, **23**, 588 (1955); J. E. Wertz and J. L. Vivo, *ibid.*, **23**, 2441 (1955).

79. L. Michaelis, G. F. Boeker, and R. K. Reber, *J. Am. Chem. Soc.*, **60**, 202 (1938).

80. L. Michaelis, M. P. Schubert, R. K. Reber, J. A. Kuck, and S. Granick, *ibid.*, **60**, 1678 (1938).

81. L. Michaelis, *ibid.*, **63**, 2446 (1941).

82. L. Michaelis and S. Granick, *ibid.*, **65**, 1747 (1943).

83. E. A. Boudreaux and E. Boulet, *ibid.*, **80**, 1588 (1958).

84. L. Michaelis, *Chem. Revs.*, **16**, 243 (1935); L. Michaelis and M. P. Schubert, *ibid.*, **22**, 437 (1938).

85. O. H. Muller, *Ann. N. Y. Acad. Sci.*, **40**, 91 (1940).

86. H. W. Melville, *Disc. Faraday Soc.*, No. **17**, 9 (1954).

87. R. G. W. Norrish and G. Porter, *ibid.*, No. **17**, 40 (1954).

88. G. B. Kistiakowsky and P. H. Kydd, *J. Am. Chem. Soc.*, **79**, 4825 (1957).

89. *Cf.* the discussion of this problem in A. A. Frost and R. G. Pearson, *Kinetics and Mechanism*, Wiley, New York, 1953, pp. 257–265.

90. F. R. Duke, *J. Am. Chem. Soc.*, **69**, 3054 (1947).

91. J. E. Taylor, *ibid.*, **75**, 3912 (1953).

92. G. J. Buist and C. A. Bunton, *J. Chem. Soc.*, **1957**, 4580.

93. A. Lapworth, *ibid.*, **1904**, 30.

94. R. P. Bell, *ibid.*, **1937**, 1637; A. Broche and R. Gibert, *Bull. Soc. Chim. France*, **22**, 131 (1955) have shown that using high concentrations of acetaldehyde, the order with respect to acetaldehyde is between one and two.

95. C. K. Ingold, *Proc. Chem. Soc.*, **1957**, 279.
96. J. Hine, *Physical Organic Chemistry*, McGraw-Hill, New York, 1956, pp. 98–112.
97. C. K. Ingold, *Structure and Mechanism in Organic Chemistry*, Cornell University Press, Ithaca, 1953, Chapter VII.
98. P. D. Bartlett, *J. Am. Chem. Soc.*, **56**, 967 (1934).
99. P. D. Bartlett and C. H. Stauffer, *ibid.*, **57**, 2580 (1935).
100. S. K. Hsü and C. L. Wilson, *J. Chem. Soc.*, **1936**, 623.
101. S. K. Hsü, C. K. Ingold, and C. L. Wilson, *ibid.*, **1938**, 78.
102. K. J. Pedersen, *J. Am. Chem. Soc.*, **51**, 2098 (1929); **58**, 240 (1936).
103. K. J. Pedersen, *J. Phys. Chem.*, **38**, 559 (1934).
104. M. L. Bender, *J. Am. Chem. Soc.*, **73**, 1626 (1951).
105. V. Henri, *Lois générales de l'action des diastases*, Hermann, Paris, 1903; L. Michaelis and M. L. Menten, *Biochem. Z.*, **49**, 333 (1913).
106. G. E. Briggs and J. B. S. Haldane, *Biochem. J.*, **19**, 338 (1925).
107. P. D. Boyer, H. Lardy, and K. Myrbäck, eds., *The Enzymes*, Vol. I, Academic Press, New York, 1959, chs. 1–3.
108. H. Gutfreund, *Disc. Faraday Soc.*, **20**, 167 (1955); H. Gutfreund and J. M. Sturtevant, *Biochem. J.*, **63**, 656 (1956).
109. H. V. Euler and A. Ölander, *Z. physik. Chem.*, **131**, 107 (1928).
110. T. W. J. Taylor, *J. Chem. Soc.*, **1930**, 2741.
111. V. K. Krieble and K. A. Holst, *J. Am. Chem. Soc.*, **60**, 2976 (1938).
112. B. S. Rabinovitch and C. A. Winkler, *Can. J. Research*, **20B**, 73 (1942).
113. J. T. Edward and S. C. R. Meacock, *J. Chem. Soc.*, **1957**, 2000.
114. R. P. Bell, A. L. Dowding, and J. A. Noble, *ibid.*, **1955**, 3106.
115. R. W. Taft, Jr., *J. Am. Chem. Soc.*, **74**, 5374 (1952); R. W. Taft, Jr., E. L. Purlee, P. Riesz, and G. A. De Fazio, *ibid.*, **77**, 1584 (1955).
116. F. A. Long, J. G. Pritchard, and F. E. Stafford, *ibid.*, **79**, 2362 (1957).
117. See A. H. Fainberg and S. Winstein, *ibid.*, **78**, 2770 (1956); **79**, 1597 (1957); E. M. Kosower, *ibid.*, **80**, 3267 (1958).
118. E. D. Hughes and C. K. Ingold, *J. Chem. Soc.*, **1935**, 244; C. K. Ingold, *Structure and Mechanism in Organic Chemistry*, Cornell University Press, 1953, pp. 345–350.
119. J. B. Conant and W. R. Kirner, *J. Am. Chem. Soc.*, **46**, 232 (1924).
120. G. M. Bennett and B. Jones, *J. Chem. Soc.*, **1935**, 1815.
121. L. C. Bateman, E. D. Hughes, and C. K. Ingold, *ibid.*, **1940**, 960.
122. A. A. Frost and R. G. Pearson, *Kinetics and Mechanism*, Wiley, New York, 1953, p. 138.
123. L. C. Bateman, E. D. Hughes, and C. K. Ingold, *J. Chem. Soc.*, **1940**, 974.
124. L. C. Bateman, M. G. Church, E. D. Hughes, C. K. Ingold, and N. A. Taher, *ibid.*, **1940**, 979.
125. H. C. Brown and C. R. Smoot, *J. Am. Chem. Soc.*, **78**, 6255 (1956).
126. J. Hine, *Physical Organic Chemistry*, McGraw-Hill, New York, 1956, p. 103.
127. Y. Pocker, *Chem. and Ind.*, 1599 (1957).
128. W. G. Young, S. Winstein, and H. L. Goering, *J. Am. Chem. Soc.*, **73**, 1958 (1951).
129. S. Winstein, E. Clippinger, A. H. Fainberg, R. Heck, and G. C. Robinson, *ibid.*, **78**, 328 (1956).
130. S. Winstein, E. Clippinger, A. H. Fainberg, and G. C. Robinson, *ibid.*, **76**, 2597 (1954).
131. A. H. Fainberg and S. Winstein, *ibid.*, **78**, 2763 (1956).
132. A. H. Fainberg and S. Winstein, *ibid.*, **78**, 2767 (1956).

133. S. Winstein and E. Clippinger, *ibid.*, **78**, 2784 (1956).
134. S. Winstein and G. C. Robinson, *ibid.*, **80**, 169 (1958).
135. J. E. Leffler, *The Reactive Intermediates of Organic Chemistry*, Interscience, New York, 1956.
136. K. Nozaki and P. D. Bartlett, *J. Am. Chem. Soc.*, **68**, 1686 (1946).
137. M. S. Kharasch and F. R. Mayo, *ibid.*, **55**, 2468 (1933).
138. M. S. Kharasch, H. Engelmann, and F. R. Mayo, *J. Org. Chem.*, **2**, 288 (1937).
139. W. E. Vaughan and F. F. Rust, *ibid.*, **5**, 449 (1940).
140. H. L. J. Bäckström, *J. Am. Chem. Soc.*, **49**, 1460 (1927); K. Ziegler and L. Ewald, *Ann.*, **504**, 162 (1933).
141. R. L. Dannley and E. L. Kay, *J. Am. Chem. Soc.*, **77**, 1046 (1955).
142. J. F. Bunnett and J. J. Randall, *ibid.*, **80**, 6020 (1958).
143. S. D. Ross, *ibid.*, **80**, 5319 (1958).
144. O. A. Stamm and H. Zollinger, *Helv. Chim. Acta*, **40**, 1955 (1957).
145. S. S. Beichler and R. W. Taft, Jr., *J. Am. Chem. Soc.*, **79**, 4927 (1957).
146a. L. P. Hammett and A. J. Deyrup, *ibid.*, **54**, 2721 (1932); L. P. Hammett, *Chem. Revs.*, **16**, 67 (1935); L. P. Hammett, *Physical Organic Chemistry*, McGraw-Hill, New York, 1940, Chapter IX.
146b. F. A. Long and M. A. Paul, *Chem. Revs.*, **57**, 935 (1957).
147. R. W. Taft, Jr., *J. Am. Chem. Soc.*, **74**, 5372 (1952).
147a. R. A. Boyd, R. W. Taft, Jr., A. P. Wolf, and D. Christman, *ibid.*, **82**, 4729 (1960).
148. V. Gold and D. P. N. Satchell, *J. Chem. Soc.*, **1955**, 3609, 3619, 3622.
148a. A. J. Kresge and Y. Chiang, *J. Am. Chem. Soc.*, **81**, 5509 (1959).
149. N. C. Deno and C. Perizzolo, *ibid.*, **79**, 1345 (1957).
150. N. C. Deno and A. Schriesheim, *ibid.*, **77**, 3051 (1955).
151. H. C. Brown and Y. Okamoto, *ibid.*, **80**, 4986 (1958).
152. R. G. Pearson and R. L. Dillon, *ibid.*, **75**, 2439 (1953).
152a. K. Ziegler and L. Ewald, *Ann.*, **473**, 163 (1929).
153. J. E. Leffler, *Science*, **117**, 340 (1953).
154. L. C. Bateman and E. D. Hughes, *J. Chem. Soc.*, **1940**, 945.
155. L. P. Hammett, *Physical Organic Chemistry*, McGraw-Hill, New York, 1940, Chapter VII.
156. H. H. Jaffé, *Chem. Revs.*, **53**, 191 (1953).
157. J. D. Roberts, J. K. Sanford, F. L. J. Sixma, H. Cerfontain, and R. Zagt, *J. Am. Chem. Soc.*, **76**, 4525 (1954).
158. P. B. D. de la Mare, *J. Chem. Soc.*, **1954**, 4450.
159. H. C. Brown and Y. Okamoto, *J. Am. Chem. Soc.*, **79**, 1913 (1957).
160. E. Berliner and L. C. Monack, *ibid.*, **74**, 1574 (1952).
161. J. F. Bunnett, F. Draper, Jr., P. R. Ryason, P. Noble, Jr., R. G. Tonkyn, and R. E. Zahler, *ibid.*, **75**, 642 (1953).
162. J. Hine, *Physical Organic Chemistry*, McGraw-Hill, New York, 1956, p. 148.
163. P. Ballinger, P. B. D. de la Mare, G. Kohnstam, and B. M. Prestt, *J. Chem. Soc.*, **1955**, 3641.
164. P. D. Bartlett and R. R. Hiatt, *J. Am. Chem. Soc.*, **80**, 1398 (1958).
165. P. D. Bartlett and L. H. Knox, *ibid.*, **61**, 3184 (1939).
166. W. von E. Doering *et al.*, *ibid.*, **75**, 1008 (1953).
167. P. D. Bartlett and F. D. Greene, *ibid.*, **76**, 1088 (1954).
168. P. D. Bartlett and G. F. Woods, *ibid.*, **62**, 2933 (1940).
169. M. S. Kharasch, F. Engelmann, and W. H. Urry, *ibid.*, **65**, 2428 (1943).

169a. A. Rajbenback and M. Szwarc, *Proc. Chem. Soc.*, **1958**, 347.
170. H. C. Brown and R. S. Fletcher, *J. Am. Chem. Soc.*, **71**, 1845 (1949); H. C. Brown and A. Stern, *ibid.*, **72**, 5068 (1950); H. C. Brown and H. L. Berneis, *ibid.*, **75**, 10 (1953).
171. F. Brown, T. D. Davies, I. Dostrovsky, O. J. Evans, and E. D. Hughes, *Nature*, **167**, 987 (1951).
172. P. D. Bartlett and M. S. Swain, *J. Am. Chem. Soc.*, **77**, 2801 (1955); P. D. Bartlett and E. B. Lefferts, *ibid.*, **77**, 2804 (1953); P. D. Bartlett and M. Stiles, *ibid.*, **77**, 2806 (1955).
173. J. D. Roberts and V. C. Chambers, *ibid.*, **73**, 5034 (1951).
174. H. C. Brown, R. S. Fletcher, and R. B. Johannesen, *ibid.*, **73**, 212 (1951).
175. H. C. Brown and M. Borkowski, *ibid.*, **74**, 1894 (1952).
176. H. C. Brown and G. Ham, *ibid.*, **78**, 2735 (1956).
177. V. Prelog and M. Kobelt, *Helv. Chim. Acta*, **32**, 1187 (1949).
178. W. H. Saunders, Jr., and R. A. Williams, *J. Am. Chem. Soc.*, **79**, 3712 (1957); C. H. DePuy and D. H. Froemsdorf, *ibid.*, **79**, 3710 (1957).
179. P. S. Skell and C. R. Hauser, *ibid.*, **67**, 1661 (1945).
180. V. J. Shiner, Jr., and M. L. Smith, *ibid.*, **80**, 4095 (1958).
181. S. Winstein, E. Grunwald *et al.*, *ibid.*, **70**, 812, 816, 821, 828 (1948).
182. J. C. Martin and W. G. Bentrude, *Chem. and Ind.*, 192 (1959).
183. E. R. Garrett, *J. Am. Chem. Soc.*, **79**, 3401 (1957).
184. H. Morawetz and P. E. Zimmering, *J. Phys. Chem.*, **58**, 753 (1954).
185. M. L. Bender, *J. Am. Chem. Soc.*, **79**, 1258 (1957).
186. F. Brown, E. D. Hughes, C. K. Ingold, and J. F. Smith, *Nature*, **168**, 65 (1951).
187. S. Winstein, B. K. Morse, E. Grunwald, K. C. Schreiber, and J. Corse, *J. Am. Chem. Soc.*, **74**, 1113 (1952).
188. S. Winstein, M. Shatavsky, C. Norton, and R. B. Woodward, *ibid.*, **77**, 4183 (1955).
189. W. G. Woods, R. A. Carboni, and J. D. Roberts, *ibid.*, **78**, 5653 (1956).
190. R. Breslow, *ibid.*, **79**, 5318 (1957).
191. S. Winstein *et al.*, *ibid.*, **74**, 1127 (1952).
192. F. H. Westheimer and N. Nicolaides, *ibid.*, **71**, 25 (1949).
193. This subject has recently been reviewed by H. Zollinger, *Angew. Chem.*, **70**, 204 (1958).
194. D. B. Denney and P. P. Klemchuk, *J. Am. Chem. Soc.*, **80**, 3285 (1958); P. G. Farrell and S. F. Hason, *Nature*, **183**, 250 (1959).
195. G. S. Hammond, *J. Am. Chem. Soc.*, **77**, 334 (1955).
196. E. Grovenstein, Jr., and D. C. Kilby, *ibid.*, **79**, 2972 (1957).
197. H. Zollinger, *Helv. Chim. Acta*, **38**, 1597, 1617 (1955).
198. C. G. Swain and A. D. Ketley, *J. Am. Chem. Soc.*, **77**, 3410 (1955).
199. E. L. Purlee and R. W. Taft, Jr., *ibid.*, **78**, 5807 (1956).
200. E. S. Lewis and C. E. Boozer, *ibid.*, **74**, 6306 (1952).
201. V. J. Shiner, Jr., *ibid.*, **75**, 2925 (1953).
202. E. S. Lewis and G. M. Coppinger, *ibid.*, **76**, 4495 (1954).
203. V. J. Shiner, Jr., and C. J. Verbanic, *ibid.*, **79**, 373 (1957).
204. C. G. Swain, J. E. C. Knee, and A. J. Kresge, *ibid.*, **79**, 505 (1957).
205. V. J. Shiner, Jr., and S. Cross, *ibid.*, **79**, 3599 (1957).
206. K. Mislow, S. Borčić, and V. Prelog, *Helv. Chim. Acta*, **40**, 2477 (1957).
207. W. H. Saunders, Jr., S. Ašperger, and D. H. Edison, *Chem. and Ind.*, 1417 (1957).

208. A. Streitwieser, Jr., and R. C. Fahey, *ibid.*, 1417 (1957).

209. R. R. Johnson and E. S. Lewis, *Proc. Chem. Soc.*, **1958**, 52.

210. J. F. Bunnett, E. W. Garbisch, Jr., and K. M. Pruitt, *J. Am. Chem. Soc.*, **79**, 385 (1957).

211. F. C. Whitmore, *Ind. Eng. Chem.*, **26**, 94 (1934).

212. W. von E. Doering, R. G. Buttery, R. G. Laughlin, and N. Chaudhuri, *J. Am. Chem. Soc.*, **78**, 3224 (1956).

213. H. C. Brown and C. R. Smoot, *ibid.*, **78**, 6255 (1956); H. C. Brown and C. W. McGary, Jr., *ibid.*, **77**, 2300 (1955).

214. I. E. Muskat and H. E. Northrup, *ibid.*, **52**, 4043 (1930).

215. A. N. Pudovik, *Zhur. Obshchei Khim.*, **19**, 1179 (1949).

216. J. Meisenheimer and G. Beutter, *Ann.*, **508**, 58 (1933).

217. A. G. Catchpole, E. D. Hughes, and C. K. Ingold, *J. Chem. Soc.*, **1948**, 8.

218. See H. E. Zimmerman and T. E. Nevins, *J. Am. Chem. Soc.*, **79**, 6559 (1957), and H. E. Zimmerman and T. W. Cutshall, *ibid.*, **80**, 2893 (1958) for the formation of the less stable stereoisomers in the ketonization of enols and the tautomerism of aci-nitro to nitro compounds under kinetically controlled conditions.

219. J. E. Leffler, *The Reactive Intermediates of Organic Chemistry*, Interscience, New York, 1956, p. 221.

220. D. A. McCaulay and A. P. Lien, *J. Am. Chem. Soc.*, **74**, 6246 (1952).

221. K. A. Cooper, E. D. Hughes, C. K. Ingold, and B. J. MacNulty, *J. Chem. Soc.*, **1948**, 2038.

222. J. G. Hawke and V. R. Stimson, *ibid.*, **1956**, 4676.

223. E. D. Hughes, C. K. Ingold, and L. I. Woolf, *ibid.*, **1948**, 2084.

224. F. R. Jensen and H. C. Brown, *J. Am. Chem. Soc.*, **80**, 3039 (1958).

224a. F. Paneth and W. Hofeditz, *Ber.*, **62**, 1335 (1929); F. Paneth and W. Lautsch, *Ber.*, **64B**, 2702 (1931); *J. Chem. Soc.*, **1935**, 380.

225. F. O. Rice, W. R. Johnston, and B. L. Evering, *J. Am. Chem. Soc.*, **54**, 3529 (1932); F. O. Rice, *ibid.*, **53**, 1959 (1931); F. O. Rice and A. L. Glasebrook, *ibid.*, **56**, 2381 (1934).

226. J. H. Raley, F. F. Rust, and W. E. Vaughan, *ibid.*, **70**, 88 (1948).

227. S. L. Cosgrove and W. A. Waters, *J. Chem. Soc.*, **1951**, 388.

228. T. W. Campbell and G. M. Coppinger, *J. Am. Chem. Soc.*, **74**, 1469 (1952).

229. C. E. Boozer, G. S. Hammond, C. E. Hamilton, and J. N. Sen, *ibid.*, **77**, 3233 (1955).

230. G. S. Hammond and L. M. Soffer, *ibid.*, **72**, 4711 (1950).

231. G. S. Hammond, J. N. Sen, and C. E. Boozer, *ibid.*, **77**, 3244 (1955).

232. A. W. Francis, *ibid.*, **47**, 2340 (1925).

233. S. Winstein and R. E. Buckles, *ibid.*, **65**, 613 (1943).

234. R. M. Roberts, J. Corse, R. Boschan, D. Seymour, and S. Winstein, *ibid.*, **80**, 1247 (1958).

235. P. Dyson and D. L. Hammick, *J. Chem. Soc.*, **1937**, 1724; M. R. F. Ashworth, R. P. Daffern, and D. L. Hammick, *ibid.*, **1939**, 809.

236. H. Conroy and R. A. Firestone, *J. Am. Chem. Soc.*, **75**, 2530 (1953).

237. C. E. Walling, E. R. Briggs, W. Cummings, and F. R. Mayo, *ibid.*, **72**, 48 (1950).

238. R. L. Dannley and E. L. Kay, *ibid.*, **77**, 1046 (1955).

239. F. C. Whitmore, *ibid.*, **54**, 3274 (1932).

240. See G. W. Wheland, *Advanced Organic Chemistry*, Wiley, New York, 1949, ch. 12, for a detailed discussion of 1,2-shifts.

241. H. S. Bloch, H. Pines, and L. Schmerling, *J. Am. Chem. Soc.*, **68**, 153 (1946).

242. G. Wittig and W. Happe, *Ann.*, **557**, 205 (1947); S. W. Kantor and C. R. Hauser, *J. Am. Chem. Soc.*, **73**, 4122 (1951).
243. W. H. Urry and N. Nicolaides, *ibid.*, **74**, 5163 (1952); D. Y. Curtin and M. J. Hurwitz, *ibid.*, **74**, 5381 (1952).
244. R. C. Fuson, C. C. Price, and D. M. Burness, *J. Org. Chem.*, **11**, 475 (1946).
245. S. D. Ross, *J. Am. Chem. Soc.*, **69**, 2982 (1947).
246. J. F. Bunnett and T. K. Brotherton, *ibid.*, **78**, 155 (1956).
247. A. G. Davies and J. Kenyon, *Quart. Revs.*, **9**, 203 (1955).
248. E. D. Hughes, C. K. Ingold, and S. Masterman, *J. Chem. Soc.*, **1937**, 1196.
249. E. D. Hughes, C. K. Ingold, and A. D. Scott, *ibid.*, **1937**, 1201.
250. W. von E. Doering and H. H. Zeiss, *J. Am. Chem. Soc.*, **75**, 4733 (1953).
251. A. Streitwieser, Jr., *Chem. Revs.*, **56**, 571 (1956).
252. See C. A. Bunton and D. R. Llewellyn, *J. Chem. Soc.*, **1957**, 3402; A. Streitwieser, Jr., and W. D. Schaeffer, *J. Am. Chem. Soc.*, **79**, 2888 (1957), for recent examples and discussion on these points.
253. W. A. Cowdrey, E. D. Hughes, and C. K. Ingold, *J. Chem. Soc.*, **1937**, 1208.
254. S. Winstein and H. J. Lucas, *J. Am. Chem. Soc.*, **61**, 1576 (1939).
255. I. Roberts and G. E. Kimball, *ibid.*, **59**, 947 (1937).
256. S. Winstein and H. J. Lucas, *ibid.*, **61**, 1576, 2845 (1939).
257. S. Winstein, E. Grunwald, and L. L. Ingraham, *ibid.*, **70**, 821 (1948).
258. D. J. Cram, *ibid.*, **71**, 3863, 3875, 3883 (1949).
259. S. Winstein and D. S. Trifan, *ibid.*, **71**, 2953 (1949); **74**, 1154 (1952).
260. S. Winstein and K. C. Schreiber, *ibid.*, **74**, 2165 (1952).
261. S. Winstein and D. Trifan, *ibid.*, **74**, 1154 (1952).
262. H. L. Goering, T. D. Nevitt, and E. F. Silversmith, *ibid.*, **77**, 5026 (1955).
263. H. C. Brown, M. S. Kharasch, and T. H. Chao, *ibid.*, **62**, 3435 (1940).
264. W. von E. Doering, M. Farber, M. Sprecher, and K. B. Wiberg, *ibid.*, **74**, 3000 (1952).
265. S. K. Hsü and C. L. Wilson, *J. Chem. Soc.*, **1936**, 623.
266. N. Kornblum, N. N. Lichtin, J. T. Patton, and D. C. Iffland, *J. Am. Chem. Soc.*, **69**, 307 (1947).
266a. R. L. Letsinger, *ibid.*, **72**, 4842 (1950).
267. E. Ott, A. Behr, and R. Schroter, *Ber.*, **61**, 2124 (1928).
268. J. F. Lane and S. E. Ulrich, *J. Am. Chem. Soc.*, **72**, 5132 (1950).
269. E. LeGoff, S. E. Ulrich, and D. B. Denney, *ibid.*, **80**, 622 (1958).
270. A survey of literature in this field is given in J. G. Burr, Jr., *Tracer Applications for the Study of Organic Reactions*, Interscience, New York, 1957. See also Chapter XXVI.
271. O. Beeck, J. W. Otvos, D. P. Stevenson, and C. D. Wagner, *J. Chem. Phys.*, **16**, 255 (1948).
272. J. D. Roberts, R. E. McMahon, and J. S. Hine, *J. Am. Chem. Soc.*, **72**, 4237 (1950).
273. J. D. Roberts, C. C. Lee, and W. H. Saunders, Jr., *ibid.*, **76**, 4501 (1954).
274. J. D. Roberts and R. H. Mazur, *ibid.*, **73**, 3542 (1951).
275. C. G. Bergstrom and S. Siegel, *ibid.*, **74**, 145 (1952).
276. J. D. Roberts and J. A. Yancey, *ibid.*, **74**, 5943 (1952).
277. J. D. Roberts and C. M. Regan, *ibid.*, **75**, 2069 (1953); J. D. Roberts and M. Halmann, *ibid.*, **75**, 5759 (1953).
278. C. J. Collins and W. A. Bonner, *ibid.*, **77**, 92, 99 (1955).
279. W. A. Bonner and D. D. Tanner, *ibid.*, **80**, 1447 (1958).

280. R. B. Loftfield, *ibid.*, **72**, 632 (1950); **73**, 4707 (1951).

281. J. D. Roberts, H. E. Simmons, Jr., L. A. Carlsmith, and C. W. Vaughan, *ibid.*, **75**, 3290 (1953); J. D. Roberts, D. A. Semenow, H. E. Simmons, Jr., and L. A. Carlsmith, *ibid.*, **78**, 601 (1956).

282. F. Scardiglia and J. D. Roberts, *Tetrahedron*, **1**, 343 (1957).

282a. S. V. Vitt and R. V. Kudryavtsey, *Zhur. Obshchei Khim.*, **27**, 2799 (1957).

283. D. B. Denney and M. A. Greenbaum, *J. Am. Chem. Soc.*, **78**, 877 (1956); **79**, 3701 (1957).

284. D. B. Denney, *ibid.*, **77**, 1706 (1955).

285. D. B. Denney and B. Goldstein, *ibid.*, **79**, 4948 (1957).

286. S. Winstein and G. C. Robinson, *ibid.*, **80**, 180 (1958).

287. M. L. Bender, Y.-L. Chow, and F. Chloupek, *ibid.*, **80**, 5380 (1958).

288. M. L. Bender, F. Chloupek, and M. C. Neveu, *ibid.*, **80**, 5384 (1958).

289. M. L. Bender and M. C. Neveu, *ibid.*, **80**, 5388 (1958).

290. This work has been summarized in J. A. Bassham and M. Calvin, *The Path of Carbon in Photosynthesis*, Prentice-Hall, Englewood Cliffs, N. J., 1957.

291. M. L. Bender, *J. Am. Chem. Soc.*, **73**, 1626 (1951).

292. M. L. Bender, R. D. Ginger, and K. C. Kemp, *ibid.*, **76**, 3350 (1954).

293. C. A. Bunton, T. A. Lewis, and D. H. Llewellyn, *Chem. and Ind.*, 1154 (1954).

294. M. L. Bender, R. D. Ginger, and J. P. Unik, *J. Am. Chem. Soc.*, **80**, 1044 (1958).

295. C. A. Bunton, T. Hadwick, D. R. Llewellyn, and Y. Pocker, *Chem. and Ind.*, 547 (1956); *J. Chem. Soc.*, **1958**, 403.

295a. I. Dostrovsky and F. S. Klein, *ibid.*, **1955**, 791.

296. C. K. Ingold, E. de Salas, and C. L. Wilson, *ibid.*, **1936**, 1328.

297. S. K. Hsü, C. K. Ingold, and C. L. Wilson, *ibid.*, **1938**, 78.

298. S. J. Cristol and D. D. Fix, *J. Am. Chem. Soc.*, **75**, 2647 (1953).

299. J. Hine, R. C. Peck, Jr., and B. D. Oakes, *ibid.*, **76**, 827 (1954).

300. K. F. Bonhoeffer and W. D. Walters, *Z. physik. Chem.*, **181A**, 441 (1938).

301. R. P. Bell and M. J. Smith, *J. Chem. Soc.*, **1958**, 1691.

302. C. G. Swain and M. M. Kreevoy, *J. Am. Chem. Soc.*, **77**, 1122 (1955).

303. S. Winstein, E. Clippinger, A. H. Fainberg, R. Heck, and G. C. Robinson, *ibid.*, **78**, 328 (1956).

304. R. Bolton, J. Miller, and A. J. Parker, *Chem. and Ind.*, 1026 (1960).

305. J. Miller and A. J. Parker, *J. Am. Chem. Soc.*, **83**, 117 (1961).

306. H. Holzer and K. Beaucamp, *Angew. Chem.*, **71**, 776 (1959); *Biochem. Biophys. Acta*, **46**, 225 (1961).

307. G. L. Carlson and G. M. Brown, *J. Biol. Chem.*, **236**, 2099 (1961); *ibid.*, **235**, PC 3 (1960).

308. L. H. Piette and W. C. Landgraf, *J. Chem. Phys.*, **32**, 1107 (1960).

309. R. S. Berry, G. N. Spokes, and M. Stiles, *J. Am. Chem. Soc.*, **82**, 5240 (1960).

310. H. Theorell, *Acta Chem. Scand.*, **14**, 933 (1960).

311. B. Vigneron, P. Crooy, F. Kezdy, and A. Bruylants, *Bull. Soc., Chim. Belges*, **69**, 616 (1961).

312. S. A. Bernhard, A. Berger, J. H. Carter, E. Katchalski, M. Sela, and Y. Shalitin, *J. Am. Chem. Soc.*, **84**, 2421 (1962).

313. R. M. Etter, H. S. Skovronek, and P. S. Skell, *J. Am. Chem. Soc.*, **81**, 1008 (1959).

314. K. R. Kopecky, G. S. Hammond, and P. A. Leermakers, *J. Am. Chem. Soc.*, **83**, 2397 (1961).

315. S. Winstein, J. Sonnenberg, and L. De Vries, *J. Am. Chem. Soc.*, **81**, 6523 (1959); S. Winstein and J. Sonnenberg, *ibid.*, **83**, 3235, 3244 (1961).

316. T. C. Bruice and J. L. York, *J. Am. Chem. Soc.*, **83**, 1382 (1961).
317. J. Halpern, B. R. James, and A. L. W. Kemp, *J. Am. Chem. Soc.*, **83**, 4097 (1961).
318. H. C. Brown and S. Nishida, *Abstracts of 139th Meeting of Am. Chem. Soc.*, St. Louis, Mo., 2-O (March, 1961).
319. H. C. Brown, Strained transition states, *Symposium on the Transition State, Anniversary Meeting of the Chemical Society*, Sheffield, England (April, 1962).
320. D. C. Kleinfelter, P. von R. Schleyer, and H. G. Richey, Jr., *Abstracts of 142nd Meeting of Am. Chem. Soc.*, Atlantic City, N. J., 56-Q (Sept., 1962).

General References

Frost, A. A. and Pearson, R. G., *Kinetics and Mechanism*, 2nd ed., Wiley, New York, 1961.
Gould, E. S., *Mechanism and Structure in Organic Chemistry*, Holt, New York, 1959.
Hammett, L. P., *Physical Organic Chemistry*, McGraw-Hill, New York, 1940.
Hine, J., *Physical Organic Chemistry*, McGraw-Hill, New York, 1956.
Ingold, C. K., *Structure and Mechanism in Organic Chemistry*, Cornell University Press, Ithaca, 1954.
Leffler, J. E., *The Reactive Intermediates of Organic Chemistry*, Interscience, New York, 1956.
Steacie, E. W. R., *Atomic and Free Radical Reactions*, 2nd ed., Reinhold, New York, 1954.
Walling, C., *Free Radicals in Solution*, Wiley, New York, 1957.

CHAPTER XXVI

USE OF ISOTOPES AND TAGGED GROUPS

WILLIAM H. SAUNDERS, JR., *University of Rochester*

I. Introduction 1519
II. Carbon Isotopes 1520
1. General 1520
2. The Claisen Rearrangement 1521
3. Isotopic vs. Non-Isotopic Methods 1524
4. Some Carbonium Ion Rearrangements 1524
III. Oxygen-18 1529
1. Ester Hydrolysis 1529
2. Oxygen Exchange with Alcohols 1530
3. Formation and Decomposition of Peroxy Compounds 1531
4. Ion-Pair Intermediates 1531
IV. Nitrogen-15 1533
1. Reaction of Azide Ion with Diazonium Salts 1533
2. The Fischer Indole Synthesis 1534
3. Miscellaneous Studies 1534
V. Hydrogen Isotopes 1535
1. Enolization and Related Reactions 1535
2. Elimination Reactions 1535
3. Deuterium Exchange by Aromatic Hydrocarbons 1537
4. Deuterium Exchange by Aliphatic Hydrocarbons 1538
5. Rates of Proton Transfers 1538
6. Deuterium-Induced Asymmetry 1538
VI. Isotopes of Other Elements 1539
1. Isotopes of the Halogens 1539
2. Sulfur-35 1539
VII. Some Practical Aspects of Tracer Work 1541
1. Preparation of Labeled Compounds 1541
2. Measurement of Deuterium 1541
3. Stable Isotopes Other Than Deuterium 1542
4. Radioactive Isotopes 1543
5. Pitfalls in Tracer Work 1544
References 1545

I. INTRODUCTION

Any well-planned study of a reaction mechanism will usually employ a variety of physical and chemical methods. A knowledge of the kinetics of the reaction is often only a starting point from which a more complete

picture of the reaction may be approached by non-kinetic means. Many reactions are not amenable to kinetic studies at all, so that other techniques must, in these cases, provide our only basis for mechanistic conclusions. An important group of techniques involving the use of isotopes of the common elements has become increasingly popular in recent years.

These techniques may be divided into a number of categories. The most widely publicized use of isotopes is as tracers. In this application, the isotope is used to "tag" an atom, which otherwise is (or could become) indistinguishable from other atoms of its kind in the molecule. One is thus able to follow the fate of the particular atom through a chemical reaction. Often, though by no means always, non-isotopic methods can furnish similar information. For example, if the point in question is the symmetry of an intermediate, stereochemical methods may also be useful. Later, there will be described a number of instances in which both isotopic and non-isotopic methods were employed to gain the same information. Studies of isotope-exchange reactions (reactions in which an atom in a molecule is replaced by another atom differing only isotopically from the first) have also been very useful. Finally, the effect of isotopes on the rates of chemical reactions is perhaps the most direct and powerful method available for studying the behavior of individual bonds in a molecule during a chemical reaction. This topic is discussed elsewhere in the present volume (Chapter IX).

The literature on isotopic tracers is by now far too extensive to be covered exhaustively in a single chapter. Consequently, the plan of the succeeding pages will be to discuss certain key cases in detail and to make brief reference to a wider variety of work, so that the reader may further satisfy his curiosity on any particular topic. Even at that, no claim for comprehensiveness is made, and apologies are tendered in advance to those whose work has been ignored, but might just as well have been included.

II. CARBON ISOTOPES

1. General

Probably the most frequent use of isotopic carbon (mostly C^{14}) tracers has been in molecular rearrangements. A knowledge of the locations of particular carbon atoms in reactants and products is often of great help in formulating the nature of the intermediate(s) involved. The information may be of a simple type giving, for example, the extent of rearrangement of a compound or the symmetry of an intermediate. More subtle applications may provide information on otherwise unapproachable steps

in complex reactions, and allow one to establish the relative contributions of various possible reaction paths.

2. The Claisen Rearrangement

A good example to begin with is the Claisen rearrangement, which has been the subject of numerous recent investigations. A point of particular interest is that many of the significant discoveries have been made by both isotopic and non-isotopic procedures. We can thus compare isotopic tracer methods with more conventional approaches and assess the advantages and disadvantages of each.

The first point to come under consideration was the inversion or non-inversion of the migrating allyl group. Two workers (1,2) showed almost simultaneously that the *ortho*-rearrangement proceeds with inversion, as in I → II (here, and elsewhere in this chapter, the * represents an isotopi-

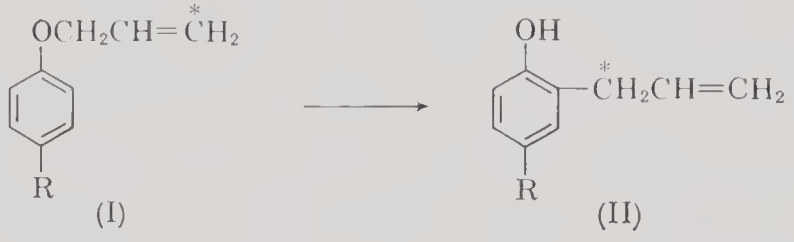

(I) (II)

cally labeled position). Now this may seem to be a trivial point, since it had been known for some time that inversion is the rule (3); for example see (III → IV).

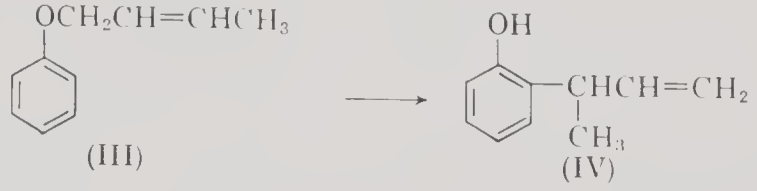

(III) (IV)

Actually the isotopic demonstration enables one to limit more severely any possible non-inversion by reason of the essentially complete absence of activity in the γ-carbon of II.

Next, the same workers showed that the allyl group migrated with net retention (1, 4) in the *para* Claisen rearrangement, V → VI. This was

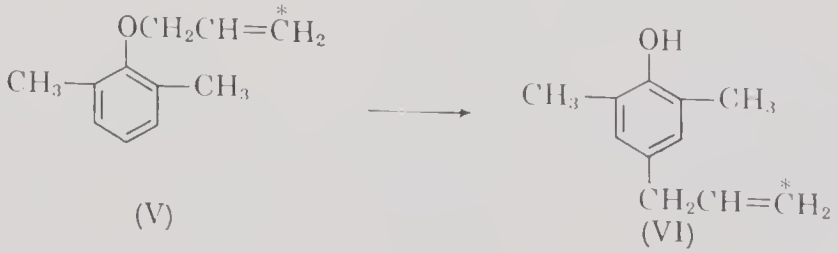

(V) (VI)

a point on which the earlier literature had been conflicting. The conflict was shortly resolved by the demonstration (5) that both VII and VIII,

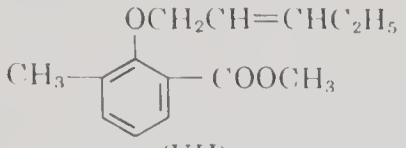

(VII)

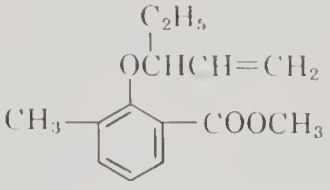

(VIII)

contrary to previous reports, undergo the *para* rearrangement with retention.

That the *para* rearrangement is intramolecular was shown (4) by rearranging a mixture of V and IX. The X recovered from the reaction mix-

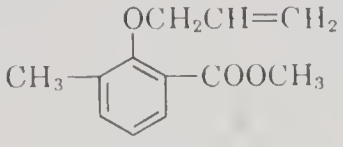

(IX)

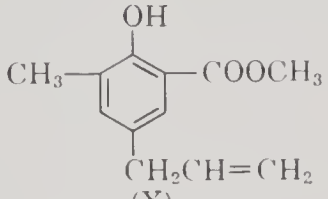

(X)

ture contained only 0.02% of the radioactivity of V; hence no appreciable fraction of the allyl groups from molecules of V wound up in X. An analogous non-isotopic demonstration of intramolecularity was obtained by rearranging mixtures of XI and XII (6). No cross products were detect-

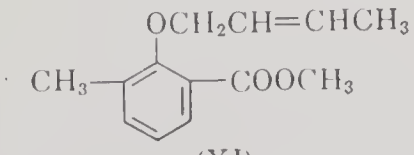

(XI)

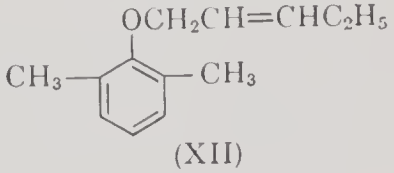

(XII)

able. In both of the above demonstrations, the two compounds used in each case were shown to rearrange separately at comparable rates, a fundamental prerequisite for the meaningfulness of such "cross-over" experiments.

The evidence thus far advanced is consistent with the sequence of XIII → XIV → XV for the *ortho* rearrangement. A logical mechanism for the

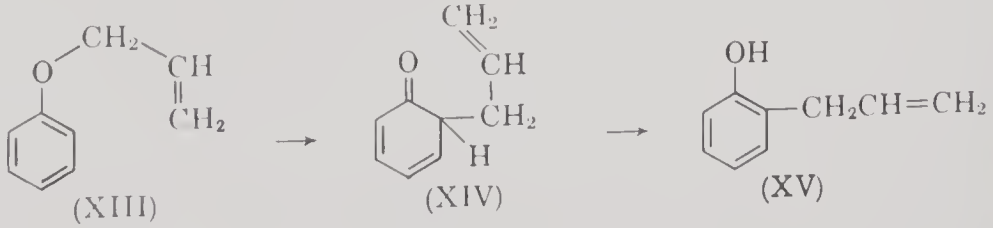

(XIII) (XIV) (XV)

para rearrangement involves an intermediate (XVI) (analogous to XIV). Evidence for the intermediate (XVI) was soon forthcoming. The rearrangement of XIX gave XXI, having the activity distribution to be expected for XX as intermediate (7). Similar evidence was obtained from the study of XXII and XXIII (A = allyl and M = 2-methylallyl) (8), where the indicated sequence of reactions was shown to occur:

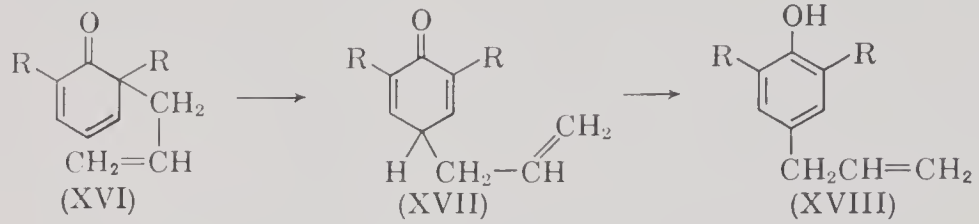

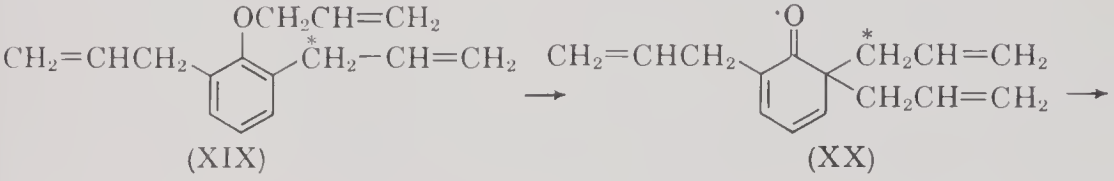

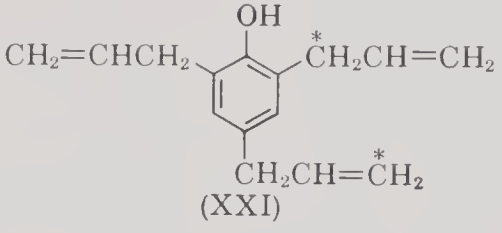

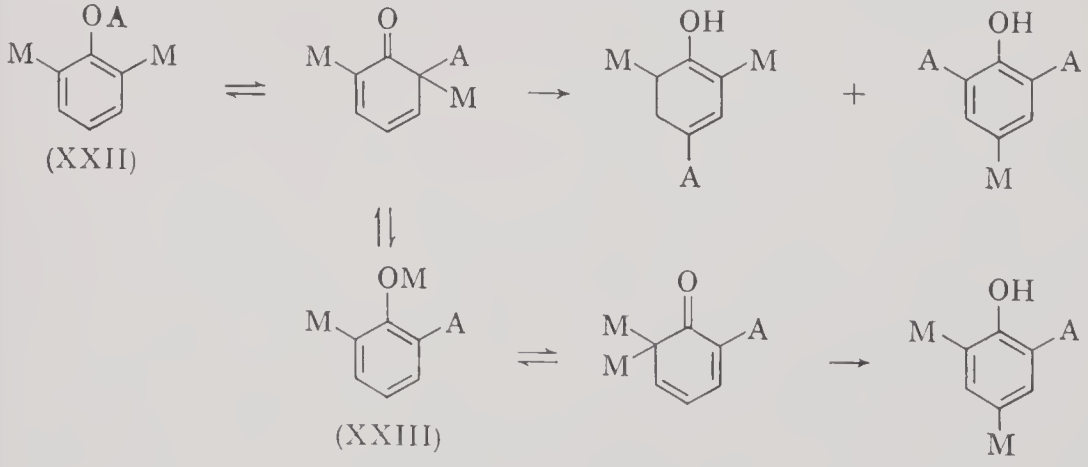

The slow interconversion of XXII and XXIII also demonstrates the reversibility of the dienone-forming reaction. The reversibility of the *para* rearrangement has been shown with C^{14}-labeled material (9). More recent work has been concerned with the preparation and rearrangement of the dienone intermediate (10) and with the relative values of the rate constants for the various individual steps (10,11).

3. Isotopic vs. Non-Isotopic Methods

The above account has shown a number of ways in which isotopic tracers can provide evidence on mechanism, as well as some instructive parallels to non-isotopic methods for acquiring similar information. Obvious advantages of the isotopic methods are less difficulty in product isolation (only enough pure product to count is needed) and, usually, a more precise answer. In addition, the interpretation of results is often simpler (8), since one is dealing with molecules differing only isotopically. Where there are structural differences, these may have substantial effects on rates of the various steps. On the other hand, the synthesis and degradation of isotopically labeled materials may at times be troublesome. A tracer investigation is reliable only to the extent that synthetic and degradative procedures are unambiguous. Some possible pitfalls in tracer investigations will be discussed in a later section.

4. Some Carbonium Ion Rearrangements

Tracer methods have been particularly prominent in recent developments in carbonium ion rearrangements. Much evidence bearing on "nonclassical" or "bridged" carbonium ions has resulted from this work.

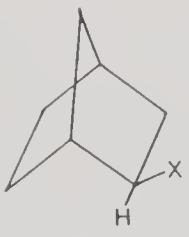

(XXIV)

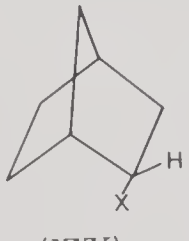

(XXV)

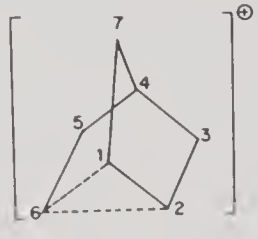

(XXVI)

Winstein and Trifan (12) noted that both *exo*- (XXIV) and *endo*-norbornyl (XXV) derivatives solvolyzed to *exo* products. When optically active starting materials were used, XXIV gave complete, and XXV nearly complete, racemization. These (and other) results require a symmetrical intermediate, which is shielded from *endo* attack. The conditions are best, though not uniquely, fulfilled by XXVI. In order to provide further evidence, Roberts (13) undertook the study of C^{14}-labeled norbornyl derivatives.

If XXVI is the only intermediate, solvolysis of XXIVa and XXVa should lead to a product in which 50% of the activity has rearranged away from the 2,3-positions.

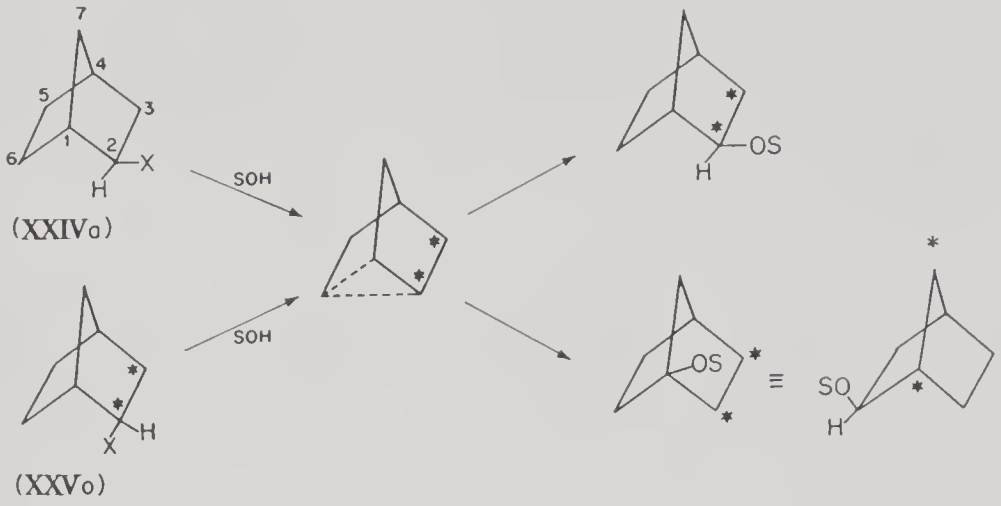

(XXIVo) (XXVo)

Under certain conditions, the extent of rearrangement approximated the predicted 50%. Under other conditions, however, the extent of rearrangement was as high as 66–69%. In these cases, activity is also found in positions 5 and 6 of the product. These data require a 2,6-hydrogen shift and are consistent with the intermediate (XXVII) (or its equivalent) formed competitively with XXVI or from XXVI. Attack at positions 1, 2, or 6 can occur with equal probability, leading to $66^2/_3\%$ rearrangement, and to activity in positions 5 and 6 of the product.

Additional impetus to the search for non-classical carbonium ions was given by Cram's (14) studies on the 3-phenyl-2-butyl and related systems, which furnished convincing stereochemical evidence for a phenonium ion intermediate (XXVIII).

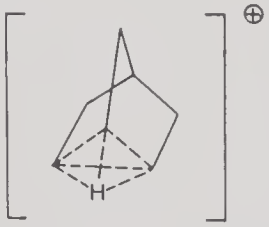

(XXVII)

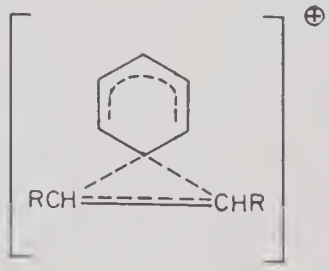

(XXVIII)

Among the subjects investigated was the deamination of amines of the type XXIX, which might proceed through the carbonium-ion intermediate XXX to give rearrangement of the C^{14}-activity. When R is hydrogen or

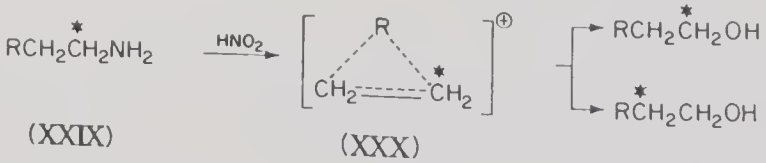

(XXIX) (XXX)

alkyl (15), however, little or no rearrangement occurs. Only when R is phenyl or substituted phenyl (15e) is there appreciable rearrangement.

Even a rearranged product does not necessarily indicate XXX as intermediate, for the same consequences would follow from an equilibrium between classical ions:

$$RCH_2\overset{*}{C}H_2^{\oplus} \rightleftharpoons R\overset{*}{C}H_2CH_2^{\oplus}$$

Although the systems mentioned in the previous paragraph do not allow a distinction between bridged ions and equilibrating open ions, this is possible in some cases. The first example was the pentamethylethyl system (XXXI) (16). Here a bridged ion (XXXII) can open in either of

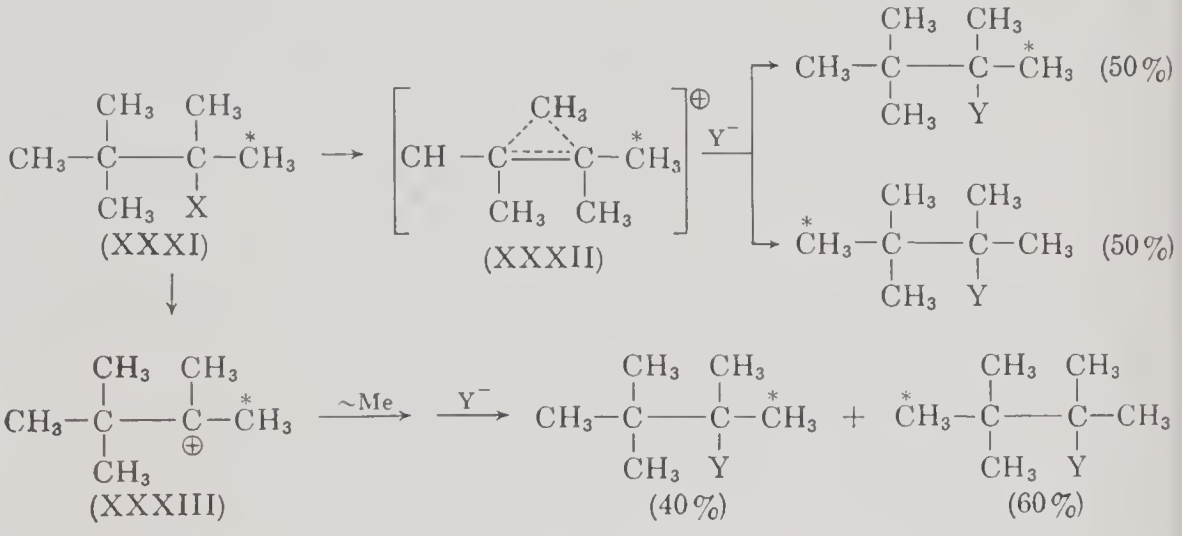

two directions with equal probability, giving a product in which the C^{14}-methyl is 50% on the carbon bearing the functional group and 50% on the adjacent carbon. If, on the other hand, equilibrating open ions of the type XXXIII are involved, the activity will become statistically distributed among the methyl groups and thus 40% of the C^{14}-methyls will be on C-1 (two methyls) and 60% on C-2 (three methyls) of the pentamethylethyl system.

Unfortunately, the experiments did not yield the desired information since, under conditions where the products formed irreversibly, only a small (12–16%) amount of C^{14}-rearrangement was observed. The figures given refer to treatment of the alcohol (XXXI, X = OH) with concentrated hydrochloric acid at 0°C. That the product chloride was formed irreversibly was shown by the fact that it underwent negligible exchange with HCl^{36} under the same conditions. With Lucas reagent ($HCl + ZnCl_2$) the 60:40 C^{14}-distribution is observed, but there is also complete exchange of chloride. Thus the product can return to carbonium ion many times and the equilibrium C^{14}-distribution results irrespective of mechanism.

A way around the problem of incomplete rearrangement in irreversible reactions was devised by Collins (17). The system employed in his studies was triphenylethyl (XXXIV) with C^{14}-labels in the benzene rings (XXXIVa) and in the carbon chain (XXXIVb). The bridged ions from XXXIVa predict a 50% rearrangement of activity, whereas equilibrating classical ions predict $66^2/_3$% rearrangement. With XXXIVb however, 50% rearrangement is a consequence of either mechanism (16).

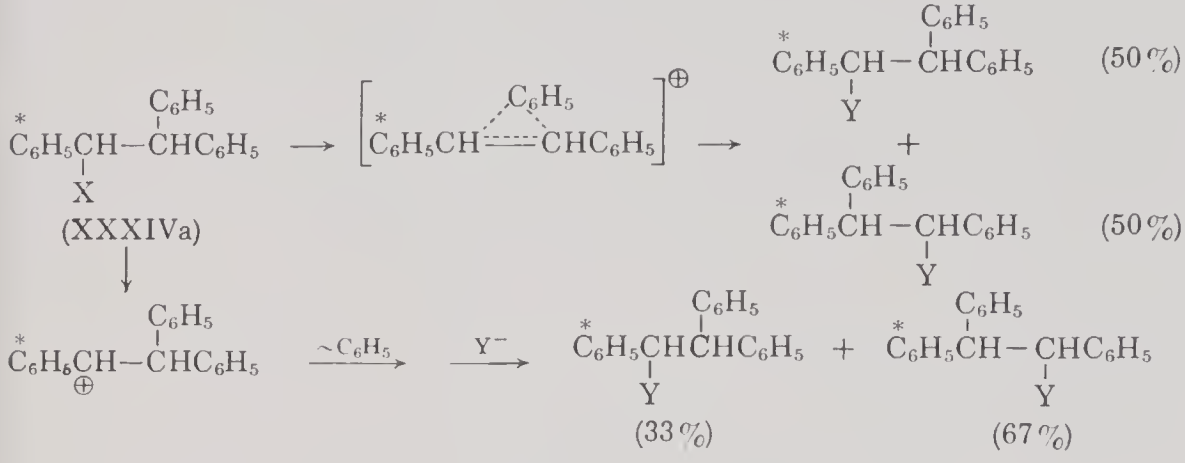

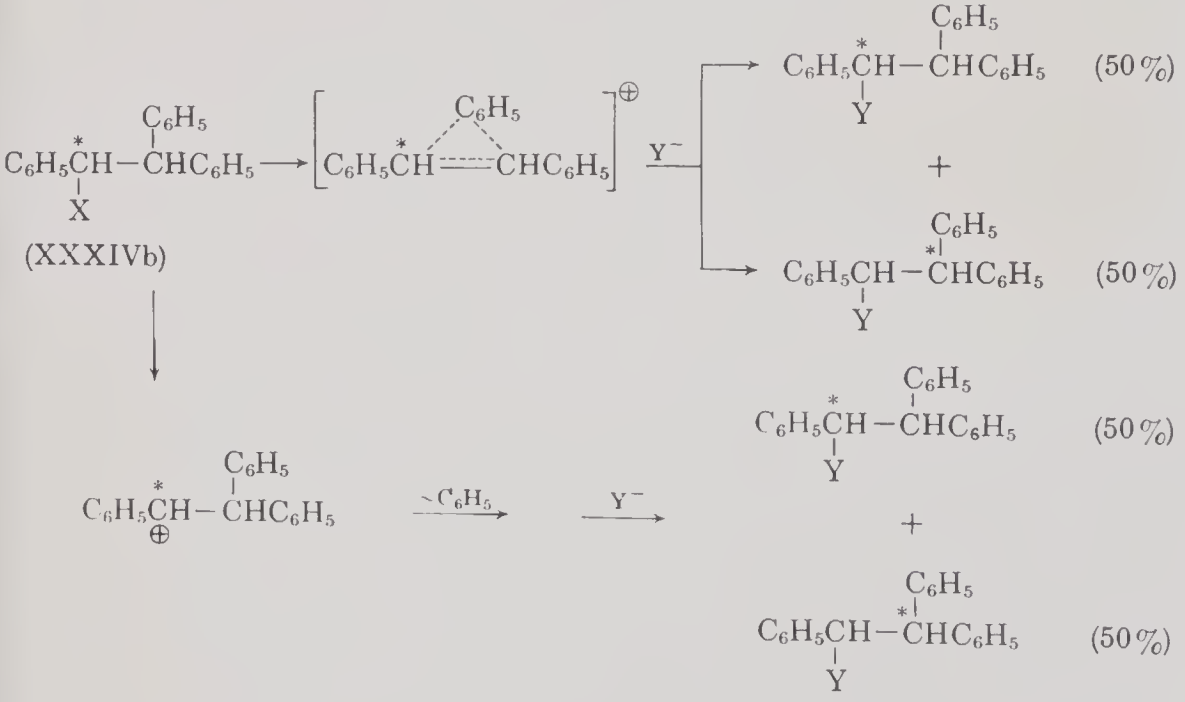

Now, in an irreversible reaction of XXIV, part of the reaction may be a non-rearranging replacement, as was found with XXXI. If the bridged ion is the sole rearranging intermediate, such rearrangement as does occur will proceed at the same rate for both XXXIVa and XXXIVb. The extents of rearrangement should therefore be identical. If, however, equilibrating open ions are involved, the rate of rearrangement for XXXIVa

should be faster than for XXXIVb, the numerical value of the ratio of rates being easily predictable (17). In fact, the rearrangement of a number of derivatives (alcohol, acetate, tosylate) of XXXIV fit the prediction excellently. Hence, rearrangements of XXXIV must proceed, at least predominantly, through open ions. The phenyl migration occurring in nitrous acid deamination of 1,2,2-triphenylethylamine was also shown to proceed through open ions (18).

Collins has, in subsequent work, made still more subtle use of the potentialities of C^{14}-labeling. In the pinacol rearrangement of triphenylethylene glycol (19), a number of reaction paths are

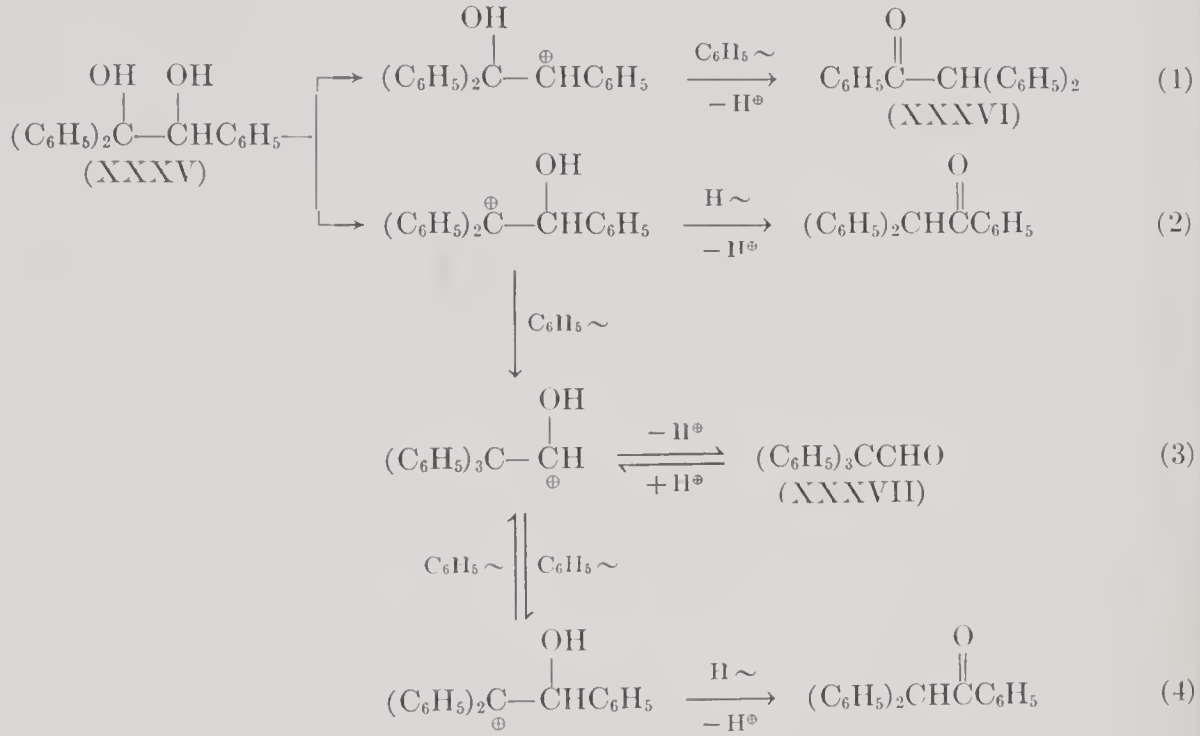

available. Normally, it would be possible only to distinguish path (3) from the rest, since it is the only one yielding a structurally different product. Using XXXV labelled in a phenyl group (XXXVa) and in the carbon chain (XXXVb), the remaining three paths can be disentangled. For

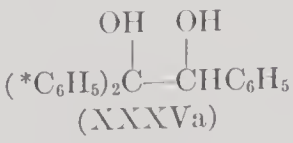

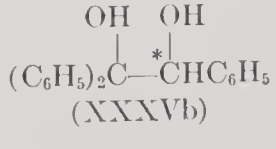

example, XXXVb would give complete rearrangement by path (1), but no rearrangement by paths (2) or (4). The reader can easily verify that the predicted extents of rearrangement for XXXVa would be 50% for path (1), 0% for path (2), and $33^1/_3$% for path (4). Thus, if one knows the yield of XXXVII and the per cent rearrangement for XXXVa and XXXVb, the contribution of each of the four paths can be calculated

(20). From these, one can calculate the migration aptitude of phenyl relative to hydrogen, which is given simply by [path (3) + path (4)]/path (2). The results turned out to be very interesting, since changes in reaction conditions produced large changes in the ratio. The C_6H_5/H migration ratio varied from 7.3 in concentrated sulfuric acid to 0.041 in dioxane-water-hydrochloric acid.

Many other applications of C^{14} to rearrangement reactions may be found in the literature. Most of these applications involve principles already covered in the preceding pages. Since little additional enlightenment would result from further multiplication of examples, the discussion will turn to isotopes of other common elements.

III. OXYGEN-18

1. Ester Hydrolysis

The only isotope of oxygen that has been used in tracer work is the stable O^{18} (there are no radioactive isotopes). This occurs to the extent of 0.20% in normal oxygen, and the usual enrichment for tracer work runs around several per cent.

Among the earliest of all organic tracer studies was the investigation by Polanyi and Szabo (21) of the alkaline hydrolysis of amyl acetate in O^{18}-enriched water. They observed that the amyl alcohol produced was isotopically normal and concluded that acyl-oxygen fission had occurred. This conclusion is undoubtedly correct, but Kursanov (22) has recently pointed out that the evidence is probably meaningless. Polanyi and Szabo dehydrated their amyl alcohol over alumina, and then carried out density measurements on the water obtained. Since water exchanges oxygen rapidly with alumina under the conditions used (23), the water would have been isotopically normal regardless of the isotopic composition of the amyl alcohol from which it was derived. Kursanov (22) provided an unequivocal demonstration of acyl-oxygen fission in the alkaline hydrolysis of ethyl propionate labeled with O^{18} in the ether oxygen. Other workers have applied O^{18} labeling to the hydrolysis of β-lactones (24), γ-lactones (25), and various esters (26–29). Exceptions to the rule of acyl-oxygen fission have been observed with tertiary acetates (26–28) and β-lactones (24). Alkyl-oxygen fission is generally favored by conditions promoting carbonium ion formation.

Closely allied to these studies have been efforts to determine the nature of the intermediate in ester hydrolysis. The reaction may be considered to occur by a direct displacement [Eq. (4)] or stepwise [Eq. (5)]. If

$$\mathrm{RCOR' + H_2O \rightarrow \left[H_2O \ldots C(=O)(R) \ldots OR' \right] \rightarrow HO{-}C(=O)(R) + HOR'}$$

$$\mathrm{RCOR' + H_2O \rightleftharpoons R{-}C(OH)_2{-}OR' \rightarrow RCOH + HOR'} \qquad (5)$$

Equation (5) is correct, and the intermediate returns to reactant at a rate comparable to that of its decomposition to products, the use of water-O^{18} should lead to incorporation of O^{18} in the carbonyl group of the unreacted ester.

This subject has been thoroughly investigated by Bender (30), who found that Equation (5) does correctly represent the mechanism in most instances. The ratio of the rate of hydrolysis (k_H) to the rate of exchange (k_E) of various benzoates ranges from 2.7 to 10.6 depending on the nature of the alkyl group and on whether the reaction is acid- or base-catalyzed. Exchange still occurs with methyl-2,4,6-trimethylbenzoate (31) ($k_H/k_E = 6.8$), methyl-β-phenylpropionate (32) ($k_H/k_E = 9.5$), and benzoyl L-phenylalanine ethyl ester (12) ($k_H/k_E = 15.6$). The last two compounds were subjected to hydrolysis catalyzed by α-chymotrypsin. In contrast to the non-enzymatic hydrolysis, no detectable exchange was found (32). Other studies of O^{18}-exchange in ester hydrolysis have been performed by Bunton (27,33). The basic hydrolysis of benzamide is accompanied by exchange, but the acid hydrolysis is not (34).

2. Oxygen Exchange with Alcohols

Examination of rates of oxygen exchange of various alcohols with enriched water has contributed valuable mechanistic information. The rate of exchange of *tert*-butyl alcohol with acidic H_2O^{18} exceeds the rate of dehydration (35). This fact suggests slow formation of a carbonium ion which then either returns to alcohol or goes on to olefin. For *n*-butyl alcohol exchange likewise goes faster than decomposition, but for neopentyl alcohol the reverse is true (36). This is interpreted as exchange via an S_N2 attack of water on the conjugate acid of the primary alcohol. The rate of this process should, of course, be much less for neopentyl alcohol than for *n*-butyl alcohol. A comparison of rates of racemization and exchange of 1-phenylethanol gave results between those predicted for S_N1 and S_N2 processes (37). Evidently the departing water molecule partially shields the frontside of the intermediate. Another interesting observation along

this line is that pinacol exchanges oxygen with aqueous acid (38) faster than it rearranges to pinacolone.

An ingenious use of O^{18}-enriched water was made by Long and Pritchard (39) in their study of the hydrolysis of propylene and isobutylene oxides. Examination of the mass spectra of the product glycols enabled them to deduce the proportion of glycol resulting from ring opening in each of the two possible directions.

3. Formation and Decomposition of Peroxy Compounds

The mode of formation of derivatives of hydrogen peroxide has been the subject of several tracer studies. Formation and hydrolysis of organic peroxyacids involves acyl-oxygen rather than oxygen-oxygen fission (40). Likewise, the oxygen-oxygen bond retains its integrity in the formation of hydroperoxides from alcohols and aqueous acidic hydrogen peroxide (41).

The use of O^{18}-labeled compounds has shed light on the mechanisms of a number of rearrangements involving peroxides or peroxyacids. For example, treatment with a peroxyacid of a ketone labeled in the carbonyl oxygen leads to an ester in which the label remains entirely in the carbonyl (40,42). The most reasonable mechanism consistent with this fact is Equation (6). In the acid-catalyzed rearrangement of 1-phenylethyl hydroperoxide (41) [Eq. (7)], no exchange of oxygen between the solvent

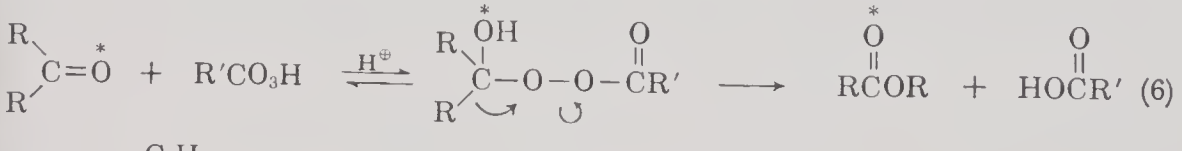

(6)

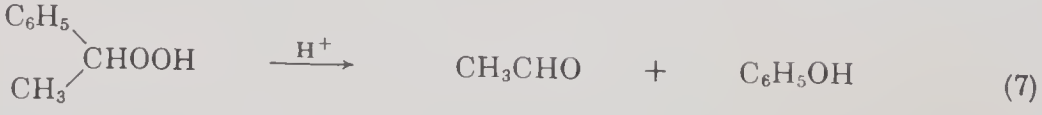

(7)

and unreacted hydroperoxide is observed. Bunton (41) argues from this that cleavage of the oxygen-oxygen bond and migration of phenyl must be concerted, since an intermediate $RO^{\oplus}$ ion should be able to react with the enriched solvent to produce isotopically altered hydroperoxide.

4. Ion-Pair Intermediates

Denney has examined some reactions that appear to involve ion-pair intermediates. His first work was on the rearrangement of labeled 9-decalyl hydroperoxide benzoate [Eq. (8)] (43). The absence of "scrambling" of the label shows that the benzoate oxygens never become equivalent (as they would in free benzoate ion). Thus any ion-pair intermediate must

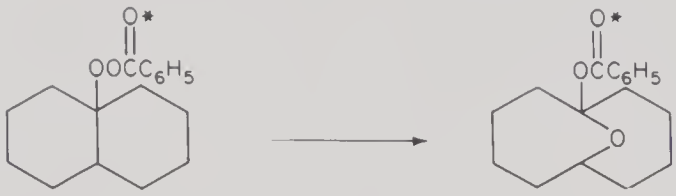

(8)

be one in which the component ions are quite specifically oriented with respect to each other. An analogous result was obtained in the rearrangement of *p*-methoxy-*p*-nitrobenzoyl peroxide (44).

The dangers in generalizing the result of a few tracer experiments are demonstrated by the complex pattern that has emerged from Denney's more recent investigations. Thus, the reaction of triphenylphosphine with benzoyl peroxide [Eq. (9)] gave an isotopic distribution consistent with a

$$(C_6H_5)_3P + C_6H_5C(=O^*)OOC(=O^*)C_6H_5 \longrightarrow C_6H_5C(=O^*)-O^{*/2}-C(=O^{*/2})-C_6H_5 + (C_6H_5)_3PO \quad (9)$$

$[C_6H_5CO_2P(C_6H_5)_3]^{\oplus}$ $[C_6H_5CO_2]^{\ominus}$ ion pair in which the oxygens of the benzoate anion become equivalent. The isotopic distribution also shows that the oxygen of the phosphine oxide must come from a peroxidic rather than a carbonyl oxygen. The mechanism of the reaction of acid anhydrides with nucleophiles appears to depend on the specific circumstances. In Equation (10) the fate of a carbonyl label depends on the relative values of the rate

$$\begin{array}{l} RC(=O)OC(=O)R + R'NH_2 \underset{k_{-1}}{\overset{k_1}{\rightleftharpoons}} RC(=O)\overset{\oplus}{N}H_2R' + RCO_2^{\ominus} \\ \qquad\qquad\qquad\qquad\qquad\qquad\qquad\qquad\qquad\qquad \Big\downarrow k_2 \\ \qquad\qquad\qquad\qquad\qquad\qquad\qquad\qquad\qquad\qquad RC(=O)NHR' + RCO_2H \end{array} \quad (10)$$

constants. If $k_2 \gg k_{-1}$ (no ion-pair return), half the label will be in the amide and half in the acid. This was observed in the reaction of benzoic anhydride with ammonia (45). For the case where $k_{-1} \gg k_2$, complete equilibration of the label results, so that the amide contains one-third, and the acid two-thirds, of the oxygen-18. Variations in the reaction conditions, the anhydride, and the nucleophile gave results varying from one extreme to the other. In the reaction of benzoic anhydride with aniline, for example, complete equilibration of the label resulted.

A subject of spirited discussion for some time has been the nature of the ion-pair intermediates in solvolyses of alkyl sulfonates. 2-Phenyl-1-propyl-*p*-bromobenzenesulfonate (labeled in the ether oxygen) was found to rearrange in acetic acid to 1-phenyl-2-propyl-*p*-bromobenzenesulfonate [Eq. (11)]. Partial equilibration of the label occurred (46). The related

$$C_6H_5\underset{\displaystyle CH_3}{\underset{|}{CH}}CH_2\overset{*}{O}SO_2Ar \xrightarrow{AcOH} ArS\overset{*}{O}_2\overset{*}{O}\underset{\displaystyle CH_3}{\underset{|}{CH}}CH_2C_6H_5 \qquad (11)$$

compound 2-*p*-methoxyphenyl-1-propyl-*p*-toluenesulfonate should form a more stable carbonium ion and hence a "looser" ion pair. In agreement with this reasoning, complete equilibration of the label was observed (i.e., only one-third of the O^{18} remained in the ether oxygen). In these ion pairs the sulfonate ion seems to be partly or completely free to rotate. The mixed nature of the results, however, disallows any effort toward generalization without further experiments.

IV. NITROGEN-15

1. Reaction of Azide Ion with Diazonium Salts

Tracer studies involving nitrogen have been relatively few. A considerable amount of work in this field has been carried out by Clusius and his collaborators. Some of their work will be described in this section.

The reaction of azide ion with benzenediazonium ion yields phenyl azide. *A priori*, this reaction is most reasonably viewed as a simple displacement of nitrogen by azide ion. Tracer studies showed, however, that this "obvious" mechanism is not the correct one. Experiments using $(C_6H_5\text{-}N^{15} \equiv N)^+$, $(C_6H_5N{\equiv}N^{15})^+$, and $(N^{15} = N = N^{15})$ showed the distribution of the nitrogen atoms was (47):

$$\overset{a\ b}{C_6H_5N}{\equiv}\overset{c}{N} + \overset{d\ e}{N{=}N{=}N} \longrightarrow \begin{cases} \xrightarrow{83\%} \overset{a\ b\ c\ d\ e}{C_6H_5N{=}N{=}N + N{\equiv}N} & (12) \\ \xrightarrow{17\%} \overset{a\ c\ d\ b\ e}{C_6H_5N{=}N{=}N + N{\equiv}N} & (13) \end{cases}$$

Scheme (12) clearly involves a linear pentazole intermediate (I), whereas scheme (13) probably involves a cyclic pentazole (II). Since II can split in either of two ways (dotted lines), the isotopic results require 66% reaction through I and 34% through II.

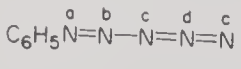

(I)

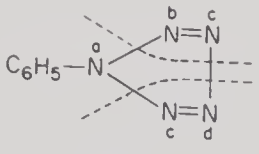

(II)

Kinetic studies of this reaction by Huisgen and Ugi (48) also revealed the existence of two reaction paths. These paths differed in rate of nitrogen evolution by a factor of about 10^4 and reaction by path (12) compared

to path (13) stood in a ratio of 65:35. This observation requires the competitive formation of two distinct intermediates, each of which then loses nitrogen at its own rate.

Collaboration between the two groups provided further confirmation (49). The reaction of $C_6H_5N{\equiv}N^{15}Cl$ with lithium azide in methyl cellosolve at $-25°$ gave 74% of the calculated yield of nitrogen. This nitrogen contained no excess N^{15}, as predicted for the intermediate (I). When the temperature of the reaction mixture was raised to 0–10°, the remaining 26% of nitrogen was evolved. This nitrogen contained the amount of N^{15} predicted by the intermediate (II).

Various substituted benzenediazonium salts (50) have also been examined. With most of the compounds employed, both paths contributed. Path (12) always predominated and was the exclusive mode of reaction with 2,4-dinitrobenzenediazonium chloride.

2. The Fischer Indole Synthesis

Apparently the earliest use of N^{15} in a mechanisms problem was by Allen and Wilson (51), who studied the mechanism of the Fischer indole synthesis. Results in agreement with the Robinson mechanism [Eq. (14)] were ob-

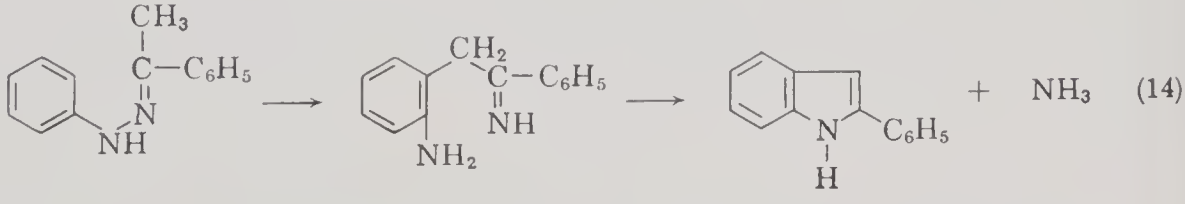

(14)

tained. Additional confirmation (using $C_6H_5NH{-}N^{15}H_2$) has been more recently provided by Clusius (52), who also examined the related reaction of phenylhydrazine with potassium thiocyanate.

3. Miscellaneous Studies

Other mechanistic work by the Swiss group includes the reaction of benzenediazonium perbromide with ammonia (53), the rearrangement of diazoaminobenzene to *p*-aminoazobenzene (54), the thermal decomposition of phenylhydrazine (55) and 1,1-diphenylhydrazine (56), and the reaction of benzenediazonium ion with phenylhydrazine to yield aniline and phenyl azide (57). The reader is referred to the original articles for details of these studies.

V. HYDROGEN ISOTOPES

1. Enolization and Related Reactions

Because of its long history, deuterium has found extensive and varied tracer applications. It is now seldom used to tag particular carbon atoms in a molecule, since C^{14} is generally more convenient. Deuterium is still useful, however, in studying the many organic reactions that involve the transfer, abstraction, or migration of hydrogen.

Among early tracer uses of deuterium was the demonstration that phenyl *sec*-butyl ketone has identical rates of racemization and deuterium uptake in dioxane—D_2O containing sodium hydroxide (58). Enolization, therefore, involves proton transfers with solvent rather than direct hydrogen migration. Other tracer studies of prototropic shifts have included the methyleneazomethine isomerization [Eq. (15)]. The initial rates of race-

$$\underset{\text{(I)}}{p\text{-}C_6H_5C_6H_4\underset{\displaystyle C_6H_5}{\underset{|}{C}}H\text{—}N{=}CHC_6H_5} \rightleftharpoons \underset{\text{(II)}}{p\text{-}C_6H_5C_6H_4\underset{\displaystyle C_6H_5}{\underset{|}{C}}{=}N\text{—}CH_2C_6H_5} \qquad (15)$$

mization, isomerization and deuterium uptake are all equal (59). Here proton loss from one carbon and deuteron uptake by another are evidently concerted. A carbanion intermediate could take up a deuteron at either carbon to give the product (II) or racemized starting material (I), thus leading to rates of racemization and exchange greater than the rate of isomerization. Deuterium exchange with the nitrile (III) does proceed considerably faster than isomerization to IV (60).

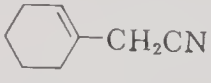

(III)

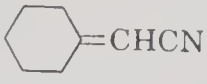

(IV)

2. Elimination Reactions

Deuterium exchange has been used to distinguish between two possible mechanisms of bimolecular elimination, the *E*2 and the *E*1cb (or carbanion) mechanisms (61). If the *E*1cb mechanism operates and k_2 is not large

$$E2: \quad B + H\text{—}\overset{|}{\underset{|}{C}}\text{—}\overset{|}{\underset{|}{C}}\text{—}X \xrightarrow{k} BH^+ + {>}C{=}C{<} + X^- \qquad (16)$$

$$E1cb: \quad B + H\text{—}\overset{|}{\underset{|}{C}}\text{—}\overset{|}{\underset{|}{C}}\text{—}X \underset{k_{-1}}{\overset{k_1}{\rightleftharpoons}} BH^+ + {}^{\ominus}\overset{|}{\underset{|}{C}}\text{—}\overset{|}{\underset{|}{C}}\text{—}X \qquad (17)$$

$$^{\ominus}\overset{|}{\underset{|}{C}}\text{—}\overset{|}{\underset{|}{C}}\text{—}X \xrightarrow{k_2} {>}C{=}C{<} + X^-$$

compared to k_{-1}, starting material recovered from partial reaction in a deuterated solvent should contain deuterium.

The first experiments along these lines involved the base-promoted conversion of 2-phenylethyl bromide to styrene in a deuterium oxide-methanol solvent (62). Recovered starting material contained no deuterium. Thus either the $E2$ mechanism, or a version of the $E1cb$ in which $k_2 \gg k_{-1}$, must operate. The same conclusions have resulted from work on eliminations promoted by potassium amide in liquid ammonia (62,63) and the reaction of 2-phenylethyldimethylsulfonium-2,2-d_2 bromide with ethoxide ion in ethanol (64). There is slight but apparently significant deuterium uptake when β-benzene hexachloride is treated with sodium ethoxide in ethanol-O-d (65). The action of base on 1,1,2,2-tetrachloroethane-1,2-d_2 gives a product containing less than the predicted deuterium content (66). This result is not unambiguous, since the product (1,1,2-trichloroethylene-2-d_2) is itself capable of exchange.

Another use of deuterium in eliminations has been to distinguish normal β-elimination [Eq. (18)] from α-elimination with hydrogen migration [Eq. (19)]. β-Deuterated halide would, of course, permit the same distinction. Some α-elimination was observed with deuterated 1-octyl halides and potassium amide in liquid ammonia (63).

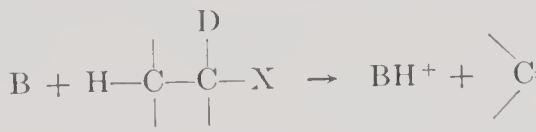

(18)

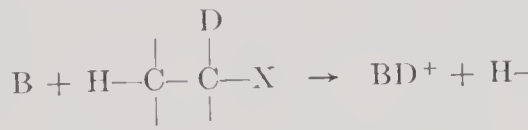

(19)

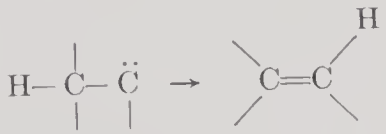

An especially noteworthy application of deuterium tracers was made by Curtin and Kellom (67). They prepared *erythro*- and *threo*-1,2-diphenylethanol-2-d by opening *trans*- and *cis*-stilbene oxides, respectively, with lithium aluminum deuteride. They next studied elimination reactions of various derivatives of these alcohols and were able to tell whether the eliminations were *cis* or *trans* by whether hydrogen or deuterium was lost. For example, *trans* elimination from the *threo* isomer [Eq. (20)] leads to loss

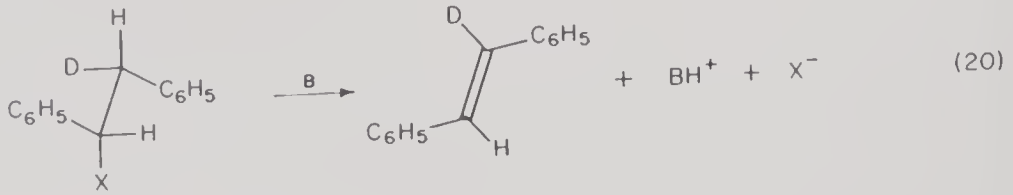

(20)

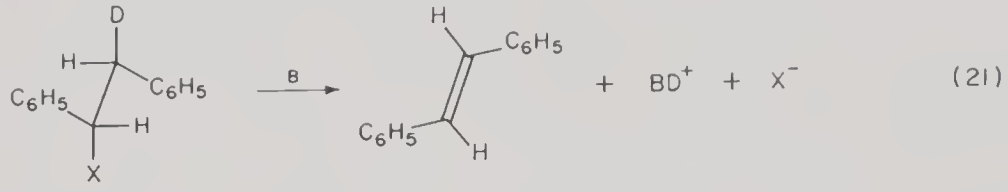

(21)

of hydrogen, whereas *trans* elimination from the *erythro* isomer [Eq. (21)] leads to loss of deuterium (in each case a *trans*-stilbene is the product). When the reaction was not completely stereospecific, the difference in the ratio (deuterium loss/hydrogen loss) for *threo* vs. *erythro* allowed simultaneous estimates of the degree of stereospecificity and the deuterium isotope effect.

3. Deuterium Exchange by Aromatic Hydrocarbons

Deuterium exchange between aromatic hydrocarbons and acids has been found to show the characteristics of electrophilic aromatic substitutions (68). Electron-repelling substituents aid the reaction, and it proceeds more readily the stronger the acid. Determination of rate of exchange at a particular position in the aromatic is easily studied if the rate of loss of deuterium to light solvent from reactant deuterated in that position is determined (69).

Particularly extensive studies of the exchange reactions have been made by Gold and Satchell (70). They found rates depended on the Hammett acidity function (71) rather than on the acid concentration, and suggested the mechanism depicted in [Eq. (22)]. They call the intermediates (V) and (VI) the "outer complex" and "inner complex," respectively (72).

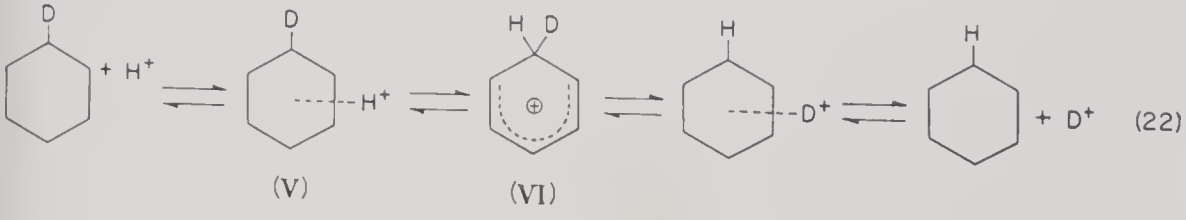

(V) (VI) (22)

Another interesting point is that exchange between toluene and sulfuric acid (70) proceeds as rapidly in the *ortho* as in the *para* position.

A different type of exchange involving aromatic hydrocarbons is the reaction of potassium amide in liquid ammonia with certain deuterated benzene derivatives (73). For the substituents fluorine, trifluoromethyl, and methoxyl, rates of exchange fell in the order *ortho* > *meta* > *para*. Evidently electrostatic effects on proton abstraction are involved here.

4. Deuterium Exchange by Aliphatic Hydrocarbons

Deuterium exchange in aliphatic hydrocarbons has been observed under various conditions. Of particular interest have been studies of the exchange between aliphatic hydrocarbons and acidic catalysts of the type normally used to promote isomerizations. Exchange with sulfuric acid was first noted by Ingold (74) and later extended by two groups (75,76).

Appreciable exchange occurs only with alkanes possessing tertiary hydrogens. Only hydrogens on carbon atoms occur adjacent to the tertiary carbon exchange, the tertiary hydrogen itself remaining untouched. The exchange with (+)-3-methylheptane is much faster than either racemization or isomerization to 2-methylheptane. These and other observations are consistent with the mechanism (76) of Equations (23–25).

$$(CH_3)_3CH \xrightarrow[\text{slow}]{\text{oxidation}} (CH_3)_3C^{\oplus} \tag{23}$$

$$(CH_3)_3C^{\oplus} \xrightarrow[\text{fast}]{D_2SO_4} (CD_3)_3C^{\oplus} \tag{24}$$

$$(CD_3)_3C^{\oplus} + (CH_3)_3CH \rightarrow (CD_3)_3CH + (CH_3)_3C^{\oplus} \tag{25}$$

The non-exchange of the tertiary hydrogen with solvent is strong evidence that it is transferred as hydride ion rather than as a proton. Similar evidence for hydride transfers has been adduced in the Cannizzaro reaction (77) and in oxidation-reduction processes akin to the Meerwein-Ponndorf-Verley reaction (78).

5. Rates of Proton Transfers

Doering and Hoffmann (79) showed that tetramethylammonium ion exchanged with basic D_2O much more slowly than did tetramethylphosphonium or trimethylsulfonium ions. Evidently the zwitterions resulting from proton abstraction are stabilized by resonance involving *d*-orbitals of sulfur and phosphorus (but not, of course, of nitrogen). Another exchange study of interest is that of Swain (80), who examined the mechanism of exchange of hydrogen between ammonium salts and alcohols.

6. Deuterium-Induced Asymmetry

A particularly ingenious use of deuterium was made by Streitwieser, who prepared various 1-butyl-1-*d* derivatives by stereospecific procedures (81). The resulting substances possessed sufficient optical activity that they could be used to determine the stereochemistry of solvolyses at the primary carbon. As might be anticipated, predominant or exclusive in-

version usually resulted. Under some conditions, however, surprisingly large amounts of racemization occurred, showing that a carbonium ion (or its stereochemical equivalent) can be involved even in primary solvolyses (82).

VI. ISOTOPES OF OTHER ELEMENTS

1. Isotopes of the Halogens

The use of isotopes of the halogens has been rather limited so far, but in a few instances has provided mechanistic information of great importance.

Key evidence for inversion of configuration in S_N2 displacements came from the demonstration that (+)-2-octyl iodide racemizes twice as fast as it exchanges with radioactive iodide ion in acetone solution. Inversion (to produce a molecule of opposite configuration and hence to give a *dl* pair) accounts uniquely for this observation (83). Similar evidence for inversion was obtained in the reaction between 1-phenylethyl bromide and radioactive bromide ion (84). Streitwieser (85) made noteworthy use of this technique to demonstrate the reality of the deuterium-induced optical activity of a sample of 1-bromobutane-1-*d*. The rate of racemization was equal to twice the rate of bromide exchange. The activity thus could not have been due to contamination with secondary bromide, since a secondary bromide would have racemized much more slowly.

Recently, de la Mare (86) has investigated the rates of the exchange reactions of a variety of primary, secondary, and tertiary halides. The data were compared with theoretical calculations (87) of rates of S_N2 displacements. Halide exchange possesses obvious advantages for theoretical interpretations, since the entering and leaving groups are spherically symmetrical and of the same size.

Isotopic halogens have also been used in the study of halogen exchanges proceeding via free radical mechanisms. Of particular interest is a study of the reaction of optically active 2-iodobutane with radioactive iodine (88). The rate of racemization was 1.54 times the rate of exchange, proving that part of the reaction involved inversion of configuration. This observation strongly suggests a backside attack on the butyl iodide by iodine atoms and is the first clear-cut example of stereospecificity in a radical displacement.

2. Sulfur-35

The main use of radioactive sulfur has been in the study of persulfate-induced polymerization. Smith (89) found that use of radioactive persul-

fate to promote the emulsion polymerization of styrene gave a polymer containing 0.46–2.3 atoms of sulfur per polymer molecule.

Somewhat more detailed work on the polymerization of tetrafluoroethylene (90) yielded interesting results. The use of labeled potassium persulfate alone, with iron powder, or with sodium bisulfite (inactive) and ferrous ion gave inactive polymers. Persulfate-bisulfite mixtures in which the bisulfite is labeled gave radioactive polymers, as did labeled bisulfite and ferric ion. Thus a fragment from the persulfate either is not incorporated in the polymer or else is, and is then removed by hydrolysis during washing. Possible reactions satisfying the facts are:

$$S_2O_8^{2-} + Fe^{2+} \rightarrow SO_4^{2-} + SO_4\dot{-} + Fe^{3+} \quad (26)$$

$$S_2O_8^{2-} + HSO_3^- \rightarrow SO_4^{2-} + SO_4\dot{-} + HSO_3\cdot \quad (27)$$

$$SO_4\dot{-} + H_2O \rightarrow HSO_4^- + HO\cdot \quad (28)$$

$$HSO_3^- + Fe^{3+} \rightarrow HSO_3\cdot + Fe^{3+} \quad (29)$$

If one assumes that each polymer molecule contains two fragments from the bisulfite, the measured radioactivity can be used to calculate the average molecular weight. Since the polymer is insoluble in all common solvents, other methods of molecular-weight determination cannot be used.

The conversion of chloroprene to neoprene type GN in the presence of various additives has been examined with isotopic sulfur (91). Elemental sulfur is incorporated to the extent of *ca.* 30 sulfur atoms per molecule. Potassium persulfate initiator is likewise incorporated, but there is only one persulfate fragment per 8–17 polymer molecules. There must thus be extensive chain transfer with monomer. When dodecyl mercaptan is used as a chain-transfer agent, each polymer molecule contains *ca.* 1.3 mercaptan units. Evidently mercaptan is incorporated not only through chain initiation by addition of RS· to monomer (which would give one RSH per molecule), but by some other process as well.

Another use of S^{35}-labeled mercaptans was made by Walling (92). Chain-transfer contants for a number of monomers were evaluated by a technique involving the use of radioactive butyl mercaptan.

The kinetics of the reaction between thiols and disulfides has been examined using labeled disulfide and inactive mercaptan (93):

$$R—\overset{*}{S}—\overset{*}{S}—R + RSH \rightleftharpoons R—\overset{*}{S}—S—R + R\overset{*}{S}H \quad (30)$$

The isotopic exchange is obviously much simpler to study than would be a reaction in which the alkyl groups of the thiol and the disulfide were not identical.

VII. SOME PRACTICAL ASPECTS OF TRACER WORK

1. Preparation of Labeled Compounds

Labeled compounds for organic tracer studies can usually be prepared by standard synthetic procedures. Departures from these standard procedures, when necessary, arise from several causes, chiefly that it is usually expensive and impractical to use the labeled reagent in excess. For example, carbonation of a Grignard reagent with carbon-C^{14}-dioxide cannot employ the customary large excess of carbon dioxide. Similarly, one often wishes to prepare labeled samples of simple organic compounds that, in unlabeled form, have been available for so long that directions for their laboratory preparation are likely to be of considerable antiquity. One is therefore sometimes faced with a development problem in modernizing procedures and adapting them to use available labeled starting materials.

Difficulties of the type mentioned above become less and less important as the literature of tracer work expands. Perhaps the best policy is to search the literature carefully to see if the desired labeled compound, or a close analogue, has been prepared. Several books describe preparative techniques employing isotopes (94). Many labeled organic compounds are commercially available. The "mark-up" on these is usually considerable but, if a relatively small amount is needed, purchase is often preferable to time-consuming practice on synthetic procedures. It is, incidentally, almost always advisable to do a "cold run" (with unlabeled materials) on syntheses designed to prepare labeled compounds.

2. Measurement of Deuterium

Numerous methods are available for deuterium analysis. These methods vary widely in generality and convenience. This section will be devoted mainly to procedures of particular usefulness to the organic chemist.

In some cases, measurements may be made directly on the deuterium-containing organic compound. If the compound is sufficiently volatile, direct introduction into a mass spectrometer is feasible. Infrared spectra of deuterated and undeuterated compounds differ in the C—H stretching and bending regions (95). Completely deuterated standards are necessary for this procedure. Sometimes it is even possible to analyze mixtures of species having deuterium in two different positions. For example, the compositions of mixtures of 2-phenylethanol-1,1-d_2 and 2-phenylethanol-2,-2-d_2 were successfully determined by infrared methods (96).

Most routine methods of deuterium analysis involve combustion of the organic compound to water. Direct measurement of the water in a mass

spectrometer is not recommended, since water adheres tenaciously to the walls of the inlet system. A "memory effect" results in which a sample is contaminated by the residue from the previous sample. Conversion of the water to hydrogen gas by reduction, or to an alkane by reaction with an organometallic may be used, but care must be exercised to obtain complete reaction so as to avoid altering the sample composition by isotopic fractionation. Unless one is restricted to very small samples, mass spectrometric procedures are generally less convenient than those described below.

Most analyses of deuterium-containing water involve direct or indirect density measurements. Perhaps the most sensitive of these is the "falling-drop" method (97). The rate of fall of a measured drop of water through a column of an organic medium (usually *o*-fluorotoluene) is compared with the dropping rates of various standard mixtures of deuterium oxide and water. A direct, though not quite linear, relation between drop rate and deuterium content is found. A rather precise constant-temperature bath is required, but otherwise the apparatus is quite simple and inexpensive. Another convenient density-measurement procedure involves the use of the gradient density tube (98).

3. Stable Isotopes Other Than Deuterium

Stable isotopes of particular interest to the organic chemist are C^{13}, O^{18}, and N^{15}. Mass spectrometry is the only technique of any importance for determination of these isotopes. Since mass spectrometry is discussed elsewhere in this series (99), the present section will be limited mainly to sample-preparation techniques.

The handling of C^{13}-labeled compounds presents few difficulties. Methods for combusting organic compounds quantitatively to carbon dioxide are well-developed (see Section VII.4), and carbon dioxide can be easily purified for introduction in the mass spectrometer. When the label is in a carboxyl group (or another group convertible to a carboxyl), reaction with hydrazoic and sulfuric acids is a convenient way of obtaining carbon dioxide.

Conversion of O^{18}-labeled compounds to a form suitable for measurement is somewhat more difficult. The most common general procedure involves pyrolysis of the organic compound to carbon monoxide, which is, in turn, oxidized to carbon dioxide with iodine pentoxide (100). Another method that is reported to be quite general consists of pyrolysis of the organic compound in the presence of mercuric chloride, or cuprous chloride, removal of the hydrogen chloride, and analysis of the remaining carbon dioxide (101). Another procedure was devised for alcohols, but should be applicable to

other compounds containing exchangeable oxygens. The alcohol and carbon dioxide are heated in a sealed tube containing a little sulfuric acid until equilibration between the alcoholic oxygen and the oxygen of the carbon dioxide has occurred (102).

Nitrogen-15 is usually measured in the mass spectrometer as molecular nitrogen. Ammonia can be converted to nitrogen by oxidation with hypobromite (103). Conversion of organic nitrogen to ammonia is best accomplished by the Kjeldahl procedure. Sometimes simpler, but less general, sample preparation methods are satisfactory (104). Finally, an ingenious spectroscopic determination of N^{15} in molecular nitrogen has been reported (105). This is said to be reproducible within 2% (adequate for most tracer measurements) and to be insensitive to common impurities.

4. Radioactive Isotopes

The measurement of radioactivity is covered elsewhere in this series (106), so that present section will be confined mainly to sample preparation and to suggestions from the author's practical experience.

Carbon-14 compounds are almost always burned to CO_2 before measurement. The usual "dry" combustion in oxygen has been employed by some workers (107,108). More widely used at present and perhaps more convenient is the "wet" combustion of Van Slyke (109), which involves treatment of the sample with a mixture of chromic, iodic, sulfuric, and phosphoric acids. A very simple sample-preparation line using this procedure has been described (110).

Scintillation counting constitutes an exception to the rule that combustion precedes measurement. Here the organic compound may often be dissolved as such in a suitable fluorescent liquid or solution. A discussion of scintillation counting is given elsewhere in this series (106).

Carbon-C^{14} dioxide may be measured directly in an ionization chamber or, with admixture of a suitable counting gas, in a proportional or Geiger-Müller counter tube. In the author's experience, the ionization chamber is considerably more convenient and dependable for routine work. Ionization chambers and the vibrating reed electrometer used to amplify the ion current are commercially available (111).

The carbon-C^{14} dioxide may also be converted to barium carbonate and measured as a solid sample. A windowless counter tube must be used because of the low penetrating power of the β-radiation from C^{14}. Although the equipment is less costly than that for ionization chamber work, higher activity samples are necessary since part of the radiation is absorbed by the solid sample ("self-absorption") and never reaches the sensitive volume of the counter.

Relatively few investigations using tritium as a tracer have been reported, but this isotope can be expected to become increasingly popular because of its low cost and the ease of introducing it as a label in organic compounds. Tritium-containing compounds can be measured directly in a scintillation counter (112), as can samples of tritiated water. For measurement in an ionization chamber, the compound is usually converted to hydrogen gas, either directly (113), or via combustion to water and subsequent reduction of the water (114). Some workers have converted tritiated water to alkanes via the Grignard reagents (117).

Methods for less frequently used isotopes will be mentioned briefly. Sulfur-35 may be measured in the ionization chamber as SO_2, or in the solid state as $BaSO_4$. Free halogens or volatile inorganic halogen compounds are too corrosive to be used in gas phase apparatus. Consequently, halogens are counted in the solid state, usually as the silver halides.

5. Pitfalls in Tracer Work

A tracer investigation must always include evidence that extraneous isotope exchange or isotope-position rearrangement does not vitiate the conclusions drawn. There is also the possibility of contamination by other labeled species. Means of dealing with these problems will be discussed in this section.

Evidence that the starting material is in fact labeled in the intended position should be obtained through degradation. This also serves to test the degradative procedure. A check should be made on the reliability of the methods used to degrade the reaction products. For this purpose, it is usually necessary to synthesize unambiguously labeled samples of the products. Close analogy to control experiments performed in other investigations may sometimes constitute adequate evidence, but it is always safer to carry out independent controls.

In isotope-exchange work, the main object is to establish the stage of the reaction at which the exchange occurs. One should therefore examine reactants, products, and any isolable intermediates for exchange. A demonstration is required that the exchange is not an artifact that occurs during isolation or purification of the substances examined. The position of isotopic substitution must, of course, also be shown.

In addition, there is, with radioactive substances, a special set of pitfalls arising from the fact that a sample may, in certain circumstances, contain impurities differing greatly in specific activity from the main component. How this may come about will be described in the next paragraph.

Let us assume that a radioactive compound A* is the product of a sequence of reactions carried out on a small scale at high specific activity

(115). In order to isolate A*, it is diluted 100-fold with inactive A. Now, if A* contained 10% of an active impurity B*, the diluted A* will contain only 0.1% *by weight* of B*, but this B* will still constitute 10% of the total activity of A*. The B* might well remain undetected by the usual criteria of purity, yet it may cause erroneous results in subsequent degradations of A*.

Suitable techniques enable one to minimize the danger from this source of error. An obvious precaution is to dilute, at the beginning of a synthesis, approximately to the activity level required in the final product. The probability that an impurity will be carried through a sequence of several reactions is much less than the probability that it will be carried through a simple isolation procedure. Closely allied to this is the desirability of performing the tracer investigation and the control experiments at similar activity levels. Degradations of materials having specific activities close to background activity (say within a factor of 10) are particularly likely to give erroneous results. Similarly, the common practice of diluting material to be degraded (so as to have a large quantity for more convenient handling) should be engaged in only with restraint and moderation.

Other methods for avoiding contaminants of high specific activity come under the heading of purification procedures. It is, for example, unlikely that the impurity will behave in precisely the same manner as the major component during purification. If the specific activity of the sample does not change through several (preferably different) purifications, one can usually assume that it contains no active impurities.

When the nature of the active impurity is known, the "hold-back carrier" technique is useful. Here one adds an inactive sample of the suspected impurity and reisolates it. This process is repeated until the material isolated is inactive. The hold-back carrier method is particularly useful in separating isomeric labeled compounds or in dealing with mixtures of similar products obtained in competition experiments (116).

References

1. J. P. Ryan and P. R. O'Connor, *J. Am. Chem. Soc.*, **74**, 5866 (1952).
2. H. Schmid and K. Schmid, *Helv. Chim. Acta*, **35**, 1879 (1952).
3. D. S. Tarbell, "The Claisen Rearrangement," in R. Adams, ed., *Organic Reactions*, Vol. II, Wiley, New York, 1944.
4. H. Schmid and K. Schmid, *Helv. Chim. Acta*, **36**, 489 (1953).
5. S. J. Rhoads, R. Rawlins, and R. D. Reynolds, *J. Am. Chem. Soc.*, **76**, 3456 (1954).
6. S. J. Rhoads and R. L. Crecelius, *ibid.*, **77**, 5060 (1955).
7. K. Schmid, W. Haegele, and H. Schmid, *Helv. Chim. Acta*, **37**, 1080 (1954).
8. D. Y. Curtin and H. W. Johnson, Jr., *J. Am. Chem. Soc.*, **78**, 2611 (1956).
9. T. Kalberer, K. Schmid, and H. Schmid, *Helv. Chim. Acta*, **39**, 555 (1956).

10. D. Y. Curtin and R. J. Crawford, *J. Am. Chem. Soc.*, **79**, 3156 (1957).

11. T. Kalberer and H. Schmid, *Helv. chim. Acta*, **40**, 13 (1957).

12. S. Winstein and D. Trifan, *J. Am. Chem. Soc.*, **71**, 2953 (1949); **74**, 1147, 1154 (1952).

13. J. D. Roberts and C. C. Lee, *ibid.*, **73**, 5009 (1951); J. D. Roberts, C. C. Lee, and W. H. Saunders, Jr., *ibid.*, **76**, 4501 (1954).

14. D. J. Cram, *ibid.*, **71**, 3863 (1949), and numerous subsequent papers.

15. (a) J. D. Roberts and J. A. Yancey, *ibid.*, **74**, 5493 (1952); (b) J. D. Roberts and M. Halmann, *ibid.*, **75**, 5759 (1953); (c) A. W. Fort and J. D. Roberts, *ibid.*, **78**, 584 (1956); (d) W. H. Saunders, Jr., *ibid.*, **78**, 5127 (1956); (e) J. D. Roberts and C. M Regan, *ibid.*, **75**, 2069 (1953).

16. J. D. Roberts and J. A. Yancey, *ibid.*, **77**, 5558 (1955).

17. C. J. Collins and W. A. Bonner, *ibid.*, **77**, 92 (1955).

18. W. A. Bonner and C. J. Collins, *ibid.*, **78**, 5587 (1956).

19. C. J. Collins, *ibid.*, **77**, 5517 (1955).

20. See Ref. 19 for a sample calculation. As stated above, this may seem like four unknowns and only three equations. Actually, of course, the fourth equation is provided by the restriction that the percentages must add up to 100%.

21. M. Polanyi and A. L. Szabo, *Trans. Far. Soc.*, **30**, 508 (1934).

22. D. N. Kursanov and R. V. Kudryavtsev, *Zhur. Obshchei Khim.*, **26**, 1040 (1956).

23. G. A. Mills and S. C. Hindin, *J. Am. Chem. Soc.*, **72**, 5549 (1950).

24. A. R. Olson and J. L. Hyde, *ibid.*, **63**, 2459 (1941).

25. F. A. Long and L. Friedman, *ibid.*, **72**, 3692 (1950).

26. C. A. Bunton and A. Konasiewicz, *J. Chem. Soc.*, **1955**, 1354.

27. C. A. Bunton, A. E. Comyns, J. Graham, and J. R. Quayle, *ibid.*, **1955**, 3817.

28. C. A. Bunton and J. L. Wood, *ibid.*, **1955**, 1522.

29. C. A. Bunton and V. A. Welch, *ibid.*, **1956**, 3240; C. A. Bunton and Y. Frei, *ibid.*, **1951**, 1872.

30. M. L. Bender, *J. Am. Chem. Soc.*, **73**, 1626 (1951).

31. M. L. Bender and R. S. Dewey, *ibid.*, **78**, 317 (1956).

32. M. L. Bender and K. C. Kemp, *ibid.*, **79**, 111 (1957).

33. C. A. Bunton and D. N. Spatcher, *J. Chem. Soc.*, **1956**, 1079.

34. M. L. Bender and R. D. Ginger, *J. Am. Chem. Soc.*, **77**, 348 (1955).

35. I. Dostrovsky and F. S. Klein, *J. Chem. Soc.*, **1955**, 791.

36. I. Dostrovsky and F. S. Klein, *ibid.*, **1955**, 4401.

37. E. Grunwald, A. Heller, and F. S. Klein, *ibid.*, **1957**, 2604.

38. C. A. Bunton, F. Hadwick, D. R. Llewellyn, and Y. Pocker, *Chem. & Ind.*, **1956**, 547.

39. F. A. Long and J. G. Pritchard, *J Am. Chem. Soc* , **78**, 2663 (1956).

40. C. A. Bunton, T. A. Lewis, and D. R. Llewellyn, *J. Chem. Soc.*, **1956**, 1226.

41. M. Bassey, C. A. Bunton, A. G. Davies, T. A. Lewis, and D. R. Llewellyn, *ibid.*, **1955**, 2471.

42. W. von E. Doering and E. Dorfman, *J. Am. Chem. Soc.*, **75**, 5595 (1953).

43. D. B. Denney, *ibid.*, **77**, 1706 (1955); D. B. Denney, *ibid.*, **79**, 4806 (1957).

44. D. B. Denney, *ibid.*, **78**, 590 (1956).

45. D. B. Denney and M. A. Greenbaum, *ibid.*, **78**, 877 (1956).

46. D. B. Denney and B. Goldstein, *ibid.*, **79**, 4948 (1957).

47. K. Clusius and H. Hürzeler, *Helv. chim. Acta*, **37**, 798 (1954).

48. R. Huisgen and I. Ugi, *Angew. Chem.*, **68**, 705 (1956).

49. I. Ugi, R. Huisgen, K. Clusius, and M. Vecchi, *ibid.*, **68**, 753 (1956).

50. K. Clusius and M. Vecchi, *Helv. chim. Acta*, **39**, 1469 (1956).
51. C. F. H. Allen and C. V. Wilson, *J. Am. Chem. Soc.*, **65**, 611 (1943).
52. K. Clusius and H. H. Weisser, *Helv. chim. Acta*, **35**, 400 (1952).
53. K. Clusius and H. Hürzeler, *ibid.*, **37**, 383 (1954).
54. K. Clusius and H. R. Weisser, *ibid.*, **35**, 1523 (1952).
55. K. Clusius and M. Hock, *ibid.*, **33**, 2212 (1950).
56. K. Clusius and M. Vecchi, *ibid.*, **36**, 933 (1953).
57. K. Clusius and R. Craubner, *ibid.*, **38**, 1060 (1955).
58. S. K. Hsu, C. K. Ingold, and C. L. Wilson, *J. Chem. Soc.*, **1938**, 78.
59. R. Perez Ossorio and E. D. Hughes, *ibid.*, **1952**, 426.
60. C. K. Ingold, E. de Salas, and C. L. Wilson, *ibid.*, **1936**, 1328.
61. C. K. Ingold, *Structure and Mechanism in Organic Chemistry*, Cornell University Press, Ithaca, 1953, Chapter VIII.
62. P. S. Skell and C. R. Hauser, *J. Am. Chem. Soc.*, **67**, 1661 (1945); D. G. Hill, B. Stewart, S. W. Kantor, W. A. Judge, and C. R. Hauser, *ibid.*, **74**, 5599 (1952).
63. D. G. Hill, W. A. Judge, P. S. Skell, S. W. Kantor, and C. R. Hauser, *ibid.*, **74**, 5599 (1952).
64. W. H. Saunders, Jr., and D. H. Edison, *ibid.*, **82**, 138 (1960).
65. S. J. Cristol and D. D. Fix, *ibid.*, **75**, 2647 (1953).
66. L. C. Leitch and H. J. Bernstein, *Can. J. Research*, **28B**, 35 (1950).
67. D. Y. Curtin and D. B. Kellom, *J. Am. Chem. Soc.*, **75**, 6011 (1953).
68. C. K. Ingold, C. G. Raisin, and C. L. Wilson, *J. Chem. Soc.*, **1936**, 1637.
69. W. M. Lauer and J. T. Day, *J. Am. Chem. Soc.*, **77**, 1904 (1955).
70. V. Gold and D. P. N. Satchell, *J. Chem. Soc.*, **1956**, 2734; **1955**, 3609, 3619, 3622.
71. L. P. Hammett, *Physical Organic Chemistry*, McGraw-Hill, New York, 1940, Chap. IX.
72. V and VI might better be called "π-complex" and "σ-complex" as suggested by H. C. Brown and J. D. Brady, *J. Am Chem. Soc.*, **74**, 3570 (1952).
73. G. E. Hall, R. Piccolini, and J. D. Roberts, *ibid.*, **77**, 4540 (1955).
74. C. K. Ingold, C. G. Raisin, and C. L. Wilson, *J. Chem. Soc.*, **1936**, 1643.
75. R. L. Burwell, Jr., and G. S. Gordon, III, *J. Am. Chem. Soc.*, **70**, 3128 (1948); **71**, 2355 (1949).
76. J. W. Otvos, D. P. Stevenson, C. D. Wagner, and O. Beeck, *ibid.*, **73**, 5741 (1951); D. P. Stevenson, C. D. Wagner, O. Beeck, and J. W. Otvos, *ibid.*, **74**, 3269 (1952).
77. W. von E. Doering, T. I. Taylor, and E. F. Schoenwalt, *ibid.*, **70**, 455 (1948).
78. W. von E. Doering and T. C. Aschner, *ibid.*, **75**, 393 (1953).
79. W. von E. Doering and A. K. Hoffmann, *ibid.*, **77**, 521 (1955).
80. C. G. Swain and M. M. Labes, *ibid.*, **79**, 1084 (1957); C. G. Swain, J. T. McKnight, and V. P. Kreiter, *ibid.*, **79**, 1088 (1957).
81. A. Streitwieser, Jr., *ibid.*, **77**, 1117 (1955).
82. A. Streitwieser, Jr., and W. D. Schaeffer, *ibid.*, **79**, 2888, 6233 (1957).
83. E. D. Hughes, T. Juliusberger, S. Masterman, B. Topley, and J. Weiss, *J. Chem. Soc.*, **1935**, 1525.
84. E. D. Hughes, T. Juliusberger, A. D. Scott, B. Topley, and J. Weiss, *ibid.*, **1936**, 1173.
85. A. Streitwieser, Jr., *J. Am Chem. Soc.*, **75**, 5014 (1953).
86. P. B. D. de la Mare, *J. Chem. Soc.*, **1955**, 3169, 3180, 3196.
87. P. B. D. de la Mare, L. Fowden, E. D. Hughes, C. K. Ingold, and J. D. H. Mackie, *ibid.*, **1955**, 3200.
88. R. A. Herrmann and R. M. Noyes, *J. Am. Chem. Soc.*, **78**, 5764 (1956).

89. W. V. Smith and H. U. Campbell, *J. Chem. Phys.*, **15**, 338 (1947); W. V. Smith, *J. Am. Chem. Soc.*, **71**, 4077 (1949).

90. K. L. Berry and J. H. Peterson, *ibid.*, **73**, 5195 (1951).

91. W. E. Mochel and J. H. Peterson, *ibid.*, **71**, 1426 (1949).

92. C. Walling, *ibid.*, **70**, 2561 (1948).

93. A. Fava, A. Iliceto, and E. Camera, *ibid.*, **79**, 833 (1947).

94. M. Calvin, C. Heidelberger, J. C. Reid, B. M. Tolbert, and P. F. Yankwich, *Isotopic Carbon*, Wiley, New York, 1949; A. Murray, III, and D. L. Williams, *Organic Syntheses with Isotopes*, Interscience, New York, 1958.

95. F. A. Miller, in H. Gilman, *Organic Chemistry*, Vol. III, Wiley, New York, 1953, p. 144.

96. W. H. Saunders, Jr., S. Asperger, and D. H. Edison, *J. Am. Chem. Soc.*, **80**, 2421 (1958).

97. W. von E. Doering and A. K. Hoffmann, *ibid.*, **77**, 521 (1955); A. S. Keston, D. Rittenberg, and R. Schoenheimer, *J. Biol. Chem.*, **122**, 227 (1937).

98. C. Anfinsen in O. W. Wilson, A. O. C. Nier, and S. R. Reimann, eds., *Preparation and Measurement of Isotopic Tracers*, J. W. Edwards, Ann Arbor, 1946, pp. 61–65.

99. D. W. Stewart in A. Weissberger, ed., *Physical Methods of Organic Chemistry*, Interscience, New York, 1960, Vol. I, Part IV, Chap. LI.

100. W. von E. Doering and E. Dorfman, *J. Am. Chem. Soc.*, **75**, 5595 (1953).

101. D. Rittenberg and L. Ponticorvo, *J. of Applied Radiation and Isotopes*, **1**, 208 (1956).

102. M. Anbar, I. Dostrovsky, F. S. Klein, and D. Samuel, *J. Chem. Soc.*, **1955**, 155.

103. D. Rittenberg, in O. W. Wilson, A. O. C. Nier, and S. R. Reimann, *Preparation and Measurement of Isotopic Tracers*, J. W. Edwards, Ann Arbor, 1946, p. 31; D. Rittenberg, A. S. Keston, F. Rosebury, and R. Schoenheimer, *J. Biol. Chem.*, **127**, 291 (1939).

104. W. R. Vaughan, W. T. Boyd, D. R. McCane, and G. J. Sloan, *Anal. Chem.*, **23**, 508 (1951).

105. M. Hoch and H. Weisser, *Helv. Chim. Acta*, **33**, 2128 (1950).

106. W. F. Bale and J. F. Bonner in A. Weissberger, ed., *Physical Methods of Organic Chemistry*, Interscience, New York, 1949 and 1954, Volume I, Part II, Chap. XXX, and Part III, Chap. XXX.

107. J. D. Roberts, W. Bennett, E. W. Holroyd, and C. H. Fugitt, *Anal. Chem.*, **20**, 904 (1948).

108. R. C. Anderson, Y. Delabarre, and A. A. Bothner-By, *ibid.*, **24**, 1298 (1952).

109. D. D. Van Slyke, R. Steele, and J. Plazin, *J. Biol. Chem.*, **192**, 769 (1951); D. D. Van Slyke and J. Folch, *ibid.*, **136**, 509 (1940).

110. O. K. Neville, *J. Am. Chem. Soc.*, **70**, 3501 (1948).

111. Applied Physics Corp., 362 W. Colorado St., Pasadena 1, California.

112. See, for example, C. G. Swain and E. E. Pegues, *J. Am. Chem. Soc.*, **80**, 812 (1958).

113. K. E. Wilzbach, L. Kaplan, and W. G. Brown, *Science*, **118**, 522 (1953).

114. C. G. Swain, V. P. Kreiter, and W. A. Sheppard, *Anal. Chem.*, **27**, 1157 (1955).

115. The remainder of this discussion is based largely on G. A. Ropp, *J. Chem. Ed.*, **34**, 60 (1957).

116. E. J. DeWitt, C. T. Lester, and G. A. Ropp, *J. Am. Chem. Soc.*, **78**, 2101 (1956).

117. R. F. Glascock, *Nucleonics*, **9**, 5, 28 (1951).

Stereochemistry and Mechanism of Reactions

S. L. Friess, *U. S. Naval Medical Research Institute*

I. Introduction 1549
II. Substitution Reactions 1550
1. Nucleophilic Substitution Processes 1551
III. Addition and Elimination Reactions 1555
1. Addition Reactions 1555
2. Elimination Reactions 1557
IV. Molecular Rearrangements 1561
1. Claisen Rearrangement 1561
2. Acyl Migrations in Cyclic Systems 1562
3. 1,2-Rearrangements 1563
4. 1,3-Rearrangements 1566
5. Rearrangement of α-Phenylethyl Aryl Ethers 1568
V. Free Radical Processes 1568
VI. Redox Reactions 1570
1. Oxidations 1570
2. Reduction Processes 1571
VII. Miscellaneous Reactions 1574
1. Decarboxylations 1574
2. Generation and Stability of Carbanions 1575
VIII. Enzymatic Processes 1576
References 1579
General References 1582

I. INTRODUCTION

Historically, one of the earliest tools available to the chemist for the probing of fine structure in organic molecules was found in the existence of asymmetric centers, and their ready detection by means of a physical variable, which could be precisely measured. This variable, optical rotatory power, is usually a sensitive function of the degree of stereochemical purity of the asymmetric structural element, and in recent years has been shown to be of expanded utility in mirroring over-all molecular asymmetry, in addition to its classic role of pinpointing the discrete rotatory power of isolated atomic centers of asymmetry. Accordingly, as increasing emphasis has been directed toward investigation of the mechanisms of reactions involving subtle structural changes on proceeding from reactants to products, the tracing of intimate molecular details of these transformations through

corresponding changes in the stereochemical configurations at *and near* the reactive centers became a natural and powerful technique. In general, the mechanistic inferences gained by use of this technique have of necessity been supplemented by kinetic, thermodynamic, and isotopic tracer results to achieve comparatively full understanding of a given process, but, in the synthesis of arguments leading to the deduction of mechanism, a potent contribution of stereochemistry lies in its information bearing on transitions that occur within well-localized regions of the molecular backbone.

The broad field of steric effects and their theoretical implications with respect to organic reaction mechanisms has recently been surveyed (1,2) in admirable fashion by eminent workers in the field. It only remains for the present treatment to categorize the techniques involved under the headings of the major reactions to which they have been applied, with appropriate examples of both the obvious and subtle approaches now available and the types of mechanistic information to be obtained from their use. Additionally, the specific advantages of stereochemistry as a technique in illuminating molecular details of enzymatically catalyzed organic reactions of biochemical and physiological significance are briefly reviewed.

II. SUBSTITUTION REACTIONS

1. Nucleophilic Substitution Processes

Certainly one of the most straightforward applications of stereochemistry to the understanding of a widely studied organic reaction has been made in the specific instance of the nucleophilic displacement process

$$Y: \; + -\overset{|}{\underset{|}{C^*}}-X \; \rightarrow \; Y-\overset{|}{\underset{|}{C^*}}- + X: \qquad (1)$$

In the simplest case of a direct nucleophilic displacement of the S_N2 type, a wealth of literature exists on examples attesting to the clean-cut nature of the inversion accompanying displacement at C*. Perhaps the earliest unequivocal demonstration, free of excessive complications produced by ionized functional groups (3) and neighboring group effects in general, can be cited in the classical work of Kenyon and Phillips (4) on acetate-tosylate displacement. With high stereochemical purity apparently maintained in all members of the reaction sequence (2), the inference is quite clear that, in the sole bond-breaking bond-making process (*a*) involving the asymmetric C* atoms, the displacement of $OTos^-$ by OAc^- is accompanied by inversion. This demonstration is wholly optical in charac-

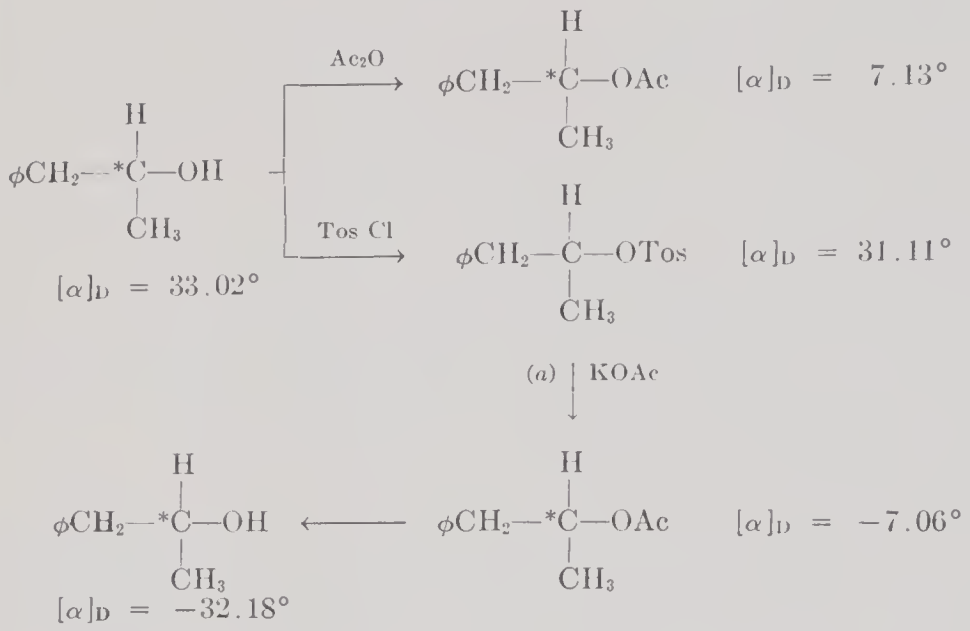

(2)

ter on the face of it, but the interplay of techniques to establish that each displacement act results in inversion is seen in the kinetic requirement that step (*a*) be proven bimolecular before the stereochemical results can be uniquely interpreted.

A somewhat more complete experimental demonstration of this mechanistic point by stereochemical and allied techniques is to be found in the symmetrical exchange studies of Hughes and co-workers (5,6). For the second-order displacement process involving optically active *sec*-octyl iodide R*I,

$$R^*I + I^- \underset{}{\overset{k_1}{\rightleftharpoons}} RI + I^- \qquad \text{(inversion at C*)}$$

and the corresponding reaction with inactive RI and radiotracer iodide ion,

$$RI + \overset{*}{I}^- \underset{}{\overset{k_2}{\rightleftharpoons}} RI^* + I^- \qquad \text{(isotope exchange)}$$

the observation that the specific rate of inversion k_1 (leading to net racemization) is equal to the specific rate k_2 of the exchange process clearly establishes that each bimolecular encounter resulting in exchange is accompanied by inversion at the displacement center.

Greater complications arise in those nucleophilic displacement processes characterized by first-order kinetics and designated as S_N1 reactions in the terminology of the English school. The picture has been discussed in detail by Ingold (7) and others, and it suffices for present purposes to treat several representative examples illustrating this complexity, with emphasis on the theoretical implications of the stereochemical data.

In the general pathway ascribed to the first order nucleophilic displacement, an initial rate-determining ionization of RX to the discrete species R^+ is normally facilitated by secondary or tertiary structure in R leading to

$$R^*\text{—}X \xrightarrow{\text{slow}} \overset{*}{R}^+ + X^- \qquad (3)$$

$$\overset{*}{R}^+ \xrightarrow[Y^-]{\text{fast}} RY \qquad \overset{*}{R}^+ \xrightarrow[SOH]{\text{fast}} ROS$$

stabilization of the carbonium ion. Fortunately, these same structural requirements can furnish potential asymmetry at the carbon center undergoing net displacement, and result in a fortuitous opportunity to study gross events in the generation and disposition of R^+ through the fate of the optical activity in the original R—X asymmetric center. Noteworthy use of this technique has been made in studies of the solvolysis of optically active 2-*n*-octyl bromide (8,9), methylethylisohexylcarbinyl chloride (9), and α-bromopropionic acid (10) and its esters. The optical results with those solvolyses of R*—X that are demonstrably unimolecular (without regard to molecularity of the solvent species concerned) are fairly unequivocal when R contains no ionizable groups such as —COOH in immediate proximity to the reaction center. Generally, there is found predominant inversion, but accompanied by a good bit of racemization. The implication might therefore be drawn that R^+, as formed, is in part protected by solvent so that tetrahedral configuration is maintained and subsequent backside attack of the nucleophilic entity yields inversion at C*, but in part is sufficiently free that the carbonium ion reverts to planar configuration and leads to racemic product. This explanation is not unique, however, in the sense that partition of the total solvolytic process into a fraction proceeding by S_N1 with racemization and another by S_N2 with solvent species could likewise account for the stereochemical results.

A most dramatic optical contrast with the above behavior is seen in the solvolysis of compounds like active α-bromopropionic acid (10,11), under conditions in which the acid function is ionized. For example, solvolysis in water at neutral pH leads unambiguously to clear *retention* of configuration at C*, in a reaction which is now generally interpreted as proceeding through an α-lactone-type intermediate, which permits complete optical protection at the active site. Essentially, an intramolec-

$$CH_3\text{—}{}^*CH(Br)\text{—}COO^- \rightarrow CH_3\text{—}CH\text{—}C(=O)(O^-) \xrightarrow{H_2O} CH_3\text{—}{}^*CH(OH)\text{—}COO^- + Br^- \qquad (4)$$

ular displacement (S_Ni) by carboxylate ion coincident with the ionization of bromide could lead to the intermediate with complete inversion, and the following nucleophilic displacement by solvent in a second act of inversion

would give the over-all result of complete retention. Interestingly, running the solvolysis in acid medium (or solvolyzing the methyl ester) leads to loss of the configuration-protecting COO^- function and reversion to the standard inversion-racemization S_N1 behavior.

The detection of S_Ni processes at a single carbon center continues to be almost uniquely achieved by use of stereochemical techniques. For example, starting with the work of Kenyon and co-workers (12) on the observed retention of configuration in the low temperature reaction of optically active alcohols with thionyl chloride,

$$\phi\text{—}{}^*\underset{\displaystyle CH_3}{\underset{|}{CH}}\text{—OH} + SOCl_2 \rightarrow \phi\text{—}{}^*\underset{\displaystyle CH_3}{\underset{|}{CH}}\text{—Cl} + SO_2 + HCl$$

considerable effort (13,14) has been expended in studying the optical fate of the intermediate chlorosulfite esters. The retention of configuration via some internal nucleophilic process such as (5), in which the Cl function

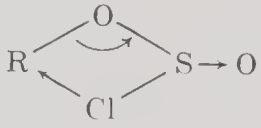

(5)

exerts a front-face displacement action on carbon, has been suggested as a general property of aromatic and secondary aliphatic chlorosulfite esters. However, the concerted process depicted in (5) is not completely established by the stereochemical demonstration of retention, since formation of the ion pair $R^+SO_2Cl^-$, with simultaneous protection of one face (accompanied by inversion) of the asymmetric center by solvent molecules, followed by a second inverting attack of Cl^- ion derived from the ($R^+SO_2Cl^- \longleftrightarrow ROSO^+ Cl^-$) entity, could also lead to over-all retention of configuration through a net double inversion. For the aliphatic esters, solvent effects on stereochemical results militate against the simple cyclic mechanism in (5).

Certainly one of the most penetrating and thorough applications of stereochemistry to the understanding of molecular-level events in nucleophilic displacement reactions has been made in the study of neighboring group effects on these processes. Largely in the hands of Winstein and co-workers (15) during the past two decades, the stereochemistry of two adjacent asymmetric C centers has been manipulated to reveal details of displacements at one center as influenced by functional groups at the second. A prototype of the procedures employed with the —OMe function as neighboring group is illustrated in Equation (6). Forearmed with knowledge of the configurations at C_α and C_β in a particular starting stereomer, these workers observed that a single inversion of C_β in the course of reac-

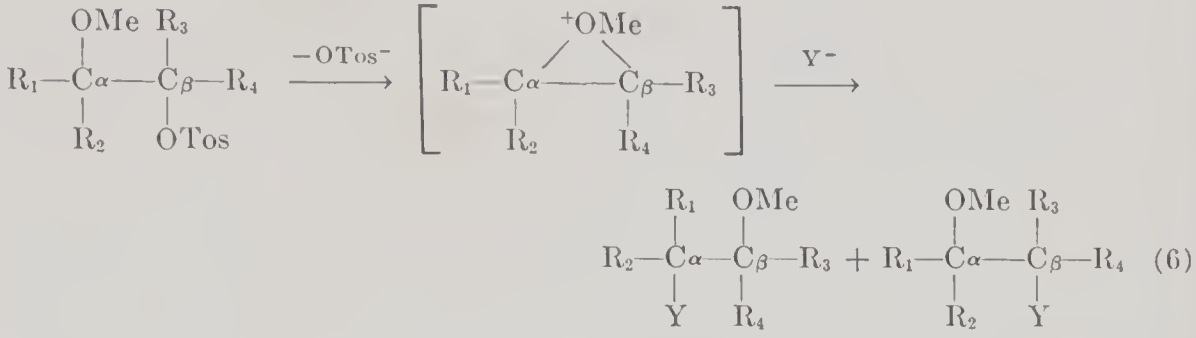

tion by the neighboring group at C_α essentially establishes and protects configurations at *both* centers; the subsequent inverting displacement by Y^- or solvent at either C_α or C_β leads to products in which structure and optical configuration neatly tag the nature and sequence of the inverting displacements. In some cases, e.g., the neighboring acetate function (16), the intermediate produced by preliminary nucleophilic displacement may even be of sufficient stability in selected solvents to warrant its synthesis or isolation and the study of subsequent displacements as separate steps.

Recent work by Cram and associates in this area of study has been characterized by high technical skill in selection of test systems for solvolysis, and elegant demonstrations of technique in complete resolution of small quantities of racemates and fractionation of diastereomeric mixtures. For example (17), in studies of the solvolysis of tosylates in the 3-phenyl-2-butyl system, judicious application of stereochemical techniques alone was sufficient to demonstrate the intervention of bridged carbonium ion intermediates between starting materials and solvolyzed products. Taking the L-*threo* and L-*erythro* starting materials I and II, respectively, in the acetolyses noted in Equation (7) it was found that the L-*threo* derivative (I)

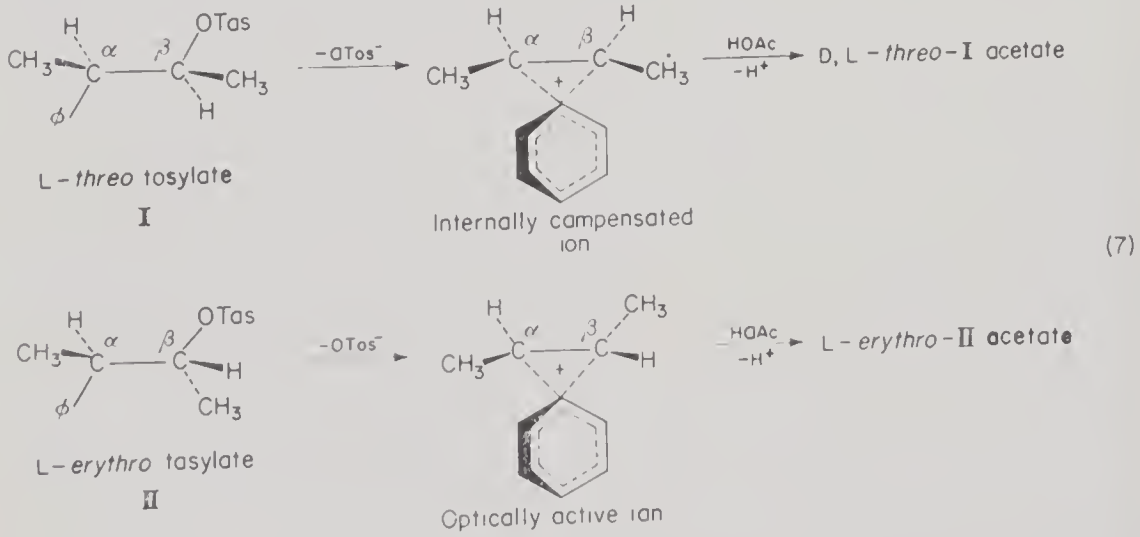

leads solely to *racemic threo* acetate, whereas the L-*erythro* tosylate (II) leads to fully optically active acetate with the same configuration as the

starting material. These facts can only be accommodated by the intermediate formation of bridged ethylenephenonium ions by highly stereospecific displacements of the phenyl group on C_β. The bridged ion in the *threo* series is fully symmetrical and therefore internally compensated, so that the subsequent inverting displacement by acetate at either C_α or C_β can only lead to *threo* racemate of high optical purity, as demonstrated by a quantitative resolution. On the other hand, the bridged ion from the *erythro* series would still be optically active, and subsequent displacement at either C_α or C_β would furnish the same acetate product with the same configuration as the starting *erythro* material, with high optical purity being realized in the course of the sequence of inverting displacements.

In the discussion to this point, attention has been devoted to stereochemical techniques as applied to nucleophilic substitution processes on aliphatic carbon atoms, since optical tools have proved highly successful in mechanistic studies of this class of reactions. In comparison, the direct electrophilic substitution process on saturated carbon has received but scant attention in the aliphatic series, where stereochemical techniques might apply, owing to the paucity of unambiguous examples known that are completely free of complicating rearrangement steps. Therefore, further discussion of techniques and their applicability to reactions involving some electrophilic facet will be reserved for later categories of reactions.

III. ADDITION AND ELIMINATION REACTIONS

1. Addition Reactions

Stereochemistry has played a major role in the understanding of processes associated with electrophilic additions to the carbon-carbon double bond. In a sense, the applications of the technique anteceded the principles of how to interpret the results of its use, since it was found early in the game that simple additions (e.g., halogenations) lead nearly exclusively to products that could only be rationalized on the basis of a *trans* addition process. For example, the additions of Br_2 and Cl_2 to maleic and fumaric acids (18) are largely *trans* under acidic conditions, and the early reports (19,20) on halogenation of the corresponding ions also indicated high stereospecificity of the addition process. In the light of these results and the pioneering work of Bartlett and Tarbell (21) pointing to the intermediate formation of X^- and a positively charged organic ion in reactions of X_2 with the ethylenic linkage, it remained for Roberts and Kimball (22) to offer an interpretation of how stereochemical purity in a *trans* adduct

might be attained. In their view, the intermediate ion formed by nucleophilic attack of olefin on X_2 is of the onium type

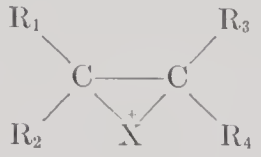

in which configuration at both C atoms is maintained by the bridging halogen entity; subsequent nucleophilic attack of X^- or SOH at the back face of either carbon could then lead to the variety of products observed by a net *trans* addition. In essence, this proposal could well account for the directed stereochemical results in bromination, with a generalization of the bridged cation reflecting contributions from forms IIIa–IIIc. However,

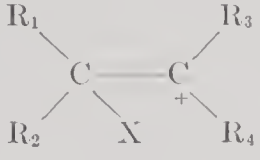

(IIIa)

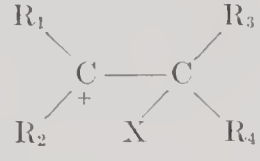

(IIIb)

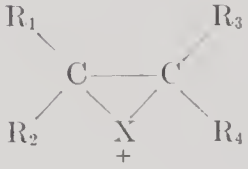

(IIIc)

following the observation by Winstein and Grumwald that a neighboring Cl function shows little driving force in assisting ionization reactions, it becomes less likely that the intermediate in chlorination could possess appreciable bivalent bridging character of halogens, as in IIIc. In this event, the stereochemical results could still be accommodated [for leading references see Winstein and Morse (23), Ingold (24)] by a dynamic pair of interconvertible, isomeric cations of the form IIIa and IIIb; these could afford sufficient stereochemical protection of both carbons to ensure exclusively backside attack by a nucleophilic entity and result in over-all *trans* addition.

From the emphasis placed on the ubiquity of preferential *trans* addition processes to the carbon-carbon double bond so far, it should not be presumed that these occur to the exclusion of the alternate *cis* mode of addition. Indeed, high stereospecificity in the sense of *cis* addition has been observed in a variety of additions, with one of the more recent and spectacular examples to be found in the work of Brown and Zweifel (24a) on hydroboration of the double bond. Here, the reaction of B_2H_6 with the double bond of cyclopentene and cyclohexene derivatives, followed by oxidation of the resulting alkylboron compound with H_2O_2 and a basic hydrolysis, furnishes a net hydration product in which the elements of water have been added cleanly to the olefin in *cis* fashion. Also, the fact that hydration in this reaction appears to take place predominantly from the less hindered side of the double bond is seen in the observation that its application to norbornene furnishes *exo*-norborneol exclusively (24a).

Nucleophilic additions to the double bond of the carbonyl group have also been studied in penetrating fashion by stereochemical tools. Indeed, the literature is replete with examples in which the directed course of 1,2-addition to this unsaturated system is shown to be powerfully controlled by the steric and configurational properties of its immediate molecular

environment. For a wide variety of such reactions in which the non-catalyzed addition of reagent results in mixtures of diastereomeric alcohols [e.g., the Grignard process pictured in Equation (8) with Newman projection formulae], Cram (25) has deduced an important generalization on the steric influence of one center in dictating the steric course of reaction at another adjacent to it. Expressed as his rule for stereochemical direction of asymmetric induction in reactions of type (8), "that diastereomer will

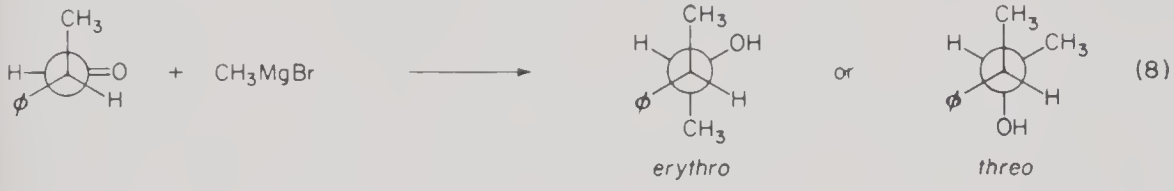

(8)

predominate which would be formed by the approach of the entering group from the least hindered side of the double bond when the rotational conformation of the C—C bond is such that the double bond is flanked by the two least bulky groups attached to the adjacent asymmetric center." In example (8), flanking of the double bond by CH_3 and H is shown, and application of the rule with respect to orientation of the incoming CH_3 group should lead to a preponderance of the *erythro* diastereomer, which was actually observed. In a sense then, the direct observation of the stereochemical results of such an addition process can be taken as a diagnostic of the steric factors that lead to a preferred mode of reaction. But, in a practical vein, too, selection of starting structures can be made in accordance with the rule so as to assure a predominance of a given stereoisomer, in a directed addition to the carbonyl group.

2. Elimination Reactions

The course of elimination reactions of both the E_2 and E_1 varieties can also be probed readily by stereochemical procedures. For example, very early studies in the stilbene dibromide series (26) on the elimination of H . . . X with basic reagents pointed to specificity in the process, with the

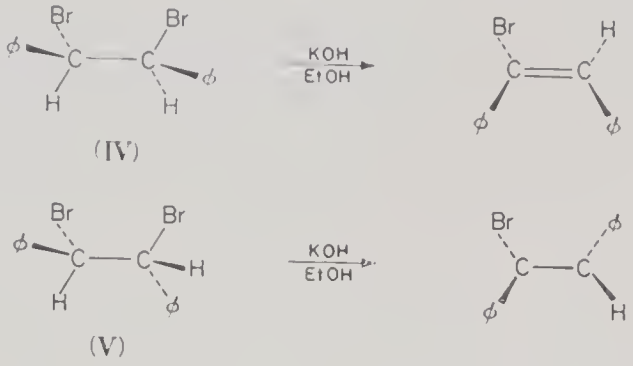

meso-dibromide (IV) furnishing predominately *cis* olefin, and D,L-dibromide (V) leading to *trans* olefin. These results point unequivocally to a *trans* elimination process, and have been amplified in recent years by a variety of stereochemical studies on HX elimination, all interpreted in terms of *trans* elimination mechanisms. In the elimination of HBr from dibromides by iodide ion in acetone, Winstein, Pressman, and Young (27) found a stereospecific *trans* elimination in a concerted process; Curtin and Kellom (28) observed clear *trans* elimination of H—OCOR in the action of potassium *tert*-butoxide on *threo* and *erythro* esters; and Cram and co-workers (29) likewise demonstrated *trans* elimination of H . . . X (X = Cl, Br, OTos) from pure diastereomers under the action of ethoxide ion in ethanol. Especially interesting in the light of these results attesting to a generality of *trans* elimination as a favored mechanism was the observation by Cristol *et al.* (30) that dehydrohalogenation under E_2 conditions of the β-isomer of benzene hexachloride (in which all Cl atoms are *trans* to one another) is an extremely slow process compared to the rates for the other known diastereomers. This apparent reluctance to undergo a smooth, concerted elimination process such as

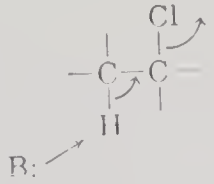

accords well with the structural facts that, in this isomer, all adjacent H and Cl pairs are *cis* to one another, and therefore the *trans* pathway above is not available for use.

The E_1 elimination process is somewhat complex, and has been scrutinized with the aid of stereochemical techniques in some detail. Some representative systems that might be considered to illustrate the power of the combined attack by stereochemical and kinetic techniques include the early work of Vavon and Barbier (31) on acid-catalyzed elimination of water from 2-alkylcyclohexanols, and later work on solvolysis and elimination by Cram (32), Winstein and co-workers (33), Ingold *et al.* (34), and Nevitt and Ham-

mond (35). In the first of these studies, attention was directed to relative rates of elimination of water from the *cis* and *trans* isomers of 2-alkylcyclohexanols under mild acid catalysis, with the net observation that *cis* structures (in which adjacent H and OH functions are *trans* to one another) eliminate much more rapidly than the corresponding *trans* isomers. A more quantitative version of the same dehydration study by Price and Karabinos (36), using the isomers of 2-phenylcyclohexanol and characterizing the proportions of 1,2- vs. 2,3-olefin that resulted, again indicated that H and OH functions *trans* to one another lead to facile elimination; with the *cis* derivative (VI) sterically accommodating the *trans* elimination process at positions 1-2, a ratio of VII/VIII of about 7 was observed; with the

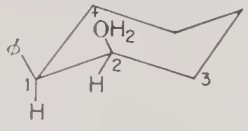

$\xrightarrow{-H_2O}$ 1, 2-olefin + 2, 3-olefin (10)

(VI) (VII) (VIII)

corresponding *trans* alcohol the lack of favored configuration at positions 1-2 causes a shift in the direction of 3-olefin product via 2-3 *trans* elimination and a resultant ratio of about 1.

Elimination of HX under E_1 conditions from menthyl and neomenthyl tosylates (33) and chlorides (34) has shown the rates of these first-order processes to depend markedly on configuration at the 3-carbon. In acetolysis and solvolysis of the tosylates, the neo isomer is the faster by a factor

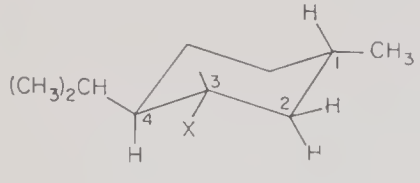

Menthyl-X

(IX)

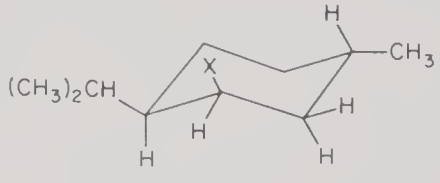

Neomenthyl-X

(X)

of about 170 and furnishes 3-menthene almost exclusively, whereas the menthyl isomer yields a mixture of 2- and 3-menthene, with the latter predominating. Elimination of HX from the chlorides under E_1 conditions (34) is also characterized by a high rate factor in favor of the neomenthyl isomer. Interpretation of these rate differences on the basis of steric direction of the elimination process rests (33) on the axial-axial disposition of H . . . X at positions 3-4 in the neo isomer, whereas the disposition is axial-equatorial in the menthyl series; accordingly, the participation of neighboring H could well facilitate ionization of X in the neo as compared with the menthyl series. Curiously though, in E_1 elimination (35) from the

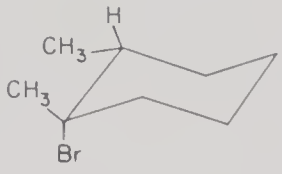

(XI) *trans*

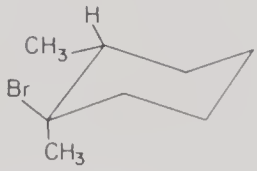

(XII) *cis*

cis-trans pair (XI)-(XII), the rates are essentially identical so that there is no evidence for participation of neighboring H in the ionization process. In contrast, working with *erythro* and *threo* tosylates in the 3-phenyl-2-butyl series, Cram (37) uncovered evidence for at least three competing elimination processes, one of which was stereospecific and characterized by *trans* elimination, with presumptive participation of neighboring hydrogen of the form:

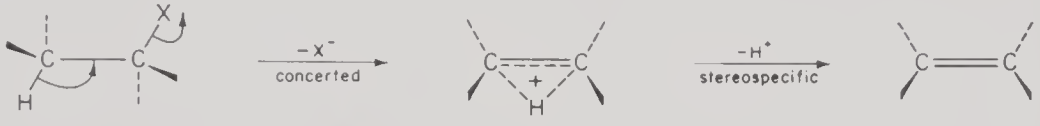

(11)

Combinations of the same kinetic and stereochemical procedures used in the E_1 and E_2 studies above have been employed in detailed analysis of events in pyrolytic eliminations. The Chugaev elimination applied to xanthate esters in the 3-phenyl-2-butyl (38) and menthyl-neomenthyl (39) systems appears to be predominantly stereospecific, with a favored *cis* mode of elimination presumably proceeding through an oriented transition state of form (XIII) (38), which recalls the earlier postulations (40,41) of

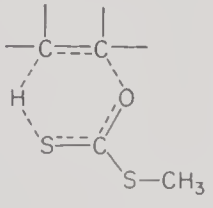

(XIII)

pyrolytic eliminations in esters via planar, cyclic transition states. Indeed, the over-all specificity in ester elimination has been elegantly assayed by Curtin and Kellom (28) in the series exemplified by (XIV), using a happy combination of stereochemical and tracer techniques. In the instance

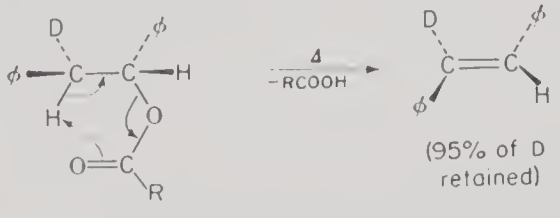

(12)

(XIV) *erythro*

cited, only predominant *cis* elimination of the type shown could account simultaneously for the configuration of the olefin product and the observed results on retention of tracer D. From a total consideration of configurational and isotopic results, these authors estimated a factor of about 8, in favor of a stereospecific *cis* elimination over the *trans* variety, in thermal eliminations from these esters.

Strikingly high degrees of stereospecificity have also been observed in the formation of olefins by thermal cracking of amine oxides (42,43). So unidirectional is the steric course of events in both cyclic and acyclic amine oxide eliminations that almost unique predictions of olefin product configuration can be drawn from application of *cis* elimination (with both leaving groups as eclipsed as possible) to a given starting configuration in the oxide.

IV. MOLECULAR REARRANGEMENTS

Optical techniques have been widely used in attempts to assess the character and relative degrees of freedom of migrating entities, as well as the general nature of transition states encountered during the course of rearrangements centered about C—C, C—N, and C—O linkages. To a considerable extent, these experiments using asymmetry as a tracer have provided key information on molecular level events attending the rearrangements, but it is probably fair to say, for the bulk of the studies in this field, that supplementary results with allied techniques (kinetic salt effects, electronic effects of substituents, etc.) have usually been required to reach unambiguous mechanistic interpretations. The power of the stereochemical methods in adding to the understanding of rearrangement mechanisms will be illustrated briefly in the subsequent discussion by examples from major classes of reactions that have received some experimental attention.

1. Claisen Rearrangement

In a straightforward application of the stereochemical tracer technique, Alexander and Kluiber (44) were able to shed considerable light on the relative freedom of the migrating entity in the *o*- and *p*-Claisen rearrangements. In the processes noted in Equations (13), considerable optical

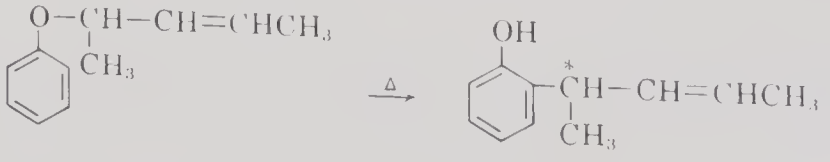

(13a)

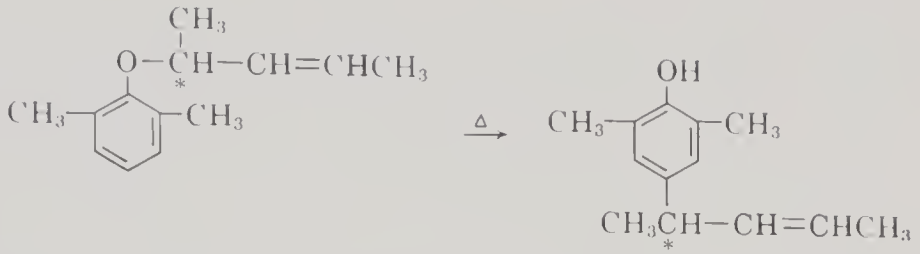

(13b)

activity was retained in the rearranged products, although the ultimate (predominant) configurations in C* were not established. Viewed from the more recent radiotracer (45) and other (46) evidence pointing to intermediates of the form XV in these rearrangements, carbonium ion character

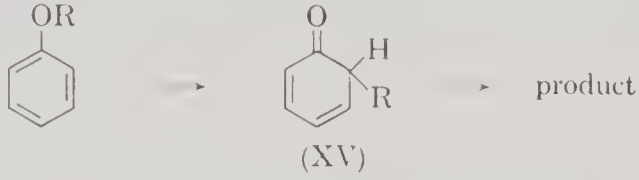

(14)

(XV)

in the migrating group during the dienone-forming step is a distinct possibility. However, should this be the case, the stereochemical results in (13) militate against a completely free allylic carbonium ion with sufficient life span as a separate entity to go completely planar and result in racemic product. Rather the same conclusion is forced, too, by the virtual absence of any "cross-products" in a mixed Claisen rearrangement with two different starting ethers (47). Finally, taking into consideration the well-known (48) inversion of the allyl group in the *ortho* rearrangement, it would appear that retention of activity (with inversion of the allyl entity) in (13a) must involve a well-oriented attack of the terminal allylic carbon at the *ortho* position to yield an active intermediate, of the form XV, and an active end product.

2. Acyl Migrations in Cyclic Systems

A pattern of equally high specificity to that noted above appears to characterize certain acyl migrations in alicyclic systems. For an example of the controlling role played by over-all conformation in aiding or opposing migration, one might cite the work of Fodor and colleagues (49) on rearrangements in the nortropine and nor-ψ-tropine series. This acid-catalyzed migration of an acetyl or benzoyl function from N $\rightarrow$ O in the nor-ψ-tropine derivatives (XVI) is quite facile, and reversed in basic medium. This is in accord with the spatial proximity of the migrating group to the adjacent OH function, as dictated by ring geometry in the fused system. In contrast, with the corresponding derivatives in the *N*-acyl-nortropine series where the orientation of H and OH functions is

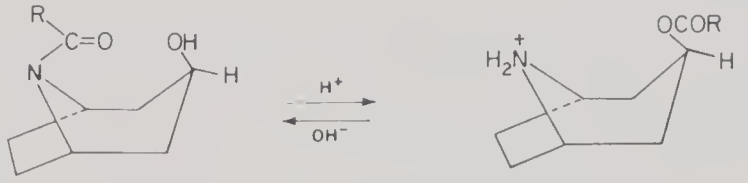

R = CH_3, C_6H_5 (XVI) (15)

reversed and the proximity relationship altered radically, no migration at all is observed under these same conditions.

These representative results on control of reactivity through the geometry imposed by molecular configuration have, as a whole, interesting analogs in reactions outside the rearrangement sphere. As a single example, the labilization (50) of acetate ester bonds in amino-cyclitol derivatives appears to be a sterically controlled phenomenon in which overall conforma-

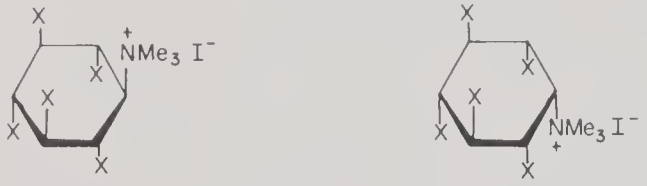

(XVII) *scyllo* X = OAc (XVIII) *myo*

tion plays the dominant role. Derivatives in the *scyllo* series (XVII) for example, display pronounced increments of hydrolysis rates in neutra aqueous medium over the corresponding rates for isomers with the *myo* configuration (XVIII).

3. 1,2-Rearrangements

A most penetrating analysis has been given by Cram (1) which pinpoints the precise information that stereochemical techniques can furnish in regard to the 1,2-rearrangement process:

$$\begin{matrix} C\text{—}B \\ | \\ A \end{matrix} \rightarrow \begin{matrix} C\text{—}B \\ | \\ A \end{matrix} \qquad (16)$$

For an especially large and important segment of this generalized reaction, which involves intermediates that are electrophilic in character, these techniques have been used with varying degrees of success to check the fate of initial asymmetry in the migrating entity A, the migration point of origin C, and the migration terminus B. This category of rearrangements includes such important reactions as the Wagner-Meerwein rearrangement, all the rearrangements proceeding via the so-called Whitmore mechanism, and the well-known rearrangements (Curtius, Lossen, Beckmann, etc.) in which the terminus B is an atom other than carbon, e.g., nitrogen or

oxygen. Considered as a group, these 1,2-rearrangement processes have, as events in common, the creation of electron deficiency or positive character at B, the migration of nucleophilic group A, and the ultimate discharge of the resulting deficiency at C by loss of a proton, electron redistribution, or combination with another nucleophilic entity. The relative sequence and timing of these events are the prime problems to which stereochemical and other techniques have been applied with increasing intensity during the past quarter century.

First, in line with the Whitmore concept that group A migrates with its bonding pair of electrons and therefore could be expected to maintain configuration at that center, it has indeed been observed for intramolecular rearrangements, and A = alkyl, that retention in the migrating group is the rule. Chiefly tested in the C → N rearrangement system, clear retention of configuration in the migrating alkyl group A has been found in the Curtius (51), Schmidt (52), Lossen (53), Beckmann (54), and Wolff (55) rearrangements, with subsequent and rather general acceptance of the idea that R: (freedom unspecified) is the migrating species. From the work of Turner (56) on the Baeyer-Villiger reaction of cyclic ketones with organic peracids [Eq. (17)], which has been viewed as involving C → O

(17)

migration of the cycloalkyl group, the observation of complete retention of configuration of the migrating group would also be in harmony with a 1,2-rearrangement involving R:. However, recent work with the powerful agent peroxytrifluoracetic acid acting on a variety of ketones in the Baeyer-Villiger reaction led Hawthorne and co-workers (57) initially to postulation of relative cationic character of the migrating entity for the benzyl group at least, and a transition state resembling a heterocyclic "phenonium ion" (XIX) for the migrating aryl function. But, reconsideration of structural influences on the reaction, in terms of steric rather than electronic

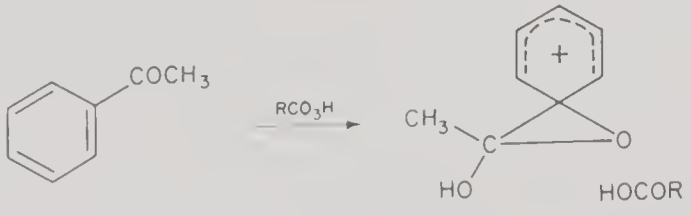

(18)

(XIX)

effects, has served to eliminate the requirement of positive character in the migrating moiety.

The fate of configuration at the migration starting point C is, in many instances, linked with the optical results at the terminus B (e.g., the work (17) on bridged phenonium ions during solvolysis-rearrangement of the Wagner-Meerwein type, in which bridging controls the stereochemistry at both carbons C and B), but in at least two instances of Wagner-Meerwein rearrangements in the terpene series, the stereochemical results at C are clear. For the stereospecific rearrangements (58) of camphene·HCl and pinene·HCl to isobornyl and bornyl chlorides, clean inversion of the carbon finally bearing the chlorine function is known to occur.

And finally, with regard to configurational change in the terminal atom B during the course of 1,2-nucleophilic rearrangement, one can cite stereochemical evidence (in both C → N and C → C rearrangements of A) pointing strongly to mechanistic detail in these processes. The first of these reactions is the classical Beckmann rearrangement in which *anti* migration has been unequivocally demonstrated (59), leading to rather general belief that A, migrating with an electron pair to N in this case, executes a back side displacement of the ester or halide function on N, as in Equation

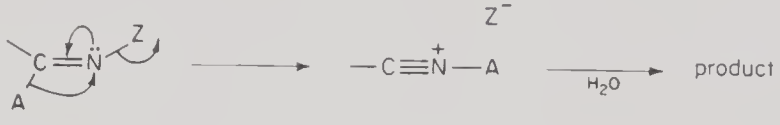

(19)

(19). Comprehensive examples of the optical fate of B in saturated systems are found in the studies of semipinacolic deamination by Bernstein and Whitmore (60), and Curtin and co-workers (61). Here, noting that in general (61) steric orientation appears more important than electronic effects in controlling migration aptitudes, reference can be made to the simplified case (60) in which only one migrating group is possible, e.g., compound XX as starting material, with the carbon bearing the amino function acting as the terminus of migration by a phenyl group. The

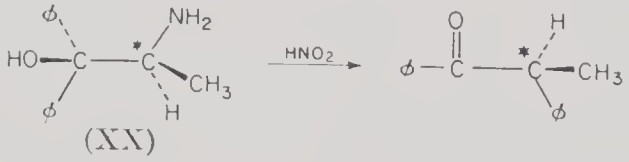

(XX) (20)

optical purity of C* in the product, and the proof of its optical configuration by ingenious synthetic and degradation procedures, resulted in a clear proof that C* is inverted in the deamination-migration sequence.

These stereochemical observations in the triad system A—C—B, especially for the Wagner-Meerwein process in which B is carbon, have been important elements in the discussion (e.g., Reference 1) of general mechanisms

attending the myriad of 1,2-nucleophilic rearrangements recorded in the literature.

In contrast with the wealth of thought and stereochemical evidence bearing on 1,2-rearrangements in which A has nucleophilic properties, the corresponding classification in which A is electrophilic finds few examples *in toto*, and only one possible member in which stereochemical techniques have added to study of mechanism. The controversial reaction in question is the Stevens rearrangement of quaternary ammonium salts under the action of strong bases, and the stereochemical test was applied (62) to the optically active starting material XXI. High retention of the optical con-

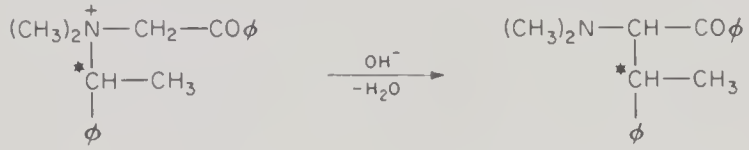

(21)

(XXI)

figuration at C* in the α-phenylethyl migrating group was observed, which only adds fuel to the general uncertainty as to whether the migrating group leaves its bonding to N with or without an electron pair. Certainly the reaction of base with an α-H atom yielding an anion (Eq. 22) might be expected to set the stage for migration of R in an electron-deficient state, but in this event the stereochemical result is puzzling since considerable racemization could conceivably occur in cationic R. A satisfying rationale

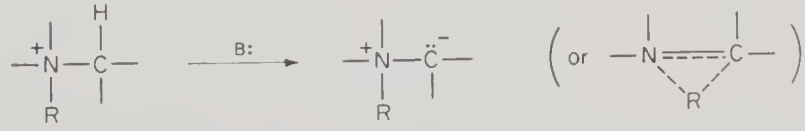

(22)

that accommodates the optical finding may well lie (1) in the reversion of the bipolar ion to the cycle indicated in Equation (22), followed by cleavage to product with retention of configuration in R by what amounts to an S_Ni shift.

4. 1,3-Rearrangements

One of the best known examples of allylic rearrangements in which optical techniques have been used to advantage for elucidation of mechanistic detail is found in the work of Balfe and Kenyon (63) on allylic esters. Specifically, the thermal 1,3-rearrangement of ester XXII in solution (or more slowly on standing as pure crystals) has been shown to proceed with considerable retention of optical activity in the allylic product, in contrast with the methanolysis of XXII, which leads to a nearly inactive mixture of the two ethers. This observation carries the strong implication that the

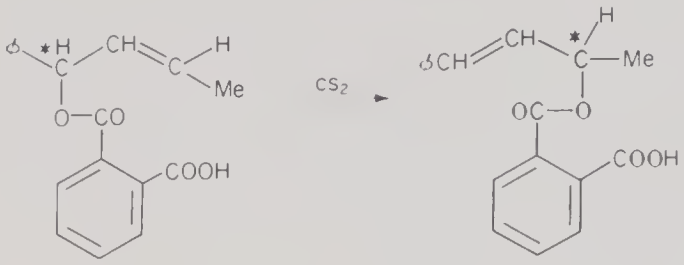

(XXII) (-)- (+)- and some D, L (23)

rearrangement proceeds through a cyclic transition state of the form XXIII, characterized by precise orientation in the nucleophilic attack of oxygen

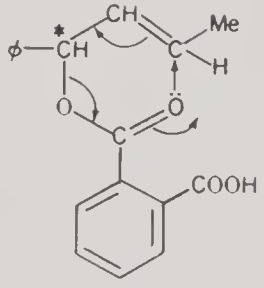

(XXIII)

on carbon, to account for specificity in the final attachment of the ester function.

Another venerable 1,3-rearrangement of the allylic type, which has been scrutinized by stereochemical techniques, is the methyleneazomethine rearrangement. In an early example (64) shown in Equation (24), the

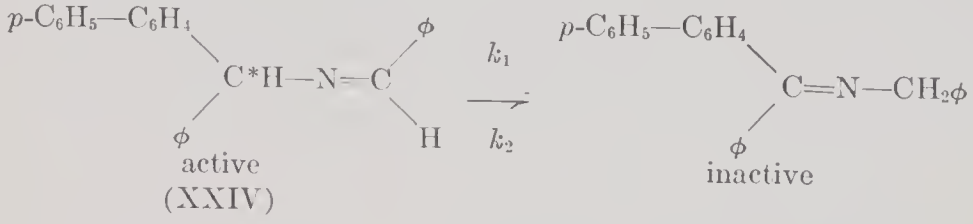

active (XXIV) inactive (24)

base-catalyzed forward rate constant k_1 for the rearrangement process has been shown equal to the observed specific rate of racemization. In the most likely explanation (65) advanced for these results, the operation of a Lowry mechanism to simultaneously remove a proton at the optical C* center by a base B: and return it to the other end of the triad with the conjugate acid BH^+, concomitant with allylic migration of the electron pair, would remove optical activity and XXIV from solution at the same rates. Any reversion of product to XXIV would be expected to give racemic starting material. Neat as this explanation may appear, however, it is complicated by the tracer observation (66) that deuterium exchange between solvent and the reaction components is appreciably faster than the rearrangement or racemization velocities.

5. Rearrangement of α-Phenylethyl Aryl Ethers

In a thorough study formally similar to the Claisen rearrangement treated in III.1. above, Hart and Eleuterio (67) used stereochemical tags to probe the processes shown in prototype in Equations (25).

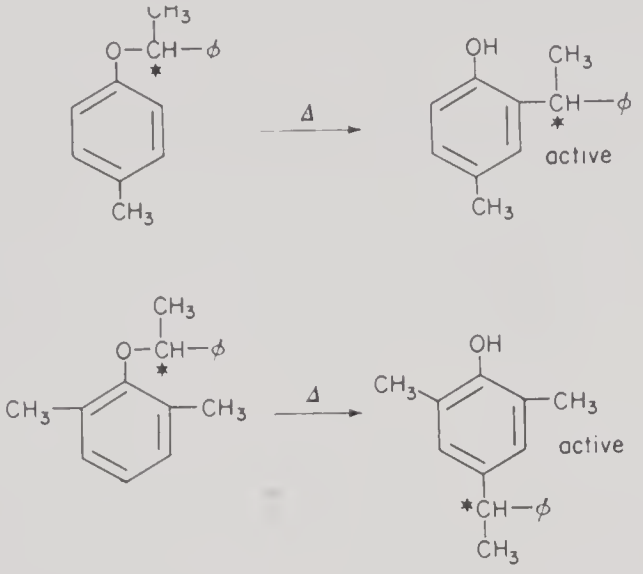

(25)

In general, the reactions were found to be about 20% stereospecific, with predominant retention of configuration in the α-phenylethyl migrating group. By reaction mixture studies with added phenolic receptors, considerable evidence for intermolecular transfer of the tagged groups was also obtained, pointing to some freedom of the migrating group. Hence, these workers were led to a rationale involving essentially the production of an ion pair with sufficient lability to account for intra- and inter-molecular transfer of the migrating group, but sufficient restrictions on freedom within

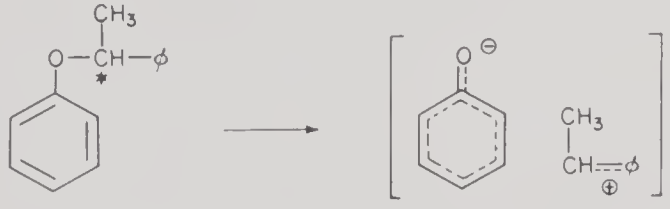

(26)

the ion pair to permit collapse to rearranged product with some degree of retention of configuration at C*.

V. FREE RADICAL PROCESSES

To a considerably lesser extent than that represented in the sampling of heterolytic processes discussed in Sections I–IV, applications of stereochemical methods to problems of mechanism in free radical reactions have been

made in certain scattered instances. These examples on the average tend to demonstrate that R•, however generated, is relatively incapable of retaining optical configuration in end products which incorporate it, but there are exceptions to this rule.

For example, Wallis and Adkins (68) made an early application of stereochemistry to the Kolbe electrolysis procedure with the optically active salt (XXV), and achieved synthesis of the totally inactive hydrocarbon

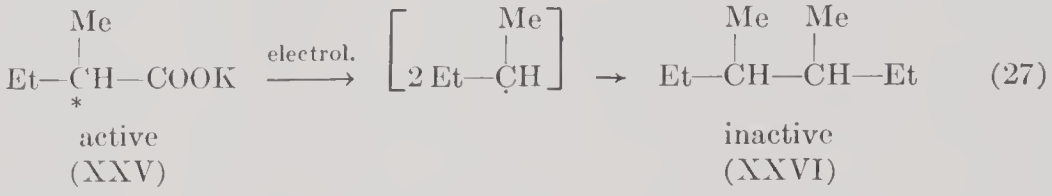

(27)

XXVI, implying that any intermediate free radicals were incapable of retaining tetrahedral configuration. Likewise, Wilken (69) found that oxidation of the active hydrocarbon (XXVII) with acetyl peroxide led to a

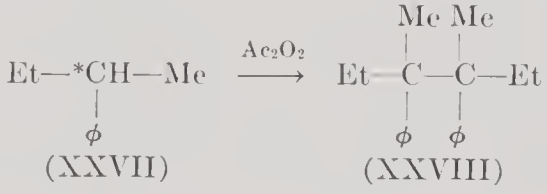

(27a)

mixture of *meso* and DL-XXVIII, with no indications of any survival of R· in optically active form.

In contrast, Kharasch and co-workers (70) were able to find evidence that R· can retain configuration in certain cases by study of the pyrolysis of the active diacyl peroxide (XXIX). In this example though, at least one-half

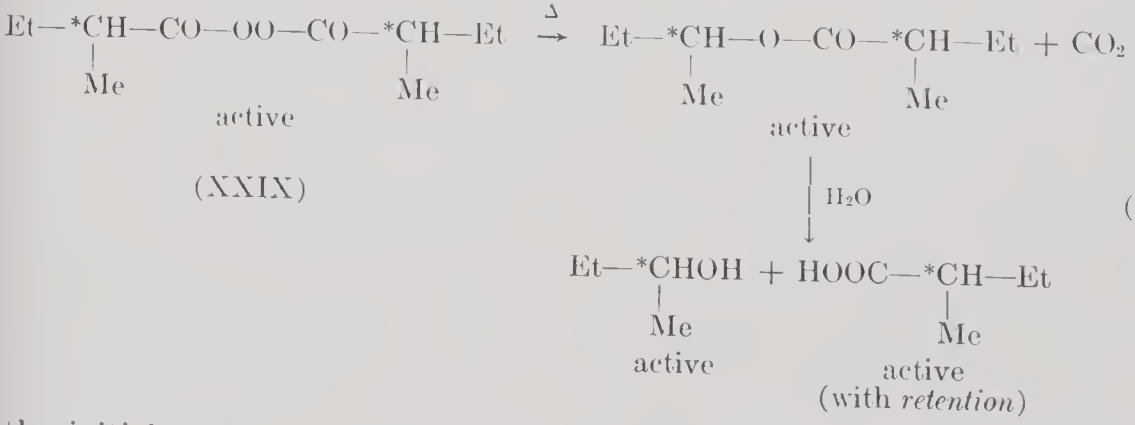

(28)

the initial ester product could have resulted from a radical of the form R*—COO·, and recovery of activity in the sense of retention of configuration in the final acid (upon hydrolysis of the ester) is therefore not too surprising.

For the photochemical chlorination (71) of active XXX via the free radical chain reaction shown in Equation (29), the stereochemical inferences

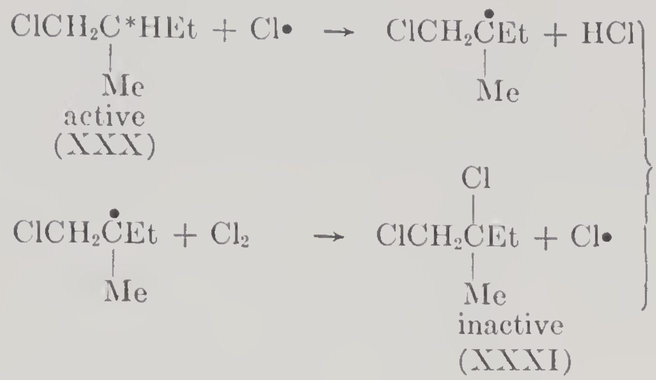

(29)

are clear. The complete inactivity of XXXI indicates that all activity must be lost at the level of the free radical.

A final and somewhat equivocal point of discussion on activity in R· centers about the Hunsdieker reaction of optically active acids. In a straightforward stereochemical test of the course of events with active XXXII, Arcus, Kenyon, and co-workers (72) found the organic halide

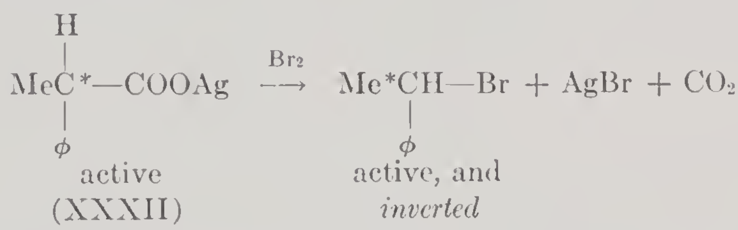

(30)

product to be active and inverted in configuration, and proposed an ionic reaction course in which Br^+ exerts a backside electrophilic attack on the asymmetric carbon of the intermediate acyl hypobromite. Yet, on repetition of this study with the same silver salt, other investigators (73) obtained the salt XXXIII as the chief product. Since XXXIII is quite

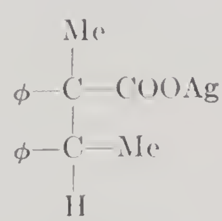

(XXXIII)

probably a product with free radical antecedents, it is not entirely clear as to whether the optical results summarized in (30) have any relationship to the question of optical stability of R· as a transient intermediate in the first studies (72), or indeed whether the reaction course is of the ionic type initially postulated.

VI. REDOX REACTIONS

1. Oxidations

Two stereospecific oxidation processes are so universally known and utilized as diagnostic aids in evaluating structures and reactivities that they

require only passing attention at this point. Some of the highlights in this category may be pointed out, though, with further reference of the reader to the comprehensive reviews presently available.

The extensive use (74) of periodate oxidation of α-glycols, α-diketones, α-ketoaldehydes, etc., in structure proofs has served to point out many details of specificity in action of this reagent. Its feature of enhanced rates of reaction with 1,2-*cis* glycolic structures as compared (75) with *trans* configurations results in highly practical application as an analytical tool, and has simultaneously led to interpretation of the mechanism of oxidative action in terms of intermediate formation of paraperiodate esters. Similarly, the pioneer studies of Criegee and co-workers (76) on directed oxidations with lead tetraacetate have pointed up a high degree of stereospecificity in response, attributable to varying degrees of ease in formation and decomposition of intermediate lead esters.

2. Reduction Processes

Somewhat greater mechanistic variety resides in organic reductions that proceed by stereospecific pathways than that found in the general field of oxidations, so that the following selection of examples covers a wider area of application than that in VI.1.

First, the selective reduction of the carbonyl group by aluminum alkoxides in the Meerwein-Ponndorf-Verley reaction appears to involve elements of stereospecificity in certain cases, which can be interpreted in terms of a possible oriented transfer of hydride ion in a complex of the type (XXXIV). An early example of this selectivity is found in the reduction

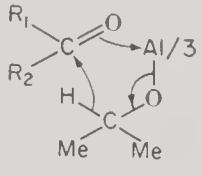

(XXXIV)

of benzil or benzoin (77) with aluminum isopropoxide, leading to 90% of *meso*-hydrobenzoin and the virtual exclusion of the other possible diastereomer. Yet, the specificity breaks down (77) and mixtures of diastereomers are obtained in many reductions, e.g., those of camphor, borneol, and isoborneol.

A formally similar, stereospecific reduction via a cyclic intermediate has recently been observed by Mosher and LaCombe (78) in the reaction with optically active Grignard reagent shown in (31). The product (XXXV) is characterized by possession of 8–11% of the possible enantiomeric purity, and represents a phenomenon in which a dying optical center from R*MgX

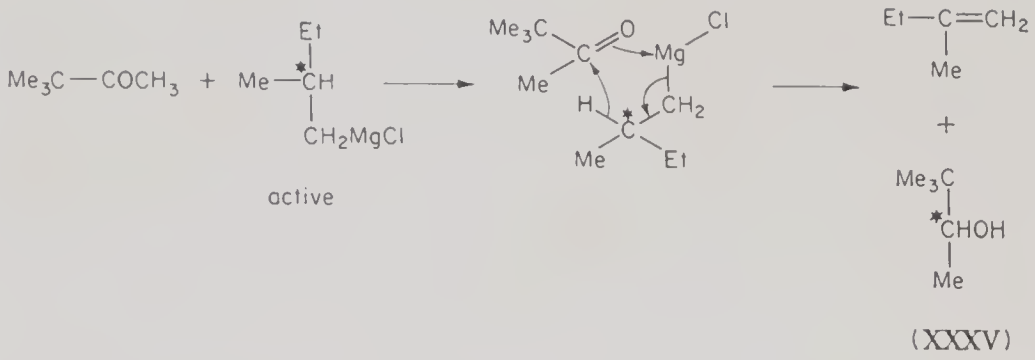

(31)

(XXXV)

has passed its activity in part to the newly formed asymmetric center by oriented transfer of hydride.

Scattered instances of stereospecificity have also been evidenced in heterogeneous reductions and hydrogenolysis processes catalyzed by noble metals. The well-known *cis* reductions of the C=C double bond by H_2 and Pt form a case in point, with the generally accepted concept being adsorption of olefin to the surface and addition of H atoms in the only (*cis*) mode of addition available. However, the optical results can vary in hydrogenolysis reactions with the structure of reactant used. For example (79), in desulfuration processes using Raney nickel, Bonner observed that both the active sulfide XXXVI and its sulfoxide yield inactive amide (XXXVII), but the corresponding active sulfone of XXXVI furnishes

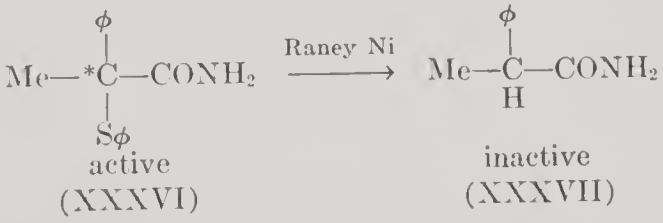

(32)

XXVII which is highly active (90% of maximum purity) and inverted in configuration. As a contrasting case of hydrogenolysis, Bonner and coworkers (80) found that reaction of XXXVIII with Raney Ni catalyst furnished the ester (XXXIX) in active form, with *retention* of optical con-

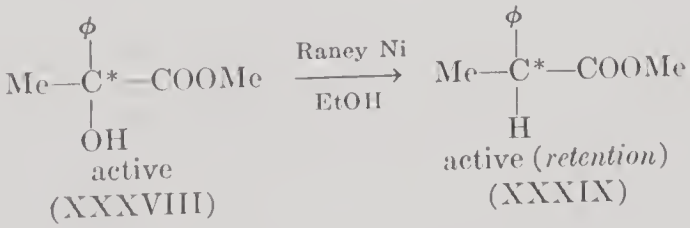

(33)

figuration. Hence, over-all specificity in the catalytic act is apparent in these processes, but the lack of uniformity of configurational results rules out postulation of a unique molecular mechanism at this point.

Reductions in homogeneous solution with the relatively new reagents $NaBH_4$ and $LiAlH_4$ offer a powerful technique for accomplishment of key

synthesis steps, and an understanding of the degrees of stereospecificity inherent in the use of each agent is therefore important from both the synthetic and mechanistic standpoints. The first of these reducing agents is of sufficient solubility and stability in aqueous medium (and mixed solvents) to extend its utility greatly in reduction of a wide variety of both polar and non-polar compounds. Accordingly, it has been possible to test its stereospecificity in reductive transfer of hydride on an assortment of structures, with the following representative results:

In the reduction of 2-dimethylaminocyclopentanone (or the corresponding cyclohexanone) in aqueous alcohol (81), little or no oriented transfer of hydride is involved, since roughly equal quantities of the *cis*- and *trans*-2-dimethylaminocyclanols are obtained. However, in the reduction of XL in aqueous methanol, Cram and Greene (82) observed considerable specificity of reaction involving directed transfer of the hydride entity in accordance with the "Rule of Steric Control of Asymmetric Induction" (Section II); a preponderance of the *threo* diastereomer (XLI) was ob-

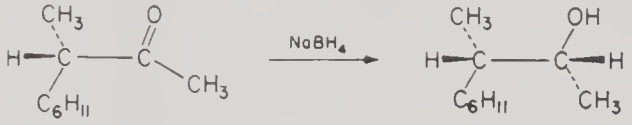

(34)

threo

(XL) (XLI)

tained, as qualitatively predicted by the rule. At the final limits of contrast, complete stereospecificity (and production of only one of the two possible enantiomers) was found by Gates (83) in the $NaBH_4$ reduction of codeinone to codeine, or 1-bromocodeinone to 1-bromocodeine, speaking for a highly oriented relationship between the polycyclic molecule and the reducing agent in the hydride transfer process. Similarly, the 3-keto function in a host of steroid derivatives has been shown to undergo highly stereospecific reduction to the alcohol, with resultant α- or β-configuration depending on the immediate molecular architecture of the steroid nucleus.

The reducing agent $LiAlH_4$ must of necessity be used in nonaqueous medium, but, within this limitation, it has been employed in a number of reductions with interesting stereochemical facets. For example, high specificity in reduction of the carbonyl group can be displayed (84); camphor is reduced almost exclusively to isoborneol, benzil (at $-80°$) is converted better than 90% to the single diastereomer, mesohydrobenzoin, and amidone is reduced (85) with virtually complete stereospecificity. Of somewhat greater mechanistic interest though is the stereospecific reduction of oxides. Trevoy and Brown (84) found strong evidence for directed *trans* opening of oxides in the cyclopentane and cyclohexane series, and attributed this mechanistically to backside nucleophilic displacement by

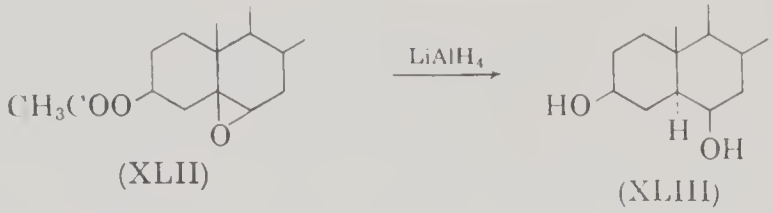

(XLII) (XLIII) (35)

a hydride entity derived from AlH_4^-. Similarly, Plattner, Heusser, and Feurer (86) found a 60% yield of product XLIII resulting from the *trans* opening of XLII. When the oxides are unsymmetrical, the direction of opening of the ring appears subject to strong steric influence (e.g., the work of Fuchs and Vander Werf (87) on opening in 3,4-epoxy-1-butene), but there seems to be little doubt that each reductive act is of the S_N2 type.

Halide reductions with $LiAlH_4$ have been studied by means of optical tools, with complex results. Eliel and Freeman (88) carried out reduction of the active chloro acid (XLIV) and obtained the spectrum of products indicated in Equation (36). The carbinol (XLV) was largely racemized,

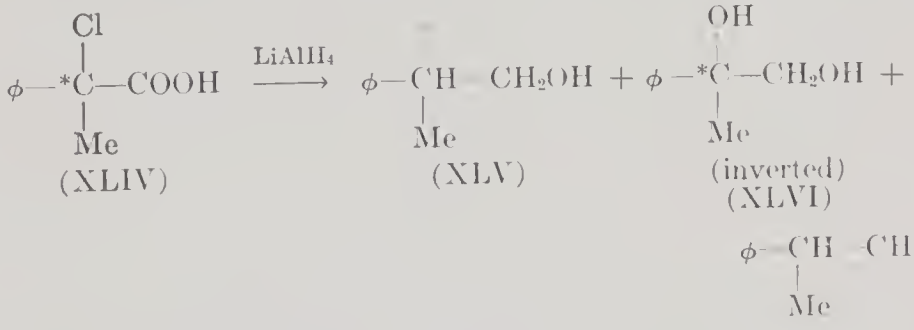

(XLIV) (XLV) (inverted) (XLVI) (36)

but XLVI was formed with nearly complete inversion. The interpretation is somewhat complicated by the probability of intermediate formation of α-lactone from XLIV, but the clean inversion evident in XLVI has been explained on the basis of one inversion in the process of α-lactone formation, and retention in the subsequent reduction of the α-lactone by acyl-oxygen fission. Somewhat simpler is the earlier observation of Eliel (89) on reduction of optically active phenylmethylcarbinyl chloride with $LiAlD_4$ leading to optically active α-deuteroethyl benzene; here the absolute configuration of the product was not ascertained, but inversion in the course of reduction was suspected by analogy with the oxide (84) work.

VII. MISCELLANEOUS REACTIONS

1. Decarboxylations

Analysis by configurational change has played an important role in understanding decarboxylations in homogeneous solution. Starting with the work of Kohler, Peterson, and Bickel (90) on decarboxylation in boiling

pyridine solution of the *erythro* and *threo* diastereomers of α-phenyl-β-benzoyl-β-bromopropionic acid, it was observed that the *erythro* isomer (XLVI) decarboxylates smoothly, whereas the *threo* does not and follows a course of HBr elimination only. These facts accord with a *trans* elimination process pictured in Equation (37), with an initial rotational con-

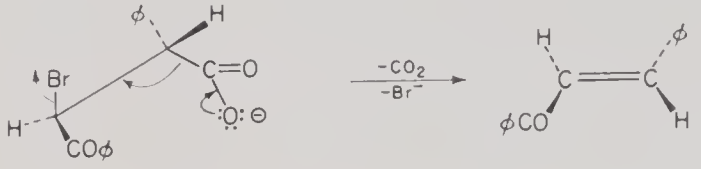

(37)

(XLVI)

formation such as to give minimum eclipsing of the bulky groups, and contrast with the *threo* structure in which no such alignment for *trans* elimination of the carboxyl function can occur.

More recently, Cristol and Norris (91) and Grovenstein and Lee (92) have found evidence for both stereospecific and nonstereospecific decarboxylations in the cinnamic acid dihalides, with interpretation of the former on the basis of a concerted *trans* elimination as in Equation (37), and of the latter in terms of a preliminary ionization (involving loss of specific configuration at the β-carbon atom) to the carbonium ion species ϕ-C^+H-$CHBrCOO^-$, with subsequent loss of CO_2 yielding mixtures of *cis* and *trans* olefin.

2. Generation and Stability of Carbanions

The problem of the generation of carbanions in unsaturated and saturated systems and the inherent stabilities of these species has also been approached with stereochemical techniques. For example, Curtin and Harris (93) studied the dehalogenation with *n*-butyl lithium of the represen-

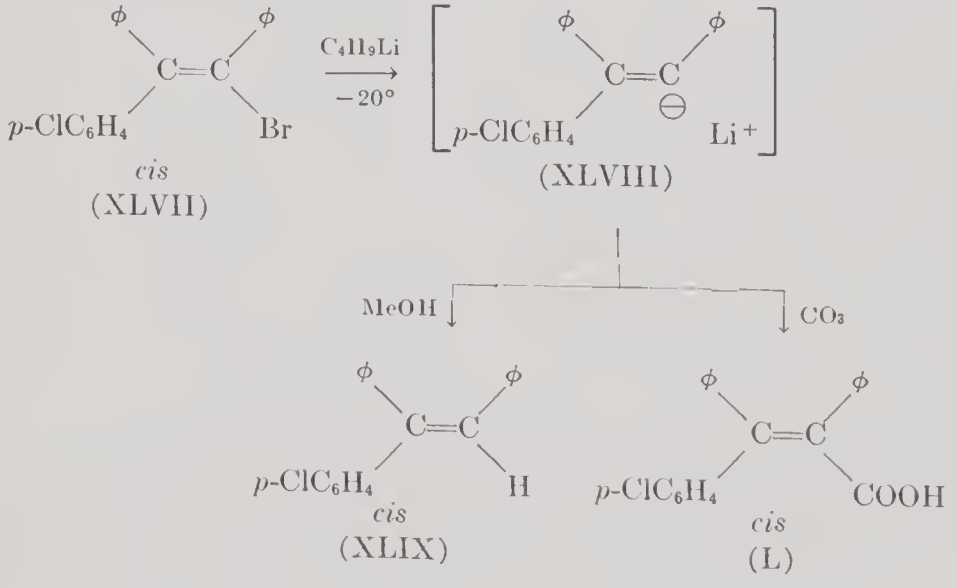

(37a)

cis
(XLVII)

(XLVIII)

cis
(XLIX)

cis
(L)

tative *cis* olefin (XLVII) and viewed the stability of the intermediate carbanion (XLVIII) in terms of the purity and configuration of its conversion products (XLIX and L). Since *cis* starting material leads to high yields of pure *cis* products through the organic salt stage, it is reasoned that a stable intermediate carbanion retains its configuration well at low temperature. A similar stereochemical result was also obtained (93) starting with *trans* XLVII.

Related work (94) in a saturated system has dealt with the low temperature metalation of optically active *sec*-octyl iodide by means of reaction with *sec*-butyl lithium, followed by carbonation. Carbonation of the

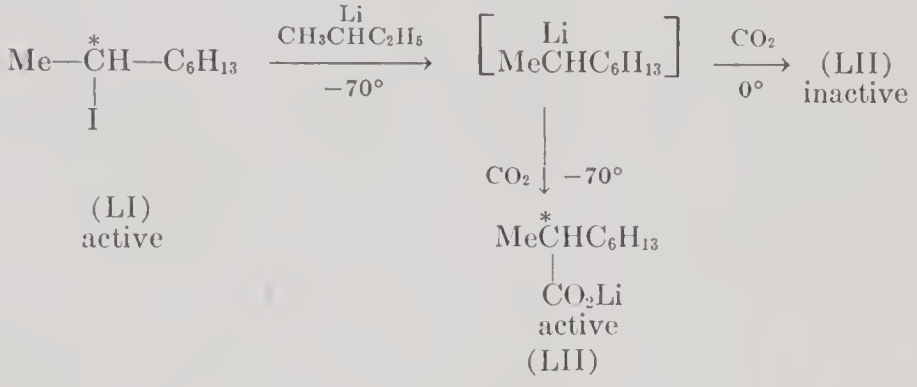

(38)

intermediate carbanion at −70° gave partially active LII (about 20% active) with retention of configuration, whereas warming to 0° and carbonation gave totally inactive LII. The logical interpretation of these results was made in terms of limited optical stability of the saturated carbanion at −70°, and its racemization at the higher temperature.

VIII. ENZYMATIC PROCESSES

The group of organic reactions known to be catalyzed by enzyme systems has expanded tremendously in the past two decades, as fundamental research into processes of biological importance has proliferated and prospered. Much of the success in probing the mechanisms of these processes is due to application of the physical and chemical techniques developed in allied disciplines, and few of these have proved more fruitful in evaluating mechanistic detail than the use of stereochemical methods. The problems of precise orientation in enzymatic processes are even more complicated than those found in uncatalyzed (by protein) reactions, since the steric needs and surface requirements of co-factors and the enzymes themselves are added to the conformational requirements of the essential reactants. Accordingly, it would be slighting the power of stereochemical techniques in application to mechanism studies if one did not at least briefly survey their utility in studying representative classes of enzymatic processes centered about organic reactions.

In the first of these classes to be considered, the organic reactions concerned are of the redox variety, reversible, and said to be linked with DPN (diphosphopyridine nucleotide) as a coenzyme in the sense that the mobile couple (Eq. 39) is continually cycled metabolically to provide electron

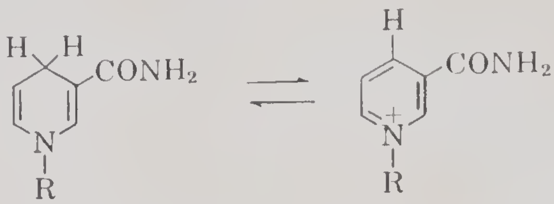

(DPNH) (DPN$^+$) $+ H^+ + 2e^-$ (39)

carriers between the ultimate electron donors and acceptors. Two reactions in this category that well illustrate the manner in which stereochemical and tracer techniques combine to elicit precise mechanistic information are found in the alcohol dehydrogenase and lactic dehydrogenase catalyzed processes below (Eq. 40, 41).

$$CH_3CH_2OH + DPN^+ \underset{}{\overset{\text{alcohol dehydrogenase}}{\rightleftharpoons}} CH_3CHO + DPNH + H^+ \qquad (40)$$

$$CH_3CHOHCOO^- + DPN^+ \overset{\text{lactic dehydrogenase}}{\rightleftharpoons} CH_3COCOO^- + DPNH + H^+ \qquad (41)$$

Much of the elegant work in this area has been that of Westheimer, Vennesland, and colleagues (95), and was carried out with highly purified catalyst systems.

In the alcohol dehydrogenase (A.D.) system, it was found in deuterium labeling experiments that hydrogen atoms are transferred reversibly from reduced substrate to DPN$^+$ in a direct process with no participation of solvent. Further, the enzyme is stereospecific (96) for *one* of the two enantiomorphs of ethanol-1-*D;* it will only accept as substrate that optical antipode produced by reaction (42), and not that resulting from (43). Also,

$$CH_3CHO + DPND + H^+ \xrightarrow{\text{A. D.}} CH_3\text{—}\overset{\overset{\displaystyle OH}{|}}{\underset{\underset{\displaystyle D}{|}}{C}}\text{—}H \qquad (42)$$

by deuterium tracer work, it was found that the H atoms in position 4 of

$$CH_3CDO + DPNH + H^+ \xrightarrow{\text{A. D.}} H\text{—}\overset{\overset{\displaystyle OH}{|}}{\underset{\underset{\displaystyle D}{|}}{C}}\text{—}CH_3 \qquad (43)$$

DPNH are not exchangeable with solvent, and that the yeast enzyme is highly stereospecific (97) with respect to removal of 4-hydrogen from, or its replacement on, *only one side of the pyridine ring.* All these elements

of stereospecificity add up to an oriented arrangement on the enzymatic surface in which H is transferred in highly direct fashion from substrate to coenzyme, or vice versa. Virtually the same elements of stereospecificity were found (98) in the lactic dehydrogenase system (41), and for this particular transfer process Vennesland and Westheimer introduced (95) the graphic pictorialization LIII.

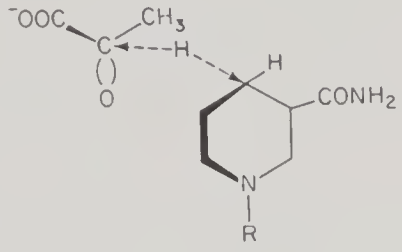

(LIII)

A second group of enzymes in which stereochemical considerations have led to important mechanistic information includes the proteases and hydrolases. For illustrative purposes and as indications of the nature of the methods employed, representative work with α-chymotrypsin (Chy) and with acetylcholinesterase (AChE) will be considered.

The first of these enzymes shows high specificity with respect to the neighborhood of a peptide or ester linkage that can be accommodated on the catalytic protein surface. In one category (LIV) of esters whose hydrolysis is markedly catalyzed by Chy, specificity resides (99) in both the optical character of the central asymmetric atom and in the nature of the group R. Normally, only compounds of the L-series are accepted by the enzyme as substrates, and the relative rates of the k_3 cleavage step decrease

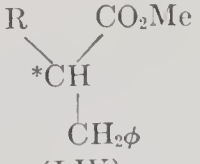

(LIV)

in the series R = ϕCONH, OH, Cl, H. These results have been interpreted (99) in terms of three-point binding of the substrate to Chy, i.e., through the ester function, the asymmetric region, and the R group, with an over-all requirement of highly oriented "lock-and-key" fit to the conformation of the catalytic surface for very effective catalysis of the cleavage with water.

In the studies of cleavage of acetylcholine by AChE, much information on the stereochemical requirements of the catalytic surface has been gleaned from work with competitive inhibitors tailored stereospecifically for the job. For example, the hydrolysis process is inhibited mildly by 1,2-quaternary aminoalcohols in the cyclohexane (100) and cyclopentane (101)

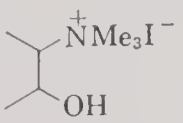
(LV)

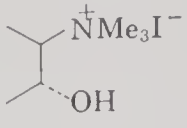
(LVI)

series, and in each instance the *cis* isomer LV is appreciably stronger in action than its *trans* relative. This has been interpreted in terms of a picture of binding to enzyme via two-pointed interaction with the two polar loci in LV–LVI, and an optimum distance between N and O functions for best interaction with the surface. That the protein region between the sites may also display surface contours with built-in stereospecificity can be inferred from recent studies (102,103) on inhibition with the optical

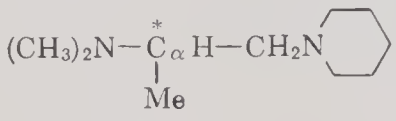
(LVII)

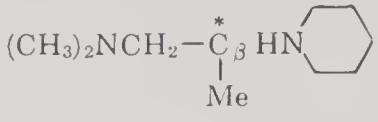
(LVIII)

antipodes of LVII and LVIII. The enzyme responds sensitively to the configuration employed at the α-carbon in LVII, with the (+)-rotatory isomer producing (102) the more powerful inhibition, but is completely insensitive in differentiating between the two optical antipodes at the β-carbon atom in LVIII (103).

References

1. D. J. Cram, in M. S. Newman, ed., *Steric Effects in Organic Chemistry*, Wiley, New York, 1956, Chapters 5 and 6.
2. P. B. D. de la Mare, in W. Klyne, ed., *Progress in Stereochemistry, Vol. 1*, Academic, London, 1954, Chapter 3.
3. P. Walden, *Ber.*, **28**, 1287 (1895).
4. H. Phillips, *J. Chem. Soc.*, **1923**, 44.
5. E. D. Hughes, F. Juliusberger, A. D. Scott, B. Topley, and J. Weiss, *ibid.*, **1936**, 1173.
6. W. A. Cowdrey, E. D. Hughes, T. P. Nevell, and C. L. Wilson, *ibid.*, **1938**, 209.
7. C. K. Ingold, *Structure and Mechanism in Organic Chemistry*, Cornell University Press, Ithaca, 1953.
8. E. D. Hughes, C. K. Ingold, and S. Masterman, *J. Chem. Soc.*, **1937**, 1196.
9. E. D. Hughes, C. K. Ingold, R. J. L. Martin, and D. F. Meigh, *Nature*, **166**, 679 (1950).
10. W. A. Cowdrey, E. D. Hughes, and C. K. Ingold, *J. Chem. Soc.*, **1937**, 1208.
11. S. Winstein and H. J. Lucas, *J. Am. Chem. Soc.*, **61**, 1576 (1939).
12. J. Kenyon, H. Phillips, and F. M. H. Taylor, *J. Chem. Soc.*, **1931**, 382.
13. E. S. Lewis and C. E. Boozer, *J. Am. Chem. Soc.*, **74**, 308 (1952); *ibid.*, **75**, 3182 (1953).
14. D. J. Cram, *ibid.*, **75**, 332 (1953).
15. For leading references see S. Winstein *et al.*, *J. Am. Chem. Soc.*, **64**, 2796 (1942); *ibid.*, **68**, 119 (1946); *Bull. soc. chim. France*, **18**, C55 (1951).

16. S. Winstein *et al.*, *J. Am. Chem. Soc.*, **64**, 2780, 2787 (1942); *ibid.*, **75**, 613 (1943)
17. D. J. Cram, *ibid.*, **71**, 3863 (1949).
18. A. McKenzie, *J. Chem. Soc.*, **1912**, 1196.
19. E. M. Terry and L. Eichelberger, *J. Am. Chem. Soc.*, **47**, 1067 (1925).
20. R. Kuhn and T. Wagner-Jauregg, *Ber.*, **61**, 519 (1928).
21. P. D. Bartlett and D. S. Tarbell, *J. Am. Chem. Soc.*, **58**, 466 (1936); *ibid.*, **59**, 407 (1937).
22. I. Roberts and G. E. Kimball, *ibid.*, **59**, 947 (1937).
23. S. Winstein and B. K. Morse, *ibid.*, **74**, 1134 (1952).
24. C. K. Ingold, reference 7, p. 662.
24a. H. C. Brown and G. Zweifel, *J. Am. Chem. Soc.*, **81**, 247 (1959).
25. D. J. Cram and F. A. A. Elhafez, *ibid.*, **74**, 5828 (1952).
26. P. Pfeiffer, *Z. physik. Chem.*, **48**, 40 (1904).
27. S. Winstein, D. Pressman, and W. G. Young, *J. Am. Chem. Soc.*, **61**, 1645 (1939).
28. D. Y. Curtin and D. B. Kellom, *ibid.*, **75**, 6011 (1953).
29. D. J. Cram, *ibid.*, **74**, 2149 (1952); D. J. Cram and F. A. A. Elhafez, *ibid.*, **74**, 5851 (1952).
30. S. J. Cristol *et al.*, *ibid.*, **69**, 340 (1947); *ibid.*, **73**, 674 (1951); *ibid.*, **75**, 2647 (1953).
31. G. Vavon and M. Barbier, *Bull. soc. chim. France*, [4], **49**, 567 (1931).
32. D. J. Cram, *J. Am. Chem. Soc.*, **75**, 2137 (1952).
33. S. Winstein, B. K. Morse, E. Grunwald, H. W. Jones, J. Corse, D. Trifan, and H. Marshall, *ibid.*, **74**, 1127 (1952).
34. E. D. Hughes, C. K. Ingold, and J. B. Rose, *J. Chem. Soc.*, **1953**, 3839.
35. T. D. Nevitt and G. S. Hammond, *J. Am. Chem. Soc.*, **76**, 4124 (1954).
36. C. C. Price and J. V. Karabinos, *ibid.*, **62**, 1159 (1940).
37. D. J. Cram, *ibid.*, **75**, 2137 (1952).
38. D. J. Cram, *ibid.*, **71**, 3883 (1949); D. J. Cram and F. A. A. Elhafez, *ibid.*, **74**, 5828 (1952).
39. W. Hückel, W. Tappe, and G. Legutke, *Ann.*, **543**, 191 (1940).
40. D. H. R. Barton, *J. Chem. Soc.*, **1949**, 2174.
41. E. R. Alexander and A. Mudrak, *J. Am. Chem. Soc.*, **72**, 1810 (1950).
42. A. C. Cope, R. A. Pike, and C. F. Spenser, *ibid.*, **75**, 3212 (1953).
43. D. J. Cram and J. McCarty, *ibid.*, **76**, 5740 (1954).
44. E. R. Alexander and R. W. Kluiber, *ibid.*, **73**, 4304 (1951).
45. K. Schmid, W. Haegele, and H. Schmid, *Helv. Chim. Acta*, **37**, 1080 (1954).
46. D. Y. Curtin and H. W. Johnson, Jr., *J. Am. Chem. Soc.*, **78**, 2611 (1956).
47. S. J. Rhoads and R. L. Crecelius, *ibid.*, **77**, 5060 (1955).
48. D. S. Tarbell, "The Claisen Rearrangement," in *Organic Reactions*, Vol. II, Wiley, New York, 1944.
49. G. Fodor and K. Nador, *J. Chem. Soc.*, **1953**, 721; G. Fodor and O. Kovacs, *ibid.*, **1953**, 724.
50. G. F. Holland, R. C. Durant, S. L. Friess, and B. Witkop, *J. Am. Chem. Soc.*, **80**, 6031 (1958).
51. L. W. Jones and E. S. Wallis, *ibid.*, **48**, 169 (1926).
52. J. V. Braun and E. Frichmelt, *Ber.*, **66**, 684 (1933).
53. E. S. Wallis and R. D. Dripps, *J. Am. Chem. Soc.*, **55**, 1701 (1933).
54. J. Kenyon and D. P. Young, *J. Chem. Soc.*, **1941**, 263.
55. J. F. Lane and E. S. Wallis, *J. Am. Chem. Soc.*, **63**, 1674 (1941).
56. R. B. Turner, *ibid.*, **72**, 878 (1952).

57. M. F. Hawthorne, W. D. Emmons, and K. S. McCallum, *ibid.*, **80**, 6393 (1958).
58. H. Meerwein *et al.*, *Ber.*, **53**, 1815 (1920); *ibid.*, **55**, 2500 (1922); *Ann.*, **435**, 174 (1923); *ibid.*, **453**, 16 (1927).
59. J. Meisenheimer, *Ber.*, **54**, 3206 (1921); O. L. Brady and G. Bishop, *J. Chem. Soc.*, **1925**, 1357.
60. H. I. Bernstein and F. C. Whitmore, *J. Am. Chem. Soc.*, **61**, 1324 (1939).
61. D. Y. Curtin *et al.*, *ibid.*, **72**, 961 (1950); *ibid.*, **73**, 3453 (1951); *ibid.*, **77**, 354 (1955).
62. A. Campbell, A. H. J. Houston, and J. Kenyon, *J. Chem. Soc.*, **1947**, 93.
63. M. P. Balfe and J. Kenyon, *Trans. Faraday Soc.*, **37**, 721 (1941).
64. S. K. Hsü, C. K. Ingold, and C. L. Wilson, *J. Chem. Soc.*, **1935**, 1778.
65. C. K. Ingold and C. L. Wilson, *ibid.*, **1934**, 93.
66. E. de Salas and C. L. Wilson, *ibid.*, **1938**, 319.
67. H. Hart and H. S. Eleuterio, *J. Am. Chem. Soc.*, **76**, 519 (1954).
68. E. S. Wallis and F. H. Adkins, *ibid.*, **55**, 3838 (1933).
69. P. H. Wilken, Ph.D. Thesis, Notre Dame, 1955; quoted by E. L. Eliel in reference 1, chapter 2.
70. M. S. Kharasch, J. G. Kuderna, and W. Nudenberg, *J. Org. Chem.*, **19**, 1283 (1954).
71. H. C. Brown, M. S. Kharasch, and T. H. Chao, *J. Am. Chem. Soc.*, **62**, 3435 (1940).
72. C. L. Arcus, A. Campbell, and J. Kenyon, *J. Chem. Soc.*, **1949**, 1510; C. L. Arcus and G. V. Boyd, *ibid.*, **1951**, 1580; J. Kenyon, *Bull. soc. chim. France*, C64–71 (1951).
73. D. C. Abbott and C. L. Arcus, *J. Chem. Soc.*, **1952**, 3195; J. Cason, M. J. Kalm, and R. H. Mills, *J. Org. Chem.*, **18**, 1670 (1953).
74. Reviewed by E. L. Jackson, *Organic Reactions*, Vol. II, Wiley, New York, 1944, Chapter 8.
75. C. C. Price and M. Knell, *J. Am. Chem. Soc.*, **64**, 552 (1942); C. C. Price and H. Kroll, *ibid.*, **60**, 2726 (1938).
76. For early papers in this sequence see: R. Criegee, *Ann.*, **481**, 275 (1930); *ibid.*, **495**, 211 (1932); *Ber.*, **64**, 260 (1931); *Angew. Chem.*, **50**, 153 (1937).
77. H. Lund, *Ber.*, **70B**, 1520 (1937).
78. H. S. Mosher and E. LaCombe, *J. Am. Chem. Soc.*, **72**, 3994 (1950).
79. W. A. Bonner, *ibid.*, **74**, 1034, 5089 (1952).
80. W. A. Bonner, J. A. Zderic, and G. A. Casaletto, *ibid.*, **74**, 5086 (1952).
81. S. L. Friess and H. D. Baldridge, *ibid.*, **78**, 2482 (1956).
82. D. J. Cram and F. D. Greene, *ibid.*, **75**, 6005 (1953).
83. M. Gates, *ibid.*, **75**, 4340 (1953).
84. L. W. Trevoy and W. G. Brown, *ibid.*, **71**, 1675 (1949).
85. M. E. Speeter, W. M. Byrd, L. C. Cheney, and S. B. Binkley, *ibid.*, **71**, 57 (1949).
86. P. A. Plattner, H. Heusser, and M. Feurer, *Helv. Chim. Acta*, **32**, 587 (1949).
87. R. Fuchs and C. A. Vander Werf, *J. Am. Chem. Soc.*, **74**, 5917 (1952).
88. E. L. Eliel and J. P. Freeman, *ibid.*, **74**, 923 (1952).
89. E. L. Eliel, *ibid.*, **71**, 3970 (1949).
90. E. P. Kohler, W. D. Peterson, and C. L. Bickel, *ibid.*, **56**, 2000 (1934).
91. S. J. Cristol and W. P. Norris, *ibid.*, **75**, 632, 2645 (1953).
92. E. Grovenstein, Jr., and D. E. Lee, *ibid.*, **75**, 2639 (1953).
93. D. Y. Curtin and E. E. Harris, *ibid.*, **73**, 2716 (1951).
94. R. L. Letsinger, *ibid.*, **72**, 4842 (1950).

95. B. Vennesland and F. H. Westheimer, in W. D. McElroy and B. Glass, eds., *The Mechanism of Enzyme Action*, Johns Hopkins Press, Baltimore, 1954, p. 357.

96. F. A. Loewus, F. H. Westheimer, and B. Vennesland, *J. Am. Chem. Soc.*, **75**, 5018 (1953).

97. H. F. Fisher, E. E. Conn, B. Vennesland, and F. H. Westheimer, *J. Biol. Chem.*, **202**, 687 (1953).

98. F. A. Loewus, P. Ofner, H. F. Fisher, F. H. Westheimer, and B. Vennesland, *ibid.*, **202**, 699 (1953).

99. J. E. Snoke and H. Neurath, *ibid.*, **182**, 577 (1950).

100. H. D. Baldridge, W. J. McCarville, and S. L. Friess, *J. Am. Chem. Soc.*, **77**, 739 (1955).

101. S. L. Friess and H. D. Baldridge, *ibid.*, **78**, 2482 (1956).

102. S. L. Friess, E. R. Whitcomb, B. T. Hogan, and P. A. French, *Arch. Biochem. Biophys.*, **74**, 451 (1958).

103. S. L. Friess, E. R. Whitcomb, R. C. Durant, and P. A. French, *ibid.*, **83**, 419 (1959).

General References

Hammett, L. P., *Physical Organic Chemistry*, McGraw-Hill, New York, 1940.

Ingold, C. K., *Structure and Mechanism in Organic Chemistry*, Cornell University Press, Ithaca, 1953.

Newman, M. S., *Steric Effects in Organic Chemistry*, Wiley, New York, 1956.

Klyne, W., *Progress in Stereochemistry, Volume 1*, Academic, London, 1954.

CUMULATIVE SUBJECT INDEX
PART I, pp. 1–702; PART II, pp. 703–1582

A

Absorption cross section, 955, 1017
Absorption spectra, flash photolysis, 1074–5
Absorption spectrophotometry
  enzyme reaction rate measurement, 1238–41
  relaxation methods, 975–6
Acetal hydrolysis, 231–2
  mechanism, 1395–6
Acetaldehyde, aldol condensation, 1448, 1502
  thermal decomposition, 451, 452, 483–6
Acetic acid, esterification with ethanol, mechanism, 1429
  proton transfer reactions with, 1040
  recombination rate constant, 816, 833
Acetone, alkaline bromination, 1447–8
  photolysis, 478–9
Acetone and cyclohexene, competitive catalytic hydrogenation, 690–2, 693
Acetyl peroxide, competing reactions, 365, 366
Acetylacetone, proton transfer reactions with, 1040
Acetylcholinesterase, stereochemistry, 1587–9
Acetylsalicylamide, base-catalyzed isomerization, 616–17
Acid-base catalysis, isotope effects in, 404–7, 412–14
Acid-base equilibria, 532–4
  extinction coefficients, 1079
Acid-base reactions, 384, 385–6
  in aqueous solution, 385–6
  fluorescent study of, 852, 856–60
  in fused salts, 384
Acidity function. *See* Hammett acidity function
Acids, carboxylic, competing reactions, 375–6
  dimerization, 939, 947, 963, 1047
Acids, organic, catalytic esterification, 673
Acoustic interferometer, relaxation studies, 1009–10
Acoustics, relaxation methods, 1005–16
Acridine, fluorescence, 856–8
Acrylonitrile, copolymerization with methyl methacrylate, 1191
Activated complex, 501, 502, 509–10, 632
Activity coefficient, 29–31, 511, 512–13, 514–15, 1399–1403
  measurement, 514–15
  of solute, 512–13
Acyl migrations, in cyclic systems, 1562–3
Acyl peroxides, decomposition of, 1421
Addition compounds, as reactive intermediates, 1435
Addition reactions, stereochemical studies, 1555–7
Affinity, 929
Alcohol dehydrogenase, kinetics of, 1273–7
  deuterium studies, 1577
Alcohols, ionization, 1401
  oxygen exchange with, 1530–1
  secondary, catalytic dehydrogenation, 657–8, 671–2, 683–4, 699–701
Aldehydes, oxidation, 1133
Aldolization and dealdolization, 552–3
sec-Alkyl chlorosulfites, decomposition, 1474
Alkyl halides, solvolysis, 240–2, 383
Allyl compounds, rate of polymerization, 1172
Aluminum chloride, in Friedel-Crafts reactions, 652–3
Amides, acid-catalyzed hydrolysis, 601–2, 1450–1
Amino acids, proton transfer reactions in, 1040
Ammonia, sound absorption curve, 1020
Ammonium cyanate, urea source, 1399
Amplifiers, chopper, 737–8
  direct-coupled, 738
  photocell, 761–2
Amplitude dispersion method, 994–1001

tert-Amyl chlorides, solvolysis, 1474
Anthracene, flash photolysis, 1091
Apparent competitive inhibition, in enzyme systems, 1287
Aquo complexes, binuclear, 1043
  inner-sphere, 1042
Arditron lamp, in flash photolysis, 1087–8
Aroyl peroxides, 1422
Arrhenius complex, 664–5, 666, 1430
Arrhenius equation, 32–3, 113, 454–6, 505, 667, 675
Arrhenius parameters, tables for
  acetaldehyde decompositions, 485
  Diels-Alder reactions, 465
  dimerization ractions, 465
  isomerizations, 463
  metathetical reactions, 479
  unimolecular elimination halides, 462
Arylmethyl chlorides, solvolysis, 561–2
Asymmetry, deuterium-induced, 1538–9
  relation to mechanism, 1549–79
Atactic polymers, 1204
Attenuation constant, sound, 1005
Autocatalysis, 193
Autoxidation, competitive, 373
  isotope effects in, 408–9
Azide ion, reaction with diazonium salts, 1533–4
Azo compounds, free radical source, 1168–9
Azobenzene, recombination rate constant, 818
Azoisobutyronitrile, extraction, 1142
  polymerization initiator, 1170–1

B

Baeyer-Villiger reaction, 1564
Beer-Lambert law. *See* Lambert-Beer law
Benton's equation, 453
β–Benzenehexachloride, elimination reaction, 1502
Benzenesulfonates, rates of acetolysis, 1456
Benzophenone, ESR investigation, 891
  photolysis of, 382
Benzoquinuclidine, reactions, 263
Benzoyl chloride, solvolysis, 559–61
Benzoyl peroxide, decomposition, 1458, 1482
  free radical source, 1168
  reaction with triphenylphosphine, 1532
Benzoyloxy radical, behavior, 1421
Benzyne intermediates, 1486, 1496, 1505
Bigeleisen theory, 390–7
Bimolecular reactions, F-factor, 935
  rate measurements
    flow method, 717–18, 724
    polarographic, 808–9, 811–12, 815
    rapid thermal method, 767, 773, 775
Bloch equations, 872–4
Block copolymers, ionic copolymerization, 1203
  synthesis, 1189–92
Bodenstein steady state approximation, 138–43
Bohr magneton, 888
Boltzmann distribution, 26
Boltzmann expression, 1362
Bond dissociation energy, 476–7, table, 477
Briggs-Haldane equation, 1250
Bromination, 357, 361, 379, 477
  by *N*-bromosuccinimide, 379
  electrophilic aromatic, 361
  photochemical, 357, 379, 477
1-Bromo-2-arylethanes, elimination reactions, 1469
  base-induced, 1396
Bromonium ion, 1488
α–Bromopropionate ion, solvolysis, 1487–8
N-Bromosuccinimide, bromination with, 379
Bromotriptycene, reactions, 262
Brønsted-Bjerrum equation, 502, 514, 520–2
Brønsted catalysis law, 211, 230–40, 245, 518, 604–5, 1399
Brønsted equation, 31, 599–602
Brønsted rate law, 1374
Brønsted theory of acids and bases, 156–8
Butadiene, dimerization, 453, 1377
tert-Butoxy radicals, competing reactions, 363
tert-Butyl bromide, salt effect, 520, 1453
tert-Butyl chloride, solvolysis, 519, 563

thermal decomposition, 450
tert-Butyl halides, solvolysis, 519, 528–9, 563
tert-Butyl peresters, thermal decomposition, 1386–8, 1467
tert-Butyl phenylperacetate, thermal decomposition, 1387
tert-Butyl propionate, thermal decomposition, 450

C

Cage effect, 1169
Calorimetry, isothermal, polymerization, reaction rate of, 1167
Caprolactone, polymerization reaction, 1150
Carbanions, 1433–4, 1460
generation and stability, 1575–6
Carbenes, product criterion, 1416–17
Carbon-13, isotope effects with, 415, 419, 1498
analytical methods, 1542
Carbon-14, isotope effects with, 414–19, 1492–6, 1520–9
analytical methods, 1543
Carbon dioxide, NMR measurement of hydration rate, 883
Carbon tetrachloride, dimerization, 1044
Carbonic acid, dehydration, 725–6
Carbonium ion, 566–9, 1432–4, 1468
bridged, 1471
ionic polymerization, 1197–1200
nonclassical, 1433, 1493–4
partitioning of, 1454
rearrangement, carbon-14 studies of, 1524–9
Carbonyl group, nucleophilic additions to, 1557
reduction in Meerwein-Ponndorf-Verley reaction, 1571
Carboxypeptidase, kinetics of, 1263–4
competitive inhibition, 1280
heat and entropy of activation, 1299
Catalase, catalase-hydrogen peroxide complex, 730
kinetics, 1322
peroxidatic reactions of, 1323–32
preparative procedures of Keilin and Hartree, 728
reactions with hydrogen peroxide, 1332–43
Catalysis, 154–9, 211, 230–40, 245, 386, 404–7, 412–14, 579–626, 650–701, 1457–60
acids and bases, 156–8
autocatalytic reactions, 653
Brønsted law, 211, 230–40, 245
enzymes. *See* Enzyme reactions
general acid. *See* General acid catalysis.
general base. *See* General base catalysis.
of heterogeneous reactions. *See* Heterogeneous catalysis
in homogeneous solutions. *See* Solution catalysis.
hydrogen ion. *See* Hydrogen ion catalysis
hydroxyl ion. *See* Hydroxyl ion catalysis
isotope effects in, 404–7, 412–14
nucleophilic. *See* Nucleophilic catalysis
specific hydroxide ion (lyate ion) catalysis, 234–6, 386
specific oxonium ion (lyonium ion) catalysis, 230–4
Catalyst-reactant intermediate, 585–6, 586–96
detection, 586–96
formation, 585–6
Catalysts, 163, 579–80, 660–1
definition, 579–80
negative, 163
Cathode follower, flash photolysis apparatus, 1069
Cavitation, 716
Cell metabolism, 323–5
Cellulose, hydrolytic degradation, 1210–13
molecular structure, 1212
Chain length, 354, 362
Chain reaction, 168–71, 354–5, 457–9, 471–3, 475–8, 480–2, 569–73. *See also* Free radicals, reactions
branching, 168–71
inhibition by nitric oxide, 471–2

inhibition by propylene, 472–3
initiation, 475–8, 1109–10
oxidation of hydrocarbons, 569–73
termination, 480–2, 1131
Chance apparatus. *See under* Flow apparatus
Chemical equilibria. *See* Equilibria
Chemical relaxation. *See* Relaxation, chemical
Chlorination, 355–7, 362, 378–80
by *N*-chlorosuccinimide, 378–9
photochemical, 355–7, 362, 379
solvent effect, 380
by sulfuryl chloride, 380
Chlorine, photochemical reaction with oxygen, 1078
Chlorobenzene, dimerization, 1044
Chloroform, base-catalyzed deuterium exchange, 1502
N-Chlorosuccinimide, chlorination with, 378–9
Christiansen formulation, 350–1
Chromatography, high-polymer separation, 1144–6
Chronopotentiometry, 824–33
apparatus, 830–2
Chymotrypsin, heat and entropy of activation for, 1299
stereochemisty, 1578
volume changes during reaction, 1303
Chymotrypsinogen, thermodynamic values for thermal denaturation of, 1297
Cinnamyl chloride, acetolysis, 1478
Cis-trans isomerization, gas phase studies, 1378–80
Claisen rearrangement, carbon-14 studies of, 1521–3
intermediate, 1483–4
stereochemical studies, 1561–2
Clark electrode, 786
Collision, 16–24, 29, 32–4, 460, 480–1, 501, 632
bimolecular, 29
diameter, 18, 22
energy of activation, 18–21
frequency, 16–18, 23–4
in condensed phases, 23–4
solvent effects, 23–4
frequency factor, 34
in heterogeneous reactions, 632
of methyl radicals in chain ending, 480–1
probability factor, 34
steric or probability factor, 21–3
three-body, 29
Collision theory, 16–24, 32–4, 501
comparison with transition state theory, 32–4, 1294
enzyme systems, 1292–3
Common ion effect, 383
Competing reactions, 343–86, 503–4, 682–6
chain reactions, 354–5
consecutive reactions, 346–51
determination of relative reaction rates, 355–73
evaluation of reaction rates in complex reactions, 381–6
identification of intermediates, 378–80
induced reactions, 351–4
mathematical treatment, 344–55
quantitative analysis, 373–8
Competitive inhibition, in enzyme systems, 1278–80, 1287
Complex formation, fluorescence, 852, 855–6
relaxation studies, 1041, 1043
Compressibility, adiabatic, 944, 953
isothermal, 932, 944
Computers, 285–326
computer theorem, 297
definition, 286–8
design, 288–90
electronic analog computers, 290–1, 293
electronic digital computers, 291–3
general types of enzyme reaction mechanisms, 311–33
intermediates, 306, 327
Johnson Foundation electronic analog computer, 299–302
linear intermediate, 318
Michaelis-Menten mechanism for enzyme reactions, 302–11
"off" region, 308
"on" region, 306
principles of use, 297–8
reflection coefficients, application to induced steady state example, 336–7

steady state region, 307–8, 327–8
Univac I electronic digital computer, 322–5
Concentration effects, 31
enzyme reactions, 1246–8
Concentration measurements, 67–84, 967–9
Condensation polymerization, 1140, 1149–60
interchange reactions, 1156
kinetics, 1153–4
rate constants, 1151–2
Consecutive reactions, 346–61
common reagent, 346–8
reactive intermediate, 348–51
Constant γ plates, flash photolysis, 1076–7
Continuous-flow methods, 1240
Continuous-flow stirred reactor, 66–7, 593–4
Copolymerization, 371–3, 1181–93
intermediates, study of, 1484
ionic, 1203
rates of reaction, 1186–9
Copper, oxidation, 647–8
Correlation time, NMR, 869
Coupled cathode follower, flash photolysis apparatus, 1069
Crabtree effect, 325
p-Cresol, catalytic dehydration, 674–5
Critical experiments, 145–7
Crystals, sublimation or melting of, 644–5
Cupric sulfate, sound absorption curve, 1021
Cyclic reactions, 150–3
Cyclobutanone, decomposition, 450
Cyclohexene, addition of CCl_3Br, 1173
Cyclohexene, catalytic hydrogenation, 695
Cyclohexene and acetone, competitive catalytic hydrogenation, 690–2, 693
cis-Cyclohexeneacetoxonium ion, formation, 1483
Cyclohexyne intermediate, 1496
Cylindrical resonator, relaxation studies, 1009

D

Darzen's condensation, isolation of intermediate, 1440–1
Debye-Hückel theory, 44, 605
Debye-Sears effect, 1011–12
Decarboxylation, isotope effects in, 414–415, 418
stereochemical studies, 1574–5
Decay constant, sound, 1005
Degradation, polymers, 1210–20
hydrolytic, 1210–14
mechanical, 1217–18
oxidative, 1218–20
photochemical, 1216–17
thermal, 1214–16
Degree of dissociation, 934, 937
Degree of transformation, 934, 937
Density, polymerization reaction rate measurement, 1165–7
Depolymerization, definition, 1210
Deuterium, isotope effects with, 356–7, 379, 393–6, 397–414, 1535–9
in aliphatic substitutions, 356–7
analytical methods, 1541–2
intermediates, study of, 1473–5, 1501–3
photohalogenation, 356–7, 379
Diacetone alcohol, depolymerization, 235
Diamagnetic susceptibility, polymerization reaction rate measurement, 1164
Diazoalkanes, polymerization, 1209
Diazomethane, carbene source, 1416–17
Diazonium salts, reaction with azide ion, 1533–4
Di-*tert*-butyl peroxide, competing reactions, 363
decomposition, 1481
p-Dichlorobenzene, arylation, 1422–3
Dicyclopentadiene, dissociation, 1377
Dielectric constant measurements, 82–3
Diels-Alder reaction, 360, 451, table, 465
mechanism, 1376–8
Diethylene glycol, polymerization with adipic acid, 1154
Differential rate equation, 451–2, 510–11
Differential spectrophotometry, 1276
Digeranyl, oxidation, 1135
Dilatometry, polymerization reaction rate, 1165–7, 1196, 1207–8
Dimerization, carboxylic acids, 939, 947, 963, 1020, 1044
relaxation studies, 1044
α, α-Dimethyallyl chloride, acetolysis, 1455

Dimethylacetamide, inner rotation, 883
Dimethylaniline, in heterogeneous catalysis, 694
p, p'-Dimethylbenzhydryl chloride, solvolysis, 1453–4, 1480
1,3-Dimethylcyclopentane, oxidative degradation, 1218–19
Dimethylformamide, inner rotation, 883
2,4-Dinitrochlorobenzene, reaction with aniline, 180
1,2-Diols, oxidation by periodic acid, 1447
Diphenyldiazomethane (DDM), competing reactions, 375–6
Diphenylpyruvic acid, recombination rate constant, 816
Diphosphopyridine nucleotide, 731
Dipolar equilibria, relaxation studies, 1025–9
Displacements, nucleophilic 245–9
  Edwards' equations, 247–9
  Swain-Scott equation, 245–7
Dissociation constant, 936
Dissociation field effect, 940–1
Downing galvanometer, 761–3
Dropping mercury electrode, enzyme kinetics, 1242, 1322
  flow methods, 785
Duroquinone, flash photolysis, 1096–9, 1101

E

Echo method, relaxation studies, 1015
Edwards' equations, 247–9
Effective concentration, 633
Effective dielectric constant, 582–3
Electrical permittivity, 945
Electric field-pulse method, 988–1001
  amplitude dispersion method, 994–1001
  square pulse method, 992–4
Electrolysis, under constant current, 824–33
Electron spin resonance, 865–6
  apparatus, 755–7
  enzyme kinetics, 1323
  isolation of intermediates, 1444, 1505
  rate constant determination, 888–91
Electrostriction, coefficient of, 932
Elimination reactions, deuterium-exchange studies, 400–1, 1535–7
  product criterion, 1410–13
  stereochemical studies, 1557–61
  sulfur, isotope effect with, 419–20
Energy levels, 1363–4, 1366
Energy of activation, 18–21, 24–7, 33, 199–204, 504–8, diagrams, 19, 25
  calculation, 199–204
  degree of freedom, 20
  errors in calculation, 504–8
  square terms, 20
  variation with temperature, 202
Energy transfer, fluorescence, 852, 855–6
Enolization, isotope effects in, 397, 412–14
  of ketones, 233
  mechanism, 1535
Enthalpy of activation, 33, 205–10, 1371–2
  entropy-enthalpy relationship, 205–10
  variations with solvent, 1390
Entropy, relation to temperature, 942–4
Entropy of activation, 33–34, 39–40, 199–204, 205–10, 1371–83
  calculation, 39–40, 199–204
  enthalpy-entropy relationship, 205–10
  intermediates, formation of, 1452
  variations with solvent, 1390–1
Entropy of reaction, 1380–92
Environmental control, 55, 59–61
Environmental effects, 518–36
Enzyme reactions, 302–35, 385, 620–6, 1450
  concentration effects, 1246–8
  electrophilicity of substrates, 625
  enzyme-substrate complex, 1243–4
  general characteristics, 1233–5
  inhibition, 624, 1277–87
  intermediates, 625–6
  kinetics, 1232–1303, 1314–57
  Michaelis-Menten mechanism. *See* Michaelis-Menten enzyme catalysis
  pH effects, 1287
  pressure effects, 1301–3
  R group specificity, 621–2
  stereochemical studies, 1576–9
  stoichiometric reflection coefficient, 334–5
  temperature effects, 1292–1301
Enzyme-substrate complex, 1243–4
  Michaelis-Menten equation, 1248–51
Epoxidation, 377

Epoxides, hydrolysis, 158–9, 1396
Equations of state, chemical equilibrium, 941–8
  dynamic, 948
Equilibria, 33–4, 149–50, 501, 502
  relaxation studies, 1022
  thermodynamic relations, 928–63
Equilibrium constant, in terms of partition functions, 1361–3
ESR. *See* Electron spin resonance
Esters, aminolysis, 272–3
  hydrolysis, 221–6, 601–2, 605, 614–16
    acid-catalyzed, 601–2, 605
    base-catalyzed, 615–16
    imidazole-catalyzed, 614
    isotopic oxygen exchange, 1450
    oxygen-18 studies of, 1529–30
    use of Taft's equations, 221–6
Esters, pyrolysis, 1412–13
Ethane, thermal decomposition, 479–80
Ethanol, dehydration, 663–4
  NMR spectrum, 875–6
  photooxidation, 1220
Ethyl benzoate, alkaline hydrolysis, mechanism, 1499–1500
Ethyl bromide, decomposition, 461–3
Ethyl formate, rotational isomerism, 1049
Ethyl linoleate, oxidation, 1135
Ethylene, polymerization, 1205–7, 1209
  reaction with bromine, 1483
Ethylene glycol, in flash photolysis, 1066
Ethylene oxide, hydration, 1397–8, 1403
Explosions, 168–71
Extent of reaction, 929
Extinction coefficient, determination by flash photolysis, 1078–9

F

Favorskii reaction, 1495
Figure of merit, enzymic activity, 1321
Fischer indole synthesis, nitrogen-15 studies, 1534
Flash lamp, construction, 1063
Flash photolysis, 1001, 1056–1104
  apparatus, 1058–71
    modifications, 1087–8
  definition, 1057
  intermediates, study of, 1505
  iodine radical recombination, 848–9
  kinetic studies with, 1088–9, 1103–4
Flash spectroscopy, 1060–1, 1063
  apparatus, 1070–1
  operating characteristics, 1072
Flow, 714–20
  equations
    Poiseuille's equation, 718
    Prandtl's equation, 718
    Reynolds' formula, 715
  stream-line, 718–19
  turbulent, 715, 718–19
Flow apparatus, 708–11, 724, 728–57
  accelerated, 729, 731
    enzyme kinetics, 1240, 1322, 1347
  Chance, 731, 733–41, 742
  Dalziel and O'Brien, 731, 745–8
  Forrest, 731
  Gibson, 731, 740, 741–5, 748
  LuValle, 731
  rapid, 728, 731
  regenerative, 749–54, 757
    applications, 754–7
    intermittent type, 751
  spectrophotometric, 731
  stopped, 729, 731, 741, 748
  Trowse, 731
Flow measurement, apparatus. *See* Flow apparatus
  errors
    deviation from mass flow, 717–20
    mixing time and slit length, 720–4
Fluorescence, quenching, 852, 855
  rate constant determination, 850–60
Fluorescent intensity, measurement, 853–4
Fluorophotometry, relaxation methods, 976
Forced solutions, relaxation equations, 917
Forcing function, damped harmonic, 922–3, 994
  exponential, 920–1
  general, 923
  harmonic, 924
  linear, 920
  rectangular pulse, 921–2
  rectangular step, 918–19, 981
  relaxation equations, 917
Forcing parameters, 928–9
Formic acid, ionization, 1384
Forms of reactants, 183–4
Fractionation, high-polymer extraction, 1142–4

Free energy, 33, 210–49, 518
linear relationships, 210–49, 518
Free energy of activation, 33, 221, 1371–2
variations with solvent, 1391
Free radical reactions, 363, 364, 366, 368, 407–10, 465–86, table, 481
addition of CCl_3Br to cyclohexene, 1173
inhibition, 471–3
initiation, 475–8
isotope effects in, 407–10
methyl radicals, 480–3, table, 481
product criterion, 1417–24
propagation, 478–80
sensitization, 470
stereochemical studies, 1568–70
termination, 480–2
Free radicals
addition polymerization. *See* Radical addition polymerization
compounds producing, 1168–9
detection, 465–70
isotopic tracers, use of, 468–9
mass spectrometry, 467–8
mirror technique, 465–6
entrapment, 1439, 1480–2
nonuniformity of propagation, 1122–4
Freeze-drying, high-polymer separation, 1149
Friedel-Crafts reactions, 652–3
Fructo-furanosidase, water in reactions of, 1245
Fugacity, 30–1, 512–13
Fumarase, pK values, 1291
Fundamental vibrational frequency, 1366

G

Galvanostat, chronopotentiometry, 830
F-factor, 934–6
Gas phase reactions, apparatus, 428–37
manometer, 433–4
reaction vessel, 431–2
thermostat, 428–31
vacuum line, 432–4
Arrhenius equation, 454–6
differential rate equation, 451–2
flow systems for rate measurements, 436–7, 445–6
free radical reactions, 465–86
homogeneous, 427–87
integrated rate equation, 447–51
rate constant calculation, 446–56
rate measurements, 438–46, 1376–80
static systems for rate measurements, 435–6
temperature control, 428–31
General acid catalysis, 230–4, 602–5
hydration of epoxides, 1396
hydrolysis of esters, 605
water in, 1389
General base catalysis, 234–6, 386, 613, 1460
Gibbs-Duhem equation, for solutions, 514
Glass electrode, rapid reactions, 784–5
Glucose, mutarotation mechanism, 823–4
Glucose metabolism, 323–5
Glycerol, polymerization with dibasic acids, 1159–60
Graft copolymers, synthesis, 1192–3
Grunwald-Winstein mY relationship, 240–5, 519, 521, 528–9, table, 243
solvent parameter (Y), 242–4, table, 243
Guggenheim method for reaction rate analysis, 507, 545

H

Half-wave potential, dropping mercury electrode, 812
Halobenzenes, nitration, isotopic dilution analysis, 1415
Halogenation, 236, 273–5, 355–7, 361, 362, 369, 378–80, 397–9, 409–10, 414, 418, 477
aromatic, 398–9, 418
electrophilic aromatic, 361
free-radical, 409–10
of ketones, 236, 397, 414
of phenol, 273–5
photochemical, 355–7, 362, 369, 477
Halogens, dissociation and recombination, 846–7
hydrolysis, 1037
isotope studies with, 1539
quantum yield, measurement, 848
α-Halosulfones, 266–7
Hammett acidity function, 521–2, 532–4, 1400, 1460–3
Hammett reaction constant (ρ), 211, 213–20, 220–9, 1465–6, table, 216

Hammett $\rho\sigma$ relationships, 211, 213–20, 220–9, 257, 518
Hammett substituent constant (σ), 211, 213–20, 220–9, 1465, table, 215
Hammett's rule, 45–7
Hammond's postulate, 398, 1394–5
Hanging mercury drop electrode, 839
Heat capacity, chemical contribution to, 942
Heat of activation, 57–9, 113
Heat of reaction, measurements, 544–8
Hemoglobin, disoxygenation of, 719–20, 740–1, 744, 747
  first kinetic measurements on, 706
  thermal studies, 773
Heterogeneous catalysis, 650–701
  activating agent, 651–4
  catalyst, 660–1
  closed systems, 654–7
  competitive reactions, 682–6, 690–4
  complex reactions, 678–90
  consecutive reactions, 686–9
  flow systems, 658–60 662
  measurements, 661
  modifier effect, 692–4
  open systems, 657–8
  simple reactions, 668–78
  solvent effect, 690–2
  temperature effect, 675–8
Heterogeneous reactions, 634–50
  fluid phases only, 636–8
  solid phases, 639–50
Hirschfelder rules, 39
Homogeneity of reaction, test for, 432
Homogeneous catalysis. *See* Solution catalysis
Hunsdieker reaction, stereochemical studies, 1570
Hydrocarbons, deuterium-exchange studies, 1537
  oxidation, product criterion, 1418–21
  photochlorination, 1423–4
Hydrogen bonding, 584
Hydrogen bromide, formation, 119, 150–3
Hydrogen chloride, formation, 161–3
Hydrogen electrode, rapid reactions, 783
Hydrogen iodide, formation, 149–50
Hydrogen ion catalysis, 597–602
  Brønsted rate equation, 599–602
  h_0 function, 598–9
Hydrogen peroxide, decomposition by ferrous ion, 1169
  reaction with catalase, 1332–43
Hydrogen transfer, isotope effects in, 393–5, 397–8, 407–11, 1535–9
Hydrolysis. *See* Solvolysis.
Hydrolytic degradation of polymers, 1210–14
Hydroperoxides, formation mechanism, 1418–19, 1531
Hydroxyl ion, reaction with glass, 182
Hydroxyl ion catalysis, 606–7
Hydroxylamine, reduction by ferrous ion, 806–7
Hyperconjugation, isotope effects in, 402–3

I

Indole, formation, nitrogen-15 studies, 1534
Induced reactions, 159–61, 351–4
Induction factor, 159, 351
Induction period, 163, 474–5
Inductive effects. 225, 260
Infinity value, 199
Inhibition, 161–4
  enzyme reactions, 1277–87
  intermediates, isolation of, 1441
Inhibition index, enzyme systems, 1282
Inhibitors, 162
  enzyme reactions, 1277–8
  polymerization initiation, 1169–70
Initial rate evaluation, 122
Integrated rate equation, 7, 447–51, 513
Interface, 632, 634, 639–50
Intermediates, 2, 12–13, 49–50, 83, 143–4, 146, 164, 378–80, 1373
  carbon, divalent, 1416–17
  classification, 1429–32
  cyclic, 1487
  definition, 1428, 1435
  detection of, 12–13, 83, 1439–46
  determination of, 1107–36
  diversion with radical traps, 13
  evidence for formation, 1447–1503
  flow sheets for, diagrams, 143, 144, 164

identification in competing reactions, 378–80
ion-pair. *See* Ion pairs
isolation, 146
linear intermediate, 318
partitioning of, 1449–50, 1454
isotopic exchange studies of, 1499
product criterion, 1412
reactive, 1432–5
transient, spectra, 1074–5
Intermittent illumination, experimental methods, 1126–30
free radical rate determination, 1111–30
theory, 1111–26
Internal rotation, partition function, 1369–70
Iodine, dissociation and recombination, 848–9
Iodonium ion, 1488
Ion-pair dissociations, 1382–3
Ion pairs, 1456, 1490–1, 1498
oxygen-18 studies, 1531–3
Ionic media, 530–6
Ionic polymerization, 1197–1203
anionic, 1200–1
carbonium-ion initiated, 1197–1200
Ionic reactions, 44–5
product criterion, 1410–16
rate constants, 904
recombination, 960
relaxation studies, 1023–5
volume of reaction, 939
Ionic strength, 44, 519, 520–1
Ionization, of enzymes, 1287–8
Irradiation, initiation of chemical reactions, 1056
Isobutene, hydration, 1384–5
Isochoric systems, 26
Isochromates, method of, 1012
Isokinetic relationship, 204–10
Isokinetic temperature, 207–10
Isomerization, 442–3, 447, 448–9, 461, 463
of allyl vinyl ether, 442–3
Arrhenium parameters, table, 463
cis-trans, 1378–80
of cyclobutene, 442–3
of cyclopropane, 461
of isopropenyl allyl ether, 448–9
of *cis*-methyl cinnamate, 447
Isooctene, catalytic hydrogenation, 656–7
Isotactic polymers, 1204
Isothermal calorimetry polymerization, reaction rate of, 1167
Isotope effects, 9, 40–3, 389–425, 356–7, 379
acid-base catalysis, 404–7, 412–14
autoxidation, 408–9
Bigelseisen theory, 390–7
carbon. *See* Carbon, isotope effects with
decarboxylation, 414–15, 418
deuterium. *See* Deuterium, isotope effects with
elimination reactions, 400–1, 419–21
enolization, 397, 412–14
free radical reactions, 407–10
halogenation
aromatic, 398–9, 418
of ketones, 397, 414
Hammond's postulate, 398
hydrogen transfer, 393–5, 397–8, 407–11
intermediates, formation of, 1472–5
intermolecular, 396–7, 415
intramolecular, 396–7, 409, 415
nitrogen. *See* Nitrogen, isotope effects with
oxidation, 398, 408, 410–11
oxygen. *See* Oxygen, isotope effects with
proton transfer, 397–8
on reaction rate, 9
redox reactions, 410–11
secondary, 395, 401–4
of solvent, 404–7
solvolysis, 402–4, 405, 416
substitutions
aliphatic nucleophilic, 402–5, 416
aromatic electrophilic, 398–400
aromatic nucleophilic, 421
sulfur. *See* Sulfur, isotope effects with
theory, 389–97
tritium. *See* Tritium, isotope effects with
zero-point energy, 40–1, 43
Isotopic dilution analysis, aromatic substitution, 1414–15
Isotopic exchange, alcohols, 1530–1
intermediates, formation of, 1499
Isotopic tracers, 10, 11, 43, 147, 468–9, 1519–45

enzyme reaction rate measurement, 1237–8
intermediates, study of, 1492–9

J

Johnson Foundation electronic analog computer, 299–302

K

Ketenes, carbene source, 1416–17
Ketones, 233, 236
enolization, 233
halogenation, 236
Kinetic current, 804
chronopotentiometry, 827–8
Kinetic data recording. *See under* Time measurements
Kinetic isotope effects, 1472–5
Kinetic spectrophotometry, 1060–1, 1063, 1080–4
Kinetics. *See* Rate of reaction
Kinetics experiments. *See* Rate measurements
Kolbe electrolysis, stereochemical studies, 1569

L

Lactic dehydrogenase, stereochemistry, 1578
β-Lactones, catalytic hydrolysis, 613
Lambert-Beer law, 77, 541–2
flash photolysis, 1076, 1082–4
relaxation methods, 973–4
Least squares method, for rate constant determination, 450
for reaction rate analysis, 507–8
Lifetime, fluorescent, 854
Lifetime of reaction chain, 1110–11
intermittent illumination, 1116
Lindemann mechanism, 460
Lineweaver-Burk equation, 1252–3
London forces, 256, 270, 581–2
Longitudinal relaxation time, NMR, 870

M

Magnesium sulfate, sound absorption curve, 1021
Magnetometry, enzyme kinetics, 1323
Maleic acid, addition of bromine, 1488
recombination, rate constant, 816
Manometry, enzyme kinetics, 1241–2
Mass action law, 294, 303, 519
Massieu function, 930
Maxwell-Boltzmann equation, 19
Mechanism of reaction
bimolecular reactions, 465
chain mechanism, 457–9
complex reactions, 3, 4–6, 10–12
computers in determination of, 285–326
deduction from kinetic data, 271–8
definition, 2
determination, 1–14, 145–8
critical experiments, 145–7
necessary data, 145
tracer methods for, 10, 11
enzymes, 623–4
free radical reactions, 465–86
homogeneous gas phase reactions, 457–86
intermediates, 2, 12–13
kinetic concepts, 110, 501–3, 516–18, 1361–1403
postulation, 136–45
Bodenstein steady state approximation, 138–43
exact, 136–8
miscellaneous methods, 143–5
numerical approximation, 138
product criterion, 1407–24
quasiheterolytic reactions, 464
reliability, 147–8
simple reactions, 3–4, 9–10
stereochemistry and, 10, 11, 1549–79
transition state, 2, 3–6
unimolecular reactions, 460–4
Meerwein-Ponndorf-Verley reaction, 1571
Mesomeric effects, 218, 260
Metallic sulfides, oxidation, 644
Metathetical reactions, 478–9, table, 479
Methallyl chloride, dimerization mechanism, 1173–4
Methyl ammonium chloride, NMR analysis, reaction kinetics, 881–2
Methyl ketones, base-catalyzed reactions, 1478

Methyl methacrylate, copolymerization with acrylonitrile, 1191
polymerization
in benzene, 1174
termination mechanism, 1172
Methyl radicals, 364, 366, 480–3
recombination, 480–3, table, 481
rate, 1133
Methylation, α- and β-, effect on dehydrohalogenation, 463–4, table, 464
Methylene glycol, dehydration, 818, 823
Methyleneazomethine rearrangement, 1567
Methylisopropylcarbinyl acetate, pyrolysis, 1412–13
Methylmercuric iodide, acid cleavage, 1384
Michaelis constant, 1251
ratio of for two substrates, 1254
Michaelis-Menten enzyme catalysis, 302–11, 334, 666, 1248–51, 1317–21
computers in study of, 302–11
one substrate, 1260–1, 1270–1
stoichiometric reflection coefficient, 334
two substrates, 1271–3
Minimum structural change, principle of, 1393
Mirror-trapping method, 1481
Modifiers, in heterogeneous catalysis, 692–4
Molecular relaxation. *See* Relaxation, molecular
Molecularity, 457
Moment of inertia, rotational, 1364
Monochromator, double replica-grating type, 735–7
flash photolysis, 1068
Hilger D246, 745
Monomer activity ratio, 1182–3
determination, 1184–6
Monomolecular reactions, F-factor, 935
rate measurements
flow method, 717–18, 723
polarographic, 807–8
rapid thermal method, 773, 775
Mutarotation, glucose, mechanism, 823–4
Myoglobin, 728

N

Naphthalene, flash photolysis, 1091–4
Neighboring group, 1469–70
Nickel sulfate, sound absorption curve, 1021
Nitration, 276–8, 251, 554–6
of alkylbenzenes, 251
aromatic, 276–8
Nitric oxide, decomposition, 139–43, 455–6
inhibition of chain reactions by, 471–2
Nitrobenzene, catalytic hyrogenation, 662–3, 696–9
p-Nitrofluorobenzene, aromatic nucleophilic substitution, 1503
Nitrogen-15, isotope effects with, 421–2, 1533–4
analytical methods, 1543
Nitromethane, neutralization, 559
Nitronium ion, 546, 555
Nitrophenyl esters, catalytic hydrolysis, 589, 607–12, 623–4
Nitrosohydroxylamine, recombination rate constant, 816
Noncompetitive inhibition, in enzyme systems, 1280–4
Normal modes, 1364
Nuclear magnetic resonance, 865–6
rate constant evaluation, 876, 881–7
theory, 866–75
Nuclear quadrupole moments, 872
Nucleation, 640–50
Nucleophilic catalysis, 239–40, 607–12, 613–17
Nylon, extraction, 1144–5
polymerization reaction, 1150

O

1-Octene, catalytic hydrogenation, 695
2-Octene, catalytic hydrogenation, 656–7
Olefins, hydration, 566–9, 1403
oxidation, 1133
Order of reaction, 111, 120–5, 188–9, 446–7, tables, 114–15, 120–5
complex reactions, 123–5
Ostwald isolation method, 125
determination, 120–5
enzyme system, 1264–6, 1327–30
simple reactions, 120–2
half-time, 121
Outgassing of solutions, 1065

Oxidation, 398, 408, 410–11, 569–73.
See also Autoxidation
determination of active intermediates, 1133–6
of hydrocarbons, 569–73
isotope effects in, 398, 408, 410–11
stereochemical studies, 1570–1
Oxidative degradation of polymers, 1218–20
Oxygen, photochemical reaction with chlorine, 1078
Oxygen-18, isotope effects with, 419, 1496–8, 1501, 1529–33
analytical methods, 1542–3
Oxygen exchange, alcohols, 1530–1
Oxygen metabolism, 323–5

P

Paneth mirror technique, 378, 465–6
Paper-strip chromatography, high-polymer separation, 1146
Paramagnetic pulse procedure, 885–7
Partially competitive inhibition, in enzyme systems, 1287
Partition functions, 1364–70
equilibrium constants, 1361–3
internal rotation, 1369–70
rate constants, 1371
in solution, 1380–2
translational, 1367
vibrational, 1368–9
Pepsin, heat and entropy of activation for, 1299
Peroxidase, 1343–54
kinetics, 1322–3
Peroxides, decomposition of, 1168, 1421–3
Peroxy compounds, 1531
Peroxysulfate ion, reduction by vanadyl or chromic ions, 155–6
pH, effect on enzyme activity, 1287
on catalase activity, 1330–1, 1342–3
Phase constant, sound, 1005
Phase memory time, NMR, 870
Phase velocity, sound. 954
Phenol, dehydration, catalytic, 678–82
hydrogenation, catalytic, 688
iodination, 273–5
proton transfer reactions with 1040
Phenonium ion, 1489
α-Phenyl aryl ethers, rearrangement, 1568
Phenyl azide, formation, 1533–4
Phenyl–*sec*-butyl ketone, halogenation, 1449–50
α-Phenylethyl halides, 528–9
1-Phenylethyl hydroperoxide, rearrangement, 1531
Phenylpyruvic acid, recombination rate constant, 816
Photochemical reactions, 1459
Photolysis, of benzophenone, 382
entrapment of radicals, 1439–40
flash photolysis technique, 1056–1104
Photomultiplier tube, 975, 1068–9
Pinacol rearrangement, carbon-14 studies of, 1528–9
Pinsent's quenching apparatus, 780–1
Planck's function, 929
Platinum microelectrode, 785–6
Poiseuille's equation, 718
Polarimetry, relaxation methods, 976–7
Polarization of reaction, 930
Polarography, 801–23
catalase-hydrogen peroxide decomposition, 786–7
enzyme kinetics, 1242, 1322–3
oxygen determination, 785–6
Polyfunctional catalysis, 1234–5
Polymerization, 164–8, 363, 367, 371–3, 1149–1210
condensation polymerization, 1149–60
copolymerization, 1181–93
emulsion polymerization, 1193–7
intermediates, study of, 1484
ionic polymerization, 1197–1203
persulfate-induced, 1539–40
radical addition polymerization, 1160–81
stereospecific polymerization, 1204–10
vinyl, chain transfer, 363
Polymers, block copolymers, 1189–92
condensation, 1213
degradation, 1210–20
graft copolymers, 1192–3
isolation and purification
chromatography, 1144–6
drying, 1148–9
fractionation, 1142–4
precipitation, 1141–2
living polymers, 1201–2
tacticity, 1204–5

three-dimensional, 1157–60
Polymethyl methacrylate, degradation, 1216
purification, 1142–3
Polysarcasine dimethylamide, separation, 1146
Polystyrene, polymerization in chlorobenzene, 1174
purification, 1142, 1145–6
Polyvinyl acetate, degradation, 1216
Potential energy, 24–5, 36–9, diagrams, 25, 37, 41, 42
Potential energy surface, 36–9, 509
Prandtl's equation, 718
Precipitation, polymer separation, 1141–2
Pressure, effect on enzyme systems, 1301-3
gaseous systems, 74–5
Pressure-jump methods, 983–8
Pressure measurements, 441–2, 564–6
Pressure-shock methods, 981–8
Primary salt effects, in solution catalysis, 605–6
Product criterion, 1407–24
intermediates, formation of, 1475–86
Product distribution, 1476–7
Propagation constant, sound, 1005
Propionyl peroxide, decomposition of, 1421
Propionyloxy radical, behavior, 1421
n-Propyl bromide,dehydrobromination,449
Propylene, inhibition of chain reactions by, 472–3
Proteins, thermal denaturation of, 1295–7
Proteolytic coefficient, 1269–70
Protolytic reactions, relaxation studies, 1033–7
Proton transfer, isotope effects in, 397–8
relaxation studies of, 1038–40
Pulse radiolysis, 1102
Pyrene, fluorescence in benzene, 855–6
Pyridinoprotein dehydrogenases, 1238–9
Pyrolysis. *See* Thermal decomposition *under specific substances*
Pyruvic acid, recombination rate constant, 816
reaction layer concept, 801–3

Q

Quadrupole relaxation pulse method, 887–8
Quantity measurements, 67–84
Quantum yield, measurement, 847–8
flash photolysis, 1072
Quenching of fluorescence, 24, 35–6, 852, 855
Quinaldinic acid, decarboxylation, 1483
Quinolinate, recombination rate constant, 816
Quinones, kinetics, 1094–1102
electron transfer reactions, 1041

R

Radiation pressure, relaxation studies, 1013
Radical addition polymerization, 1160–81
initiation reaction of, 1167–71, 1179
reaction rate, measurement of, 1163–7
termination mechanism of, 1172–3
transfer mechanism of, 1173–5
Random copolymers, 1203
Rankine balance, 750
application of flow apparatus, 754–5
Rapid reactions, electrometric measurements, 781–7
flow measurement, 703–57. *See also* Flow measurement
gasometric method, 787–8
quenching, 779–81
thermal measurement, 758–78. *See also* Rapid thermal method
ultrafiltration method, 788–91
Rapid thermal method, 758–78
accuracy, 765–7
apparatus, 759–63
applications, 775
reactions studied, 773–5
Rate constant, 22, 58, 111, 112, 126–36, 195–6, 199, 293–7, 298, 446–56, 504–8
calculation, 126–36, 451–2, 454–6
analytical methods, 127–32
differential rate equation, 451–2
flow method, 453–4
graphic methods, 126–7
indirect, 134–6
least squares method, 131–2, 134
long-interval method, 127–8
method of averages, 130–1
short-interval method, 128–9

computers in calculation of, 293–7, 298
derivation from data, 195–6
determination, 446–56. *See also* Rate constant, calculation
fluorescence, determinations with, 850–60
fractional times, 450–1
graphical, 448–50
least squares method, 450
potentiostatics, 839
errors in calculation, 504–8
infinity value, 199
partition functions, 1371
statistical treatment of rate data, 132–4
Rate-determining steps, 5, 49, 155, 517
Rate equations for correlation with environment, 522–8
differential, 451–2, 510–11
empirical, 111–19, 136–45
Arrhenius equation, 113
comparison to postulated mechanism, 136–45
complex reactions, 119
half-time, 112, tables, 114–15
isochoric, isothermal systems, 111–13, table, 118
nonisochoric, nonisothermal systems, 113 -19, table, 118
order of reaction, 111, tables, 114–15
integrated, 7, 447–51, 513
linearized, 901–2
Rate measurements
accuracy, 55–9, 504–8
of aldolization and dealdolization, 552–3
analytical method, 181–3
apparatus for, 72–7, 79, 81, 428–37
calorimeter, 75–7, 79
dilatometer, 72–3
interferometer, 73–4
manometer, 74–5, 433–4
polarimeter, 81
reaction vessel, 431–2
thermostat, 428–31
vacuum line, 432–4
calorimetry, 544–7
chemical analysis, 68
chronopotentiometry, 833
closed systems, 537–9
colorimetry, 79–80
complex reactions, 196–9
conductometry, 556–62
defects in experiments. *See* Rate measurements, errors
density of liquids, 71–3
differential thermal analysis, 547–8
dilatometry, 548–56
electrical conductivity, 81–2
electron spin resonance, 84, 888–91
environmental control, 55, 59–61
enzyme reactions, 1236–43
errors, 56–9, 178–98, 190–3, 504–8
evaluation, 178–99
flow systems, 64–7, 436–7, 445–6
stirred reactors, 66–7
straight tubes, 64–6
of fluorescence, 80
gas evolution methods, 69–70
gas phase chromatography, 68
of gas phase reactions, 438–46, 563–73
gravimetric methods, 70
indirect, 62, 70–84
infrared analysis, 80
initiating and quenching reactions, 62–3
kinetic considerations, 6–7
kinetic plot, 190–3
light absorption, 71, 77–80
mass spectrography, 68
mass spectrometry, 84, 437–8, 444
nitration, 554–6
nuclear magnetic resonance, 881–7
open systems, 536–7
optical methods, 442–4
optical rotation, 80–1
oxidation of hydrocarbons, 569–73
photometric methods, 442–4
polarimetry, 80–1, 540–1
polarography, 539, 807–9, 819–22
precision, 504–8
pressure, 74–5, 441–2
refractive index, 73–4
reproducibility of data, 193–4
rotating-disk electrode, 836
significance of data, 189–90
spectrophotometry, 77–9, 541–4
static systems, 435–6, 440–4
stationary field method, 837–8
temperature of adiabatic systems, 75–7
vacuum line technique, 538
vapor phase chromatography, 437–8, 444

volumetric analysis, 536
yield, 250–5
Rate of reaction, absolute calculation, 35–40
absolute reaction rate, theory of, 2, 8, 36, 40–7, 501, 502, 509–14, 528–9
addition polymerization, 1162–7, 1169
Arrhenius hypothesis, 32–3
bimolecular reaction, 529–30
catalysis, 154–9
chain reactions, 161–4, 168–71
comparison of reactions with dissimilar mechanism, 529–30
constant. *See* Rate constant
copolymerization, 1186–9
cyclic reactions, 150–3
environmental effects on, 518–36
enzymes, 1314–57
equations. *See* Rate equations
equilibria, 33–4, 149–50, 501, 502
evaluation in complex reactions, 381–6
explosions, 168–71
forms of reactants, 183–4
frequency factor, 28
Hammett's rule, 45–7
in heterogeneous reactions, 642–7
induced reactions, 159–61
induction period, 474–5
initial, 515–16
interpretation of data, 110–71, 178–278
ionic media, 530–6
ionic reactions, 44–5
isokinetic relationship, 204–10
mathematical analysis, 506–8
Guggenheim method, 507
least squares method, 507–8
measurements. *See* Rate measurements
nucleophilic displacements, 245–7
polymerization, 164–8
potential energy, 24–5, 36–8, diagrams, 25, 37, 41, 42
prediction, 34, 35
recombination of protons with ions of weak acids, 815–18
salt effect on, 43–5, 519–20
slow reactions, 7
in solutions, 500–73
solvent effects on, 208–519
structural effects on, 8–9, 208, 255–71, 518
temperature coefficient, 22–3
temperature control, 186
temperature dependence, 528
theories, 15–50, 501–2
transmission coefficient, 28–9, 33
Rate-product criterion, 1480
Reaction layer concept, 801–7
chronopotentiometry, 827–8
Reaction mechanism. *See* Mechanism of reaction
Reaction rate. *See* Rate of reaction.
Reaction steps, 47–50, 166, 475–82
initiation, 166, 475–8, 1056–7, 1109–10, 1418
propagation, 166, 478–80, 1418
termination, 166, 480–2
Reactions
autocatalytic, 653
bimolecular, 465, 529–30
chain. *See* Chain reactions.
competing. *See* Competing reactions.
consecutive. *See* consecutive reactions.
cyclic, 150–3
free-radical. *See* Free radical reactions.
heterogeneous. *See* Heterogeneous reactions.
identification, 179–80
induced. *See* Induced reactions.
ionic. *See* Ionic reactions.
metathetical, 478–9
quasiheterolytic, 464
redox, 410–11
sequential catalytic, 591–4
series, 204–5
unimolecular, 460–4
Rearrangement reactions
carbon-14 studies of, 1521–9
intermediates in, 1484–6
stereochemical studies, 1561–8
1,2-Rearrangements, stereochemical studies, 1563–6
1,3-Rearrangements, stereochemical studies, 1563–6
Red blood cell, life-span of, 1237–8
Redox potentials, rapid thermal method, 785
stereochemical studies, 1570–4

Redox reactions, isotope effects in, 410–11
relaxation studies, 1039
Reduction, stereochemical studies, 1571–4
Reduction activation, 1169
Refractive index, polymerization reaction rate measurement, 1164–5
Regenerative flow apparatus. *See under* Flow apparatus
Relaxation, chemical, 896–7
Relaxation, molecular, 896
Relaxation methods, 869–1049
experimental techniques, 966–1029
stationary. *See* Stationary relaxation methods
theory, 901–66
transient. *See* Transient relaxation methods
Relaxation spectrum, 913
analysis, 914–15
characteristic equation, 908
transformation matrix, 909
Relaxation time, 896–7, 901
measurement, 917
thermodynamics, 905–14, 948, 950
Resonators, relaxation studies, 1007–10
Reverberation, relaxation studies, 1010–11
Reversibility of reactions, 192
Reynolds' formula, 715
Rotating-disk electrode, 834–7
Rotating sector method, 1131
Rotational isomerism, 1019
mechanism, 1048
relaxation studies, 1044, 1049
Rubber, oxidative degradation, 1218

S

Salt effect, 43–5, 277–8, 519–21
intermediates, formation of, 1453–7
special, 1456–7
Scanning spectrophotometer, flash photolysis technique, 1061
Semipinacolic deamination, 1565
Semiquinones, kinetics, 1094–1102
Shielding constant, 875
Shielding effect, 1487
Shock-tube technique, 1056
Sigma complex, 1434
Silicone oil, in flash photolysis, 1066
Sing-around system, relaxation studies, 1015
Smiles rearrangement, 267–8
Solute-solvent interaction, 525–6, 527
Solution catalysis, 579–626
adsorption rate, 588
catalyst-reactant intermediate, 585–96
charge-charge interactions, 582–4
complex formation, 589–6
continuous flow stirred reactor, 593–4
dipolar interactions, 582–4
dispersion forces, 581–2
entropy of complex formation, 584–5
enzymes. *See* Enzyme catalysis
equilibration between solvent phase and catalyst phase, 588–90
general acid. *See* General acid catalysis
general base. *See* General base catalysis
hydrogen bonding, 584
hydrogen ion. *See* Hydrogen ion catalysis
hydroxyl ion. *See* Hydroxyl ion catalysis
inhibition, 594–6
intermediate complexes, 585–96
London forces, 581–2
multifunctional, 617–20
nucleophilic. *See* Nucleophilic catalysis
primary salt effect, 605–6
proton transfer, 602–5
sequential catalytic reactions 591–4
Solutions, 500–73
activity coefficient of solute, 512–13
choice of solvent, 504
fugacity of solute, 512–13
specific techniques for rate measurements, 536–73
Solvent effects, 23–4, 30–1, 208, 404–7, 519, 690–2
in heterogeneous catalysis, 690–2
intermediates, formation of, 1452–3
isotope effect of, 404–7
Solvolysis, 240–4, 358, 361–2, 377–81, 383, 402–4, 405, 416, 519
of alkyl halides, 240–2, 358, 361–2, 377, 383, 1453–4
of alkyl sulfonates, 1532–3
of arylmethyl chlorides, 561–2

of benzhydryl halides, 379–80, table, 380
of benzoyl chloride, 559–61
of butenyl chlorides, 381
of *tert*-butyl halides, 528–9, 563
common ion effect, 383
of esters, 377
of halogens, 1037
isotope effects in, 402–4, 405, 416
methoxymercuration, 377–8
of α-phenylethyl halides, 528–9
stereochemical studies, 1552, 1554
Sound, velocity of, 953–5
Sound absorption, relaxation studies, 1006–22
Sound intensity, definition, 1016
Sound propagation, propagation constant, 1005
wave equation, 952
Sound pulse technique, relaxation studies, 1014–15
Special salt effects, 1456–7
Specific heat, chemical contribution to, 942–3
Specific interaction of ions, 44–5
Spectraphone method, relaxation studies, 1014
Spectrograph, in flash photolysis, 1070
Spectrophotometer
Beckman, 731
in flow apparatus of Dalziel and O'Brien, 745–6
sensitivity, 747
enzyme reactions, 729–31
double-beam system, 730–1
rapid recording, 752
relaxation methods, 973–6
Spectrophotometry enzyme kinetics, 1238–41, 1322,1336–8, 1344–5
isolation of intermediates, 1442–4
Spectroscopy, flash photolysis, 1060–1
Spherical resonator, relaxation studies, 1008–9
Spin-lattice relaxation time, NMR, 869, 872
Spin-spin interaction, 876
Spin-spin relaxation time, NMR, 871–2
Spin temperature, NMR, 869
Square pulse method, 992–4
Square wave light pulses, 1124–6
Stability constant, 936
Standard state, 29, 30, 512–13
Stationary high-field techniques, 1022
Stationary relaxation methods, 924–8, 951, 1004–29
Statistical thermodynamics, and reaction mechanism, 1361–75
Steady state, 138–43, 307–8, 327–30, 336–7, 338–41, 349–50, 352–3, 386, 688
Bodenstein approximation, 138–43
changes, 329–30
induced steady state, 328–9, 336–7
kinetic information from, 845–6
kinetic steady state (steady state region), 327–8
Steady state analysis, ionic polymerization rates, 1197, 1199
Steady state region, 307–8, 338–41
in computer solutions of reaction mechanisms, 307–8
superposition principle, 338–41
Stereochemistry, relation to reaction mechanism, 1549–79
Stereospecific polymerization, 1204–10
Steric effects, 222, 259, 261–2, 265–6, 267–8
intermediates, formation of, 1468, 1486–92
steric acceleration, 267–8
Stevens rearrangement, 1566
Stirred reactor. *See* Continuous flow stirred reactor.
Stoichiometric reflection coefficients, 327–41, 929
definition, 330–1
linear chain, 333–2
Michaelis-Menten system, 334
properties, 331–2
Stoichiometry, 180, 293–7, 298–9, 327–41, 437–8, 503–4
of homogeneous gas phase reactions, 437–8
use of computers in study of, 293–7, 298–9
Stopped-flow method, 705, 707
apparatus, 729, 731, 741, 748
electrometric measurements with, 782–4
enzyme catalysis, 1450
enzyme kinetics, 1240, 1322, 1347

rapid thermal measurements with, 777–8
Strain-entropy rule, 1388
Streaming mercury electrode, 840
Structural effects, 8–9, 208, 255–71, 518
cis effect, 265–6
conformational effects, 268–9
intermediates, formation of, 1463–72
London forces, 256, 270
neighboring group participation, 258, 263
d-orbital resonance, 267
ortho effects, 226–7, 269–70, table, 227
recognition of, 256–70
Smiles rearrangement, 267–8
substituent effects, 257
Styrene, depolymerization of, 1420
living polymers, 1202
polymerization
by potassamide, 1201
by stannic chloride, 1198
Substitution, 276–8, 398–400, 402–4, 407–10, 416, 421, 517. *See also* Displacements.
aliphatic nucleophilic, 517, 402–4, 405, 416
isotope effects in, 402–4, 405, 416
aromatic electrophilic, isotope effects in, 398–400
aromatic nucleophilic, 276–8, 421
isotope effects in, 421
free-radical, isotope effects in, 407–10
silicon, nucleophilic, 277–8
stereochemical studies, 1550–5
Sugars, reduction, 823
Sulfur ion, autoxidation, 163–4
Sulfur, liquid, ESR, 889–90
Sulfur-35, isotope effects with, 419–21, 1539–40
analytical methods, 1544
Sulfuric acid, acidity functions, 1402
Superposition principle, 338–41
Swain-Scott equation, 245–7
Syndiotactic polymers, 1205

T

Taft-Hammett parameter, 1397
Taft's equations, 220–9, 257, 269–70
inductive effects, 225
ortho effects, 226–7, 269–70, table, 227
reaction constants, table, 224
steric effects, 222
substituent constants, tables, 223, 227
Techniques for rate measurements. *See under* Rate measurements
Temperature, effect in enzyme systems, 1292–1301
relation to entropy, 942–4
Temperature coefficient, 22–3, 113
Temperature control, 59–61, 186, 428–31
in homogeneous gas phase reactions, 428–31
thermostat, 60–1, 428–31
Temperature dependence of reaction rate, 528
Temperature-jump methods, 969–81
enzyme kinetics, 1323
equipment, 977–81
Tetrabutylammonium picrate, entropy of dissociation, 1383
Tetralin and *p*-xylene, competitive catalytic hydrogenation, 685–6
Tetramethylammonium picrate, entropy of dissociation, 1383
Theory of absolute reaction rates. *See under* Reaction rates
Thermal degradation of polymers, 1214–16
Thermocouple, 761
Thermodynamics, and rate mechanism, 1361–1403
Thioglycol, proton transfer reactions with, 1040
Thiosulfate, oxidation by peroxide, 154–5
Thunberg tubes, 1240
Time measurements, 61–7, 89–108, 186–7, 446
in flow systems, 64–7
stirred reactors, 66–7
straight tubes, 64–6
interval timers, 92–4
recording instruments, 94–108
analog timers, 93–4
cathode-ray oscillograph, 100–7
digital timers, 92–3, 108
electrical oscillators, 90
EPUT meter, 93
galvanometric, 97–8

kymograph, 95
loop galvanometer, 99–100
magnetic tape, 107–8
photographic, 99–100
printer bar recorder, 97–8
stopclock, 92
strip chart recorders, 96
universal time, 91
Toluene, dimerization, 1044
mercuration, 1414
Trace impurities, 187–8
metal ions, 187
oxygen, 187
water, 188
Tracer studies. *See* Isotopic tracers
Transfer function, 924–8
thermodynamic conditions, 948, 950
Transient intermediates, absorption spectra, 1074–5
enzyme reactions, 1248
Transient relaxation methods, 967–1003
Transient state enzyme kinetics, 1245–6, 1314–57
Transient solution, relaxation equations, 916
Transition state, 2, 3–6, 24–31, 32–4, 390, 501–2, 509, 1435–9
activity coefficient, 29–31
Boltzmann distribution, 26
condensed systems, 29–31, 34
energy of activation, 24–5, 26–7, diagram, 25
fugacities, 30–1
monomolecular reactions, 30
rate of transformation, 27-8
reaction coordinate, 27–8
transition complex, 24, 25, 27–8
Transition state theory, comparison with collision theory, 32–4, 1294
enzyme systems, 1294–1301
Transition time, chronopotentiometry, 824–6
Translational energy, 1367
Translational partition function, 1367
Transmission coefficient, 28–9, 33, 510, 511–12, 524–5
Trichloromethyl radicals, competing reactions, 368
Triethylamine, sound absorption curve, 1020
Triphenylethyl glycol, pinacol rearrangement, carbon-14 studies of, 1528–9
Triphenylmethyl chloride, hydrolysis in H_2O-dioxane, 1455
ionization in liquid SO_2, 1434
Triplet state, 1089
kinetics, 1090
Tritium, isotope effects with, 393–6, 397–414
analytical methods, 1544
Trypsin, heat and entropy of activation for, 1299
thermodynamic values for thermal denaturation of, 1297
volume changes during reaction, 1303
Tuning fork resonator, relaxation studies, 1007–8
Tunnel effect, 43, 390, 392, 394

U

Ultrafiltration, 788–91
Uncompetitive inhibition, in enzyme systems, 1287
Unimolecular reactions. *See* Monomolecular reactions
Univac I electronic digital computer, 322–5
β,γ-Unsaturated nitrile, isomerization, 1501–2
Uranyl ferrioxalate, in flash photolysis, 1072
Uranyl oxalate, absorption spectrum, 1072
Uranyl uranate, oxidation, 644, 646–7

V

van't Hoff complex, 664, 1430
Verdoperoxidase, 1345–6
Vibrational energy, 1366
Vibrational partition function, 1368–9
Vinyl acetate, polymerization in benzene, 1174
Vinyl ethers, polymerization by iodine, 1199
Vinyl octyl ether, ionic polymerization, 1198
Viscosity measurements, polymer degradation, 1211

Volume change measurements, 548–56, 564
Volume magnetic susceptibility,
detection of, 754
method, 751
Volume of activation, 1375

W

Water formation, mechanism, 144–5
Wien effect, 988
relaxation studies, 1023
Wurtz reaction, 1492

X

o-Xylene, catalytic hydrogenation, 656
p-Xylene and tetralin, competitive catalytic hydrogenation, 685–6

Y

Yield, 11–12, 250–5

Z

Zero-point vibrational energy, 1392–3
Zucker-Hammett hypothesis, 521

T. P. I. LIBRARY, MYSORE

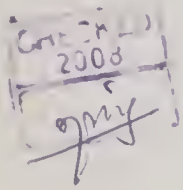

CFTRI-MYSORE
5578

Investigation of

E1, 5:f"n, 1, N49
Call No. N48:2B
FREISS and
others
nique of
mistry
II